

Resource-Economical Synthesis by Selective Metal-Catalyzed C–H Activations

Dissertation

for the award of the degree

“Doctor rerum naturalium” (Dr.rer.nat.)

of the Georg-August-Universität Göttingen



within the doctoral program of chemistry
of the Georg-August-Universität School of Science (GAUSS)

Submitted by
Uttam Dhawa
From Kolkata, India

Göttingen, 2021

Thesis Committee

Prof. Dr. Lutz Ackermann, Institute of Organic and Biomolecular Chemistry

Prof. Dr. Manuel Alcarazo, Institute of Organic and Biomolecular Chemistry

Members of the Examination Board

Reviewer: Prof. Dr. Lutz Ackermann, Institute of Organic and Biomolecular Chemistry

Second Reviewer: Prof. Dr. Manuel Alcarazo, Institute of Organic and Biomolecular Chemistry

Further members of the Examination Board

Prof. Dr. Dr. h.c.mult. Lutz F. Tietze, Institute of Organic and Biomolecular Chemistry

Prof. Dr. Ricardo Mata, Institute of Physical Chemistry

Dr. Michael John, Institute of Organic and Biomolecular Chemistry

Dr. Daniel Janßen-Müller, Institute of Organic and Biomolecular Chemistry

Date of the oral examination: 15.04.2021

List of Abbreviations

Å	Ångström
Ac	acetyl
acac	acetyl acetate
Alk	alkyl
AMLA	ambiphilic metal-ligand activation
$[\alpha]_D$	specific rotation at 589 nm
aq.	aqueous
Ar	aryl
atm	atmospheric pressure
BHT	2,6- <i>di-tert</i> -butyl-4-methylphenol
BIES	base-assisted internal electrophilic substitution
Bn	benzyl
Boc	<i>tert</i> -butyloxycarbonyl
Bu	butyl
Bz	benzoyl
calc.	calculated
<i>cat.</i>	catalytic
CMD	concerted-metalation-deprotonation
conv.	conversion
Cp*	pentamethylcyclopentadienyl
Cy	cyclohexyl
CyH	cyclohexane
δ	chemical shift
d	doublet
DCE	1,2-dichloroethane
dd	doublet of doublet
DFT	density functional theory
DG	directing group
DME	dimethoxyethane
DMF	<i>N,N</i> -dimethylformamide
dt	doublet of triplet
EI	electron ionization

equiv	equivalent
ES	electrophilic substitution
ESI	electrospray ionization
Et	ethyl
FG	functional group
g	gram
GC	gas chromatography
h	hour
Hal	halogen
Het	hetero atom
Hept	heptyl
Hex	hexyl
HFIP	hexafluoro-2-propanol
HPLC	high performance liquid chromatography
HR-MS	high resolution mass spectrometry
Hz	Hertz
<i>i</i>	<i>iso</i>
IR	infrared spectroscopy
IES	internal electrophilic substitution
<i>J</i>	coupling constant
KIE	kinetic isotope effect
L	ligand
<i>m</i>	<i>meta</i>
m	multiplet
M	molar
[M] ⁺	molecular ion peak
Me	methyl
Mes	mesityl
mg	milligram
MHz	megahertz
min	minute
mL	milliliter
mmol	millimol

M. p.	melting point
MS	mass spectrometry
<i>m/z</i>	mass-to-charge ratio
NCTS	<i>N</i> -cyano-4-methyl- <i>N</i> -phenyl benzenesulfonamide
NMC	<i>N</i> -Methylcaprolactam
NMTS	<i>N</i> -cyano- <i>N</i> -(4-methoxy)phenyl- <i>p</i> -toluenesulfonamide
NMP	<i>N</i> -methylpyrrolidinone
NMR	nuclear magnetic resonance
<i>o</i>	<i>ortho</i>
OA	oxidative addition
OPV	oil pump vacuum
<i>p</i>	<i>para</i>
Ph	phenyl
PhMe	toluene
PMP	<i>para</i> -methoxyphenyl
Piv	pivaloyl
ppm	parts per million
Pr	propyl
PTSA	<i>p</i> -Toluenesulfonic acid
py	pyridyl
pym	pyrimidine
pyr	pyrazol
q	quartet
RT	room temperature
s	singlet
sat.	saturated
SPS	solvent purification system
<i>t</i>	<i>tert</i>
t	triplet
T	temperature
THF	tetrahydrofuran
TLC	thin layer chromatography
TM	transition metal

TMP	3,4,5-trimethoxyphenyl
TMS	trimethylsilyl
Ts	<i>para</i> -toluenesulfonyl
TS	transition state
<i>t_r</i>	retention time
<i>wt%</i>	weight percentage
UV	ultraviolet
X	(pseudo)halide

Table of Contents

1. Introduction	1
1.1. Transition Metal-Catalyzed C–H Activation	1
1.2. Transition Metal-Catalyzed C–F/C–H Functionalization	6
1.2.1. Precious Transition Metal-Catalyzed C–F Functionalization	6
1.3. Enantioselective C–H Activation	11
1.3.1. Palladium Catalysis	11
1.3.2. Rhodium Catalysis	20
1.3.3. Iridium Catalysis	26
1.3.4. Ruthenium Catalysis	35
1.3.5. Nickel Catalysis	36
1.3.6. Cobalt Catalysis	39
1.3.7. Iron Catalysis	42
1.4. Transition Metal-Catalyzed Oxidative C–H Activation towards Resource Economy.	44
1.4.1.1. Palladium-Catalyzed C–H Olefinations with Chemical Oxidants	44
1.4.1.2. Cobalt-Catalyzed C–H Activations with Chemical Oxidants	48
1.4.1.3. Copper-Catalyzed C–H activations with Chemical Oxidants	52
1.4.2. Electrochemical Transition Metal-Catalyzed C–H Activation	56
1.4.2.1. Palladium Catalysis	57
1.4.2.2. Cobalt Catalysis	61
1.4.2.3. Copper Catalysis	67
2. Objectives	69
3. Results and Discussion	74
3.1. Manganese(I)-Catalyzed (Per)Fluoro-Allylative and Alkenylative C–F/C–H Functionalizations	74
3.1.1. Optimization Studies	74
3.1.2. Substrate Scope and Limitations	76
3.1.3. Proposed Catalytic Cycle	83
3.2. Ruthenium(II)-Catalyzed <i>E</i> -Selective Allylative C–F/C–H Functionalization	85
3.2.1. Optimization Studies	85
3.2.2. Substrate Scope	89
3.2.3. Mechanistic Studies	93
3.2.4. Proposed Catalytic Cycle	95

3.3. Enantioselective Cobalt(III)-Catalyzed C–H Activation	97
3.3.1. Optimization Studies	97
3.3.3. Effect of <i>N</i> -Substitution Pattern	100
3.3.4. Substrate Scope and Limitations	102
3.3.5. Mechanistic Studies	107
3.3.6. Proposed Catalytic Cycle	111
3.4. Ruthenium(II)-Catalyzed Enantioselective C–H Activation	113
3.4.1. Optimization Studies	113
3.4.2. Effect of <i>N</i> -Substitution Pattern	117
3.4.3. Substrate Scope	119
3.4.4. Mechanistic Studies	121
3.4.5. Proposed Catalytic Cycle	123
3.5. Copper-Catalyzed Alkyne Annulation by C–H Alkynylation	125
3.5.1. Optimization Studies	126
3.5.2. Substrate Scope and Limitations	126
3.5.3. Proposed Catalytic Cycle	131
3.6. Electrochemical Cobalt-catalyzed C–H Allylation	133
3.6.1. Optimization Studies	133
3.6.2. Substrate Scope and Limitations	135
3.6.3. Mechanistic Studies	140
3.6.4. Proposed Catalytic Cycle	143
3.7. Enantioselective Palladaelectro-Catalyzed C–H Activations	146
3.7.1. Optimization Studies	146
3.7.2. Substrate Scope	148
3.7.3. Mechanistic Studies	154
3.7.4. Product Diversification	157
4. Summary and Outlook	162
5. Experimental Part	169
5.1. General Remarks	169
5.2. General Procedures	172
5.3. Manganese(I)-Catalyzed Allylative C–H/C–F Functionalization	177
5.3.1. Characterization Data	177
5.3.2. Removal of Directing Group	195
5.4. Ruthenium(II)-catalyzed C–F/C–H functionalization	196

5.4.1. Characterization Data.....	196
5.4.2. Mechanistic Studies	210
5.5. Enantioselective Cobalt(III)-catalyzed C–H activation	214
5.5.1. Analytical Data of Novel Chiral Acids	214
5.5.2. Characterization Data of the Alkylated Products.....	218
5.5.3. Removable of the Directing Group	232
5.5.4. Mechanistic Studies	234
5.6. Ruthenium(II)-Catalyzed Enantioselective C–H Activation	239
5.6.1. Characterization Data.....	239
5.6.2. Mechanistic Studies	245
5.7. Copper-catalyzed Alkyne Annulation by C–H Alkynylation	249
5.7.1. Characterization Data.....	249
5.8. Electrochemical Cobalt-catalyzed C–H Allylation.....	263
5.8.1. Characterization Data.....	263
5.8.2. Mechanistic Studies	273
5.9 Enantioselective Palladaelectro-Catalyzed C–H Activations	277
5.9.1. Characterization Data.....	277
5.9.2. Late stage Diversification	289
5.9.3. Mechanistic Studies for the Atroposelective C–H Activation	299
5.10. Crystallographic Data.....	302
6. References	312
Acknowledgements	333
Annexes	335

1. Introduction

Organic synthesis has paramount importance in science and society. Since the emergence of organic synthesis in early 19th century as marked by revolutionary discovery of the preparation of urea by Wöhler in 1828 in Germany,^[1] organic synthesis has changed the world with its gigantic applications for the benefit of society.^[2] Organic synthesis has direct impact on several new domains ranging from the development of modern medicines to the production of nutritional goods, cosmetics, functional materials, including polymers, plastic, among others. Despite the vast applications of organic synthesis in resolving societal issues, there are rising concerns for the economical and environmental impact of its processes. Consumption of nonrenewable resources, including energy and materials, emissions of toxic and hazardous waste have detrimental effect on the environment.^[3]

Thus, efforts have been devoted to the discovery and emergence of resource-economical, environmentally-benign strategies in the field of organic synthesis,^[4] providing the guidelines of green chemistry as put forwarded by *Anastas* and *Warner* in their 12 Principles of Green Chemistry.^[5] Among these guidelines, the application of catalytic processes rather than stoichiometric transformations, easily available starting materials, minimization of waste formations, mild reactions conditions are of prime importance to elevate the power of organic transformations to the standards of Nature and beyond.^[6]

1.1. Transition Metal-Catalyzed C–H Activation

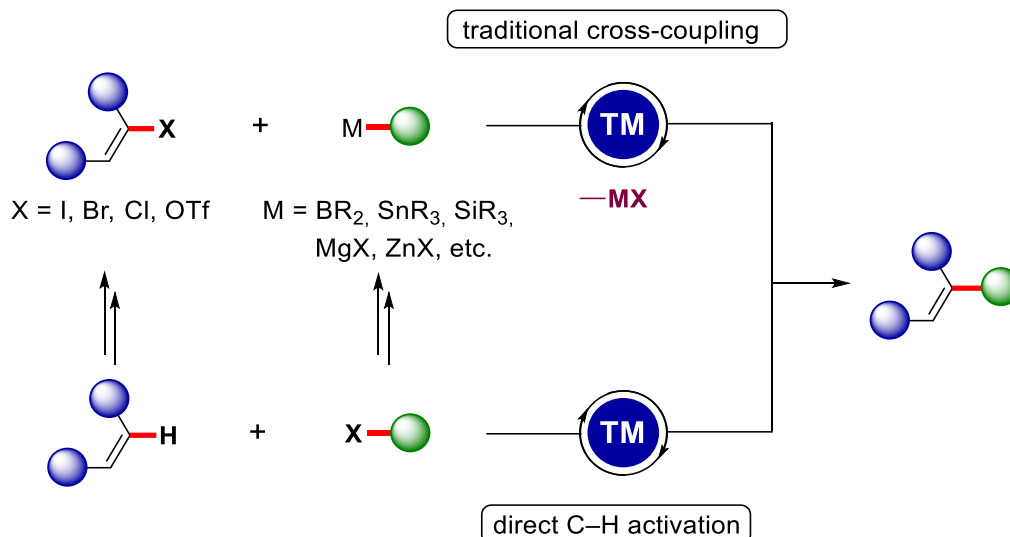
Initial discoveries in the rich history of transition metal-catalyzed cross-coupling reactions^[7] originate from the pioneering, 150 years old, reactions by Glaser^[8] and Ullman^[9] on copper-promoted or -catalyzed cross-coupling reactions. These intriguing studies set the stage for metal-catalyzed C–C/C–Het bond forming reactions between two structural units.^[10] Nevertheless, starting from the 1950s palladium started to gain its market value with the development of well known palladium on charcoal^[11] and Lindlar catalysts.^[12] Later, Hafner discovered the famous Wacker process for the syntheses of acetaldehyde which became a benchmark study on exhibiting the potential of palladium in the synthesis of organic molecules.^[13] Meanwhile, Heck found the application of palladium catalyst in cross-coupling reactions with organomercurial compounds.^[14] Few years later, almost at the same time, Mizoroki^[15] and later Heck^[16] independently demonstrated palladium-catalyzed cross couplings between organic halides and alkenes, the *Mizoroki–Heck* reaction. With this pioneering study, the last five decades have witnessed a gigantic progress in metal-catalyzed

1. Introduction

cross-coupling reactions. A broad range of organometallic coupling partners has been employed, which has originated in a series of named reactions, like *Suzuki–Miyaura*,^[17] *Negishi*,^[18] *Kumada–Corriu*,^[19] *Hiyama*,^[20] *Stille*^[21] and *Sonogashira–Hagihara*^[22] cross-coupling reactions. Furthermore, the *Tsuji–Trost* reaction^[23] and the *Buchwald–Hartwig* amination^[24] should be mentioned in the context of palladium-catalyzed chemistry. These important discoveries and their highly practical applications both in academia and in industry were recognized with the 2010 Nobel Prize to Heck, Negishi and Suzuki for palladium catalyzed cross-coupling reactions.^[25]

Despite enormous developments, transition metal-catalyzed cross-coupling reactions^[26] associated with several limitations. The need of the pre-functionalized starting materials as well as air- and moisture-sensitive organometallic coupling partners jeopardize the atom-economy and sustainability of this otherwise powerful approach. More importantly, the generation of stoichiometric, potentially toxic organometallic compounds as by-products are highly undesirable to conserve the environmental integrity.

In stark contrast, metal-catalyzed direct C–H activation represents a more sustainable approach towards excellent atom- and step-economy, given the ubiquitous presence of C–H bonds in organic molecules.^[27] Thereby, C–H activation offers more environmentally-benign, practical approaches for large-scale syntheses without the lengthy prefunctionalization of starting materials, thereby providing improved step-economy and preventing concurrent undesired waste generation. Thus over the past years, transition metal catalyzed C–H activation has surfaced as a powerful tool to improve the efficacy of molecular synthesis with notable applications in late-stage diversification,^[28] material sciences,^[29] and pharmaceutical industries,^[30] among others. Nevertheless, the applications of cost-effective Earth-abundant 3d transition metals^[31] further enhance the sustainability of the C–H activation^[32] approach (Scheme 1).

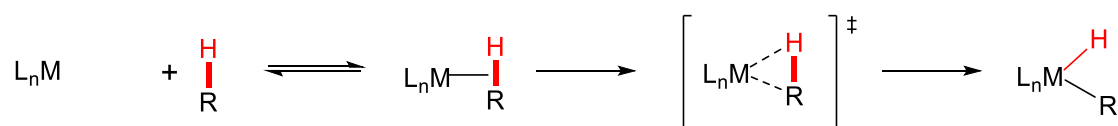


Scheme 1. Traditional cross-coupling vs C–H Activation.

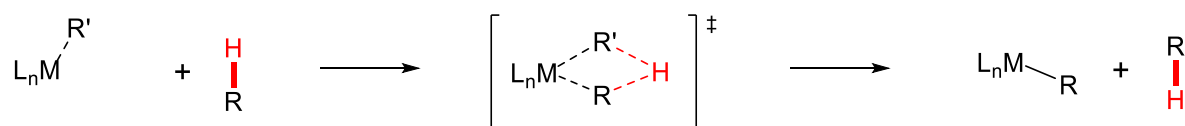
Despite the enormous importance of organometallic C–H activation approach, the formation of C–Metal bond from C–H bond is far more challenging as the C–H bond is generally stronger than the C–X bond.^[33] Thus, over the past years several studies have been directed towards elucidating the mechanistic pathways of the key C–H activation step to enable better catalytic processes. In this respect, different modes of action have been proposed for the elementary C–H metalation event.^[34] These include: a) the oxidative addition pathway is more feasible for late transition metal at lower oxidation states, where achieving higher oxidation states are much easier (Scheme 2a). b) In contrast, σ -bond metathesis is more prominent for early transition metals where concerted breaking of C–H bond and formation of C–Met bond occurs (Scheme 2b). c) Electrophilic substitution pathway is proposed for late transition metals in high oxidation states usually in polar medium (Scheme 2c). d) Like σ -bond metathesis, 1,2-addition pathways are more feasible for early transition metals featuring multiple unsaturated double bonds (Scheme 2d). This type of pathway operates *via* $[2\sigma+2\pi]$ reaction. e) Finally, the most common pathway is the base-assisted C–H cleavage, where generally carboxylate bases^[34a] are involved in the proton abstraction (Scheme 2e).

1. Introduction

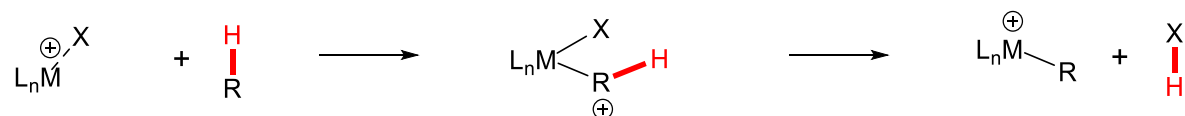
(a) oxidative addition



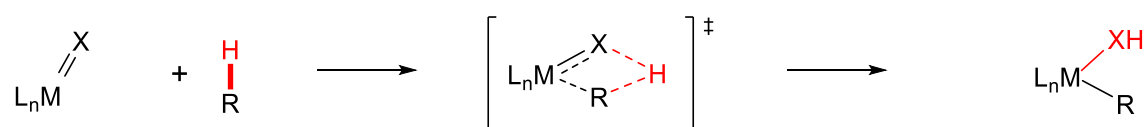
(b) σ -bond metathesis



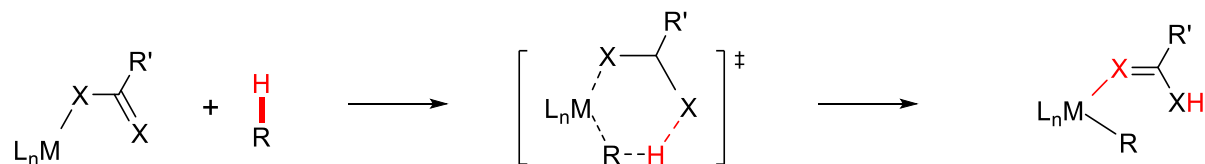
(c) electrophilic substitution



(d) 1,2-addition

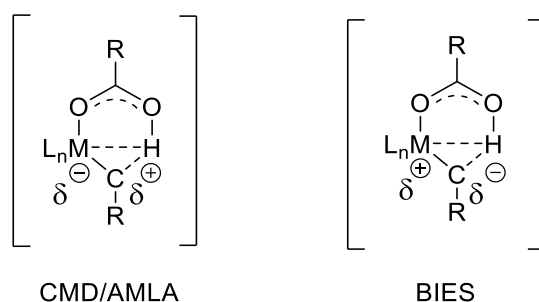


(e) base assisted metalation



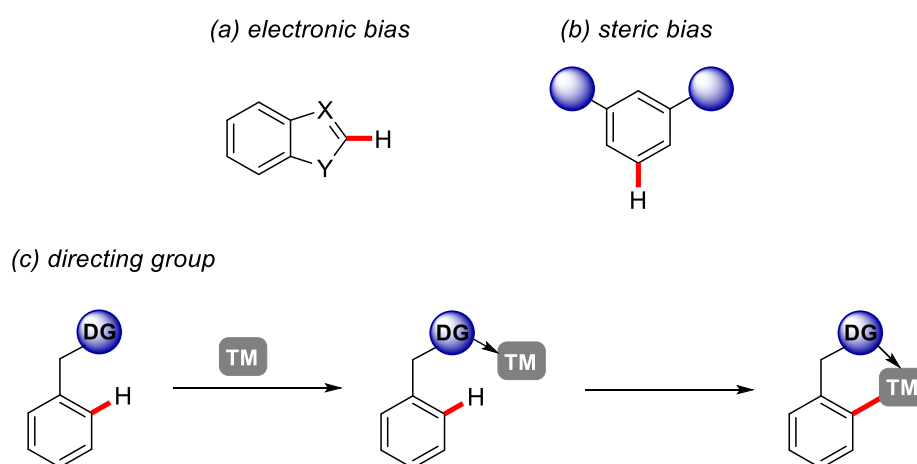
Scheme 2. Mechanistic pathways for organometallic C–H activation.

Consequently, base-assisted C–H metalation has been studied in greater details, giving rise to several distinct pathways. Among them, CMD (concerted metalation deprotonation) or AMLA (ambiphilic metal-ligand activation) and BIES (base-assisted internal electrophilic substitution) pathways have been suggested. The term CMD was named by Fagnou/Gorelsky,^[35] whereas AMLA was disclosed through computational studies by MacGregor/Davies,^[36] although both mechanism presents similar six-membered transition state, where both metalation and deprotonation occur simultaneously. While for BIES mechanism^[37] which was introduced by Ackermann, electrophilic substitution type C–H activation occurs by carboxylate additives. In contrast to CMD/AMLA, the selectivity of BIES type C–H activation is not controlled by kinetic C–H acidity (Scheme 3).



Scheme 3. Comparison of transition state structures in base-assisted metalation.

The control of regioselectivity remains an arduous task owing to subtle reactivity difference of omnipresent C–H bonds. Nonetheless, in recent years several strategies have evolved to address this challenging issue. These include: a) the substrate’s electronic bias by exploiting its inherent more acidic positions. b) Likewise, steric bias forces the activation at the less hindered C–H bond. Unfortunately, these strategies depend on the nature of the substrates, thereby minimizing its generality. In this regard, introduction of directing group (DG)^[27d, 38] with Lewis basic functionalities plays a crucial role for proximity-induced C–H activations (Scheme 4). In addition, the elegant use of the functional groups embedded within the molecules, as directing groups is an alternative atom-economical approach. Thus, considerable efforts have been made towards weakly co-ordinating^[39] and removable directing groups.^[40]



Scheme 4. Selectivity-control in C–H activation.

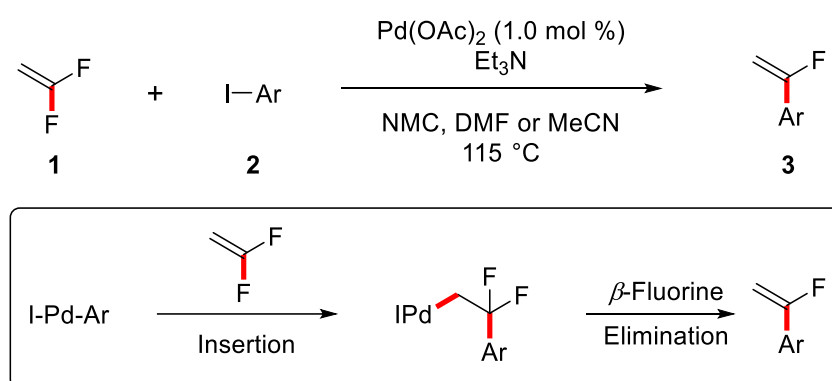
Moreover, recently transient directing groups have gained considerable attention as it avoids the additional steps to install and remove the DG, instead it generates *in situ* DG in a reversible transient manner.^[41]

1.2. Transition Metal-Catalyzed C–F/C–H Functionalization

Fluorinated organic compounds have gained considerable attention in pharmaceutical, agrochemical and material sciences due to their unique chemical and physical properties.^[42] The installation of the small, highly electronegative fluorine atom on organic compounds significantly enhances their solubility and metabolic stability.^[43] Notably, fluoroalkenes are considered as important fluorinated molecules due to their enhanced biological properties.^[44] Therefore, there is a strong demand to get access to the fluorinated building blocks. Among various routes to synthesis fluorinated scaffolds, transition metal-catalyzed fluorination reactions have emerged as a promising approach.^[43a, 45] Alternatively, the selective activation of C–F bonds is step-economical route to synthesize highly functionalized fluorinated molecules.^[42a, 42b] In this context readily available polyfluorinated molecules can be selectively derivatized to form the C–C bonds by transition metal-mediated C–F bond activation.^[46]

1.2.1. Precious Transition Metal-Catalyzed C–F Functionalization

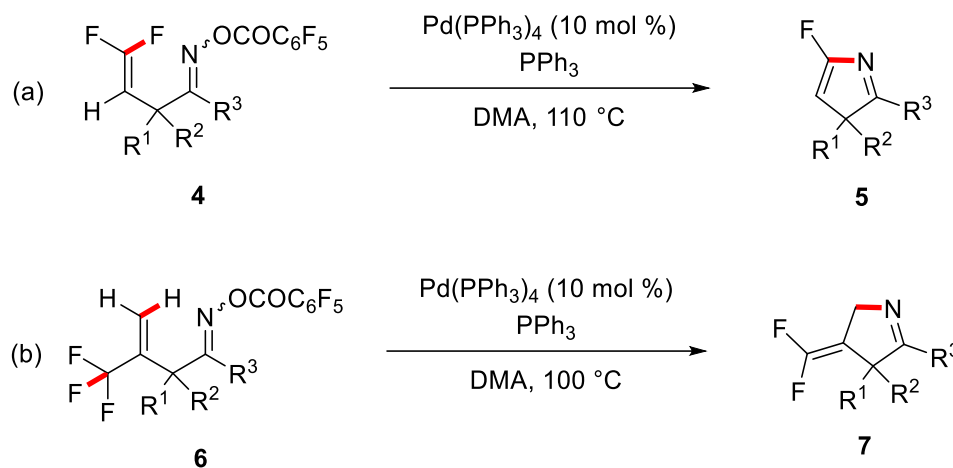
An early example of defluorinative coupling of 1,1-difluoroethylene with aryl halides was elegantly achieved using palladium as catalyst by Heitz in 1991.^[47] In their pioneering contribution, an arylpalladium(II) iodide species was formed in the presence of triethylamine which underwent insertion into 1,1-difluoroethylene **1** to form β,β -difluorinated phenethylpalladium(II) species (Scheme 5). Thus, the formed palladium(II) species readily underwent β -fluorine elimination to furnish α -fluorostyrenes **3**, synthetically valuable building blocks for fluoropolymers.



Scheme 5. Palladium-catalyzed defluorinative coupling through β -fluoro elimination.

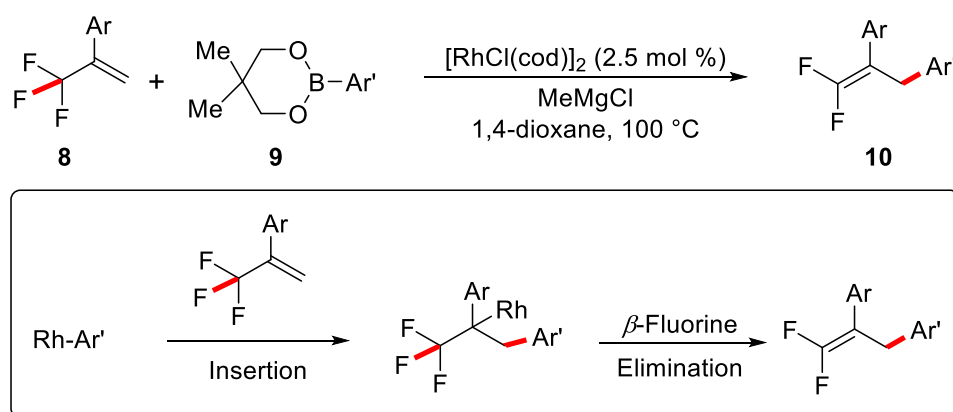
After a decade, in 2005 Ichikawa reported an intramolecular Heck-type 5-*endo*-trig cyclization of oxime derivatives containing 1,1-difluoro-1-alkene motifs **4**.^[48] A combination of Pd(PPh₃)₄ and PPh₃ enabled the facile β -fluorine elimination for the synthesis of 5-fluoro-3*H*-pyrroles **5** (Scheme 6a). Later, the same group extended this strategy to 2-(trifluoromethyl)allyl ketone *O*-

pentafluorobenzoyloximes **6** for Heck-type of cyclization to form *exo*-difluoromethylene **7** unit via exclusively β -fluorine elimination (Scheme 6b).^[49] These elegant findings through fluorine elimination set the stage for further developments in the area of transition metal-catalyzed C–F bond activation.



Scheme 6. Heck-type 5-*endo*-cyclization.

Taking inspiration from these studies, insertion of fluoroalkenes into metal species have been intensively studied in recent years.^[46] Transmetalation of organometallic reagents from main group elements to transition metals is the key step, preceding the insertion into the fluoroalkenes. It is noteworthy to mention that this type of reactivity is largely restricted to organosilicon and organoboron compounds. In an early report in 2008, Murakami showed the potential of rhodium catalysis for the formation of arylrhodium(I) species with aryl boronic esters **9** which underwent insertion into C–C double bond and subsequently selective β -fluorine elimination delivered *gem*-difluoroalkenes **10** (Scheme 7).^[50]

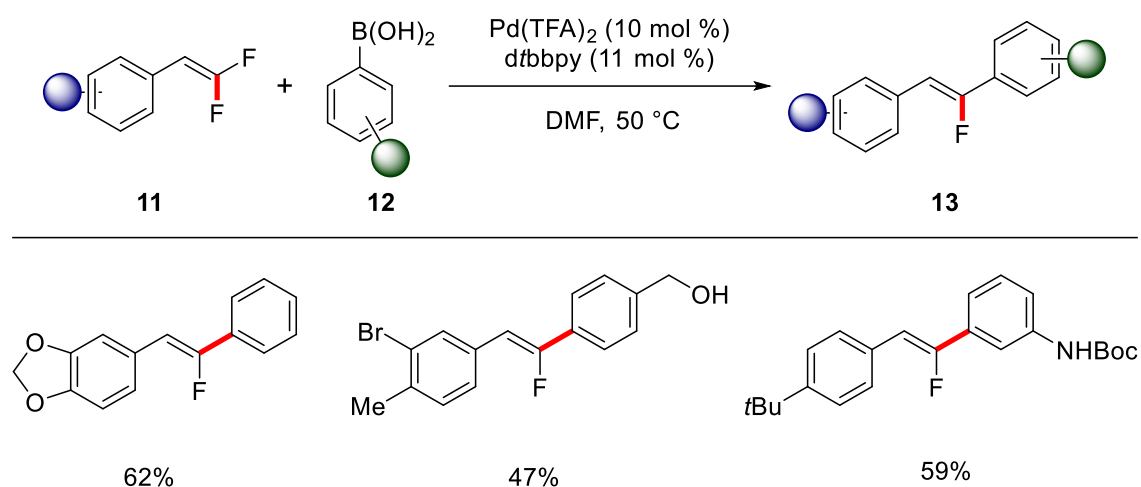


Scheme 7. Rhodium-catalyzed arylation by β -fluorine elimination.

Later, Toste described redox-neutral process for the palladium-catalyzed defluorinative coupling of 1-aryl-2,2-difluoroalkenes **11** with boronic acids **12** via β -fluoride elimination to

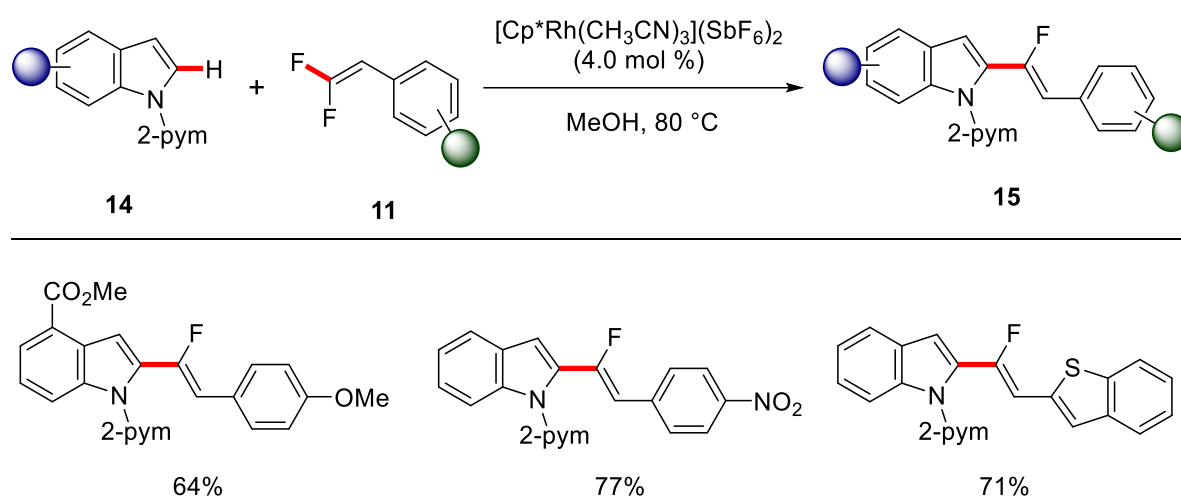
1. Introduction

synthesis monofluoroalkene **13** building blocks (Scheme 8).^[51] Notably, these mild reaction conditions tolerated various sensitive functional groups to afford monofluorostilbene products with excellent diastereoselectivity.



Scheme 8. Palladium-catalyzed defluorinative coupling.

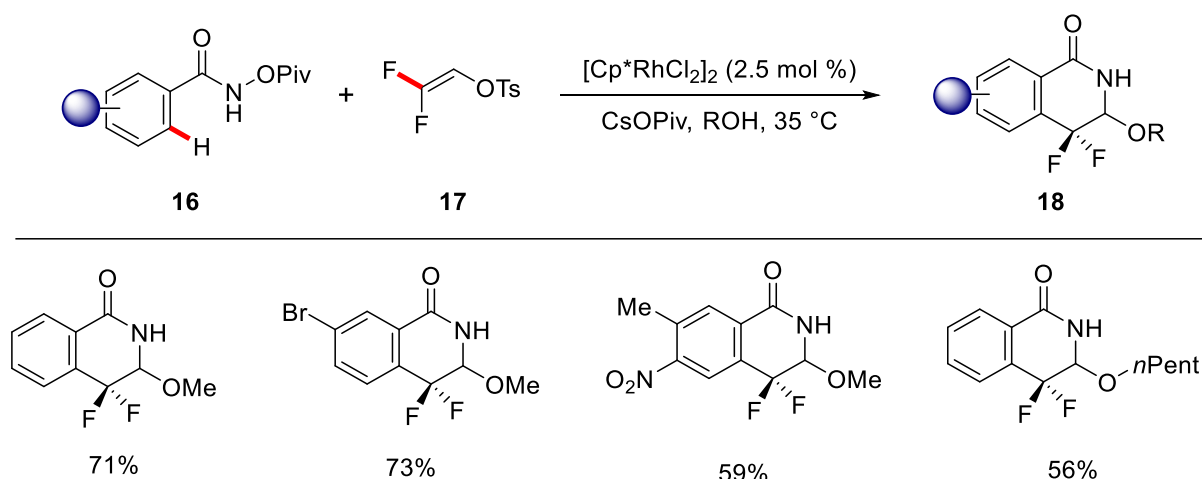
Recently, the merger of C–F activation with challenging C–H cleavage has become a research area of topical interest for the synthesis of highly valuable fluorinated scaffolds. Loh made a significant advancement in this research area by achieving C–F/C–H activation using Cp*Rh(III) catalyst (Scheme 9).^[52] The authors utilized redox-neutral conditions for the α -fluoroalkenylation with 1,1-difluoro-1-alkenes **11** through chelation-directed rhodium(III)-catalyzed C–H bond cleavage of (hetero)arenes **14**. Notably, *in situ* generated hydrogen fluoride had beneficial effect in the outcome of the reaction possibly due to the hydrogen bond involvement in the activation of C–F bond.



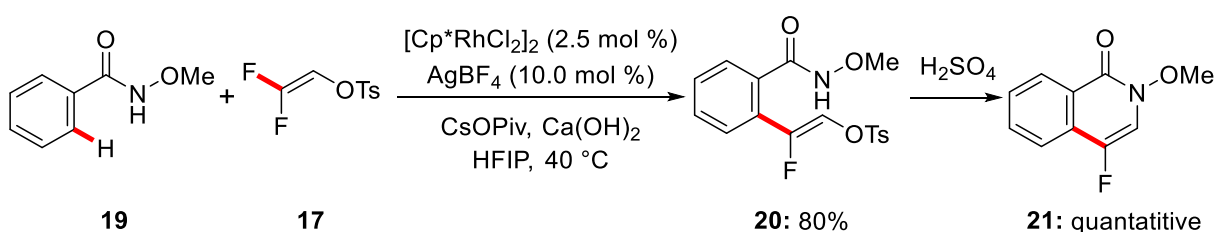
Scheme 9. Rhodium-catalyzed C–H/C–F activation.

In 2017, Li and Wang achieved the synthesis of different types of fluorinated heterocycles by directing group governed distinct reactivities (Scheme 10).^[53] The authors employed a Cp*Rh(III) complex with 2,2-difluorovinyl tosylate **17** as the coupling partner to control the selectivity over C–N formation versus β -fluorine elimination, by using N–OMe and N–OPiv benzamides **16** and **19**. Annulated dihydroisoquinolin-1(2*H*)-ones **18** bearing a *gem*-difluorides substituent at the C4 position were formed when N–OPiv benzamides were used whereas for N–OMe benzamide, mono fluoroalkene **20** was formed by β -fluorine elimination which was further treated under acidic condition to afford 4-fluoroisoquinolin-1(2*H*)-one **21**. In addition, this reaction protocol tolerated a wide range of functional groups under mild reaction conditions.

(a) Synthesis of *gem*-difluorinated dihydroisoquinolin-1(2*H*)-ones



(b) Synthesis of 4-fluoroisoquinolin-1(2*H*)-ones

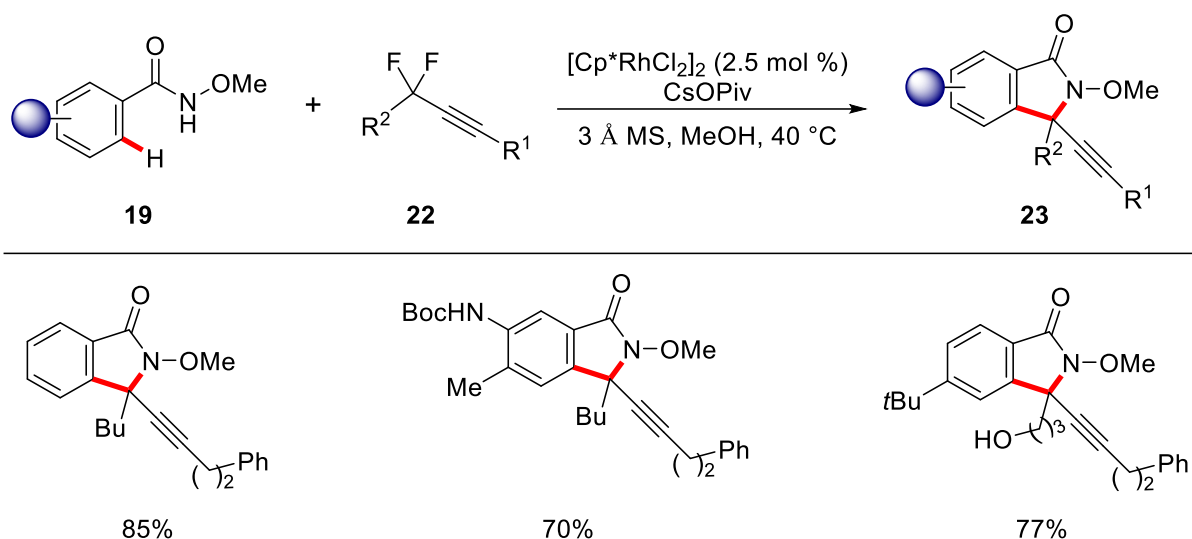


Scheme 10. Rhodium-catalyzed coupling of benzamides with 2,2-difluorovinyl tosylate **17**.

Shortly thereafter, Wang and Loh presented a unique way to synthesize five membered lactams **23** using α,α -difluoromethylene alkynes **22** via Cp*Rh(III)-catalyzed two fold C–F bond cleavage (Scheme 11).^[54] Oxidant-free reaction conditions were employed for the defluorinative [4+1] annulation reaction for the synthesis of alkynyl substituted isoindolin-1-ones **23**. A plethora of α,α -difluoromethylene alkynes **22** worked efficiently as one carbon reaction partner with a migration of C–C triple bond. It should be duly noted that this

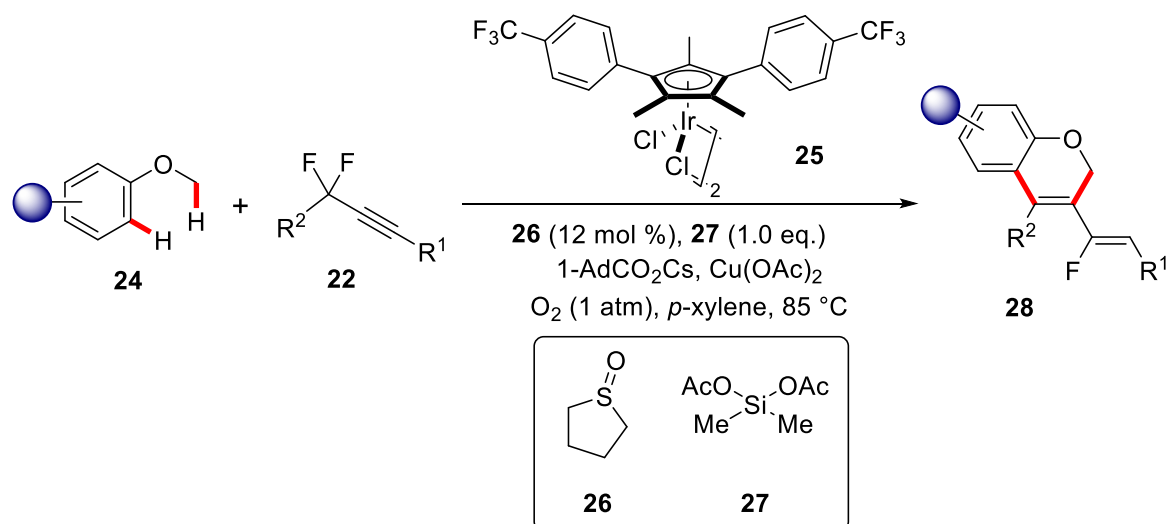
1. Introduction

methodology presents one of the scarce examples in the literature where sp carbon atom of alkyne was used as a one-carbon coupling partner.



Scheme 11. Cp^{*}Rh(III)-catalyzed [4+1] annulation via C–F Bond activation.

In 2018, an iridium(III)-catalyzed double C–H functionalization of C(sp²)–H and C(sp³)–H bonds of anisoles was reported (Scheme 12).^[55] A catalytic combination of Cp^{*}Ir(III) complex **25** and ancillary sulfoxide ligand **26** was employed to enable the sequential cleavage of C–H bonds of anisoles **24**. The authors propose a β -fluorine elimination which leads to the formation of fluoroallene species and in the following steps, subsequent β -H elimination delivered the chromene scaffolds **28**. Likewise, a wide array of anisoles **24** and difluoroalkynes **22** were tested which were efficiently coupled to form the chromene products **28**.

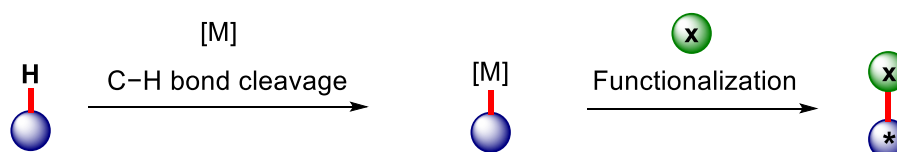


Scheme 12. Iridium-catalyzed double C–H bond activation of anisoles **24**.

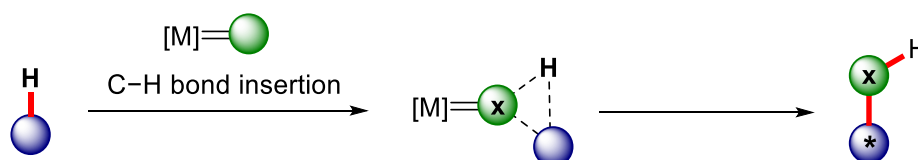
1.3. Enantioselective C–H Activation

The direct activation of inert C–H bonds represents a very attractive, atom- and step-economic approach for providing new synthetic transformations.^[27, 56] However, enantioselective C–H functionalization represents a valuable strategy for the construction of complex chiral compounds from simple precursors by selectively activating particular C–H bonds. Thus, over the past years transition metal complexes have been identified as powerful catalysts for the enantioselective C–H functionalization reactions.^[57] In this context, 4d and 5d transition metals were mainly employed to enable full selectivity control.^[58] With the rising concerns for the prices and toxicities of precious transition metals, recent focus has shifted towards Earth-abundant and cost-effective transition metals^[31] for successful execution of stereocontrolled organometallic C–H activations.^[59] In addition to organometallic C–H activations, outer-sphere processes have also been realized which do not involve the formation of direct metal-carbon bond.^[60] This type of mechanism is more prominent for metal-carbenoid and –nitrenoid insertion reactions (Scheme 13).^[61] So, outer-sphere mechanisms are not discussed here.

(a) *Inner-sphere mechanism*



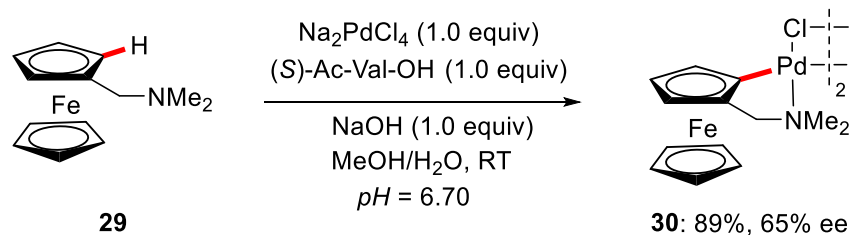
(b) *Outer-sphere mechanism*



Scheme 13. Mechanistic classification for enantioselective C–H activations.

1.3.1. Palladium Catalysis

Since the pioneering studies by Sokolov in 1977 on the introduction of mono-protected chiral amino acids for the enantioselective stoichiometric C–H palladation (Scheme 14),^[62] palladium has become the most commonly applied transition metal for enantioselective organometallic C–H activations. Consequently, a large variety of chiral ligands have evolved for a successful outcome of palladium-catalyzed C–H activation reactions, with commonly used phosphorus-based ligands, such as TADDOL, BINOL and BINAP as well as monoprotected amino acids (MPAA).^[63]

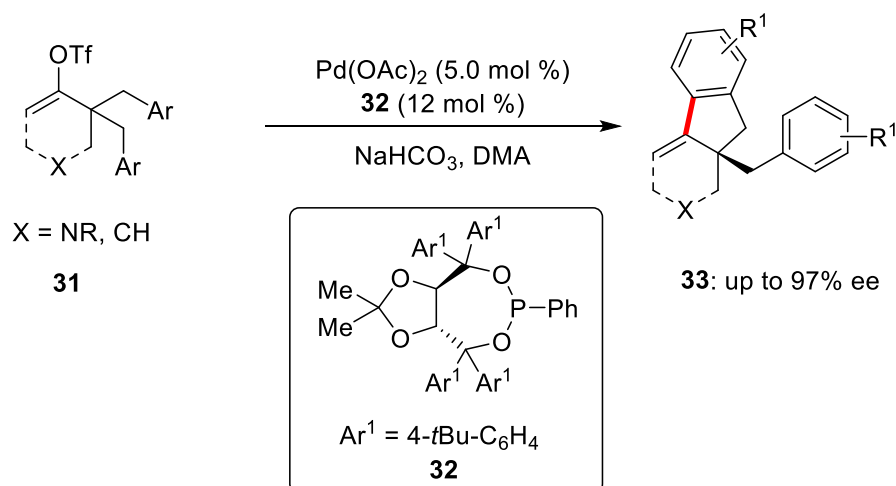


Scheme 14. Enantioselective stoichiometric C–H palladation of ferrocene **29**.

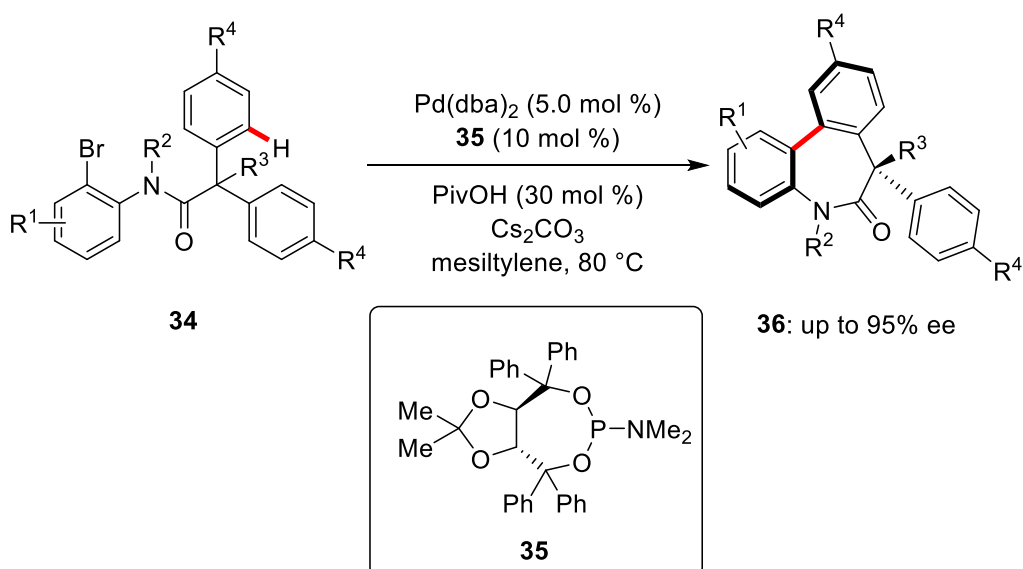
1.3.1.1. Phosphorus-Based Ligands

In 2009, Cramer achieved enantioselective palladium(0)/palladium(II) C–H functionalization in an intramolecular desymmetrization reaction.^[64] The authors utilized a TADDOL-derived monodentate phosphine **32** ligand to induce high enantioselectivity for intramolecular arylation with vinyl triflates **31**. This protocol provided access to a wide variety of chiral indane motifs **33** containing quaternary stereogenic centers with high enantioselectivities (Scheme 15a). Later, a phosphoramidite-type of TADDOL based ligand **35** proved viable for the arylation of bromides **34** in the formation of dibenzazepinones **36** (Scheme 15b).^[65]

(a) Arylation with vinyl triflates

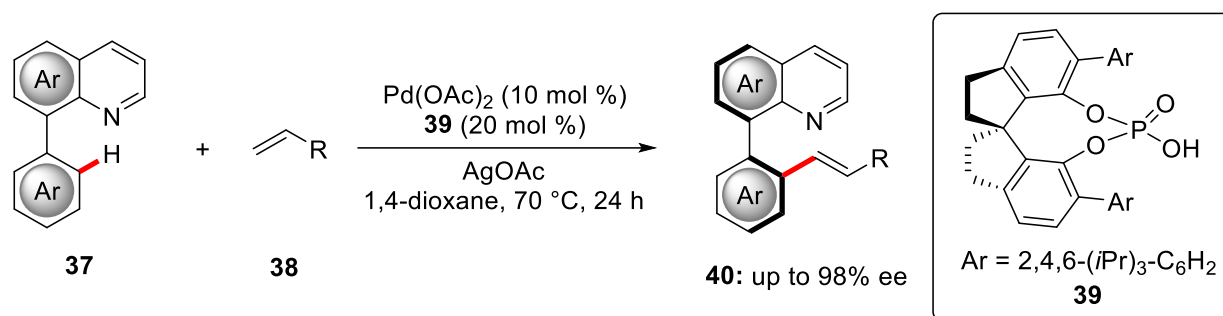


(b) Asymmetric synthesis of dibenzazepinones

**Scheme 15.** Palladium-catalyzed enantioselective intramolecular arylation.

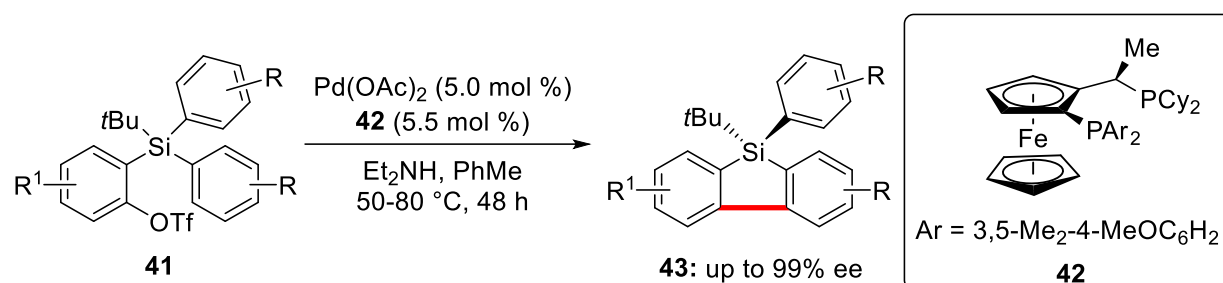
The potential of TADDOL-based ligands was also shown towards the formation of *P*-stereogenic phosphinic amides, as independently reported by Duan^[66] and Ma.^[67] Also, Gu reported TADDOL ligand-facilitated asymmetric induction in an atroposelective cyclization protocol.^[68]

In addition, SPINOL-derived chiral phosphoric acid **39** was found as the best ligand for the palladium-catalyzed atroposelective olefination of arenes **37** (Scheme 16).^[69] Later, the same strategy was employed to free amine (-NH₂) substrates.^[70]



Scheme 16. Palladium-catalyzed atroposelective olefination of arene **37**.

Furthermore, the Josiphos-type ligand **42** was utilized in combination with palladium catalysis for the intramolecular C–H arylation to syntheses highly enantio-enriched silicon-based ring systems **43** (Scheme 17).^[71]

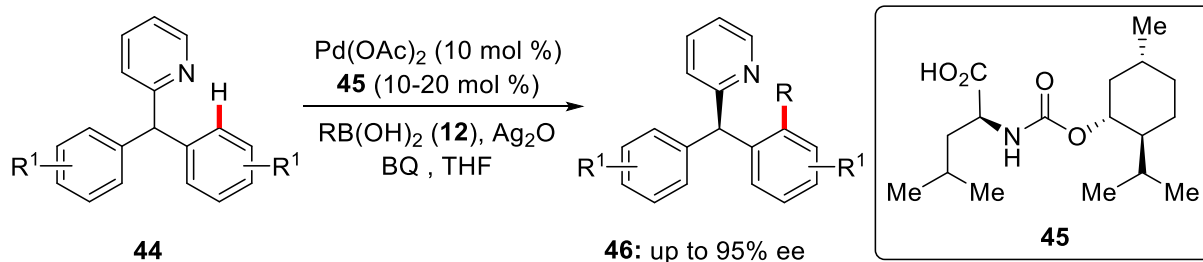


Scheme 17. Palladium-catalyzed desymmetrization of 2-(arylsilyl)aryl triflates **41**.

It is noteworthy that a bifunctional phosphine-carboxylate ligand was also applied for enantioselective palladium-catalyzed arylation reactions by Baudoin.^[72] In 2017, Cramer reported C–H alkenylation of ketene aminal phosphate with a phosphine ligand, containing both point and axial chirality.^[73]

1.3.1.2 Monoprotected Amino Acids as Chiral Ligands

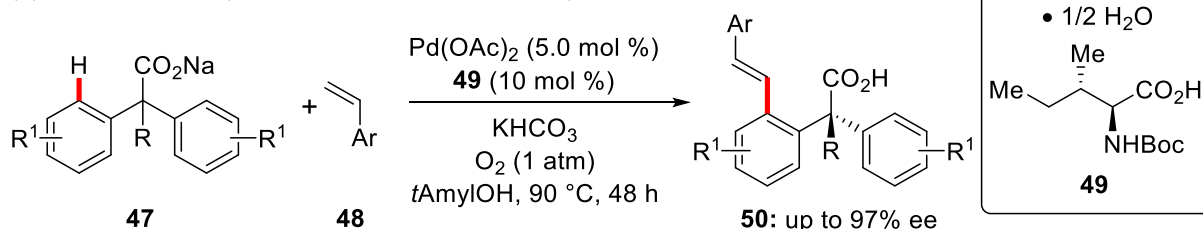
Since the introduction of mono-protected amino acids (MPAA) by Sokolov as chiral ligands,^[62] their application in combination with palladium catalysis has significantly propelled this emerging research area.^[63a] An elegant study by Yu in 2008 demonstrated the potential of MPAA as viable ligands for this class of transformations. The utilization of a bulky menthol-derived amino acid ligand **45** enabled the desymmetrization of diaryl(2-pyridyl)methane derivatives **44** with alkyl boronic acids **12** with high enantioselectivities (Scheme 18).^[74]



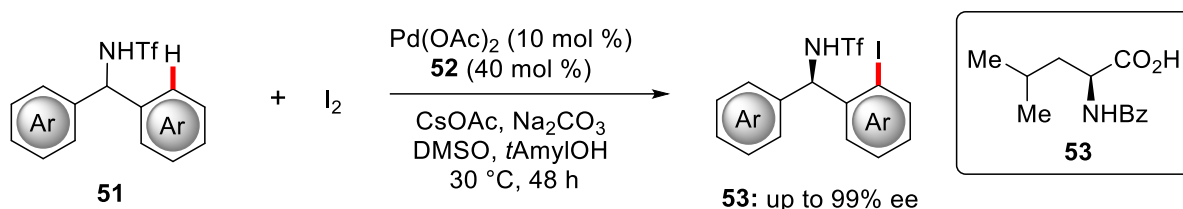
Scheme 18. Palladium-catalyzed desymmetrization using MPAA **45**.

Later, Yu achieved desymmetrization of α,α -diphenylacetates^[75] and diarylmethylamines^[76] by merging similar type of MPAA complex with palladium catalysis. In the former case, sodium salt **47** was reacted with styrene derivatives **48** under oxygen atmosphere (Scheme 19a). Later, the same group extended this approach to diarylmethylamines **51** using molecular iodine as both a reagent and an oxidant using leucine derivative **53** as the chiral ligand (Scheme 19b).

(a) Palladium-catalyzed olefination of α,α -diphenylacetates



(b) Palladium-catalyzed C–H iodination of diarylmethylamines

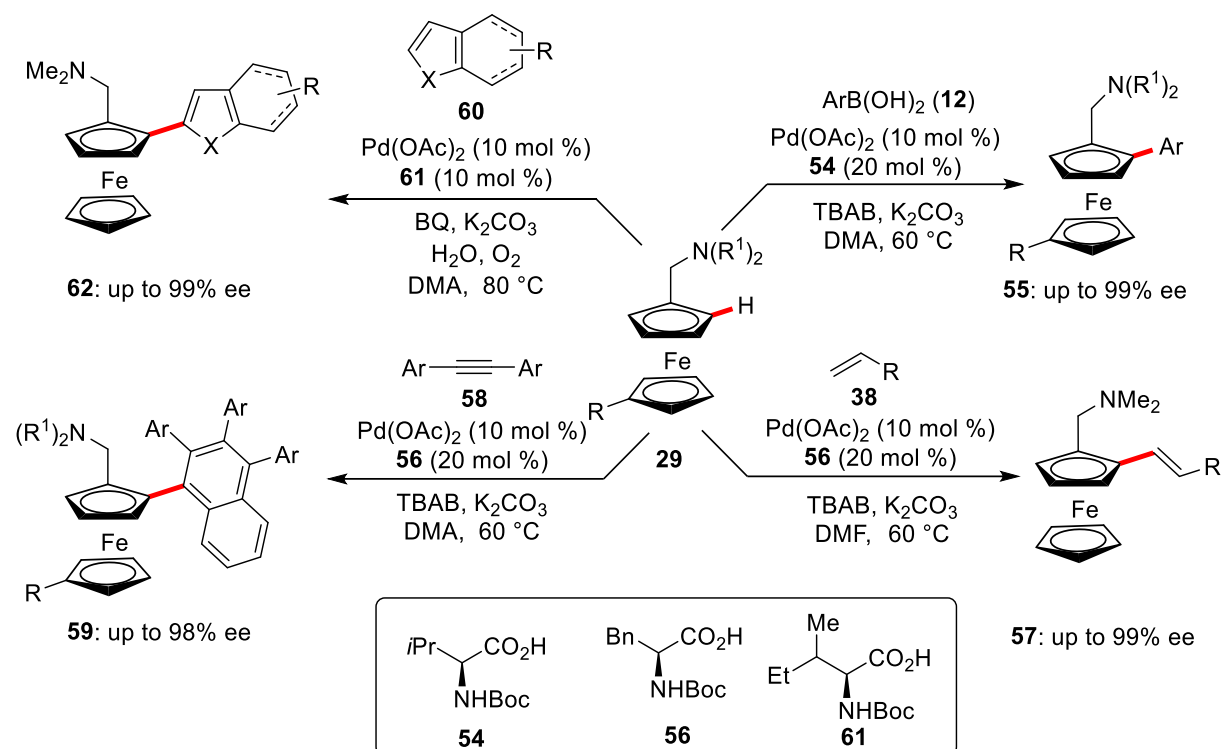


Scheme 19. Palladium-catalyzed olefination of α,α -diphenylacetates **47** and iodination of diarylmethylamines **51**.

In subsequent studies, MPAAAs have emerged as powerful ligands for palladium-catalyzed desymmetrization of diarylmethylamines^[77] and diarylphosphinamides^[78] with arylboronic acid pinacol esters, providing the desymmetrized products with high enantioselectivities.

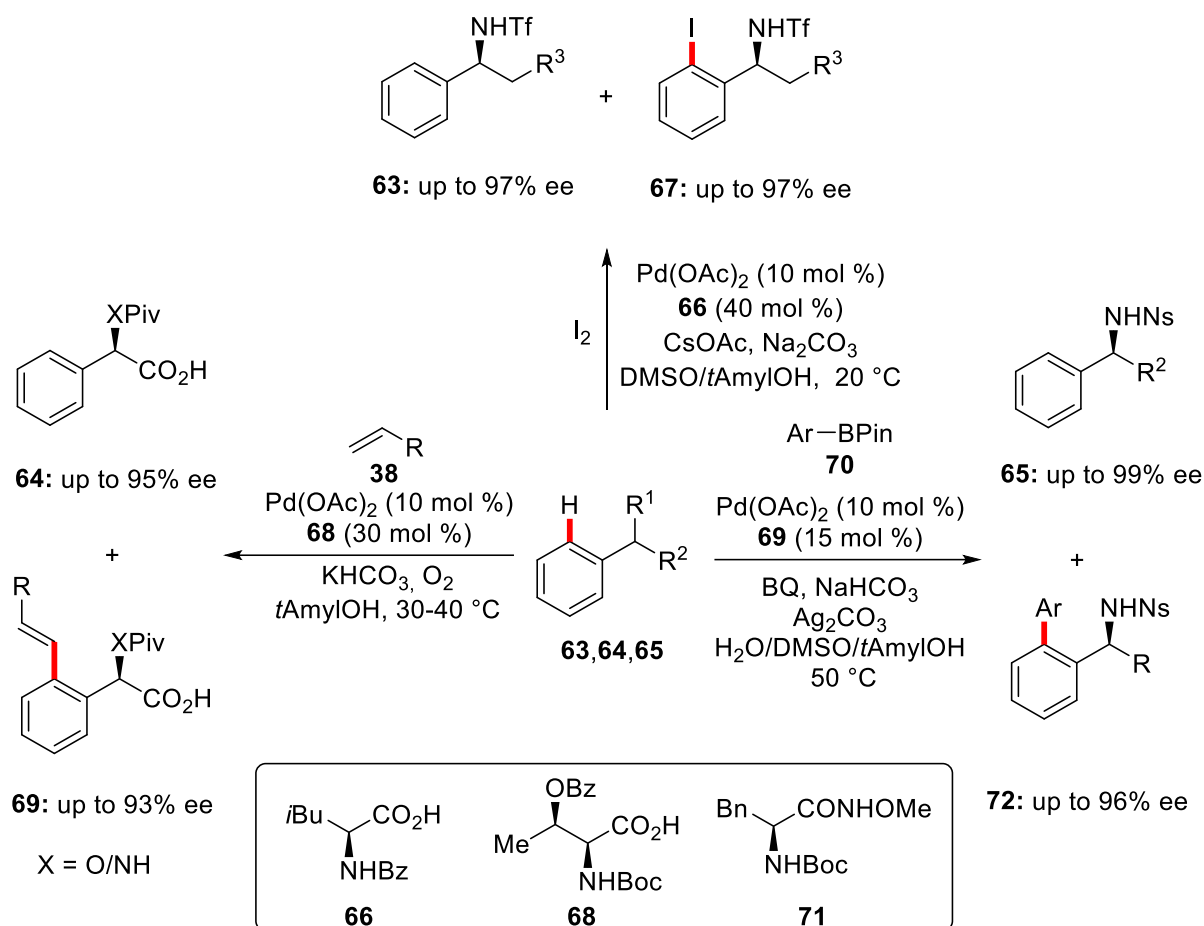
Enantioselective transformations of ferrocenes *via* direct C–H activation are a key subject area to synthesize planer chiral ferrocenes in a step-economical way (Scheme 20). Consequently, building on the great success of MPAAAs ligands, enantioselective arylation with arylboronic acids^[79] **12** as well as olefination of ferrocenes^[80] **29** have been feasible by the judicious choice of MPAAAs ligand. In addition, You developed further transformations towards enantioselective biaryl couplings of ferrocenes **29** with heteroarenes **60**.^[81]

1. Introduction



Scheme 20. Palladium-catalyzed asymmetric functionalization of ferrocenes **29**.

In 2016, Yu made a contribution towards the development of palladium-catalyzed iodination of chiral arylalkylamines as well as β -amino acid and β -amino alcohol derivatives utilizing MPAAAs as chiral ligands (Scheme 11).^[82] This protocol was not restricted to the iodination, the same group extended this strategy towards olefins^[83] **38** and arylboronic acid pinacol esters^[84] **70** as the coupling partners. (Scheme 21).



Scheme 21. Palladium-catalyzed enantioselective functionalization of arenes using MPAA auxiliaries.

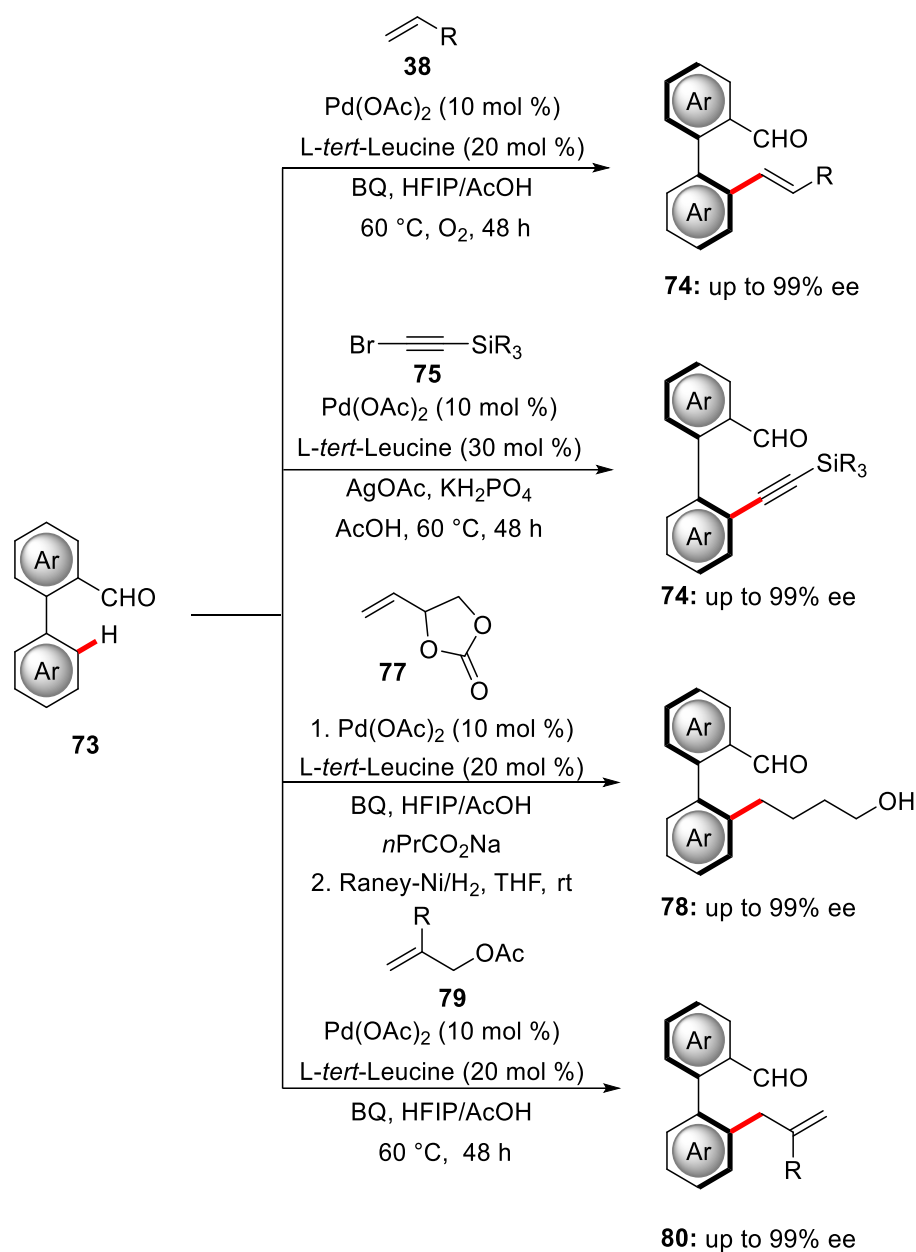
Subsequently, synthesis of axially chiral biaryls *via* kinetic resolution was disclosed by palladium-catalyzed C–H iodination using MPAA auxiliaries.^[85] Similar strategy enabled the atroposelective olefination of biaryls containing P(O)Ph₂ as the directing group.^[86] In a recent study, Shi employed L-pyroglutamic acid as chiral ligand for the atroposelective synthesis of axially chiral styrenes.^[87]

1.3.1.3 Chiral Transient Auxiliaries

Since the contribution by Yu on enantioselective C(sp³)–H activations^[88] by transient directing group (TDG), novel methods have evolved over the past years for chiral transient directing group^[41] approaches in synergistic C–H activation. In this context, Shi efficiently employed chiral TDGs for the synthesis of axially chiral biaryls. In 2017, Shi reported atroposelective olefination of racemic biaryl containing aldehydes **73** in the presence of commercially available *L*-tert-leucine as the chiral TDG using oxygen as the terminal oxidant.^[89] Later, this efficient protocol was successfully extended by Shi to various other coupling partners including olefins

1. Introduction

38,^[89] protected alkynyl bromides **75**,^[90] allyl acetate derivatives **79**^[91] and 4-vinyl-1,1-dioxolan-2-one **77**^[91] (Scheme 22).

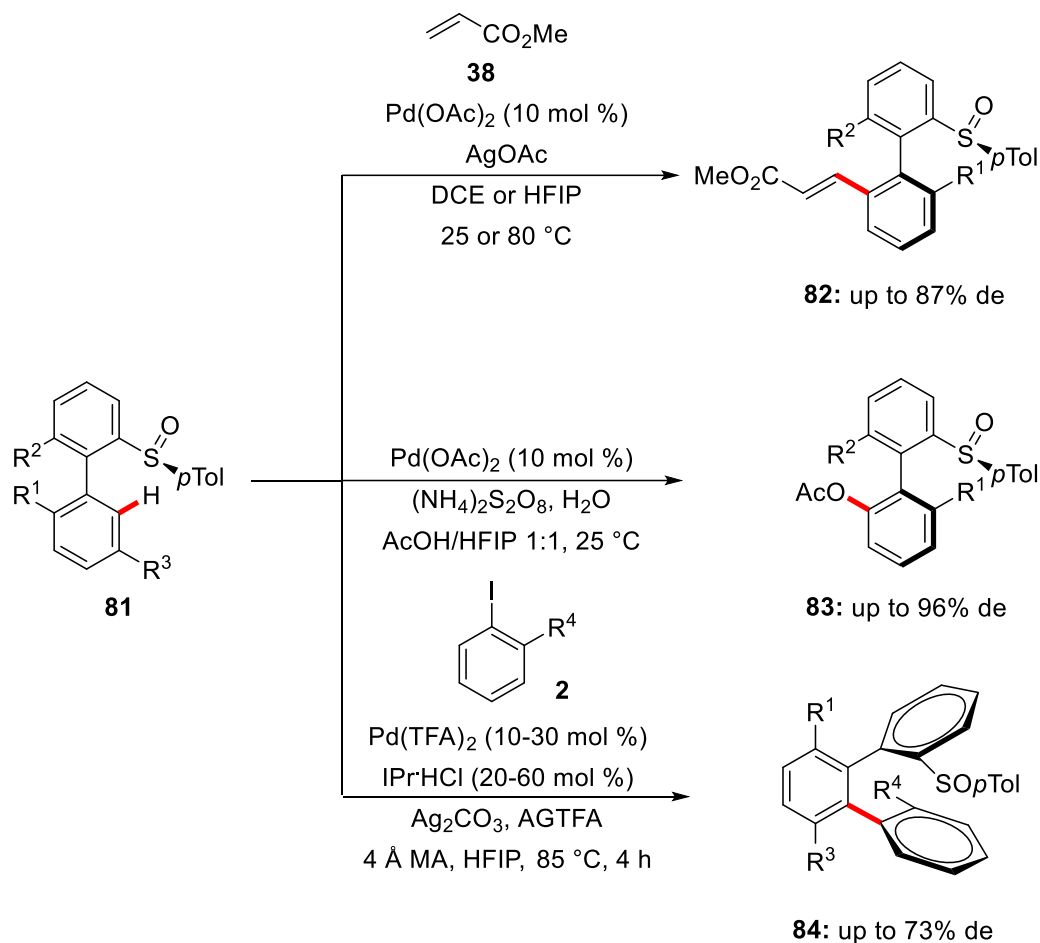


Scheme 22. Palladium-catalyzed atroposelective transformations of biaryls using TDG strategy.

Concurrently, related reaction conditions were employed for the synthesis of N–C axially chiral scaffolds by Shi^[92] and Xie.^[93]

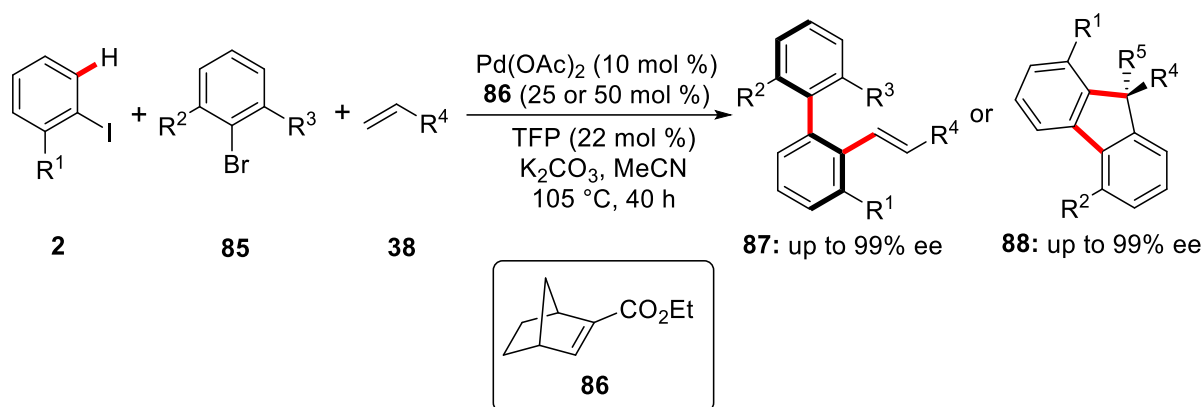
Another powerful approach was demonstrated for the synthesis of axially chiral scaffolds by introducing chiral auxiliaries. This strategy was mainly explored by the groups of Colobert and Wencel-Delord. Enantio-enriched sulfoxides **81** containing sulfur as the stereogenic center,

were used as chiral auxiliaries for successful olefination,^[94] acetoxylation and halogenation,^[95] as well as arylation^[96] reactions (Scheme 23).



Scheme 23. Palladium-catalyzed diastereoselective C–H activation of biaryls **81**.

In 2018, an interesting strategy was put into practice by Yu for the enantioselective remote *meta*-C–H activation using a chiral norbornene as a transient mediator.^[97] This concept was further applied by Zhou for three-component coupling reactions involving aryl iodides **2**, aryl bromides **85** and variety of terminating reagents **38** including olefins, alkynes, cyanide, boronic acids and ketones (Scheme 24).^[98]

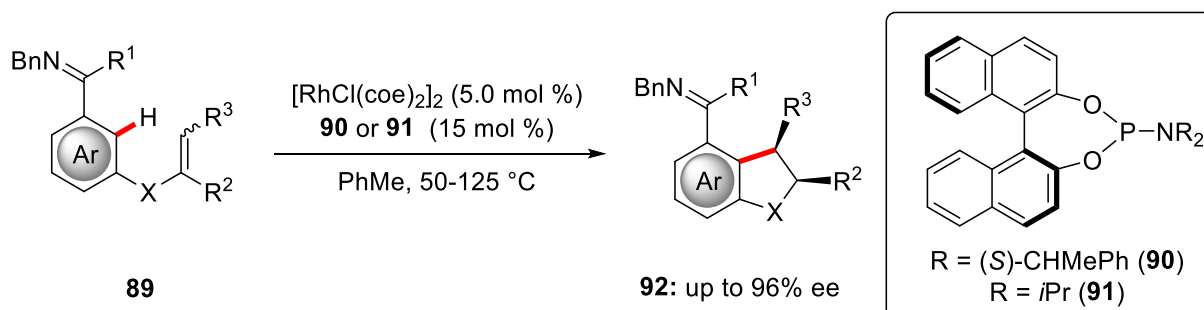


Scheme 24. Palladium/chiral norbornene cooperative catalysis towards chiral biaryls.

1.3.2. Rhodium Catalysis

1.3.2.1. Ligand-Induced Asymmetric C–H Activation

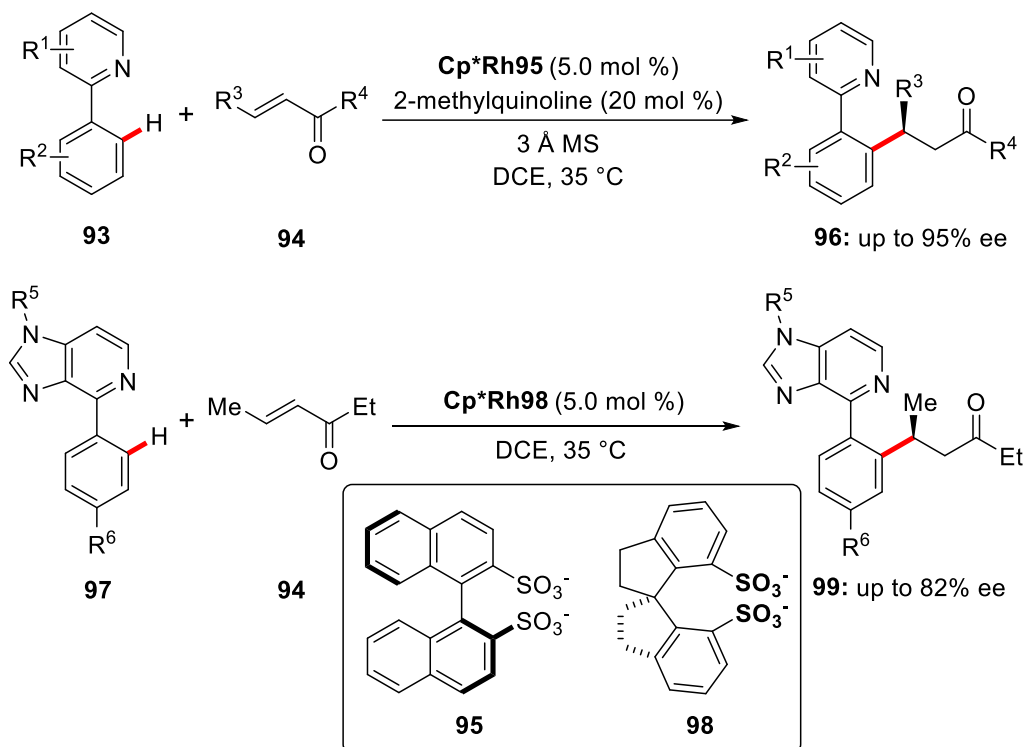
Early pioneering studies on rhodium(I)-catalyzed enantioselective C–H activations can be traced back to the elegant contributions of Murai^[99] and Ellman/Bergman.^[100] Murai applied a monodentate phosphine ligand for a rhodium(I)-catalyzed enantioselective hydroarylation protocol.^[99] Later, Ellman/Bergman presented intramolecular imine-directed hydroarylation of ketimines **89** (Scheme 25). The key to success was the use of BINOL-based chiral ligands **90** or **91** to achieve high enantioselectivities for this cyclization protocol.



Scheme 25. Rhodium-catalyzed hydroarylation of ketimine **89**.

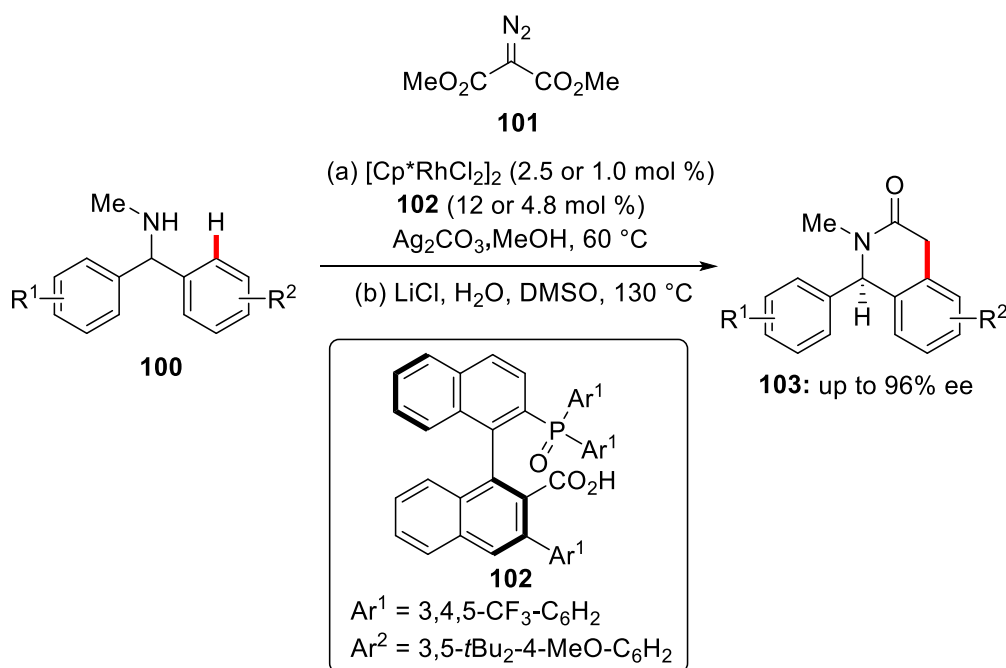
This early pioneering studies have set the stage for various enantioselective annulation reactions using alkynes and alkenes as coupling partners by the aid of chiral biphosphine ligands.^[101]

Considering the high importance of enantioselective hydroarylation reactions, a number of reports have been documented in the literature. In a recent study, Matsunaga employed a hybrid catalyst, namely a 1:1 mixture of Cp**Rh*(III) and (*S*)-BINSate anion for the addition of 2-phenylpyridine **93** with α,β -unsaturated ketones **94**.^[102] Also the scope was further extended to 6-arylpyridines **97** with a modified (*R*)-SPISate spirocyclic anion based catalyst (Scheme 26).



Scheme 26. Rhodium-catalyzed C–H activation using chiral anions.

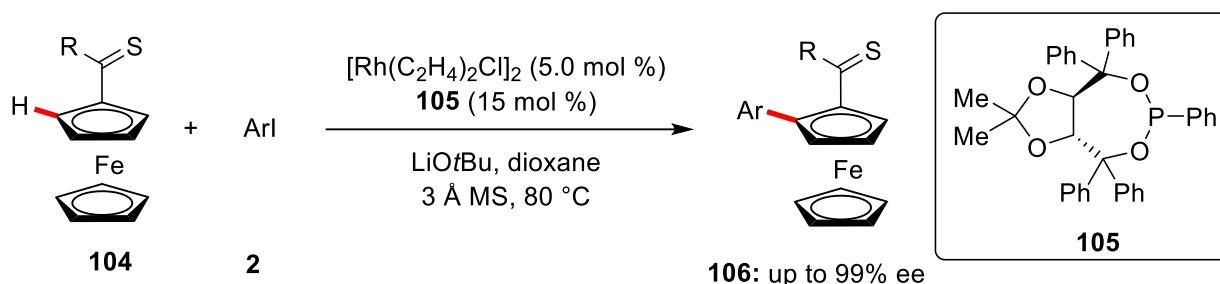
Subsequently, Matsunaga reported the merger of a chiral carboxylic acid **102** with $\text{Cp}^*\text{Rh(III)}$ complex for the synthesis of 1,4-dihydroisoquinolin-3(2*H*)-one derivatives **103** *via* a desymmetrization process (Scheme 27).^[103]



Scheme 27. Rhodium-catalyzed C–H activation using chiral carboxylic acid **100**.

1. Introduction

In 2019, a protocol for highly enantioselective arylation of ferrocenes **104** was reported by You.^[104] The authors employed a TADDOL-based chiral ligand **105** to synthesis planar chiral ferrocenes **106** by thioetone directed C–H activation (Scheme 28).



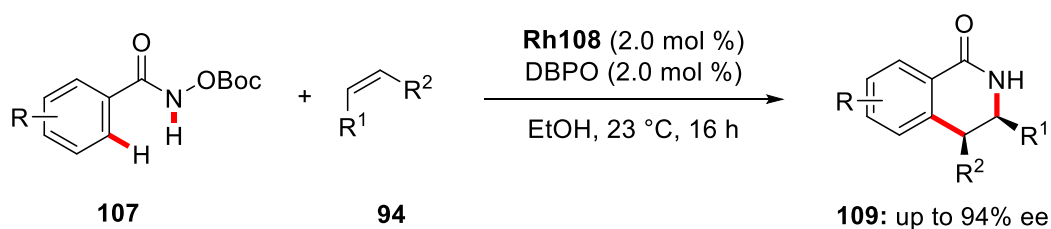
Scheme 28. Rhodium-catalyzed C–H arylation of ferrocenes.

TADDOL-derived monodentate phosphonite has also been applied by You in atroposelective C–H arylation reactions to synthesis highly enantioenriched chiral biaryls.^[105]

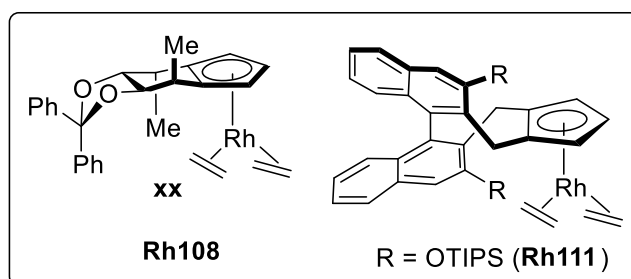
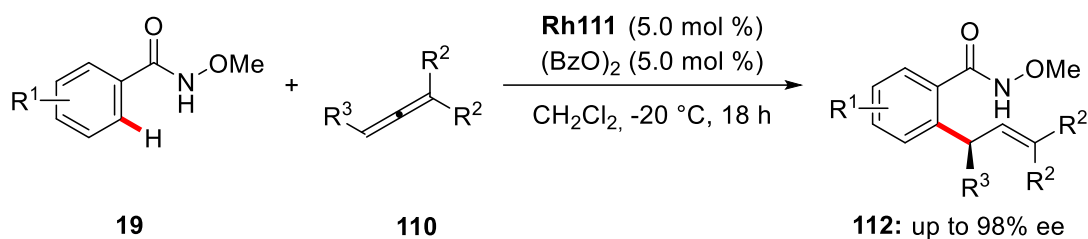
1.3.2.2. Chiral Cp^x-Based Catalysts

Apart from the use of exogenous chiral ligands with Cp^{*}Rh(III) complexes, another powerful approach involves the use of chiral cyclopentadienyl-based (Cp^x) complex to gain high levels of selectivity control.^[106] The application of these complexes was demonstrated by Cramer for the annulation of hydroxamic acid derivatives **107** with olefins **94** to provide the annulated products **109** with excellent enantioselectivities (Scheme 29a).^[107] Using a bulky OTIPS substituent on Cp^x complex **Rh111** enabled the functionalization of hydroxymates **19** with allenes **110** in high enantioselectivity (Scheme 29b).^[108]

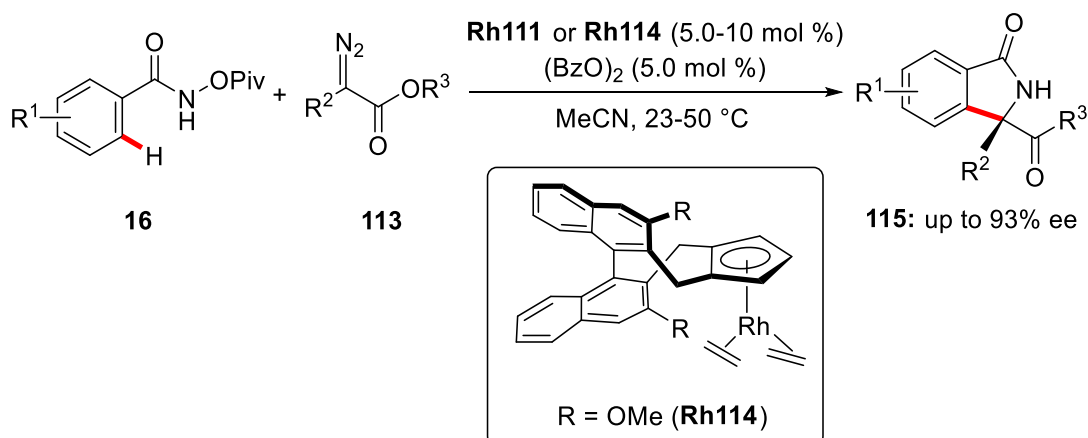
(a) Rhodium-catalyzed enantioselective C–H annulation



(b) Rhodium-catalyzed enantioselective C–H allylation

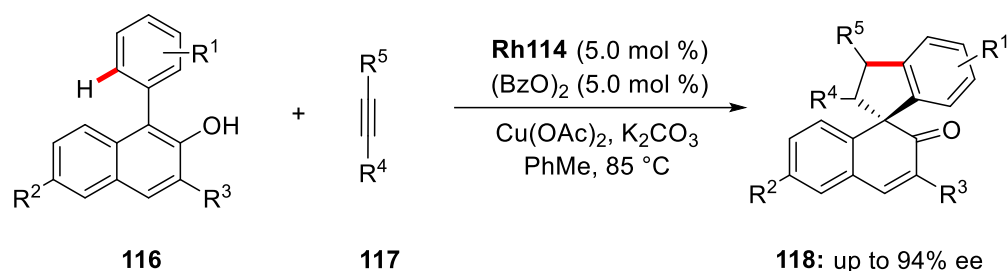
**Scheme 29.** Rhodium-catalyzed enantioselective C–H annulation.

In subsequent reports, similar chiral Cp^x complexes have found application in enantioselective intramolecular reactions to synthesize cyclized scaffold.^[109] Later, chiral isoindolone derivatives **115** were synthesized using diazo compounds **113** *via* rhodium-catalyzed C–H activation (Scheme 30).^[110]

**Scheme 30.** Rhodium-catalyzed enantioselective synthesis of isoindolones **115**.

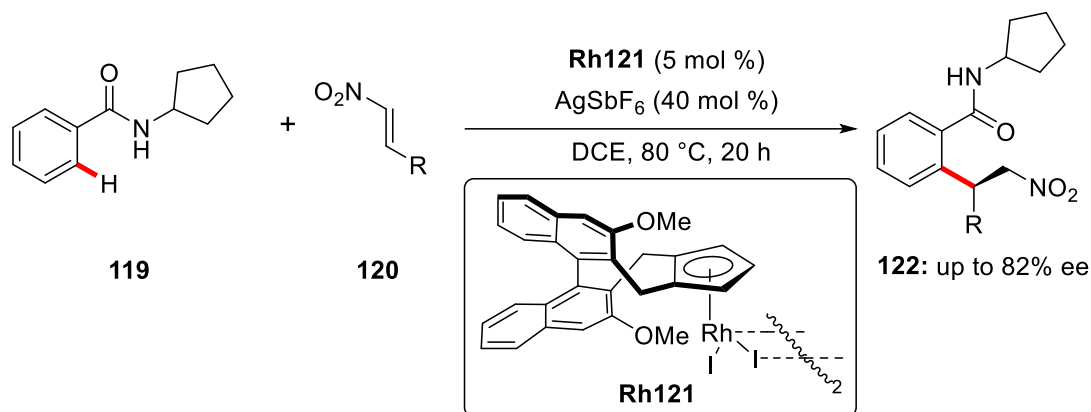
1. Introduction

Chiral Cp^x complex was also effective for enantioselective [3+2] spiroannulation reactions as demonstrated by You. Quaternary stereogenic centers **118** were formed under oxidative conditions (Scheme 31).^[111]



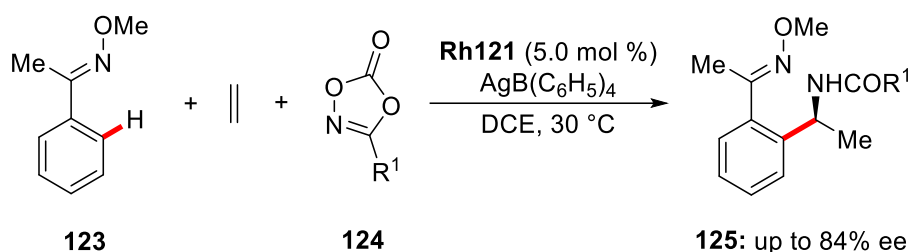
Scheme 31. Rhodium-catalyzed spiroannulations.

In 2017, Ellman showed the potential of similar type of chiral Cp^x complex **Rh121** for enantioselective rhodium(III)-catalyzed C–H bond addition to nitroalkenes **120** (Scheme 32).^[112]



Scheme 32. Rhodium-catalyzed enantioselective dual C–H activation.

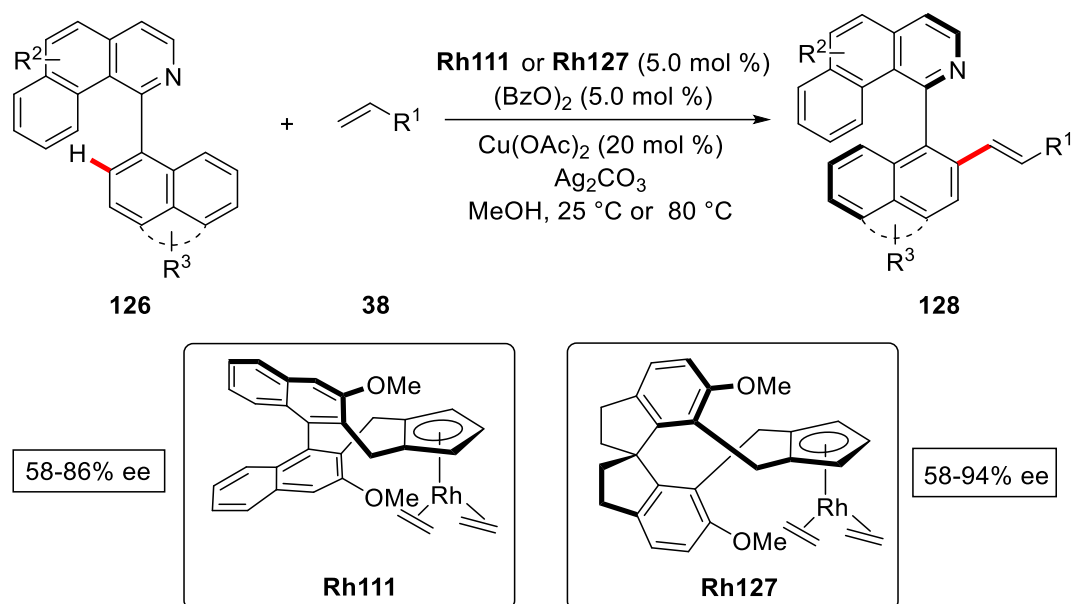
Later, a three component reaction involving arene, terminal alkenes, and aminating agent was achieved by the same group. The authors utilized the same chiral rhodium complex **Rh121** for the synthesis of α -methyl branched amines **125** with moderate to good enantioselectivities (Scheme 33).^[113]



Scheme 33. Rhodium-catalyzed enantioselective three component reaction.

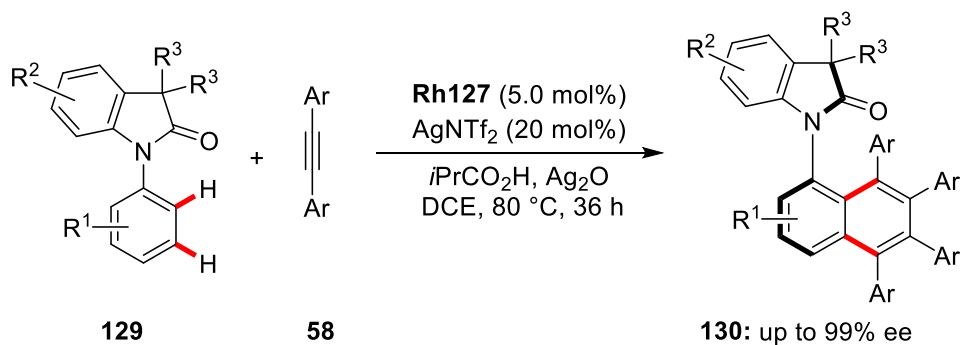
You also showed the application of chiral Cp^x rhodium complexes **Rh111** for successful atroposelective C–H olefination reactions with alkenes **38** (Scheme 34).^[114] In subsequent

studies, a SPINOL-type ligand **Rh127** provided improved enantioselectivities as shown by the same group.^[115]



Scheme 34. Rhodium-catalyzed atroposelective C–H olefination.

Later, in 2019, Wang employed the same chiral rhodium(III) complex **Rh127** for the synthesis atropo-stable indolinone derivatives **130** via dual C–H activation in an oxidative alkyne annulation conditions (Scheme 35).^[116]



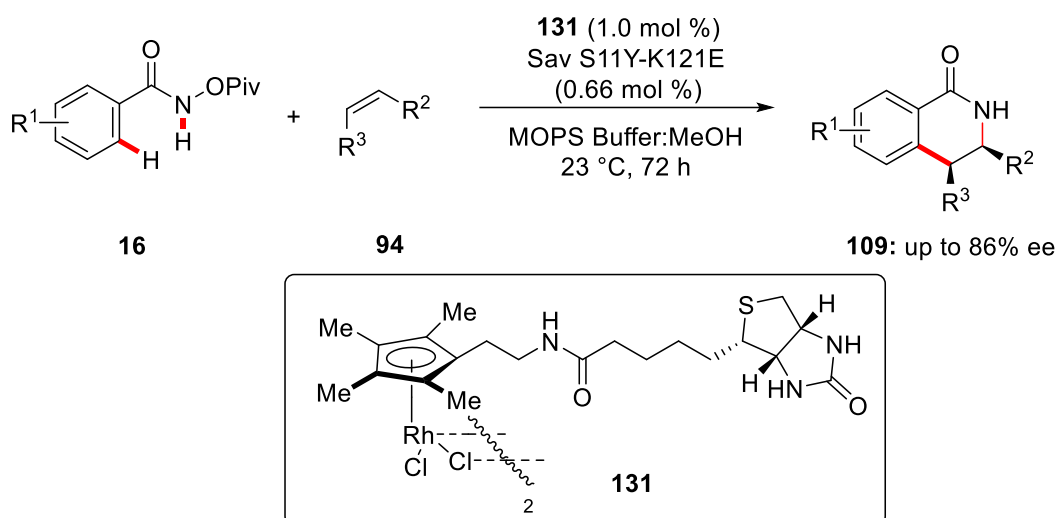
Scheme 35. Rhodium-catalyzed atroposelective synthesis of C–N axially chiral biaryls.

In addition to the aforementioned reports, successful approaches have been described for the atroposelective synthesis of biaryls using chiral Cp^x complex with notable contributions from Li,^[117] as well as Antonchick and Waldmann.^[118]

Despite significant advances, it is noteworthy to mention that the multi-step syntheses of chiral Cp^x and pre-coordination to metal catalysts limit the atom-economy of this strategy.

1.3.2.3. Other Strategies

In 2012, Ward and Rovis devised a completely different approach to enantioselective C–H activation using rhodium catalysis. Here, a Cp* ligand was linked with biotin derivative that binds to streptavidin in a host-guest type interaction typical for enzymes providing environment for asymmetric induction. The initial potential of this catalytic system was tested for enantioselective annulation of hydroxymates **16** and olefins **94** at room temperature (Scheme 36).^[119] Later, the same group improved the versatility of this catalytic system towards the synthesis of δ -lactams in high yields and enantioselectivity.^[120]



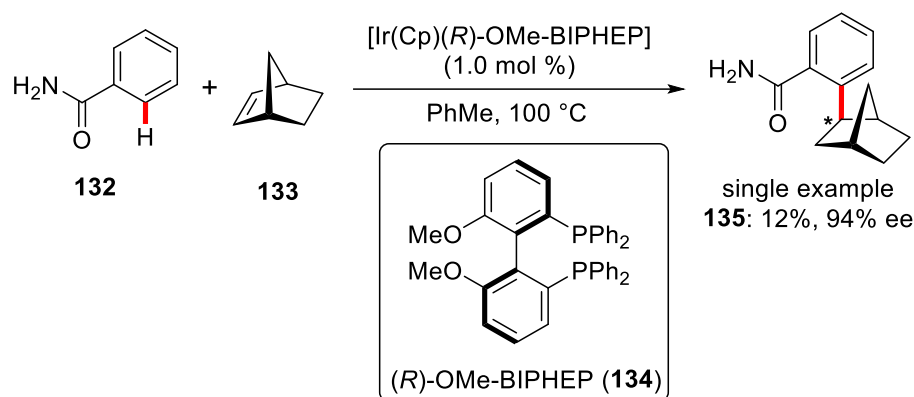
Scheme 36. Rhodium-catalyzed C–H activation with artificial metalloenzymes.

The use of chiral transient directing group was largely limited to palladium catalysis, until recently, Wang employed this strategy to rhodium catalysis in their enantioselective synthesis of chiral phthalides from simple aldehydes.^[121]

1.3.3. Iridium Catalysis

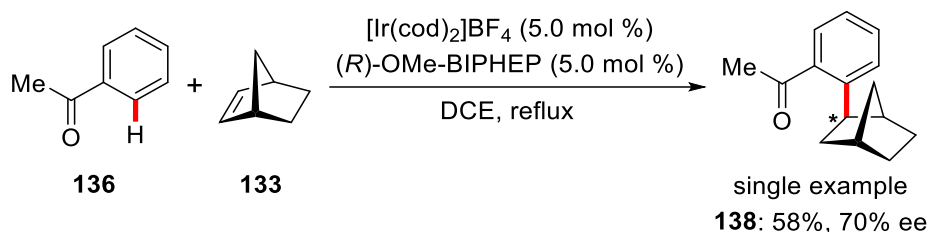
Over the past years, owing to unique properties of iridium catalysts, there has been a considerable increase in the use of iridium complexes for the development of novel and selective enantioselective C–H transformations.^[122]

In 2000, Togni documented an early example of an iridium-catalyzed enantioselective C–H hydroarylation of norbornene **132** with benzamide **133**.^[123] An iridium complex bearing cyclopentadienyl (Cp) and chiral ligand (*R*)-MeO-BIPHEP **134** enabled the intermolecular enantioselective hydroarylation to provide the alkylated product **135** in 94% ee, albeit with a low yield of 12% (Scheme 37).



Scheme 37. Early example of iridium-catalyzed enantioselective hydroarylation of norbornene **133**.

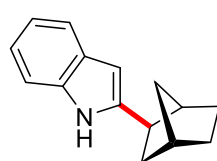
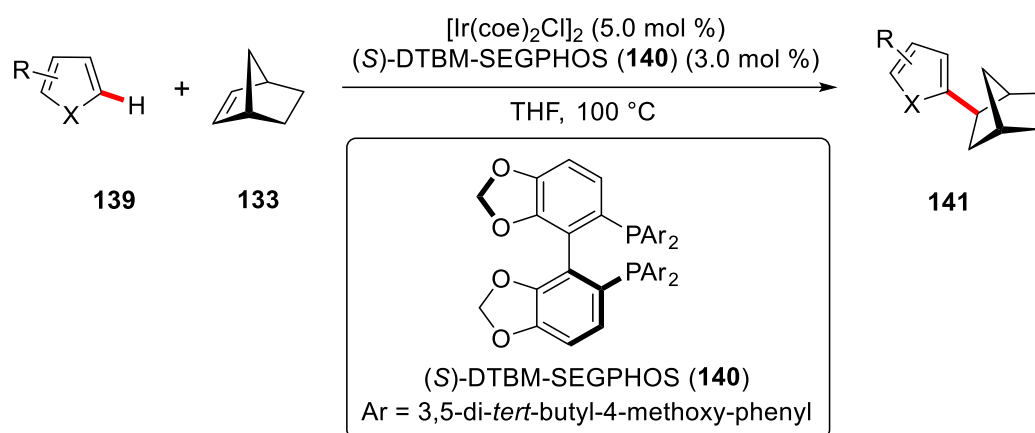
In 2008, in a related study Shibata employed $[\text{Ir}(\text{cod})_2]\text{BF}_4$ as the catalyst and $(R)\text{-MeO-BIPHEP 137}$ as the chiral ligand to achieve a single example of enantioselective C–H addition of 2'-methylacetophenone **136** to norbornene **133** with 58% yield and 70% ee (Scheme 38).^[124]



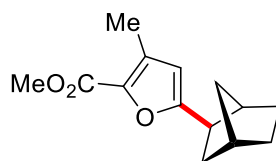
Scheme 38. Iridium-catalyzed enantioselective hydroarylation 2'-methylacetophenone **136**.

In 2013, Hartwig disclosed enantioselective C–H additions of heteroarenes to bicycloalkenes **133** with the cooperation of $(S)\text{-DTBM-SEGPHOS 140}$ as the chiral ligand to provide highly enantioenriched alkylated products **141** (Scheme 39).^[125] Notably, the reaction occurred efficiently with heteroarenes, including indoles, thiophenes, pyrroles and furans, selectively reacting on the C–H bonds adjacent to the heteroatoms. Even for unprotected indoles, C2 alkylation was observed in contrast to its typical reactivity at the C3 position. A broad range of functional groups was tolerated to form the alkylated products with good yields and excellent enantioselectivities.

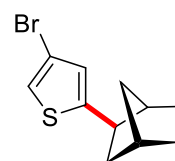
1. Introduction



93%, 96% ee



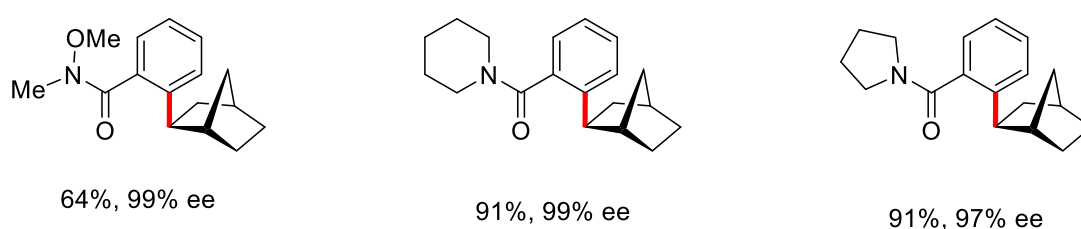
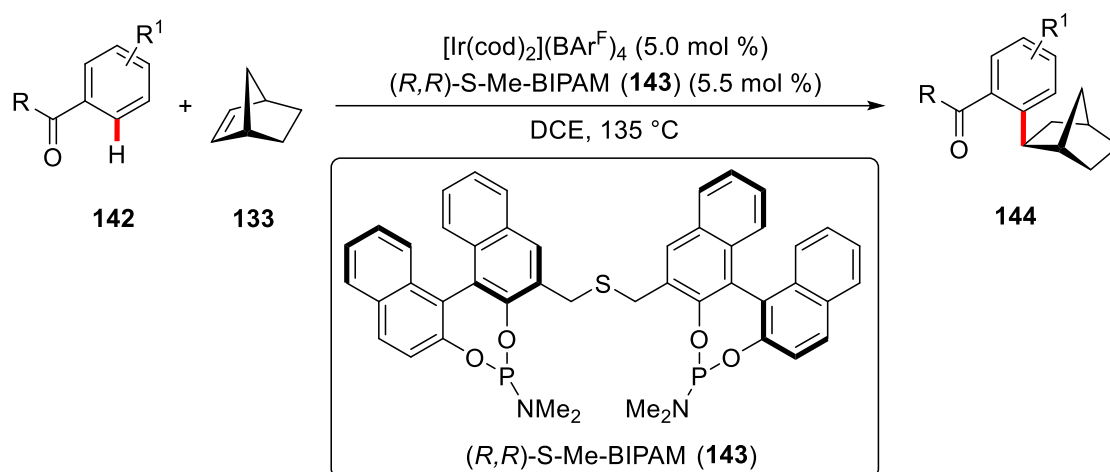
87%, 78% ee



95%, 98% ee

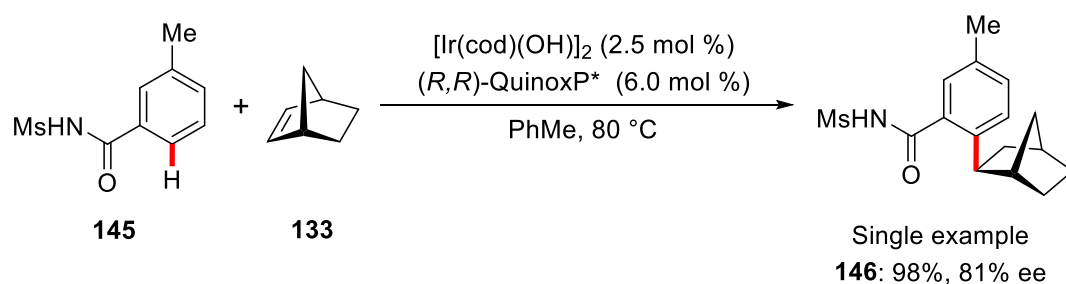
Scheme 39. Iridium-catalyzed enantioselective hydroarylation of bicycloalkanes.

Thereafter, a combination of cationic iridium complex and newly designed sulfur linked bis(phosphoramidite) ligand [(*R,R*)-S-Me-BIPAM] **143** was applied by Yamamoto for amide- and ketone-directed **142** enantioselective C–H hydroarylation of bicycloalkanes **133** (Scheme 40).^[126]



Scheme 40. Enantioselective additions to norbornenes **133**.

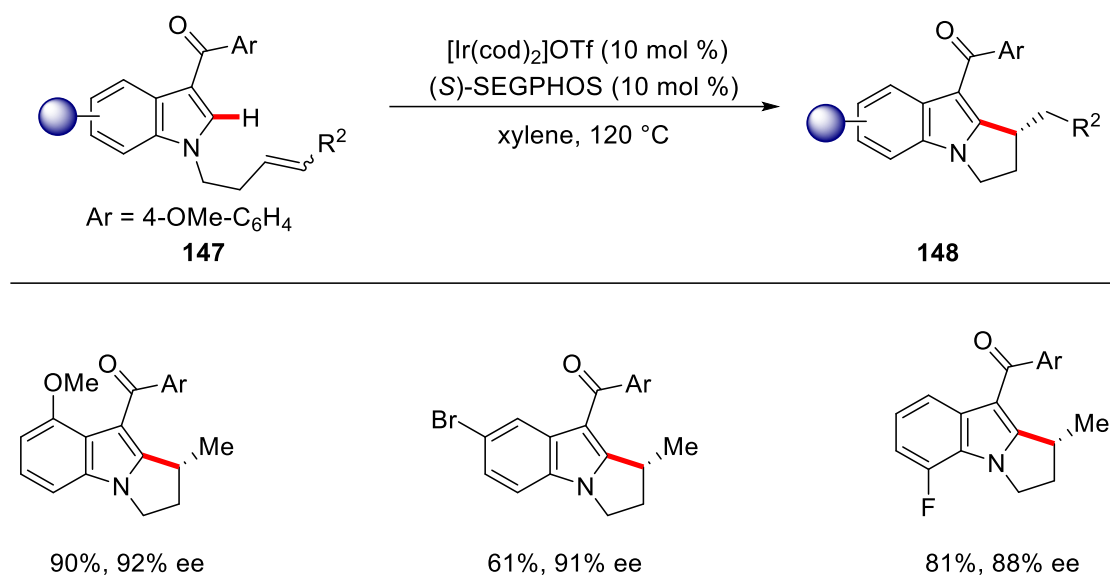
Later, Nishimura observed a similar reactivity in an example of enantioselective C–H alkylation of *N*-sulfonylbenzamides **145** using (R,R) -QuinoxP* as the chiral ligand (Scheme 41).^[127]



Scheme 41. Enantioselective C–H alkylation of *N*-sulfonylbenzamides **145**.

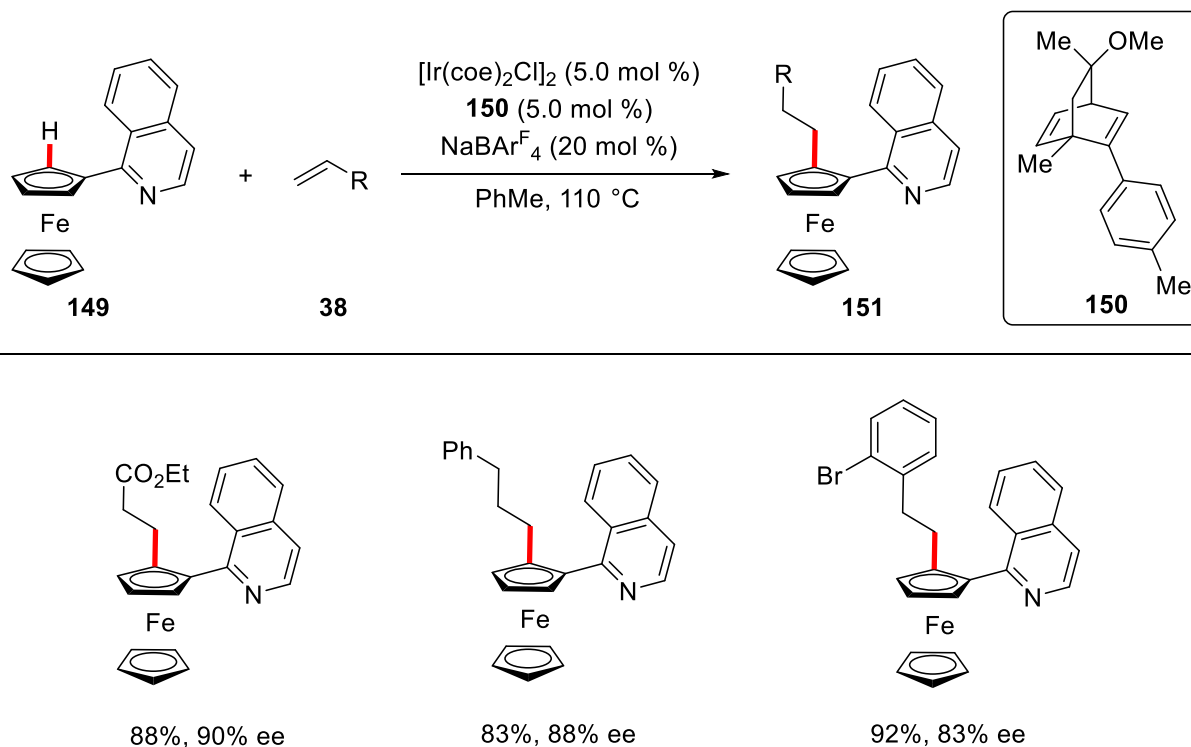
While early enantioselective transformations were mainly limited to bicycloalkenes as olefin coupling partners, recently a broad variety of olefin partners has been employed. Intrigued by their previous racemic work on intermolecular C2-alkylation of *N*-protected indoles with terminal alkenes,^[128] in 2015 Shibata applied a combination of iridium(I) catalyst and chiral diphosphine ligands (*S*)-SEGPHOS or (*S*)-Xyl-BINAP to enable the highly enantioselective intramolecular version of this protocol (Scheme 42).^[129] C3-substituted ketone directed intramolecular C2 alkylations were achieved with this catalytic system to furnish highly enantioenriched annulated indoles **148** with high yields and enantioselectivities.

1. Introduction



Scheme 42. Enantioselective C–H alkylation of indole derivatives **148**.

The same group reported a catalytic system which set the stage for first iridium-catalyzed enantioselective C(sp²)–H alkylation of ferrocene by the aid of 1-isoquinolyl moiety **149** as the directing group (Scheme 43).^[130] The key to success was represented by the use of a combination of iridium(I) complex and an analogue of Carreira's diene ligand **150** to introduce planer chirality in ferrocene.^[131] Thus various sensitive functional groups on olefin coupling partners **38** were tolerated to afford the alkylated products **151** in good yields and excellent enantioselectivities.

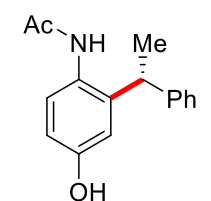
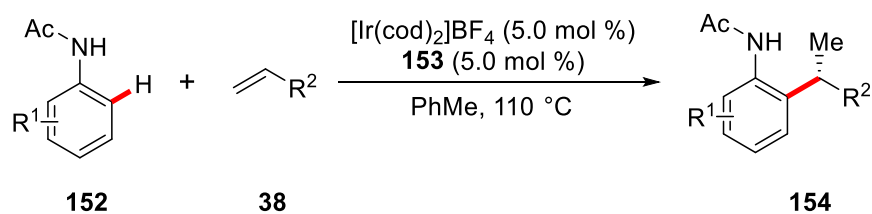


Scheme 43. Enantioselective C–H alkylation of ferrocenes **149**.

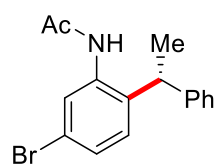
In contrast, efficient branch-selective, highly enantioselective iridium-catalyzed hydroarylations of styrenes and α -olefins of anilides were disclosed.^[132] Key to success for achieving anilide **152** directed enantioselective *ortho*-C–H activation was the development of a chiral bisphosphite ligand **153** to generate tertiary benzylic stereocenters in high enantioselectivity and high atom economy (Scheme 44a). Also, the authors extended this strategy to hydroheteroarylation of terminal olefins **38** with thiophene **155** using a ferrocene-based bisphosphonate ligand **156**. With this tailored ligand **157**, a diverse range of α -olefins **38** were found as amenable substrates to provide the alkylated thiophenes **157** without compromising the yields and selectivities (Scheme 44b).

1. Introduction

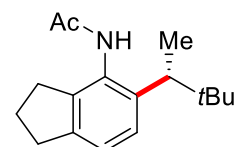
(a) Enantioselective alkene hydroarylation



82%, 92.5:7.5 e.r.

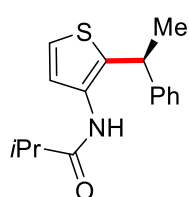
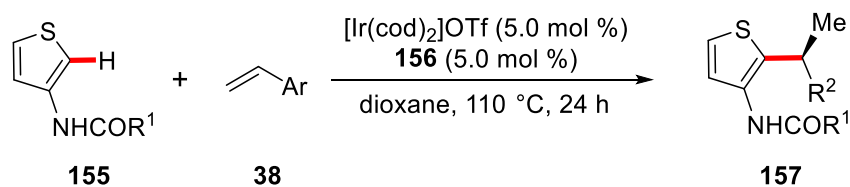


69%, 94:6 e.r.

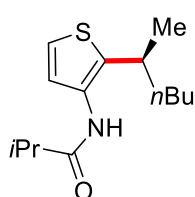


81%, 95:5 e.r.

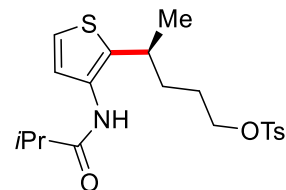
(b) Enantioselective alkene hydroarylation



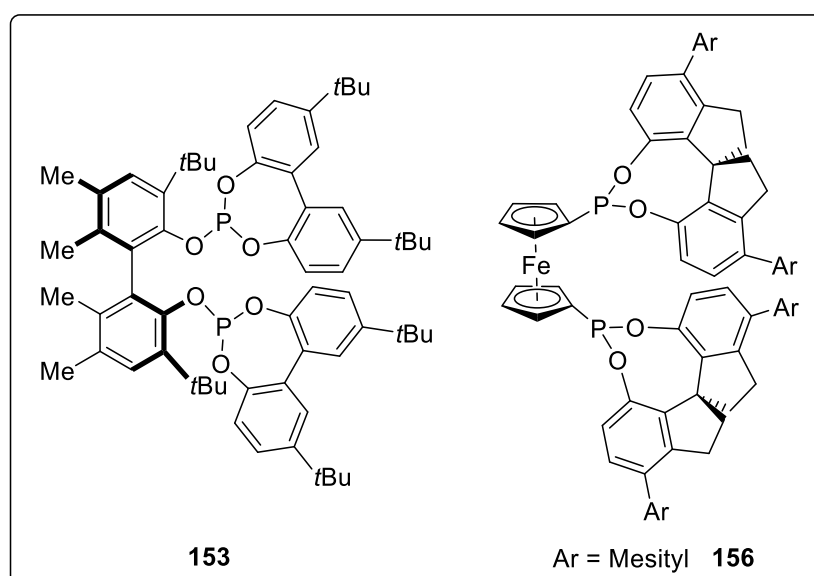
77%, 97.5:2.5 e.r.



83%, 98:2 e.r.

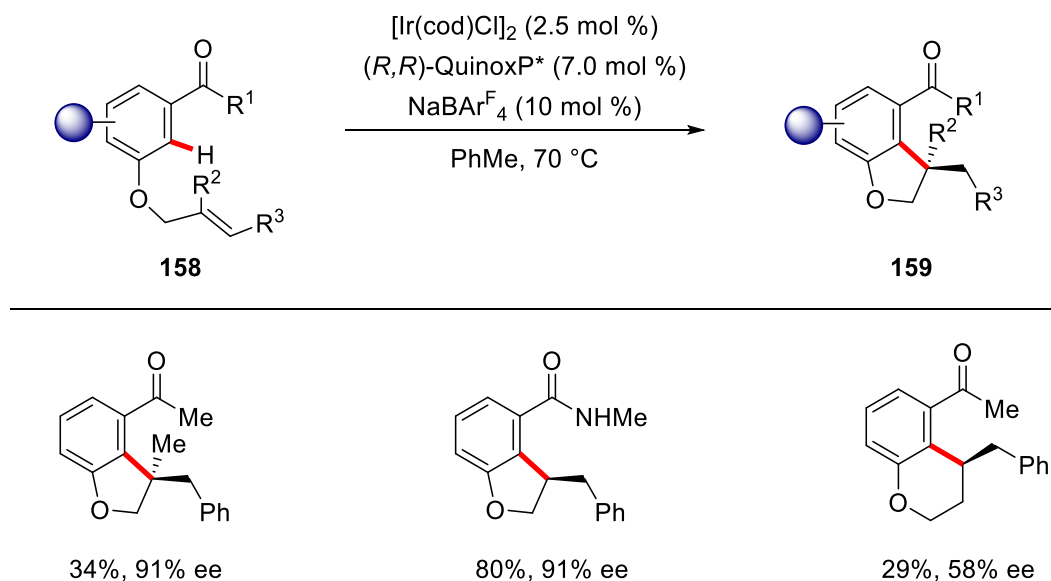


82%, 92:8 e.r.



Scheme 44. Enantioselective hydroarylation of terminal olefins **38**.

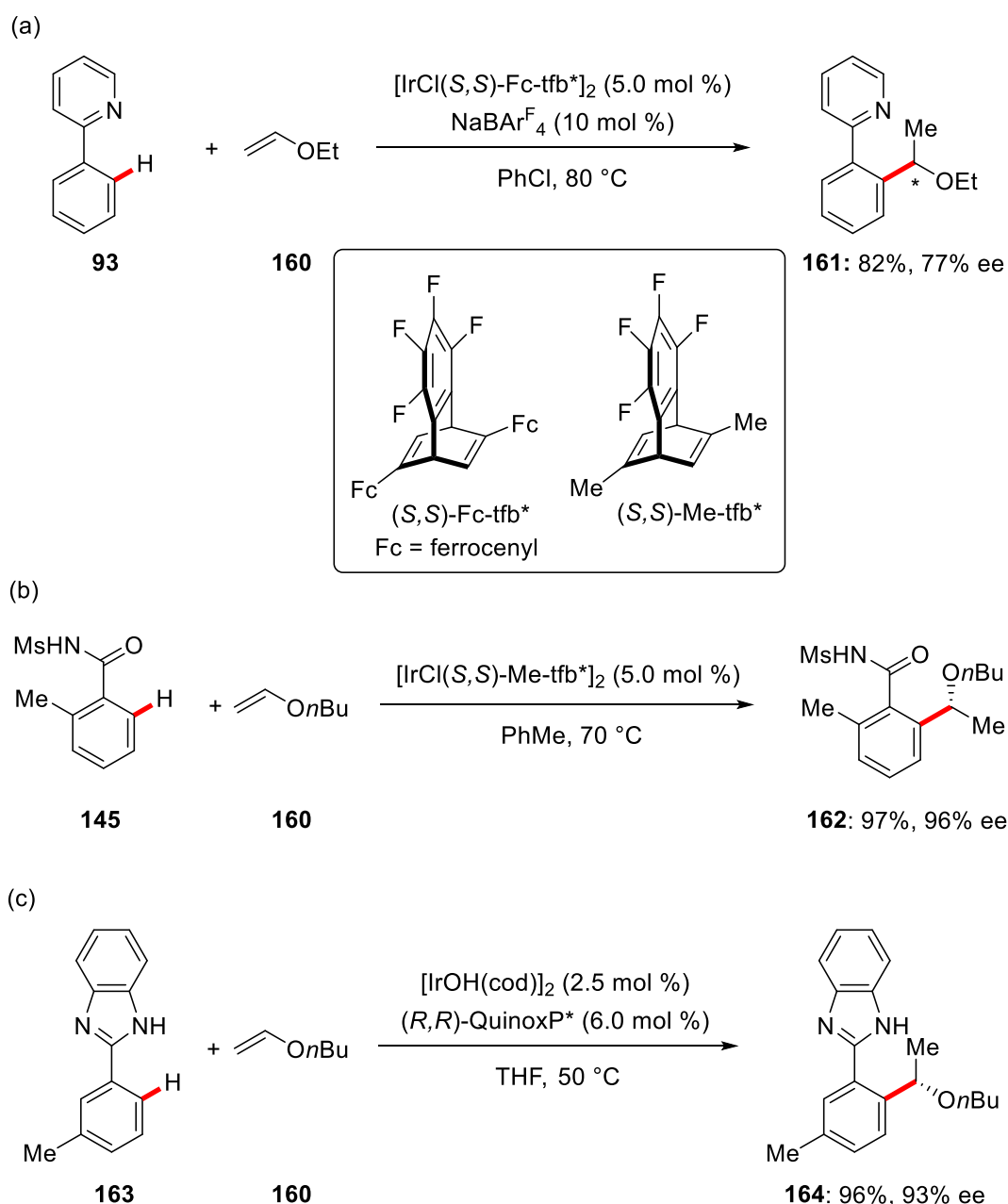
In line with intramolecular hydroarylations, Rueping and Cavallo, very recently, expanded this approach towards oxygen tethered internal olefins **158** through amide and ketone directed C–H activation (Scheme 45).^[133] Here the use of (*R,R*)-QuinoxP* as chiral ligand proved to be crucial to achieve high enantioselectivities with the combination of a cationic iridium(I) catalyst. Thus, biologically relevant chiral dihydrobenzofurans **159** were obtained. Notably, this protocol also provided access to quaternary stereocenter with high enantioselectivity, albeit with lower yield.



Scheme 45. Enantioselective intramolecular C–H alkylation.

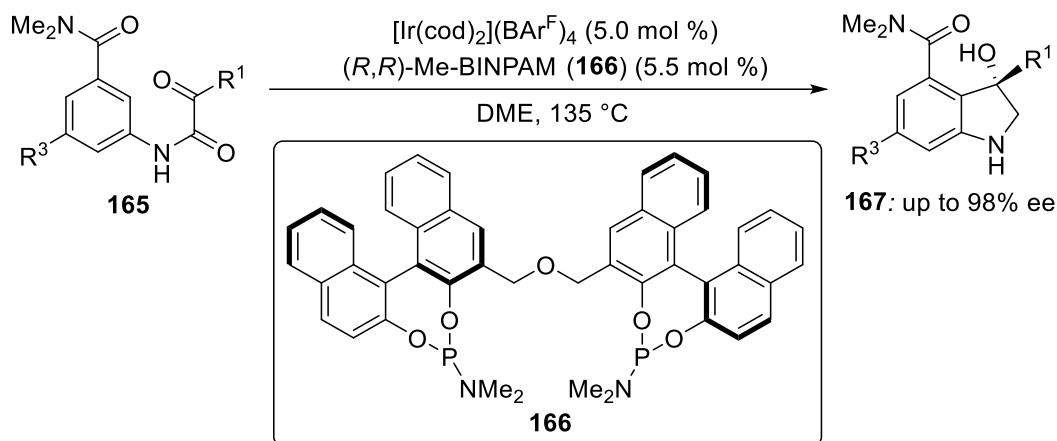
Besides numerous reports on enantioselective C–H alkylations, enantioselective hydroarylations of electron rich olefins using iridium complexes have remained elusive until very recently.^[134] In 2015, Nishimura developed iridium catalyzed hydroarylation of vinyl ethers **160** *via* directed C–H activation. Promising results were obtained after initial screening with chiral diene (*S,S*)-Fc-tfb*, which provided the desired chiral ether **161** with 77% ee (Scheme 46a). Later the same group succeeded to achieve highly enantioselective alkylation of *N*-sulfonylbenzamides **145** with vinyl ethers **160** utilizing an iridium complex bearing the chiral diene (*S,S*)-Me-tfb* (Scheme 46b). Moreover, the authors were able to expand this methodology to azoles containing N–H bonds by the aid of a (*R,R*)-QuinoxP* ligand (Scheme 46c).

1. Introduction



Scheme 46. Enantioselective hydroarylation of electron-rich olefins **160**.

On a different note, the Shibata group in 2009 reported for the first time iridium-catalyzed enantioselective addition to carbon–heteroatom double bonds.^[135] A moderate enantioselectivity of 72% ee was observed when a chiral bisphosphine ligand was employed to synthesize enantioenriched oxindole derivative. Later, Yamamoto and coworkers were able to extend this protocol to high enantioselectivity using a chiral bidentate bis-phosphoramidite ligand **166** by the aid of an amide directing group (Scheme 47).^[136]



Scheme 47. Enantioselective intramolecular C–H additions.

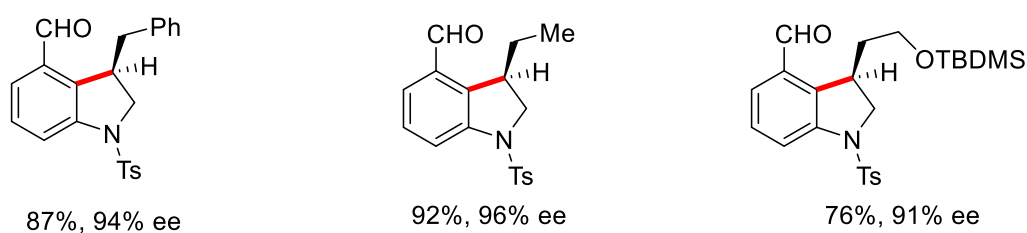
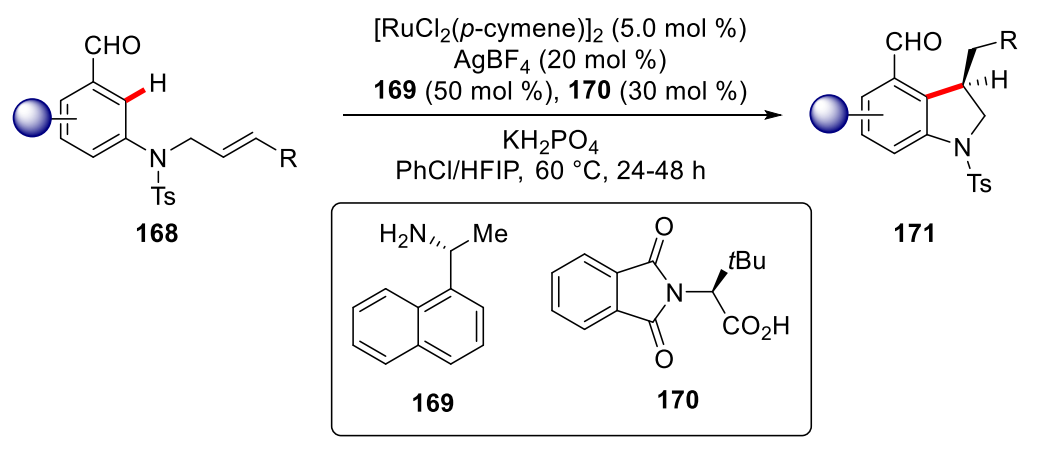
1.3.4. Ruthenium Catalysis

Over the past decades, versatile and cost-effective ruthenium(II) arene complexes^[137] have shown enormous success in various C–H activation reactions.^[27t, 39, 138] Despite of these major advances, enantioselective C–H transformations with comparatively inexpensive ruthenium catalysts remains considerably underdeveloped.

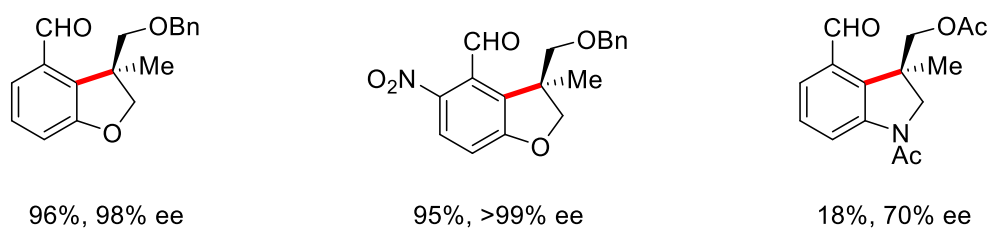
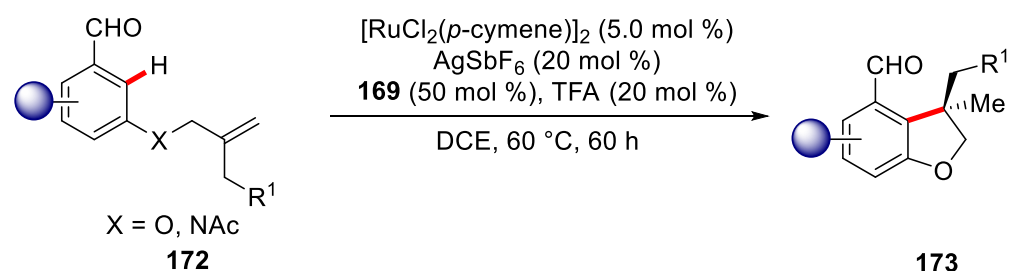
Very recently, Cui and co-workers developed enantioselective ruthenium(II)-catalyzed intramolecular C–H hydroarylations of nitrogen-tethered olefin aldehydes **168** (Scheme 48a).^[139] The key to success was represented by the use of a commercially available α -methylamines **169** as chiral TDG for the synthesis of highly enantioenriched indoline derivatives **171**. The optimization studies showed that addition of catalytic amounts of protected chiral carboxylic acid **170** was beneficial for the outcome of the reaction. Shortly after, Wang and coworkers concurrently achieved similar reactivities with the oxygen-tethered olefin aldehydes **172** by the aid of an α -chiral amine as the chiral TDG (Scheme 48b).^[140] This methodology set the stage for the highly efficient synthesis of 2,3-dihydrobenzofurans **173**, containing all-carbon quaternary stereocenters in high yields and excellent enantioselectivities.

1. Introduction

(a) Synthesis of indoline derivatives



(b) Synthesis of 2,3-dihydrobenzofurans



Scheme 48. Enantioselective ruthenium(II)-catalyzed C–H alkylation.

1.3.5. Nickel Catalysis

The complexes of nickel have emerged as efficient catalysts for their versatile applications in C–H activation reactions^[141] with notable applications in hydroarylations^[142] type reactivity.^[32c]

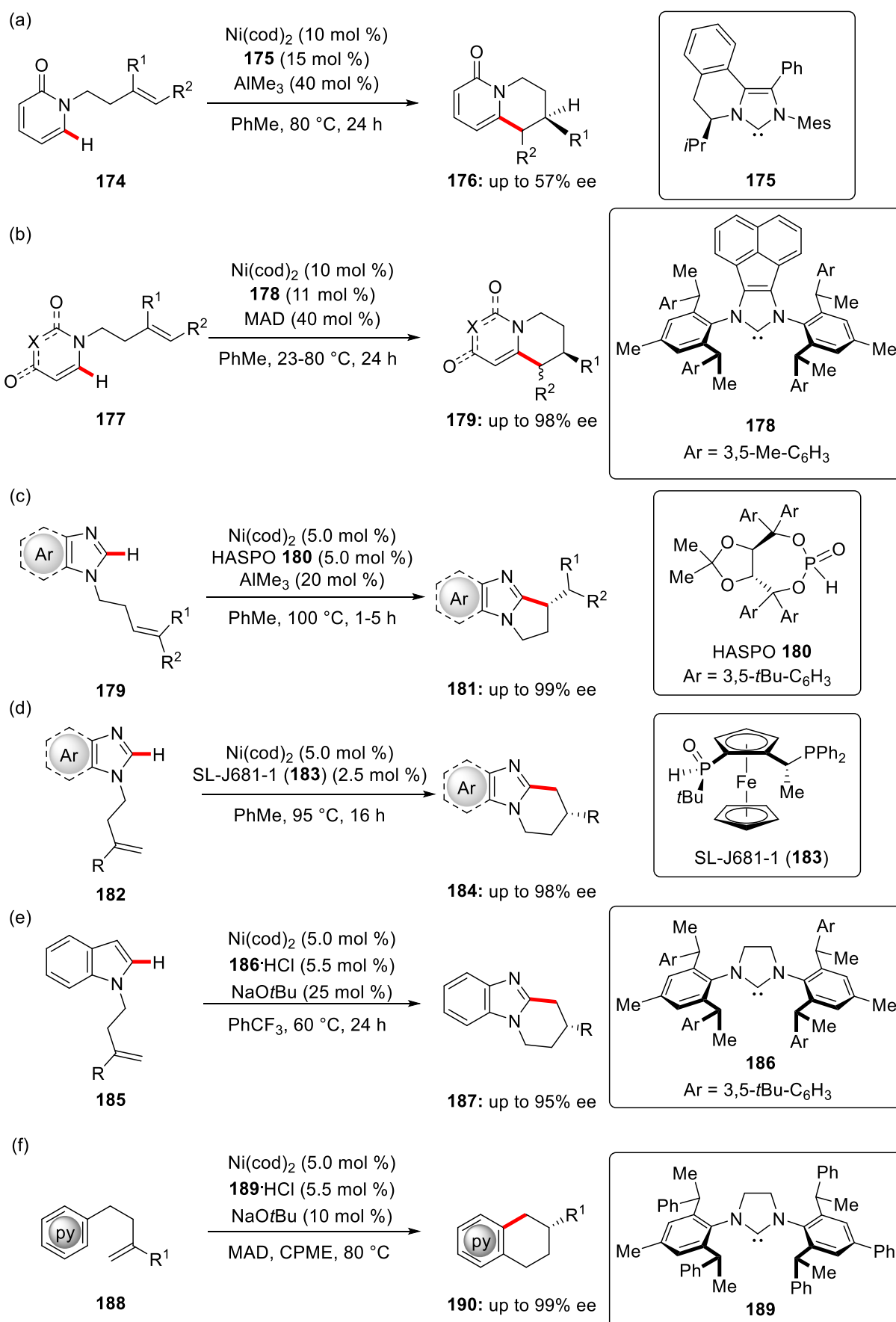
1.3.5.1. Intramolecular Reactions

Over the past years, a significant progress has been observed for the nickel-catalyzed enantioselective intramolecular C–H activations. In 2009, Nakao and Hiyama reported a racemic protocol for intramolecular C–H alkylation of pyridines with tethered olefins by a cooperative nickel/Lewis acid manifold.^[143] Later, Cramer achieved preliminary success in enantioselective version of this protocol by using a chiral isoquinoline-based N-heterocyclic carbene^[144] **176** to provide *endo*-cyclized products **174** in 78.5:21.5 e.r. (Scheme 49a).^[145] Later, further improvement of this protocol was reported by the same group. A modified acenaphthene backbone contained NHC ligand **178**, which was developed based on previous ligand design by Gawley,^[146] was found to be crucial to achieve excellent enantioselectivities in the presence of MAD (methylaluminium bis(2,6-di-*tert*-butyl 4-methylphenoxide) as a Lewis acid (Scheme 49b).^[147] Further developments in this direction were reported by Ye, where TADDOL-based HASPOs **180** were employed to promote nickel-aluminum bimetallic catalysis for highly enantioselective *exo*-selective intramolecular C–H cyclization of imidazole derivatives **181** (Scheme 49c).^[148]

Despite these advances, enantioselective cyclizations were limited to the use of pyrophoric organoaluminium reagents as additives^[149] which significantly restrict the substrate scope. To address this issue, Ackermann realized an aluminum-free reaction conditions for nickel catalyzed intramolecular highly enantioselective transformation. The unprecedented use of nickel/JoSPOphos^[150] manifold enabled the *endo*-cyclization of imidazoles with unactivated alkenes **182** (Scheme 49d).^[151]

Later, Cramer employed chiral SIPR ligand **186** with bulky flanking groups for highly enantioselective nickel(0)-catalyzed *endo*-cyclization of indoles and pyrrole **185** (Scheme 49e).^[152] This approach was further extended by Shi to pyridines **188** utilizing a bulky chiral NHC ligand **189** in the presence of MAD as Lewis acid (Scheme 49f).^[153] Shortly thereafter, the same group devised similar strategy in the presence of a bulky chiral NHC ligand to synthesis enantioenriched fluorotetralins by achieving *endo*-selective C–H annulation of polyfluoroarenes with excellent enantioselectivities.^[154]

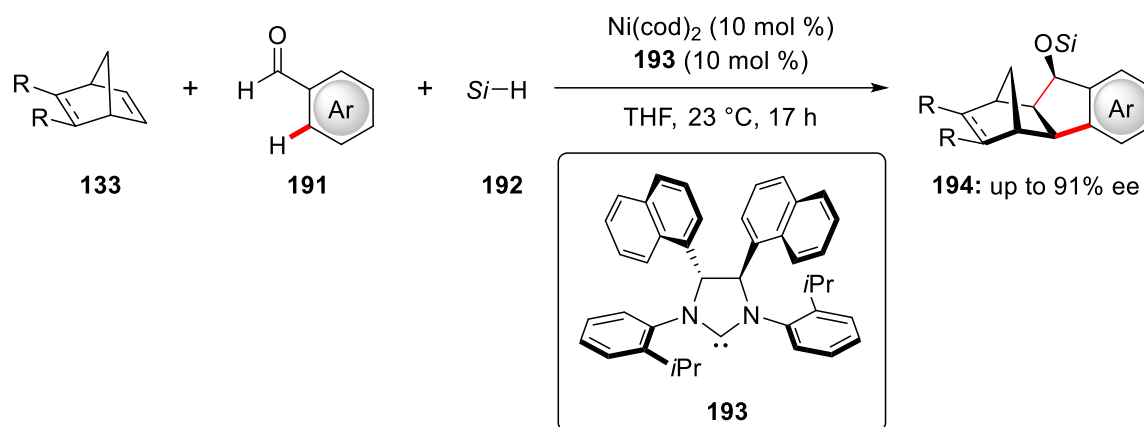
1. Introduction



Scheme 49. Nickel-catalyzed enantioselective intramolecular C–H activations.

1.3.5.2. Intermolecular Reactions

Although numerous studies have been conducted on nickel-catalyzed intramolecular enantioselective hydroarylations, enantioselective intermolecular C–H activations remain extremely scarce in the literature. Inspired by the previous racemic work on nickel/NHC catalyzed three-component coupling by Fukuzawa,^[155] an enantioselective version of this protocol was reported by Cramer and coworkers using a novel chiral NHC ligand **193** (Scheme 50).^[156] The key to success was the use of flanking *N*-aryl substituted Grubbs-type chiral NHC^[157] **193** to provide annulated indanols **194** in a highly enantioselective fashion.



Scheme 50. Enantioselective reductive three-component coupling.

1.3.6. Cobalt Catalysis

Over the last few decades, cobalt complexes have turned out to be among most promising 3d metals with numerous application to the functionalization of inert C–H bonds.^[31, 32d, 32f, 32g, 32j] In general, these reactions can be performed by two strategies. (a) So-called low-valent cobalt catalysis:^[32i] These are commonly performed under reductive conditions, where readily available cobalt(II) salt are reduced *in situ* to form either a cobalt(0) complex or, more commonly, a cobalt(I)-complex, which undergoes oxidative addition to promote the functionalization. (b) Cobalt(III) catalysis is mainly performed using bench-stable high-valent cobalt(III) catalysts with cyclopentadienyl ligands.^[32f] Early developments in the field of enantioselective cobalt-catalyzed C–H functionalizations have been realized using low-valent cobalt chemistry.

1.3.6. 1. Cobalt Catalysis under Reductive Conditions

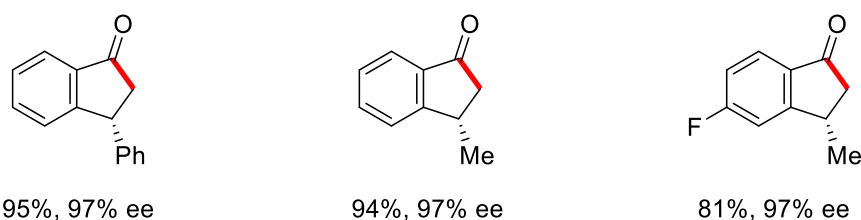
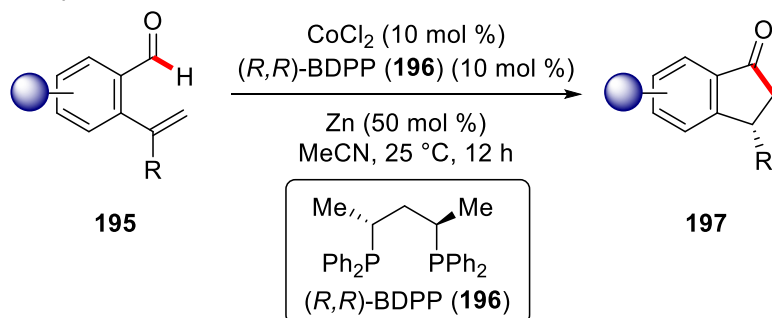
In 2014, Yoshikai utilized a combination of CoCl_2 as the catalyst and (*R,R*)-BDPP as the optimal chiral phosphine ligand to promote intramolecular hydroacylation of 2-

1. Introduction

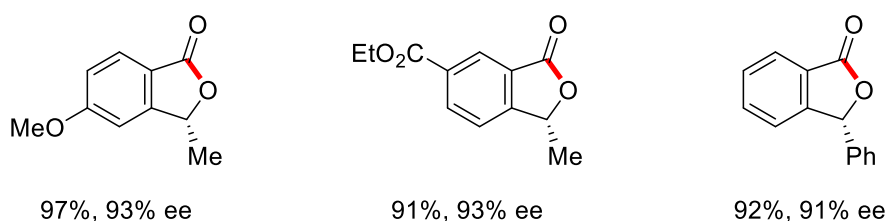
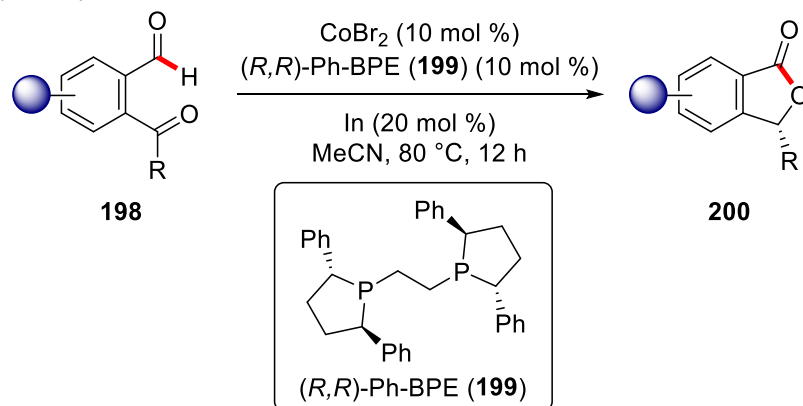
alkenylbenzaldehydes **195** to deliver highly enantioenriched indanones **197** (Scheme 51a).^[158]

The authors further extended this protocol to 2-acylbenzaldehydes **198** using a catalytic system of CoBr₂ and (*R,R*)-Ph-BPE for the synthesis of phthalides **200** building blocks in high enantioselectivity (Scheme 51b). Cobalt-chiral diposphine catalytic systems provided the phthalide and indanone derivatives in good yields and with high enantio-control.

(a) Hydroacylation of olefins



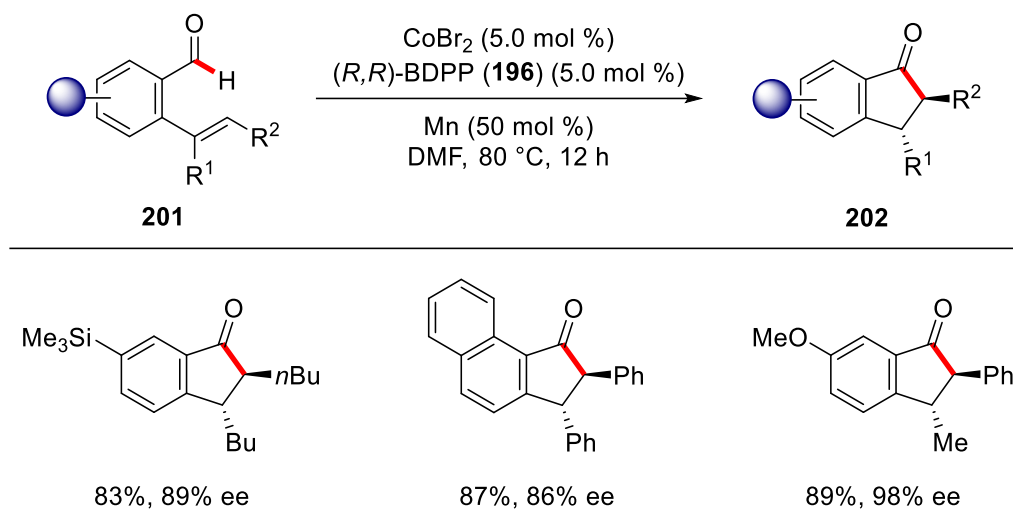
(b) Hydroacylation of ketones



Scheme 51. Enantioselective cobalt-catalyzed intramolecular hydroacylations.

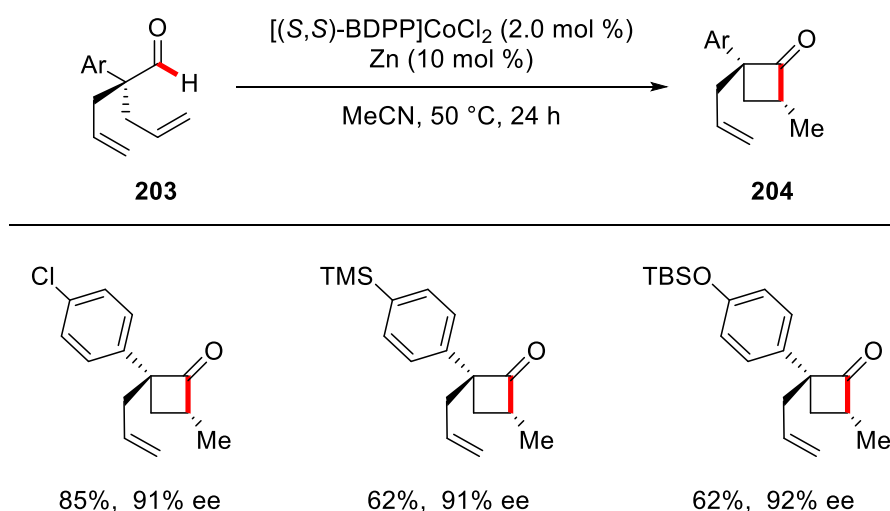
Later, the same group extended this approach to more challenging trisubstituted alkenes for the step-economical synthesis of 2,3-disubstituted indanones **202** (Scheme 52).^[159] The authors achieved hydroacylations of 2-alkenylbenzaldehydes **201** bearing a trisubstituted olefin by

using a catalytic system of CoBr_2 and (R,R) -BDPP to provide the corresponding chiral cyclic ketones **202** in high yields and enantioselectivities. Notably, the outcome of the reaction was only hardly influenced by the E/Z ratio of the starting olefin substrates.



Scheme 52. Hydroacylation of trisubstituted alkenes **201**.

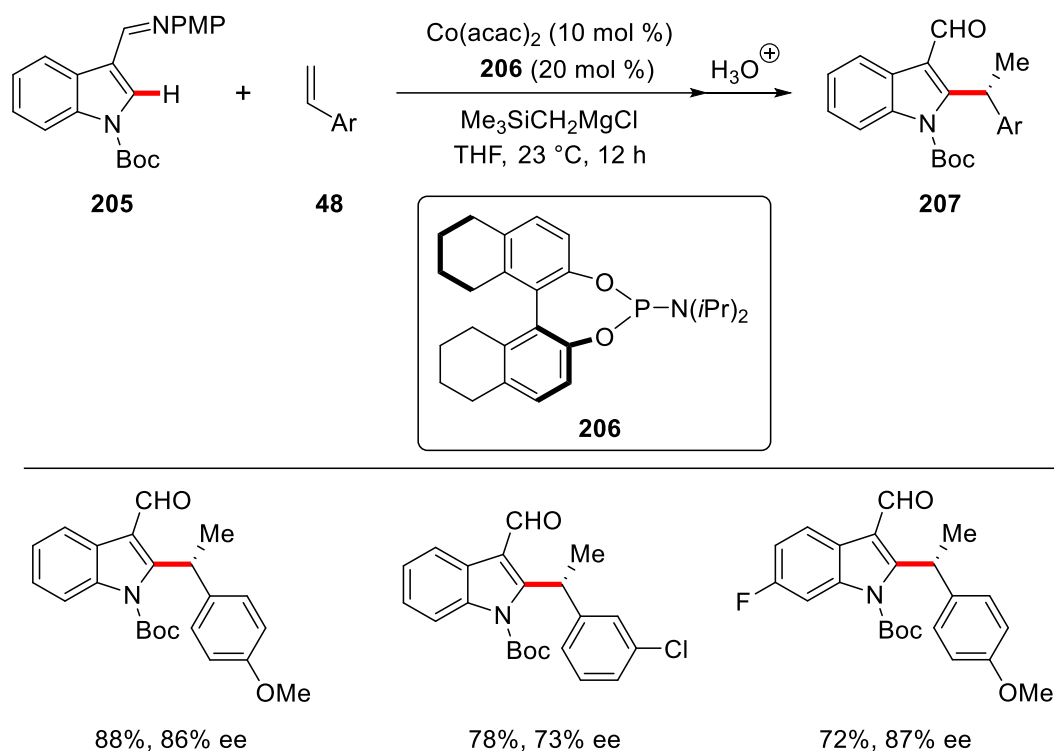
Shortly thereafter, the versatile cobalt catalysis was applied by Dong and coworkers for a unique desymmetrization protocol for the intramolecular hydroacylation process to construct strained four-membered cyclobutanone derivatives **204** (Scheme 53).^[160] The authors were able to control the regioselectivity to enable the formation of four-membered cyclobutanone **204** in preference to the five-membered regioisomers. A cobalt catalyst derived from chiral diphosphine ligand (S,S) -BDPP enabled the synthesis of strained cyclobutanones **204** from α -substituted dienyl aldehydes **203** with quaternary and tertiary stereogenic centers in high yields and with high enantioselectivities.



Scheme 53. Enantioselective hydroacylation towards cyclobutanones **204**.

1. Introduction

In 2016, Yoshikai unraveled the low-valent cobalt catalyzed enantioselective C–H alkylation of indole derivatives **205** with styrenes **48**.^[161] Imine-directed C–H alkylation was achieved in the presence of $\text{Co}(\text{acac})_2$ as catalyst and BINOL-derived phosphoramidates **206** as chiral ligand. Thus, enantioenriched 1,1-diarylethane derivatives were obtained in high yields and with high enantioselectivities.



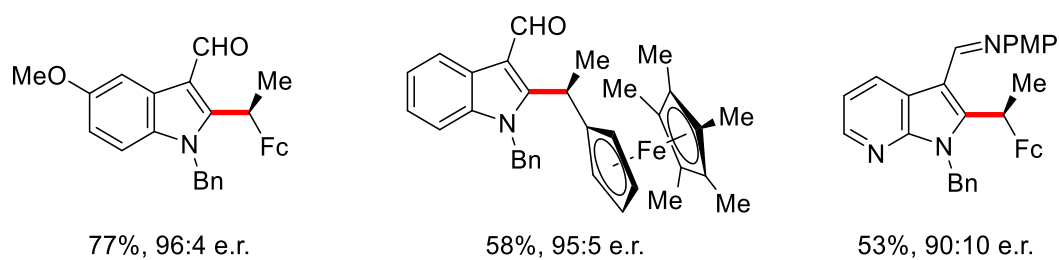
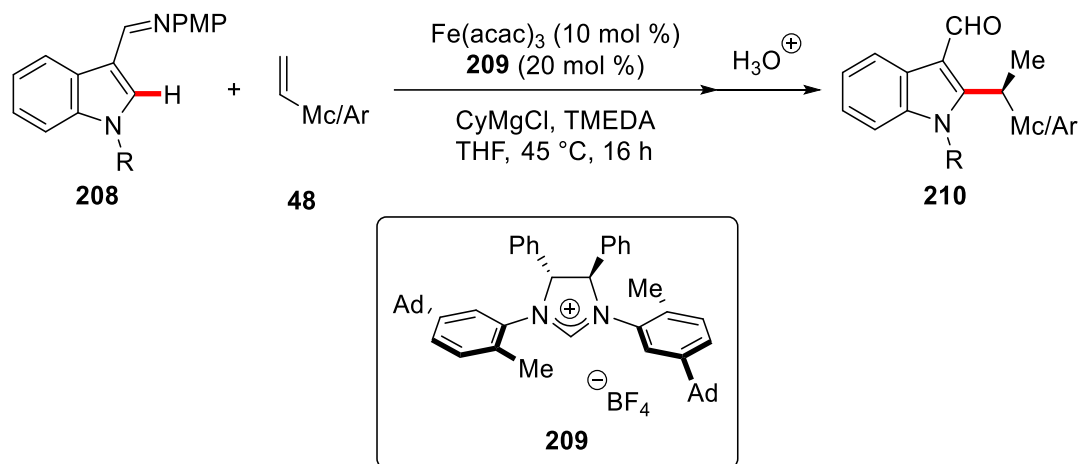
Scheme 54. Enantioselective cobalt-catalyzed hydroarylation of styrenes **48**.

1.3.7. Iron Catalysis

Iron is by far the most naturally abundant transition metal on Earth. Iron chemistry is promoted by low cost and low toxicities as well as a broad array of various oxidation states. This has been reflected in the increasing use of iron catalysts in molecular syntheses, pharmaceutical and agrochemical industries.^[162] This has set the stage for catalytic iron-catalyzed organometallic C–H functionalization processes. While the field of iron-catalyzed C–H activation is emerging, still the development of enantioselective C–H transformation is highly desirable.

On this note, in 2018 Ackermann succeeded to achieve first highly enantioselective iron-catalyzed organometallic C–H activation (Scheme 55).^[163] The authors reported enantioselective C–H secondary alkylation of (aza)indoles by the design of a novel bulky *meta*-1-adamantyl substituted NHC **209** ligand which proved to be crucial for a high level of

enantiocontrol. A plethora of diversely substituted indoles and azaindoles **208** were tested with styrenes and vinylmetallocenes **48** under the optimized reaction conditions. Thus, chiral C2-alkylated products **210** were obtained in excellent yields and enantioselectivities.



Scheme 55. Enantioselective iron-catalyzed C–H secondary alkylation.

1.4. Transition Metal-Catalyzed Oxidative C–H Activation towards Resource Economy

Transition metal-catalyzed C–H activation has emerged as viable tool for molecular synthesis due to its high atom- and step-economy.^[27, 56] In this regard, oxidative C–H transformations are particularly attractive as they avoid the use of prefunctionalization. Yet, oxidant economy significantly contradicts the sustainable nature of synthetically attractive oxidative C–H transformations. Unfortunately, oxidative C–H activations heavily rely on expensive and toxic chemical oxidants including hypervalent iodine(III) and copper(II) or silver(I) salts, generating stoichiometric amounts of undesired chemical waste. Also, in recent years use of molecular oxygen has gained certain attention as terminal oxidant^[164] but its use with highly flammable organic solvents imposes safety issues.^[165]

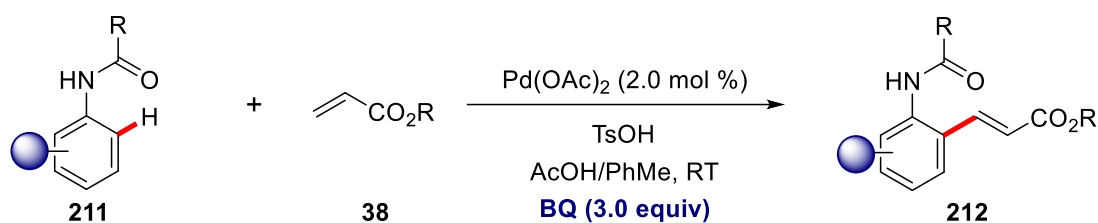
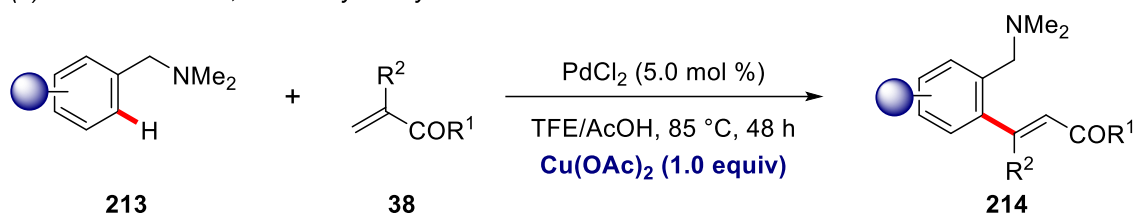
1.4.1.1. Palladium-Catalyzed C–H Olefinations with Chemical Oxidants

Mizoroki-Heck couplings have huge impact on synthetic chemistry for C–C bond formation reactions.^[15b, 166] Given the significantly high importance of olefination reactions, Fujiwara–Moritani reaction even offers a better strategy for the introduction of olefins into arene C–H bonds as it avoids the preactivation of the substrates.^[167] Yet, the use of large excess of substrates and lack of site-selectivity have jeopardized the application of Fujiwara–Moritani reaction to an extent. Thus, over the past decades directing group assisted C–H activation has become an attractive strategy to control the regioselectivity.^[27d, 38] Consequently, these oxidative transformations are largely depended on the use of chemical oxidants for the reoxidation of metal centers. Here few representative examples have been provided to highlight the necessity of the expensive and toxic chemical oxidants for successful outcome of the palladium-catalyzed olefination reactions.

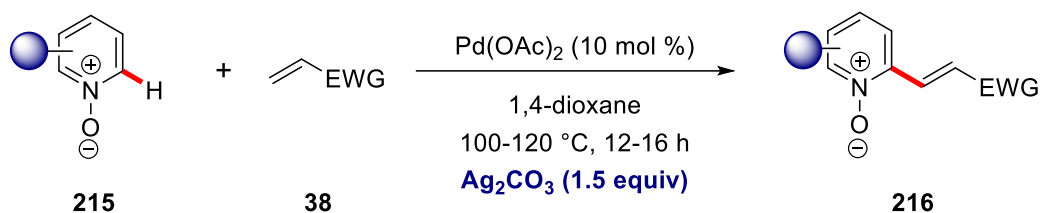
In an elegant study by De Vries and Van Leeuwen in 2002, palladium-catalyzed oxidative olefinations of anilides **211** were achieved at room temperature (Scheme 56a).^[168] 2.0 mol% Pd(OAc)₂ was employed as catalyst in combination with 3.0 equiv of BQ as terminal oxidant to obtain optimal yields for the olefination protocol.

In a related study, Shi reported palladium-catalyzed *ortho*-olefination of *N,N*-dimethylbenzylamines **213** (Scheme 56b).^[169] Among a series of tested chemical oxidants, stoichiometric amounts Cu(OAc)₂ was found to be the best oxidant for this transformation.

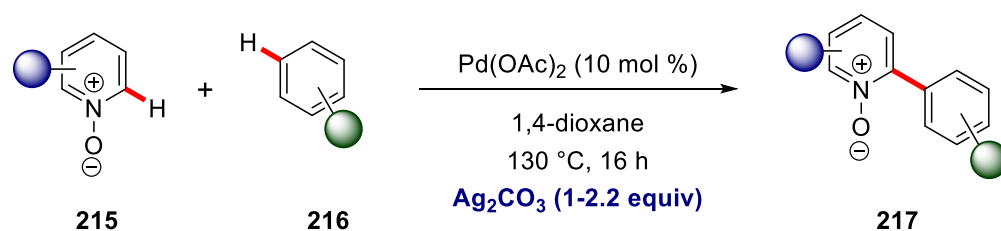
(a) Olefination of anilides

(b) Olefination of *N,N*-dimethylbenzylamines**Scheme 56.** Palladium-catalyzed *ortho*-olefination in presence of chemical oxidants.

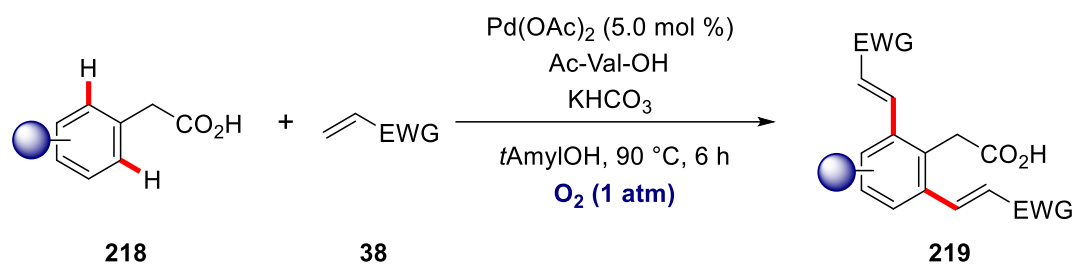
Later, Chang disclosed oxidative alkenylation and arylation of pyridine *N*-oxides **215** in the presence of silver based oxidant (Scheme 57).^[170]

(a) alkenylation of pyridine *N*-oxide

(b) arylation with arenes

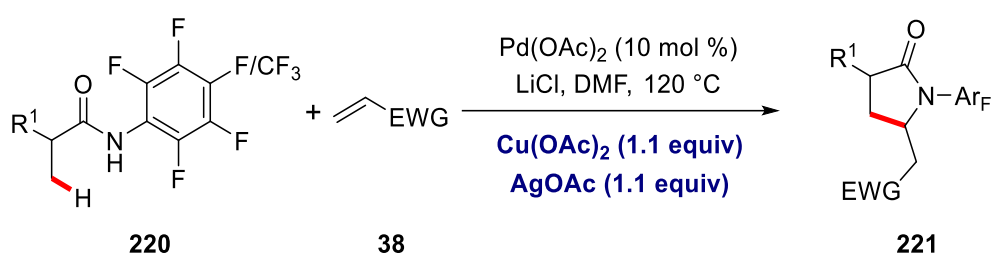
**Scheme 57.** Palladium-catalyzed oxidative alkenylation and arylation with silver-based oxidants.

In 2010, *ortho*-C–H olefination reaction for phenylacetic acids **218** was disclosed using oxygen at atmospheric pressure as the terminal oxidant (Scheme 58).^[171]



Scheme 58. Oxygen as terminal oxidant in *ortho*-C–H olefination reaction.

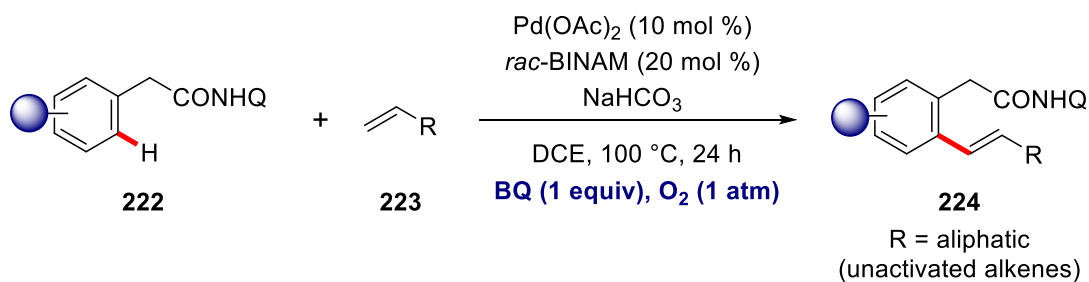
In 2010, a protocol for palladium-catalyzed C(sp³)–H olefination was documented (Scheme 59).^[172] A superstoichiometric mixture of Cu(OAc)₂ and AgOAc as oxidants provided the highest yield for this olefination protocol with a fancy directing group.



Scheme 59. Palladium-catalyzed oxidative C(sp³)–H olefination.

These examples set the stage for the further developments in palladium-catalyzed oxidative transformations with chemical oxidants with notable contributions from Gevorgyan,^[173] Shi,^[174] Yu,^[175] among others.^[27m]

Despite these advances, the vast majority of C–H olefination reactions required activated or electronically-biased olefins, such as acrylates and styrenes. In 2014, Maiti reported C–H olefination reactions with unactivated alkenes **223** as coupling partners (Scheme 60).^[176] The authors disclosed palladium-catalyzed chelation-assisted C–H alkenylation of phenylacetic acid derivatives **222** with unbiased aliphatic alkenes **223** by the aid of 8-aminoquinoline as the directing group. The key to success was the use of *rac*-BINAM as the ligand for this oxidative alkenylation protocol with 1 equiv of BQ under atmospheric pressure of oxygen as the oxidant.



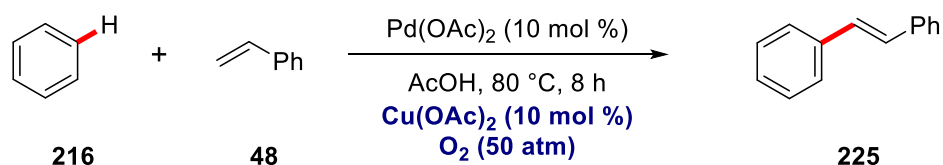
Scheme 60. Palladium-catalyzed C–H olefination with unbiased olefins under oxygen atmosphere.

In addition to the aforementioned reports, oxidative olefinations have also emerged as an attractive strategy for the enantioselective transformations including desymmetrization reactions and atroposelective transformations which have been comprehensively discussed in the previous chapter (*cf.* chapter 1.3.1.).^[41a, 57-58, 63a]

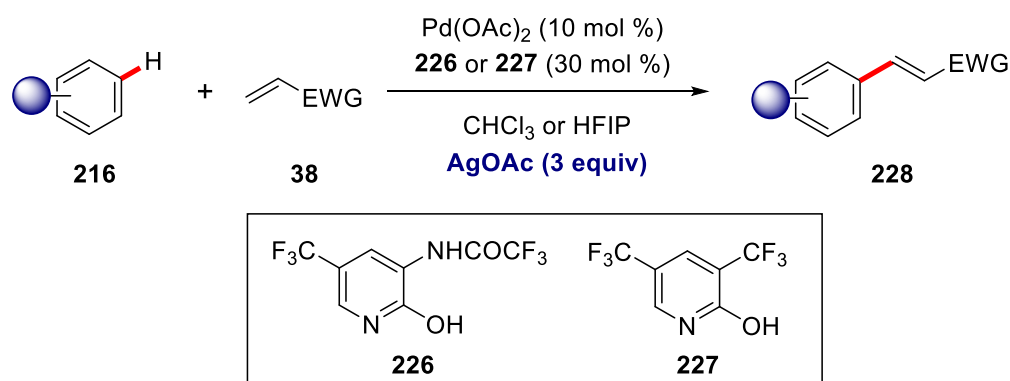
Other than directing group assisted C–H activation,^[27d, 38] ligand-assisted palladium catalyzed Fujiwara–Moritani type reaction has recently gained certain momentum.^[177] In 1969, in a pioneering work palladium-catalyzed Fujiwara–Moritani reaction was reported to form C–C bonds under oxidative conditions (Scheme 61a).^[167a, 178] Later, Yu’s study disclosed oxidative olefinations of electron-deficient arenes in the presence of 2,6-dialkylpyridine ligands. Significant contributions have also been made in the ligand-accelerated C–H olefination reactions by Yu,^[179] Sanford,^[180] Stahl.^[181] In these studies mainly pyridines **226** or **227** have been identified as the best ligands for the Fujiwara–Moritani reactions of simple arenes (Scheme 61b). Very recently, Fernández-Ibáñez identified inexpensive bidentate S,O-ligands^[37a, 182] **229** for non-directed C–H olefination reactions of electron-rich and electron-poor arenes **216** (Scheme 61c).^[183] Similarly, these oxidative transformations are also limited to the use of superstoichiometric amounts of chemical oxidants which impeded the sustainability of this approach.

1. Introduction

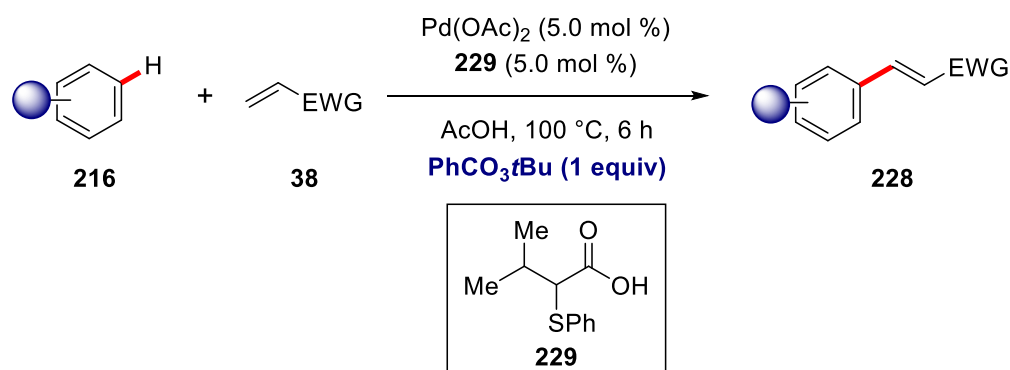
(a) Early example of the Pd-catalyzed Fujiwara–Moritani reaction



(b) 2-Pyridone ligand-accelerated non-directed C–H functionalization



(c) S,O-Ligand-promoted non-directed C–H functionalization



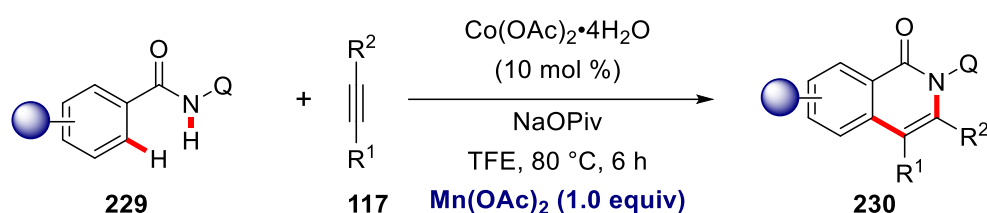
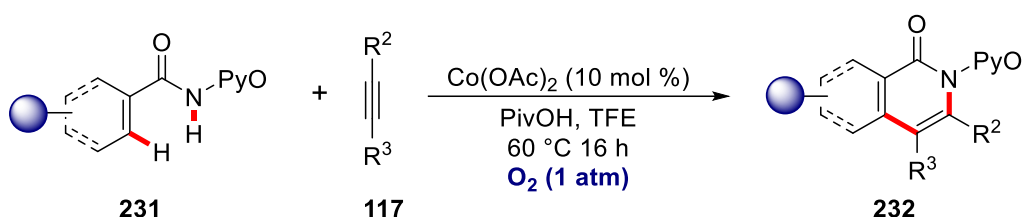
Scheme 61. Non-directed C–H activation under oxidative conditions.

1.4.1.2. Cobalt-Catalyzed C–H Activations with Chemical Oxidants

Among the 3d transition metals, bench-stable cobalt(II) salts have gained wide applications due to their commercial availability, easy set up and robustness.^[32a] Starting from Daugulis's work on C–H/N–H annulation of benzamides **229** with the aid of 8-aminoquinoline as the directing group (Scheme 62a),^[184] cobalt-catalyzed oxidative C–H/X–H annulation has emerged as a versatile step-economical way to synthesis decorated heterocycles.^[164d, 185]

In this context, in 2016 the Ackermann group utilized for the first time molecular oxygen as the terminal oxidant to achieve the oxidative cobalt-catalyzed synthesis of isoindolones **232** (Scheme 62b).^[164d]

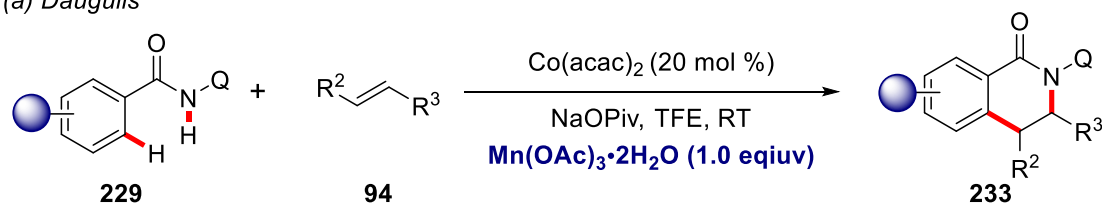
(a) C–H/N–H Activation by Daugulis

(b) O_2 as the sole oxidant by Ackermann

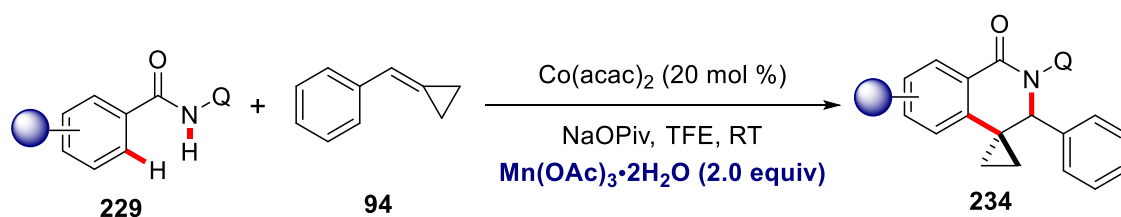
Scheme 62. C–H/N–H annulation of benzamides **231** with internal alkynes **117** under oxidative conditions.

Besides annulation with alkynes **117**, alkenes **38/94** and allenes **110/236** have also found suitable application in the annulation protocol in the presence of chemical oxidants, with notable contributions from Daugulis,^[186] Ackermann,^[185f] Cheng,^[187] Volla/Maiti (Scheme 63 and 64).^[188]

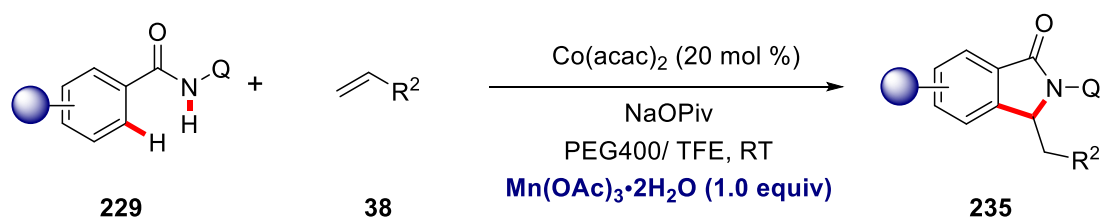
(a) Daugulis



(b) Volla

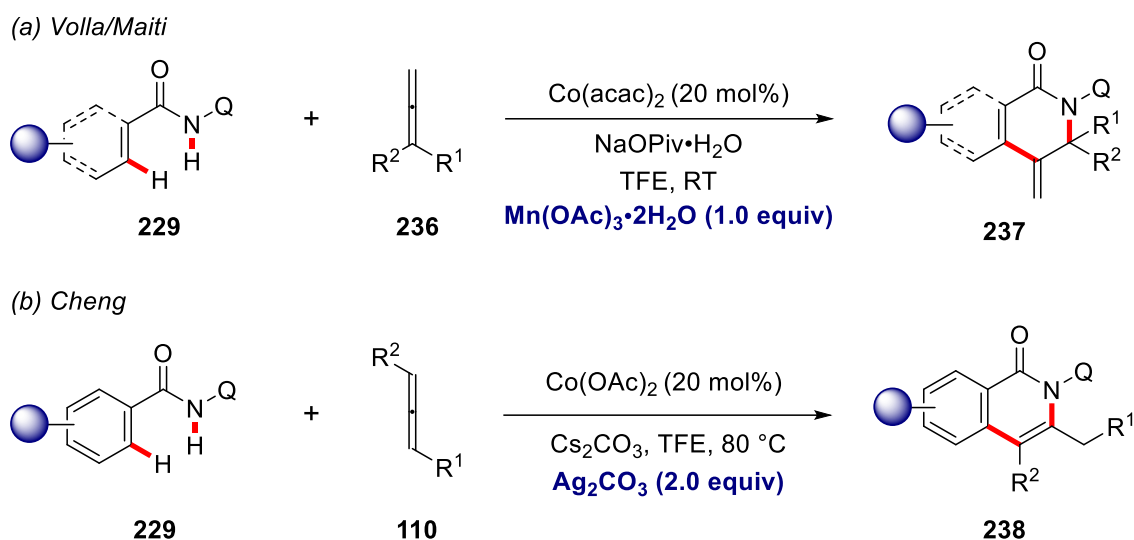


(c) Ackermann



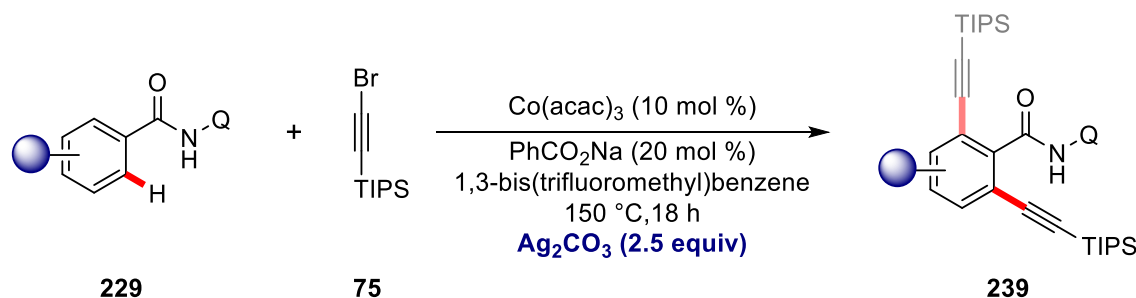
Scheme 63. Cobalt-catalyzed oxidative C–H/N–H annulation with alkenes **38** and **94**.

1. Introduction



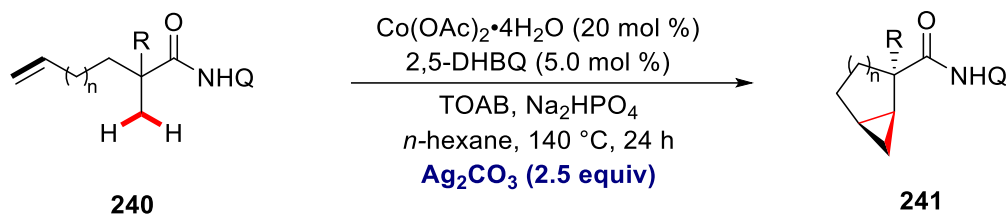
Scheme 64. Cobalt-catalyzed oxidative C–H/N–H annulation with allenes **236** and **110**.

Oxidative cobalt(II)-catalyzed C–H activation was not limited to annulation reactions. Indeed, various C–C and C–Het bond forming reactions have been well studied in the literature. Balaraman reported the oxidative C–H alkylation by the aid of 8-aminoquinoline as the directing group in the presence of $\text{Co}(\text{acac})_3$ as the catalyst and superstoichiometric amounts of Ag_2CO_3 to obtain the alkynylated products **239** (Scheme 65).^[189]



Scheme 65. Cobalt(II)-catalyzed oxidative C–H alkylation.

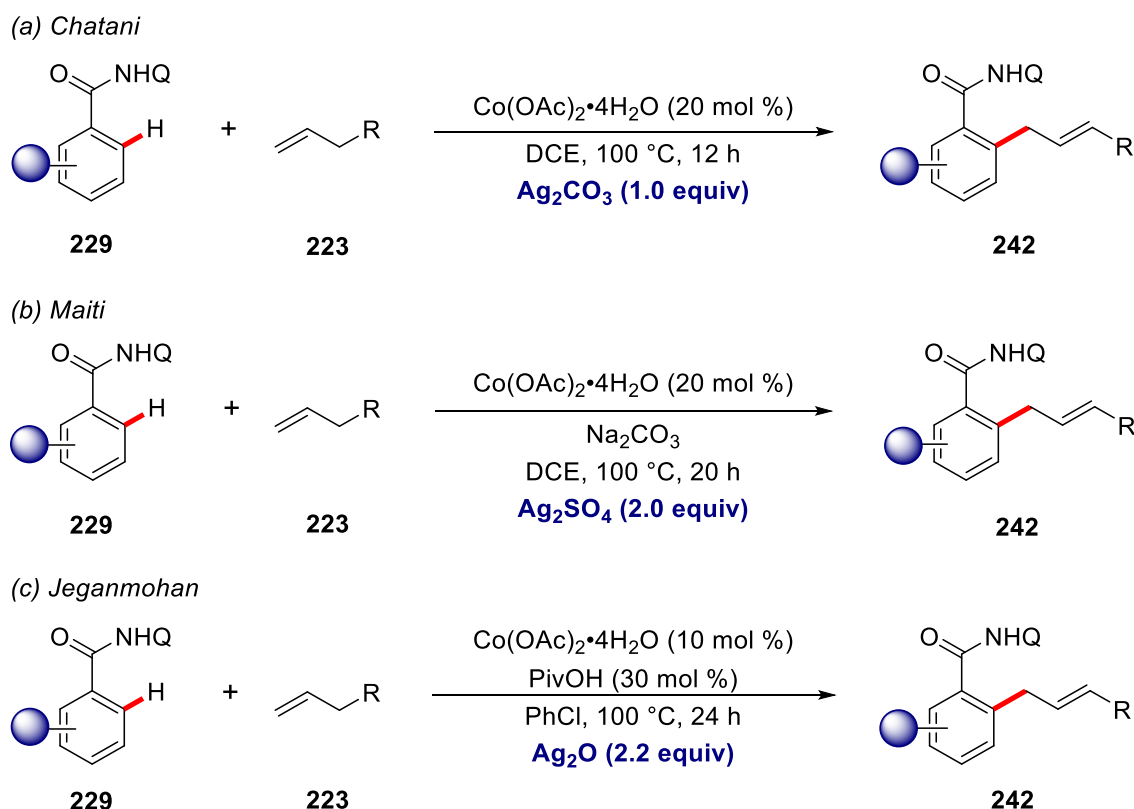
Recently, a protocol for the synthesis of the bicyclo[n.1.0] ring system **241** was realized by Shi through oxidative multiple $\text{C}(\text{sp}^3)\text{--H}$ functionalization strategy in the presence of superstoichiometric amounts of Ag_2CO_3 as the oxidant (Scheme 66).^[190]



Scheme 66. Cobalt-catalyzed oxidative $\text{C}(\text{sp}^3)\text{--H}$ functionalization.

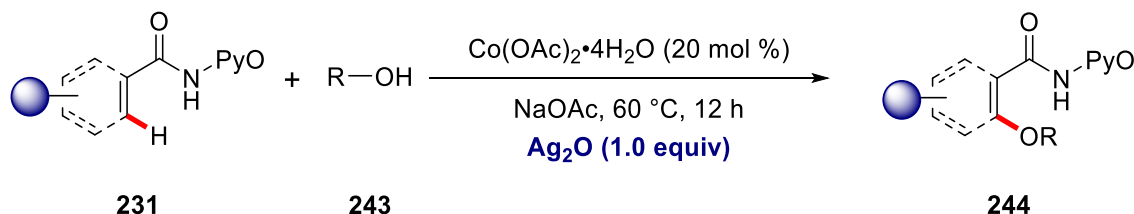
Almost at the same time three independent reports were documented for the allylation of quinolinamides **229** with unbiased alkenes **223** under cobalt(II) catalysis by the groups of

Jeganmohan,^[191] Chatani,^[192] and Maiti.^[193] Silver based chemical oxidants were employed for this oxidative allylation protocol. Jeganmohan used Ag₂O as the oxidant, whereas Chatani employed Ag₂CO₃ as the oxidant in the presence of Co(OAc)₂·4H₂O as the catalyst. Maiti observed optimal reactivity using Ag₂SO₄ as the oxidant in DCE as the solvent. Notably, all these studies provided allylic selectivity over styrenyl-type reactivity (Scheme 67).



Scheme 67. Cobalt-catalyzed C–H allylation in the presence of silver based oxidants.

In addition, versatile cobalt catalysis was discovered as a viable tool to realize C–Het bond forming reactions. Song and Niu reported oxidative cobalt-catalyzed C(sp²)–H alkoxylation of amides **231** by the aid of a bidentate directing group (Scheme 68).^[194]



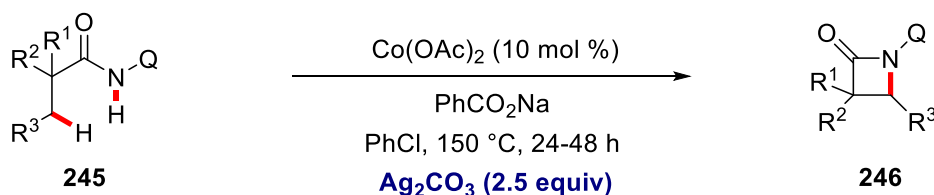
Scheme 68. Oxidative C(sp²)–H alkoxylation of amides **231**.

An intramolecular dehydrogenative C–H amination was reported by Ge.^[195] This protocol proved viable for the synthesis of β - and γ -lactams **246** by C(sp³)–H bond activation (Scheme 69a). A silver based oxidant was found to be the most efficient for this amination protocol. Later, Song and Niu devised intermolecular C(sp²)–H amination.^[196] With the aid of a bidentate

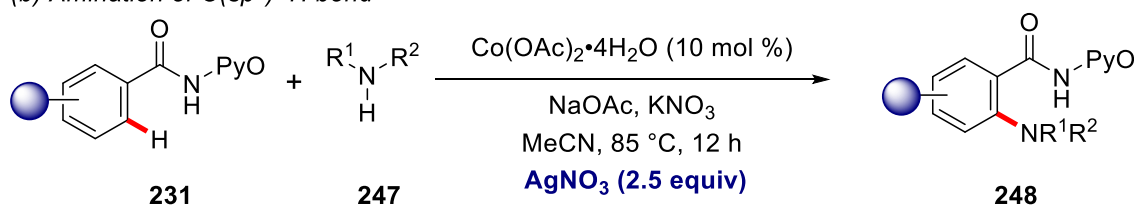
1. Introduction

N,O-auxiliary, *ortho*-C–H aminations were feasible with secondary alkyl amines **247** (Scheme 69b). Here, AgNO₃ was found to be the optimal oxidant in this reaction.

(a) Intramolecular dehydrogenative amination



(b) Amination of C(sp²)-H bond

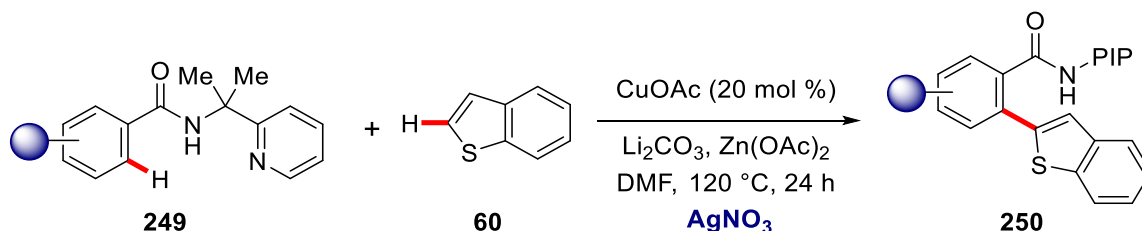


Scheme 69. Oxidative cobalt-catalyzed C–H amination.

1.4.1.3. Representative Examples on Copper-Catalyzed C–H activations with Chemical Oxidants

Building upon elegant studies by Ullmann and Goldberg,^[9, 197] copper complexes have been widely applied for C–C and C–Het bond forming reactions. In this context, copper-catalyzed C–H arylation with aryl halides have been well studied by Daugulis,^[198] Miura^[199] and Ackermann^[200] utilizing copper(I) catalysts. Besides aryl halides, diaryliodonium salts have been well investigated as arylating agents with copper complexes, with key reports by Gaunt,^[201] Glorius,^[202] Shi^[203] and among others.

Moreover, oxidative C–H/C–H couplings are an attractive strategy, which avoids prefunctionalized starting materials. Consequently, several examples have been documented on oxidative cross-coupling reactions in the presence of chemical oxidants.^[204] In a recent example, Shi utilized 2-(pyridin-2-yl) isopropyl amine (PIP) as directing group for oxidative coupling between benzamides **249** and thiophenes **60** using AgNO₃ as oxidant (Scheme 70).^[205]

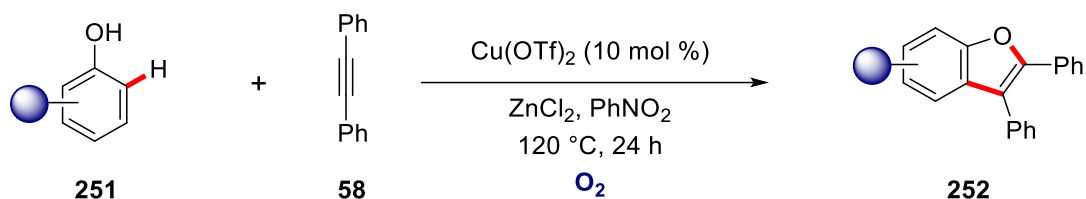


Scheme 70. Copper-catalyzed oxidative C–H/C–H coupling.

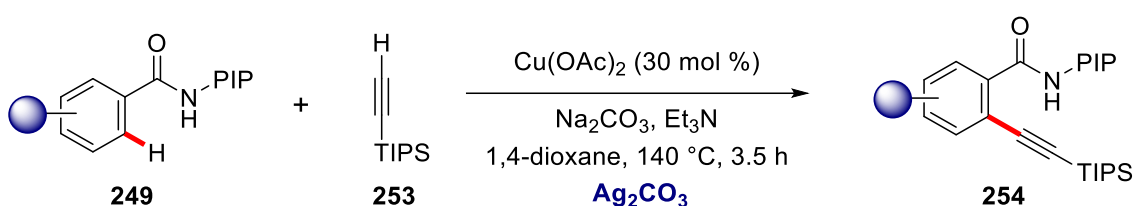
In the light of oxidative transformations, copper catalyzed alkyne annulations represent a step-economical way to synthesis complex molecules. In this context, Jiang reported copper-

catalyzed annulation between phenols **251** and internal alkynes **58** to synthesize benzofurans **252** under an atmosphere of oxygen (Scheme 71a).^[206] It is noteworthy to mention that *ortho*-alkynylation was achieved using PIP as the bidentate directing group and silver-based chemical oxidant (Scheme 71b).^[207]

(a) annulation of phenols with alkynes



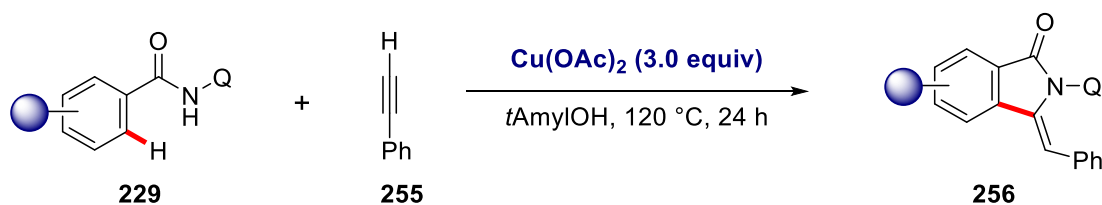
(b) *ortho*-alkynylation of amides



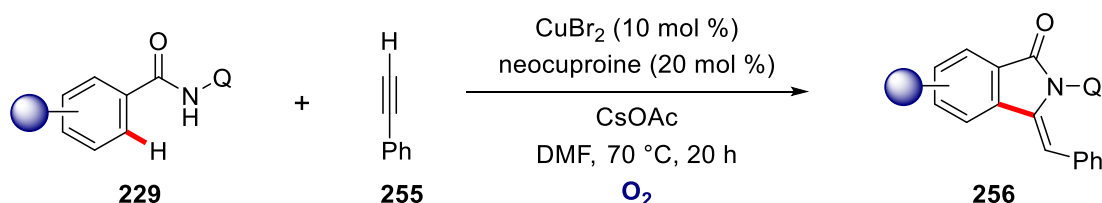
Scheme 71. Copper catalyzed oxidative annulation and alkenylation.

You reported copper-mediated 8-aminoquinoline assisted C–H/N–H annulation to synthesize 3-methyleneisoindolin-1-ones derivatives **256** (Scheme 72a).^[208] Later, a related protocol was disclosed using catalytic amounts of CuBr_2 and O_2 as the sacrificial oxidant (Scheme 72b).^[209]

(a) copper-mediated *ortho*-C–H activation

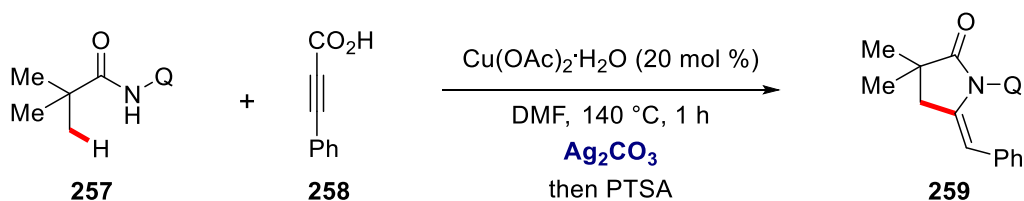


(b) copper-catalyzed *ortho*-C–H activation



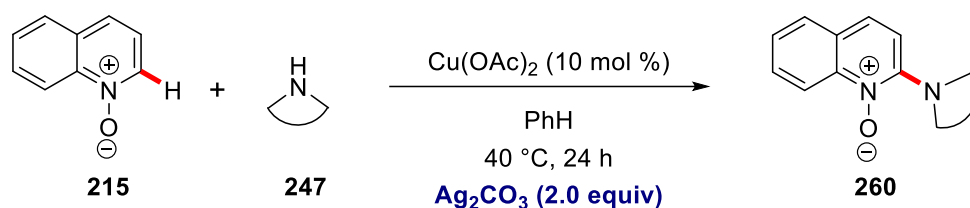
Scheme 72. Copper catalyzed synthesis of isoindolinones.

This protocol was further extended to challenging $\text{C}(\text{sp}^3)\text{-H}$ activations.^[210] Here a combination of a copper(II) salt and Ag_2CO_3 was exploited for the alkenylation with alkynyl carboxylic acids **258** (Scheme 73).



Scheme 73. C(sp³)-H bond activation with alkynyl carboxylic acids.

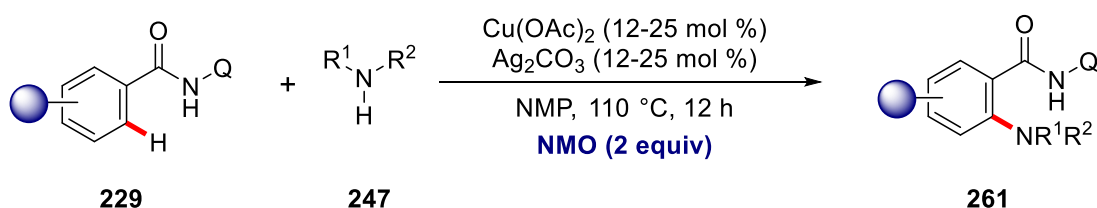
Likewise, copper catalysis has also been extensively used in C-Het bond forming reactions. Considering the importance of C-N bonds, numerous reports have been documented for copper-catalyzed C-H amination reactions using various amination sources.^[211] Furthermore, oxidative C-H/N-H coupling have been realized between quinoline-*N*-oxide **215** and cyclic amines **247** in the presence of stoichiometric silver(I) oxidant (Scheme 74).^[212]



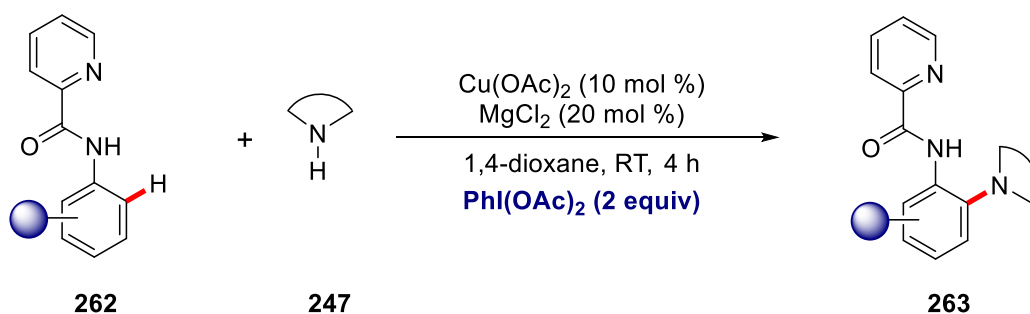
Scheme 74. Copper-catalyzed oxidative C-H amination.

In 2013, *ortho*-amination of benzamides **229** have been reported by the Daugulis groups by the aid of 8-aminoquinoline as the directing group.^[213] This amination protocol required NMO as oxidant in the presence of cocatalytic Ag₂CO₃ as additive to improve the outcome of the reaction (Scheme 75a). In a related study, copper-catalyzed C-H aminations have also been reported using PIDA as oxidant using picolinamide as the directing group (Scheme 75b).^[214]

(a) amination of C(sp²)-H bond using NMO as oxidant

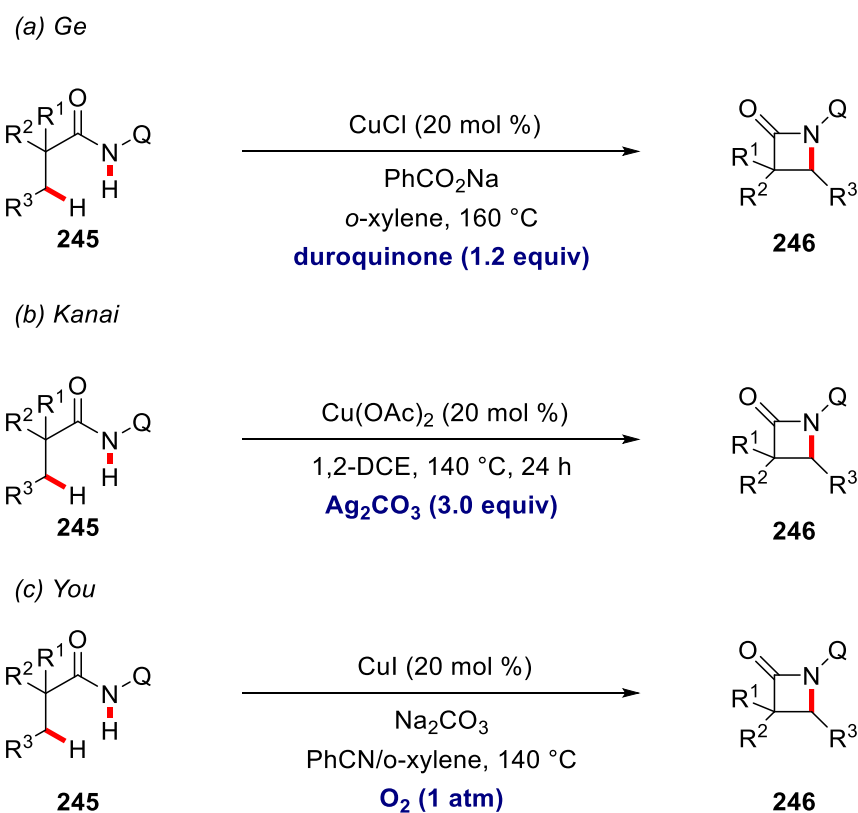


(b) amination of C(sp²)-H bond using PIDA as oxidant



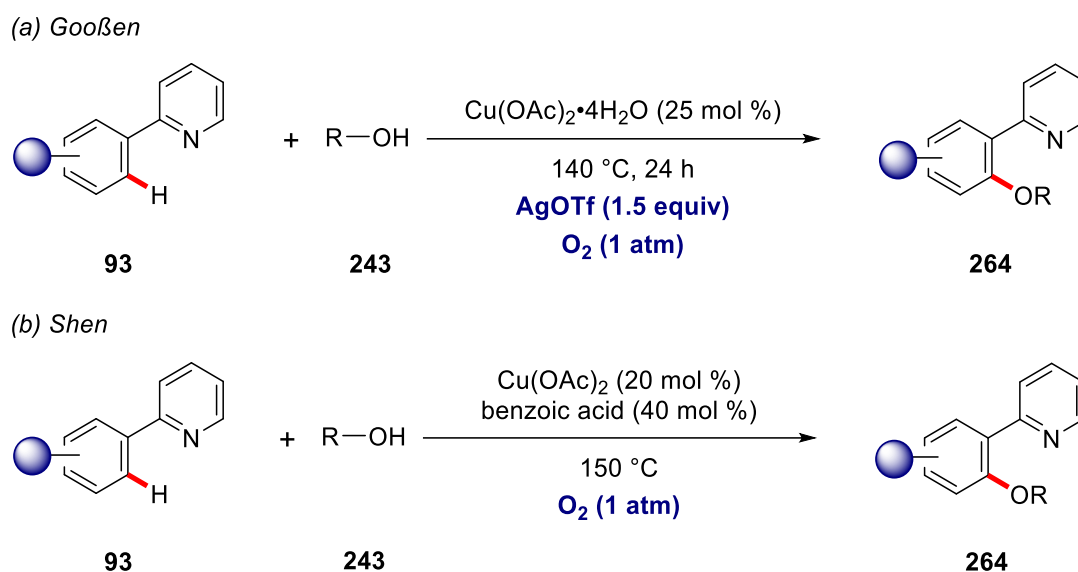
Scheme 75. Copper catalyzed C(sp²)-H aminations with chemical oxidants.

Furthermore, intramolecular C(sp³)-H amidations have been independently reported by Kuninobo/Kanai,^[215] Ge^[216] and You (Scheme 76).^[217] These transformations were also limited to the use of chemical oxidants or O₂ as the terminal oxidant.



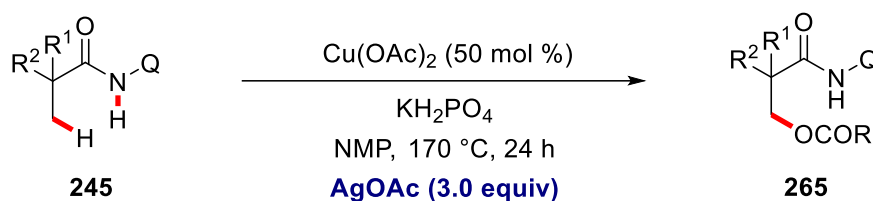
Scheme 76. Intramolecular C(sp³)-H amidations.

Likewise, copper-catalyzed oxygenation has been well studied under oxidative conditions. Goosen employed AgOTf as the oxidant for *ortho*-alkoxylation of 2-phenyl pyridine **93** (Scheme 77a).^[218] A further study was published using O₂ as the terminal oxidant (Scheme 77b).^[219]



Scheme 77. copper-catalyzed oxidative oxygenation.

The low cost of copper catalysts has led to the development of various copper-promoted C–H activation reactions. In this context, Ge disclosed copper-promoted C–H oxygenation of C(sp³)–H bond directed by bidentate 8-aminoquinoline group (Scheme 78).^[220]



Scheme 78. Copper-promoted C–H oxygenation.

1.4.2. Electrochemical Transition Metal-Catalyzed C–H Activation.

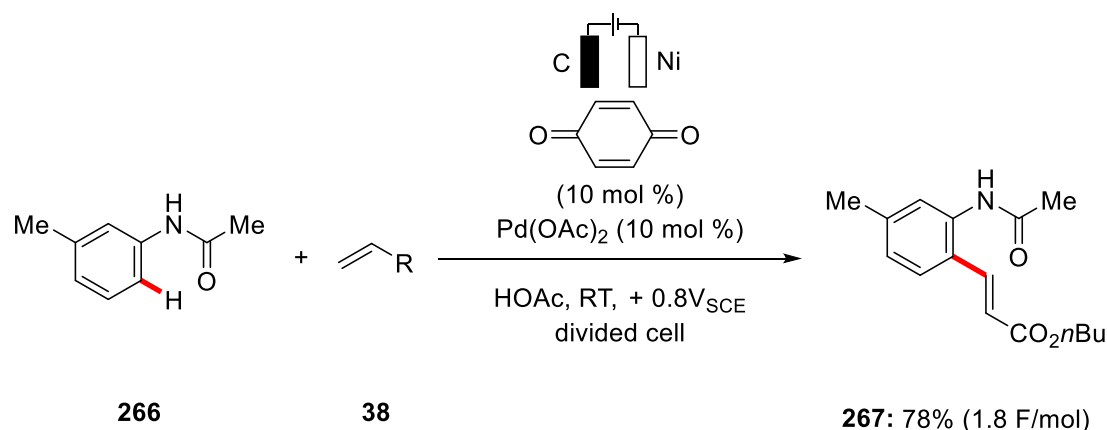
In modern era there is an increasing demands for renewable energy sources, including the wind and solar energies.^[221] Thus, the use of electricity is highly desirable for chemical synthesis which opens up a new avenue for environmentally-benign strategy towards improved molecular synthesis.^[222] Moreover, chemical oxidants operate at a fixed potential, whereas electricity offers to control the potential and current for the desired transformation, thus enabling better selectivities of the reactions^[223] with optimal resource-economy.^[224]

Building upon pioneering works of Kolbe^[225] and Shono,^[226] organic electrocatalysis^[227] has undergone a significant renaissance. Over the few decades there has been significant developments in organic electrocatalysis, exploiting the innate reactivity of organic molecules. Consequently, electrochemical and metal-free transformations exploiting the inherent reactivity have been well studied with notable contributions from Waldvogel,^[228] Baran,^[229]

Yoshida,^[230] and Xu,^[231] among others. In this context, the merger of transition metal catalysis with electrosynthesis^[232] has shown an enormous potential for the activation of strong C–H bonds. Thus, electrochemistry holds unique potential towards the development of environmentally-benign diverse C–H functionalizations to form C–C or C–Het bonds, using electrons as green terminal oxidants in lieu of expensive chemical oxidants.^[232]

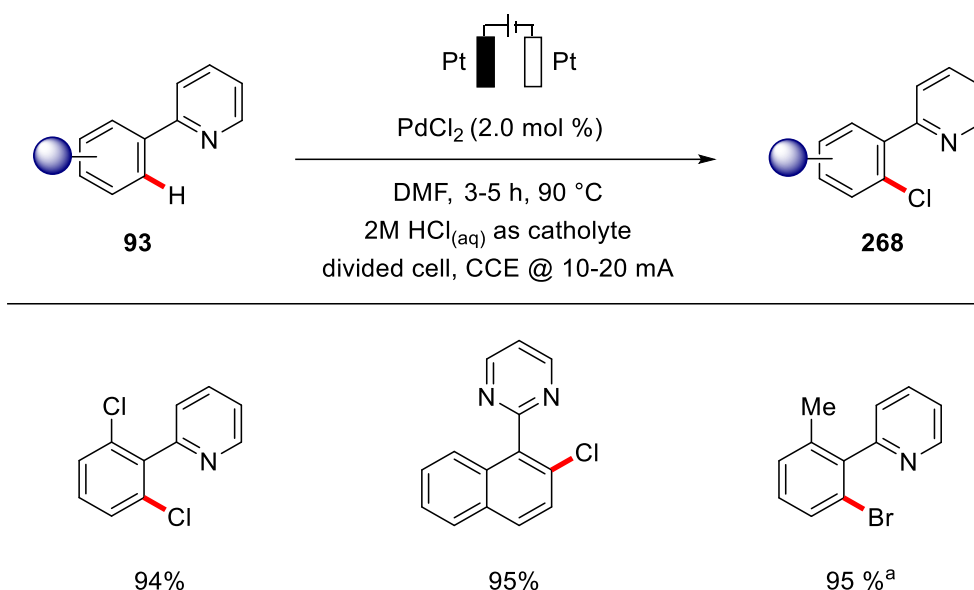
1.4.2.1. Palladium Catalyzed Electrochemical C–H Activation

In 2007, Amatore and Jutand documented the merger of palladium-catalyzed C–H activation with electrosynthesis. Hence, the authors reported on Fujiwara-Moritani-type^[167] C–H alkenylation reaction of *N*-acetylanilines **266** in AcOH as reaction media (Scheme 79).^[233] Co-catalytic amounts of *p*-benzoquinone were beneficial as redox mediators for this reaction, which was regenerated at the anode to recycle the palladium(II) species in the catalytic cycle. This early study set the stage for further developments in electrochemical palladium-catalyzed C–H activation.



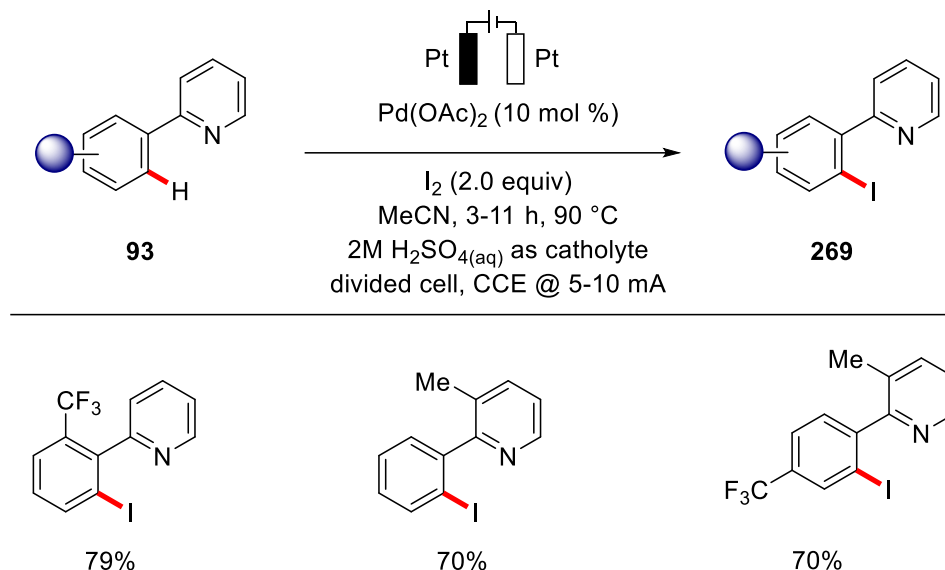
Scheme 79. Electrocatalytic Fujiwara-Moritani reaction.

In 2009, Kakiuchi exploited electrochemistry for the palladium-catalyzed halogenation of 2-phenyl pyridine **93** with hydrogen halides.^[234] This protocol enabled the incorporation of synthetically useful halo groups on the aromatic rings without expensive halogenation reagents (Scheme 80). Instead, electricity was solely responsible to form the electrophilic Cl⁺ species to enable improved direct halogenations.



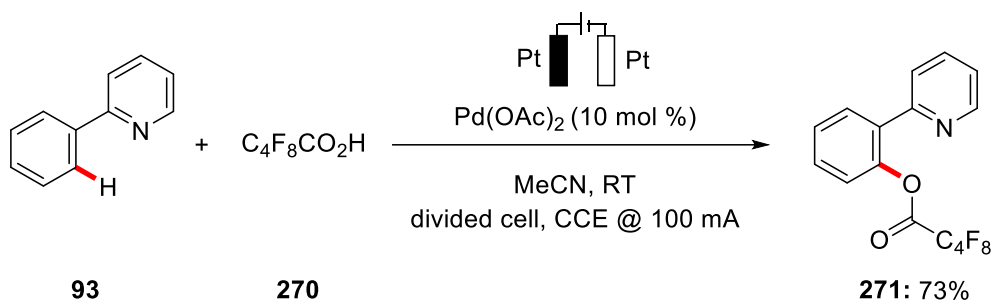
Scheme 80. Electrochemical palladium-catalyzed halogenation of phenylpyridines **93**.
^a PdBr₂ (2.0 mol %) and 2M HBr_(aq) used.

In a related approach, later the same group extended the C–H halogenation approach to C–H iodinations (Scheme 81).^[235] Here, the authors utilized elemental iodine as the iodonium source to enable the C–H iodinations in MeCN as reaction media. Notably, this iodination protocol was also compatible with KI as iodonium source.



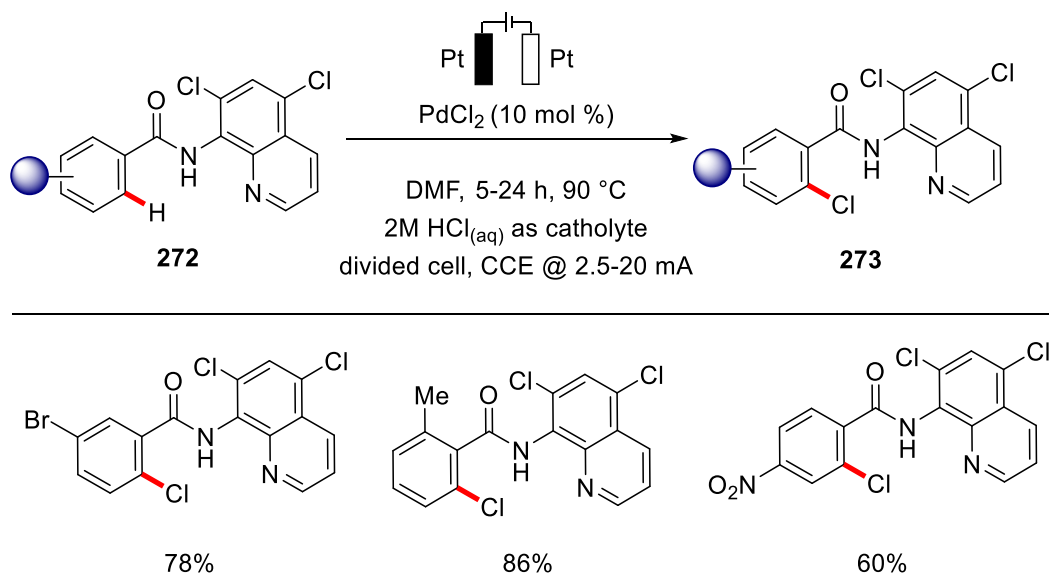
Scheme 81. Electrochemical palladium-catalyzed iodination.

Later, *ortho*-C–H perfluoroalkoxylation of phenyl pyridines **93** with perfluoroalkylated acids **270** was reported under mild reaction conditions (Scheme 82).^[236] This was an early example of electrochemical metal-catalyzed direct C–H oxygenation reactions.^[60, 237]



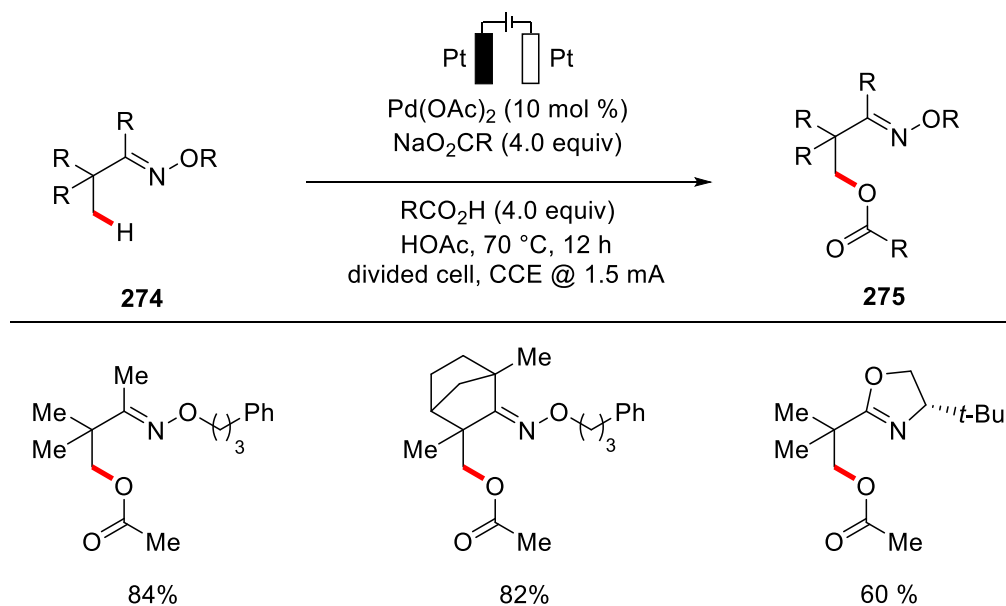
Scheme 82. Palladium-catalyzed electrochemical C–H perfluoroxylation.

Until recently, strongly-coordinating phenylpyridines and anilides were substrates of choice in the early developments of electrochemical transformations. In this context, Kakuichi later succeeded to achieve *ortho*-selective chlorination of electron-poor benzamides **272** by a modified chlorinated bidentate 8-aminoquinoline directing group (Scheme 83).^[238]



Scheme 83. Electrochemical bidentate directing group assisted C–H chlorination.

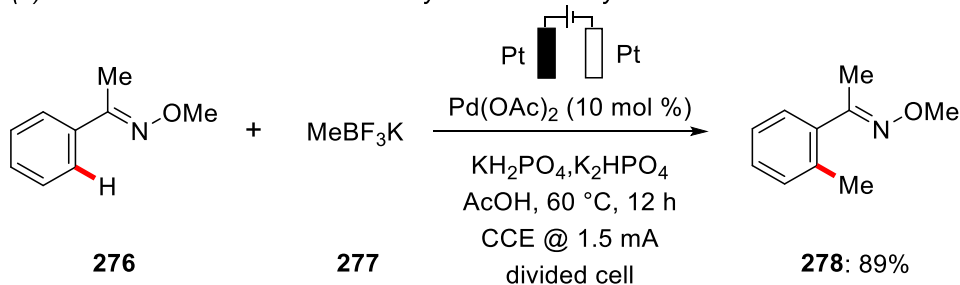
In 2017, a major contribution was achieved by Mei in electrochemical palladium catalyzed C–H activation. Thus, Mei reported palladium-catalyzed C(sp³)–H oxygenation of oxime derivatives **274** (Scheme 84).^[239] It is noteworthy to mention that this protocol offered a broad scope of synthetically useful oxime derivatives **275** under rather mild reaction conditions.



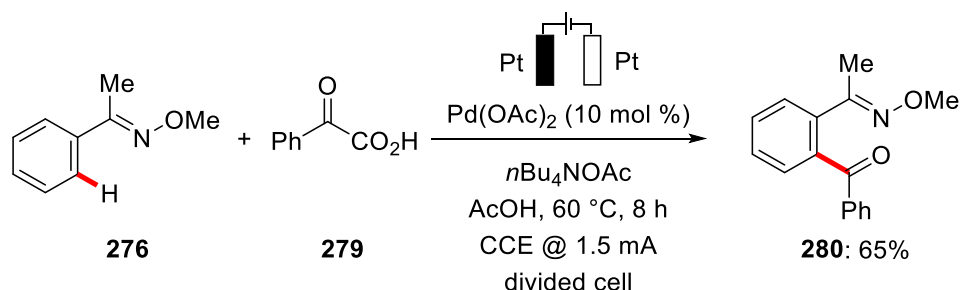
Scheme 84. Palladium-catalyzed C(sp³)-H oxygenation.

In subsequent efforts, the same group reported efficient palladium-catalyzed oxidative *ortho*-C(sp²)-H methylation and benzoylation of oximes **276** with methyltrifluoroborates **277** and benzoyl acetic acids **279** as the coupling partners respectively (Scheme 85a and 85b).^[240] Also, the authors prepared cyclometalated palladacycle which was found to be a competent catalyst for the C-H methylation reactions.

(a) *Electrochemical Palladium-Catalyzed C-H Methylation*

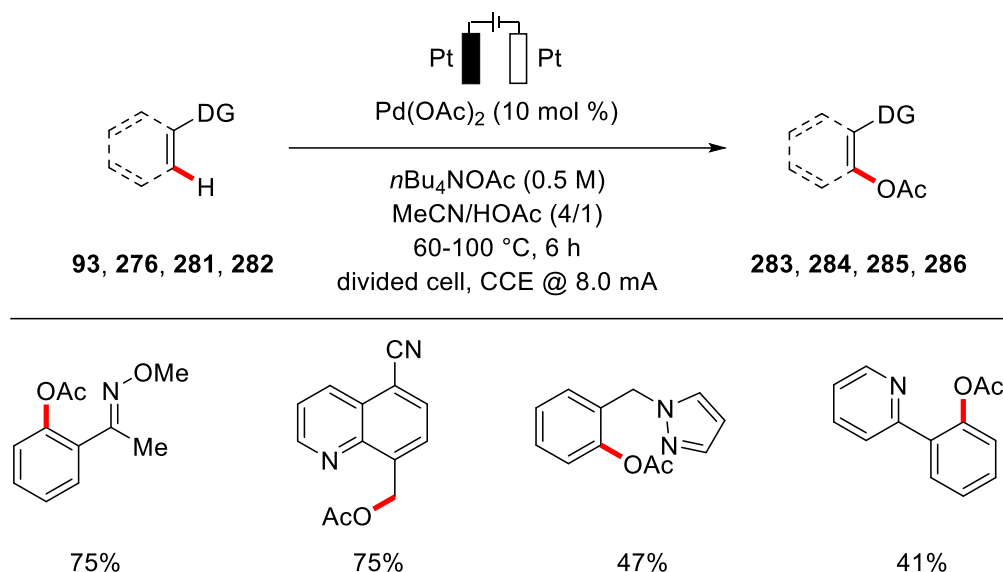


(b) *Palladium-Catalyzed Oxidative Benzoylation*



Scheme 85. Palladium-catalyzed C-H alkylation and benzoylation.

In subsequent study, Sanford reported related electrochemical C(sp²)-H and C(sp³)-H oxygenations (Scheme 86).^[241] A broad range of directing groups was also found amenable in this protocol. In addition, this transformation tolerated an array of sensitive functional groups.



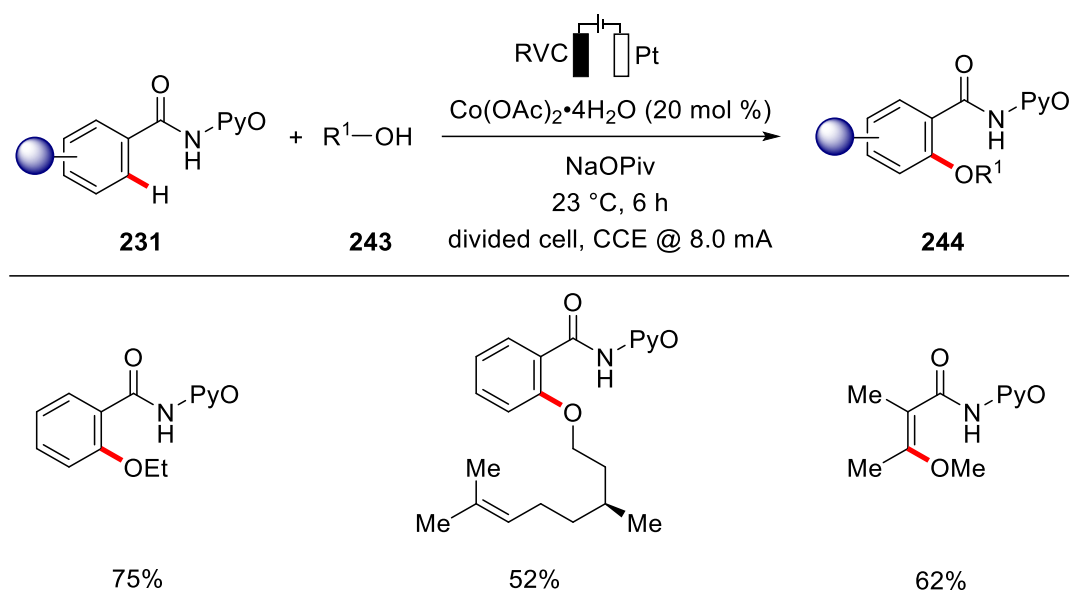
Scheme 86. Electrochemical C(sp²)-H and C(sp³)-H oxygenation.

1.4.2.2. Cobalt-Catalyzed Electrochemical C-H Activation

Over the past decades C-H electrosynthesis has largely relied on precious 4d and 5d transition metals, prominently featuring expensive palladium, rhodium,^[242] iridium^[243] and ruthenium^[244] complexes. In recent years, the prices of precious transition metals have increased significantly which has led to a growing demand in the use of Earth-abundant and cost-efficient 3d metals as viable catalysts for molecular C-H transformations.^[232c]

1.4.2.2.1. C-H Oxygenation

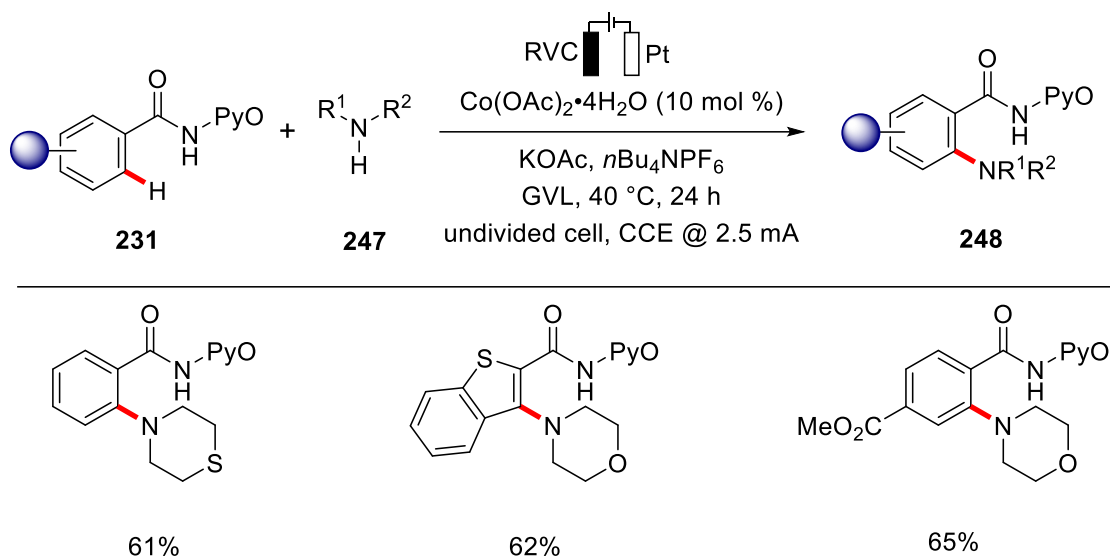
Recently, versatile cobalt catalysts have become a powerful tool for oxidative electrochemical C-H activations with notable contributions by Ackermann.^[32a, 245] In 2017, Ackermann reported the first electrochemical cobalt catalyzed C-H oxygenation.^[246] To the best of my knowledge, this is the first example for electrochemical C-H activation by Earth-abundant 3d transition metals. Here, the authors elegantly employed a combination of Cp*-free Co(OAc)₂·4H₂O as the inexpensive catalyst and NaOPiv as base for the electrochemical C-H oxygenation of benzamides **231** with aliphatic alcohols **243** enabled by a *N,O*-bidentate directing group (Scheme 87). The key characteristic of this protocol was high levels of functional group tolerance at room temperature.



Scheme 87. Electrochemical cobalt-catalyzed C–H oxygenation.

1.4.2.2.2. C–N Bond Formation

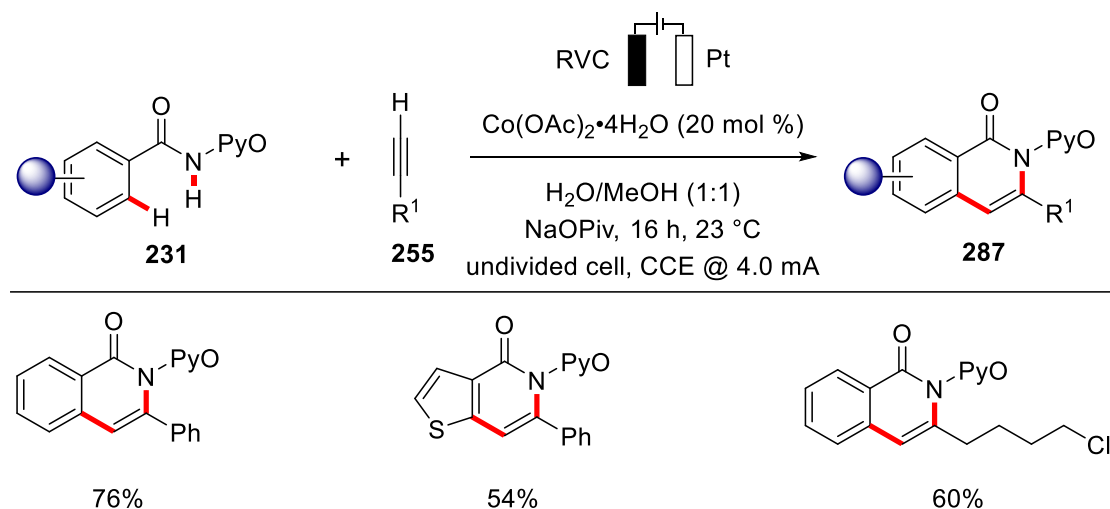
Intrigued by the pioneering C–H oxygenation,^[246] the electrooxidative direct C–H amination of otherwise inert C–H bonds of aromatic benzamides **231** was reported by Ackermann.^[247] The reaction was performed in the renewable solvent γ -valerolactone (GVL) at 40 °C in the absence of expensive and toxic metal oxidants. It should be duly noted that this was the first report for the use of biomass-derived solvent in electrocatalysis.^[6, 248] The amination of benzamides **231** proceeded with diverse set of secondary amines **247** with H_2 as the only stoichiometric byproduct, produced by cathodic reduction (Scheme 88). Thereafter, Lei reported similar reactivity utilizing 8-AQ as directing group for the C–H amination with cyclic secondary amines in a divided cell set up.^[249]



Scheme 88. Cobalt-catalyzed electrooxidative C–H amination.

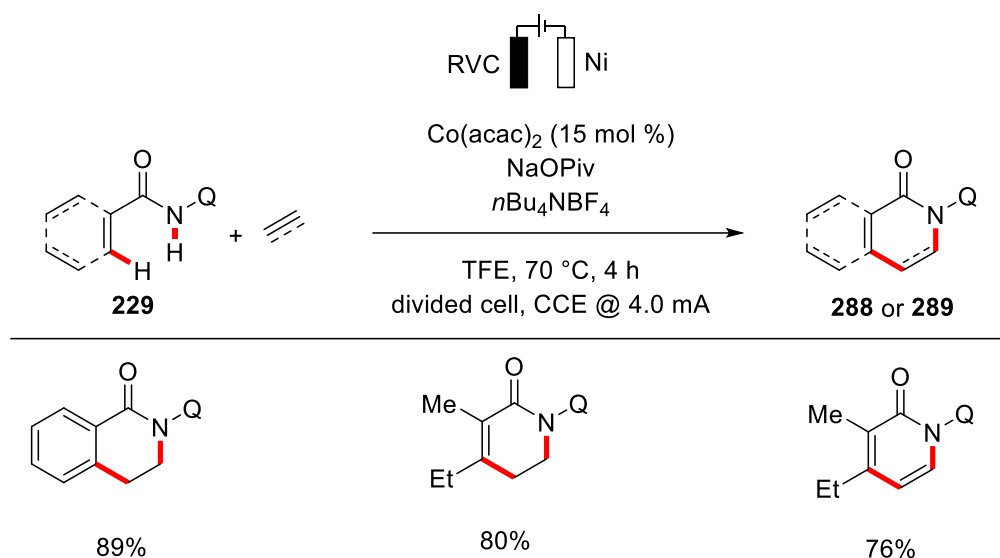
1.4.2.2.3. C–H Activation for Annulations.

In 2018, an unprecedented electrochemical annulation of C–H and N–H bond with alkynes **255** was disclosed by Ackermann (Scheme 89).^[250] Notably, versatile and robust cobalt catalysis enabled the synthesis of isoquinolone motifs **287** by C–H/N–H annulation of benzamides **231** in H₂O as the reaction medium. A broad range of substrates was tolerated in this annulation protocol at room temperature, including benzamides, heterocycles, and alkenes bearing pyridine *N*-oxide as the directing group.



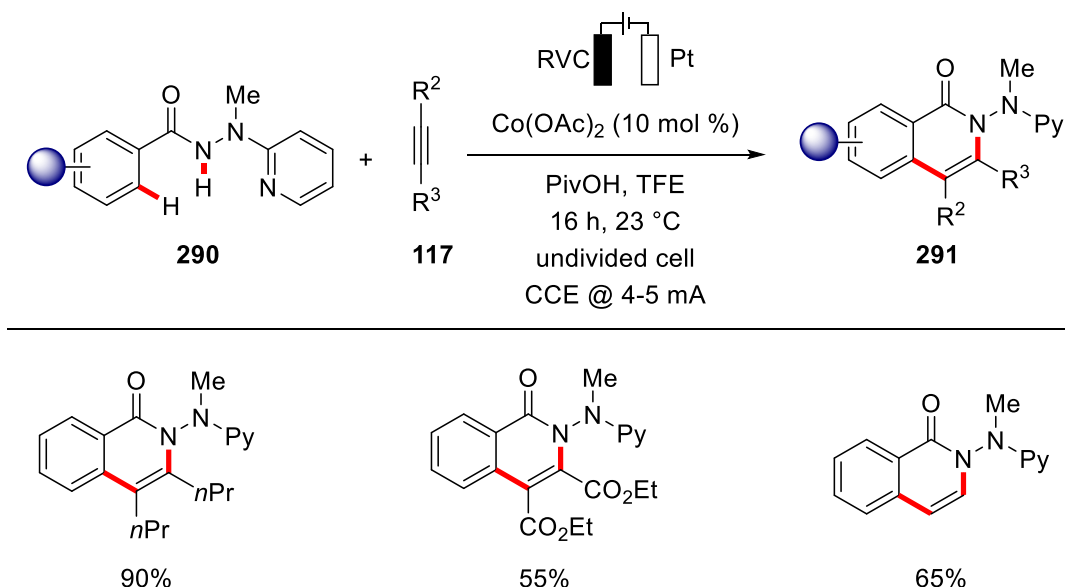
Scheme 89. Electrooxidative C–H/N–H annulation.

In subsequent reports, Lei extended this approach towards the [4+2] C–H/N–H annulation of amides **229** with gaseous ethylene and ethyne (Scheme 90).^[251] Here, 8-aminoquinoline was found as the directing group of choice for efficient annulation reactions.



Scheme 90. Electrooxidative C–H/N–H annulation with ethyne and ethylene.

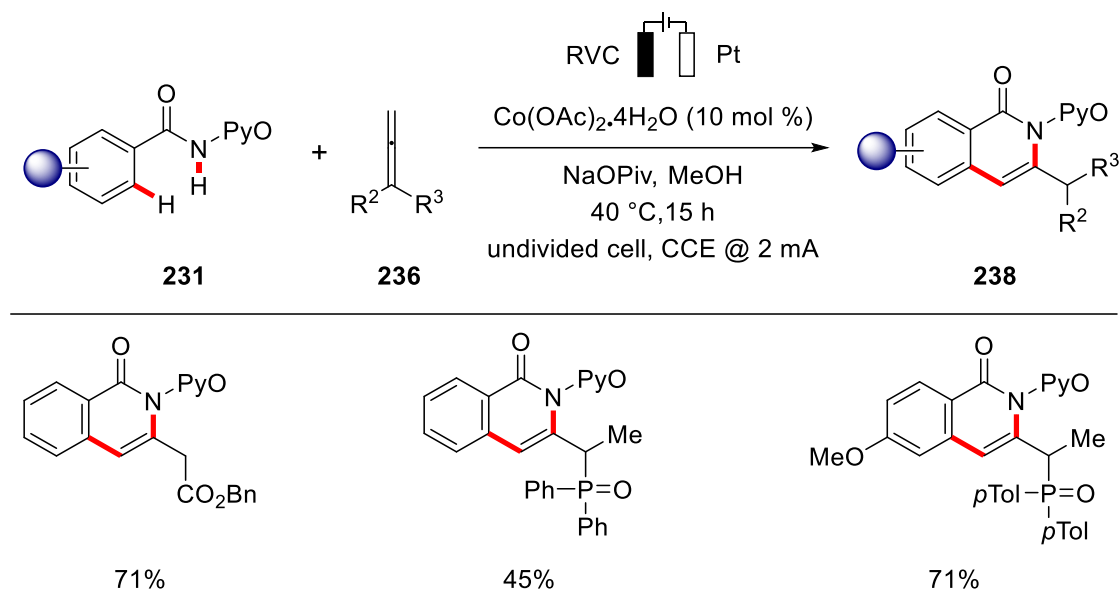
In contrast to the previous reports, which were mainly limited to terminal alkynes, Ackermann showed the versatility of cobalt catalysis towards internal alkynes **117** for electrooxidative C–H/N–H annulations (Scheme 91).^[252] A traceless hydrazide directing group enabled the annulation process at room temperature. Likewise, a wide range of internal alkynes **117** were found as suitable substrates. A key feature of this transformation was represented by the electroreductive hydrazide cleavage, using catalytic amounts of SmI₂ to remove the benzhydrazide in a traceless manner.



Scheme 91. Electrochemical C–H/N–H activation with internal alkynes **117**.

Subsequently, a step-economical annulation was unraveled by Ackermann by the direct use of allenes **236** for electrochemical C–H/N–H annulation process.^[253] Notably, various diversely

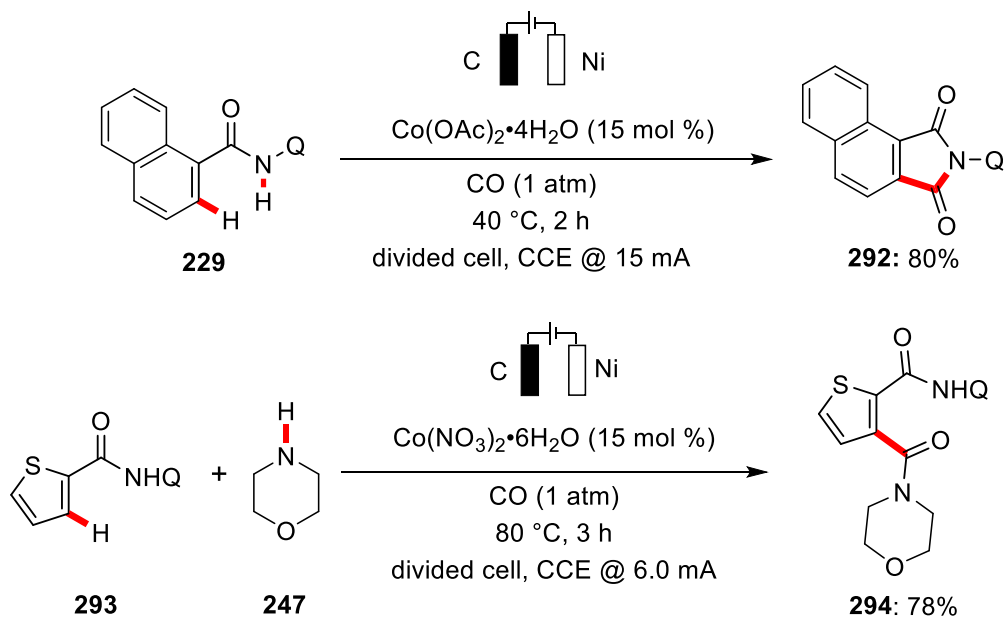
substituted allenes **236** were tolerated and provided the corresponding products **238** with high regioselectivity (Scheme 92).



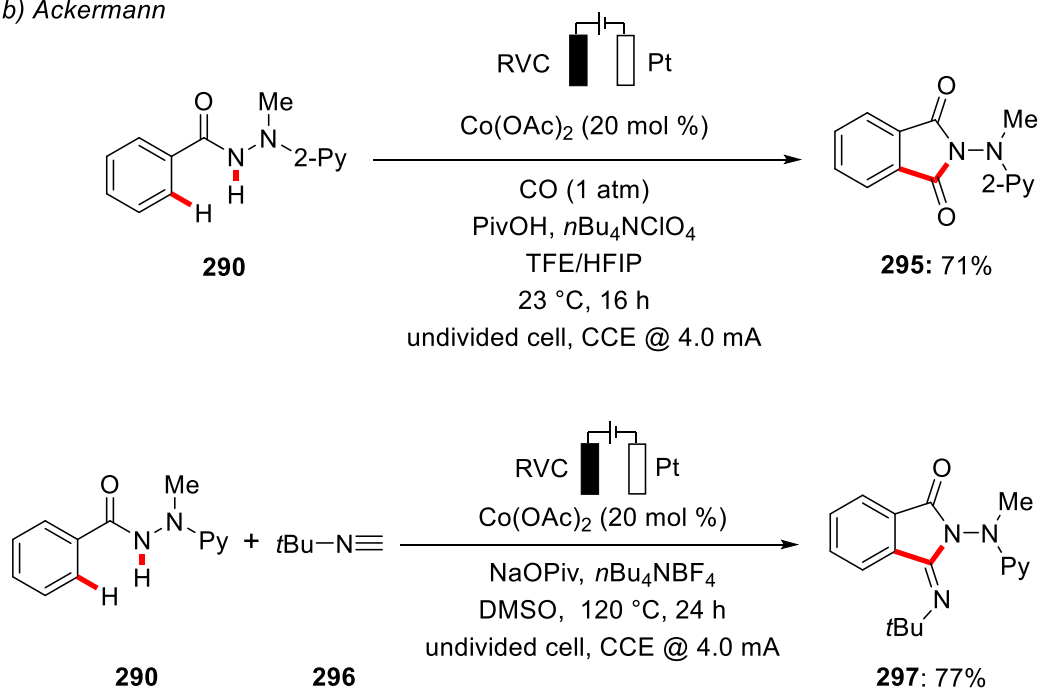
Scheme 92. Cobaltacatalyzed electrochemical C–H activation with allenes.

In addition to annulations with alkynes **117/255** and allenes **236**, Lei and Ackermann independently reported the oxidative C–H/N–H carbonylation with gaseous carbon monoxide. Lei utilized 8-aminoquinoline as the directing group for the C–H/N–H carbonylation in the presence of catalytic amounts of cobalt catalyst.^[254] Likewise, the reaction was further extended to intermolecular variant in the presence of secondary amines (Scheme 93a). In addition to carbon monoxide, Ackermann also showed the versatility of cobalt catalysis with synthetically useful isocyanides **296** for C–H/N–H annulation with benzhydrazides **290** (Scheme 93b).^[255]

a) Lei



b) Ackermann

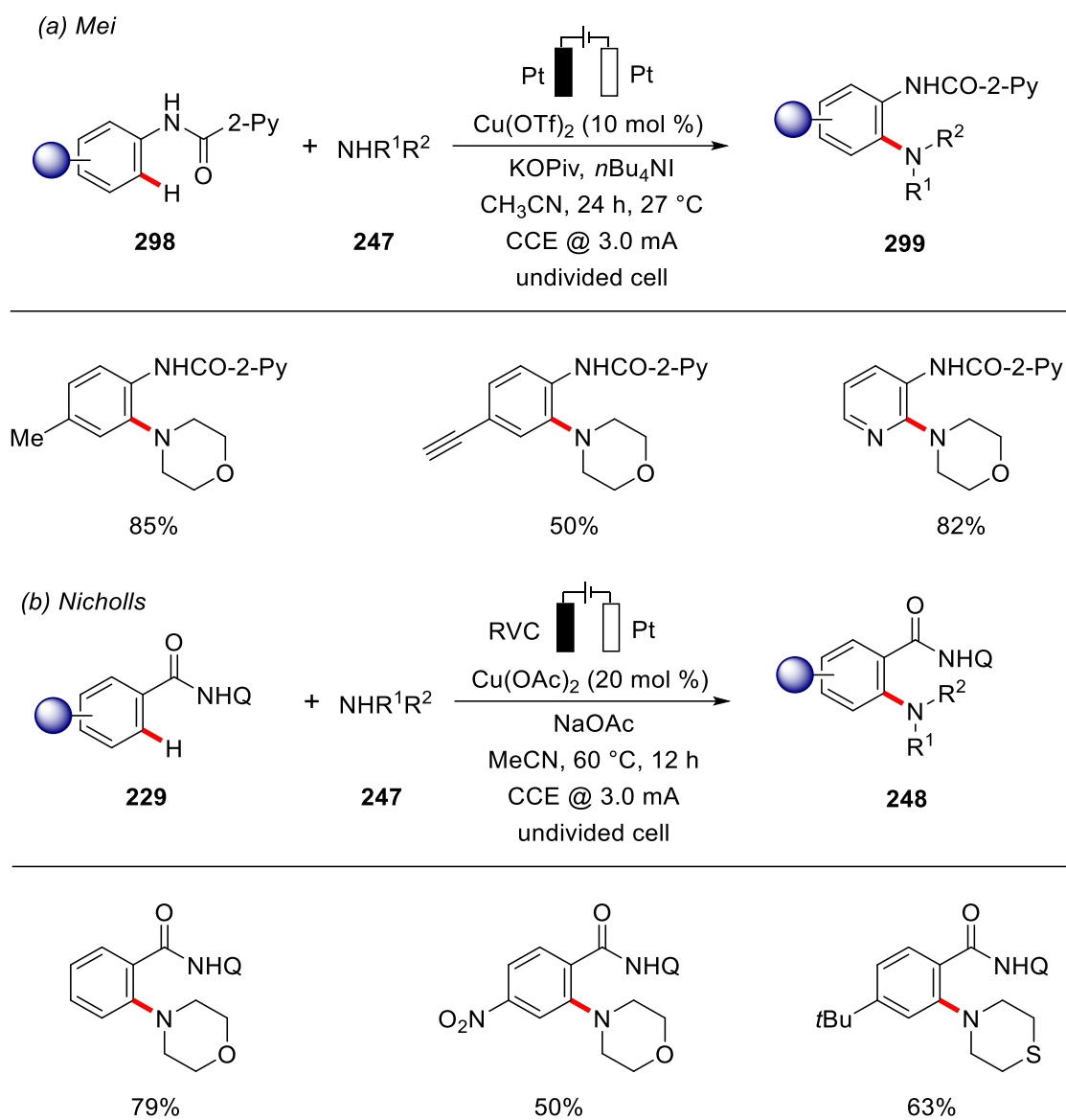


Scheme 93. Cobalt-catalyzed electrochemical C–H/N–H annulation with carbon monoxide and isocyanides.

1.4.2.3. Copper Catalyzed Electrochemical C–H Activation

While notable advances have been reported on Earth-abundant cobalt catalysis for sustainable electrocatalysis,^[31] a recent trend has shifted to other Earth-abundant metalla-electrocatalyzed C–H transformations. Recently, Mei exploited the potential of copper catalysis for electrochemical C–H amination reactions. It is noteworthy to mention that the authors achieved direct C–H aminations of electron-rich anilides **298** at room temperature using electricity as green oxidant (Scheme 95a).^[256] The optimized electrocatalyst proved broadly applicable and showed high functional group tolerance. Shortly thereafter, in a related work, Nicholls and coworkers disclosed similar reactivity by the aid of 8-aminoquinoline directing group.^[257] The authors succeeded in achieving electro-oxidative aminations of amides **229** with amines **247** producing H₂ as the sole byproduct (Scheme 95b).

1. Introduction

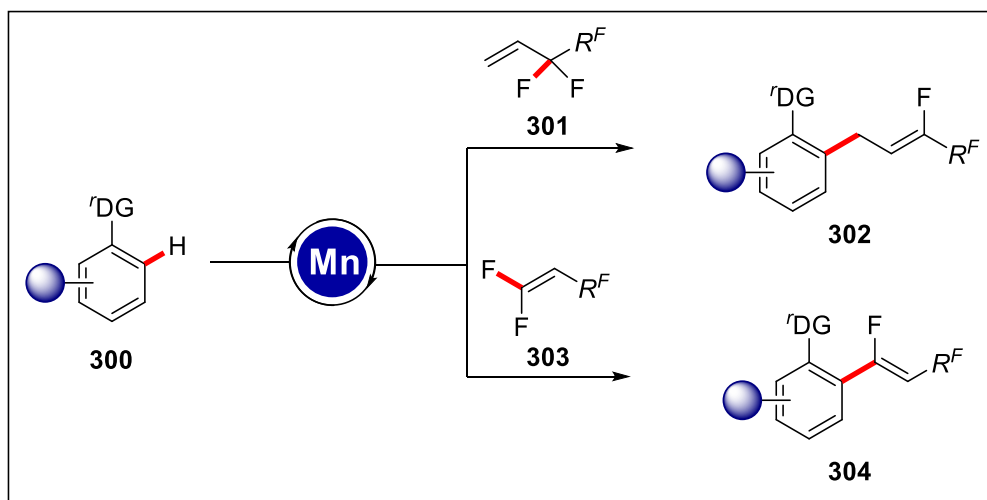


Scheme 94. Copper-catalyzed electrochemical C–H amination.

2. Objectives

Transition metal-catalyzed C–H activation has been continuously evolving as an increasingly powerful approach in the emerging field of synthetic chemistry.^[27, 56] The development of new molecular reactions continues to be highly desirable in the advent of organic synthesis to elevate the productivity at lower cost. Thus, the objective of this thesis was to aim on the development of cost-effective and environmentally-benign metal-catalyzed selective C–H activation reactions with olefins and alkynes with a major emphasis on the identification of resource-economical conditions. In addition, a considerable focus has been placed on the mechanistic understandings of these C–H activations.

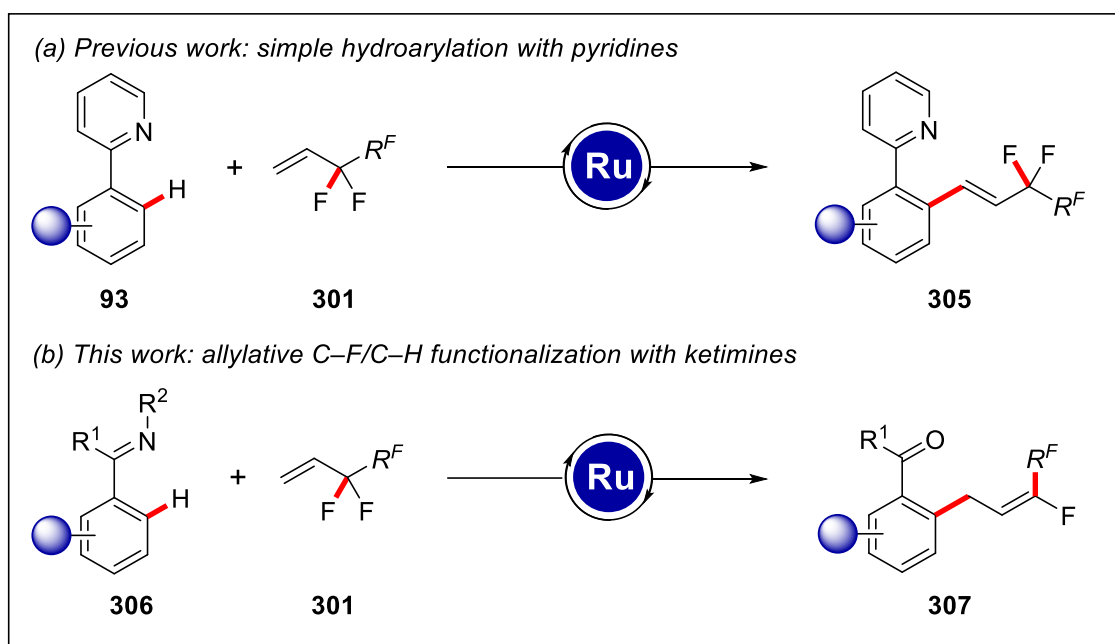
Over the past years, C–F functionalization has emerged as a viable tool for the incorporation of fluorinated scaffolds into organic molecules.^[42a, 42b] Thus we became interested in exploiting the potential of inexpensive and versatile manganese catalysis for unprecedented C–F/C–H functionalization through β -fluoride elimination (Scheme 95). Particularly, a broad substrate scope and mild reaction conditions should be of prime importance for the synthesis of diverse fluorinated scaffolds.



Scheme 95. Manganese(I)-catalyzed C–F/C–H functionalization.

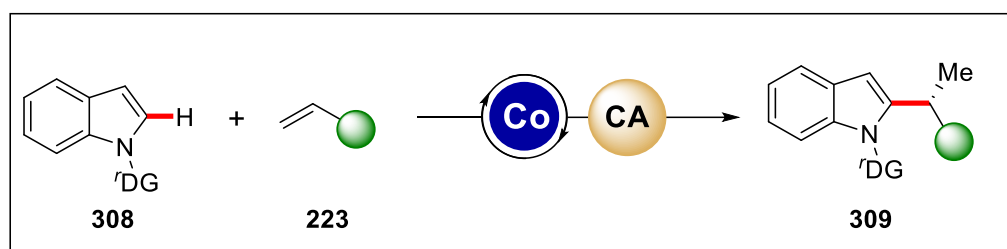
Despite enormous advances in the application of ruthenium catalysts in organometallic C–H activations,^[27t, 39, 138] challenging C–F functionalization by ruthenium catalysis remained elusive. In this context, related studies of hydroarylations were achieved with unactivated alkenes and perfluoroalkylalkenes by Ackermann,^[258] which set the stage for the merger of C–H activation with C–F functionalization. In this regard, our aim was to develop a ligand enabled new strategy for a switch in chemoselectivity towards challenging C–F functionalization, along with mechanistic studies (Scheme 96).

2. Objectives



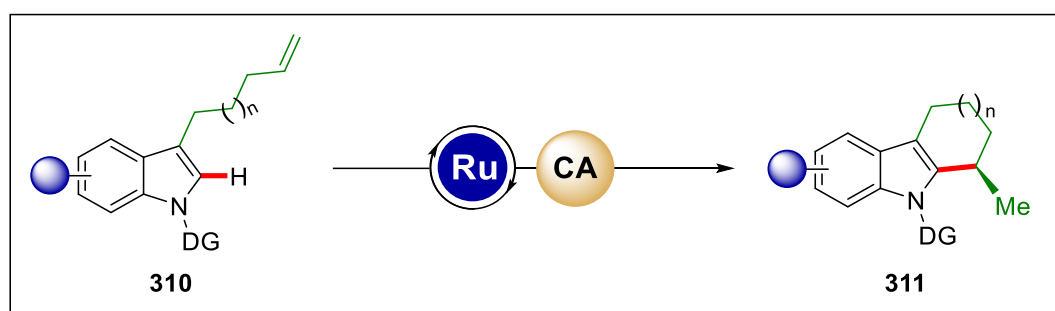
Scheme 96. *E*-selective C–H/C–F functionalization by ruthenium (II) catalysis.

The fascinating research area of enantioselective C–H activation remains primarily dominated by 4d and 5d transition metals.^[58] Recent efforts have been directed more towards non-toxic Earth-abundant transition metals.^[59] Considering the importance of efficient and step-economical assembly of chiral molecules, novel enantioselective transformations utilizing cost-effective transition metals should be developed under sustainable reaction conditions. In this context, numerous studies on cobalt(III)-catalyzed C–H activation have been developed due to their significant versatility.^[31, 32d, 32f, 32g, 32j] Still enantioselective transformations with cobalt(III) catalysts have remained elusive and unexplored at the outset of this work. In this context, a combination of Cp*Co(III) catalyst with a novel chiral acid was investigated for achieving high enantioselectivities in C–H alkylation reactions. Furthermore, detailed mechanistic and computational studies were performed to unravel the mode of action (Scheme 97).



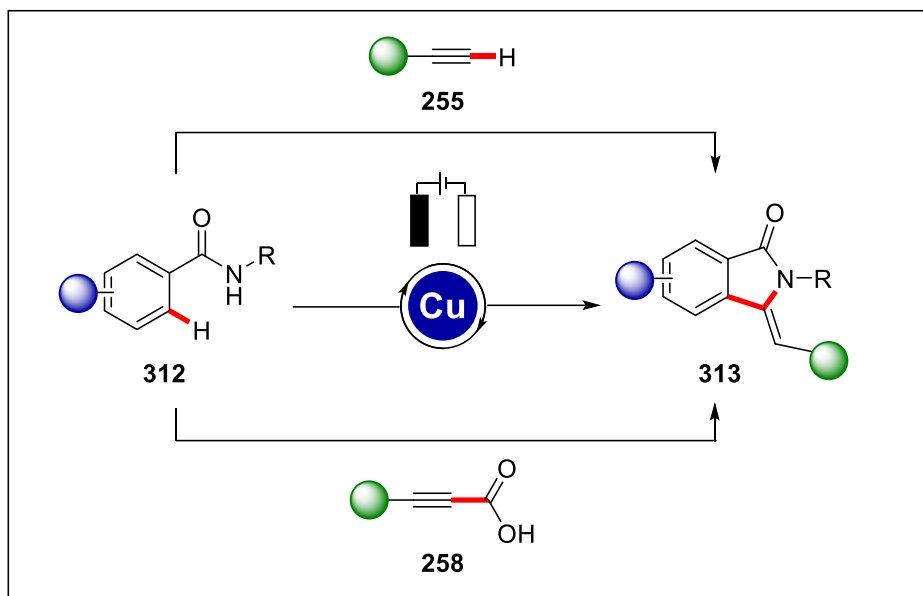
Scheme 97. Enantioselective cobalt(III)-catalyzed C–H activation enabled by chiral carboxylic acid cooperation.

In this regard, we also became interested in the development of new enantioselective transformations utilizing cost-effective ruthenium as the catalyst. While organometallic ruthenium catalyzed C–H activations are well-investigated,^[27t, 39, 138] the enantioselective transformations remain underdeveloped. Thus, we decided to explore the versatility of ruthenium catalysts for the enantioselective C–H alkylation reactions with the combination of a chiral acid, along with detailed mechanistic studies (Scheme 98).



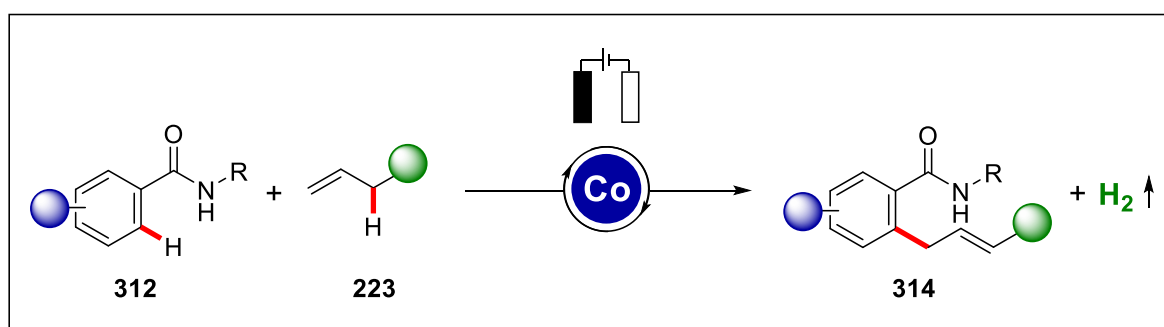
Scheme 98. Enantioselective ruthenium(II)-catalyzed C–H alkylation.

To harness the full potential of C–H activation, metallaelectrocatalysis provides excellent resource economy for sustainable organic synthesis.^[224] Over the past years, the merger of C–H activation and electrosynthesis has emerged as a potent strategy, albeit early contributions were limited to palladium catalysis.^[232] In this context, the use of less toxic and inexpensive copper in oxidative electrochemical transformations offers an attractive strategy towards improved resource economy using electrons as green oxidant. Thus, inexpensive copper catalyst was intended to utilize in electrochemical conditions for oxidative annulation reactions with alkynes **255** and **258** (Scheme 99).



Scheme 99. Cupraelectro-catalyzed alkyne annulation.

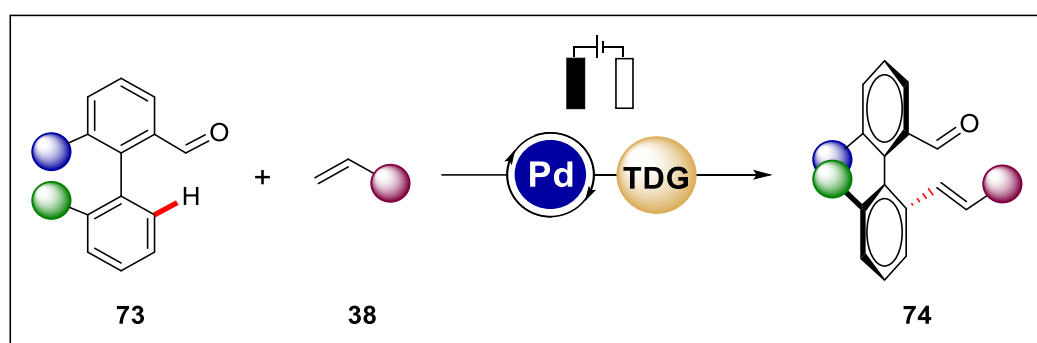
In 2017, Ackermann reported the first cobalt-catalyzed electrochemical C–H activation where electro-oxidation of the cobalt catalyst is the key step.^[246] Since then, electrochemical oxidative transformations with Earth-abundant cobalt have gained enormous attention, employing electrons as traceless oxidant.^[32a, 245] In this context, 4d and 5d transition metal-catalyzed electrochemical transformations remained restricted to the use of activated alkenes as coupling partners. Thus, within this thesis, a new protocol for electrochemical C–H allylation with unactivated alkenes was intended to address utilizing inexpensive and Earth-abundant cobalt catalysts. Detailed mechanistic studies were performed to delineate the unique reactivity with unbiased olefins (Scheme 100).



Scheme 100. Cobalt-catalyzed electrochemical C–H allylation.

To unleash the full potential of electrocatalysis towards perfect resource economy, enantioselective electrosynthesis is highly desirable as a new sustainable tool for the construction of chiral molecules.^[232] Despite significant advances in electrosynthesis, enantioselective metallaelectro-catalyzed C–H activation remained unprecedented,

showcasing the challenges in asymmetric electrocatalysis. Consequently, our focus was to develop the first enantioselective metallaelectro-catalyzed C–H activation. Thus, our approach was directed towards electrochemical atroposelective synthesis of axially-chiral biaryls. In this regard, a sustainable protocol for the enantioselective electrochemical C–H activation was addressed by the cooperation of transient directing group utilizing palladium as catalyst under mild reaction conditions. Furthermore, a major focus of our strategy was the late-stage diversification of axially chiral compounds to access target structures of value to asymmetric catalysis (Scheme 101).

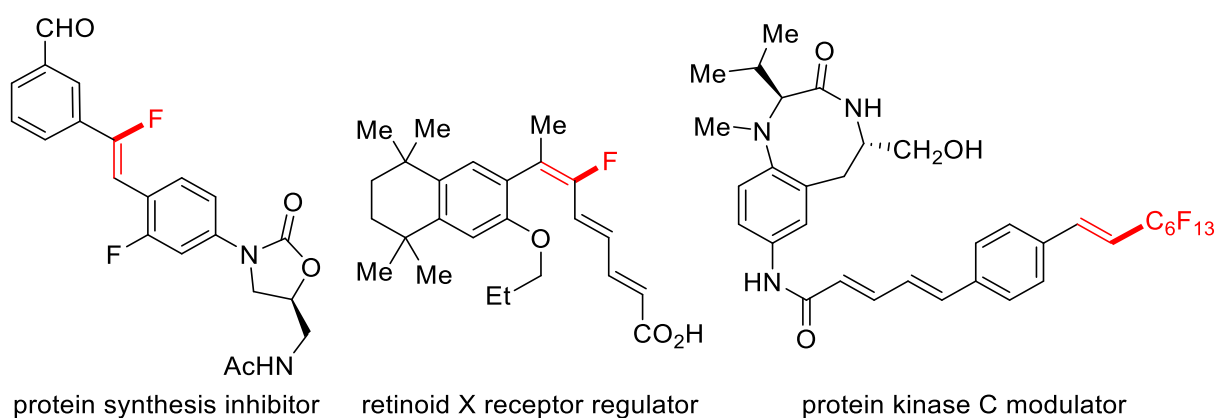


Scheme 101. Enantioselective metallaelectro-catalyzed C–H activation.

3. Results and Discussion

3.1. Manganese(I)-Catalyzed (Per)Fluoro-Allylative and Alkenylative C–F/C–H Functionalizations

In recent years, manganese catalysts have gained considerable attention owing to their inexpensive nature and low toxicities^[32g, 259] with significant numbers of studies for various C–H additions onto C–C or C–Het multiple bonds and C–H allylations reactions *via* β -oxygen or -carbon elimination.^[260] Recently, transition metal mediated β -fluorine elimination has become a viable tool for the transformation of C–F bonds.^[46] Consequently, the merger of C–F activation with challenging C–H cleavages presents a sustainable and atom-economical approach to enable the selective synthesis of fluorinated molecules.^[52–55] Thus, we were interested in the development of catalytic C–F/C–H activations by the aid of inexpensive and less toxic manganese catalysis.



Scheme 102. Examples of bioactive fluoroalkenes

3.1.1. Optimization Studies

After initial optimization studies by *Dr. D. Zell* for the allylative C–H/C–F functionalizations of indole **315**, almost quantitative yield was observed when indole **315a** was reacted with perfluoroalkylalkene **301a** in the presence of catalytic amounts of $\text{MnBr}(\text{CO})_5$ and 2.0 equiv of K_2CO_3 in dioxane (Table 1, entry 1). It is noteworthy to mention that in the absence of the base, the yield of the desired product **316aa** was significantly reduced, being suggestive of the formation of the corresponding fluoride salt which is possibly the driving force of the reaction (entry 2). Moreover, in a recent study the group of Ichikawa showed the potential of Lewis-acids to enable the activation of inert sp^3 C–F bond of the CF_3 group through a Friedel–Crafts-type mechanism.^[261] Thus, a series of Lewis acids, including AlCl_3 , Et_2AlCl , $\text{BF}_3 \cdot \text{OEt}_2$, TiCl_4 , ZrCl_4 , and FeCl_3 were tested under our optimized reaction conditions (entry 3–8), which,

however failed to provide the desired C–F/C–H functionalization product **316aa**; highlighting the necessity of $\text{MnBr}(\text{CO})_5$ as the effective catalyst for this challenging transformation.

Table 1. Optimization for manganese(I)-catalyzed allylative C–F/C–H functionalization.^[a]

Entry	Variation of the standard conditions	316aa [%] ^[b]
1	none	97
2	in the absence of K_2CO_3	7
3	AlCl_3 in place of [Mn]	--- ^[c]
4	Et_2AlCl in place of [Mn]	--- ^[c]
5	$\text{BF}_3 \cdot \text{OEt}_2$ in place of [Mn]	--- ^[c]
6	TiCl_4 in place of [Mn]	--- ^[c]
7	ZrCl_4 in place of [Mn]	--- ^[c,d]
8	FeCl_3 in place of [Mn]	--- ^[c,d]

[a] Reaction conditions: **315a** (0.50 mmol), **301a** (1.00 mmol), $[\text{MnBr}(\text{CO})_5]$ (10 mol %), K_2CO_3 (0.50 mmol), solvent (0.50 mL), 80 °C, 20 h. [b] isolated yield. [c] Lewis acid (1.0 equiv). [d] Performed by *Mr. V. Müller*.

Next, we were interested in the incorporation of the α -fluoroalkenyl motifs in to arenes using *gem*-difluoroalkenes **11** as the coupling partner, which is a very appealing class of synthetic intermediates with highly polarized C–C double bonds. A comprehensive optimization study with indole **315a** reflected the necessity of acetate base for increasing the reactivity to large extent, revealing 20 mol % NaOAc as additive to be optimal (Table 2, entry 1-3). Similarly, after probing various reaction temperatures, optimal reactivity was observed at 100 °C, while higher reaction temperatures were detrimental to the yield of the desired product **317aa** (entry 4-7). Notably, higher concentration of *gem*-difluoroalkenes improved the reactivity, albeit the overall difference in reactivity was less striking (entry 8-9).

Table 2. Optimization for manganese(I)-catalyzed alkenylative C–F/C–H functionalization.^[a]

Entry	NaOAc [mol %]	Temperature [°C]	Yield [%] ^[b]
1	30	100	77
2	10	100	74
3	20	100	81
4	20	90	40
5	20	95	68
6	20	105	70
7	20	120	57
8	20	100	60 ^[c]
9	20	100	85 ^[d]

[a] Reaction conditions: **315a** (0.50 mmol), **11a** (1.00 mmol), [MnBr(CO)₅] (10 mol %), K₂CO₃ (0.50 mmol), NaOAc (10–30 mol %), 1,4-dioxane (0.50 mL), 20 h. [b] isolated yield. [c] **11a** (0.60 mmol). [d] **11a** (1.50 mmol).

3.1.2. Substrate Scope and Limitations of C–H/C–F Functionalizations

With the optimized reaction condition in hand, we next investigated the versatility and robustness of allylative C–H/C–F functionalizations (Table 3). Initially, a gram-scale reaction was carried out and the desired product **316aa** was obtained without any significant loss of efficacy (entry 1). Next, various C5-substituted 2-pyridylindoles were tested under the optimized reaction condition (entries 2–4). Both electron-rich and electron-deficient indoles provided the desired products **316** in excellent yields and with good diastereoselectivities, albeit acetate base facilitated the reactivity for the substrate **315d** (entry 4). Importantly, sterically-hindered C3 substituted indoles also afforded the corresponding desired products in good to excellent yields (entries 5–7). To our delight, challenging 7-azaindole **315g**, which is a key structural motif present in various anticancer drug molecules, was very efficiently converted to provide the desired allylative C–H/C–F product **316ga** in good yield and with good diastereoselectivity, although addition of acetate base and higher concentration of **301a**

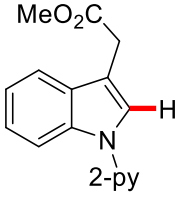
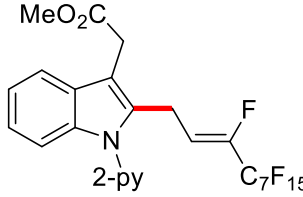
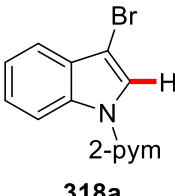
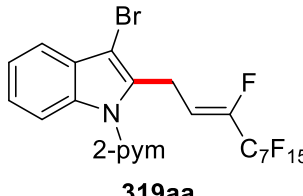
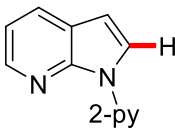
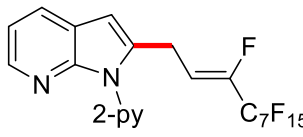
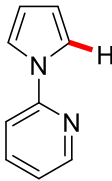
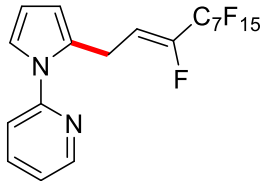
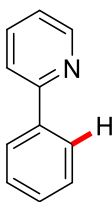
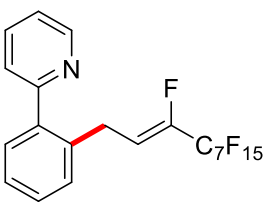
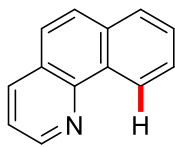
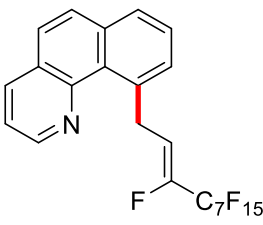
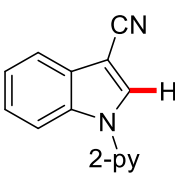
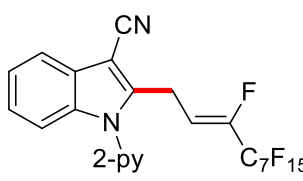
were needed (entry 8). Furthermore, 1-(pyridin-2-yl)-1*H*-pyrrole (**320a**), 2-phenylpyridines (**93a**), benzo[*h*]quinoline (**323a**) also delivered the desired products in good yields under slightly modified reaction conditions (entries 9-11). However, cyano and nitro-substituted indoles **315h** and **315i** remained untouched under the optimized condition (entries 12-13). In addition, 1-(pyridin-2-yl)-1*H*-benzo[*d*]imidazole (**324a**) and 9-(pyridin-2-yl)-9*H*-carbazole (**326a**) did not react under otherwise identical reaction conditions (entries 14-15).

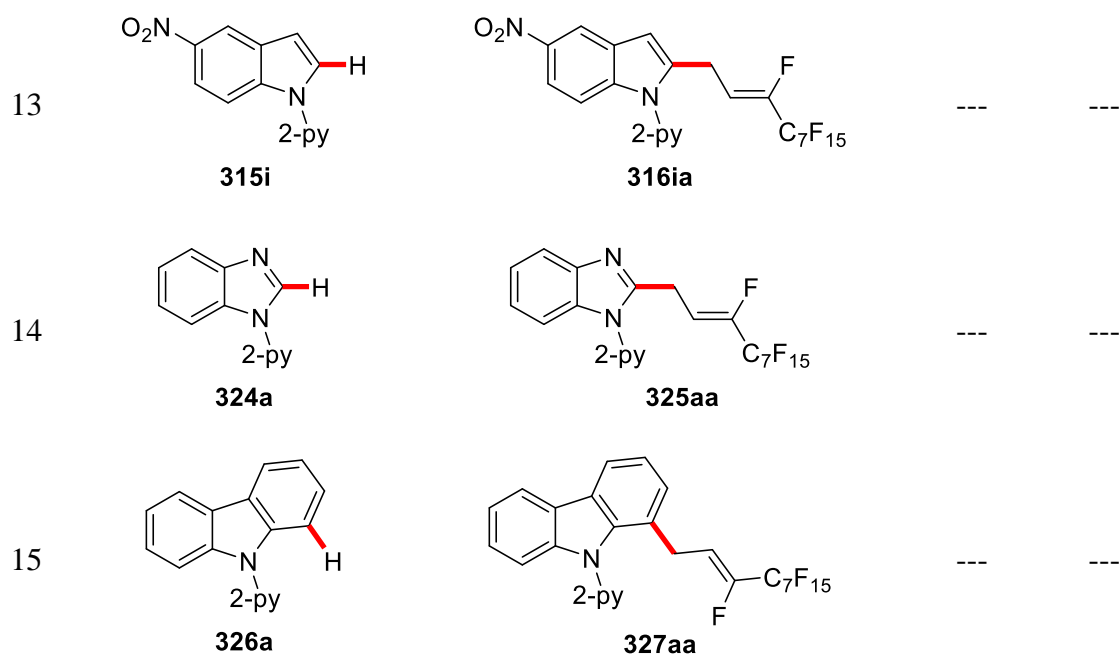
Table 3. Scope of the manganese(I)-catalyzed allylative C–H/C–F functionalization.^[a]

Reaction scheme showing the conversion of indole **315** (with DG) and perfluoroalkyl acrylate **301a** to the allylated product **316** using $[\text{MnBr}(\text{CO})_5]$ (7.5 mol %), K_2CO_3 , 1,4-dioxane, 100 °C, 20 h.

Entry	Indole	Product	<i>E/Z</i>	Yield ^[b]
1			10:90 10:90	97% 91% ^[c]
2			10:90	85%
3			10:90	93%
4			12:88	90% ^[d]
5			12:88	90%

3. Results and Discussion

6	 <p>315f</p>	 <p>316fa</p>	10:90	62%
7	 <p>318a</p>	 <p>319aa</p>	12:88	89% ^[d,e]
8	 <p>315g</p>	 <p>316ga</p>	20:80	82% ^[d,e]
9	 <p>320a</p>	 <p>321aa</p>	13:87	62%
10	 <p>93a</p>	 <p>322aa</p>	14:86	58% ^[d,f]
11	 <p>323a</p>	 <p>324aa</p>	4:96	54% ^[d-f]
12	 <p>315h</p>	 <p>316ha</p>	---	---



[a] Reaction conditions: **315** (0.50 mmol), **301a** (0.60 mmol), $[\text{MnBr}(\text{CO})_5]$ (7.5 mol %), K_2CO_3 (0.50 mmol), 1,4-dioxane (0.5 mL), 20 h. [b] Yield of isolated product. [c] Reaction carried on 3.0 mmol scale. [d] NaOAc (30 mol %) as additive. [e] **301a** (1.0 mmol). [f] 120 °C.

Furthermore, different perfluoroalkyl chain lengths were investigated under the optimized reaction conditions (Table 4). 1*H*,1*H*,2*H*-Perfluorohexene (**301b**) and 1*H*,1*H*,2*H*-perfluorododecene (**301c**) reacted efficiently with indole **315a** and 2-phenylpyridine **93b** to furnish the corresponding products **316ab-316ac** and **322bc** in good yields respectively (entries 1-3). In the latter case, an elevated reaction temperature and a higher concentration of **301c** were necessary (entry 3).

3. Results and Discussion

Table 4. Scope of the manganese(I)-catalyzed C–H/C–F functionalization with perfluoroalkylalkene.^[a]

Entry	Perfluoroalkylalkene	Product	<i>E/Z</i>	Yield ^[b]
1			10:90	76%
2			11:89	84%
3			8:92	57% ^[c,d]

[a] Reaction conditions: **315/93** (0.50 mmol), **301** (0.60 mmol), [MnBr(CO)₅] (7.5 mol %), K₂CO₃ (0.50 mmol), 1,4-dioxane (0.50 mL), 20 h. [b] Yield of isolated product. [c] NaOAc (30 mol %) as additive. [d] **301c** (2.0 equiv) [e] 120 °C.

Next, we turned our attention towards direct functionalization of peptides which holds significant potential in biomolecular chemistry for chemoselective ligation of peptide (Table 5). To our delight, protected amino acids **328a-328b** underwent C–F/C–H functionalization without racemization of the stereogenic centers, reflecting the mildness and versatility of the developed methodology (entries 1-2). In addition, more structurally complex dipeptide **328c** also delivered the desired product **329ca** with high levels of site-selectivity, albeit higher catalyst loading was needed to increase the turnover number (entry 3).

Table 5. C–H/C–F functionalization with amino acids.^[a]

Reaction scheme showing the C–H/C–F functionalization of indole **328** with perfluoroalkene **301a** to form product **329**. Conditions: $[\text{MnBr}(\text{CO})_5]$ (10 mol %), K_2CO_3 , 1,4-dioxane, 100 °C, 20 h.

Entry	Indole	Product	<i>E/Z</i>	Yield ^[b]
1	<p>328a</p>	<p>329aa</p>	2:98	83% ^[c,d]
2	<p>328b</p>	<p>329ba</p>	10:90	85% ^[c,d]
3	<p>328c</p>	<p>329ca</p>	10:90	64% ^[c,e]

[a] Reaction conditions: **328a** (0.50 mmol), **301a** (0.60 mmol), $[\text{MnBr}(\text{CO})_5]$ (10 mol %), K_2CO_3 (0.50 mmol), 1,4-dioxane (0.50 mL), 20 h. [b] Yield of isolated product. [c] NaOAc (30 mol %) as additive. [d] **301a** (2.0 equiv) [e] **301a** (3.0 equiv), $[\text{Mn}]$ (20 mol %).

Moreover, on a pleasing note, challenging perfluoroalkenes **303** were found as suitable substrates for C–H perfluoroalkenylations (Table 6). Indole **315a** and sterically-demanding C3-substituted indole **315e** provided the desired perfluoroalkenylation products in good yields and selectively delivered the *E*-isomers (entry 1-2). Even more challenging protected amino acids **328a-328b** were also identified as amenable substrates for the perfluoroalkenylation, showcasing the versatility of our method (entries 3-4). However, higher catalyst loading was necessary for the pyrazole derivative **332a** to afford the desired product **333ab** in synthetically

3. Results and Discussion

useful yield (entry 5). It is noteworthy to mention that all the perfluoroalkenylation products were selectively obtained as the *E*-isomer.

Table 6. Alkenylative C–F/C–H functionalizations with perfluoroalkenes.^[a]

$\text{315/328/332} + \text{303} \xrightarrow[\text{K}_2\text{CO}_3, \text{1,4-dioxane, 100 }^\circ\text{C, 20 h}]{[\text{MnBr}(\text{CO})_5] \text{ (10 mol \%)}} \text{330/331/333}$

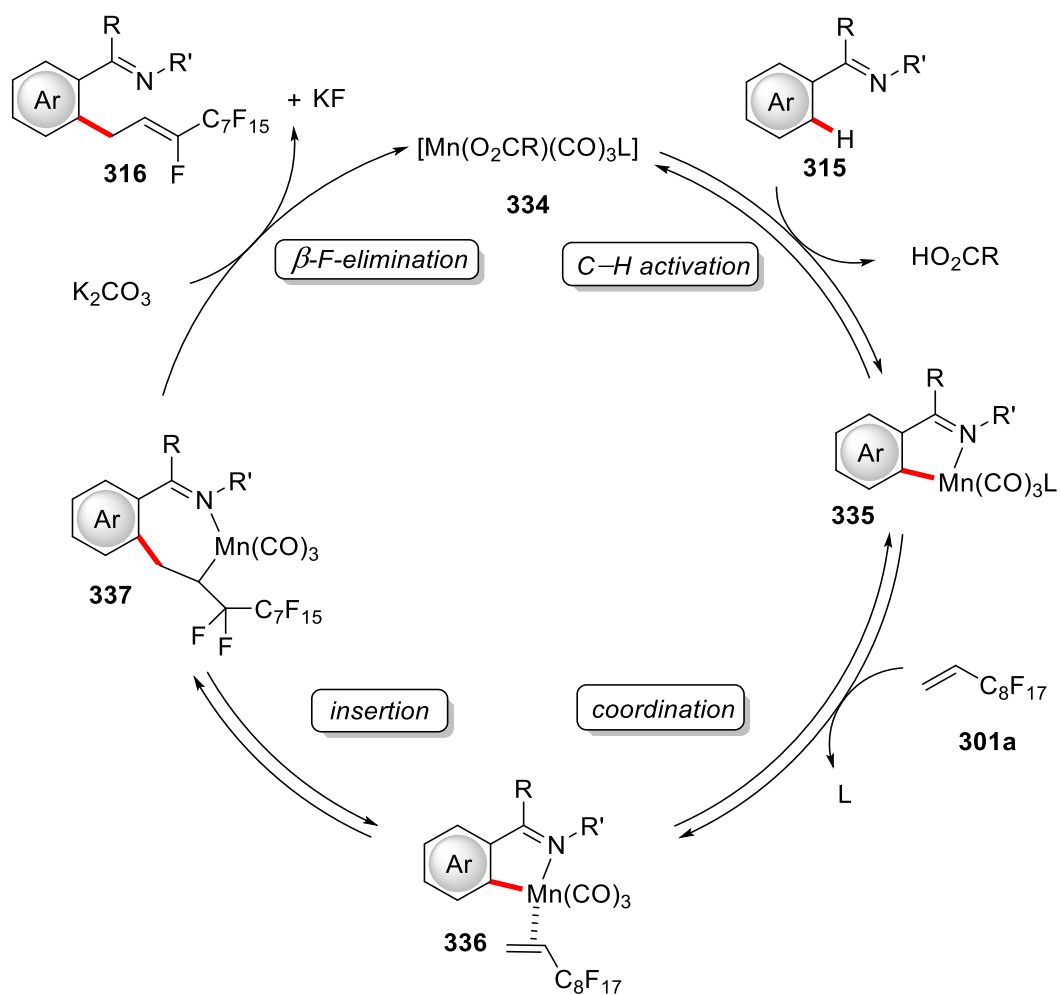
Entry	Indole	Perfluoroalkenes	Product	Yield ^[b]
1				85%
2				86% ^[c]
3				57% ^[c,d]
4				48% ^[c]
5				68% ^[c]

[a] Reaction conditions: **315/328/332** (0.50 mmol), **303** (0.60 mmol), [MnBr(CO)₅] (10 mol %), K₂CO₃ (0.50 mmol), 1,4-dioxane (0.50 mL), 20 h. [b] Yield of isolated product. [c] NaOAc (30 mol %) as additive. [d] [Mn] (15 mol %).

3.1.3. Proposed Catalytic Cycle

Detailed mechanistic studies by *Dr. D. Zell* revealed a significant amount of H/D exchange at C2-position of the reisolated starting material **315a**, which is suggestive of a reversible C–H bond activation step. In addition KIE experiments by *Dr. D. Zell* and DFT studies by *M. Bursch* and *Prof. S. Grimme* supported a facile and reversible BIES-type C–H metalation event.

Thus, the proposed catalytic cycle initiates *via* a carbonate-assisted facile BIES C–H activation step to form the manganacycle **335** (Scheme 103). Then, fast coordination of perfluoroalkylalkene **301a** with the manganacycle **335** and subsequent migratory insertion into the manganese-carbon bond forms intermediate **337**. Next, rate-determining β -F elimination by the carbonate base preferentially forms the *Z*-configured product **316** as supported from DFT-calculations by *M. Bursch* and regenerates the initially formed bicarbonate complex **334** and completes the cycle. Formation of the potassium fluoride is possibly the driving force for the reaction, as in the absence of carbonate base the reactivity is significantly reduced.



Scheme 103. Proposed catalytic cycle for the allylative C-F/C-H functionalization.

3.2. Ruthenium(II)-Catalyzed *E*-Selective Allylative C–F/C–H Functionalization

During last two decades ruthenium(II) complexes have been extensively studied in catalytic C–H bond activation due to their cost-effectiveness as well as their robust and versatile reactivity.^[27t, 39, 138] Furthermore, metal-catalyzed hydroarylations reactions^[262] are particularly attractive because of their perfect atom-economy with significant progress realized by versatile ruthenium catalysts.^[7] In this context, early contributions were primarily realized with relatively unstable and expensive low-valent ruthenium catalysts such as [RuH₂(CO)(PPh₃)₃], [RuH₂(PPh₃)₄], [Ru(CO)₂(PPh₃)₃] or [RuH₂(H₂)₂(PCy₃)₂]. However, recently bench-stable [Ru(O₂CR)₂(*p*-cymene)] complex has been identified as powerful catalyst for various direct C–H bond arylations, hydroarylations and oxidative annulation reactions.^[263] Thus far simple hydroarylations were reported with unactivated alkenes and perfluoroalkylalkenes by ruthenium(II)biscarboxylate catalysts.^[258] Despite significant advancement of atom-economical hydroarylations, ruthenium(II)-catalyzed C–F bond activations remains largely underexplored.

On this note, developments of step-economical protocols for the site-selective installation of fluorine-containing moieties into organic molecules are in great demand. Thereby, we were interested to achieve challenging ruthenium catalyzed C–F/C–H functionalization-based C–H allylations reactions *via* β -fluorine elimination.

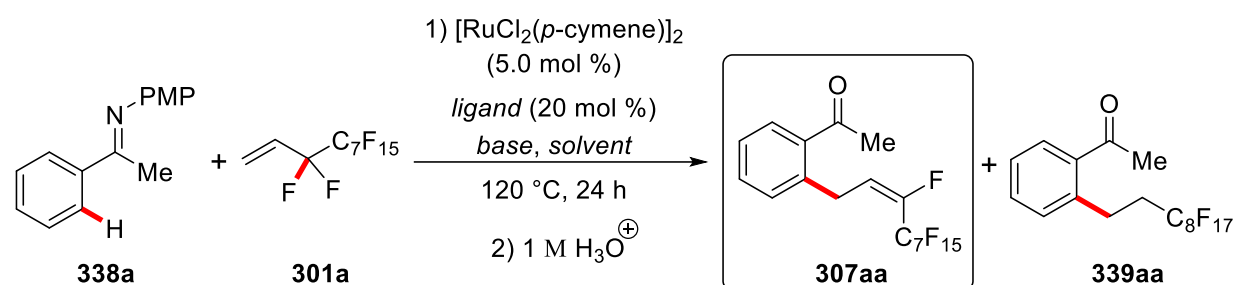
3.2.1. Optimization Studies

The optimization study was commenced by probing various reaction conditions for the envisioned C–F/C–H functionalization with synthetically useful ketimine **338** (Table 7). Initial study under ligand-free conditions did not deliver the desired product **307aa** (Table 7, entry 1). Subsequently, we tested a set of representative ligands and solvents. Cyclohexane turned out to be the optimal solvent for the C–F/C–H functionalization among other typical organic solvents (entries 2-9). It is noteworthy to mention that the presence of strong base delivered the hydroarylation product selectively under ligand-free conditions which was previously achieved by the Ackermann group using a pyridine directing group (entry 10).^[258] Among a variety of bases, K₃PO₄ provided slightly improved yields of the desired ketone **307aa** upon one-pot hydrolysis (entries 11-16). Subsequently, a variety of electron-rich and electron-deficient phosphines were tested in cyclohexane. The best catalytic efficiency was realized in the presence of electron-deficient P(4-C₆H₄F)₃ as ligand (entries 17-23), particularly employing the trimethoxyphenylketimine **340a** as the substrate (entries 26-27). Moreover, higher or lower

3. Results and Discussion

reaction temperatures failed to improve the yields of the desired product **307aa** (entries 24-25). Finally, control experiment in the absence of the catalyst showed the necessity of the ruthenium catalyst for the envisioned C–F/C–H functionalization (entry 29). The *E/Z*-diastereoselectivities were slightly influenced by the choice of the ligand, generally favoring the *E*-diastereomer, while only very minor amounts of the corresponding hydroarylation products **339aa** of less than 2% were observed under the optimized reaction condition.

Table 7. Optimization for the ruthenium(II)-catalyzed allylative C–F/C–H functionalization.^[a]



Entry	Ligand	Base	Solvent	<i>E/Z</i>	Yield	307aa:339aa
1	---	K ₂ CO ₃	CyH	---	---	---
2	PPh ₃	K ₂ CO ₃	NMP	---	---	---
3	PPh ₃	K ₂ CO ₃	HFIP	---	---	---
4	PPh ₃	K ₂ CO ₃	H ₂ O	---	---	---
5	PPh ₃	K ₂ CO ₃	DME	---	---	---
6	PPh ₃	K ₂ CO ₃	PhMe	2.7	40%	84:16
7	PPh ₃	K ₂ CO ₃	<i>m</i> -xylene	2.0	42%	80:20
8	PPh ₃	K ₂ CO ₃	1,4-dioxane	2.0	45%	80:20
9	PPh ₃	K ₂ CO ₃	CyH	2.5	42%	80:20
10	---	KOH	1,4-dioxane	---	70%	0:100
11	PPh ₃	Cs ₂ CO ₃	CyH	2.7	35%	80:20
12	PPh ₃	KH ₂ PO ₄	CyH	2.4	38%	85:15
13	PPh ₃	KHCO ₃	CyH	---	---	---
14	PPh ₃	Na ₂ CO ₃	CyH	---	---	---
15	PPh ₃	K ₃ PO ₄	CyH	2.8	53%	84:16
16	PPh ₃	K ₃ PO ₄	PhMe	1.7	38%	87:13

17	PCy ₃	K ₃ PO ₄	CyH	2.0	8%	80:20
18	dppf	K ₃ PO ₄	CyH	---	---	---
19	P(Cy)Ph ₂	K ₃ PO ₄	CyH	2.7	35%	60:40
20	P(4-C ₆ H ₄ Cl) ₃	K ₃ PO ₄	CyH	2.0	25%	87:13
21	P(4-C ₆ H ₄ Me) ₃	K ₃ PO ₄	CyH	2.3	27%	80:20
22	P(4-C ₆ H ₄ OMe) ₃	K ₃ PO ₄	CyH	3.0	28%	94:6
23 ^[b]	P(4-C ₆ H ₄ F) ₃	K ₃ PO ₄	CyH	3.5	65%	98:2
24 ^[b,c]	P(4-C ₆ H ₄ F) ₃	K ₃ PO ₄	CyH	5.3	54%	98:2
25 ^[b,d]	P(4-C ₆ H ₄ F) ₃	K ₃ PO ₄	CyH	3.7	59%	97:3
26 ^[e]	P(4-C ₆ H ₄ F) ₃	K ₃ PO ₄	CyH	3.0	65%	96:4
27^[b,e]	P(4-C₆H₄F)₃	K₃PO₄	CyH	3.5	73%	98:2
28 ^[f]	P(4-C ₆ H ₄ F) ₃	K ₃ PO ₄	CyH	3.3	72%	97:3
29 ^[g]	P(4-C ₆ H ₄ F) ₃	K ₃ PO ₄	CyH	---	---	---

[a] Reaction conditions: **338a** (0.50 mmol), **301a** (0.60 mmol), [RuCl₂(*p*-cymene)]₂ (5.0 mol %), ligand (20 mol %), base (2.0 equiv), solvent (1.0 mL), 120 °C, 24 h, isolated yields. [b] TMP-ketimine **340a**. [c] 110 °C. [d] 140 °C. [e] **301a** (1.50 mmol). [f] Base (3.0 equiv). [g] Without [Ru].

Next, we tested different directing groups for the envisioned allylative C–F/C–H functionalization (Table 8). However, no conversion was observed with challenging aldimines **341a** and **343a** (entries 1-2). Also, *N*-(pivaloyloxy)benzamide **16a** and *o*-toluic acid **346a** failed to promote C–F/C–H functionalization (entries 3-4).

3. Results and Discussion

Table 8. Attempted directing groups for allylative C–F/C–H functionalization.^[a]

$[\text{RuCl}_2(p\text{-cymene})]_2$ (5.0 mol %) / $\text{P}(4\text{-C}_6\text{H}_4\text{F})_3$ (20 mol %) / K_3PO_4 , CyH, 120 °C, 24 h

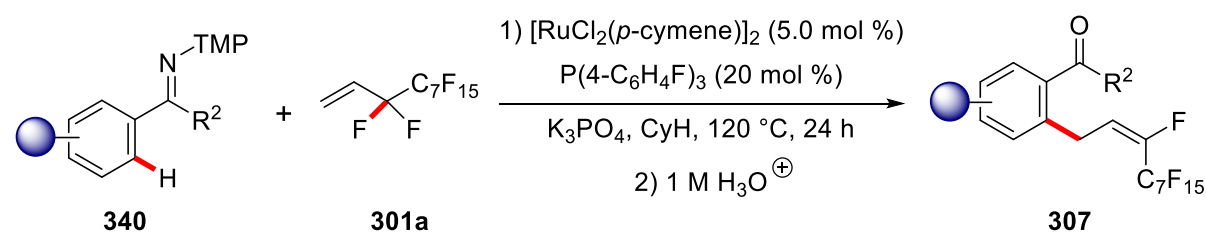
Entry	Directing Groups	Product	Yield [%]
1	 341a	 342aa	n.r.
2	 343a	 344aa	n.r.
3	 16a	 345aa	n.r.
4	 346a	 347aa	n.r.

[a] Reaction conditions: Imine (0.50 mmol), **301a** (1.50 mmol), $[\text{RuCl}_2(p\text{-cymene})]_2$ (5.0 mol %), $\text{P}(4\text{-C}_6\text{H}_4\text{F})_3$ (20 mol %), K_3PO_4 (2.0 equiv), CyH (1.0 mL), 120 °C, 24 h, isolated yields. n.r. = No Reaction.

3.2.2. Substrate Scope of C–F/C–H Functionalization

Diversely substituted valuable ketimines **340** were tested under the optimized catalytic reaction conditions (Table 9). Both electron-rich and electron-poor arenes **340** were well tolerated under the reaction condition furnishing the desired products **307** in moderate to good yields with moderate *E/Z* ratio. The robust ruthenium(II)catalysis manifold permitted C–F/C–H functionalizations in high levels of chemo-, site- and regio-selectivity. Methyl and ethyl substituted ketimines **340a** and **340b** both furnished the products in good yields under the optimized reaction conditions (entries 1-2). Subsequently, various *para*-substituted ketimines **340c-340h** were tested, providing the corresponding products **307ca-307ha** in moderate to good yields (entries 3-8). Notably, the robust ruthenium(II)catalysis manifold proved to be tolerant of a set of synthetically meaningful electrophilic functional groups, including chloro and ester substituents (entries 7-8), which should prove invaluable for further late-stage diversification. The site selectivity was largely governed by steric repulsion for the *meta*-substituted arene **340i** (entry 9). However, the versatile ruthenium(II)catalyst also showed limitations. Nitro and cyano-substituted ketimines **340j** and **340k** did not furnish the products **340ja** and **340ka** respectively, under the optimized reaction condition (entries 10-11). Also, heteroarene **348a** failed to undergo the C–F/C–H functionalizations (entry 12).

Table 9. Scope of the allylative C–H/C–F functionalizations.^[a]



Entry	Ketimine	Product	<i>E/Z</i>	307:339	Yield
1	 340a	 307aa	78:22	98:2	73%

3. Results and Discussion

2	 340b	 307ba	75:25	99:1	63%
3	 340c	 307ca	84:16	92:8	62%
4	 340d	 307da	80:20	99:1	53%
5	 340e	 307ea	75:25	98:2	58%
6	 340f	 307fa	72:28	97:3	54%
7	 340g	 307ga	70:30	99:1	48%
8	 340h	 307ha	83:17	98:2	59%

9	 340i	 307ia	74:26	91:9	63%
10	 340j	 307ja	---	---	n.r.
11	 340k	 307ka	---	---	n.r.
12	 348a	 349aa	---	---	n.r.

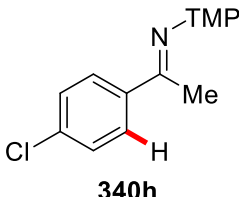
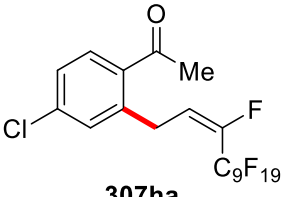
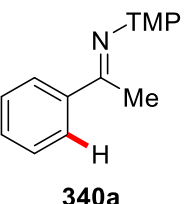
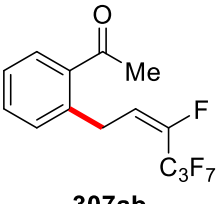
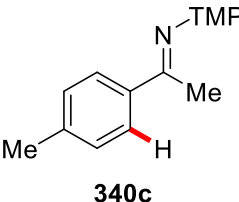
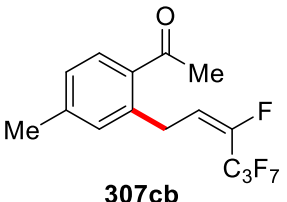
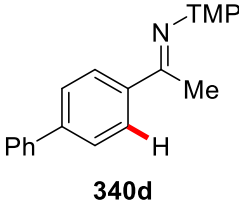
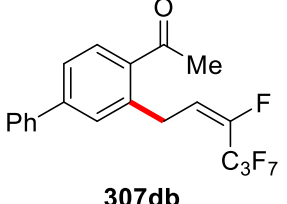
[a] Reaction conditions: **340** (0.50 mmol), **301a** (1.50 mmol), $[\text{RuCl}_2(p\text{-cymene})]_2$ (5.0 mol %), $\text{P}(4\text{-C}_6\text{H}_4\text{F})_3$ (20 mol %), K_3PO_4 (2.0 equiv), CyH (1.0 mL), 120 °C, 24 h, isolated yields.

The versatile ruthenium(II)-catalyzed C–F/C–H functionalization was subsequently tested with other perfluoroalkylalkenes **301** (Table 10). Thereby, 1*H*,1*H*,2*H*-perfluoro-1-dodecene **301c** was likewise smoothly converted into the corresponding products **307** with various substituted ketimines **340** in good yields and with good diastereoselectivities (entries 1-7), exploiting the removable nature of the ketimine within a user-friendly one-pot procedure. Similarly, a considerable variability with respect to the perfluoroalkyl chain length was observed. Likewise, 1*H*,1*H*,2*H*-perfluoro-1-hexene **301b** was tested under the reaction conditions with various unsubstituted **340a** and *para*-substituted ketimines **340c-340d**, furnishing the corresponding products with high levels of chemo-, diastereo-, and position-selectivities (entries 8-10).

3. Results and Discussion

Table 10. C–F/C–H functionalization with perfluoroalkylalkenes **301**.^[a]

Entry	Ketimine	301	Product	<i>E/Z</i>	307:339	Yield
1		301c		79:21	99:1	65%
2		301c		83:17	94:6	64%
3		301c		82:18	98:2	60%
4		301c		73:27	87:13	61%
5		301c		82:18	98:2	56%
6		301c		73:27	100:0	54%

7	 <p>340h</p>	301c	 <p>307ha</p>	76:24	99:1	60%
8	 <p>340a</p>	301b	 <p>307ab</p>	89:11	91:9	48%
9	 <p>340c</p>	301b	 <p>307cb</p>	81:19	99:1	49%
10	 <p>340d</p>	301b	 <p>307db</p>	84:16	99:1	52%

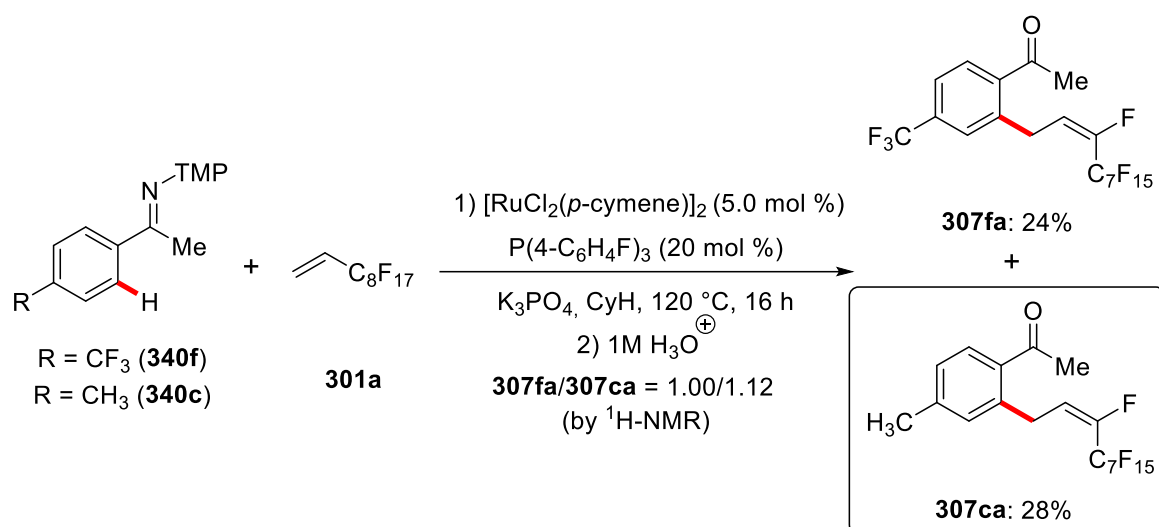
[a] Reaction conditions: **340** (0.50 mmol), **301** (1.50 mmol), $[\text{RuCl}_2(p\text{-cymene})]_2$ (5.0 mol %), $\text{P}(4\text{-C}_6\text{H}_4\text{F})_3$ (20 mol %), K_3PO_4 (2.0 equiv), CyH (1.0 mL), 120 °C, 24 h, isolated yields.

3.2.3. Mechanistic Studies

Considering the unique selectivity features of the ruthenium(II)-catalyzed C–F/C–H functionalization, we became then intrigued to delineating its mode of action.

3.2.3.1. Intermolecular Competition Experiment

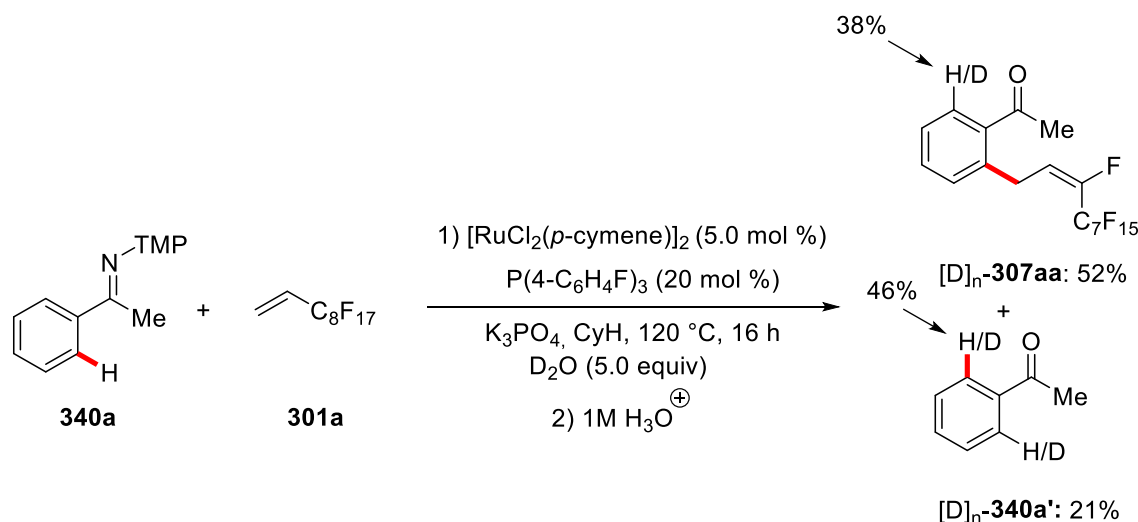
To this end, we performed an intermolecular competition experiment between electron-rich and electron-deficient arenes **340c** and **340f**, which revealed a preferential reactivity in favor of the more electron-rich substrate **340c** (Scheme 104). This finding is in disagreement with a CMD/AMLA-type C–H activation. Instead, a base-assisted internal electrophilic substitution (BIES)-type C–H metalation is rather operative for the allylative C–F/C–H functionalization.



Scheme 104. Competition experiment between electron-rich and electron-deficient arenes.

3.2.3.2. Deuterium Labeling Experiments

Subsequently, we performed deuterium labeling experiments to gain insights into the C–H ruthenation step (Scheme 105). The ruthenium(II)-catalyzed C–F/C–H functionalization was performed in the presence of the isotopically-labeled D_2O as co-solvent (Scheme 105). Here, we observed a considerable H/D exchange at the *ortho*-positions of the allylated product $[\text{D}]_n\text{-307aa}$ and the hydrolyzed starting material $[\text{D}]_n\text{-340a}'$.

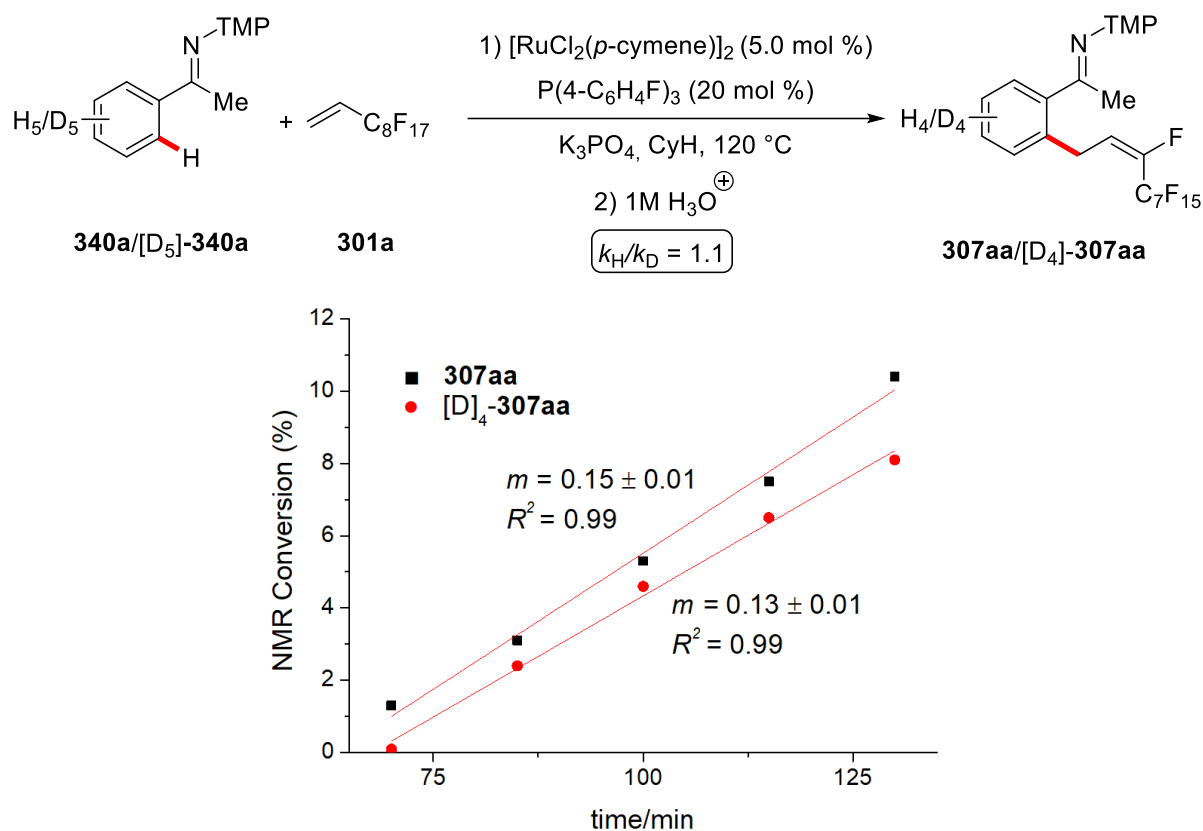


Scheme 105. Deuterium labeling experiments for C–F/C–H functionalization.

3.2.3.3. KIE Study

Moreover, to gain further mechanistic understanding of the C–H activation step, independent KIE-experiments were performed (Scheme 106). Thus, the substrate 340a and its deuterated analogue $[\text{D}]_5\text{-340a}$ were employed for independent kinetic experiments (Scheme 106). We

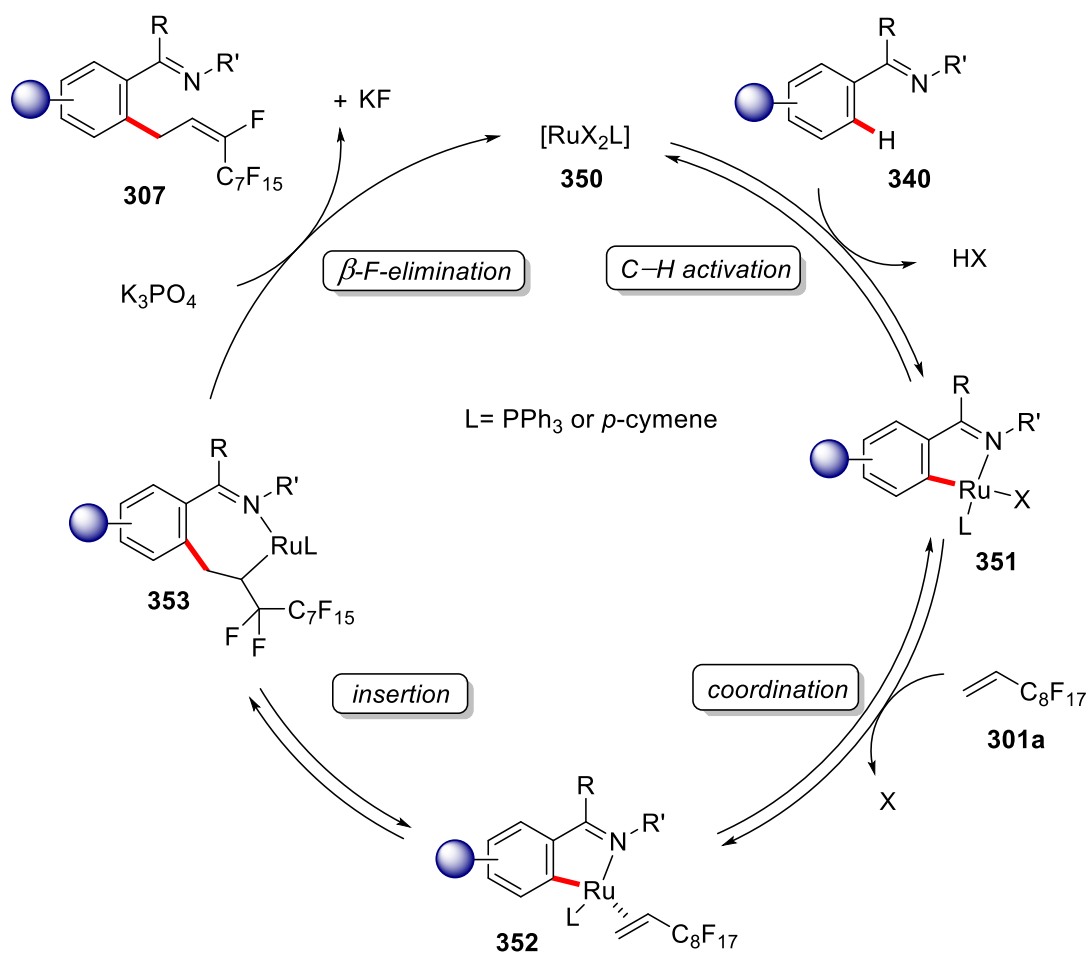
observed a very minor kinetic isotope effect (KIE) of $k_H/k_D = 1.1$, suggestive of a facile and not turnover-limiting C–H metalation event of the ruthenium(II)-catalyzed C–F/C–H functionalization.



Scheme 106. Intramolecular KIE by independent experiments.

3.2.4. Proposed Catalytic Cycle

Based on our detailed mechanistic studies, the allylative ruthenium(II)-catalyzed C–H/C–F functionalization of ketimines **340** is proposed to be initiated by a reversible and facile BIES-type C–H cleavage to form the ruthenacycle **351** (Scheme 107). In the subsequent step, the ruthenacycle **351** is then coordinated by the perfluoroalkylalkene **301a** in a fast and reversible step. In the following step, a migratory insertion into the ruthenium-carbon bond forms seven-membered ruthenacycle intermediate **353** in a possibly irreversible process as there was no H/D exchange in the perfluoroalkylalkenes **301a**. Finally, diastereo-selective base-mediated β -F-elimination delivers the desired product **307**, along with a subsequent ligand exchange regenerating the catalytically active species **350**.



Scheme 107. Proposed catalytic cycle ruthenium-catalyzed C-F/C-H functionalization.

3.3. Enantioselective Cobalt(III)-Catalyzed C–H Activation

Despite numerous reports on precious 4d and 5d transition metal-catalyzed^[57] enantioselective C–H activations,^[58] full selectivity control with 3d metal catalysts remains a challenging area of research (*cf.* chapter 1.3.). However, this area has gained major attention during the course of this doctoral thesis.^[59]

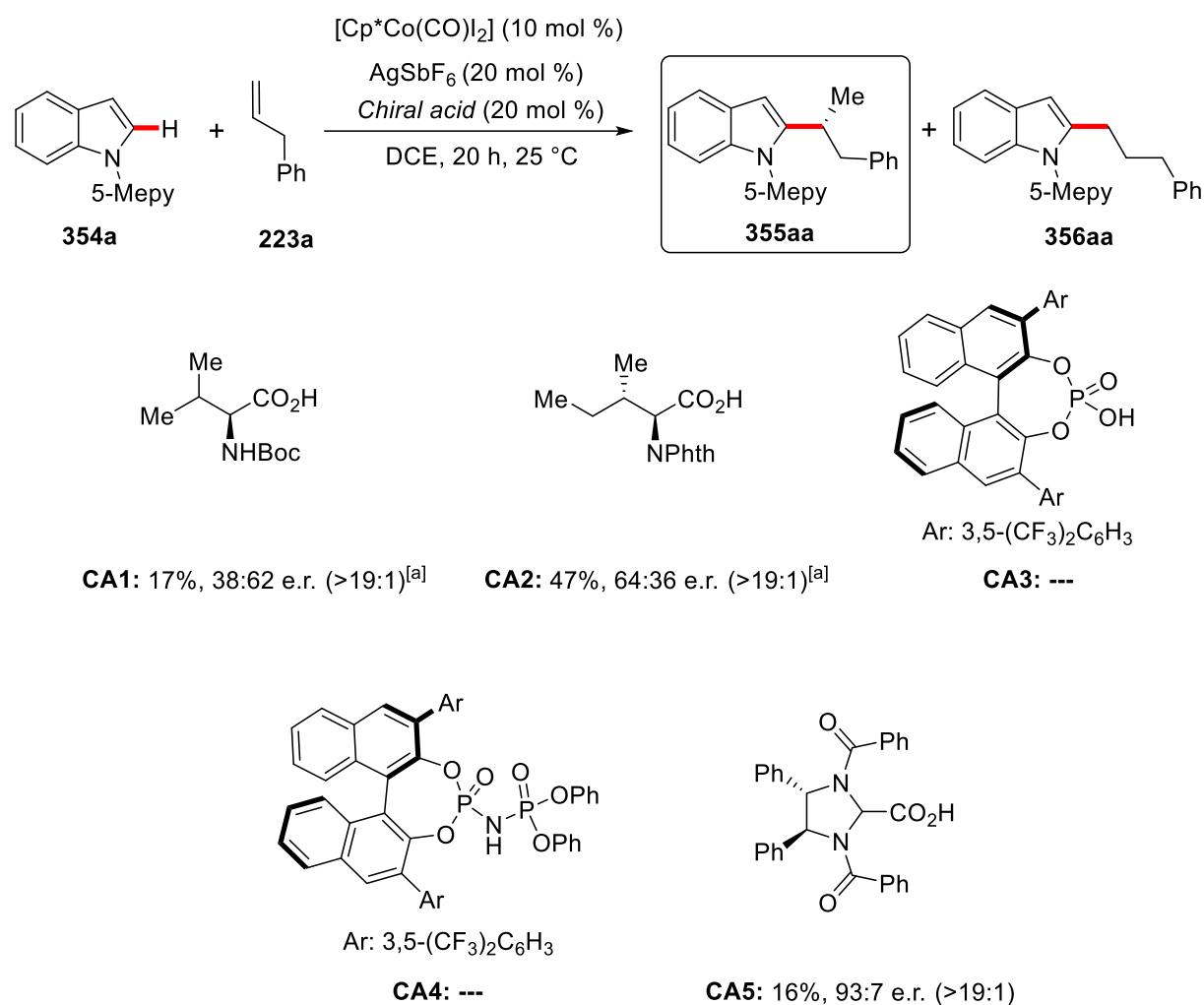
In this context, enantioselective C–H alkylations by 3d transition metals were thus far largely achieved with superstoichiometric amounts of reactive Grignard reagent, which jeopardized the functional group tolerance of these transformations. It is noteworthy to mention that the Yoshikai group achieved the enantioselective cobalt(II)-catalyzed C–H alkylation by the use of BINOL-derived phosphoramidites,^[161] whereas, the Ackermann group reported the first highly enantioselective iron-catalyzed C–H secondary alkylation of (aza)indoles through the design of a novel bulky *meta*-1-adamantyl substituted chiral NHC ligand.^[163] But these transformations still required the use of superstoichiometric amounts of reactive Grignard reagent.

Despite significant advances in the use of cobalt(III) complexes in recent years for various C–H activation reactions,^[264] asymmetric cobalt(III)-catalyzed C–H activation remained unexplored at the outset of this work, although very few examples of enantioselective cobalt(II)-catalyzed C–H transformations have been reported under reductive conditions (*cf.* chapter 1.3.6.).^[59] Furthermore, the Ackermann group reported a racemic highly branch-selective cobalt(III)-catalyzed C–H alkylation using stoichiometric amounts of Brønsted acid.^[265] Drawing inspiration from these studies, we were interested in the development of the first highly enantioselective cobalt(III)-catalyzed C–H activation.

3.3.1. Optimization Studies

After extensive optimization with commonly used chiral carboxylic acids,^[63, 266] initial results by *Dr. F. Pesciaioli* showed the quest for the development of novel chiral acids for the challenging enantioselective cobalt(III)-catalyzed C–H alkylation. Here is a brief overview of the initial studies from *Dr. F. Pesciaioli* (Scheme 108).

3. Results and Discussion

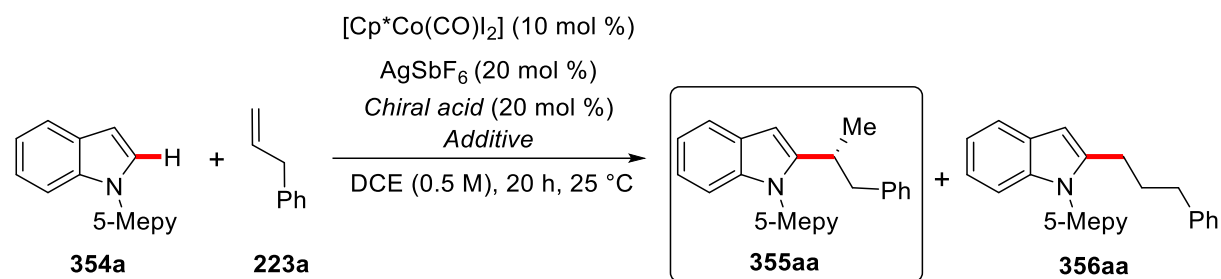


Scheme 108. Enantioselective cobalt(III)-catalyzed C–H alkylation performed by *Dr. F. Pesciaoli*. [a] Chiral acid (1.0 equiv). Markovnikov:*anti*-Markovnikov selectivities in parentheses.

After identifying the novel chiral acid scaffold **CA5**,^[267] further probing of additives and diversely substituted novel chiral acid **CA5** were performed for achieving high levels of enantiocontrol (Table 11). Amberlyst 15 was found to have a beneficial effect for improving the catalytic efficacy as well as the enantioselectivity (entry 3). Further modifications to the phenyl rings on the chiral acids failed to increase the enantioselectivity (entries 4-5). Gratifyingly, by increasing the reaction temperature and prolonging the reaction time to 65 hours we were able to access the product **355aa** in synthetically useful 61% yield and with high enantioselectivity (92:8 e.r.) (entry 6). However, a slight decrease in yield was observed when a reduced amount of acid additive was employed (entry 7). The use of $[\text{Cp}^*\text{CoI}_2]_2$ as the catalyst also showed similar reactivity in terms of catalytic efficiency and enantioselectivity (entry 8). It is noteworthy to mention that a decrease in yield was observed when the reaction was

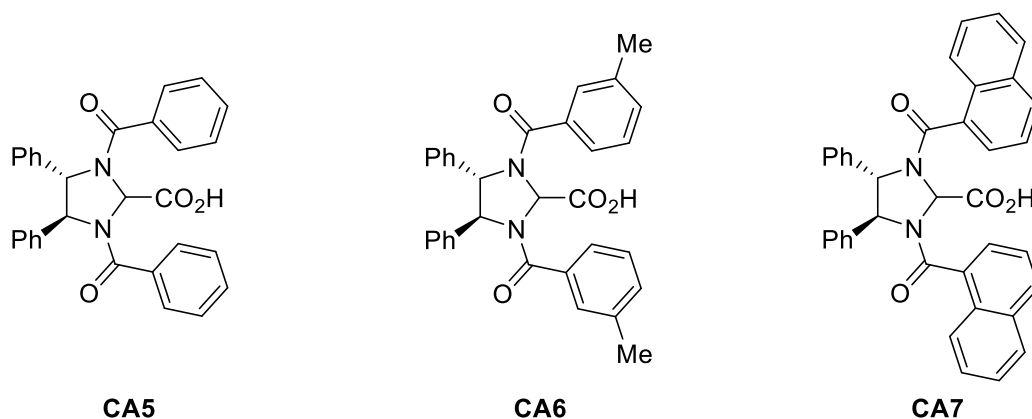
performed for a shorter reaction time (entry 9), highlighting the need of longer reaction time for achieving synthetically useful yields of this challenging transformation.

Table 11. Asymmetric cobalt(III)-catalyzed C–H alkylation.^[a]



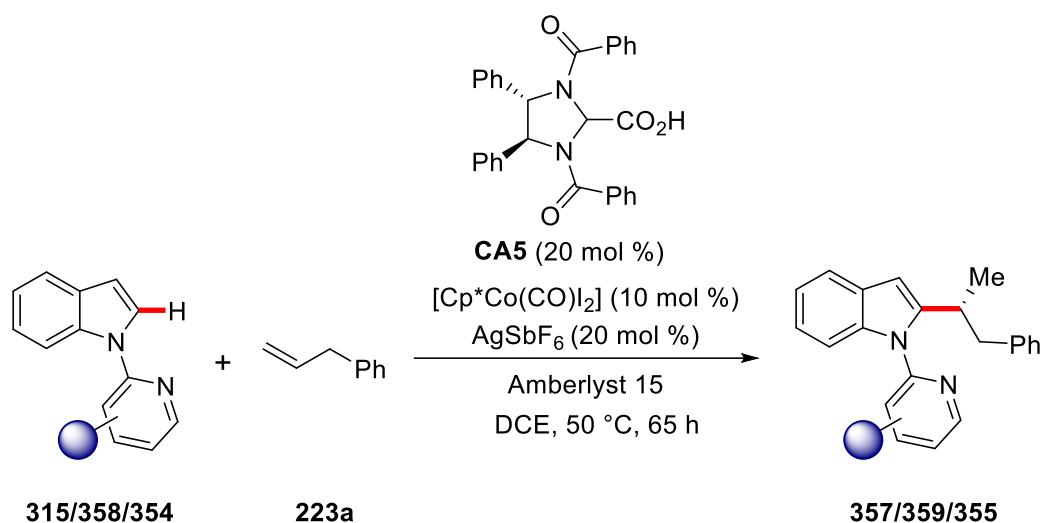
Entry	Acid	Additive	Yield [%]	355aa:356aa	e.r.
1	1-AdCO ₂ H	---	32	>19:1	50:50 ^[b]
2	CA5	---	16	>19:1	93:7 ^[c]
3	CA5	Amberlyst 15	22	>19:1	96:4 ^[c]
4	CA6	Amberlyst 15	25	>19:1	91:9
5	CA7	Amberlyst 15	7	>19:1	58:42
6	CA5	Amberlyst 15	61	11:1	92:8^[c,e,f]
7	CA5	Amberlyst 15	56	11:1	92:8 ^[d,e,f]
8	CA5	Amberlyst 15	60	11:1	92:8 ^[e,f,g]
9	CA5	Amberlyst 15	48	11:1	92:8 ^[e,f,h]

[a] Reaction conditions: **354a** (0.50 mmol), **223a** (1.50 mmol), [Co] (10 mol %), AgSbF_6 (20 mol %), chiral acid (20 mol %), additive (1.50 equiv), DCE (0.50 M), 25 °C, 20 h, conversion determined by ¹H-NMR with Ph₃CH as the internal standard. [b] Acid (1.0 equiv). [c] performed by *Dr. F. Pesciaioli*. [d] Amberlyst 15 (1.0 equiv). [e] DCE (1.0 M), 65 h. [f] Isolated yields. [g] $[\text{Cp}^*\text{CoI}_2]$ (5.0 mol %). [h] 48 h.



3.3.3. Effect of the *N*-Substitution Pattern

With the optimized reaction conditions in hand, we next examined the effect of substituents on the pyridyl group for the enantioselective C–H alkylation (Table 12). Unsubstituted pyridine **315a** provided the product **357aa** in nearly identical yield, but with lower enantioselectivity (entry 1). The same held true for 4-methyl-substituted pyridine, which provided the product **359ba** in marginally lower yield and with decreased enantioselectivity (entry 2). Thus, 5-methylpyridine (5-Mepy) was identified as being slightly superior in terms of enantioselectivities (entry 3).

Table 12. *N*-substitution pattern in asymmetric C–H alkylation.^[a]

Entry	Indole	Product	M:AM ^[b]	Yield ^[c]	e.r. ^[d]
1	 315a	 357aa	82:18	59%	88:12
2	 358a	 359ba	85:15	50%	87:13 ^[e]
3	 354a	 355aa	92:8	61%	92:8 ^[e]

[a] Reaction conditions: Indole (0.50 mmol), **223a** (1.50 mmol), [Cp*Co(CO)I₂] (10 mol %), AgSbF₆ (20 mol %), **CA5** (20 mol %), Amberlyst 15 (1.50 equiv), DCE (0.50 mL, 1.0 M), 50 °C, 65 h. [b] All Markovnikov:anti-Markovnikov selectivities determined by ¹H-NMR spectroscopy. [c] Yield of isolated product. [d] Determined by chiral HPLC analysis. [e] Performed by *Dr. F. Pesciaioli*.

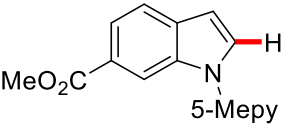
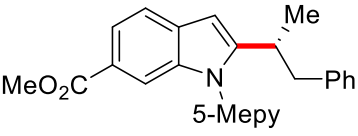
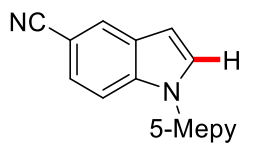
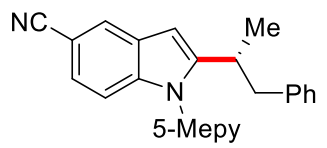
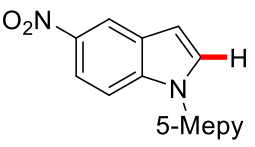
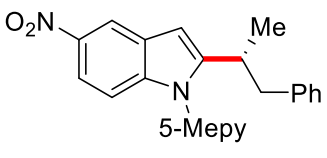
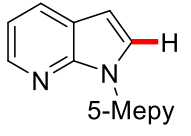
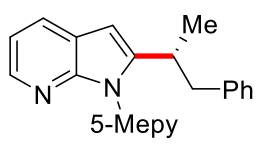
3.3.4. Substrate Scope and Limitations of Asymmetric C–H Activation

With the identified best catalyst, we tested the effect of the substitution on indoles **354** (Table 13). Our robust catalyst provided the desired C2 alkylated products **355** with high branched selectivities and with high level of enantiocontrol. Halogens at C5, including sensitive bromide and iodide, furnished the desired products **355ba** and **355ca** in high enantioselectivities (entries 2-3). Furthermore, the substrate **354d** bearing an ester group was also tolerated under our mild and Grignard-free condition, delivering the C2 alkylated product **355da** in good yield and with high levels of enantiocontrol (entry 4). Unfortunately, both cyano- and nitro-motifs **354e** and **354f** were however not acceptable under our optimized reaction condition (entries 5-6). In addition, azaindole **354g** did not react and failed to provide the C2 alkylated product (entry 7).

Table 13. Asymmetric C–H activation with indoles **354**.^[a]

CA5 (20 mol %)
[Cp*Co(CO)₂] (10 mol %)
AgSbF₆ (20 mol %)
 Amberlyst 15
 DCE, 50 °C, 65 h

Entry	Indole	Product	Yield ^[b,c]	e.r. ^[d]
1			61% (92:8)	92:8
2			66% (94:6)	93:7
3			65% (96:4)	92:8

4	 354d	 355da	73% (96:4)	92:8
5	 354e	 355ea	---	---
6	 354f	 355fa	---	---
7	 354g	 355ga	---	---

[a] Reaction conditions: indole (0.50 mmol), **223a** (1.50 mmol), [Cp*Co(CO)I₂] (10 mol %), AgSbF₆ (20 mol %), **CA5** (20 mol %), Amberlyst 15 (1.50 equiv), DCE (0.50 mL, 1.0 M), 50 °C, 65 h. [b] Yield of isolated product. [c] Markovnikov:*anti*-Markovnikov selectivities in parentheses; determined by ¹H-NMR spectroscopy. [d] Determined by chiral HPLC analysis.

Subsequently, we surveyed various unactivated olefins **223** to examine the effect of the substitution on the aryl ring (Table 14). Methyl substitution at the *para*-position furnished the desired product **355ab** in slightly lower yield and enantioselectivity (entry 1). However, a methoxy substituent in the *para*-position provided the corresponding product **355ac** in a similar yield and enantioselectivity as compared to compound **355ab** (entry 2). Similarly, *para*-phenyl and fluoro gave the desired products **355ad** and **355ae** respectively in moderate yields and with good enantioselectivities (entries 3-4). Electron-rich disubstituted methoxy substituted olefin **223f** was also tolerated, delivering the C2 alkylated product **355af** in good yield and with high enantioselectivity (entry 5). Chloro (**223g**) and bromo (**223i**) groups did not hamper the reactivity, highlighting the mildness of our reaction conditions (entries 6 and 8). However, in the case of pentafluoro benzene **223h** we observed a significant decrease in the enantioselectivity (entry 7). Other functionalities were tested, such as acetate, triflate, and ester,

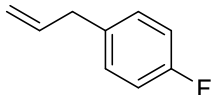
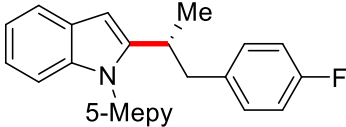
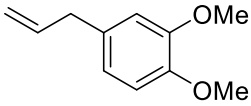
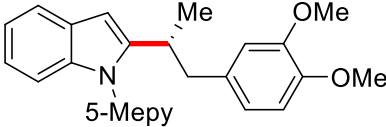
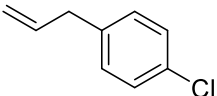
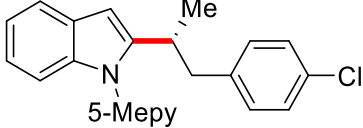
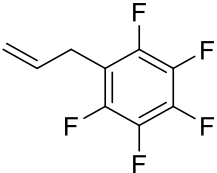
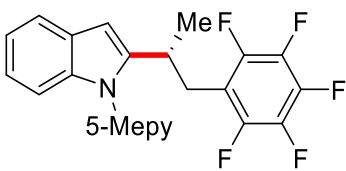
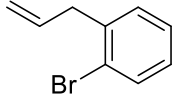
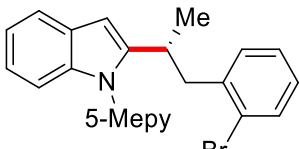
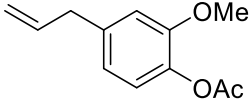
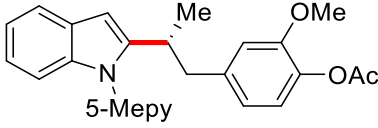
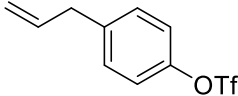
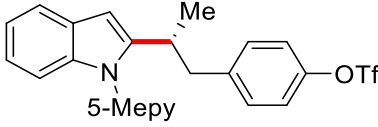
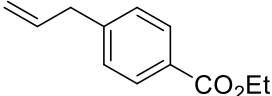
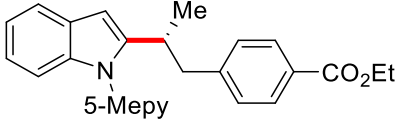
3. Results and Discussion

which afforded the products **355aj-355al** in moderate yields and with good enantioselectivities (entries 9-11). However the acetate-substituted phenyl ring (**223j**) required a higher temperature to achieve good conversion (entry 9). At 60 °C, product **355aj** was formed in 55% isolated yield and 88:12 er. As observed before, at a higher temperature the ratio of linear to branched product also increased significantly.^[265] Unfortunately, in case of the unactivated alkyl substituted alkenes **223n** and **223o**, we observed the products **355an** and **355ao** respectively in significantly decreased yields and enantioselectivities, reflecting the challenges of this transformation (entries 13-14). In addition, 2-substituted hydroxyl group failed to deliver the desired product **355ap** in synthetically useful yields (entry 15).

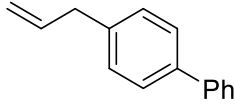
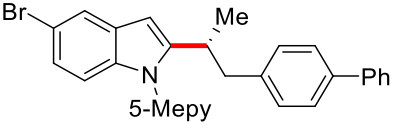
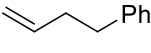
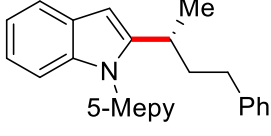
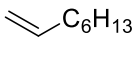
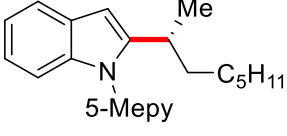
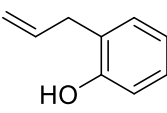
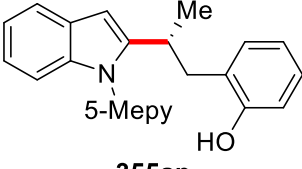
Table 14. Asymmetric C–H activation with alkenes **223**.^[a]

$\text{354a} + \text{223} \xrightarrow[\text{DCE, 50 } ^\circ\text{C, 65 h}]{\text{CA5 (20 mol \%), [Cp}^*\text{Co(CO)I}_2\text{] (10 mol \%), AgSbF}_6\text{ (20 mol \%), Amberlyst 15}}$ **355**

Entry	Alkene	Product	Yield ^[b,c]	e.r. ^[d]
1			46% (97:3)	90:10
2			61% (92:8)	91:9
3			51% (92:8)	89:11

4	 223e	 355ae	52% (94:6)	92:8
5	 223f	 355af	63% (91:9)	92:8
6	 223g	 355ag	41% (93:7)	88:12
7	 223h	 355ah	55% (96:4)	83:17
8	 223i	 355ai	49% (86:14)	92:8 ^[e]
9	 223j	 355aj	55% (75:25)	88:12 ^[f]
10	 223k	 355ak	42% (96:4)	87:13
11	 223l	 355al	56% (86:14)	86:14

3. Results and Discussion

12			53% (92:8)	89:11 ^[g]
	223m	355bm		
13			34% (80:20)	67:33
	223n	355an		
14			37% (90:10)	72:28
	223o	355ao		
15			<10%	---
	223p	355ap		

[a] Reaction conditions: **354** (0.50 mmol), **223** (1.50 mmol), [Cp*Co(CO)I₂] (10 mol %), AgSbF₆ (20 mol %), **CA5** (20 mol %), Amberlyst 15 (1.50 equiv), DCE (0.50 mL, 1.0 M), 50 °C, 65 h. [b] Yield of isolated product. [c] Markovnikov:*anti*-Markovnikov selectivities in parentheses; determined by ¹H-NMR spectroscopy. [d] Determined by chiral HPLC analysis. [e] Performed by *Dr. F. Pescioli*. [f] at 60 °C. [g] **354b** instead of **354a**.

Furthermore, we were able to remove the pyridine orienting groups in a traceless fashion to generate the free indoles **357** (Table 15). Other than simple indole **355aa**, dimethoxy **355da** and ester substituted C2 alkylated products **355af** were also transformed into the free indoles **357** by hydrogenation without erosion of the enantioselectivities (entries 1-3). Furthermore, single crystal X-ray diffraction confirmed that **357da** was the (*R*)-enantiomer, and the other products were assigned by analogy.

Table 15. Traceless removal of directing group.^[a]

Entry	Substrate	Product	Yield ^[b,c]	e.r. ^[d]
	<p>1) MeOTf (1.2 equiv) CH₂Cl₂, 0 °C to 25 °C, 6 h</p> <p>2) Pd(OH)₂/C (10 wt.-%) HCO₂NH₄ (10 equiv) MeOH, 60 °C, 6 h</p> <p>355 → 357</p>			
1	<p>355aa</p>	<p>357aa</p>	86% (92:8)	92:8
2	<p>355da</p>	<p>357da</p>	79% (92:8)	93:7
3	<p>355af</p>	<p>357af</p>	82% (92:8)	91:9

[a] Reaction conditions: (1) **355** (0.20 mmol), MeOTf (0.22 mmol), CH₂Cl₂ (0.50 mL), 0 °C to 25 °C, 6 h. (2) Pd(OH)₂/C (10 wt.-%), HCO₂NH₄ (2.0 mmol), MeOH (1.0 mL), 60 °C, 6 h.

[b] Yield of isolated product. [c] Markovnikov:*anti*-Markovnikov selectivities in parentheses; determined by ¹H-NMR spectroscopy. [d] Determined by chiral HPLC analysis.

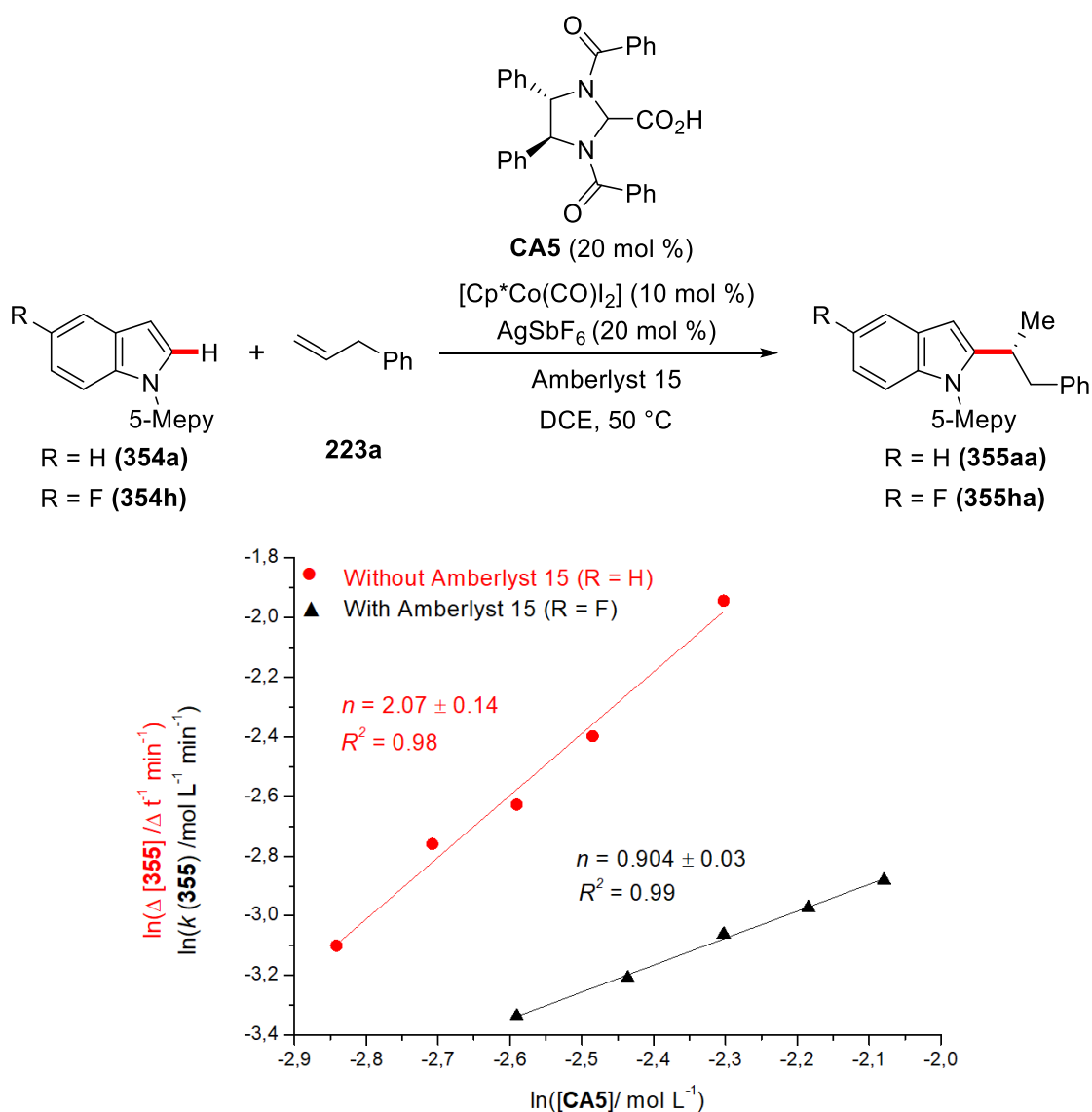
3.3.5. Mechanistic Studies

Given the novelty of the chiral acid **CA5** and the high levels of enantioselectivity generated in this transformation, we were keen to delineate its mode of action. Therefore, detailed experimental and computational mechanistic studies were performed in order to gain insights into the reaction mechanism.

3.3.5.1. Kinetic Reaction Orders

3.3.5.1.1. Reaction Order with respect to Chiral Acid CA5.

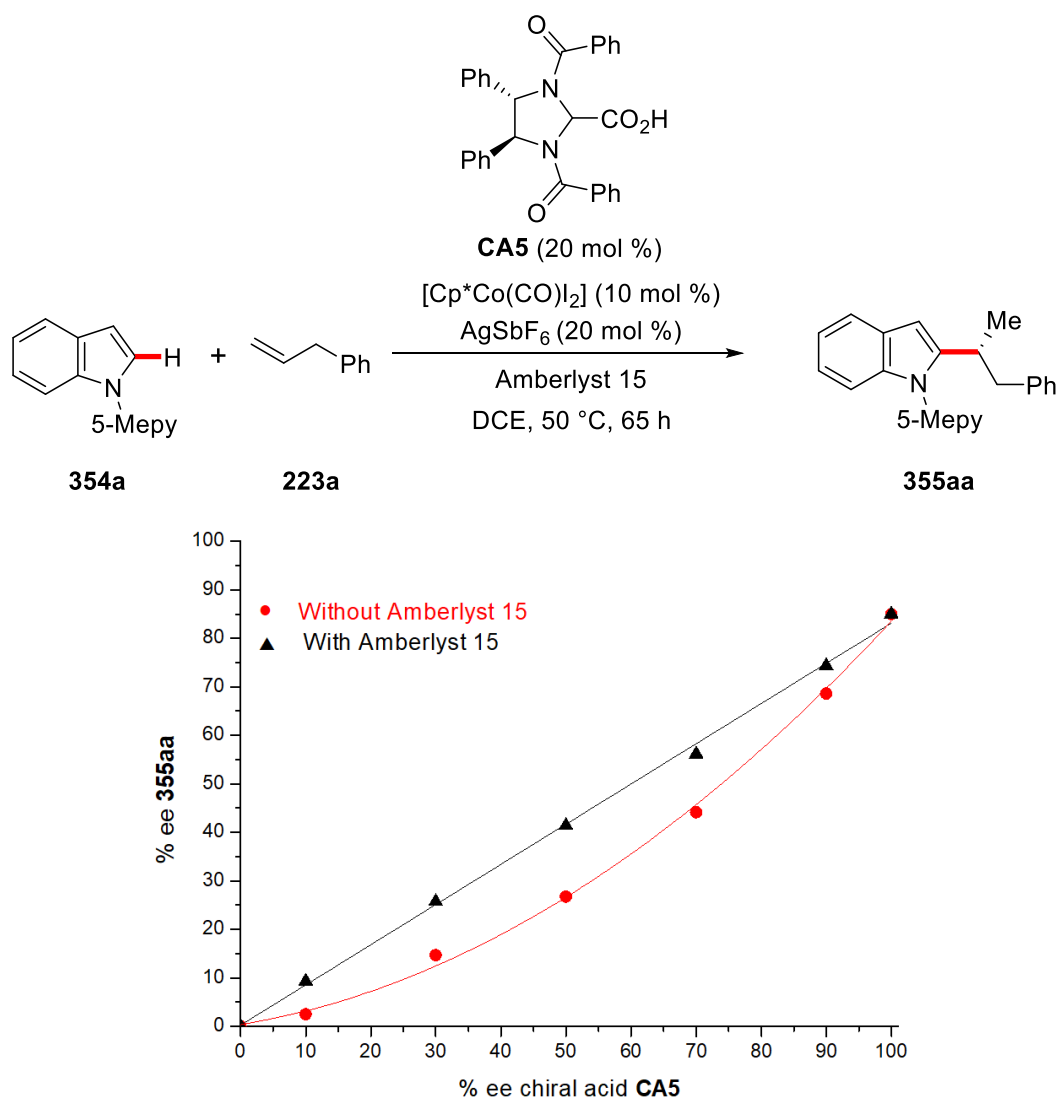
Initially, we determined the kinetic order of the reaction under the optimized reaction conditions with respect to the concentration of the chiral acid **CA5** which was equal to $n = 0.904 \pm 0.03$, indicating a first order dependence on the concentration of chiral acid (Scheme 109). Next, we tested the order of the chiral acid under modified reaction conditions in the absence of the Amberlyst 15 additive. Quite strikingly, we found the order of the chiral acid without Amberlyst 15 was equal to $n = 2.07 \pm 0.14$, which corresponds to an order of two. These findings suggest that the chiral acid **CA5** may form a dimeric species in solution which is also in accordance with our non-linear effect study.



Scheme 109. Order in chiral acid **CA5** with and without Amberlyst 15.

3.3.5.2. Non-Linear Effect Studies

The deviation from the proportionality between the enantiomeric excess of the chiral ligand and the enantiomeric induction of the transformation was next investigated. We studied the non-linear effect in our enantioselective transformation in two distinct sets of conditions. In the first instance, the absence of a non-linear effect (NLE) excludes the formation of a multiligand containing catalyst or catalytically competent oligomer in the enantioselective Co(III)-catalyzed C–H alkylation. Then, the effect of the enantiomeric excess of the chiral acid **CA5** over the enantiomeric induction of the transformation was investigated under Amberlyst 15-free reaction conditions, which gave a considerable negative non-linear-effect. This arguably relates to the existence of a dimeric species in solution.



Scheme 110. Non-linear effect studies with and without Amberlyst 15.

3.3.5.3. Diffusion NMR Study

To further investigate the presence of a dimeric chiral acid species in solution, we performed detailed diffusion controlled NMR spectroscopy in collaboration with *Dr. Michael John* (Figure 1). As diffusion NMR experiments resolve different compounds depending on their size and shape of the molecules, we prepared two NMR samples of chiral acid with and without the external acid TFA. Indeed, the diffusion coefficients were different and the ratio of diffusion coefficients indicated the formation of dimers in the absence of TFA. These findings can be rationalized by a hydrogen bond-stabilized dimeric resting state of the chiral acid which are supported by detailed NLE study and kinetic studies (*vide supra*).

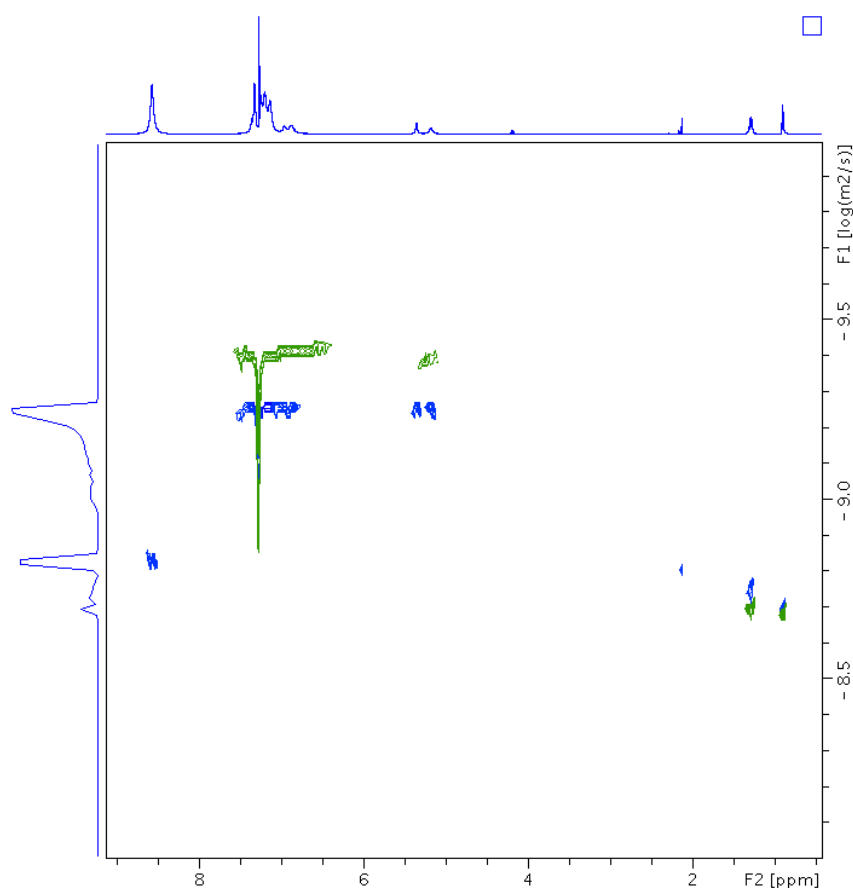
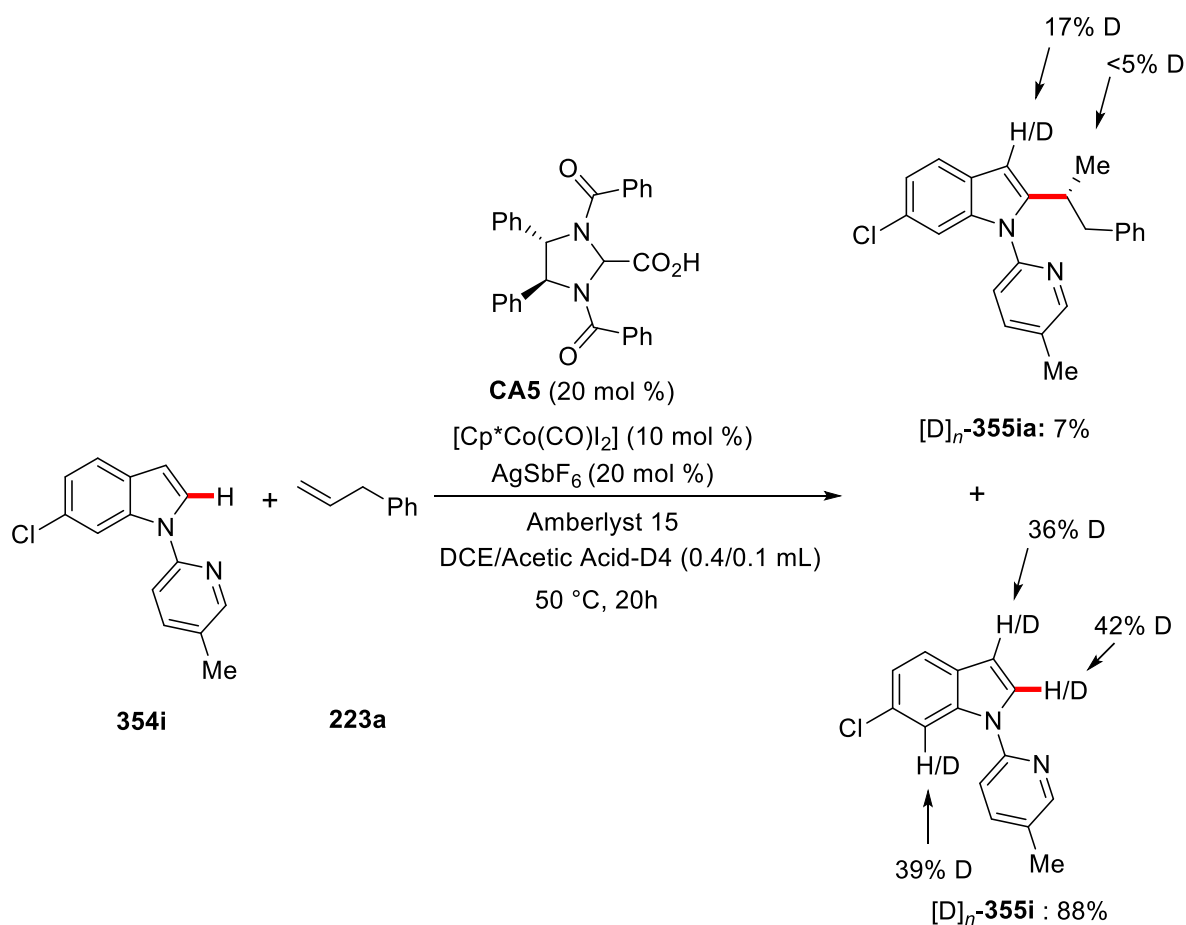


Figure 1. Overlay of DOSY spectra (500 MHz, 25 °C, CDCl₃) of **CA5** (8 mg, 0.017 mmol, in 700 mL of CDCl₃) in the presence (blue) and absence (green) of 0.063 mmol of TFA. The ratio of diffusion coefficients ($5.5 \times 10^{-10} \pm 0.2 \times 10^{-10} \text{ m}^2\text{s}^{-1} / 4.0 \times 10^{-10} \pm 0.2 \times 10^{-10} \text{ m}^2\text{s}^{-1} = 1.375$) indicates the formation of dimers in the absence of TFA. DOSY spectra were recorded on a Bruker Avance III HD 500 MHz instrument equipped with a Cryoprobe Prodigy. The pulse sequence *dsteppgp3s* was used, and the diffusion delay (*d20*) and gradient duration (*p30*) were set to 150 and 1 ms, respectively. *n*Hexane was used as internal standard.

3.3.5.4. H/D Exchange Experiment

Next, we performed a H/D exchange experiment with $\text{CD}_3\text{CO}_2\text{D}$ as the co-solvent to probe the C–H activation elementary step (Scheme 111). As a result, a significant deuterium incorporation was observed at the C3-position of the product **355ia** as well as at the C3- and C7 positions in the starting material in accordance with previously reported racemic branched-selective cobalt(III)-catalyzed C–H alkylations.^[265] Notably, we observed a significant H/D scrambling in the C2-position of the re-isolated starting material **355i** which clearly suggests a facile and reversible C–H metalation step to be involved.

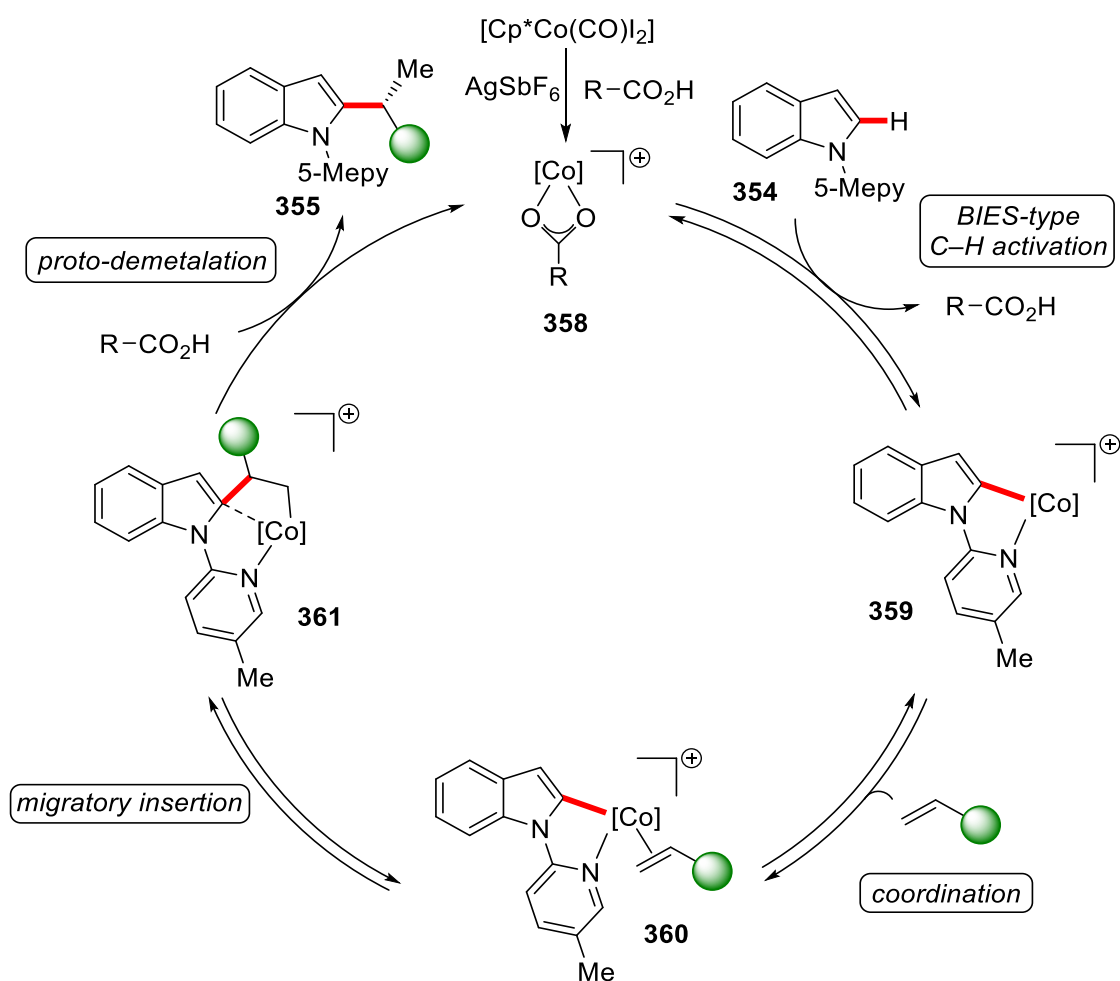


Scheme 111. H/D scrambling experiment for cobalt(III)-catalyzed C–H alkylation.

3.3.6. Proposed Catalytic Cycle

To gain deeper mechanistic insight into the enantioselective cobalt(III)-catalyzed C–H alkylation by the co-operation of the novel chiral carboxylic acid **CA5**, detailed DFT-studies were performed by *Dr. J. C. A. Oliveira*. Given that the H/D exchange experiment clearly suggested a reversible C–H metalation step to be involved, migratory insertion and protodemetalation steps were interrogated by means of computational DFT studies.

On the basis of our detailed mechanistic studies, we propose a plausible catalytic cycle initiated by a reversible and facile C–H metalation to form the intermediate **359** (Scheme 112). Then, and following co-ordination of the alkene **223**, a reversible migratory insertion into the cobalt-carbon bond proceeds to form racemic intermediate **361**. Afterwards, in line with our DFT-studies, the turnover-limiting proto-demetalation step proceeds with chiral acid **CA5**, which acts as the proton source in the enantio-determining step. Thus, the (*R*)-enantiomer of intermediate **361** undergoes selective proto-demetalation with C2-symmetric chiral acid **CA5** to generate the enantioenriched product **355**.



Scheme 112. Proposed catalytic cycle for the enantioselective C–H alkylation.

3.4. Ruthenium(II)-Catalyzed Enantioselective C–H Activation

Ruthenium(II) complexes have been recognized as powerful catalysts for various C–H activation reactions, in particular for hydroarylation reactions.^[27], 39, 138] Despite significant advancements, ruthenium-catalyzed enantioselective C–H activations remain rare.^[268] This can be largely attributed to the absence of reactivity of pentamethylcyclopentadienyl ruthenium(II) complexes, which significantly jeopardizes the use of chiral Cp^x ligands to achieve full selectivity control.^[269] Furthermore, it is noteworthy that the multi-step syntheses of Cp^x-ligands and pre-coordination to metal catalysts reduce the atom- and step economy to large extent.^[106]

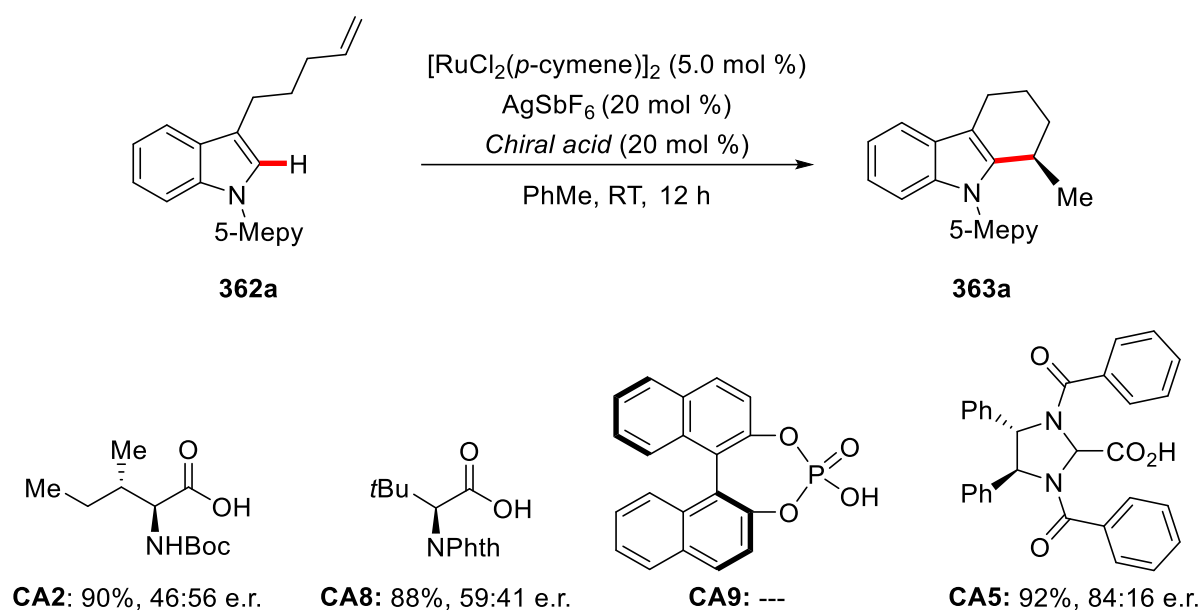
In light of enantioselective C–H activation, the cooperative combination of chiral carboxylic acids (CCAs) with transition metals has become a successful tool for efficient enantioinduction.^[34a, 58a] While ruthenium-catalyzed enantioselective transformations are scarce in literature, in very recent reports, the groups of Cui^[139] and Wang^[140] independently reported ruthenium(II)-catalyzed enantioselective intramolecular hydroarylations by the cooperation of a chiral amine as the directing group^[41] where the enantio-induction was primarily governed by the chiral amine. Intrigued by our previous development of the first cobalt(III)-catalyzed enantioselective C–H alkylations by the design of a novel C2-symmetric chiral acid,^[270] we became interested in devising a new enantioselective strategy for ruthenium-catalyzed asymmetric C–H activations. Particularly the design of novel chiral carboxylic acids was envisioned to control the enantio-determining proto-demetalation step.^[63a, 271]

3.4.1. Optimization Studies

The optimization studies were initiated by probing the effect of various classes of typical Brønsted acids for the enantioselective C2-selective intramolecular C–H alkylation of olefin-tethered indole **362a** (Scheme 113). Over the past years, *N*-protected amino acids have evolved as powerful ligands particularly for palladium-catalyzed enantioselective C–H functionalizations.^[63a] Thus, we initially started our optimization with this class of ligands in the presence of catalytic amounts of [RuCl₂(*p*-cymene)]₂ to furnish the desired cyclized indole derivative **363a** at room temperature. The reaction worked very efficiently with both Boc- **CA2** and phthaloyl- protected **CA8** amino acids, enabling the cyclization with almost quantitative yields, albeit very poor levels of enantiocontrol were observed. Furthermore, well-defined chiral phosphoric acids **CA9**^[266] which have been broadly used in the enantioselective C–H

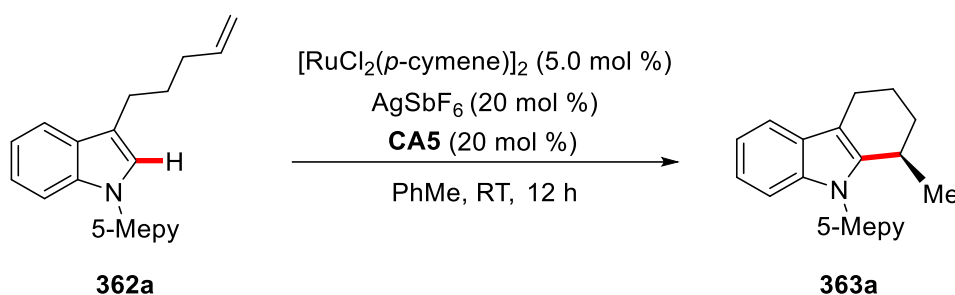
3. Results and Discussion

transformations failed to provide any reactivity, reflecting the quest for the development of novel chiral carboxylic acids for organometallic ruthenium-catalyzed enantioselective C–H activation strategies. Recently we achieved the highly enantioselective cobalt(III)-catalyzed C–H activation through the design of a novel C₂-symmetric chiral carboxylic acid.^[270] Intrigued by this result, we surveyed this class of chiral carboxylic acids in the ruthenium-catalyzed enantioselective C–H alkylation. We were pleased to observe an excellent yield of the desired cyclized product with C₂-symmetric chiral acid **CA5** with a promising enantioselectivity.



Scheme 113. Chiral acid screening for the enantioselective C–H alkylation.

Next, various representative solvents were tested, but fell short in delivering the product **363a** in improved enantioselectivity (Table 16, entries 1-5). Thus, toluene was found to be the optimal solvent (entry 5). Furthermore, we also probed the effect of additives for enantioselective ruthenium-catalyzed C–H alkylations (entries 6-9). Nonetheless, in stark contrast to our previous report,^[270] Amberlyst 15 did not show a beneficial effect on the outcome of the reaction (entry 6). Similar results were obtained for other acid additives which provided the desired product **363a** in almost quantitative yields, but lower levels of enantiocontrol were observed (entry 7-9).

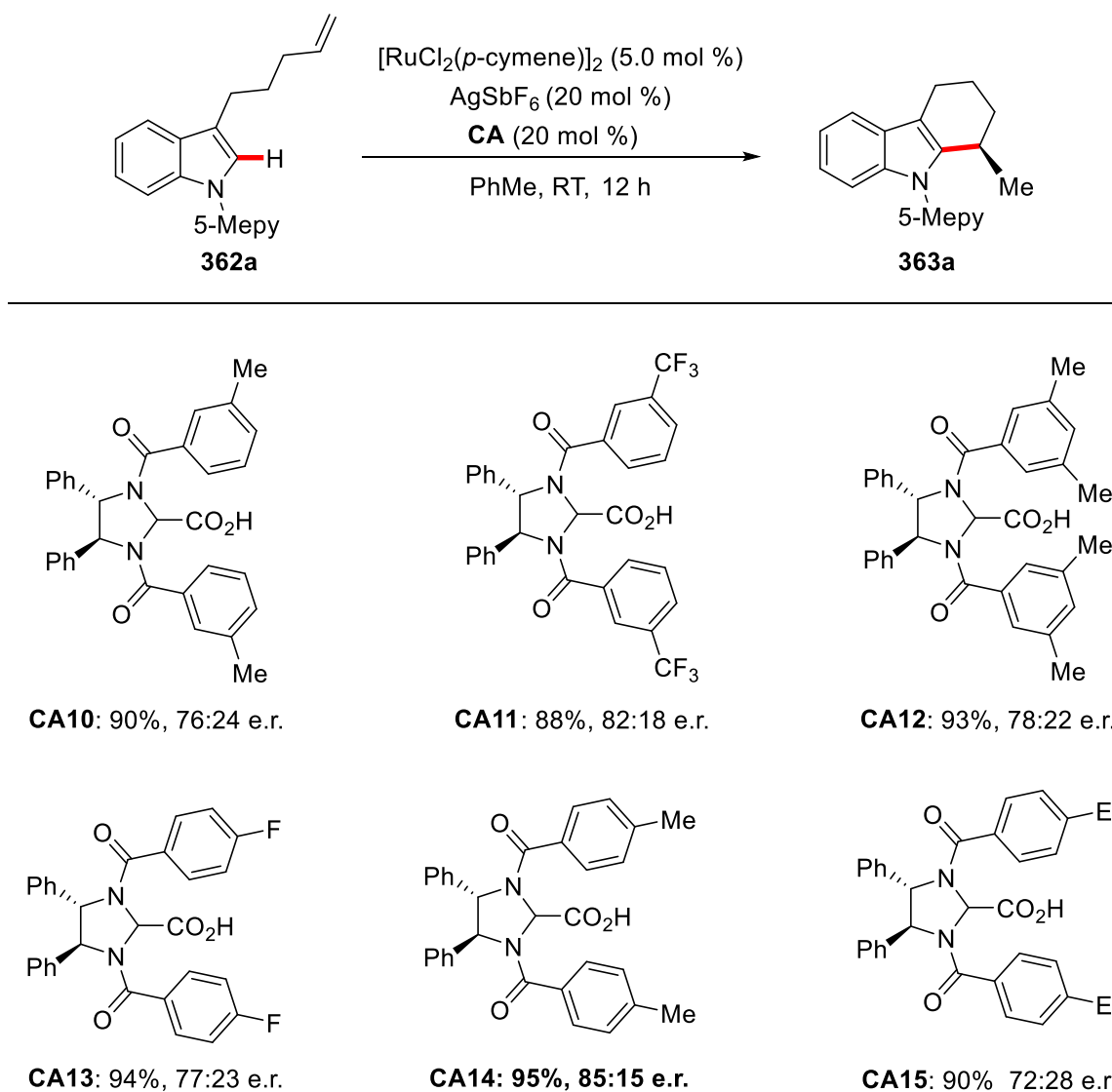
Table 16. Asymmetric ruthenium(II)-catalyzed C–H activation.^[a]

Entry	Additive	Solvent	Yield [%]	e.r. ^[b]
1	---	1,2-DCE	93	76:24
2	---	<i>o</i> -xylene	55	70:30
3	---	1,4-dioxane	52	62:38
4	---	PhCF ₃	90	71:29
5	---	PhMe	92	84:16
6	Amberlyst 15	PhMe	94	84:16
7	Amberlite CG50	PhMe	88	77:23
8	Citric Acid	PhMe	95	78:22
9	MS13X	PhMe	90	84:16

[a] Reaction conditions: **362a** (0.25 mmol), [Ru] (10 mol %), AgSbF₆ (20 mol %), **CA5** (20 mol %), Additive (1.50 equiv), PhMe (0.50 mL), RT, 12 h, isolated yields. [b] Enantioselectivities determined by chiral HPLC.

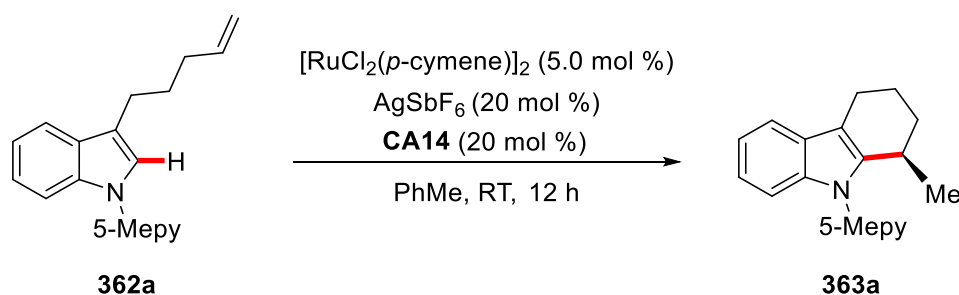
Thereafter, diversely substituted novel chiral carboxylic acids were newly synthesized and probed in the envisioned enantioselective transformations of indoles (Scheme 114). Variation in *meta*-substitution provided the product **363a** in lower enantioselectivity for both methyl **CA10** and trifluoromethyl substituted arenes **CA11**. Similarly, 3,5-disubstituted methyl **CA12** also failed to improve the enantioselectivity. However, we observed a beneficial effect of *para*-phenyl substituted chiral acids in improving the enantioselectivity. Among the tested electron-rich and electron-deficient chiral scaffolds, *para*-methyl substituted chiral acid **CA14** turned out to be superior for achieving high levels of enantiocontrol. Slightly bulkier ethyl-substituted **CA15** was tested as well but provided inferior results compared to the methyl group.

3. Results and Discussion



Scheme 114. Chiral acid screening for the enantioselective C–H alkylation of indoles **362a**.

Next, we tested several variations of our standard conditions (Table 17). Remarkably, the reaction also occurred under silver-free reaction conditions using NaSbF₆ or NaPF₆ as the additive, albeit with slightly lower yields (entries 2-3). As previously observed, Amberlyst 15 did not improve the enantioselectivity, although the reactivity was not influenced (entry 4). Next, a series of several other metal catalysts, such as, [OsCl₂(*p*-cymene)]₂, [Cp*Co(CO)I₂], Pd(OAc)₂, [Cp*IrCl₂]₂ and [Cp*RhCl₂]₂ were tested, which failed to deliver the desired tetrahydrocarbazole derivative **363a** in considerable enantioselectivity (entry 5-9). Likewise, *ent*-**CA14** afforded the (*S*)-enantiomer of the tetrahydrocarbazole (entry 10).

Table 17. Asymmetric ruthenium(II)-catalyzed C–H activation.^[a]

Entry	Variation of Standard Condition	Yield[%]	e.r. ^[b]
1	none	95	85:15
2	NaSbF_6 instead of AgSbF_6	37 ^[c]	77:23
3	NaPF_6 instead of AgSbF_6	20 ^[c]	83:17
4	Amberlyst 15 as additive	94	85:15
5	$[\text{OsCl}_2(p\text{-cymene})]_2$ as catalyst	---	---
6	$[\text{Cp}^*\text{Co}(\text{CO})\text{I}_2]$ as catalyst	<5	n.d.
7	$\text{Pd}(\text{OAc})_2$ as catalyst	---	---
8	$[\text{Cp}^*\text{IrCl}_2]_2$ as catalyst	---	---
9	$[\text{Cp}^*\text{RhCl}_2]_2$ as catalyst	90	58:42
10	<i>ent</i> - CA14 was used	94	15:85

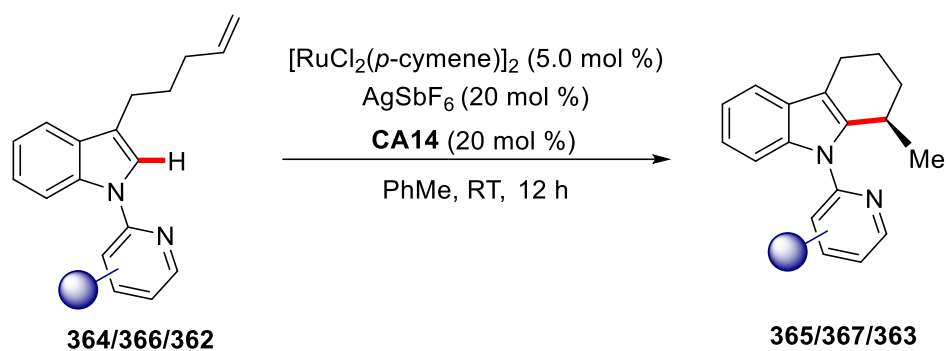
[a] Reaction conditions: **362a** (0.25 mmol), [Ru] (10 mol %), AgSbF_6 (20 mol %), **CA14** (20 mol %), PhMe (0.50 mL), RT, 12 h, isolated yields. [b] Determined by chiral HPLC. [c] Conversion determined by $^1\text{H-NMR}$ using Ph_3CH as the internal standard. n.d. = not determined.

3.4.2. Effect of N-Substitution Pattern

Subsequently, we surveyed the substitution pattern on the pyridyl directing group for the enantioselective C–H alkylation (Table 18). Hence, a similar yield was observed for the unsubstituted pyridine **364a**, albeit lower enantioselectivity of the cyclized product **365a** was obtained (entry 1). The 4-methyl-substituted pyridine **366a** provided a marginally lower yield compared to the 5-methyl substituted substrate **362a** as well as a lower enantioselectivity (entry 2). Thus, 5-methylpyridine (5-Mepy) **362a** furnished the desired product **363a** with the highest enantioselectivity (entry 3).

3. Results and Discussion

Table 18. Effect of *N*-substitution pattern on asymmetric C–H alkylation.^[a]



Entry	Indole	Product	Yield [%]	e.r. ^[b]
1			88	76:24
2			90	81:19
3			95	85:15

[a] Reaction conditions: Indole (0.25 mmol), [Ru] (10 mol %), AgSbF_6 (20 mol %), **CA14** (20 mol %), PhMe (0.50 mL), RT, 12 h, isolated yields. [b] Determined by chiral HPLC.

3.4.3. Substrate Scope of Asymmetric C–H Alkylation

With the optimized catalyst in hand, various C5 and C6 substituted indoles **362** were tested (Table 19). Our approach provided the desired C2-cyclized products **363** in excellent yields and with good enantiocontrol independent of varying the sterics and electronics of the substituents. Both electron-rich and electron-deficient substrates furnished the desired products with good enantioselectivity under exceedingly mild reaction conditions (entries 1-5). Remarkably, halogens including fluoride and bromide were well tolerated in the versatile ruthenium(II) catalysis, which would prove invaluable for further late-stage diversifications (entries 4-5). Thus the desired products **363d-363e** were obtained in high yields and moderate enantioselectivities. Furthermore, the reaction was also performed on a 1 mmol scale with bromo substrate **362e**, furnishing the product in an identical yield of 86% with 83:17 e.r. (entry 5). Additionally, the product **363e** was recrystallized from dichloromethane, and analyzed by single crystal X-ray diffraction, clearly revealing the (*R*)-conformation of the stereocenter. The other products **363** were assigned by analogy. Thereafter, an extensive study of the scope of this enantioselective transformation was studied by *Dr. R. Connon* and *Mr. R. Steinbock*.

Table 19. Asymmetric C–H alkylation with indoles **362**.^[a]

Entry	Indole	Product	Yield [%]	e.r. ^[b]
1	 362a	 363a	95	85:15

3. Results and Discussion

2	 362b	89	85:15
3	 362c	95	84:16
4	 362d	66	86:14
5	 362e	88 86 ^[c]	82:18 83:17 ^[c]

[a] Reaction conditions: **362** (0.25 mmol), [Ru] (10 mol %), AgSbF₆ (20 mol %), **CA14** (20 mol %), PhMe (0.50 mL), RT, 12 h, isolated yields. [b] Determined by chiral HPLC. [c] Performed on 1 mmol scale.

We further became interested to extend this approach to the synthesis of larger rings (Table 20). Under our optimized reaction conditions, we observed a rather low conversion for the formation of seven-membered ring **369**, albeit Amberlyst 15 proved to be beneficial here (entries 1-2). Further optimization was performed by *Mr. R. Steinbock*, showcasing that prolonged reaction time could provide cyclohepta[*b*]indole derivative **369** in a synthetically useful yield of 51% with a good enantioselectivity of 82:18 e.r. (entry 3). Unfortunately, larger than 7-membered rings could not be formed under otherwise identical reaction conditions (entry 4).

Table 20. Enantioselective C–H alkylation for larger rings.^[a]

Entry	n	Variation of Standard Condition	Yield [%]	e.r. ^[b]
1	1	none	17	82:18
2	1	Amberlyst 15 as additive	25	82:18 ^[c]
3	1	Amberlyst 15 as additive and 72 h	51	82:18^[c]
4	2	none	---	---

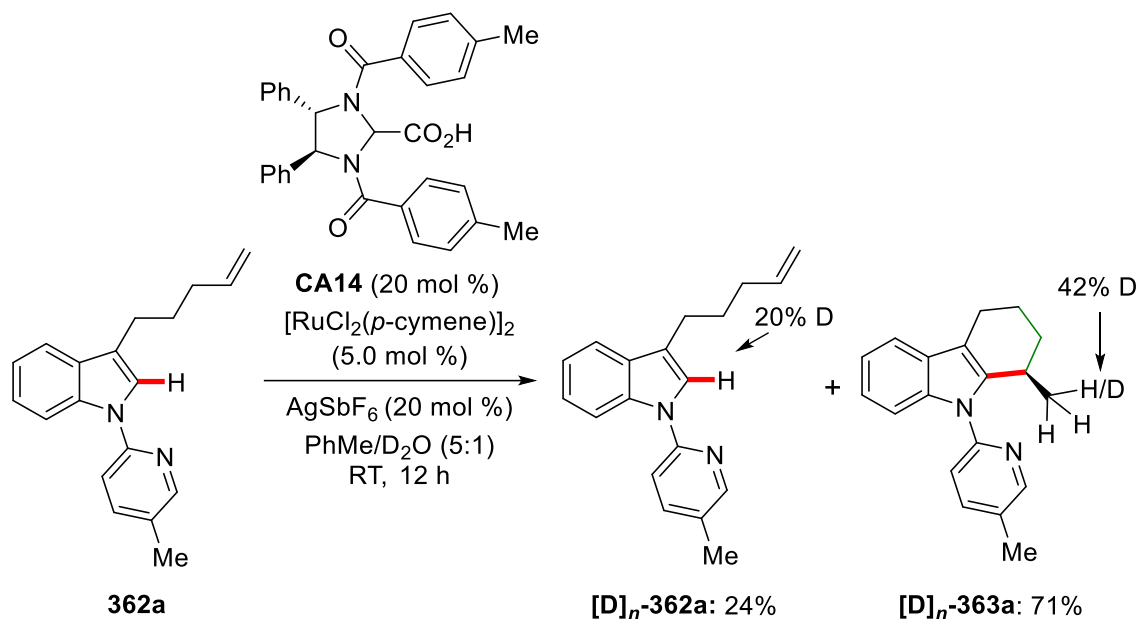
[a] General reaction conditions: **368/370** (0.10 mmol), [Ru] (10 mol %), AgSbF₆ (20 mol %), **CA14** (20 mol %), PhMe (0.50 mL), RT, 20 h, isolated yields. [b] Enantioselectivities determined by chiral HPLC. [c] Performed by *Mr. R. Steinbock*.

3.4.4. Mechanistic Studies

Given the unique selectivity shown by the chiral carboxylic acid **CA14** for the intramolecular enantioselective C–H alkylation in ruthenium(II)-catalysis, we were interested to unravel its mode of action. Therefore, detailed experimental and computational mechanistic studies were performed in order to gain insights into the reaction mechanism.

3.4.4.1. H/D Exchange Experiment

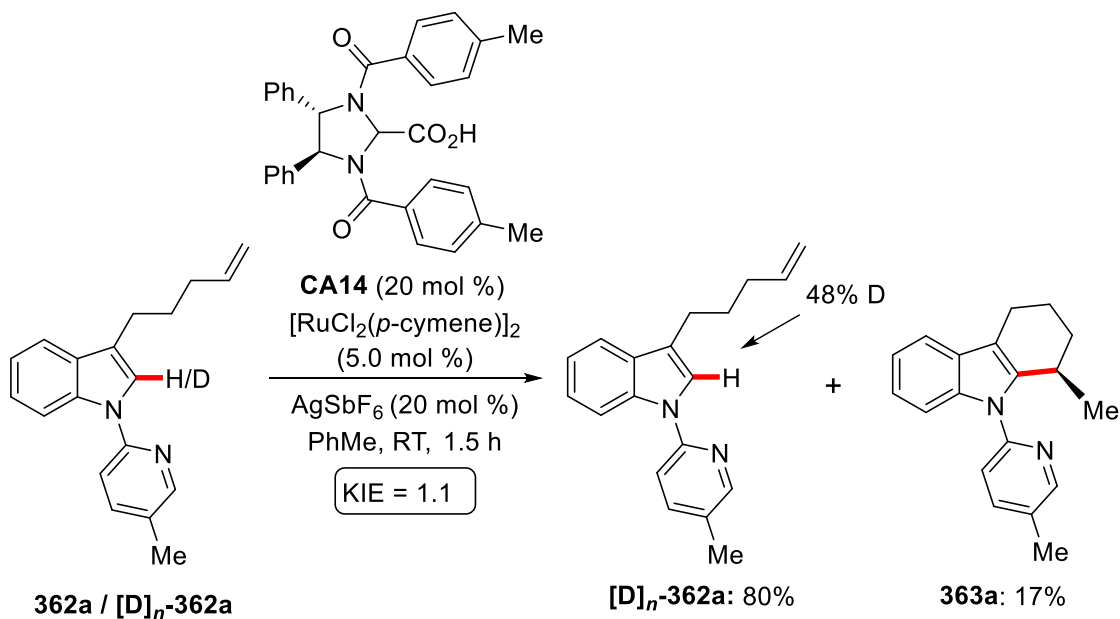
Initially, a H/D exchange experiment was conducted in toluene with isotopically-labeled D₂O as the co-solvent to probe the C–H activation step (Scheme 115). Significant H/D exchange was observed in the methyl-group in **363a** and in the recovered starting material **362a**. This observation can be rationalized by a facile and reversible C–H ruthenation step.



Scheme 115. H/D exchange experiment of the enantioselective C–H alkylation.

3.4.4.2. KIE Studies

Furthermore, the intramolecular kinetic isotope effect (KIE) was determined for the substrate **362** and isotopically-labelled substrate **[D]_n-362a**, which showed a KIE of $k_{\text{H}}/k_{\text{D}} \approx 1.1$, which is in good agreement with the H/D exchange experiment, being suggestive of a fast and non rate-determining C–H ruthenation (Scheme 116).

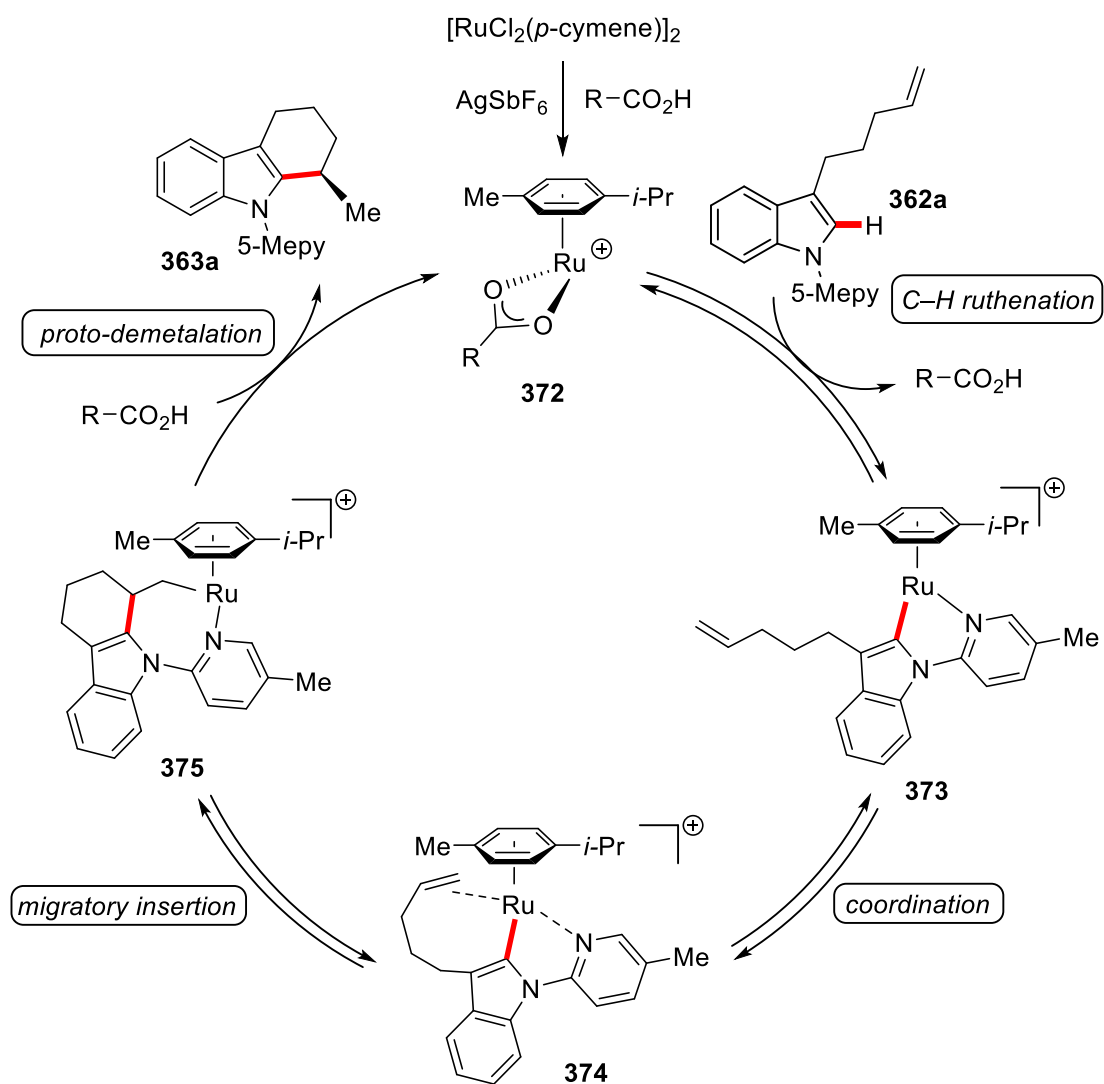


Scheme 116. KIE studies of the enantioselective C–H alkylation.

3.4.5. Proposed Catalytic Cycle

In addition to these experimental mechanistic studies, detailed DFT-studies were performed by *Dr. J. C. A. Oliveira* to gain mechanistic insights of enantioselective ruthenium(II)-catalyzed C–H alkylation.

On the basis of our mechanistic studies, we propose a plausible catalytic cycle to commence with a fast C–H activation step, as supported by the H/D exchange experiments and the KIE study, to form the intermediate **373** (Scheme 117). Then, the generated ruthenacycle **373** undergoes a reversible alkene coordination to form **374**, followed by a reversible migratory insertion into the ruthenium-carbon bond to form racemic intermediate **375**. In accordance with the computational studies, a process involving the turnover-limiting proto-demetalation step proceeds with chiral acid **CA14**, which acts as the proton source in the enantio-determining step. Finally, selective proto-demetalation occurs from the (*R*)-enantiomer of intermediate **375** with the chiral carboxylic acid **CA14** to regenerate the catalytically active species **372** and releases the enantioenriched cyclized indole **363**.



Scheme 117. Proposed catalytic cycle for enantioselective ruthenium(II)-catalyzed C-H alkylation.

3.5. Copper-Catalyzed Alkyne Annulation by C–H Alkynylation

In the last decade electro-organic synthesis has witnessed a considerable renaissance in order to achieve new reactivity towards improved resource economy.^[224] While early contributions on the synergistic merger of oxidative metal catalysis with electrosynthesis were limited to the use of expensive 4d and 5d transition metals, recent trends have shifted towards inexpensive 3d transition metal catalysis.^[232] In this context, copper is one of the most abundant 3d transition metals in the Earth's crust.^[31] Consequently, copper catalysts have emerged in the past few years as powerful tools for cost-effective C–H activation reactions. Among others, copper catalysts have been widely used for C–H arylations, aminations and alkyne annulation reactions (*cf.* chapter 1.4.1.3). However, oxidative copper-catalyzed C–H activations such as aminations or alkyne annulations had largely required toxic and expensive sacrificial oxidants, which jeopardize the atom-economy of the overall strategy.^[31]

Surprisingly, electrochemical copper-catalyzed C–H activation was largely unexplored. Yet very recently, Mei reported copper-catalyzed electrochemical aminations with anilides through a proposed single electron transfer (SET) mechanism.^[256] Subsequently, similar electrooxidative aminations were independently reported by Nicholls^[257] using 8-aminoquinoline as the directing group. However, electrochemical copper-catalyzed C–H alkynylations^[209, 272] have thus far proven elusive. Thus, we became interested in the development of copper-catalyzed electro-oxidative alkyne annulation enabled by C–H alkynylations of synthetically valuable benzamides to deliver bioactive five-membered isoindolones. It is noteworthy that isoindolones are core structural motifs of various pharmaceutical drugs and natural products with distinct biological activity. Hence, sustainable methods to synthesize highly functionalized isoindolones scaffolds are highly desirable (Figure 2).

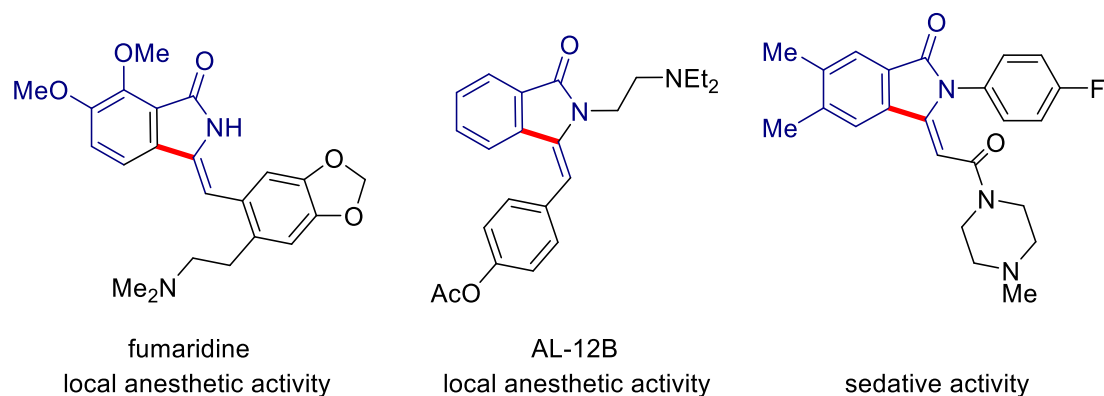
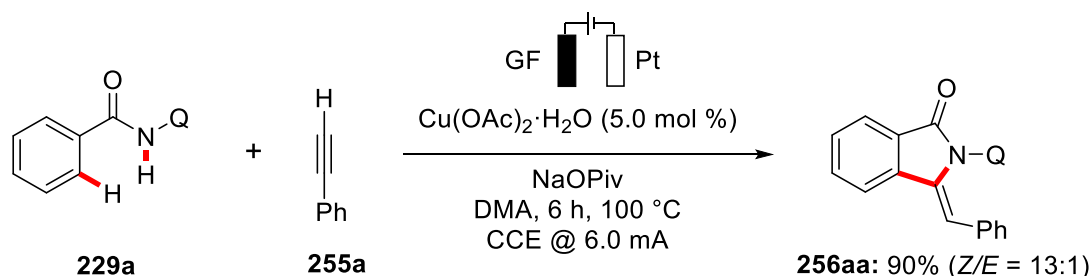


Figure 2. Examples of biologically important 3-methyleneisoindolin-1-ones derivatives.

3.5.1. Optimization of the Copper-Catalyzed Electrochemical C–H Annulation

Initial optimized reaction conditions for the envisioned copper-catalyzed electrochemical C–H annulation were obtained by *Dr. C. Tian*, in that benzamide **229a** was reacted with phenyl acetylene **255a** in an undivided cell set-up in the presence of 5.0 mol % of $\text{Cu}(\text{OAc})_2 \cdot \text{H}_2\text{O}$, one equiv of NaOPiv in DMA at 100 °C with a combination of graphite felt as anode and platinum as cathode. A constant current of 6.0 mA was applied to thereby provide the desired alkyne annulated product **256aa** with 90% yield (*Z/E* = 13:1) (Scheme 118).



Scheme 118. Copper-catalyzed electrochemical C–H annulation.

3.5.2. Substrate Scope and Limitations of the Electrochemical Copper-Catalyzed Alkyne Annulation

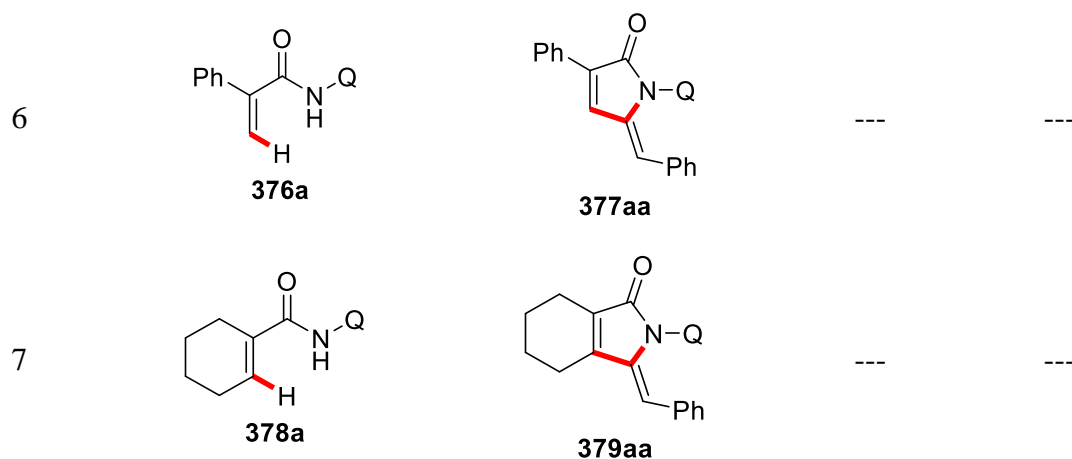
With the optimized reaction conditions in hand, we tested the versatility of differently substituted benzamides **229** for the electrochemical copper-catalyzed C–H cascade annulation to test the generality and limitations of this reaction (Table 21). To our delight, sterically crowded *ortho*-substituted benzamides **229b** and **229c** efficiently provided the desired annulated products **256ba** and **256ca** in good yields, while for bulky *ortho*-phenyl-substituted benzamide **229c**, an increased catalyst loading was required to improve the catalytic efficiency (entries 2-3). Even *para*-nitro substituted benzamide **229d** was well tolerated by our robust catalysis (entry 4). Unfortunately, electron-rich 2-methoxybenzamide **229e** failed to show any

reactivity (entry 5). In addition, 2-phenyl-*N*-(quinolin-8-yl)acrylamide **376a** and cyclohexene benzamide **378a** remained untouched (entries 6-7).

Table 21. Cupraelectro-catalyzed C–H annulation with benzamides **229**.^[a]

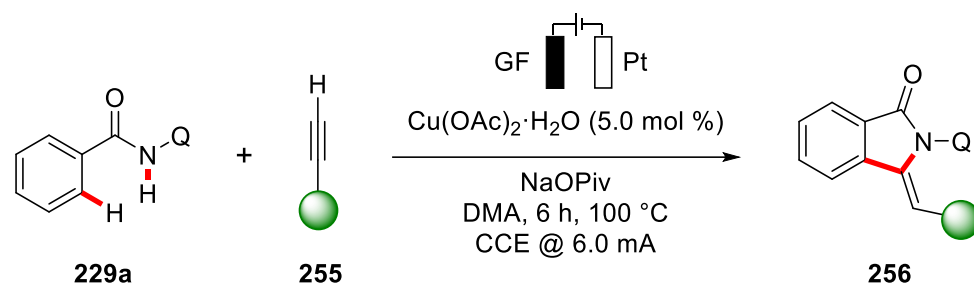
Entry	Benzamide	Product	<i>E/Z</i>	Yield [%]
1			1:13	88
2			1:10	65
3			1:2.8	51 ^[b]
4			1:3	58 ^[b]
5			---	---

3. Results and Discussion



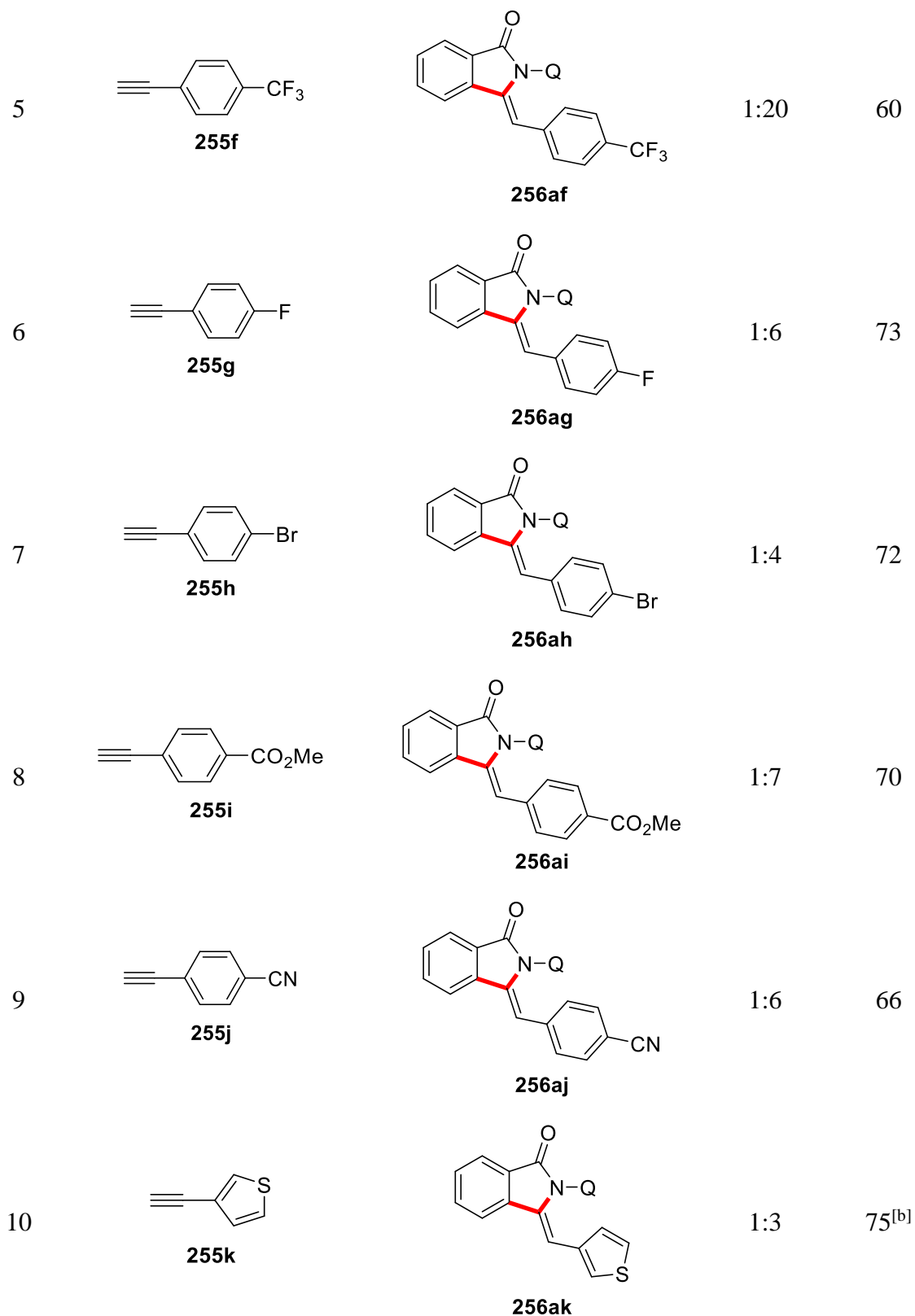
[a] Reaction conditions: **229** (0.25 mmol), **255a** (0.50 mmol), Cu(OAc)₂·H₂O (5.0 mol %), NaOPiv (1.0 equiv), DMA (4.0 mL), 100 °C, constant current at 6.0 mA, 6 h, GF anode (10 mm × 15 mm × 6 mm), Pt-plate cathode (10 mm × 15 mm × 0.25 mm), undivided cell, isolated yields. [b] Cu(OAc)₂·H₂O (10 mol %).

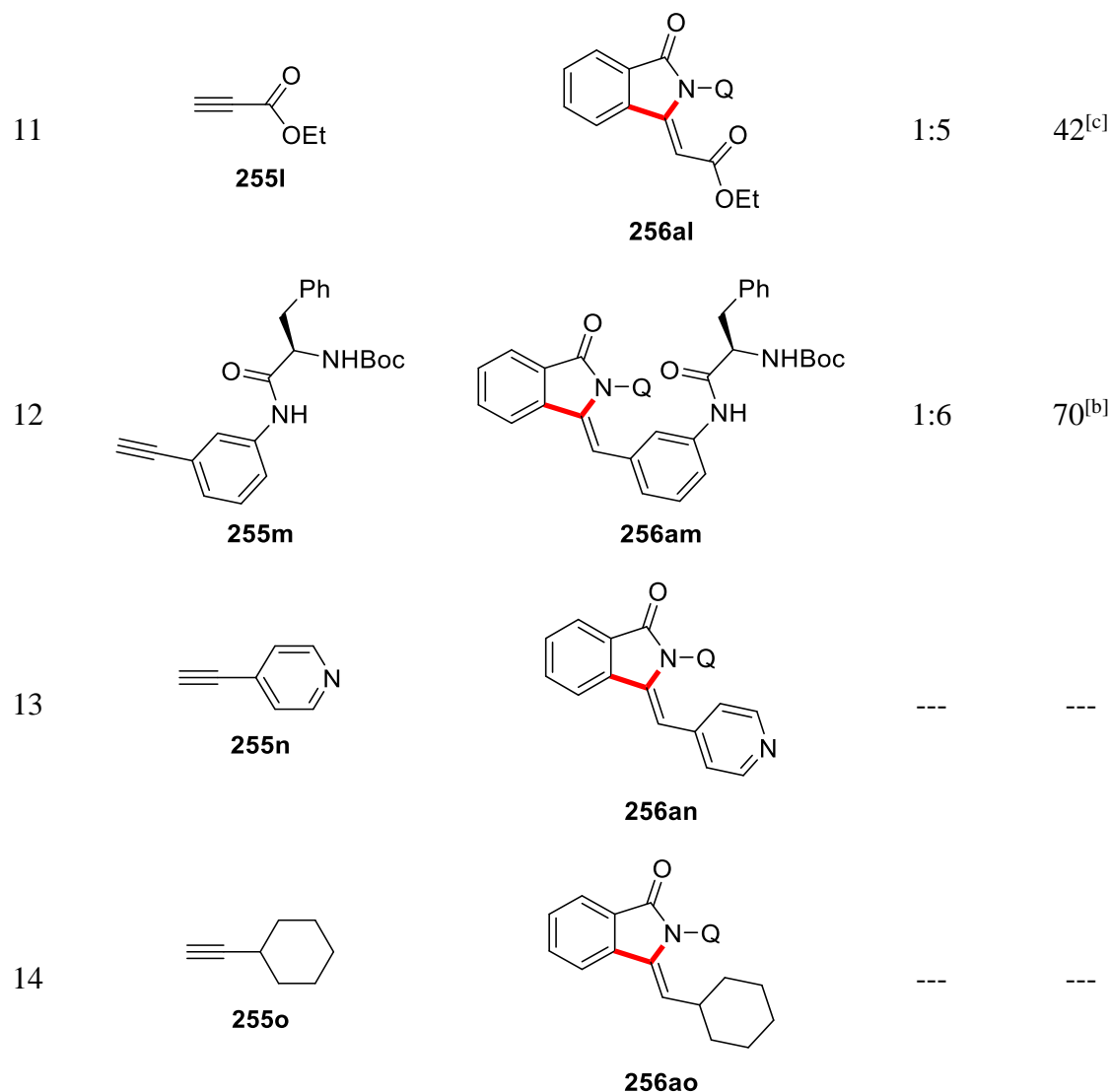
Likewise, a broad range of *ortho*-, *meta*- and *para*- substituted terminal alkynes **255** was tested under our optimized electrochemical reaction conditions to demonstrate the robustness of our catalyst (Table 22). In general, electron-rich 4-ethynyltoluene **255b**, 4-ethynylanisole **255c** and 2-ethynylanisole **255d** were smoothly converted with good yields to the corresponding products **256ab-256ad** (entries 1-3). Moreover, *meta*-chlorophenylacetylene **255e** was also found as an amenable substrate, while electron-poor 4-ethynyltrifluoroluene **255f** showed slightly lower reactivity (entries 4-5). To our satisfaction, a series of *para*-substituted halo groups was well tolerated, which should prove invaluable for late-stage diversification (entries 6-7). In addition, ester **255i** and cyano-containing alkyne **255j** were also chemo-selectively converted to deliver the desired isoindolinones **256ai** and **256aj** in good yields (entries 8-9). Electron-rich heterocycle thiophene acetylene **255k** was also found to be amenable substrate in the cupraelectro-catalyzed annulation manifold, albeit higher catalyst loading was employed to improve the conversion (entry 10). A significant drop in reactivity was observed for the aliphatic alkyne **255l** (entry 11), whereas the robustness of the copper-catalyzed annulation allowed excellent efficacy with alkyne bearing Boc-protected amino acid **255m** (entry 12). As a limitation of the substrate scope, 4-ethynylpyridine **255n** and ethynylcyclohexane **255o** remained unreacted under the optimized reaction conditions, as the remaining starting materials were recovered in almost quantitative yields (entries 13-14).

Table 22. Cupraelectro-catalyzed C–H annulation with terminal alkynes **255**.^[a]

Entry	Alkyne	Product	<i>E/Z</i>	Yield [%]
1	 255b	 256ab	1:6	77
2	 255c	 256ac	1:1.4	72
3	 255d	 256ad	1:4	73
4	 255e	 256ae	1:4	70

3. Results and Discussion





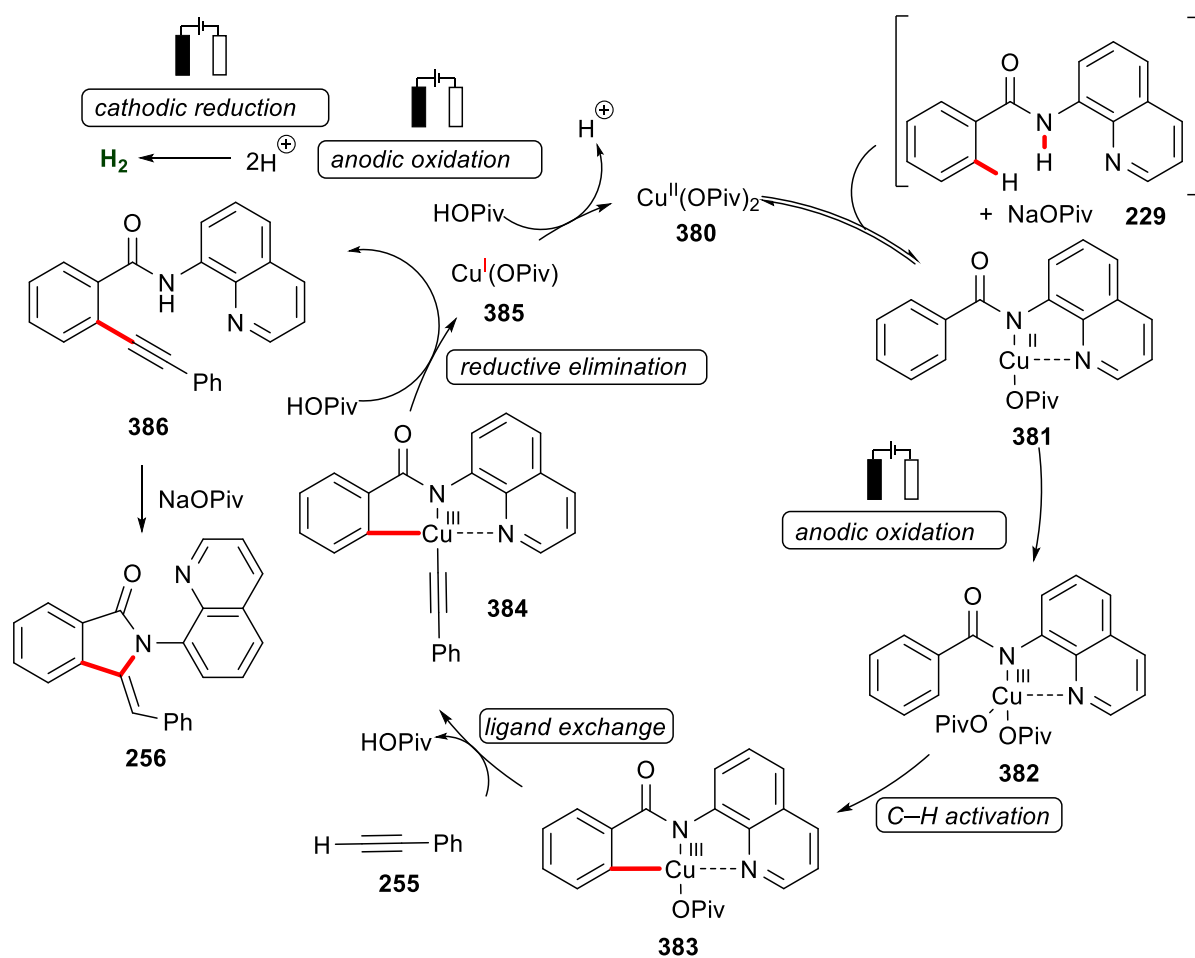
[a] Reaction conditions: **229a** (0.25 mmol), **255** (0.50 mmol), Cu(OAc)₂·H₂O (5.0 mol %), NaOPiv (1.0 equiv), DMA (4.0 mL), 100 °C, constant current at 6.0 mA, 6 h, GF anode (10 mm × 15 mm × 6 mm), Pt-plate cathode (10 mm × 15 mm × 0.25 mm), undivided cell, isolated yields. [b] Cu(OAc)₂·H₂O (10 mol %). [c] Cu(OAc)₂·H₂O (20 mol %).

3.5.3. Proposed Catalytic cycle for Copper-Catalyzed Electrochemical C–H Annulation

Based on the mechanistic studies from *Dr. C. Tian* and cyclic voltammetry analysis from *Mr. A. Scheremetjew*, we have proposed a plausible catalytic cycle for the copper-catalyzed electrochemical C–H annulation (Scheme 119). First, the catalytic cycle initiates with the benzamide co-ordination to form copper(II) intermediate **381**, which readily undergoes anodic oxidation to form catalytically competent copper(III) carboxylate species **382**. Second, the catalytically competent species **382** undergoes facile carboxylate assisted C–H activation to form **383**. Third, ligand exchange with alkyne **255** forms species **384** and subsequent reductive

3. Results and Discussion

elimination affords the alkenylated arene **386**, which undergoes facile base-assisted cyclization to form the annulated product **256**.



Scheme 119. Proposed catalytic cycle for cupraelectro-catalyzed alkyne annulation.

3.6. Electrochemical Cobalt-catalyzed C–H Allylation

In recent years significant momentum was gained by the merger of transition metal-catalyzed oxidative C–H activation with electrochemistry, enabling the use of electrons as sustainable redox equivalents.^[232] Since the pioneering report on cobalt-catalyzed oxidative C–H oxygenation by the Ackermann group in 2017,^[246] electrochemical cobalt catalyzed C–H activation has been well studied by Ackermann and others.^[32a, 245] Moreover, electrochemical palladium-,^[233] rhodium-,^[242e, 242f] iridium-^[243b] and ruthenium-^[244h]catalyzed organometallic C–H activations are mainly restricted to activated alkenes, such as styrenes and acrylates. In sharp contrast, electrochemical C–H activation with unactivated aliphatic alkenes is unexplored. Thus, Lei developed cobalt-catalyzed electrochemical C–H/N–H annulations with simple ethylene, delivering solely the cyclized product.^[251] Considering that the control of chemo-selectivity is an important endeavor in organic synthesis, we became interested to study cobalt-catalyzed electrochemical C–H activation with unactivated alkenes.

Direct C–H allylations have really become an important method in terms of step-economy, and, consequently, there has been a significant development in *ortho*-C–H allylations. Over the past years, the synthetic community has witnessed a significant advancement in transition metal-catalyzed C–H allylations primarily with prefunctionalized coupling partners, such as allyl halides or acetates.^[273] While very recently unactivated allylic coupling partners have been employed for oxidative C–H allylation reactions, this approach largely required superstoichiometric amounts of chemical oxidants, which jeopardized its synthetic utility.^[191-193] In this context, it is noteworthy that electrocatalyzed C–H allylations are as of yet unknown. Thus we were interested to develop cobalt-electro-catalyzed C–H allylations of synthetically meaningful benzamides and challenging unactivated alkenes.

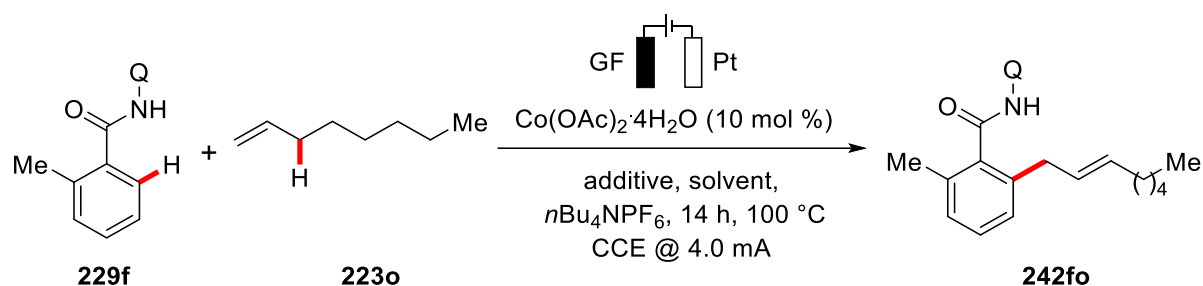
3.6.1. Optimization of the Electrochemical Cobalt(II)-Catalyzed C–H Allylation

We initiated our optimization for the envisioned cobalt(II)-catalyzed C–H allylation with *ortho*-substituted benzamide **229f** as the model substrate (Table 23). We performed our initial test reaction with benzamide **229f** and unactivated alkene **223o** in a user-friendly undivided cell set-up under a constant current electrolysis. We were pleased to exclusively observe allylated product **242fo** with a catalytic amounts of inexpensive Co(OAc)₂·4H₂O in the presence of NaOAc as the additive (entry 1). Next, we tested various carboxylate and carbonate additives, among which, NaOPiv was ideal, providing the desired allylated product **242fo** in

3. Results and Discussion

60% yield (entries 1-5). Then, a series of representative solvents was tested (entries 5-10). To our delight, biomass-derived renewable γ -valerolactone (GVL) provided the optimal results (entry 5).^[6, 248] Among other typical solvents, DCE gave comparable reactivity (entry 6), while other solvents showed either low conversion or no reaction at all (entries 7-10). It is noteworthy that a deep eutectic solvent system of choline chloride and urea was able to furnish the desired product **242fo**, albeit in lower yield (entry 11). Furthermore, different reaction temperatures were tested, which revealed the optimal reactivity at 100 °C, while higher or lower reaction temperatures reduced the yields (entries 12-13). Control experiments highlighted the necessity of the cobalt(II)-catalyst and the electricity (entries 14-15). It is noteworthy that *ortho*-unsubstituted benzamides afforded the corresponding products in lower yields with a mixture of styrenyl and allylic isomers. This revealed the necessity for the *ortho*-substitution to provide exclusively the β -H elimination product from the allylic proton in a unique manner *via* a conformationally-strained 7-membered metallacycle.

Table 23. Optimization studies for electrochemical cobalt(II)-catalyzed C–H allylation.^[a]



Entry	Additive	Solvent	Yield [%]
1	NaOAc	GVL	12
2	KOAc	GVL	8
3	Na ₂ CO ₃	GVL	19
4	PivOH	GVL	49
5	NaOPiv	GVL	60
6	NaOPiv	DCE	58
7	NaOPiv	TFE	28
8	NaOPiv	MeCN	27

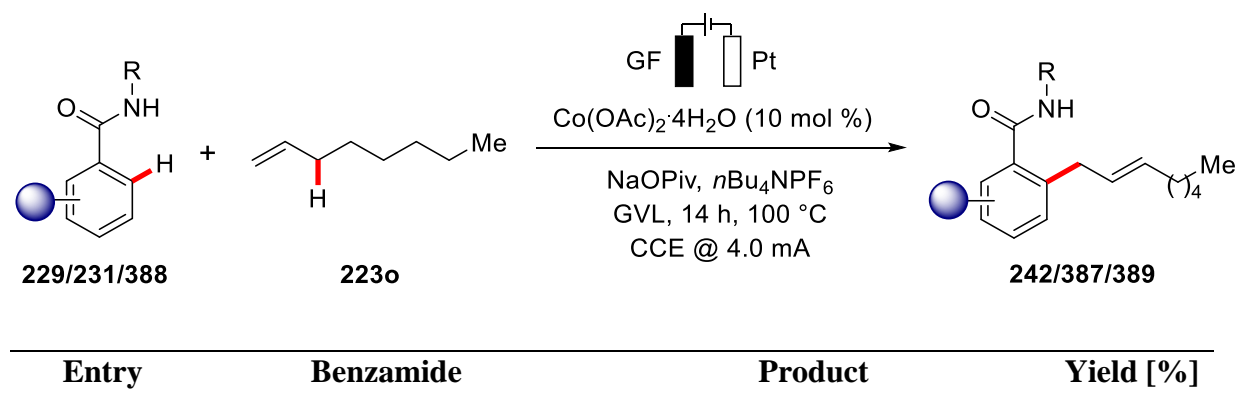
9	NaOPiv	MeOH/H ₂ O	---
10	NaOPiv	<i>t</i> BuOH/H ₂ O	---
11	NaOPiv	Choline chloride/Urea (1:2)	25 ^[b]
12	NaOPiv	GVL	52 ^[c]
13	NaOPiv	GVL	42 ^[d]
14	NaOPiv	GVL	--- ^[e]
15	NaOPiv	GVL	5 ^[f]

[a] General reaction conditions: **229f** (0.50 mmol), **223o** (1.50 mmol), Co(OAc)₂·4H₂O (10 mol %), additive (1.0 equiv), solvent (4.0 mL), *n*Bu₄NPF₆ (0.50 equiv), 100 °C, constant current at 4.0 mA, 14 h, GF anode (10 mm × 15 mm × 6 mm), Pt-plate cathode (10 mm × 15 mm × 0.25 mm), undivided cell, isolated yields. [b] In absence of *n*Bu₄NPF₆. [c] 120 °C. [d] 80 °C. [e] In absence of cobalt source. [f] No electricity.

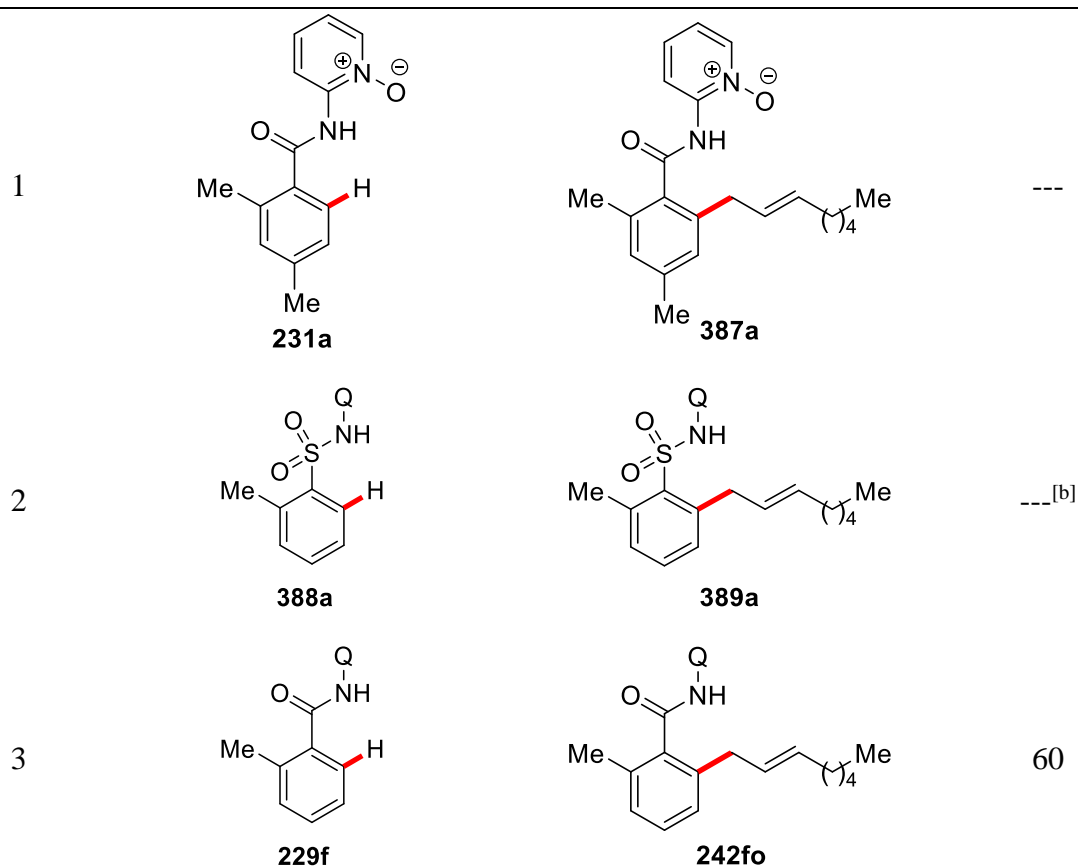
3.6.2. Substrate Scope and Limitations of the Electrochemical Cobalt-Catalyzed C–H Allylation

After establishing the optimized reaction conditions, we next tested various *N*-amide substituents in the cobalt-electro-catalyzed C–H allylation (Table 24). Pyridine-*N*-oxide **231a** which worked very efficiently for electrochemical cobalt-catalyzed C–H oxygenation,^[246] failed to deliver the allylated product **387a** (entry 1). In addition, the recently used sulfonamide **388a** for cobalt-catalyzed electrochemical alkyne annulation,^[274] proved to be inefficient for the desired C–H allylation reaction (entry 2).

Table 24. Effect of the orienting group on the electrochemical C–H allylation.^[a]



3. Results and Discussion

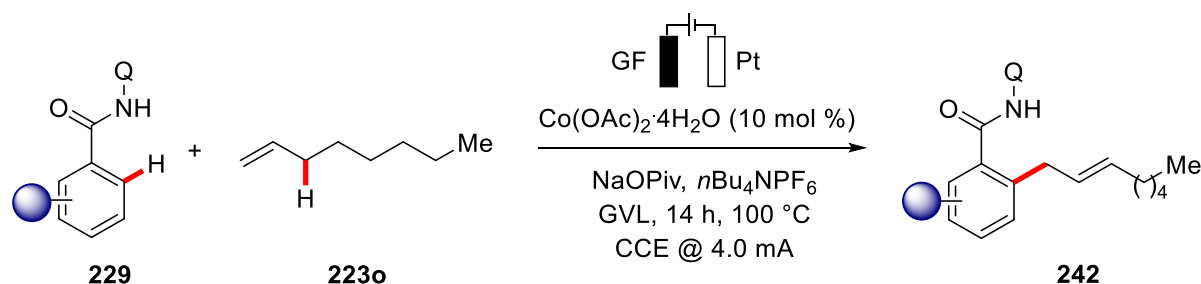


[a] Reaction conditions: Benzamide (0.50 mmol), **223o** (1.50 mmol), $\text{Co}(\text{OAc})_2 \cdot 4\text{H}_2\text{O}$ (10 mol %), NaOPiv (2.0 equiv), $n\text{Bu}_4\text{NPF}_6$ (0.50 equiv), GVL (4.0 mL), 100 °C, constant current at 4.0 mA, 14 h, GF anode (10 mm × 15 mm × 6 mm), Pt-plate cathode (10 mm × 15 mm × 0.25 mm), undivided cell, isolated yields. [b] Performed by *W. Li*.

With the optimized reaction conditions in hand, we next decided to assess the generality of the electrochemical cobalt-catalyzed C–H allylation (Table 25). The mild reaction conditions in undivided cell set-up proved viable for sterically-hindered benzamides and various functional groups. Initially, the robustness of the *ortho*-substituted benzamides **229** was explored with challenging *n*-octene, and independent of the steric influence, the desired products **242** were formed with excellent allylic selectivity. To our delight, and in contrast to previous work on cobalt-electro-catalyzed C–H oxygenations,^[246] which was severely limited to *ortho*-substituted benzamides, in this present study larger substituents including methoxy, trifluoromethyl and phenyl provided the corresponding products with excellent levels of allylic selectivity (entries 2-4). Fortunately, electron-rich and electron-deficient arenes were smoothly converted with high chemo-selectivity. Even sterically-bulky substituents at the 5-position of the benzamides **229i** and **229j** did not affect the selectivity, and only a slight decrease in yields

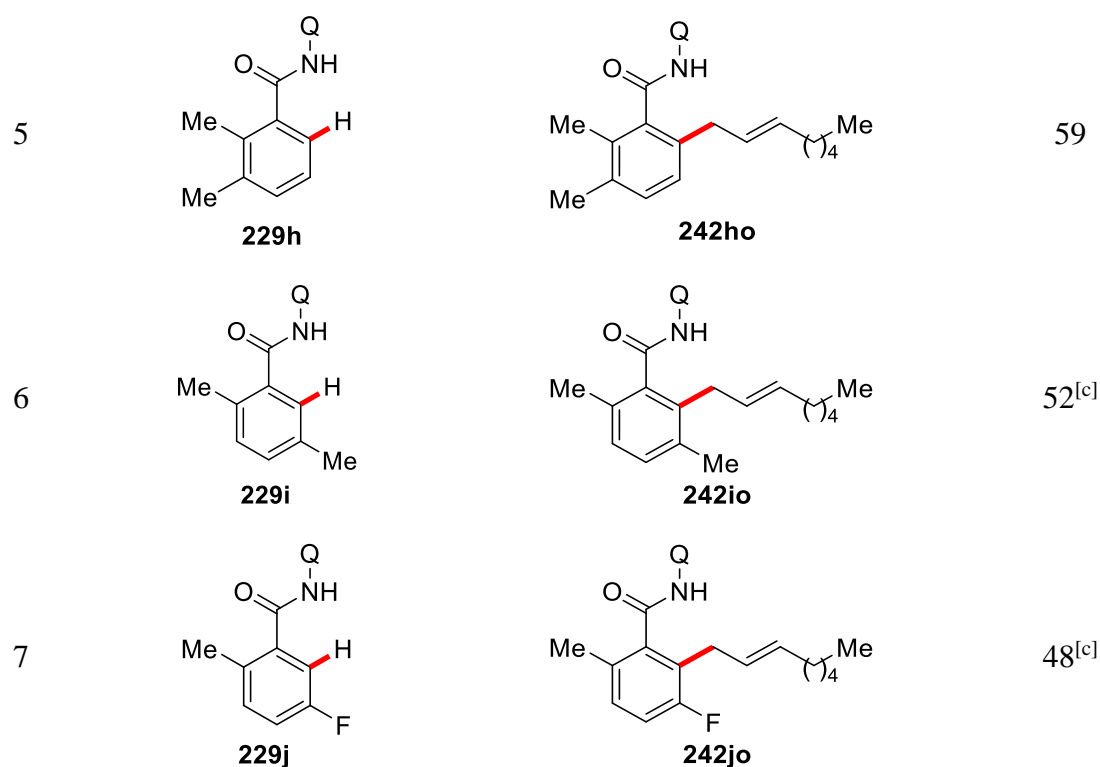
was observed (entries 6-7). In addition, halo-groups were tolerated, delivering the corresponding product **242jo** which should prove invaluable for further late-stage diversifications, highlighting the potential of the cobalt-electro-catalyzed C–H allylation approach.

Table 25. Cobalt-electro-catalyzed C–H allylation with benzamides **229**.^[a]



Entry	Benzamide	Product	Yield [%]
1	<p>229f</p>	<p>242fo</p>	60
2	<p>229e</p>	<p>242eo</p>	55 ^[b]
3	<p>229g</p>	<p>242go</p>	52
4	<p>229c</p>	<p>242co</p>	55

3. Results and Discussion

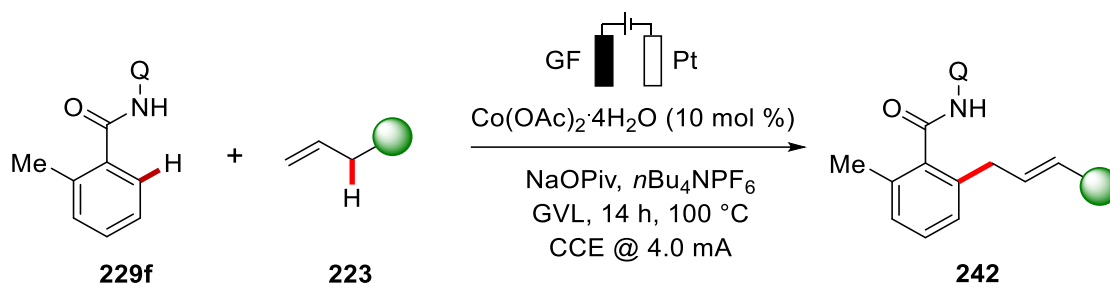


[a] Reaction conditions: **229** (0.50 mmol), **223o** (1.50 mmol), Co(OAc)₂·4H₂O (10 mol %), NaOPiv (2.0 equiv), *n*Bu₄NPF₆ (0.50 equiv), GVL (4.0 mL), 100 °C, constant current at 4.0 mA, 14 h, GF anode (10 mm × 15 mm × 6 mm), Pt-plate cathode (10 mm × 15 mm × 0.25 mm), undivided cell, isolated yields. [b] Co(OAc)₂·4H₂O (20 mol %). [c] Performed by Dr. C. Tian.

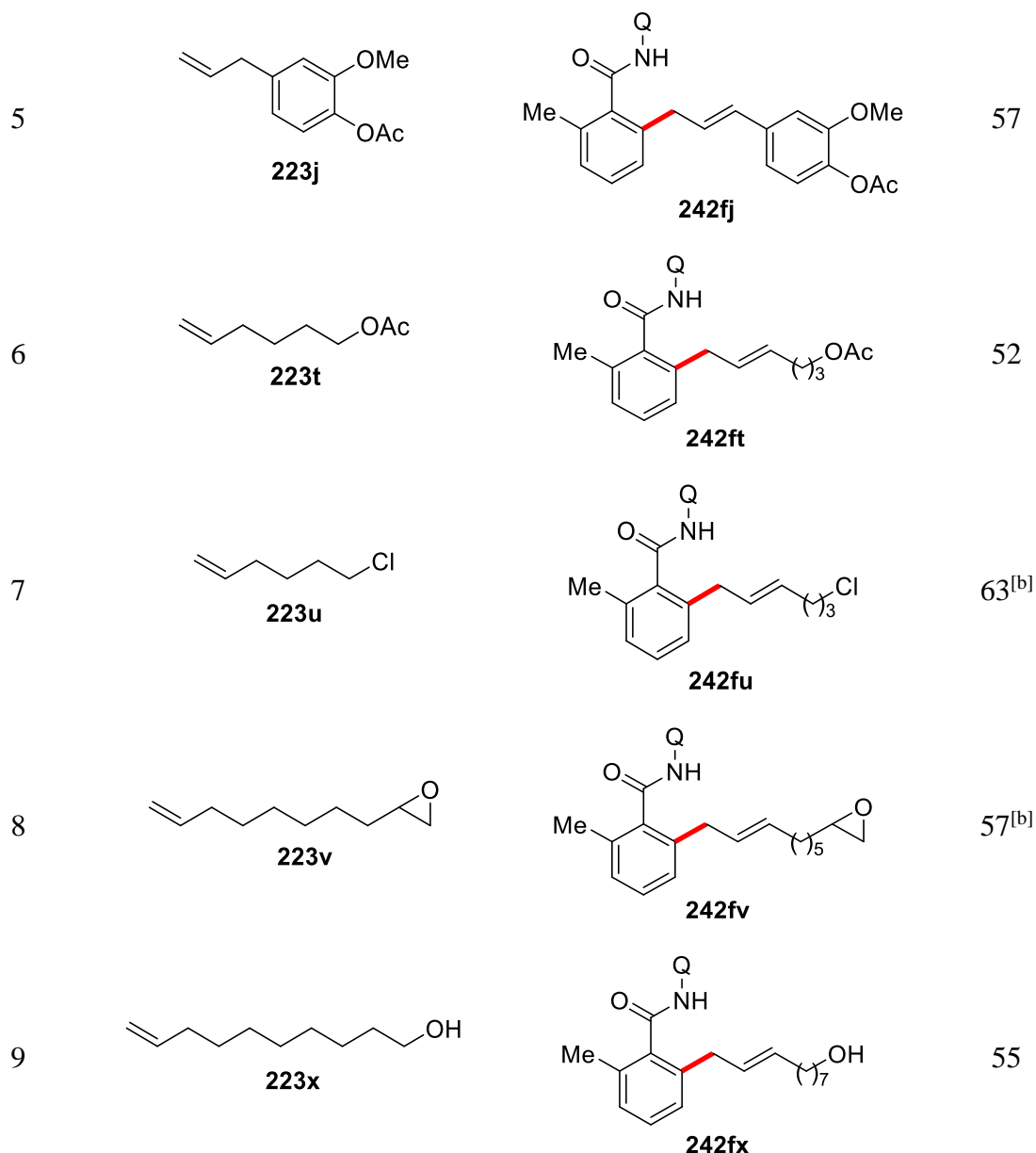
Next, we evaluated the viable substrate scope for unactivated alkenes **223** to demonstrate the synthetic utility of our transformation (Table 26). Interestingly, a variation in the extended alkyl chain length did not influence the efficacy of the electrocatalytic transformation. Under the optimized reaction conditions, both 1-decene **223q** and 1-nonene **223r** delivered the desired products **242fq** and **242fr**, respectively, in good yields (entries 1-2). Likewise, allyl benzene **223a** was exclusively transformed into the desired allylated product **242fa** (entry 3). Gratifyingly, the cobalt-electrocatalyzed C–H allylation proved applicable to the chemoselective mono-functionalization of diene **223s** to deliver allylated benzamide product **242fs**, demonstrating the unique selectivity features of this transformation without isomerization of the additional double bond (entry 4). Notably, various sensitive functional groups were fully tolerated by the versatile cobalt catalysis. Acetate-containing substrates **223j** and **223t** were efficiently converted to provide the corresponding allylated benzamides **242fj** and **242ft** in good yields (entries 5-6). It is noteworthy that chloro and epoxy groups were fully

tolerated, albeit a higher catalyst loading was employed here (entries 7-8). More delightfully, challenging the free hydroxyl group **223x** on the alkene was also well accepted (entry 9).

Table 26. Cobalt electro-catalyzed C–H allylation with unactivated alkenes **223**.^[a]



Entry	Alkene	Product	Yield [%]
1	 223q	 242fq	62
2	 223r	 242fr	64
3	 223a	 242fa	53
4	 223s	 242fs	53 ^[b]



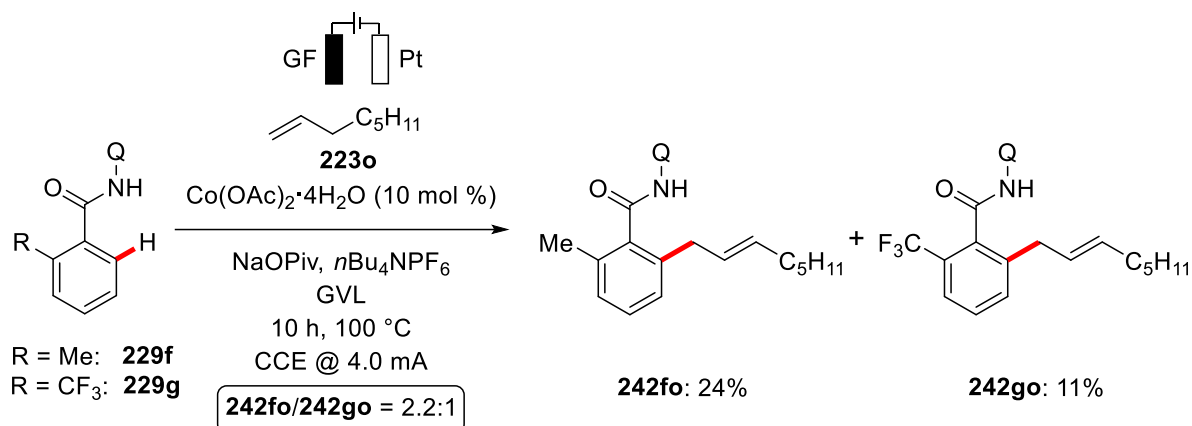
[a] Reaction conditions: **229f** (0.50 mmol), **223** (1.50 mmol), $\text{Co}(\text{OAc})_2 \cdot 4\text{H}_2\text{O}$ (10 mol %), NaOPiv (2.0 equiv), $n\text{Bu}_4\text{NPF}_6$ (0.50 equiv), GVL (4.0 mL), 100 °C, constant current at 4.0 mA, 14 h, GF anode (10 mm × 15 mm × 6 mm), Pt-plate cathode (10 mm × 15 mm × 0.25 mm), undivided cell, isolated yields. [b] $\text{Co}(\text{OAc})_2 \cdot 4\text{H}_2\text{O}$ (20 mol %).

3.6.3. Mechanistic Studies

After establishing the versatility of the first electrocatalytic C–H allylation, we were intrigued to delineate the catalyst's mode of action.

3.6.3.1. Competition Experiments

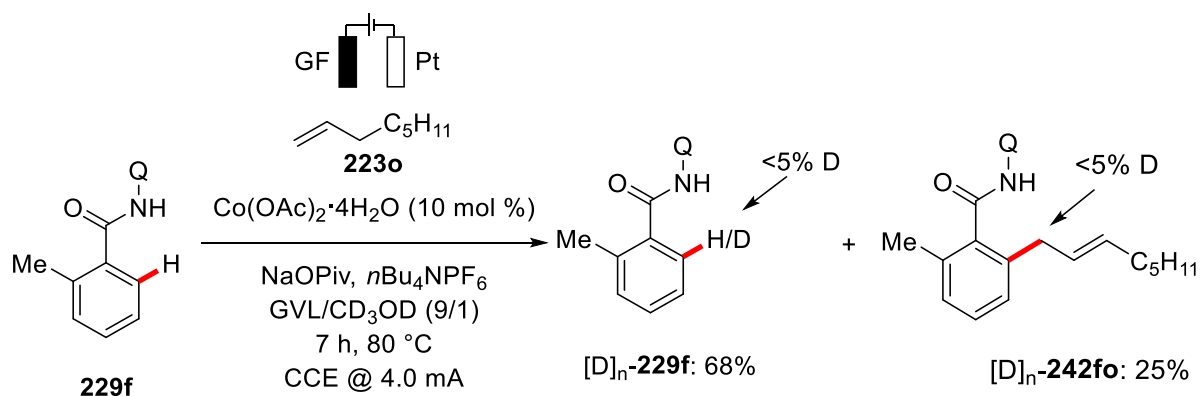
To this end, we carried out an intermolecular competition experiment with electronically distinct benzamides **229f** and **229g**, which clearly showed a preference for the electron-rich arene **242fo** to react inherently faster than the electron-poor analogue **242go** (Scheme 120). This supports a BIES mechanism.



Scheme 120. Competition experiments for cobalt-electrocatalyzed C–H allylation.

3.6.3.2. H/D Exchange Experiment

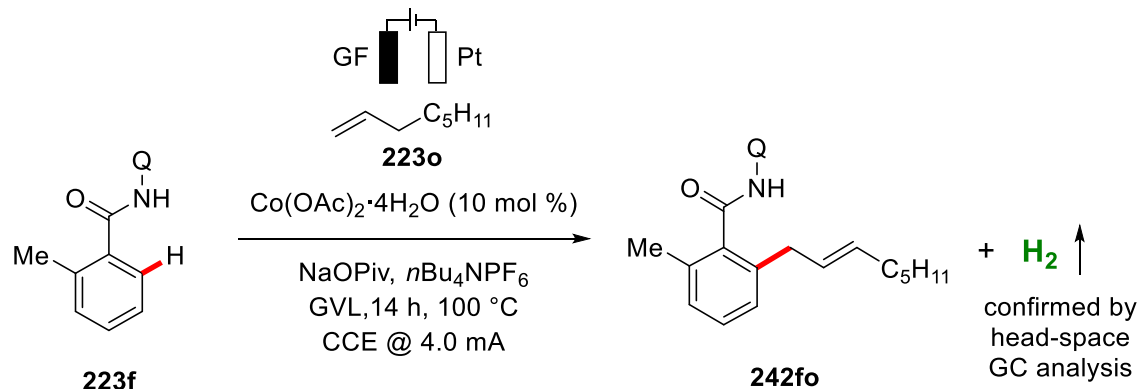
In addition, a H/D-exchange experiment was conducted using isotopically-labeled CD_3OD as the deuterated co-solvent under the optimized reaction condition, which showed no H/D crossover either in the product **242fo** or in the isolated starting material **229f** (Scheme 121). This observation suggests an irreversible C–H activation event to be operative for the cobalt-catalyzed C–H allylation.



Scheme 121. H/D exchange experiment for cobalt-electrocatalyzed C–H allylation.

3.6.3.3. Gas-Chromatographic Head-Space Analysis

Finally, *Dr. C. Tian* observed the formation of molecular hydrogen by gas-chromatographic head-space analysis, highlighting molecular hydrogen as the sole by-product formed through cathodic reduction (Scheme 122).



Scheme 122. Gas-chromatographic head-space analysis.

3.6.3.4. Cyclic Voltammetry Studies

Furthermore, detailed cyclic voltammetry studies were conducted by *Dr. C. Tian* in acetonitrile on the electrochemical cobalt(II)-catalyzed C–H allylation (Figure 3). While the amide substrate **229f** was oxidized at 1.46 V_{SCE}, interestingly the alkene **223o** did not show any relevant oxidation event. Finally, the *in-situ* generated cobalt catalyst showed a lower oxidation potential at 1.19 V_{SCE}. This observation strongly supports an initial anodic cobalt(II/III) single-electron oxidation.

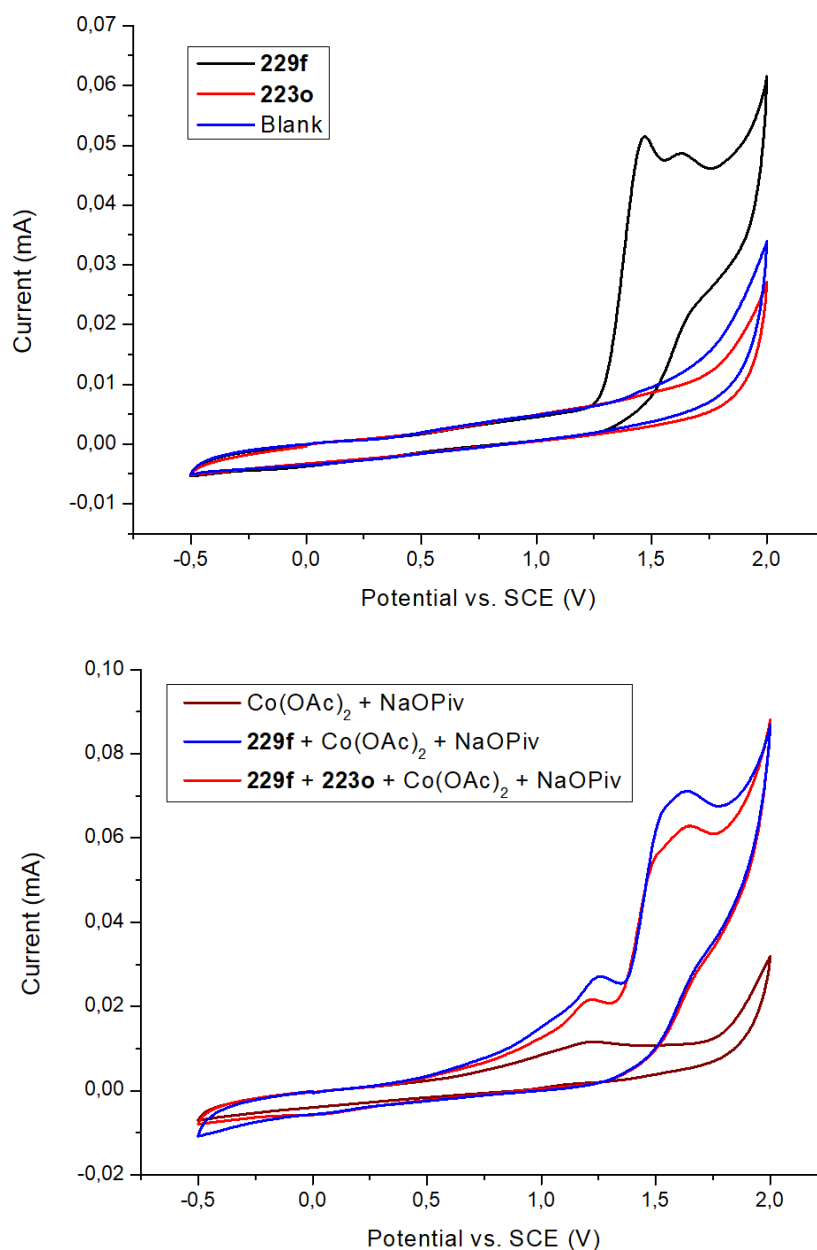


Figure 3. Cyclic voltammetry.

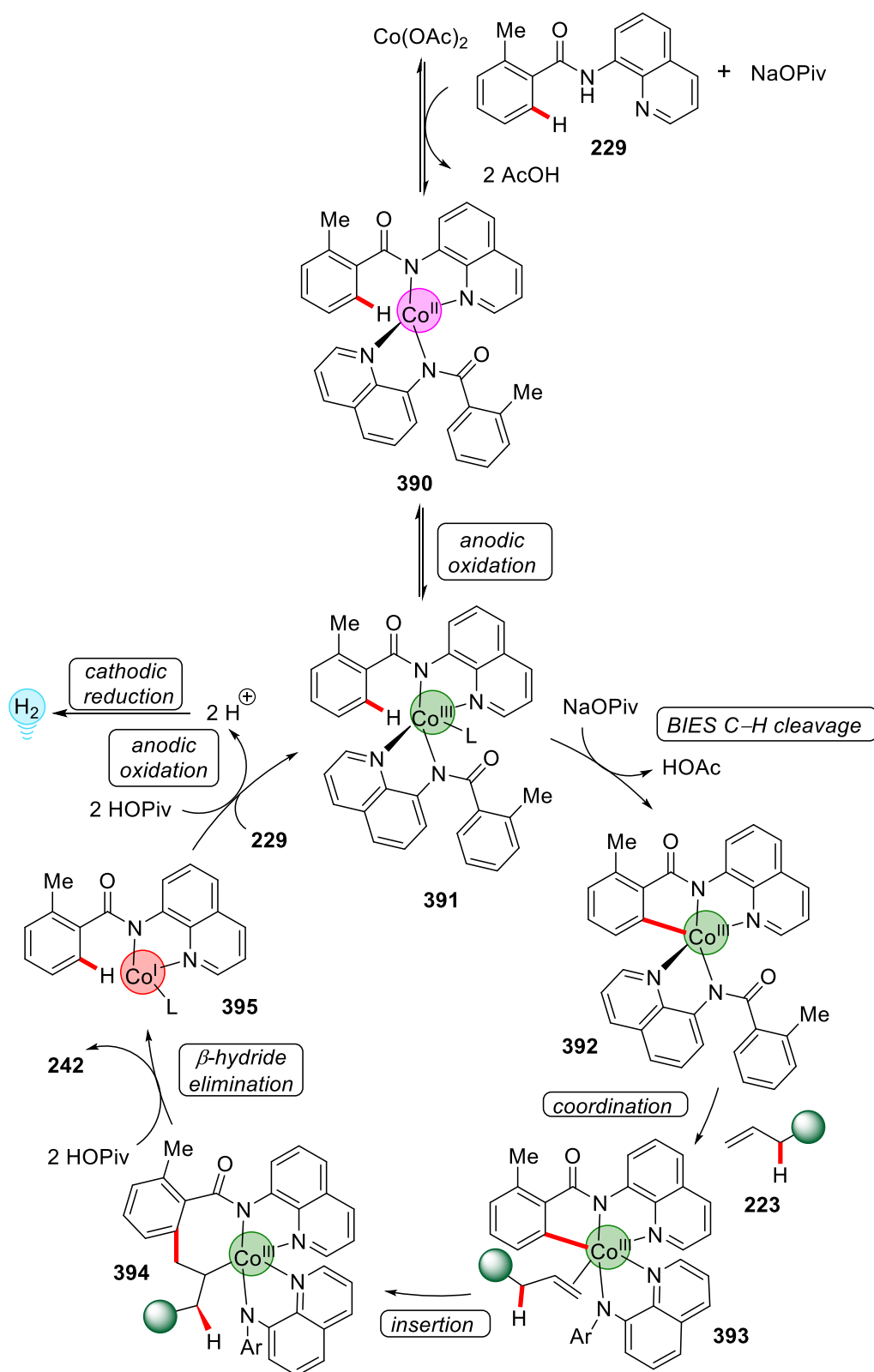
General condition: DMA, 0.1 M *n*Bu₄NPF₆, 5 mM HOAc, 5 mM substrates, 100 mV/s.

3.6.4. Proposed Catalytic Cycle

In accordance with recent findings^[275] and on the basis of our mechanistic findings, we have depicted a plausible catalytic cycle for the cobalt-catalyzed electrochemical C–H allylation (Scheme 123). Here electrochemical cobalt(II)-catalyzed C–H allylation is likely initiated by anodic cobalt oxidation to generate the cobalt(III) species **391**. After generation of the active cobalt(III) species **391**, the carboxylate-assisted C–H scission occurs by irreversible, BIES-

3. Results and Discussion

type mechanistic pathways to form the 5-membered cobaltacycle **392** as supported by H/D-exchange experiment and competition experiment. Thus formed cyclometalated cobalt complex undergoes alkene co-ordination to afford **393** and subsequent 1,2-migratory insertion with the non-activated alkene **223** forms the conformationally strained 7-membered metallacycle **394**. Next the 7-membered metallacycle **394** undergoes β -hydride elimination exclusively from the allylic proton, releasing the desired product **242** with allylic selectivity. Finally, the cobalt(I) species **395** is oxidized to the active cobalt(III) catalyst **391** by anodic oxidation to complete the catalytic cycle. Notably, the cathodic half-reaction formed H₂ as the sole stoichiometric byproduct, showcasing the sustainability of the electrochemical oxidative allylation.



Scheme 123. Proposed catalytic cycle for cobalt electro-catalyzed C-H allylation.

3.7. Enantioselective Palladaelectro-Catalyzed C–H Activations

Electrochemical oxidations have been well studied for the last few decades, since they offer an attractive approach by the utilization of electric current to obviate the use of toxic and expensive reagents. In recent years, significant advances have been realized by the merger of electrocatalysis with organometallic C–H activations, using electrons as green redox equivalents.^[232] Major progresses in electrochemical palladium catalyzed C–H activations have been realized by strong *N*-directing groups.^[234-236, 238-239, 240b, 241, 276] Despite these significant advances, electrochemical enantioselective C–H activations are thus far unknown.^[277] Possibly cathodic catalyst reduction as well as electrochemical degradation of the chiral ligands make the asymmetric metallaelectro-catalysis an extremely challenging research area.

Considering the importance of axially-chiral biaryls as key structural motifs in various catalysts,^[278] ligands^[279] and natural products,^[280] we were interested in the development of the first electrochemical enantioselective synthesis of axially chiral biaryls. It is noteworthy that since the early, albeit moderately selective report on rhodium(I)-catalyzed C–H alkylations of arylpyridines, atroposelective syntheses of axially-chiral biaryls have become a major research area (*cf.* chapter 1.3.1.).^[281] Notably, Shi employed chiral transient directing groups for the efficient synthesis of axially-chiral biaryls.^[41a] Despite these advances, these transformations are often limited to the use of toxic oxidants. Hence, we became interested in the development of an atroposelective synthesis of axially-chiral biaryls with the aid of transient directing groups, employing electricity as the redox agent. Furthermore, it should be duly noted that transient directing groups had never been used before in electrochemical C–H activation reactions.

3.7.1. Optimization Studies

For the development of the first enantioselective electrochemical metal-catalyzed C–H activation, we were interested in the advancement of atroposelective C–H activation of biaryls under sustainable electrochemical conditions (Table 27). We began our investigations by evaluating a series of weakly-coordinating transient directing groups for the envisioned atroposelective electrocatalyzed C–H olefination of biaryls **73a** with *n*-butyl acrylate **38a**. We started our optimization with several α -amino acids to access highly enantioenriched axially chiral biaryls **74aa** with synthetically useful formyl groups (entries 1-5). Thus, we found that *L*-*tert*-leucine was the best TDG for this atroposelective transformation, delivering the desired product with 53% yield and 97% ee (entry 5). Electrolytes always play a significant role in the

outcome of electrochemical reactions. Thus, we tested other electrolyte additives, such as NaOAc, KOAc, NaOPiv and *n*Bu₄NPF₆, which provided inferior results as compared to LiOAc (entries 6-9). This finding suggested that the additive played an important role for the successful outcome of the reaction, thus operating both as an electrolyte and a base for the carboxylate-assisted C–H bond cleavage (*vide infra*). It is noteworthy that AcOH has been found as a commonly used solvent for palladium-catalyzed electrochemical C–H activation reactions. In line with previous literatures, we observed AcOH indeed to be the optimal solvent, possibly playing a crucial role in the *in situ* formation of the imine species. When we employed only TFE as the reaction medium, we did not observe any reactivity whereas a mixture of TFE and AcOH provided the product **74aa** in moderate yield and with high enantioselectivity (entries 10-11). Prolonging the reaction time, delivered the C–H olefinated product in 71% yield and 97% ee (entry 12). Notably, the enantioselective metallaelectro-catalysis also occurred under an inert atmosphere, albeit with reduced efficiency (entry 14). In stark contrast to the use of chemical oxidants,^[89] a redox mediator was not required for efficient metallaelectro-catalysis, as we observed that commonly used redox mediators such as benzoquinone, failed to improve the reactivity to a large extent. Control experiments confirmed the necessity of the TDG, the electricity and the palladium catalyst (entries 15-17).

Table 27. Optimization of the atroposelective electrocatalyzed C–H olefination.^[a]

Entry	TDG	Additive	Solvent	Yield [%]	ee [%] ^[b]
1	L-valine	LiOAc	AcOH	35	48 ^[c]
2	L-Phenylglycine	LiOAc	AcOH	37	40
3	L-tryptophan	LiOAc	AcOH	21	68 ^[c]
4	H-Asp(<i>O</i> tBu)-OH	LiOAc	AcOH	55	20
5	L- <i>tert</i> -leucine	LiOAc	AcOH	53	97
6	L- <i>tert</i> -leucine	NaOAc	AcOH	47	99

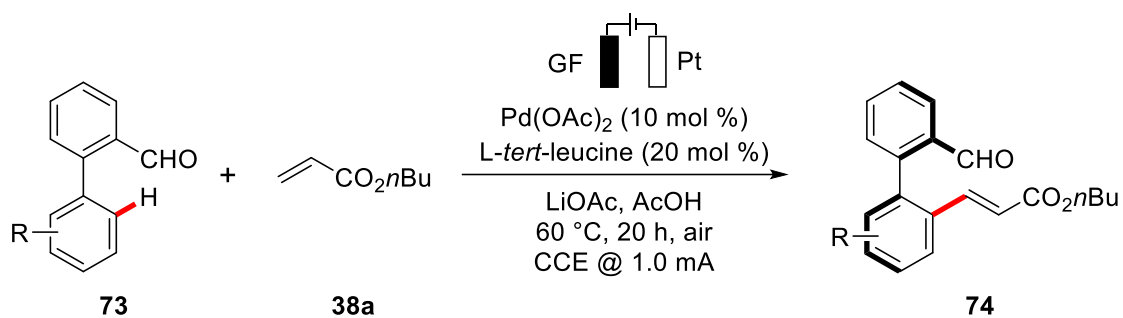
3. Results and Discussion

7	<i>L-tert-leucine</i>	KOAc	AcOH	45	98
8	<i>L-tert-leucine</i>	NaOPiv	AcOH	50	96
9	<i>L-tert-leucine</i>	<i>n</i> Bu ₄ NPF ₆	AcOH	48	99
10	<i>L-tert-leucine</i>	---	TFE	---	---
11	<i>L-tert-leucine</i>	---	TFE/AcOH	46	99
12	<i>L-tert-leucine</i>	LiOAc	AcOH	71	97^[d]
13	<i>L-tert-leucine</i>	LiOAc	AcOH	66	97 ^[d,e]
14	<i>L-tert-leucine</i>	LiOAc	AcOH	43	97 ^[d,f]
15	---	LiOAc	AcOH	---	---
16	<i>L-tert-leucine</i>	LiOAc	AcOH	25	97 ^[g]
17	<i>L-tert-leucine</i>	LiOAc	AcOH	---	--- ^[h]

[a] Reaction conditions: Undivided cell, **73a** (0.20 mmol), **38a** (0.60 mmol), [Pd] (10 mol %), TDG (20 mol %), additive (2.0 equiv), solvent (4.5 mL), 60 °C, constant current at 1.0 mA, 14 h, GF anode (10 mm × 15 mm × 6 mm), Pt-plate cathode (10 mm × 15 mm × 0.25 mm), isolated yields. [b] Enantioselectivities determined by chiral HPLC. [c] Performed by *Dr. C. Tian*. [d] 20 h. [e] **38a** (2.0 equiv). [f] Under N₂. [g] Without electricity. [h] No palladium.

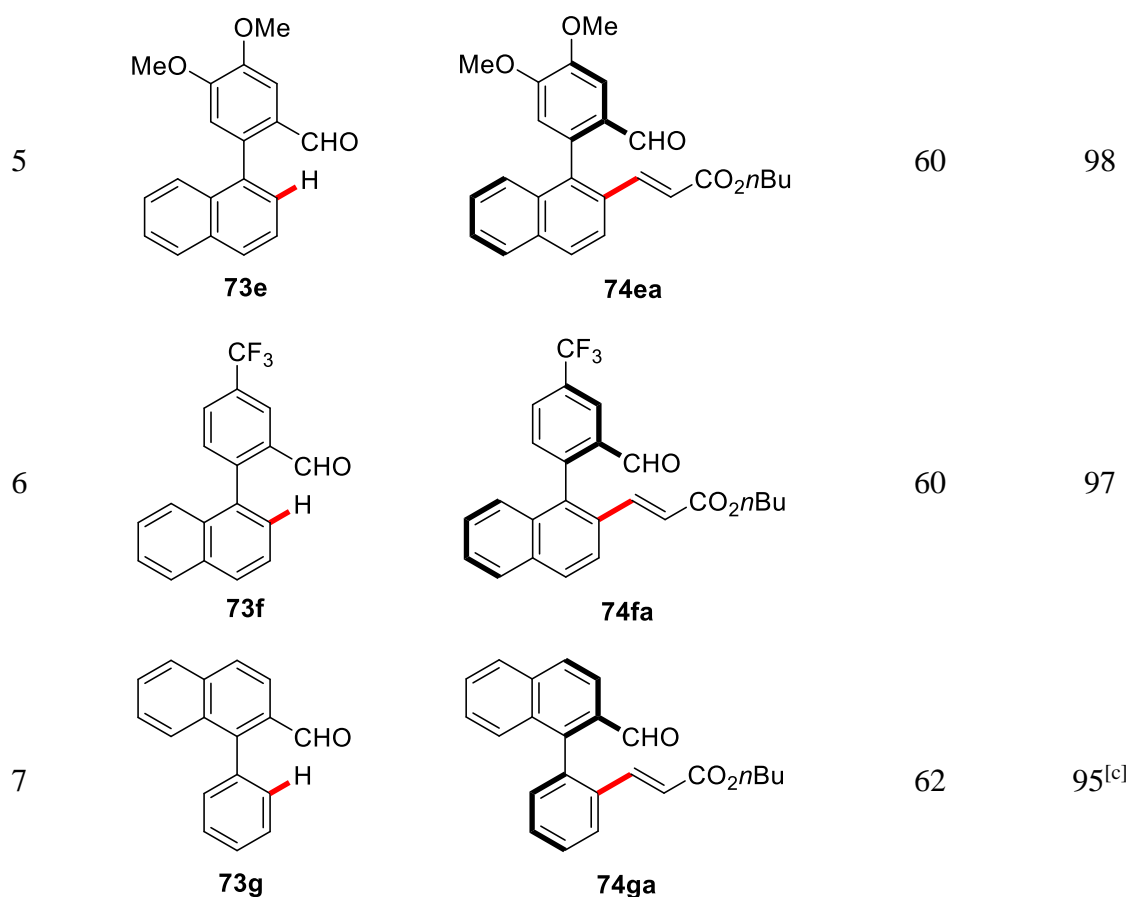
3.7.2. Substrate Scope of Atroposelective Electrocatalyzed C–H Olefination

With the optimized reaction conditions in hand, we explored the generality of the enantioselective palladaelectro-catalysis (Table 28). First, electron-rich and electron-deficient racemic biaryls **73** were tested. To our delight, all the corresponding axially chiral compounds **74** were formed with good yields and in excellent enantioselectivities, reflecting very little effect of the electronic properties of the substituents on the outcome of the electrocatalysis (entries 1-7).

Table 28. Atroposelective electro-catalyzed C–H olefination of biaryls **73**.^[a]

Entry	Biaryl	Product	Yield [%]	<i>ee</i> [%] ^[b]
1			71	97
2			66	95
3			71	95
4			54	99

3. Results and Discussion



[a] Reaction conditions: Undivided cell, **73** (0.20 mmol), **38a** (0.60 mmol), Pd(OAc)₂ (10 mol %), *L-tert*-Leucine (20 mol %), LiOAc (2.0 equiv), AcOH (4.5 mL), 60 °C, constant current at 1.0 mA, 20 h, GF anode (10 mm × 15 mm × 6 mm), Pt-plate cathode (10 mm × 15 mm × 0.25 mm), isolated yields. [b] Enantioselectivities determined by chiral HPLC. [c] Performed by *J. Hao*.

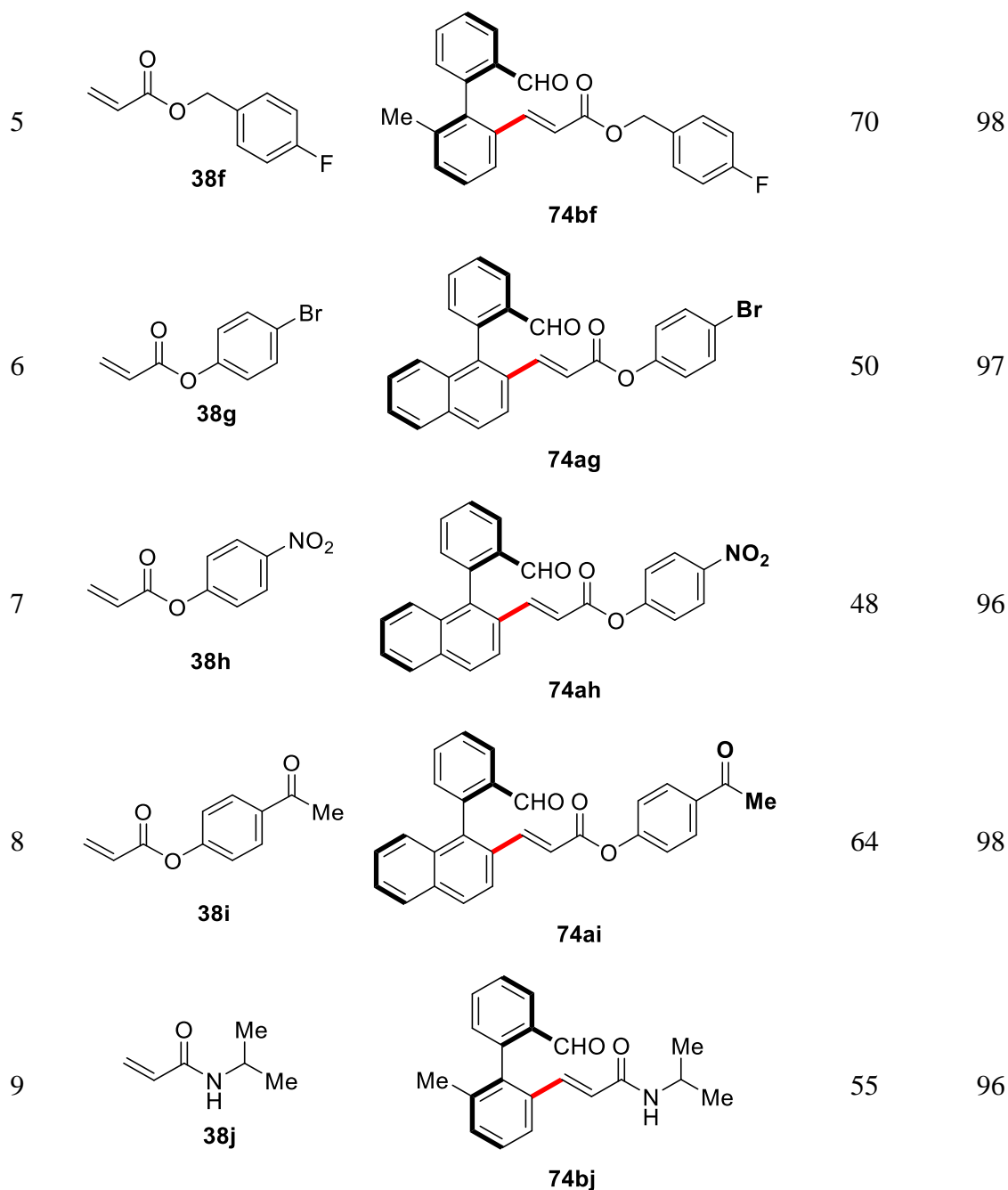
Second, a broad range of alkene coupling partners was investigated under our optimized electrochemical conditions (Table 29). α,β -Unsaturated olefins **38** served as particularly effective coupling partners in this reaction conditions. Vinyl sulfone **38b** and vinyl phosphonate **38c** were efficiently installed through atroposelective C–H activation in moderate to good yields and in excellent enantioselectivities (entries 1-2). Notably, methyl vinyl ketone **38d** was also compatible, delivering the olefinated product **74bd** in high enantioselectivity (entry 3). To our delight, various sensitive functional groups, like fluoro- (**38f**), bromo- (**38g**), nitro- (**38h**) and carbonyl (**38i**) substituents, on the arene were well tolerated, which should prove invaluable for further late stage modifications. In contrast, alkenes containing bromo- (**38j**) or nitro- (**38h**) groups exhibited lower reactivity to deliver the corresponding products

(entries 4-8). Remarkably, acrylamide (**38j**) was also compatible with our robust catalyst to furnish the axially-chiral biaryl **74bj** with very high levels of enantio-induction (entry 9).

Table 29. Atroposelective palladaelectro-catalysis with alkenes **38**.^[a]

Entry	Alkene	Product	Yield [%]	<i>ee</i> [%] ^[b]
1	 38b	 74ab	52	98
2	 38c	 74ac	68	99
3	 38d	 74bd	64	98
4	 38e	 74ae	68	98

3. Results and Discussion



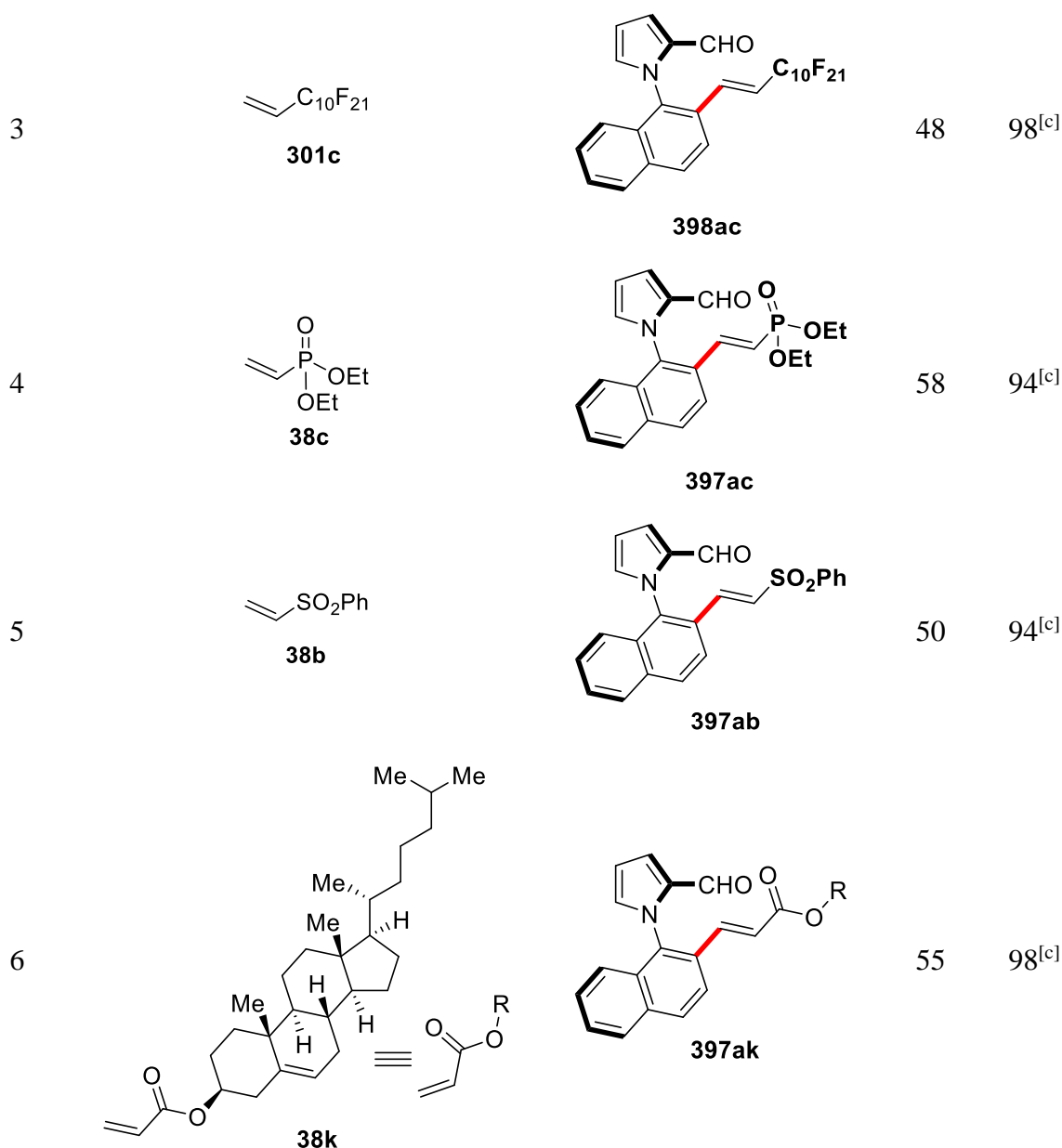
[a] Reaction conditions: Undivided cell, **73** (0.20 mmol), **38** (0.60 mmol), Pd(OAc)₂ (10 mol %), *L-tert*-Leucine (20 mol %), LiOAc (2.0 equiv), AcOH (4.5 mL), 60 °C, constant current at 1.0 mA, 20 h, GF anode (10 mm × 15 mm × 6 mm), Pt-plate cathode (10 mm × 15 mm × 0.25 mm), isolated yields. [b] Enantioselectivities determined by chiral HPLC.

We were pleased to observe that the palladaelectro-catalysis was not only limited to the conversion of racemic biaryls **73**. Indeed, the electrocatalysis also set the stage for the synthesis of N–C axially-chiral motifs^[92a, 93] (Table 30). To improve the conversion, a slightly higher loading of TDG was employed for the synthesis of axially chiral N–C scaffold **397** and **398**.

To demonstrate the generality of our transformation, we tested the scope of olefin coupling partners with *N*-aryl pyrrole **396** as the model substrate. Thus, *N*-C axially-chiral *N*-aryl pyrroles **397** and **398** were obtained under the electrochemical conditions in a site- and highly enantio-selective fashion (entry 1). Other than α,β -unsaturated olefins, perfluoroalkylalkenes **301a** and **301c** were also compatible to enable unprecedented C–H perfluoroalkenylations (entries 2-3). Thus, this protocol provided a highly enantioselective strategy to deliver synthetically useful axially-chiral fluorinated heterobiaryls **398aa** and **398ac** in moderate to good yields. Similarly, vinyl phosphonate (**38c**), vinyl sulfone (**38b**) and cholesterol derivative (**38k**) were also identified as suitable coupling partners for the synthesis of versatile *N*-C axially chiral scaffolds with high levels of enantio-induction (entries 4-6).

Table 30. Atroposelective palladaelectro-catalyzed C–H olefination of *N*-aryl pyrroles.^[a]

Entry	Alkene	Product	Yield [%]	<i>ee</i> [%] ^[b]
1	 38a	 397aa	56	99
2	 301a	 398aa	52	98



[a] Reaction conditions: Undivided cell, **396** (0.20 mmol), **38/301** (0.60 mmol), Pd(OAc)₂ (10 mol %), *L*-*tert*-Leucine (30 mol %), LiOAc (2.0 equiv), AcOH (4.5 mL), 60 °C, constant current at 1.0 mA, 20 h, GF anode (10 mm × 15 mm × 6 mm), Pt-plate cathode (10 mm × 15 mm × 0.25 mm), isolated yields. [b] Enantioselectivities determined by chiral HPLC. [c] Performed by *J. Hao*.

3.7.3. Mechanistic Studies

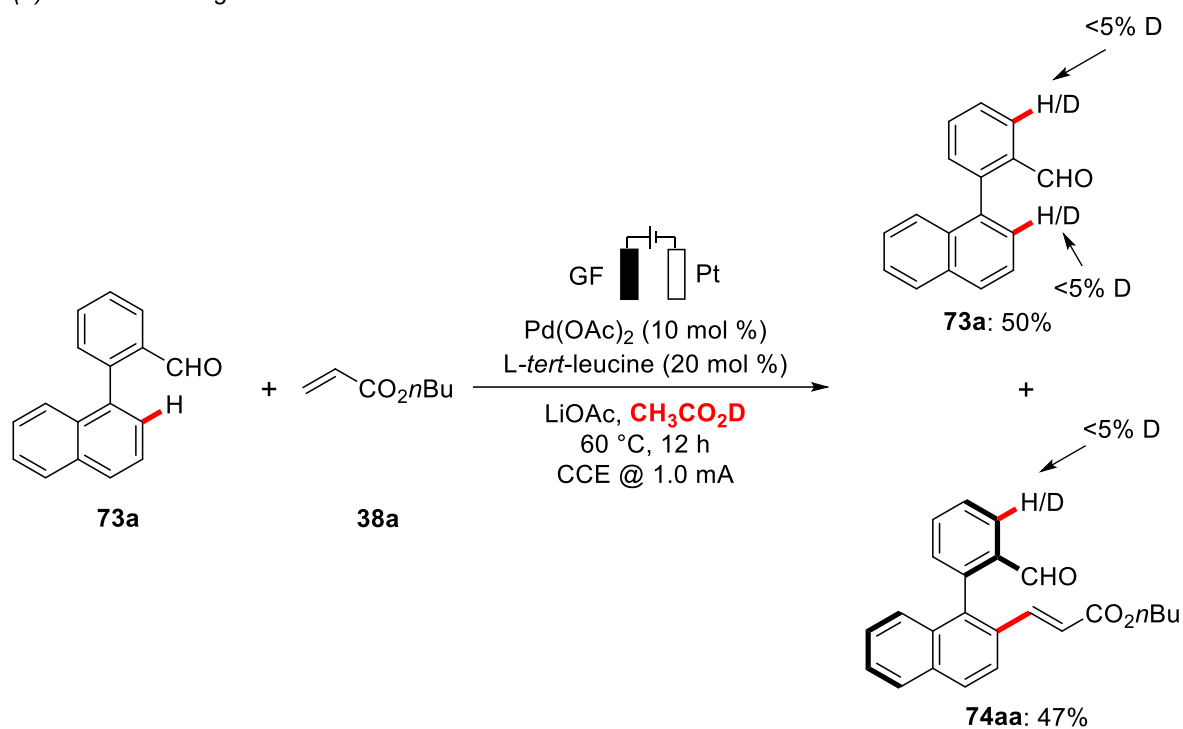
After establishing a broad scope for the first atroposelective pallada-electrocatalyzed C–H activation, detailed experimental and computational mechanistic studies were performed to gain insights into its mode of action.

3.7.3.1. H/D Scrambling and KIE Studies

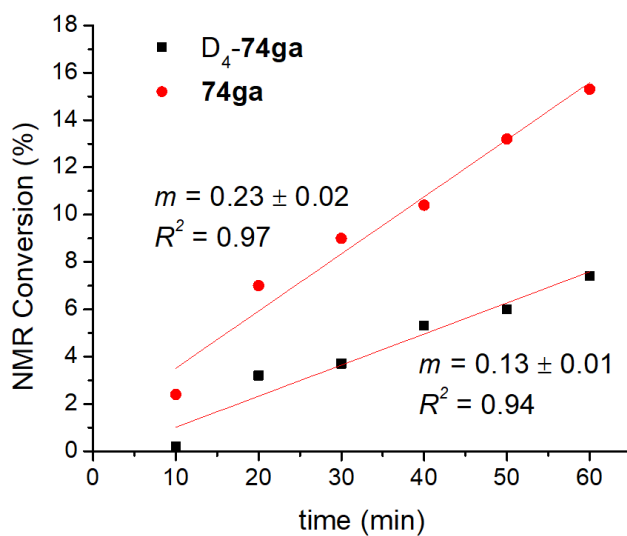
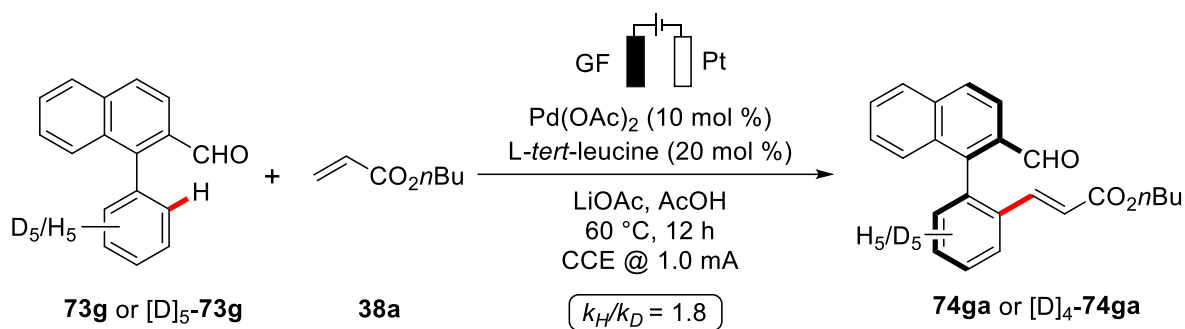
First, a H/D exchange experiment was conducted using AcOD as the solvent (Scheme 124a). We did not observe a H/D scrambling neither in the product **74aa** nor in the recovered starting material **73a**. Second, a KIE was studied by two independent reactions with isotopically labeled compound [D]₅-**73g**, which showed a KIE of $k_H/k_D \approx 1.8$ (Scheme 124b). These findings from H/D scrambling experiments and KIE experiments suggests the C–H cleavage step is the rate-determining step.

3. Results and Discussion

(a) H/D scrambling



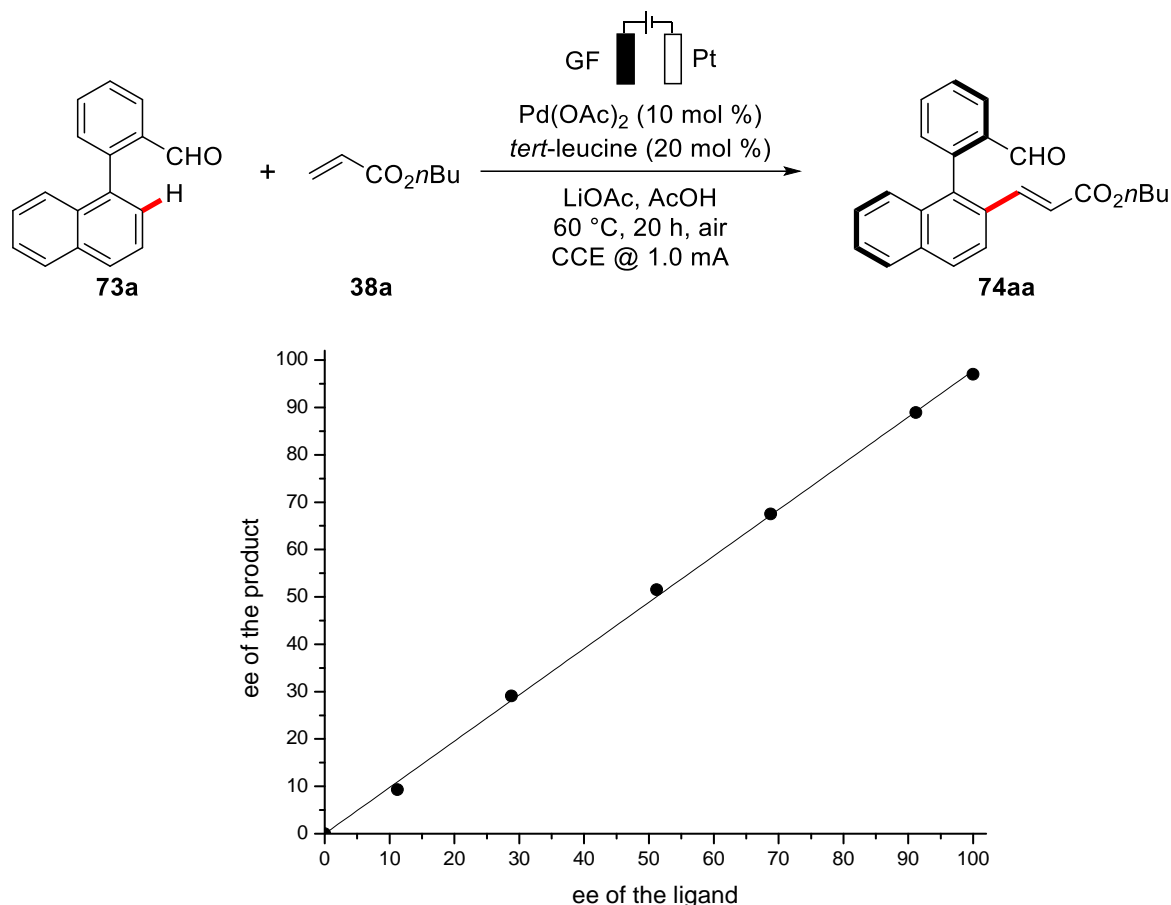
(b) KIE Studies



Scheme 124. H/D scrambling and KIE studies for the pallada-electrocatalysis.

3.7.3.2. Non-Linear Effect Studies

To gain insights into the ligand-to-metal ratio in the atroposelective pallada-electrocatalysis, the effect of the enantiomeric excess of *L-tert*-Leucine on the enantiomeric induction of the electrochemical transformation was studied (Scheme 125). Here, we did not observe a non-linear effect (NLE), which excludes a multi-ligand containing catalyst or oligomeric species, instead it is indicative of the enantio-determining step involving a metal to ligand ratio of 1:1.



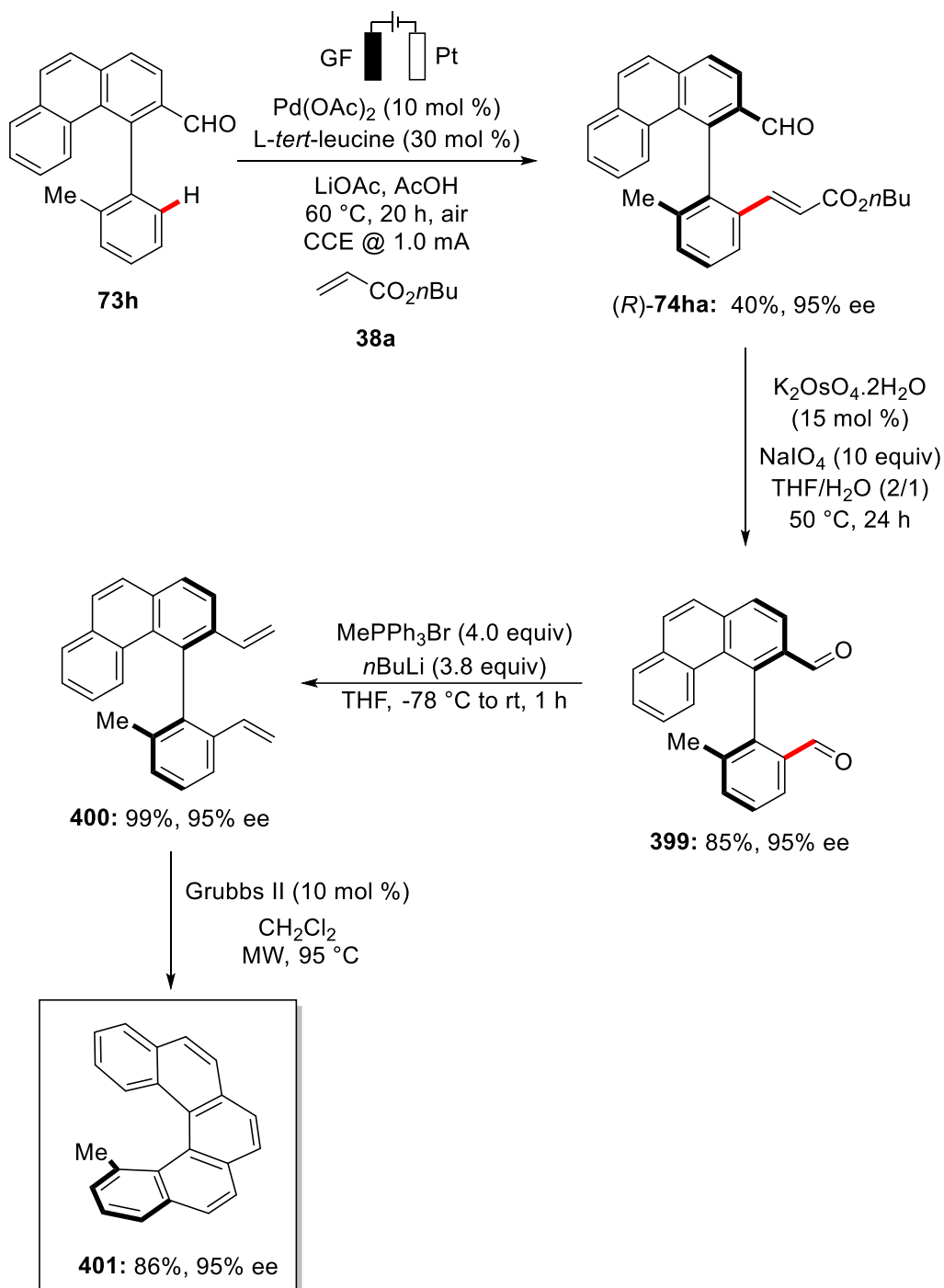
Scheme 125. Non-linear effect studies for the pallada-electrocatalysis.

3.7.4. Product Diversification

As previously described axially chiral compounds are very important building blocks,^[278-280] thus the synthetic value of the palladium-catalyzed electrochemical C–H olefination was demonstrated by the late-stage diversification of thus-obtained highly enantiomerically-enriched biaryls (Scheme 126-128). In this context, straightforward asymmetric synthesis of enantiopure helicenes are in high demand.^[282] To this end, we performed a kinetic resolution on conformationally stable aldehyde **73h** under otherwise optimal reaction conditions. The desired olefinated product **74ha** was obtained with 95% ee. Then, the addition of K₂O₈O₄ and

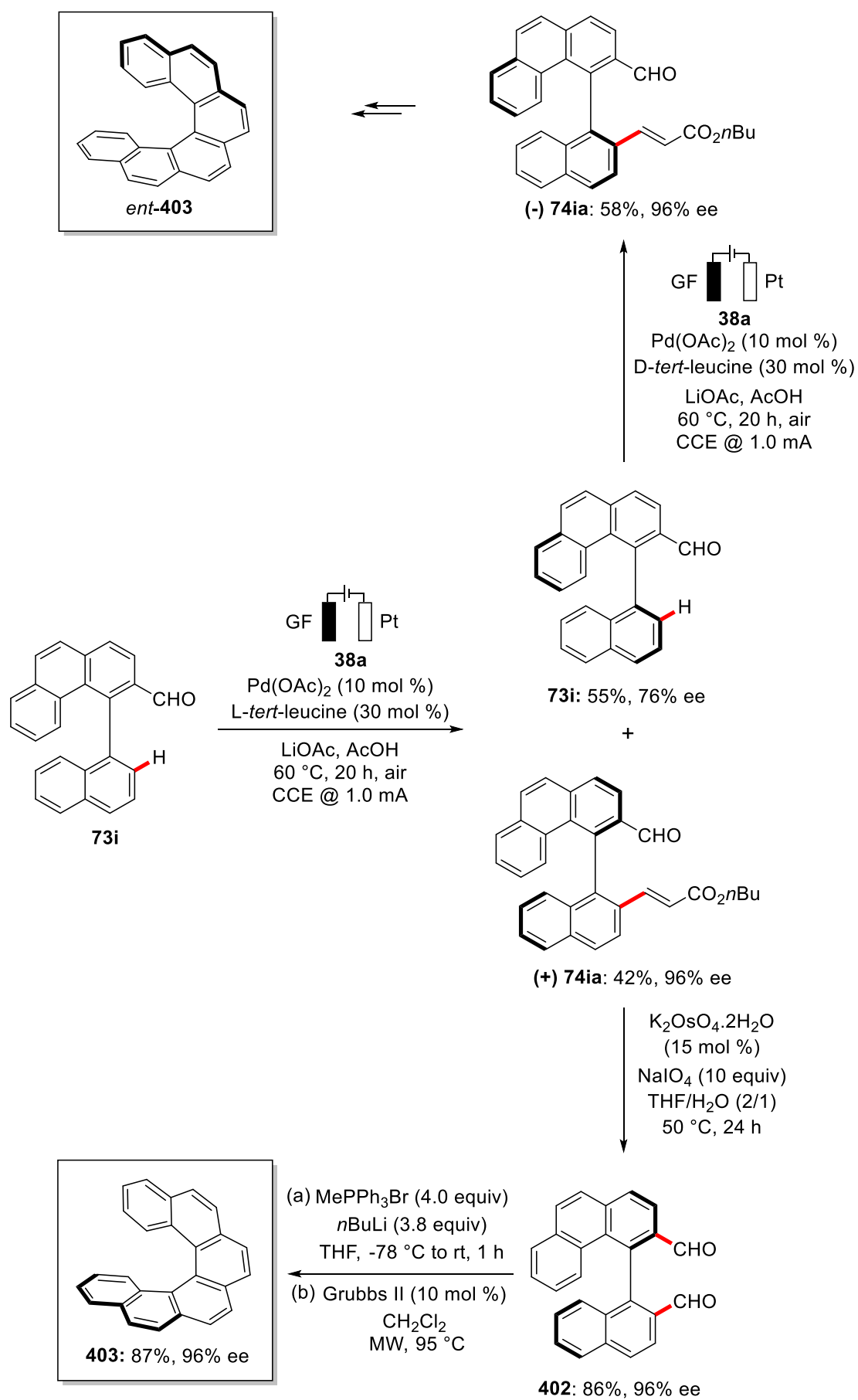
3. Results and Discussion

NaIO₄ enabled the preparation of dialdehyde **399** in high yield by oxidative double bond cleavage. Subsequently, a Wittig reaction and a catalyzed olefin- metathesis provided the highly enantioenriched [5]-helicene **401** in overall good yield and in excellent optical yield (Scheme 126). Likewise, a similar strategy was followed for the synthesis of chiral [6]-helicene starting from conformationally stable aldehyde **73i**. Here [6]-helicene **403** was obtained in overall high yield and enantioselectivity (Scheme 127). In addition, the recovered starting material **73i**, after the kinetic resolution, was treated under the optimized reaction conditions using *D-tert*-Leucine as the TDG. Subsequently, the opposite enantiomer of the olefinated product **74ia** was obtained which can be converted to the opposite enantiomer *ent*-[6]-helicene **403** following the same path. Furthermore, the synthetic utility of our method was reflected by the synthesis of chiral dicarboxylic acid **404** and chiral BINOL **405** (Scheme 128). Dialdehyde **402** was treated under Pinnick oxidation conditions, delivering the dicarboxylic acid **404** while Baeyer-Villiger-oxidation gave the chiral BINOL **405**. These new chiral molecules should find various applications as ligands for asymmetric catalysis.

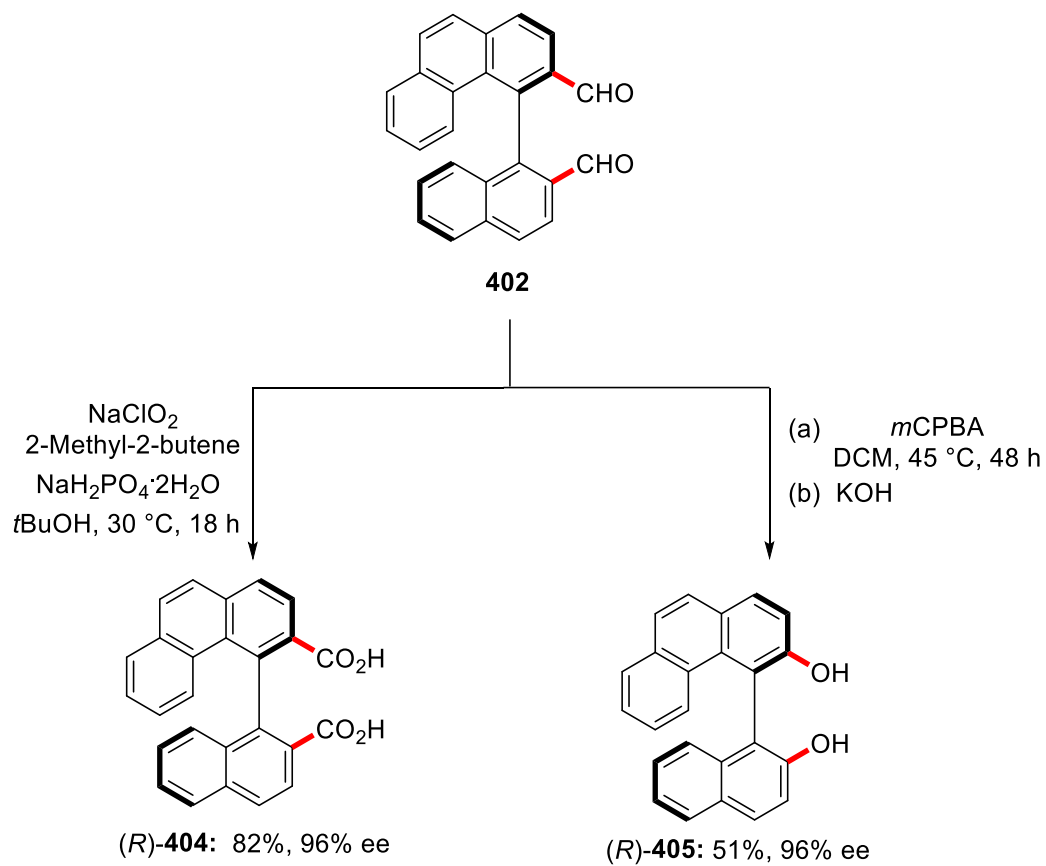


Scheme 126. Synthesis of enantioenriched [5]-helicene.

3. Results and Discussion



Scheme 127. Synthesis of enantioenriched [6]-helicene.

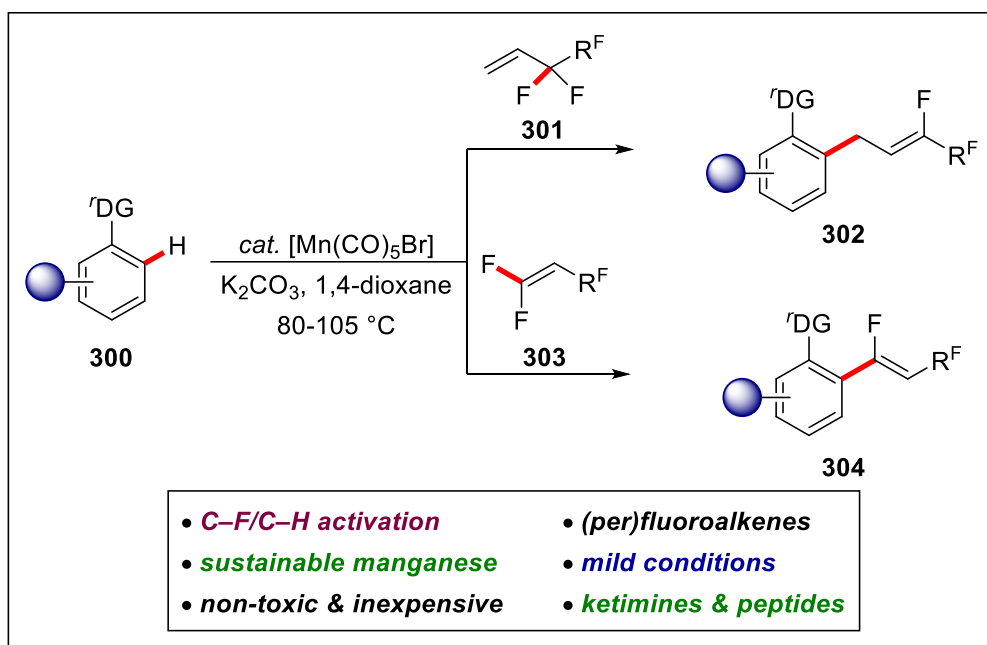


Scheme 128. Late-stage diversification to chiral diacid and substituted BINOL.

4. Summary and Outlook

The advent of new synthetic strategies has enriched the synthetic organic chemistry to access molecules with tremendous complexity. In this context, transition metal-catalyzed C–H activation has emerged as a powerful tool for highly step- and atom- economical synthesis that avoids laborious prefunctionalizations of starting materials.^[27, 56] In this thesis, the primary focus was the development of novel and sustainable methods by direct C–H activation to synthesize value-added synthetic targets of biological importance.

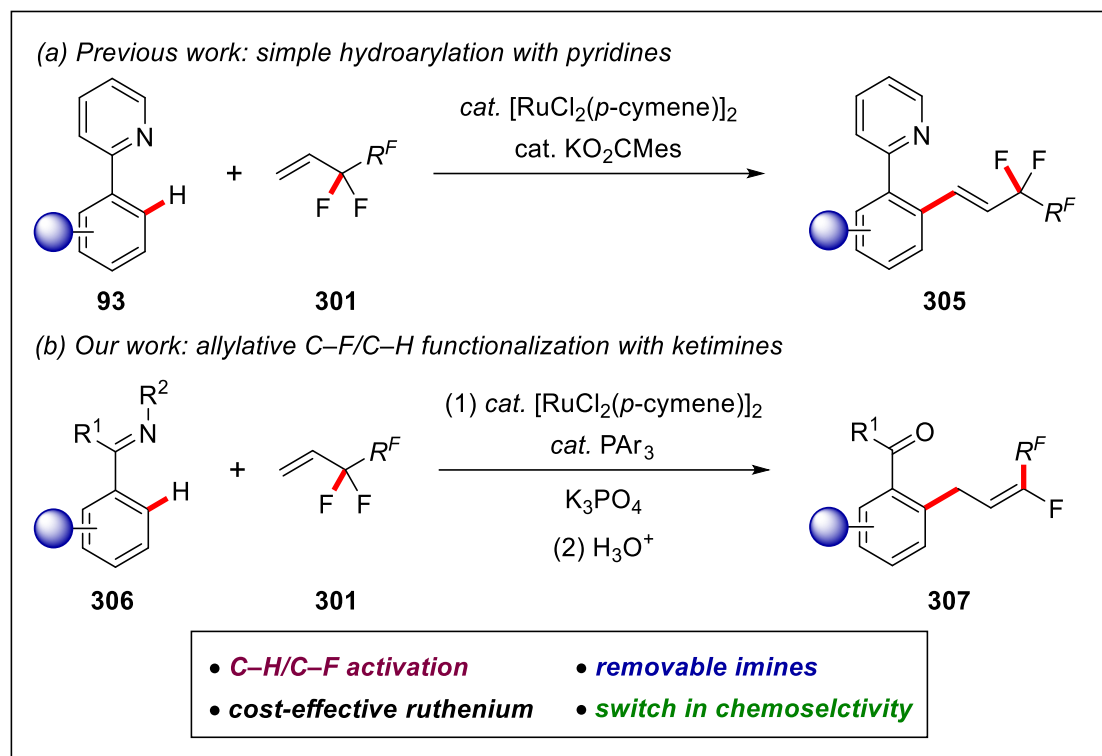
In the first project, the unprecedented use of a manganese(I) complex was demonstrated for challenging C–F/C–H functionalizations (Scheme 129).^[283] Robust reaction conditions and ample substrate scope are some of the key characteristics of this approach. This method proved to be viable for synthetically meaningful ketimines. Thus, versatile manganese(I)-catalyzed C–F/C–H functionalization allowed for the synthesis of diverse fluorinated scaffolds. In addition to allylations and alkenylations, we also identified the potential of manganese catalysis in C–H perfluoroalkenylation using challenging perfluoroalkenes. It is noteworthy that even amino acids and peptides underwent C–F/C–H functionalizations under racemization-free conditions.



Scheme 129. Manganese(I)-catalyzed C–F/C–H functionalizations.

In the second project, the versatility of ruthenium catalysis was shown towards C–F/C–H functionalization (Scheme 130).^[284] Previously our group reported on the ruthenium-catalyzed C–H hydroarylations with unactivated alkenes and perfluoroalkenes. In the present method, by

the judicious choice of a tertiary phosphine ligand, a switch in chemoselectivity was observed towards challenging C–F functionalization. More pleasingly, ketimines were found as amenable substrates for the envisioned C–F/C–H functionalization to synthesis fluorinated ketones by a one-pot hydrolysis. This approach allowed for highly chemo- and position-selective β -fluorine eliminations with a broad range of substituted ketimines and perfluoroalkenes. Considering the importance of fluorinated building blocks, these studies are expected to inspire related developments in the field of transition metal catalysis.

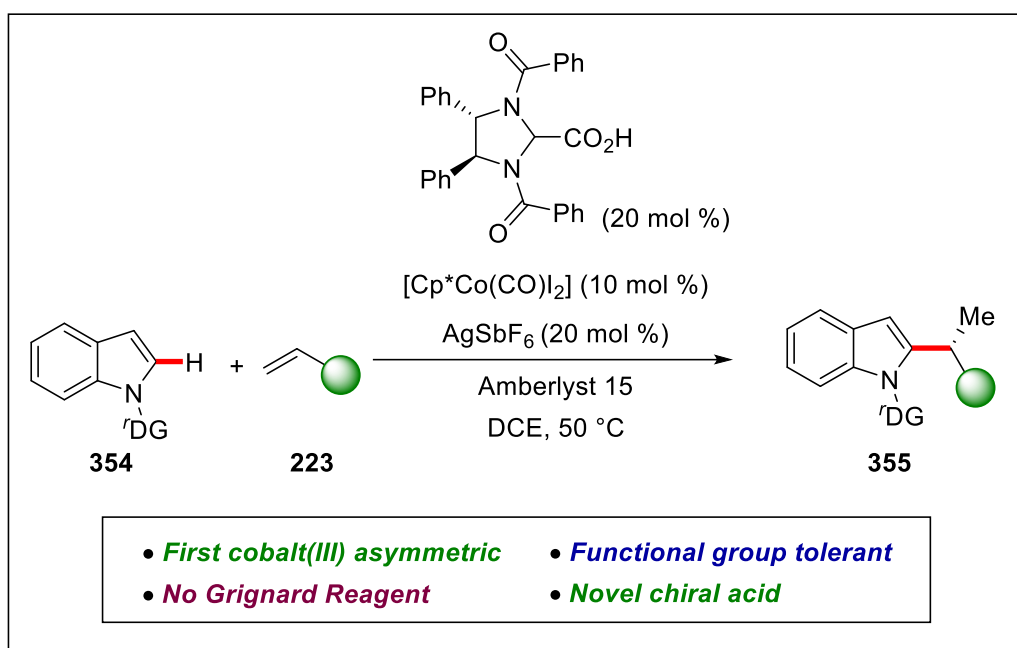


Scheme 130. *E*-selective C–H/C–F functionalization by ruthenium(II) catalysis.

As with fluorinated scaffolds, chiral molecules represent a class of highly desirable building blocks. Thus, the next part of the thesis focused on the development of sustainable enantioselective transformations using cost-effective transition metals. In the third project, we developed a novel chiral carboxylic acid **CA5** to realize the first cobalt(III)-catalyzed enantioselective C–H activation (Scheme 131).^[270] Initial studies with commonly used mono protected amino acids and chiral phosphoric acids failed to provide high levels of enantiocontrol. In contrast, the design of novel chiral carboxylic acid **CA5** enabled the first highly enantioselective cobalt(III)-catalyzed C–H alkylation with unactivated alkenes **223** by organometallic chelation assisted C–H activation. The mild Grignard-free reaction conditions tolerated a wide array of sensitive functional groups on the indoles **354** as well as on the alkene coupling partners **223**. Moreover, the directing groups were removed in a traceless fashion

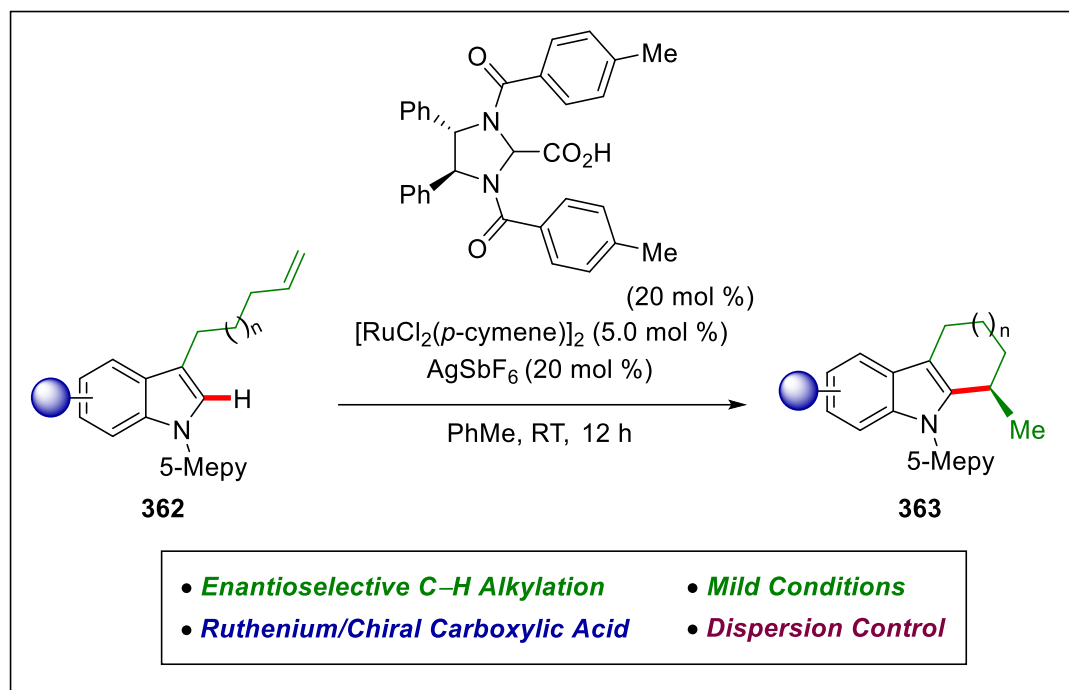
4. Summary and Outlook

under hydrogenation conditions without any erosion of the enantiomeric excess. Detailed mechanistic studies by kinetic experiments and non-linear effect studies provided evidence for dimeric hydrogen bond stabilized resting state of the chiral carboxylic acid. This study on cooperative cobalt(III)/chiral acid manifold set the stage for subsequent developments in the enantioselective cobalt(III)-catalyzed C–H activation, as further reports were documented by Matsunaga^[271a] and Cramer.^[285]



Scheme 131. Enantioselective cobalt(III)-catalyzed C–H alkylation by chiral carboxylic acid cooperation.

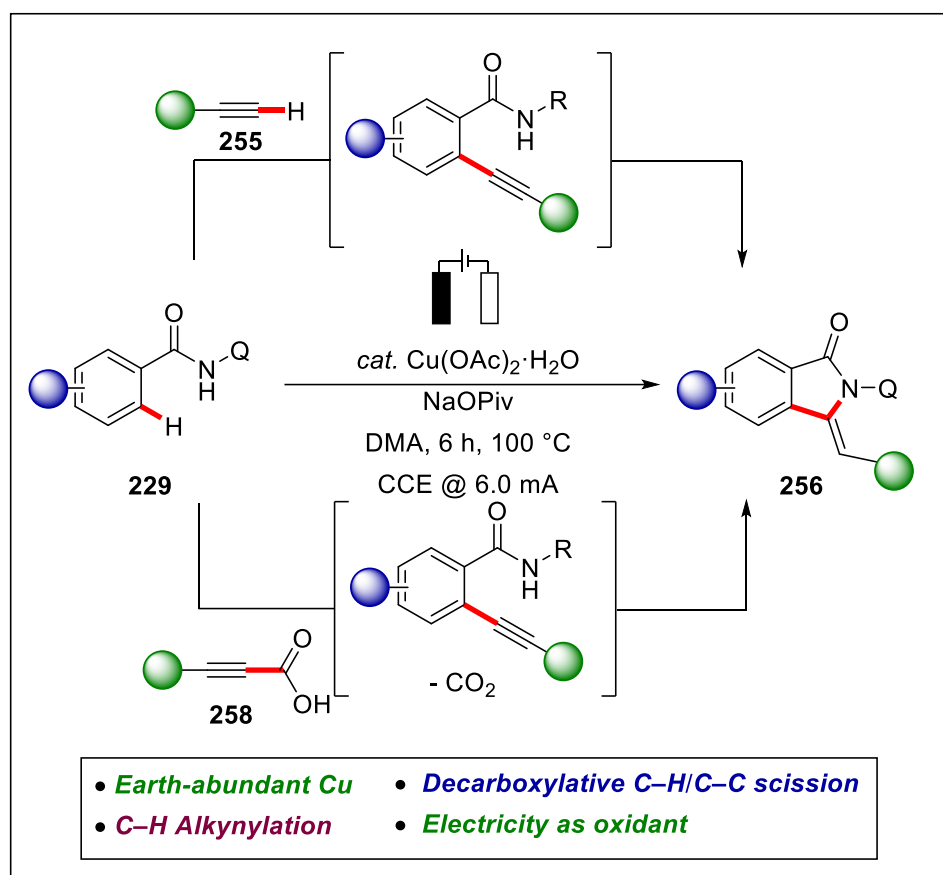
Thereafter, we became interested in the development of ruthenium-catalyzed enantioselective organometallic C–H activation with the combination of a chiral acid. In contrast to the significant advances in the ruthenium catalyzed C–H activation, organometallic enantioselective transformations remain largely underdeveloped. In this project we succeeded to achieve enantioselective ruthenium-catalyzed organometallic C–H alkylation, employing a C2 symmetrical chiral acid **CA14** to control the enantio-induction (Scheme 132).^[286] Cost-effective and bench-stable $[\text{RuCl}_2(p\text{-cymene})]_2$ was successfully employed with a chiral carboxylic acid to synthesis enantioenriched tetrahydrocarbazoles and cyclohepta[*b*]indoles derivatives by intramolecular cyclization at room temperature. C2-symmetric chiral acid was found to be crucial for enantioselective intramolecular C–H alkylation while other commonly used chiral acids failed in this protocol. Detailed kinetic and DFT studies unraveled a reversible C–H metalation step and an enantio-determining proto-demetalation step by the chiral acid. DFT studies provided support for the presence of weak secondary dispersive interactions to control enantio-induction.



Scheme 132. Enantioselective ruthenium-catalyzed organometallic C–H alkylation

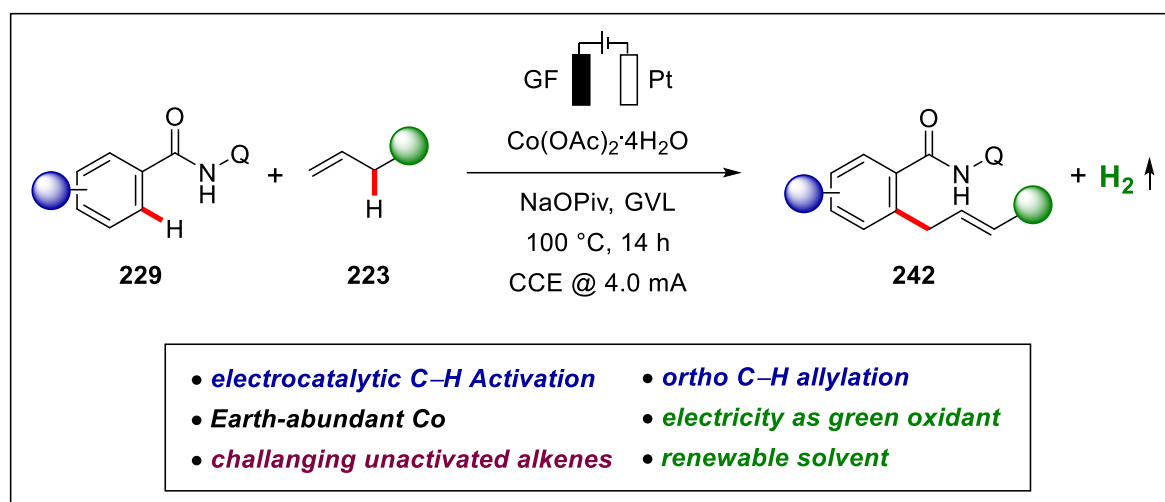
Resource-economy is another important aspect in molecular syntheses.^[224] Consequently, a large portion of the doctoral thesis was focused on addressing improved sustainability and resource-economy for the activation of inert C–H bonds. Over the past years, early examples of electrochemical C–H activations were largely restricted to the use of palladium. In 2017, Ackermann realized the first electrochemical 3d transition metal-catalyzed C–H activation using inexpensive cobalt as a catalyst for oxygenation reactions,^[246] which has set the stage for the development of electrochemical transformations with Earth-abundant transition metals.^[232]

In the fifth project, we realized electrochemical copper-catalyzed sequential alkyne annulations with benzamides to synthesis isoindolone motifs **256** in the absence of any chemical oxidants (Scheme 133).^[287] Inexpensive $\text{Cu}(\text{OAc})_2$ was employed as the catalyst for the electrooxidative alkylation protocol by the assistance of 8-aminoquinoline as the directing group. Furthermore, our reaction conditions were found to be suitable for the decarboxylative C–H/C–C cleavage with alkynyl carboxylic acids. This study showed the unique potential of copper catalysts in electrochemical transformations, which is expected to inspire related developments in the near future.



Scheme 133. Copper-catalyzed electrochemical alkyne annulation.

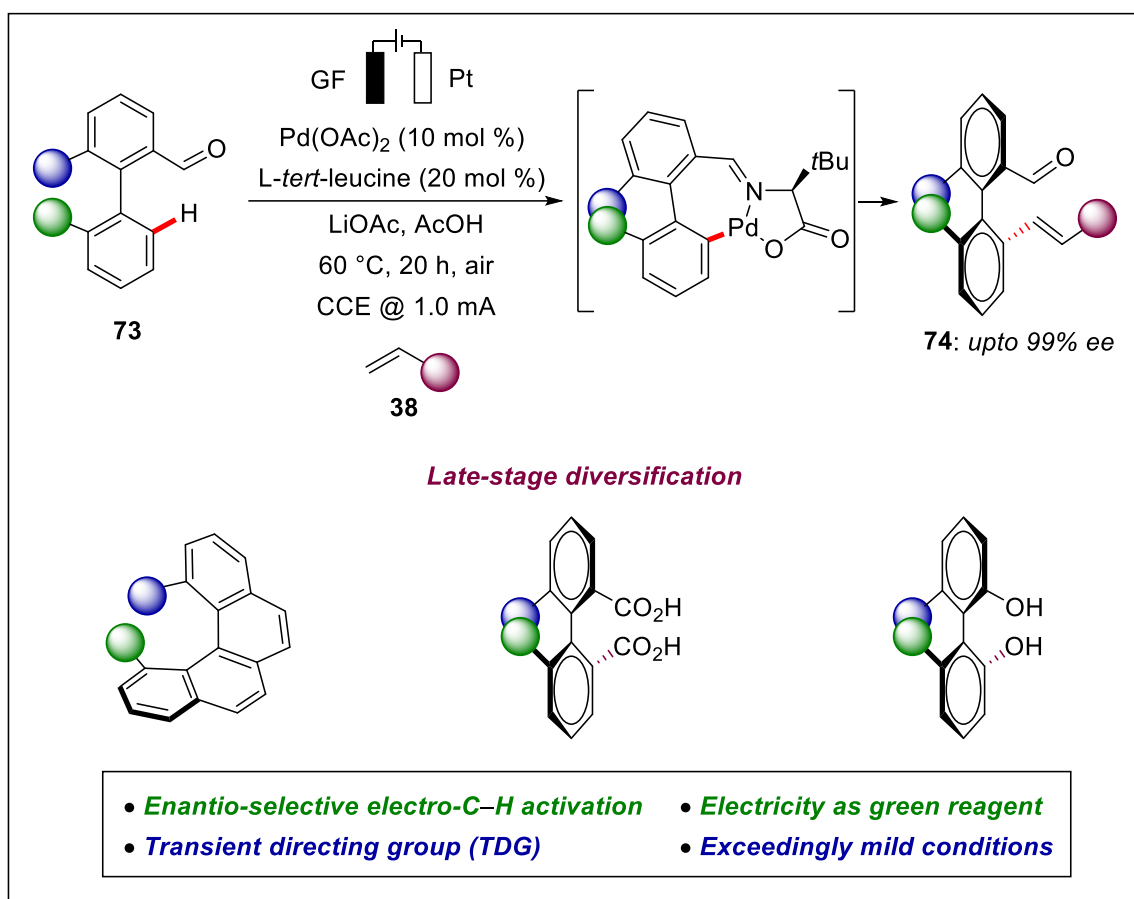
Thus far, all the reported electrochemical transformations with precious 4d and 5d transition metals were limited to activated alkenes, such as styrenes and acrylates. In the subsequent project, we showed the versatility of oxidative cobalt catalysis in electrocatalytic C–H allylations with unbiased olefins (Scheme 134).^[288] A key characteristic of our strategy was the use of the biomass-derived solvent γ -valerolactone as the reaction media. Electro-oxidative cobalt catalysis provided the chelation-assisted *ortho*-C–H allylation by the assistance of 8-aminoquinoline as the directing group, generating molecular hydrogen as the sole stoichiometric by-product. A plethora of sensitive functional groups were fully tolerated, providing exclusively the allylic selectivity. Competition experiment provided evidence for a base-assisted internal electrophilic-type substitution mechanism for the C–H metalation event. This turns out to be one of the scarce example for the application of unactivated olefins in electrochemical C–H activation reactions.



Scheme 134. Cobalt-catalyzed electrochemical C–H allylation

The merger of electrosynthesis with transition metal catalysis provides enormous potential towards perfect resource economy. Despite substantial progress, enantioselective metallaelectro-catalyzed C–H activation was not realized before. To address the full potential of electrochemistry and considering practical importance of chiral building blocks, we achieved the first asymmetric metallaelectro-catalyzed C–H activation under exceedingly mild reaction conditions (Scheme 135).^[289] We employed inexpensive *L-tert*-leucine as a transient directing group to enable electrochemical atroposelective organometallic C–H activation. This was the unprecedented report for the application of transient directing group in electrochemical transformations. The combination of Pd(OAc)_2 and *L-tert*-leucine provided excellent enantioselectivities for the atroposelective olefination reactions to furnish axially-chiral biaryls. On a pleasing note, similar reaction conditions were also effective for the synthesis of N–C axially-chiral motifs in excellent enantioselectivities. Detailed kinetic studies shed light on the C–H metalation step, being suggestive of the C–H activation as the rate-determining step. In addition, DFT studies showed preference for the formation of seven membered ring over the five-membered metallacycle to enable the axial chirality. This metallaelectro-catalyzed enantioselective protocol provided a step-economical strategy to the synthesis of highly enantio-enriched BINOLs, dicarboxylic acids and helicenes. Given the topical interest in the development of new approach for enantioselective transformations, this sustainable protocol paves the path for further developments in this research area.

4. Summary and Outlook



Scheme 135. Metallaelectro-catalyzed enantioselective C–H activation.

5. Experimental Part

5.1. General Remarks

All reactions involving air- and/or moisture-sensitive compounds were conducted under a dry nitrogen atmosphere using pre-dried glassware and standard Schlenk techniques. If not otherwise noted, yields refer to isolated compounds which were estimated to be >95% pure based on $^1\text{H-NMR}$.

Vacuum

The following average pressure was measured on the used rotary vane pump RD4 from Vacuubrand®: $0.8 \cdot 10^{-1}$ mbar (uncorrected value).

Melting Points

Melting points were measured on a Stuart® Melting Point Apparatus SMP3 from Barloworld Scientific. Values are uncorrected.

Chromatography

Analytical thin layer chromatography (TLC) was performed on silica gel 60 F254 aluminium sheets from Merck. Plates were either visualized under irradiation at 254 nm or 365 nm or developed by treatment with a potassium permanganate solution followed by careful warming. Chromatographic purifications were accomplished by column chromatography on Merck Geduran® silica gel, grade 60 (40–63 μm , 70–230 mesh ASTM).

Gel permeation chromatography (GPC)

GPC purifications were performed on a JAI system (JAI-LC-9260 II NEXT) equipped with two sequential columns (JAIGEL-2HR, gradient rate: 5.000; JAIGEL-2.5HR, gradient rate: 20.000; internal diameter = 20 mm; length = 600 mm; Flush rate = 10.0 mL/min and chloroform (HPLC-quality with 0.6% ethanol as stabilizer) was used as the eluent.

Infrared Spectroscopy

IR spectra were recorded using a Bruker® Alpha-P ATR spectrometer. Liquid samples were measured as film and solid samples neat. Spectra were recorded in the range from 4000 to 400 cm^{-1} . Analysis of the spectral data was carried out using Opus 6. Absorption is given in wave numbers (cm^{-1}).

Nuclear Magnetic Resonance Spectroscopy

NMR spectra were recorded on Mercury Plus 300, VNMRS 300, Inova 500 and 600 from Varian®, or Avance 300, Avance III 300 and 400, Avance III HD 400 and 500 from Bruker®. Chemical shifts are reported in δ -values in ppm relative to the residual proton peak or carbon peak of the deuterated solvent.

The coupling constants J are reported in hertz (Hz). Analysis of the recorded spectra was carried out using MestReNova 10.0 software.

	¹ H-NMR	¹³ C-NMR
CDCl ₃	7.26	77.16
CD ₃ CO ₂ D	11.65	179.0

Gas Chromatography

Monitoring of reaction process *via* gas chromatography or coupled gas chromatography-mass spectrometry was performed using a 7890 GC-system with/without mass detector 5975C (Triple-Axis-Detector) or a 7890B GC-system coupled with a 5977A mass detector, both from Agilent Technologies®.

Mass Spectrometry

Electron ionization (EI) and EI high resolution mass spectra (HR-MS) were measured on a time-of-flight mass spectrometer AccuTOF from JEOL. Electrospray ionization (ESI) mass spectra were recorded on an Io-Trap mass spectrometer LCQ from Finnigan, a quadrupole time-of-flight maXis from Bruker Daltonic or on a time-of-flight mass spectrometer microTOF from Bruker Daltonic. ESI-HR-MS spectra were recorded on a Bruker Apex IV or Bruker Daltonic 7T, Fourier transform ion cyclotron resonance (FTICR) mass spectrometer. The ratios of mass to charge (m/z) are indicated, intensities relative to the base peak ($I = 100$) are written in parentheses.

Chiral HPLC

Chiral HPLC chromatograms were recorded on an Agilent 1290 Infinity using CHIRALPAK® IA-3, IB-3, IC-3, ID-3, IE-3 and IF-3 columns (3.0 μ m particle size; ϕ : 4.6 mm and 250 mm length) at ambient temperature.

Specific Rotations

Optical rotations were measured on an Anton Paar MCP 150 polarimeter using a 10 cm cell with a Na 589 nm filter. Concentrations are indicated in g/100 mL.

Solvents

All solvents for reactions involving air- and/or moisture-sensitive reagents were dried, distilled and stored under an inert atmosphere (dry nitrogen) according to the following standard procedures.

1,2-Dichloroethane (DCE) and toluene (PhMe) were dried over CaH₂ for 8 h, degassed and distilled under reduced pressure. 1,4-Dioxane and di-*n*-butylether (*n*Bu₂O) were dried over Na for 8 h, degassed and distilled under reduced pressure.

CH₂Cl₂, DMF, THF, Et₂O were obtained from a MBRAUN MB SPS-800 solvent purification system.

Chemicals

Chemicals obtained from commercial sources with a purity >95% were used as received without further purification.

The following compounds were known from the literature and synthesized according to previously known methods: Indoles **315** and **354**^[290] and **362**,^[291] ketimines **340**^[292], Benzamides **229**^[293], Biaryl aldehydes **73**.^[89]

The following compounds were kindly synthesized and provided by the persons listed below: Karsten Rauch: IMes·HCl, IPr·HCl, [RuCl₂(*p*-cymene)]₂, [Cp*RhCl₂]₂, dry and/or degassed solvents (DCE, *t*AmOH, 1,4-dioxane, PhMe).

Dr. Daniel Zell: Indole **354e**.

Valentine Müller: *gem*-Difluorostyrene **11a**.

Dr. Fabio Pesciaioli: Chiral acid **CA5**.

Dr. Cong Tian: Benzamide **229d**.

Nikolaos Kaplaneris: Indole **328a-328c**, Alkene **38e-38j** and **38k**, **255m**, Ligand **CA2** and **CA8**.

Rongxin Yin: Indole **354b-354c**, ketimine **340f**.

Julia Struwe: 2-Phenyl pyridines **93b**.

Becky Bongsuiru Jei: Chiral acid **CA13** and **CA15**.

5.2. General Procedures

5.2.1. General Procedure A: Manganese(I)-Catalyzed Allylative C–H/C–F Functionalization

A suspension of heteroarene **315** (0.50 mmol, 1.00 equiv), 1*H*,1*H*,2*H*-perfluoroalkene **301** (0.60 mmol, 1.20 equiv), [MnBr(CO)₅] (10.3 mg, 7.5 mol %) and K₂CO₃ (69.1 mg, 0.50 mmol, 1.00 equiv) in 1,4-dioxane (0.50 mL, 1.00 M) was stirred at 80 °C for 20 h. At ambient temperature, the mixture was diluted with EtOAc (3.0 mL) and the solvents were removed *in vacuo* and the remaining residue was purified by column chromatography on silica gel to afford the desired products **316**.

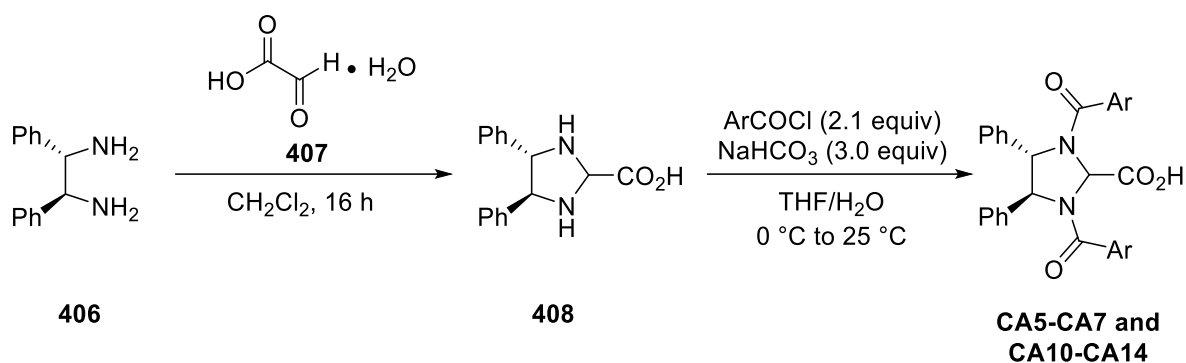
5.2.2. General Procedure B: Manganese(I)-Catalyzed C–H/C–F Functionalization of Heteroarenes with Perfluoroalkenes

A suspension of heteroarene **315/328/332** (0.50 mmol, 1.00 equiv), perfluoroalkene **303** (1.50 mmol, 3.00 equiv), [MnBr(CO)₅] (13.7 mg, 10.0 mol %) and K₂CO₃ (69.0 mg, 0.50 mmol, 1.00 equiv) in 1,4-dioxane (0.50 mL, 1.00 M) was stirred at 100 °C for 20 h. At ambient temperature, the solvent was removed *in vacuo* and the remaining residue was purified by column chromatography on silica gel to afford the desired products **328/331/333**.

5.2.3. General Procedure C: Ruthenium(II)-Catalyzed C–F/C–H Functionalization

A suspension of ketimine **340** (0.50 mmol, 1.0 equiv), 1*H*,1*H*,2*H*-perfluoroalkene **301** (1.50 mmol, 3.0 equiv), [RuCl₂(*p*-cymene)]₂ (15.3 mg, 5.0 mol %), P(4-C₆H₄F)₃ (31.6 mg, 20 mol %) and K₃PO₄ (212 mg, 1.0 mmol, 2.0 equiv) in cyclohexane (1.0 mL) was stirred under N₂ at 120 °C for 24 h in pressure tube. At ambient temperature, the reaction mixture was diluted with EtOAc (5.0 mL) and HCl (5.0 mL, 1 M) was added. The mixture was stirred for 3 h and extracted with EtOAc (3 x 10.0 mL). After removal of the solvents *in vacuo*, the remaining residue was purified by column chromatography on silica gel to afford the desired products **307**.

5.2.4. General Procedure D: Synthesis of the chiral acid CA5-CA7 and CA10-CA14.



To a solution of (*S,S*)-diphenylethanediamine (212.3 mg, 1.00 mmol) in CH_2Cl_2 (4.0 mL) was added an equimolar amount of glyoxylic acid monohydrate (92.1 mg, 1.00 mmol) under vigorous stirring. After 16 h, the solvent was removed to afford (*4S,5S*)-4,5-diphenylimidazolidine-2-carboxylic acid **408** (265.3 mg, 99% yield) as a yellow solid.

To a solution of **408** in THF/ H_2O (5 mL, 1:1) at 0 °C, NaHCO_3 (252 mg, 3.00 mmol) and acyl chloride (2.10 mmol, 2.1 equiv) were added, and the reaction was allowed to reach ambient temperature. After 16 h, the reaction mixture was diluted with CH_2Cl_2 (10 mL) and washed with HCl (1 M, 10 mL) solution. The aqueous phase was extracted with CH_2Cl_2 (3 x 10 mL). The combined organic phase was washed with brine and dried over Na_2SO_4 and the solvent was removed under *vacuum*. The crude mixture was purified *via* flash chromatography (CH_2Cl_2 100% to $\text{CH}_2\text{Cl}_2\text{:CH}_3\text{OH} = 90\text{:}10$) to afford chiral acids **CA5-CA7** and **CA10-CA14**.

5.2.5. General Procedure E: Cobalt(III)-Catalyzed Asymmetric C–H Alkylation

A suspension of indole **354** (0.50 mmol, 1.00 equiv), alkene **223** (1.50 mmol, 3.00 equiv), $[\text{Cp}^*\text{Co}(\text{CO})\text{I}_2]$ (23.8 mg, 50.0 μmol , 10.0 mol %), AgSbF_6 (34.4 mg, 100 μmol , 20.0 mol %), chiral acid **CA5** (48.0 mg, 100 μmol , 20.0 mol %) and Amberlyst 15 (160 mg, 1.50 equiv) in DCE (0.5 mL, 1.0 M) were stirred at 50 °C for 65 h. At ambient temperature, the reaction mixture was diluted with EtOAc (2.0 mL) and Et_3N (0.5 mL) was added. The mixture was stirred for 0.5 h and filtered through a short pad of silica and the solvents were removed *in vacuo*. The crude mixture was purified by flash column chromatography on silica gel to afford the desired product **355**.

5.2.6. General Procedure F: Synthesis of Racemic Products for Cobalt(III)-Catalyzed C–H Alkylation

A suspension of indole **354** (0.50 mmol, 1.00 equiv), alkene **223** (1.50 mmol, 3.00 equiv), $[\text{Cp}^*\text{Co}(\text{CO})\text{I}_2]$ (23.8 mg, 50.0 μmol , 10.0 mol %), AgSbF_6 (34.4 mg, 100 μmol , 20.0 mol %), 1-AdCO₂H (48.0 mg, 100 μmol , 20.0 mol %) in DCE (0.5 mL, 1.0 M) were stirred at 50 °C for 20 h. At ambient temperature, the reaction mixture was diluted with EtOAc (2.0 mL) and the

solvents were removed *in vacuo*. The crude mixture was purified by flash column chromatography on silica gel to afford the racemic product **355**.

5.2.7. General Procedure G: Traceless Removable of Directing Group for Cobalt(III)-Catalyzed C–H Alkylated Products

To a solution of **355** (0.2 mmol, 1.00 equiv) in CH₂Cl₂ (0.5 mL) was added MeOTf (36.1 mg, 1.10 equiv) dropwise at 0 °C. After 30 min, the mixture was allowed to warm up to 25 °C and stirred for 6 h. After removal of the solvent *in vacuo*, Pd(OH)₂/C (7.7 mg, 10 wt.-%) and ammonium formate (126 mg, 2.00 mmol, 10.0 equiv) were added. The mixture was diluted with MeOH (1.0 mL) and stirred at 60 °C for 6 h. After addition of EtOAc (5.0 mL) at ambient temperature, the mixture was filtered through a short pad of celite[®] and the solvents were removed *in vacuo*. The crude mixture was purified by flash column chromatography on silica gel to yield **357**.

5.2.8. General Procedure H: Ruthenium(II)-Catalyzed Asymmetric C–H Alkylation for the Synthesis of Tetrahydrocarbazoles

A suspension of indole **362** (0.25 mmol, 1.00 equiv), [RuCl₂(*p*-cymene)]₂ (7.7 mg, 5.0 mol %), AgSbF₆ (17.2 mg, 20 mol %), chiral acid **CA14** (25.2 mg, 20 mol %) in PhMe (0.50 mL) were stirred at 25 °C for 12 h. The reaction mixture was diluted with EtOAc (2.0 mL) and the solvent was removed *in vacuo*. The crude mixture was purified by column chromatography on silica gel to afford the desired product **363**.

5.2.9. General Procedure I: Synthesis of Racemic Products for Ruthenium(II)-Catalyzed C–H Alkylation

A suspension of indole **362** (0.10 mmol, 1.00 equiv), [RuCl₂(*p*-cymene)]₂ (3.1 mg, 5.0 mol %), AgSbF₆ (6.9 mg, 100 μmol, 20 mol %), 1-AdCO₂H (18.0 mg, 1 equiv) in PhMe (0.50 mL) were stirred at 50 °C for 12 h. At ambient temperature, the reaction mixture was diluted with EtOAc (2.0 mL) and the solvents were removed *in vacuo*. The crude mixture was purified by column chromatography on silica gel to afford the racemic products *rac*-**363**.

5.2.10. General Procedure J: Copper-catalyzed Alkyne Annulation by C–H Alkynylation

The electrocatalysis was carried out in an undivided cell, with a RVC anode (10 mm × 15 mm × 6 mm) and a platinum cathode (10 mm × 15 mm × 0.25 mm). Benzamide **229** (0.25 mmol, 1.0 equiv), alkyne **255** (0.50 mmol, 2.0 equiv), NaOPiv (31 mg, 0.25 mmol, 1.0 equiv) and

Cu(OAc)₂·H₂O (2.5 mg, 5.0 mol %) were placed in a 10 mL cell and dissolved in DMA (4.0 mL). Electrocatalysis was performed at 100 °C with a constant current of 6.0 mA maintained for 6 h. At ambient temperature, saturated aqueous NaHCO₃ (4.0 mL) was added. The RVC anode was washed with EtOAc (3 × 10 mL) in an ultrasonic bath. The washings were added to the reaction mixture and the combined phases were extracted with EtOAc (4 × 10 mL), then dried over Na₂SO₄. Evaporation of the solvent and subsequent column chromatography on silica gel afforded the corresponding products **256**.

5.2.11. General Procedure K: Cobaltaelectro-Catalyzed C–H Allylation

The electrolysis was carried out in an undivided cell with a GF anode (10 mm × 15 mm × 6 mm) and a platinum cathode (10 mm × 15 mm × 0.25 mm). Co(OAc)₂·4H₂O (12.7 mg, 0.05 mmol, 10 mol %), NaOPiv (124.0 mg, 1.0 mmol, 2.0 equiv), *n*-Bu₄NPF₆ (97.0 mg, 0.25 mmol, 0.50 equiv) and benzamide **229** (0.50 mmol, 1.0 equiv) were dissolved in GVL (4.0 mL) and the alkene **223** (1.5 mmol, 3.0 equiv) was added sequentially. At 100 °C, electrolysis was conducted with a constant current of 4.0 mA for 14 h. The mixture was transferred to a flask and the electrodes were rinsed with acetone (3 × 5.0 mL). Then the combined solvent was removed under reduced pressure, the residue was diluted with EtOAc (10 mL) and stirred with NaOH (aq) (2 M, 20 mL) for 2 h. The mixture was extracted with water (3 × 20 mL) and successively with EtOAc (3 × 20 mL), then the organic layer was dried over Na₂SO₄. After evaporation of the solvent *under vacuo*, subsequent column chromatography on silica gel (*n*-hexane/EtOAc) yielded the desired product **242**.

5.2.12. General Procedure L: Atroposelective Palladaelectro-catalyzed C–H Olefination

The electrocatalysis was carried out in an undivided cell, with a GF anode (10 mm × 15 mm × 6 mm) and a platinum cathode (10 mm × 15 mm × 0.25 mm). Biaryls **73** or **396** (0.20 mmol, 1.0 equiv), acrylates **38** (0.60 mmol, 3 equiv), Pd(OAc)₂ (4.49 mg, 10 mol %), *L*-*tert*-leucine (5.24 mg, 20 %) and LiOAc (26.4 mg, 2 equiv) were placed in a 10 mL cell and dissolved in AcOH (4.5 mL). Electrocatalysis was performed at 60 °C with a constant current of 1.0 mA maintained for 20 h. At ambient temperature, the reaction mixture was diluted with EtOAc. The GF anode was washed with EtOAc (3 × 10 mL) in an ultrasonic bath. The combined washings were added to the reaction mixture and the solvents were removed *in vacuo*. The crude mixture was purified by column chromatography on silica gel to yield **74** or **397**.

5.2.13. General Procedure M: General Procedure for the Synthesis of Racemic Products

The racemic compounds were prepared using *rac*-D/*L*-valine as the transient directing groups instead of *L*-*tert*-leucine, following the general procedure **L**.

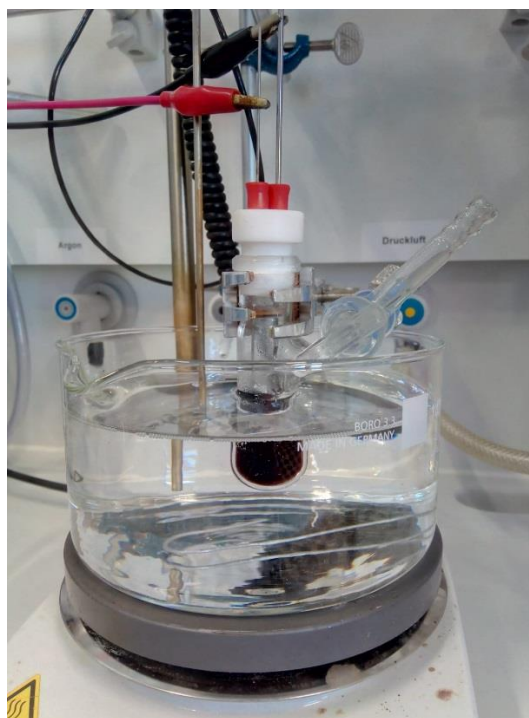
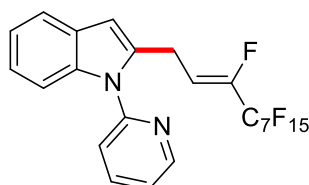


Figure 4. Electrochemical Reaction set up.

5.3. Manganese(I)-Catalyzed Allylative C–H/C–F Functionalization

5.3.1. Characterization Data



(Z)-2-(1H,1H,2H-Perfluorodec-2-en-1-yl)-1-(pyridin-2-yl)-1H-indole (316aa): The general procedure **A** was followed using 1-(pyridin-2-yl)-1H-indole (**315a**) (97.1 mg, 0.50 mmol) and 1H,1H,2H-perfluorodec-1-ene (**301a**) (268 mg, 0.60 mmol). Isolation by column chromatography (*n*-hexane/EtOAc: 10:1) yielded **316aa** (301 mg, 97%, *Z/E* = 90:10) as a yellow oil.

¹H-NMR (300 MHz, CDCl₃): δ = 8.64 (ddd, *J* = 4.9, 1.9, 0.9 Hz, 1H), 7.88 (ddd, *J* = 7.9, 7.6, 1.9 Hz, 1H), 7.61 (ddd, *J* = 6.4, 4.9, 1.9 Hz, 1H), 7.41 (ddd, *J* = 7.9, 1.0, 0.9 Hz, 1H), 7.38 (ddd, *J* = 7.4, 4.3, 2.6 Hz, 1H), 7.31 (ddd, *J* = 7.1, 4.9, 0.9 Hz, 1H), 7.25–7.12 (m, 2H), 6.50 (dd, *J* = 0.9, 0.9 Hz, 1H), 6.16 (dt, *J* = 22.3, 8.1 Hz, 0.10H, *E*), 5.82 (dt, *J* = 33.0, 7.5 Hz, 0.90H, *Z*), 3.90 (ddt, *J* = 7.5, 4.2, 1.8 Hz, 1.80H, *Z*), 3.84 (ddt, *J* = 8.1, 4.5, 1.8 Hz, 0.20H, *E*).

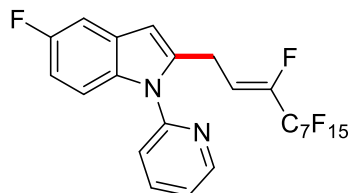
¹³C-NMR (125 MHz, CDCl₃): δ = 150.8 (C_q), 149.6 (CH), 146.1 (dt, ¹*J*_{C–F} = 261 Hz, ²*J*_{C–F} = 29.1 Hz, C_q), 138.3 (CH), 137.1 (C_q), 136.1 (C_q), 128.3 (C_q), 122.4 (CH), 122.1 (CH), 121.0 (CH), 120.5 (CH), 120.0 (CH), 117.0 (dt, ¹*J*_{C–F} = 288 Hz, ²*J*_{C–F} = 31.3 Hz, C_q), 113.3 (td, ²*J*_{C–F} = 8.1 Hz, ³*J*_{C–F} = 4.2 Hz, CH), 112.4 (m, C_q), 110.9 (m, C_q), 110.7 (m, C_q), 110.5 (m, C_q), 108.6 (m, C_q), 108.3 (m, C_q), 110.1 (CH), 106.7 (CH), 22.7 (d, ³*J*_{C–F} = 4.3 Hz, CH₂).

¹⁹F-NMR (282 MHz, CDCl₃): δ = –80.9 (m), –115.0 (m), –117.5 (m), –122.0 (m), –122.8 (m), –123.0 (m), –126.3 (m), –130.8 (m).

IR (ATR): 3061, 1589, 1472, 1455, 1439, 1197, 1107, 736 cm^{–1}.

MS (ESI) *m/z* (relative intensity): 643 ([M + Na⁺], 20), 621 ([M + H]⁺, 100).

HR-MS (ESI): *m/z* calcd. for [C₂₃H₁₂F₁₆N₂ + H]⁺ 621.0818, found 621.0809.



(Z)-2-(1H,1H,2H-Perfluorodec-2-en-1-yl)-5-fluoro-1-(pyridin-2-yl)-1H-indole (316ba):

The general procedure **A** was followed using 5-fluoro-1-(pyridin-2-yl)-1H-indole (**315b**) (106 mg, 0.50 mmol) and 1H,1H,2H-perfluoro-1-decene (**301a**) (268 mg, 0.60 mmol).

5. Experimental Part

Isolation by column chromatography (*n*-hexane/EtOAc = 10:1) yielded **316ba** (271 mg, 85%, *Z/E* = 90:10) as a white solid. M.p.: 95 °C.

¹H-NMR (500 MHz, CDCl₃): δ = 8.63 (ddd, *J* = 4.9, 2.0, 0.8 Hz, 1H), 7.88 (ddd, *J* = 7.7, 7.5, 2.0 Hz, 1H), 7.43 (ddd, *J* = 8.0, 1.0, 0.8 Hz, 1H), 7.32 (ddd, *J* = 7.5, 4.8, 1.0 Hz, 1H), 7.27 (dd, *J* = 8.9, 4.4 Hz, 1H), 7.25–7.21 (m, 1H), 6.90 (dt, *J* = 9.1, 2.6 Hz, 1H), 6.44 (d, *J* = 0.9 Hz, 1H), 6.12 (dt, *J* = 22.2, 8.2 Hz, 0.10H, *E*), 5.78 (dt, *J* = 32.6, 7.5 Hz, 0.90H, *Z*), 3.85 (ddt, *J* = 7.7, 3.9, 2.0 Hz, 1.80H, *Z*), 3.80 (ddt, 7.7, 4.1, 1.9 Hz, 0.20H, *E*).

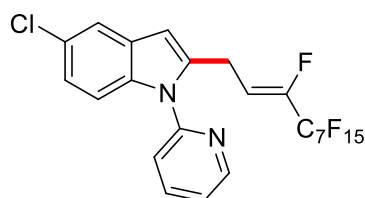
¹³C-NMR (125 MHz, CDCl₃): δ = 158.5 (d, ¹*J*_{C-F} = 236 Hz, C_q), 150.7 (C_q), 149.8 (CH), 146.2 (dt, ¹*J*_{C-F} = 261, ²*J*_{C-F} = 29.0 Hz, C_q), 138.6 (CH), 137.7 (C_q), 133.7 (C_q), 128.8 (d, ³*J*_{C-F} = 10.3 Hz, C_q), 122.4 (CH), 120.4 (CH), 117.2 (dt, ¹*J*_{C-F} = 285 Hz, ²*J*_{C-F} = 33.3 Hz, C_q), 113.7 (m, C_q), 113.0 (dt, ²*J*_{C-F} = 8.5 Hz, ³*J*_{C-F} = 4.4 Hz, CH), 112.4 (m, C_q), 110.9 (d, ²*J*_{C-F} = 9.5 Hz, CH), 110.5 (d, ²*J*_{C-F} = 26.0 Hz, CH), 110.4 (m, C_q), 110.0 (m, C_q), 108.6 (m, C_q), 108.2 (m, C_q), 105.4 (d, ²*J*_{C-F} = 23.7 Hz, CH), 103.5 (d, ³*J*_{C-F} = 4.3 Hz, CH), 22.7 (d, ³*J*_{C-F} = 4.3 Hz, CH₂).

¹⁹F-NMR (470 MHz, CDCl₃): δ = -81.0 (m), -117.6 (m), -122.1 (m), -122.9 (m), -123.0 (m) - 123.4 (m), -123.5 (m), -126.3 (m), -130.5 (m).

IR (ATR): 1473, 1450, 1439, 1235, 1143, 776, 663 cm⁻¹.

MS (ESI) *m/z* (relative intensity): 661 ([M + Na]⁺, 15), 639 ([M + H]⁺, 100).

HR-MS (ESI): *m/z* calcd. for [C₂₃H₁₁F₁₇N₂ + H]⁺ 639.0724, found 639.0731.



(*Z*)-2-(1*H*,1*H*,2*H*-Perfluorodec-2-en-1-yl)-5-chloro-1-(pyridin-2-yl)-1*H*-indole (**316ca**):

The general procedure **A** was followed using 5-chloro-1-(pyridin-2-yl)-1*H*-indole (**315c**) (114 mg, 0.50 mmol) and 1*H*,1*H*,2*H*-perfluoro-1-decene (**301a**) (268 mg, 0.60 mmol). Isolation by column chromatography (*n*-hexane/EtOAc: 10:1) yielded **316ca** (303 mg, 93%, *Z/E* = 90:10) as a white solid. M.p.: 95 °C.

¹H-NMR (400 MHz, CDCl₃): δ = 8.63 (ddd, *J* = 4.8, 2.0, 0.8 Hz, 1H), 7.94–7.84 (m, 1H), 7.54 (d, *J* = 2.0 Hz, 1H), 7.41 (d, *J* = 7.9 Hz, 1H), 7.33 (dd, *J* = 7.7, 4.8 Hz, 1H), 7.25 (d, *J* = 8.7 Hz, 1H), 7.10 (dd, *J* = 8.7, 2.1 Hz, 1H), 6.41 (s, 1H), 6.11 (dt, *J* = 22.2, 8.3 Hz, 0.10H, *E*), 5.77 (dt, *J* = 32.6, 7.1 Hz, 0.90H, *Z*), 3.85 (ddt, *J* = 7.5, 4.2, 2.1 Hz, 1.80H, *Z*), 3.80 (ddt, *J* = 7.5, 4.2, 2.1 Hz, 0.20H, *E*).

¹³C-NMR (100 MHz, CDCl₃): δ = 150.5 (C_q), 149.8 (CH), 146.4 (dt, ¹*J*_{C-F} = 261, ²*J*_{C-F} = 29.1 Hz, C_q), 138.6 (CH), 137.6 (C_q), 135.6 (C_q), 129.3 (C_q), 126.6 (C_q), 122.6 (d, ²*J*_{C-F} = 13.5 Hz,

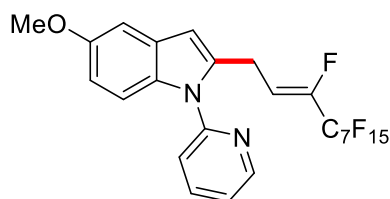
CH), 120.6 (CH), 120.5 (CH), 119.8 (CH), 117.1 (dt, $^1J_{C-F} = 285$ Hz, $^2J_{C-F} = 33.3$ Hz, C_q), 113.4 (m, C_q), 112.9 (dt, $^2J_{C-F} = 8.7$ Hz, $^3J_{C-F} = 4.5$ Hz, CH), 111.2 (d, $^4J_{C-F} = 2.8$ Hz, CH), 110.6 (m, C_q), 110.2 (m, C_q), 108.6 (m, C_q), 108.2 (m, C_q), 107.9 (m, C_q), 103.1 (CH), 22.7 (d, $^3J_{C-F} = 4.4$ Hz, CH₂).

^{19}F -NMR (470 MHz, CDCl₃): $\delta = -80.8$ (m), -117.5 (m), -122.0 (m), -122.8 (m), -122.9 (m), -123.4 (m), -126.1 (m), -130.2 (m).

IR (ATR): 3069, 1588, 1471, 1235, 1051, 781, 707, 528 cm⁻¹.

MS (ESI) m/z (relative intensity): 655 ([M + H]⁺, 100), 621 (15).

HR-MS (ESI): m/z calcd. for [C₂₃H₁₁ClF₁₆N₂ + H]⁺ 655.0428, found 655.0436.



(Z)-2-(1H,1H,2H-Perfluorodec-2-en-1-yl)-5-methoxy-1-(pyridin-2-yl)-1H-indole (316da):

The general procedure **A** was followed using 5-methoxy-1-(pyridin-2-yl)-1H-indole (**315d**) (112 mg, 0.50 mmol), 1H,1H,2H-perfluoro-1-decene (**301a**) (268 mg, 0.60 mmol) and NaOAc (12.3 mg, 30 mol %). Isolation by column chromatography (*n*-hexane/EtOAc = 10:1) yielded **316da** (292 mg, 90%, *Z/E* = 88:12) as a colorless oil.

^1H -NMR (400 MHz, CDCl₃): $\delta = 8.60$ (ddd, $J = 4.8, 2.0, 0.9$ Hz, 1H), 7.86 (ddd, $J = 7.7, 7.5, 2.0$ Hz, 1H), 7.44 (ddd, $J = 8.0, 1.0, 0.9$ Hz, 1H), 7.32–7.19 (m, 2H), 7.05 (d, $J = 2.5$ Hz, 1H), 6.81 (dd, $J = 9.0, 2.5$ Hz, 1H), 6.40 (d, $J = 1.0$ Hz, 1H), 6.13 (dt, $J = 22.3, 8.2$ Hz, 0.12H, *E*), 5.79 (dt, $J = 32.8, 7.5$ Hz, 0.88H, *Z*), 3.87 (ddt, $J = 7.5, 4.0, 2.3$ Hz, 2H), 3.84 (s, 3H).

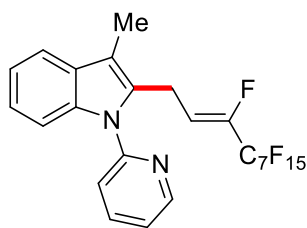
^{13}C -NMR (75 MHz, CDCl₃): $\delta = 155.1$ (C_q), 151.0 (C_q), 149.8 (CH), 146.0 (dt, $^1J_{C-F} = 261$ Hz, $^2J_{C-F} = 29.0$ Hz, C_q), 138.5 (CH), 136.6 (C_q), 132.2 (C_q), 128.9 (C_q), 121.9 (CH), 120.2 (CH), 116.7 (dt, $^1J_{C-F} = 285$ Hz, $^2J_{C-F} = 33.3$ Hz, C_q), 113.3 (dt, $^2J_{C-F} = 8.4$ Hz, $^3J_{C-F} = 4.5$ Hz, CH), 112.1 (CH), 111.8 (m, C_q), 111.0 (CH), 110.7 (m, C_q), 110.2 (m, C_q), 107.7 (m, C_q), 107.2 (m, C_q), 106.6 (m, C_q), 103.6 (CH), 102.4 (CH), 55.8 (CH₃), 22.8 (d, $J = 4.3$ Hz, CH₂).

^{19}F -NMR (376 MHz, CDCl₃): $\delta = -80.9$ (m), -117.5 (m), -122.0 (m), -122.8 (m), -122.9 (m), -123.4 (m), -126.2 (m), -130.9 (m).

IR (ATR): 1474, 1450, 1438, 1237, 1201, 1146, 907, 729, 649 cm⁻¹.

MS (ESI) m/z (relative intensity): 673 ([M + Na]⁺, 20), 651 ([M + H]⁺, 100), 381 (15).

HR-MS (ESI): m/z calcd. for [C₂₄H₁₄F₁₆N₂O + H]⁺ 651.0923, found 651.0917.



(Z)-2-(1H,1H,2H-Perfluorodec-2-en-1-yl)-3-methyl-1-(pyridin-2-yl)-1H-indole (316ea):

The general procedure **A** was followed using 3-methyl-1-(pyridin-2-yl)-1H-indole (**315e**) (104 mg, 0.50 mmol) and 1H,1H,2H-perfluoro-1-decene (**301a**) (268 mg, 0.60 mmol). Isolation by column chromatography (*n*-hexane/EtOAc = 10:1) yielded **316ea** (285 mg, 90%, *Z/E* = 88:12) as a white solid. M.p.: 65 °C.

¹H-NMR (300 MHz, CDCl₃): δ = 8.60 (ddd, *J* = 4.8, 1.9, 0.8 Hz, 1H), 7.86 (ddd, *J* = 8.1, 7.5, 2.0 Hz, 1H), 7.58–7.53 (m, 1H), 7.45 (ddd, *J* = 8.0, 1.0, 0.8 Hz, 1H), 7.37–7.31 (m, 1H), 7.28 (ddd, *J* = 7.5, 4.9, 1.0 Hz, 1H), 7.19–7.14 (m, 2H), 5.92 (dt, *J* = 23.2, 7.5 Hz, 0.12H, *E*), 5.69 (dt, *J* = 33.3, 7.4 Hz, 0.88H, *Z*), 3.86 (ddt, *J* = 7.5, 3.9, 2.3 Hz, 2H), 2.32 (s, 3H).

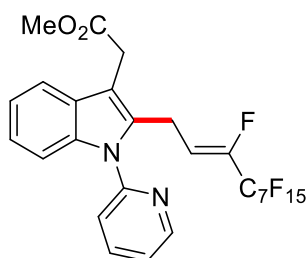
¹³C-NMR (125 MHz, CDCl₃): δ = 151.2 (C_q), 149.7 (CH), 145.3 (dt, ¹*J*_{C-F} = 261 Hz, ²*J*_{C-F} = 29.0 Hz, C_q), 138.3 (CH), 136.4 (C_q), 131.2 (C_q), 129.3 (C_q), 122.7 (CH), 121.8 (CH), 120.6 (CH), 120.4 (CH), 118.7 (CH), 116.6 (dt, ¹*J*_{C-F} = 285 Hz, ²*J*_{C-F} = 33.3 Hz, C_q), 113.9 (dt, ²*J*_{C-F} = 8.2 Hz, ³*J*_{C-F} = 4.5 Hz, CH), 112.9 (m, C_q), 111.7 (C_q), 110.6 (m, C_q), 110.5 (m, C_q), 110.3 (m, C_q), 109.9 (CH), 108.7 (m, C_q), 108.2 (m, C_q), 20.4 (d, ³*J*_{C-F} = 4.5 Hz, CH₂), 8.6 (CH₃).

¹⁹F-NMR (282 MHz, CDCl₃): δ = -80.8 (m), -117.4 (m), -122.1 (m), -122.8 (m), -122.8 (m), -123.3 (m), -126.1 (m), -131.7 (m).

IR (ATR): 3066, 1587, 1472, 1147, 906, 728 cm⁻¹.

MS (ESI) *m/z* (relative intensity): 657 ([M + Na]⁺, 15), 635 ([M + H]⁺, 100), 633 (20).

HR-MS (ESI): *m/z* calcd. for [C₂₄H₁₄F₁₆N₂ + H]⁺ 635.0974, found 635.0973.



(Z)-Methyl-2-[(1H,1H,2H-Perfluorodec-2-en-1-yl)-1-(pyridin-2-yl)-1H-indole-3-

yl]acetate (316fa): The general procedure **A** was followed using methyl 2-(1-(pyridin-2-yl)-1H-indol-3-yl)acetate (**315f**) (134 mg, 0.50 mmol) and 1H,1H,2H-perfluoro-1-decene (**301a**) (268 mg, 0.60 mmol). Isolation by column chromatography (*n*-hexane/EtOAc = 10:1) yielded **316fa** (214 mg, 62%, *Z/E* = 90:10) as a yellow solid. M.p.: 68 °C.

$^1\text{H-NMR}$ (500 MHz, CDCl_3): δ = 8.62 (ddd, J = 4.9, 1.9, 0.8 Hz, 1H), 7.87 (ddd, J = 7.7, 7.5, 1.9 Hz, 1H), 7.65 (ddd, J = 8.1, 3.2, 1.7 Hz, 1H), 7.47 (ddd, J = 7.9, 1.0, 0.8 Hz, 1H), 7.40–7.27 (m, 2H), 7.26–7.15 (m, 2H), 6.04 (dt, J = 22.8, 7.2 Hz, 0.10H, *E*), 5.77 (dt, J = 33.4, 7.4 Hz, 0.90H, *Z*), 3.94 (ddt, J = 7.4, 4.4, 2.2 Hz, 2H), 3.81 (s, 2H), 3.69 (s, 3H).

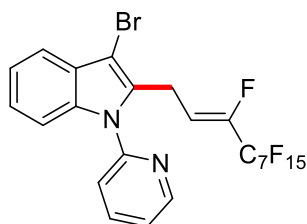
$^{13}\text{C-NMR}$ (125 MHz, CDCl_3): δ = 171.7 (C_q), 150.7 (C_q), 149.7 (CH), 145.4 (dt, $^1J_{\text{C-F}}$ = 260 Hz, $^2J_{\text{C-F}}$ = 29.1 Hz, C_q), 138.4 (CH), 136.4 (C_q), 133.4 (d, $^4J_{\text{C-F}}$ = 2.0 Hz, C_q), 128.1 (C_q), 122.9 (CH), 122.2 (CH), 121.1 (CH), 120.7 (CH), 118.8 (CH), 116.7 (dt, $^1J_{\text{C-F}}$ = 282 Hz, $^2J_{\text{C-F}}$ = 33.0 Hz, C_q), 113.7 (dt, $^2J_{\text{C-F}}$ = 8.1 Hz, $^3J_{\text{C-F}}$ = 4.3 Hz, CH), 112.6 (m, C_q), 112.3 (m, C_q), 110.1 (CH), 110.7 (m, C_q), 110.4 (m, C_q), 108.7 (C_q), 108.5 (m, C_q), 108.2 (m, C_q), 52.0 (CH_3), 30.1 (CH_2), 20.3 (d, $^3J_{\text{C-F}}$ = 4.2 Hz, CH_2).

$^{19}\text{F-NMR}$ (376 MHz, CDCl_3): δ = -80.9 (m), -117.5 (m), -122.1 (m), -122.9 (m), -123.4 (m), -124.1 (m), -126.2 (m), -130.4 (m).

IR (ATR): 1740, 1472, 1439, 1200, 1108, 733, 663 cm^{-1} .

MS (ESI) m/z (relative intensity): 693 [$\text{M} + \text{H}^+$], (100).

HR-MS (ESI): m/z calcd. for $[\text{C}_{26}\text{H}_{16}\text{F}_{16}\text{N}_2\text{O}_2 + \text{H}]^+$ 693.1029, found 693.1025.



(Z)-2-(1H,1H,2H-Perfluorodec-2-en-1-yl)-3-bromo-1-(pyridin-2-yl)-1H-indole (319aa): A modified general procedure **A** was followed using 3-bromo-1-(pyrimidin-2-yl)-1H-indole (**318a**) (136 mg, 0.50 mmol), 1H,1H,2H-perfluoro-1-decene (**301a**) (446 mg, 1.00 mmol), $[\text{MnBr}(\text{CO})_5]$ (13.7 mg, 10 mol %) and NaOAc (12.3 mg, 30 mol %). Isolation by column chromatography (*n*-hexane/EtOAc = 10:1) yielded **319aa** (310 mg, 89%, *Z/E* = 88:12) as a colorless oil.

$^1\text{H-NMR}$ (500 MHz, CDCl_3): δ = 8.63 (ddd, J = 4.9, 2.0, 0.8 Hz, 1H), 7.89 (ddd, J = 7.7, 7.7, 2.0 Hz, 1H), 7.64–7.58 (m, 1H), 7.48–7.42 (m, 1H), 7.37–7.32 (m, 2H), 7.27–7.23 (m, 2H), 5.96 (dt, J = 22.4, 7.3 Hz, 0.12H, *E*), 5.68 (dt, J = 32.7, 7.3 Hz, 0.88H, *Z*), 3.98 (ddt, J = 7.5, 3.9, 2.0 Hz, 2H).

$^{13}\text{C-NMR}$ (125 MHz, CDCl_3): δ = 150.2 (d, $^4J_{\text{C-F}}$ = 2.5 Hz, C_q), 149.8 (CH), 145.7 (dt, $^1J_{\text{C-F}}$ = 261 Hz, $^2J_{\text{C-F}}$ = 29.1 Hz, C_q), 138.4 (CH), 135.9 (d, $^3J_{\text{C-F}}$ = 8.8 Hz, C_q), 132.8 (d, $^4J_{\text{C-F}}$ = 2.0 Hz, C_q), 127.2 (C_q), 123.7 (d, $^3J_{\text{C-F}}$ = 5.7 Hz, CH), 122.5 (d, $^2J_{\text{C-F}}$ = 10.1 Hz, CH), 121.6 (d, $^3J_{\text{C-F}}$ = 3.8 Hz, CH), 120.4 (CH), 119.2 (CH), 117.2 (dt, $^1J_{\text{C-F}}$ = 283 Hz, $^2J_{\text{C-F}}$ = 33.0 Hz,

5. Experimental Part

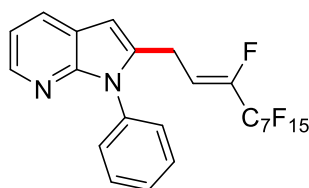
^{13}C -NMR (100 MHz, CDCl_3): $\delta = 112.7$ (m, C_q), 112.5 (dt, $^2J_{\text{C-F}} = 8.5$ Hz, $^3J_{\text{C-F}} = 4.4$ Hz, CH), 110.7 (m, C_q), 110.6 (m, C_q), 110.2 (CH), 110.1 (m, C_q), 109.8 (m, C_q), 108.4 (m, C_q), 95.0 (C_q), 21.1 (d, $^3J_{\text{C-F}} = 4.3$ Hz, CH_2).

^{19}F -NMR (470 MHz, CDCl_3): $\delta = -80.9$ (m), -117.5 (m), -122.0 (m), -122.8 (m), -123.2 (m), -123.4 (m), -126.2 (m), -130.1 (m).

IR (ATR): $1469, 1453, 1235, 1108, 738, 663$ cm^{-1} .

MS (ESI) m/z (relative intensity): 699 ($[\text{M}^{(79}\text{Br}) + \text{H}]^+$, 100), 619 (10).

HR-MS (ESI): m/z calcd. for $[\text{C}_{22}\text{H}_{11}^{79}\text{BrF}_{16}\text{N}_3 + \text{H}]^+$ 699.9875 , found 699.9918 .



(Z)-2-(1H,1H,2H-Perfluorohex-2-en-1-yl)-1-(pyridin-2-yl)-1H-7-azaindole (316ga): A modified general procedure A was followed using 1-(pyridin-2-yl)-1H-pyrrolo[2,3-*b*]pyridine (**315g**) (98.0 mg, 0.50 mmol), 1H,1H,2H-perfluoro-1-decene (**301a**) (446 mg, 1.00 mmol), $[\text{MnBr}(\text{CO})_5]$ (13.7 mg, 10 mol %) and NaOAc (12.3 mg, 30 mol %). Isolation by column chromatography (*n*-hexane/EtOAc = 10:1) yielded **316ga** (254 mg, 82%, *Z/E* = 80:20) as a colorless oil.

^1H -NMR (300 MHz, CDCl_3) $\delta = 8.58$ (ddd, $J = 4.9, 1.9, 0.9$ Hz, 1H), 8.28 (dt, $J = 4.8, 1.8$ Hz, 1H), 7.95 – 7.82 (m, 3H), 7.30 (ddd, $J = 6.7, 4.9, 2.0$ Hz, 1H), 7.12 (ddd, $J = 7.8, 4.8, 1.9$ Hz, 1H), 6.42 (dt, $J = 2.0, 0.9$ Hz, 1H), 6.17 (dt, $J = 22.3, 8.2$ Hz, 0.20 H, *E*), 5.83 (dt, $J = 32.8, 7.5$ Hz, 0.80H, *Z*), 4.00 (ddt, $J = 7.5, 3.6, 2.0$ Hz, 2H).

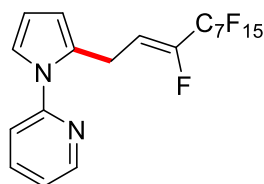
^{13}C -NMR (100 MHz, CDCl_3): $\delta = 149.8$ (C_q), 148.8 (CH, *Z*), 148.7 (CH, *E*), 146.5 (dt, $^1J_{\text{C-F}} = 262$ Hz, $^2J_{\text{C-F}} = 29.6$ Hz, C_q), 143.1 (CH), 138.1 (CH), 137.3 (C_q), 128.1 (CH), 122.1 (CH), 121.7 (CH), 119.0 (C_q), 117.4 (CH), 116.5 (dt, $^1J_{\text{C-F}} = 286$ Hz, $^2J_{\text{C-F}} = 32.7$ Hz, C_q), 115.2 (C_q), 113.0 (dt, $^2J_{\text{C-F}} = 8.7$ Hz, $^3J_{\text{C-F}} = 4.5$ Hz, CH), 112.6 (m, C_q), 111.5 (m, C_q), 111.0 (m, C_q), 110.4 (m, C_q), 107.9 (m, C_q), 106.7 (m, C_q), 101.5 (CH), 23.3 (d, $^3J_{\text{C-F}} = 4.4$ Hz, CH_2).

^{19}F -NMR (282 MHz, CDCl_3): $\delta = -81.0$ (m), -117.6 (m), -122.1 (m), -122.1 (m), -122.9 (m), -123.0 (m), -126.3 (m), -130.4 (m).

IR (ATR): $3073, 2852, 1590, 1471, 1236, 805, 663$ cm^{-1} .

MS (ESI) m/z (relative intensity): 622 ($[\text{M} + \text{H}]^+$, 100), 602 (15).

HR-MS (ESI): m/z calcd. for $[\text{C}_{22}\text{H}_{11}\text{F}_{16}\text{N}_3 + \text{H}]^+$ 622.0770 , found 622.0769 .



(Z)-2-[2-(1H,1H,2H-Perfluorodec-2-en-1-yl)-1H-pyrrol-1-yl]pyridine (321aa): The general procedure A was followed using 2-(1H-pyrrol-1-yl)pyridine (**320a**) (72.0 mg, 0.50 mmol) and 1H,1H,2H-perfluoro-1-decene (**301a**) (268 mg, 0.60 mmol). Isolation by column chromatography (*n*-hexane/EtOAc = 10:1) yielded **321aa** (177 mg, 62%, *Z/E* = 87:13) and **321aa'** (59.1 mg, 12%, *Z/E* = 87:13) as yellow oils.

¹H-NMR (400 MHz, CDCl₃): δ = 8.47 (ddd, *J* = 4.9, 1.9, 0.9 Hz, 1H), 7.77 (ddd, *J* = 8.2, 7.5, 1.9 Hz, 1H), 7.28 (dt, *J* = 8.2, 0.9 Hz, 1H), 7.18 (ddd, *J* = 7.5, 4.9, 0.9 Hz, 1H), 7.01 (ddd, *J* = 3.1, 1.8, 0.5 Hz, 1H), 6.24 (ddd, *J* = 3.1, 2.6, 0.5 Hz, 1H), 6.16 (dt, *J* = 22.7, 8.2 Hz, 0.13H, *E*), 6.12–6.09 (m, 1H) 5.81 (dt, *J* = 33.4, 7.5 Hz, 0.87H, *Z*), 3.88 (ddt, *J* = 7.5, 3.9, 2.0 Hz, 1.74H, *Z*), 3.83 (ddt, *J* = 7.5, 4.0, 2.0 Hz, 0.26H, *E*).

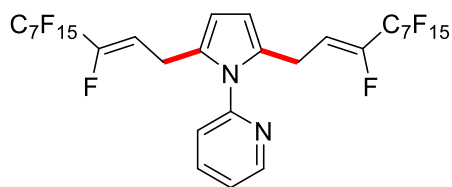
¹³C-NMR (100 MHz, CDCl₃): δ = 152.5 (C_q), 148.6 (CH), 145.4 (dt, ¹*J*_{C-F} = 260 Hz, ²*J*_{C-F} = 30.1 Hz, C_q), 138.5 (CH), 129.1 (C_q), 121.2 (CH), 121.0 (CH), 116.9 (dt, ¹*J*_{C-F} = 285 Hz, ²*J*_{C-F} = 33.3 Hz, C_q), 116.6 (CH), 114.6 (dt, *J* = 8.3, 4.3 Hz, CH), 112.2 (m, C_q), 111.3 (m, C_q), 111.2 (m, C_q), 110.9 (m, C_q), 110.7 (CH), 109.7 (CH), 108.6 (m, C_q), 107.8 (C_q), 22.9 (d, ³*J*_{C-F} = 4.2 Hz, CH₂).

¹⁹F-NMR (376 MHz, CDCl₃): δ = –80.8 (m), –117.5 (m), –122.0 (m), –122.8 (m), –123.0 (m), –123.5 (m), –126.2 (m), –132.3 (m).

IR (ATR): 1523, 1504, 1325, 1182, 992, 754 cm⁻¹.

MS (ESI) *m/z* (relative intensity): 593 ([M + Na]⁺, 20), 571 ([M + H]⁺, 100).

HR-MS (ESI): *m/z* calcd. for [C₁₉H₁₀F₁₆N₂ + H]⁺ 571.0661, found 571.0668.



(Z)-2-[2,5-Di-(1H,1H,2H-perfluorodec-2-en-1-yl)-1H-pyrrol-1-yl]pyridine (321aa'):

¹H-NMR (300 MHz, CDCl₃): δ = 8.58 (ddd, *J* = 4.9, 1.9, 0.9 Hz, 1H), 7.84 (ddd, *J* = 8.2, 7.5, 2.0 Hz, 1H), 7.34 (dt, *J* = 8.2, 0.9 Hz, 1H), 7.23 (ddd, *J* = 7.5, 4.9, 0.9 Hz, 1H), 6.03–5.92 (m, 2H), 5.80 (dt, *J* = 22.7, 8.2 Hz, 0.26H, *E*), 5.61 (dt, *J* = 33.4, 7.5 Hz, 1.74H, *Z*), 3.45 (ddt, *J* = 7.5, 3.9, 2.0 Hz, 4H).

5. Experimental Part

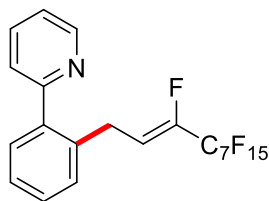
^{13}C -NMR (100 MHz, CDCl_3): $\delta = 150.7$ (C_q), 149.8 (CH), 145.7 (dt, $^1J_{\text{C-F}} = 259$ Hz, $^2J_{\text{C-F}} = 30.1$ Hz, C_q), 138.4 (CH), 129.1 (C_q), 123.1 (CH), 121.9 (CH), 117.4 (dt, $^1J_{\text{C-F}} = 288$ Hz, $^2J_{\text{C-F}} = 33.3$ Hz, C_q), 112.6 (dt, $J = 8.3, 4.3$ Hz, CH), 111.2 (m, C_q), 110.8 (m, C_q), 110.2 (m, C_q), 109.7 (m, C_q), 108.8 (m, C_q), 108.2 (m, C_q), 107.8 (CH), 21.3 (d, $^3J_{\text{C-F}} = 4.1$ Hz, CH_2).

^{19}F -NMR (376 MHz, CDCl_3): $\delta = -81.2$ (m), -117.7 (m), -121.9 (m), -122.2 (m), -123.1 (m), -123.1 (m), -126.4 (m), -131.8 (m).

IR (ATR): 2960, 2924, 1473, 1235, 1143, 1047, 735, 559 cm^{-1} .

MS (ESI) m/z (relative intensity): 997 ($[\text{M} + \text{H}]^+$, 100), 573 (20), 545 (15).

HR-MS (ESI): m/z calcd. for $[\text{C}_{29}\text{H}_{12}\text{F}_{32}\text{N}_2 + \text{H}]^+$ 997.0562, found: 997.0553



(Z)-2-[2-(1H,1H,2H-Perfluorodec-2-en-1-yl)phenyl]pyridine (322aa): A modified procedure **A** was followed using 2-phenylpyridine (**93a**) (78.0 mg, 0.50 mmol), 1H,1H,2H-perfluoro-1-decene (**301a**) (268 mg, 0.60 mmol) and NaOAc (12.3 mg, 30 mol %) at 120 °C. Isolation by column chromatography (*n*-hexane/EtOAc = 10:1) yielded **322aa** (169 mg, 58%, *Z/E* = 86:14) as a yellow oil.

^1H -NMR (300 MHz, CDCl_3): $\delta = 8.67$ (ddd, $J = 4.9, 1.9, 0.9$ Hz, 1H), 7.74 (dt, $J = 7.7, 1.8$ Hz, 1H), 7.48–7.17 (m, 6H), 6.05 (dt, $J = 23.1, 8.2$ Hz, 0.14H), 5.76 (dt, $J = 33.4, 7.7$ Hz, 0.86H), 3.73 (ddt, $J = 7.7, 4.0, 2.3$ Hz, 2H).

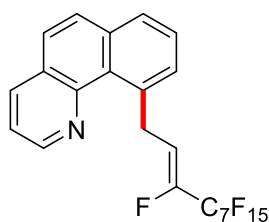
^{13}C -NMR (125 MHz, CDCl_3): $\delta = 159.3$ (C_q), 149.0 (CH), 145.4 (dt, $^1J_{\text{C-F}} = 258$ Hz, $^2J_{\text{C-F}} = 29.0$ Hz, C_q), 140.3 (C_q), 136.4 (d, $^2J_{\text{C-F}} = 7.4$ Hz, CH), 135.7 (C_q), 130.0 (d, $^2J_{\text{C-F}} = 7.8$ Hz, CH), 128.7 (d, $^3J_{\text{C-F}} = 3.2$ Hz, CH), 127.0 (d, $^3J_{\text{C-F}} = 4.2$ Hz, CH), 123.9 (CH), 123.8 (d, $^2J_{\text{C-F}} = 10.8$ Hz, CH), 121.9 (d, $^4J_{\text{C-F}} = 2.2$ Hz, CH), 117.0 (dt, $^1J_{\text{C-F}} = 285$ Hz, $^2J_{\text{C-F}} = 33.3$ Hz, C_q), 115.7 (m, CH), 112.7 (m, C_q), 112.4 (m, C_q), 110.9 (m, C_q), 110.7 (m, C_q), 108.5 (m, C_q), 108.3 (m, C_q), 27.8 (d, $^3J_{\text{C-F}} = 3.5$ Hz, CH_2).

^{19}F -NMR (282 MHz, CDCl_3): $\delta = -81.0$ (m), -117.5 (m), -122.2 (m), -123.0 (m), -123.5 (m), -124.5 (m), -126.3 (m), -132.7 (m).

IR (ATR): 1235, 1198, 1105, 748, 663 cm^{-1} .

MS (ESI) m/z (relative intensity): 582 $[\text{M} + \text{H}]^+$, (100).

HR-MS (ESI): m/z calcd. for $[\text{C}_{21}\text{H}_{11}\text{F}_{16}\text{N} + \text{H}]^+$ 582.0709, found 582.0718.



(Z)-10-(1H,1H,2H-Perfluorodec-2-en-1-yl)benzo[h]quinolone (324aa): A modified general procedure **A** was followed using benzo[h]quinolone (**323a**) (90.0 mg, 0.50 mmol), 1H,1H,2H-perfluoro-1-decene (**301a**) (446 mg, 1.00 mmol), [MnBr(CO)₅] (13.7 mg, 10 mol %) and NaOAc (12.3 mg, 30 mol %) at 120 °C. Isolation by column chromatography (*n*-hexane/EtOAc = 10:1) yielded **324aa** (163 mg, 54%, *Z/E* = 96:4) as a yellow oil.

¹H-NMR (400 MHz, CDCl₃): δ = 8.97 (ddd, *J* = 4.3, 1.9, 0.9 Hz, 1H), 8.25–8.09 (m, 1H), 7.85 (dd, *J* = 7.3, 1.9 Hz, 1H), 7.80 (d, *J* = 8.8 Hz, 1H), 7.67 (d, *J* = 8.8 Hz, 1H), 7.64–7.56 (m, 2H), 7.49 (ddd, *J* = 8.0, 4.3, 0.6 Hz, 1H), 6.50 (dt, *J* = 24.3, 8.0 Hz, 0.04H, *E*), 6.20 (dt, *J* = 35.0, 7.4 Hz, 0.96H, *Z*), 4.80 (ddt, *J* = 7.4, 3.8, 2.3 Hz, 2H).

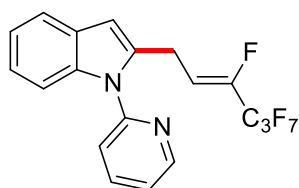
¹³C-NMR (100 MHz, CDCl₃): δ = 147.8 (C_q), 147.4 (CH), 145.0 (dt, ¹*J*_{C-F} = 261 Hz, ²*J*_{C-F} = 29.1 Hz, C_q), 137.4 (C_q), 135.7 (CH), 135.5 (C_q), 131.2 (CH), 129.2 (C_q), 128.8 (CH), 128.2 (CH), 127.7 (CH), 127.5 (C_q), 125.8 (CH), 121.0 (CH), 117.6 (CH), 116.9 (dt, ¹*J*_{C-F} = 275 Hz, ²*J*_{C-F} = 32.3 Hz, C_q), 113.4 (m, C_q), 111.3 (m, C_q), 110.9 (m, C_q), 110.7 (m, C_q), 108.6 (m, C_q), 108.0 (m, C_q), 33.0 (d, ³*J*_{C-F} = 3.8 Hz, CH₂).

¹⁹F-NMR (376 MHz, CDCl₃): δ = -80.8 (m), -117.2 (m), -122.0 (m), -122.1 (m), -122.8 (m), -122.9 (m), -126.2 (m), -133.7 (m).

IR (ATR): 1235, 1200, 1146, 833, 663 cm⁻¹.

MS (ESI) *m/z* (relative intensity): 606 ([M + H]⁺, 100), 582 (20).

HR-MS (ESI): *m/z* calcd. for [C₂₃H₁₁F₁₆N + H]⁺ 606.0709, found 606.0704.



(Z)-2-(1H,1H,2H-Perfluorohex-2-en-1-yl)-1-(pyridin-2-yl)-1H-indole (316ab): The general procedure **A** was followed using 1-(pyridin-2-yl)-1H-indole (**315a**) (97.1 mg, 0.50 mmol) and 1H,1H,2H-perfluoro-1-hexene (**301b**) (148 mg, 0.60 mmol). Isolation by column chromatography (*n*-hexane/EtOAc = 10:1) yielded **316ab** (160 mg, 76%, *Z/E* = 90:10) as a colourless oil.

5. Experimental Part

$^1\text{H-NMR}$ (400 MHz, CDCl_3): δ = 8.68 (ddd, J = 4.9, 2.0, 0.9 Hz, 1H), 7.93 (ddd, J = 7.6, 7.6, 2.0 Hz, 1H), 7.72–7.60 (m, 1H), 7.52 (d, J = 8.0 Hz, 1H), 7.45–7.32 (m, 2H), 7.25–7.18 (m, 2H), 6.54 (d, J = 0.9 Hz, 1H), 6.20 (dt, J = 22.5, 8.3 Hz, 0.10H, *E*), 5.85 (dt, J = 32.9, 7.5 Hz, 0.90H, *Z*), 3.93 (ddt, J = 6.9, 3.3, 2.4 Hz, 2H).

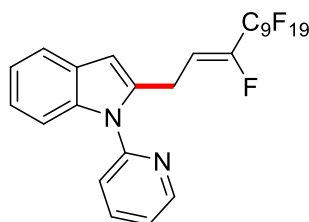
$^{13}\text{C-NMR}$ (100 MHz, CDCl_3): δ = 150.9 (C_q), 149.7 (CH), 145.9 (dt, $^1J_{\text{C-F}}$ = 262 Hz, $^2J_{\text{C-F}}$ = 29.8 Hz, C_q), 138.4 (CH), 137.1 (C_q), 136.1 (C_q), 128.3 (C_q), 122.4 (CH), 122.2 (CH), 121.0 (CH), 120.5 (CH), 120.4 (CH), 117.9 (dt, $^1J_{\text{C-F}}$ = 285 Hz, $^2J_{\text{C-F}}$ = 33.0 Hz, C_q), 113.3 (dt, $^2J_{\text{C-F}}$ = 8.3 Hz, $^3J_{\text{C-F}}$ = 4.3 Hz, CH), 110.1 (CH), 109.6 (m, C_q), 107.7 (m, C_q), 103.7 (CH), 22.7 (d, $^3J_{\text{C-F}}$ = 4.3 Hz, CH₂).

$^{19}\text{F-NMR}$ (376 MHz, CDCl_3): δ = -80.8 (m), -115.9 (m, *E*), -118.5 (m, *Z*), -127.4 (m, *Z*), -127.9 (m, *E*), -131.0 (m).

IR (ATR): 3059, 1587, 1119, 782, 737 cm^{-1} .

MS (ESI) m/z (relative intensity): 443 ($[\text{M} + \text{Na}]^+$, 10), 421 (100).

HR-MS (ESI): m/z calcd. for $[\text{C}_{19}\text{H}_{12}\text{F}_8\text{N}_2 + \text{H}]^+$ 421.0946, found 421.0950.



(Z)-2-(1H,1H,2H-Perfluorododec-2-en-1-yl)-1-(pyridin-2-yl)-1H-indole (316ac): The general procedure **A** was followed using 1-(pyridin-2-yl)-1H-indole (**315a**) (97.1 mg, 0.50 mmol) and 1H,1H,2H-perfluoro-1-dodecene (**301c**) (328 mg, 0.60 mmol). Isolation by column chromatography (*n*-hexane/EtOAc = 10:1) yielded **316ac** (302 mg, 84%, *Z/E* = 89:11) as a colorless oil.

$^1\text{H-NMR}$ (500 MHz, CDCl_3): δ = 8.64 (ddd, J = 4.8, 2.0, 0.8 Hz, 1H), 7.87 (ddd, J = 7.7, 7.5, 2.0 Hz, 1H), 7.63–7.58 (m, 1H), 7.48 (dt, J = 8.0, 1.0 Hz, 1H), 7.40–7.36 (m, 1H), 7.31 (ddd, J = 7.5, 4.9, 1.0 Hz, 1H), 7.20–7.15 (m, 2H), 6.50 (d, J = 0.9 Hz, 1H), 6.15 (dt, J = 22.4, 8.2 Hz, 0.11H, *E*), 5.81 (dt, J = 32.8, 7.5 Hz, 0.89H, *Z*), 3.90 (ddt, J = 7.5, 4.0, 2.2 Hz, 1.78H, *Z*), 3.85 (ddt, J = 7.5, 4.0, 2.2 Hz, 0.22H, *E*).

$^{13}\text{C-NMR}$ (125 MHz, CDCl_3): δ = 150.8 (C_q), 149.7 (CH), 146.2 (dt, $^1J_{\text{C-F}}$ = 261 Hz, $^2J_{\text{C-F}}$ = 29.0 Hz, C_q), 138.4 (CH), 137.1 (C_q), 136.1 (d, $^4J_{\text{C-F}}$ = 2.0 Hz, C_q), 128.3 (C_q), 122.4 (CH), 122.2 (CH), 121.1 (CH), 120.6 (CH), 120.4 (CH), 117.2 (dt, $^1J_{\text{C-F}}$ = 290 Hz, $^2J_{\text{C-F}}$ = 33.1 Hz, C_q), 113.3 (dt, $^2J_{\text{C-F}}$ = 8.5 Hz, $^3J_{\text{C-F}}$ = 4.4 Hz, CH), 112.7 (m, C_q), 110.8 (m, C_q), 110.6 (m, C_q),

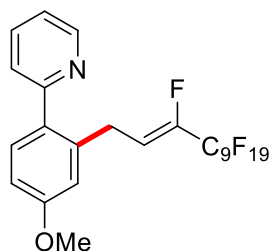
110.1 (CH), 108.8 (m, C_q), 108.5 (m, C_q), 108.2 (m, C_q), 106.3 (m, C_q), 106.1 (m, C_q), 103.7 (CH), 22.7 (d, ³J_{C-F} = 4.3 Hz, CH₂).

¹⁹F-NMR (470 MHz, CDCl₃): δ = -81.0 (m), -117.6 (m), -121.8 (m), -122.0 (m), -122.0 (m), -122.2 (m), -122.9 (m), -123.0 (m), -126.3 (m), -130.9 (m).

IR (ATR): 1471, 1438, 1200, 1105, 735, 556, 528 cm⁻¹.

MS (ESI) *m/z* (relative intensity): 721 ([M + H]⁺, 100), 621 (10).

HR-MS (ESI): *m/z* calcd. for [C₂₅H₁₂F₂₀N₂ + H]⁺ 721.0754, found 721.0755.



(Z)-4-Methoxy-2-[2-(1H,1H,2H-perfluorododec-2-en-1-yl)phenyl]pyridine (322bc): A modified general procedure **A** was followed using 2-(4-methoxyphenyl)pyridine (**93b**) (93.0 mg, 0.50 mmol), 1H,1H,2H-perfluoro-1-dodecene (**301c**) (546 mg, 1.00 mmol) and [MnBr(CO)₅] (13.7 mg, 10 mol %) at 120 °C. Isolation by column chromatography (*n*-hexane/EtOAc = 10:1) yielded **322bc** (201 mg, 57%, *Z/E* = 92:8) as a pale yellow solid. M.p.: 55 °C.

¹H-NMR (300 MHz, CDCl₃): δ = 8.63 (ddd, *J* = 4.9, 1.9, 0.9 Hz, 1H), 7.80–7.57 (m, 1H), 7.37–7.34 (m, 1H), 7.34–7.31 (m, 1H), 7.20 (ddd, *J* = 7.6, 4.9, 1.2 Hz, 1H), 6.86 (dd, *J* = 8.4, 2.6 Hz, 1H), 6.80 (d, *J* = 2.6 Hz, 1H), 6.05 (dt, *J* = 23.0, 8.2 Hz, 0.08H, *E*), 5.76 (dt, *J* = 33.4, 7.7 Hz, 0.92H, *Z*), 3.82 (s, 3H), 3.72 (ddt, *J* = 7.4, 3.8, 2.3 Hz, 2H).

¹³C-NMR (125 MHz, CDCl₃): δ = 159.8 (C_q), 159.1 (C_q), 149.0 (CH), 145.3 (dt, ¹J_{C-F} = 258 Hz, 29.0 Hz, C_q), 137.2 (C_q), 136.4 (CH), 132.9 (C_q), 131.3 (CH), 123.7 (CH), 121.5 (CH), 117.1 (dt, ¹J_{C-F} = 289 Hz, ²J_{C-F} = 33.2 Hz, C_q), 115.7 (C_q), 115.5 (CH), 112.4 (CH), 112.2 (m, C_q), 110.7 (m, C_q), 110.6 (m, C_q), 110.5 (m, C_q), 108.8 (m, C_q), 108.5 (m, C_q), 108.2 (m, C_q), 55.3 (CH₃), 28.1 (d, ⁴J_{C-F} = 3.4 Hz, CH₂).

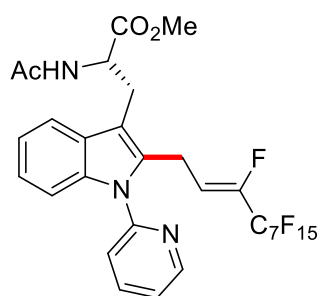
¹⁹F-NMR (282 MHz, CDCl₃): δ = -80.9 (m), -117.5 (m), -121.7 (m), -121.8 (m), -122.0 (m), -122.2 (m), -122.8 (m), -123.0 (m), -126.2 (m), -132.7 (m).

IR (ATR): 1609, 1467, 1429, 1201, 1147, 1045, 786, 529 cm⁻¹.

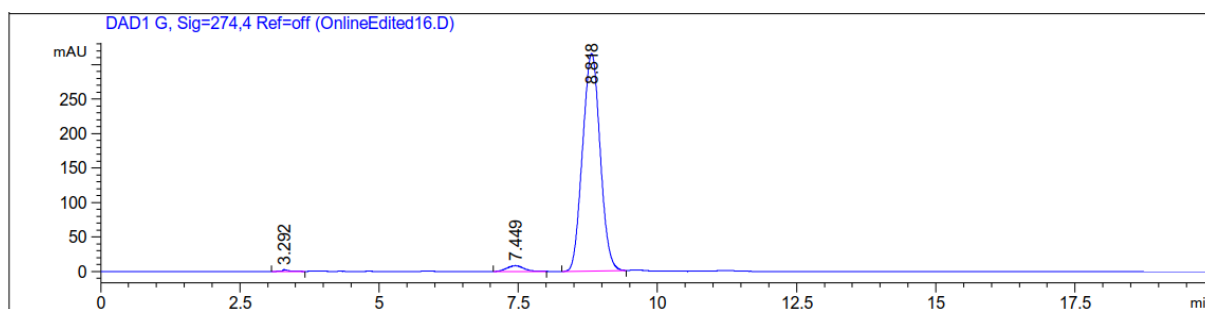
MS (ESI) *m/z* (relative intensity): 712 ([M + H]⁺, 100).

HR-MS (ESI): *m/z* calcd. for [C₂₄H₁₃F₂₀NO + H]⁺ 712.0751, found 712.0756.

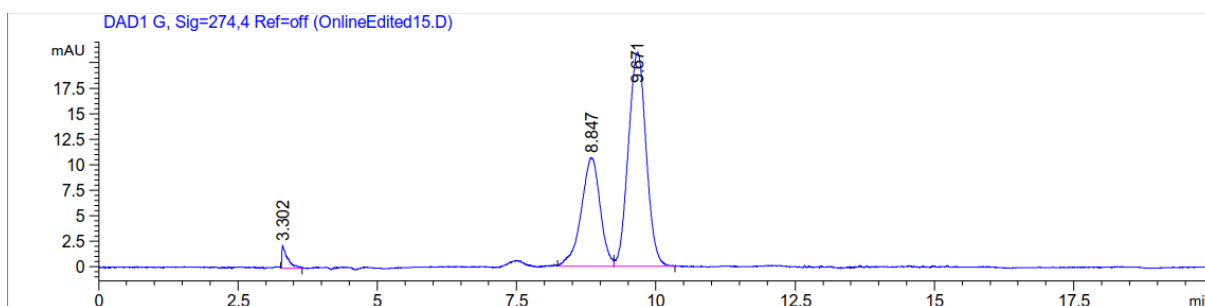
5. Experimental Part



(Z)- Methyl acetyl-1-(pyridin-2-yl)-2-(1H,1H,2H-perfluorodec-2-en-1-yl)-L-tryptophanate (329aa): A modified general procedure A was followed using methyl acetyl-1-(pyridin-2-yl)-L-tryptophanate (**328a**) (168 mg, 0.50 mmol), 1H,1H,2H-perfluoro-1-decene (**301a**) (446 mg, 1.00 mmol), [MnBr(CO)₅] (13.7 mg, 10 mol %) and NaOAc (12.3 mg, 30 mol %). Isolation by column chromatography (*n*-hexane/EtOAc = 1:1) yielded **329aa** (317 mg, 83%, *Z/E* = 98:2) as a white solid. M.p.: 118 °C.



Reaction with **328a** (*ee* = 35%):



¹H-NMR (500 MHz, CDCl₃): δ = 8.64–8.53 (m, 1H), 7.85 (ddd, *J* = 7.5, 7.5, 1.9 Hz, 1H), 7.58–7.51 (m, 1H), 7.42 (dt, *J* = 8.0, 1.0 Hz, 1H), 7.34–7.26 (m, 2H), 7.19–7.11 (m, 2H), 6.26 (d, *J* = 8.0 Hz, 1H), 5.78 (dt, *J* = 22.7, 7.0 Hz, 0.02H, *E*), 5.47 (dt, *J* = 33.1, 7.2 Hz, 0.98H, *Z*), 4.96 (ddd, *J* = 8.0, 6.4, 5.0 Hz, 1H), 4.01–3.77 (m, 2H), 3.66 (s, 3H), 3.42–3.25 (m, 2H), 1.94 (s, 3H).

¹³C-NMR (125 MHz, CDCl₃): δ = 172.4 (C_q), 169.8 (C_q), 150.6 (C_q), 149.7 (CH), 145.5 (dt, ¹*J*_{C-F} = 262 Hz, ²*J*_{C-F} = 29.3 Hz, C_q), 138.4 (CH), 136.6 (C_q), 133.6 (C_q), 128.5 (C_q), 122.9 (CH), 122.3 (CH), 120.9 (CH), 120.6 (CH), 118.6 (CH), 116.9 (dt, ¹*J*_{C-F} = 292 Hz, ²*J*_{C-F} = 31.8 Hz, C_q), 113.6 (CH), 112.4 (m, C_q), 112.1 (m, C_q), 110.6 (m, C_q), 110.3 (m, C_q), 110.0

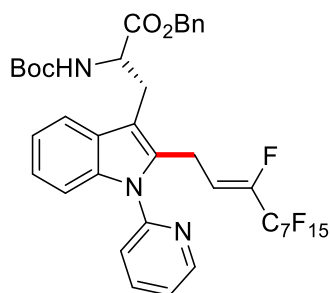
(CH), 109.9 (C_q), 108.5 (m, C_q), 108.1 (m, C_q), 52.8 (CH), 52.4 (CH₃), 26.9 (d, ⁴J_{C-F} = 4.1 Hz, CH₂), 23.0 (CH₃), 20.1 (CH₂).

¹⁹F-NMR (470 MHz, CDCl₃): δ = -80.9 (m), -117.4 (m), -121.0 (m), -121.1 (m), -122.9 (m), -123.0 (m), -126.3 (m), -130.2 (m).

IR (ATR): 1725, 1472, 1439, 1201, 1147, 1106, 908, 707 cm⁻¹.

MS (ESI) *m/z* (relative intensity): 786 ([M + Na]⁺, 20), 764 ([M + H]⁺, 100).

HR-MS (ESI): *m/z* calcd. for [C₂₉H₂₁F₁₆N₃O₃ + H]⁺ 764.1400, found 764.1392.



(Z)- Benzyl *tert*-butyloxycarbonyl-1-(pyridin-2-yl)-2-(1*H*,1*H*,2*H*-perfluorodec-2-en-1-yl)-L-tryptophanate (329ba): A modified general procedure A was followed using benzyl *tert*-butyloxycarbonyl-1-(pyridin-2-yl)-L-tryptophanate (**328b**) (236 mg, 0.50 mmol), 1*H*,1*H*,2*H*-perfluoro-1-decene (**301a**) (446 mg, 1.00 mmol), [MnBr(CO)₅] (13.7 mg, 10 mol %) and NaOAc (12.3 mg, 30 mol %). Isolation by column chromatography (*n*-hexane/EtOAc = 20:1) yielded **329ba** (381 mg, 85%, *Z/E* = 90:10) as a white solid. M.p.: 63 °C.

¹H-NMR (300 MHz, CDCl₃): δ = 8.60 (ddd, *J* = 4.8, 1.9, 0.9 Hz, 1H), 7.85 (ddd, *J* = 7.7, 7.6, 1.9 Hz, 1H), 7.68–7.48 (m, 1H), 7.41–7.26 (m, 6H), 7.23–7.11 (m, 4H), 5.84 (dt, *J* = 23.1, 8.4 Hz, 0.10H, *E*), 5.53 (dt, *J* = 33.0, 7.1 Hz, 0.90H, *Z*), 5.21 (d, *J* = 8.3 Hz, 1H), 5.14–4.96 (m, 2H), 4.80–4.68 (m, 1H), 3.95–3.78 (m, 2H), 3.34 (d, *J* = 6.0 Hz, 2H), 1.41 (s, 9H).

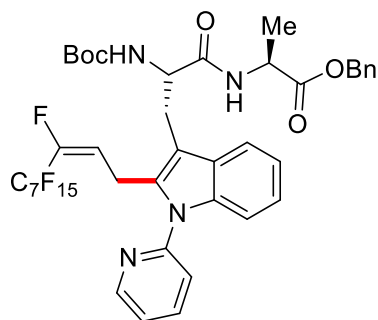
¹³C-NMR (125 MHz, CDCl₃): δ = 171.8 (C_q), 154.9 (C_q), 150.6 (C_q), 149.5 (CH), 145.7 (dt, ¹J_{C-F} = 261 Hz, ²J_{C-F} = 29.0 Hz, C_q), 138.2 (CH), 136.6 (C_q), 134.9 (C_q), 133.6 (C_q), 128.2 (CH), 122.8 (CH), 122.1 (CH), 120.7 (d, ²J_{C-F} = 39.7 Hz, CH), 118.8 (CH), 113.7 (CH), 110.1 (C_q), 110.0 (CH), 79.9 (CH₂), 67.3 (C_q), 54.2 (CH), 28.2 (CH₃), 27.6 (CH₂), 20.3 (d, ³J_{C-F} = 4.0 Hz, CH₂).

¹⁹F-NMR (282 MHz, CDCl₃): δ = -80.9 (m), -117.3 (m), -122.1 (m), -122.1 (m), -122.8 (m), -123.2 (m), -126.2 (m), -130.2 (m).

IR (ATR): 1707, 1472, 1238, 1149, 906, 649 cm⁻¹.

MS (ESI) *m/z* (relative intensity): 920 ([M + Na]⁺, 20), 898 ([M + H]⁺, 100).

HR-MS (ESI): *m/z* calcd. for [C₃₈H₃₁F₁₆N₃O₄ + H]⁺ 898.2132, found: 898.2122.



Benzyl [(S)-2-(tert-butoxycarbonyl)amino-3-{2-((Z)-1H,1H,2H-perfluorodec-2-en-1-yl)-1-(pyridin-2-yl)-1H-indol-3-yl}propanoyl]-L-alaninate (329ca): A modified general procedure A was followed using benzyl *N*-(tert-butoxycarbonyl)-1-(pyridin-2-yl)-L-tryptophyl-L-alaninate (**328c**) (54.2 mg, 0.10 mmol), 1*H*,1*H*,2*H*-perfluoro-1-decene (**301a**) (134 mg, 0.30 mmol), NaOAc (2.4 mg, 30 mol %) and [MnBr(CO)₅] (5.6 mg, 20 mol %). Isolation by column chromatography (*n*-hexane/EtOAc = 1:1) yielded **329ca** (62.0 mg, 64%, *Z/E* = 90:10) as a pale yellow solid. M.p.: 140 °C.

¹H-NMR (400 MHz, CDCl₃): δ = 8.63 (ddd, *J* = 4.9, 2.0, 0.9 Hz, 1H), 7.90 (ddd, *J* = 7.6, 7.5, 1.9 Hz, 1H), 7.77–7.64 (m, 1H), 7.49 (d, *J* = 8.1 Hz, 1H), 7.39–7.31 (m, 5H), 7.28 (t, *J* = 3.8 Hz, 2H), 7.19 (dd, *J* = 6.1, 3.1 Hz, 2H), 6.33 (d, *J* = 7.1 Hz, 1H), 5.89 (dt, *J* = 22.9, 7.2 Hz, 0.10H, *E*), 5.59 (dt, *J* = 33.2, 7.2 Hz, 0.90H, *Z*), 5.31 (bs, 1H), 5.05 (d, *J* = 2.8 Hz, 2H), 4.64–4.33 (m, 2H), 3.93 (ddt, *J* = 7.4, 3.8, 2.3 Hz, 2H), 3.47–3.13 (m, 2H), 1.45 (s, 9H), 1.33 (d, *J* = 7.1 Hz, 3H).

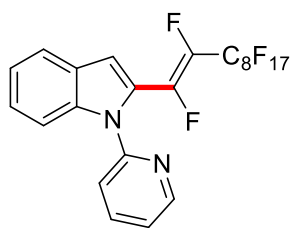
¹³C-NMR (100 MHz, CDCl₃): δ = 172.0 (C_q), 170.8 (C_q), 155.1 (C_q), 150.8 (C_q), 149.7 (CH), 145.2 (dt, ¹*J*_{C-F} = 260 Hz, ²*J*_{C-F} = 29.1 Hz, C_q), 138.4 (CH), 136.8 (C_q), 135.3 (C_q), 133.8 (C_q), 128.6 (CH), 128.4 (CH), 128.2 (C_q), 128.0 (CH), 122.9 (CH), 122.3 (CH), 121.1 (CH), 120.9 (CH), 118.9 (CH), 117.0 (dt, ¹*J*_{C-F} = 288 Hz, ²*J*_{C-F} = 33.0 Hz, C_q), 113.7 (dt, *J* = 8.3, 4.3 Hz, CH), 113.2 (m, C_q), 112.7 (m, C_q), 111.0 (m, C_q), 110.9 (m, C_q), 110.7 (m, C_q), 110.4 (C_q), 110.1 (CH), 107.9 (m, C_q), 80.1 (C_q), 67.0 (CH₂), 54.9 (CH), 48.3 (CH), 28.2 (CH₃), 27.7 (CH₂), 20.2 (d, ³*J*_{C-F} = 4.6 Hz, CH₂), 18.4 (CH₃).

¹⁹F-NMR (375 MHz, CDCl₃): δ = –80.8 (m), –117.3 (m), –122.0 (m), –122.0 (m), –122.8 (m), –122.8 (m), –126.1 (m), –130.5 (m).

IR (ATR): 3303, 2982, 1658, 1472, 1458, 1238, 1202, 1148 cm⁻¹.

MS (ESI) *m/z* (relative intensity): 991 ([M + Na]⁺, 30), 969 ([M + H]⁺, 100).

HR-MS (ESI): *m/z* calcd. for [C₄₁H₃₆F₁₆N₄O₅ + H]⁺ 969.2503, found: 969.2497.



(E)-1-(Pyridin-2-yl)-2-(perfluorodec-2-en-1-yl)-1H-indole (330aa): The general procedure **B** was followed using 1-(pyridin-2-yl)-1H-indole (**315a**) (58.2 mg, 0.30 mmol) and perfluorodec-1-ene (**303a**) (450 mg, 0.90 mmol). Isolation by column chromatography (*n*-hexane/EtOAc = 20:1) yielded **330aa** (172 mg, 85%).

$^1\text{H-NMR}$ (500 MHz, CDCl_3): δ = 8.58 (ddd, J = 4.9, 1.9, 0.9 Hz, 1H), 7.88 (ddd, J = 7.7, 5.9, 1.9 Hz, 1H), 7.71 (dt, J = 7.9, 1.0 Hz, 1H), 7.58 (dd, J = 8.5, 0.9 Hz, 1H), 7.46 (dt, J = 8.0, 1.0 Hz, 1H), 7.37–7.28 (m, 2H), 7.24 (dt, J = 7.4, 1.0 Hz, 1H), 7.19 (dd, J = 2.1, 1.1 Hz, 1H).

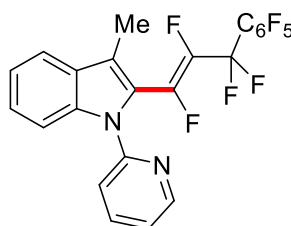
$^{13}\text{C-NMR}$ (125 MHz, CDCl_3): δ = 150.5 (C_q), 149.4 (CH), 148.9 (ddt, $^1J_{\text{C-F}}$ = 255 Hz, $^2J_{\text{C-F}}$ = 41.0 Hz, $^3J_{\text{C-F}}$ = 3.2 Hz, C_q), 138.3 (CH), 137.9 (C_q), 137.2 (dtd, $^1J_{\text{C-F}}$ = 250 Hz, $^2J_{\text{C-F}}$ = 46.0 Hz, $^2J_{\text{C-F}}$ = 29.7 Hz, C_q), 127.4 (C_q), 125.5 (CH), 124.2 (dd, $^2J_{\text{C-F}}$ = 23.5 Hz, $^3J_{\text{C-F}}$ = 5.3 Hz, C_q), 122.3 (CH), 122.0 (CH), 122.0 (CH), 120.7 (m, C_q), 119.0 (CH), 116.9 (m, C_q), 113.1 (m, C_q), 112.7 (m, C_q), 112.3 (m, C_q), 111.4 (dd, $^3J_{\text{C-F}}$ = 7.7 Hz, $^4J_{\text{C-F}}$ = 5.3 Hz, CH), 110.9 (CH), 110.3 (m, C_q), 108.5 (m, C_q), 108.2 (m, C_q).

$^{19}\text{F-NMR}$ (282 MHz, CDCl_3): δ = -80.9 (m), -116.7 (m), -122.1 (m), -122.1 (m), -122.2 (m), -122.8 (m), -123.7 (m), -126.2 (m), -135.0 (dtt, J = 140, 26.5, 7.2 Hz), -162.9 (dt, J = 140, 12.6 Hz).

IR (ATR): 1470, 1441, 1198, 1145, 737, 708 cm^{-1} .

MS (ESI) m/z (relative intensity): 675 ($[\text{M} + \text{H}]^+$, 100).

HR-MS (ESI): m/z calcd. for $[\text{C}_{23}\text{H}_9\text{F}_{19}\text{N}_2 + \text{H}]^+$ 675.0535, found: 675.0539.



(E)-3-Methyl-1-(pyridin-2-yl)-2-(1,2,3,3-tetrafluoro-3-phenylprop-1-en-1-yl)-1H-indole (330eb): The general procedure **B** was followed using 3-methyl-1-(pyridin-2-yl)-1H-indole (**315e**) (62.4 mg, 0.30 mmol), 3-(pentafluorophenyl)pentafluoroprop-1-ene (**303b**) (286 mg, 0.90 mmol) and NaOAc (7.4 mg, 30 mol %). Isolation by column chromatography (*n*-hexane/EtOAc = 15:1) yielded **330eb** (126 mg, 86%).

5. Experimental Part

$^1\text{H-NMR}$ (500 MHz, CDCl_3): δ = 8.53 (ddd, J = 4.9, 1.9, 0.9 Hz, 1H), 7.84 (ddd, J = 8.0, 7.5, 1.9 Hz, 1H), 7.68 (d, J = 8.1 Hz, 1H), 7.65 (dt, J = 8.4, 0.9 Hz, 1H), 7.41 (dt, J = 8.1, 0.9 Hz, 1H), 7.34 (ddd, J = 8.4, 7.2, 1.1 Hz, 1H), 7.29–7.21 (m, 2H), 2.41 (dd, J = 3.1, 2.2 Hz, 3H).

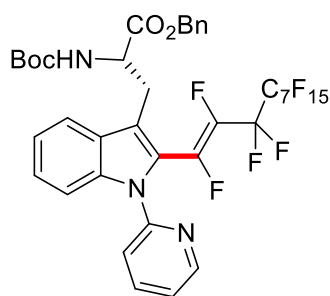
$^{13}\text{C-NMR}$ (125 MHz CDCl_3): δ = 150.6 (C_q), 149.3 (CH), 145.3 (m, C_q), 145.2 (dt, $^1J_{\text{C-F}}$ = 250 Hz, $^2J_{\text{C-F}}$ = 4.6 Hz, C_q), 141.9 (m, C_q), 138.0 (m, C_q), 138.3 (CH), 137.3 (C_q), 136.8 (m, C_q), 128.5 (C_q), 125.6 (CH), 121.7 (CH), 121.4 (CH), 121.1 (dd, $^2J_{\text{C-F}}$ = 22.8 Hz, $^3J_{\text{C-F}}$ = 3.5 Hz, C_q), 120.9 (C_q), 120.3 (CH), 118.3 (CH), 112.8 (C_q), 111.1 (CH), 108.8 (m, C_q), 9.4 (d, $^4J_{\text{C-F}}$ = 3.2 Hz, CH_3).

$^{19}\text{F-NMR}$ (283 MHz, CDCl_3): δ = -93.4 (m), -130.3 (dt, J = 146, 15.4 Hz), -139.4 (m), -148.5 (m), -159.4 (m), -160.5 (m).

IR (ATR): 1592, 1580, 1528, 1506, 1282, 1187, 929, 745 cm^{-1} .

MS (ESI) m/z (relative intensity): 509 ($[\text{M} + \text{Na}]^+$, 10), 487 ($[\text{M} + \text{H}]^+$, 100), 467 (15).

HR-MS (ESI): m/z calcd. for $[\text{C}_{23}\text{H}_{11}\text{F}_9\text{N}_2 + \text{H}]^+$ 487.0851, found: 487.0859.



Benzyl (S,E)-2-(tert-butoxycarbonyl)amino-3-{2-(perfluorodec-2-en-1-yl)-1-(pyridin-2-yl)-1H-indol-3-yl}propanoate (331bc): A modified general procedure **B** was followed using benzyl *tert*-butyloxycarbonyl-1-(pyridin-2-yl)-L-tryptophanate (**328b**) (142 mg, 0.30 mmol), perfluorodec-1-ene (**303c**) (450 mg, 0.90 mmol), $[\text{MnBr}(\text{CO})_5]$ (12.3 mg, 15 mol %) and NaOAc (7.4 mg, 30 mol %). Isolation by column chromatography (*n*-hexane/EtOAc = 10:1) yielded **331bc** (135 mg, 57%).

$^1\text{H-NMR}$ (400 MHz, CDCl_3): δ = 8.53 (ddd, J = 4.8, 1.9, 0.9 Hz, 1H), 7.83 (m, 1H), 7.80–7.73 (d, J = 8.0 Hz, 1H), 7.65–7.54 (d, J = 8.4 Hz, 1H), 7.39–7.33 (t, J = 7.3 Hz, 2H), 7.31–7.22 (m, 5H), 7.20–7.12 (m, 2H), 5.16–5.07 (dd, J = 11.3, 5.1 Hz, 2H), 5.05–4.96 (d, J = 12.4 Hz, 1H), 4.83–4.73 (q, J = 7.3 Hz, 1H), 3.52–3.13 (d, J = 6.6 Hz, 2H), 1.54–1.15 (s, 9H).

$^{13}\text{C-NMR}$ (125 MHz, CDCl_3): δ = 171.9 (C_q), 155.0 (C_q), 150.1 (C_q), 149.5 (CH), 147.9 (dd, $^1J_{\text{C-F}}$ = 257 Hz, $^2J_{\text{C-F}}$ = 44.5 Hz, C_q), 138.4 (CH), 137.9 (m, C_q), 137.4 (C_q), 135.1 (CH), 128.5 (CH), 128.2 (CH), 128.0 (CH), 127.7 (CH), 125.9 (CH), 122.2 (CH), 121.9 (C_q), 120.7 (C_q), 119.1 (m, C_q), 118.7 (CH), 117.0 (dt, $^1J_{\text{C-F}}$ = 287 Hz, $^2J_{\text{C-F}}$ = 33.9 Hz, C_q), 113.4 (m, C_q), 112.8

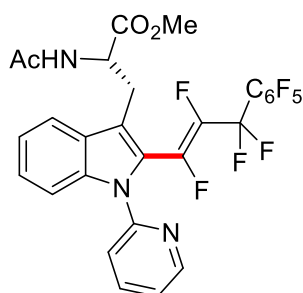
(m, C_q), 111.2 (CH), 110.9 (m, C_q), 110.7 (m, C_q), 110.4 (m, C_q), 108.8 (m, C_q), 108.3 (m, C_q), 79.9 (CH₂), 67.2 (C_q), 53.8 (CH), 28.4 (CH₂), 27.6 (CH₃).

¹⁹F-NMR (376 MHz, CDCl₃): δ = -80.8 (m), -116.7 (m), -121.8 (m), -121.9 (m), -122.1 (m), -122.7 (m), -123.3 (m), -121.1 (m), -126.8 (dt, *J* = 146, 23.6 Hz), -160.3 (dt, *J* = 146, 12.3 Hz).

IR (ATR): 3362, 2957, 1587, 1569, 1450, 1383, 1212, 996 cm⁻¹.

MS (ESI) *m/z* (relative intensity): 974 ([M + Na]⁺, 70), 952 ([M + H]⁺, 100), 896 (20).

HR-MS (ESI): *m/z* calcd. for [C₃₈H₂₈F₁₉N₃O₄ + H]⁺ 952.1849, found: 952.1833.



(E)-Methyl acetyl-1-(pyridin-2-yl)-2-[3-(pentafluorophenyl)tetrafluoroprop-1-en-1-yl]-L-tryptophanate (331ab): The general procedure **B** was followed using methyl acetyl-1-(pyridin-2-yl)-L-tryptophanate (**328a**) (101 mg, 0.30 mmol), 3-(pentafluorophenyl)pentafluoroprop-1-ene (**303b**) (178 mg, 0.60 mmol) and NaOAc (7.4 mg, 30 mol %). Isolation by column chromatography (*n*-hexane/EtOAc = 1:1) yielded **331ab** (148 mg, 48%) as a yellow solid. M.p.: 122 °C.

¹H-NMR (400 MHz, CDCl₃): δ = 8.50 (ddd, *J* = 4.8, 1.8, 0.9 Hz, 1H), 7.85 (ddd, *J* = 7.7, 7.5, 1.9 Hz, 1H), 7.75 (d, *J* = 8.0 Hz, 1H), 7.57 (d, *J* = 8.4 Hz, 1H), 7.41 (d, *J* = 8.0 Hz, 1H), 7.32 (d, *J* = 7.4 Hz, 1H), 7.30–7.27 (m, 1H), 7.27–7.20 (m, 1H), 6.11 (d, *J* = 8.0 Hz, 1H), 4.98 (dt, *J* = 8.0, 6.0 Hz, 1H), 3.62 (s, 3H), 3.35 (d, *J* = 6.0 Hz, 2H), 1.92 (s, 3H).

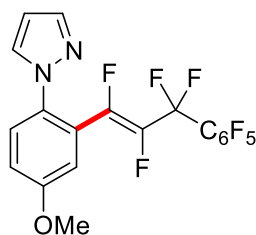
¹³C-NMR (100 MHz, CDCl₃): δ = 171.9 (C_q), 169.7 (C_q), 150.2 (C_q), 149.4 (CH), 146.2 (m, C_q), 143.7 (m, C_q), 141.8 (m, C_q), 139.1 (m, C_q), 138.4 (CH), 137.3 (d, ⁴*J*_{C-F} = 2.0 Hz, C_q), 136.6 (C_q), 127.7 (d, ⁴*J*_{C-F} = 1.7 Hz, C_q), 125.8 (CH), 122.5 (C_q), 122.2 (CH), 121.9 (CH), 120.5 (CH), 118.9 (CH), 118.7 (m, C_q), 112.7 (m, C_q), 111.3 (CH), 100.0 (m, C_q), 52.4 (CH₃), 52.4 (CH), 27.7 (CH₂), 22.9 (CH₃).

¹⁹F-NMR (375 MHz, CDCl₃): δ = -94.0 (m), -128.5 (dt, *J* = 146, 16.7 Hz), -139.4 (m), -148.2 (m), -157.9 (dt, *J* = 146, 18.5 Hz), -160.1 (m).

IR (ATR): 3285, 2957, 1744, 1657, 1527, 1506, 1371, 993, 741 cm⁻¹.

MS (ESI) *m/z* (relative intensity): 638 ([M + Na]⁺, (20)), 616 ([M + H]⁺, 100), 596 (10).

HR-MS (ESI): *m/z* calcd. for [C₂₈H₁₈F₉N₃O₃ + H]⁺ 616.1265, found 616.1277.

**(E)-1-[4-methoxy-2-(1,2,3,3-tetrafluoro-3-phenylprop-1-en-1-yl)phenyl]-1H-pyrazole**

(333ab): A modified general procedure **B** was followed using 1-(4-methoxyphenyl)-1H-pyrazole (**332a**) (52.2 mg, 0.30 mmol), 3-(pentafluorophenyl)pentafluoroprop-1-ene (**303b**) (286 mg, 0.90 mmol) and NaOAc (7.4 mg, 30 mol %). Isolation by column chromatography (*n*-hexane/EtOAc = 15:1) yielded **333ab** (96.3 mg, 68%).

$^1\text{H-NMR}$ (400 MHz, CDCl_3): δ = 7.58 (d, J = 1.8 Hz, 1H), 7.56 (d, J = 2.4 Hz, 1H), 7.43 (d, J = 8.5 Hz, 1H), 7.09 (ddd, J = 8.5, 2.8, 2.4 Hz, 1H), 7.07 (dd, J = 2.8, 1.3 Hz, 1H), 6.35 (dd, J = 2.4, 1.8 Hz, 1H), 3.86 (s, 3H).

$^{13}\text{C-NMR}$ (125 MHz CDCl_3): δ = 158.7 (C_q), 149.4 (dt, $^1J_{\text{C-F}}$ = 255 Hz, $^2J_{\text{C-F}}$ = 45.0 Hz, $^3J_{\text{C-F}}$ = 7.3 Hz, C_q), 146.0 (m, C_q), 144.1 (m, C_q), 142.9 (m, C_q), 140.8 (CH), 138.1 (m, C_q), 132.6 (C_q), 129.5 (CH), 126.9 (CH), 123.1 (dd, $^2J_{\text{C-F}}$ = 22.8 Hz, $^3J_{\text{C-F}}$ = 4.2 Hz, C_q), 117.8 (CH), 115.5 (CH), 112.7 (m, C_q), 108.5 (m, C_q), 107.0 (CH), 55.8 (CH_3).

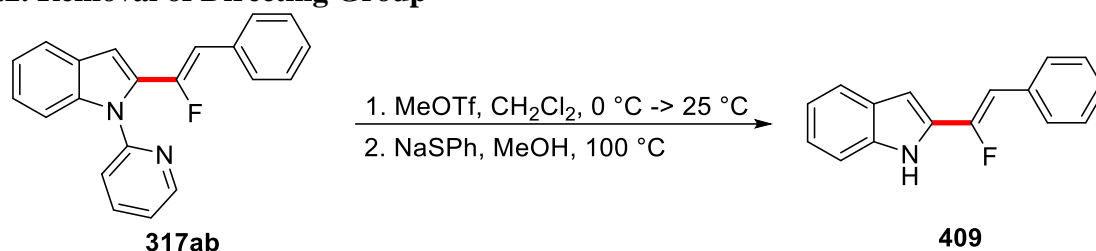
$^{19}\text{F-NMR}$ (376 MHz, CDCl_3): δ = -94.2 (m), -132.8 (dt, J = 141, 16.3 Hz), -139.1 (m), -148.6 (m), -160.3 (m), -162.4 (m).

IR (ATR): 2946, 1524, 1505, 1326, 1182, 1043, 993, 755 cm^{-1} .

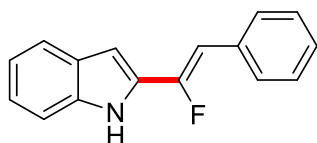
MS (ESI) m/z (relative intensity): 475 ($[\text{M} + \text{Na}]^+$, 20), 453 ($[\text{M} + \text{H}]^+$, 100), 433 (10).

HR-MS (ESI): m/z calcd. for $[\text{C}_{19}\text{H}_9\text{F}_9\text{N}_2\text{O} + \text{H}]^+$ 453.0644, found: 453.0646.

5.3.2. Removal of Directing Group



Methyl trifluoromethanesulfonate (98.4 mg, 66 μ L, 0.60 mmol, 1.20 equiv) was added dropwise to a solution of **317ab** (157 mg, 0.50 mmol, 1.00 equiv) in CH_2Cl_2 (7.5 mL) at 0 $^\circ\text{C}$, and the resulting solution was stirred for 12 h at 25 $^\circ\text{C}$. After removal of the solvent, PhSNa (330 mg, 2.50 mmol, 5.00 equiv) and MeOH (5.0 mL) were added and the resulting mixture was stirred at 100 $^\circ\text{C}$ for 24 h with a reflux condenser. The solvents were removed, and the resulting residue was neutralized using HCl (1.0 M) and extracted with CH_2Cl_2 (4 \times 20 mL). The combined organic layers were washed with brine, dried over Na_2SO_4 and concentrated *in vacuo*. The remaining residue was purified by column chromatography on silica gel (n-hexane/EtOAc: 20:1) to afford the desired product **409** (71.4 mg, 60%) as a white solid.



(Z)-2-(1-Fluoro-2-phenylvinyl)-1H-indole (409): M.p.: 135 $^\circ\text{C}$.

$^1\text{H-NMR}$ (400 MHz, CDCl_3): δ = 8.31 (bs, 1H), 7.63–7.58 (m, 3H), 7.40–7.34 (m, 3H), 7.29–7.21 (m, 2H), 7.13 (ddd, J = 7.9, 7.5, 0.9 Hz, 1H), 6.84 (d, J = 1.7 Hz, 1H), 6.50 (d, J = 20.8 Hz, 0.10H, *E*), 6.23 (d, J = 39.9 Hz, 0.90H, *Z*).

$^{13}\text{C-NMR}$ (100 MHz, CDCl_3): δ = 151.5 (d, J = 253 Hz, C_q), 136.5 (CH), 133.2 (d, $^3J_{\text{C-F}}$ = 3.3 Hz, C_q), 130.7 (d, $^2J_{\text{C-F}}$ = 31.3 Hz, C_q), 128.8 (d, $^4J_{\text{C-F}}$ = 7.5 Hz, CH), 128.7 (CH), 128.5 (C_q), 127.5 (C_q), 123.4 (CH), 121.0 (CH), 120.7 (CH), 111.1 (CH), 105.6 (d, $^2J_{\text{C-F}}$ = 8.8 Hz, CH), 101.5 (d, $^3J_{\text{C-F}}$ = 3.8 Hz, CH).

$^{19}\text{F-NMR}$ (376 MHz, CDCl_3): δ = –109.4 (d, J = 20.8 Hz, *E*), –118.3 (d, J = 39.9 Hz, *Z*).

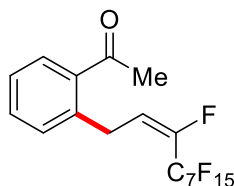
IR (ATR): 3425, 3052, 1653, 1446, 1024, 944, 589 cm^{-1} .

MS (ESI) m/z (relative intensity): 238 ($[\text{M} + \text{H}]^+$, 80), 163 (100).

HR-MS (ESI): m/z calcd. for $[\text{C}_{16}\text{H}_{12}\text{FN} + \text{H}]^+$ 238.1027, found 238.1036.

5.4. Ruthenium(II)-catalyzed C–F/C–H functionalization

5.4.1. Characterization Data



(E)-1-[2-(1H,1H,2H-Perfluorodec-2-en-1-yl)phenyl]ethan-1-one (307aa): The general procedure **C** was followed using *N*-(3,4,5-trimethoxyphenyl)-1-phenylethan-1-imine (**340a**) (143 mg, 0.50 mmol) and 1*H*,1*H*,2*H*-perfluorodec-1-ene (**301a**) (669 mg, 1.50 mmol). Isolation by column chromatography (*n*-hexane/EtOAc: 25/1) yielded **307aa** (199 mg, 73%, *E/Z* = 78:22, **307aa/339aa** = 98:2) as a yellow oil.

¹H-NMR (300 MHz, CDCl₃): δ = 7.84 (dd, *J* = 7.4, 1.4 Hz, 1H), 7.49 (ddd, *J* = 7.6, 7.4, 1.4 Hz, 1H), 7.39 (ddd, *J* = 7.6, 7.5, 1.4 Hz, 1H), 7.28 (dd, *J* = 7.5, 1.4 Hz, 1H), 6.18 (dt, *J* = 23.1, 8.4 Hz, 0.78H, *E*), 5.95 (dt, *J* = 33.7, 7.8 Hz, 0.22H, *Z*), 3.84 (ddt, *J* = 8.3, 4.1, 2.3 Hz, 2H), 3.20–3.10 (m, 0.04H, **339aa**), 2.64 (s, 2.34H, *E*), 2.63 (s, 0.66H, *Z*).

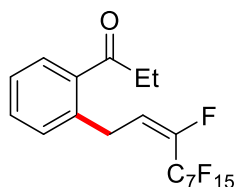
¹³C-NMR (75 MHz, CDCl₃): δ = 201.1 (C_q), 144.4 (dt, ¹*J*_{C–F} = 257.1 Hz, ²*J*_{C–F} = 29.1 Hz, C_q), 138.3 (C_q), 136.6 (C_q), 132.4 (CH), 131.2 (CH), 130.2 (CH), 127.1 (CH), 120.8 (dt, ¹*J*_{C–F} = 288.3 Hz, ²*J*_{C–F} = 34.2 Hz, C_q), 119.0 (d, ²*J*_{C–F} = 16.8 Hz, CH), 115.2 (m, C_q), 113.6 (m, C_q), 111.1 (m, C_q), 110.6 (m, C_q), 108.2 (m, C_q), 106.6 (m, C_q), 29.2 (CH₃), 28.4 (m, CH₂).

¹⁹F-NMR (282 MHz, CDCl₃): δ = –80.9 (m), –114.5 (m, *E*), –117.5 (m, *Z*), –122.1 (m), –122.8 (m), –123.4 (m), –124.0 (m), –126.2 (m), –132.4 (m).

IR (ATR): 1690, 1357, 1226, 1199, 1143, 1116, 759, 732 cm^{–1}.

MS (ESI) *m/z* (relative intensity): 569 ([M + Na]⁺, 100), 547 ([M + H]⁺, 45), 381 (15).

HR-MS (ESI): *m/z* calcd. for [C₁₈H₁₀F₁₆O + H]⁺ 547.0549, found 547.0554.



(E)-1-[2-(1H,1H,2H-perfluorodec-2-en-1-yl)phenyl]propan-1-one (307ba): The general procedure **C** was followed using *N*-(3,4,5-trimethoxyphenyl)-1-phenylpropan-1-imine (**340b**) (150 mg, 0.50 mmol) and 1*H*,1*H*,2*H*-perfluorodec-1-ene (**301a**) (669 mg, 1.50 mmol). Isolation by column chromatography (*n*-hexane/EtOAc: 25/1) yielded **307ba** (176 mg, 63%, *E/Z* = 75:25, **307ba/339ba** = 99:1) as a yellow oil.

$^1\text{H-NMR}$ (500 MHz, CDCl_3): $\delta = 7.72$ (dd, $J = 8.0, 1.4$ Hz, 1H), 7.43 (ddd, $J = 7.7, 7.5, 1.4$ Hz, 1H), 7.33 (ddd, $J = 8.0, 7.5, 1.4$ Hz, 1H), 7.22 (dd, $J = 7.7, 1.4$ Hz, 1H), 6.15 (dt, $J = 23.1, 8.4$ Hz, 0.75H, *E*), 5.93 (dt, $J = 33.7, 7.8$ Hz, 0.25H, *Z*), 3.75 (ddt, $J = 7.4, 4.1, 2.0$ Hz, 2H), 3.10–3.00 (m, 0.02H, **339ba**), 2.94 (q, $J = 7.2$ Hz, 2H), 1.19 (t, $J = 7.3$ Hz, 3H).

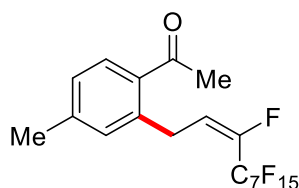
$^{13}\text{C-NMR}$ (125 MHz, CDCl_3): $\delta = 204.4$ (C_q), 143.9 (dt, $^1J_{\text{C-F}} = 256.2$ Hz, $^2J_{\text{C-F}} = 27.3$ Hz, C_q), 137.8 (C_q), 137.1 (C_q), 131.9 (CH), 131.1 (CH), 129.0 (CH), 127.0 (CH), 119.0 (d, $^2J_{\text{C-F}} = 8.2$ Hz, CH), 117.2 (dt, $^1J_{\text{C-F}} = 287.7$ Hz, $^2J_{\text{C-F}} = 31.3$ Hz, C_q), 113.4 (m, C_q), 112.9 (m, C_q), 112.0 (m, C_q), 110.7 (m, C_q), 110.4 (m, C_q), 108.5 (m, C_q), 34.4 (CH_2), 28.3 (m, CH_2), 8.2 (CH_3).

$^{19}\text{F-NMR}$ (471 MHz, CDCl_3): $\delta = -80.9$ (m), -114.4 (m, *E*), -117.4 (m, *Z*), -122.0 (m), -122.8 (m), -123.3 (m), -123.9 (m), -126.2 (m), -132.5 (m).

IR (ATR): 1709, 1340, 1291, 1259, 1143, 1121, 721, 700 cm^{-1} .

MS (ESI) m/z (relative intensity): 583 ($[\text{M} + \text{Na}]^+$, 100), 561 ($[\text{M} + \text{H}]^+$, 10).

HR-MS (ESI): m/z calcd. for $[\text{C}_{19}\text{H}_{12}\text{F}_{16}\text{O} + \text{H}]^+$ 561.0705, found 561.0708.



(E)-1-[4-Methyl-2-(1H,1H,2H-perfluorodec-2-en-1-yl)phenyl]ethan-1-one (307ca): The general procedure **C** was followed using 1-(4-methylphenyl)-*N*-(3,4,5-trimethoxyphenyl)-1-phenylethan-1-imine (**340c**) (150 mg, 0.50 mmol) and 1H,1H,2H-perfluorodec-1-ene (**301a**) (669 mg, 1.50 mmol). Isolation by column chromatography (*n*-hexane/EtOAc: 25/1) yielded **307ca** (174 mg, 62%, *E/Z* = 84:16, **307ca/339ca** = 92:8) as a yellow oil.

$^1\text{H-NMR}$ (500 MHz, CDCl_3): $\delta = 7.71$ (d, $J = 8.0$ Hz, 1H), 7.15 (dd, $J = 8.0, 1.4$ Hz, 1H), 7.05 (d, $J = 1.4$ Hz, 1H), 6.14 (dt, $J = 23.3, 8.3$ Hz, 0.84H, *E*), 5.91 (dt, $J = 32.5, 8.3$ Hz, 0.16H, *Z*), 3.80 (ddt, $J = 7.5, 4.0, 2.2$ Hz, 2H), 3.20–3.03 (m, 0.16H, **339ca**), 2.58 (s, 2.52H, *E*), 2.57 (s, 0.48H, *Z*), 2.36 (s, 3H).

$^{13}\text{C-NMR}$ (125 MHz, CDCl_3): $\delta = 200.5$ (C_q), 143.9 (dt, $^1J_{\text{C-F}} = 260.3$ Hz, $^2J_{\text{C-F}} = 27.5$ Hz, C_q), 143.2 (C_q), 138.6 (C_q), 133.7 (C_q), 132.1 (CH), 130.7 (CH), 127.6 (CH), 119.1 (d, $^2J_{\text{C-F}} = 18.3$ Hz, CH), 117.1 (dt, $^1J_{\text{C-F}} = 289.1$ Hz, $^2J_{\text{C-F}} = 33.8$ Hz, C_q), 113.2 (m, C_q), 112.1 (m, C_q), 111.0 (m, C_q), 110.7 (m, C_q), 109.7 (m, C_q), 108.6 (m, C_q), 29.1 (CH_3), 28.5 (m, CH_2), 21.3 (CH_3).

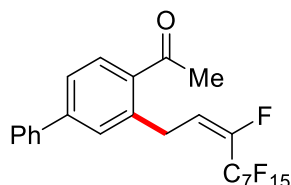
$^{19}\text{F-NMR}$ (471 MHz, CDCl_3): $\delta = -80.9$ (m), -114.5 (m, *E*), -117.5 (m, *Z*), -122.0 (m), -122.8 (m), -123.4 (m), -124.4 (m), -126.3 (m), -132.8 (m).

5. Experimental Part

IR (ATR): 1695, 1395, 1243, 1200, 1155, 1103, 749, 710 cm^{-1} .

MS (ESI) m/z (relative intensity): 583 ($[\text{M} + \text{Na}]^+$, 100), 561 ($[\text{M} + \text{H}]^+$, 20).

HR-MS (ESI): m/z calcd. for $[\text{C}_{19}\text{H}_{12}\text{F}_{16}\text{O} + \text{H}]^+$ 561.0705, found 561.0708.



(E)-1-[4-Phenyl-2-(1H,1H,2H-perfluorodec-2-en-1-yl)phenyl]ethan-1-one (307da): The general procedure **C** was followed using 1-([1,1'-biphenyl]-4-yl)-*N*-(3,4,5-trimethoxyphenyl)ethan-1-imine (**340d**) (188 mg, 0.50 mmol) and 1*H*,1*H*,2*H*-perfluorodec-1-ene (**301a**) (669 mg, 1.50 mmol). Isolation by column chromatography (*n*-hexane/EtOAc: 25/1) yielded **307da** (165 mg, 53%, *E/Z* = 80:20, **307da**/**339da** = 99:1) as a yellow oil.

$^1\text{H-NMR}$ (300 MHz, CDCl_3): δ = 7.88 (d, J = 8.1 Hz, 1H), 7.72–7.52 (m, 3H), 7.54–7.35 (m, 4H), 6.21 (dt, J = 23.0, 8.2, 0.7 Hz, 0.80H, *E*), 5.98 (dt, J = 33.7, 10.5, 1.2 Hz, 0.20H, *Z*), 3.91 (ddt, J = 6.1, 4.2, 2.1 Hz, 2H), 3.41–3.06 (m, 0.02H, **339da**), 2.64 (s, 2.40H, *E*), 2.63 (s, 0.60H, *Z*).

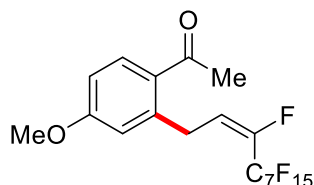
$^{13}\text{C-NMR}$ (125 MHz, CDCl_3): δ = 200.1 (C_q), 144.9 (C_q), 144.3 (dt, $^1J_{\text{C-F}}$ = 251 Hz, $^2J_{\text{C-F}}$ = 29.4 Hz, C_q), 139.1 (C_q), 138.8 (C_q), 134.8 (C_q), 130.8 (CH), 129.9 (CH), 128.7 (CH), 128.1 (CH), 129.0 (CH), 126.9 (CH), 125.3 (CH), 118.7 (d, $^2J_{\text{C-F}}$ = 8.9 Hz, CH), 116.8 (dt, $^1J_{\text{C-F}}$ = 288.5 Hz, $^2J_{\text{C-F}}$ = 32.3 Hz, C_q), 112.7 (m, C_q), 111.8 (m, C_q), 110.8 (m, C_q), 110.5 (m, C_q), 110.5 (m, C_q), 108.4 (m, C_q), 29.0 (CH_3), 28.6 (m, CH_2).

$^{19}\text{F-NMR}$ (282 MHz, CDCl_3): δ = –80.8 (m), –114.4 (m, *E*), –117.4 (m, *Z*), –121.9 (m), –122.7 (m), –123.0 (m), –123.3 (m), –123.7 (m), –126.1 (m), –132.5 (m).

IR (ATR): 1693, 1452, 1257, 1233, 1143, 1057, 961, 749 cm^{-1} .

MS (ESI) m/z (relative intensity): 645 ($[\text{M} + \text{Na}]^+$, 100), 623 ($[\text{M} + \text{H}]^+$, 30).

HR-MS (ESI): m/z calcd. for $[\text{C}_{24}\text{H}_{14}\text{F}_{16}\text{O} + \text{H}]^+$ 623.0862, found 623.0867.



(E)-1-[4-Methoxy-2-(1H,1H,2H-perfluorodec-2-en-1-yl)phenyl]ethan-1-one (307ea): The general procedure **C** was followed using 1-(4-methoxyphenyl)-*N*-(3,4,5-trimethoxyphenyl)-1-phenylethan-1-imine (**340e**) (158 mg, 0.50 mmol) and 1*H*,1*H*,2*H*-perfluorodec-1-ene (**301a**)

(669 mg, 1.50 mmol). Isolation by column chromatography (*n*-hexane/EtOAc: 25/1) yielded **307ea** (167 mg, 58%, *E/Z* = 75:25, **307ea/339ea** = 98:2) as a yellow oil.

¹H-NMR (500 MHz, CDCl₃): δ = 7.82 (d, *J* = 8.7 Hz, 1H), 6.82 (dd, *J* = 8.7, 2.7 Hz, 1H), 6.72 (d, *J* = 2.7 Hz, 1H), 6.17 (dt, *J* = 23.5, 8.8 Hz, 0.75H, *E*), 5.92 (dt, *J* = 33.9, 7.8 Hz, 0.25H, *Z*), 3.86 (ddt, *J* = 7.0, 4.1, 1.6 Hz, 2H), 3.83 (s, 3H), 3.20–3.00 (m, 0.04H, **339ea**) 2.56 (s, 2.25H, *E*), 2.55 (s, 0.75H, *Z*).

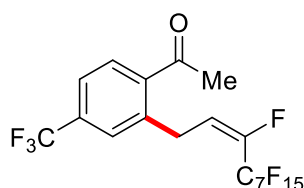
¹³C-NMR (125 MHz, CDCl₃): δ = 199.1 (C_q), 162.5 (C_q), 144.1 (dt, ¹*J*_{C-F} = 256.2 Hz, ²*J*_{C-F} = 27.3 Hz, C_q), 141.5 (C_q), 133.1 (CH), 128.8 (C_q), 118.8 (d, ²*J*_{C-F} = 8.9 Hz, CH), 117.5 (dt, ¹*J*_{C-F} = 287 Hz, ²*J*_{C-F} = 31.3 Hz, C_q), 117.0 (CH), 116.5 (CH), 112.8 (m, C_q), 112.6 (m, C_q), 111.6 (CH), 110.9 (m, C_q), 110.7 (m, C_q), 110.2 (m, C_q), 55.3 (CH₃), 29.0 (m, CH₂), 28.8 (CH₃).

¹⁹F-NMR (471 MHz, CDCl₃): δ = -80.7 (m), -114.3 (m, *E*), -117.3 (m, *Z*), -121.9 (m), -122.9 (m), -123.3 (m), -124.0 (m), -126.1 (m), -132.5 (m).

IR (ATR): 1686, 1604, 1585, 1235, 1199, 1144, 1106, 733, 706 cm⁻¹.

MS (ESI) *m/z* (relative intensity): 599 ([M + Na]⁺, 100), 577 ([M + H]⁺, 30).

HR-MS (ESI): *m/z* calcd. for [C₁₉H₁₂F₁₆O₂ + H]⁺ 577.0655, found 577.0653.



(*E*)-1-[4-Trifluoromethyl-2-(1*H*,1*H*,2*H*-perfluorodec-2-en-1-yl)phenyl]ethan-1-one

(307fa): The general procedure **C** was followed using 1-[4-trifluoromethyl-*N*-(3,4,5-trimethoxyphenyl)-1-phenyl]ethan-1-one (**340f**) (177 mg, 0.50 mmol) and 1*H*,1*H*,2*H*-perfluorodec-1-ene (**301a**) (669 mg, 1.50 mmol). Isolation by column chromatography (*n*-hexane/EtOAc: 25/1) yielded **307fa** (166 mg, 54%, *E/Z* = 72:28, **307fa/339fa** = 97:3) as a yellow oil.

¹H-NMR (300 MHz, CDCl₃): δ = 7.88 (d, *J* = 8.1 Hz, 1H), 7.65 (dd, *J* = 8.1, 1.4 Hz, 1H), 7.53 (d, 1.4 Hz, 1H), 6.10 (dt, *J* = 22.6, 8.5 Hz, 0.72H, *E*), 5.87 (dt, *J* = 33.5, 7.5 Hz, 0.28H, *Z*), 3.86 (ddt, *J* = 7.0, 4.0, 2.0 Hz, 2H), 3.30–3.20 (m, 0.06H, **339fa**), 2.66 (s, 2.16H, *E*), 2.65 (s, 0.84H, *Z*).

¹³C-NMR (75 MHz, CDCl₃): δ = 200.4 (C_q), 145.3 (dt, ¹*J*_{C-F} = 261.2 Hz, ²*J*_{C-F} = 29.5 Hz, C_q), 139.7 (C_q), 138.8 (C_q), 133.7 (q, ²*J*_{C-F} = 33.0 Hz, C_q), 130.0 (CH), 127.8 (q, ³*J*_{C-F} = 3.8 Hz, CH), 125.0 (d, ¹*J*_{C-F} = 273.3 Hz, C_q), 124.0 (q, ³*J*_{C-F} = 3.7 Hz, CH), 118.0 (dt, ¹*J*_{C-F} = 376.1 Hz, ²*J*_{C-F} = 22.3 Hz, C_q), 117.7 (d, ²*J*_{C-F} = 7.8 Hz, CH), 114.0 (m, C_q), 111.5 (m, C_q), 110.8 (m, C_q), 110.2 (m, C_q), 108.0 (m, C_q), 107.5 (m, C_q), 29.3 (CH₃), 28.1 (m, CH₂).

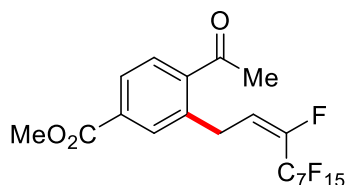
5. Experimental Part

^{19}F -NMR (282 MHz, CDCl_3): $\delta = -63.6$ (m), -81.0 (m), -114.7 (m), -117.7 (m), -122.1 (m), -122.9 (m), -123.2 (m), -123.4 (m), -126.4 (m), -130.7 (m).

IR (ATR): 1719, 1311, 1263, 1223, 1140, 1100, 720, 700 cm^{-1} .

MS (ESI) m/z (relative intensity): 637 ($[\text{M} + \text{Na}]^+$, 100), 615 ($[\text{M} + \text{H}]^+$, 40).

HR-MS (ESI): m/z calcd. for $[\text{C}_{19}\text{H}_9\text{F}_{19}\text{O} + \text{Na}]^+$ 637.0242, found 637.0241.



(E)-Methyl-4-acetyl-3-(1H,1H,2H-perfluorodec-2-en-1-yl)benzoate (307ga): The general procedure **C** was followed using methyl-4-(1-((3,4,5-trimethoxyphenyl)imino)ethyl)benzoate (**340g**) (172 mg, 0.50 mmol) and 1H,1H,2H-perfluorodec-1-ene (**301a**) (669 mg, 1.50 mmol). Isolation by column chromatography (*n*-hexane/EtOAc: 25/1) yielded **307ga** (145 mg, 48%, *E/Z* = 70:30, **307ga/339ga** = 99:1) as a yellow oil.

^1H -NMR (500 MHz, CDCl_3): $\delta = 8.00$ (d, $J = 7.7$ Hz, 1H), 7.90 (dd, $J = 7.7, 1.9$ Hz, 1H), 7.79 (d, $J = 1.9$ Hz, 1H), 6.10 (dt, $J = 22.8, 8.7, 0.70$ Hz, *E*), 5.87 (dt, $J = 33.4, 7.7$ Hz, 0.30H, *Z*), 3.92 (s, 3H), 3.81 (ddt, $J = 7.4, 4.5, 2.1$ Hz, 2H), 3.30–3.20 (m, 0.02H, **339ga**), 2.61 (s, 2.10H, *E*), 2.60 (s, 0.90H, *Z*).

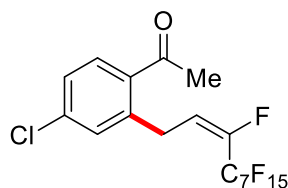
^{13}C -NMR (125 MHz, CDCl_3): $\delta = 200.9$ (C_q), 165.7 (C_q), 144.5 (dt, $^1J_{\text{C-F}} = 256.2$ Hz, $^2J_{\text{C-F}} = 27.9$ Hz, C_q), 140.3 (C_q), 138.1 (C_q), 133.1 (C_q), 132.3 (CH), 129.6 (CH), 128.2 (CH), 118.0 (d, $^2J_{\text{C-F}} = 8.1$ Hz, CH), 115.0 (dt, $^1J_{\text{C-F}} = 281$ Hz, $^2J_{\text{C-F}} = 31.3$ Hz, C_q), 112.6 (m, C_q), 111.6 (m, C_q), 110.9 (m, C_q), 110.6 (m, C_q), 110.4 (m, C_q), 108.5 (m, C_q), 52.4 (CH₃), 29.5 (CH₃), 28.1 (m, CH₂).

^{19}F -NMR (471 MHz, CDCl_3): $\delta = -80.8$ (m), -114.5 (m, *E*), -117.4 (m, *Z*), -121.9 (m), -122.7 (m), -122.9 (m), -123.3 (m), -126.1 (m), -131.1 (m).

IR (ATR): 1725, 1663, 1222, 1205, 1156, 1100, 701 cm^{-1} .

MS (ESI) m/z (relative intensity): 627 ($[\text{M} + \text{Na}]^+$, 100), 605 ($[\text{M} + \text{H}]^+$, 10).

HR-MS (ESI): m/z calcd. for $[\text{C}_{20}\text{H}_{12}\text{F}_{16}\text{O}_3 + \text{H}]^+$ 605.0604, found 605.0601.



(E)-1-[4-Chloro-2-(1H,1H,2H-perfluorodec-2-en-1-yl)phenyl]ethan-1-one (307ha): The general procedure **C** was followed using 1-(4-chlorophenyl)-*N*-(3,4,5-trimethoxyphenyl)-1-phenylethan-1-imine (**340h**) (160 mg, 0.50 mmol) and 1*H*,1*H*,2*H*-perfluorodec-1-ene (**301a**) (669 mg, 1.50 mmol). Isolation by column chromatography (*n*-hexane/EtOAc: 25/1) yielded **307ha** (171 mg, 59%, *E/Z* = 83:17, **307ha/339ha** = 98:2) as a yellow oil.

¹H-NMR (300 MHz, CDCl₃): δ = 7.76 (dd, *J* = 8.4, 1.9 Hz, 1H), 7.37 (dd, *J* = 8.4, 2.1 Hz, 1H), 7.29 (dd, 2.1, 1.9 Hz, 1H), 6.16 (dt, 22.3, 8.7 Hz, 0.83H, *E*), 5.92 (dt, *J* = 33.4, 7.7 Hz, 0.17H, *Z*), 3.80 (ddt, *J* = 7.8, 4.1, 2.0 Hz, 2H), 3.20–3.10 (m, 0.04H, **339ha**) 2.62 (s, 2.49H, *E*), 2.61 (s, 0.51H, *Z*).

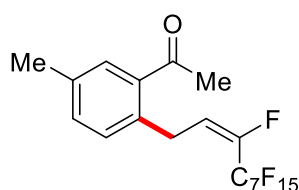
¹³C-NMR (75 MHz, CDCl₃): δ = 199.8 (C_q), 145.1 (dt, ¹*J*_{C-F} = 275 Hz, ²*J*_{C-F} = 28.5 Hz, C_q), 140.4 (C_q), 138.5 (C_q), 134.7 (CH), 131.6 (CH), 131.2 (CH), 127.2 (C_q), 118.2 (dt, ¹*J*_{C-F} = 285.2 Hz, ²*J*_{C-F} = 35.3 Hz, C_q), 118.0 (d, ²*J*_{C-F} = 7.2 Hz, CH), 115.2 (m, C_q), 114.5 (m, C_q), 114.3 (m, C_q), 112.4 (m, C_q), 111.5 (m, C_q), 111.1 (m, C_q), 29.1 (CH₃), 28.2 (m, CH₂).

¹⁹F-NMR (282 MHz, CDCl₃): δ = -80.8 (m), -114.5 (m, *E*), -117.5 (m, *Z*), -122.0 (m), -122.7 (m), -123.0 (m), -123.3 (m), -126.2 (m), -131.2 (m).

IR (ATR): 1695, 1345, 1279, 1259, 1153, 1102, 741, 721 cm⁻¹.

MS (ESI) *m/z* (relative intensity): 603 ([M + Na]⁺, 100), 581 ([M + H]⁺, 55).

HR-MS (ESI): *m/z* calcd. for [C₁₈H₉³⁵ClF₁₆O + H]⁺ 581.0159, found 581.0163.



(E)-1-[5-Methyl-2-(1H,1H,2H-perfluorodec-2-en-1-yl)phenyl]ethan-1-one (307ia): The general procedure **C** was followed using 1-(3-methylphenyl)-*N*-(3,4,5-trimethoxyphenyl)-1-phenylethan-1-imine (**340i**) (150 mg, 0.50 mmol) and 1*H*,1*H*,2*H*-perfluorodec-1-ene (**301a**) (669 mg, 1.50 mmol). Isolation by column chromatography (*n*-hexane/EtOAc: 25/1) yielded **307ia** (176 mg, 63%, *E/Z* = 74:26, **307ia/339ia** = 91:9) as a yellow oil.

¹H-NMR (300 MHz, CDCl₃): δ = 7.61 (d, *J* = 2.7 Hz, 1H), 7.32 (dd, 8.4, 2.7 Hz, 1H), 7.17 (dd, *J* = 8.4 Hz, 2.7 Hz, 1H), 6.17 (dt, *J* = 23.2, 8.7 Hz, 0.74H, *E*), 5.94 (dt, *J* = 33.8, 7.8 Hz, 0.26H,

5. Experimental Part

Z), 3.79 (ddt, $J = 7.4, 4.2, 2.2$ Hz, 2H), 3.22–2.97 (m, 0.18H, **339ia**), 2.62 (s, 2.22H, *E*), 2.61 (s, 0.78H, *Z*) 2.42 (s, 3H).

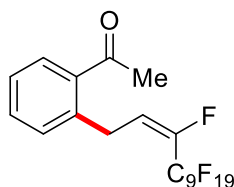
^{13}C -NMR (75 MHz, CDCl_3): $\delta = 201.2$ (C_q), 144.1 (dt, $^1J_{\text{C-F}} = 258.1$ Hz, $^2J_{\text{C-F}} = 28.3$ Hz, C_q), 136.8 (C_q), 136.5 (C_q), 135.1 (C_q), 133.0 (CH), 131.1 (CH), 130.7 (CH), 119.9 (dt, $^1J_{\text{C-F}} = 288.2$ Hz, $^2J_{\text{C-F}} = 34.1$ Hz, C_q), 119.2 (d, $^2J_{\text{C-F}} = 17.5$ Hz, CH), 115.2 (m, C_q), 112.1 (m, C_q), 111.6 (m, C_q), 110.7 (m, C_q), 108.6 (m, C_q), 108.2 (m, C_q), 29.1 (CH_3), 27.9 (m, CH_2), 20.8 (CH_3).

^{19}F -NMR (282 MHz, CDCl_3): $\delta = -80.9$ (m), -114.4 (m, *E*), -117.5 (m, *Z*), -122.0 (m), -122.8 (m), -123.4 (m), -124.3 (m), -126.2 (m), -132.7 (m).

IR (ATR): 1679, 1607, 1582, 1251, 1185, 1134, 1106, 733, 716 cm^{-1} .

MS (ESI) m/z (relative intensity): 583 ($[\text{M} + \text{Na}]^+$, 100), 561 ($[\text{M} + \text{H}]^+$, 40).

HR-MS (ESI): m/z calcd. for $[\text{C}_{19}\text{H}_{12}\text{F}_{16}\text{O} + \text{H}]^+$ 561.0705, found 561.0710.



(E)-1-[4-Methyl-2-(1H,1H,2H-perfluorododec-2-en-1-yl)phenyl]ethan-1-one (307ac): The general procedure **C** was followed using 1-(4-methylphenyl)-*N*-(3,4,5-trimethoxyphenyl)-1-phenylethan-1-imine (**340a**) (150 mg, 0.50 mmol) and 1H,1H,2H-perfluorododec-1-ene (**301c**) (820 mg, 1.50 mmol). Isolation by column chromatography (*n*-hexane/EtOAc: 25/1) yielded **307ac** (210 mg, 64%, *E/Z* = 83:17, **307ac/339ac** = 94:6) as a yellow oil.

^1H -NMR (300 MHz, CDCl_3): $\delta = 7.75$ (d, $J = 8.0$ Hz, 1H), 7.18 (dd, $J = 8.0, 1.9$ Hz, 1H), 7.08 (d, $J = 1.9$ Hz, 1H), 6.20 (dt, $J = 25.3, 8.1$ Hz, 0.83H, *E*), 5.95 (dt, $J = 33.9, 4.4$ Hz, 0.17H, *Z*), 3.84 (ddt, $J = 7.3, 4.1, 2.1$ Hz, 2H), 3.21–3.03 (m, 0.12H, **339ac**), 2.61 (s, 2.49H, *E*), 2.60 (s, 0.51H, *Z*), 2.40 (s, 3H).

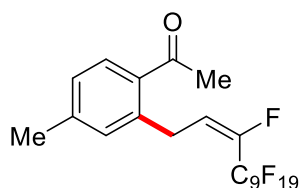
^{13}C -NMR (75 MHz, CDCl_3): $\delta = 200.4$ (C_q), 144.6 (dt, $^1J_{\text{C-F}} = 255.1$ Hz, $^2J_{\text{C-F}} = 25.3$ Hz, C_q), 143.2 (C_q), 138.6 (C_q), 133.6 (C_q), 132.0 (CH), 130.7 (CH), 127.6 (CH), 119.7 (dt, $^1J_{\text{C-F}} = 275.3$ Hz, $^2J_{\text{C-F}} = 37.3$ Hz, C_q), 119.1 (d, $^2J_{\text{C-F}} = 9.8$ Hz, CH), 115.1 (m, C_q), 111.6 (m, C_q), 110.8 (m, C_q), 110.7 (m, C_q), 110.1 (m, C_q), 108.6 (m, C_q), 107.5 (m, C_q), 107.1 (m, C_q), 29.0 (CH_3), 28.4 (m, CH_2), 21.2 (CH_3).

^{19}F -NMR (282 MHz, CDCl_3): $\delta = -80.9$ (m), -114.5 (m, *E*), -117.5 (m, *Z*), -121.9 (m), -122.8 (m), -123.0 (m), -123.1 (m), -123.4 (m), -124.4 (m), -126.3 (m), -132.8 (m).

IR (ATR): 1700, 1355, 1249, 1210, 1195, 1100, 730, 695 cm^{-1} .

MS (ESI) m/z (relative intensity): 683 ($[\text{M} + \text{Na}]^+$, 100), 661 ($[\text{M} + \text{H}]^+$, 30).

HR-MS (ESI): m/z calcd. for $[C_{21}H_{12}F_{20}O + H]^+$ 661.0642, found 661.0641.



(E)-1-[4-Methyl-2-(1H,1H,2H-perfluorododec-2-en-1-yl)phenyl]ethan-1-one (307cc): The general procedure **C** was followed using 1-(4-methylphenyl)-*N*-(3,4,5-trimethoxyphenyl)-1-phenylethan-1-imine (**340c**) (150 mg, 0.50 mmol) and 1*H*,1*H*,2*H*-perfluorododec-1-ene (**301c**) (820 mg, 1.50 mmol). Isolation by column chromatography (*n*-hexane/EtOAc: 25/1) yielded **307cc** (210 mg, 64%, *E/Z* = 83:17, **307cc/339cc** = 94:6) as a yellow oil.

$^1\text{H-NMR}$ (300 MHz, CDCl_3): δ = 7.75 (d, J = 8.0 Hz, 1H), 7.18 (dd, J = 8.0, 1.9 Hz, 1H), 7.08 (d, J = 1.9 Hz, 1H), 6.20 (dt, J = 25.3, 8.1 Hz, 0.83H, *E*), 5.95 (dt, J = 33.9, 4.4 Hz, 0.17H, *Z*), 3.84 (ddt, J = 7.3, 4.1, 2.1 Hz, 2H), 3.21–3.03 (m, 0.12H, **339cc**), 2.61 (s, 2.49H, *E*), 2.60 (s, 0.51H, *Z*), 2.40 (s, 3H).

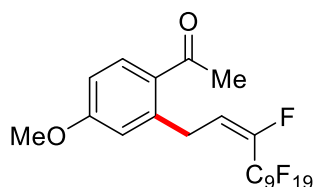
$^{13}\text{C-NMR}$ (75 MHz, CDCl_3): δ = 200.4 (C_q), 144.6 (dt, $^1J_{\text{C-F}}$ = 255.1 Hz, $^2J_{\text{C-F}}$ = 25.3 Hz, C_q), 143.2 (C_q), 138.6 (C_q), 133.6 (C_q), 132.0 (CH), 130.7 (CH), 127.6 (CH), 119.7 (dt, $^1J_{\text{C-F}}$ = 275.3 Hz, $^2J_{\text{C-F}}$ = 37.3 Hz, C_q), 119.1 (d, $^2J_{\text{C-F}}$ = 9.8 Hz, CH), 115.1 (m, C_q), 111.6 (m, C_q), 110.8 (m, C_q), 110.7 (m, C_q), 110.1 (m, C_q), 108.6 (m, C_q), 107.5 (m, C_q), 107.1 (m, C_q), 29.0 (CH_3), 28.4 (m, CH_2), 21.2 (CH_3).

$^{19}\text{F-NMR}$ (282 MHz, CDCl_3): δ = –80.9 (m), –114.5 (m, *E*), –117.5 (m, *Z*), –121.9 (m), –122.8 (m), –123.0 (m), –123.1 (m), –123.4 (m), –124.4 (m), –126.3 (m), –132.8 (m).

IR (ATR): 1700, 1355, 1249, 1210, 1195, 1100, 730, 695 cm^{-1} .

MS (ESI) m/z (relative intensity): 683 ($[\text{M} + \text{Na}]^+$, 100), 661 ($[\text{M} + \text{H}]^+$, 30).

HR-MS (ESI): m/z calcd. for $[C_{21}H_{12}F_{20}O + H]^+$ 661.0642, found 661.0641.



(E)-1-[4-Methoxy-2-(1H,1H,2H-perfluorododec-2-en-1-yl)phenyl]ethan-1-one (307ec): The general procedure **C** was followed using 1-[4-methoxy-*N*-(3,4,5-trimethoxyphenyl)-1-phenylethan-1-imine (**340e**) (160 mg, 0.50 mmol) and 1*H*,1*H*,2*H*-perfluorododec-1-ene (**301c**) (820 mg, 1.50 mmol). Isolation by column chromatography (*n*-hexane/EtOAc: 25/1) yielded **307ec** (203 mg, 60%, *E/Z* = 82:18, **307ec/339ec** = 98:2) as a yellow solid. M.p.: 52 °C.

5. Experimental Part

$^1\text{H-NMR}$ (500 MHz, CDCl_3): δ = 7.81 (d, J = 8.5 Hz, 1H), 6.81 (dd, J = 8.5, 2.7 Hz, 1H), 6.71 (d, J = 2.7 Hz, 1H), 6.16 (dt, J = 27.5, 7.8 Hz, 0.82H, *E*), 5.92 (dt, J = 32.7, 7.5 Hz, 0.18H, *Z*), 3.85 (ddt, J = 7.3, 3.6, 1.6 Hz, 2H), 3.82 (s, 3H), 3.20–3.00 (m, 0.04H, **339ec**), 2.55 (s, 2.46H, *E*), 2.54 (s, 0.54H, *Z*).

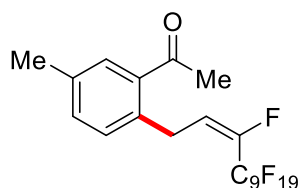
$^{13}\text{C-NMR}$ (125 MHz, CDCl_3): δ = 199.1 (C_q), 162.4 (C_q), 144.0 (dt, $^1J_{\text{C-F}}$ = 235.3 Hz, $^2J_{\text{C-F}}$ = 28.1 Hz, C_q), 141.4 (C_q), 133.0 (CH), 128.7 (C_q), 118.7 (d, $^2J_{\text{C-F}}$ = 8.5 Hz, CH), 117.5 (dt, $^1J_{\text{C-F}}$ = 273.2 Hz, $^2J_{\text{C-F}}$ = 30.9 Hz, C_q), 117.0 (CH), 112.7 (m, C_q), 112.6 (m, C_q), 112.5 (m, C_q), 111.5 (CH), 111.4 (m, C_q), 110.8 (m, C_q), 110.6 (m, C_q), 110.1 (m, C_q), 108.4 (m, C_q), 55.2 (CH_3), 28.9 (m, CH_2), 28.7 (CH_3).

$^{19}\text{F-NMR}$ (282 MHz, CDCl_3): δ = -80.8 (m), -114.3 (m, *E*), -117.4 (m, *Z*), -121.8 (m), -122.7 (m), -123.0 (m), -123.1 (m), -123.3 (m), -124.0 (m), -126.1 (m), -132.5 (m).

IR (ATR): 1720, 1450, 1335, 1229, 1209, 1104, 720, 607 cm^{-1} .

MS (ESI) m/z (relative intensity): 699 ($[\text{M} + \text{Na}]^+$, 100), 677 (80).

HR-MS (ESI): m/z calcd. for $[\text{C}_{21}\text{H}_{12}\text{F}_{20}\text{O}_2 + \text{H}]^+$ 677.0591, found 677.0584.



(*E*)-1-[5-Methyl-2-(1*H*,1*H*,2*H*-perfluorododec-2-en-1-yl)phenyl]ethan-1-one (307ic): The general procedure **C** was followed using 1-(3-methylphenyl)-*N*-(3,4,5-trimethoxyphenyl)-1-phenylethan-1-imine (**340i**) (150 mg, 0.50 mmol) and 1*H*,1*H*,2*H*-perfluorododec-1-ene (**301c**) (820 mg, 1.50 mmol). Isolation by column chromatography (*n*-hexane/EtOAc: 25/1) yielded **307ic** (201 mg, 61%, *E/Z* = 73:27, **307ic/339ic** = 87:13) as a yellow oil.

$^1\text{H-NMR}$ (300 MHz, CDCl_3): δ = 7.61 (d, J = 2.5 Hz, 1H), 7.31 (dd, 8.0, 2.5 Hz, 1H), 7.16 (d, J = 8.0 Hz, 1H), 6.18 (dt, J = 25.4, 6.3, 0.73H, *E*), 5.93 (dt, J = 33.4, 4.2 Hz, 0.27H, *Z*), 3.79 (ddt, J = 7.7, 4.2, 2.2 Hz, 2H), 3.22–2.97 (m, 0.27H, **339ic**), 2.62 (s, 2.19H, *E*), 2.61 (s, 0.81H, *Z*), 2.42 (s, 3H).

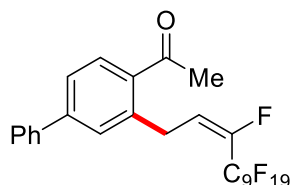
$^{13}\text{C-NMR}$ (75 MHz, CDCl_3): δ = 201.2 (C_q), 144.2 (dt, $^1J_{\text{C-F}}$ = 255.3 Hz, $^2J_{\text{C-F}}$ = 28.1 Hz, C_q), 136.8 (C_q), 136.6 (C_q), 135.1 (C_q), 133.0 (CH), 131.1 (CH), 130.7 (CH), 119.6 (dt, $^1J_{\text{C-F}}$ = 288.2 Hz, $^2J_{\text{C-F}}$ = 34.1 Hz, C_q), 119.2 (d, $^2J_{\text{C-F}}$ = 7.5 Hz, CH), 115.1 (m, C_q), 112.1 (m, C_q), 111.6 (m, C_q), 111.2 (m, C_q), 110.7 (m, C_q), 110.1 (m, C_q), 108.1 (m, C_q), 107.5 (m, C_q), 29.2 (CH_3), 27.9 (m, CH_2), 20.9 (CH_3).

$^{19}\text{F-NMR}$ (282 MHz, CDCl_3): δ = -80.9 (m), -114.5 (m, *E*), -117.5 (m, *Z*), -121.9 (m), -122.8 (m), -123.0 (m), -123.1 (m), -123.4 (m), -124.4 (m), -126.3 (m), -132.8 (m).

IR (ATR): 1712, 1355, 1243, 1223, 1155, 1130, 725, 695 cm^{-1} .

MS (ESI) m/z (relative intensity): 683 ($[\text{M} + \text{Na}]^+$, 100), 661 ($[\text{M} + \text{H}]^+$, 20).

HR-MS (ESI): m/z calcd. for $[\text{C}_{21}\text{H}_{12}\text{F}_{20}\text{O} + \text{H}]^+$ 661.0642, found 661.0639.



(E)-1-[4-Phenyl-2-(1H,1H,2H-perfluorododec-2-en-1-yl)phenyl]ethan-1-one (307dc): The general procedure **C** was followed using 1-([1,1'-biphenyl]-4-yl)-*N*-(3,5-dimethoxy-4-methylphenyl)ethan-1-imine (**340d**) (188 mg, 0.50 mmol) and 1*H*,1*H*,2*H*-perfluorododec-1-ene (**301c**) (820 mg, 1.50 mmol). Isolation by column chromatography (*n*-hexane/EtOAc: 25/1) yielded **307dc** (202 mg, 56%, *E/Z* = 82:18, **307dc/339dc** = 98:2) as a yellow solid. M.p.: 67 °C.

$^1\text{H-NMR}$ (300 MHz, CDCl_3): δ = 7.92 (d, J = 8.1 Hz, 1H), 7.66–7.58 (m, 3H), 7.55–7.43 (m, 4H), 6.25 (dt, J = 23.5, 8.2 Hz, 0.82H, *E*), 6.02 (dt, J = 33.7, 7.8 Hz, 0.18H, *Z*), 3.90 (ddt, J = 8.5, 4.1, 2.0 Hz, 2H), 3.27–3.15 (m, 0.02H, **339dc**), 2.68 (s, 2.46H, *E*), 2.67 (s, 0.54H, *Z*).

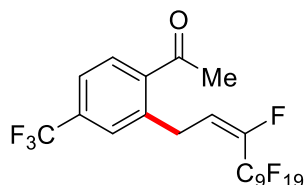
$^{13}\text{C-NMR}$ (75 MHz, CDCl_3): δ = 200.5 (C_q), 145.2 (dt, $^1J_{\text{C-F}}$ = 251.3 Hz, $^2J_{\text{C-F}}$ = 29.4 Hz, C_q), 144.4 (C_q), 139.4 (C_q), 139.1 (C_q), 134.9 (C_q), 131.1 (CH), 130.2 (CH), 130.0 (CH), 128.9 (CH), 128.3 (CH), 127.2 (CH), 125.6 (CH), 119.0 (d, $^2J_{\text{C-F}}$ = 8.1 Hz, CH), 118.1 (dt, $^1J_{\text{C-F}}$ = 288.2 Hz, $^2J_{\text{C-F}}$ = 32.3 Hz, C_q), 115.2 (m, C_q), 114.4 (m, C_q), 114.1 (m, C_q), 111.6 (m, C_q), 110.8 (m, C_q), 110.1 (m, C_q), 107.6 (m, C_q), 107.1 (m, C_q), 29.1 (CH_3), 28.7 (m, CH_2).

$^{19}\text{F-NMR}$ (282 MHz, CDCl_3): δ = –80.8 (m), –114.4 (m, *E*), –117.4 (m, *Z*), –121.9 (m), –122.7 (m), –123.0 (m), –123.3 (m), –123.4 (m), –123.7 (m), –126.1 (m), –132.5 (m).

IR (ATR): 1693, 1370, 1265, 1230, 1179, 1121, 710, 630 cm^{-1} .

MS (ESI) m/z (relative intensity): 745 ($[\text{M} + \text{Na}]^+$, 100), 740 (30), 723 ($[\text{M} + \text{H}]^+$, 20).

HR-MS (ESI): m/z calcd. for $[\text{C}_{26}\text{H}_{14}\text{F}_{20}\text{O} + \text{H}]^+$ 723.0798, found 723.0786.



(E)-1-[4-Trifluoromethyl-2-(1H,1H,2H-perfluorododec-2-en-1-yl)phenyl]ethan-1-one

(307fc): The general procedure **C** was followed using 1-[4-trifluoromethyl-*N*-(3,4,5-trimethoxyphenyl)-1-phenyl]ethan-1-one (**340f**) (177 mg, 0.50 mmol) and 1*H*,1*H*,2*H*-

5. Experimental Part

perfluorododec-1-ene (**301c**) (820 mg, 1.50 mmol). Isolation by column chromatography (*n*-hexane/EtOAc: 25/1) yielded **307fc** (193 mg, 54%, *E/Z* = 73:27) as a yellow oil.

¹H-NMR (300 MHz, CDCl₃): δ = 7.87 (d, *J* = 8.0 Hz, 1H), 7.64 (dd, *J* = 8.0, 1.4 Hz, 1H), 7.52 (d, *J* = 1.4 Hz, 1H), 6.10 (dt, *J* = 25.6, 8.5 Hz, 0.73H, *E*), 5.87 (dt, *J* = 33.4, 7.8 Hz, 0.27H, *Z*), 3.86 (ddt, *J* = 7.5, 4.0, 2.0 Hz, 2H), 2.65 (s, 2.19H, *E*), 2.64 (s, 0.81H, *Z*).

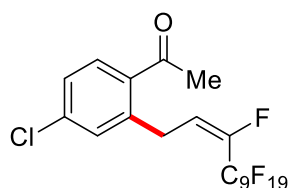
¹³C-NMR (100 MHz, CDCl₃): δ = 200.4 (C_q), 145.1 (dt, ¹*J*_{C-F} = 261.2 Hz, ²*J*_{C-F} = 29.5 Hz, C_q), 139.9 (C_q), 138.9 (CH), 133.9 (q, ²*J*_{C-F} = 33.1 Hz, C_q), 130.0 (CH), 127.9 (q, ³*J*_{C-F} = 3.8 Hz, CH), 125.0 (d, ¹*J*_{C-F} = 273.5 Hz, C_q), 124.1 (d, ²*J*_{C-F} = 7.3 Hz, C_q), 117.5 (dt, ¹*J*_{C-F} = 275.2 Hz, ²*J*_{C-F} = 22.3 Hz, C_q), 116.9 (d, ²*J*_{C-F} = 7.8 Hz, CH), 114.1 (m, C_q), 113.2 (m, C_q), 111.6 (m, C_q), 110.8 (m, C_q), 110.5 (m, C_q), 110.2 (m, C_q), 108.7 (m, C_q), 108.6 (m, C_q), 29.4 (CH₃), 28.1 (m, CH₂).

¹⁹F-NMR (376 MHz, CDCl₃): δ = -63.6 (m), -81.0 (m), -114.6 (m, *E*), -117.6 (m, *Z*), -121.9 (m), -122.0 (m), -122.3 (m), -122.5 (m), -123.2 (m), -123.4 (m), -126.3 (m), -130.7 (m).

IR (ATR): 1712, 1412, 1238, 1212, 1155, 1114, 711, 601 cm⁻¹.

MS (ESI) *m/z* (relative intensity): 737 ([M + Na]⁺, 100), 722 (20).

HR-MS (ESI): *m/z* calcd. for [C₂₁H₉F₂₃O + Na]⁺ 737.0178, found 737.0170.



(E)-1-[4-Chloro-2-(1H,1H,2H-perfluorododec-2-en-1-yl)phenyl]ethan-1-one (307ha): The general procedure **C** was followed using 1-(4-chlorophenyl)-*N*-(3,4,5-trimethoxyphenyl)-1-phenylethan-1-imine (**340h**) (160 mg, 0.50 mmol) and 1*H,1H,2H*-perfluorododec-1-ene (**301c**) (820 mg, 1.50 mmol). Isolation by column chromatography (*n*-hexane/EtOAc: 25/1) yielded **307ha** (204 mg, 60%, *E/Z* = 76:24, **307ha/339ha** = 99:1) as a yellow oil.

¹H-NMR (300 MHz, CDCl₃): δ = 7.76 (d, *J* = 8.4 Hz, 1H), 7.37 (dd, *J* = 8.4, 1.6 Hz, 1H), 7.22 (d, 1.6 Hz, 1H), 6.14 (dt, *J* = 24.7, 8.7 Hz, 0.76H, *E*), 5.92 (dt, *J* = 35.4, 7.8 Hz, 0.24H, *Z*), 3.86 (ddt, *J* = 7.8, 4.1, 2.0 Hz, 2H), 3.26–3.03 (m, 0.02H, **339ha**), 2.62 (s, 2.28H, *E*), 2.61 (s, 0.72H, *Z*).

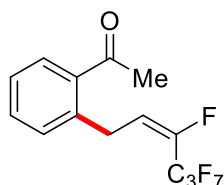
¹³C-NMR (75 MHz, CDCl₃): δ = 199.7 (C_q), 144.5 (dt, ¹*J*_{C-F} = 259.1 Hz, ²*J*_{C-F} = 28.4 Hz, C_q), 140.1 (C_q), 138.5 (C_q), 134.7 (C_q), 131.5 (CH), 131.2 (CH), 127.2 (CH), 118.3 (dt, ¹*J*_{C-F} = 288.3 Hz, ²*J*_{C-F} = 32.3 Hz, C_q), 118.0 (d, ²*J*_{C-F} = 8.9 Hz, CH), 114.5 (C_q), 113.3 (C_q), 112.1 (C_q), 111.5 (C_q), 111.1 (C_q), 110.5 (C_q), 108.0 (C_q), 107.1 (C_q), 29.1 (CH₃), 28.1 (m, CH₂).

^{19}F -NMR (282 MHz, CDCl_3): $\delta = -80.9$ (m), -114.5 (m, *E*), -117.5 (m, *Z*), -122.0 (m), -122.8 (m), -123.1 (m), -123.3 (m), -123.4 (m), -123.8 (m), -126.2 (m), -132.4 (m).

IR (ATR): 1699, 1379, 1269, 1232, 1181, 1123, 711, 630 cm^{-1} .

MS (ESI) m/z (relative intensity): 703 ($[\text{M} + \text{Na}]^+$, 100), 698 (10), 685 (20).

HR-MS (ESI): m/z calcd. for $[\text{C}_{20}\text{H}_9\text{ClF}_{20}\text{O} + \text{Na}]^+$ 702.9915, found 702.9905.



(*E*)-1-[2-(1*H*,1*H*,2*H*-Perfluorohex-2-en-1-yl)phenyl]ethan-1-one (307ab): The general procedure **C** was followed using *N*-(3,4,5-trimethoxyphenyl)-1-phenylethan-1-imine (**340a**) (143 mg, 0.50 mmol) and 1*H*,1*H*,2*H*-perfluorohex-2-en-1-yl (**301b**) (370 mg, 1.50 mmol). Isolation by column chromatography (*n*-hexane/EtOAc: 25/1) yielded **307ab** (83 mg, 48%, *E/Z* = 89:11, **307ab**/**339ab** = 91:9) as a yellow oil.

^1H -NMR (300 MHz, CDCl_3): $\delta = 7.82$ (dd, $J = 7.5, 1.6$ Hz, 1H), 7.50 (ddd, $J = 7.7, 7.5, 1.6$ Hz, 1H), 7.39 (ddd, $J = 7.7, 7.6, 1.6$ Hz, 1H), 7.27 (dd, 7.6, 1.6 Hz, 1H), 6.18 (dt, $J = 23.1, 8.3$ Hz, 0.89H, *E*), 5.95 (dt, $J = 33.8, 7.8$ Hz, 0.11H, *Z*), 3.80 (ddt, $J = 7.8, 4.0, 2.0$ Hz, 2H), 3.20–3.10 (m, 0.18H, **339ab**), 2.64 (s, 2.67H, *E*), 2.64 (s, 0.33H, *Z*).

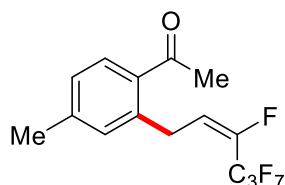
^{13}C -NMR (75 MHz, CDCl_3): $\delta = 201.1$ (C_q), 141.5 (dt, $^1J_{\text{C-F}} = 259.2$ Hz, $^2J_{\text{C-F}} = 28.4$ Hz, C_q), 138.2 (C_q), 136.6 (C_q), 132.4 (CH), 131.2 (CH), 130.2 (CH), 127.1 (CH), 119.3 (dt, $^1J_{\text{C-F}} = 288.1$ Hz, $^2J_{\text{C-F}} = 32.3$ Hz, C_q), 118.3 (d, $^2J_{\text{C-F}} = 8.9$ Hz, CH), 115.8 (m, C_q), 111.1 (m, C_q), 29.3 (CH_3), 28.3 (m, CH_2).

^{19}F -NMR (282 MHz, CDCl_3): $\delta = -80.7$ (m), -115.4 (m, *E*), -118.5 (m, *Z*), -124.1 (m, *E*), -127.8 (m, *Z*), -132.6 (m).

IR (ATR): 1709, 1425, 1255, 1232, 1189, 1104, 781, 651 cm^{-1} .

MS (ESI) m/z (relative intensity): 381 ($[\text{M} + \text{Na}]^+$, 100), 369 (80).

HR-MS (ESI): m/z calcd. for $[\text{C}_{14}\text{H}_{10}\text{F}_8\text{O} + \text{Na}]^+$ 369.0496, found 369.0497.



(*E*)-1-[4-Methyl-2-(1*H*,1*H*,2*H*-perfluorohex-2-en-1-yl)phenyl]ethan-1-one (307cb): The general procedure **C** was followed using 1-(4-methylphenyl)-*N*-(3,4,5-trimethoxyphenyl)-1-phenylethan-1-imine (**340c**) (150 mg, 0.50 mmol) and 1*H*,1*H*,2*H*-perfluorohex-2-en-1-yl

5. Experimental Part

(301b) (370 mg, 1.50 mmol). Isolation by column chromatography (*n*-hexane/EtOAc: 25/1) yielded **307cb** (88 mg, 49%, *E/Z* = 81:19, **307cb/339cb** = 99:1) as a yellow oil.

¹H-NMR (300 MHz, CDCl₃): δ = 7.75 (dd, *J* = 1.8 Hz, 0.8 Hz, 1H), 7.19 (dd, *J* = 8.0, 1.8 Hz, 1H), 7.17 (dd, 8.0, 0.8 Hz, 1H), 6.18 (dt, *J* = 23.3, 8.3 Hz, 0.81H, *E*), 5.95 (dt, *J* = 32.9, 7.8 Hz, 0.19H, *Z*), 3.83 (ddt, *J* = 8.4, 4.8, 2.2 Hz, 2H), 3.30–3.15 (m, 0.02H, **339cb**), 2.62 (s, 2.43H, *E*), 2.61 (s, 0.57H, *Z*), 2.40 (s, 3H).

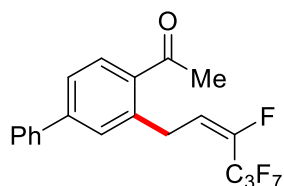
¹³C-NMR (75 MHz, CDCl₃): δ = 200.5 (C_q), 144.2 (dt, ¹*J*_{C-F} = 259.1 Hz, ²*J*_{C-F} = 28.4 Hz, C_q), 143.2 (C_q), 138.6 (C_q), 133.6 (C_q), 132.1 (CH), 130.7 (CH), 127.6 (CH), 119.1 (dt, ¹*J*_{C-F} = 288.3 Hz, ²*J*_{C-F} = 32.3 Hz, C_q), 118.3 (d, ²*J*_{C-F} = 8.7 Hz, CH), 112.8 (m, C_q), 108.3 (m, C_q), 29.0 (CH₃), 28.4 (m, CH₂), 21.3 (CH₃).

¹⁹F-NMR (282 MHz, CDCl₃): δ = -80.7 (m), -115.4 (m, *E*), -118.4 (m, *Z*), -124.5 (m, *E*), -127.8 (m, *Z*), -133.0 (m).

IR (ATR): 1720, 1470, 1267, 1232, 1189, 1131, 711, 630 cm⁻¹.

MS (ESI) *m/z* (relative intensity): 383 ([M + Na]⁺, 100), 333 (10).

HR-MS (ESI): *m/z* calcd. for [C₁₅H₁₂F₈O + H]⁺ 361.0833, found 361.0828.



(E)-1-[4-Phenyl-2-(1H,1H,2H-perfluorohex-2-en-1-yl)phenyl]ethan-1-one (307db): The general procedure **C** was followed using 1-([1,1'-biphenyl]-4-yl)-*N*-(3,5-dimethoxy-4-methylphenyl)ethan-1-imine (**340d**) (188 mg, 0.50 mmol) and 1*H*,1*H*,2*H*-Perfluorohex-2-en-1-yl (**301b**) (370 mg, 1.50 mmol). Isolation by column chromatography (*n*-hexane/EtOAc: 25/1) yielded **307db** (110 mg, 52%, *E/Z* = 84:16, **307db/339db** = 99:1) as a yellow oil.

¹H-NMR (300 MHz, CDCl₃): δ = 7.90 (d, *J* = 8.1 Hz, 1H), 7.60–7.55 (m, 3H), 7.52–7.40 (m, 4H), 6.23 (dt, *J* = 23.1, 8.4 Hz, 0.84H, *E*), 6.00 (dt, *J* = 33.7, 7.8 Hz, 0.16H, *Z*), 3.87 (ddt, *J* = 8.3, 4.2, 2.1 Hz, 2H), 3.23–3.12 (m, 0.02H, **339db**), 2.65 (s, 2.52H, *E*), 2.66 (s, 0.48H, *Z*).

¹³C-NMR (75 MHz, CDCl₃): δ = 200.5 (C_q), 145.2 (dt, ¹*J*_{C-F} = 259.9 Hz, ²*J*_{C-F} = 28.4 Hz, C_q), 144.5 (C_q), 139.4 (C_q), 139.0 (C_q), 134.9 (C_q), 131.1 (CH), 130.2 (CH), 129.9 (CH), 129.0

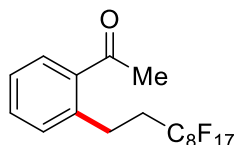
(CH), 128.4 (CH), 127.1 (CH), 125.6 (CH), 119.0 (d, $^2J_{C-F} = 7.8$ Hz, CH), 117.4 (dt, $^1J_{C-F} = 288.1$ Hz, $^2J_{C-F} = 32.3$ Hz, C_q), 111.5 (m, C_q), 108.8 (m, C_q), 29.2 (CH₃), 28.6 (m, CH₂).

^{19}F -NMR (282 MHz, CDCl₃): $\delta = -80.6$ (m), -115.3 (m, *E*), -118.4 (m, *Z*), -124.0 (m, *E*), -127.7 (m, *Z*), -132.4 (m).

IR (ATR): 1711, 1410, 1237, 1212, 1199, 1111, 701, 600 cm⁻¹.

MS (ESI) *m/z* (relative intensity): 445 ([M + Na]⁺, 100), 423 ([M + H]⁺, 20).

HR-MS (ESI): *m/z* calcd. for [C₂₀H₁₄F₈O + H]⁺ 423.0990, found 423.0996.



1-(2-(3,3,4,4,5,5,6,6,7,7,8,8,9,9,10,10-heptafluorodecyl)phenyl)ethan-1-one

(339aa):

A suspension of ketimine **340a** (0.50 mmol, 1.0 equiv), 1*H*,1*H*,2*H*-perfluoroalkene **301a** (1.50 mmol, 3.0 equiv), [RuCl₂(*p*-cymene)]₂ (15.3 mg, 5.0 mol %), NaOAc (12.3 mg, 30 mol %) and K₂CO₃ (104 mg, 0.75 mmol, 1.50 equiv) in 1,4-dioxane (0.50 mL, 1 M) was stirred under nitrogen at 120 °C for 16 h. At ambient temperature, the reaction mixture was diluted with EtOAc (5.0 mL) and HCl (5.0 mL, 1 M) was added. The mixture was stirred for 3 h and extracted with EtOAc (3 x 10 mL). After removal of the solvents *in vacuo*, the remaining residue was purified by column chromatography on silica gel to afford the desired product **339aa**.

^1H -NMR (300 MHz, CDCl₃): $\delta = 7.76$ (dd, $J = 7.8, 1.6$ Hz, 1H), 7.44 (ddd, $J = 7.7, 7.5, 1.6$ Hz, 1H), 7.33 (ddd, $J = 7.8, 7.5, 1.6$ Hz, 1H), 7.28 (dd, $J = 7.7, 1.6$ Hz, 1H), 3.38–2.77 (m, 2H), 2.59 (s, 3H), 2.56–2.24 (m, 2H).

^{13}C -NMR (125 MHz, CDCl₃): $\delta = 201.0$ (C_q), 140.0 (C_q), 137.0 (C_q), 132.2 (CH), 131.8 (CH), 130.1 (CH), 126.8 (CH), 121.0–108.2 (m, -C₈F₁₇), 32.7 (t, $^2J_{C-F} = 22$ Hz, CH₂), 29.2 (CH₃), 25.7 (t, $^3J_{C-F} = 5$ Hz, CH₂).

^{19}F -NMR (282 MHz, CDCl₃): $\delta = -80.9$ (m), -114.6 (m), -121.7 (m), -122.0 (m), -122.8 (m), -123.5 (m), -126.1 (m), -126.3 (m).

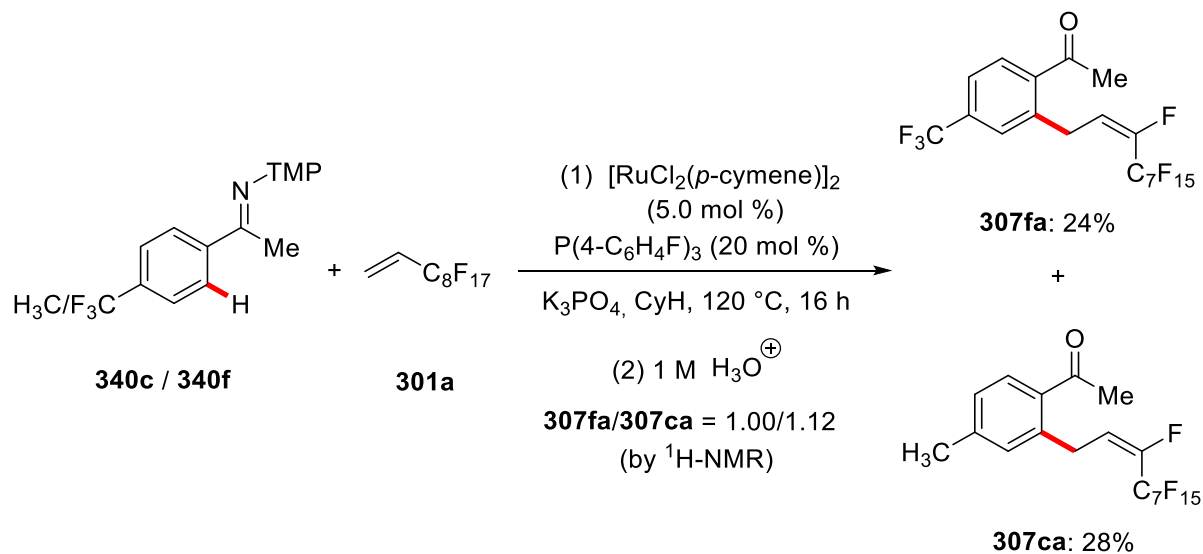
IR (ATR): 1701, 1419, 1257, 1233, 1155, 1121, 711, 610 cm⁻¹.

MS (ESI) *m/z* (relative intensity): 589 ([M + Na]⁺, 100), 584 (10), 569 (40).

HR-MS (ESI): *m/z* calcd. for [C₁₈H₁₁F₁₇O + Na]⁺ 589.0431, found 589.0432.

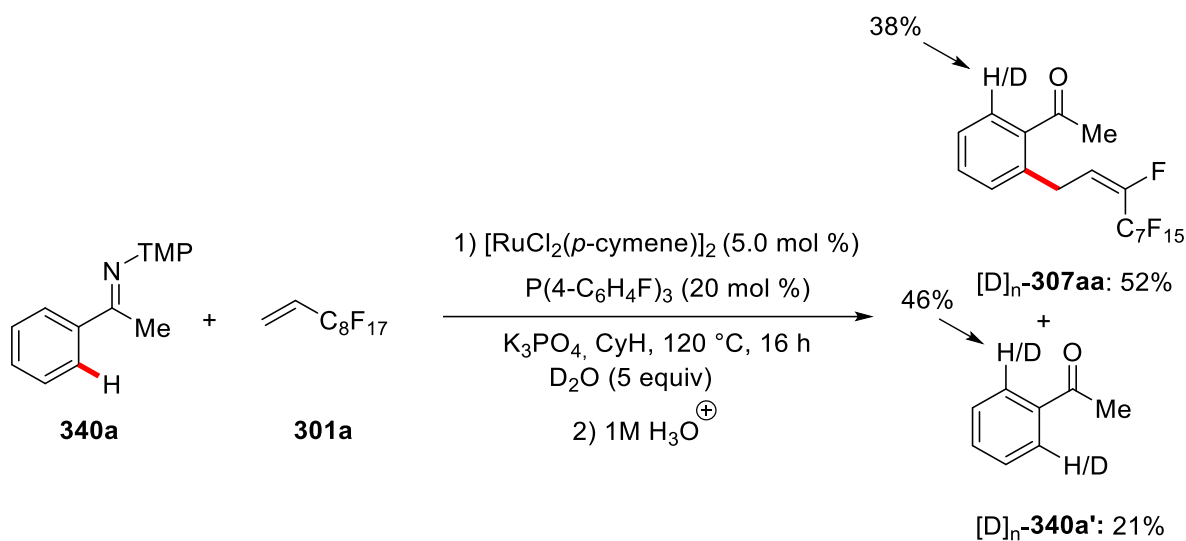
5.4.2. Mechanistic Studies

5.4.2.1. Intermolecular competition experiment

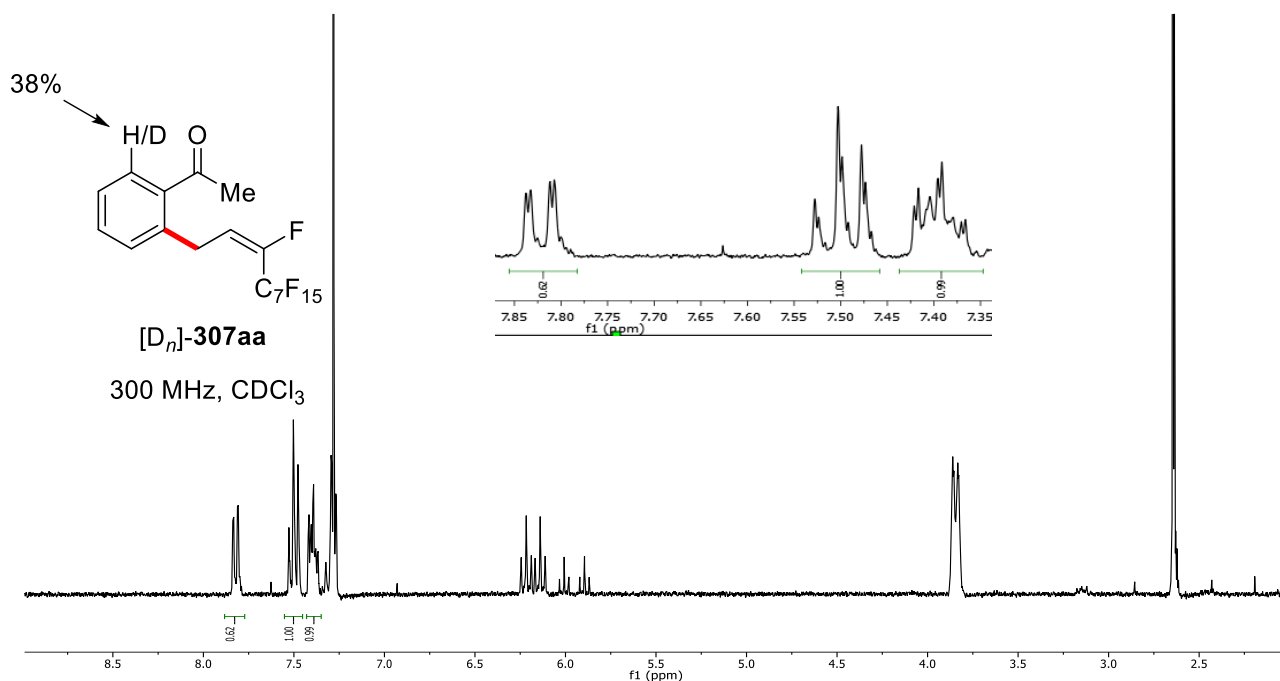


1-(4-methylphenyl)-N-(3,4,5-trimethoxyphenyl)-1-phenylethan-1-imine (**340c**) (150 mg, 0.50 mmol), 1-[4-trifluoromethyl-N-(3,4,5-trimethoxyphenyl)-1-phenyl]ethan-1-one (**340f**) (177 mg, 0.50 mmol), 1H,1H,2H-perfluoroalkene (**301a**) (446 mg, 1.0 mmol), $[\text{RuCl}_2(p\text{-cymene})]_2$ (15.3 mg, 5.0 mol %), $\text{P}(4\text{-C}_6\text{H}_4\text{F})_3$ (31.6 mg, 20 mol %) and K_3PO_4 (212 mg, 1.0 mmol) were stirred in cyclohexane (1.0 mL) at 120 °C for 16 h. At ambient temperature, the reaction mixture was diluted with EtOAc (10.0 mL), and HCl (5 mL, 1 M) was added. The mixture was stirred for 3 h and extracted with EtOAc (3 x 10.0 mL). After removal of the solvents *in vacuo*, **307fa** and **307ca** were isolated together by column chromatography on silica gel. The ratio of **307fa** and **307ca** was determined by means of $^1\text{H-NMR}$ spectroscopy which corresponds to **307fa** 24% and **307ca** 28%.

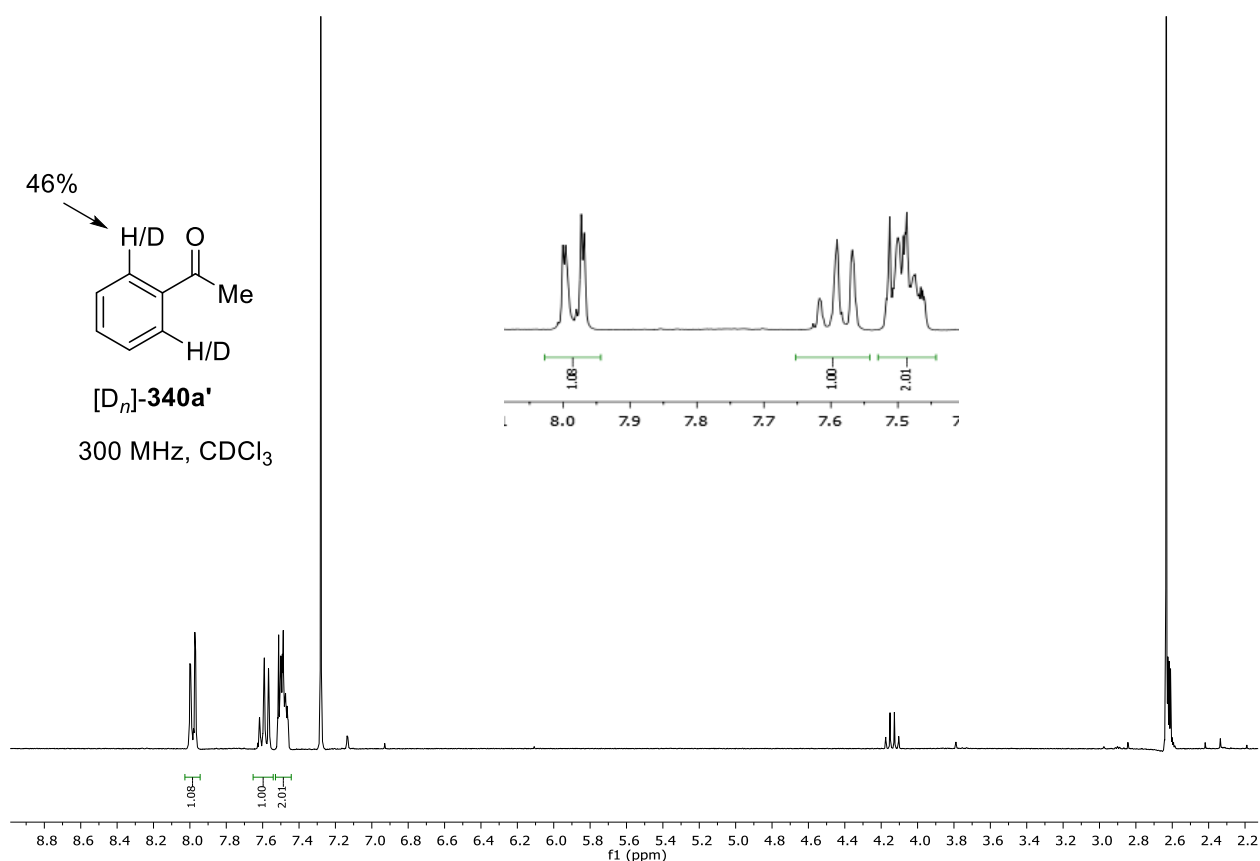
5.4.2.2. H/D Exchange Experiments



Ketimine **340a** (143 mg, 0.50 mmol), 1H,1H,2H-perfluoroalkene (**301a**) (669 mg, 1.50 mmol), $[RuCl_2(p\text{-cymene})]_2$ (15.3 mg, 5.0 mol %), $P(4\text{-C}_6\text{H}_4\text{F})_3$ (31.6 mg, 20.0 mol %) and K_3PO_4 (212 mg, 1.0 mmol) were stirred in cyclohexane (1.0 mL) and D_2O (5 equiv) at 120 °C for 16 h. At ambient temperature, the reaction mixture was diluted with EtOAc (5.0 mL) and HCl (5.0 mL, 1 M) was added. The mixture was stirred for 3 h and extracted with EtOAc (3 x 10.0 mL). After removal of the solvents *in vacuo*, purification by flash column chromatography on silica gel yielded $[D]_n$ -**340a** (21%) and $[D]_n$ -**307aa** (52%).

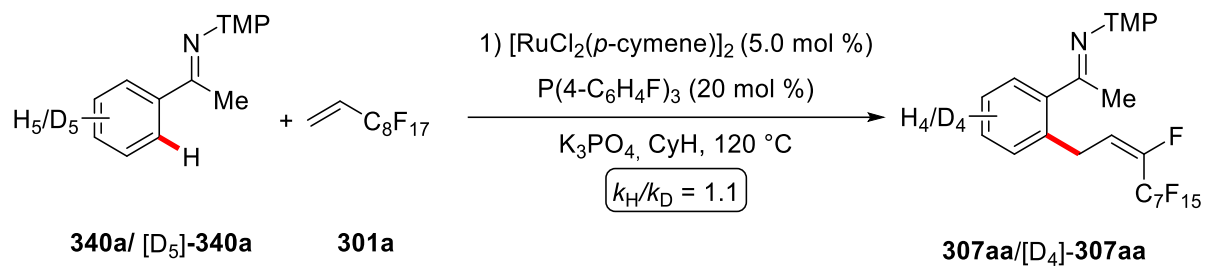


5. Experimental Part



5.4.2.3. Intermolecular KIE by Independent Experiments

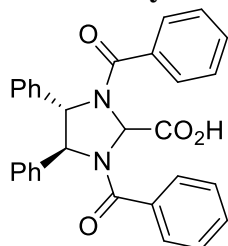
Two parallel reactions with **340a** and [D]₅-**340a** were performed to determine the corresponding KIE value. **340a** (143 mg, 0.50 mmol) or [D]₅-**340a** (145 mg, 0.50 mmol), [RuCl₂(*p*-cymene)]₂ (15.3 mg, 5.0 mol %), P(4-C₆H₄F)₃ (31.6 mg, 20.0 mol %), 1,3,5-trimethoxybenzene (84 mg, 0.50 mmol) and K₃PO₄ (212 mg, 1.0 mmol) were stirred in cyclohexane (1.0 mL) at 120 °C. A periodic aliquot (0.02 mL) was removed by syringe and analyzed by ¹H-NMR spectroscopy to provide the following conversions:

**Table 31.** Conversion-time table for determination of the KIE.

Time (min)	70	85	100	115	130
307aa	1.2	3.1	5.3	7.5	10.4
[D] ₅ - 307aa	0.1	2.4	4.3	6.6	8.3

5.5. Enantioselective Cobalt(III)-catalyzed C–H activation

5.5.1. Analytical Data of Novel Chiral Acids



(4*S*,5*S*)-1,3-Dibenzoyl-4,5-diphenylimidazolidine-2-carboxylic acid (CA5): General procedure **D** was followed using benzoyl chloride (295 mg, 2.10 mmol) to afford (4*S*,5*S*)-1,3-dibenzoyl-4,5-diphenylimidazolidine-2-carboxylic acid **CA5** (309.4 mg, 65% yield) as a white solid.

¹H-NMR (600 MHz, CD₃CO₂D): δ = 7.74–7.06 (m, 19H), 7.15–6.84 (m, 2H), 5.50 (s, 1H), 5.24 (s, 1H).

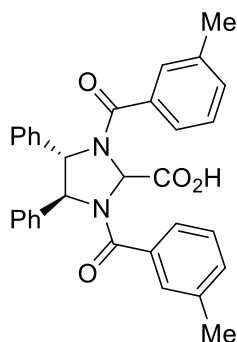
¹³C-NMR (125 MHz, CD₃CO₂D): (one carbon resonance is missing due to overlap): δ = 173.2 (C_q), 172.6 (C_q), 171.5 (C_q), 141.0 (C_q), 139.1 (C_q), 135.7 (C_q), 134.7 (C_q), 131.7 (CH), 131.5 (CH), 129.9 (CH), 129.7 (CH), 129.2 (CH), 129.1 (CH), 129.1 (CH), 127.8 (CH), 127.7 (CH), 127.2 (CH), 126.7 (CH), 73.9 (CH), 72.8 (CH), 71.0 (CH).

IR (ATR): 3060, 1645, 1602, 1495, 1447, 1388, 867, 754, 698, 551 cm⁻¹.

$[\alpha]_D^{20}$: -76.0 (*c* = 1.00, CHCl₃).

MS (ESI) *m/z* (relative intensity): 499 (80) [M + Na]⁺, 477 (100) [M + H]⁺, 425 (20).

HR-MS (ESI): *m/z* calcd. for [C₃₀H₂₄N₂O₄ + H]⁺ 477.1807 found 477.1809.



(4*S*,5*S*)-1,3-Bis(3-methylbenzoyl)-4,5-diphenylimidazolidine-2-carboxylic acid (CA6): General procedure **D** was followed using *m*-tolouyl chloride (323 mg, 2.10 mmol) to afford (4*S*,5*S*)-1,3-bis(3-methylbenzoyl)-4,5-diphenylimidazolidine-2-carboxylic acid **CA6** (352.8 mg, 70% yield) as a white solid.

¹H-NMR (500 MHz, CD₃CO₂D): δ = 7.49–7.19 (m, 9H), 7.18–7.03 (m, 8H), 7.02–6.88 (m, 2H), 5.49 (s, 1H), 5.22 (s, 1H), 2.20 (s, 3H), 2.13 (s, 3H).

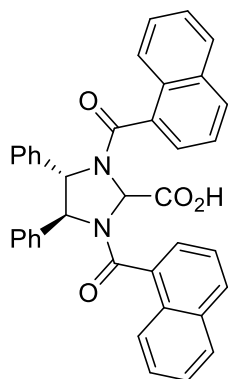
^{13}C -NMR (125 MHz, $\text{CD}_3\text{CO}_2\text{D}$): (one carbon resonance is missing due to overlap): $\delta = 173.7$ (C_q), 172.9 (C_q), 171.6 (C_q), 141.3 (C_q), 139.5 (C_q), 139.4 (C_q), 139.3 (C_q), 139.2 (C_q), 135.8 (C_q), 135.4 (CH), 134.8 (CH), 132.5 (CH), 132.3 (CH), 131.4 (CH), 130.0 (CH), 129.8 (CH), 129.4 (CH), 129.3 (CH), 129.2 (CH), 129.1 (CH), 128.5 (CH), 128.2 (CH), 127.4 (CH), 126.9 (CH), 125.0 (CH), 124.8 (CH), 73.8 (CH), 72.8 (CH), 70.8 (CH), 21.2 (CH_3), 21.1 (CH_3).

IR (ATR): 3030, 1642, 1585, 1495, 1384, 1211, 1092, 749, 698, 663 cm^{-1} .

$[\alpha]_D^{20}$: -67.8 ($c = 1.10$, CHCl_3).

MS (ESI) m/z (relative intensity): 527 (80) $[\text{M} + \text{Na}]^+$, 505 (100) $[\text{M} + \text{H}]^+$, 341 (20).

HR-MS (ESI): m/z calcd. for $[\text{C}_{32}\text{H}_{28}\text{N}_2\text{O}_4 + \text{H}]^+$ 505.2122 found 505.2119.



(4S,5S)-1,3-Di(1-naphthoyl)-4,5-diphenylimidazolidine-2-carboxylic acid (CA7): General procedure **D** was followed using 1-naphthoyl chloride (399 mg, 2.10 mmol) to afford (4S,5S)-1,3-bis(3-methylbenzoyl)-4,5-diphenylimidazolidine-2-carboxylic acid **CA7** (392.1 mg, 68% yield) as a white solid.

^1H -NMR (400 MHz, $\text{CDCl}_3 + 1\%$ TFA): $\delta = 9.00$ – 8.40 (m, 5H), 8.00 – 7.53 (m, 3H), 7.52 – 7.40 (m, 1H), 7.39 – 7.26 (m, 3H), 7.20 – 6.89 (m, 9H), 6.76 – 6.57 (m, 2H), 6.56 – 6.24 (m, 2H), 4.91 (s, 1H), 4.71 (s, 1H).

^{13}C -NMR (125 MHz, $\text{CD}_3\text{CO}_2\text{D}$): (four carbon resonance is missing due to overlap): $\delta = 172.6$ (C_q), 172.3 (C_q), 172.1 (C_q), 140.5 (CH), 139.0 (C_q), 138.9 (C_q), 135.1 (CH), 134.9 (C_q), 134.0 (C_q), 133.9 (C_q), 133.1 (C_q), 132.6 (C_q), 132.6 (C_q), 132.3 (CH), 131.0 (CH), 129.6 (CH), 129.2

5. Experimental Part

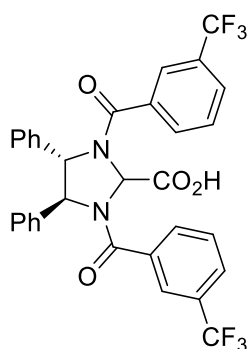
(CH), 129.0 (CH), 128.8 (CH), 127.9 (CH), 127.5 (CH), 127.3 (CH), 127.2 (CH), 126.7 (CH), 126.7 (CH), 125.6 (CH), 125.4 (CH), 75.3 (CH), 73.9 (CH), 71.9 (CH).

IR (ATR): 3054, 1637, 1508, 1457, 1299, 778, 750, 697, 655 cm^{-1} .

$[\alpha]_{\text{D}}^{20}$: -94.9 ($c = 1.18$, CHCl_3).

MS (ESI) m/z : 599 $[\text{M} + \text{Na}]^+$.

HR-MS (ESI): m/z calcd. for $[\text{C}_{38}\text{H}_{28}\text{N}_2\text{O}_4 + \text{H}]^+$ 577.2122 found 577.2112.



(4S,5S)-4,5-Diphenyl-1,3-bis[3-(trifluoromethyl)benzoyl]imidazolidine-2-carboxylic acid

(CA11): General procedure **D** was followed using 3-(trifluoromethyl)benzoyl chloride (436.8 mg, 2.10 mmol) to afford **CA11** (367.1 mg, 60% yield) as a white solid. M.p.: >200 $^{\circ}\text{C}$.

$^1\text{H-NMR}$ (600 MHz, $\text{CD}_3\text{CO}_2\text{D}$): $\delta = 7.62\text{--}7.48$ (m, 5H), 7.42–7.34 (m, 2H), 7.29–7.13 (m, 9H), 7.11–6.99 (m, 2H), 6.98–6.83 (m, 1H), 5.35 (s, 1H), 5.17 (bs, 1H).

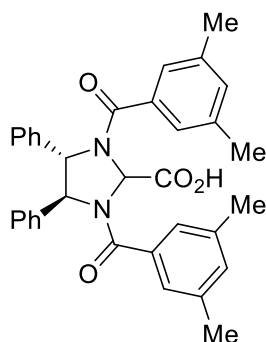
$^{13}\text{C-NMR}$ (100 MHz, $\text{CD}_3\text{CO}_2\text{D}$) (one carbon resonances are missing due to overlap): $\delta = 171.7$ (C_q), 171.6 (C_q), 170.9 (C_q), 140.0 (C_q), 138.7 (C_q), 137.0 (C_q), 136.1 (C_q), 131.5 (q, $^2J_{\text{C-F}} = 32.4$ Hz, C_q), 131.4 (q, $^2J_{\text{C-F}} = 32.4$ Hz, C_q), 131.4 (CH), 130.3 (CH), 130.2 (CH), 130.1 (CH), 129.9 (CH), 129.5 (CH), 128.2 (CH), 128.2 (CH), 128.0 (CH), 127.6 (CH), 127.4 (CH), 124.9 (CH), 124.9 (CH), 124.7 (q, $^1J_{\text{C-F}} = 271.8$ Hz, C_q), 124.6 (q, $^1J_{\text{C-F}} = 271.8$ Hz, C_q), 74.5 (CH), 73.3 (CH), 71.6 (CH).

$^{19}\text{F-NMR}$ (377 MHz, $\text{CD}_3\text{CO}_2\text{D}$): $\delta = -63.7$ (m), -63.8 (m).

IR (ATR): 3066, 3033, 1651, 1456, 1386, 1326, 1280, 1121, 1072, 750, 699 cm^{-1} .

$[\alpha]_{\text{D}}^{20}$: -49.2 ($c = 1.00$, CHCl_3). MS (ESI) m/z (relative intensity): 1247 (20) $[2\text{M} + \text{Na}]^+$, 635 (100) $[\text{M} + \text{Na}]^+$, 613 (15) $[\text{M} + \text{H}]^+$.

HR-MS (ESI): m/z calcd. for $[\text{C}_{32}\text{H}_{22}^{19}\text{F}_6\text{N}_2\text{O}_4 + \text{Na}]^+$ 635.1376 found 635.1361.



(4*S*,5*S*)-1,3-Bis(3,5-dimethylbenzoyl)-4,5-diphenylimidazolidine-2-carboxylic acid

(CA12): General procedure **D** was followed using 3,5-dimethylbenzoyl chloride (352.8 mg, 2.10 mmol) to afford **CA12** (329.0 mg, 62% yield) as a white solid. M.p.: 180–186 °C.

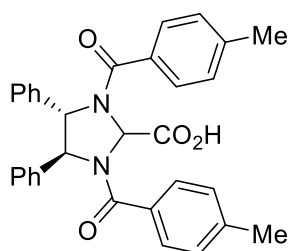
¹H-NMR (400 MHz, CD₃CO₂D): δ = 7.46–7.27 (m, 8H), 7.25–7.08 (m, 2H), 7.04–6.67 (m, 7H), 5.51 (s, 1H), 5.24 (bs, 1H), 2.19 (s, 6H), 2.14 (s, 6H).

¹³C-NMR (100 MHz, CD₃CO₂D) (two carbon resonances are missing due to overlap): δ = 172.9 (C_q), 171.9 (C_q), 170.3 (C_q), 140.2 (C_q), 138.5 (C_q), 138.1 (C_q), 138.1 (C_q), 134.6 (C_q), 133.7 (C_q), 132.2 (CH), 132.0 (CH), 128.9 (CH), 128.6 (CH), 128.1 (CH), 128.0 (CH), 126.4 (CH), 125.8 (CH), 124.6 (CH), 124.5 (CH), 72.6 (CH), 71.7 (CH), 69.6 (CH), 20.0 (CH₃), 20.0 (CH₃). IR (ATR): 3030, 2920, 1651, 1602, 1455, 1390, 1345, 858, 753, 698, 664 cm⁻¹.

[α]_D²⁰: –97.7 (c = 1.00, CHCl₃).

MS (ESI) *m/z* (relative intensity): 1087 (10) [2M+Na]⁺, 533 (100) [M+H]⁺.

HR-MS (ESI): *m/z* calcd. for [C₃₄H₃₂N₂O₄+H]⁺ 533.2435 found 533.2436.



(4*S*,5*S*)-1,3-Bis(4-methylbenzoyl)-4,5-diphenylimidazolidine-2-carboxylic acid (CA14):

General procedure **D** was followed using 4-methylbenzoyl chloride (323.0 mg, 2.10 mmol) to afford (4*S*,5*S*)-1,3-dibenzoyl-4,5-diphenylimidazolidine-2-carboxylic acid **CA14** (352.0 mg, 70% yield) as a white solid. M.p.: 168–175 °C.

¹H-NMR (400 MHz, CD₃CO₂D): δ = 7.49 (d, *J* = 7.4 Hz, 2H), 7.45–7.40 (m, 2H), 7.39–7.35 (m, 1H), 7.35–7.21 (m, 7H), 7.21–7.12 (m, 2H), 7.13–6.91 (m, 5H), 5.59 (s, 1H), 5.32 (bs, 1H), 2.30 (s, 3H), 2.27 (s, 3H).

¹³C-NMR (100 MHz, CD₃CO₂D): δ = 173.8 (C_q), 173.0 (C_q), 171.4 (C_q), 142.8 (C_q), 142.4 (C_q), 141.4 (C_q), 139.3 (C_q), 132.9 (C_q), 131.8 (C_q), 130.1 (CH), 130.0 (CH), 129.9 (CH), 129.9

5. Experimental Part

(CH), 129.3 (CH), 129.2 (CH), 128.2 (CH), 128.1 (CH), 127.3 (CH), 126.7 (CH), 73.4 (CH), 72.7 (CH), 70.9 (CH), 21.4 (CH₃), 21.4 (CH₃).

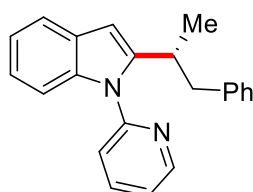
IR (ATR): 3061, 3008, 1635, 1455, 1377, 1388, 1211, 1182, 828, 752, 697 cm⁻¹.

$[\alpha]_{\text{D}}^{20}$: -57.4 (c = 1.00, CHCl₃).

MS (ESI) m/z (relative intensity): 1031 (10) [2M+Na]⁺, 527 (100) [M+Na]⁺, 505 (20) [M+H]⁺.

HR-MS (ESI): m/z calcd. for [C₃₂H₂₈N₂O₄+Na]⁺ 527.1941 found 527.1929.

5.5.2. Characterization Data of the Alkylated Products



(R)-2-(1-Phenylpropan-2-yl)-1-(pyridin-2-yl)-1H-indole (357aa): The general procedure **E** was followed using 1-(pyridin-2-yl)-1H-indole (**315a**) (97.1 mg, 0.50 mmol) and allylbenzene (**223a**) (177 mg, 1.50 mmol). Isolation by column chromatography (*n*-hexane/EtOAc = 30:1) yielded **357aa** (92 mg, 59%, M/AM = 82:18) as a yellow oil.

¹H-NMR (300 MHz, CDCl₃): δ = 8.74 (ddd, J = 4.9, 2.0, 0.8 Hz, 1H), 7.89 (ddd, J = 7.7, 2.0 Hz, 1H), 7.70–7.60 (m, 1H), 7.38 (ddd, J = 7.5, 4.9, 1.1 Hz, 1H), 7.33 (dd, J = 8.4, 1.2 Hz, 1H), 7.28 (d, J = 3.2 Hz, 1H), 7.24–7.12 (m, 5H), 6.99–6.92 (m, 2H), 6.58 (d, J = 0.9 Hz, 1H), 3.68–3.49 (m, 0.82H, M), 3.05 (dd, J = 13.3, 5.3 Hz, 1H), 2.95 (t, J = 7.7 Hz, 0.36H, AM), 2.60 (dd, J = 13.3, 7.5 Hz, 1H), 1.28 (d, J = 6.9 Hz, 3H).

¹³C-NMR (75 MHz, CDCl₃): δ = 151.6 (C_q), 149.7 (CH), 146.5 (C_q), 140.3 (C_q), 138.4 (CH), 137.3 (C_q), 129.1 (CH), 128.3 (C_q), 128.1 (CH), 125.9 (CH), 122.3 (CH), 121.8 (CH), 121.7 (CH), 120.6 (CH), 120.1 (CH), 109.9 (CH), 100.5 (CH), 43.9 (CH₂), 32.9 (CH), 19.4 (CH₃).

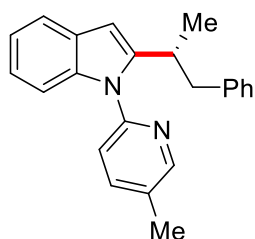
IR (ATR): 3025, 2965, 1595, 1585, 1468, 1452, 741 cm⁻¹.

MS (EI) m/z (relative intensity): 312 (20) [M]⁺, 221 (35), 207 (100).

HR-MS (EI⁺): m/z calcd. For [C₂₂H₂₀N₂]⁺ 312.1626, found 312.1621.

$[\alpha]_{\text{D}}^{20}$: +16.0 (c = 1.00, CHCl₃).

HPLC separation (Chiralpak[®] IB-3, *n*-hexane/EtOAc 90:10, 1.0 mL/min, detection at 280 nm): t_r (major) = 7.9 min, t_r (minor) = 9.5 min, t_r (AM) = 10.2 min, 88:12 e.r.



(R)-1-(5-Methylpyridin-2-yl)-2-(1-phenylpropan-2-yl)-1H-indole (355aa): The general procedure **E** was followed using 1-(5-methylpyridin-2-yl)-1H-indole (**354a**) (104.1 mg, 0.50 mmol) and allylbenzene (**223a**) (177 mg, 1.50 mmol). Isolation by column chromatography (*n*-hexane/EtOAc = 30:1) yielded **355aa** (99.4 mg, 61%, M/AM = 92:8) as a yellow oil.

¹H-NMR (300 MHz, CDCl₃): δ = 8.54 (dd, J = 2.4, 0.8 Hz, 1H), 7.69–7.60 (m, 2H), 7.28–7.20 (m, 3H), 7.20–7.09 (m, 4H), 7.04–6.89 (m, 2H), 6.54 (d, J = 0.8 Hz, 1H), 3.72–3.43 (m, 0.92H, M), 3.07 (dd, J = 13.3, 5.2 Hz, 1H), 2.90 (t, J = 7.5 Hz, 0.16H, AM), 2.61 (dd, J = 13.4, 9.0 Hz, 1H), 2.46 (s, 3H), 1.26 (d, J = 6.8 Hz, 3H).

¹³C-NMR (125 MHz, CDCl₃): δ = 149.7 (CH), 149.0 (C_q), 146.3 (C_q), 140.2 (C_q), 138.7 (CH), 137.3 (C_q), 131.9 (C_q), 128.9 (CH), 128.3 (C_q), 127.9 (CH), 125.8 (CH), 121.4 (CH), 121.1 (CH), 120.3 (CH), 119.9 (CH), 109.9 (CH), 99.9 (CH), 43.7 (CH₂), 32.9 (CH), 19.5 (CH₃), 18.1 (CH₃).

IR (ATR): 2925, 1596, 1482, 1455, 1396, 1346, 1314, 785, 748, 699 cm⁻¹.

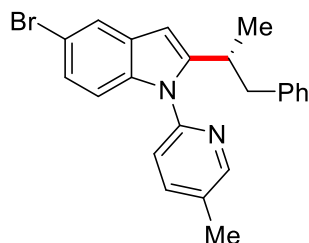
MS (ESI) m/z (relative intensity): 349 (20) [M + Na]⁺, 327 (100) [M + H]⁺.

HR-MS (ESI): m/z calcd. for [C₂₃H₂₂N₂ + H]⁺ 327.1859 found 327.1856.

$[\alpha]_D^{20}$: +9.2 (c = 0.90, CHCl₃).

HPLC separation (Chiralpak[®] IB-3, *n*-hexane/*i*-PrOH 95:5, 0.75 mL/min, detection at 273 nm):

t_r (major) = 8.9 min, t_r (minor) = 10.0 min, t_r (AM) = 10.7 min, 92:8 e.r.



(R)-5-Bromo-1-(5-methylpyridin-2-yl)-2-(1-phenylpropan-2-yl)-1H-indole (355ba): The general procedure **E** was followed using 5-bromo-1-(5-methylpyridin-2-yl)-1H-indole (**354b**) (143 mg, 0.50 mmol) and allylbenzene (**223a**) (177 mg, 1.50 mmol). Isolation by column chromatography (*n*-hexane/EtOAc = 30:1) yielded **355ba** (133.3 mg, 66%, M/AM = 94:6) as a yellow oil.

5. Experimental Part

$^1\text{H-NMR}$ (300 MHz, CDCl_3): δ = 8.50 (dd, J = 2.5, 0.8 Hz, 1H), 7.71 (ddd, J = 7.5, 7.2, 2.5 Hz, 1H), 7.64 (ddd, J = 7.2, 2.5, 0.8 Hz, 1H), 7.21–7.12 (m, 4H), 7.10–7.00 (m, 2H), 6.95–6.88 (m, 2H), 6.44 (d, J = 0.8 Hz, 1H), 3.53–3.36 (m, 0.94H, M), 3.00 (dd, J = 13.3, 5.5 Hz, 1H), 2.83 (t, J = 7.7 Hz, 0.12H, AM), 2.59 (dd, J = 13.3, 8.7 Hz, 1H), 2.44 (s, 3H), 1.23 (d, J = 6.9 Hz, 3H).

$^{13}\text{C-NMR}$ (125 MHz, CDCl_3): δ = 149.8 (CH), 148.5 (C_q), 147.6 (C_q), 139.9 (C_q), 138.9 (CH), 136.0 (C_q), 132.3 (C_q), 130.0 (C_q), 128.9 (CH), 128.0 (CH), 125.9 (CH), 124.1 (CH), 122.3 (CH), 121.0 (CH), 113.4 (C_q), 111.4 (CH), 99.4 (CH), 43.6 (CH_2), 32.9 (CH), 19.6 (CH_3), 18.1 (CH_3).

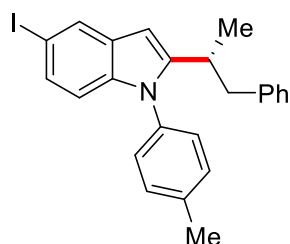
IR (ATR): 2964, 1595, 1575, 1481, 1450, 747 cm^{-1} .

MS (ESI) m/z (relative intensity): 405 (100) [$\text{M} + \text{H}$, ^{79}Br] $^+$, 327 (20), 289 (10).

HR-MS (ESI): m/z calcd. for $[\text{C}_{23}\text{H}_{21}^{79}\text{BrN}_2 + \text{H}]^+$ 405.0957, found 405.0961.

$[\alpha]_{\text{D}}^{20}$: -12.0 (c = 1.00, CHCl_3).

HPLC separation (Chiralpak[®] ID-3, *n*-hexane/*i*-PrOH 99:1, 1.00 mL/min, detection at 273 nm): t_r (major) = 17.3 min, t_r (minor) = 20.2 min, t_r (AM) = 24.0 min, 93:7 e.r.



(R)-5-Iodo-1-(5-methylpyridin-2-yl)-2-(1-phenylpropan-2-yl)-1H-indole (355ca): The general procedure **E** was followed using 5-iodo-1-(5-methylpyridin-2-yl)-1H-indole (**354c**) (167.1 mg, 0.50 mmol) and allylbenzene (**223a**) (177 mg, 1.50 mmol). Isolation by column chromatography (*n*-hexane/EtOAc = 30:1) yielded **355ca** (146.9 mg, 65%, M/AM = 96:4) as a yellow oil.

$^1\text{H-NMR}$ (500 MHz, CDCl_3): δ = 8.49 (dd, J = 2.4, 0.9 Hz, 1H), 7.91 (dd, J = 1.6, 0.9 Hz, 1H), 7.63 (ddd, J = 8.0, 2.4, 0.9 Hz, 1H), 7.34 (dd, J = 8.6, 1.6 Hz, 1H), 7.21–7.11 (m, 3H), 7.06 (d, J = 8.0 Hz, 1H), 6.94 (d, J = 8.6 Hz, 1H), 6.92–6.86 (m, 2H), 6.41 (d, J = 0.8 Hz, 1H), 3.50–3.36 (m, 0.96H, M), 2.98 (dd, J = 13.4, 5.5 Hz, 1H), 2.80 (t, J = 7.9 Hz, 0.08H, AM), 2.58 (dd, J = 13.4, 8.6 Hz, 1H), 2.44 (s, 3H), 1.21 (d, J = 6.8 Hz, 3H).

$^{13}\text{C-NMR}$ (125 MHz, CDCl_3): δ = 149.9 (CH), 148.5 (C_q), 147.3 (C_q), 139.9 (C_q), 139.0 (CH), 136.5 (C_q), 132.4 (C_q), 130.8 (C_q), 129.7 (CH), 129.0 (CH), 128.7 (CH), 128.1 (CH), 125.9 (CH), 121.1 (CH), 112.0 (CH), 99.1 (CH), 83.8 (C_q), 43.6 (CH_2), 32.8 (CH), 19.5 (CH_3), 18.1 (CH_3).

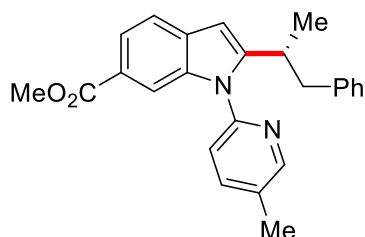
IR (ATR): 3024, 1594, 1495, 1481, 1453, 790, 748 cm^{-1} .

MS (ESI) m/z (relative intensity): 475 (100) $[\text{M} + \text{Na}]^+$, 453 (70) $[\text{M} + \text{H}]^+$, 397 (10).

HR-MS (ESI): m/z calcd. for $[\text{C}_{23}\text{H}_{21}\text{N}_2 + \text{Na}]^+$ 475.0646, found 475.0642.

$[\alpha]_{\text{D}}^{20}$: -23.3 ($c = 1.03$, CHCl_3).

HPLC separation (Chiralpak[®] ID-3, *n*-hexane/*i*-PrOH 98:2, 0.75 mL/min, detection at 273 nm): t_r (major) = 16.6 min, t_r (minor) = 19.4 min, t_r (AM) = 23.3 min, 92:8 e.r.



(R)-Methyl 1-(5-methylpyridin-2-yl)-2-(1-phenylpropan-2-yl)-1H-indole-6-carboxylate

(355da): The general procedure **E** was followed using methyl 1-(5-methylpyridin-2-yl)-1H-indole-5-carboxylate (**354d**) (192.1 mg, 0.50 mmol) and allylbenzene (**223a**) (177 mg, 1.50 mmol). Isolation by column chromatography (*n*-hexane/EtOAc = 10:1) yielded **355da** (140.2 mg, 73%, M/AM = 94:6) as a yellow oil.

¹H-NMR (400 MHz, CDCl_3): δ = 8.51 (dd, $J = 2.4, 0.7$ Hz, 1H), 7.88 (dd, $J = 1.5, 0.7$ Hz, 1H), 7.85–7.77 (m, 1H), 7.67 (ddd, $J = 8.0, 2.4, 0.7$ Hz, 1H), 7.59 (dd, $J = 8.0, 0.7$ Hz, 1H), 7.20–7.06 (m, 4H), 6.97–6.84 (m, 2H), 6.54 (d, $J = 0.7$ Hz, 1H), 3.86 (s, 3H), 3.52–3.35 (m, 0.94H, M), 3.02 (dd, $J = 13.3, 5.5$ Hz, 1H), 2.85 (t, $J = 7.7$ Hz, 0.12H, AM), 2.61 (dd, $J = 13.3, 8.7$ Hz, 1H), 2.45 (s, 3H), 1.24 (d, $J = 6.8$ Hz, 3H).

¹³C-NMR (100 MHz, CDCl_3): δ = 168.1 (C_q), 150.1 (C_q), 150.0 (CH), 148.4 (C_q), 139.9 (C_q), 139.1 (CH), 136.8 (C_q), 132.7 (C_q), 132.1 (C_q), 129.0 (CH), 128.1 (CH), 126.1 (CH), 123.1 (C_q), 121.6 (CH), 121.4 (CH), 119.5 (CH), 112.2 (CH), 100.2 (CH), 51.8 (CH₃), 43.6 (CH₂), 33.0 (CH), 19.5 (CH₃), 18.1 (CH₃).

IR (ATR): 3026, 1710, 1614, 1534, 1444, 1288, 743 cm^{-1} .

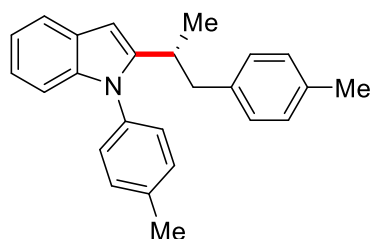
MS (ESI) m/z (relative intensity): 407 (30) $[\text{M} + \text{Na}]^+$, 385 (100) $[\text{M} + \text{H}]^+$, 269 (10).

HR-MS (ESI): m/z calcd. for $[\text{C}_{25}\text{H}_{24}\text{N}_2\text{O}_2 + \text{Na}]^+$ 407.1729, found 407.1730.

$[\alpha]_{\text{D}}^{20}$: $+12.0$ ($c = 0.67$, CHCl_3).

HPLC separation (Chiralpak[®] IA-3, *n*-hexane/*i*-PrOH 99:1, 1.0 mL/min, detection at 273 nm): t_r (major) = 25.1 min, t_r (minor) = 27.5 min, t_r (AM) = 42.9 min, 92:8 e.r.

5. Experimental Part



(R)-1-(5-Methylpyridin-2-yl)-2-[1-(*p*-tolyl)propan-2-yl]-1*H*-indole (355ab): The general procedure **E** was followed using 1-(5-methylpyridin-2-yl)-1*H*-indole (**354a**) (104.1 mg, 0.50 mmol) and 1-allyl-4-methylbenzene (**223b**) (198.3 mg, 1.50 mmol). Isolation by column chromatography (*n*-hexane/EtOAc = 30:1) yielded **355ab** (78.2 mg, 46%, M/AM = 97:3) as a yellow oil.

¹H-NMR (400 MHz, CDCl₃): δ = 8.51 (dd, J = 2.5, 0.8 Hz, 1H), 7.65 (ddd, J = 8.0, 2.5, 0.8 Hz, 1H), 7.61–7.57 (m, 1H), 7.23–7.17 (m, 2H), 7.14–7.09 (m, 2H), 6.99 (d, J = 7.8 Hz, 2H), 6.83 (d, J = 7.8 Hz, 2H), 6.50 (d, J = 0.8 Hz, 1H), 3.58–3.38 (m, 0.97H, M), 2.99 (dd, J = 13.4, 5.1 Hz, 1H), 2.86 (t, J = 7.6 Hz, 0.06H, AM), 2.60 (dd, J = 13.4, 7.8 Hz, 1H), 2.44 (s, 3H), 2.28 (s, 3H), 1.21 (d, J = 6.8 Hz, 3H).

¹³C-NMR (100 MHz, CDCl₃): δ = 149.8 (CH), 149.2 (C_q), 146.6 (C_q), 138.8 (CH), 137.4 (C_q), 137.2 (C_q), 135.2 (C_q), 132.0 (C_q), 128.9 (CH), 128.7 (CH), 128.4 (C_q), 121.4 (CH), 121.2 (CH), 120.3 (CH), 120.0 (CH), 109.9 (CH), 99.9 (CH), 43.2 (CH₂), 32.8 (CH), 20.9 (CH₃), 19.3 (CH₃), 18.1 (CH₃).

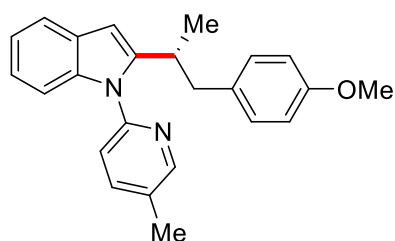
IR (ATR): 3014, 1596, 1482, 1456, 899, 802, 737 cm⁻¹.

MS (ESI) m/z (relative intensity): 363 (20) [M + Na]⁺, 341 (100) [M + H]⁺, 251 (10).

HR-MS (ESI): m/z calcd. for [C₂₄H₂₄N₂ + Na]⁺ 363.1830, found 363.1832.

[α]_D²⁰: +11.5 (c = 1.04, CHCl₃).

HPLC separation (Chiralpak[®] ID-3, *n*-hexane/*i*-PrOH 99:1, 0.50 mL/min, detection at 273 nm): t_r (major) = 31.6 min, t_r (minor) = 34.0 min, t_r (AM) = 38.9 min, 90:10 e.r.



(R)-2-[1-(4-Methoxyphenyl)propan-2-yl]-1-(5-methylpyridin-2-yl)-1*H*-indole (355ac):

The general procedure **E** was followed using 1-(5-methylpyridin-2-yl)-1*H*-indole (**354a**) (104.1 mg, 0.50 mmol), 1-allyl-4-methoxybenzene (**223c**) (222 mg, 1.50 mmol). Isolation by

column chromatography (*n*-hexane/EtOAc = 10:1) yielded **355ac** (108.6 mg, 61%, M/AM = 92:8) as a yellow oil.

¹H-NMR (300 MHz, CDCl₃): δ = 8.51 (dd, *J* = 2.5, 0.8 Hz, 1H), 7.68 (ddd, *J* = 7.9, 7.5, 2.1 Hz, 1H) 7.66–7.55 (m, 1H), 7.23–7.09 (m, 4H), 6.85 (d, *J* = 8.6 Hz, 2H), 6.72 (d, *J* = 8.7 Hz, 2H), 6.49 (d, *J* = 0.8 Hz, 1H), 3.75 (s, 3H), 3.55–3.35 (m, 0.92H, M), 2.96 (dd, *J* = 13.5, 5.2 Hz, 1H), 2.84 (t, *J* = 7.6 Hz, 0.16H, AM), 2.53 (dd, *J* = 13.5, 8.8 Hz, 1H), 2.45 (s, 3H), 1.22 (d, *J* = 6.9 Hz, 3H).

¹³C-NMR (125 MHz, CDCl₃): δ = 157.7 (C_q), 149.7 (CH), 149.1 (C_q), 146.4 (C_q), 138.7 (CH), 137.3 (C_q), 132.3 (C_q), 131.9 (C_q), 129.8 (CH), 128.3 (C_q), 121.4 (CH), 121.1 (CH), 120.2 (CH), 120.0 (CH), 113.4 (CH), 109.9 (CH), 99.9 (CH), 55.2 (CH₃), 42.8 (CH₂), 33.0 (CH), 19.5 (CH₃), 18.1 (CH₃).

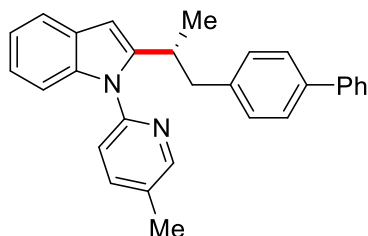
IR (ATR): 2961, 1688, 1511, 1483, 1456, 811, 747 cm⁻¹.

MS (ESI) *m/z* (relative intensity): 379 (20) [M + Na]⁺, 357 (100) [M + H]⁺, 211 (10).

HR-MS (ESI): *m/z* calcd. for [C₂₄H₂₄N₂O + Na]⁺ 357.1959, found 357.1961.

[α]_D²⁰: +5.0 (c = 0.80, CHCl₃).

HPLC separation (Chiralpak[®] ID-3, *n*-hexane/*i*-PrOH 98:2, 0.75 mL/min, detection at 273 nm): *t_r* (major) = 25.6 min, *t_r* (minor) = 29.7 min, *t_r* (AM) = 35.4 min, 91:9 e.r.



(R)-2-[1-[(1,1'-Biphenyl)-4-yl]propan-2-yl]-1-(5-methylpyridin-2-yl)-1H-indole (355ad):

The general procedure **E** was followed using 1-(5-methylpyridin-2-yl)-1H-indole (**354a**) (104.1 mg, 0.50 mmol), 4-allyl-1,1'-biphenyl (**223d**) (291.2 mg, 1.50 mmol). Isolation by column chromatography (*n*-hexane/EtOAc = 20:1) yielded **355ad** (102.6 mg, 51%, M/AM = 92:8) as a yellow oil.

¹H-NMR (500 MHz, CDCl₃): δ = 8.53 (dd, *J* = 2.2, 0.9 Hz, 1H), 7.69–7.60 (m, 2H), 7.59–7.54 (m, 2H), 7.45–7.40 (m, 4H), 7.36–7.30 (m, 1H), 7.24–7.21 (m, 1H), 7.18 (d, *J* = 8.1 Hz, 1H), 7.14 (ddd, *J* = 7.2, 5.0, 1.7 Hz, 2H), 7.03–6.98 (m, 2H), 6.55 (d, *J* = 0.8 Hz, 1H), 3.63–3.50 (m, 0.92H, M), 3.07 (dd, *J* = 13.4, 5.4 Hz, 1H), 2.90 (t, *J* = 7.9 Hz, 0.16H, AM), 2.65 (dd, *J* = 13.4, 8.7 Hz, 1H), 2.45 (s, 3H), 1.29 (d, *J* = 6.8 Hz, 3H).

¹³C-NMR (125 MHz, CDCl₃): δ = 149.8 (CH), 149.1 (C_q), 146.4 (C_q), 140.9 (C_q), 139.4 (C_q), 138.8 (CH), 138.7 (C_q), 137.4 (C_q), 132.0 (C_q), 129.4 (CH), 128.7 (CH), 128.4 (C_q), 127.0

5. Experimental Part

(CH), 126.8 (CH), 126.7 (CH), 121.5 (CH), 121.2 (CH), 120.4 (CH), 120.0 (CH), 109.9 (CH), 100.0 (CH), 43.4 (CH₂), 32.8 (CH), 19.5 (CH₃), 18.1 (CH₃).

IR (ATR): 3025, 1596, 1482, 1470, 1455, 748, 697 cm⁻¹.

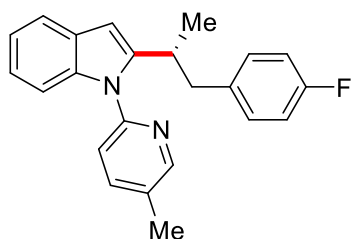
MS (ESI) m/z (relative intensity): 425 (15) [M + Na]⁺, 403 (100) [M + H]⁺, 381 (10).

HR-MS (ESI): m/z calcd. for [C₂₉H₂₆N₂ + Na]⁺ 425.1987, found 425.1988.

[α]_D²⁰: +20.0 (c = 0.80, CHCl₃).

HPLC separation (Chiralpak[®] ID-3, *n*-hexane/*i*-PrOH 98:2, 1.0 mL/min, detection at 273 nm):

t_r (major) = 16.1 min, t_r (minor) = 17.7 min, t_r (AM) = 22.0 min, 89:11 e.r.



(R)-2-[1-(4-Fluorophenyl)propan-2-yl]-1-(5-methylpyridin-2-yl)-1H-indole (355ae): The general procedure **A** was followed using 1-(5-methylpyridin-2-yl)-1H-indole (**354a**) (104.1 mg, 0.50 mmol) and 1-allyl-4-fluorobenzene (**223e**) (204.2 mg, 1.50 mmol). Isolation by column chromatography (*n*-hexane/EtOAc = 20:1) yielded **355ae** (89.5 mg, 52%, M/AM = 94:6) as a yellow oil.

¹H-NMR (400 MHz, CDCl₃): δ = 8.51 (dd, J = 2.4, 0.8 Hz, 1H), 7.65 (ddd, J = 8.0, 7.4, 2.4 Hz, 1H), 7.62–7.58 (m, 1H), 7.22 (dd, J = 2.6, 0.8 Hz, 1H), 7.18 (dd, J = 8.0, 0.7 Hz, 1H), 7.15–7.10 (m, 2H), 6.88 (d, J = 3.8 Hz, 2H), 6.86 (d, J = 3.8 Hz, 2H), 6.49 (d, J = 0.9 Hz, 1H), 3.54–3.44 (m, 0.94H, M), 2.99 (dd, J = 13.5, 5.5 Hz, 1H), 2.89–2.80 (t, J = 7.9 Hz, 0.12H, AM), 2.59 (dd, J = 13.5, 8.5 Hz, 1H), 2.44 (s, 3H), 1.24 (d, J = 6.9 Hz, 3H).

¹³C-NMR (100 MHz, CDCl₃): δ = 161.4 (d, ¹ J_{C-F} = 244.2 Hz, C_q), 149.8 (CH), 149.1 (C_q), 146.1 (C_q), 138.8 (CH), 137.3 (C_q), 135.8 (C_q), 132.0 (C_q), 130.4 (d, ³ J_{C-F} = 8.2 Hz, CH), 128.3 (C_q), 121.5 (CH), 121.1 (CH), 120.4 (CH), 120.0 (CH), 114.7 (d, ² J_{C-F} = 24.2 Hz, CH), 109.9 (CH), 100.1 (CH), 42.8 (CH₂), 32.8 (CH), 19.4 (CH₃), 18.0 (CH₃).

¹⁹F-NMR (375 MHz, CDCl₃): δ = -117.5 (m, 1F).

IR (ATR): 2965, 1597, 1508, 1482, 1456, 1218, 747 cm⁻¹.

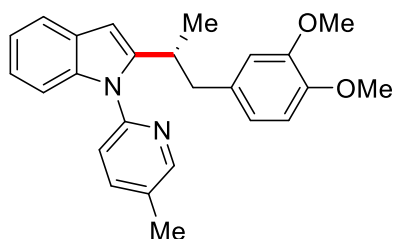
MS (ESI) m/z (relative intensity): 367 (15) [M + Na]⁺, 345 (100) [M + H]⁺, 211 (10).

HR-MS (ESI): m/z calcd. for [C₂₃H₂₁FN₂ + Na]⁺ 367.1578, found 367.1581.

[α]_D²⁰: +11.2 (c = 1.07, CHCl₃).

HPLC separation (Chiralpak[®] IA-3, *n*-hexane/*i*-PrOH 99:1, 1.0 mL/min, detection at 273 nm):

t_r (minor) = 13.3 min, t_r (major) = 14.4 min, t_r (AM) = 18.3 min, 8:92 e.r.



(R)-2-[1-(3,4-Dimethoxyphenyl)propan-2-yl]-1-(5-methylpyridin-2-yl)-1H-indole

(355af): The general procedure **E** was followed using 1-(5-methylpyridin-2-yl)-1H-indole (**354a**) (104.1 mg, 0.50 mmol), 4-allyl-1,2-dimethoxybenzene (**223f**) (267.2 mg, 1.50 mmol). Isolation by column chromatography (*n*-hexane/EtOAc = 5:1) yielded **355af** (121.7 mg, 63%, M/AM = 91:9) as a yellow oil.

¹H-NMR (500 MHz, CDCl₃): δ = 8.48 (dd, *J* = 2.6, 0.8 Hz, 0.91H, M), 8.46 (dd, *J* = 2.6, 0.8 Hz, 0.09H, AM), 7.62 (ddd, *J* = 8.0, 2.6, 0.8 Hz, 1H), 7.60–7.54 (m, 1H), 7.21–7.15 (m, 1H), 7.14–7.06 (m, 3H), 6.65 (d, *J* = 8.0 Hz, 1H), 6.51–6.43 (m, 2H), 6.29 (d, *J* = 1.9 Hz, 1H), 3.81 (s, 3H), 3.62 (s, 3H), 3.53–3.43 (m, 1H), 2.87 (dd, *J* = 13.4, 5.7 Hz, 1H), 2.53 (dd, *J* = 13.4, 6.9 Hz, 1H), 2.42 (s, 3H), 1.27 (d, *J* = 6.9 Hz, 3H).

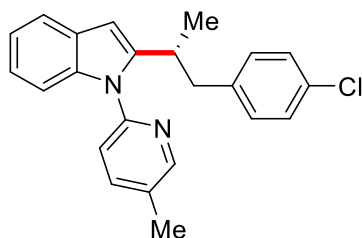
¹³C-NMR (125 MHz, CDCl₃): δ = 149.6 (CH), 149.1 (C_q), 148.3 (C_q), 147.1 (C_q), 146.2 (C_q), 138.7 (CH), 137.3 (C_q), 132.7 (C_q), 131.9 (C_q), 128.3 (C_q), 121.4 (CH), 121.2 (CH), 120.9 (CH), 120.3 (CH), 119.9 (CH), 111.9 (CH), 110.7 (CH), 109.8 (CH), 100.1 (CH), 55.8 (CH₃), 55.4 (CH₃), 43.5 (CH₂), 32.9 (CH), 19.3 (CH₃), 18.0 (CH₃).

IR (ATR): 2933, 1590, 1515, 1442, 1410, 817, 787 cm⁻¹.

MS (ESI) *m/z* (relative intensity): 409 (15) [M + Na]⁺, 387 (100) [M + H]⁺, 211 (10). HR-MS (ESI): *m/z* calcd. for [C₂₅H₂₆N₂O₂ + Na]⁺ 409.1888, found 409.1886.

[α]_D²⁰: +20.0 (*c* = 1.00, CHCl₃).

HPLC separation (Chiralpak[®] IA-3, *n*-hexane/*i*-PrOH 90:10, 1.00 mL/min, detection at 273 nm): *t_r* (major) = 10.4 min, *t_r* (minor) = 11.4 min, *t_r* (AM) = 14.4 min, 92:8 e.r.



(R)-2-[1-(4-Chlorophenyl)propan-2-yl]-1-(5-methylpyridin-2-yl)-1H-indole (355ag): The general procedure **E** was followed using 1-(5-methylpyridin-2-yl)-1H-indole (**354a**) (104.1 mg, 0.50 mmol), 1-allyl-4-chlorobenzene (**223g**) (228 mg, 1.50 mmol). Isolation by

5. Experimental Part

column chromatography (*n*-hexane/EtOAc = 20:1) yielded **355ag** (73.8 mg, 41%, M/AM = 93:7) as a yellow oil.

¹H-NMR (400 MHz, CDCl₃): δ = 8.49 (dd, *J* = 2.4, 0.8 Hz, 1H), 7.65 (ddd, *J* = 8.0, 2.4, 0.7 Hz, 1H), 7.60–7.57 (m, 1H), 7.22–7.18 (m, 1H), 7.18–7.14 (m, 1H), 7.14–7.09 (m, 4H), 6.83 (d, *J* = 8.1 Hz, 2H), 6.48 (d, *J* = 0.8 Hz, 1H), 3.57–3.41 (m, 0.93H, M), 2.96 (dd, *J* = 13.4, 5.7 Hz, 1H), 2.80 (t, *J* = 8.4 Hz, 0.14H, AM), 2.58 (dd, *J* = 13.4, 8.3 Hz, 1H), 2.44 (s, 3H), 1.23 (d, *J* = 6.9 Hz, 3H).

¹³C-NMR (100 MHz, CDCl₃): δ = 149.8 (CH), 149.1 (C_q), 145.9 (C_q), 138.8 (CH), 138.6 (C_q), 137.3 (C_q), 132.0 (C_q), 131.6 (C_q), 130.3 (CH), 128.3 (C_q), 128.1 (CH), 121.6 (CH), 121.1 (CH), 120.4 (CH), 120.0 (CH), 110.0 (CH), 100.2 (CH), 43.1 (CH₂), 32.7 (CH), 19.5 (CH₃), 18.1 (CH₃).

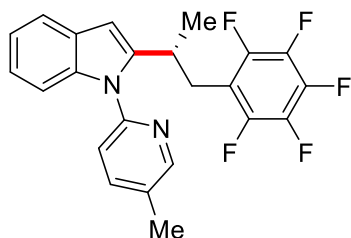
IR (ATR): 2965, 1687, 1483, 1456, 1216, 839, 738 cm⁻¹.

MS (ESI) *m/z* (relative intensity): 383 (15) [M + Na, ³⁵Cl]⁺, 361 (100) [M + H, ³⁵Cl]⁺, 211 (10), 173 (5).

HR-MS (ESI): *m/z* calcd. for [C₂₃H₂₁³⁵ClN₂ + Na]⁺ 383.1284, found 383.1285.

[α]_D²⁰: +8.0 (c = 1.0, CHCl₃).

HPLC separation (Chiralpak[®] IA-3, *n*-hexane/*i*-PrOH 95:5, 0.75 mL/min, detection at 273 nm): *t_r* (minor) = 11.6 min, *t_r* (major) = 12.3 min, *t_r* (AM) = 14.4 min, 12:88 e.r.



(R)-1-(5-methylpyridin-2-yl)-2-[1-(perfluorophenyl)propan-2-yl]-1H-indole (355ah): The general procedure **E** was followed using 1-(5-methylpyridin-2-yl)-1H-indole (**354a**) (104.1 mg, 0.50 mmol), 1-allyl-2,3,4,5,6-pentafluorobenzene (**223h**) (312.2 mg, 1.50 mmol). Isolation by column chromatography (*n*-hexane/EtOAc = 20:1) yielded **355ah** (114.4 mg, 55%, M/AM = 96:4) as a yellow oil.

¹H-NMR (400 MHz, CDCl₃): δ = 8.47 (dd, *J* = 2.4, 0.8 Hz, 1H), 7.68 (ddd, *J* = 8.0, 7.5, 2.4 Hz, 1H), 7.62–7.55 (m, 1H), 7.27–7.22 (m, 1H), 7.22–7.17 (m, 1H), 7.14–7.07 (m, 2H), 6.54 (d, *J* = 0.8 Hz, 1H), 3.68–3.50 (m, 0.96H, M), 3.03 (dd, *J* = 13.6, 6.1 Hz, 1H), 2.88 (t, *J* = 7.9 Hz, 0.08H, AM), 2.78 (dd, *J* = 13.6, 8.8 Hz, 1H), 2.45 (s, 3H), 1.28 (d, *J* = 7.0 Hz, 3H).

¹³C-NMR (100 MHz, CDCl₃): δ = 150.0 (CH), 148.8 (C_q), 145.2 (dm, ¹*J*_{C-F} = 243.2 Hz, C_q), 144.8 (C_q), 139.9 (dm, ¹*J*_{C-F} = 253.2 Hz, C_q), 138.8 (CH), 137.4 (C_q), 137.2 (dm, ¹*J*_{C-F} = 251.2

Hz, C_q), 132.2 (C_q), 128.2 (C_q), 121.9 (CH), 120.8 (CH), 120.5 (CH), 120.2 (CH), 113.2 (t, ²J_{C-F} = 24.2, C_q), 110.0 (CH), 100.2 (CH), 30.6 (CH), 30.1 (CH₂), 19.5 (CH₃), 18.0 (CH₃).

¹⁹F-NMR (375 MHz, CDCl₃): δ = -142.7 (m, 2F), -157.4 (m, 1F), -163.0 (m, 2F).

IR (ATR): 2974, 1596, 1519, 1502, 1146, 971, 789 cm⁻¹.

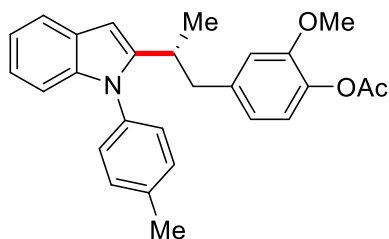
MS (ESI) *m/z* (relative intensity): 439 (15) [M + Na]⁺, 417 (100) [M + H]⁺, 211 (10).

HR-MS (ESI): *m/z* calcd. for [C₂₃H₁₇F₅N₂ + H]⁺ 417.1380, found 417.1385.

[α]_D²⁰: +4.0 (c = 1.00, CHCl₃).

HPLC separation (Chiralpak[®] IA-3, *n*-hexane/*i*-PrOH 95:5, 1.0 mL/min, detection at 273 nm):

t_r (major) = 6.5 min, *t_r* (minor) = 7.9 min, *t_r* (AM) = 17.6 min, 83:17 e.r.



(R)-2-Methoxy-5-(2-(1-(5-methylpyridin-2-yl)-1H-indol-2-yl)propyl)phenyl acetate

(355aj): A modified general procedure **E** was followed using 5-bromo-1-(5-methylpyridin-2-yl)-1H-indole (**354a**) (104.1 mg, 0.50 mmol), 5-allyl-2-methoxyphenyl acetate (**223j**) (309.2 mg, 1.50 mmol) at 60 °C. Isolation by column chromatography (*n*-hexane/EtOAc = 5:1) yielded **355aj** (113.9 mg, 55%, M/AM = 75:25) as a yellow oil.

Major isomer (M): ¹H-NMR (500 MHz, CDCl₃): δ = 8.46 (dd, *J* = 2.4, 0.8 Hz, 1H), 7.64–7.60 (m, 1H), 7.60–7.55 (m, 1H), 7.15 (dd, *J* = 7.2, 0.8 Hz, 1H), 7.13–7.10 (m, 1H), 7.09–7.08 (m, 1H), 7.03 (d, *J* = 8.0 Hz, 1H), 6.77 (d, *J* = 8.0 Hz, 1H), 6.52 (d, *J* = 0.8 Hz, 1H), 6.45–6.41 (m, 1H), 6.34 (d, *J* = 1.9 Hz, 1H), 3.51 (s, 3H), 3.49–3.41 (m, 1H), 2.91–2.80 (m, 1H), 2.72–2.54 (m, 1H), 2.40 (s, 3H), 2.27 (s, 3H), 1.31 (d, *J* = 6.8 Hz, 3H).

¹³C-NMR (125 MHz, CDCl₃): δ = 169.2 (C_q), 150.4 (CH), 149.6 (CH), 148.9 (C_q), 146.0 (C_q), 140.9 (C_q), 139.1 (C_q), 138.9 (CH), 137.8 (C_q), 137.2 (C_q), 131.9 (C_q), 128.3 (C_q), 122.0 (CH), 121.5 (CH), 121.1 (CH), 120.3 (CH), 119.9 (CH), 112.9 (CH), 109.9 (CH), 99.9 (CH), 55.4 (CH₃), 44.2 (CH₂), 32.9 (CH), 20.6 (CH₃), 19.7 (CH₃), 18.0 (CH₃).

Minor isomer (AM): (one carbon signal less due to overlapping with major isomer) ¹H-NMR (500 MHz, CDCl₃): δ = 8.43 (dd, *J* = 2.4, 0.8 Hz, 1H), 7.65 (dd, *J* = 2.4, 0.8 Hz, 1H), 7.56–7.55 (m, 1H), 7.28–7.25 (m, 1H), 7.25–7.24 (m, 1H), 7.08–7.06 (m, 2H), 6.88 (d, *J* = 8.0 Hz, 1H), 6.68 (d, *J* = 1.9 Hz, 1H), 6.65 (dd, *J* = 8.0, 1.9 Hz, 1H), 6.46 (d, *J* = 1.9 Hz, 1H), 3.76 (s, 3H), 2.93–2.82 (m, 2H), 2.68–2.55 (m, 2H), 2.41 (s, 3H), 2.29 (s, 3H), 1.86 (ddd, *J* = 15.3, 8.3, 7.0 Hz, 2H).

5. Experimental Part

^{13}C -NMR (125 MHz, CDCl_3): δ = 169.2 (C_q), 150.6 (C_q), 149.8 (CH), 148.9 (C_q), 146.0 (C_q), 141.0 (C_q), 138.8 (CH), 137.6 (C_q), 137.3 (C_q), 131.8 (C_q), 128.4 (C_q), 122.3 (CH), 120.5 (CH), 120.4 (CH), 120.4 (CH), 119.8 (CH), 112.5 (CH), 110.0 (CH), 101.9 (CH), 99.9 (CH), 55.7 (CH_3), 35.2 (CH_2), 30.1 (CH_2), 26.8 (CH_2), 17.8 (CH_3).

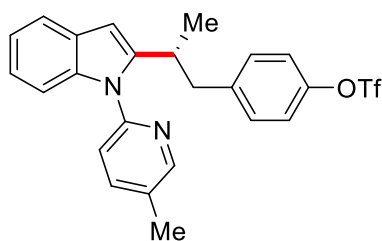
IR (ATR): 3011, 1762, 1598, 1482, 1456, 1197, 1034, 749 cm^{-1} .

MS (ESI) m/z (relative intensity): 437 (10) $[\text{M} + \text{Na}]^+$, 415 (100) $[\text{M} + \text{H}]^+$, 275 (10).

HR-MS (ESI): m/z calcd. for $[\text{C}_{26}\text{H}_{26}\text{N}_2\text{O}_3 + \text{H}]^+$ 415.2010, found 415.2016.

$[\alpha]_{\text{D}}^{20}$: +3.9 ($c = 1.02$, CHCl_3).

HPLC separation (Chiralpak[®] ID-3, *n*-hexane/*i*-PrOH 90:10, 1.0 mL/min, detection at 273 nm): t_r (minor) = 15.5 min, t_r (major) = 16.5 min, t_r (AM) = 32.8 min, 12:88 e.r.



(*R*)-4-[2-{1-(5-Methylpyridin-2-yl)-1*H*-indol-2-yl}propyl]phenyl

trifluoromethanesulfonate (355ak): The general procedure **E** was followed using 1-(5-methylpyridin-2-yl)-1*H*-indole (**354a**) (104.1 mg, 0.50 mmol), ethyl 4-allylphenyl trifluoromethanesulfonate (**223k**) (399.2 mg, 1.50 mmol). Isolation by column chromatography (*n*-hexane/EtOAc = 30:1) yielded **355ak** (99.5 mg, 42%, M/AM = 96:4) as a yellow oil.

^1H -NMR (400 MHz, CDCl_3): δ = 8.48 (dd, $J = 2.4, 0.8$ Hz, 1H), 7.65 (ddd, $J = 8.0, 2.4, 0.8$ Hz, 1H), 7.60–7.57 (m, 1H), 7.21–7.16 (m, 1H), 7.14–7.09 (m, 3H), 7.05 (d, $J = 8.7$ Hz, 2H), 6.97 (d, $J = 8.7$ Hz, 2H), 6.48 (d, $J = 0.8$ Hz, 1H), 3.59–3.40 (m, 0.96H, M), 3.02 (dd, $J = 13.4, 5.9$ Hz, 1H), 2.85 (t, $J = 7.5$ Hz, 0.08H, AM), 2.65 (dd, $J = 13.4, 8.2$ Hz, 1H), 2.44 (s, 3H), 1.25 (d, $J = 7.0$ Hz, 3H).

^{13}C -NMR (100 MHz, CDCl_3): δ = 149.8 (CH), 148.9 (C_q), 147.8 (C_q), 145.6 (C_q), 140.9 (C_q), 138.9 (CH), 137.3 (C_q), 132.1 (C_q), 130.7 (CH), 128.3 (C_q), 121.7 (CH), 121.0 (CH), 120.8 (CH), 120.5 (CH), 120.1 (CH), 119.2 (q, $^1J_{\text{C-F}} = 319.1$ Hz, C_q), 109.9 (CH), 100.3 (CH), 43.2 (CH_2), 32.7 (CH), 19.6 (CH_3), 18.0 (CH_3).

^{19}F -NMR (375 MHz, CDCl_3): δ = -73.0 (m, 1F).

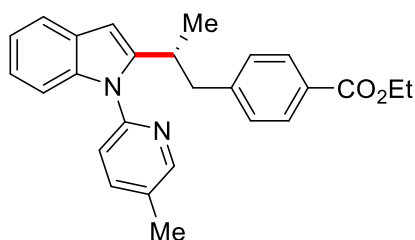
IR (ATR): 2967, 1596, 1483, 1456, 1208, 888, 710 cm^{-1} .

MS (ESI) m/z (relative intensity): 497 (10) $[\text{M} + \text{Na}]^+$, 475 (100) $[\text{M} + \text{H}]^+$.

HR-MS (ESI): m/z calcd. for $[\text{C}_{24}\text{H}_{21}\text{F}_3\text{N}_2\text{O}_3\text{S} + \text{Na}]^+$ 497.1119, found 497.1117.

$[\alpha]_{\text{D}}^{20}$: +4.4 ($c = 0.90$, CHCl_3).

HPLC separation (Chiralpak[®] ID-3, *n*-hexane/*i*-PrOH 99:1, 0.75 mL/min, detection at 273 nm): t_r (minor) = 21.0 min, t_r (major) = 23.2 min, t_r (AM) = 32.6 min, 13:87 e.r.



(R)-Ethyl 4-[2-{1-(5-methylpyridin-2-yl)-1H-indol-2-yl}propyl]benzoate (355al): The general procedure **E** was followed using 1-(5-methylpyridin-2-yl)-1H-indole (**354a**) (104.1 mg, 0.50 mmol), ethyl 4-allylbenzoate (**2231**) (286.5 mg, 1.50 mmol). Isolation by column chromatography (*n*-hexane/EtOAc = 10:1) yielded **355al** (111.7 mg, 56%, M/AM = 86:14) as a yellow oil.

¹H-NMR (300 MHz, CDCl_3): $\delta = 8.54$ (dd, $J = 2.4, 0.8$ Hz, 1H), 7.93–7.84 (m, 2H), 7.74–7.55 (m, 2H), 7.27–7.12 (m, 4H), 7.08–6.98 (m, 2H), 6.53 (d, $J = 0.8$ Hz, 1H), 4.39 (q, $J = 7.1$ Hz, 2H), 3.66–3.49 (m, 0.86H, M), 3.10 (dd, $J = 13.4, 5.5$ Hz, 1H), 2.89 (t, $J = 7.6$ Hz, 0.28H, AM), 2.70 (dd, $J = 13.4, 6.5$ Hz, 1H), 2.48 (s, 3H), 1.41 (t, $J = 7.1$ Hz, 3H), 1.27 (d, $J = 6.8$ Hz, 3H).

¹³C-NMR (75 MHz, CDCl_3): $\delta = 166.7$ (C_q), 149.9 (CH), 149.1 (C_q), 145.9 (C_q), 145.7 (C_q), 138.9 (CH), 137.4 (C_q), 132.2 (C_q), 129.4 (CH), 129.1 (CH), 128.4 (C_q), 128.3 (C_q), 121.7 (CH), 121.1 (CH), 120.5 (CH), 120.1 (CH), 110.0 (CH), 100.3 (CH), 60.8 (CH_2), 43.8 (CH_2), 32.7 (CH), 19.5 (CH_3), 18.1 (CH_3), 14.4 (CH_3).

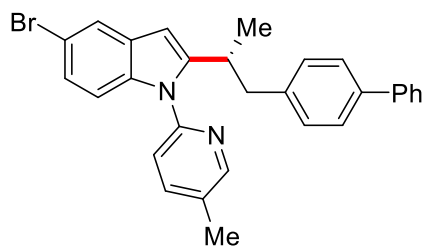
IR (ATR): 2976, 1722, 1609, 1483, 1275, 844 cm^{-1} .

MS (ESI) m/z (relative intensity): 421 (30) $[\text{M} + \text{Na}]^+$, 399 (100) $[\text{M} + \text{H}]^+$, 381 (5), 211 (10).

HR-MS (ESI): m/z calcd. for $[\text{C}_{26}\text{H}_{26}\text{N}_2\text{O}_2 + \text{Na}]^+$ 421.1887, found 421.1886.

$[\alpha]_{\text{D}}^{20}$: +3.6 ($c = 1.10$, CHCl_3).

HPLC separation (Chiralpak[®] IB-3, *n*-hexane/EtOAc 90:10, 1.0 mL/min, detection at 280 nm): t_r (major) = 9.9 min, t_r (minor) = 12.1 min, t_r (AM) = 17.3 min, 86:14 e.r.



(R)-2-(1-([1,1'-Biphenyl]-4-yl)propan-2-yl)-5-bromo-1-(5-methylpyridin-2-yl)-1H-indole (355bm): The general procedure **E** was followed using 5-bromo-1-(5-methylpyridin-2-yl)-1H-

5. Experimental Part

indole (**354b**) (143 mg, 0.50 mmol), 4-allyl-1,1'-biphenyl (**223m**) (291.2 mg, 1.50 mmol). Isolation by column chromatography (*n*-hexane/EtOAc = 20:1) yielded **355bm** (127.2 mg, 53%, M/AM = 92:8) as a yellow oil.

¹H-NMR (300 MHz, CDCl₃): δ = 8.54 (dd, *J* = 2.4, 0.9 Hz, 1H), 7.74 (d, *J* = 1.9 Hz, 1H), 7.66 (ddd, *J* = 8.31, 2.4, 0.9 Hz, 1H), 7.60–7.54 (m, 2H), 7.50–7.45 (m, 4H), 7.40–7.35 (m, 1H), 7.21 (dd, *J* = 8.7, 1.9 Hz, 1H), 7.15–7.04 (m, 2H), 7.03–6.95 (m, 2H), 6.49 (s, 1H), 3.61–3.44 (m, 0.92H, M), 3.04 (dd, *J* = 13.3, 5.7 Hz, 1H), 2.89 (t, *J* = 7.9 Hz, 0.16H, AM) 2.68 (dd, *J* = 13.3, 8.4 Hz, 1H), 2.48 (s, 3H), 1.30 (d, *J* = 6.9 Hz, 3H).

¹³C-NMR (75 MHz, CDCl₃): δ = 145.0 (CH), 148.7 (C_q), 147.7 (C_q), 141.0 (C_q), 139.2 (C_q), 139.0 (CH), 138.9 (C_q), 136.1 (C_q), 132.5 (C_q), 130.1 (CH), 129.5 (CH), 128.8 (CH), 127.1 (C_q), 126.9 (CH), 126.8 (CH), 124.3 (CH), 122.5 (CH), 121.2 (CH), 113.6 (C_q), 111.5 (CH), 99.6 (CH), 43.4 (CH₂), 32.9 (CH), 19.7 (CH₃), 18.1 (CH₃).

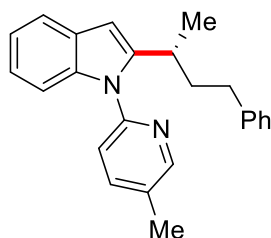
IR (ATR): 3026, 1595, 1482, 1207, 1034, 791, 697 cm⁻¹.

MS (ESI) *m/z* (relative intensity): 503 (10) [M + Na, ⁷⁹Br]⁺, 481 (100) [M + H, ⁷⁹Br]⁺, 403 (10).

HR-MS (ESI): *m/z* calcd. for [C₂₉H₂₅⁷⁹BrN₂ + Na]⁺ 503.1098, found 503.1093.

[α]_D²⁰: -8.9 (c = 0.90, CHCl₃).

HPLC separation (Chiralpak[®] ID-3, *n*-hexane/*i*-PrOH 98:2, 1.0 mL/min, detection at 273 nm): *t_r* (major) = 17.1 min, *t_r* (minor) = 19.5 min, *t_r* (AM) = 25.8 min, 89:11 e.r.



(R)-1-(5-Methylpyridin-2-yl)-2-(4-phenylbutan-2-yl)-1H-indole (355an): The general procedure **E** was followed using 1-(5-methylpyridin-2-yl)-1H-indole (**354a**) (104.1 mg, 0.50 mmol), 4-Phenyl-1-butene (**223n**) (198 mg, 1.50 mmol). Isolation by column chromatography (*n*-hexane/EtOAc = 30:1) yielded **355an** (57.8 mg, 34%, M/AM = 80:20) as a yellow oil.

¹H-NMR (300 MHz, CDCl₃): δ = 8.45 (d, *J* = 2.4 Hz, 1H), 7.71–7.64 (m, 1H), 7.64–7.59 (m, 1H), 7.28 (d, *J* = 3.3 Hz, 1H), 7.27–7.23 (m, 2H), 7.23–7.20 (m, 1H), 7.20–7.16 (m, 1H), 7.16–7.11 (m, 2H), 7.09–7.04 (m, 2H), 6.52 (s, 1H), 3.31–3.11 (m, 0.90H, M), 2.87 (t, *J* = 4.0 Hz, 0.10H, AM), 2.59 (t, *J* = 7.6 Hz, 2H), 2.47 (s, 3H), 2.10–1.94 (m, 1H), 1.83–1.70 (m, 1H), 1.33 (d, *J* = 6.9 Hz, 3H).

^{13}C -NMR (100 MHz, CDCl_3): $\delta = 150.0$ (CH), 149.1 (C_q), 146.9 (C_q), 142.3 (C_q), 138.8 (CH), 137.5 (C_q), 132.0 (C_q), 128.5 (C_q), 128.4 (CH), 128.2 (CH), 125.5 (CH), 121.4 (CH), 121.2 (CH), 120.4 (CH), 120.0 (CH), 110.1 (CH), 99.7 (CH), 38.8 (CH), 33.4 (CH_2), 30.3 (CH_2), 20.6 (CH_3), 18.1 (CH_3).

IR (ATR): 2955, 1593, 1481, 1435, 1399, 1366, 1324, 765, 758, 670 cm^{-1} .

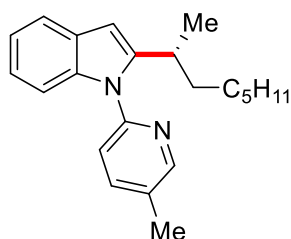
MS (ESI) m/z (relative intensity): 363 (80) $[\text{M} + \text{H}]^+$, 341(15) $[\text{M} + \text{H}]^+$.

HR-MS (ESI): m/z calcd. for $[\text{C}_{24}\text{H}_{24}\text{N}_2 + \text{H}]^+$ 341.2012 found 341.2011.

$[\alpha]_{\text{D}}^{20}$: +16.0 ($c = 1.25$, CHCl_3)

HPLC separation (Chiralpak® IF-3, *n*-hexane/EtOAc 95:5, 1.00 mL/min, detection at 273 nm):

t_r (major) = 8.1 min, t_r (minor) = 7.5 min, t_r (AM) = 7.8 min, 68:32 e.r.



(R)-1-(5-Methylpyridin-2-yl)-2-(octan-2-yl)-1H-indole (355ao): The general procedure **E** was followed using 1-(5-methylpyridin-2-yl)-1H-indole (**354a**) (104.1 mg, 0.50 mmol), 1-octene (**223o**) (168 mg, 1.50 mmol). Isolation by column chromatography (*n*-hexane/EtOAc = 30:1) yielded **355ao** (59.2 mg, 37%, M/AM = 90:10) as a yellow oil.

^1H -NMR (300 MHz, CDCl_3): $\delta = 8.52$ (d, $J = 2.5$ Hz, 1H), 7.72 (dd, $J = 8.1, 2.5$, 1H), 7.64–7.56 (m, 1H), 7.33 (d, $J = 8.1$ Hz, 1H), 7.26–7.18 (m, 1H), 7.18–7.04 (m, 2H), 6.46 (s, 1H), 3.23–3.08 (m, 0.90H, M), 2.82 (t, $J = 7.6$ Hz, 0.10H, AM) 2.47 (s, 3H), 1.73–1.52 (m, 1H), 1.50–1.06 (m, 12H), 0.87 (t, $J = 6.9$ Hz, 3H).

^{13}C NMR (125 MHz, CDCl_3) $\delta = 149.9$ (CH), 149.2 (C_q), 147.5 (C_q), 138.7 (CH), 137.4 (C_q), 131.9 (C_q), 128.4 (C_q), 121.3 (CH), 121.2 (CH), 120.2 (CH), 119.8 (CH), 109.9 (CH), 99.3 (CH), 37.0 (CH_2), 31.6 (CH_2), 30.7 (CH), 29.2 (CH_2), 27.0 (CH_2), 22.6 (CH_2), 20.5 (CH_3), 18.0 (CH_3), 14.0 (CH_3).

IR (ATR): 2935, 1591, 1472, 1465, 1366, 1321, 1310, 787, 741, 689 cm^{-1} .

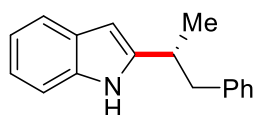
MS (ESI) m/z (relative intensity): 321 (100) $[\text{M} + \text{H}]^+$, 342 (15) $[\text{M} + \text{Na}]^+$.

HR-MS (ESI): m/z calcd. for $[\text{C}_{22}\text{H}_{28}\text{N}_2 + \text{H}]^+$ 321.2325 found 321.2328.

$[\alpha]_{\text{D}}^{20}$: +25.0 ($c = 0.8$, CHCl_3).

HPLC separation (Chiralpak® IF-3, *n*-hexane/EtOAc 90:10, 1.00 mL/min, detection at 280 nm): t_r (major) = 6.3 min, t_r (minor) = 5.5 min, t_r (AM) = 7.8 min, 72:28 e.r.

5.5.3. Removable of the Directing Group



(R)-2-(1-Phenylpropan-2-yl)-1H-indole (357aa): The general procedure **G** was followed using (*R*)-1-(5-Methylpyridin-2-yl)-2-(1-phenylpropan-2-yl)-1*H*-indole (**355aa**) (65.2 mg, 0.20 mmol, e.r. 92:8). Isolation by column chromatography (*n*-hexane/EtOAc = 10:1) yielded **357aa** (40.4 mg, 86%, M/AM = 92:8) as a brown solid. M. P.: 75–78 °C.

¹H-NMR (600 MHz, CDCl₃): δ = 7.65 (s, 1H), 7.60 (dd, *J* = 7.7, 1.2 Hz, 1H), 7.34–7.29 (m, 2H), 7.27 (dd, *J* = 7.8, 1.7 Hz, 2H), 7.19–7.15 (m, 3H), 7.16–7.10 (m, 1H), 6.25 (d, *J* = 0.8 Hz, 0.92H, M), 6.23 (d, *J* = 0.8 Hz, 0.08H, M), 3.21 (m, 1H), 3.06 (dd, *J* = 13.3, 6.6 Hz, 1H), 2.90 (dd, *J* = 13.3, 7.6 Hz, 1H), 1.38 (d, *J* = 6.9 Hz, 3H).

¹³C-NMR (125 MHz, CDCl₃): δ = 143.9 (C_q), 139.9 (C_q), 135.5 (C_q), 128.9 (CH), 128.4 (C_q), 128.2 (CH), 126.1 (CH), 120.9 (CH), 119.9 (CH), 119.5 (CH), 110.3 (CH), 98.2 (CH), 43.8 (CH₂), 35.2 (CH), 19.9 (CH₃).

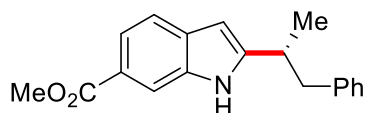
IR (ATR): 3399, 3025, 1676, 1454, 1301, 1029, 748 cm⁻¹.

MS (ESI) *m/z* (relative intensity): 258 (30) [M + Na]⁺, 236 (100) [M + H]⁺, 209 (5), 201 (10).

HR-MS (ESI): *m/z* calcd. for [C₁₇H₁₇N + H]⁺ 236.1430, found 236.1434.

[α]_D²⁰: –30.0 (*c* = 0.80, CHCl₃).

HPLC separation (Chiralpak[®] IA-3, *n*-hexane/*i*-PrOH 99:1, 0.75 mL/min, detection at 273 nm): *t_r* (major) = 23.9 min, *t_r* (minor) = 26.2 min, *t_r* (AM) = 36.9 min, 92:8 e.r.



(R)-Methyl 2-(1-phenylpropan-2-yl)-1H-indole-6-carboxylate (357da): The general procedure **G** was followed using (*R*)-methyl 1-(5-methylpyridin-2-yl)-2-(1-phenylpropan-2-yl)-1*H*-indole-6-carboxylate (**355da**) (76.8 mg, 0.20 mmol, e.r. 92:8). Isolation by column chromatography (*n*-hexane/EtOAc = 10:1) yielded **357da** (46.5 mg, 79%, M/AM = 94:6) as a yellow solid. M. P.: 145–149 °C.

¹H-NMR (500 MHz, CDCl₃): δ = 8.24 (s, 1H), 8.04 (dd, *J* = 1.6, 0.8 Hz, 1H), 7.77 (dd, *J* = 8.4, 1.6 Hz, 1H), 7.53 (d, *J* = 8.4 Hz, 1H), 7.30–7.16 (m, 3H), 7.12–7.02 (m, 2H), 6.31 (dd, *J* = 2.1, 1.0 Hz, 1H), 3.91 (s, 3H), 3.23 (m, 0.94H, M), 3.03 (dd, *J* = 13.4, 7.1 Hz, 1H), 2.89 (dd, *J* = 13.4, 7.5 Hz, 1H), 2.79 (t, *J* = 7.6 Hz, 0.12H, AM), 1.37 (d, *J* = 6.9 Hz, 3H).

^{13}C -NMR (125 MHz, CDCl_3): δ = 168.5 (C_q), 148.1 (C_q), 139.8 (C_q), 134.9 (C_q), 132.4 (C_q), 129.1 (CH), 128.4 (CH), 126.4 (CH), 122.5 (C_q), 120.8 (CH), 119.4 (CH), 112.9 (CH), 98.9 (CH), 52.0 (CH_3), 43.7 (CH_2), 35.4 (CH), 19.7 (CH_3).

IR (ATR): 3342, 3025, 1687, 1619, 1546, 1314, 743 cm^{-1} .

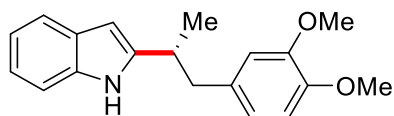
MS (ESI) m/z (relative intensity): 316 (30) $[\text{M} + \text{Na}]^+$, 294 (100) $[\text{M} + \text{H}]^+$, 117 (5).

HR-MS (ESI): m/z calcd. for $[\text{C}_{19}\text{H}_{19}\text{NO}_2 + \text{H}]^+$ 294.1484, found 294.1489.

$[\alpha]_{\text{D}}^{20}$: -72.9 ($c = 0.93$, CHCl_3).

HPLC separation (Chiralpak[®] IF-3, *n*-hexane/*i*-PrOH 95:5, 1.0 mL/min, detection at 273 nm):

t_r (major) = 14.1 min, t_r (minor) = 16.0 min, t_r (AM) = 23.9 min, 92:8 e.r.



(*R*)-2-(1-(3,4-Dimethoxyphenyl)propan-2-yl)-1*H*-indole (357af): The general procedure **G** was followed using (*R*)-2-(1-(3,4-dimethoxyphenyl)propan-2-yl)-1-(5-methylpyridin-2-yl)-1*H*-indole (**355af**) (77.2 mg, 0.20 mmol). Isolation by column chromatography (*n*-hexane/EtOAc = 5:1) yielded **357af** (48.4 mg, 82%, M/AM = 92:8) as a yellow oil.

^1H -NMR (500 MHz, CDCl_3): δ = 7.73 (s, 1H), 7.57–7.47 (m, 1H), 7.27–7.18 (m, 1H), 7.08 (dd, $J = 8.1, 1.4$ Hz, 2H), 6.76 (d, $J = 8.1$ Hz, 1H), 6.66 (dd, $J = 8.1, 2.0$ Hz, 1H), 6.49 (d, $J = 2.0$ Hz, 1H), 6.26 (dd, $J = 2.1, 0.9$ Hz, 1H), 3.85 (s, 3H), 3.65 (s, 3H), 3.15 (m, 0.91H, M), 2.93 (dd, $J = 13.5, 7.2$ Hz, 1H), 2.83 (dd, $J = 13.5, 7.0$ Hz, 1H), 2.76 (t, $J = 7.5$ Hz, 0.18H, AM), 1.36 (d, $J = 6.9$ Hz, 3H). ^{13}C -NMR (125 MHz, CDCl_3): δ = 148.6 (C_q), 147.4 (C_q), 144.0 (C_q), 135.5 (C_q), 132.5 (C_q), 128.4 (C_q), 121.0 (CH), 121.0 (CH), 119.8 (CH), 119.5 (CH), 112.1 (CH), 110.9 (CH), 110.3 (CH), 98.3 (CH), 55.8 (CH_3), 55.6 (CH_3), 43.5 (CH_2), 35.3 (CH), 19.7 (CH_3).

IR (ATR): 3368, 3004, 1589, 1305, 1140, 1026, 784 cm^{-1} .

MS (ESI) m/z (relative intensity): 318 (100) $[\text{M} + \text{Na}]^+$, 295 (30) $[\text{M} + \text{H}]^+$, 209 (5).

HR-MS (ESI): m/z calcd. for $[\text{C}_{19}\text{H}_{21}\text{NO}_2 + \text{H}]^+$ 296.1641, found 296.1645.

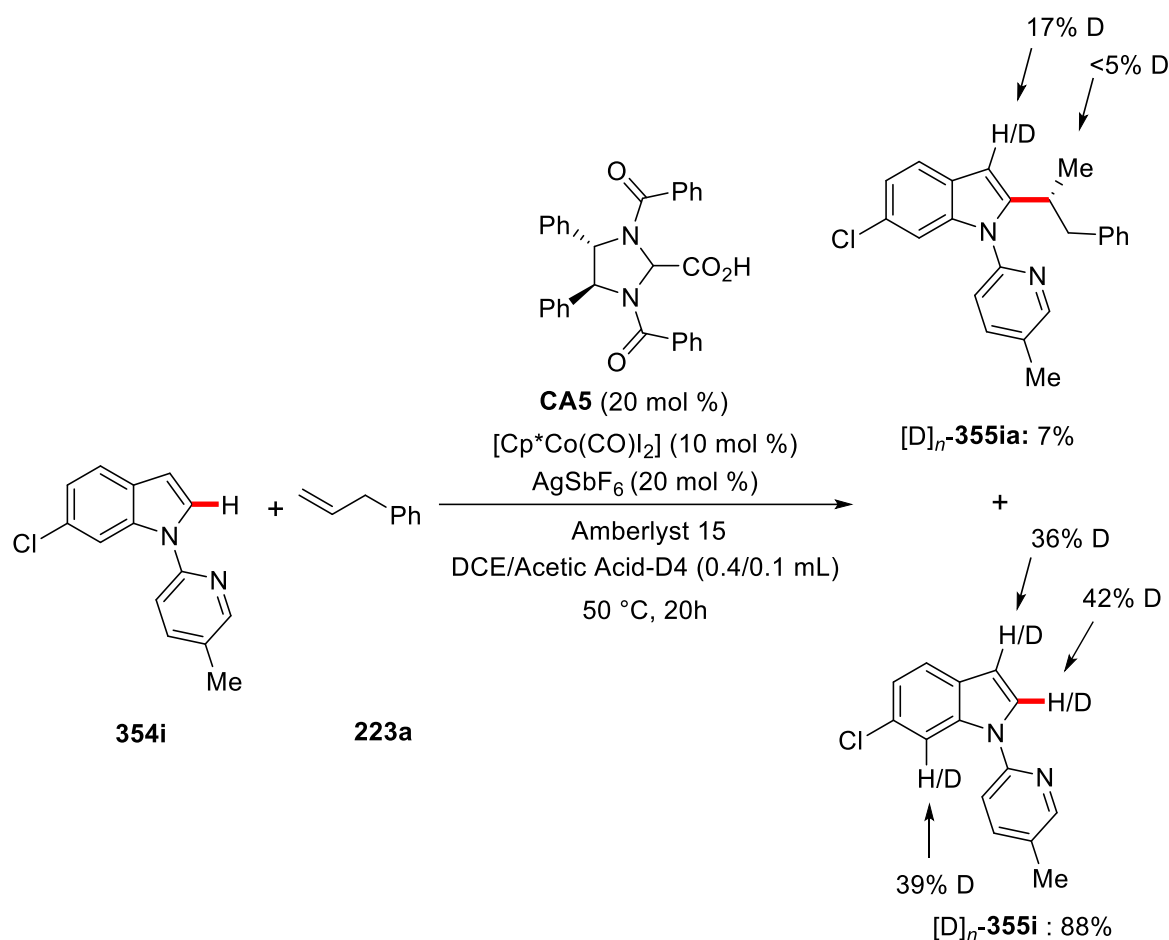
$[\alpha]_{\text{D}}^{20}$: -88.4 ($c = 0.95$, CHCl_3).

HPLC separation (Chiralpak[®] IF-3, *n*-hexane/*i*-PrOH 98:2, 1.0 mL/min, detection at 273 nm):

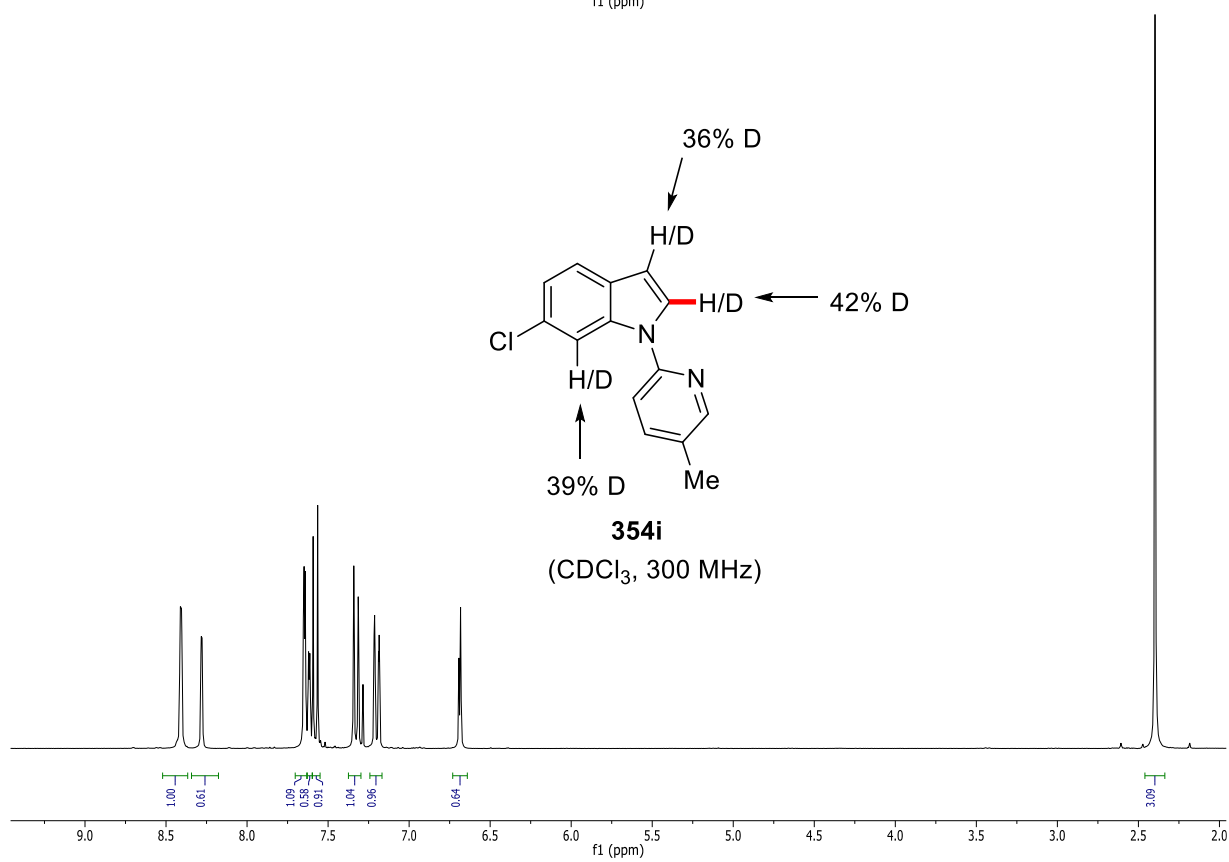
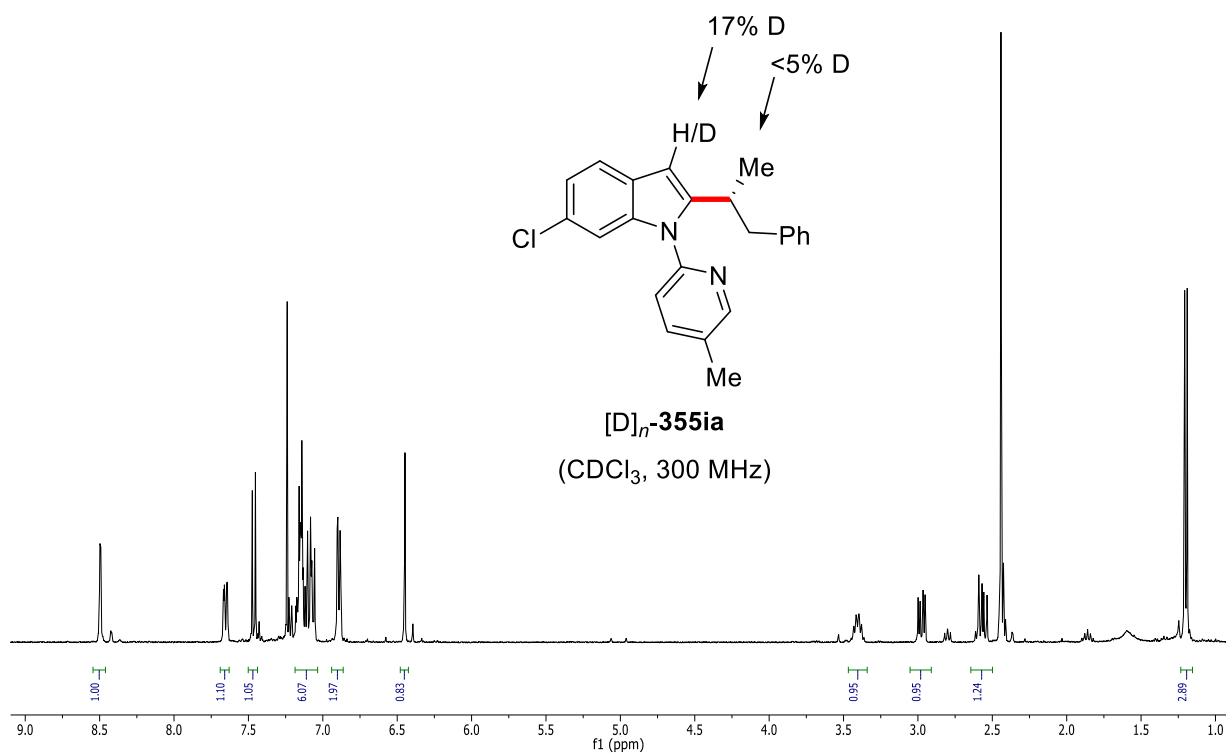
t_r (major) = 19.5 min, t_r (minor) = 21.8 min, t_r (AM) = 23.0 min, 92:8 e.r.

5.5.4. Mechanistic Studies

5.5.4.1. H/D-exchange for the asymmetric C–H alkylation



The representative procedure **E** was followed using **354i** (121 mg, 0.50 mmol, 1 equiv), allylbenzene (**223a**) (177 mg, 1.50 mmol, 1.50 equiv), $[\text{Cp}^*\text{Co}(\text{CO})\text{I}_2]$ (23.8 mg, 10.0 mol %) and AgSbF_6 (34.4 mg, 20.0 mol %) in DCE (0.4 mL) and $\text{CD}_3\text{CO}_2\text{D}$ (0.1 mL) for 20 h. At ambient temperature, the reaction mixture was diluted with EtOAc (2.0 mL) and Et_3N (0.5 mL) was added. The mixture was stirred for 0.5 h and filtered through a short pad of silica and the solvents were removed *in vacuo*. The crude mixture was purified by flash column chromatography on silica gel to afford the desired product $[\text{D}]_n$ -**355ia** (12 mg, 7%) and $[\text{D}]_n$ -**355i** (106 mg, 88% reis.) as yellow oils.



5.5.4.2. Kinetic Studies

5.3.4.2.1. Determination of the reaction order with respect to the concentration of CA5:

The reaction order was examined using the initial rate method. Five parallel independent reactions of **354h** (56.6 mg, 0.25 mmol), **223a** (88.5 mg, 0.75 mmol), [Cp*Co(CO)I₂] (11.9 mg, 25.0 μmol), AgSbF₆ (17.2 mg, 50 μmol), Amberlyst 15 (80 mg, 0.38 mmol) and **CA5** (0.0375, 0.0435, 0.05, 0.05625, 0.0625 mmol) were heated at 50 °C in DCE (0.50 mL). After cooling to ambient temperature, ¹⁹F-NMR conversions were measured by using 1-fluorononane as the internal standard.

Table 32. Reaction order in **CA5** for the asymmetric C–H alkylation

Entry	$c / \text{mol L}^{-1}$	$k / \text{mol L}^{-1} \text{min}^{-1}$	$\ln(c / \text{mol L}^{-1})$	$\ln(k / \text{mol L}^{-1} \text{min}^{-1})$
1	0.075	0.0357	-2.59027	-3.3326
2	0.0875	0.0404	-2.43612	-3.20893
3	0.10	0.0468	-2.30259	-3.06187
4	0.1125	0.0512	-2.1848	-2.97202
5	0.125	0.0483	-2.07944	-2.88062

5.5.4.2.2. Determination of the reaction order with respect to the concentration of CA5 without Amberlyst 15:

The reaction order was examined using the change of the vibration between the range of 1497-1478 cm⁻¹ with the React-IR. A solution of **354a** (104.1 mg, 0.50 mmol), **223a** (177 mg, 1.50 mmol), [Cp*Co(CO)I₂] (23.8 mg, 50.0 μmol), AgSbF₆ (34.5 mg, 100 μmol) and **CA5** (0.0875, 0.1, 0.1125, 0.125, 0.15 mmol) were heated at 50 °C in DCE (0.50 mL) and a diamond probe connected to a Mettler Toledo ReactIR. Every three minutes during 2 h an IR spectrum was recorded. The slope for the vibration between the range of 1497-1478 cm⁻¹ was determined during the interval between 3 min and 30 min.

Table 33. Reaction order in **CA5** for the asymmetric C–H alkylation without Amberlyst 15.

Entry	$c / \text{mol L}^{-1}$	$k / \text{mol L}^{-1} \text{min}^{-1}$	$\ln(c / \text{mol L}^{-1})$	$\ln(k / \text{mol L}^{-1} \text{min}^{-1})$
1	0.058	0.045	-2.84158	-3,10109
2	0.067	0.0633	-2.70805	-2,75987
3	0.075	0.0722	-2.59026	-2,62832
4	0.083	0.0909	-2.48490	-2,398

5	0.1	0.1431	-2.30258	-1,94421
---	-----	--------	----------	----------

5.5.4.3. Nonlinear Effect Study

5.3.4.3.1. Nonlinear effect study in presence of Amberlyst 15

Six parallel independent reactions of **354a** (56.6 mg, 0.25 mmol), **223a** (88.6 mg, 0.75 mmol), [Cp*Co(CO)I₂] (11.9 mg, 25.0 μmol), AgSbF₆ (17.2 mg, 50 μmol), Amberlyst 15 (80 mg, 0.38 mmol) and **CA5** (10–100% *ee*, 24.0 mg, 50.0 μmol) were heated at 50 °C in DCE (0.50 mL) for 65 h. At ambient temperature, the reaction mixture was diluted with EtOAc (2 mL) and Et₃N (0.50 mL) was added. The mixture was stirred for 0.5 h and filtered through a short pad of silica and the solvents were removed *in vacuo*. The crude mixture was purified by flash column chromatography on silica gel to afford the desired product **355aa**. The enantiomeric excess was determined by HPLC with chiral stationary phase.

Table 34. Nonlinear effect study for the asymmetric C–H alkylation.

Entry	<i>ee</i> of the chiral acid [CA5]	<i>ee</i> of the product [355aa]
1	0	0
2	10	9.3
3	30	25.7
4	50	41.4
5	70	56.1
6	90	74.4
7	100	84.0

5.5.4.3.2. Nonlinear effect study in absence of Amberlyst 15

Six parallel independent reactions of **354a** (56.6 mg, 0.25 mmol), **223a** (88.6 mg, 0.75 mmol), [Cp*Co(CO)I₂] (11.9 mg, 25.0 μmol), AgSbF₆ (17.2 mg, 50.0 μmol) and **CA5** (10–100% *ee*, 24.0 mg, 50.0 μmol) were heated at 50 °C in DCE (0.50 mL) for 65 h. At ambient temperature, the reaction mixture was diluted with EtOAc (2 mL) and the solvents were removed *in vacuo*. The crude mixture was purified by flash column chromatography on silica gel to afford the desired product **355aa**. The enantiomeric excess was determined by HPLC with chiral stationary phase.

5. Experimental Part

Table 35. Nonlinear effect study for the asymmetric C–H alkylation without Amberlyst 15.

Entry	<i>ee</i> of the chiral acid [CA5]	<i>ee</i> of the product [355aa]
1	0	0
2	10	2.5
3	30	14.7
4	50	26.8
5	70	44.1
6	90	68.6
7	100	84.0

5.5.4.4. DOSY Experiment:

Comparison of two NMR Samples:

- 1) 8 mg chiral acid CA5 in 700 μL of CDCl_3 + 1 μL of *n*-hexane.
- 2) 8 mg chiral acid CA5 in 700 μL of CDCl_3 + 5 μL of TFA + 1 μL of *n*-hexane.

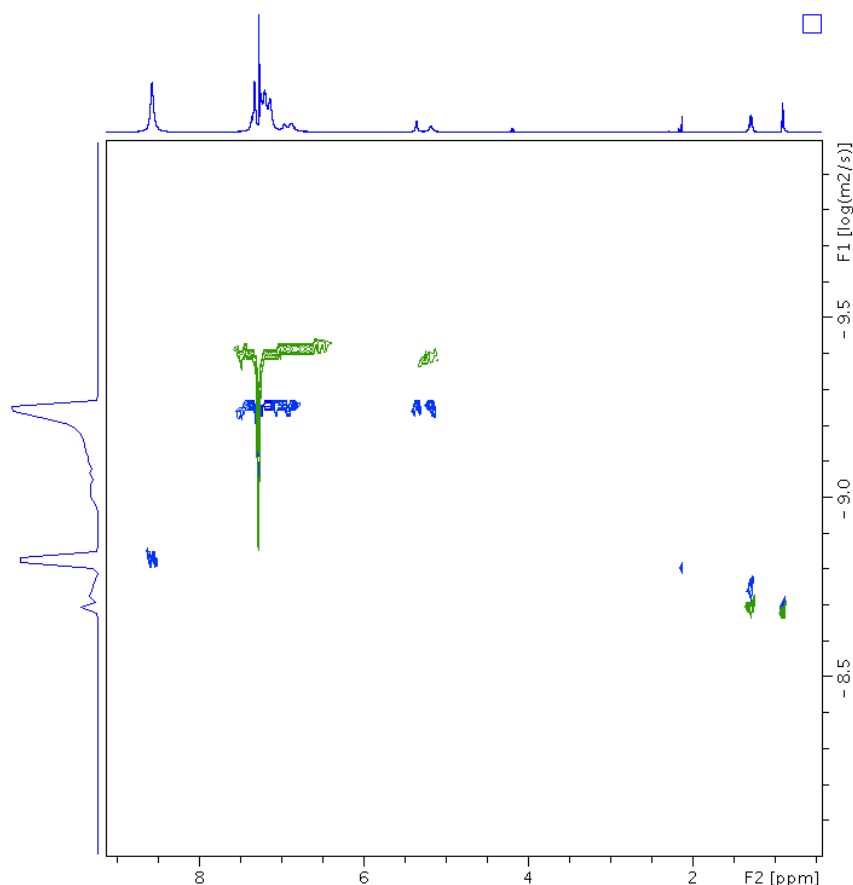
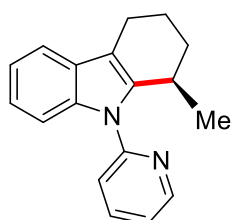


Figure 4. Overlay of DOSY spectra (500 MHz, 25 °C, CDCl₃) of **CA5** (8 mg, 0.017 mmol, in 700 mL of CDCl₃) in the presence (blue) and absence (green) of 0.063 mmol of TFA. The ratio of diffusion coefficients ($5.5 \times 10^{-10} \pm 0.2 \times 10^{-10} \text{ m}^2\text{s}^{-1} / 4.0 \times 10^{-10} \pm 0.2 \times 10^{-10} \text{ m}^2\text{s}^{-1} = 1.375$) indicates formation of dimers in the absence of TFA. DOSY spectra were recorded on a Bruker Avance III HD 500 MHz instrument equipped with a Cryoprobe Prodigy. The pulse sequence *dstebpgp3s* was used, and the diffusion delay (*d20*) and gradient duration (*p30*) were set to 150 and 1 ms, respectively. *n*Hexane was used as internal standard.

5.6. Ruthenium(II)-Catalyzed Enantioselective C–H Activation

5.6.1. Characterization Data



(R)-1-Methyl-9-(pyridin-2-yl)-2,3,4,9-tetrahydro-1H-carbazole (365a): The general procedure **H** was followed using 3-(pent-4-en-1-yl)-1-(pyridin-2-yl)-1H-indole (**364a**)

5. Experimental Part

(65.5 mg, 0.25 mmol). Isolation by column chromatography (*n*-hexane/EtOAc = 20:1) yielded **365a** (57.7 mg, 88%) as a yellow solid. M.p.: 77–82 °C.

¹H-NMR (400 MHz, CDCl₃): δ = 8.62 (ddd, *J* = 4.9, 2.0, 0.9 Hz, 1H), 7.85 (ddd, *J* = 8.0, 7.4, 2.0 Hz, 1H), 7.52–7.49 (m, 1H), 7.45 (dd, *J* = 8.0, 0.9 Hz, 1H), 7.40–7.37 (m, 1H), 7.26 (ddd, *J* = 7.4, 4.9, 0.9 Hz, 1H), 7.16–7.10 (m, 2H), 3.57–3.47 (m, 1H), 2.84–2.67 (m, 2H), 2.16–2.05 (m, 1H), 1.98–1.81 (m, 2H), 1.69–1.58 (m, 1H), 0.83 (d, *J* = 6.9 Hz, 3H).

¹³C-NMR (100 MHz, CDCl₃): δ = 152.1 (C_q), 149.5 (CH), 140.2 (C_q), 138.2 (CH), 136.8 (C_q), 128.3 (C_q), 121.8 (CH), 121.4 (CH), 120.2 (CH), 120.2 (CH), 118.1 (CH), 112.6 (C_q), 109.8 (CH), 31.9 (CH₂), 27.2 (CH), 21.5 (CH₂), 20.3 (CH₃), 19.9 (CH₂).

IR (ATR): 2959, 2929, 1584, 1471, 1437, 1372, 738 cm⁻¹.

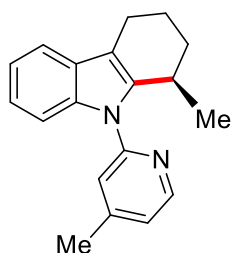
MS (ESI) *m/z* (relative intensity): 285 (25) [M+Na]⁺, 263 (100) [M+H]⁺.

HR-MS (ESI): *m/z* calcd. for [C₁₈H₁₈N₂+H]⁺ 263.1543 found 263.1542.

[α]_D²⁰: –70.5 (c = 1.0, CHCl₃).

HPLC separation (Chiralpak[®] IF-3, *n*-hexane/EtOAc 95:5, 1.0 mL/min, detection at 273 nm):

t_r (major) = 11.7 min, *t_r* (minor) = 10.5 min, 76:24 e.r.



(R)-1-Methyl-9-(4-methylpyridin-2-yl)-2,3,4,9-tetrahydro-1H-carbazole (367a): The general procedure **H** was followed using 1-(4-methylpyridin-2-yl)-3-(pent-4-en-1-yl)-1H-indole (**366a**) (69.0 mg, 0.25 mmol). Isolation by column chromatography (*n*-hexane/EtOAc = 20:1) yielded **367a** (62.0 mg, 90%) as a colourless oil.

¹H-NMR (400 MHz, CDCl₃): δ = 8.47 (d, *J* = 5.1 Hz, 1H), 7.53–7.46 (m, 1H), 7.40–7.34 (m, 1H), 7.27 (d, *J* = 1.5 Hz, 1H), 7.16–7.09 (m, 3H), 3.59–3.45 (m, 1H), 2.86–2.67 (m, 2H), 2.47 (s, 3H), 2.17–2.05 (m, 1H), 1.98–1.80 (m, 2H), 1.68–1.58 (m, 1H), 0.84 (d, *J* = 6.9 Hz, 3H).

¹³C-NMR (100 MHz, CDCl₃): δ = 152.0 (C_q), 149.9 (C_q), 149.0 (CH), 140.2 (C_q), 136.9 (C_q), 128.3 (C_q), 122.6 (CH), 121.7 (CH), 120.9 (CH), 120.1 (CH), 118.1 (CH), 112.5 (C_q), 109.8 (CH), 31.8 (CH₂), 27.2 (CH), 21.5 (CH₂), 21.2 (CH₃), 20.3 (CH₃), 19.9 (CH₂).

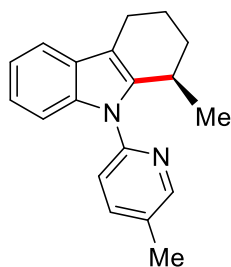
IR (ATR): 2930, 1601, 1478, 1454, 1224, 824, 736 cm⁻¹.

MS (ESI) *m/z* (relative intensity): 299 (10) [M+Na]⁺, 277 (100) [M+H]⁺.

HR-MS (ESI): *m/z* calcd. for [C₁₉H₂₀N₂+Na]⁺ 299.1519 found 299.1519.

[α]_D²⁰: –82.2 (c = 1.0, CHCl₃).

HPLC separation (Chiralpak[®] IB-3, *n*-hexane/EtOAc 95:5, 1.0 mL/min, detection at 273 nm): t_r (major) = 13.9 min, t_r (minor) = 9.5 min, 81:19 e.r.



(R)-1-Methyl-9-(5-methylpyridin-2-yl)-2,3,4,9-tetrahydro-1H-carbazole (363a): The general procedure **H** was followed using 1-(5-methylpyridin-2-yl)-3-(pent-4-en-1-yl)-1H-indole (**362a**) (69.0 mg, 0.25 mmol). Isolation by column chromatography (*n*-hexane/EtOAc = 20:1) yielded **363a** (65.7 mg, 95%) as a colourless oil.

¹H-NMR (400 MHz, CDCl₃): δ = 8.45 (d, J = 2.4, 0.8 Hz, 1H), 7.68 (ddd, J = 8.1, 2.4, 0.8 Hz, 1H), 7.54–7.47 (m, 1H), 7.38–7.32 (m, 2H), 7.16–7.09 (m, 2H), 3.60–3.40 (m, 1H), 2.86–2.66 (m, 2H), 2.43 (s, 3H), 2.17–2.05 (m, 1H), 2.00–1.80 (m, 2H), 1.71–1.59 (m, 1H), 0.85 (d, J = 6.8 Hz, 3H).

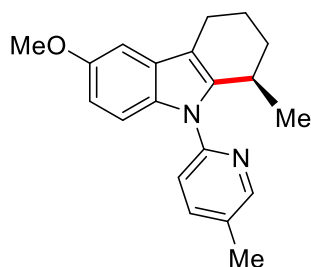
¹³C-NMR (100 MHz, CDCl₃): δ = 149.7 (CH), 149.7 (C_q), 140.2 (C_q), 138.8 (CH), 137.0 (C_q), 131.1 (C_q), 128.1 (C_q), 121.7 (CH), 120.0 (CH), 119.8 (CH), 118.0 (CH), 112.1 (C_q), 109.7 (CH), 31.8 (CH₂), 27.1 (CH), 21.5 (CH₂), 20.3 (CH₃), 19.9 (CH₂), 18.0 (CH₃).

IR (ATR): 2928, 1570, 1483, 1385, 1224, 1028, 833, 737 cm⁻¹.

MS (ESI) m/z (relative intensity): 299 (10) [M+Na]⁺, 277 (100) [M+H]⁺.

HR-MS (ESI): m/z calcd. for [C₁₉H₂₀N₂+H]⁺ 277.1699 found 277.1700.

$[\alpha]_D^{20}$: -95.3 (c = 1.0, CHCl₃). HPLC separation (Chiralpak[®] ID-3, *n*-hexane/EtOAc 90:10, 1.0 mL/min, detection at 273 nm): t_r (major) = 7.5 min, t_r (minor) = 5.8 min, 85:15 e.r.



(R)-6-Methoxy-1-methyl-9-(5-methylpyridin-2-yl)-2,3,4,9-tetrahydro-1H-carbazole (363b): The general procedure **H** was followed using 5-methoxy-1-(5-methylpyridin-2-yl)-3-(pent-4-en-1-yl)-1H-indole (**362b**) (76.5 mg, 0.25 mmol). Isolation by column chromatography (*n*-hexane/EtOAc = 10:1) yielded **363b** (68.0 mg, 89%) as a yellow oil.

5. Experimental Part

$^1\text{H-NMR}$ (400 MHz, CDCl_3): δ = 8.43 (d, J = 2.3 Hz, 1H), 7.65 (dd, J = 8.1, 2.3 Hz, 1H), 7.31 (d, J = 8.1 Hz, 1H), 7.26 (d, J = 8.8 Hz, 1H), 6.96 (d, J = 2.5 Hz, 1H), 6.77 (dd, J = 8.8, 2.5 Hz, 1H), 3.87 (s, 3H), 3.55–3.40 (m, 1H), 2.80–2.64 (m, 2H), 2.41 (s, 3H), 2.20–2.02 (m, 1H), 2.01–1.80 (m, 2H), 1.68–1.56 (m, 1H), 0.84 (d, J = 6.9 Hz, 3H).

$^{13}\text{C-NMR}$ (100 MHz, CDCl_3): δ = 154.5 (C_q), 149.8 (C_q), 149.6 (CH), 140.9 (C_q), 138.8 (CH), 132.1 (C_q), 130.9 (C_q), 128.6 (C_q), 119.5 (CH), 111.9 (C_q), 111.0 (CH), 110.6 (CH), 100.6 (CH), 56.0 (CH_3), 31.8 (CH_2), 27.2 (CH), 21.5 (CH_2), 20.3 (CH_3), 19.9 (CH_2), 18.0 (CH_3).

IR (ATR): 2930, 1596, 1483, 1440, 1388, 1156, 820 cm^{-1} .

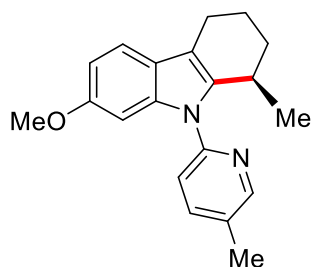
MS (ESI) m/z (relative intensity): 329 (25) $[\text{M}+\text{Na}]^+$, 307 (100) $[\text{M}+\text{H}]^+$.

HR-MS (ESI): m/z calcd. for $[\text{C}_{20}\text{H}_{22}\text{N}_2\text{O}+\text{H}]^+$ 307.1805 found 307.1808.

$[\alpha]_{\text{D}}^{20}$: -51.6 (c = 1.0, CHCl_3).

HPLC separation (Chiralpak[®] ID-3, *n*-hexane/EtOAc 90:10, 1.0 mL/min, detection at 273 nm):

t_r (major) = 13.6 min, t_r (minor) = 8.6 min, 85:15 e.r.



(R)-7-Methoxy-1-methyl-9-(5-methylpyridin-2-yl)-2,3,4,9-tetrahydro-1H-carbazole

(363c): The general procedure **H** was followed using 6-methoxy-1-(5-methylpyridin-2-yl)-3-(pent-4-en-1-yl)-1H-indole (**362c**) (76.5 mg, 0.25 mmol). Isolation by column chromatography (*n*-hexane/EtOAc = 10:1) yielded **363c** (72.0 mg, 95%) as a yellow oil.

$^1\text{H-NMR}$ (300 MHz, CDCl_3): δ = 8.46 (d, J = 2.4 Hz, 1H), 7.67 (dd, J = 8.1, 2.4 Hz, 1H), 7.37 (d, J = 8.5 Hz, 1H), 7.32 (d, J = 8.1 Hz, 1H), 6.90 (d, J = 2.3 Hz, 1H), 6.79 (dd, J = 8.5, 2.3 Hz, 1H), 3.79 (s, 3H), 3.46–3.34 (m, 1H), 2.83–2.60 (m, 2H), 2.43 (s, 3H), 2.15–2.00 (m, 1H), 1.95–1.80 (m, 2H), 1.69–1.56 (m, 1H), 0.82 (d, J = 6.8 Hz, 3H).

$^{13}\text{C-NMR}$ (100 MHz, CDCl_3): δ = 156.4 (C_q), 149.8 (C_q), 149.8 (CH), 139.0 (C_q), 138.9 (CH), 137.8 (C_q), 131.1 (C_q), 122.6 (C_q), 119.7 (CH), 118.5 (CH), 112.1 (C_q), 109.0 (CH), 94.7 (CH), 55.9 (CH_3), 31.8 (CH_2), 27.2 (CH), 21.5 (CH_2), 20.4 (CH_3), 20.0 (CH_2), 18.1 (CH_3).

IR (ATR): 2930, 1596, 1475, 1406, 1227, 1203, 1025, 796 cm^{-1} .

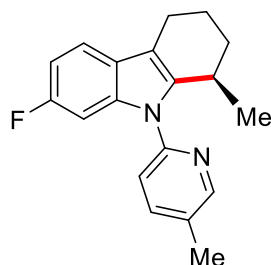
MS (ESI) m/z (relative intensity): 329 (10) $[\text{M}+\text{Na}]^+$, 307 (100) $[\text{M}+\text{H}]^+$.

HR-MS (ESI): m/z calcd. for $[\text{C}_{20}\text{H}_{22}\text{N}_2\text{O}+\text{Na}]^+$ 329.1624 found 329.1622.

$[\alpha]_{\text{D}}^{20}$: -65.1 (c = 1.0, CHCl_3).

HPLC separation (Chiralpak® ID-3, *n*-hexane/EtOAc 90:10, 1.0 mL/min, detection at 273 nm):

t_r (major) = 13.8 min, t_r (minor) = 9.6 min, 84:16 e.r.



(R)-7-Fluoro-1-methyl-9-(5-methylpyridin-2-yl)-2,3,4,9-tetrahydro-1H-carbazole (363d):

The general procedure **H** was followed using 6-fluoro-1-(5-methylpyridin-2-yl)-3-(pent-4-en-1-yl)-1H-indole (**362d**) (73.5 mg, 0.25 mmol). Isolation by column chromatography (*n*-hexane/EtOAc = 30:1) yielded **363d** (49 mg, 66%) as a yellow oil.

¹H-NMR (400 MHz, CDCl₃): δ = 8.47 (d, J = 2.3 Hz, 1H), 7.71 (dd, J = 8.1, 2.3 Hz, 1H), 7.41 (dd, J = 8.5, 5.4 Hz, 1H), 7.33 (d, J = 8.0 Hz, 1H), 7.07 (dd, J = 9.5, 2.3 Hz, 1H), 6.90 (ddd, J = 9.5, 8.5, 2.3 Hz, 1H), 3.55–3.38 (m, 1H), 2.84–2.66 (m, 2H), 2.45 (s, 3H), 2.16–2.05 (m, 1H), 2.00–1.81 (m, 2H), 1.69–1.59 (m, 1H), 0.85 (d, J = 6.8 Hz, 3H).

¹³C-NMR (75 MHz, CDCl₃): δ = 160.1 (d, ¹ J_{C-F} = 234.1 Hz, C_q), 149.9 (CH), 149.4 (C_q), 140.5 (d, ⁴ J_{C-F} = 3.4 Hz, C_q), 139.0 (CH), 137.1 (d, ³ J_{C-F} = 12.2 Hz, C_q), 131.5 (C_q), 124.6 (C_q), 119.6 (CH), 118.5 (d, ³ J_{C-F} = 9.9 Hz, CH), 112.1 (C_q), 108.1 (d, ² J_{C-F} = 24.1 Hz, CH), 97.0 (d, ² J_{C-F} = 27.2 Hz, CH), 31.7 (CH₂), 27.2 (CH), 21.4 (CH₂), 20.3 (CH₃), 19.9 (CH₂), 18.1 (CH₃).

¹⁹F-NMR (377 MHz, CDCl₃): δ = -121.5.

IR (ATR): 2929, 1596, 1473, 1484, 1387, 1142, 825, 797 cm⁻¹.

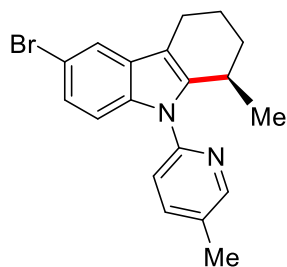
MS (ESI) m/z (relative intensity): 295 (100) [M+H]⁺.

HR-MS (ESI): m/z calcd. for [C₁₉H₁₉¹⁹FN₂+H]⁺ 295.1605 found 295.1612.

$[\alpha]_D^{20}$: -78.6 (c = 1.0, CHCl₃).

HPLC separation (Chiralpak® ID-3, *n*-hexane/EtOAc 90:10, 1.0 mL/min, detection at 273 nm):

t_r (major) = 7.2 min, t_r (minor) = 5.3 min, 86:14 e.r.



(R)-6-Bromo-1-methyl-9-(5-methylpyridin-2-yl)-2,3,4,9-tetrahydro-1H-carbazole (363e):

The general procedure **H** was followed using 5-bromo-1-(5-methylpyridin-2-yl)-3-(pent-4-en-

5. Experimental Part

1-yl)-1*H*-indole (**362e**) (88.5 mg, 0.25 mmol). Isolation by column chromatography (*n*-hexane/EtOAc = 15:1) yielded **363e** (78.0 mg, 88%) as a yellow solid. M.p.: 110–115 °C.

¹H-NMR (300 MHz, CDCl₃): δ = 8.44 (d, *J* = 2.4 Hz, 1H), 7.68 (dd, *J* = 8.2, 2.4 Hz, 1H), 7.60 (d, *J* = 1.3 Hz, 1H), 7.29 (d, *J* = 8.2 Hz, 1H), 7.23–7.10 (m, 2H), 3.52–3.34 (m, 1H), 2.81–2.59 (m, 2H), 2.43 (s, 3H), 2.15–2.01 (m, 1H), 1.97–1.80 (m, 2H), 1.74–1.55 (m, 1H), 0.83 (d, *J* = 6.8 Hz, 3H).

¹³C-NMR (100 MHz, CDCl₃): δ = 149.9 (CH), 149.3 (C_q), 141.6 (C_q), 139.0 (CH), 135.7 (C_q), 131.7 (C_q), 129.9 (C_q), 124.3 (CH), 120.7 (CH), 119.8 (CH), 113.2 (C_q), 111.7 (C_q), 111.3 (CH), 31.6 (CH₂), 27.1 (CH), 21.3 (CH₂), 20.2 (CH₃), 19.8 (CH₂), 18.1 (CH₃).

IR (ATR): 2929, 1572, 1483, 1455, 1402, 1027, 792 cm⁻¹.

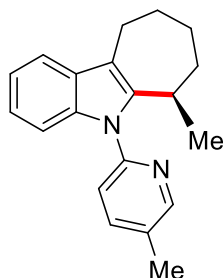
MS (ESI) *m/z* (relative intensity): 377 (25) [M+Na]⁺, 355 (100) [M+H]⁺.

HR-MS (ESI): *m/z* calcd. for [C₁₉H₁₉⁷⁹BrN₂+Na]⁺ 377.0624 found 377.0620.

[α]_D²⁰: –50.5 (c = 1.0, CHCl₃).

HPLC separation (Chiralpak[®] ID-3, *n*-hexane/EtOAc 90:10, 1.0 mL/min, detection at 273 nm): *t_r* (major) = 8.6 min, *t_r* (minor) = 5.7 min, 82:18 e.r.

1 mmol scale reaction: A modified procedure **H** was followed using 5-bromo-1-(5-methylpyridin-2-yl)-3-(pent-4-en-1-yl)-1*H*-indole (**362e**) (354.0 mg, 1.0 mmol), [RuCl₂(*p*-cymene)]₂ (30.6 mg, 5.0 mol %), AgSbF₆ (68.8 mg, 20 mol %) and chiral acid **CA14** (100.4 mg, 20 mol %) in PhMe (2.0 mL) at 25 °C for 36 h. The reaction mixture was diluted with EtOAc (5.0 mL) and the solvent was removed *in vacuo*. The crude mixture was purified by flash column chromatography (*n*-hexane/EtOAc = 15:1) on silica gel to afford the desired product **363e**. (304.2 mg, 86%) as a yellow solid. HPLC separation (Chiralpak[®] ID-3, *n*-hexane/EtOAc 90:10, 1.0 mL/min, detection at 273 nm): *t_r* (major) = 8.5 min, *t_r* (minor) = 5.7 min, 83:17 e.r.



(*R*)-6-Methyl-5-(5-methylpyridin-2-yl)-5,6,7,8,9,10-hexahydrocyclohepta[*b*]indole

(369a): The general procedure **H** was followed using 3-(hex-5-en-1-yl)-1-(5-methylpyridin-2-yl)-1*H*-indole (**368a**) (29.0 mg, 0.10 mmol). Isolation by column chromatography (*n*-hexane/EtOAc = 30:1) yielded **369a** (5.0 mg, 17%) as a yellow oil.

$^1\text{H-NMR}$ (600 MHz, CDCl_3): δ = 8.45 (dd, J = 2.5, 0.8 Hz, 1H), 7.67–7.61 (m, 1H), 7.51–7.44 (m, 1H), 7.22 (d, J = 7.0 Hz, 1H), 7.10 (dd, J = 8.0, 0.8 Hz, 1H), 7.07 (ddd, J = 8.0, 7.0, 1.2 Hz, 1H), 7.03 (ddd, J = 8.0, 7.0, 1.2 Hz, 1H), 3.26–3.18 (m, 1H), 3.06 (ddd, J = 15.4, 5.8, 2.6 Hz, 1H), 2.67 (ddd, J = 15.4, 12.4, 2.6 Hz, 1H), 2.40 (s, 3H), 2.06–1.99 (m, 1H), 1.96–1.87 (m, 2H), 1.84–1.74 (m, 2H), 1.56–1.50 (m, 1H), 1.17 (d, J = 7.2 Hz, 3H).

$^{13}\text{C-NMR}$ (100 MHz, CDCl_3): δ = 150.0 (CH), 149.5 (C_q), 143.1 (C_q), 138.7 (CH), 136.3 (C_q), 131.8 (C_q), 128.8 (C_q), 121.6 (CH), 121.2 (CH), 119.8 (CH), 117.7 (CH), 114.6 (C_q), 110.0 (CH), 33.2 (CH_2), 30.5 (CH), 28.7 (CH_2), 25.4 (CH_2), 24.1 (CH_2), 18.4 (CH_3), 18.1 (CH_3).

IR (ATR): 2920, 1596, 1570, 1483, 1459, 1384, 1201, 738 cm^{-1} .

MS (ESI) m/z (relative intensity): 313 (10) $[\text{M}+\text{Na}]^+$, 291 (100) $[\text{M}+\text{H}]^+$.

HR-MS (ESI): m/z calcd. for $[\text{C}_{20}\text{H}_{22}\text{N}_2+\text{H}]^+$ 291.1856 found 291.1858.

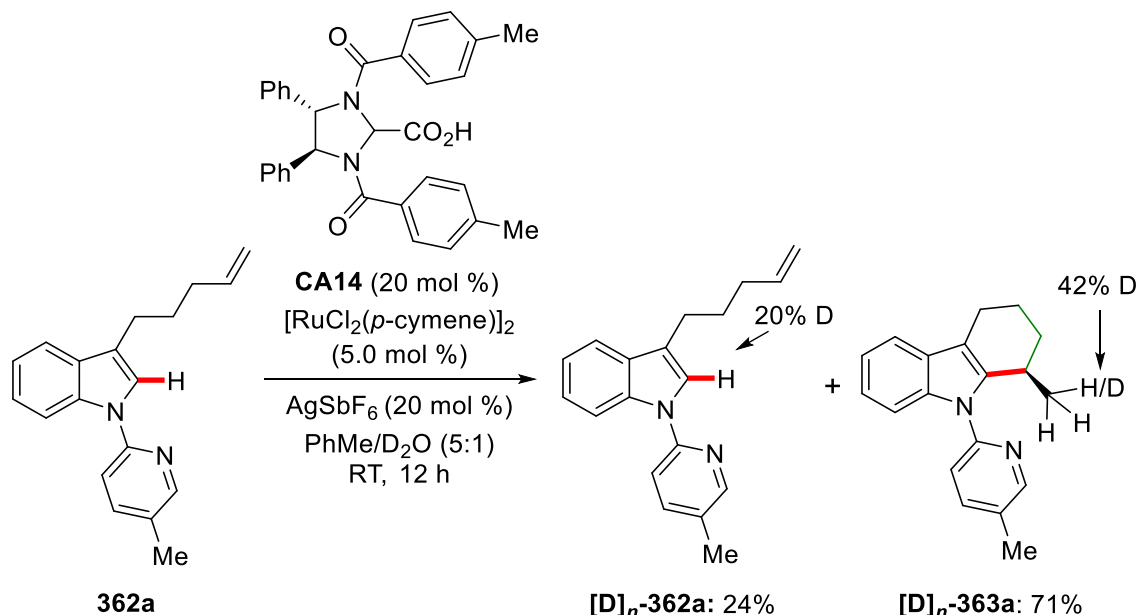
$[\alpha]_D^{20}$: -7.4 (c = 1.0, CHCl_3).

HPLC separation (Chiralpak[®] ID-3, *n*-hexane/EtOAc 90:10, 1.0 mL/min, detection at 273 nm):

t_r (major) = 7.6 min, t_r (minor) = 6.0 min, 82:18 e.r.

5.6.2. Mechanistic Studies

5.6.2.1. H/D Exchange Experiment



The representative procedure **H** was followed using **362a** (69.0 mg, 0.25 mmol, 1 equiv), $[\text{RuCl}_2(p\text{-cymene})]_2$ (7.7 mg, 5.0 mol %), AgSbF_6 (17.2 mg, 20 mol %), **CA14** (25.2 mg, 20 mol %) in PhMe (0.50 mL) and D_2O (0.10 mL) at 25 °C for 12 h. At ambient temperature, the reaction mixture was diluted with EtOAc (2.0 mL) and the solvents was removed *in vacuo*.

5. Experimental Part

The crude mixture was purified by flash column chromatography on silica gel to afford the desired product $[D]_n\text{-363a}$ (48.0 mg, 71%) and $[D]_n\text{-362a}$ (17.0 mg, 24%) as yellow oils.

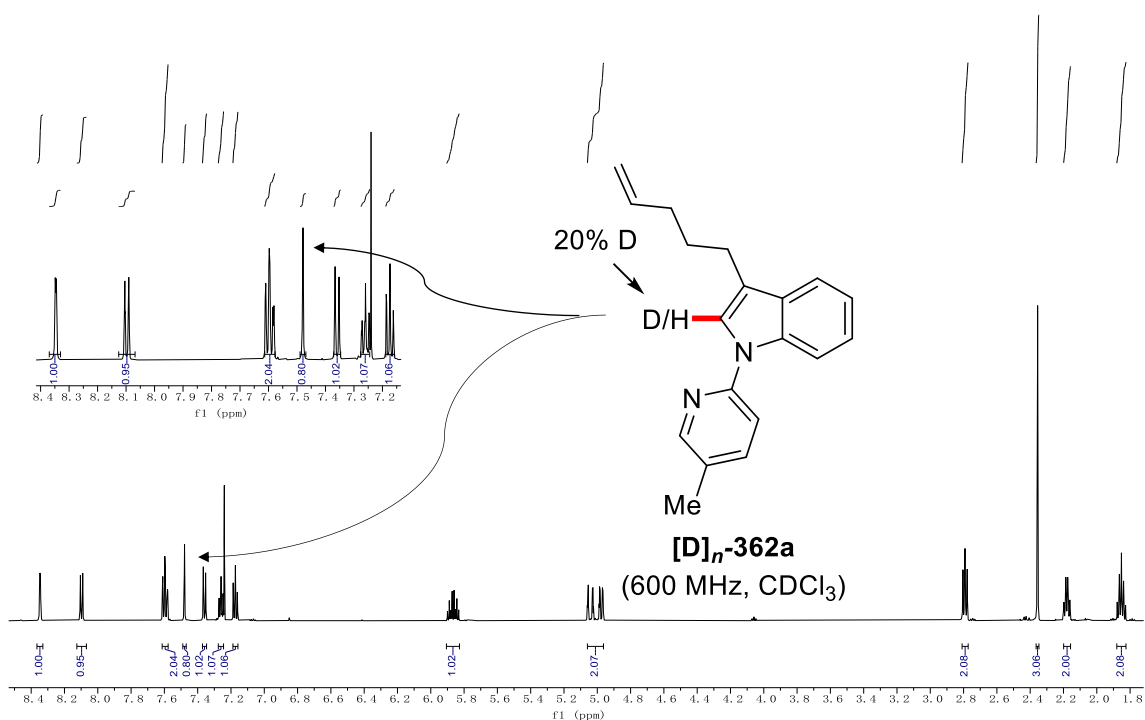


Figure 5. $^1\text{H-NMR}$ of reisolated $[D]_n\text{-362}$ from the deuteration study.

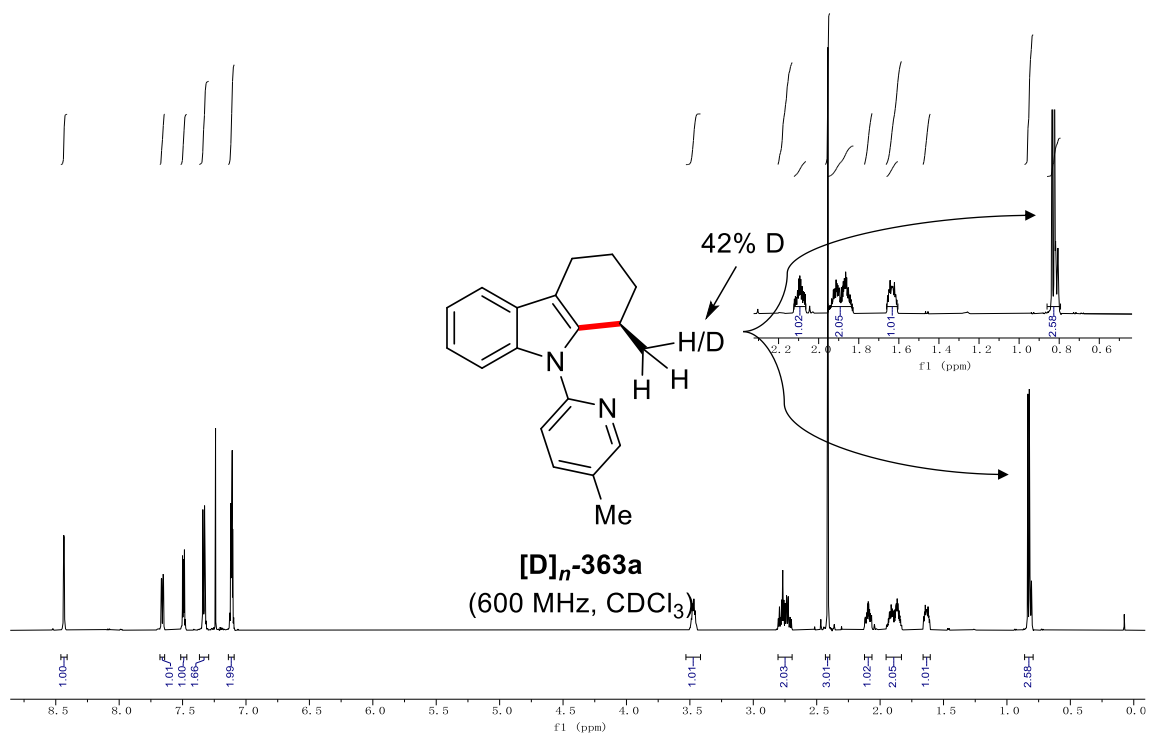
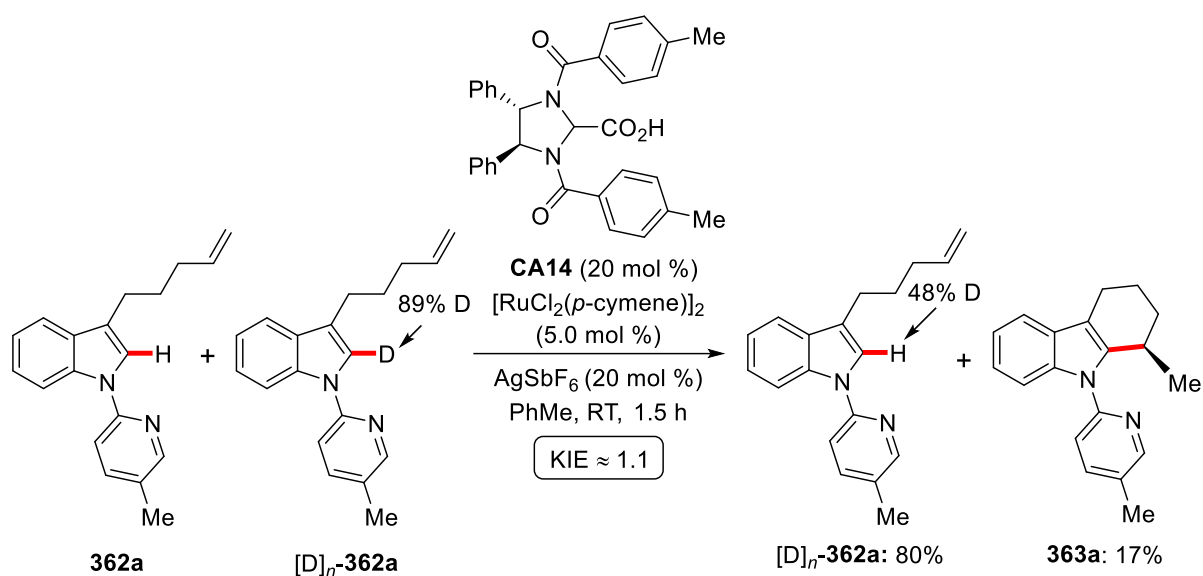


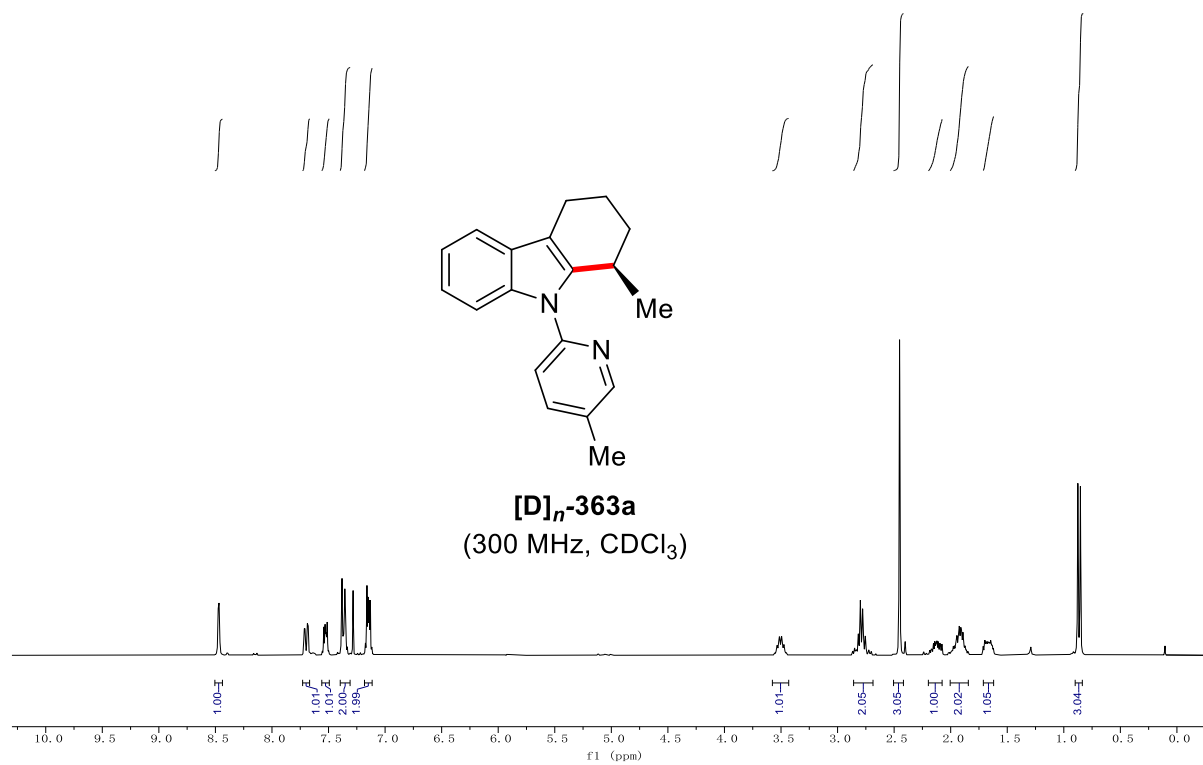
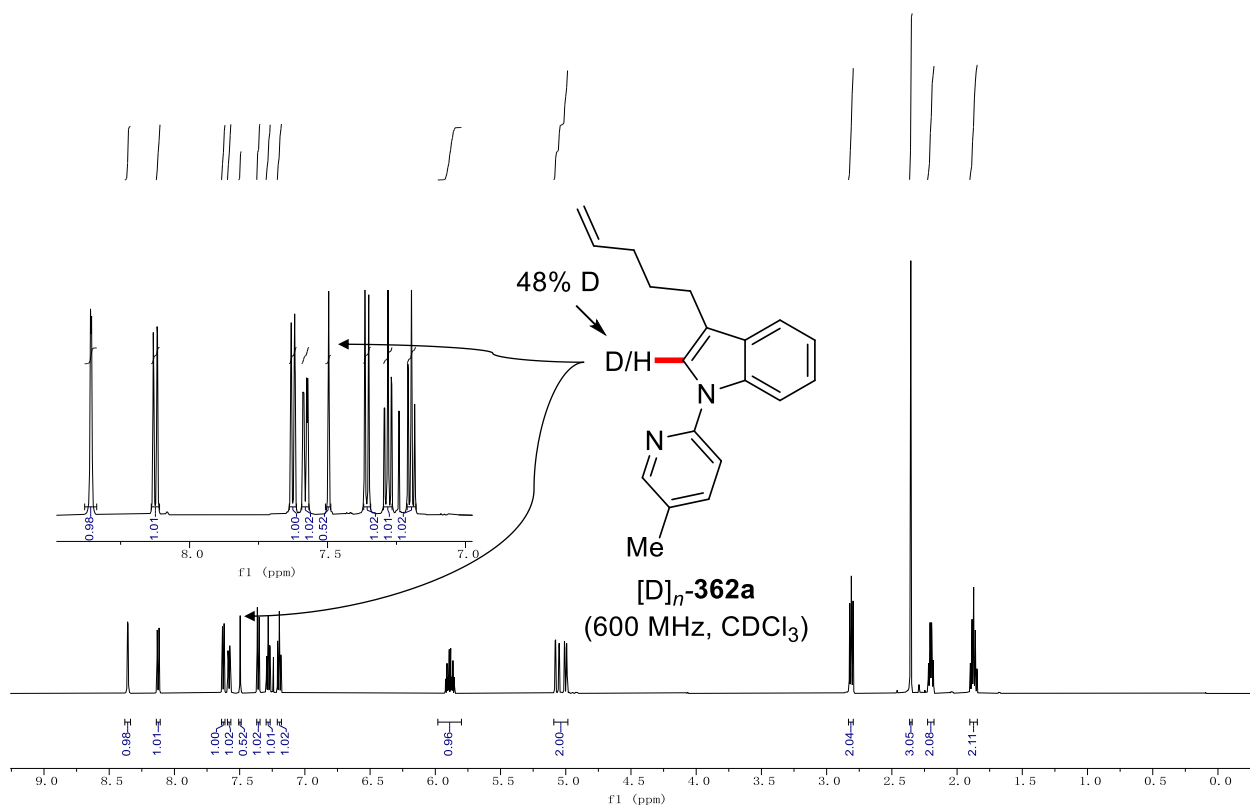
Figure 6. $^1\text{H-NMR}$ of $[D]_n\text{-363}$ from the deuteration study.

5.6.2.2. Intramolecular Competition KIE Experiment



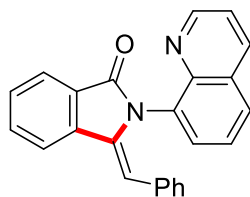
The representative procedure **A** was followed using **362a** (53.8 mg, 0.195 mmol, 1 equiv), $[\text{D}]_n\text{-362a}$ (69.3 mg, 0.25 mmol, 1 equiv), $[\text{RuCl}_2(p\text{-cymene})]_2$ (13.7 mg, 10 mol %), AgSbF_6 (30.5 mg, 20 mol %) and **CA14** (44.8 mg, 20 mol %) in PhMe (1.5 mL) at 25 °C for 1.5 h. The reaction mixture was diluted with EtOAc (5.0 mL) and the solvent was removed *in vacuo*. The crude mixture was purified by flash column chromatography on silica gel to afford the desired product **363a** (21.0 mg, 17%) and $[\text{D}]_n\text{-362a}$ (98.0 mg, 80%) as yellow oils. The kinetic isotope effect of this reaction was determined to be $k_{\text{H}}/k_{\text{D}} \approx 52/48 \approx 1.1$ as estimated by $^1\text{H-NMR}$ spectroscopy, based on the recovered starting material.

5. Experimental Part



5.7. Copper-catalyzed Alkyne Annulation by C–H Alkynylation

5.7.1. Characterization Data



(Z)-3-Benzylidene-2-(quinolin-8-yl) isoindolin-1-one (256aa): The general procedure **J** was followed using benzamide **229a** (62 mg, 0.25 mmol) and alkyne **255a** (51 mg, 0.50 mmol). Purification by column chromatography on silica gel (*n*-hexane/EtOAc: 5/1) yielded **256aa** (78.7 mg, 90%, *E/Z* = 1:13) as a white solid. M. p.: 210–215 °C.

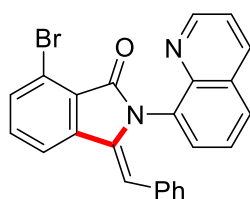
Resonances are reported for (*Z*)-**256aa**. ¹H-NMR (300 MHz, CDCl₃): δ = 8.85 (dd, *J* = 4.2, 1.7 Hz, 1H), 8.02–7.94 (m, 2H), 7.88 (d, *J* = 7.7 Hz, 1H), 7.68 (td, *J* = 7.5, 1.2 Hz, 1H), 7.61–7.53 (m, 2H), 7.48 (dd, *J* = 7.4, 1.5 Hz, 1H), 7.34–7.27 (m, 2H), 6.81 (s, 0.93H, *Z*), 6.71–6.64 (m, 1H), 6.60–6.48 (m, 4H), 6.02 (s, 0.07H, *E*).

¹³C-NMR (125 MHz, CDCl₃): δ = 167.9 (C_q), 150.2 (CH), 144.3 (C_q), 138.6 (C_q), 136.0 (C_q), 135.6 (CH), 134.1 (C_q), 133.4 (C_q), 132.1 (CH), 129.9 (CH), 128.9 (CH), 128.7 (C_q), 128.2 (C_q), 128.2 (CH), 128.0 (CH), 126.2 (CH), 125.9 (CH), 125.5 (CH), 123.8 (CH), 121.1 (CH), 119.5 (CH), 107.2 (CH).

IR (ATR): 3061, 1704, 1596, 1472, 1377, 1221, 1024, 716 cm⁻¹.

MS (ESI) *m/z* (relative intensity): 371 (10) [M+Na]⁺, 349 (60) [M+H]⁺.

HR-MS (ESI) *m/z* calcd for C₂₄H₁₇N₂O [M+H]⁺: 349.1335, found: 349.1324. The analytical data correspond with those reported in the literature.^[208]



(Z)-3-Benzylidene-7-bromo-2-(quinolin-8-yl)isoindolin-1-one (256ba): The general procedure **J** was followed using benzamide **229b** (82 mg, 0.25 mmol) and alkyne **255a** (51 mg, 0.50 mmol). Purification by column chromatography on silica gel (*n*-hexane/EtOAc: 2/1) yielded **256ba** (69.2 mg, 65%, *E/Z* = 1:10) as a yellow solid. M. p.: 200–205 °C.

Resonances are reported for (*Z*)-**256ba**.

¹H-NMR (400 MHz, CDCl₃): δ = 8.83 (dd, *J* = 4.2, 1.7 Hz, 1H), 8.02–7.93 (m, 2H), 7.90–7.85 (m, 1H), 7.67 (dd, *J* = 7.8, 1.2 Hz, 1H), 7.56 (dd, *J* = 7.5, 1.2 Hz, 2H), 7.46 (dd, *J* = 7.4, 1.4

5. Experimental Part

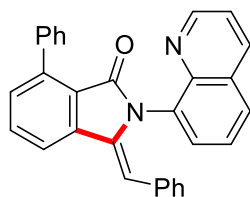
Hz, 1H), 7.31–7.26 (m, 2H), 6.79 (s, 0.90H, Z), 6.70–6.61 (m, 1H), 6.60–6.43 (m, 3H), 6.00 (s, 0.10H, E).

^{13}C -NMR (100 MHz, CDCl_3): δ = 168.1 (C_q), 150.3 (CH), 144.4 (C_q), 138.7 (C_q), 136.1 (C_q), 135.7 (CH), 135.5 (C_q), 135.3 (C_q), 134.2 (C_q), 133.6 (C_q), 132.2 (CH), 130.0 (CH), 129.1 (CH), 128.8 (C_q), 128.1 (CH), 126.3 (CH), 126.0 (CH), 125.6 (CH), 123.9 (CH), 121.2 (CH), 119.6 (CH), 107.3 (CH).

IR (ATR): 3048, 1714, 1650, 1500, 1473, 1070, 757, 693 cm^{-1} .

MS (ESI) m/z (relative intensity): 449 (30) $[\text{M}(^{79}\text{Br})+\text{Na}]^+$, 427 (100) $[\text{M}(^{79}\text{Br})+\text{H}]^+$.

HR-MS (ESI): m/z calcd for $\text{C}_{24}\text{H}_{16}^{79}\text{BrN}_2\text{O}$ $[\text{M}+\text{H}]^+$: 427.0441, found: 427.0448.



(Z)-3-Benzylidene-7-phenyl-2-(quinolin-8-yl)isoindolin-1-one (256ca): The general procedure **J** was followed using benzamide **229c** (81 mg, 0.25 mmol) and alkyne **255a** (51 mg, 0.50 mmol) with $\text{Cu}(\text{OAc})_2 \cdot \text{H}_2\text{O}$ (5.0 mg, 10 mol %). Purification by column chromatography on silica gel (*n*-hexane/EtOAc: 2/1) yielded **256ca** (54.3 mg, 51%, *E/Z* = 1:3) as a yellow oil. Resonances reported for **(Z)-256ca**: ^1H -NMR (400 MHz, CDCl_3): δ = 8.82 (dd, J = 4.2, 1.6 Hz, 1H), 7.95–7.86 (m, 2H), 7.71 (d, J = 7.7 Hz, 1H), 7.63 (d, J = 1.7 Hz, 1H), 7.61 (d, J = 1.2 Hz, 1H), 7.54 (d, J = 1.3 Hz, 1H), 7.48 (dd, J = 7.5, 1.0 Hz, 2H), 7.43–7.39 (m, 2H), 7.38–7.35 (m, 2H), 7.26 (d, J = 1.7 Hz, 1H), 6.83 (s, 1H), 6.64 (t, J = 7.3 Hz, 1H), 6.60–6.55 (m, 2H), 6.51 (d, J = 7.5 Hz, 2H).

^{13}C -NMR (125 MHz, CDCl_3): δ = 167.2 (C_q), 150.2 (CH), 144.3 (C_q), 141.1 (C_q), 139.7 (C_q), 137.2 (C_q), 135.6 (C_q), 135.6 (CH), 134.2 (C_q), 133.6 (C_q), 131.7 (CH), 131.1 (CH), 130.2 (CH), 129.7 (CH), 129.4 (CH), 128.7 (C_q), 128.4 (CH), 128.1 (CH), 127.5 (CH), 126.1 (CH), 125.8 (CH), 125.5 (CH), 124.0 (C_q), 121.0 (CH), 118.6 (CH), 106.7 (CH).

Resonances reported for **(E)-256ca**: ^1H -NMR (400 MHz, CDCl_3): δ = 8.92 (dd, J = 4.2, 1.6 Hz, 1H), 8.20 (dd, J = 8.3, 1.6 Hz, 1H), 7.95–7.89 (m, 1H), 7.81 (dd, J = 7.3, 1.4 Hz, 1H), 7.66 (d, J = 7.8 Hz, 1H), 7.60 (d, J = 1.6 Hz, 1H), 7.58 (t, J = 1.4 Hz, 1H), 7.51–7.45 (m, 1H), 7.43–7.38 (m, 1H), 7.38–7.35 (m, 2H), 7.35–7.32 (m, 4H), 7.32–7.27 (m, 3H), 7.24 (s, 1H), 6.01 (s, 1H).

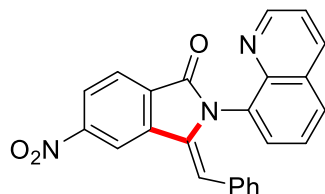
^{13}C -NMR (125 MHz, CDCl_3) (two carbon peak less due to overlap): δ = 166.1 (C_q), 151.1 (CH), 144.9 (C_q), 141.0 (C_q), 138.1 (C_q), 137.4 (C_q), 136.6 (C_q), 136.1 (CH), 135.5 (C_q), 132.8

(C_q), 131.5 (CH), 131.3 (CH), 129.7 (CH), 129.4 (C_q), 129.2 (CH), 128.1 (CH), 127.7 (CH), 127.6 (CH), 127.5 (CH), 127.4 (CH), 126.2 (CH), 122.2 (CH), 121.7 (CH), 111.5 (CH).

IR (ATR): 3055, 1719, 1595, 1473, 1377, 825, 759 cm⁻¹.

MS (ESI) *m/z* (relative intensity): 447 (10) [M+Na]⁺, 425 (100) [M+H]⁺.

HR-MS (ESI): *m/z* calcd for C₃₀H₂₀N₂ONa [M+Na]⁺: 447.1468, found: 447.1473.



(Z)-3-Benzylidene-5-nitro-2-(quinolin-8-yl) isoindolin-1-one (256da): The general procedure **J** was followed using benzamide **229d** (73 mg, 0.25 mmol) and alkyne **255a** (51 mg, 0.50 mmol) with Cu(OAc)₂·H₂O (5.0 mg, 10 mol %). Purification by column chromatography on silica gel (*n*-hexane/EtOAc: 1/1) yielded **256da** (57 mg, 58%, *E/Z* = 1:3) as a yellow oil.

Resonances reported for **(Z)-256da**. ¹H-NMR (400 MHz, CDCl₃): δ = 8.84 (dd, *J* = 4.2, 1.6 Hz, 1H), 8.78 (d, *J* = 1.8 Hz, 1H), 8.44 (dd, *J* = 8.3, 1.9 Hz, 1H), 8.17 (d, *J* = 8.3 Hz, 1H), 8.01 (dd, *J* = 8.3, 1.6 Hz, 1H), 7.65 (dd, *J* = 8.2, 1.4 Hz, 1H), 7.53 (dd, *J* = 7.4, 1.3 Hz, 1H), 7.38–7.31 (m, 2H), 6.99 (s, 1H), 6.74 (dd, *J* = 8.9, 5.3 Hz, 1H), 6.59 (dd, *J* = 7.1, 6.4 Hz, 4H).

¹³C-NMR (100 MHz, CDCl₃): δ = 166.0 (C_q), 150.8 (C_q), 150.5 (CH), 144.0 (C_q), 139.5 (C_q), 135.9 (CH), 134.6 (C_q), 133.5 (C_q), 132.7 (C_q), 132.5 (C_q), 130.0 (CH), 129.9 (CH), 129.7 (C_q), 128.1 (CH), 126.7 (CH), 126.5 (CH), 125.7 (CH), 125.2 (CH), 124.0 (CH), 121.5 (CH), 115.6 (CH), 110.4 (CH).

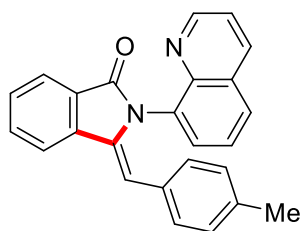
Resonances reported for **(E)-256da**. ¹H-NMR (400 MHz, CDCl₃): δ = 8.94 (dd, *J* = 4.2, 1.6 Hz, 1H), 8.41–8.34 (m, 2H), 8.30 (dd, *J* = 8.3, 1.7 Hz, 1H), 8.15 (d, *J* = 8.1 Hz, 2H), 8.05 (dd, *J* = 8.3, 1.4 Hz, 1H), 7.90 (dd, *J* = 7.3, 1.4 Hz, 1H), 7.76 (dd, *J* = 8.2, 7.3 Hz, 1H), 7.50 (dd, *J* = 8.4, 4.3 Hz, 1H), 7.42 (dd, *J* = 6.6, 2.5 Hz, 4H), 6.23 (s, 1H).

¹³C-NMR (100 MHz, CDCl₃) (two peaks overlap): δ = 164.9 (C_q), 151.4 (CH), 150.3 (C_q), 144.6 (C_q), 137.3 (C_q), 136.4 (CH), 136.2 (C_q), 134.8 (C_q), 134.1 (C_q), 132.1 (C_q), 131.2 (CH), 129.3 (CH), 128.9 (CH), 128.7 (CH), 126.4 (CH), 124.8 (CH), 124.3 (CH), 122.1 (CH), 119.0 (CH), 115.0 (CH).

IR (ATR): 2955, 1712, 1645, 1596, 1342, 1180, 827, 790 cm⁻¹.

MS (ESI) *m/z* (relative intensity): 416 (20) [M+Na]⁺, 394 (100) [M+H]⁺.

HR-MS (ESI): *m/z* calcd for C₂₄H₁₆N₃O₃ [M+H]⁺: 394.1186, found: 394.1188.



(Z)-3-(4-Methylbenzylidene)-2-(quinolin-8-yl) isoindolin-1-one (256ab): The general procedure **J** was followed using benzamide **229a** (62 mg, 0.25 mmol) and alkyne **255b** (58 mg, 0.50 mmol). Purification by column chromatography on silica gel (*n*-hexane/EtOAc: 2/1) yielded **256ab** (69.7 mg, 77%, *E/Z* = 1:6) as a yellow oil.

Resonances reported for (*Z*)-**256ab**. $^1\text{H-NMR}$ (400 MHz, CDCl_3): δ = 8.82 (d, J = 3.2 Hz, 1H), 7.97 (d, J = 7.2 Hz, 2H), 7.86 (d, J = 7.8 Hz, 1H), 7.66 (t, J = 7.6 Hz, 1H), 7.61–7.55 (m, 1H), 7.52 (dd, J = 7.5, 0.8 Hz, 1H), 7.45 (dd, J = 7.4, 1.2 Hz, 1H), 7.33–7.24 (m, 2H), 6.77 (s, 1H), 6.41 (d, J = 7.8 Hz, 2H), 6.30 (d, J = 7.8 Hz, 2H), 2.00 (s, 3H).

$^{13}\text{C-NMR}$ (100 MHz, CDCl_3): δ = 168.1 (C_q), 150.3 (CH), 144.4 (C_q), 138.7 (C_q), 135.8 (C_q), 135.8 (CH), 135.6 (C_q), 134.3 (C_q), 132.1 (CH), 130.5 (C_q), 130.0 (CH), 129.1 (CH), 128.9 (CH), 128.8 (C_q), 128.2 (C_q), 128.0 (CH), 126.9 (CH), 125.6 (CH), 123.9 (CH), 121.2 (CH), 119.6 (CH), 107.5 (CH), 20.8 (CH_3).

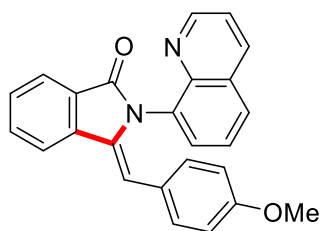
Resonances reported for (*E*)-**256ab**. $^1\text{H-NMR}$ (400 MHz, CDCl_3): δ = 8.91 (dd, J = 4.2, 1.5 Hz, 1H), 8.22 (dd, J = 8.1, 1.3 Hz, 1H), 7.99–7.93 (m, 2H), 7.82 (dd, J = 7.3, 1.2 Hz, 1H), 7.71–7.68 (m, 1H), 7.52–7.51 (m, 1H), 7.50–7.47 (m, 1H), 7.43–7.36 (m, 2H), 7.25 (d, J = 3.7 Hz, 2H), 7.14 (d, J = 7.9 Hz, 2H), 5.98 (s, 1H), 2.35 (s, 3H).

$^{13}\text{C-NMR}$ (100 MHz, CDCl_3): δ = 167.0 (C_q), 151.2 (CH), 145.0 (C_q), 138.5 (C_q), 137.4 (C_q), 136.2 (CH), 135.6 (C_q), 132.9 (C_q), 132.2 (C_q), 131.6 (CH), 131.4 (CH), 130.4 (C_q), 129.6 (C_q), 129.4 (CH), 129.2 (CH), 128.0 (CH), 126.9 (CH), 126.3 (CH), 123.7 (CH), 123.3 (CH), 121.8 (CH), 112.3 (CH), 21.3 (CH_3).

IR (ATR): 2922, 1718, 1630, 1565, 1255, 1203, 891, 724 cm^{-1} .

MS (ESI) m/z (relative intensity): 385 (10) $[\text{M}+\text{Na}]^+$, 363 (100) $[\text{M}+\text{H}]^+$.

HR-MS (ESI): m/z calcd for $\text{C}_{25}\text{H}_{19}\text{N}_2\text{O}$ $[\text{M}+\text{H}]^+$: 363.1495, found: 363.1492. The analytical data correspond with those reported in the literature.^[208]



(Z)-3-(4-Methoxybenzylidene)-2-(quinolin-8-yl) isoindolin-1-one (256ac): The general procedure **J** was followed using benzamide **229a** (62 mg, 0.25 mmol) and alkyne **255c** (66 mg, 0.50 mmol). Purification by column chromatography on silica gel (*n*-hexane/EtOAc: 1/1) yielded **256ac** (68.1 mg, 72%, *E/Z* = 1:1.4) as a white solid. M. p.: 185–190 °C.

Resonances reported for (*Z*)-**256ac**. ¹H-NMR (400 MHz, CDCl₃): δ = 8.83 (dd, *J* = 4.2, 1.7 Hz, 1H), 8.00–7.92 (m, 2H), 7.85 (dd, *J* = 7.8, 1.5 Hz, 1H), 7.72–7.58 (m, 2H), 7.57–7.49 (m, 1H), 7.49–7.43 (m, 1H), 7.34–7.26 (m, 2H), 6.75 (s, 1H), 6.50–6.43 (m, 2H), 6.10–6.02 (m, 2H), 3.81 (s, 3H).

¹³C-NMR (100 MHz, CDCl₃): δ = 168.1 (C_q), 157.7 (C_q), 150.3 (CH), 144.5 (C_q), 138.8 (C_q), 135.7 (CH), 135.5 (C_q), 134.4 (C_q), 132.1 (CH), 130.7 (CH), 129.6 (C_q), 129.4 (CH), 128.9 (C_q), 128.8 (CH), 128.2 (CH), 126.0 (C_q), 125.7 (CH), 123.9 (CH), 121.2 (CH), 119.5 (CH), 111.9 (CH), 107.2 (CH), 55.1 (CH₃).

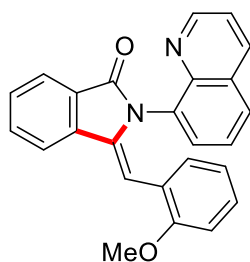
Resonances reported for (*E*)-**256ac**. ¹H-NMR (400 MHz, CDCl₃): δ = 8.90 (dd, *J* = 4.2, 1.7 Hz, 1H), 8.22 (dd, *J* = 8.2, 1.7 Hz, 1H), 8.00–7.92 (m, 2H), 7.82 (dd, *J* = 7.3, 1.5 Hz, 1H), 7.72–7.58 (m, 1H), 7.57–7.49 (m, 1H), 7.49–7.43 (m, 1H), 7.43–7.36 (m, 2H), 7.34–7.26 (m, 2H), 6.91–6.84 (m, 2H), 5.96 (s, 1H), 3.54 (s, 3H).

¹³C-NMR (100 MHz, CDCl₃): δ = 166.9 (C_q), 159.1 (C_q), 151.2 (CH), 145.0 (C_q), 138.3 (C_q), 136.2 (CH), 135.6 (C_q), 133.0 (C_q), 131.6 (CH), 131.4 (CH), 129.9 (CH), 129.2 (CH), 128.2 (CH), 128.2 (C_q), 127.5 (C_q), 123.7 (CH), 123.1 (CH), 121.8 (CH), 127.5 (C_q), 126.3 (CH), 113.9 (CH), 112.0 (CH), 55.3 (CH₃).

IR (ATR): 3022, 1712, 1610, 1555, 1243, 1103, 791, 754 cm⁻¹.

MS (ESI) *m/z* (relative intensity): 401 (10) [M+Na]⁺, 379 (100) [M+H]⁺.

HR-MS (ESI): *m/z* calcd for C₂₅H₁₉N₂O₂ [M+H]⁺: 379.1441, found: 379.1458. The analytical data correspond with those reported in the literature.^[208]



(Z)-3-(2-Methoxybenzylidene)-2-(quinolin-8-yl) isoindolin-1-one (256ad): The general procedure **J** was followed using benzamide **229a** (62 mg, 0.25 mmol) and alkyne **255d** (66 mg, 0.50 mmol). Purification by column chromatography on silica gel (*n*-hexane/EtOAc: 1/1) yielded **256ad** (62.0 mg, 66%, *E/Z* = 1:4) as a white solid. M. p.: 172–180 °C.

Resonances are reported for (*Z*)-**256ad**. ¹H-NMR (300 MHz, CDCl₃): δ = 8.88 (dd, *J* = 4.1, 1.5 Hz, 1H), 8.06–7.96 (m, 2H), 7.94 (d, *J* = 8.0 Hz, 1H), 7.70 (t, *J* = 7.5 Hz, 1H), 7.58 (d, *J* = 7.4 Hz, 2H), 7.51 (dd, *J* = 7.4, 1.3 Hz, 1H), 7.34–7.28 (m, 2H), 6.79 (s, 1H), 6.70 (dd, *J* = 7.8, 1.8 Hz, 1H), 6.33 (t, *J* = 7.6 Hz, 2H), 5.95 (t, *J* = 7.6 Hz, 1H), 3.61 (s, 3H).

¹³C-NMR (125 MHz, CDCl₃): δ = 167.9 (C_q), 155.9 (C_q), 150.0 (CH), 144.4 (C_q), 138.5 (C_q), 136.1 (C_q), 135.6 (CH), 133.9 (C_q), 131.9 (CH), 129.8 (CH), 129.7 (CH), 128.7 (CH), 128.5 (C_q), 128.21 (C_q), 128.1 (CH), 127.7 (CH), 125.2 (CH), 123.6 (CH), 122.3 (C_q), 120.8 (CH), 119.8 (CH), 118.3 (CH), 108.6 (CH), 103.6 (CH), 54.9 (CH₃).

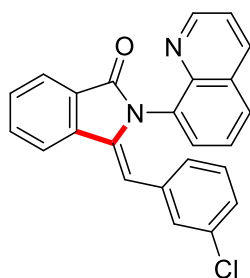
Resonances are reported for (*E*)-**256ad**. ¹H-NMR (300 MHz, CDCl₃): δ = 8.95 (dd, *J* = 4.2, 1.5 Hz, 1H), 8.25 (dd, *J* = 8.4, 1.6 Hz, 1H), 8.00 (dd, *J* = 8.4, 1.2 Hz, 2H), 7.96–7.88 (m, 1H), 7.69 (dd, *J* = 7.6, 1.1 Hz, 1H), 7.61–7.55 (m, 1H), 7.54–7.49 (m, 1H), 7.44 (dd, *J* = 7.5, 1.2 Hz, 2H), 7.37–7.28 (m, 2H), 7.03–6.94 (m, 1H), 6.89 (d, *J* = 8.2 Hz, 1H), 6.02 (s, 1H), 3.72 (s, 3H).

¹³C-NMR (125 MHz, CDCl₃): δ = 166.8 (C_q), 157.3 (C_q), 150.9 (CH), 144.9 (C_q), 138.2 (C_q), 136.0 (CH), 132.9 (C_q), 131.5 (CH), 131.2 (CH), 131.1 (CH), 130.3 (C_q), 129.4 (C_q), 129.3 (CH), 129.1 (CH), 129.0 (CH), 126.2 (CH), 123.9 (C_q), 123.5 (CH), 123.1 (CH), 122.3 (C_q), 121.6 (CH), 120.1 (CH), 110.6 (CH), 108.7 (CH), 55.4 (CH₃).

IR (ATR): 3048, 1709, 1595, 1398, 1243, 791 cm⁻¹.

MS (ESI) *m/z* (relative intensity): 401 (25) [M+Na]⁺, 379 (100) [M+H]⁺.

HR-MS (ESI): *m/z* calcd for C₂₅H₁₈N₂O₂Na [M+Na]⁺: 401.1260, found: 401.1262. The analytical data correspond with those reported in the literature.^[208]



(Z)-3-(3-Chlorobenzylidene)-2-(quinolin-8-yl) isoindolin-1-one (256ae): The general procedure **J** was followed using benzamide **229a** (62 mg, 0.25 mmol) and alkyne **255e** (68 mg, 0.50 mmol). Purification by column chromatography on silica gel (*n*-hexane/EtOAc: 2/1) yielded **256ae** (66.6 mg, 70%, *E/Z* = 1:4) as a white solid. M. p.: 170–177 °C.

Resonances are reported for (*Z*)-**256ae**. ¹H-NMR (400 MHz, CDCl₃): δ = 8.84 (dd, *J* = 4.2, 1.7 Hz, 1H), 7.99–7.95 (m, 2H), 7.84 (dd, *J* = 7.6, 1.2 Hz, 1H), 7.69–7.64 (m, 1H), 7.60 (dd, *J* = 8.3, 1.4 Hz, 1H), 7.56 (dd, *J* = 7.5, 0.9 Hz, 1H), 7.46 (dd, *J* = 7.5, 1.4 Hz, 1H), 7.35–7.29 (m, 2H), 7.26 (dd, *J* = 1.4, 0.4 Hz, 1H), 6.66 (s, 1H), 6.63 (dd, *J* = 7.6, 1.6 Hz, 1H), 6.50–6.47 (m, 1H), 6.46–6.44 (m, 1H).

¹³C-NMR (100 MHz, CDCl₃): δ = 168.0 (C_q), 150.5 (CH), 144.2 (C_q), 138.4 (C_q), 137.0 (C_q), 135.9 (CH), 135.4 (C_q), 133.9 (C_q), 132.4 (C_q), 132.3 (CH), 129.2 (CH), 129.3 (CH), 129.0 (C_q), 128.6 (CH), 128.4 (CH), 128.3 (C_q), 127.4 (CH), 126.3 (CH), 126.0 (CH), 125.7 (CH), 124.0 (CH), 121.4 (CH), 119.7 (CH), 105.3 (CH).

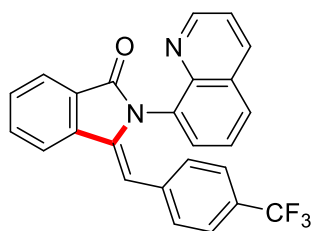
Resonances are reported for (*E*)-**256ae**. ¹H-NMR (400 MHz, CDCl₃): δ = 8.90 (dd, *J* = 4.2, 1.7 Hz, 1H), 8.22 (dd, *J* = 8.3, 1.7 Hz, 1H), 8.01 (d, *J* = 1.7 Hz, 2H), 7.81 (dd, *J* = 7.3, 1.4 Hz, 1H), 7.71–7.64 (m, 1H), 7.51 (dd, *J* = 7.5, 1.4 Hz, 1H), 7.43–7.39 (m, 1H), 7.35 (dd, *J* = 2.3, 1.8 Hz, 2H), 6.52 (d, *J* = 7.6 Hz, 1H), 6.55–6.50 (m, 3H), 5.89 (s, 1H).

¹³C-NMR (100 MHz, CDCl₃): δ = 166.9 (C_q), 151.2 (CH), 144.9 (C_q), 139.6 (C_q), 137.2 (C_q), 136.2 (CH), 135.2 (C_q), 134.3 (C_q), 132.6 (C_q), 131.9 (CH), 131.3 (CH), 130.5 (C_q), 129.8 (CH), 129.7 (CH), 129.7 (CH), 129.5 (C_q), 129.4 (CH), 127.6 (CH), 127.6 (CH), 126.3 (CH), 123.9 (CH), 123.1 (CH), 121.9 (CH), 110.1 (CH).

IR (ATR): 3058, 1716, 1652, 1593, 1500, 1397, 827, 757 cm⁻¹.

MS (ESI) *m/z* (relative intensity): 405 (10) [M+Na]⁺, 383 (100) [M+H]⁺.

HR-MS (ESI): *m/z* calcd for C₂₄H₁₅³⁵ClN₂ONa [M+Na]⁺: 405.0765, found: 405.0762.

**(Z)-2-(Quinolin-8-yl)-3-(4-(trifluoromethyl)benzylidene)isoindolin-1-one (256af)**

The general procedure **J** was followed using benzamide **229a** (73 mg, 0.25 mmol) and alkyne **255f** (85 mg, 0.50 mmol). Purification by column chromatography on silica gel (*n*-hexane/EtOAc: 2/1) yielded **256af** (62.6 mg, 60%, *E/Z* = 1:20) as a yellow oil.

Resonances are reported for (*Z*)-**256af**: ¹H-NMR (400 MHz, CDCl₃): δ = 8.82 (dd, *J* = 4.2, 1.7 Hz, 1H), 8.03 (dd, *J* = 7.6, 1.0 Hz, 1H), 7.95 (dd, *J* = 8.3, 1.7 Hz, 1H), 7.91 (dd, *J* = 7.8, 1.0 Hz, 1H), 7.73 (dd, *J* = 7.6, 1.2 Hz, 1H), 7.62 (dd, *J* = 7.8, 1.2 Hz, 2H), 7.56 (dd, *J* = 7.6, 1.4 Hz, 1H), 7.37 (dd, *J* = 8.3, 7.6 Hz, 1H), 7.31 (dd, *J* = 8.3, 4.2 Hz, 1H), 6.80–6.72 (m, 3H), 6.68–6.61 (m, 2H).

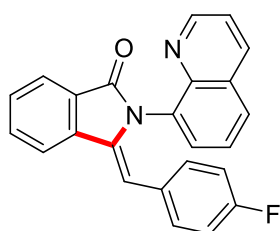
¹³C-NMR (100 MHz, CDCl₃): δ = 167.9 (C_q), 150.4 (CH), 144.1 (C_q), 138.3 (C_q), 137.5 (C_q), 137.4 (C_q), 135.9 (CH), 133.9 (C_q), 132.5 (CH), 130.2 (CH), 129.5 (CH), 128.9 (C_q), 128.7 (CH), 128.4 (C_q), 128.2 (CH), 127.7 (q, ²*J*_{C-F} = 34.2 Hz, C_q), 125.8 (CH), 124.1 (CH), 123.4 (q, ¹*J*_{C-F} = 270 Hz, C_q), 122.8 (q, ³*J*_{C-F} = 3.4 Hz, CH), 121.4 (CH), 119.8 (CH), 105.2 (CH).

¹⁹F-NMR (375 MHz, CDCl₃): δ = -63.1 (m).

IR (ATR): 3022, 1711, 1609, 1511, 1221, 827, 798, 728 cm⁻¹.

MS (ESI) *m/z* (relative intensity): 417 (100) [M+H]⁺.

HR-MS (ESI): *m/z* calcd for C₂₅H₁₆F₃N₂O [M+H]⁺: 417.1209, found: 417.1218.



(Z)-3-(4-Fluorobenzylidene)-2-(quinolin-8-yl)isoindolin-1-one (256ag): The general procedure **J** was followed using benzamide **229a** (62 mg, 0.25 mmol) and alkyne **255g** (60 mg, 0.50 mmol). Purification by column chromatography on silica gel (*n*-hexane/EtOAc: 2/1) yielded **256ag** (66.9 mg, 73%, *E/Z* = 1:6) as a yellow oil.

Resonances are reported for (*Z*)-**256ag**: ¹H-NMR (400 MHz, CDCl₃): δ = 8.83 (dd, *J* = 4.2, 1.7 Hz, 1H), 8.03–7.97 (m, 2H), 7.87 (dd, *J* = 7.8, 0.9 Hz, 1H), 7.68 (t, *J* = 7.8 Hz, 1H), 7.64 (dd, *J* = 8.3, 1.4 Hz, 1H), 7.56 (dd, *J* = 7.4, 0.9 Hz, 1H), 7.49 (dd, *J* = 7.4, 1.4 Hz, 1H), 7.38–7.28 (m, 2H), 6.71 (s, 1H), 6.57–6.47 (m, 2H), 6.26–6.18 (m, 2H).

^{13}C -NMR (100 MHz, CDCl_3): $\delta = 168.0$ (C_q), 161.0 (d, $^1J_{\text{C-F}} = 240$ Hz, C_q), 150.4 (CH), 144.3 (C_q), 138.5 (C_q), 136.4 (C_q), 135.8 (CH), 134.1 (C_q), 132.3 (CH), 130.1 (CH), 129.7 (d, $^3J_{\text{C-F}} = 8.1$ Hz, CH), 129.5 (d, $^4J_{\text{C-F}} = 2.9$ Hz, C_q), 129.2 (CH), 128.8 (C_q), 128.4 (CH), 128.3 (C_q), 125.7 (CH), 123.9 (CH), 121.3 (CH), 119.6 (CH), 113.1 (d, $^2J_{\text{C-F}} = 22.9$ Hz, CH), 106.0 (CH).
 ^{19}F -NMR (375 MHz, CDCl_3): $\delta = -115.6$ (m).

Resonances are reported for (*E*)-**256ag**: ^1H -NMR (400 MHz, CDCl_3): $\delta = 8.90$ (dd, $J = 4.2, 1.7$ Hz, 1H), 8.22 (dd, $J = 8.4, 1.7$ Hz, 1H), 7.96–7.94 (m, 2H), 7.82 (dd, $J = 7.4, 1.5$ Hz, 1H), 7.51–7.49 (m, 1H), 7.44–7.42 (m, 1H), 7.42–7.39 (m, 3H), 7.38–7.28 (m, 2H), 7.08–6.98 (m, 2H), 5.92 (s, 1H).

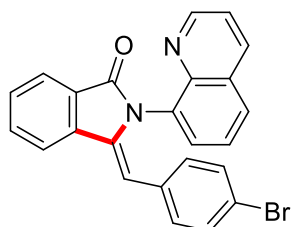
^{13}C -NMR (100 MHz, CDCl_3): $\delta = 167.0$ (C_q), 161.5 (d, $^1J_{\text{C-F}} = 247.5$ Hz, C_q), 151.2 (CH), 144.9 (C_q), 139.1 (C_q), 136.2 (CH), 135.3 (C_q), 132.8 (C_q), 131.8 (CH), 131.4 (CH), 131.2 (d, $^3J_{\text{C-F}} = 8.0$ Hz, CH), 131.2 (C_q), 130.5 (C_q), 129.5 (d, $^4J_{\text{C-F}} = 2.9$ Hz, C_q), 129.6 (CH), 126.3 (CH), 123.9 (CH), 123.8 (CH), 123.1 (CH), 121.8 (CH), 115.5 (d, $^2J_{\text{C-F}} = 21.5$ Hz, CH), 1107 (CH).

^{19}F -NMR (375 MHz, CDCl_3): $\delta = -113.9$ (m).

IR (ATR): 3048, 1715, 1655, 1596, 1397, 1227, 829 cm^{-1} .

MS (ESI) m/z (relative intensity): 389 (15) $[\text{M}+\text{Na}]^+$, 367 (100) $[\text{M}+\text{H}]^+$.

HR-MS (ESI): m/z calcd for $\text{C}_{24}\text{H}_{16}\text{N}_2\text{O}$ $[\text{M}+\text{H}]^+$: 367.1241, found: 367.1253. The analytical data correspond with those reported in the literature.^[210]



(Z)-3-(4-Bromobenzylidene)-2-(quinolin-8-yl) isoindolin-1-one (256ah): The general procedure **J** was followed using benzamide **229a** (62 mg, 0.25 mmol) and alkyne **255h** (91 mg, 0.50 mmol). Purification by column chromatography on silica gel (*n*-hexane/EtOAc: 2/1) yielded **256ah** (76.7 mg, 72%, *E/Z* = 1:4) as a yellow oil.

Resonances are reported for (*Z*)-**256ah**: ^1H -NMR (400 MHz, CDCl_3): $\delta = 8.80$ (dd, $J = 4.2, 1.7$ Hz, 1H), 8.05–7.97 (m, 2H), 7.84 (d, $J = 7.8$ Hz, 1H), 7.70–7.63 (m, 2H), 7.55 (dd, $J = 7.4, 0.9$ Hz, 1H), 7.49 (dd, $J = 7.4, 1.4$ Hz, 1H), 7.37–7.27 (m, 2H), 6.66 (s, 1H), 6.59 (d, $J = 8.3$ Hz, 2H), 6.37 (d, $J = 8.3$ Hz, 2H).

^{13}C -NMR (100 MHz, CDCl_3): $\delta = 167.9$ (C_q), 150.4 (CH), 144.3 (C_q), 138.4 (C_q), 136.8 (C_q), 135.8 (CH), 134.1 (C_q), 132.4 (C_q), 132.3 (CH), 131.6 (CH), 131.2 (CH), 130.1 (CH), 129.5

5. Experimental Part

(CH), 129.1 (CH), 128.9 (C_q), 128.5 (CH), 128.3 (C_q), 124.0 (CH), 121.4 (CH), 120.0 (C_q), 119.7 (CH), 105.7 (CH).

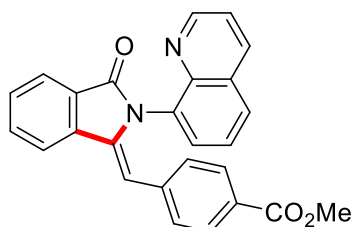
Resonances are reported for (*E*)-**256ah**: ¹H-NMR (400 MHz, CDCl₃): δ = 8.95 (d, *J* = 4.3 Hz, 1H), 8.27 (dd, *J* = 8.4, 1.6 Hz, 1H), 8.06 (d, *J* = 1.6 Hz, 1H), 7.91–7.83 (m, 1H), 7.73 (d, *J* = 1.3 Hz, 2H), 7.51–7.49 (m, 2H), 7.48–7.44 (m, 2H), 7.30–7.26 (m, 4H), 5.87 (s, 1H).

¹³C-NMR (100 MHz, CDCl₃): δ = 166.9 (C_q), 151.2 (CH), 144.9 (C_q), 139.2 (C_q), 136.3 (CH), 135.2 (C_q), 134.3 (C_q), 134.2 (CH), 132.7 (C_q), 131.9 (CH), 131.4 (CH), 130.5 (C_q), 129.6 (CH), 129.6 (C_q), 129.5 (CH), 129.3 (CH), 126.3 (CH), 123.9 (CH), 123.1 (CH), 121.9 (CH), 121.6 (C_q), 110.4 (CH).

IR (ATR): 3049, 1713, 1595, 1472, 1302, 827, 759, 718 cm⁻¹.

MS (ESI) *m/z* (relative intensity): 449 (10) [M(⁷⁹Br)+Na]⁺, 427 (100) [M(⁷⁹Br)+H]⁺.

HR-MS (ESI): *m/z* calcd for C₂₄H₁₅⁷⁹BrN₂ONa [M+Na]⁺: 449.0260, found: 449.0270.



(*Z*)-Methyl 4-[(3-oxo-2-(quinolin-8-yl)isoindolin-1-ylidene)methyl]benzoate (**256ai**): The general procedure **J** was followed using benzamide **229a** (62 mg, 0.25 mmol) and alkyne **255i** (80 mg, 0.50 mmol). Purification by column chromatography on silica gel (*n*-hexane/EtOAc: 2/1) yielded **256ai** (71.7 mg, 70%, *E/Z* = 1:7) as a yellow solid. M. p.: 185–190 °C.

Resonances are reported for (*Z*)-**256ai**. ¹H-NMR (400 MHz, CDCl₃): δ = 8.81 (dd, *J* = 4.2, 1.7 Hz, 1H), 7.97 (dd, *J* = 7.6, 1.2 Hz, 1H), 7.93 (d, *J* = 8.2 Hz, 1H), 7.86 (d, *J* = 7.8 Hz, 1H), 7.67 (t, *J* = 7.4 Hz, 1H), 7.59–7.53 (m, 2H), 7.48 (d, *J* = 7.4, 1H), 7.31–7.25 (m, 2H), 7.21–7.15 (m, 2H), 6.73 (s, 1H), 6.62–6.54 (m, 2H), 3.79 (3H).

¹³C-NMR (100 MHz, CDCl₃): δ = 168.0 (C_q), 166.6 (C_q), 150.4 (CH), 144.2 (C_q), 138.6 (C_q), 138.4 (C_q), 137.2 (C_q), 135.8 (CH), 134.0 (C_q), 132.4 (CH), 130.0 (CH), 129.4 (CH), 128.8 (C_q), 128.5 (CH), 128.3 (C_q), 128.1 (CH), 127.4 (CH), 127.3 (C_q), 125.7 (CH), 124.0 (CH), 121.4 (CH), 119.7 (CH), 105.7 (CH), 51.9 (CH₃).

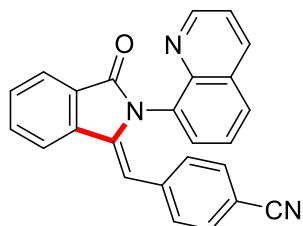
Resonances are reported for (*E*)-**256ai**: ¹H-NMR (400 MHz, CDCl₃): δ = 8.90 (dd, *J* = 4.2, 1.7 Hz, 1H), 8.23 (dd, *J* = 8.3, 1.7 Hz, 1H), 8.02–7.99 (m, 2H), 7.82 (dd, *J* = 7.3, 1.4 Hz, 1H), 7.67 (t, *J* = 7.4 Hz, 1H), 7.51 (dd, *J* = 7.4, 1.0 Hz, 1H), 7.46–7.42 (m, 3H), 7.41–7.37 (m, 1H), 7.31–7.25 (m, 2H), 7.21–7.15 (m, 2H), 5.96 (s, 1H), 3.81 (3H).

^{13}C -NMR (100 MHz, CDCl_3): δ = 167.0 (C_q), 166.7 (C_q), 151.3 (CH), 144.9 (C_q), 140.4 (C_q), 139.8 (C_q), 136.3 (CH), 135.2 (C_q), 132.6 (C_q), 131.9 (CH), 131.4 (CH), 130.5 (C_q), 129.8 (CH), 129.7 (CH), 129.6 (CH), 129.5 (CH), 129.1 (C_q), 127.3 (C_q), 126.3 (CH), 123.9 (CH), 123.2 (CH), 121.9 (CH), 110.6 (CH), 52.1 (CH_3).

IR (ATR): 3050, 1712, 1604, 1472, 1276, 1107, 791, 732 cm^{-1} .

MS (ESI) m/z (relative intensity): 429 (10) $[\text{M}+\text{Na}]^+$, 407 (100) $[\text{M}+\text{H}]^+$.

HR-MS (ESI): m/z calcd for $\text{C}_{26}\text{H}_{19}\text{N}_2\text{O}_3$ $[\text{M}+\text{H}]^+$: 407.1390, found: 407.1397.



(Z)-4-[(3-Oxo-2-(quinolin-8-yl) isoindolin-1-ylidene) methyl] benzonitrile (256aj): The general procedure **J** was followed using benzamide **229a** (62 mg, 0.25 mmol) and alkyne **255j** (64 mg, 0.50 mmol). Purification by column chromatography on silica gel (*n*-hexane/EtOAc: 1/1) yielded **256aj** (61.5 mg, 66%, *E/Z* = 1:6) as a white solid. M. p.: 235–242 °C.

Resonances are reported for (*Z*)-**256aj**. ^1H -NMR (400 MHz, CDCl_3): δ = 8.83 (dd, J = 4.2, 1.7 Hz, 1H), 8.06–7.97 (m, 2H), 7.89 (d, J = 7.7 Hz, 1H), 7.72 (t, J = 7.6 Hz, 1H), 7.67 (dd, J = 8.2, 1.4 Hz, 1H), 7.65–7.59 (m, 1H), 7.54 (d, J = 6.5 Hz, 1H), 7.41–7.30 (m, 2H), 6.80 (d, J = 8.2 Hz, 2H), 6.71 (s, 1H), 6.66 (d, J = 8.2 Hz, 2H).

^{13}C -NMR (100 MHz, CDCl_3): δ = 167.9 (C_q), 150.5 (CH), 144.1 (C_q), 138.8 (C_q), 138.2 (C_q), 138.0 (C_q), 136.0 (CH), 133.9 (C_q), 132.6 (CH), 130.1 (CH), 129.8 (CH), 128.9 (C_q), 128.8 (CH), 128.7 (CH), 128.3 (C_q), 125.8 (CH), 124.1 (CH), 121.6 (CH), 119.9 (CH), 118.7 (C_q), 109.5 (CH), 109.2 (C_q), 104.6 (CH).

Resonances are reported for (*E*)-**256aj**. ^1H -NMR (400 MHz, CDCl_3): δ = 8.93 (dd, J = 4.2, 1.7 Hz, 1H), 8.27 (dd, J = 8.3, 1.7 Hz, 1H), 8.05–8.02 (m, 2H), 7.85 (dd, J = 7.3, 1.4 Hz, 1H), 7.72 (dd, J = 7.5, 1.1 Hz, 1H), 7.66–7.59 (m, 2H), 7.58–7.55 (m, 1H), 7.52–7.42 (m, 5H), 5.93 (s, 1H).

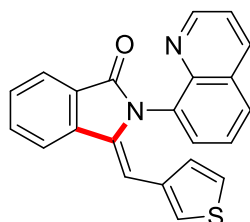
^{13}C -NMR (100 MHz, CDCl_3): δ = 166.9 (C_q), 151.3 (CH), 144.9 (C_q), 140.6 (C_q), 140.4 (C_q), 138.8 (C_q), 136.4 (CH), 136.0 (CH), 134.9 (C_q), 132.5 (C_q), 132.2 (CH), 132.1 (CH), 131.4 (CH), 130.6 (C_q), 130.3 (CH), 130.2 (CH), 129.8 (CH), 129.6 (C_q), 126.4 (CH), 123.0 (CH), 122.0 (CH), 118.8 (CH), 111.0 (C_q).

IR (ATR): 3047, 1704, 1650, 1597, 1470, 1144, 754 cm^{-1} .

MS (ESI) m/z (relative intensity): 396 (20) $[\text{M}+\text{Na}]^+$, 374 (100) $[\text{M}+\text{H}]^+$.

5. Experimental Part

HR-MS (ESI): m/z calcd for $C_{25}H_{16}N_3O$ $[M+H]^+$: 374.1288, found: 374.1295. The analytical data correspond with those reported in the literature.^[208]



(Z)-2-(Quinolin-8-yl)-3-(thiophen-3-ylmethylene) isoindolin-1-one (256ak): The general procedure **J** was followed using benzamide **229a** (73 mg, 0.25 mmol) and alkyne **255k** (54 mg, 0.50 mmol) with $Cu(OAc)_2 \cdot H_2O$ (5.0 mg, 10 mol %). Purification by column chromatography on silica gel (*n*-hexane/EtOAc: 2/1) yielded **256ak** (66 mg, 75%, *E/Z* = 1:3) as a yellow solid. M. p.: 170–175 °C.

Resonances reported for (*Z*)-**256ak**: 1H -NMR (300 MHz, $CDCl_3$): δ = 8.83 (dd, J = 4.1, 1.8 Hz, 1H), 8.04 (dd, J = 8.4, 1.7 Hz, 1H), 7.96 (d, J = 7.7 Hz, 1H), 7.84 (d, J = 7.9 Hz, 1H), 7.68 (dd, J = 8.0, 5.8 Hz, 2H), 7.56–7.52 (m, 2H), 7.39 (d, J = 7.9 Hz, 1H), 7.37–7.28 (m, 1H), 6.65 (s, 1H), 6.54 (dd, J = 5.0, 3.0 Hz, 1H), 6.20 (d, J = 4.3 Hz, 2H).

^{13}C -NMR (100 MHz, $CDCl_3$): δ = 168.0 (C_q), 150.5 (CH), 144.6 (C_q), 138.6 (C_q), 136.2 (C_q), 135.9 (CH), 134.2 (C_q), 133.8 (C_q), 132.2 (CH), 129.8 (CH), 129.0 (CH), 128.9 (C_q), 128.5 (CH), 128.2 (C_q), 127.9 (CH), 125.8 (CH), 123.9 (CH), 123.0 (CH), 122.8 (CH), 121.4 (CH), 119.5 (CH), 101.8 (CH).

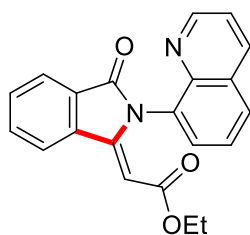
Resonances reported for (*E*)-**256ak**: 1H -NMR (300 MHz, $CDCl_3$): δ = 8.91 (dd, J = 4.1, 1.8 Hz, 1H), 8.23 (dd, J = 8.4, 1.7 Hz, 1H), 7.96 (d, J = 7.7 Hz, 2H), 7.84 (d, J = 7.9 Hz, 1H), 7.73–7.61 (m, 2H), 7.54 (t, J = 7.4 Hz, 1H), 7.49–7.42 (m, 2H), 7.37–7.27 (m, 2H), 7.07 (d, J = 5.0 Hz, 1H), 5.85 (s, 1H).

^{13}C -NMR (100 MHz, $CDCl_3$): δ = 166.9 (C_q), 151.3 (CH), 145.0 (C_q), 139.2 (C_q), 136.3 (CH), 135.5 (C_q), 134.2 (C_q), 132.8 (C_q), 131.8 (CH), 131.4 (CH), 130.3 (C_q), 129.6 (C_q), 129.5 (CH), 129.4 (CH), 128.9 (CH), 126.3 (CH), 125.7 (CH), 124.0 (CH), 123.8 (CH), 123.2 (CH), 121.8 (CH), 106.2 (CH).

IR (ATR): 3021, 1709, 1501, 1473, 1397, 827, 789 cm^{-1} .

MS (ESI) m/z (relative intensity): 377 (10) $[M+Na]^+$, 355 (100) $[M+H]^+$.

HR-MS (ESI): m/z calcd for $C_{22}H_{15}N_2OS$ $[M+H]^+$: 355.0900, found: 355.0902.



(Z)-Ethyl 2-(3-oxo-2-(quinolin-8-yl) isoindolin-1-ylidene)acetate (256al): The general procedure **J** was followed using benzamide **229a** (73 mg, 0.25 mmol) and alkyne **2551** (49 mg, 0.50 mmol) with $\text{Cu}(\text{OAc})_2 \cdot \text{H}_2\text{O}$ (10.0 mg, 20 mol %). Purification by column chromatography on silica gel (*n*-hexane/EtOAc: 1/3) yielded **256al** (36.2 mg, 42%, *E/Z* = 1:5) as a yellow oil.

Resonances are reported for (*Z*)-**256al**: $^1\text{H-NMR}$ (400 MHz, CDCl_3): δ = 8.88 (dd, J = 4.4, 1.7 Hz, 1H), 8.24 (dd, J = 8.3, 1.7 Hz, 1H), 7.99 (dd, J = 7.5, 1.0 Hz, 1H), 7.94 (dd, J = 8.3, 1.4 Hz, 1H), 7.83 (dd, J = 7.3, 1.0 Hz, 1H), 7.78 (dd, J = 7.3, 1.4 Hz, 1H), 7.74–7.64 (m, 3H), 7.43 (dd, J = 8.3, 4.2 Hz, 1H), 5.98 (s, 1H), 3.45 (dq, J = 10.9, 7.1 Hz, 1H), 3.26 (dq, J = 10.9, 7.1 Hz, 1H), 0.72 (t, J = 7.1, 0.7 Hz, 3H).

$^{13}\text{C-NMR}$ (100 MHz, CDCl_3): δ = 168.4 (C_q), 164.3 (C_q), 150.6 (CH), 144.9 (C_q), 144.0 (C_q), 138.0 (C_q), 136.2 (CH), 134.5 (C_q), 132.9 (CH), 130.9 (CH), 129.4 (CH), 128.9 (C_q), 128.7 (CH), 128.2 (C_q), 126.1 (CH), 124.3 (CH), 121.5 (CH), 120.4 (CH), 95.5 (CH), 60.1 (CH_2), 13.6 (CH_3).

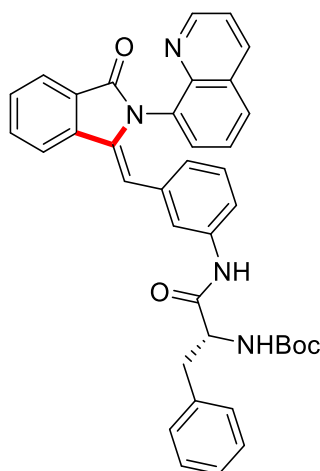
Resonances are reported for (*E*)-**256al**: $^1\text{H-NMR}$ (400 MHz, CDCl_3): δ = 9.23 (dd, J = 7.9, 0.9 Hz, 1H), 8.90 (d, J = 1.6 Hz, 1H), 8.30–8.26 (m, 1H), 8.07–8.00 (m, 2H), 7.75 (dd, J = 6.5, 1.1 Hz, 3H), 7.73–7.62 (m, 1H), 7.48 (dd, J = 8.3, 4.2 Hz, 1H), 5.25 (s, 1H), 4.18 (qd, J = 7.1, 3.8 Hz, 2H), 1.24 (t, J = 7.0 Hz, 3H).

$^{13}\text{C-NMR}$ (100 MHz, CDCl_3): δ = 167.6 (C_q), 166.1 (C_q), 151.5 (CH), 150.8 (C_q), 144.7 (C_q), 136.3 (CH), 134.3 (C_q), 133.3 (CH), 131.9 (C_q), 131.4 (CH), 131.3 (CH), 130.3 (C_q), 130.0 (CH), 129.6 (C_q), 128.4 (CH), 126.4 (CH), 123.7 (CH), 122.1 (CH), 100.2 (CH), 60.3 (CH_2), 14.2 (CH_3).

IR (ATR): 3010, 1705, 1601, 1533, 1290, 855, 770, 728 cm^{-1} .

MS (ESI) m/z (relative intensity): 345 (100) $[\text{M}+\text{H}]^+$.

HR-MS (ESI): m/z calcd for $\text{C}_{21}\text{H}_{17}\text{N}_2\text{O}_3$ $[\text{M}+\text{H}]^+$: 345.1234, found: 345.1232.



(*S,Z*)-tert-Butyl-((1-oxo-1-((3-((3-oxo-2-(quinolin-8-yl) isoindolin-1-ylidene) methyl) phenyl) amino)-3-phenylpropan-2-yl) carbamate (256am): The general procedure **J** was followed using benzamide **229a** (73 mg, 0.25 mmol) and alkyne **255m** (182 mg, 0.50 mmol) with $\text{Cu}(\text{OAc})_2 \cdot \text{H}_2\text{O}$ (5.0 mg, 10 mol %). Purification by column chromatography on silica gel (*n*-hexane/EtOAc: 2/1) yielded **256am** (106.7 mg, 70%, *E/Z* = 1:6) as a yellow oil.

Resonances are reported for (*Z*)-**256am**: $^1\text{H-NMR}$ (400 MHz, CDCl_3): δ = 8.78 (dd, J = 4.0, 1.1 Hz, 1H), 7.95 (d, J = 7.5 Hz, 1H), 7.86–7.78 (m, 2H), 7.69–7.61 (m, 1H), 7.54 (t, J = 7.5 Hz, 1H), 7.48–7.43 (m, 1H), 7.38 (d, J = 7.1 Hz, 1H), 7.32–7.27 (m, 3H), 7.24–7.14 (m, 5H), 6.85 (d, J = 8.0 Hz, 1H), 6.68 (s, 1H), 6.52–6.40 (m, 2H), 6.26 (dd, J = 12.6, 7.6 Hz, 1H), 5.06 (s, 1H), 4.31 (s, 1H), 3.14–2.92 (m, 2H), 1.43 (s, 9H).

$^{13}\text{C-NMR}$ (100 MHz, CDCl_3): δ = 167.9 (C_q), 167.8 (C_q), 167.1 (C_q), 149.4 (CH), 143.3 (C_q), 137.6 (C_q), 135.5 (CH), 135.5 (C_q), 134.9 (CH), 134.8 (CH), 134.7 (C_q), 133.3 (C_q), 133.1 (C_q), 131.3 (CH), 129.0 (C_q), 128.4 (C_q), 128.3 (CH), 128.2 (CH), 128.0 (CH), 127.4 (CH), 127.3 (C_q), 126.0 (CH), 124.8 (CH), 124.7 (CH), 123.4 (CH), 123.0 (CH), 120.3 (CH), 120.2 (CH), 118.9 (CH), 118.7 (CH), 105.6 (CH), 79.7 (C_q), 55.5 (CH), 37.1 (CH₂), 27.3 (CH₃).

Resonances are reported for (*E*)-**256am**: $^1\text{H-NMR}$ (400 MHz, CDCl_3): δ = 8.88 (dd, J = 4.0, 1.1 Hz, 1H), 8.21 (d, J = 7.9 Hz, 1H), 7.95 (d, J = 7.4 Hz, 2H), 7.89–7.75 (m, 2H), 7.65 (t, J = 7.4 Hz, 1H), 7.50 (d, J = 1.1 Hz, 1H), 7.43–7.36 (m, 3H), 7.35–7.24 (m, 2H), 7.22–7.14 (m, 2H), 7.11 (d, J = 6.9 Hz, 2H), 7.07–6.98 (m, 3H), 5.90 (s, 1H), 5.13 (s, 1H), 4.42 (s, 1H), 3.15–2.91 (m, 2H), 1.36 (s, 9H).

$^{13}\text{C-NMR}$ (100 MHz, CDCl_3): δ = 168.7 (C_q), 166.1 (C_q), 154.8 (CH), 150.3 (CH), 144.0 (C_q), 138.1 (C_q), 136.6 (C_q), 135.7 (CH), 135.6 (CH), 135.3 (C_q), 135.1 (C_q), 134.3 (C_q), 133.3 (C_q), 131.8 (CH), 130.9 (CH), 130.4 (C_q), 129.4 (CH), 128.5 (CH), 128.5 (C_q), 127.8 (CH), 126.2 (C_q), 125.9 (CH), 125.4 (CH), 124.6 (CH), 122.8 (CH), 122.5 (CH), 120.9 (CH), 119.9 (CH), 118.2 (CH), 116.9 (CH), 116.8 (CH), 110.6 (CH), 79.7 (C_q), 55.5 (CH), 37.3 (CH₂), 27.3 (CH₃).

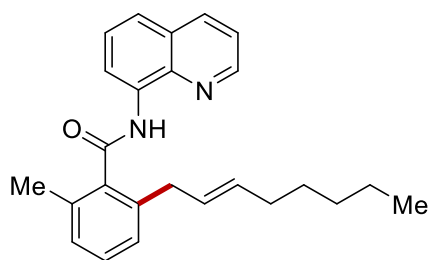
IR (ATR): 3022, 1721, 1652, 1542, 1244, 872, 791, 711 cm^{-1} .

MS (ESI) m/z (relative intensity): 633 (10) $[\text{M}+\text{Na}]^+$, 611 (100) $[\text{M}+\text{H}]^+$.

HR-MS (ESI): m/z calcd for $\text{C}_{38}\text{H}_{34}\text{N}_4\text{O}_4\text{Na}$ $[\text{M}+\text{Na}]^+$: 633.2472, found: 633.2475.

5.8. Electrochemical Cobalt-catalyzed C–H Alkylation

5.8.1. Characterization Data



(E)-2-Methyl-6-(oct-2-en-1-yl)-N-(quinolin-8-yl)benzamide (242fo): The general procedure **K** was followed using 2-methyl-*N*-(quinolin-8-yl)benzamide (**229f**) (131.1 mg, 0.50 mmol) and *n*-octene (**223o**) (168.0 mg, 1.5 mmol). Isolation by column chromatography (*n*-hexane/EtOAc = 10:1) yielded **242fo** (112.0 mg, 60%) as a colourless oil.

$^1\text{H-NMR}$ (400 MHz, CDCl_3): δ = 9.90 (s, 1H), 8.98 (dd, J = 7.4, 1.7 Hz, 1H), 8.72 (dd, J = 4.2, 1.7 Hz, 1H), 8.15 (dd, J = 8.3, 1.7 Hz, 1H), 7.61–7.57 (m, 1H), 7.54 (dd, J = 8.3, 1.7 Hz, 1H), 7.42 (dd, J = 8.3, 4.2 Hz, 1H), 7.26 (dd, J = 7.4, 1.7 Hz, 1H), 7.16–7.07 (m, 2H), 5.54 (dtt, J = 14.7, 6.6, 1.4 Hz, 1H), 5.40 (dtt, J = 14.7, 6.6, 1.4 Hz, 1H), 3.43 (d, J = 6.6 Hz, 2H), 2.42 (s, 3H), 1.88–1.73 (m, 2H), 1.18–1.06 (m, 6H), 0.77 (t, J = 6.2 Hz, 3H).

$^{13}\text{C-NMR}$ (100 MHz, CDCl_3): δ = 168.7 (C_q), 148.2 (CH), 138.5 (C_q), 137.8 (C_q), 137.7 (C_q), 136.3 (CH), 134.7 (C_q), 134.4 (C_q), 132.5 (CH), 129.1 (CH), 128.1 (CH), 128.1 (CH), 128.0 (C_q), 127.4 (CH), 127.0 (CH), 121.9 (CH), 121.6 (CH), 116.8 (CH), 36.7 (CH_2), 32.4 (CH_2), 31.4 (CH_2), 28.9 (CH_2), 22.4 (CH_2), 19.5 (CH_3), 14.0 (CH_3).

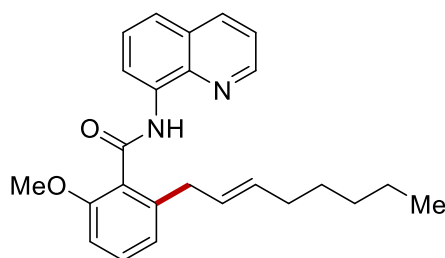
IR (ATR): 2947, 1675, 1582, 1429, 1296, 970, 800, 710 cm^{-1} .

MS (ESI) m/z (relative intensity): 395 (20) $[\text{M}+\text{Na}]^+$, 373 (100) $[\text{M}+\text{H}]^+$.

HR-MS (ESI): m/z calcd. for $[\text{C}_{25}\text{H}_{28}\text{N}_2\text{O}+\text{Na}]^+$ 395.2094 found 395.2087.

The analytical data correspond with those reported in the literature.^[193]

5. Experimental Part



(E)-2-Methoxy-6-(oct-2-en-1-yl)-N-(quinolin-8-yl)benzamide (242eo): A modified general procedure **K** was followed using 2-methoxy-*N*-(quinolin-8-yl)benzamide (**229e**) (140.0 mg, 0.50 mmol) and *n*-octene (**223o**) (168.0 mg, 1.5 mmol) with Co(OAc)₂·4H₂O (25.4 mg, 0.1 mmol, 20 mol %). Isolation by column chromatography (*n*-hexane/EtOAc = 5:1) yielded **242eo** (106.5 mg, 55%) as a yellow oil.

¹H-NMR (400 MHz, CDCl₃): δ = 10.04 (s, 1H), 8.99 (dd, *J* = 7.5, 1.5 Hz, 1H), 8.72 (dd, *J* = 4.2, 1.5 Hz, 1H), 8.14 (dd, *J* = 8.3, 1.5 Hz, 1H), 7.58 (dd, *J* = 8.3, 7.5 Hz, 1H), 7.51 (dd, *J* = 8.3, 1.5 Hz, 1H), 7.41 (dd, *J* = 8.3, 4.2 Hz, 1H), 7.32 (dd, *J* = 8.3, 7.5 Hz, 1H), 6.90 (dd, *J* = 7.7, 1.0 Hz, 1H), 6.84 (dd, *J* = 8.4, 0.9 Hz, 1H), 5.55 (dt, *J* = 15.2, 6.6, 1.2 Hz, 1H), 5.42 (dt, *J* = 15.2, 6.6, 1.2 Hz, 1H), 3.82 (s, 3H), 3.49–3.41 (m, 2H), 1.87–1.76 (m, 2H), 1.18–1.04 (m, 6H), 0.76 (t, *J* = 6.4 Hz, 3H).

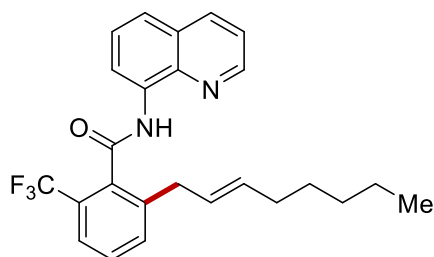
¹³C-NMR (100 MHz, CDCl₃): δ = 166.3 (C_q), 156.4 (C_q), 148.0 (CH), 140.3 (C_q), 138.5 (C_q), 136.2 (CH), 134.8 (C_q), 132.5 (CH), 130.2 (CH), 128.0 (C_q), 127.9 (CH), 127.4 (CH), 126.9 (C_q), 122.0 (CH), 121.6 (CH), 121.5 (CH), 116.7 (CH), 108.8 (CH), 55.8 (CH₃), 36.4 (CH₂), 32.3 (CH₂), 31.3 (CH₂), 28.8 (CH₂), 22.4 (CH₂), 14.0 (CH₃).

IR (ATR): 2922, 1656, 1590, 1492, 1322, 998, 850, 730 cm⁻¹.

MS (ESI) *m/z* (relative intensity): 411 (80) [M+Na]⁺, 389 (100) [M+H]⁺.

HR-MS (ESI): *m/z* calcd. for [C₂₅H₂₈N₂O₂+Na]⁺ 411.2043 found 411.2040.

The analytical data correspond with those reported in the literature.^[193]



(E)-2-(Oct-2-en-1-yl)-N-(quinolin-8-yl)-6-(trifluoromethyl)benzamide (242go): The general procedure **K** was followed using *N*-(quinolin-8-yl)-2-(trifluoromethyl)benzamide (**229g**) (158.4 mg, 0.50 mmol) and *n*-octene (**223o**) (168.0 mg, 1.5 mmol). Isolation by column chromatography (*n*-hexane/EtOAc = 20:1) yielded **242go** (110.3 mg, 52%) as a yellow oil.

$^1\text{H-NMR}$ (400 MHz, CDCl_3): δ = 9.98 (s, 1H), 8.95 (dd, J = 7.1, 1.7 Hz, 1H), 8.71 (dd, J = 4.2, 1.7 Hz, 1H), 8.15 (dd, J = 8.3, 1.7 Hz, 1H), 7.64–7.56 (m, 3H), 7.55–7.48 (m, 2H), 7.42 (dd, J = 8.3, 4.2 Hz, 1H), 5.59–5.49 (m, 1H), 5.48–5.38 (m, 1H), 3.49 (d, J = 6.8 Hz, 2H), 1.86–1.78 (m, 2H), 1.20–1.07 (m, 6H), 0.79 (t, J = 6.2 Hz, 3H).

$^{13}\text{C-NMR}$ (100 MHz, CDCl_3) (one resonance is missing due to overlap): δ = 165.5 (C_q), 148.3 (CH), 139.9 (C_q), 138.4 (C_q), 136.3 (CH), 135.1 (q, $^3J_{\text{C-F}}$ = 1.9 Hz, C_q), 134.1 (C_q), 133.4 (CH), 129.3 (CH), 128.0 (C_q), 127.4 (CH), 127.4 (q, $^2J_{\text{C-F}}$ = 30.1 Hz, C_q), 127.1 (CH), 124.0 (q, $^3J_{\text{C-F}}$ = 4.7 Hz, CH), 123.8 (q, $^1J_{\text{C-F}}$ = 270.4, C_q), 122.2 (CH), 121.7 (CH), 116.9 (CH), 36.3 (CH_2), 32.3 (CH_2), 31.3 (CH_2), 28.7 (CH_2), 22.4 (CH_2), 14.0 (CH_3).

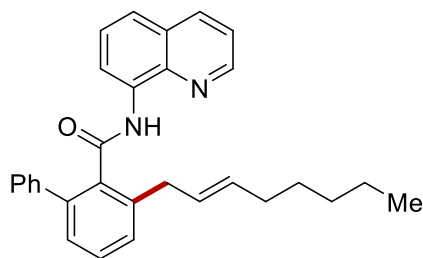
$^{19}\text{F-NMR}$ (375 MHz, CDCl_3): δ = -58.8.

IR (ATR): 3328, 1720, 1670, 1532, 1422, 1350, 980, 720, cm^{-1} .

MS (ESI) m/z (relative intensity): 449 (70) $[\text{M}+\text{Na}]^+$, 427 (100) $[\text{M}+\text{H}]^+$.

HR-MS (ESI): m/z calcd. for $[\text{C}_{25}\text{H}_{25}\text{N}_2\text{O}_2\text{F}_3+\text{Na}]^+$ 449.1811 found 449.1804.

The analytical data correspond with those reported in the literature.^[192]



(E)-3-(Oct-2-en-1-yl)-N-(quinolin-8-yl)-[1,1'-biphenyl]-2-carboxamide (242co): The general procedure **K** was followed using *N*-(quinolin-8-yl)-[1,1'-biphenyl]-2-carboxamide (**229c**) (162.0 mg, 0.50 mmol) and *n*-octene (**223o**) (168.0 mg, 1.5 mmol). Isolation by column chromatography (*n*-hexane/EtOAc = 10:1) yielded **242co** (119.1 mg, 55%) as a yellow oil.

$^1\text{H-NMR}$ (400 MHz, CDCl_3): δ = 9.66 (s, 1H), 8.80 (dd, J = 7.4, 1.8 Hz, 1H), 8.63 (dd, J = 4.2, 1.8 Hz, 1H), 8.09 (dd, J = 8.3, 1.8 Hz, 1H), 7.59–7.45 (m, 5H), 7.40–7.34 (m, 3H), 7.24 (d, J = 7.7 Hz, 2H), 7.18–7.07 (m, 1H), 5.73–5.58 (m, 1H), 5.56–5.40 (m, 1H), 3.61 (d, J = 6.7 Hz, 2H), 1.95–1.75 (m, 2H), 1.27–1.05 (m, 6H), 0.80 (t, J = 6.6 Hz, 3H).

$^{13}\text{C-NMR}$ (100 MHz, CDCl_3): δ = 168.1 (C_q), 147.9 (CH), 140.4 (C_q), 139.8 (C_q), 139.0 (C_q), 138.4 (C_q), 136.6 (C_q), 136.0 (CH), 134.4 (C_q), 132.6 (CH), 129.3 (CH), 128.8 (CH), 128.7 (CH), 128.2 (CH), 128.0 (CH), 128.0 (CH), 127.8 (C_q), 127.3 (CH), 127.3 (CH), 121.6 (CH), 121.4 (CH), 116.5 (CH), 36.8 (CH_2), 32.4 (CH_2), 31.4 (CH_2), 28.9 (CH_2), 22.4 (CH_2), 14.0 (CH_3).

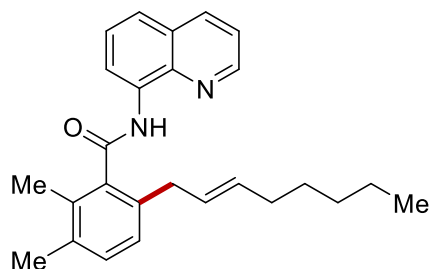
IR (ATR): 2955, 1678, 1522, 1502, 1472, 1290, 932, cm^{-1} .

MS (ESI) m/z (relative intensity): 457 (30) $[\text{M}+\text{Na}]^+$, 435 (100) $[\text{M}+\text{H}]^+$.

5. Experimental Part

HR-MS (ESI): m/z calcd. for $[C_{30}H_{30}N_2O+Na]^+$ 457.2256 found 457.2252.

The analytical data correspond with those reported in the literature.^[192]



(E)-2,3-Dimethyl-6-(oct-2-en-1-yl)-N-(quinolin-8-yl)benzamide (242ho): The general procedure **K** was followed using 2,3-dimethyl-*N*-(quinolin-8-yl)benzamide (**229h**) (138.1 mg, 0.50 mmol) and *n*-octene (**223o**) (168.0 mg, 1.5 mmol). Isolation by column chromatography (*n*-hexane/EtOAc = 30:1) yielded **242ho** (114.0 mg, 59%) as a yellow oil.

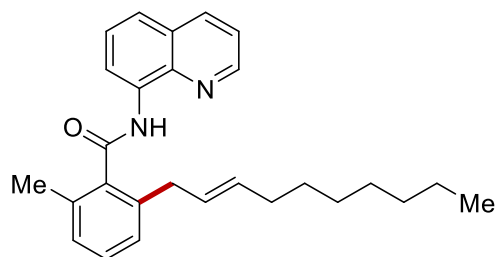
¹H-NMR (300 MHz, CDCl₃): δ = 9.90 (s, 1H), 9.00 (dd, J = 7.3, 1.7 Hz, 1H), 8.70 (dd, J = 4.2, 1.7 Hz, 1H), 8.15 (dd, J = 8.3, 1.7 Hz, 1H), 7.60 (dd, J = 8.3, 7.2 Hz, 1H), 7.54 (dd, J = 8.3, 1.7 Hz, 1H), 7.42 (dd, J = 8.3, 4.2 Hz, 1H), 7.16 (d, J = 7.8 Hz, 1H), 7.04 (d, J = 7.8 Hz, 1H), 5.53 (dtt, J = 15.2, 6.2, 1.2 Hz, 1H), 5.38 (dtt, J = 15.2, 6.2, 1.2 Hz, 1H), 3.40 (d, J = 6.2 Hz, 2H), 2.31 (s, 3H), 2.29 (s, 3H), 1.85–1.72 (m, 2H), 1.20–1.06 (m, 6H), 0.78 (t, J = 6.8 Hz, 3H).
¹³C-NMR (125 MHz, CDCl₃): δ = 169.1 (C_q), 148.0 (CH), 138.4 (C_q), 137.9 (C_q), 136.2 (CH), 135.1 (C_q), 134.8 (C_q), 134.4 (C_q), 132.8 (C_q), 132.1 (CH), 130.4 (CH), 128.2 (CH), 128.0 (C_q), 127.3 (CH), 126.7 (CH), 121.7 (CH), 121.5 (CH), 116.7 (CH), 36.6 (CH₂), 32.4 (CH₂), 31.4 (CH₂), 28.9 (CH₂), 22.5 (CH₂), 20.0 (CH₃), 16.7 (CH₃), 14.1 (CH₃).

IR (ATR): 2045, 1710, 1668, 1552, 1473, 1224, 1175, 865, cm⁻¹.

MS (ESI) m/z (relative intensity): 409 (90) [M+Na]⁺, 387 (100) [M+H]⁺.

HR-MS (ESI): m/z calcd. for $[C_{26}H_{30}N_2O+Na]^+$ 409.2250 found 409.2251.

The analytical data correspond with those reported in the literature.^[192]



(E)-2-(Dec-2-en-1-yl)-6-methyl-N-(quinolin-8-yl)benzamide (242fq): The general procedure **K** was followed using 2-methyl-*N*-(quinolin-8-yl)benzamide (**229f**) (131.1 mg, 0.50 mmol) and *n*-decene (**223q**) (210.1 mg, 1.5 mmol). Isolation by column chromatography (*n*-hexane/EtOAc = 10:1) yielded **242fq** (124.0 mg, 62%) as a yellow oil.

$^1\text{H-NMR}$ (600 MHz, CDCl_3): δ = 9.92 (s, 1H), 8.99 (dd, J = 7.5, 1.3 Hz, 1H), 8.71 (dd, J = 4.2, 1.7 Hz, 1H), 8.15 (dd, J = 8.3, 1.7 Hz, 1H), 7.61–7.58 (m, 1H), 7.54 (dd, J = 8.3, 1.4 Hz, 1H), 7.42 (dd, J = 8.3, 4.2 Hz, 1H), 7.27 (dd, J = 7.7, 1.4 Hz, 1H), 7.17–7.10 (m, 2H), 5.56 (dt, J = 16.5, 6.7, 1.3 Hz, 1H), 5.41 (dt, J = 16.5, 6.7, 1.3 Hz, 1H), 3.45 (d, J = 6.7 Hz, 2H), 2.43 (s, 3H), 1.87–1.77 (m, 2H), 1.25–1.20 (m, 2H), 1.17–1.07 (m, 8H), 0.84 (t, J = 7.3 Hz, 3H).

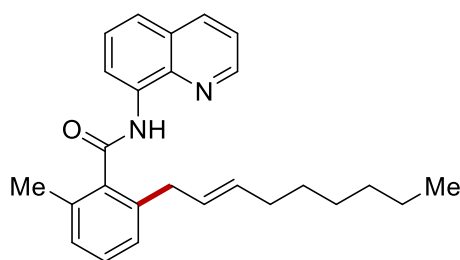
$^{13}\text{C-NMR}$ (125 MHz, CDCl_3): δ = 168.5 (C_q), 148.1 (CH), 138.4 (C_q), 137.6 (C_q), 137.6 (C_q), 136.2 (CH), 134.5 (C_q), 134.3 (C_q), 132.3 (CH), 129.0 (CH), 128.0 (CH), 127.9 (CH), 127.9 (C_q), 127.3 (CH), 126.9 (CH), 121.8 (CH), 121.5 (CH), 116.7 (CH), 36.7 (CH_2), 32.4 (CH_2), 31.8 (CH_2), 29.2 (CH_2), 29.1 (CH_2), 29.1 (CH_2), 22.7 (CH_2), 19.5 (CH_3), 14.1 (CH_3).

IR (ATR): 2977, 1688, 1533, 1405, 1299, 973, 850, 719 cm^{-1} .

MS (ESI) m/z (relative intensity): 423 (40) $[\text{M}+\text{Na}]^+$, 401 (100) $[\text{M}+\text{H}]^+$.

HR-MS (ESI): m/z calcd. for $[\text{C}_{27}\text{H}_{32}\text{N}_2\text{O}+\text{H}]^+$ 401.2587 found 401.2589.

The analytical data correspond with those reported in the literature.^[193]



(E)-2-Methyl-6-(non-2-en-1-yl)-N-(quinolin-8-yl)benzamide (242fr): The general procedure **K** was followed using 2-methyl-*N*-(quinolin-8-yl)benzamide (**229f**) (131.1 mg, 0.50 mmol) and *n*-nonene (**223r**) (189.0 mg, 1.5 mmol). Isolation by column chromatography (*n*-hexane/EtOAc = 10:1) yielded **242fr** (124.1 mg, 64%) as a yellow oil.

$^1\text{H-NMR}$ (600 MHz, CDCl_3): δ = 9.93 (s, 1H), 9.01 (dd, J = 7.6, 1.4 Hz, 1H), 8.72 (dd, J = 4.2, 1.7 Hz, 1H), 8.15 (dd, J = 8.3, 1.7 Hz, 1H), 7.60 (dd, J = 7.9 Hz, 1.7 Hz, 1H), 7.55 (dd, J = 8.3, 1.4 Hz, 1H), 7.42 (dd, J = 8.3, 4.2 Hz, 1H), 7.28 (dd, J = 7.7, 1.4 Hz, 1H), 7.15 (dd, J = 7.8, 1.2 Hz, 1H), 7.13 (d, J = 7.7 Hz, 1H), 5.57 (dt, J = 14.9, 6.7, 1.5 Hz, 1H), 5.41 (dt, J = 14.9, 6.6, 1.5 Hz, 1H), 3.46 (dd, J = 6.8, 1.5 Hz, 2H), 2.44 (s, 3H), 1.88–1.79 (m, 2H), 1.22–1.07 (m, 8H), 0.82 (t, J = 7.3 Hz, 3H).

$^{13}\text{C-NMR}$ (125 MHz, CDCl_3): δ = 168.5 (C_q), 148.0 (CH), 138.4 (C_q), 137.6 (C_q), 137.6 (C_q), 136.1 (CH), 134.5 (C_q), 134.3 (C_q), 132.3 (CH), 128.9 (CH), 128.0 (CH), 127.9 (CH), 127.9 (C_q), 127.3 (CH), 126.9 (CH), 121.8 (CH), 121.5 (CH), 116.7 (CH), 36.7 (CH_2), 32.4 (CH_2), 31.6 (CH_2), 29.1 (CH_2), 28.8 (CH_2), 22.6 (CH_2), 19.5 (CH_3), 14.1 (CH_3).

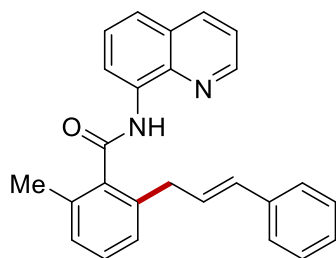
IR (ATR): 2912, 1666, 1545, 1492, 1287, 890, 811, 765 cm^{-1} .

MS (ESI) m/z (relative intensity): 409 (20) $[\text{M}+\text{Na}]^+$, 387 (100) $[\text{M}+\text{H}]^+$.

5. Experimental Part

HR-MS (ESI): m/z calcd. for $[C_{26}H_{30}N_2O+Na]^+$ 409.2250 found 409.2248.

The analytical data correspond with those reported in the literature.^[193]



(E)-2-Cinnamyl-6-methyl-N-(quinolin-8-yl)benzamide (242fa): The general procedure **K** was followed using 2-methyl-*N*-(quinolin-8-yl)benzamide (**229f**) (131.1 mg, 0.50 mmol) and allylbenzene (**223a**) (177.0 mg, 1.5 mmol). Isolation by column chromatography (*n*-hexane/EtOAc = 10:1) yielded **242fa** (100.1 mg, 53%) as a yellow oil.

¹H-NMR (600 MHz, CDCl₃): δ = 9.98 (s, 1H), 9.02 (dd, J = 7.9, 1.3 Hz, 1H), 8.48 (dd, J = 4.3, 1.7 Hz, 1H), 8.10 (dd, J = 8.3, 1.7 Hz, 1H), 7.60 (dd, J = 7.9, 1.3 Hz, 1H), 7.53 (dd, J = 8.3, 1.3 Hz, 1H), 7.34–7.29 (m, 2H), 7.22–7.20 (m, 1H), 7.17 (d, J = 7.6 Hz, 1H), 7.14–7.10 (m, 2H), 7.10–7.07 (m, 3H), 6.41–6.27 (m, 2H), 3.66 (d, J = 6.5 Hz, 2H), 2.47 (s, 3H).

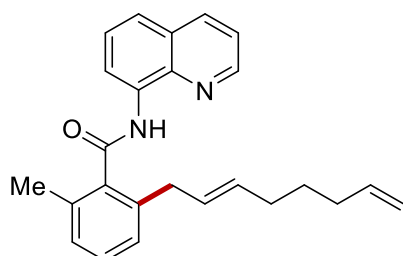
¹³C-NMR (125 MHz, CDCl₃): δ = 168.4 (C_q), 148.0 (CH), 138.2 (C_q), 137.8 (C_q), 137.1 (C_q), 136.6 (C_q), 136.0 (CH), 134.8 (C_q), 134.2 (C_q), 131.2 (CH), 129.1 (CH), 128.5 (CH), 128.3 (CH), 128.0 (CH), 127.8 (C_q), 127.2 (CH), 127.2 (CH), 126.7 (CH), 125.9 (CH), 121.9 (CH), 121.5 (CH), 116.6 (CH), 37.1 (CH₂), 19.5 (CH₃).

IR (ATR): 2952, 1671, 1570, 1477, 1223, 899, 801, 734 cm⁻¹.

MS (ESI) m/z (relative intensity): 401 (30) [M+Na]⁺, 379 (100) [M+H]⁺.

HR-MS (ESI): m/z calcd. for $[C_{26}H_{22}N_2O+H]^+$ 379.1805 found 379.1804.

The analytical data correspond with those reported in the literature.^[192]



(E)-2-Methyl-6-(octa-2,7-dien-1-yl)-N-(quinolin-8-yl)benzamide (242fs): A modified procedure **K** was followed using 2-methyl-*N*-(quinolin-8-yl)benzamide (**229f**) (131.1 mg, 0.50 mmol) and 1,7-octadiene (**223s**) (167.0 mg, 1.5 mmol) with Co(OAc)₂·4H₂O (25.4 mg,

0.1 mmol, 20 mol %). Isolation by column chromatography (*n*-hexane/EtOAc = 10:1) yielded **242fs** (98.0 mg, 53%) as a yellow oil.

¹H-NMR (600 MHz, CDCl₃): δ = 9.92 (s, 1H), 8.99 (dd, *J* = 7.6, 1.4 Hz, 1H), 8.71 (dd, *J* = 4.2, 1.7 Hz, 1H), 8.15 (dd, *J* = 8.3, 1.7 Hz, 1H), 7.62–7.58 (m, 1H), 7.55 (dd, *J* = 8.3, 1.4 Hz, 1H), 7.42 (dd, *J* = 8.3, 4.2 Hz, 1H), 7.28 (t, *J* = 7.6 Hz, 1H), 7.15–7.11 (m, 2H), 5.65 (dtt, *J* = 16.9, 10.2, 6.7 Hz, 1H), 5.58 (dtt, *J* = 15.0, 6.7, 1.4 Hz, 1H), 5.40 (dtt, *J* = 15.0, 6.7, 1.4 Hz, 1H), 5.03–4.74 (m, 2H), 3.45 (dd, *J* = 6.7, 1.4 Hz, 2H), 2.43 (s, 3H), 1.95–1.77 (m, 4H), 1.30–1.24 (m, 2H).

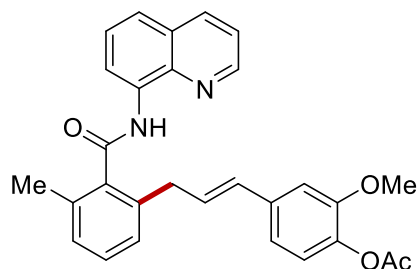
¹³C-NMR (125 MHz, CDCl₃): δ = 168.5 (C_q), 148.1 (CH), 138.6 (CH), 138.4 (C_q), 137.6 (C_q), 137.5 (C_q), 136.2 (CH), 134.6 (C_q), 134.3 (C_q), 131.8 (CH), 129.0 (CH), 128.4 (CH), 128.0 (CH), 127.9 (C_q), 127.3 (CH), 126.9 (CH), 121.8 (CH), 121.5 (CH), 116.7 (CH), 114.2 (CH₂), 36.7 (CH₂), 33.2 (CH₂), 31.8 (CH₂), 28.4 (CH₂), 19.5 (CH₃).

IR (ATR): 2910, 1651, 1561, 1432, 1297, 907, 809, 720 cm⁻¹.

MS (ESI) *m/z* (relative intensity): 393 (25) [M+Na]⁺, 371 (100) [M+H]⁺.

HR-MS (ESI): *m/z* calcd. for [C₂₅H₂₆N₂O+Na]⁺ 393.1937 found 393.1931.

The analytical data correspond with those reported in the literature.^[193]



(E)-2-Methoxy-4-{3-[3-methyl-2-(quinolin-8-ylcarbamoyl)phenyl]prop-1-en-1-yl}phenyl acetate (242fj): A modified general procedure **K** was used with 2-methyl-*N*-(quinolin-8-yl)benzamide (**229f**) (131.1 mg, 0.50 mmol) and eugenol acetate (**223j**) (309.1 mg, 1.5 mmol). After electrolysis, the mixture was transferred to a flask and the electrodes were rinsed with acetone (3 × 5.0 mL). Then the combined solvent was removed under reduced pressure and subsequent column chromatography on silica gel (*n*-hexane/EtOAc = 5:1) yielded **242fj** (132.1 mg, 57%) as a yellow oil.

¹H-NMR (400 MHz, CDCl₃): δ = 9.93 (s, 1H), 8.97 (dd, *J* = 7.5, 1.5 Hz, 1H), 8.39 (dd, *J* = 4.2, 1.7 Hz, 1H), 8.08 (dd, *J* = 8.3, 1.7 Hz, 1H), 7.58 (dd, *J* = 8.3, 7.5 Hz, 1H), 7.52 (dd, *J* = 8.3, 1.5 Hz, 1H), 7.37–7.32 (m, 1H), 7.32–7.28 (m, 1H), 7.20–7.14 (m, 2H), 6.74 (d, *J* = 8.0 Hz, 1H), 6.63–6.55 (m, 2H), 6.34–6.15 (m, 2H), 3.65 (s, 3H), 3.62 (d, *J* = 5.6 Hz, 2H), 2.44 (s, 3H), 2.27 (s, 3H).

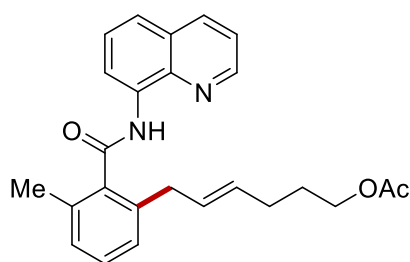
5. Experimental Part

^{13}C -NMR (100 MHz, CDCl_3): δ = 169.0 (C_q), 168.5 (C_q), 150.7 (C_q), 148.3 (CH), 138.6 (C_q), 138.3 (C_q), 138.0 (C_q), 136.5 (C_q), 136.3 (C_q), 136.0 (CH), 135.0 (C_q), 134.3 (C_q), 130.6 (CH), 129.2 (CH), 128.9 (CH), 128.5 (CH), 127.9 (C_q), 127.4 (CH), 127.2 (CH), 122.3 (CH), 122.0 (CH), 121.7 (CH), 118.5 (CH), 116.7 (CH), 109.6 (CH), 55.6 (CH_3), 37.1 (CH_2), 20.7 (CH_3), 19.5 (CH_3).

IR (ATR): 2940, 1682, 1577, 1321, 1277, 960, 808, 659 cm^{-1} .

MS (ESI) m/z (relative intensity): 489 (100) $[\text{M}+\text{Na}]^+$, 467 (90) $[\text{M}+\text{H}]^+$.

HR-MS (ESI): m/z calcd. for $[\text{C}_{29}\text{H}_{26}\text{N}_2\text{O}_4+\text{Na}]^+$ 489.1785 found 489.1777.



(E)-6-[3-Methyl-2-(quinolin-8-ylcarbamoyl)phenyl]hex-4-en-1-yl acetate (242ft): A modified general procedure **K** was used with 2-methyl-*N*-(quinolin-8-yl)benzamide (**229f**) (131.1 mg, 0.50 mmol) and hex-5-en-1-yl acetate (**223t**) (177.0 mg, 1.5 mmol). After electrolysis, the mixture was transferred to a flask and the electrodes were rinsed with acetone (3×5.0 mL). Then the combined solvent was removed under reduced pressure and subsequent column chromatography on silica gel (*n*-hexane/EtOAc = 3:1) yielded **242ft** (104.0 mg, 52%) as a yellow oil.

^1H -NMR (600 MHz, CDCl_3): δ = 9.90 (s, 1H), 8.97 (dd, J = 7.5, 1.4 Hz, 1H), 8.71 (dd, J = 4.2, 1.7 Hz, 1H), 8.15 (dd, J = 8.3, 1.7 Hz, 1H), 7.60–7.57 (m, 1H), 7.54 (dd, J = 8.3, 1.4 Hz, 1H), 7.42 (dd, J = 8.3, 4.2 Hz, 1H), 7.27 (t, J = 7.5 Hz, 1H), 7.13–7.10 (m, 2H), 5.60 (dtt, J = 15.0, 6.7, 1.5 Hz, 1H), 5.37 (dtt, J = 15.0, 6.7, 1.5 Hz, 1H), 3.89 (t, J = 6.7 Hz, 2H), 3.47–3.41 (m, 2H), 2.42 (s, 3H), 1.96 (s, 3H), 1.92–1.87 (m, 2H), 1.53–1.47 (m, 2H).

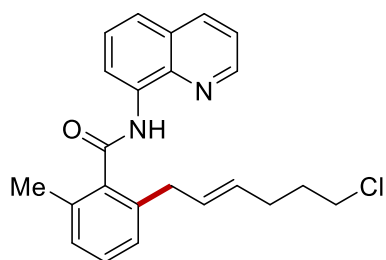
^{13}C -NMR (125 MHz, CDCl_3): δ = 170.8 (C_q), 168.4 (C_q), 148.1 (CH), 138.4 (C_q), 137.6 (C_q), 137.2 (C_q), 136.2 (CH), 134.6 (C_q), 134.2 (C_q), 130.5 (CH), 129.2 (CH), 129.0 (CH), 128.0 (CH), 127.9 (C_q), 127.3 (CH), 126.9 (CH), 121.8 (CH), 121.5 (CH), 116.7 (CH), 63.9 (CH_2), 36.6 (CH_2), 28.7 (CH_2), 28.1 (CH_2), 21.0 (CH_3), 19.5 (CH_3).

IR (ATR): 3011, 1650, 1555, 1423, 1276, 903, 801, 689 cm^{-1} .

MS (ESI) m/z (relative intensity): 425 (70) $[\text{M}+\text{Na}]^+$, 403 (90) $[\text{M}+\text{H}]^+$.

HR-MS (ESI): m/z calcd. for $[\text{C}_{25}\text{H}_{26}\text{N}_2\text{O}_3+\text{Na}]^+$ 425.1836 found 425.1829.

The analytical data correspond with those reported in the literature.^[192]



(E)-2-(6-Chlorohex-2-en-1-yl)-6-methyl-N-(quinolin-8-yl)benzamide (242fu): A modified general procedure **K** was used with 2-methyl-*N*-(quinolin-8-yl)benzamide (**229f**) (131.1 mg, 0.50 mmol) and 6-chlorohexene (**223u**) (177.0 mg, 1.5 mmol) with $\text{Co}(\text{OAc})_2 \cdot 4\text{H}_2\text{O}$ (25.4 mg, 0.1 mmol, 20 mol %). After electrolysis, the mixture was transferred to a flask and the electrodes were rinsed with acetone (3×5.0 mL). Then the combined solvent was removed under reduced pressure and subsequent column chromatography on silica gel (*n*-hexane/EtOAc = 5:1) yielded **242fu** (119.0 mg, 63%) as a yellow oil.

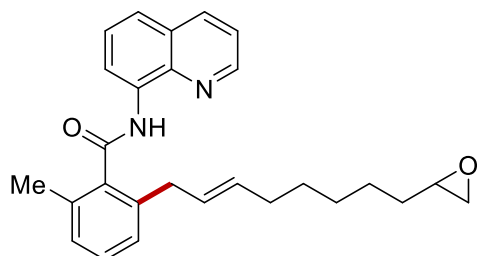
$^1\text{H-NMR}$ (400 MHz, CDCl_3): δ = 9.94 (s, 1H), 9.02 (dd, J = 7.4, 1.7 Hz, 1H), 8.77 (dd, J = 4.2, 1.7 Hz, 1H), 8.21 (dd, J = 8.3, 1.7 Hz, 1H), 7.64 (dd, J = 7.4, 1.6 Hz, 1H), 7.60 (dd, J = 8.3, 1.6 Hz, 1H), 7.47 (dd, J = 8.3, 4.2 Hz, 1H), 7.34–7.30 (m, 1H), 7.20–7.10 (m, 2H), 5.67 (dtt, J = 15.0, 6.7, 1.5 Hz, 1H), 5.38 (dtt, J = 15.0, 6.7, 1.5 Hz, 1H), 3.48 (d, J = 6.7 Hz, 2H), 3.42–3.33 (m, 2H), 2.47 (s, 3H), 2.07–1.97 (m, 2H), 1.70–1.62 (m, 2H).

$^{13}\text{C-NMR}$ (100 MHz, CDCl_3): δ = 168.6 (C_q), 148.3 (CH), 138.5 (C_q), 137.7 (C_q), 137.3 (C_q), 136.4 (CH), 134.8 (C_q), 134.4 (C_q), 130.0 (CH), 129.9 (CH), 129.2 (CH), 128.2 (CH), 128.0 (C_q), 127.4 (CH), 127.1 (CH), 122.0 (CH), 121.7 (CH), 116.8 (CH), 44.4 (CH_2), 36.7 (CH_2), 31.9 (CH_2), 29.5 (CH_2), 19.5 (CH_3).

IR (ATR): 2937, 1645, 1502, 1444, 1238, 780 cm^{-1} .

MS (ESI) m/z (relative intensity): 401 (100) $[\text{M}+\text{Na}]^+$, 379 (90) $[\text{M}+\text{H}]^+$.

HR-MS (ESI): m/z calcd. for $[\text{C}_{23}\text{H}_{23}\text{N}_2\text{O}^{35}\text{Cl}+\text{Na}]^+$ 401.1391 found 401.1394.



(E)-2-Methyl-6-[8-(oxiran-2-yl)oct-2-en-1-yl]-N-(quinolin-8-yl)benzamide (242fv): A modified general procedure **K** was used with 2-methyl-*N*-(quinolin-8-yl)benzamide (**229f**) (131.1 mg, 0.50 mmol) and 1,2-epoxy-9-decene (**223v**) (232.0 mg, 1.5 mmol) with $\text{Co}(\text{OAc})_2 \cdot 4\text{H}_2\text{O}$ (25.4 mg, 0.1 mmol, 20 mol %). After electrolysis, the mixture was transferred

5. Experimental Part

to a flask and the electrodes were rinsed with acetone (3×5.0 mL). Then the combined solvent was removed under reduced pressure and subsequent column chromatography on silica gel (*n*-hexane/EtOAc = 4:1) yielded **242fv** (118.0 mg, 57%) as a yellow oil.

$^1\text{H-NMR}$ (600 MHz, CDCl_3): δ = 9.89 (s, 1H), 8.97 (dd, J = 7.5, 1.4 Hz, 1H), 8.71 (dd, J = 4.2, 1.7 Hz, 1H), 8.16 (dd, J = 8.3, 1.7 Hz, 1H), 7.61–7.57 (m, 1H), 7.55 (dd, J = 8.3, 1.4 Hz, 1H), 7.43 (dd, J = 8.3, 4.2 Hz, 1H), 7.26 (t, J = 7.7 Hz, 1H), 7.13–7.08 (m, 2H), 5.55 (dtt, J = 15.0, 6.7, 1.4 Hz, 1H), 5.38 (dtt, J = 15.0, 6.7, 1.4 Hz, 1H), 3.46–3.41 (m, 2H), 2.82 (tdd, J = 5.7, 4.0, 2.7 Hz, 1H), 2.69 (dd, J = 5.1, 4.0 Hz, 1H), 2.42 (s, 3H), 2.40 (dd, J = 5.1, 2.7 Hz, 1H), 1.82 (d, J = 6.5 Hz, 2H), 1.43–1.38 (m, 2H), 1.34–1.22 (m, 2H), 1.20–1.14 (m, 4H).

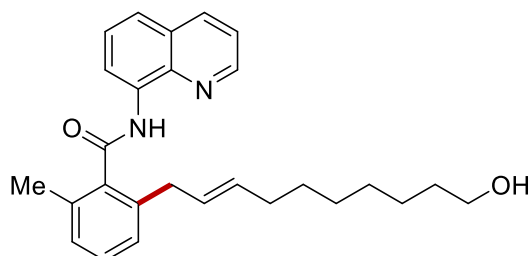
$^{13}\text{C-NMR}$ (150 MHz, CDCl_3): δ = 168.6 (C_q), 148.2 (CH), 138.5 (C_q), 137.7 (C_q), 136.3 (CH), 134.7 (C_q), 134.4 (C_q), 132.1 (CH), 129.1 (CH), 128.4 (CH), 128.1 (CH), 128.0 (C_q), 127.4 (CH), 127.0 (CH), 121.9 (CH), 121.6 (CH), 116.8 (CH), 52.3 (CH), 47.1 (CH_2), 36.7 (CH_2), 32.4 (CH_2), 32.2 (CH_2), 29.0 (CH_2), 28.9 (CH_2), 25.7 (CH_2), 19.5 (CH_3).

IR (ATR): 2921, 1688, 1566, 1430, 1154, 903, 810, 737 cm^{-1} .

MS (ESI) m/z (relative intensity): 437 (50) $[\text{M}+\text{Na}]^+$, 415 (100) $[\text{M}+\text{H}]^+$.

HR-MS (ESI): m/z calcd. for $[\text{C}_{27}\text{H}_{30}\text{N}_2\text{O}_2+\text{Na}]^+$ 437.2199 found 437.2196.

The analytical data correspond with those reported in the literature.^[193]



(E)-2-(10-Hydroxydec-2-en-1-yl)-6-methyl-N-(quinolin-8-yl)benzamide (242fx): A modified general procedure **K** was used with 2-methyl-*N*-(quinolin-8-yl)benzamide (**229f**) (131.1 mg, 0.50 mmol) and 9-decenol (**223x**) (234.0 mg, 1.5 mmol). After electrolysis, the mixture was transferred to a flask and the electrodes were rinsed with acetone (3×5.0 mL). Then the combined solvent was removed under reduced pressure and subsequent column chromatography on silica gel (*n*-hexane/EtOAc = 2:1) yielded **242fx** (114.0 mg, 55%) as a yellow oil.

$^1\text{H-NMR}$ (600 MHz, CDCl_3): δ = 9.92 (s, 1H), 8.98 (dd, J = 7.5, 1.4 Hz, 1H), 8.70 (dd, J = 4.2, 1.7 Hz, 1H), 8.14 (dd, J = 8.3, 1.7 Hz, 1H), 7.61–7.56 (m, 1H), 7.53 (dd, J = 8.3, 1.4 Hz, 1H), 7.41 (dd, J = 8.3, 4.2 Hz, 1H), 7.26 (t, 1H), 7.14–7.08 (m, 2H), 5.58–5.51 (m, 1H), 5.43–5.33

(m, 1H), 3.58–3.50 (m, 2H), 3.43 (d, $J = 6.9$ Hz, 2H), 2.42 (s, 3H), 1.83–1.78 (m, 2H), 1.49–1.42 (m, 2H), 1.24–1.18 (m, 2H), 1.16–1.07 (m, 6H).

^{13}C -NMR (125 MHz, CDCl_3): $\delta = 168.5$ (C_q), 148.0 (CH), 138.3 (C_q), 137.6 (C_q), 137.5 (C_q), 136.1 (CH), 134.5 (C_q), 134.2 (C_q), 132.2 (CH), 128.9 (CH), 128.0 (CH), 127.9 (CH), 127.9 (CH), 127.2 (CH), 126.9 (C_q), 121.8 (CH), 121.5 (CH), 116.7 (CH), 62.8 (CH_2), 36.7 (CH_2), 32.7 (CH_2), 32.3 (CH_2), 29.1 (CH_2), 29.1 (CH_2), 29.0 (CH_2), 25.6 (CH_2), 19.5 (CH_3).

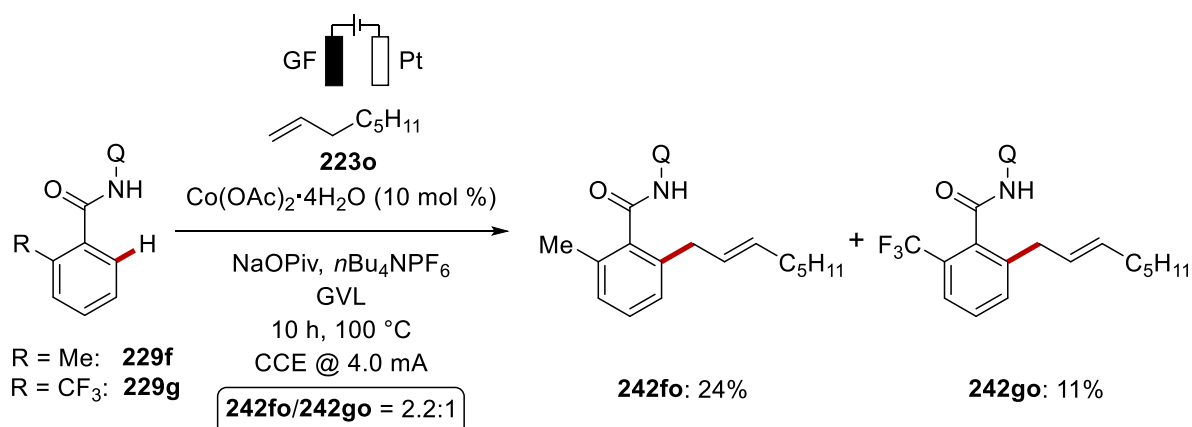
IR (ATR): 2923, 1670, 1535, 1437, 1255, 987, 850, 719 cm^{-1} .

MS (ESI) m/z (relative intensity): 439 (70) $[\text{M}+\text{Na}]^+$, 417 (100) $[\text{M}+\text{H}]^+$.

HR-MS (ESI): m/z calcd. for $[\text{C}_{27}\text{H}_{32}\text{N}_2\text{O}_2+\text{H}]^+$ 417.2537 found 417.2535.

5.8.2. Mechanistic Studies

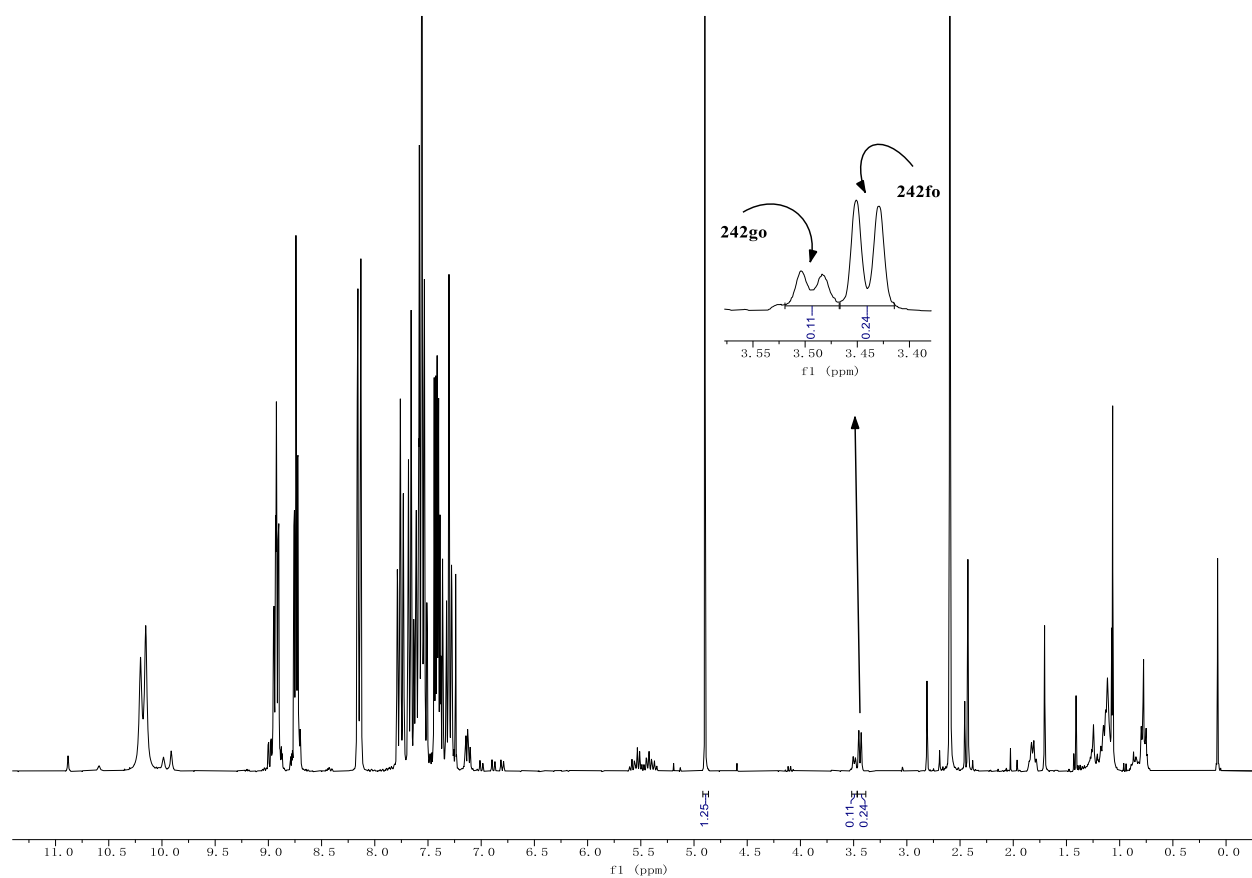
5.8.2.1. Competition Experiments



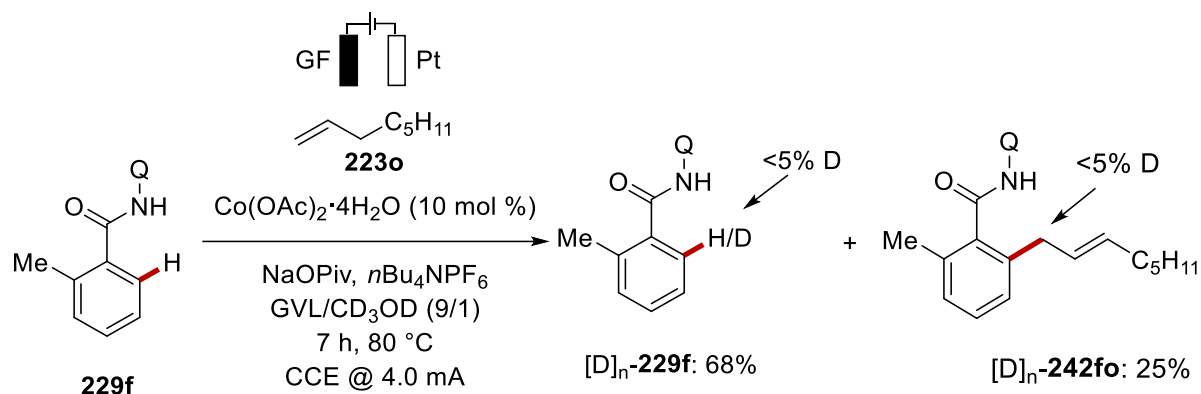
The electrocatalysis was carried out in an undivided cell with a GF anode (10 mm \times 15 mm \times 6 mm) and a Pt cathode (10 mm \times 15 mm \times 0.25 mm). Benzamide **229f** (157.2 mg, 0.60 mmol), and benzamide **229g** (189.6 mg, 0.60 mmol), *n*-octene **223o** (22.4 mg, 0.20 mmol), NaOPiv (49.6 mg, 0.40 mmol), *n*Bu₄NPF₆ (97.0 mg, 0.25 mmol), and Co(OAc)₂·4H₂O (5.0 mg, 10 mol %) were placed in a 10 mL cell and dissolved in GVL (4.0 mL). Electrocatalysis was performed at 100 °C with a constant current of 4.0 mA maintained for 10 h. At ambient temperature, the mixture was transferred to a flask and the electrodes were rinsed with acetone (3 \times 5.0 mL). Then, the solvent was removed under reduced pressure and the residue was stirred with NaOH (aq) (2 M, 15 mL) for 2 h. The mixture was extracted with H₂O (3 \times 20 mL) and successively with EtOAc (3 \times 20 mL) then the organic layer was dried over Na₂SO₄. After evaporation of the solvent *under vacuo*, the crude mixture was filtered through very short silica column. After evaporation of the solvent, dibromomethane (43.5 mg,

5. Experimental Part

0.25 mmol, 1.25 equiv) was added as an internal standard. The ratio of **242fo** and **242go** was determined by means of $^1\text{H-NMR}$ which corresponds to **242fo** (24%) and **242go** (11%).

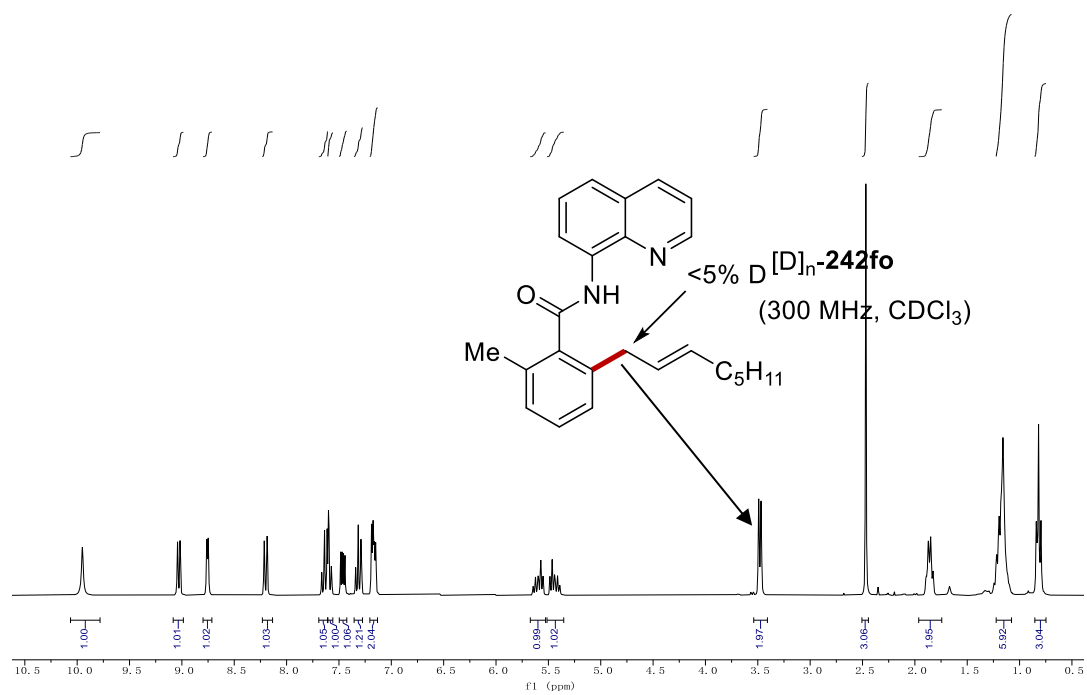
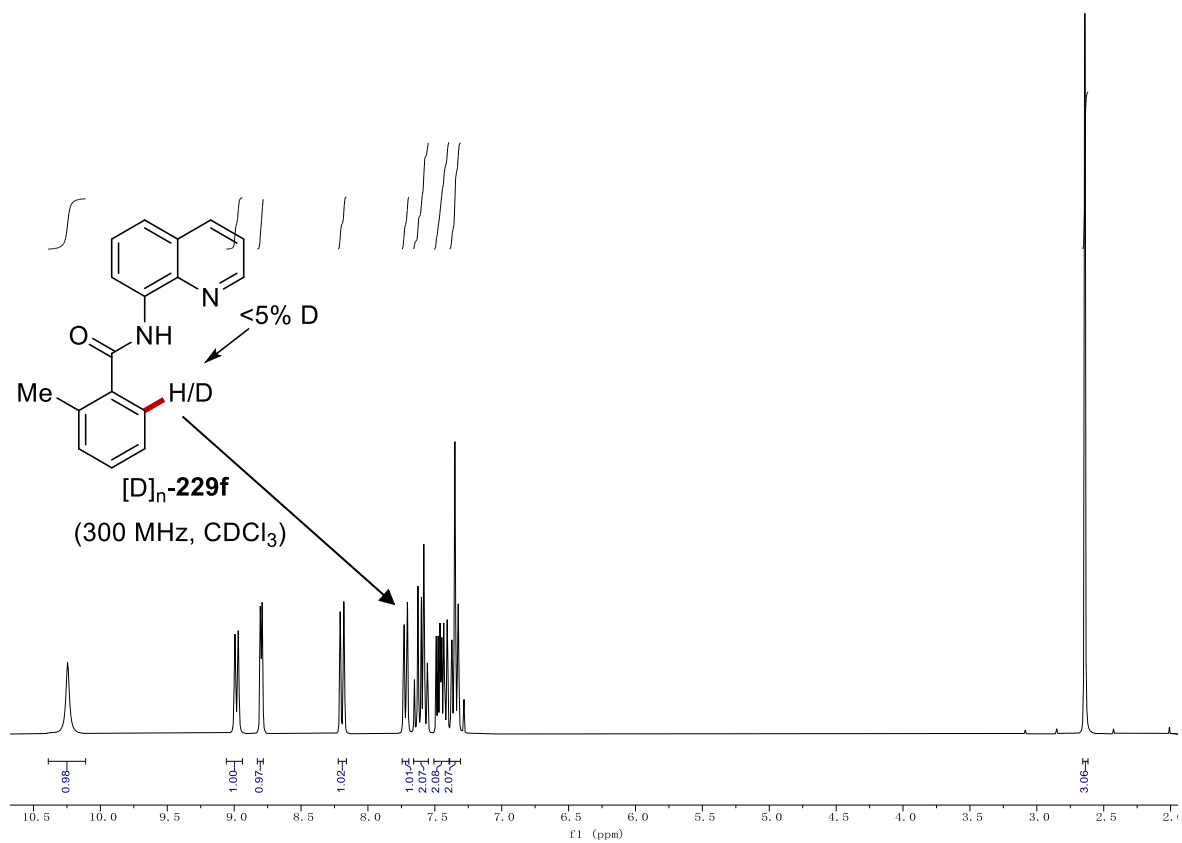


5.8.2.2. H/D Exchange Experiment



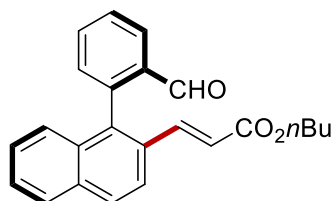
The electrocatalysis was carried out in an undivided cell with a GF anode (10 mm × 15 mm × 6 mm) and a Pt cathode (10 mm × 15 mm × 0.25 mm). Benzamide **229f** (131.1 mg, 0.50 mmol), *n*-octene **223o** (168.4 mg, 1.5 mmol), NaOPiv (124.0 mg, 1.0 mmol), $n\text{Bu}_4\text{NPF}_6$ (97.0 mg, 0.25 mmol) and $\text{Co(OAc)}_2 \cdot 4\text{H}_2\text{O}$ (12.7 mg, 10 mol %) were placed in a 10 mL cell and dissolved in GVL (3.6 mL) and CD_3OD (0.40 mL). Electrocatalysis was performed at 80 °C with a constant current of 4.0 mA maintained for 7 h. At ambient temperature, the mixture was transferred to a flask and the electrodes were rinsed with acetone (3 × 5.0 mL). Then, the combined solvent was removed under reduced pressure, the residue diluted with EtOAc (10 mL) and stirred with NaOH (aq) (2 M, 20 mL). The mixture was extracted with H_2O (3 × 20 mL) and successively with EtOAc (3 × 20 mL) then the organic layer was dried over Na_2SO_4 . After evaporation of the solvent *under vacuo* subsequently column chromatography on silica gel (*n*-hexane/EtOAc = 10:1) yielded $[\text{D}]_n$ -**229f** (89.0 mg, 68%) as a yellow solid and $[\text{D}]_n$ -**242fo** (46.6 mg, 25%) as a colorless oil. The D-incorporation was estimated by $^1\text{H-NMR}$ spectroscopy.

5. Experimental Part



5.9 Enantioselective Palladaelectro-Catalyzed C–H Activations by Transient Directing Groups

5.9.1. Characterization Data



(E)-Butyl 3-(1-(2-formylphenyl)naphthalen-2-yl)acrylate (74aa): The general procedure **L** was followed using 2-(naphthalen-1-yl)benzaldehyde (**73a**) (46.4 mg, 0.20 mmol) and *n*-butyl acrylate (**38a**) (76.9 mg, 0.60 mmol). Isolation by column chromatography (*n*-hexane/EtOAc = 5:1) yielded **74aa** (51.1 mg, 71%) as a yellow oil.

¹H-NMR (300 MHz, CDCl₃): δ = 9.49 (s, 1H), 8.19 (dd, *J* = 7.6, 0.8 Hz, 1H), 7.97 (d, *J* = 8.8 Hz, 1H), 7.93 (d, *J* = 8.1 Hz, 1H), 7.86 (d, *J* = 8.8 Hz, 1H), 7.78 (td, *J* = 8.8, 1.5 Hz, 1H), 7.69 (t, *J* = 7.4 Hz, 1H), 7.55 (d, *J* = 8.1 Hz, 1H), 7.48–7.34 (m, 3H), 7.28 (d, *J* = 8.4 Hz, 1H), 6.50 (d, *J* = 16.0 Hz, 1H), 4.13 (t, *J* = 6.5 Hz, 2H), 1.64–1.60 (m, 2H), 1.38–1.33 (m, 2H), 0.93 (t, *J* = 7.3 Hz, 3H).

¹³C-NMR (75 MHz, CDCl₃): δ = 191.3 (CH), 166.6 (C_q), 142.0 (CH), 141.3 (C_q), 136.7 (C_q), 135.3 (C_q), 134.1 (CH), 133.8 (C_q), 133.3 (C_q), 132.0 (CH), 131.2 (C_q), 129.1 (CH), 128.9 (CH), 128.2 (CH), 127.8 (CH), 127.3 (CH), 127.3 (CH), 127.0 (CH), 122.7 (CH), 120.2 (CH), 64.4 (CH₂), 30.6 (CH₂), 19.2 (CH₂), 13.7 (CH₃).

IR (ATR): 2959, 1697, 1630, 1597, 1389, 1297, 1269, 1176, 818 cm⁻¹.

MS (ESI) *m/z* (relative intensity): 381 (100) [M + Na]⁺, 359 (30) [M + H]⁺.

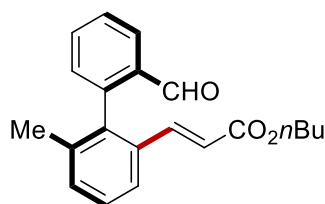
HR-MS (ESI): *m/z* calcd. for [C₂₄H₂₂O₃ + Na]⁺ 381.1461 found 381.1468.

[α]_D²⁰: –35.9 (*c* = 1.1, CHCl₃).

HPLC separation (Chiralpak[®] IA-3, *n*-hexane/*i*-PrOH 95:5, 1.0 mL/min, detection at 273 nm):

t_r (major) = 17.1 min, *t_r* (minor) = 11.2 min, 97% ee.

The analytical data correspond with those reported in the literature.^[89]



(E)-Butyl 3-(2'-formyl-6-methyl-[1,1'-biphenyl]-2-yl)acrylate (74ba)

5. Experimental Part

The general procedure **L** was followed using 2'-methyl-[1,1'-biphenyl]-2-carbaldehyde (**73b**) (39.3 mg, 0.20 mmol) and *n*-butyl acrylate (**38a**) (76.9 mg, 0.60 mmol). Isolation by column chromatography (*n*-hexane/EtOAc = 6:1) yielded **74ba** (42.6 mg, 66%) as a yellow oil. ¹H-NMR (400 MHz, CDCl₃): δ = 9.61 (s, 1H), 8.06 (dd, *J* = 7.8, 1.4 Hz, 1H), 7.69 (td, *J* = 7.5, 1.4 Hz, 1H), 7.64–7.52 (m, 2H), 7.41–7.29 (m, 2H), 7.25–7.17 (m, 2H), 6.27 (d, *J* = 15.9 Hz, 1H), 4.06 (t, *J* = 6.6 Hz, 2H), 2.00 (s, 3H), 1.64–1.46 (m, 2H), 1.39–1.20 (m, 2H), 0.89 (t, *J* = 7.4 Hz, 3H).

¹³C-NMR (100 MHz, CDCl₃): δ = 191.5 (CH), 166.5 (C_q), 142.7 (C_q), 142.4 (CH), 138.1 (C_q), 137.3 (C_q), 134.3 (CH), 134.1 (C_q), 134.0 (C_q), 131.5 (CH), 130.9 (CH), 128.5 (CH), 128.5 (CH), 128.0 (CH), 123.9 (CH), 119.9 (CH), 64.3 (CH₂), 30.6 (CH₂), 20.8 (CH₃), 19.1 (CH₂), 13.7 (CH₃).

IR (ATR): 2959, 1596, 1711, 1695, 1311, 1245, 1014, 785, 748, 699 cm⁻¹.

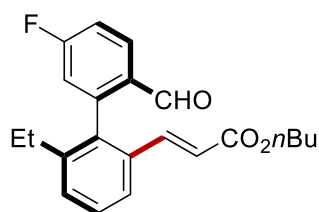
MS (ESI) *m/z* (relative intensity): 345 (100) [M + Na]⁺, 323 (5) [M + H]⁺.

HR-MS (ESI): *m/z* calcd. for [C₂₁H₂₂O₃ + Na]⁺ 345.1461 found 345.1466.

[α]_D²⁰: -35.9 (c = 1.1, CHCl₃).

HPLC separation (Chiralpak[®] IA-3, *n*-hexane/*i*-PrOH 98:2, 1.0 mL/min, detection at 273 nm): *t_r* (major) = 11.3 min, *t_r* (minor) = 10.2 min, 95% ee.

The analytical data correspond with those reported in the literature.^[89]



(E)-Butyl 3-(6-ethyl-5'-fluoro-2'-formyl-[1,1'-biphenyl]-2-yl)acrylate (74ca): The general procedure **L** was followed using 2'-ethyl-5-fluoro-[1,1'-biphenyl]-2-carbaldehyde (**73c**) (45.4 mg, 0.20 mmol) and *n*-butyl acrylate (**38a**) (76.9 mg, 0.60 mmol). Isolation by column chromatography (*n*-hexane/EtOAc = 5:1) yielded **74ca** (50.3 mg, 71%, *E/Z* = 98:2) as a yellow oil.

¹H-NMR (400 MHz, CDCl₃): δ = 9.53 (s, 1H), 8.12 (dd, *J* = 8.7, 5.9 Hz, 1H), 7.61 (dd, *J* = 7.7, 1.4 Hz, 1H), 7.50–7.35 (m, 2H), 7.34–7.23 (m, 1H), 7.19 (d, *J* = 16.0 Hz, 1H), 6.98 (dd, *J* = 8.8, 2.6 Hz, 1H), 6.31 (d, *J* = 16.0 Hz, 0.98H, *E*), 5.78 (d, *J* = 12.0 Hz, 0.02H, *Z*), 4.10 (t, *J* = 6.6 Hz, 2H), 2.35 (qd, *J* = 7.4, 3.5 Hz, 2H), 1.66–1.52 (m, 2H), 1.41–1.25 (m, 2H), 1.06 (t, *J* = 7.5 Hz, 3H), 0.92 (t, *J* = 7.4 Hz, 3H).

^{13}C -NMR (100 MHz, CDCl_3): $\delta = 189.8$ (CH), 166.4 (C_q), 166.0 (d, $^1J_{\text{C-F}} = 260.1$ Hz, C_q), 145.3 (d, $^3J_{\text{C-F}} = 8.5$ Hz, C_q), 143.1 (C_q), 142.0 (CH), 136.0 (C_q), 133.9 (C_q), 131.1 (d, $^4J_{\text{C-F}} = 2.7$ Hz, C_q), 130.7 (d, $^2J_{\text{C-F}} = 10.2$ Hz, CH) 130.1 (CH), 129.1 (CH), 123.9 (CH), 120.4 (CH), 118.2 (d, $^2J_{\text{C-F}} = 20.2$ Hz, CH), 116.2 (CH), 64.4 (CH_2), 30.6 (CH_2), 26.6 (CH_2), 19.1 (CH_2), 14.9 (CH_3), 13.7 (CH_3).

^{19}F -NMR (375 MHz, CDCl_3): $\delta = -102.4$.

IR (ATR): 2963, 1713, 1635, 1604, 1580, 1272, 1222, 1183, 799 cm^{-1} .

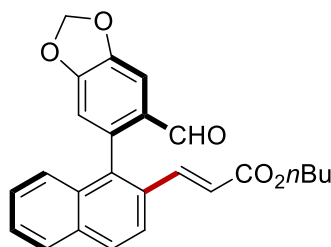
MS (ESI) m/z (relative intensity): 377 (100) $[\text{M} + \text{Na}]^+$, 355 (5) $[\text{M} + \text{H}]^+$.

HR-MS (ESI): m/z calcd. for $[\text{C}_{22}\text{H}_{23}\text{FO}_3 + \text{Na}]^+$ 377.1523 found 377.1528.

$[\alpha]_D^{20}$: -1.2 ($c = 1.2$, CHCl_3).

HPLC separation (Chiralpak® IA-3, *n*-hexane/*i*-PrOH 98:2, 1 mL/min, detection at 273 nm):

t_r (major) = 10.0 min, t_r (minor) = 8.8 min, 95% ee.



(E)-Butyl 3-(1-(6-formylbenzo[*d*][1,3]dioxol-5-yl)naphthalen-2-yl)acrylate (74da): The general procedure **L** was followed using 6-(naphthalen-1-yl)benzo[*d*][1,3]dioxole-5-carbaldehyde (**73d**) (55.2 mg, 0.20 mmol) and *n*-butyl acrylate (**38a**) (76.9 mg, 0.60 mmol). Isolation by column chromatography (*n*-hexane/EtOAc = 4:1) yielded **74da** (43.4 mg, 54%, *E/Z* = 97:3) as a yellow oil.

^1H -NMR (400 MHz, CDCl_3): $\delta = 9.34$ (s, 0.03H, *Z*), 9.23 (s, 0.97H, *E*), 7.95 (d, $J = 8.7$ Hz, 1H), 7.91 (d, $J = 8.1$ Hz, 1H), 7.84 (d, $J = 8.7$ Hz, 1H), 7.59 (s, 1H), 7.58–7.50 (m, 2H), 7.47–7.41 (m, 1H), 7.38 (d, $J = 8.5$ Hz, 1H), 6.77 (s, 1H), 6.51 (d, $J = 16.0$ Hz, 1H), 6.20 (d, $J = 3.3$ Hz, 2H), 4.16 (t, $J = 6.6$ Hz, 2H), 1.76–1.57 (m, 2H), 1.46–1.34 (m, 2H), 0.96 (t, $J = 7.4$ Hz, 3H).

^{13}C -NMR (100 MHz, CDCl_3): $\delta = 189.6$ (CH), 166.7 (C_q), 152.7 (C_q), 148.7 (C_q), 142.0 (CH), 138.5 (CH), 136.2 (C_q), 133.8 (C_q), 133.5 (C_q), 131.5 (C_q), 130.5 (C_q), 129.2 (C_q), 128.2 (CH), 127.4 (CH), 127.4 (CH), 127.0 (CH), 122.6 (CH), 120.3 (CH), 111.3 (CH), 106.4 (CH), 102.4 (CH_2), 64.5 (CH_2), 30.7 (CH_2), 19.2 (CH_2), 13.7 (CH_3).

IR (ATR): 2927, 1712, 1683, 1480, 1259, 1177, 1036, 819 cm^{-1} .

MS (ESI) m/z (relative intensity): 425 (100) $[\text{M} + \text{Na}]^+$, 403 (30) $[\text{M} + \text{H}]^+$.

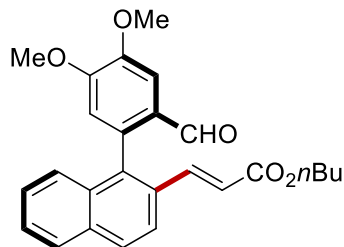
5. Experimental Part

HR-MS (ESI): m/z calcd. for $[C_{25}H_{22}O_5 + Na]^+$ 425.1359 found 425.1363.

$[\alpha]_D^{20}$: +4.0 ($c = 0.35$, $CHCl_3$).

HPLC separation (Chiralpak[®] IA-3, *n*-hexane/*i*-PrOH 90:10, 1.0 mL/min, detection at 273 nm):

t_r (major) = 16.4 min, t_r (minor) = 11.7 min, 99% ee.



(E)-Butyl 3-(1-(2-formyl-4,5-dimethoxyphenyl)naphthalen-2-yl)acrylate (74ea): The general procedure **L** was followed using 4,5-dimethoxy-2-(naphthalen-1-yl)benzaldehyde (**73e**) (58.4 mg, 0.20 mmol) and *n*-butyl acrylate (**38a**) (76.9 mg, 0.60 mmol). Isolation by column chromatography (*n*-hexane/EtOAc = 3:1) yielded **74ea** (50.3 mg, 60%) as a yellow oil. ¹H-NMR (400 MHz, CDCl₃): $\delta = 9.30$ (s, 1H), 7.96 (d, $J = 8.7$ Hz, 1H), 7.92 (d, $J = 8.1$ Hz, 1H), 7.85 (d, $J = 8.7$ Hz, 1H), 7.65 (s, 1H), 7.57–7.47 (m, 2H), 7.43 (dd, $J = 8.1, 6.6$ Hz, 1H), 7.36 (d, $J = 8.4$ Hz, 1H), 6.77 (s, 1H), 6.50 (d, $J = 15.9$ Hz, 1H), 4.14 (t, $J = 6.6$ Hz, 2H), 4.07 (s, 3H), 3.93 (s, 3H), 1.69–1.57 (m, 2H), 1.40–1.33 (h, $J = 7.4$ Hz, 2H), 0.94 (t, $J = 7.4$ Hz, 3H).

¹³C-NMR (100 MHz, CDCl₃): $\delta = 190.1$ (CH), 166.6 (C_q), 153.9 (C_q), 149.4 (C_q), 142.1 (CH), 136.4 (C_q), 136.4 (C_q), 133.8 (C_q), 133.65 (C_q), 131.5 (C_q), 129.1 (CH), 128.8 (C_q), 128.1 (CH), 127.4 (CH), 127.3 (CH), 127.1 (CH), 122.6 (CH), 120.2 (CH), 113.5 (CH), 108.5 (CH), 64.4 (CH₂), 56.4 (CH₃), 56.2 (CH₃), 30.7 (CH₂), 19.2 (CH₂), 13.7 (CH₃).

IR (ATR): 2958, 1708, 1680, 1595, 1272, 1092, 752 cm⁻¹.

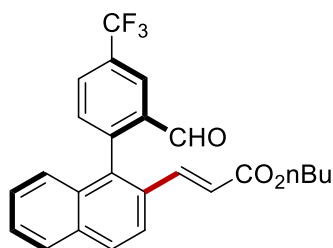
MS (ESI) m/z (relative intensity): 441 (100) [M + Na]⁺, 419 (5) [M + H]⁺.

HR-MS (ESI): m/z calcd. for $[C_{26}H_{26}O_5 + Na]^+$ 441.1672 found 441.1676.

$[\alpha]_D^{20}$: +23.7 ($c = 1.0$, $CHCl_3$).

HPLC separation (Chiralpak[®] IA-3, *n*-hexane/*i*-PrOH 95:5, 1 mL/min, detection at 273 nm): t_r (major) = 24.1 min, t_r (minor) = 21.9 min, 98% ee.

The analytical data correspond with those reported in the literature.^[89]



(E)-Butyl 3-(1-(2-formyl-4-(trifluoromethyl)phenyl)naphthalen-2-yl)acrylate (74fa): The general procedure **L** was followed using 2-(naphthalen-1-yl)-5-(trifluoromethyl)benzaldehyde (**73f**) (60.2 mg, 0.20 mmol) and *n*-butyl acrylate (**38a**) (76.9 mg, 0.60 mmol). Isolation by column chromatography (*n*-hexane/EtOAc = 5:1) yielded **74fa** (51.4 mg, 60%) as a yellow oil.

$^1\text{H-NMR}$ (400 MHz, CDCl_3): δ = 9.45 (s, 1H), 8.45–8.37 (m, 1H), 8.02–7.95 (m, 2H), 7.94–7.89 (m, 1H), 7.84 (d, J = 8.8 Hz, 1H), 7.58–7.47 (m, 2H), 7.41 (ddd, J = 8.3, 6.9, 1.3 Hz, 1H), 7.33 (d, J = 15.9 Hz, 1H), 7.16 (dd, J = 8.5, 0.9 Hz, 1H), 6.48 (d, J = 15.9 Hz, 1H), 4.09 (t, J = 6.9 Hz, 2H), 1.65–1.51 (m, 2H), 1.39–1.25 (m, 2H), 0.89 (t, J = 7.4 Hz, 3H).

$^{13}\text{C-NMR}$ (100 MHz, CDCl_3): δ = 189.7 (CH), 166.3 (C_q), 144.7 (C_q), 141.1 (CH), 135.6 (C_q), 134.8 (C_q), 133.7 (C_q), 132.9 (CH), 131.7 (C_q), 131.4 (d, $^2J_{\text{C-F}}$ = 33.8 Hz, C_q), 131.2 (C_q), 130.3 (q, $^3J_{\text{C-F}}$ = 3.2 Hz, CH), 129.7 (CH), 128.4 (CH), 127.8 (CH), 127.6 (CH), 126.4 (CH), 124.9 (q, $^3J_{\text{C-F}}$ = 3.7 Hz, CH), 123.9 (q, $^1J_{\text{C-F}}$ = 278.2 Hz, C_q), 122.7 (CH), 121.0 (CH), 64.5 (CH_2), 30.6 (CH_2), 19.1 (CH_2), 13.6 (CH_3).

$^{19}\text{F-NMR}$ (375 MHz, CDCl_3): δ = –62.9.

IR (ATR): 2961, 1701, 1615, 1330, 1173, 1131, 750, 710 cm^{-1} .

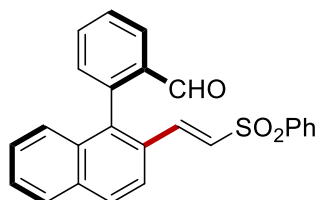
MS (ESI) m/z (relative intensity): 449 (100) $[\text{M} + \text{Na}]^+$, 427 (10) $[\text{M} + \text{H}]^+$.

HR-MS (ESI): m/z calcd. for $[\text{C}_{25}\text{H}_{21}\text{F}_3\text{O}_3 + \text{Na}]^+$ 449.1335 found 449.1336.

$[\alpha]_{\text{D}}^{20}$: –8.1 (c = 1.0, CHCl_3).

HPLC separation (Chiralpak[®] IA-3, *n*-hexane/*i*-PrOH 95:5, 1 mL/min, detection at 273 nm): t_r (major) = 11.5 min, t_r (minor) = 8.0 min, 97% ee.

The analytical data correspond with those reported in the literature.¹



(E)-2-(2-(2-(Phenylsulfonyl)vinyl)naphthalen-1-yl)benzaldehyde (74ab): The general procedure **L** was followed using 2-(naphthalen-1-yl)benzaldehyde (**73a**) (46.4 mg, 0.20 mmol) and (vinylsulfonyl)benzene (**38b**) (100.8 mg, 0.60 mmol). Isolation by column chromatography (*n*-hexane/EtOAc = 1:1) yielded **74ab** (41.4 mg, 52%) as a yellow oil.

5. Experimental Part

$^1\text{H-NMR}$ (400 MHz, CDCl_3): δ = 9.44 (s, 1H), 8.18 (dd, J = 7.7, 1.4 Hz, 1H), 7.96–7.88 (m, 2H), 7.84–7.76 (m, 3H), 7.73 (d, J = 7.6, 1.0 Hz, 1H), 7.70 (d, J = 8.5 Hz, 1H), 7.65–7.60 (m, 1H), 7.59–7.52 (m, 3H), 7.44 (dd, J = 8.2, 6.8, 1.2 Hz, 1H), 7.41–7.33 (m, 2H), 7.31 (d, J = 8.5 Hz, 1H), 6.86 (d, J = 15.6 Hz, 1H).

$^{13}\text{C-NMR}$ (100 MHz, CDCl_3): (two carbon less due to overlap) δ = 190.9 (CH), 140.4 (C_q), 140.2 (C_q), 140.1 (CH), 137.7 (C_q), 135.2 (C_q), 134.2 (CH), 134.1 (C_q), 133.5 (CH), 133.1 (C_q), 131.9 (CH), 129.6 (CH), 129.4 (CH), 129.3 (C_q), 128.3 (CH), 128.2 (CH), 127.8 (CH), 127.7 (CH), 127.6 (CH), 127.1 (CH), 122.8 (CH).

IR (ATR): 2924, 1696, 1607, 1303, 1084, 786, 742, 680 cm^{-1} .

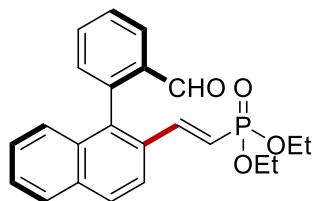
MS (ESI) m/z (relative intensity): 421 (100) $[\text{M} + \text{Na}]^+$, 399 (10) $[\text{M} + \text{H}]^+$.

HR-MS (ESI): m/z calcd. for $[\text{C}_{25}\text{H}_{18}\text{O}_3\text{S} + \text{Na}]^+$ 421.0869 found 421.0870.

$[\alpha]_D^{20}$: +20.1 (c = 1.0, CHCl_3).

HPLC separation (Chiralpak[®] IB-3, *n*-hexane/*i*-PrOH 80:20, 1 mL/min, detection at 273 nm):

t_r (major) = 20.0 min, t_r (minor) = 12.9 min, 98% ee.



(E)-Diethyl (2-(1-(2-formylphenyl)naphthalen-2-yl)vinyl)phosphonate (74ac): The general procedure **L** was followed using 2-(naphthalen-1-yl)benzaldehyde (**73a**) (46.4 mg, 0.20 mmol) and diethyl vinylphosphonate (**38c**) (98.4 mg, 0.60 mmol). Isolation by column chromatography (*n*-hexane/EtOAc = 1:9) yielded **74ac** (53.6 mg, 68%) as a yellow oil.

$^1\text{H-NMR}$ (400 MHz, CDCl_3): δ = 9.43 (s, 1H), 8.12 (dd, J = 7.8, 1.5 Hz, 1H), 7.93 (d, J = 8.7 Hz, 1H), 7.88 (dd, J = 8.2, 1.2 Hz, 1H), 7.78 (d, J = 8.7 Hz, 1H), 7.75–7.69 (m, 1H), 7.66–7.59 (m, 1H), 7.50 (ddd, J = 8.2, 6.8, 1.2 Hz, 1H), 7.37 (ddd, J = 8.2, 6.8, 1.2 Hz, 1H), 7.31 (ddd, J = 7.5, 1.2, 0.6 Hz, 1H), 7.25–7.21 (m, 1H), 7.20–7.05 (m, 1H), 6.29 (t, J = 17.7 Hz, 1H), 4.04–3.86 (m, 4H), 1.20 (dt, J = 15.2, 7.1 Hz, 6H).

$^{13}\text{C-NMR}$ (100 MHz, CDCl_3): δ = 191.2 (CH), 145.4 (d, J = 7.1 Hz, CH), 141.2 (C_q), 136.0 (C_q), 135.2 (C_q), 134.0 (CH), 133.7 (C_q), 133.2 (C_q), 131.9 (CH), 131.6 (d, J = 1.8 Hz, C_q), 129.1 (CH), 128.9 (CH), 128.1 (CH), 127.7 (CH), 127.3 (CH), 126.9 (CH), 122.5 (CH), 117.7 (CH), 115.8 (CH), 61.9 (d, J = 5.4 Hz, CH_2), 61.8 (d, J = 5.4 Hz, CH_2), 16.3 (d, J = 4.1 Hz, CH_3), 16.2 (d, J = 4.1 Hz, CH_3).

$^{31}\text{P-NMR}$ (160 MHz, CDCl_3): δ = 18.2.

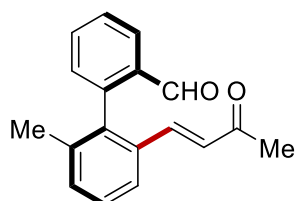
IR (ATR): 2981, 1697, 1595, 1247, 1049, 1023, 965, 770 cm^{-1} .

MS (ESI) m/z (relative intensity): 417 (100) $[\text{M} + \text{Na}]^+$, 395 (10) $[\text{M} + \text{H}]^+$.

HR-MS (ESI): m/z calcd. for $[\text{C}_{23}\text{H}_{23}\text{O}_4\text{P} + \text{Na}]^+$ 417.1226 found 417.1232.

$[\alpha]_{\text{D}}^{20}$: -6.8 ($c = 1.2$, CHCl_3).

HPLC separation (Chiralpak[®] IB-3, *n*-hexane/*i*-PrOH 95:5, 1 mL/min, detection at 273 nm): t_r (major) = 31.0 min, t_r (minor) = 28.7 min, 99% ee.



(*E*)-2'-methyl-6'-(3-oxobut-1-en-1-yl)-[1,1'-biphenyl]-2-carbaldehyde (74bd): The general procedure **L** was followed using 2'-methyl-[1,1'-biphenyl]-2-carbaldehyde (**73b**) (39.3 mg, 0.20 mmol) and but-3-en-2-one (**38d**) (42.1 mg, 0.60 mmol). Isolation by column chromatography (*n*-hexane/EtOAc = 7:1) yielded **74bd** (33.8 mg, 64%, *E/Z* = 96:4) as a colourless oil.

¹H-NMR (400 MHz, CDCl_3): $\delta = 9.63$ (s, 1H), 8.08 (dd, $J = 7.8, 1.5$, 1H), 7.71 (td, $J = 7.5, 1.5$ Hz, 1H), 7.65–7.55 (m, 2H), 7.41–7.32 (m, 2H), 7.23 (ddd, $J = 7.6, 1.3, 0.6$ Hz, 1H), 7.03 (d, $J = 16.2$ Hz, 1H), 6.53 (d, $J = 16.0$ Hz, 0.96H, *E*), 6.44 (d, $J = 12.0$ Hz, 0.04H, *Z*), 2.07 (s, 3H), 2.02 (s, 3H).

¹³C-NMR (100 MHz, CDCl_3): $\delta = 198.0$ (C_q), 191.4 (CH), 142.6 (C_q), 141.3 (CH), 138.3 (C_q), 137.3 (C_q), 134.2 (CH), 134.2 (C_q), 134.0 (C_q), 131.8 (CH), 130.9 (CH), 128.8 (CH), 128.6 (CH), 128.6 (CH), 128.0 (CH), 124.0 (CH), 27.1 (CH_3), 20.8 (CH_3).

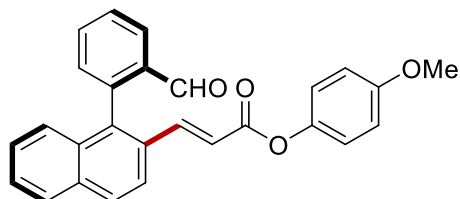
IR (ATR): 2945, 1696, 1632, 1445, 1376, 1316, 750, 701 cm^{-1} .

MS (ESI) m/z (relative intensity): 287 (100) $[\text{M} + \text{Na}]^+$, 265 (30) $[\text{M} + \text{H}]^+$.

HR-MS (ESI): m/z calcd. for $[\text{C}_{18}\text{H}_{16}\text{O}_2 + \text{Na}]^+$ 287.1043 found 287.1045.

$[\alpha]_{\text{D}}^{20}$: -26.7 ($c = 1.1$, CHCl_3).

HPLC separation (Chiralpak[®] IB-3, *n*-hexane/*i*-PrOH 95:5, 1 mL/min, detection at 273 nm): t_r (major) = 15.8 min, t_r (minor) = 11.6 min, 98% ee.



(*E*)-4-methoxyphenyl -3-(1-(2-formylphenyl)naphthalen-2-yl)acrylate (74ae): The general procedure **L** was followed using 2-(naphthalen-1-yl)benzaldehyde (**73a**) (46.4 mg, 0.20 mmol)

5. Experimental Part

and 4-methoxyphenyl acrylate (**38e**) (106.9 mg, 0.60 mmol). Isolation by column chromatography (*n*-hexane/EtOAc = 4:1) yielded **74ae** (55.5 mg, 68%, *E/Z* = 97:3) as a yellow oil.

¹H-NMR (400 MHz, CDCl₃): δ = 9.55 (s, 0.03H, *Z*), 9.53 (s, 0.97H, *E*), 8.19 (dd, *J* = 7.9, 1.4 Hz, 1H), 8.02 (d, *J* = 8.8 Hz, 1H), 7.99–7.89 (m, 2H), 7.83–7.73 (m, 1H), 7.73–7.51 (m, 3H), 7.51–7.40 (m, 2H), 7.34–7.22 (m, 2H), 6.80 (dd, *J* = 8.3, 2.5 Hz, 1H), 6.75–6.65 (m, 3H), 3.81 (s, 3H).

¹³C-NMR (100 MHz, CDCl₃): δ = 191.2 (CH), 164.8 (C_q), 160.4 (C_q), 151.6 (C_q), 144.0 (CH), 141.0 (C_q), 137.3 (C_q), 135.3 (C_q), 134.1 (CH), 133.9 (C_q), 133.3 (C_q), 131.9 (CH), 130.8 (C_q), 129.7 (CH), 129.2 (CH), 129.1 (CH), 128.2 (CH), 128.0 (CH), 127.5 (CH), 127.4 (CH), 127.1 (CH), 122.7 (CH), 119.1 (CH), 113.7 (CH), 111.7 (CH), 107.4 (CH), 55.4 (CH₃).

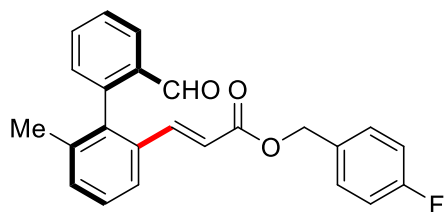
IR (ATR): 2920, 1724, 1695, 1594, 1489, 1146, 757 cm⁻¹.

MS (ESI) *m/z* (relative intensity): 431 (100) [M + Na]⁺, 409 (20) [M + H]⁺.

HR-MS (ESI): *m/z* calcd. for [C₂₇H₂₀O₄ + Na]⁺ 431.1254 found 431.1253.

[α]_D²⁰: -31.9 (c = 1.0, CHCl₃).

HPLC separation (Chiralpak[®] IA-3, *n*-hexane/*i*-PrOH 95:5, 1 mL/min, detection at 273 nm): *t_r* (major) = 15.1 min, *t_r* (minor) = 13.6 min, 98% ee.



4-Fluorobenzyl (E)-3-(2'-formyl-6-methyl-[1,1'-biphenyl]-2-yl)acrylate (74bf): The general procedure **L** was followed using 2'-methyl-[1,1'-biphenyl]-2-carbaldehyde (**73b**) (40 mg, 0.20 mmol) and 4-fluorobenzyl acrylate (**38f**) (108 mg, 0.60 mmol). Isolation by column chromatography (*n*-hexane/EtOAc = 5:1) yielded **74bf** (53 mg, 70%).

¹H-NMR (400 MHz, CDCl₃): δ = 9.61 (s, 1H), 8.06 (dd, *J* = 7.8, 1.4 Hz, 1H), 7.69 (dd, *J* = 7.5, 1.5 Hz, 1H), 7.62–7.54 (m, 2H), 7.39–7.31 (m, 2H), 7.31–7.19 (m, 4H), 7.06–6.99 (m, 2H), 6.31 (d, *J* = 16.0 Hz, 1H), 5.07 (s, 2H), 2.00 (s, 3H).

¹³C-NMR (100 MHz, CDCl₃): δ = 191.4 (CH), 166.1 (C_q), 162.5 (d, ¹*J*_{C-F} = 246.8 Hz, C_q), 143.2 (CH), 142.5 (C_q), 138.2 (C_q), 137.3 (C_q), 134.2 (CH), 134.1 (C_q), 133.7 (C_q), 131.8 (d, ⁴*J*_{C-F} = 3.2 Hz, C_q), 131.7 (CH), 130.9 (CH), 129.9 (d, ³*J*_{C-F} = 8.2 Hz, CH), 128.5 (CH), 128.5 (CH), 128.0 (CH), 123.9 (CH), 119.2 (CH), 115.4 (d, ²*J*_{C-F} = 21.6 Hz, CH), 65.4 (CH₂), 20.8 (CH₃).

^{19}F -NMR (375 MHz, CDCl_3): $\delta = -113.8$.

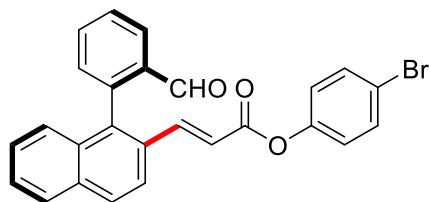
IR (ATR): 2955, 1730, 1682, 1485, 1376, 1320, 744 cm^{-1} .

MS (ESI) m/z (relative intensity): 397 (100) $[\text{M} + \text{Na}]^+$, 375 (20) $[\text{M} + \text{H}]^+$.

HR-MS (ESI): m/z calcd. for $[\text{C}_{24}\text{H}_{19}\text{FO}_3 + \text{Na}]^+$ 397.1210 found 397.1215.

$[\alpha]_{\text{D}}^{20}$: -7.0 ($c = 1.0$, CHCl_3).

HPLC separation (Chiralpak[®] IA-3, n -hexane/ i -PrOH 95:5, 1 mL/min, detection at 273 nm): t_r (major) = 12.6 min, t_r (minor) = 16.3 min, 98% ee.



(E)-4-Bromophenyl -3-(1-(2-formylphenyl)naphthalen-2-yl)acrylate (74ag): The general procedure **L** was followed using 2-(naphthalen-1-yl)benzaldehyde (**73a**) (46 mg, 0.20 mmol) and 4-bromophenyl acrylate (**38g**) (135.6 mg, 0.60 mmol). Isolation by column chromatography (n -hexane/EtOAc = 5:1) yielded **74ag** (45.6 mg, 50%) as yellow oil.

^1H -NMR (400 MHz, CDCl_3): $\delta = 9.50$ (s, 1H), 8.16 (d, $J = 7.7$ Hz, 1H), 7.99 (d, $J = 8.7$ Hz, 1H), 7.95–7.88 (m, 2H), 7.82–7.62 (m, 2H), 7.63–7.52 (m, 2H), 7.50–7.45 (m, 2H), 7.42 (t, $J = 8.5$ Hz, 1H), 7.37 (d, $J = 7.6$ Hz, 1H), 7.31–7.25 (m, 1H), 7.02–6.93 (m, 2H), 6.64 (d, $J = 16.6$ Hz, 1H).

^{13}C -NMR (100 MHz, CDCl_3): $\delta = 191.2$ (CH), 164.6 (C_q), 149.7 (C_q), 144.4 (CH), 140.9 (C_q), 137.5 (C_q), 135.3 (C_q), 134.1 (CH), 134.0 (C_q), 133.3 (C_q), 132.4 (CH), 132.0 (CH), 130.7 (C_q), 129.3 (CH), 129.1 (CH), 128.2 (CH), 128.1 (CH), 127.7 (CH), 127.5 (CH), 127.1 (CH), 123.3 (CH), 122.6 (CH), 118.8 (C_q), 118.7 (CH).

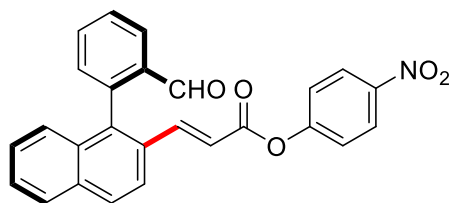
IR (ATR): 2935, 1712, 1682, 1355, 1250, 1146, 1014, 920 cm^{-1} .

MS (ESI) m/z (relative intensity): 479 (100) $[\text{M} + \text{Na}]^+$, 457 (10) $[\text{M} + \text{H}]^+$.

HR-MS (ESI): m/z calcd. for $[\text{C}_{26}\text{H}_{17}^{79}\text{BrO}_3 + \text{Na}]^+$ 479.0253 found 479.0245.

$[\alpha]_{\text{D}}^{20}$: -34.0 ($c = 1.5$, CHCl_3).

HPLC separation (Chiralpak[®] IA-3, n -hexane/ i -PrOH 95:5, 1 mL/min, detection at 273 nm): t_r (major) = 20.4 min, t_r (minor) = 23.1 min, 97% ee.



(E)-4-nitrophenyl-3-(1-(2-formylphenyl)naphthalen-2-yl)acrylate (74ah): The general procedure **L** was followed using 2-(naphthalen-1-yl)benzaldehyde (**73a**) (46.4 mg, 0.20 mmol) and 4-nitrophenyl acrylate (**38h**) (115.9 mg, 0.60 mmol). Isolation by column chromatography (*n*-hexane/EtOAc = 1:1) yielded **74ah** (40.6 mg, 48%) as a yellow oil.

$^1\text{H-NMR}$ (400 MHz, CDCl_3): δ = 9.53 (s, 1H), 8.28 (d, J = 9.1 Hz, 2H), 8.19 (d, J = 7.7 Hz, 1H), 8.03 (d, J = 8.8 Hz, 1H), 7.99–7.89 (m, 2H), 7.80 (td, J = 7.5, 1.5 Hz, 1H), 7.76–7.54 (m, 3H), 7.51–7.37 (m, 2H), 7.36–7.25 (m, 3H), 6.68 (d, J = 15.9 Hz, 1H).

$^{13}\text{C-NMR}$ (100 MHz, CDCl_3): δ = 191.2 (CH), 163.9 (C_q), 155.5 (C_q), 145.4 (CH), 145.3 (C_q), 140.8 (C_q), 137.9 (C_q), 135.3 (C_q), 134.2 (C_q), 134.1 (CH), 133.3 (C_q), 132.0 (CH), 130.5 (C_q), 129.4 (CH), 129.2 (CH), 128.3 (CH), 128.2 (CH), 127.9 (CH), 127.6 (CH), 127.2 (CH), 125.2 (CH), 122.5 (CH), 122.4 (CH), 117.9 (CH).

IR (ATR): 3018, 1696, 1661, 1215, 751, 720, 683 cm^{-1} .

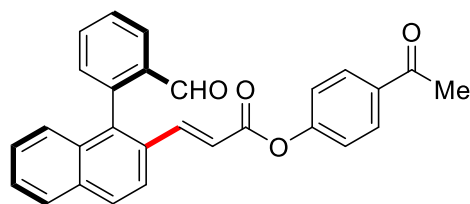
MS (ESI) m/z (relative intensity): 446 (100) $[\text{M} + \text{Na}]^+$, 424 (20) $[\text{M} + \text{H}]^+$.

HR-MS (ESI): m/z calcd. for $[\text{C}_{26}\text{H}_{17}\text{NO}_5 + \text{Na}]^+$ 446.0999 found 446.0998.

$[\alpha]_D^{20}$: -10.6 (c = 0.2, CHCl_3).

HPLC separation (Chiralpak[®] IA-3, *n*-hexane/*i*-PrOH 90:10, 1 mL/min, detection at 273 nm):

t_r (major) = 27.0 min, t_r (minor) = 42.4 min, 96% ee.



4-Acetylphenyl (E)-3-(1-(2-formylphenyl)naphthalen-2-yl)acrylate (74ai): The general procedure **L** was followed using 2-(naphthalen-1-yl)benzaldehyde (**73a**) (46 mg, 0.20 mmol) and 4-acetylphenyl acrylate (**38i**) (114 mg, 0.60 mmol). Isolation by column chromatography (*n*-hexane/EtOAc = 4:1) yielded **74ai** (54 mg, 64%) as colourless oil.

$^1\text{H-NMR}$ (400 MHz, CDCl_3): δ = 9.51 (s, 1H), 8.16 (ddd, J = 7.9, 1.5, 0.6 Hz, 1H), 8.02–7.96 (m, 3H), 7.95–7.92 (m, 1H), 7.91 (d, J = 8.8 Hz, 1H), 7.77 (td, J = 7.5, 1.5 Hz, 1H), 7.70–7.54 (m, 3H), 7.46–7.34 (m, 2H), 7.32–7.24 (m, 1H), 7.23–7.17 (m, 2H), 6.66 (d, J = 15.9 Hz, 1H), 2.59 (s, 3H).

^{13}C -NMR (100 MHz, CDCl_3): $\delta = 196.8$ (C_q), 191.2 (CH), 164.3 (C_q), 154.4 (C_q), 144.7 (CH), 140.9 (C_q), 137.6 (C_q), 135.3 (C_q), 134.6 (C_q), 134.1 (CH), 134.0 (C_q), 133.3 (C_q), 131.9 (CH), 130.7 (C_q), 129.8 (CH), 129.3 (CH), 129.1 (CH), 128.2 (CH), 128.1 (CH), 127.7 (CH), 127.5 (CH), 127.1 (CH), 122.6 (CH), 121.7 (CH), 118.5 (CH), 26.6 (CH_3).

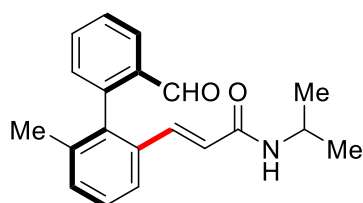
IR (ATR): 2925, 1733, 1682, 1596, 1201, 1130, 753, 658 cm^{-1} .

MS (ESI) m/z (relative intensity): 443 (100) $[\text{M} + \text{Na}]^+$, 421 (5) $[\text{M} + \text{H}]^+$.

HR-MS (ESI): m/z calcd. for $[\text{C}_{28}\text{H}_{20}\text{O}_4 + \text{Na}]^+$ 443.1254 found 443.1258.

$[\alpha]_{\text{D}}^{20}$: -29.9 ($c = 1.0$, CHCl_3).

HPLC separation (Chiralpak[®] IA-3, *n*-hexane/*i*-PrOH 70:30, 0.75 mL/min, detection at 273 nm): t_r (major) = 17.2 min, t_r (minor) = 21.4 min, 98% ee.



(*R,E*)-3-(2'-formyl-6-methyl-[1,1'-biphenyl]-2-yl)-*N*-isopropylacrylamide (74bj): The general procedure **L** was followed using 2'-methyl-[1,1'-biphenyl]-2-carbaldehyde (**73b**) (39.3 mg, 0.20 mmol) and *N*-isopropylacrylamide (**38j**) (67.9 mg, 0.60 mmol). Isolation by column chromatography (*n*-hexane/EtOAc = 1:2) yielded **74bj** (33.8 mg, 55%) as a white solid. M.P. 145–150 °C.

^1H -NMR (400 MHz, CDCl_3): $\delta = 9.59$ (s, 1H), 8.02 (d, $J = 7.8$ Hz, 1H), 7.66 (td, $J = 7.5$, 1.5 Hz, 1H), 7.58–7.48 (m, 2H), 7.38–7.24 (m, 2H), 7.24–7.12 (m, 2H), 6.16 (d, $J = 15.4$ Hz, 1H), 5.40 (d, $J = 7.9$ Hz, 1H), 4.13–4.00 (m, 1H), 1.97 (s, 3H), 1.18–1.08 (m, 6H).

^{13}C -NMR (100 MHz, CDCl_3): $\delta = 191.7$ (CH), 164.4 (C_q), 142.8 (C_q), 138.7 (CH), 137.9 (C_q), 137.3 (C_q), 134.5 (C_q), 134.4 (C_q), 134.1 (CH), 130.9 (CH), 130.8 (CH), 128.5 (CH), 128.3 (CH), 128.0 (CH), 123.7 (CH), 122.8 (CH), 41.5 (CH), 22.8 (CH_3), 22.7 (CH_3), 20.8 (CH_3).

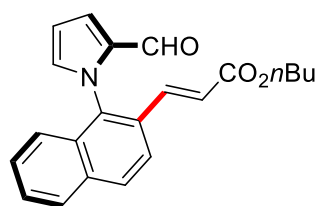
IR (ATR): 2924, 1694, 1652, 1541, 1456, 1225, 1195, 755 cm^{-1} .

MS (ESI) m/z (relative intensity): 330 (100) $[\text{M} + \text{Na}]^+$, 308 (20) $[\text{M} + \text{H}]^+$.

HR-MS (ESI): m/z calcd. for $[\text{C}_{20}\text{H}_{21}\text{NO}_2 + \text{Na}]^+$ 330.1465 found 330.1470.

$[\alpha]_{\text{D}}^{20}$: +9.2 ($c = 0.25$, CHCl_3).

HPLC separation (Chiralpak[®] IA-3, *n*-hexane/*i*-PrOH 90:10, 1 mL/min, detection at 273 nm): t_r (major) = 13.2 min, t_r (minor) = 12.0 min, 96% ee.



(E)-Butyl -3-(1-(2-formyl-1H-pyrrol-1-yl)naphthalen-2-yl)acrylate (397aa): A modified procedure **A** was followed using 1-(naphthalen-1-yl)-1H-pyrrole-2-carbaldehyde (**396a**) (44.3 mg, 0.20 mmol) and *n*-butyl acrylate (**38a**) (76.9 mg, 0.60 mmol) with *L*-*tert*-leucine (7.9 mg, 30 mol %). Isolation by column chromatography (*n*-hexane/EtOAc = 5:1) yielded **397aa** (38.9 mg, 56%) as a yellow oil.

¹H-NMR (400 MHz, CDCl₃): δ = 9.46 (s, 1H), 8.02 (d, *J* = 8.8 Hz, 1H), 7.96 (d, *J* = 8.2 Hz, 1H), 7.86 (d, *J* = 8.8 Hz, 1H), 7.65–7.56 (m, 1H), 7.56–7.46 (m, 1H), 7.37–7.28 (m, 2H), 7.18 (d, *J* = 8.5 Hz, 1H), 7.09 (s, 1H), 6.69–6.62 (m, 1H), 6.52 (d, *J* = 16.0 Hz, 1H), 4.20 (t, *J* = 6.6 Hz, 2H), 1.75–1.62 (m, 2H), 1.50–1.38 (m, 2H), 0.99 (t, *J* = 7.3 Hz, 3H).

¹³C-NMR (100 MHz, CDCl₃): δ = 178.5 (CH), 166.4 (C_q), 139.1 (C_q), 138.3 (CH), 135.6 (CH), 134.5 (C_q), 134.4 (C_q), 132.2 (CH), 131.5 (C_q), 129.7 (C_q), 129.5 (CH), 128.1 (CH), 128.0 (CH), 127.8 (CH), 123.2 (CH), 122.6 (CH), 121.6 (CH), 111.5 (CH), 64.5 (CH₂), 30.6 (CH₂), 19.1 (CH₂), 13.7 (CH₃).

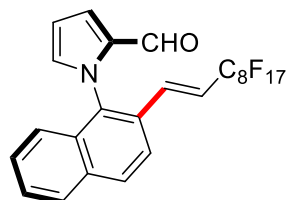
IR (ATR): 2957, 1712, 1671, 1305, 1196, 1150, 787, 741 cm⁻¹.

MS (ESI) *m/z* (relative intensity): 370 (100) [M + Na]⁺, 348 (20) [M + H]⁺.

HR-MS (ESI): *m/z* calcd. for [C₂₂H₂₁NO₃ + Na]⁺ 370.1414 found 370.1419.

[α]_D²⁰: -43.1 (c = 0.4, CHCl₃).

HPLC separation (Chiralpak[®] ID-3, *n*-hexane/*i*-PrOH 80:20, 1 mL/min, detection at 273 nm): *t_r* (major) = 15.2 min, *t_r* (minor) = 16.6 min, 99% ee. The analytical data correspond with those reported in the literature.^[276]



(E)-1-(2-(3,3,4,4,5,5,6,6,7,7,8,8,9,9,10,10,10-heptafluorodec-1-en-1-yl)naphthalen-1-yl)-1H-pyrrole-2-carbaldehyde (398aa): A modified procedure **A** was followed using 1-(naphthalen-1-yl)-1H-pyrrole-2-carbaldehyde (**396a**) (44.3 mg, 0.20 mmol) and 3,3,4,4,5,5,6,6,7,7,8,8,9,9,10,10,10-heptafluorodec-1-ene (**301a**) (267.7 mg, 0.60 mmol) with *L*-*tert*-leucine (7.9 mg, 30 mol %). Isolation by column chromatography (*n*-hexane/DCM = 1:1) yielded **398aa** (69.2 mg, 52%) as a yellow oil.

$^1\text{H-NMR}$ (400 MHz, CDCl_3): $\delta = 9.43$ (s, 1H), 7.99 (d, $J = 8.7$ Hz, 1H), 7.92 (d, $J = 8.2$ Hz, 1H), 7.72 (d, $J = 8.7$ Hz, 1H), 7.61–7.50 (m, 1H), 7.52–7.43 (m, 1H), 7.27 (dd, $J = 4.0, 1.6$ Hz, 1H), 7.15 (d, $J = 7.5$ Hz, 1H), 7.06–6.97 (m, 1H), 6.72 (dt, $J = 16.1, 2.4$ Hz, 1H), 6.60 (dd, $J = 4.0, 2.5$ Hz, 1H), 6.17 (dt, $J = 16.2, 11.8$ Hz, 1H).

$^{13}\text{C-NMR}$ (100 MHz, CDCl_3): $\delta = 178.3$ (CH), 135.4 (C_q), 134.6–134.3 (m, CH+ C_q), 134.3 (C_q), 131.9 (CH), 131.3 (C_q), 129.7 (CH), 128.7 (C_q), 128.3 (CH), 128.1 (CH), 127.9 (CH), 123.1 (CH), 122.6 (CH), 122.1 (CH), 117.8 (t, $J = 23.1$ Hz, CH- CF_2), 111.6 (CH).

$^{19}\text{F-NMR}$ (375 MHz, CDCl_3): $\delta = -80.7$ (m), -111.5 (m), -121.3 (m), -121.9 (m), -122.7 (m), -123.1 (m), -126.1 (m).

IR (ATR): 2925, 1671, 1239, 1201, 1146, 1113, 762, 746, cm^{-1} .

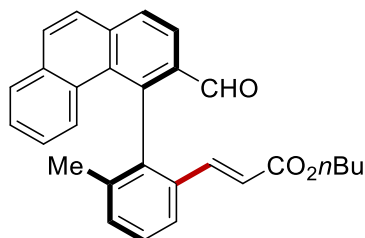
MS (ESI) m/z (relative intensity): 688 (100) $[\text{M} + \text{Na}]^+$, 666 (20) $[\text{M} + \text{H}]^+$.

HR-MS (ESI): m/z calcd. for $[\text{C}_{25}\text{H}_{12}\text{F}_{17}\text{NO} + \text{Na}]^+$ 688.0540 found 688.0535.

$[\alpha]_D^{20}$: -38.3 ($c = 0.75$, CHCl_3).

HPLC separation (Chiralpak® ID-3, *n*-hexane/*i*-PrOH 99:1, 1 mL/min, detection at 273 nm): t_r (major) = 6.1 min, t_r (minor) = 6.7 min, 98% ee.

5.9.2. Late stage Diversification



(*R*, *E*)-Butyl 3-(2-(3-formylphenanthren-4-yl)-3-methylphenyl)acrylate (74ha): A modified procedure **L** was followed using 4-(*o*-tolyl)phenanthrene-3-carbaldehyde (**73h**) (59.2 mg, 0.20 mmol) and *n*-butyl acrylate (**38a**) (76.9 mg, 0.60 mmol) with *L*-*tert*-leucine (7.9 mg, 30 mol %). Isolation by column chromatography (*n*-hexane/EtOAc = 5:1) yielded **74ha** (33.8 mg, 40%) as a yellow oil and **73h** (32.0 mg, 54%) as yellow oil.

$^1\text{H-NMR}$ (400 MHz, CDCl_3): $\delta = 9.59$ (s, 1H), 8.28 (d, $J = 8.2$ Hz, 1H), 8.09 (d, $J = 8.2$ Hz, 1H), 7.95–7.82 (m, 3H), 7.77 (d, $J = 7.9$ Hz, 1H), 7.63–7.40 (m, 4H), 7.24–7.05 (m, 2H), 6.26 (d, $J = 15.8$ Hz, 1H), 3.94 (t, $J = 6.5$ Hz, 2H), 1.86 (s, 3H), 1.52–1.38 (m, 2H), 1.24–1.10 (m, 2H), 0.83 (t, $J = 7.4$ Hz, 3H).

$^{13}\text{C-NMR}$ (100 MHz, CDCl_3): $\delta = 192.3$ (CH), 166.2 (C_q), 141.9 (CH), 141.7 (C_q), 139.4 (C_q), 137.8 (C_q), 137.4 (C_q), 134.6 (C_q), 133.7 (C_q), 133.0 (C_q), 132.4 (CH), 131.3 (C_q), 131.2 (CH), 130.0 (CH), 129.4 (CH), 129.2 (CH), 128.4 (C_q), 127.5 (CH), 127.0 (CH), 126.7 (CH), 125.6

5. Experimental Part

(CH), 124.9 (CH), 124.4 (CH), 120.5 (CH), 64.2 (CH₂), 30.5 (CH₂), 20.4 (CH₃), 19.0 (CH₂), 13.6 (CH₃).

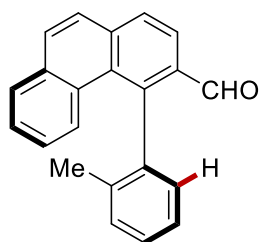
IR (ATR): 2933, 1701, 1650, 1590, 1410, 1251, 1115, 1045, 795 cm⁻¹.

MS (ESI) *m/z* (relative intensity): 445 (100) [M + Na]⁺, 423 (20) [M + H]⁺.

HR-MS (ESI): *m/z* calcd. for [C₂₉H₂₆O₃ + H]⁺ 423.1955 found 423.1959.

[α]_D²⁰: +238.1 (c = 0.8, CHCl₃).

HPLC separation (Chiralpak[®] IA-3, *n*-hexane/*i*-PrOH 99:1, 1 mL/min, detection at 273 nm): *t_r* (major) = 23.7 min, *t_r* (minor) = 22.7 min, 95% ee.



(*R*)-4-(*o*-Tolyl)phenanthrene-3-carbaldehyde (73h):

¹H-NMR (600 MHz, CDCl₃): δ = 9.69 (s, 1H), 8.21 (d, *J* = 8.3 Hz, 1H), 7.99 (dd, *J* = 8.3, 0.9 Hz, 1H), 7.90–7.82 (m, 2H), 7.80 (d, *J* = 8.8 Hz, 1H), 7.51–7.44 (m, 3H), 7.41 (dd, *J* = 7.7, 1.4, 1H), 7.38 (dd, *J* = 7.5, 1.4 Hz, 1H), 7.27 (dd, *J* = 7.5, 1.4 Hz, 1H), 7.16–7.12 (m, 1H), 1.93 (s, 3H).

¹³C-NMR (150 MHz, CDCl₃): δ = 193.1 (CH), 144.6 (C_q), 138.7 (C_q), 137.2 (C_q), 136.8 (C_q), 133.6 (C_q), 133.0 (C_q), 131.4 (C_q), 130.9 (CH), 130.8 (CH), 130.3 (CH), 129.3 (CH), 129.1 (CH), 128.8 (CH), 128.4 (C_q), 127.4 (CH), 126.9 (CH), 126.5 (CH), 126.5 (CH), 126.4 (CH), 123.9 (CH), 20.1 (CH₃).

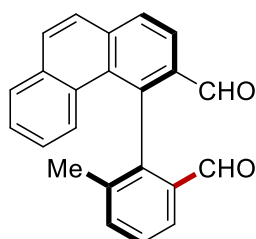
IR (ATR): 2937, 1710, 1599, 1432, 1211, 1105, 1020, 710 cm⁻¹.

MS (ESI) *m/z* (relative intensity): 319 (100) [M + Na]⁺, 297 (20) [M + H]⁺.

HR-MS (ESI): *m/z* calcd. for [C₂₂H₁₆O + Na]⁺ 319.1093 found 319.1098.

[α]_D²⁰: +21.2 (c = 1.0, CHCl₃).

HPLC separation (Chiralpak[®] IB-3, *n*-hexane/EtOAc 99:1, 1 mL/min, detection at 273 nm): *t_r* (major) = 7.3 min, *t_r* (minor) = 7.1 min, 77% ee.



(S)-4-(2-Formyl-6-methylphenyl)phenanthrene-3-carbaldehyde (399): To a solution of **74ha** (30 mg, 0.07 mmol, 1 equiv) in THF (1.8 mL) and H₂O (0.9 mL), K₂OsO₄·2H₂O (4 mg, 0.011 mmol, 15 mol %) and NaIO₄ (149 mg, 0.7 mmol, 10 equiv) were added at 25 °C, the reaction mixture was stirred at 50 °C for 16 h. The reaction mixture was then stopped by the addition with sat. aqueous Na₂S₂O₃ (5 mL) and stirred vigorously for 30 min. The biphasic reaction mixture was extracted with EtOAc (3 × 20 mL) and then the combined organic layers were washed with brine (20 mL), dried over Na₂SO₄, and concentrated. The crude product was purified by flash column chromatography (*n*-hexane/EtOAc = 3:1) to provide **399** (19.3 mg, 85%) as a yellow oil.

¹H-NMR (400 MHz, CDCl₃): δ = 9.63 (s, 1H), 9.49 (s, 1H), 8.30 (dd, *J* = 8.3, 1.2 Hz, 1H), 8.16–8.11 (m, 1H), 8.10–8.05 (m, 1H), 7.99–7.84 (m, 3H), 7.80–7.68 (m, 2H), 7.52 (ddd, *J* = 8.3, 6.9, 1.2 Hz, 1H), 7.34 (d, *J* = 9.2 Hz, 1H), 7.17 (ddd, *J* = 8.7, 7.0, 1.4 Hz, 1H), 2.01 (s, 3H).

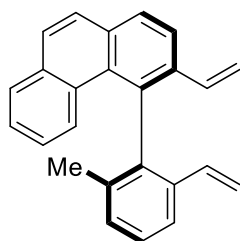
¹³C-NMR (100 MHz, CDCl₃): δ = 191.5 (CH), 190.9 (CH), 142.2 (C_q), 139.6 (C_q), 138.4 (C_q), 137.3 (C_q), 136.4 (CH), 135.2 (C_q), 133.8 (C_q), 133.4 (C_q), 131.5 (CH), 131.0 (C_q), 130.3 (CH), 129.6 (CH), 129.4 (CH), 128.8 (C_q), 127.5 (CH), 127.1 (CH), 126.9 (CH), 126.9 (CH), 125.7 (CH), 124.5 (CH), 19.9 (CH₃).

IR (ATR): 2925, 1710, 1643, 1555, 1400, 1320, 1290, 850 cm⁻¹.

MS (ESI) *m/z* (relative intensity): 347 (100) [M + Na]⁺, 325 (20) [M + H]⁺.

HR-MS (ESI): *m/z* calcd. for [C₂₃H₁₆O₂ + Na]⁺ 347.1043 found 347.1038.

[α]_D²⁰: +42.8 (c = 1.0, CHCl₃).



(S)-4-(2-Methyl-6-vinylphenyl)-3-vinylphenanthrene (400): A flame dried round bottom flask was charged with **399** (16 mg, 0.05 mmol, 1 equiv). THF (1.5 mL) was added and the mixture is stirred until dissolution of the substrate. The solution was cooled to -78 °C. A second flame dried round bottom flask was charged with methyltriphenylphosphonium bromide (71.5 mg, 0.2 mmol, 4 equiv). THF (1.5 mL) was added and the suspension was cooled to -78 °C. *n*-Butyllithium (3.8 equiv, 0.19 mmol) was added to the suspension of the phosphonium salt. The orange solution was warmed to rt for 10 min, and then cooled to -78 °C. The orange solution

5. Experimental Part

of the phosphorus ylide was slowly transferred *via* canula to the solution of **399**. The reaction mixture was warmed to rt and stirred for 1 hour. Silica gel was directly added to the reaction mixture and the solvent was evaporated under vacuum. The crude product was purified by flash column chromatography (*n*-hexane/EtOAc = 15:1) to provide **400** (15.9 mg, 99%) as a yellow oil.

¹H-NMR (400 MHz, CDCl₃): δ = 7.97 (d, *J* = 1.6 Hz, 2H), 7.89–7.73 (m, 3H), 7.68 (d, *J* = 7.8 Hz, 1H), 7.53 (d, *J* = 8.8 Hz, 1H), 7.50–7.42 (m, 2H), 7.34 (d, *J* = 7.5 Hz, 1H), 7.13 (ddd, *J* = 8.7, 6.9, 1.6 Hz, 1H), 6.45–6.31 (m, 1H), 6.27–6.15 (m, 1H), 5.76 (dd, *J* = 17.4, 1.4 Hz, 1H), 5.58 (dd, *J* = 17.4, 1.4 Hz, 1H), 5.16 (dd, *J* = 11.0, 1.5 Hz, 1H), 4.89 (dd, *J* = 11.0, 1.5 Hz, 1H), 1.80 (s, 3H).

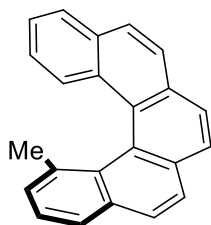
¹³C-NMR (100 MHz, CDCl₃): δ = 140.6 (C_q), 136.8 (C_q), 136.6 (C_q), 135.8 (C_q), 135.6 (C_q), 135.5 (CH), 135.0 (CH), 133.6 (C_q), 133.3 (C_q), 131.4 (C_q), 130.2 (CH), 129.1 (CH), 128.8 (C_q), 128.8 (CH), 128.0 (CH), 127.9 (CH), 127.7 (CH), 126.2 (CH), 126.0 (CH), 126.0 (CH), 124.0 (CH), 123.4 (CH), 115.5 (CH₂), 114.9 (CH₂), 20.1 (CH₃).

IR (ATR): 2932, 1550, 1472, 1355, 1259, 1231, 980, 720 cm⁻¹.

MS (EI) *m/z* (relative intensity): 320 (20), 305 (20), 276 (100), 263 (10), 228 (30).

HR-MS (EI): *m/z* calcd. for [C₂₅H₂₀] [M]⁺ 320.1560 found 320.1558.

$[\alpha]_D^{20}$: +10.8 (c = 1.0, CHCl₃).



10-Methyldibenzo[*c,g*]phenanthrene (401): A flame-dried microwave vessel, equipped with a magnetic stirrer was charged with **400** (9.6 mg, 0.03 mmol) under N₂. Anhydrous CH₂Cl₂ (1.5 mL) was added and the mixture was stirred until dissolution of all the substrates. The Grubbs II catalyst (2.5 mg, 0.003 mmol, 10 mol %) was added, the tube was sealed. The reaction vessel was irradiated in a microwave at 95 °C for 1 h. The reaction mixture is concentrated in *vacuo* and purified by flash column silica gel chromatography (*n*-hexane/EtOAc = 30:1) to afford [5]-helicene **401** (7.4 mg, 86 %) as a colourless oil.

¹H-NMR (600 MHz, CDCl₃): δ = 7.96–7.90 (m, 5H), 7.89 (d, *J* = 8.4 Hz, 1H), 7.88–7.86 (m, 1H), 7.84 (dd, *J* = 8.4, 0.7 Hz, 1H), 7.80 (d, *J* = 8.4 Hz, 1H), 7.54 (d, *J* = 7.5 Hz, 1H), 7.45 (ddd, *J* = 8.0, 6.8, 1.2 Hz, 1H), 7.21–7.17 (m, 1H), 7.12 (ddd, *J* = 8.4, 6.8, 1.4 Hz, 1H), 1.54 (s, 3H).

^{13}C -NMR (150 MHz, CDCl_3): $\delta = 136.0$ (C_q), 133.2 (C_q), 132.9 (C_q), 131.9 (C_q), 131.5 (C_q), 131.2 (C_q), 130.4 (C_q), 128.6 (CH), 128.5 (C_q), 127.8 (CH), 127.8 (CH), 127.1 (CH), 127.1 (CH), 126.3 (CH), 126.2 (CH), 126.1 (CH), 126.0 (CH), 125.6 (CH), 125.5 (CH), 125.2 (CH), 125.1 (CH), 124.9 (C_q), 23.2 (CH_3).

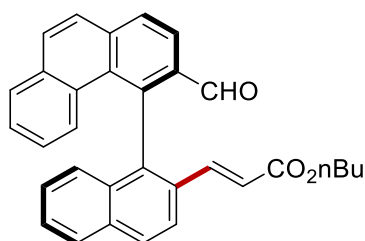
IR (ATR): 2922, 1532, 1452, 1260, 1096, 1018, 798, 695 cm^{-1} .

MS (EI) m/z (relative intensity): 292 (30), 277 (100), 261 (10), 228 (10), 138 (30).

HR-MS (EI): m/z calcd. for $\text{C}_{23}\text{H}_{16}$ $[\text{M}]^+$: 292.1252, found 292.1246.

$[\alpha]_D^{20}$: -20.4 ($c = 0.25$, CHCl_3).

HPLC separation (Chiralpak[®] IB-3, *n*-hexane/*i*-PrOH 98:2, 1 mL/min, detection at 273 nm): t_r (major) = 3.6 min, t_r (minor) = 3.9 min, 95% ee.



(+)(*E*)-*n*-Butyl-3-(1-(3-formylphenanthren-4-yl)naphthalen-2-yl)acrylate (74ia): A modified procedure **L** was followed using 4-(naphthalen-1-yl)phenanthrene-3-carbaldehyde (**73i**) (66.4 mg, 0.20 mmol) and *n*-butyl acrylate (**38a**) (76.9 mg, 0.60 mmol) with *L*-tert-leucine (7.9 mg, 30 mol %). Isolation by column chromatography (*n*-hexane/EtOAc = 5:1) yielded **74ia** (35.5 mg, 42%, *E/Z* = 96:4) as a yellow oil and **73i** (38.0 mg, 55%) as yellow solid. M.P.: 130-132 °C.

^1H -NMR (400 MHz, CDCl_3): $\delta = 9.38$ (s, 1H), 8.35 (dd, $J = 8.2, 1.7$ Hz, 1H), 8.22–8.10 (m, 2H), 8.03–7.89 (m, 4H), 7.85 (dd, $J = 7.9, 1.6$ Hz, 1H), 7.54 (dd, $J = 8.2, 1.5$ Hz, 1H), 7.40 (dd, $J = 7.5, 6.9, 1.2$ Hz, 1H), 7.32–7.17 (m, 4H), 6.94 (dd, $J = 8.6, 1.6$ Hz, 1H), 6.41 (d, $J = 15.8$ Hz, 0.96H, *E*), 5.67 (d, $J = 12.3$ Hz, 0.04H, *Z*), 3.97 (t, $J = 6.5$ Hz, 2H), 1.54–1.40 (m, 2H), 1.29–1.14 (m, 2H), 0.84 (t, $J = 6.5$ Hz, 3H).

^{13}C -NMR (100 MHz, CDCl_3): $\delta = 192.1$ (CH), 166.2 (C_q), 141.3 (CH), 140.2 (C_q), 138.1 (C_q), 137.3 (C_q), 134.2 (C_q), 134.1 (C_q), 133.7 (C_q), 133.4 (C_q), 131.8 (C_q), 131.4 (CH), 130.7 (C_q), 130.4 (CH), 129.6 (CH), 129.5 (C_q), 129.3 (CH), 128.3 (CH), 127.9 (CH), 127.8 (CH), 127.5 (CH), 127.0 (CH), 126.8 (CH), 126.6 (CH), 126.3 (CH), 124.4 (CH), 123.3 (CH), 120.7 (CH), 64.2 (CH_2), 30.5 (CH_2), 19.0 (CH_2), 13.7 (CH_3).

IR (ATR): 2933, 1698, 1652, 1559, 1421, 1222, 885 cm^{-1} .

MS (ESI) m/z (relative intensity): 481 (100) $[\text{M} + \text{Na}]^+$, 459 (10) $[\text{M} + \text{H}]^+$.

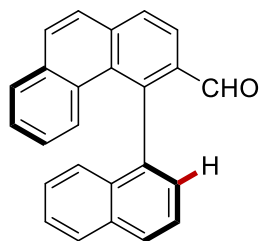
HR-MS (ESI): m/z calcd. for $[\text{C}_{32}\text{H}_{26}\text{O}_3 + \text{Na}]^+$ 481.1774 found 481.1773.

5. Experimental Part

$[\alpha]_D^{20}$: +178.2 ($c = 1.0$, CHCl_3).

HPLC separation (Chiralpak[®] IA-3, *n*-hexane/*i*-PrOH 95:5, 1.0 mL/min, detection at 273 nm):

t_r (major) = 15.4 min, t_r (minor) = 12.1 min, 96% ee.



(R)-4-(Naphthalen-1-yl)phenanthrene-3-carbaldehyde (73i): ¹H NMR (600 MHz, CDCl_3):

$\delta = 9.45$ (s, 1H), 8.27 (d, $J = 8.3$ Hz, 1H), 8.11 – 8.06 (m, 2H), 7.99 (dd, $J = 8.3, 0.9$ Hz, 1H), 7.88 (d, $J = 8.8$ Hz, 1H), 7.85 (d, $J = 8.8$ Hz, 1H), 7.81 (dd, $J = 7.8, 1.5$ Hz, 1H), 7.62 (dd, $J = 8.3, 6.9$ Hz, 1H), 7.52–7.48 (m, 1H), 7.47 (dd, $J = 6.9, 1.2$ Hz, 1H), 7.38–7.33 (m, 2H), 7.27 (ddd, $J = 8.3, 6.7, 1.0$ Hz, 1H), 7.20 (dd, $J = 8.7, 1.0$ Hz, 1H), 6.86 (ddd, $J = 8.7, 6.9, 1.5$ Hz, 1H).

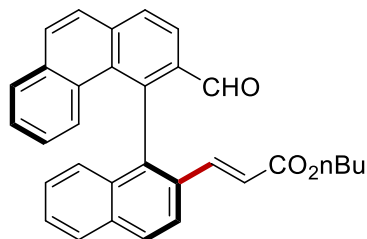
¹³C-NMR (150 MHz, CDCl_3): $\delta = 192.9$ (CH), 143.1 (C_q), 137.2 (C_q), 136.9 (C_q), 134.2 (C_q), 133.7 (C_q), 133.6 (C_q), 133.2 (C_q), 131.0 (CH), 130.8 (C_q), 129.7 (CH), 129.4 (C_q), 129.0 (CH), 128.9 (CH), 128.5 (CH), 128.3 (CH), 127.3 (CH), 127.2 (CH), 127.2 (CH), 126.7 (CH), 126.4 (CH), 126.2 (CH), 126.0 (CH), 125.9 (CH), 123.9 (CH).

IR (ATR): 2955, 1678, 1569, 1417, 1232, 685 cm^{-1} .

MS (ESI) m/z (relative intensity): 355 (100) $[\text{M} + \text{Na}]^+$, 333 (20) $[\text{M} + \text{H}]^+$.

HR-MS (ESI): m/z calcd. for $[\text{C}_{25}\text{H}_{16}\text{O} + \text{Na}]^+$ 355.1093 found 355.1095.

$[\alpha]_D^{20}$: -4.5 ($c = 1.2$, CHCl_3). HPLC separation (Chiralpak[®] ID-3, *n*-hexane/*i*-PrOH 99:1, 1.0 mL/min, detection at 273 nm): t_r (major) = 15.3 min, t_r (minor) = 16.2 min, 76% ee.



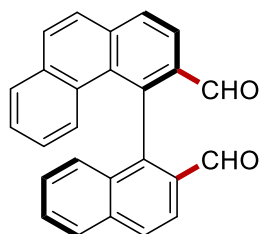
(-)-E)-n-Butyl-3-(1-(3-formylphenanthren-4-yl)naphthalen-2-yl)acrylate (74ia): A modified procedure L was followed using recovered 4-(naphthalen-1-yl)phenanthrene-3-carbaldehyde **73i** (30 mg, 0.09 mmol, 76% ee) and *n*-butyl acrylate (**38a**) (34.6 mg,

0.27 mmol) with *D*-*tert*-leucine (3.6 mg, 30 mol %). Isolation by column chromatography (*n*-hexane/EtOAc = 5:1) yielded *ent*-**74ia** (23.9 mg, 58%, *E/Z* = 96:4, 96% ee).

$[\alpha]_D^{20}$: -30.2 (*c* = 0.4).

HPLC separation (Chiralpak[®] IA-3, *n*-hexane/*i*-PrOH 95:5, 1.0 mL/min, detection at 273 nm):

t_r (major) = 11.9 min, t_r (minor) = 14.9 min, 96% ee.



4-(2-Formylnaphthalen-1-yl)phenanthrene-3-carbaldehyde (402): To a solution of **74ia** (32.1 mg, 0.07 mmol, 1 equiv) in THF (1.8 mL) and H₂O (0.9 mL), K₂OsO₄·2H₂O (4 mg, 0.011 mmol, 15 mol %) and NaIO₄ (149 mg, 0.7 mmol, 10 equiv) were added at 25 °C, the reaction mixture was stirred at 50 °C for 16 h. The reaction mixture was then quenched with sat. aqueous Na₂S₂O₃ (5 mL) and stirred vigorously for 30 min. The biphasic reaction mixture was extracted with EtOAc (3 × 20 mL) and then the combined organic layers were washed with brine (20 mL), dried over Na₂SO₄, and concentrated. The crude product was purified by column chromatography (*n*-hexane/EtOAc = 3:1) to provide **402** (22.3 mg, 86%) as a yellow oil.

¹H-NMR (400 MHz, CDCl₃): δ = 9.60 (s, 1H), 9.42 (s, 1H), 8.38 (dd, *J* = 8.3, 1.5 Hz, 1H), 8.27–8.18 (m, 3H), 8.09 (d, *J* = 8.2 Hz, 1H), 8.00–7.91 (m, 2H), 7.88 (dd, *J* = 7.9, 1.5 Hz, 1H), 7.69 (ddd, *J* = 8.3, 6.7, 1.5 Hz, 1H), 7.53–7.47 (m, 1H), 7.46–7.37 (m, 2H), 7.06 (d, *J* = 8.8 Hz, 1H), 6.94 (ddd, *J* = 8.8, 7.0, 1.2 Hz, 1H).

¹³C-NMR (100 MHz, CDCl₃): δ = 191.3 (CH), 190.9 (CH), 143.5 (C_q), 137.8 (C_q), 137.1 (C_q), 136.1 (C_q), 134.8 (C_q), 133.9 (C_q), 133.3 (C_q), 132.4 (C_q), 131.7 (CH), 130.8 (CH), 130.2 (C_q), 130.1 (C_q), 129.9 (CH), 129.9 (CH), 129.5 (CH), 128.7 (CH), 128.4 (CH), 127.3 (CH), 127.2 (CH), 126.9 (CH), 126.8 (CH), 126.6 (CH), 124.3 (CH), 123.0 (CH).

IR (ATR): 2935, 1712, 1695, 1555, 1496, 1246, 1114, 795 cm⁻¹.

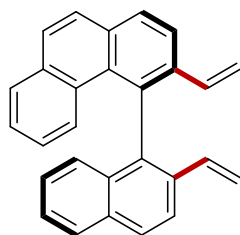
MS (ESI) *m/z* (relative intensity): 383 (100) [M + Na]⁺, 361 (30) [M + H]⁺.

HR-MS (ESI): *m/z* calcd. for [C₂₆H₁₆O₂ + Na]⁺ 383.1043 found 383.1044.

$[\alpha]_D^{20}$: -11.4 (*c* = 0.9, CHCl₃).

HPLC separation (Chiralpak[®] IA-3, *n*-hexane/*i*-PrOH 90:10, 1.0 mL/min, detection at 273 nm):

t_r (major) = 30.8 min, t_r (minor) = 12.7 min, 96% ee.



3-Vinyl-4-(2-vinylnaphthalen-1-yl)phenanthrene (402'): A flame dried round bottom flask was charged with **403** (17.8 mg, 0.05 mmol, 1 equiv). THF (1.5 mL) was added and the mixture was stirred until dissolution of the substrate. The solution was cooled to $-78\text{ }^{\circ}\text{C}$. A second flame-dried round bottom flask was charged with methyltriphenylphosphonium bromide (71.5 mg, 0.2 mmol, 4 equiv). THF (1.5 mL) was added and the suspension was cooled to $-78\text{ }^{\circ}\text{C}$. *n*-Butyllithium (3.8 equiv, 0.19 mmol) was added to the suspension of the phosphonium salt. The orange solution was warmed to rt for 10 min, and then cooled back to $-78\text{ }^{\circ}\text{C}$. The orange solution of phosphorus ylide was slowly transferred *via* canula to the solution of **402**. The reaction mixture was warmed to rt and stirred for 1 hour. Silica gel was directly added to the reaction mixture and the solvent is evaporated under vacuum. The crude product was purified by column chromatography (*n*-hexane/EtOAc = 15:1) to provide **402'** (17.7 mg, 99%) as yellow oil.

$^1\text{H-NMR}$ (400 MHz, CDCl_3): δ = 8.12–8.00 (m, 3H), 8.01–7.92 (m, 2H), 7.87 (d, J = 8.8 Hz, 1H), 7.83–7.75 (m, 2H), 7.45 (ddd, J = 8.8, 5.5, 2.4 Hz, 1H), 7.40–7.29 (m, 2H), 7.23–7.15 (m, 2H), 6.89 (ddd, J = 8.8, 6.9, 1.6 Hz, 1H), 6.38 (dd, J = 17.5, 11.0 Hz, 1H), 6.21 (dd, J = 17.5, 11.0 Hz, 1H), 5.80–5.68 (m, 2H), 5.07–4.98 (m, 2H).

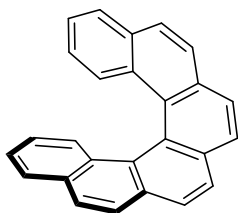
$^{13}\text{C-NMR}$ (100 MHz, CDCl_3): δ = 138.0 (C_q), 137.0 (C_q), 135.6 (CH), 134.7 (CH), 134.1 (C_q), 133.7 (C_q), 133.6 (C_q), 133.5 (C_q), 133.3 (C_q), 132.7 (C_q), 131.0 (C_q), 129.9 (C_q), 129.5 (CH), 128.7 (CH), 128.3 (CH), 128.1 (CH), 128.0 (CH), 127.6 (CH), 126.8 (CH), 126.6 (CH), 126.4 (CH), 126.3 (CH), 126.0 (CH), 125.9 (CH), 123.9 (CH), 123.1 (CH), 115.5 (CH_2), 115.4 (CH_2).

IR (ATR): 2925, 1596, 1482, 1455, 1396, 1346, 1314, 785, 748, 699 cm^{-1} .

MS (EI) m/z (relative intensity): 356 (70), 328 (80), 313 (100), 298 (70), 215 (10).

HR-MS (EI): m/z calcd. for $\text{C}_{28}\text{H}_{20}$ $[\text{M}]^+$: 356.1560, found 356.1559.

$[\alpha]_{\text{D}}^{20}$: +130.5 (c = 1.0, CHCl_3).



[6]-helicene (**403**): A flame-dried microwave vessel, equipped with a magnetic stirrer, was charged with **402'** (10.7 mg, 0.03 mmol). CH₂Cl₂ (1.5 mL) was added and the mixture was stirred until dissolution of all the substrate. Grubbs II (2.5 mg, 0.003 mmol, 10 mol %) was added, and the tube was sealed. The reaction vessel was irradiated in a microwave at 95 °C for 1 h. The reaction mixture was concentrated in *vacuo* and purified by column silica gel chromatography (*n*-hexane/EtOAc = 30:1) to afford [6]-helicene **403** (8.6 mg, 88%) as a colourless oil.

¹H-NMR (600 MHz, CDCl₃): δ = 8.02–7.94 (m, 4H), 7.94–7.88 (m, 4H), 7.83–7.79 (m, 2H), 7.58 (ddt, *J* = 8.6, 1.2, 0.6 Hz, 2H), 7.20 (ddd, *J* = 8.0, 6.8, 1.1 Hz, 2H), 6.67 (ddd, *J* = 8.4, 6.8, 1.4 Hz, 2H).

¹³C-NMR (150 MHz, CDCl₃): δ = 133.1 (C_q), 131.7 (C_q), 131.2 (C_q), 129.9 (C_q), 128.0 (C_q), 127.9 (CH), 127.7 (CH), 127.5 (CH), 127.2 (CH), 126.9 (CH), 126.2 (CH), 125.5 (CH), 124.6 (CH), 124.1 (C_q).

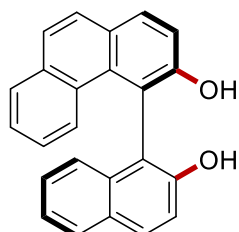
IR (ATR): 2922, 1496, 1259, 1095, 1070, 795, 749, 610 cm⁻¹.

MS (EI) *m/z* (relative intensity): 328 (80), 313 (90), 300 (100), 162 (20).

HR-MS (EI): *m/z* calcd. for C₂₆H₁₆ [M]⁺: 328.1247, found 328.1242.

[α]_D²⁰: -350.1 (c = 1.0, CHCl₃).

HPLC separation (Chiralpak[®] IB-3, *n*-hexane/*i*-PrOH 99:1, 1 mL/min, detection at 273 nm): *t_r* (major) = 7.3 min, *t_r* (minor) = 8.5 min, 96% ee.



(R)-4-(2-Hydroxynaphthalen-1-yl)phenanthren-3-ol (405): **402** (15 mg, 0.04 mmol) and *m*-chloroperbenzoic acid (*m*CPBA) (75%, 23 mg, 0.1 mmol) were refluxed in CH₂Cl₂ (1.5 mL) for 48 h. The reaction mixture was allowed to cool and then aqueous Na₂S₂O₃ was added to destroy the excess of *m*CPBA. The suspension mixture was neutralized with aqueous NaHCO₃. The solution was extracted with CH₂Cl₂ (3 × 50 mL). The combined extracts were washed with brine (4 × 100 mL) and dried with anhydrous magnesium sulfate. Removal of the solvent gave a brown solid, which was dissolved in MeOH (3 mL) and hydrolyzed under nitrogen with aqueous KOH (2.5 equiv). After 2 h MeOH was evaporated and the solution was acidified to *pH* 2 with a concentrated HCl solution. The product was finally extracted with CH₂Cl₂ and

5. Experimental Part

chromatography on silica gel (*n*-hexane/EtOAc = 1:2) provided the desired product **405** (7.0 mg, 51%) as a white solid.

¹H-NMR (600 MHz, CDCl₃): δ = 8.07–7.99 (m, 2H), 7.93 (dd, *J* = 8.1, 1.0 Hz, 1H), 7.81–7.74 (m, 2H), 7.66 (d, *J* = 8.8 Hz, 1H), 7.51–7.48 (m, 1H), 7.46 (d, *J* = 8.6 Hz, 1H), 7.40–7.36 (m, 2H), 7.34 (ddd, *J* = 7.9, 6.9, 1.1 Hz, 1H), 7.30–7.28 (m, 2H), 6.90 (ddd, *J* = 8.6, 7.0, 1.6 Hz, 1H), 5.11 (s, 1H), 5.04 (s, 1H).

¹³C-NMR (150 MHz, CDCl₃): δ = 154.0 (C_q), 151.9 (C_q), 133.7 (C_q), 132.6 (C_q), 132.5 (CH), 131.7 (CH), 130.7 (C_q), 129.89 (C_q), 129.5 (C_q), 128.6 (CH), 128.6 (C_q), 128.6 (CH), 127.9 (CH), 127.5 (CH), 126.6 (CH), 126.1 (CH), 125.8 (CH), 125.2 (CH), 124.6 (CH), 123.9 (CH), 118.2 (CH), 116.9 (CH), 114.5 (C_q), 112.4 (C_q).

IR (ATR): 2912, 1680, 1540, 1420, 1260, 846, 755 cm⁻¹.

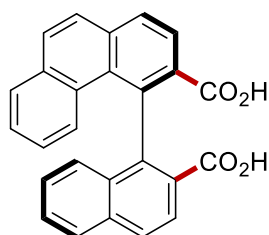
MS (ESI) *m/z* (relative intensity): 359 (100) [M + Na]⁺, 337 (10) [M + H]⁺.

HR-MS (ESI): *m/z* calcd. for [C₂₄H₁₆O₂ + Na]⁺ 359.1043 found 359.1044.

[α]_D²⁰: -4.9 (c = 0.35, CHCl₃).

HPLC separation (Chiralpak[®] IA-3, *n*-hexane/*i*-PrOH 90:10, 1.0 mL/min, detection at 273 nm):

t_r (major) = 36.8 min, *t_r* (minor) = 27.8 min, 96% ee.



(R)-4-(2-Carboxynaphthalen-1-yl)phenanthrene-3-carboxylic acid (404): To a stirred solution of compound **402** (15 mg, 0.04 mmol) and 2-methylbut-2-ene (36.4 mg, 0.52 mmol) in *t*BuOH (1.5 mL) were added a saturated solution of NaClO₂ (14.4 mg, 0.16 mmol) and NaH₂PO₄·2H₂O (31.2 mg, 0.20 mmol). The mixture was stirred at 30 °C for 18 hours. The mixture was treated with saturated NH₄Cl and extracted with EtOAc. The combined organic layers were washed with brine, dried over Na₂SO₄, filtered, concentrated, and purified by chromatography on silica gel (*n*-hexane/EtOAc/AcOH = 1:1:0.1) to give compound **404** (12.4 mg, 82%) M.p. >200 °C.

¹H-NMR (400 MHz, CD₃CO₂D): δ = 8.32 (d, *J* = 8.8 Hz, 1H), 8.25 (d, *J* = 8.3 Hz, 1H), 8.22–8.19 (m, 2H), 8.02 (d, *J* = 8.3 Hz, 1H), 7.91 (d, *J* = 8.8 Hz, 2H), 7.83 (dd, *J* = 8.1, 1.5 Hz, 1H), 7.53 (ddd, *J* = 8.1, 6.2, 1.7 Hz, 1H), 7.37–7.31 (m, 1H), 7.26–7.17 (m, 2H), 7.14 (d, *J* = 8.8 Hz, 1H), 6.87 (ddd, *J* = 8.7, 7.0, 1.7 Hz, 1H).

^{13}C -NMR (150 MHz, $\text{CD}_3\text{CO}_2\text{D}$): δ = 173.4 (C_q), 172.5 (C_q), 144.5 (C_q), 139.6 (C_q), 136.9 (C_q), 136.8 (C_q), 134.1 (C_q), 133.9 (C_q), 131.8 (C_q), 131.0 (CH), 130.9 (C_q), 130.7 (C_q), 130.1 (CH), 129.5 (CH), 129.3 (CH), 129.1 (CH), 128.4 (CH), 128.1 (CH), 128.1 (CH), 128.0 (C_q), 127.8 (CH), 127.7 (CH), 127.5 (CH), 127.3 (CH), 127.1 (CH).

IR (ATR): 2922, 1719, 1595, 1455, 1168, 1142, 748, 699 cm^{-1} .

MS (ESI) m/z (relative intensity): 415 (100) $[\text{M} + \text{Na}]^+$, 393 (10) $[\text{M} + \text{H}]^+$.

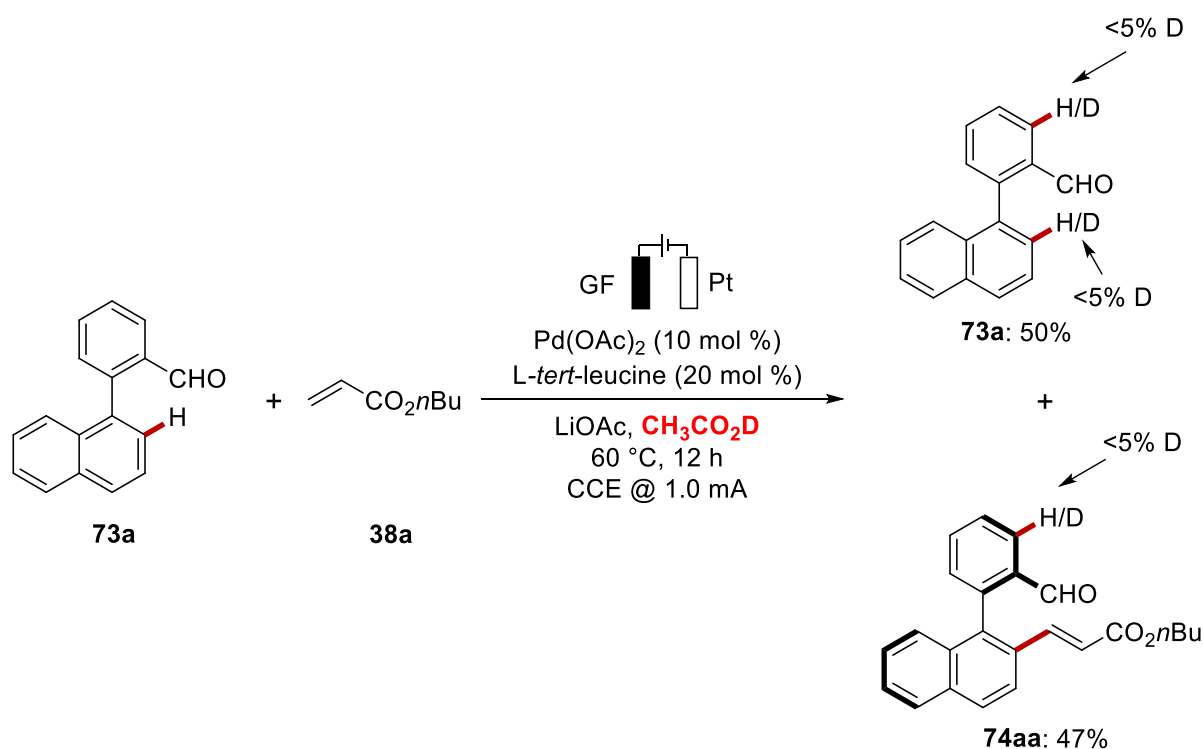
HR-MS (ESI): m/z calcd. for $[\text{C}_{26}\text{H}_{16}\text{O}_4 + \text{Na}]^+$ 415.0941 found 415.0940.

$[\alpha]_D^{20}$: -19.9 ($c = 0.8$, CHCl_3).

HPLC separation (Chiralpak[®] IB-3, *n*-hexane/*i*-PrOH/TFA 92:8:0.08, 1.0 mL/min, detection at 273 nm): t_r (major) = 18.7 min, t_r (minor) = 25.9 min, 96% ee.

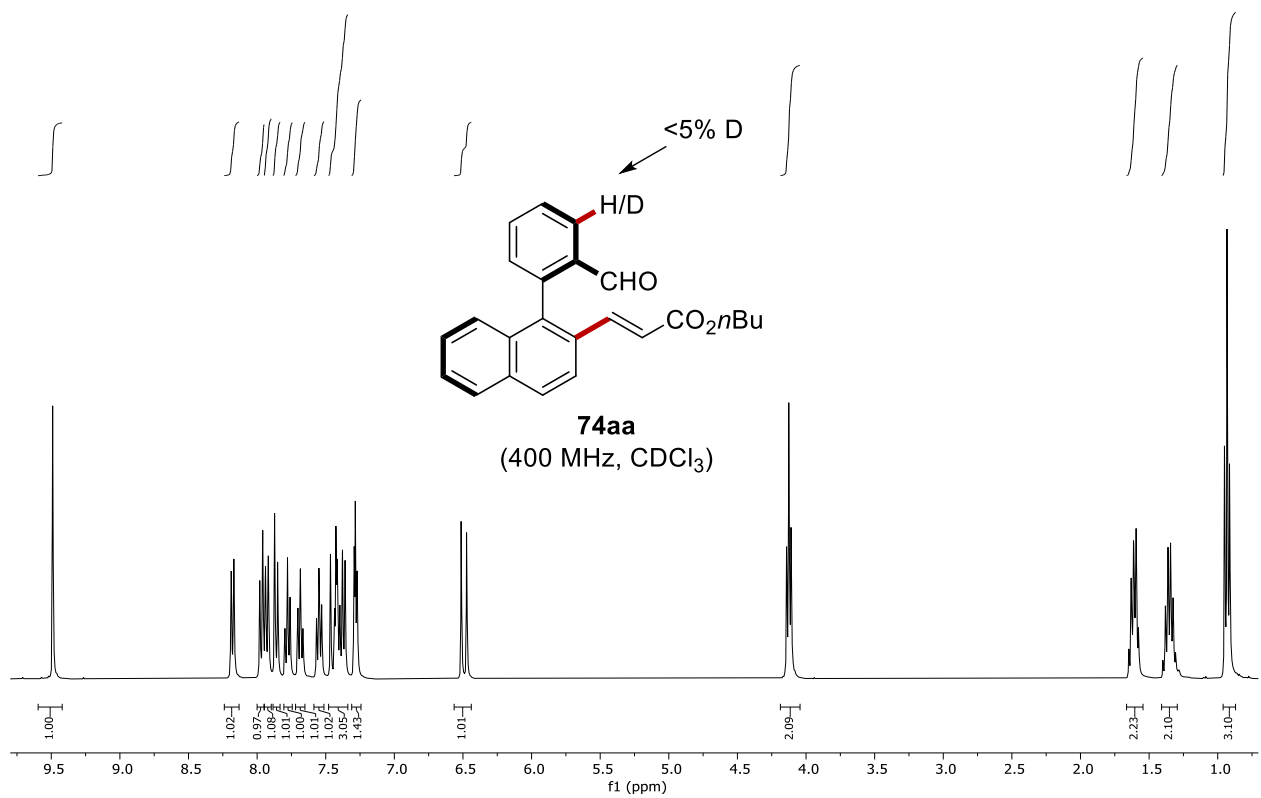
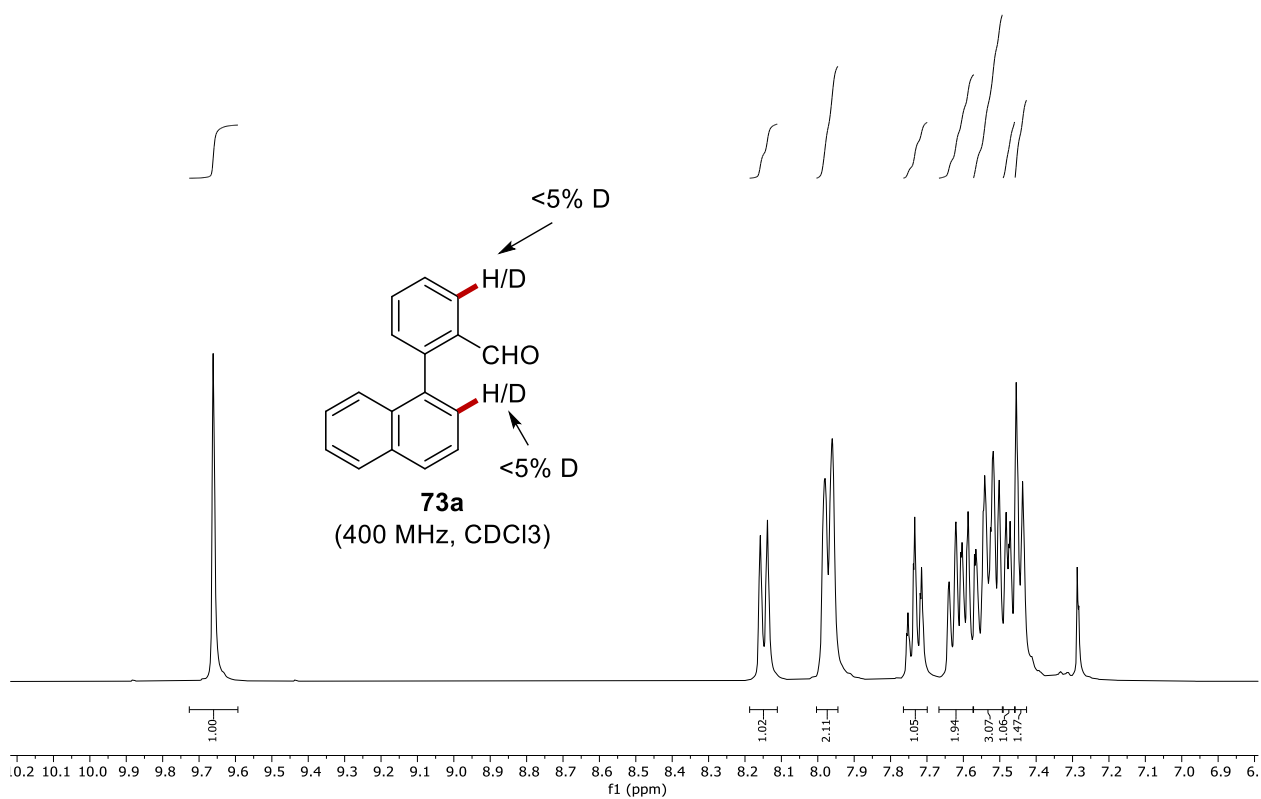
5.9.3. Mechanistic Studies for the Atroposelective C–H Activation

5.9.3.1. H/D-exchange experiment

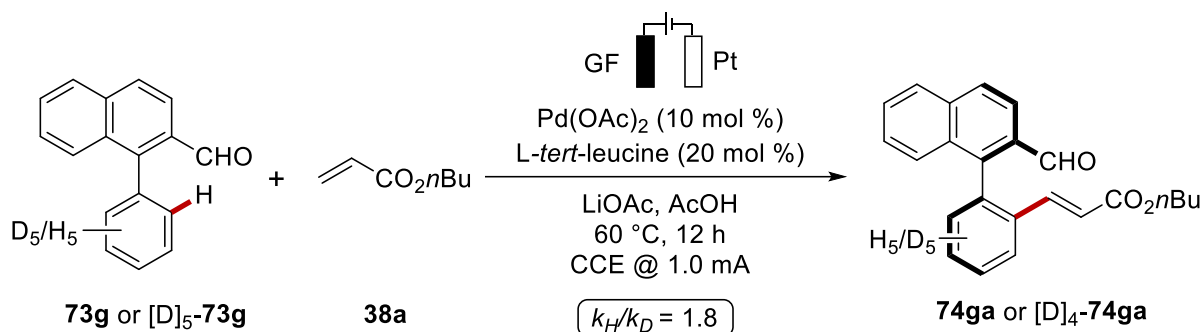


The representative procedure **L** was followed using **73a** (46.4 mg, 0.20 mmol, 1 equiv), *n*-butyl acrylate (**38a**) (76.9 mg, 0.6 mmol, 3 equiv), $\text{Pd}(\text{OAc})_2$ (4.49 mg, 10 mol %), *L*-*tert*-leucine (5.24 mg, 20 mol %) and LiOAc (26.4 mg, 2 equiv) in AcOD (4.5 mL) at 60 °C for 12 h. At ambient temperature, the reaction mixture was diluted with EtOAc (3.0 mL) and the solvents were removed *in vacuo*. The crude mixture was purified by flash column chromatography on silica gel to afford the desired product **74aa** (34 mg, 47%) and **73a** (23.2 mg, 50% reisolated).

5. Experimental Part



5.7.3.2. KIE Studies



Two parallel reactions of **73g** and **[D]₅-73g** with **38a** were performed to determine the KIE by comparison of the initial reaction rates through ¹H-NMR-analysis with triphenylmethane as the internal standard. A suspension of **73g** (46.4 mg, 0.20 mmol, 1.00 equiv) or **[D]₅-73g** (47.4 mg, 0.50 mmol, 1.00 equiv), **38a** (76.9 mg, 1.50 mmol, 3 equiv), Pd(OAc)₂ (4.49 mg, 10 mol %), *L-tert-leucine* (5.24 mg, 20 mol %) and LiOAc (26.4 mg, 2 equiv) and triphenylmethane (48.9 mg, 0.20 mmol) in AcOH (5.6 mL) was stirred at 60 °C. Aliquots (30 μL) were periodically removed to provide the following conversions as determined by ¹H-NMR:

Table 36. Conversion-time table

<i>t</i> / min	10	20	30	40	50	60
74ga / %	2.41	7.11	9.02	10.38	13.18	15.2
[D]_n-74ga / %	0.2	3.21	3.71	5.31	6.05	7.43

5.7.3.3. Nonlinear Effect Study

Six parallel independent reactions of **73a** (46.4 mg, 0.20 mmol), **38a** (76.9 mg, 0.60 mmol), Pd(OAc)₂ (4.49 mg, 10 mol %), *L-tert-leucine* (10–100% ee, 5.24 mg, 20 mol %) and LiOAc (26.4 mg, 2 equiv) were heated at 60 °C in AcOH (4.5 mL) for 20 h. At ambient temperature, the reaction mixture was diluted with EtOAc (3.0 mL) and the solvents were removed *in vacuo*. The crude mixture was purified by flash column chromatography on silica gel to afford the desired product **74aa**. The enantiomeric excess was determined by HPLC on chiral stationary phase.

Table 37. Nonlinear effect study for the asymmetric C–H olefination.

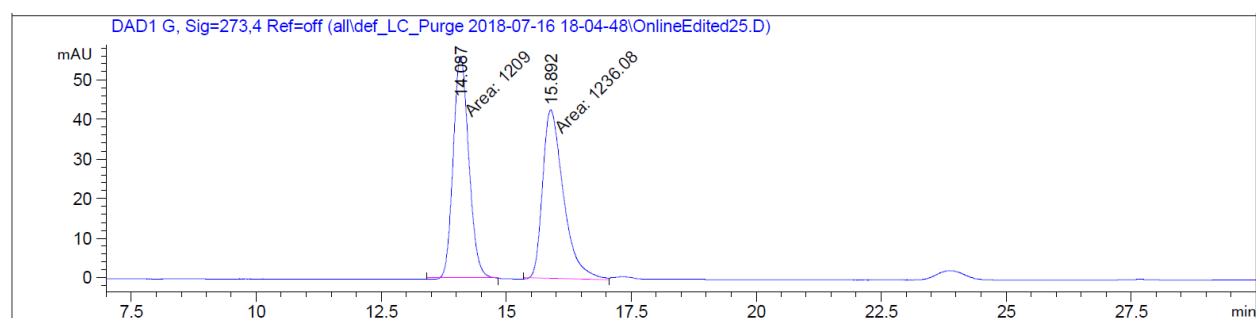
Entry	<i>ee</i> of <i>L-tert-leucine</i>	<i>ee</i> of the product [74aa]
1	0	0
2	11.2	9.3
3	28.8	29.1
4	51.2	51.5
5	68.8	67.5
6	91.2	88.9
7	100	97.3

5.10. Crystallographic Data

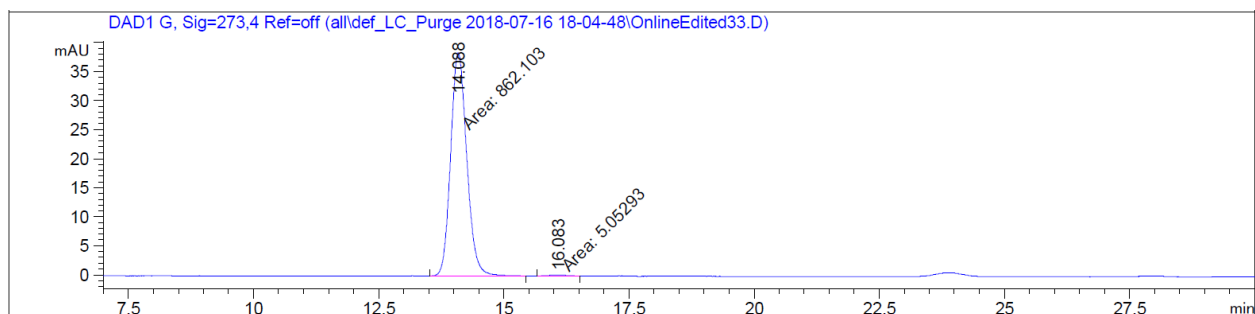
The crystal structures of **357da**, **363e** and **256aj** were measured and solved by *Dr. Christopher Golz*.

5.10.1. Determination of Absolute Stereochemistry of **357da**

357da (40 mg, 0.14 mmol, e.r. 92:8) was recrystallized from *n*-hexane/CH₂Cl₂ to furnish optically pure product (15 mg, 0.05 mmol, e.r. 99:1) as mother liquor. HPLC separation (Chiralpak® IF-3, *n*-hexane/*i*-PrOH 95:5, 1.0 mL/min, detection at 273 nm): *t_r*(major) = 14.1 min, *t_r*(minor) = 16.1 min, 99.4:0.6 e.r.



Peak #	RetTime [min]	Type	Width [min]	Area [mAU*s]	Height [mAU]	Area %
1	14.087	MM	0.3604	1208.99988	55.91126	49.4463
2	15.892	MM	0.4848	1236.07727	42.49546	50.5537



Peak #	RetTime [min]	Type	Width [min]	Area [mAU*s]	Height [mAU]	Area %
1	14.088	FM	0.3737	862.10291	38.44878	99.4173
2	16.083	MM	0.4284	5.05293	1.96560e-1	0.5827

Crystals suitable for X-Ray crystallography were grown by slow evaporation from *n*-hexane/CH₂Cl₂.

5.10.1.1. X-Ray Crystallographic Analysis of 357da

Table 38. Crystal data of 357da

Compound	357da
CCDC Number	CCDC 1857899
Empirical formula	C ₁₉ H ₁₉ NO ₂
Formula Weight	293.35
Temperature	100.03
Crystal System	monoclinic
Space group	P2 ₁
a/Å	8.3652(5)
b/Å	12.7119(8)
c/Å	14.4909(9)
α/°	90
β/°	91.7540(10)
γ/°	90

5. Experimental Part

Volume/Å ³	1540.21(16)
Z	4
$\rho_{\text{calc}}/\text{cm}^3$	1.265
μ/mm^{-1}	0.650
F(000)	624.0
Crystal size/mm ³	0.525 × 0.462 × 0.094
Radiation	CuK α ($\lambda = 1.54178$)
2 Θ range for data collection/°	6.102 to 155.35
Index ranges	-10 ≤ h ≤ 10, -16 ≤ k ≤ 16, -18 ≤ l ≤ 18
Reflections collected	6284
Independent reflections	6284 [R _{int} = 0.0300, R _{sigma} = 0.0301]
Data/restraints/parameters	6284/136/540
Goodness-of-fit on F ²	1.064
Final R indexes [I >= 2 σ (I)]	R ₁ = 0.0300, wR ₂ = 0.0827
Final R indexes [all data]	R ₁ = 0.0301, wR ₂ = 0.0827
Largest diff. peak/hole / e Å ⁻³	0.26/-0.13
Flack parameter	0.00(9)

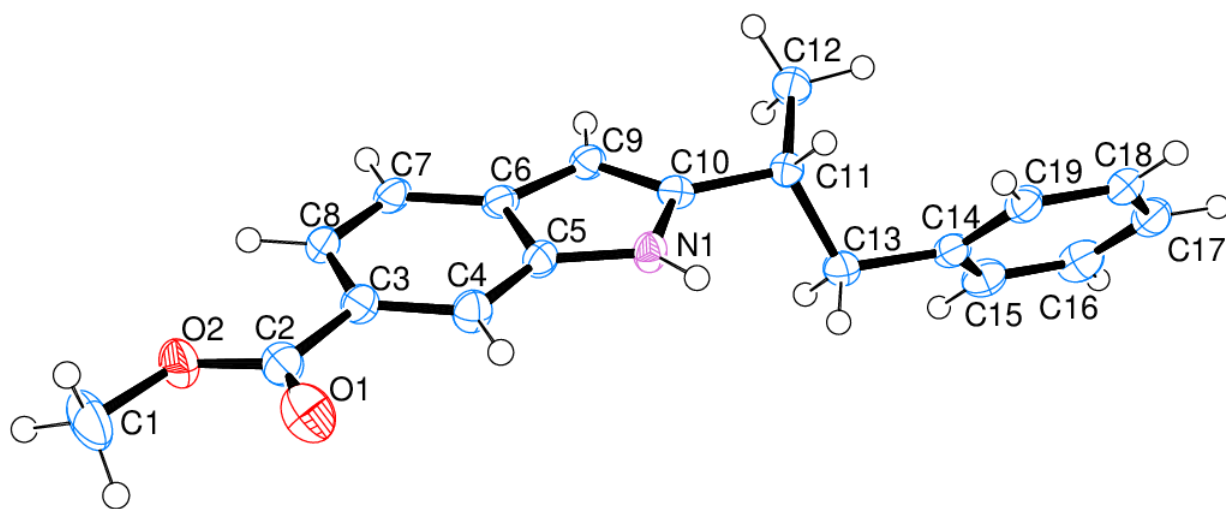


Table 39. Selected bond lengths [Å] and angles [°] for **357da**

O1-C2	1.215(3)	C2-O2-C1	117.2(2)
O2-C1	1.448(3)	C10-N1-C5	109.00(17)
O2-C2	1.338(3)	O1-C2-O2	123.1(2)
N1-C5	1.379(3)	O1-C2-C3	125.1(2)
N1-C10	1.377(3)	O2-C2-C3	111.8(2)

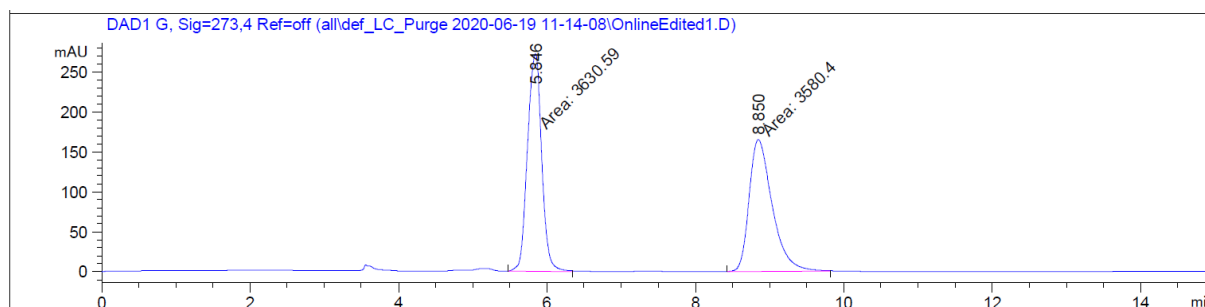
C2-C3	1.482(3)	C4-C3-C2	117.3(2)
C3-C4	1.398(3)	C4-C3-C8	120.8(2)
C3-C8	1.409(3)	C8-C3-C2	121.8(2)
C4-C5	1.391(3)	C5-C4-C3	117.7(2)
C5-C6	1.419(3)	N1-C5-C4	130.3(2)
C6-C7	1.403(3)	N1-C5-C6	107.56(18)
C6-C9	1.425(3)	C4-C5-C6	122.2(2)
C7-C8	1.381(3)	C5-C6-C9	106.59(18)
C9-C10	1.372(3)	C7-C6-C5	118.9(2)
C10-C11	1.503(3)	C7-C6-C9	134.5(2)
C11-C12	1.528(3)	C8-C7-C6	119.41(19)
C11-C13	1.547(3)	C7-C8-C3	120.99(19)
C13-C14	1.515(3)	C10-C9-C6	107.54(19)
C14-C15	1.397(3)	N1-C10-C11	120.88(18)
C14-C19	1.395(3)	C9-C10-N1	109.32(19)
C15-C16	1.386(3)	C9-C10-C11	129.80(19)
C16-C17	1.379(4)	C10-C11-C12	111.03(17)
C17-C18	1.388(3)	C10-C11-C13	110.73(16)
C18-C19	1.390(3)	C12-C11-C13	111.86(17)
		C14-C13-C11	113.08(16)
		C15-C14-C13	120.61(19)
		C19-C14-C13	121.46(18)
		C19-C14-C15	117.9(2)
		C16-C15-C14	120.8(2)
		C17-C16-C15	120.7(2)
		C16-C17-C18	119.5(2)
		C17-C18-C19	120.0(2)
		C18-C19-C14	121.16(19)

5.10.2. Determination of Absolute Stereochemistry of **363e**

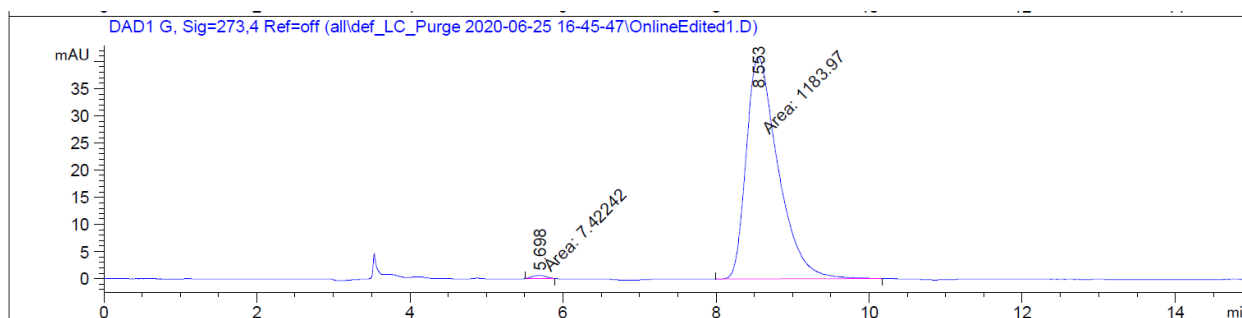
363e (70 mg, 0.20 mmol, 82:18 e.r.) was recrystallized from CH₂Cl₂ at RT by slow evaporation to obtain suitable crystals for X-Ray crystallography. HPLC separation of crystal **363e**

5. Experimental Part

(Chiralpak® ID-3, *n*-hexane/EtOAc 90:10, 1.0 mL/min, detection at 273 nm): t_r (major) = 8.6 min, t_r (minor) = 5.7 min, 99.4:0.6 e.r.

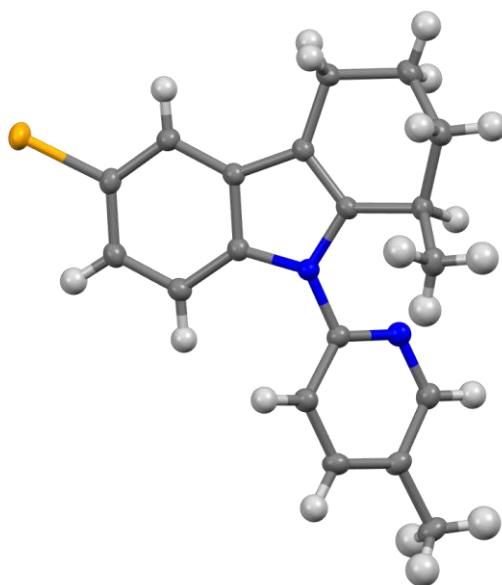


Peak #	RetTime [min]	Type	Width [min]	Area [mAU*s]	Height [mAU]	Area %
1	5.846	MM	0.2217	3630.59351	272.88000	50.3481
2	8.850	MM	0.3607	3580.39746	165.42451	49.6519



Peak #	RetTime [min]	Type	Width [min]	Area [mAU*s]	Height [mAU]	Area %
1	5.698	MM	0.2029	7.42242	6.09674e-1	0.6230
2	8.553	MM	0.4822	1183.96558	40.92201	99.3770

5.10.2.1. X-Ray Crystallographic Analysis of 363e

**Table 40.** Crystal data of **256aj**

Compound	363e
CCDC Number	CCDC 2012314
Empirical formula	C ₁₉ H ₁₉ BrN ₂
Formula Weight	355.27
Temperature	100.0
Crystal System	orthorhombic
Space group	P2 ₁ 2 ₁ 2 ₁
a/Å	9.0448(5)
b/Å	12.6834(6)
c/Å	13.7386(5)
α/°	90
β/°	90
γ/°	90
Volume/Å ³	1576.08(13)
Z	4
ρ _{calc} /cm ³	1.497
μ/mm ⁻¹	2.606
F(000)	728.0
Crystal size/mm ³	0.344 × 0.172 × 0.155
Radiation	MoKα (λ = 0.71073)
2θ range for data collection/°	4.37 to 61.036

5. Experimental Part

Index ranges	-12 ≤ h ≤ 12, -18 ≤ k ≤ 18, -19 ≤ l ≤ 18
Reflections collected	54097
Independent reflections	4808 [R _{int} = 0.0218, R _{sigma} = 0.0107]
Data/restraints/parameters	4808/0/201
Goodness-of-fit on F ²	1.067
Final R indexes [I >= 2σ (I)]	R ₁ = 0.0188, wR ₂ = 0.0501
Final R indexes [all data]	R ₁ = 0.0194, wR ₂ = 0.0509
Largest diff. peak/hole / e Å ⁻³	0.55/-0.19
Flack parameter	0.0083(14)

Table 41. Selected bond lengths [Å] and angles [°] for **363e**

Br1-C1	1.9134 (16)	C6-C1-Br1	118.57(12)
N1-C4	1.397 (2)	C6-C1-C2	123.22(15)
N1-C8	1.410 (2)	C3-C2-C1	119.93(15)
N1-C14	1.416 (2)	C2-C3-C4	118.00(15)
N2-C14	1.336 (2)	N1-C4-C5	107.50(14)
N2-C18	1.335 (2)	C3-C4-N1	130.62(15)
C1-C2	1.397 (2)	C3-C4-C5	121.88(15)
C1-C6	1.383 (2)	C4-C5-C7	107.48(14)
C2-C3	1.388 (2)	C6-C5-C4	119.67(15)
C3-C4	1.393 (2)	C6-C5-C7	132.84(15)
C4-C5	1.416 (2)	C1-C6-C5	117.24(15)
C5-C6	1.406 (2)	C5-C7-C12	128.90(14)
C5-C7	1.430 (2)	C8-C7-C5	107.64(14)
C7-C8	1.366 (2)	C8-C7-C12	123.39(14)
C7-C12	1.501 (2)	N1-C8-C9	124.30(14)
C8-C9	1.499 (2)	C7-C8-N1	109.45(14)
C9-C10	1.558 (2)	C7-C8-C9	125.96(15)
C9-C13	1.530 (2)	C8-C9-C10	107.93(14)
C10-C11	1.526 (2)	C8-C9-C13	111.97(14)
C11-C12	1.528 (2)	C13-C9-C10	108.24(14)
C14-C15	1.392 (2)	C11-C10-C9	112.86(15)
C15-C16	1.390 (2)	C10-C11-C12	110.35(15)
C16-C17	1.393 (2)	C7-C12-C11	109.53(14)

C17-C18	1.397 (2)	N2-C14-N1	115.55(14)
C17-C19	1.505 (2)	N2-C14-C15	123.07(16)
C4-N1-C8	107.92(13)	C15-C14-N1	121.38(15)
C4-N1-C14	124.61(14)	C16-C15-C14	118.31(16)
C8-N1-C14	125.71(14)	C15-C16-C17	119.87(16)
C18-N2-C14	117.42(15)	C16-C17-C18	116.58(16)
C2-C1-Br1	118.21(12)	C16-C17-C19	122.65(17)
		C18-C17-C19	120.76(16)
		N2-C18-C17	124.62(16)

5.10.3. X-Ray Crystallographic Analysis of 256aj

Table 42. Crystal data of **256aj**

Compound	256aj
CCDC Number	CCDC 1910199
Empirical formula	C ₂₅ H ₁₅ N ₃ O
Formula Weight	373.40
Temperature	99.95
Crystal System	monoclinic
Space group	C2/c
a/Å	39.582(3)
b/Å	6.6842(5)
c/Å	13.9095(8)
α/°	90
β/°	97.656(2)
γ/°	90
Volume/Å ³	3647.2(4)
Z	8
ρ _{calc} /cm ³	1.360
μ/mm ⁻¹	0.085
F(000)	1552.0
Crystal size/mm ³	0.379 × 0.351 × 0.052
Radiation	MoKα (λ = 0.71073)
2θ range for data collection/°	5.91 to 59.128
Index ranges	-54 ≤ h ≤ 54, -9 ≤ k ≤ 9, -19 ≤ l ≤ 17

5. Experimental Part

Reflections collected	31821
Independent reflections	5081 [$R_{\text{int}} = 0.0295$, $R_{\text{sigma}} = 0.0196$]
Data/restraints/parameters	5081/0/262
Goodness-of-fit on F^2	1.042
Final R indexes [$I > 2\sigma(I)$]	$R_1 = 0.0410$, $wR_2 = 0.1015$
Final R indexes [all data]	$R_1 = 0.0479$, $wR_2 = 0.1090$
Largest diff. peak/hole / $e \text{ \AA}^{-3}$	0.30/-0.25

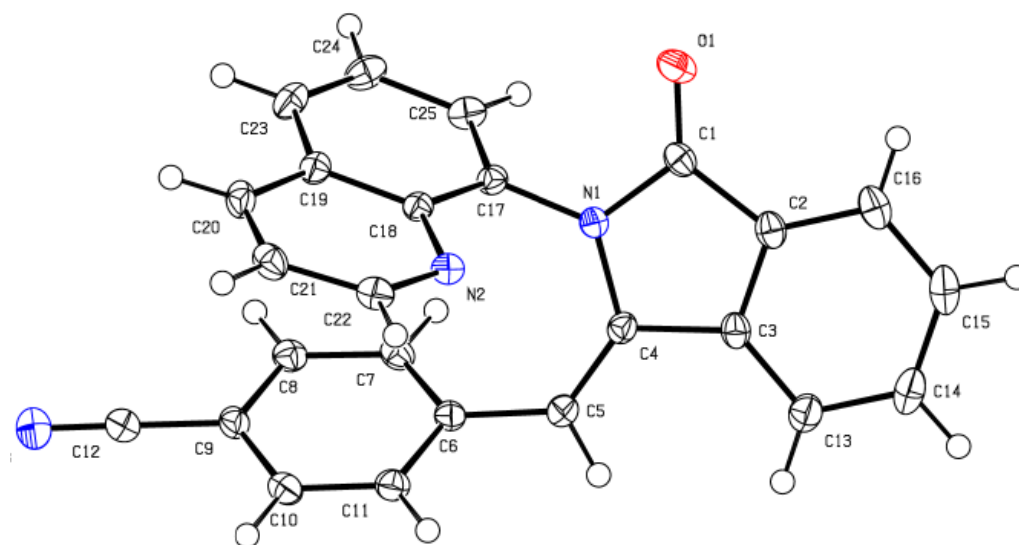


Table 43. Selected bond lengths [\AA] and angles [$^\circ$] for **256aj**

O1–C1	1.2182(13)	C9–C10	1.3996(16)
N1–C1	1.3978(13)	C9–C12	1.4425(15)
N1–C4	1.4170(13)	C10–C11	1.3817(15)
N1–C17	1.4260(13)	C13–C14	1.3925(16)
N2–C18	1.3686(13)	C14–C15	1.3961(19)
N2–C22	1.3206(14)	C15–C16	1.3907(18)
N3–C12	1.1448(16)	C17–C18	1.4228(14)
C1–C2	1.4766(15)	C17–C25	1.3735(15)
C2–C3	1.3933(15)	C18–C19	1.4227(14)
C2–C16	1.3898(15)	C19–C20	1.4185(15)
C3–C4	1.4729(14)	C19–C23	1.4182(15)
C3–C13	1.3912(15)	C20–C21	1.3652(17)
C4–C5	1.3433(14)	C21–C22	1.4141(16)
C5–C6	1.4741(14)	C23–C24	1.3673(17)

C6–C7	1.4025(15)	C24–C25	1.4092(16)
C6–C11	1.4020(14)	C1–N1–C4	112.09(9)
C7–C8	1.3859(15)	C1–N1–C17	121.05(9)
C8–C9	1.515(3)	C4–N1–C17	126.86(8)
C22–N2–C18	116.81(9)	C11–C10–C9	119.29(10)
O1–C1–N1	124.93(10)	C10–C11–C6	120.96(10)
O1–C1–C2	129.39(10)	N3–C12–C9	179.31(14)
N1–C1–C2	105.67(9)	C3–C13–C14	117.70(11)
C3–C2–C1	108.35(9)	C13–C14–C15	121.68(11)
C16–C2–C1	129.61(10)	C16–C15–C14	120.58(11)
C16–C2–C3	122.04(10)	C2–C16–C15	117.56(11)
C2–C3–C4	108.88(9)	C18–C17–N1	120.31(9)
C13–C3–C2	120.42(10)	C25–C17–N1	118.85(9)
C13–C3–C4	130.70(10)	C25–C17–C18	120.84(10)
N1–C4–C3	104.99(8)	N2–C18–C17	119.19(9)
C5–C4–N1	129.95(10)	N2–C18–C19	122.97(9)
C5–C4–C3	125.06(10)	C19–C18–C17	117.83(9)
C4–C5–C6	128.86(10)	C20–C19–C18	117.51(10)
C7–C6–C5	122.87(9)	C23–C19–C18	119.92(10)
C11–C6–C5	118.35(10)	C23–C19–C20	122.57(10)
C11–C6–C7	118.78(10)	C21–C20–C19	119.20(10)
C8–C7–C6	120.96(10)	C20–C21–C22	118.80(10)
C7–C8–C9	119.06(10)	N2–C22–C21	124.66(10)
C8–C9–C12	120.08(10)	C24–C23–C19	120.51(10)
C10–C9–C8	120.78(10)	C23–C24–C25	120.07(10)
C10–C9–C12	119.13(10)	C17–C25–C24	120.68(10)

6. References

- [1] F. Wöhler, *Ann. Phys.* **1828**, 88, 253-256.
- [2] a) K. C. Nicolaou, S. Rigol, *Angew. Chem. Int. Ed.* **2019**, 58, 11206-11241; b) K. C. Nicolaou, *Isr. J. Chem.* **2018**, 58, 104-113; c) L. F. Tietze, T. Eicher, U. Diederichsen, A. Speicher, N. Schützenmeister, *Reactions and Syntheses: In the Organic Chemistry Laboratory, Second, Completely Revised and Updated Edition*, Wiley-VCH, Weinheim, **2015**; d) K. C. Nicolaou, *Proc. R. Soc. London Ser. A* **2014**, 470, 20130690; e) K. C. Nicolaou, J. S. Chen, *Classics in total synthesis III: Further targets, strategies, methods*, Wiley-VCH, Weinheim, **2011**; f) E.-i. Negishi, A. de Meijere, *Handbook of Organopalladium Chemistry for Organic Synthesis*, Wiley, New York, **2002**.
- [3] a) S. A. Matlin, G. Mehta, H. Hopf, A. Krief, *Nat. Chem.* **2016**, 8, 393-398; b) B. H. Lipshutz, N. A. Isley, J. C. Fennewald, E. D. Slack, *Angew. Chem. Int. Ed.* **2013**, 52, 10952-10958.
- [4] a) B. M. Trost, *Angew. Chem. Int. Ed.* **1995**, 34, 259-281; b) B. M. Trost, *Science* **1991**, 254, 1471-1477.
- [5] a) P. T. Anastas, M. M. Kirchhoff, *Acc. Chem. Res.* **2002**, 35, 686-694; b) P. T. Anastas, J. C. Warner, *Green chemistry: theory and practice*, Oxford University Press, Oxford, **1998**.
- [6] P. Gandeepan, N. Kaplaneris, S. Santoro, L. Vaccaro, L. Ackermann, *ACS Sustainable Chem. Eng.* **2019**, 7, 8023-8040.
- [7] L. Ackermann, *Modern Arylation Methods*, Wiley-VCH, Weinheim, **2009**.
- [8] a) C. Glaser, *Justus Liebigs Ann. Chem.* **1870**, 154, 137-171; b) C. Glaser, *Ber. Dtsch. Chem. Ges.* **1869**, 2, 422-424.
- [9] F. Ullmann, J. Bielecki, *Ber. Dtsch. Chem. Ges.* **1901**, 34, 2174-2185.
- [10] C. C. C. Johansson Seechurn, M. O. Kitching, T. J. Colacot, V. Snieckus, *Angew. Chem. Int. Ed.* **2012**, 51, 5062-5085.
- [11] R. Mozingo, *Org. Synth.* **1946**, 26, 77-82.
- [12] H. Lindlar, *Helv. Chim. Acta* **1952**, 35, 446-450.
- [13] J. Smidt, W. Hafner, R. Jira, J. Sedlmeier, R. Sieber, H. Kojer, R. Rüttinger, *Angew. Chem.* **1959**, 71, 176-182.
- [14] a) R. F. Heck, *J. Am. Chem. Soc.* **1968**, 90, 5546-5548; b) R. F. Heck, *J. Am. Chem. Soc.* **1968**, 90, 5542-5546; c) R. F. Heck, *J. Am. Chem. Soc.* **1968**, 90, 5538-5542; d)

- R. F. Heck, *J. Am. Chem. Soc.* **1968**, *90*, 5531-5534; e) R. F. Heck, *J. Am. Chem. Soc.* **1968**, *90*, 5526-5531; f) R. F. Heck, *J. Am. Chem. Soc.* **1968**, *90*, 5518-5526.
- [15] a) K. Mori, T. Mizoroki, A. Ozaki, *Bull. Chem. Soc. Jpn.* **1973**, *46*, 1505-1508; b) T. Mizoroki, K. Mori, A. Ozaki, *Bull. Chem. Soc. Jpn.* **1971**, *44*, 581-581.
- [16] a) H. A. Dieck, R. F. Heck, *J. Am. Chem. Soc.* **1974**, *96*, 1133-1136; b) R. F. Heck, J. P. Nolley, *J. Org. Chem.* **1972**, *37*, 2320-2322.
- [17] a) N. Miyaura, A. Suzuki, *Chem. Rev.* **1995**, *95*, 2457-2483; b) N. Miyaura, K. Yamada, A. Suzuki, *Tetrahedron Lett.* **1979**, *20*, 3437-3440; c) N. Miyaura, A. Suzuki, *J. Chem. Soc., Chem. Commun.* **1979**, 866-867.
- [18] a) E. Negishi, A. O. King, N. Okukado, *J. Org. Chem.* **1977**, *42*, 1821-1823; b) A. O. King, N. Okukado, E.-i. Negishi, *J. Chem. Soc., Chem. Commun.* **1977**, 683-684.
- [19] a) K. Tamao, K. Sumitani, M. Kumada, *J. Am. Chem. Soc.* **1972**, *94*, 4374-4376; b) R. J. P. Corriu, J. P. Masse, *J. Chem. Soc., Chem. Commun.* **1972**, 144a-144a.
- [20] a) T. Hiyama, *J. Organomet. Chem.* **2002**, *653*, 58-61; b) Y. Hatanaka, T. Hiyama, *J. Org. Chem.* **1988**, *53*, 918-920.
- [21] a) J. K. Stille, *Angew. Chem. Int. Ed.* **1986**, *25*, 508-524; b) D. Milstein, J. K. Stille, *J. Am. Chem. Soc.* **1979**, *101*, 4992-4998; c) D. Milstein, J. K. Stille, *J. Am. Chem. Soc.* **1978**, *100*, 3636-3638.
- [22] a) R. Chinchilla, C. Nájera, *Chem. Soc. Rev.* **2011**, *40*, 5084-5121; b) R. Chinchilla, C. Nájera, *Chem. Rev.* **2007**, *107*, 874-922; c) K. Sonogashira, *J. Organomet. Chem.* **2002**, *653*, 46-49; d) K. Sonogashira, Y. Tohda, N. Hagihara, *Tetrahedron Lett.* **1975**, *16*, 4467-4470.
- [23] a) B. M. Trost, D. L. Van Vranken, *Chem. Rev.* **1996**, *96*, 395-422; b) B. M. Trost, P. E. Strege, *J. Am. Chem. Soc.* **1977**, *99*, 1649-1651; c) B. M. Trost, T. J. Fullerton, *J. Am. Chem. Soc.* **1973**, *95*, 292-294; d) J. Tsuji, H. Takahashi, M. Morikawa, *Tetrahedron Lett.* **1965**, *6*, 4387-4388.
- [24] a) F. Paul, J. Patt, J. F. Hartwig, *J. Am. Chem. Soc.* **1994**, *116*, 5969-5970; b) A. S. Guram, S. L. Buchwald, *J. Am. Chem. Soc.* **1994**, *116*, 7901-7902.
- [25] The nobel prize in chemistry 2010 - press release: https://www.nobelprize.org/nobel_prizes/chemistry/laureates/2010/press.html (accessed on 07.02.2021).
- [26] A. de Meijere, S. Bräse, M. Oestreich, *Metal-Catalyzed Cross-Coupling Reactions and More*, Wiley-VCH, Weinheim, **2014**.

- [27] a) S. Rej, Y. Ano, N. Chatani, *Chem. Rev.* **2020**, *120*, 1788-1887; b) A. Dey, S. K. Sinha, T. K. Achar, D. Maiti, *Angew. Chem. Int. Ed.* **2019**, *58*, 10820-10843; c) Y. Xu, G. Dong, *Chem. Sci.* **2018**, *9*, 1424-1432; d) C. Sambigiagio, D. Schönbauer, R. Blicck, T. Dao-Huy, G. Pototschnig, P. Schaaf, T. Wiesinger, M. F. Zia, J. Wencel-Delord, T. Besset, B. U. W. Maes, M. Schnürch, *Chem. Soc. Rev.* **2018**, *47*, 6603-6743; e) Y. Park, Y. Kim, S. Chang, *Chem. Rev.* **2017**, *117*, 9247-9301; f) J. R. Hummel, J. A. Boerth, J. A. Ellman, *Chem. Rev.* **2017**, *117*, 9163-9227; g) J. He, M. Wasa, K. S. L. Chan, Q. Shao, J.-Q. Yu, *Chem. Rev.* **2017**, *117*, 8754-8786; h) H. M. L. Davies, D. Morton, *ACS Cent. Sci.* **2017**, *3*, 936-943; i) T. Gensch, M. N. Hopkinson, F. Glorius, J. Wencel-Delord, *Chem. Soc. Rev.* **2016**, *45*, 2900-2936; j) P. Gandeepan, C.-H. Cheng, *Chem. Asian J.* **2015**, *10*, 824-838; k) O. Daugulis, J. Roane, L. D. Tran, *Acc. Chem. Res.* **2015**, *48*, 1053-1064; l) J. Wencel-Delord, F. Glorius, *Nat. Chem.* **2013**, *5*, 369-375; m) C. S. Yeung, V. M. Dong, *Chem. Rev.* **2011**, *111*, 1215-1292; n) I. A. I. Mkhaliid, J. H. Barnard, T. B. Marder, J. M. Murphy, J. F. Hartwig, *Chem. Rev.* **2010**, *110*, 890-931; o) T. W. Lyons, M. S. Sanford, *Chem. Rev.* **2010**, *110*, 1147-1169; p) A. Gunay, K. H. Theopold, *Chem. Rev.* **2010**, *110*, 1060-1081; q) D. A. Colby, R. G. Bergman, J. A. Ellman, *Chem. Rev.* **2010**, *110*, 624-655; r) L. Ackermann, R. Vicente, A. R. Kapdi, *Angew. Chem. Int. Ed.* **2009**, *48*, 9792-9826; s) R. G. Bergman, *Nature* **2007**, *446*, 391-393; t) L. Ackermann, *Synlett* **2007**, 507-526.
- [28] a) J. Börgel, T. Ritter, *Chem* **2020**, *6*, 1877-1887; b) W. Wang, M. M. Lorion, J. Shah, A. R. Kapdi, L. Ackermann, *Angew. Chem. Int. Ed.* **2018**, *57*, 14700-14717; c) A. F. M. Noisier, M. A. Brimble, *Chem. Rev.* **2014**, *114*, 8775-8806.
- [29] a) J.-R. Pouliot, F. Grenier, J. T. Blaskovits, S. Beaupré, M. Leclerc, *Chem. Rev.* **2016**, *116*, 14225-14274; b) D. J. Schipper, K. Fagnou, *Chem. Mater.* **2011**, *23*, 1594-1600.
- [30] a) S. D. Friis, M. J. Johansson, L. Ackermann, *Nat. Chem.* **2020**, *12*, 511-519; b) D. C. Blakemore, L. Castro, I. Churcher, D. C. Rees, A. W. Thomas, D. M. Wilson, A. Wood, *Nat. Chem.* **2018**, *10*, 383-394; c) M. Seki, *Org. Process Res. Dev.* **2016**, *20*, 867-877; d) T. Cernak, K. D. Dykstra, S. Tyagarajan, P. Vachal, S. W. Krska, *Chem. Soc. Rev.* **2016**, *45*, 546-576; e) L. Ackermann, *Org. Process Res. Dev.* **2015**, *19*, 260-269.
- [31] P. Gandeepan, T. Müller, D. Zell, G. Cera, S. Warratz, L. Ackermann, *Chem. Rev.* **2019**, *119*, 2192-2452.
- [32] a) R. Mei, U. Dhawa, R. C. Samanta, W. Ma, J. Wencel-Delord, L. Ackermann, *ChemSusChem* **2020**, *13*, 3306-3356; b) S. M. Khake, N. Chatani, *Chem* **2020**, *6*, 1056-1081; c) S. M. Khake, N. Chatani, *Trends Chem.* **2019**, *1*, 524-539; d) A. Baccalini, S.

- Vergura, P. Dolui, G. Zanoni, D. Maiti, *Org. Biomol. Chem.* **2019**, *17*, 10119-10141; e) P. M. Edwards, L. L. Schafer, *Chem. Commun.* **2018**, *54*, 12543-12560; f) T. Yoshino, S. Matsunaga, *Adv. Synth. Catal.* **2017**, *359*, 1245-1262; g) W. Liu, L. Ackermann, *ACS Catal.* **2016**, *6*, 3743-3752; h) G. Cera, L. Ackermann, *Top. Curr. Chem.* **2016**, *374*, 57; i) K. Gao, N. Yoshikai, *Acc. Chem. Res.* **2014**, *47*, 1208-1219; j) C.-L. Sun, B.-J. Li, Z.-J. Shi, *Chem. Rev.* **2011**, *111*, 1293-1314; k) A. A. Kulkarni, O. Daugulis, *Synthesis* **2009**, 4087-4109.
- [33] S. J. Blanksby, G. B. Ellison, *Acc. Chem. Res.* **2003**, *36*, 255-263.
- [34] a) L. Ackermann, *Chem. Rev.* **2011**, *111*, 1315-1345; b) D. Balcells, E. Clot, O. Eisenstein, *Chem. Rev.* **2010**, *110*, 749-823.
- [35] a) D. Lapointe, K. Fagnou, *Chem. Lett.* **2010**, *39*, 1118-1126; b) S. I. Gorelsky, D. Lapointe, K. Fagnou, *J. Am. Chem. Soc.* **2008**, *130*, 10848-10849; c) L.-C. Campeau, M. Parisien, A. Jean, K. Fagnou, *J. Am. Chem. Soc.* **2006**, *128*, 581-590.
- [36] a) Y. Boutadla, D. L. Davies, S. A. Macgregor, A. I. Poblador-Bahamonde, *Dalton Trans.* **2009**, 5887-5893; b) D. L. Davies, S. M. A. Donald, S. A. Macgregor, *J. Am. Chem. Soc.* **2005**, *127*, 13754-13755.
- [37] a) K. Naksomboon, J. Poater, F. M. Bickelhaupt, M. Á. Fernández-Ibáñez, *J. Am. Chem. Soc.* **2019**, *141*, 6719-6725; b) E. Tan, O. Quinonero, M. Elena de Orbe, A. M. Echavarren, *ACS Catal.* **2018**, *8*, 2166-2172; c) H. Wang, M. Moselage, M. J. González, L. Ackermann, *ACS Catal.* **2016**, *6*, 2705-2709; d) D. Santrač, S. Cella, W. Wang, L. Ackermann, *Eur. J. Org. Chem.* **2016**, 5429-5436; e) W. Ma, R. Mei, G. Tenti, L. Ackermann, *Chem. Eur. J.* **2014**, *20*, 15248-15251.
- [38] Z. Chen, B. Wang, J. Zhang, W. Yu, Z. Liu, Y. Zhang, *Org. Chem. Front.* **2015**, *2*, 1107-1295.
- [39] S. De Sarkar, W. Liu, S. I. Kozhushkov, L. Ackermann, *Adv. Synth. Catal.* **2014**, *356*, 1461-1479.
- [40] a) W. Ma, P. Gandeepan, J. Li, L. Ackermann, *Org. Chem. Front.* **2017**, *4*, 1435-1467; b) F. Zhang, D. R. Spring, *Chem. Soc. Rev.* **2014**, *43*, 6906-6919.
- [41] a) G. Liao, T. Zhang, Z.-K. Lin, B.-F. Shi, *Angew. Chem. Int. Ed.* **2020**, *59*, 19773-19786; b) M. I. Lapuh, S. Mazeh, T. Besset, *ACS Catal.* **2020**, *10*, 12898-12919; c) P. Gandeepan, L. Ackermann, *Chem* **2018**, *4*, 199-222.
- [42] a) T. Ahrens, J. Kohlmann, M. Ahrens, T. Braun, *Chem. Rev.* **2015**, *115*, 931-972; b) H. Amii, K. Uneyama, *Chem. Rev.* **2009**, *109*, 2119-2183; c) W. K. Hagmann, *J. Med. Chem.* **2008**, *51*, 4359-4369.

- [43] a) T. Furuya, A. S. Kamlet, T. Ritter, *Nature* **2011**, *473*, 470-477; b) K. Müller, C. Faeh, F. Diederich, *Science* **2007**, *317*, 1881-1886.
- [44] a) G. Landelle, M. Bergeron, M.-O. Turcotte-Savard, J.-F. Paquin, *Chem. Soc. Rev.* **2011**, *40*, 2867-2908; b) C. E. Jakobsche, G. Peris, S. J. Miller, *Angew. Chem. Int. Ed.* **2008**, *47*, 6707-6711.
- [45] a) Y. Ye, S. D. Schimler, P. S. Hanley, M. S. Sanford, *J. Am. Chem. Soc.* **2013**, *135*, 16292-16295; b) P. S. Fier, J. F. Hartwig, *J. Am. Chem. Soc.* **2012**, *134*, 10795-10798; c) X. Wang, L. Truesdale, J.-Q. Yu, *J. Am. Chem. Soc.* **2010**, *132*, 3648-3649; d) E. J. Cho, T. D. Senecal, T. Kinzel, Y. Zhang, D. A. Watson, S. L. Buchwald, *Science* **2010**, *328*, 1679-1681; e) D. A. Watson, M. Su, G. Teverovskiy, Y. Zhang, J. García-Fortanet, T. Kinzel, S. L. Buchwald, *Science* **2009**, *325*, 1661-1664.
- [46] T. Fujita, K. Fuchibe, J. Ichikawa, *Angew. Chem. Int. Ed.* **2019**, *58*, 390-402.
- [47] W. Heitz, A. Knebelkamp, *Makromol. Chem. Rapid Commun.* **1991**, *12*, 69-75.
- [48] K. Sakoda, J. Mihara, J. Ichikawa, *Chem. Commun.* **2005**, 4684-4686.
- [49] J. Ichikawa, R. Nadano, N. Ito, *Chem. Commun.* **2006**, 4425-4427.
- [50] T. Miura, Y. Ito, M. Murakami, *Chem. Lett.* **2008**, *37*, 1006-1007.
- [51] R. T. Thornbury, F. D. Toste, *Angew. Chem. Int. Ed.* **2016**, *55*, 11629-11632.
- [52] P. Tian, C. Feng, T.-P. Loh, *Nat. Commun.* **2015**, *6*, 7472.
- [53] J.-Q. Wu, S.-S. Zhang, H. Gao, Z. Qi, C.-J. Zhou, W.-W. Ji, Y. Liu, Y. Chen, Q. Li, X. Li, H. Wang, *J. Am. Chem. Soc.* **2017**, *139*, 3537-3545.
- [54] C.-Q. Wang, L. Ye, C. Feng, T.-P. Loh, *J. Am. Chem. Soc.* **2017**, *139*, 1762-1765.
- [55] F. Romanov-Michailidis, B. D. Ravetz, D. W. Paley, T. Rovis, *J. Am. Chem. Soc.* **2018**, *140*, 5370-5374.
- [56] a) H. Yi, G. Zhang, H. Wang, Z. Huang, J. Wang, A. K. Singh, A. Lei, *Chem. Rev.* **2017**, *117*, 9016-9085; b) Z. Dong, Z. Ren, S. J. Thompson, Y. Xu, G. Dong, *Chem. Rev.* **2017**, *117*, 9333-9403; c) G. Rouquet, N. Chatani, *Angew. Chem. Int. Ed.* **2013**, *52*, 11726-11743.
- [57] C. G. Newton, S.-G. Wang, C. C. Oliveira, N. Cramer, *Chem. Rev.* **2017**, *117*, 8908-8976.
- [58] a) T. Yoshino, S. Satake, S. Matsunaga, *Chem. Eur. J.* **2020**, *26*, 7346; b) T. K. Achar, S. Maiti, S. Jana, D. Maiti, *ACS Catal.* **2020**, 13748-13793; c) C. Zheng, S.-L. You, *RSC Adv.* **2014**, *4*, 6173-6214; d) J. Wencel-Delord, F. Colobert, *Chem. Eur. J.* **2013**, *19*, 14010-14017; e) R. Giri, B.-F. Shi, K. M. Engle, N. Maugel, J.-Q. Yu, *Chem. Soc. Rev.* **2009**, *38*, 3242-3272.

- [59] a) Ł. Woźniak, N. Cramer, *Trends Chem.* **2019**, *1*, 471-484; b) J. Loup, U. Dhawa, F. Pesciaioli, J. Wencel-Delord, L. Ackermann, *Angew. Chem. Int. Ed.* **2019**, *58*, 12803-12818.
- [60] A. R. Dick, M. S. Sanford, *Tetrahedron* **2006**, *62*, 2439-2463.
- [61] a) H. M. L. Davies, J. R. Manning, *Nature* **2008**, *451*, 417-424; b) J. T. Groves, P. Viski, *J. Am. Chem. Soc.* **1989**, *111*, 8537-8538.
- [62] V. I. Sokolov, L. L. Troitskaya, O. A. Reutov, *J. Organomet. Chem.* **1977**, *133*, C28-C30.
- [63] a) Q. Shao, K. Wu, Z. Zhuang, S. Qian, J.-Q. Yu, *Acc. Chem. Res.* **2020**, *53*, 833-851; b) K. M. Engle, J.-Q. Yu, *J. Org. Chem.* **2013**, *78*, 8927-8955.
- [64] M. R. Albicker, N. Cramer, *Angew. Chem. Int. Ed.* **2009**, *48*, 9139-9142.
- [65] T. Saget, N. Cramer, *Angew. Chem. Int. Ed.* **2013**, *52*, 7865-7868.
- [66] Z.-Q. Lin, W.-Z. Wang, S.-B. Yan, W.-L. Duan, *Angew. Chem. Int. Ed.* **2015**, *54*, 6265-6269.
- [67] L. Liu, A.-A. Zhang, Y. Wang, F. Zhang, Z. Zuo, W.-X. Zhao, C.-L. Feng, W. Ma, *Org. Lett.* **2015**, *17*, 2046-2049.
- [68] C. He, M. Hou, Z. Zhu, Z. Gu, *ACS Catal.* **2017**, *7*, 5316-5320.
- [69] J. Luo, T. Zhang, L. Wang, G. Liao, Q.-J. Yao, Y.-J. Wu, B.-B. Zhan, Y. Lan, X.-F. Lin, B.-F. Shi, *Angew. Chem. Int. Ed.* **2019**, *58*, 6708-6712.
- [70] B.-B. Zhan, L. Wang, J. Luo, X.-F. Lin, B.-F. Shi, *Angew. Chem. Int. Ed.* **2020**, *59*, 3568-3572.
- [71] R. Shintani, H. Otomo, K. Ota, T. Hayashi, *J. Am. Chem. Soc.* **2012**, *134*, 7305-7308.
- [72] L. Yang, M. Neuburger, O. Baudoin, *Angew. Chem. Int. Ed.* **2018**, *57*, 1394-1398.
- [73] D. Grosheva, N. Cramer, *ACS Catal.* **2017**, *7*, 7417-7420.
- [74] B.-F. Shi, N. Mangel, Y.-H. Zhang, J.-Q. Yu, *Angew. Chem. Int. Ed.* **2008**, *47*, 4882-4886.
- [75] B.-F. Shi, Y.-H. Zhang, J. K. Lam, D.-H. Wang, J.-Q. Yu, *J. Am. Chem. Soc.* **2010**, *132*, 460-461.
- [76] L. Chu, X.-C. Wang, C. E. Moore, A. L. Rheingold, J.-Q. Yu, *J. Am. Chem. Soc.* **2013**, *135*, 16344-16347.
- [77] B. N. Laforteza, K. S. L. Chan, J.-Q. Yu, *Angew. Chem. Int. Ed.* **2015**, *54*, 11143-11146.
- [78] Z.-J. Du, J. Guan, G.-J. Wu, P. Xu, L.-X. Gao, F.-S. Han, *J. Am. Chem. Soc.* **2015**, *137*, 632-635.

- [79] D.-W. Gao, Y.-C. Shi, Q. Gu, Z.-L. Zhao, S.-L. You, *J. Am. Chem. Soc.* **2013**, *135*, 86-89.
- [80] C. Pi, Y. Li, X. Cui, H. Zhang, Y. Han, Y. Wu, *Chem. Sci.* **2013**, *4*, 2675-2679.
- [81] D.-W. Gao, Q. Gu, S.-L. You, *J. Am. Chem. Soc.* **2016**, *138*, 2544-2547.
- [82] L. Chu, K.-J. Xiao, J.-Q. Yu, *Science* **2014**, *346*, 451-455.
- [83] K.-J. Xiao, L. Chu, J.-Q. Yu, *Angew. Chem. Int. Ed.* **2016**, *55*, 2856-2860.
- [84] K.-J. Xiao, L. Chu, G. Chen, J.-Q. Yu, *J. Am. Chem. Soc.* **2016**, *138*, 7796-7800.
- [85] D.-W. Gao, Q. Gu, S.-L. You, *ACS Catal.* **2014**, *4*, 2741-2745.
- [86] S.-X. Li, Y.-N. Ma, S.-D. Yang, *Org. Lett.* **2017**, *19*, 1842-1845.
- [87] L. Jin, Q.-J. Yao, P.-P. Xie, Y. Li, B.-B. Zhan, Y.-Q. Han, X. Hong, B.-F. Shi, *Chem* **2020**, *6*, 497-511.
- [88] F.-L. Zhang, K. Hong, T.-J. Li, H. Park, J.-Q. Yu, *Science* **2016**, *351*, 252-256.
- [89] Q.-J. Yao, S. Zhang, B.-B. Zhan, B.-F. Shi, *Angew. Chem. Int. Ed.* **2017**, *56*, 6617-6621.
- [90] G. Liao, Q.-J. Yao, Z.-Z. Zhang, Y.-J. Wu, D.-Y. Huang, B.-F. Shi, *Angew. Chem. Int. Ed.* **2018**, *57*, 3661-3665.
- [91] G. Liao, B. Li, H.-M. Chen, Q.-J. Yao, Y.-N. Xia, J. Luo, B.-F. Shi, *Angew. Chem. Int. Ed.* **2018**, *57*, 17151-17155.
- [92] a) S. Zhang, Q.-J. Yao, G. Liao, X. Li, H. Li, H.-M. Chen, X. Hong, B.-F. Shi, *ACS Catal.* **2019**, *9*, 1956-1961; b) H.-M. Chen, S. Zhang, G. Liao, Q.-J. Yao, X.-T. Xu, K. Zhang, B.-F. Shi, *Organometallics* **2019**, *38*, 4022-4028.
- [93] J. Zhang, Q. Xu, J. Wu, J. Fan, M. Xie, *Org. Lett.* **2019**, *21*, 6361-6365.
- [94] T. Wesch, F. R. Leroux, F. Colobert, *Adv. Synth. Catal.* **2013**, *355*, 2139-2144.
- [95] C. K. Hazra, Q. Dherbassy, J. Wencel-Delord, F. Colobert, *Angew. Chem. Int. Ed.* **2014**, *53*, 13871-13875.
- [96] a) Q. Dherbassy, J. P. Djukic, J. Wencel-Delord, F. Colobert, *Angew. Chem. Int. Ed.* **2018**, *57*, 4668-4672; b) Q. Dherbassy, J. Wencel-Delord, F. Colobert, *Tetrahedron* **2018**, *74*, 6205-6212.
- [97] H. Shi, A. N. Herron, Y. Shao, Q. Shao, J.-Q. Yu, *Nature* **2018**, *558*, 581-585.
- [98] Z.-S. Liu, Y. Hua, Q. Gao, Y. Ma, H. Tang, Y. Shang, H.-G. Cheng, Q. Zhou, *Nat. Catal.* **2020**, *3*, 727-733.
- [99] N. Fujii, F. Kakiuchi, A. Yamada, N. Chatani, S. Murai, *Chem. Lett.* **1997**, *26*, 425-426.
- [100] a) H. Harada, R. K. Thalji, R. G. Bergman, J. A. Ellman, *J. Org. Chem.* **2008**, *73*, 6772-6779; b) A. Watzke, R. M. Wilson, S. J. O'Malley, R. G. Bergman, J. A. Ellman, *Synlett*

- 2007**, 2383-2389; c) R. K. Thalji, J. A. Ellman, R. G. Bergman, *J. Am. Chem. Soc.* **2004**, *126*, 7192-7193.
- [101] a) D. N. Tran, N. Cramer, *Angew. Chem. Int. Ed.* **2013**, *52*, 10630-10634; b) D. N. Tran, N. Cramer, *Angew. Chem. Int. Ed.* **2011**, *50*, 11098-11102.
- [102] S. Satake, T. Kurihara, K. Nishikawa, T. Mochizuki, M. Hatano, K. Ishihara, T. Yoshino, S. Matsunaga, *Nat. Catal.* **2018**, *1*, 585-591.
- [103] L. Lin, S. Fukagawa, D. Sekine, E. Tomita, T. Yoshino, S. Matsunaga, *Angew. Chem. Int. Ed.* **2018**, *57*, 12048-12052.
- [104] Z.-J. Cai, C.-X. Liu, Q. Wang, Q. Gu, S.-L. You, *Nat. Commun.* **2019**, *10*, 4168.
- [105] Q. Wang, Z.-J. Cai, C.-X. Liu, Q. Gu, S.-L. You, *J. Am. Chem. Soc.* **2019**, *141*, 9504-9510.
- [106] J. Mas-Roselló, A. G. Herraiz, B. Audic, A. Laverny, N. Cramer, *Angew. Chem. Int. Ed.* **2021**, DOI: 10.1002/anie.202008166.
- [107] B. Ye, N. Cramer, *Science* **2012**, *338*, 504-506.
- [108] B. Ye, N. Cramer, *J. Am. Chem. Soc.* **2013**, *135*, 636-639.
- [109] a) B. Ye, P. A. Donets, N. Cramer, *Angew. Chem. Int. Ed.* **2014**, *53*, 507-511; b) B. Ye, N. Cramer, *Synlett* **2015**, *26*, 1490-1495.
- [110] B. Ye, N. Cramer, *Angew. Chem. Int. Ed.* **2014**, *53*, 7896-7899.
- [111] J. Zheng, S.-B. Wang, C. Zheng, S.-L. You, *J. Am. Chem. Soc.* **2015**, *137*, 4880-4883.
- [112] T. J. Potter, D. N. Kamber, B. Q. Mercado, J. A. Ellman, *ACS Catal.* **2017**, *7*, 150-153.
- [113] S. Maity, T. J. Potter, J. A. Ellman, *Nat. Catal.* **2019**, *2*, 756-762.
- [114] J. Zheng, S.-L. You, *Angew. Chem. Int. Ed.* **2014**, *53*, 13244-13247.
- [115] J. Zheng, W.-J. Cui, C. Zheng, S.-L. You, *J. Am. Chem. Soc.* **2016**, *138*, 5242-5245.
- [116] H. Li, X. Yan, J. Zhang, W. Guo, J. Jiang, J. Wang, *Angew. Chem. Int. Ed.* **2019**, *58*, 6732-6736.
- [117] a) F. Wang, Z. Qi, Y. Zhao, S. Zhai, G. Zheng, R. Mi, Z. Huang, X. Zhu, X. He, X. Li, *Angew. Chem. Int. Ed.* **2020**, *59*, 13288-13294; b) M. Tian, D. Bai, G. Zheng, J. Chang, X. Li, *J. Am. Chem. Soc.* **2019**, *141*, 9527-9532.
- [118] Z.-J. Jia, C. Merten, R. Gontla, C. G. Daniliuc, A. P. Antonchick, H. Waldmann, *Angew. Chem Int Edit* **2017**, *56*, 2429-2434.
- [119] T. K. Hyster, L. Knorr, T. R. Ward, T. Rovis, *Science* **2012**, *338*, 500-503.
- [120] I. S. Hassan, A. N. Ta, M. W. Danneman, N. Semakul, M. Burns, C. H. Basch, V. N. Dippon, B. R. McNaughton, T. Rovis, *J. Am. Chem. Soc.* **2019**, *141*, 4815-4819.
- [121] G. Li, J. Jiang, H. Xie, J. Wang, *Chem. Eur. J.* **2019**, *25*, 4688-4694.

6. References

- [122] Ł. Woźniak, J.-F. Tan, Q.-H. Nguyen, A. Madron du Vigné, V. Smal, Y.-X. Cao, N. Cramer, *Chem. Rev.* **2020**, *120*, 10516-10543.
- [123] R. Aufdenblatten, S. Diezi, A. Togni, *Monatsh. Chem.* **2000**, *131*, 1345-1350.
- [124] K. Tsuchikama, M. Kasagawa, Y.-K. Hashimoto, K. Endo, T. Shibata, *J. Organomet. Chem.* **2008**, *693*, 3939-3942.
- [125] C. S. Sevov, J. F. Hartwig, *J. Am. Chem. Soc.* **2013**, *135*, 2116-2119.
- [126] T. Shirai, Y. Yamamoto, *Angew. Chem. Int. Ed.* **2015**, *54*, 9894-9897.
- [127] M. Nagamoto, J.-i. Fukuda, M. Hatano, H. Yorimitsu, T. Nishimura, *Org. Lett.* **2017**, *19*, 5952-5955.
- [128] S. Pan, N. Ryu, T. Shibata, *J. Am. Chem. Soc.* **2012**, *134*, 17474-17477.
- [129] T. Shibata, N. Ryu, H. Takano, *Adv. Synth. Catal.* **2015**, *357*, 1131-1135.
- [130] T. Shibata, T. Shizuno, *Angew. Chem. Int. Ed.* **2014**, *53*, 5410-5413.
- [131] E. M. Carreira, L. Kvaerno, *Classics in Stereoselective Synthesis*, John Wiley & Sons, New York, **2009**.
- [132] S. Grélaud, P. Cooper, L. J. Feron, J. F. Bower, *J. Am. Chem. Soc.* **2018**, *140*, 9351-9356.
- [133] V. S. Shinde, M. V. Mane, L. Cavallo, M. Rueping, *Chem. Eur. J.* **2020**, *26*, 8308-8313.
- [134] a) A. Romero-Arenas, V. Hornillos, J. Iglesias-Sigüenza, R. Fernández, J. López-Serrano, A. Ros, J. M. Lassaletta, *J. Am. Chem. Soc.* **2020**, *142*, 2628-2639; b) D. Yamauchi, T. Nishimura, H. Yorimitsu, *Chem. Commun.* **2017**, *53*, 2760-2763; c) Y. Ebe, M. Onoda, T. Nishimura, H. Yorimitsu, *Angew. Chem. Int. Ed.* **2017**, *56*, 5607-5611; d) M. Hatano, Y. Ebe, T. Nishimura, H. Yorimitsu, *J. Am. Chem. Soc.* **2016**, *138*, 4010-4013; e) Y. Ebe, T. Nishimura, *J. Am. Chem. Soc.* **2015**, *137*, 5899-5902.
- [135] K. Tsuchikama, Y.-k. Hashimoto, K. Endo, T. Shibata, *Adv. Synth. Catal.* **2009**, *351*, 2850-2854.
- [136] T. Shirai, H. Ito, Y. Yamamoto, *Angew. Chem. Int. Ed.* **2014**, *53*, 2658-2661.
- [137] L. Ackermann, *Acc. Chem. Res.* **2014**, *47*, 281-295.
- [138] a) P. Nareddy, F. Jordan, M. Szostak, *ACS Catal.* **2017**, *7*, 5721-5745; b) B. Li, P. H. Dixneuf, *Chem. Soc. Rev.* **2013**, *42*, 5744-5767; c) P. B. Arockiam, C. Bruneau, P. H. Dixneuf, *Chem. Rev.* **2012**, *112*, 5879-5918.
- [139] Z.-Y. Li, H. H. C. Lakmal, X. Qian, Z. Zhu, B. Donnadiou, S. J. McClain, X. Xu, X. Cui, *J. Am. Chem. Soc.* **2019**, *141*, 15730-15736.
- [140] G. Li, Q. Liu, L. Vasamsetty, W. Guo, J. Wang, *Angew. Chem. Int. Ed.* **2020**, *59*, 3475-3479.

- [141] a) S. Z. Tasker, E. A. Standley, T. F. Jamison, *Nature* **2014**, *509*, 299-309; b) Y. Nakao, *Chem. Rec.* **2011**, *11*, 242–251.
- [142] L. Ackermann, T. B. Gunnoe, L. G. Habgood, *Catalytic hydroarylation of carbon-carbon multiple bonds*, Wiley-VCH, Weinheim, **2018**.
- [143] Y. Nakao, H. Idei, K. S. Kanyiva, T. Hiyama, *J. Am. Chem. Soc.* **2009**, *131*, 15996-15997.
- [144] D. Hirsch-Weil, K. A. Abboud, S. Hong, *Chem. Commun.* **2010**, *46*, 7525-7527.
- [145] P. A. Donets, N. Cramer, *Angew. Chem. Int. Ed.* **2015**, *54*, 633–637.
- [146] a) A. Albright, R. E. Gawley, *J. Am. Chem. Soc.* **2011**, *133*, 19680-19683; b) A. Albright, D. Eddings, R. Black, C. J. Welch, N. N. Gerasimchuk, R. E. Gawley, *J. Org. Chem.* **2011**, *76*, 7341-7351.
- [147] J. Diesel, A. M. Finogenova, N. Cramer, *J. Am. Chem. Soc.* **2018**, *140*, 4489-4493.
- [148] Y.-X. Wang, S.-L. Qi, Y.-X. Luan, X.-W. Han, S. Wang, H. Chen, M. Ye, *J. Am. Chem. Soc.* **2018**, *140*, 5360-5364.
- [149] Y.-X. Wang, M. Ye, *Sci. China Chem.* **2018**, *61*, 1004-1013.
- [150] H. Landert, F. Spindler, A. Wyss, H.-U. Blaser, B. Pugin, Y. Ribourduille, B. Gschwend, B. Ramalingam, A. Pfaltz, *Angew. Chem. Int. Ed.* **2010**, *49*, 6873-6876.
- [151] J. Loup, V. Müller, D. Ghorai, L. Ackermann, *Angew. Chem. Int. Ed.* **2019**, *58*, 1749-1753.
- [152] J. Diesel, D. Grosheva, S. Kodama, N. Cramer, *Angew. Chem. Int. Ed.* **2019**, *58*, 11044-11048.
- [153] W.-B. Zhang, X.-T. Yang, J.-B. Ma, Z.-M. Su, S.-L. Shi, *J. Am. Chem. Soc.* **2019**, *141*, 5628-5634.
- [154] Y. Cai, X. Ye, S. Liu, S.-L. Shi, *Angew. Chem. Int. Ed.* **2019**, *58*, 13433-13437.
- [155] K. Ogata, Y. Atsuumi, D. Shimada, S.-i. Fukuzawa, *Angew. Chem. Int. Ed.* **2011**, *50*, 5896-5899.
- [156] J. S. E. Ahlin, N. Cramer, *Org. Lett.* **2016**, *18*, 3242–3245.
- [157] T. J. Seiders, D. W. Ward, R. H. Grubbs, *Org. Lett.* **2001**, *3*, 3225-3228.
- [158] J. Yang, N. Yoshikai, *J. Am. Chem. Soc.* **2014**, *136*, 16748-16751.
- [159] J. Yang, A. Rérat, Y. J. Lim, C. Gosmini, N. Yoshikai, *Angew. Chem. Int. Ed.* **2017**, *56*, 2449-2453.
- [160] D. K. Kim, J. Riedel, R. S. Kim, V. M. Dong, *J. Am. Chem. Soc.* **2017**, *139*, 10208-10211.
- [161] P.-S. Lee, N. Yoshikai, *Org. Lett.* **2015**, *17*, 22-25.

- [162] a) A. Fürstner, *ACS Cent. Sci.* **2016**, *2*, 778-789; b) I. Bauer, H.-J. Knölker, *Chem. Rev.* **2015**, *115*, 3170-3387.
- [163] J. Loup, D. Zell, J. C. A. Oliveira, H. Keil, D. Stalke, L. Ackermann, *Angew. Chem. Int. Ed.* **2017**, *56*, 14197-14201.
- [164] a) S. Warratz, C. Kornhaaß, A. Cajaraville, B. Niepötter, D. Stalke, L. Ackermann, *Angew. Chem. Int. Ed.* **2015**, *54*, 5513-5517; b) J. Piera, J.-E. Bäckvall, *Angew. Chem. Int. Ed.* **2008**, *47*, 3506-3523; c) S. S. Stahl, *Angew. Chem. Int. Ed.* **2004**, *43*, 3400-3420; d) R. Mei, H. Wang, S. Warratz, S. A. Macgregor, L. Ackermann, *Chem. Eur. J.* **2016**, *22*, 6759-6763.
- [165] P. M. Osterberg, J. K. Niemeier, C. J. Welch, J. M. Hawkins, J. R. Martinelli, T. E. Johnson, T. W. Root, S. S. Stahl, *Org. Process Res. Dev.* **2015**, *19*, 1537-1543.
- [166] a) J. Le Bras, J. Muzart, *Chem. Rev.* **2011**, *111*, 1170-1214; b) K. C. Nicolaou, P. G. Bulger, D. Sarlah, *Angew. Chem. Int. Ed.* **2005**, *44*, 4442-4489; c) A. B. Dounay, L. E. Overman, *Chem. Rev.* **2003**, *103*, 2945-2964; d) I. P. Beletskaya, A. V. Cheprakov, *Chem. Rev.* **2000**, *100*, 3009-3066; e) R. F. Heck, *Acc. Chem. Res.* **1979**, *12*, 146-151.
- [167] a) Y. Fujiwara, I. Moritani, S. Danno, R. Asano, S. Teranishi, *J. Am. Chem. Soc.* **1969**, *91*, 7166-7169; b) Y. Fujiwara, I. Moritani, M. Matsuda, S. Teranishi, *Tetrahedron Lett.* **1968**, *9*, 633-636; c) I. Moritani, Y. Fujiwara, *Tetrahedron Lett.* **1967**, *8*, 1119-1122.
- [168] M. D. K. Boele, G. P. F. van Strijdonck, A. H. M. de Vries, P. C. J. Kamer, J. G. de Vries, P. W. N. M. van Leeuwen, *J. Am. Chem. Soc.* **2002**, *124*, 1586-1587.
- [169] G. Cai, Y. Fu, Y. Li, X. Wan, Z. Shi, *J. Am. Chem. Soc.* **2007**, *129*, 7666-7673.
- [170] S. H. Cho, S. J. Hwang, S. Chang, *J. Am. Chem. Soc.* **2008**, *130*, 9254-9256.
- [171] K. M. Engle, D.-H. Wang, J.-Q. Yu, *Angew. Chem. Int. Ed.* **2010**, *49*, 6169-6173.
- [172] M. Wasa, K. M. Engle, J.-Q. Yu, *J. Am. Chem. Soc.* **2010**, *132*, 3680-3681.
- [173] C. Huang, B. Chattopadhyay, V. Gevorgyan, *J. Am. Chem. Soc.* **2011**, *133*, 12406-12409.
- [174] B. Liu, H.-Z. Jiang, B.-F. Shi, *J. Org. Chem.* **2014**, *79*, 1521-1526.
- [175] G. Li, D. Leow, L. Wan, J.-Q. Yu, *Angew. Chem. Int. Ed.* **2013**, *52*, 1245-1247.
- [176] A. Deb, S. Bag, R. Kancherla, D. Maiti, *J. Am. Chem. Soc.* **2014**, *136*, 13602-13605.
- [177] S. Kancherla, K. B. Jørgensen, M. Á. Fernández-Ibáñez, *Synthesis* **2019**, *51*, 643-663.
- [178] a) C. Jia, T. Kitamura, Y. Fujiwara, *Acc. Chem. Res.* **2001**, *34*, 633-639; b) C. Jia, W. Lu, T. Kitamura, Y. Fujiwara, *Org. Lett.* **1999**, *1*, 2097-2100; c) I. Moritanl, Y. Fujiwara, *Tetrahedron Lett.* **1967**, *8*, 1119-1122.

- [179] a) L.-Y. Liu, K.-S. Yeung, J.-Q. Yu, *Chem. Eur. J.* **2019**, *25*, 2199-2202; b) P. Wang, P. Verma, G. Xia, J. Shi, J. X. Qiao, S. Tao, P. T. W. Cheng, M. A. Poss, M. E. Farmer, K.-S. Yeung, J.-Q. Yu, *Nature* **2017**, *551*, 489-493; c) P. Wang, M. E. Farmer, J.-Q. Yu, *Angew. Chem. Int. Ed.* **2017**, *56*, 5125-5129; d) Y.-H. Zhang, B.-F. Shi, J.-Q. Yu, *J. Am. Chem. Soc.* **2009**, *131*, 5072-5074.
- [180] a) A. K. Cook, M. S. Sanford, *J. Am. Chem. Soc.* **2015**, *137*, 3109-3118; b) J. B. Gary, A. K. Cook, M. S. Sanford, *ACS Catal.* **2013**, *3*, 700-703; c) A. K. Cook, M. H. Emmert, M. S. Sanford, *Org. Lett.* **2013**, *15*, 5428-5431; d) A. Kubota, M. H. Emmert, M. S. Sanford, *Org. Lett.* **2012**, *14*, 1760-1763; e) M. H. Emmert, A. K. Cook, Y. J. Xie, M. S. Sanford, *Angew. Chem. Int. Ed.* **2011**, *50*, 9409-9412.
- [181] Y. Izawa, S. S. Stahl, *Adv. Synth. Catal.* **2010**, *352*, 3223-3229.
- [182] a) W.-L. Jia, N. Westerveld, K. M. Wong, T. Morsch, M. Hakkennes, K. Naksomboon, M. Á. Fernández-Ibáñez, *Org. Lett.* **2019**, *21*, 9339-9342; b) Y. Álvarez-Casao, M. Á. Fernández-Ibáñez, *Eur. J. Org. Chem.* **2019**, 1842-1845.
- [183] K. Naksomboon, C. Valderas, M. Gómez-Martínez, Y. Álvarez-Casao, M. Á. Fernández-Ibáñez, *ACS Catal.* **2017**, *7*, 6342-6346.
- [184] L. Grigorjeva, O. Daugulis, *Angew. Chem. Int. Ed.* **2014**, *53*, 10209-10212.
- [185] a) S. Zhai, S. Qiu, X. Chen, J. Wu, H. Zhao, C. Tao, Y. Li, B. Cheng, H. Wang, H. Zhai, *Chem. Commun.* **2018**, *54*, 98-101; b) T. T. Nguyen, L. Grigorjeva, O. Daugulis, *Angew. Chem. Int. Ed.* **2018**, *57*, 1688-1691; c) Á. M. Martínez, N. Rodríguez, R. Gómez-Arrayás, J. C. Carretero, *Chem. Eur. J.* **2017**, *23*, 11669-11676; d) T. T. Nguyen, L. Grigorjeva, O. Daugulis, *ACS Catal.* **2016**, *6*, 551-554; e) L.-B. Zhang, X.-Q. Hao, Z.-J. Liu, X.-X. Zheng, S.-K. Zhang, J.-L. Niu, M.-P. Song, *Angew. Chem. Int. Ed.* **2015**, *54*, 10012-10015; f) W. Ma, L. Ackermann, *ACS Catal.* **2015**, *5*, 2822-2825.
- [186] L. Grigorjeva, O. Daugulis, *Org. Lett.* **2014**, *16*, 4684-4687.
- [187] R. Boobalan, R. Kuppusamy, R. Santhoshkumar, P. Gandeepan, C.-H. Cheng, *ChemCatChem* **2017**, *9*, 273-277.
- [188] a) A. Dey, N. Thrimurtulu, C. M. R. Volla, *Org. Lett.* **2019**, *21*, 3871-3875; b) R. Nallagonda, N. Thrimurtulu, C. M. R. Volla, *Adv. Synth. Catal.* **2018**, *360*, 255-260; c) N. Thrimurtulu, A. Dey, D. Maiti, C. M. R. Volla, *Angew. Chem. Int. Ed.* **2016**, *55*, 12361-12365.
- [189] V. G. Landge, G. Jaiswal, E. Balaraman, *Org. Lett.* **2016**, *18*, 812-815.
- [190] Z.-Z. Zhang, Y.-Q. Han, B.-B. Zhan, S. Wang, B.-F. Shi, *Angew. Chem. Int. Ed.* **2017**, *56*, 13145-13149.

- [191] R. Manoharan, G. Sivakumar, M. Jeganmohan, *Chem. Commun.* **2016**, 52, 10533-10536.
- [192] T. Yamaguchi, Y. Kommagalla, Y. Aihara, N. Chatani, *Chem. Commun.* **2016**, 52, 10129-10132.
- [193] a) A. Baccalini, S. Vergura, P. Dolui, S. Maiti, S. Dutta, S. Maity, F. F. Khan, G. K. Lahiri, G. Zanoni, D. Maiti, *Org. Lett.* **2019**, 21, 8842-8846; b) S. Maity, P. Dolui, R. Kancherla, D. Maiti, *Chem. Sci.* **2017**, 8, 5181-5185; c) S. Maity, R. Kancherla, U. Dhawa, E. Hoque, S. Pimparkar, D. Maiti, *ACS Catal.* **2016**, 6, 5493-5499.
- [194] L.-B. Zhang, X.-Q. Hao, S.-K. Zhang, Z.-J. Liu, X.-X. Zheng, J.-F. Gong, J.-L. Niu, M.-P. Song, *Angew. Chem. Int. Ed.* **2015**, 54, 272-275.
- [195] X. Wu, K. Yang, Y. Zhao, H. Sun, G. Li, H. Ge, *Nat. Commun.* **2015**, 6, 6462.
- [196] L.-B. Zhang, S.-K. Zhang, D. Wei, X. Zhu, X.-Q. Hao, J.-H. Su, J.-L. Niu, M.-P. Song, *Org. Lett.* **2016**, 18, 1318-1321.
- [197] a) J. Hassan, M. Sévignon, C. Gozzi, E. Schulz, M. Lemaire, *Chem. Rev.* **2002**, 102, 1359-1470; b) P. E. Fanta, *Chem. Rev.* **1964**, 64, 613-632; c) I. Goldberg, *Ber. Dtsch. Chem. Ges.* **1906**, 39, 1691-1692.
- [198] a) H.-Q. Do, R. M. K. Khan, O. Daugulis, *J. Am. Chem. Soc.* **2008**, 130, 15185-15192; b) H.-Q. Do, O. Daugulis, *J. Am. Chem. Soc.* **2008**, 130, 1128-1129; c) H.-Q. Do, O. Daugulis, *J. Am. Chem. Soc.* **2007**, 129, 12404-12405.
- [199] a) T. Yoshizumi, T. Satoh, K. Hirano, D. Matsuo, A. Orita, J. Otera, M. Miura, *Tetrahedron Lett.* **2009**, 50, 3273-3276; b) T. Yoshizumi, H. Tsurugi, T. Satoh, M. Miura, *Tetrahedron Lett.* **2008**, 49, 1598-1600.
- [200] a) I. Choi, V. Müller, G. Lole, R. Köhler, V. Karius, W. Viöl, C. Jooss, L. Ackermann, *Chem. Eur. J.* **2020**, 26, 3509-3514; b) F. Yang, J. Koeller, L. Ackermann, *Angew. Chem. Int. Ed.* **2016**, 55, 4759-4762; c) R. Jeyachandran, H. K. Potukuchi, L. Ackermann, *Beilstein J. Org. Chem.* **2012**, 8, 1771-1777; d) L. Ackermann, H. K. Potukuchi, D. Landsberg, R. Vicente, *Org. Lett.* **2008**, 10, 3081-3084.
- [201] a) H. A. Duong, R. E. Gilligan, M. L. Cooke, R. J. Phipps, M. J. Gaunt, *Angew. Chem. Int. Ed.* **2011**, 50, 463-466; b) C.-L. Ciana, R. J. Phipps, J. R. Brandt, F.-M. Meyer, M. J. Gaunt, *Angew. Chem. Int. Ed.* **2011**, 50, 458-462; c) R. J. Phipps, M. J. Gaunt, *Science* **2009**, 323, 1593-1597; d) R. J. Phipps, N. P. Grimster, M. J. Gaunt, *J. Am. Chem. Soc.* **2008**, 130, 8172-8174.
- [202] S. Vásquez-Céspedes, K. M. Chepiga, N. Möller, A. H. Schäfer, F. Glorius, *ACS Catal.* **2016**, 6, 5954-5961.

- [203] Y. Yang, R. Li, Y. Zhao, D. Zhao, Z. Shi, *J. Am. Chem. Soc.* **2016**, *138*, 8734-8737.
- [204] a) L.-H. Zou, J. Mottweiler, D. L. Priebbenow, J. Wang, J. A. Stubenrauch, C. Bolm, *Chem. Eur. J.* **2013**, *19*, 3302-3305; b) S. Fan, Z. Chen, X. Zhang, *Org. Lett.* **2012**, *14*, 4950-4953; c) H.-Q. Do, O. Daugulis, *J. Am. Chem. Soc.* **2011**, *133*, 13577-13586.
- [205] S. Zhao, J. Yuan, Y.-C. Li, B.-F. Shi, *Chem. Commun.* **2015**, *51*, 12823-12826.
- [206] W. Zeng, W. Wu, H. Jiang, L. Huang, Y. Sun, Z. Chen, X. Li, *Chem. Commun.* **2013**, *49*, 6611-6613.
- [207] Y.-J. Liu, Y.-H. Liu, X.-S. Yin, W.-J. Gu, B.-F. Shi, *Chem. Eur. J.* **2015**, *21*, 205-209.
- [208] J. Dong, F. Wang, J. You, *Org. Lett.* **2014**, *16*, 2884-2887.
- [209] Y. Zhang, Q. Wang, H. Yu, Y. Huang, *Org. Biomol. Chem.* **2014**, *12*, 8844-8850.
- [210] J. Zhang, D. Li, H. Chen, B. Wang, Z. Liu, Y. Zhang, *Adv. Synth. Catal.* **2016**, *358*, 792-807.
- [211] a) A. John, K. M. Nicholas, *J. Org. Chem.* **2011**, *76*, 4158-4162; b) Q. Shuai, G. Deng, Z. Chua, D. S. Bohle, C.-J. Li, *Adv. Synth. Catal.* **2010**, *352*, 632-636; c) T. Uemura, S. Imoto, N. Chatani, *Chem. Lett.* **2006**, *35*, 842-843; d) X. Chen, X.-S. Hao, C. E. Goodhue, J.-Q. Yu, *J. Am. Chem. Soc.* **2006**, *128*, 6790-6791.
- [212] G. Li, C. Jia, K. Sun, *Org. Lett.* **2013**, *15*, 5198-5201.
- [213] L. D. Tran, J. Roane, O. Daugulis, *Angew. Chem. Int. Ed.* **2013**, *52*, 6043-6046.
- [214] Q. Li, S.-Y. Zhang, G. He, Z. Ai, W. A. Nack, G. Chen, *Org. Lett.* **2014**, *16*, 1764-1767.
- [215] Z. Wang, J. Ni, Y. Kuninobu, M. Kanai, *Angew. Chem. Int. Ed.* **2014**, *53*, 3496-3499.
- [216] X. Wu, Y. Zhao, G. Zhang, H. Ge, *Angew. Chem. Int. Ed.* **2014**, *53*, 3706-3710.
- [217] C. Wang, Y. Yang, D. Qin, Z. He, J. You, *J. Org. Chem.* **2015**, *80*, 8424-8429.
- [218] S. Bhadra, C. Matheis, D. Katayev, L. J. Gooßen, *Angew. Chem. Int. Ed.* **2013**, *52*, 9279-9283.
- [219] W. Lu, H. Xu, Z. Shen, *Org. Biomol. Chem.* **2017**, *15*, 1261-1267.
- [220] X. Wu, Y. Zhao, H. Ge, *Chem. Asian J.* **2014**, *9*, 2736-2739.
- [221] a) P. Lanzafame, S. Abate, C. Ampelli, C. Genovese, R. Passalacqua, G. Centi, S. Perathoner, *ChemSusChem* **2017**, *10*, 4409-4419; b) R. Schlögl, *Angew. Chem. Int. Ed.* **2011**, *50*, 6424-6426; c) R. Schlögl, *ChemSusChem* **2010**, *3*, 209-222.
- [222] W. Leitner, E. A. Quadrelli, R. Schlögl, *Green Chem.* **2017**, *19*, 2307-2308.
- [223] N. Sauermann, T. H. Meyer, Y. Qiu, L. Ackermann, *ACS Catal.* **2018**, *8*, 7086-7103.
- [224] T. H. Meyer, I. Choi, C. Tian, L. Ackermann, *Chem* **2020**, *6*, 2484-2496.

- [225] a) H. Kolbe, E. Lautemann, *Justus Liebigs Ann. Chem.* **1860**, *115*, 157-206; b) M. Faraday, *Philos. Trans. R. Soc. London* **1825**, *115*, 440-466.
- [226] T. Shono, *Tetrahedron* **1984**, *40*, 811-850.
- [227] a) D. Pollok, S. R. Waldvogel, *Chem. Sci.* **2020**, *11*, 12386-12400; b) J. Liu, L. Lu, D. Wood, S. Lin, *ACS Cent. Sci.* **2020**, *6*, 1317-1340; c) A. Wiebe, T. Gieshoff, S. Möhle, E. Rodrigo, M. Zirbes, S. R. Waldvogel, *Angew. Chem. Int. Ed.* **2018**, *57*, 5594-5619; d) S. Tang, Y. Liu, A. Lei, *Chem* **2018**, *4*, 27-45; e) G. S. Sauer, S. Lin, *ACS Catal.* **2018**, *8*, 5175-5187; f) K. D. Moeller, *Chem. Rev.* **2018**, *118*, 4817-4833; g) M. D. Kärkäs, *Chem. Soc. Rev.* **2018**, *47*, 5786-5865; h) M. Yan, Y. Kawamata, P. S. Baran, *Chem. Rev.* **2017**, *117*, 13230-13319; i) H. Kolbe, *Justus Liebigs Ann. Chem.* **1849**, *69*, 257-294; j) M. Faraday, *Ann. Phys.* **1834**, *109*, 149-189.
- [228] a) A. Wiebe, S. Lips, D. Schollmeyer, R. Franke, S. R. Waldvogel, *Angew. Chem. Int. Ed.* **2017**, *56*, 14727-14731; b) L. J. Wesenberg, S. Herold, A. Shimizu, J.-i. Yoshida, S. R. Waldvogel, *Chem. Eur. J.* **2017**, *23*, 12096-12099; c) T. Gieshoff, A. Kehl, D. Schollmeyer, K. D. Moeller, S. R. Waldvogel, *J. Am. Chem. Soc.* **2017**, *139*, 12317-12324; d) A. Wiebe, D. Schollmeyer, K. M. Dyballa, R. Franke, S. R. Waldvogel, *Angew. Chem. Int. Ed.* **2016**, *55*, 11801-11805; e) S. Lips, A. Wiebe, B. Elsler, D. Schollmeyer, K. M. Dyballa, R. Franke, S. R. Waldvogel, *Angew. Chem. Int. Ed.* **2016**, *55*, 10872-10876; f) B. Elsler, A. Wiebe, D. Schollmeyer, K. M. Dyballa, R. Franke, S. R. Waldvogel, *Chem. Eur. J.* **2015**, *21*, 12321-12325; g) A. Kirste, B. Elsler, G. Schnakenburg, S. R. Waldvogel, *J. Am. Chem. Soc.* **2012**, *134*, 3571-3576.
- [229] a) C. Li, Y. Kawamata, H. Nakamura, J. C. Vantourout, Z. Liu, Q. Hou, D. Bao, J. T. Starr, J. Chen, M. Yan, P. S. Baran, *Angew. Chem. Int. Ed.* **2017**, *56*, 13088-13093; b) Y. Kawamata, M. Yan, Z. Liu, D.-H. Bao, J. Chen, J. T. Starr, P. S. Baran, *J. Am. Chem. Soc.* **2017**, *139*, 7448-7451; c) E. J. Horn, B. R. Rosen, Y. Chen, J. Tang, K. Chen, M. D. Eastgate, P. S. Baran, *Nature* **2016**, *533*, 77-81; d) B. R. Rosen, E. W. Werner, A. G. O'Brien, P. S. Baran, *J. Am. Chem. Soc.* **2014**, *136*, 5571-5574; e) A. G. O'Brien, A. Maruyama, Y. Inokuma, M. Fujita, P. S. Baran, D. G. Blackmond, *Angew. Chem. Int. Ed.* **2014**, *53*, 11868-11871.
- [230] a) R. Hayashi, A. Shimizu, J.-i. Yoshida, *J. Am. Chem. Soc.* **2016**, *138*, 8400-8403; b) T. Morofuji, A. Shimizu, J.-i. Yoshida, *J. Am. Chem. Soc.* **2015**, *137*, 9816-9819; c) T. Morofuji, A. Shimizu, J.-i. Yoshida, *J. Am. Chem. Soc.* **2014**, *136*, 4496-4499; d) T. Morofuji, A. Shimizu, J.-i. Yoshida, *J. Am. Chem. Soc.* **2013**, *135*, 5000-5003; e) Y. Ashikari, A. Shimizu, T. Nokami, J.-i. Yoshida, *J. Am. Chem. Soc.* **2013**, *135*, 16070-

- 16073; f) T. Morofuji, A. Shimizu, J.-i. Yoshida, *Angew. Chem. Int. Ed.* **2012**, *51*, 7259-7262; g) Y. Ashikari, T. Nokami, J.-i. Yoshida, *J. Am. Chem. Soc.* **2011**, *133*, 11840-11843.
- [231] a) P. Xiong, H.-H. Xu, J. Song, H.-C. Xu, *J. Am. Chem. Soc.* **2018**, *140*, 2460-2464; b) H.-B. Zhao, Z.-J. Liu, J. Song, H.-C. Xu, *Angew. Chem. Int. Ed.* **2017**, *56*, 12732-12735; c) P. Xiong, H.-H. Xu, H.-C. Xu, *J. Am. Chem. Soc.* **2017**, *139*, 2956-2959; d) Z.-J. Wu, H.-C. Xu, *Angew. Chem. Int. Ed.* **2017**, *56*, 4734-4738; e) A. A. Folgueiras-Amador, X.-Y. Qian, H.-C. Xu, T. Wirth, *Chem. Eur. J.* **2017**, *24*, 487-491; f) H.-B. Zhao, Z.-W. Hou, Z.-J. Liu, Z.-F. Zhou, J. Song, H.-C. Xu, *Angew. Chem. Int. Ed.* **2016**, *56*, 587-590; g) Z.-W. Hou, Z.-Y. Mao, H.-B. Zhao, Y. Y. Melcamu, X. Lu, J. Song, H.-C. Xu, *Angew. Chem. Int. Ed.* **2016**, *55*, 9168-9172.
- [232] a) R. C. Samanta, T. H. Meyer, I. Siewert, L. Ackermann, *Chem. Sci.* **2020**, *11*, 8657-8670; b) K.-J. Jiao, Y.-K. Xing, Q.-L. Yang, H. Qiu, T.-S. Mei, *Acc. Chem. Res.* **2020**, *53*, 300-310; c) P. Gandeepan, L. H. Finger, T. H. Meyer, L. Ackermann, *Chem. Soc. Rev.* **2020**, *49*, 4254-4272; d) L. Ackermann, *Acc. Chem. Res.* **2020**, *53*, 84-104; e) T. H. Meyer, L. H. Finger, P. Gandeepan, L. Ackermann, *Trends Chem.* **2019**, *1*, 63-76; f) Q.-L. Yang, P. Fang, T.-S. Mei, *Chin. J. Chem.* **2018**, *36*, 338-352; g) C. Ma, P. Fang, T.-S. Mei, *ACS Catal.* **2018**, *8*, 7179-7189; h) A. Jutand, *Chem. Rev.* **2008**, *108*, 2300-2347.
- [233] C. Amatore, C. Cammoun, A. Jutand, *Adv. Synth. Catal.* **2007**, *349*, 292-296.
- [234] F. Kakiuchi, T. Kochi, H. Mutsutani, N. Kobayashi, S. Urano, M. Sato, S. Nishiyama, T. Tanabe, *J. Am. Chem. Soc.* **2009**, *131*, 11310-11311.
- [235] H. Aiso, T. Kochi, H. Mutsutani, T. Tanabe, S. Nishiyama, F. Kakiuchi, *J. Org. Chem.* **2012**, *77*, 7718-7724.
- [236] Y. B. Dudkina, D. Y. Mikhaylov, T. V. Gryaznova, A. I. Tufatullin, O. N. Kataeva, D. A. Vicic, Y. H. Budnikova, *Organometallics* **2013**, *32*, 4785-4792.
- [237] V. S. Thirunavukkarasu, S. I. Kozhushkov, L. Ackermann, *Chem. Commun.* **2014**, *50*, 29-39.
- [238] M. Konishi, K. Tsuchida, K. Sano, T. Kochi, F. Kakiuchi, *J. Org. Chem.* **2017**, *82*, 8716-8724.
- [239] Q.-L. Yang, Y.-Q. Li, C. Ma, P. Fang, X.-J. Zhang, T.-S. Mei, *J. Am. Chem. Soc.* **2017**, *139*, 3293-3298.

6. References

- [240] a) Q.-L. Yang, C.-Z. Li, L.-W. Zhang, Y.-Y. Li, X. Tong, X.-Y. Wu, T.-S. Mei, *Organometallics* **2019**, *38*, 1208-1212; b) C. Ma, C.-Q. Zhao, Y.-Q. Li, L.-P. Zhang, X.-T. Xu, K. Zhang, T.-S. Mei, *Chem. Commun.* **2017**, *53*, 12189-12192.
- [241] A. Shrestha, M. Lee, A. L. Dunn, M. S. Sanford, *Org. Lett.* **2018**, *20*, 204-207.
- [242] a) W.-J. Kong, Z. Shen, L. H. Finger, L. Ackermann, *Angew. Chem. Int. Ed.* **2020**, *59*, 5551-5556; b) Z.-J. Wu, F. Su, W. Lin, J. Song, T.-B. Wen, H.-J. Zhang, H.-C. Xu, *Angew. Chem. Int. Ed.* **2019**, *58*, 16770-16774; c) W.-J. Kong, L. H. Finger, J. C. A. Oliveira, L. Ackermann, *Angew. Chem. Int. Ed.* **2019**, *58*, 6342-6346; d) W.-J. Kong, L. H. Finger, A. M. Messinis, R. Kuniyil, J. C. A. Oliveira, L. Ackermann, *J. Am. Chem. Soc.* **2019**, *141*, 17198-17206; e) Y. Qiu, A. Scheremetjew, L. Ackermann, *J. Am. Chem. Soc.* **2019**, *141*, 2731-2738; f) Y. Qiu, W.-J. Kong, J. Struwe, N. Sauermann, T. Rogge, A. Scheremetjew, L. Ackermann, *Angew. Chem. Int. Ed.* **2018**, *57*, 5828-5832.
- [243] a) Q.-L. Yang, Y.-K. Xing, X.-Y. Wang, H.-X. Ma, X.-J. Weng, X. Yang, H.-M. Guo, T.-S. Mei, *J. Am. Chem. Soc.* **2019**, *141*, 18970-18976; b) Y. Qiu, M. Stangier, T. H. Meyer, J. C. A. Oliveira, L. Ackermann, *Angew. Chem. Int. Ed.* **2018**, *57*, 14179-14183.
- [244] a) X. Tan, X. Hou, T. Rogge, L. Ackermann, *Angew. Chem. Int. Ed.* **2021**, DOI: 10.1002/anie.202014289; b) L. Yang, R. Steinbock, A. Scheremetjew, R. Kuniyil, L. H. Finger, A. M. Messinis, L. Ackermann, *Angew. Chem. Int. Ed.* **2020**, *59*, 11130-11135; c) L. Massignan, X. Tan, T. H. Meyer, R. Kuniyil, A. M. Messinis, L. Ackermann, *Angew. Chem. Int. Ed.* **2020**, *59*, 3184-3189; d) Z.-Q. Wang, C. Hou, Y.-F. Zhong, Y.-X. Lu, Z.-Y. Mo, Y.-M. Pan, H.-T. Tang, *Org. Lett.* **2019**, *21*, 9841-9845; e) M.-J. Luo, T.-T. Zhang, F.-J. Cai, J.-H. Li, D.-L. He, *Chem. Commun.* **2019**, *55*, 7251-7254; f) M.-J. Luo, M. Hu, R.-J. Song, D.-L. He, J.-H. Li, *Chem. Commun.* **2019**, *55*, 1124-1127; g) F. Xu, Y.-J. Li, C. Huang, H.-C. Xu, *ACS Catal.* **2018**, *8*, 3820-3824; h) Y. Qiu, C. Tian, L. Massignan, T. Rogge, L. Ackermann, *Angew. Chem. Int. Ed.* **2018**, *57*, 5818-5822; i) R. Mei, J. Koeller, L. Ackermann, *Chem. Commun.* **2018**, *54*, 12879-12882.
- [245] N. Sauermann, T. H. Meyer, L. Ackermann, *Chem. Eur. J.* **2018**, *24*, 16209-16217.
- [246] N. Sauermann, T. H. Meyer, C. Tian, L. Ackermann, *J. Am. Chem. Soc.* **2017**, *139*, 18452-18455.
- [247] N. Sauermann, R. Mei, L. Ackermann, *Angew. Chem. Int. Ed.* **2018**, *57*, 5090-5094.
- [248] T. Dalton, T. Faber, F. Glorius, *ACS Cent. Sci.* **2021**, DOI: 10.1021/acscentsci.1020c01413.
- [249] X. Gao, P. Wang, L. Zeng, S. Tang, A. Lei, *J. Am. Chem. Soc.* **2018**, *140*, 4195-4199.

- [250] C. Tian, L. Massignan, T. H. Meyer, L. Ackermann, *Angew. Chem. Int. Ed.* **2018**, *57*, 2383-2387.
- [251] S. Tang, D. Wang, Y. Liu, L. Zeng, A. Lei, *Nature Commun.* **2018**, *9*, 798.
- [252] R. Mei, N. Sauermann, J. C. A. Oliveira, L. Ackermann, *J. Am. Chem. Soc.* **2018**, *140*, 7913-7921.
- [253] a) R. Mei, X. Fang, L. He, J. Sun, L. Zou, W. Ma, L. Ackermann, *Chem. Commun.* **2020**, *56*, 1393-1396; b) T. H. Meyer, J. C. A. Oliveira, S. C. Sau, N. W. J. Ang, L. Ackermann, *ACS Catal.* **2018**, *8*, 9140-9147.
- [254] L. Zeng, H. Li, S. Tang, X. Gao, Y. Deng, G. Zhang, C.-W. Pao, J.-L. Chen, J.-F. Lee, A. Lei, *ACS Catal.* **2018**, *8*, 5448-5453.
- [255] S. C. Sau, R. Mei, J. Struwe, L. Ackermann, *ChemSusChem* **2019**, *12*, 3023-3027.
- [256] Q.-L. Yang, X.-Y. Wang, J.-Y. Lu, L.-P. Zhang, P. Fang, T.-S. Mei, *J. Am. Chem. Soc.* **2018**, *140*, 11487-11494.
- [257] S. Kathiravan, S. Suriyanarayanan, I. A. Nicholls, *Org. Lett.* **2019**, *21*, 1968-1972.
- [258] M. Schinkel, I. Marek, L. Ackermann, *Angew. Chem. Int. Ed.* **2013**, *52*, 3977-3980.
- [259] a) T. Aneeja, M. Neetha, C. M. A. Afsina, G. Anilkumar, *Catal. Sci. Technol.* **2021**, *11*, 444-458; b) R. Cano, K. Mackey, G. P. McGlacken, *Catal. Sci. Technol.* **2018**, *8*, 1251-1266; c) C. Wang, *Synlett* **2013**, *24*, 1606-1613.
- [260] a) C. Zhu, J. C. A. Oliveira, Z. Shen, H. Huang, L. Ackermann, *ACS Catal.* **2018**, *8*, 4402-4407; b) Y.-F. Liang, R. Steinbock, L. Yang, L. Ackermann, *Angew. Chem. Int. Ed.* **2018**, *57*, 10625-10629; c) Y. Hu, B. Zhou, H. Chen, C. Wang, *Angew. Chem. Int. Ed.* **2018**, *57*, 12071-12075; d) H. Wang, F. Pesciaioli, J. C. A. Oliveira, S. Warratz, L. Ackermann, *Angew. Chem. Int. Ed.* **2017**, *56*, 15063-15067; e) Y.-F. Liang, V. Müller, W. Liu, A. Münch, D. Stalke, L. Ackermann, *Angew. Chem. Int. Ed.* **2017**, *56*, 9415-9419; f) S. Sueki, Z. Wang, Y. Kuninobu, *Org. Lett.* **2016**, *18*, 304-307; g) W. Liu, S. C. Richter, Y. Zhang, L. Ackermann, *Angew. Chem. Int. Ed.* **2016**, *55*, 7747-7750; h) B. Zhou, Y. Hu, C. Wang, *Angew. Chem. Int. Ed.* **2015**, *54*, 13659-13663; i) B. Zhou, P. Ma, H. Chen, C. Wang, *Chem. Commun.* **2014**, *50*, 14558-14561; j) B. Zhou, H. Chen, C. Wang, *J. Am. Chem. Soc.* **2013**, *135*, 1264-1267; k) Y. Kuninobu, Y. Nishina, T. Takeuchi, K. Takai, *Angew. Chem. Int. Ed.* **2007**, *46*, 6518-6520.
- [261] K. Fuchibe, H. Hatta, K. Oh, R. Oki, J. Ichikawa, *Angew. Chem. Int. Ed.* **2017**, *56*, 5890-5893.
- [262] a) M. Schinkel, J. Wallbaum, S. I. Kozhushkov, I. Marek, L. Ackermann, *Org. Lett.* **2013**, *15*, 4482-4484; b) U. Helmstedt, E. Clot, *Chem. Eur. J.* **2012**, *18*, 11449-11458;

- c) N. M. Neisius, B. Plietker, *Angew. Chem. Int. Ed.* **2009**, *48*, 5752-5755; d) K. Cheng, B. Yao, J. Zhao, Y. Zhang, *Org. Lett.* **2008**, *10*, 5309-5312; e) F. Kakiuchi, H. Ohtaki, M. Sonoda, N. Chatani, S. Murai, *Chem. Lett.* **2001**, *30*, 918-919; f) S. Busch, W. Leitner, *Adv. Synth. Catal.* **2001**, *343*, 192-195.
- [263] a) S. I. Kozhushkov, L. Ackermann, *Chem. Sci.* **2013**, *4*, 886-896; b) L. Ackermann, *Isr. J. Chem.* **2010**, *50*, 652-663.
- [264] M. Moselage, J. Li, L. Ackermann, *ACS Catal.* **2015**, *6*, 498-525.
- [265] D. Zell, M. Bursch, V. Müller, S. Grimme, L. Ackermann, *Angew. Chem. Int. Ed.* **2017**, *56*, 10378-10382.
- [266] a) S.-Y. Yan, Y.-Q. Han, Q.-J. Yao, X.-L. Nie, L. Liu, B.-F. Shi, *Angew. Chem. Int. Ed.* **2018**, *57*, 9093-9097; b) H. Wang, H.-R. Tong, G. He, G. Chen, *Angew. Chem. Int. Ed.* **2016**, *55*, 15387-15391; c) L. Ackermann, R. Vicente, A. Althammer, *Org. Lett.* **2008**, *10*, 2299-2302.
- [267] a) A. I. Gerasyuto, R. P. Hsung, N. Sydorenko, B. Slafer, *J. Org. Chem.* **2005**, *70*, 4248-4256; b) N. Halland, P. S. Aburel, K. A. Jørgensen, *Angew. Chem. Int. Ed.* **2004**, *43*, 1272-1277; c) N. Halland, T. Hansen, K. A. Jørgensen, *Angew. Chem. Int. Ed.* **2003**, *42*, 4955-4957; d) N. Halland, R. G. Hazell, K. A. Jørgensen, *J. Org. Chem.* **2002**, *67*, 8331-8338; e) A. Alexakis, J.-P. Tranchier, N. Lensen, P. Mangeney, *J. Am. Chem. Soc.* **1995**, *117*, 10767-10768.
- [268] a) Q. Xing, C.-M. Chan, Y.-W. Yeung, W.-Y. Yu, *J. Am. Chem. Soc.* **2019**, *141*, 3849-3853; b) Y. Nishioka, T. Uchida, T. Katsuki, *Angew. Chem. Int. Ed.* **2013**, *52*, 1739-1742; c) E. Milczek, N. Boudet, S. Blakey, *Angew. Chem. Int. Ed.* **2008**, *47*, 6825-6828; d) F. Kakiuchi, P. Le Gendre, A. Yamada, H. Ohtaki, S. Murai, *Tetrahedron: Asymmetry* **2000**, *11*, 2647-2651.
- [269] a) S. H. Park, S.-G. Wang, N. Cramer, *ACS Catal.* **2019**, *9*, 10226-10231; b) D. Kossler, F. G. Perrin, A. A. Suleymanov, G. Kiefer, R. Scopelliti, K. Severin, N. Cramer, *Angew. Chem. Int. Ed.* **2017**, *56*, 11490-11493; c) D. Kossler, N. Cramer, *Chem. Sci.* **2017**, *8*, 1862-1866; d) D. Kossler, N. Cramer, *J. Am. Chem. Soc.* **2015**, *137*, 12478-12481.
- [270] F. Pesciaioli, U. Dhawa, J. C. A. Oliveira, R. Yin, M. John, L. Ackermann, *Angew. Chem. Int. Ed.* **2018**, *57*, 15425-15429.
- [271] a) S. Fukagawa, Y. Kato, R. Tanaka, M. Kojima, T. Yoshino, S. Matsunaga, *Angew. Chem. Int. Ed.* **2019**, *58*, 1153-1157; b) L. Lin, S. Fukagawa, D. Sekine, E. Tomita, T. Yoshino, S. Matsunaga, *Angew. Chem. Int. Ed.* **2018**, *57*, 12048-12052; c) D. Gwon, S. Park, S. Chang, *Tetrahedron* **2015**, *71*, 4504-4511.

- [272] a) W.-C. C. Lee, W. Wang, J. J. Li, *J. Org. Chem.* **2018**, *83*, 2382-2388; b) X.-X. Zheng, C. Du, X.-M. Zhao, X. Zhu, J.-F. Suo, X.-Q. Hao, J.-L. Niu, M.-P. Song, *J. Org. Chem.* **2016**, *81*, 4002-4011; c) X.-Q. Hao, C. Du, X. Zhu, P.-X. Li, J.-H. Zhang, J.-L. Niu, M.-P. Song, *Org. Lett.* **2016**, *18*, 3610-3613; d) J. Zhang, H. Chen, C. Lin, Z. Liu, C. Wang, Y. Zhang, *J. Am. Chem. Soc.* **2015**, *137*, 12990-12996; e) W. Miura, K. Hirano, M. Miura, *Org. Lett.* **2015**, *17*, 4034-4037; f) M. Shang, H.-L. Wang, S.-Z. Sun, H.-X. Dai, J.-Q. Yu, *J. Am. Chem. Soc.* **2014**, *136*, 11590-11593; g) A. E. Wendlandt, A. M. Suess, S. S. Stahl, *Angew. Chem. Int. Ed.* **2011**, *50*, 11062-11087.
- [273] a) H. Jo, S. Han, J. Park, M. Choi, S. H. Han, T. Jeong, S.-Y. Lee, J. H. Kwak, Y. H. Jung, I. S. Kim, *Tetrahedron* **2016**, *72*, 571-578; b) G. Cera, T. Haven, L. Ackermann, *Angew. Chem. Int. Ed.* **2016**, *55*, 1484-1488; c) Y. Suzuki, B. Sun, K. Sakata, T. Yoshino, S. Matsunaga, M. Kanai, *Angew. Chem. Int. Ed.* **2015**, *54*, 9944-9947; d) T. Gensch, S. Vásquez-Céspedes, D.-G. Yu, F. Glorius, *Org. Lett.* **2015**, *17*, 3714-3717; e) D.-G. Yu, T. Gensch, F. de Azambuja, S. Vásquez-Céspedes, F. Glorius, *J. Am. Chem. Soc.* **2014**, *136*, 17722-17725; f) X. Cong, Y. Li, Y. Wei, X. Zeng, *Org. Lett.* **2014**, *16*, 3926-3929.
- [274] Y. Cao, Y. Yuan, Y. Lin, X. Jiang, Y. Weng, T. Wang, F. Bu, L. Zeng, A. Lei, *Green Chem.* **2020**, *22*, 1548-1552.
- [275] T. H. Meyer, J. C. A. de Oliveira, D. Ghorai, L. Ackermann, *Angew. Chem. Int. Ed.* **2020**, *59*, 10955-10960.
- [276] a) F. Saito, H. Aiso, T. Kochi, F. Kakiuchi, *Organometallics* **2014**, *33*, 6704-6707; b) Y.-Q. Li, Q.-L. Yang, P. Fang, T.-S. Mei, D. Zhang, *Org. Lett.* **2017**, *19*, 2905-2908; c) Q.-L. Yang, X.-Y. Wang, T.-L. Wang, X. Yang, D. Liu, X. Tong, X.-Y. Wu, T.-S. Mei, *Org. Lett.* **2019**, *21*, 2645-2649.
- [277] a) K. E. Poremba, S. E. Dibrell, S. E. Reisman, *ACS Catal.* **2020**, *10*, 8237-8246; b) X. Chang, Q. Zhang, C. Guo, *Angew. Chem. Int. Ed.* **2020**, *59*, 12612-12622; c) Q. Lin, L. Li, S. Luo, *Chem. Eur. J.* **2019**, *25*, 10033-10044; d) M. Ghosh, V. S. Shinde, M. Rueping, *Beilstein J. Org. Chem.* **2019**, *15*, 2710-2746.
- [278] a) Q. Wang, Q. Gu, S.-L. You, *Angew. Chem. Int. Ed.* **2019**, *58*, 6818-6825; b) D. Parmar, E. Sugiono, S. Raja, M. Rueping, *Chem. Rev.* **2014**, *114*, 9047-9153; c) J. Yu, F. Shi, L.-Z. Gong, *Acc. Chem. Res.* **2011**, *44*, 1156-1171; d) J. M. Brunel, *Chem. Rev.* **2008**, *108*, 1170-1170; e) T. Akiyama, J. Itoh, K. Fuchibe, *Adv. Synth. Catal.* **2006**, *348*, 999-1010.

- [279] a) J. F. Teichert, B. L. Feringa, *Angew. Chem. Int. Ed.* **2010**, *49*, 2486-2528; b) Y. Chen, S. Yekta, A. K. Yudin, *Chem. Rev.* **2003**, *103*, 3155-3212; c) R. Noyori, H. Takaya, *Acc. Chem. Res.* **1990**, *23*, 345-350.
- [280] a) G. Bringmann, T. Gulder, T. A. M. Gulder, M. Breuning, *Chem. Rev.* **2011**, *111*, 563-639; b) M. C. Kozlowski, B. J. Morgan, E. C. Linton, *Chem. Soc. Rev.* **2009**, *38*, 3193-3207.
- [281] G. Liao, T. Zhou, Q.-J. Yao, B.-F. Shi, *Chem. Commun.* **2019**, *55*, 8514-8523.
- [282] a) I. G. Stará, I. Starý, *Acc. Chem. Res.* **2020**, *53*, 144-158; b) P. Redero, T. Hartung, J. Zhang, L. D. M. Nicholls, G. Zichen, M. Simon, C. Golz, M. Alcarazo, *Angew. Chem. Int. Ed.* **2020**, *59*, 23527-23531; c) J. Nejedlý, M. Šámal, J. Rybáček, I. G. Sánchez, V. Houska, T. Warzecha, J. Vacek, L. Sieger, M. Buděšínský, L. Bednárová, P. Fiedler, I. Císařová, I. Starý, I. G. Stará, *J. Org. Chem.* **2020**, *85*, 248-276; d) T. Hartung, R. Machleid, M. Simon, C. Golz, M. Alcarazo, *Angew. Chem. Int. Ed.* **2020**, *59*, 5660-5664; e) K. Dhbaibi, L. Favereau, J. Crassous, *Chem. Rev.* **2019**, *119*, 8846-8953; f) M. Gingras, *Chem. Soc. Rev.* **2013**, *42*, 1051-1095; g) Y. Shen, C.-F. Chen, *Chem. Rev.* **2012**, *112*, 1463-1535.
- [283] D. Zell, U. Dhawa, V. Müller, M. Bursch, S. Grimme, L. Ackermann, *ACS Catal.* **2017**, *7*, 4209-4213.
- [284] U. Dhawa, D. Zell, R. Yin, S. Okumura, M. Murakami, L. Ackermann, *J. Catal.* **2018**, *364*, 14-18.
- [285] K. Ozols, Y.-S. Jang, N. Cramer, *J. Am. Chem. Soc.* **2019**, *141*, 5675-5680.
- [286] U. Dhawa, R. Connon, J. C. A. Oliveira, R. Steinbock, L. Ackermann, *Org. Lett.* **2021**, DOI: 10.1021/acs.orglett.1c00615.
- [287] C. Tian, U. Dhawa, A. Scheremetjew, L. Ackermann, *ACS Catal.* **2019**, *9*, 7690-7696.
- [288] U. Dhawa, C. Tian, W. Li, L. Ackermann, *ACS Catal.* **2020**, 6457-6462.
- [289] U. Dhawa, C. Tian, T. Wdowik, J. C. A. Oliveira, J. Hao, L. Ackermann, *Angew. Chem. Int. Ed.* **2020**, *59*, 13451-13457.
- [290] L. Liang, S. Fu, D. Lin, X.-Q. Zhang, Y. Deng, H. Jiang, W. Zeng, *J. Org. Chem.* **2014**, *79*, 9472-9480.
- [291] a) A. Whyte, A. Torelli, B. Mirabi, L. Prieto, J. F. Rodríguez, M. Lautens, *J. Am. Chem. Soc.* **2020**, *142*, 9510-9517; b) R. K. Nandi, R. Guillot, C. Kouklovsky, G. Vincent, *Org. Lett.* **2016**, *18*, 1716-1719.
- [292] L. Ackermann, *Org. Lett.* **2005**, *7*, 3123-3125.
- [293] R. Ueno, S. Natsui, N. Chatani, *Org. Lett.* **2018**, *20*, 1062-1065.

Acknowledgements

First, I would like to express my sincere gratitude to my supervisor Prof. Dr. Lutz Ackermann for giving me the opportunity to carry out my PhD under his supervision, and for constant encouragement and support. His insightful suggestions, in many ways, have shaped my research career and greatly influenced the overall development as a research scholar. His unmistakable devotion, patience and strong work ethics would surely have a lasting impression on my professional career. Honestly, I could not have imagined having a better advisor and mentor for my PhD study. Thank you for all your support and guidance.

Besides my advisor, I would like to thank Prof. Dr. Manuel Alcarazo for accepting to be my second supervisor. Valuable suggestions from him has helped significantly to assess my work and improve further.

I also would like to thank Prof. Dr. Dr. h.c.mult. Lutz F. Tietze, Prof. Dr. Ricardo Mata, Dr. Michael John, Dr. Daniel Janßen-Müller for agreeing to take part in my defense.

I am thankful to Institut für Organische und Biomolekulare Chemie, Georg-August-Universität Göttingen for the work space and the instrumental facilities.

Financial assistance from DAAD, University of Göttingen and Prof. Dr. Lutz Ackermann is gratefully acknowledged.

I gratefully acknowledge Ms. Gabriele Keil-Knepel and Bianca Spitalieri for their kind assistance for the administrative works. I sincerely thank Mr. Stefan Beußhausen for taking care of all the instruments in our research group, especially the chiral HPLC, the glovebox and the GPC, which I used very often during my stay in the last fours years. Also I thank him for technical assistance with computers. I sincerely thank Mr. Karsten Rauch for his kind support and guidance to maintain safety in the lab.

My sincere thanks also goes to my fellow labmates, and all the members of our lab, past and present, for great work atmosphere, teamwork and companionship. I sincerely thank Dr. Daniel Zell, Dr. Fabio Pesciaioli, Dr. Cong Tian, Dr. Joachim Loup, Dr. Ramesh Chandra Samanta, Dr. Joao Carlos Agostinho de Oliveira, Dr. Tomasz Wdowik, Dr. Robert Connon, Dr. Ruhuai Mei, Dr. Wenbo Ma, Dr. Lars H. Finger, Nikolaos Kaplaneris, Valentin Müller, Tjark Meyer, Ralf Alexander Steinbock, Isaac Choi, Maximilian Stangier, Julia Struwe, Alexej Scheremetjew, Becky Bongsuiru Jei, Zhipeng Lin, Xiaoyan Hou, Binbin Yuan, Shintaro

Okumura, Masoom Nasiha Hussain, Weizhao Li, Rongxin Yin for their help on my PhD projects.

I would like to thank whole Ackermann family and special thank to all members in 309: Dr. Daniel Zell, Dr. Fabio Pesciaioli, Dr. Yu-Feng Liang, Dr. Debasish Ghorai, Dr. Weiping Liu, Dr. Tomasz Wdowik, Dr. Robert Connon, Dr. Cong Tian, Dr. Elżbieta Gońka, Valentin Müller, Ralf Alexander Steinbock, Long Yang, Becky Bongsuiru Jei, Isaac Maksso, Binbin Yuan Masoom Nasiha Hussain, Weizhao Li, Rongxin Yin.

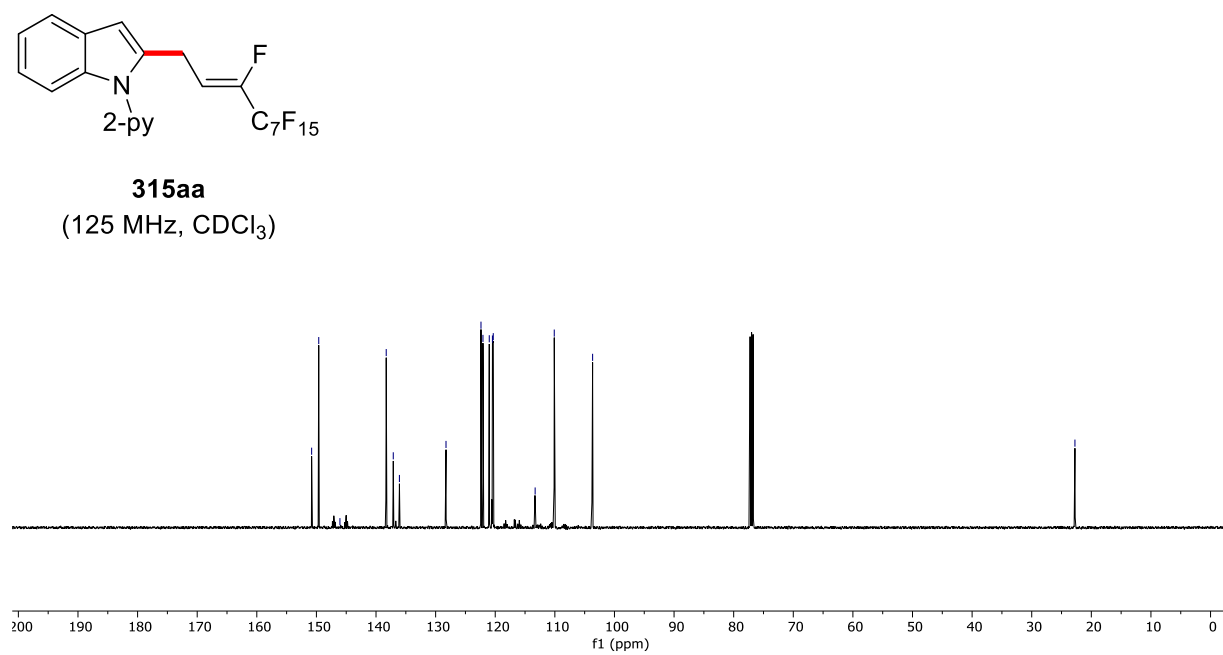
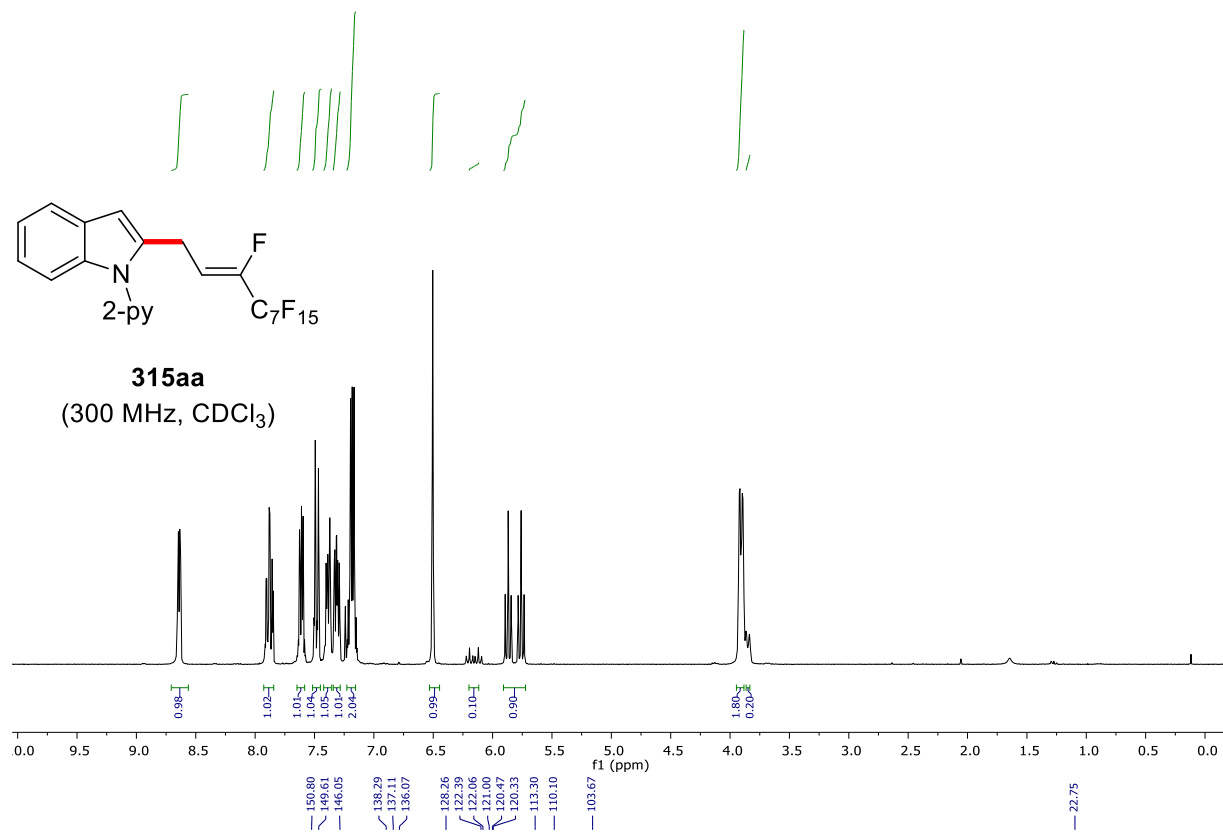
Many thanks to Dr. Robert Connon, Dr. Joao Carlos Agostinho de Oliveira, Nikolaos Kaplaneris, Dr. Tomasz Wdowik, Dr. Ramesh Chandra Samanta, Leonardo Massignan, Maximilian Stangier, Nate Ang for their time to correct this thesis. I sincerely would like to thank all the people who previously corrected manuscripts, supporting information, posters, abstracts and proposals in very short time: Nikolaos Kaplaneris, Dr. Ramesh Chandra Samanta, Dr. Joao Carlos Agostinho de Oliveira, Dr. Tomasz Wdowik, Dr. Robert Connon, Valentin Müller, Tjark Meyer, Isaac Choi, Maximilian Stangier, Dr. Yu-Feng Liang, Dr. Debasish Ghorai, Dr. Joachim Loup, Dr. Wei Wang, Dr. Gandeepan Parthasarathy, Dr. Santhi Vardhana Yetra, Dr. Mélanie Lorion, Dr. Parthasarathi Subramanian. Thank you all for your time and patience.

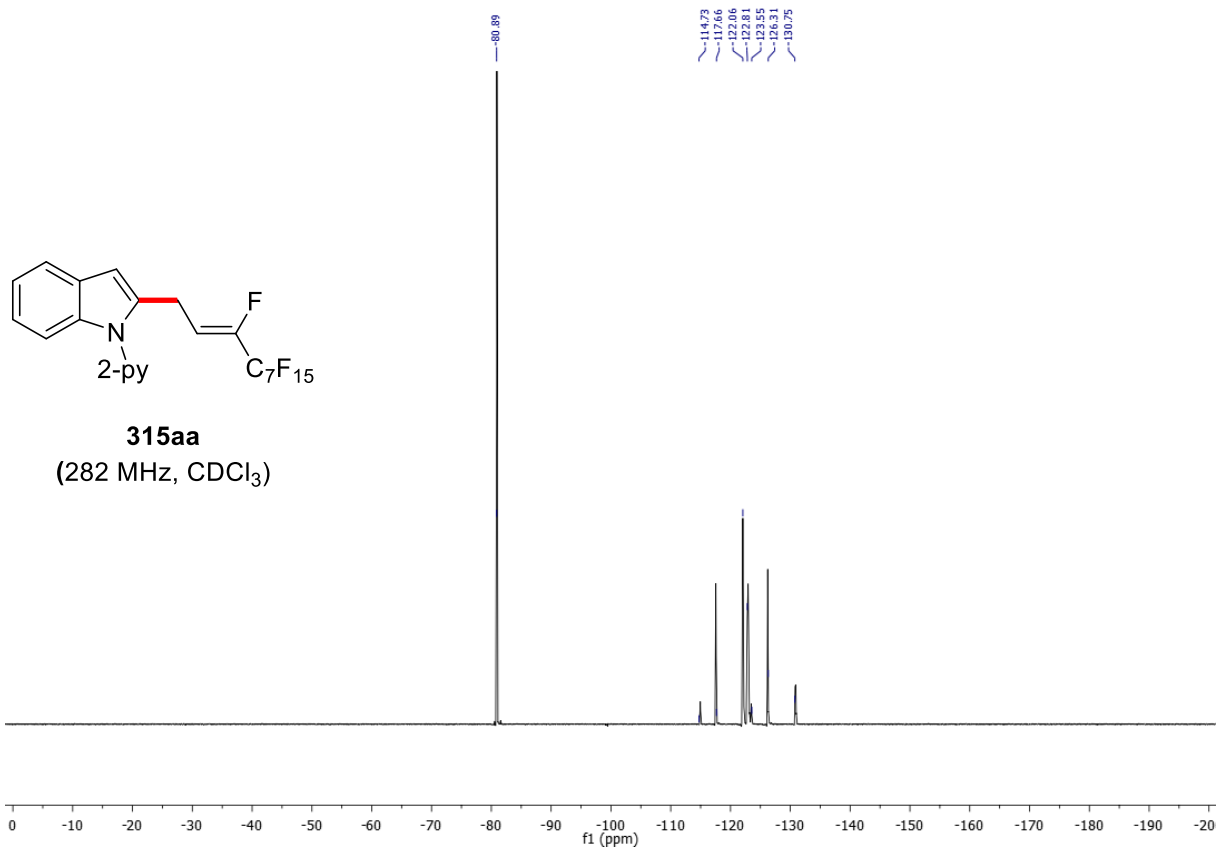
Moreover, I deeply thank to Dr. Michael John for helping me in DOSY experiment as well as in analyzing some NMR spectroscopic data. I am thankful to Dr. Christopher Golz for his assistance with X-ray diffraction analysis. I am thankful to the instrument operators, and staffs (NMR and mass spectrometry) at the IOBC for their continuous support to our research work.

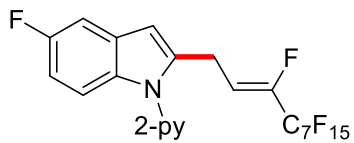
I also would like to express my gratitude to my former supervisors Prof. Dr. Debabrata Maiti and Prof. Dr. Yashwant D. Vankar for teaching me chemistry and giving me the opportunity to conduct research within their laboratories.

Last but not the least, I would like to express my deepest gratitude to my parents and my friends. Their unconditional support and encouragement made it possible to come this far.

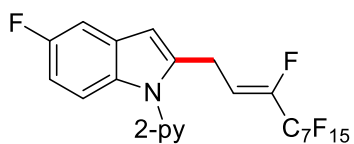
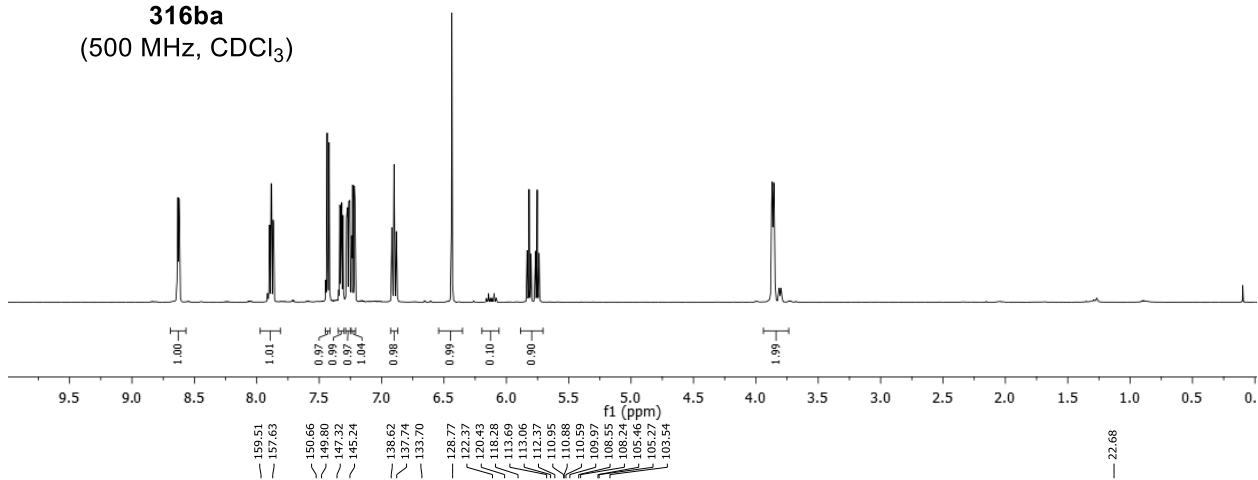
NMR Spectra and HPLC Chromatograms



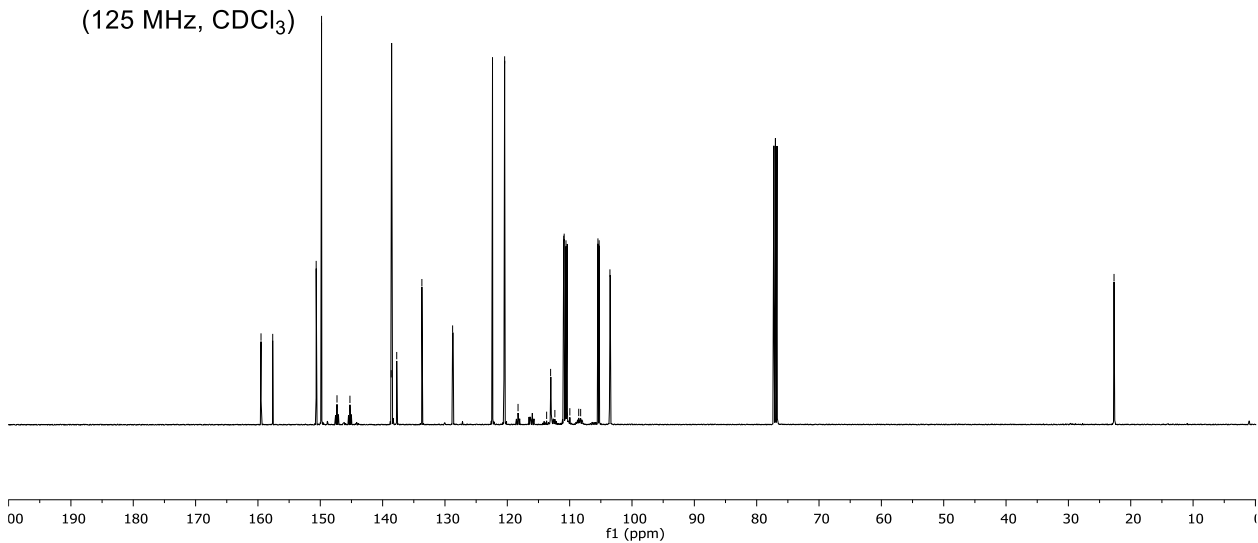


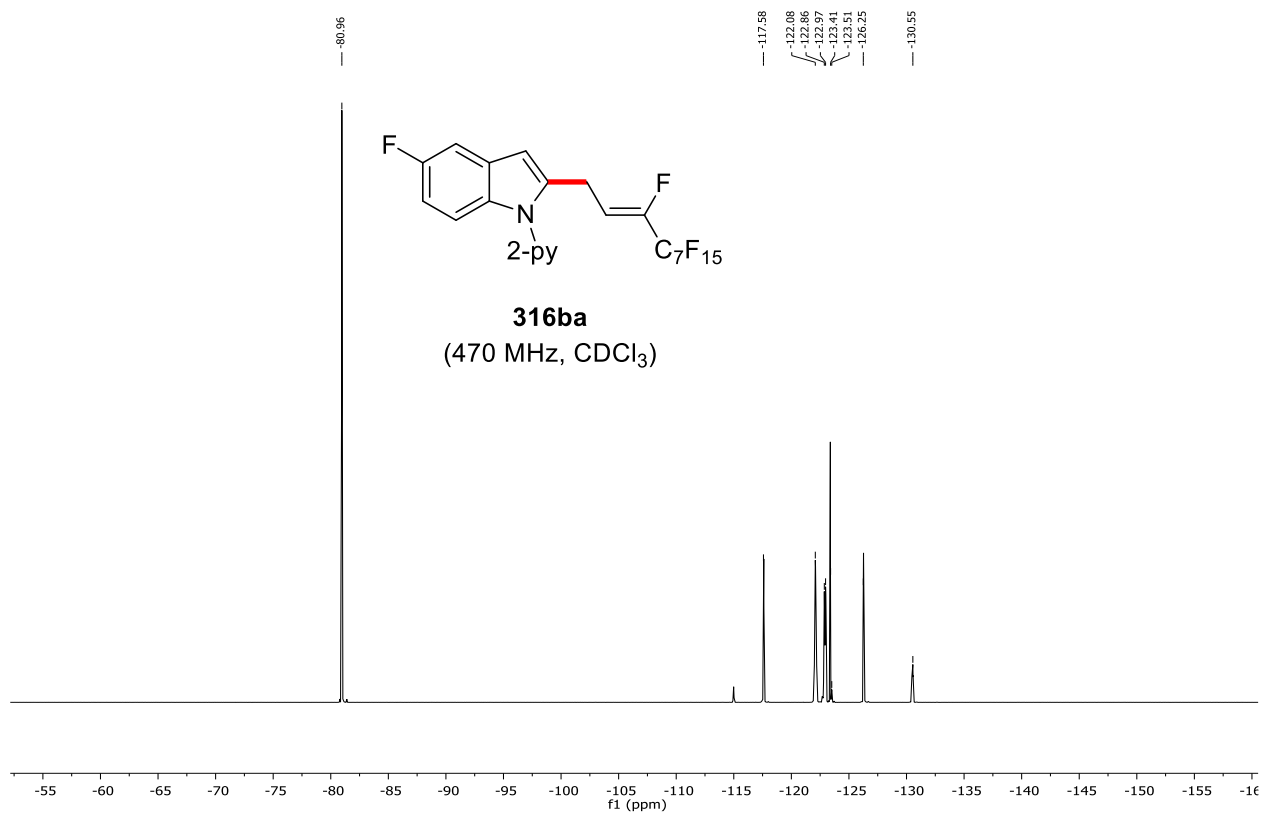


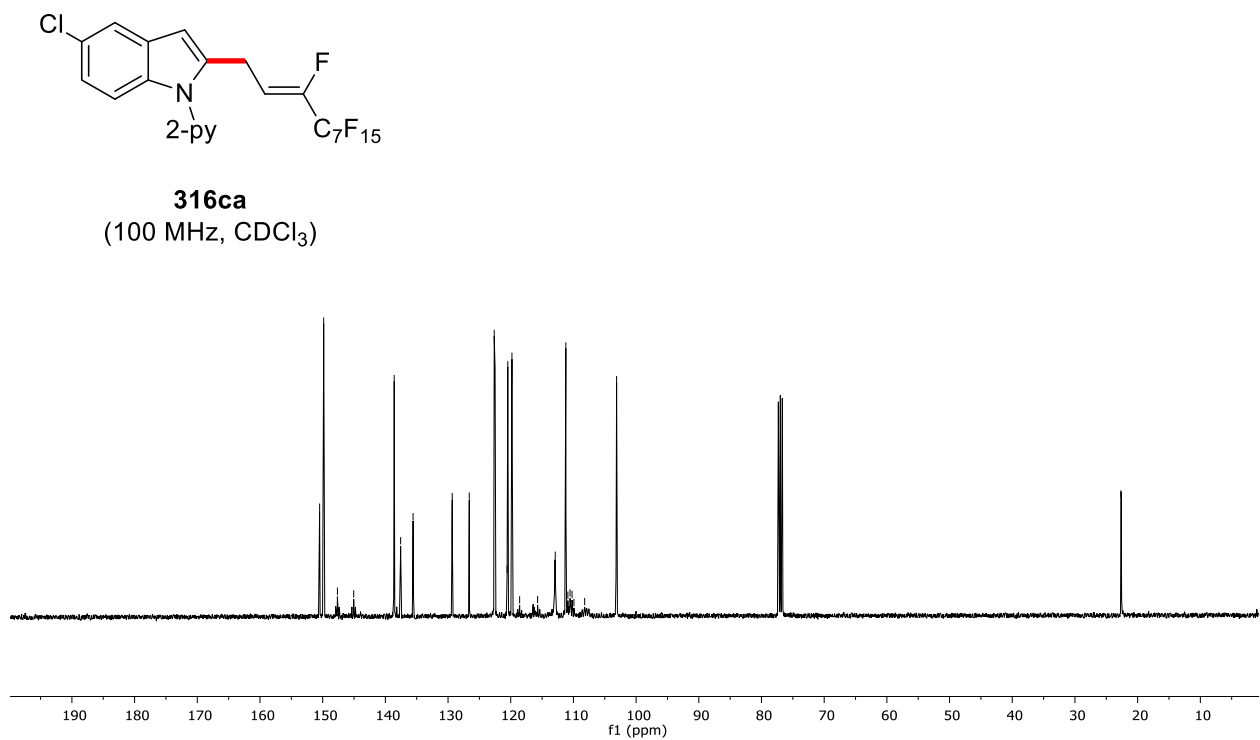
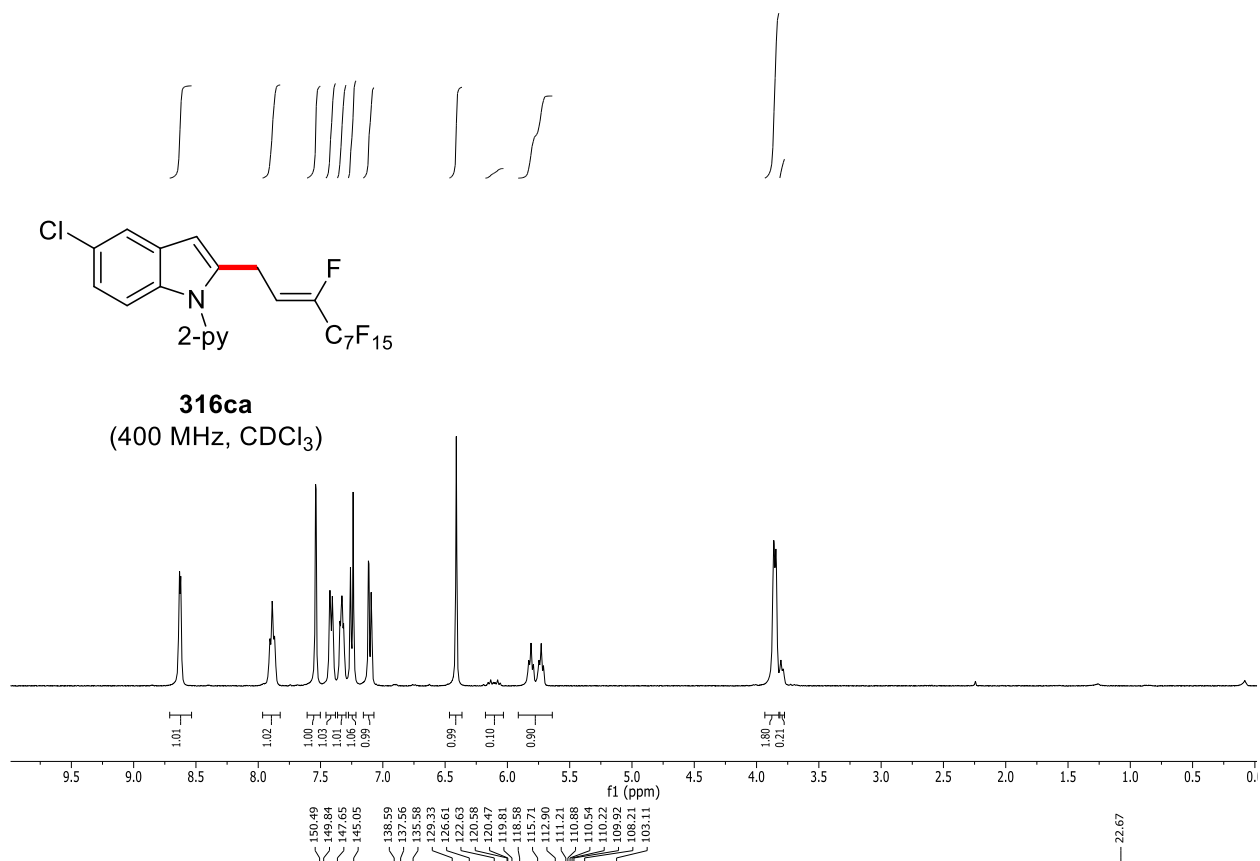
316ba
(500 MHz, CDCl₃)

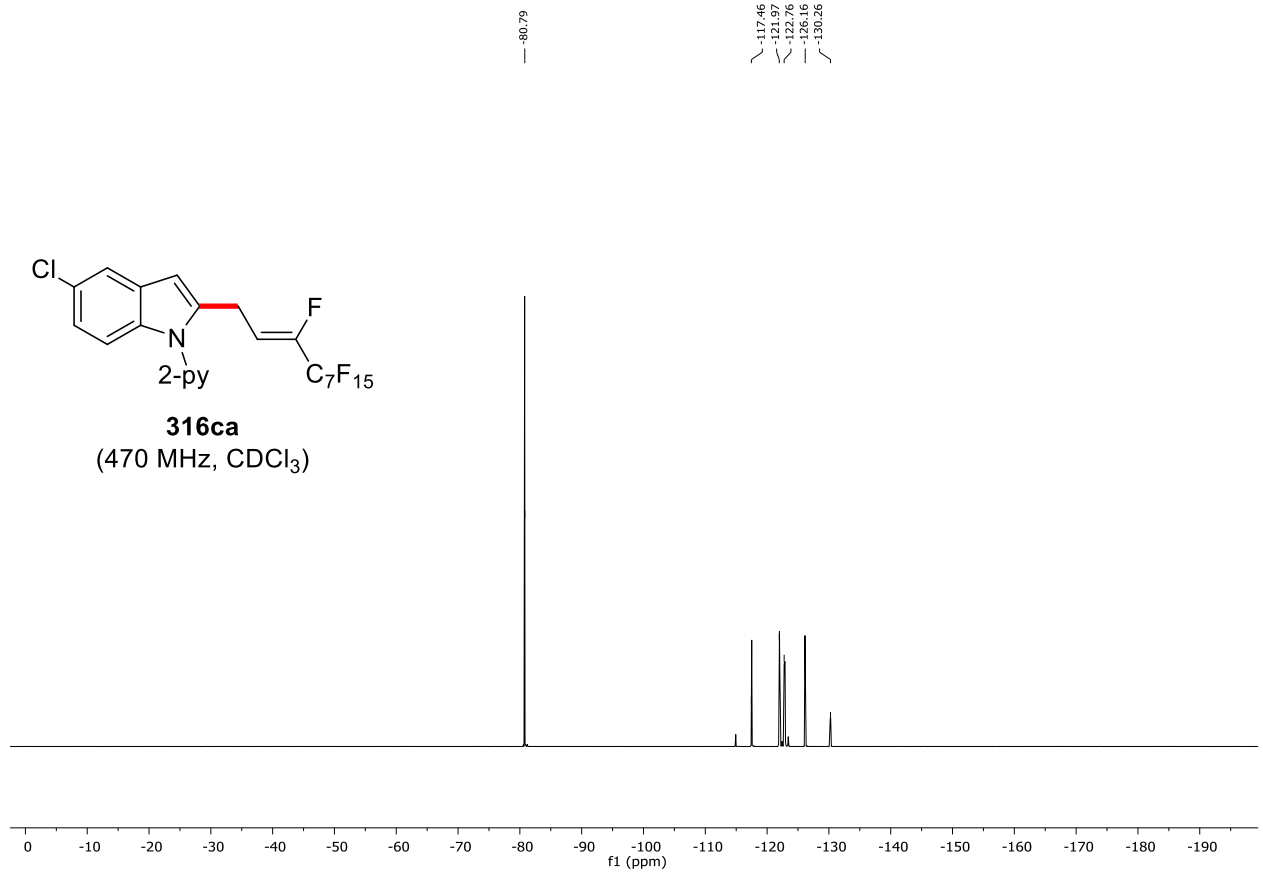


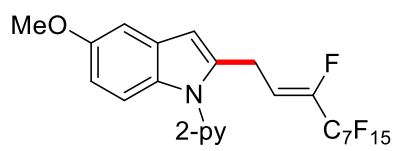
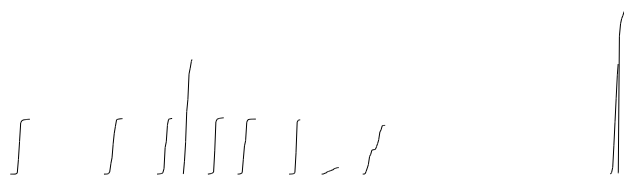
316ba
(125 MHz, CDCl₃)



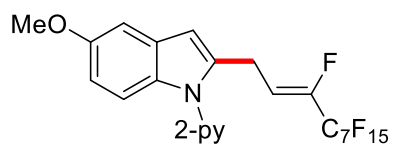
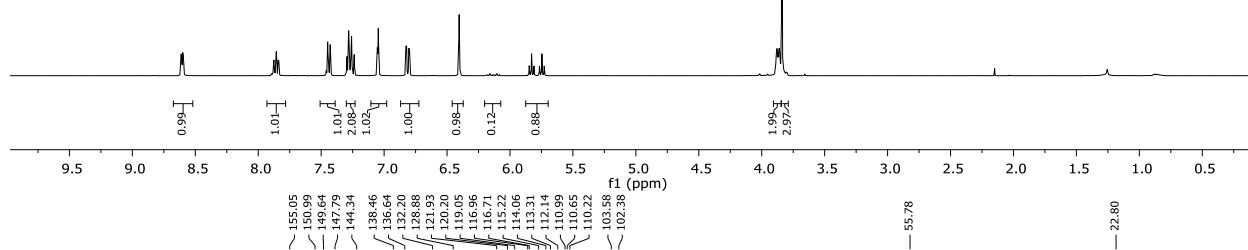




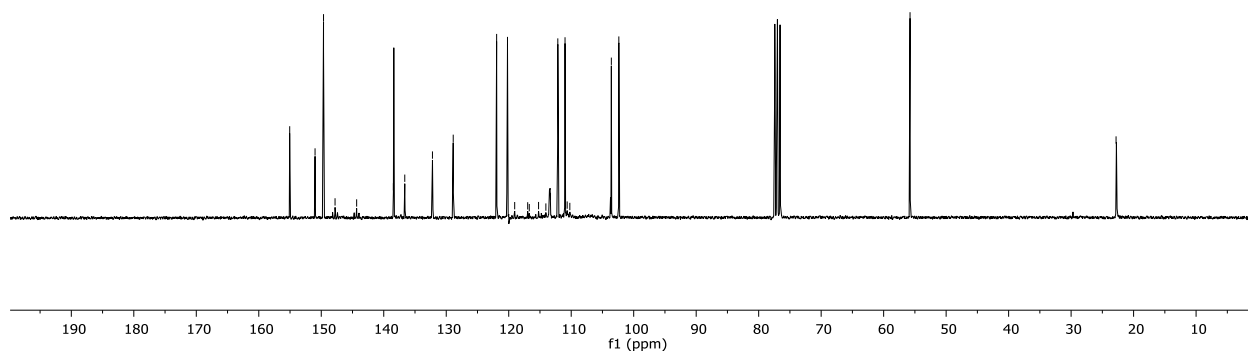


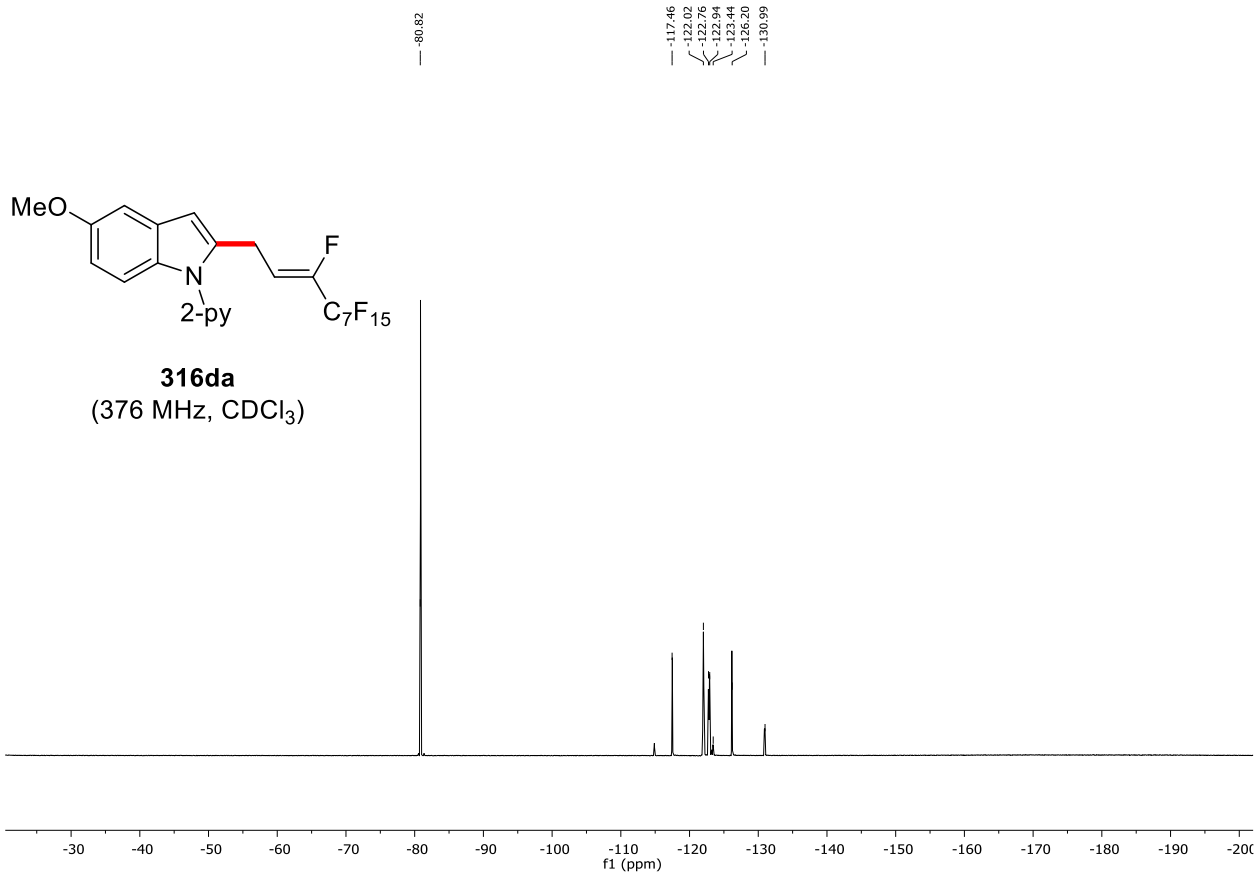


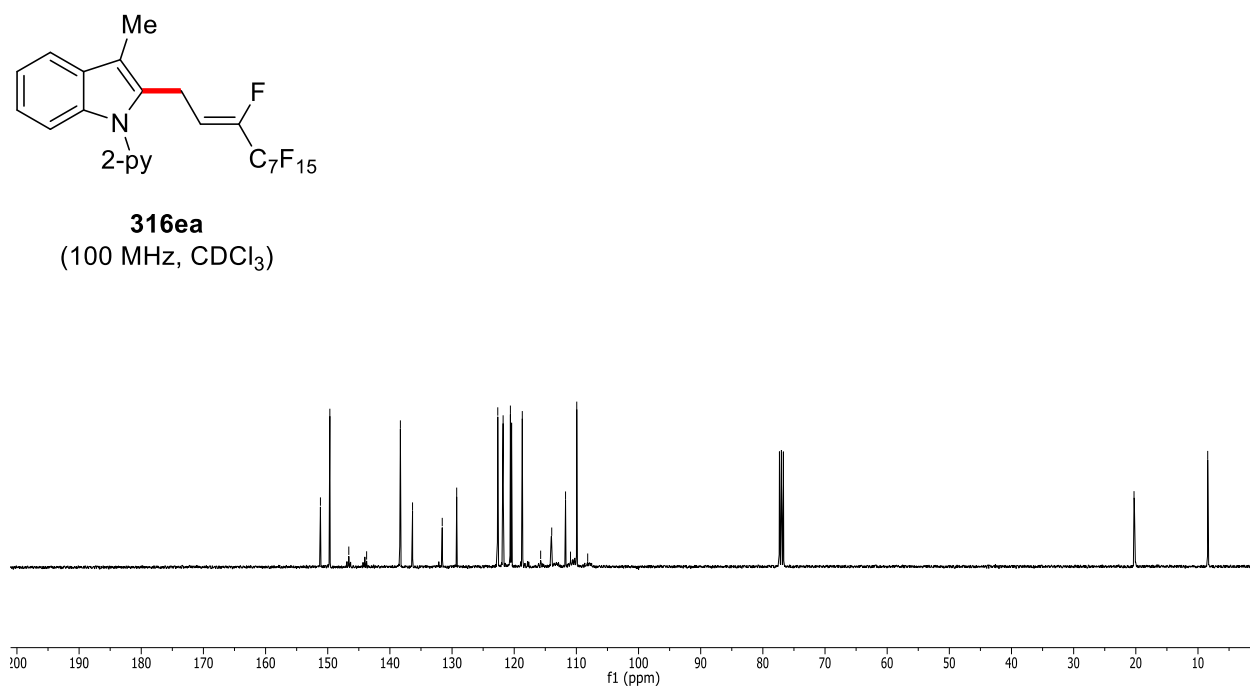
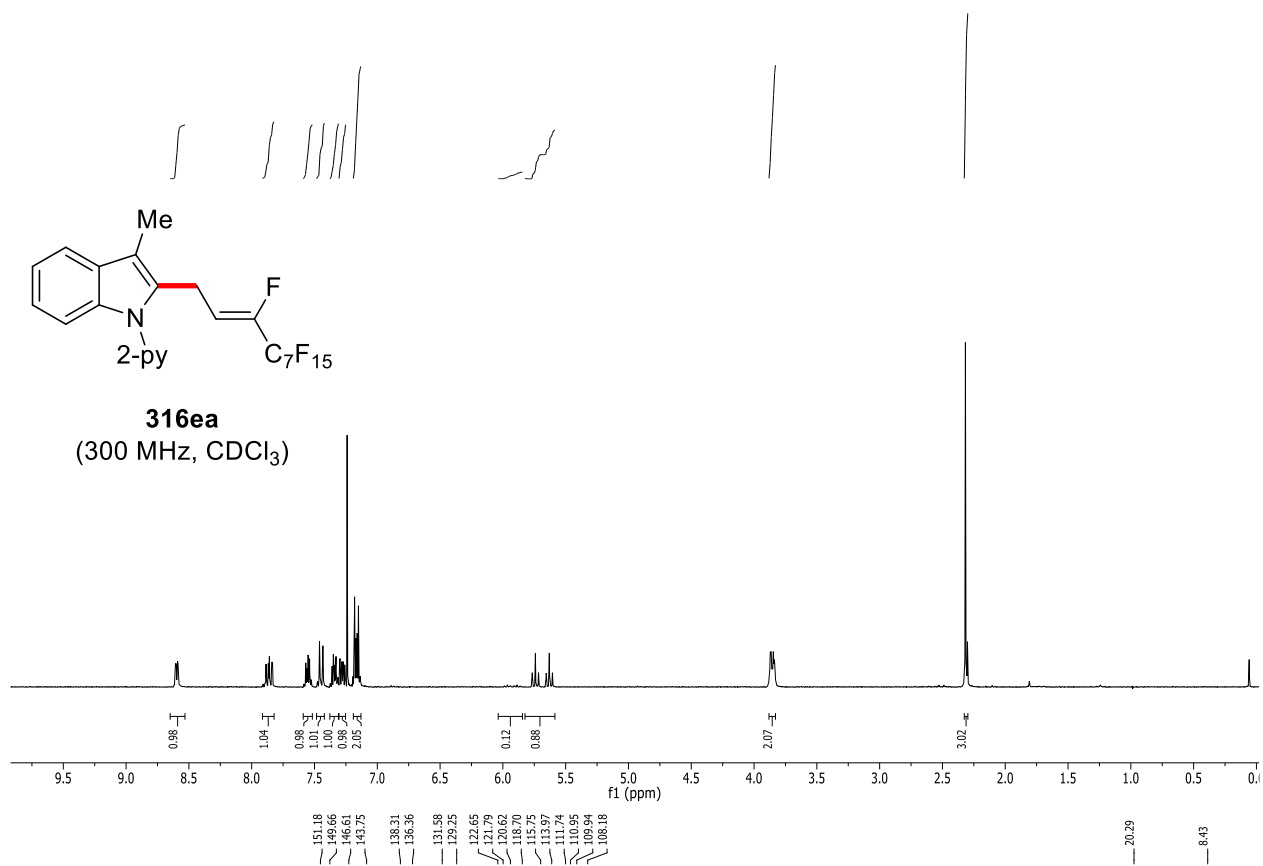
316da
(400 MHz, CDCl₃)

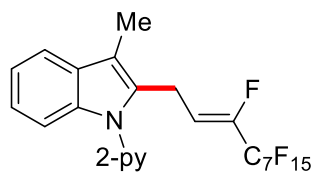


316da
(75 MHz, CDCl₃)

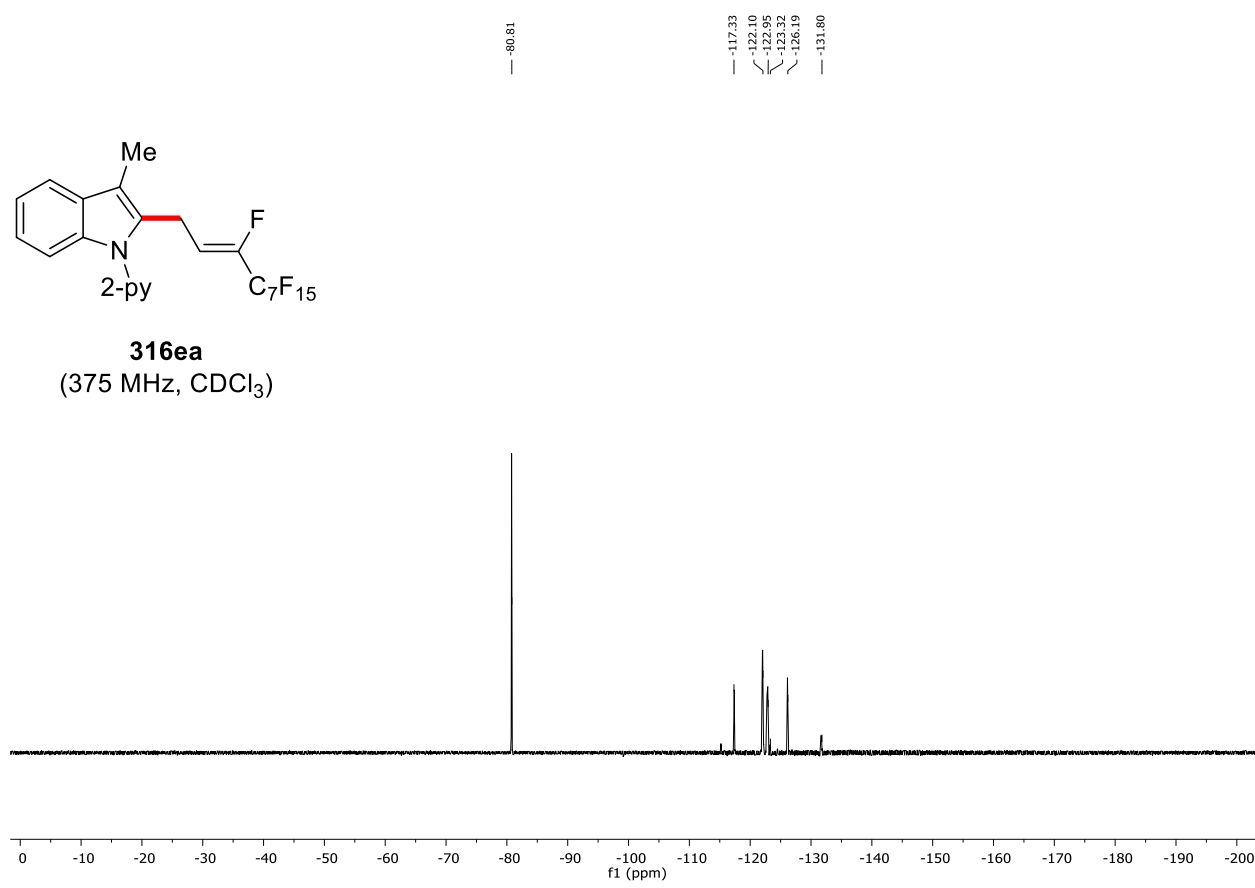


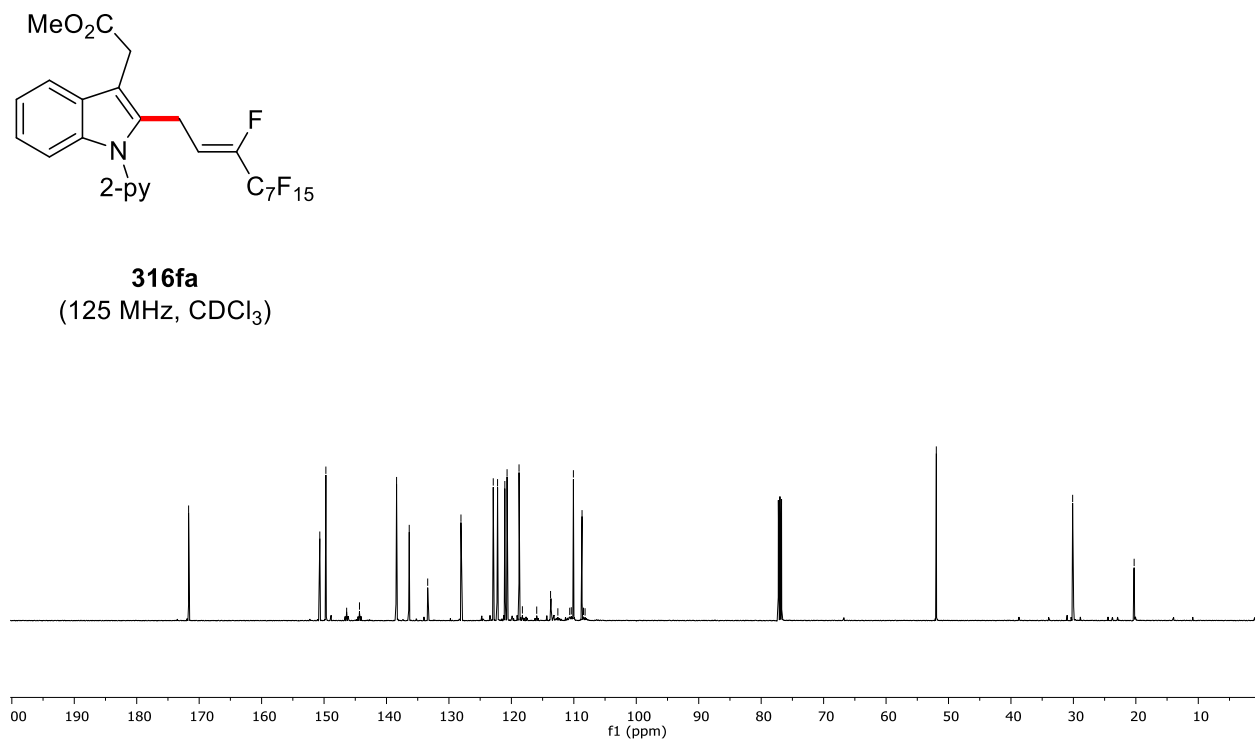
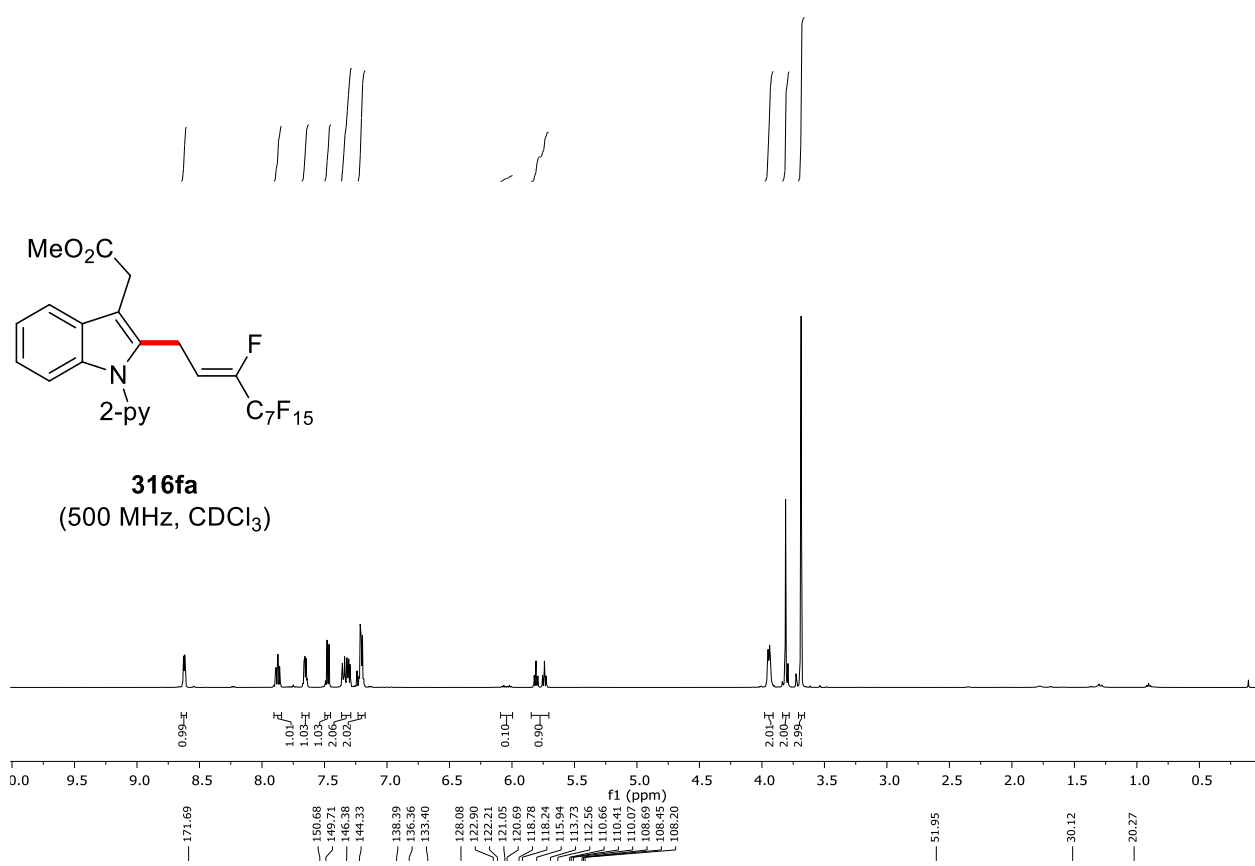


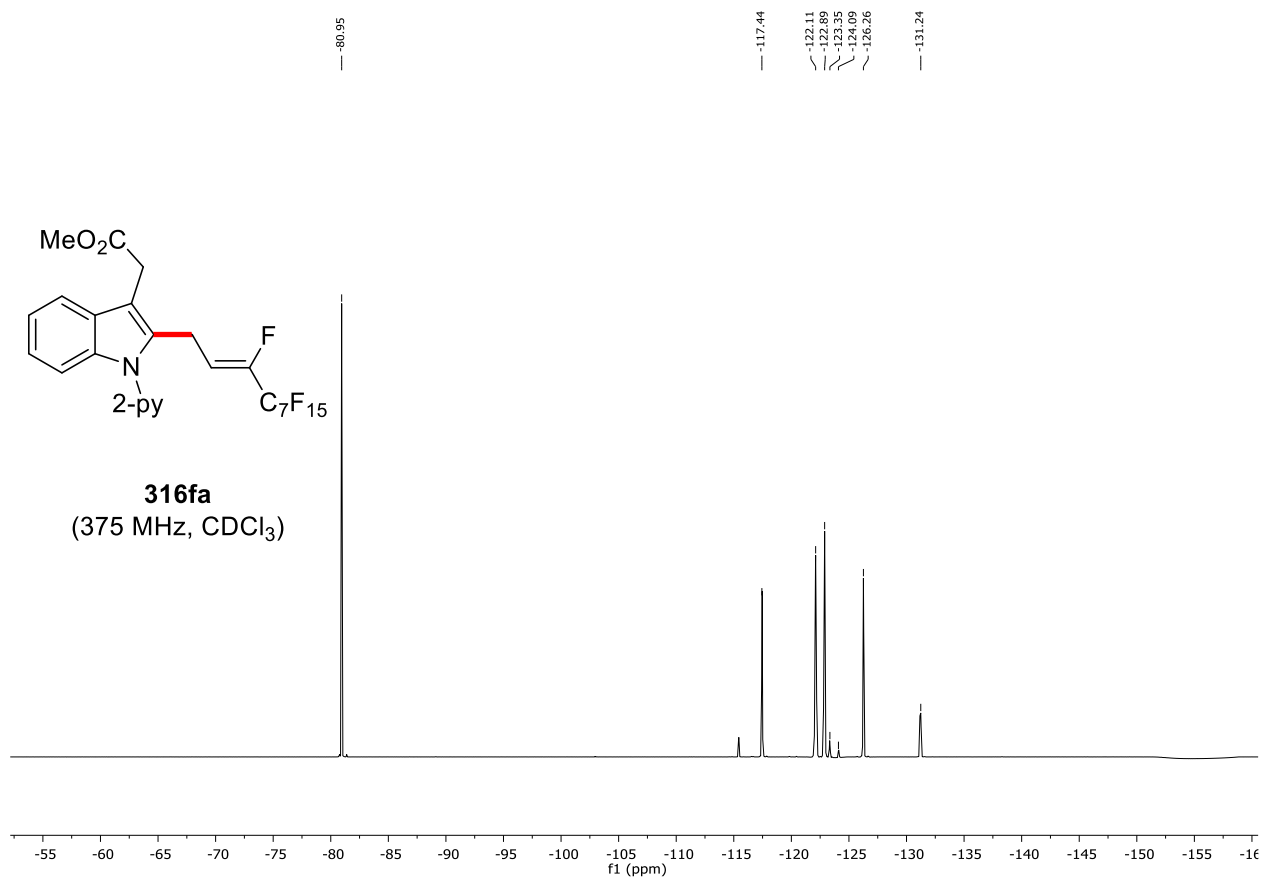


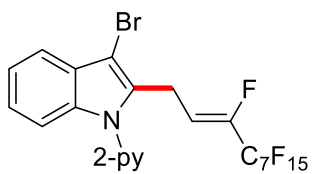


316ea
(375 MHz, CDCl₃)

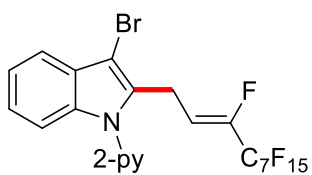
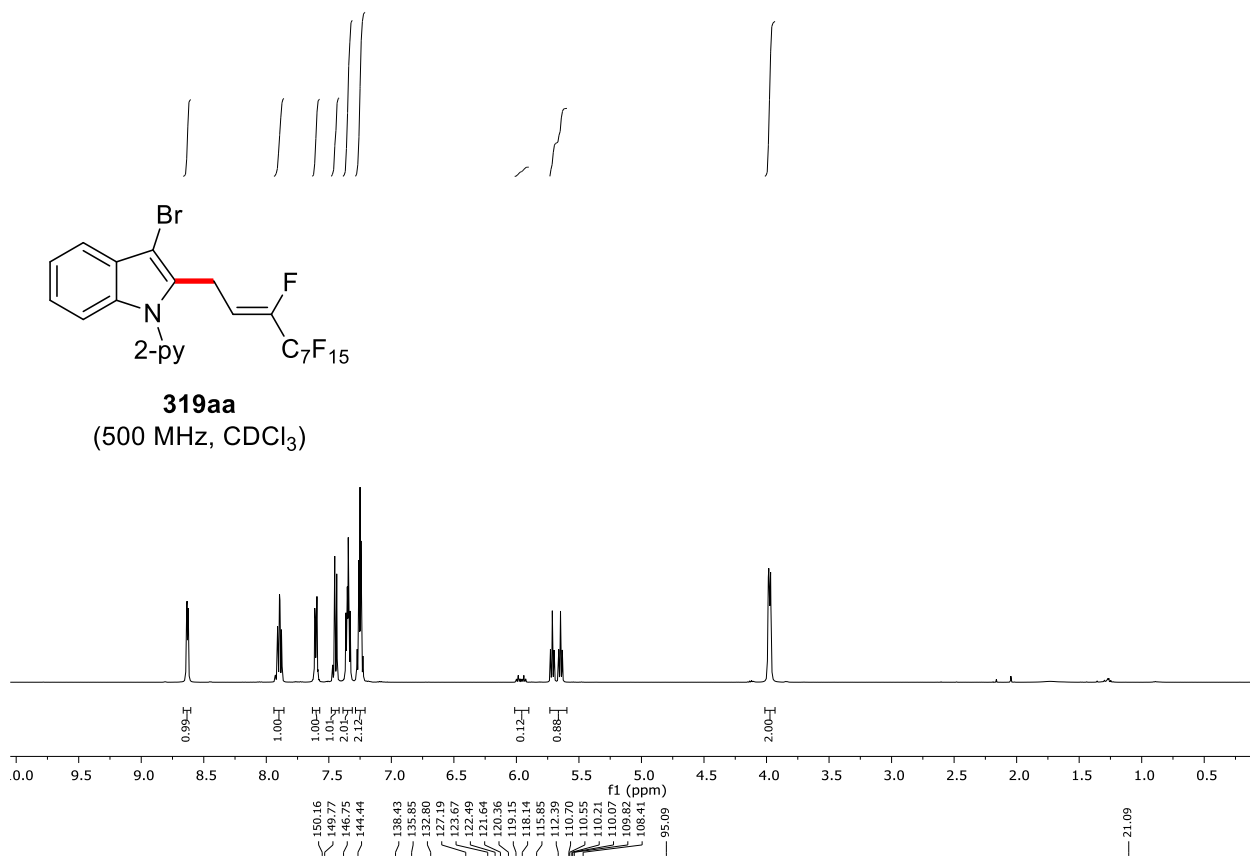




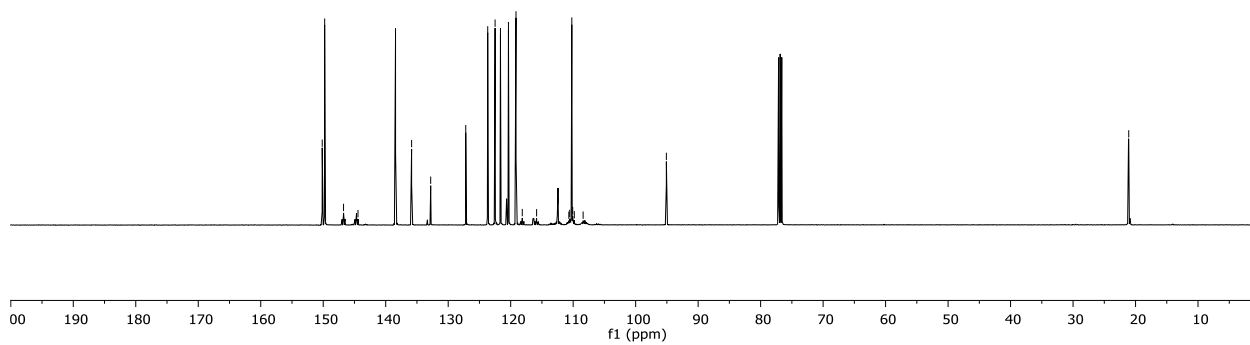


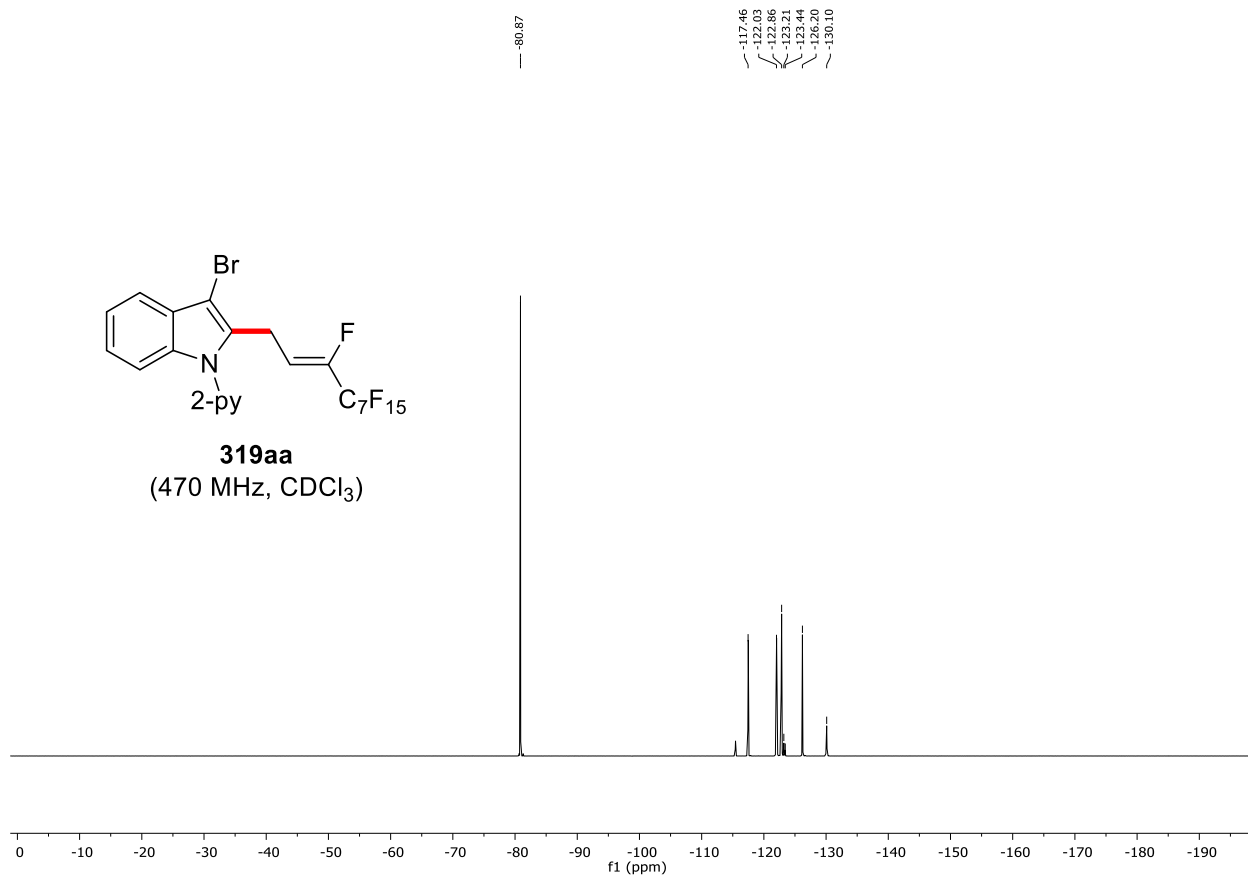


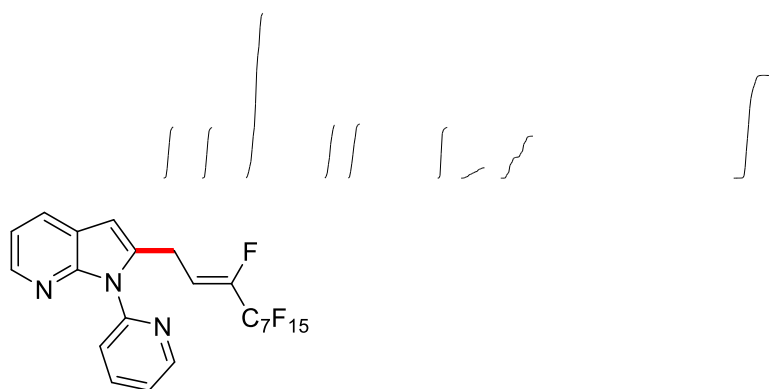
319aa
(500 MHz, CDCl₃)



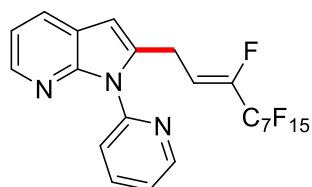
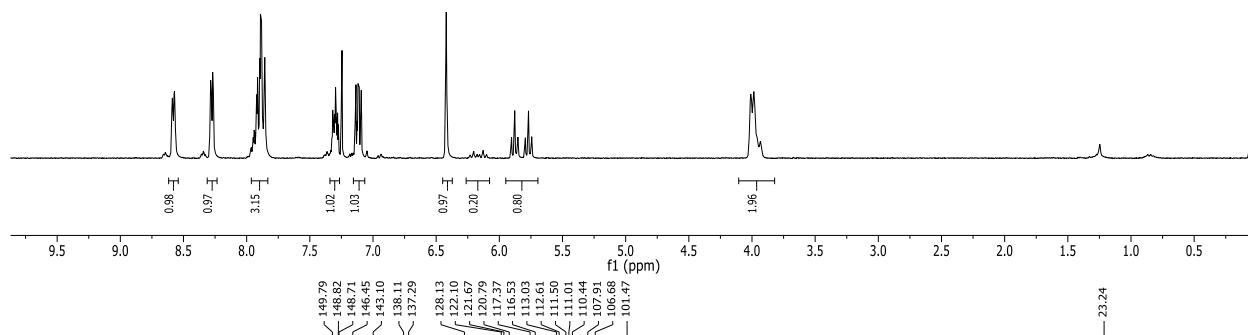
319aa
(125 MHz, CDCl₃)



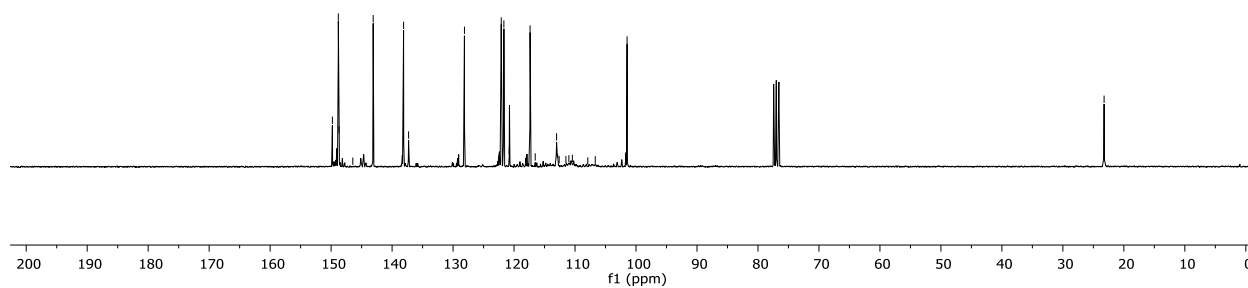


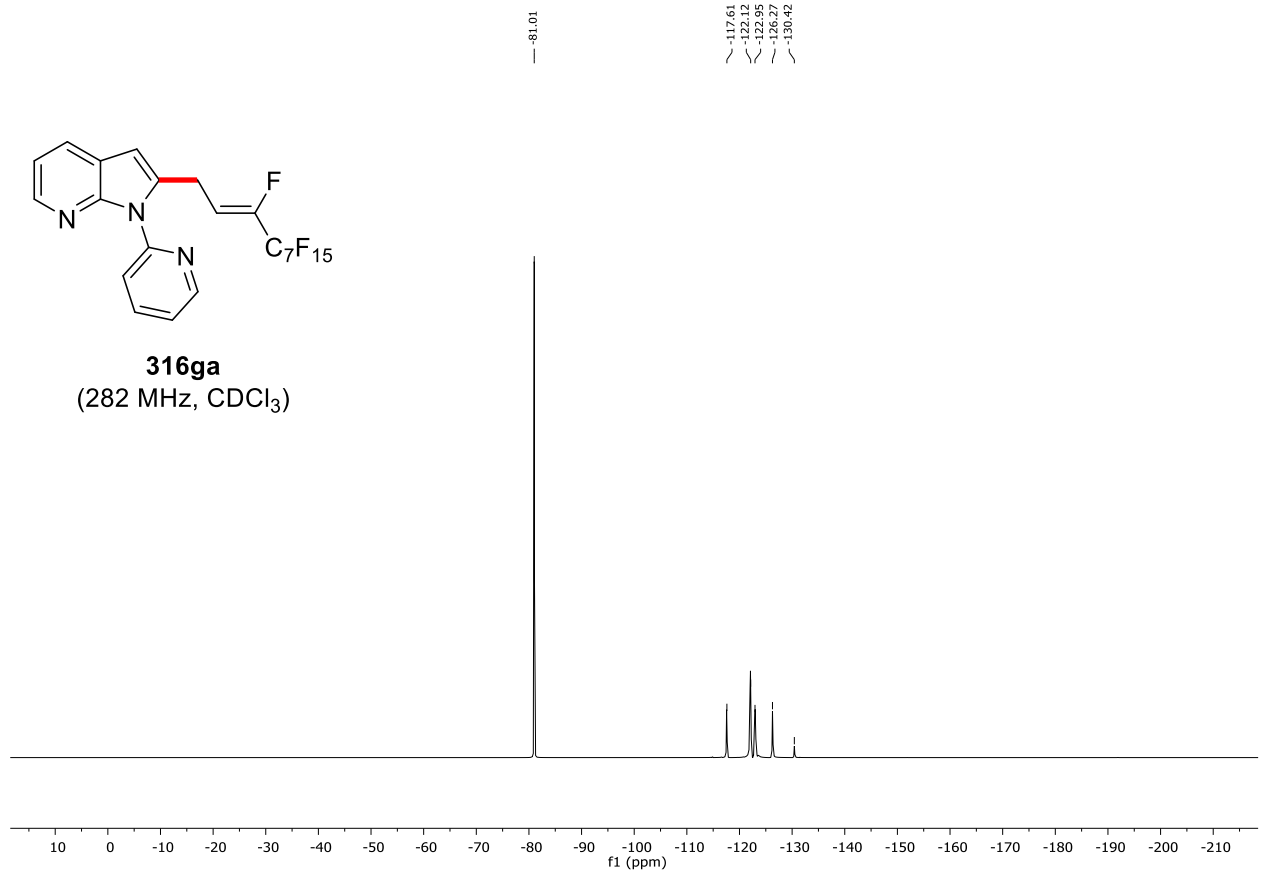


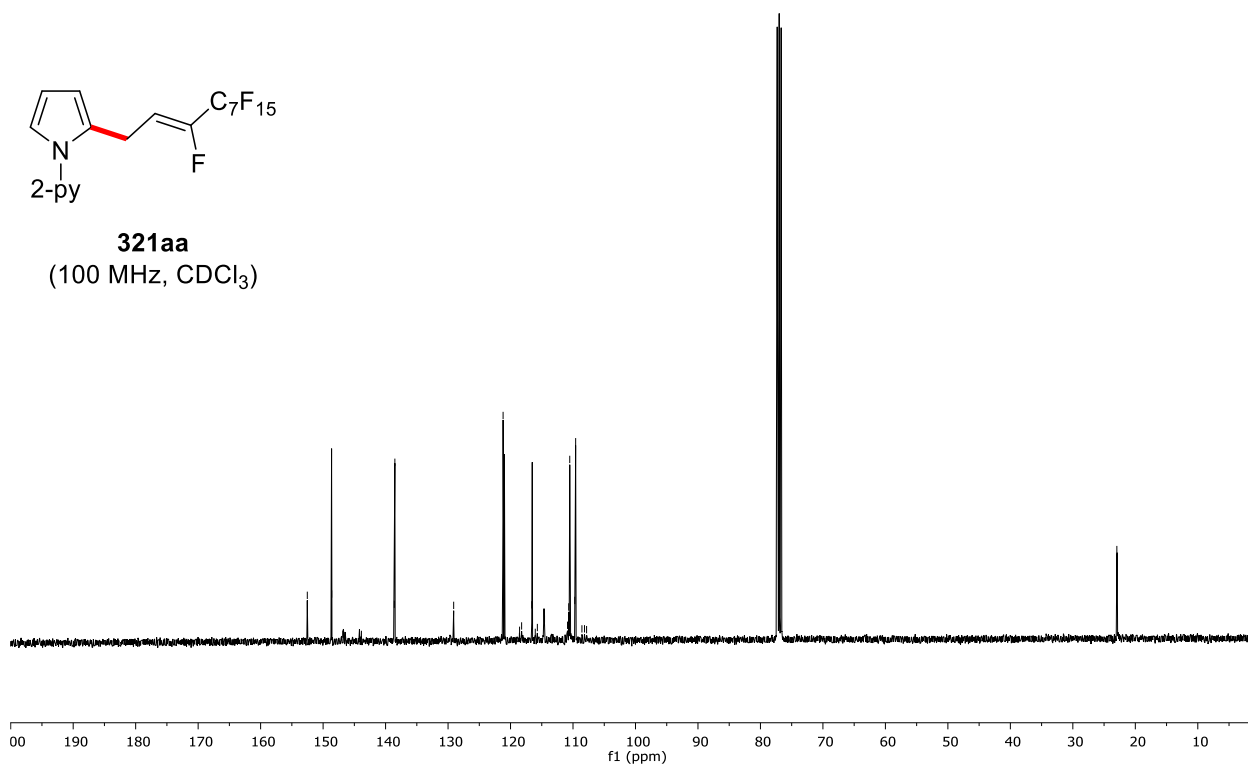
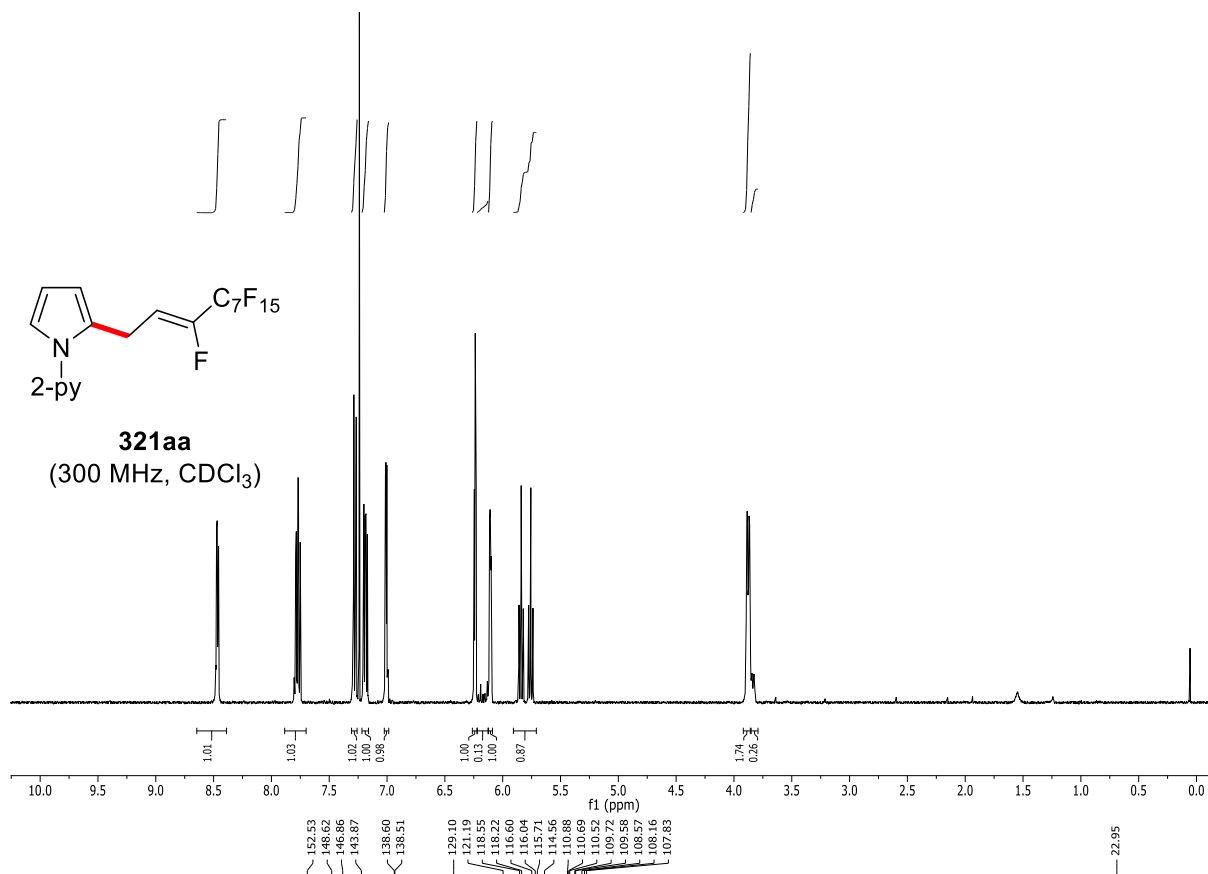
316ga
(300 MHz, CDCl₃)

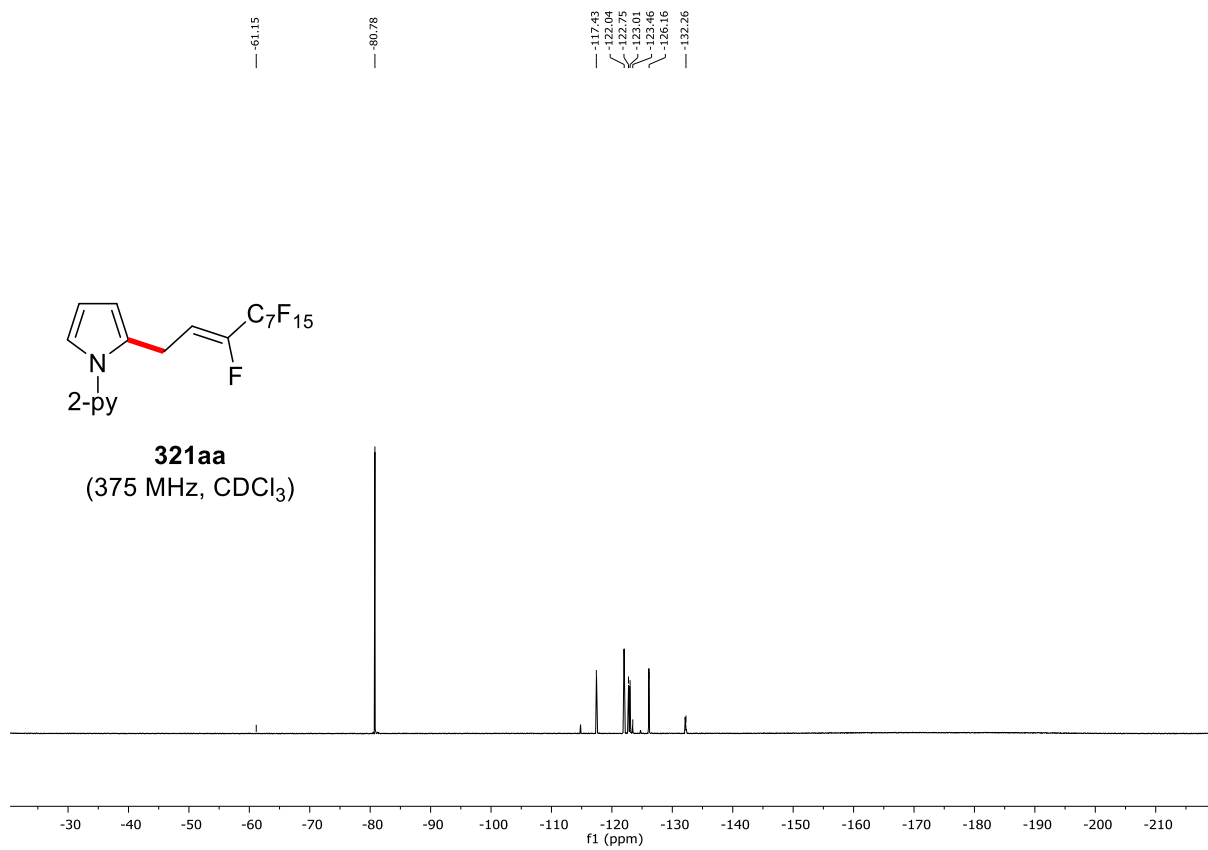


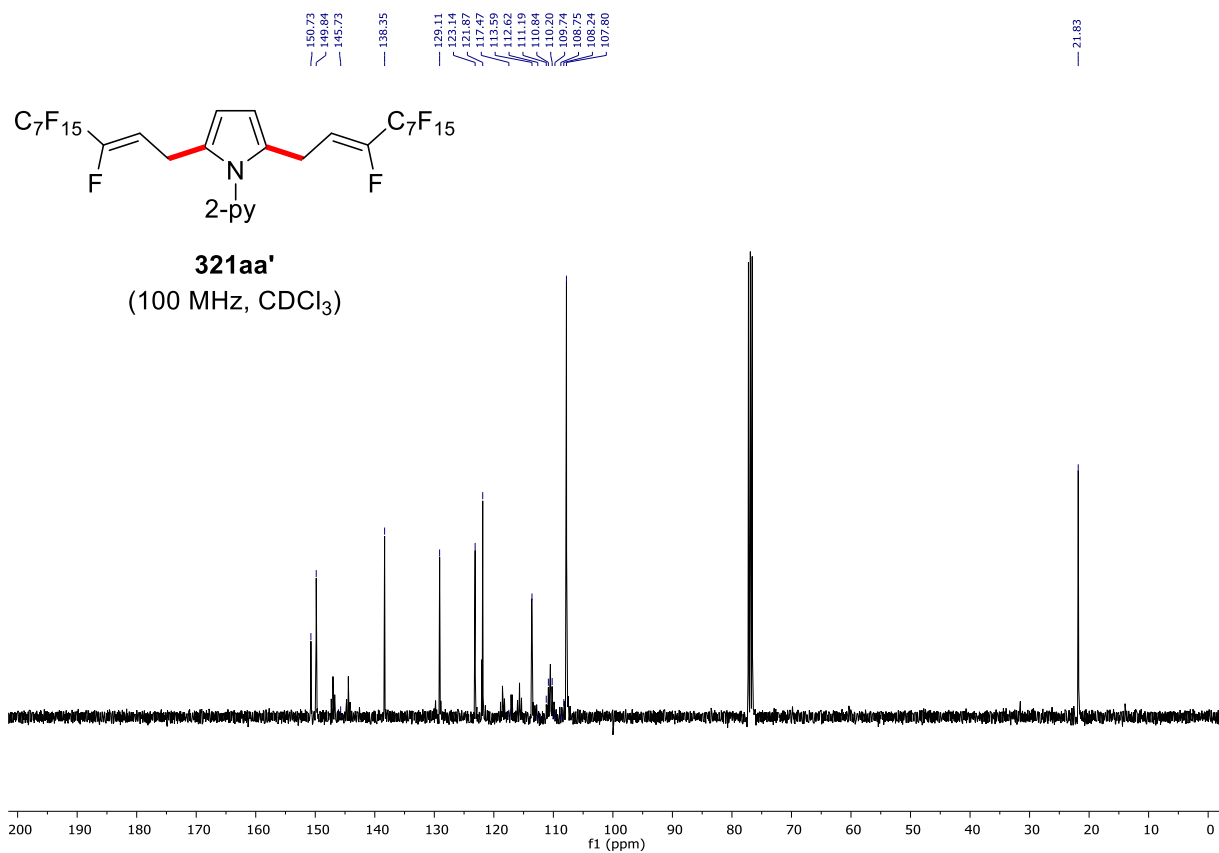
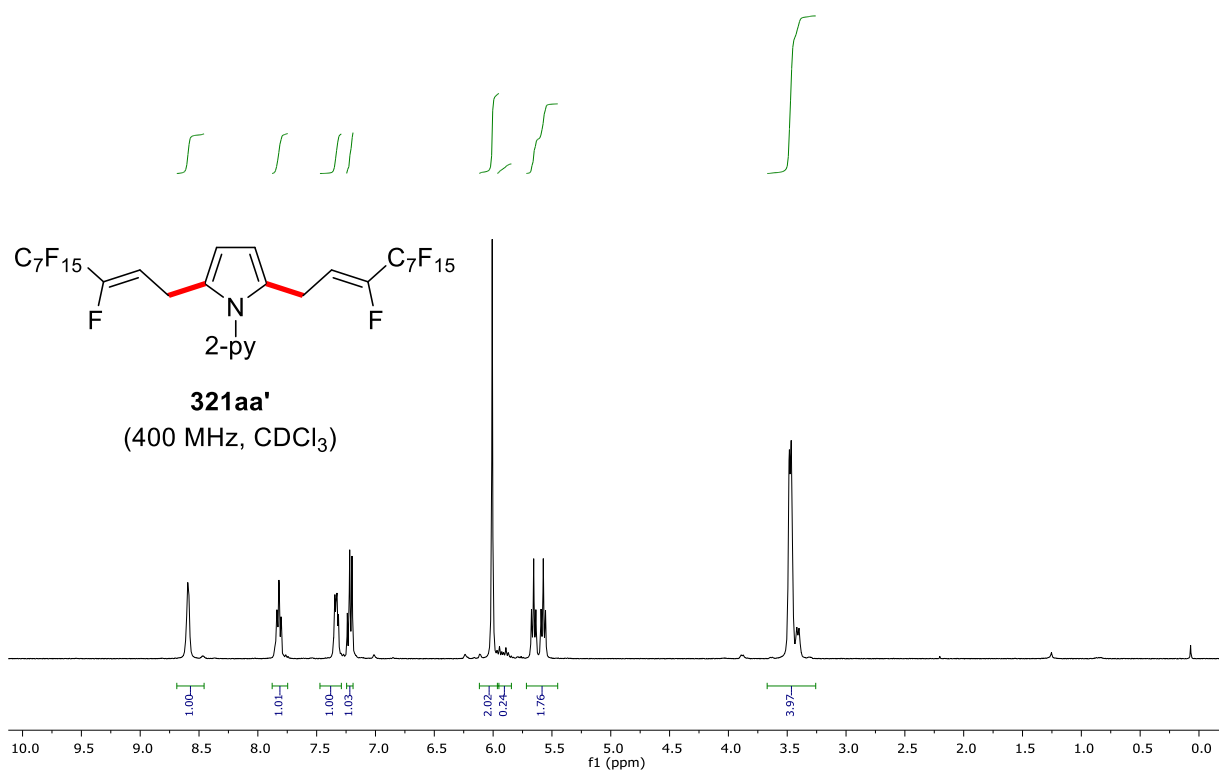
316ga
(100 MHz, CDCl₃)

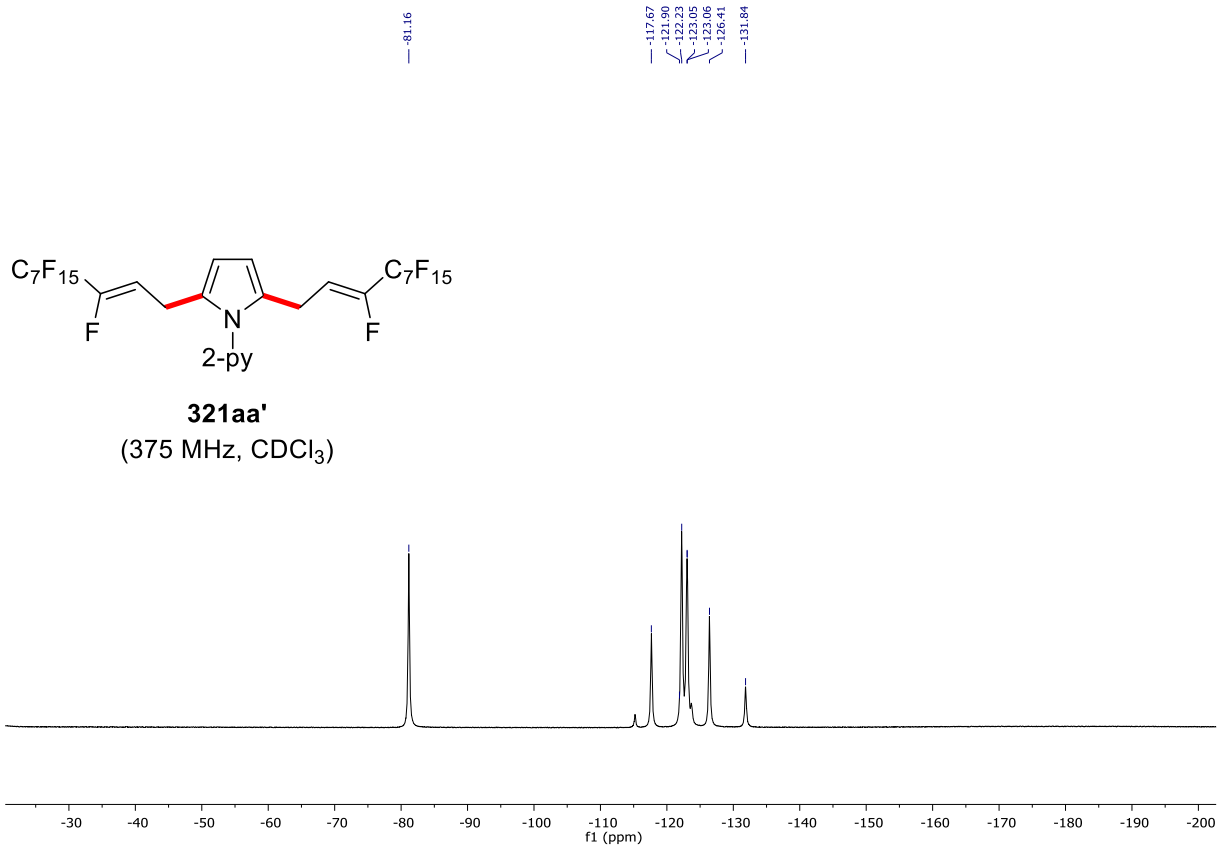


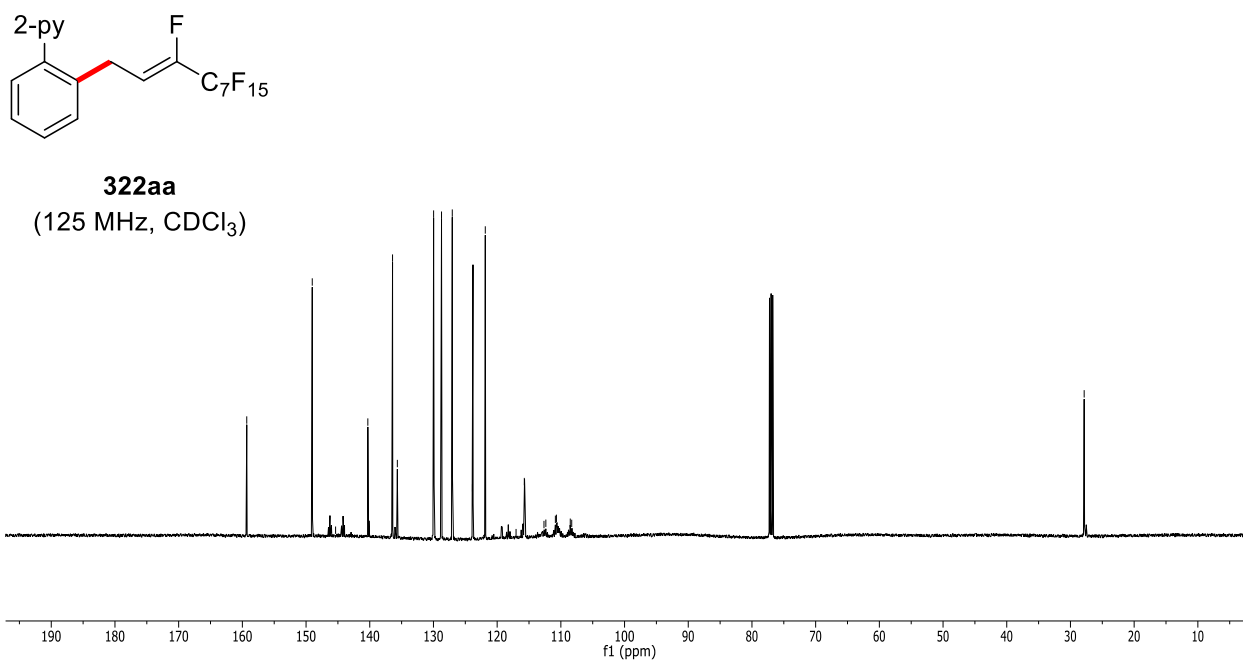
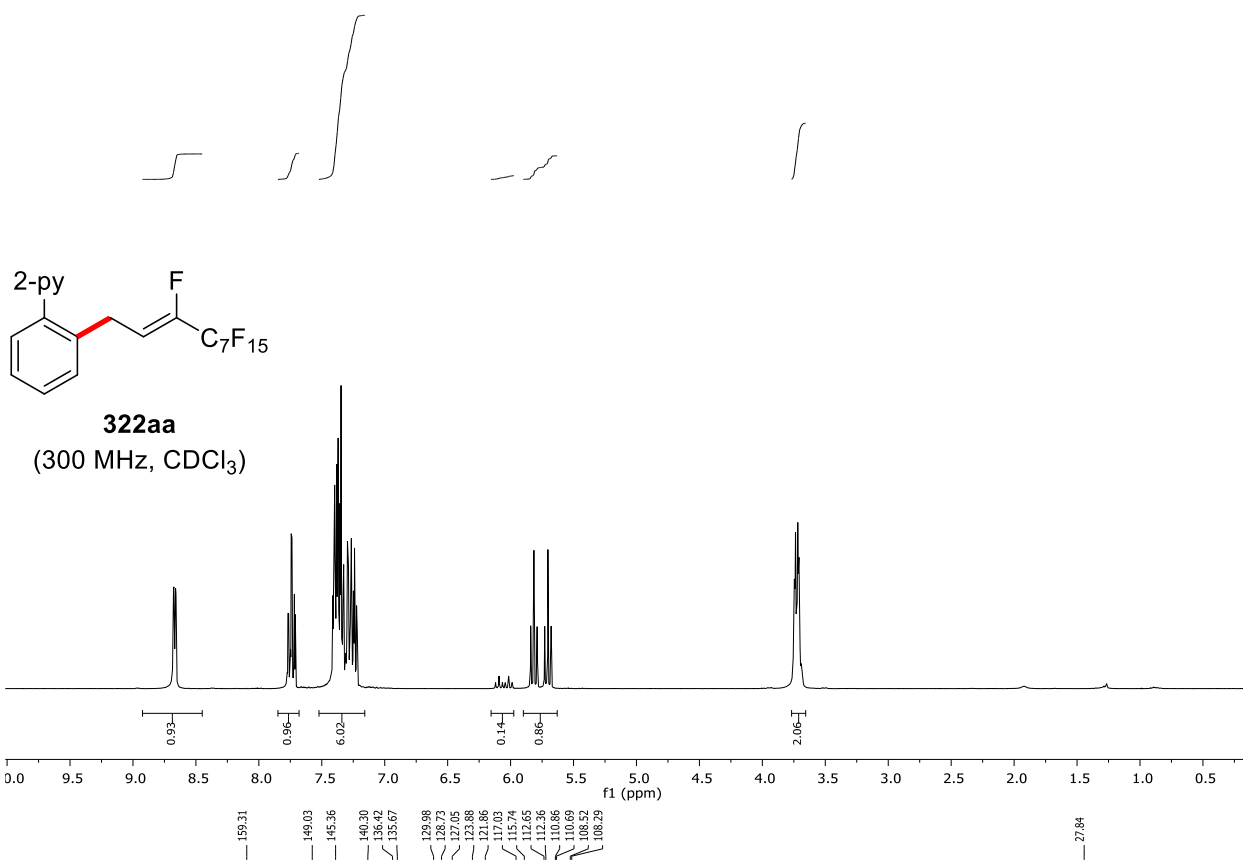


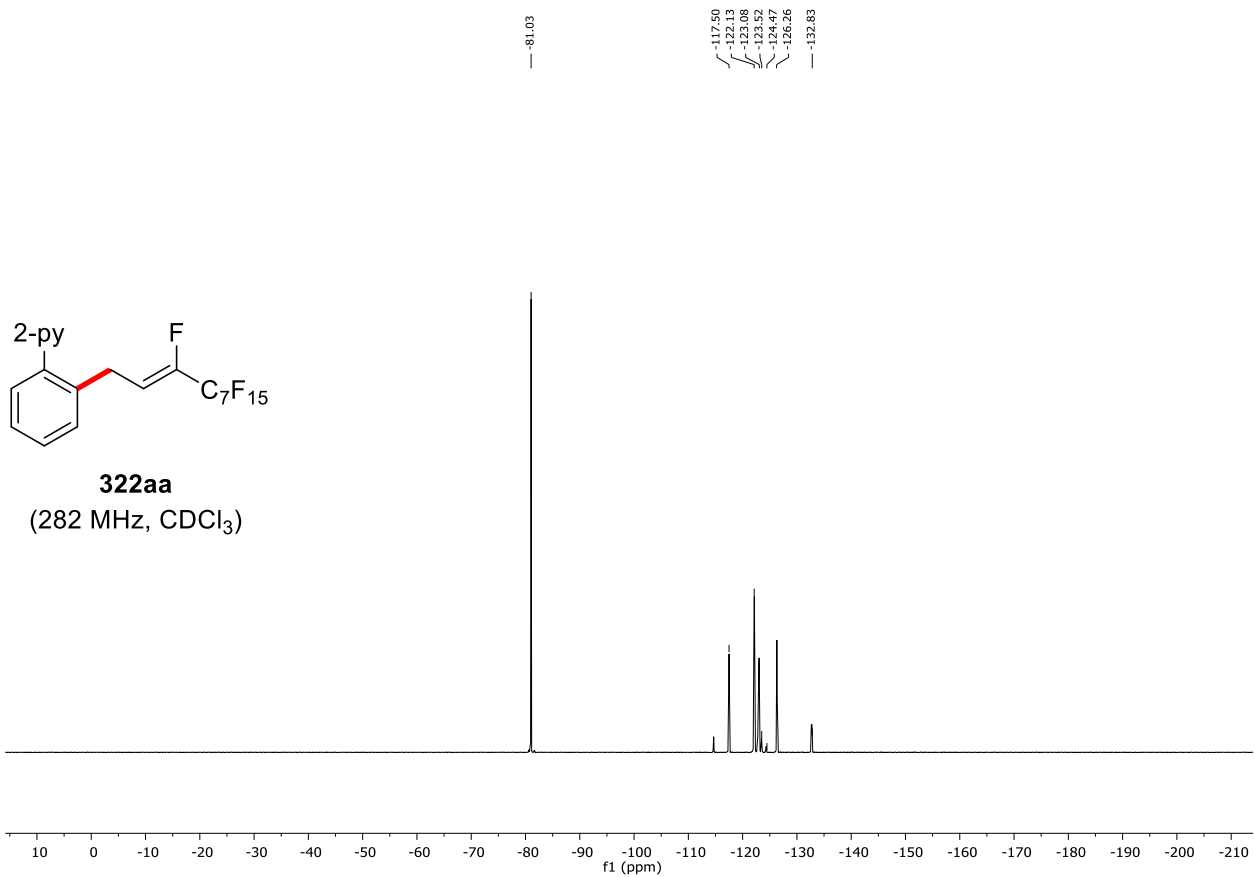


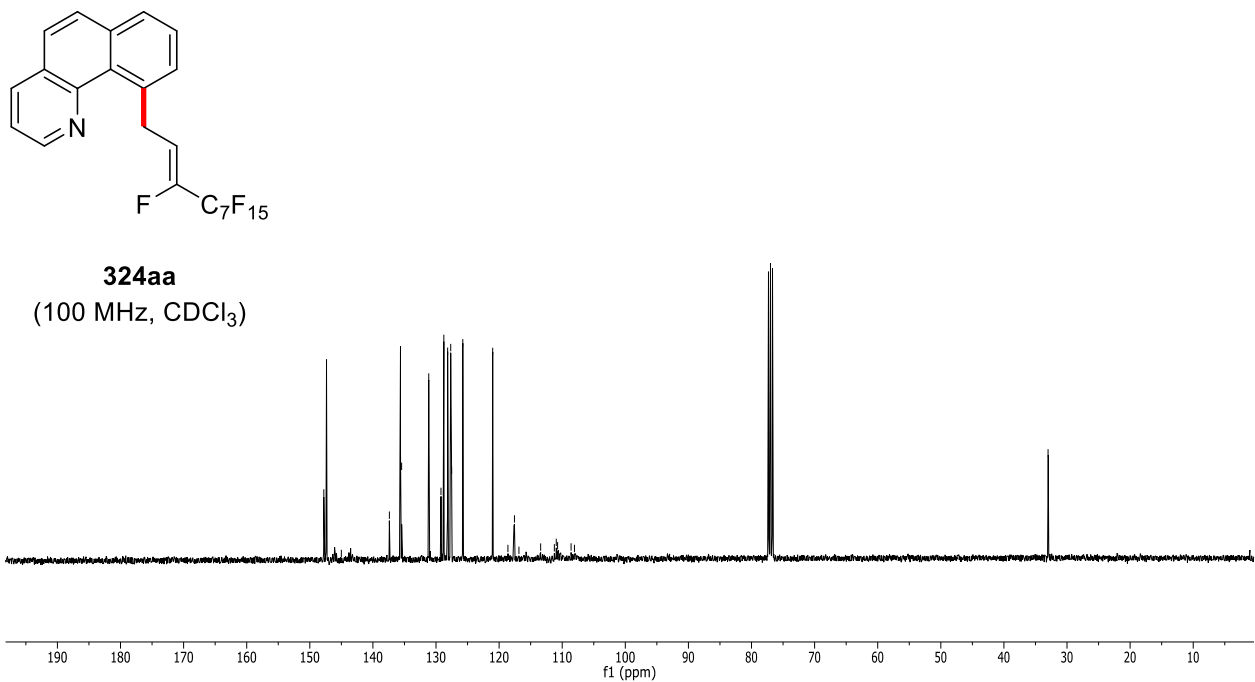
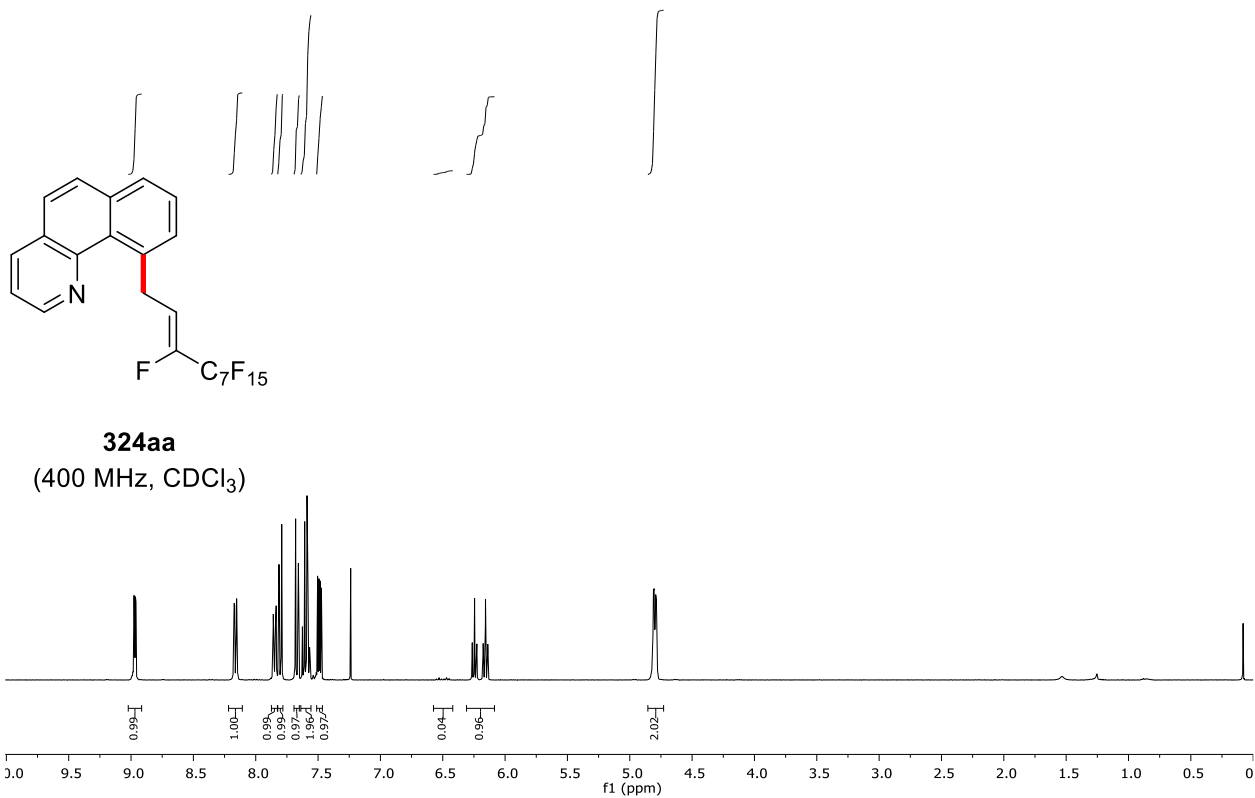


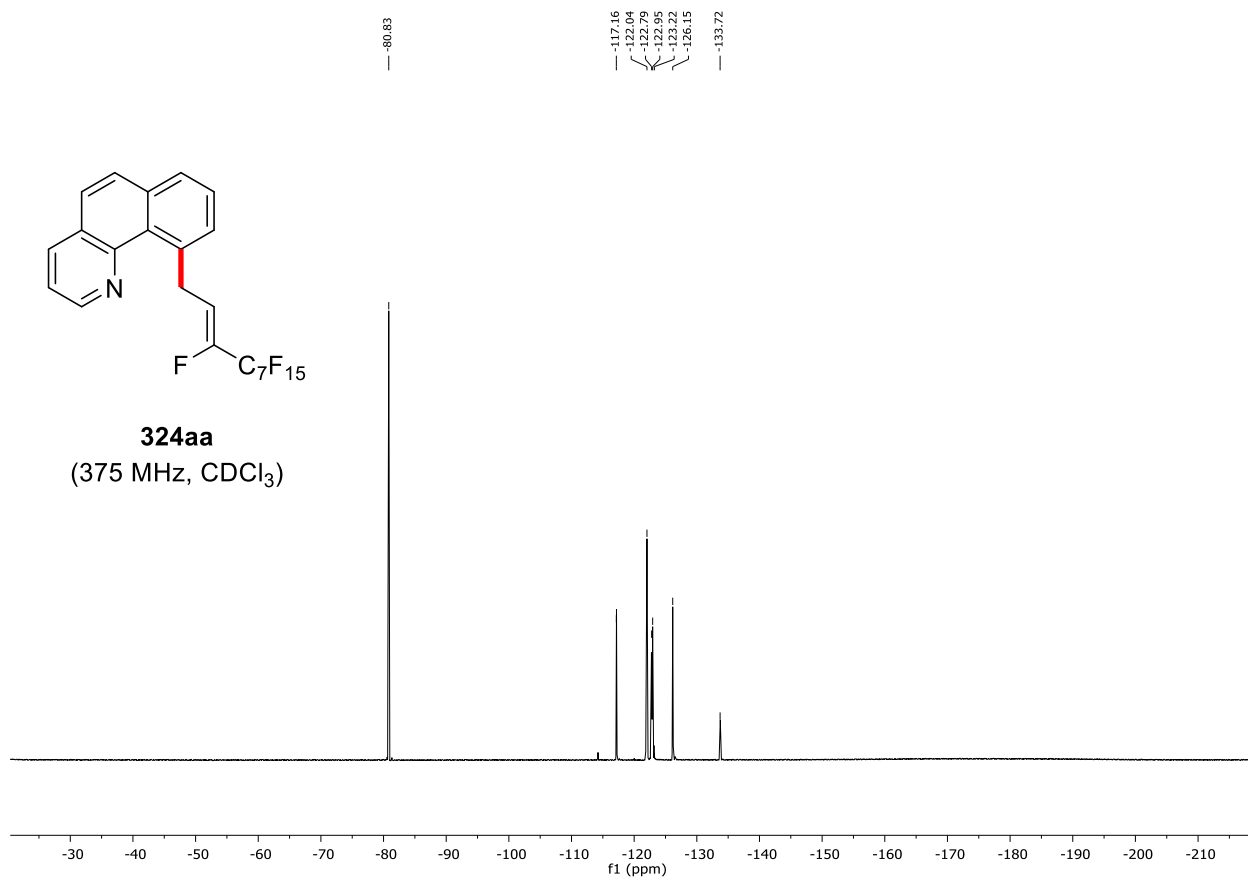


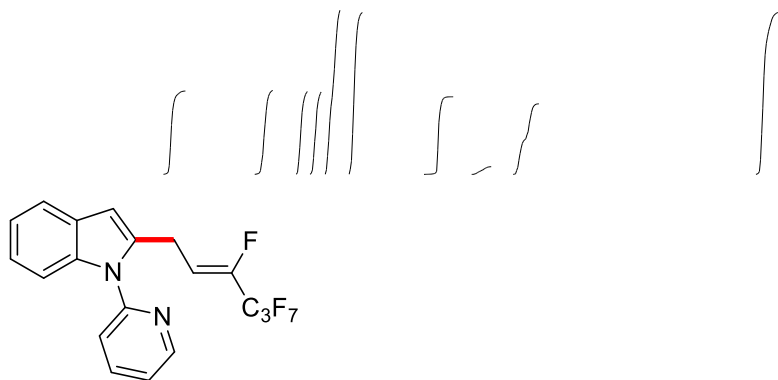




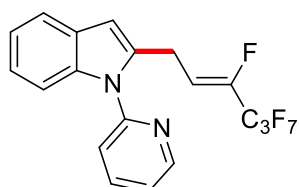
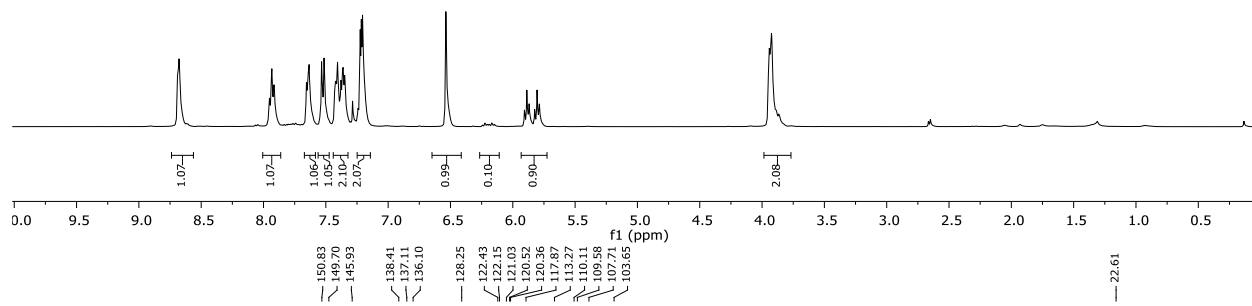




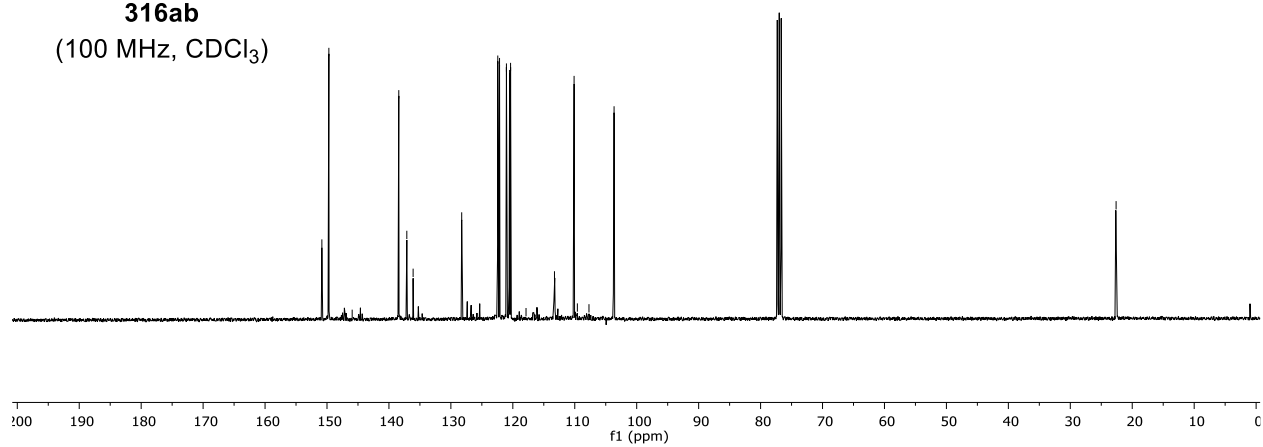


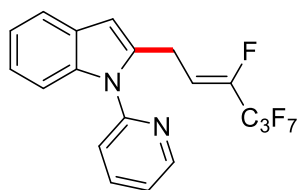


316ab
(400 MHz, CDCl₃)

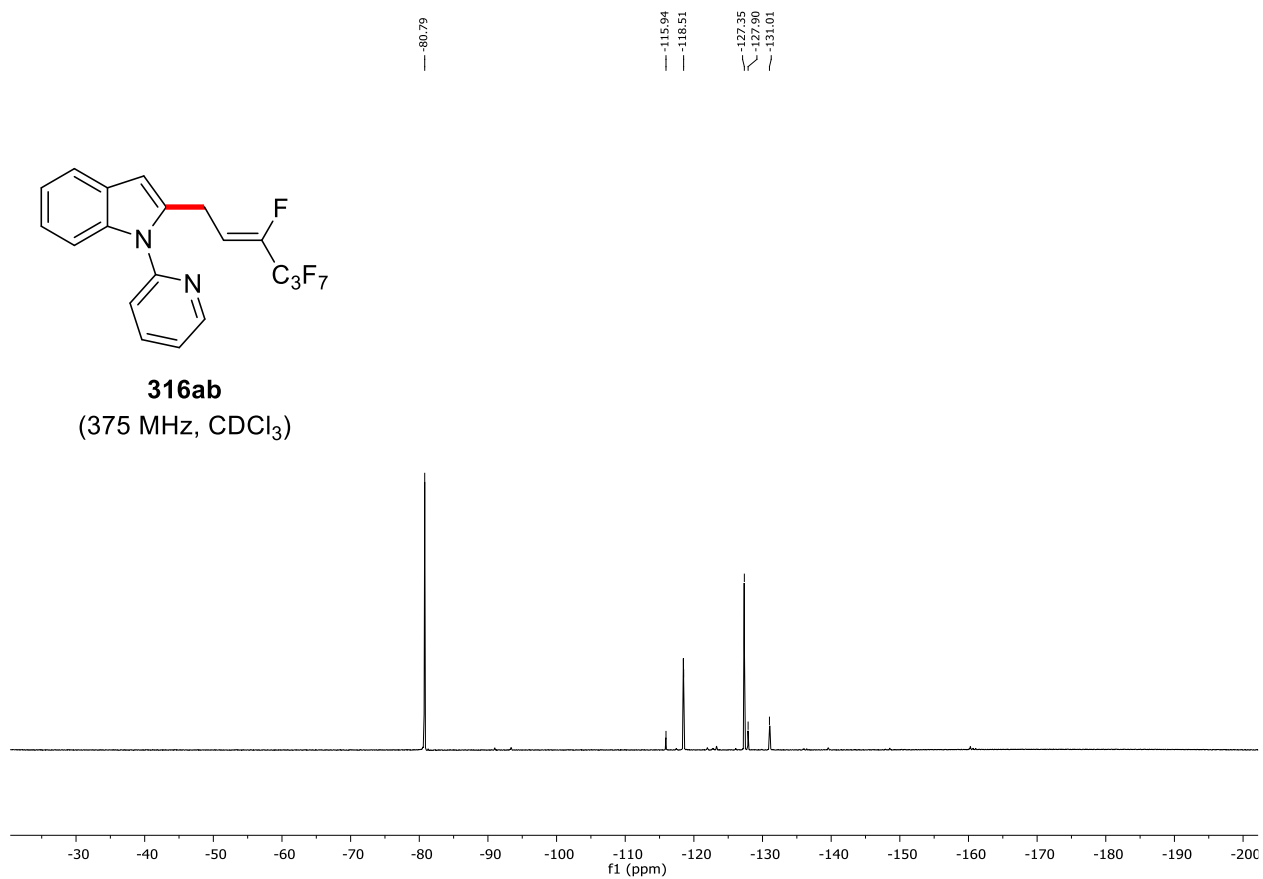


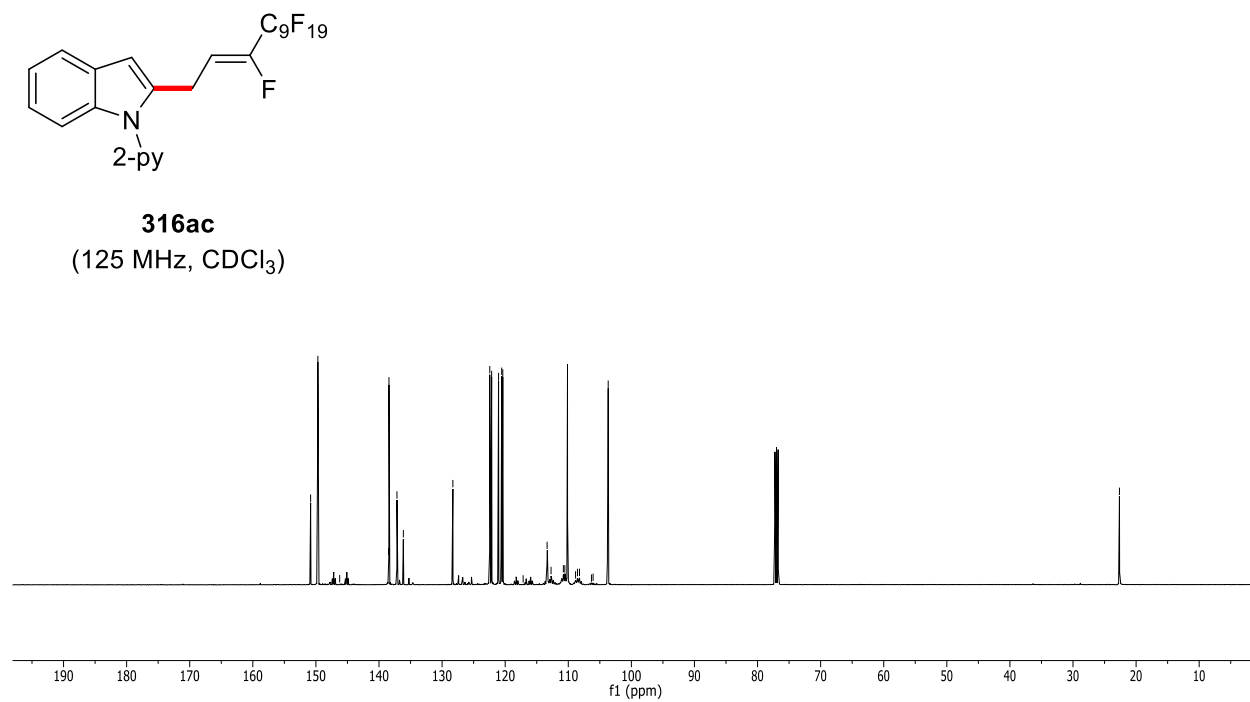
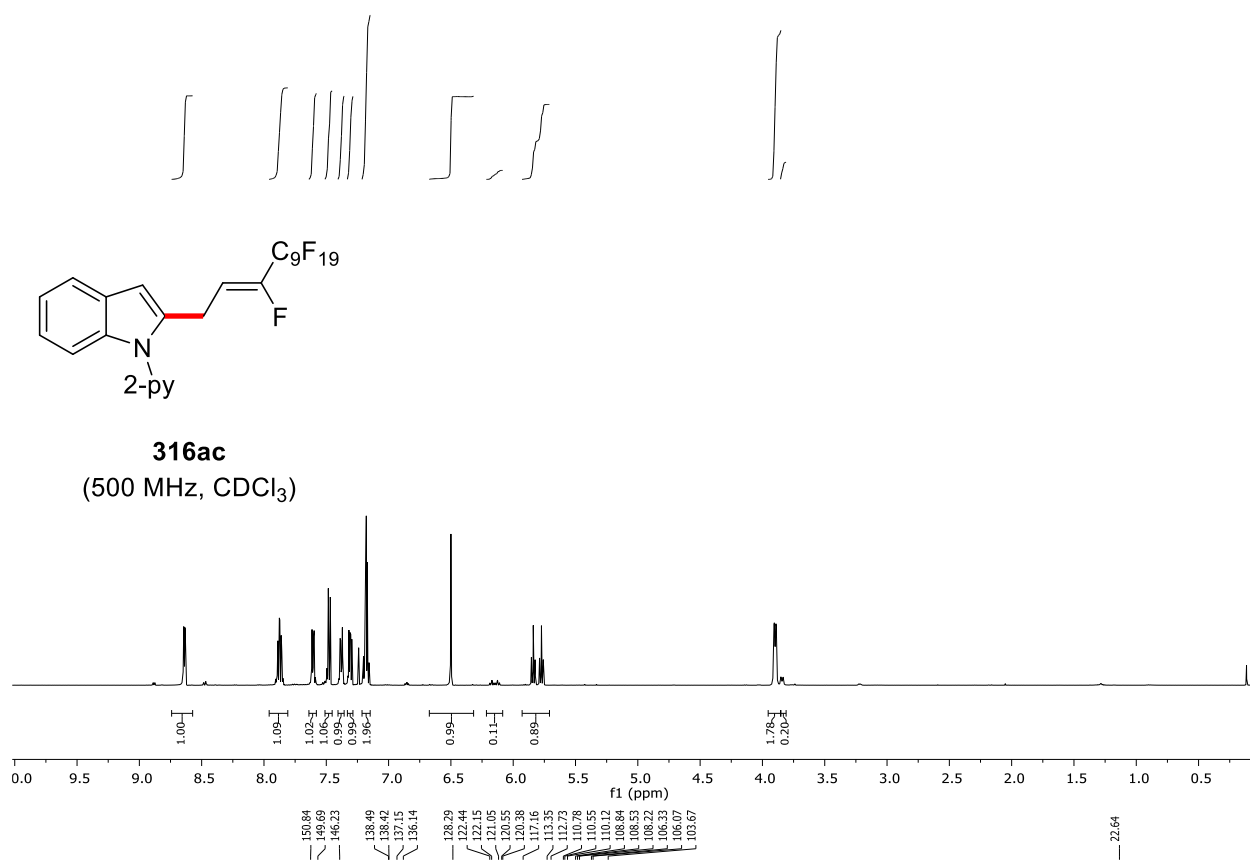
316ab
(100 MHz, CDCl₃)

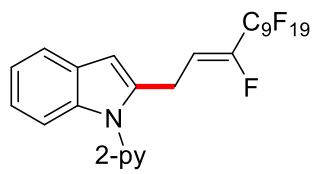




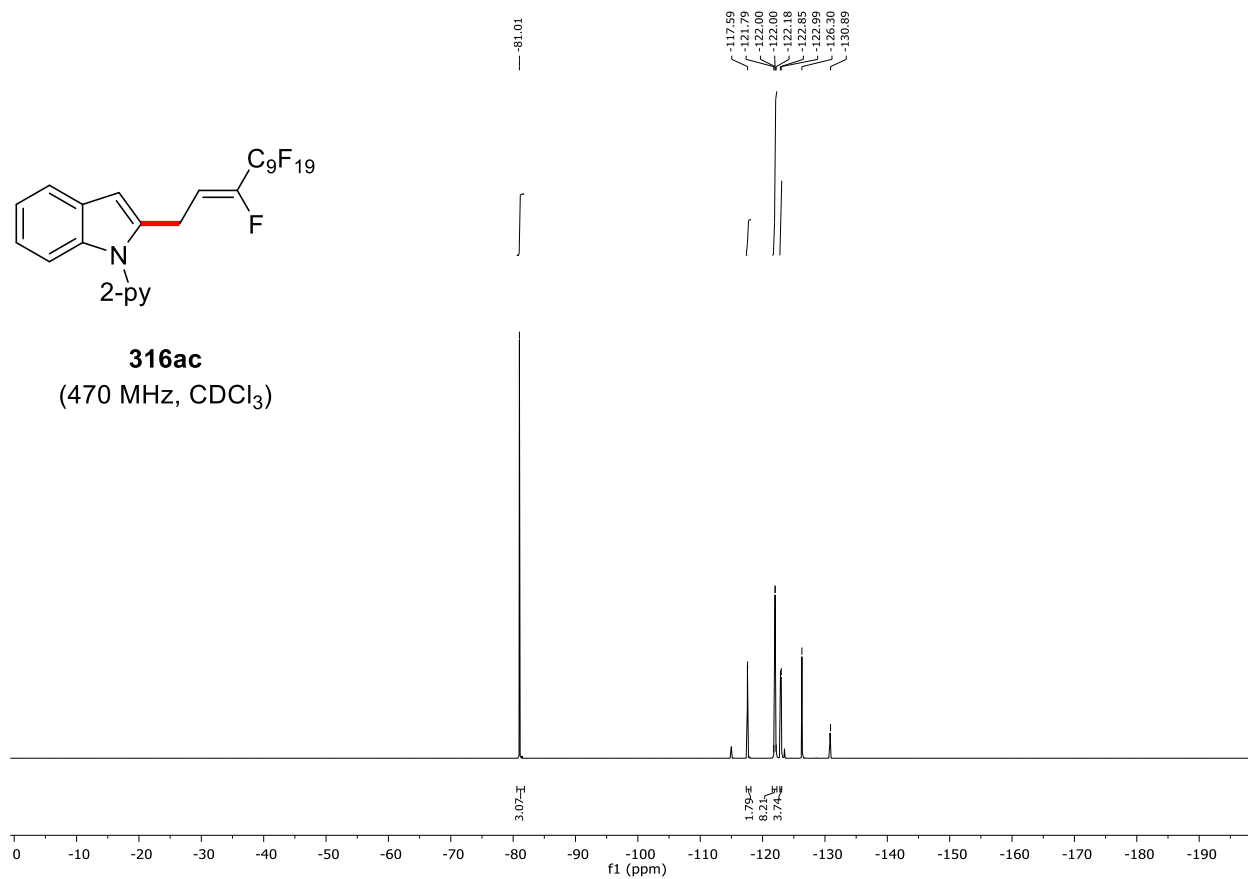
316ab
(375 MHz, CDCl₃)

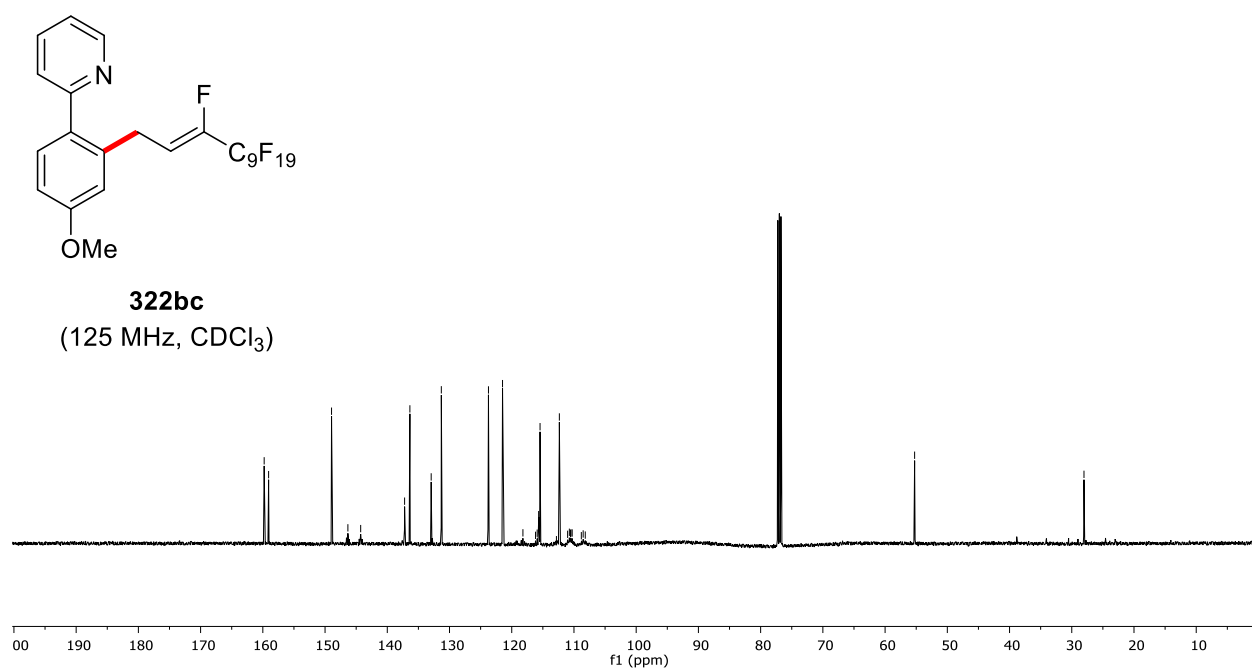
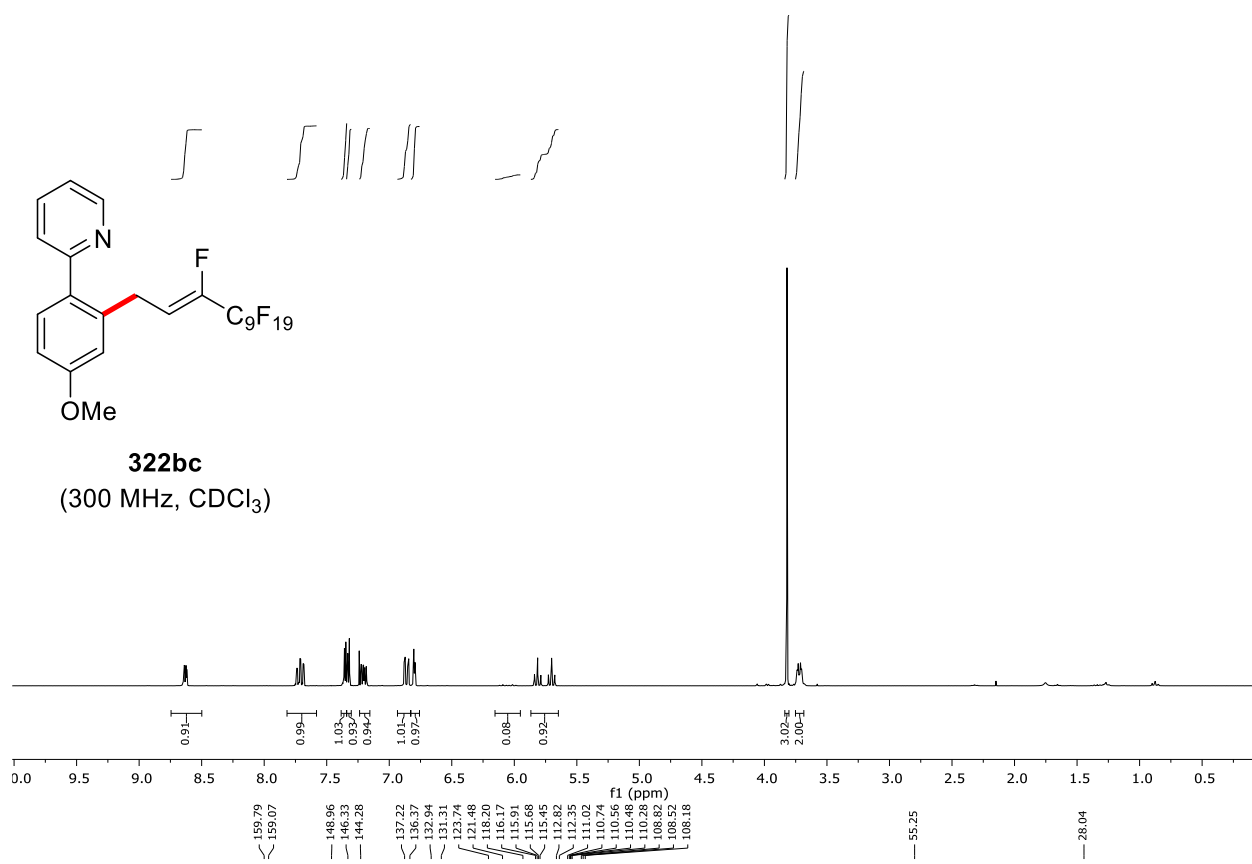


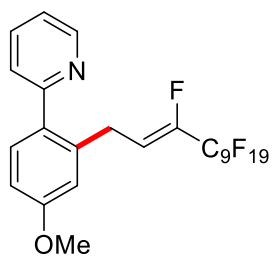




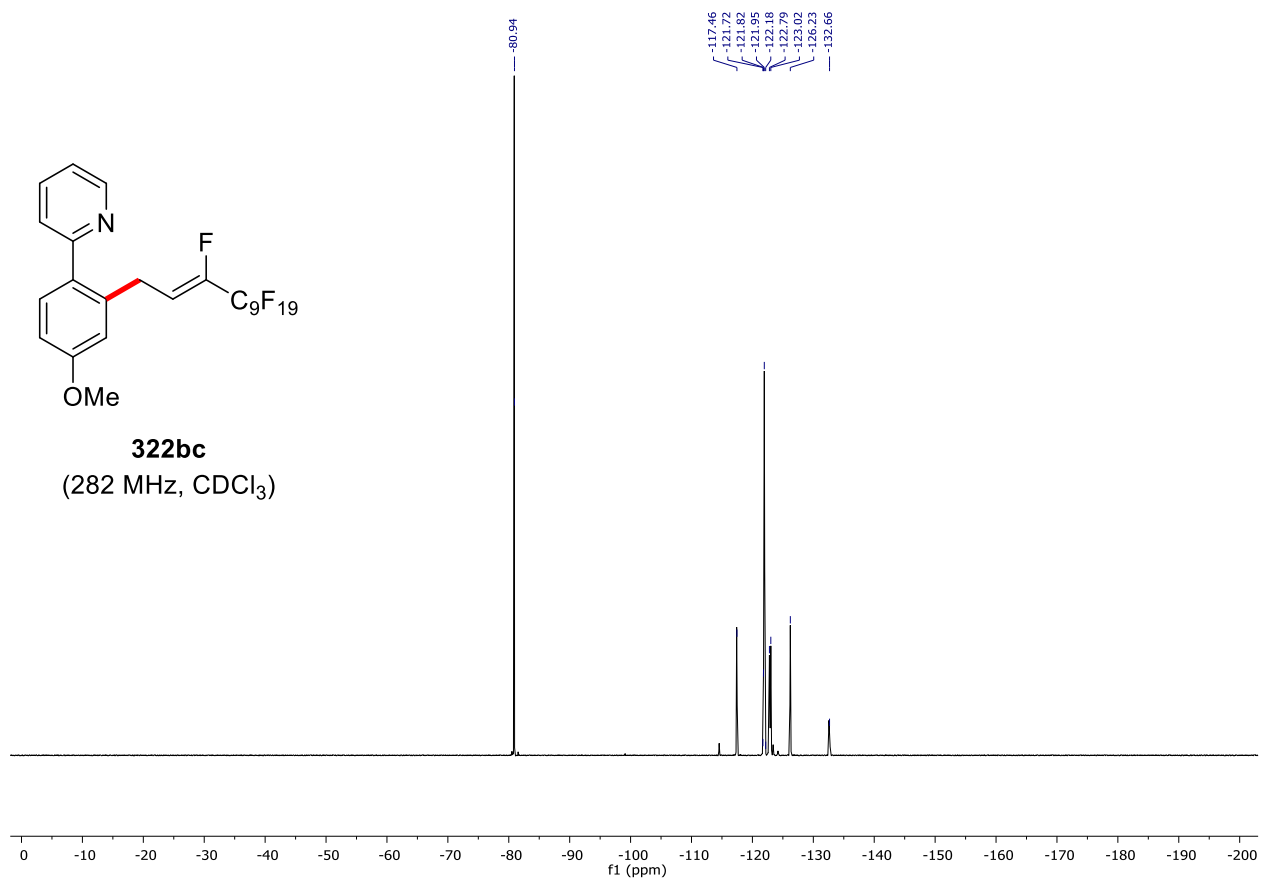
316ac
(470 MHz, CDCl₃)

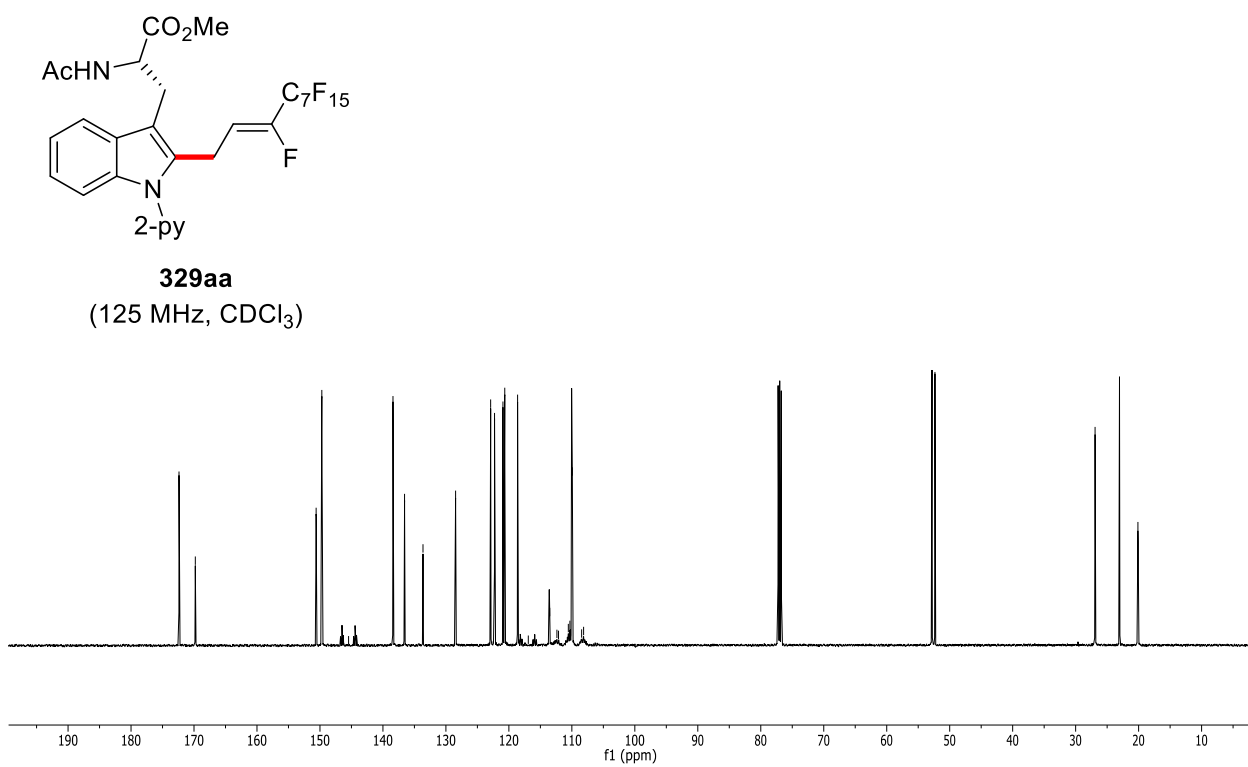
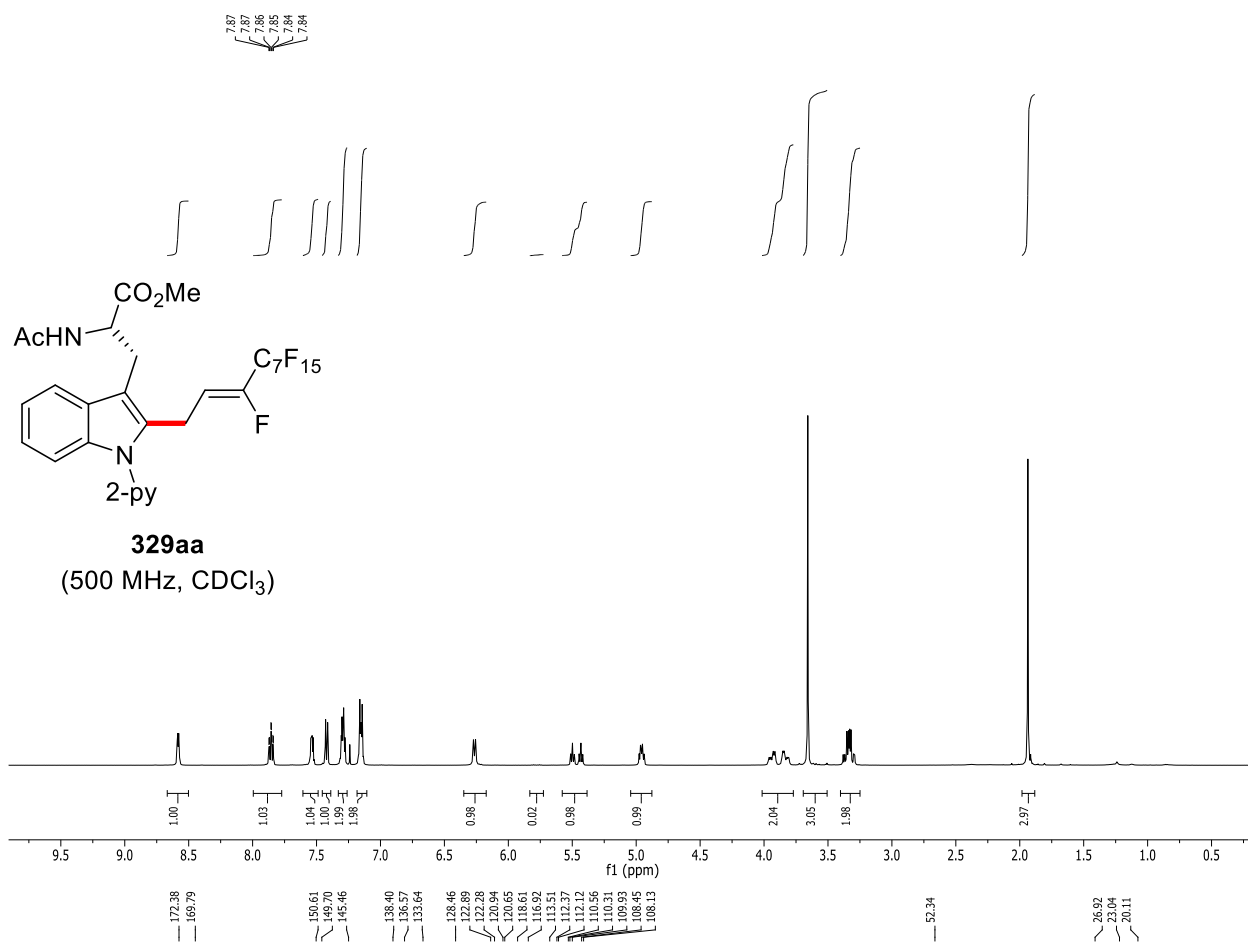


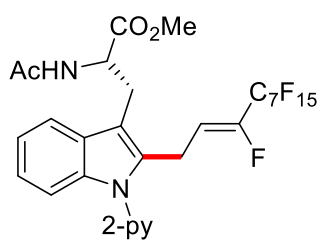




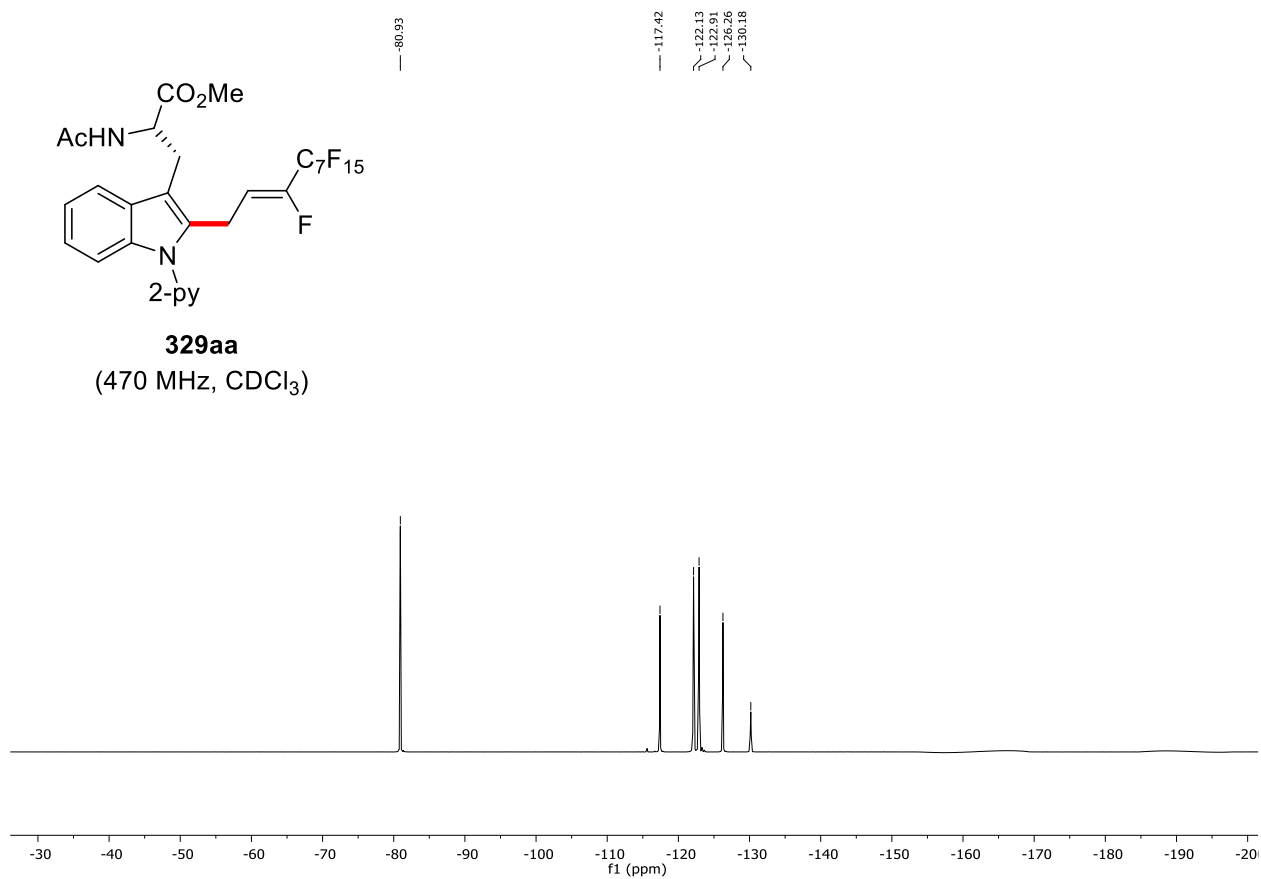
322bc
(282 MHz, CDCl₃)

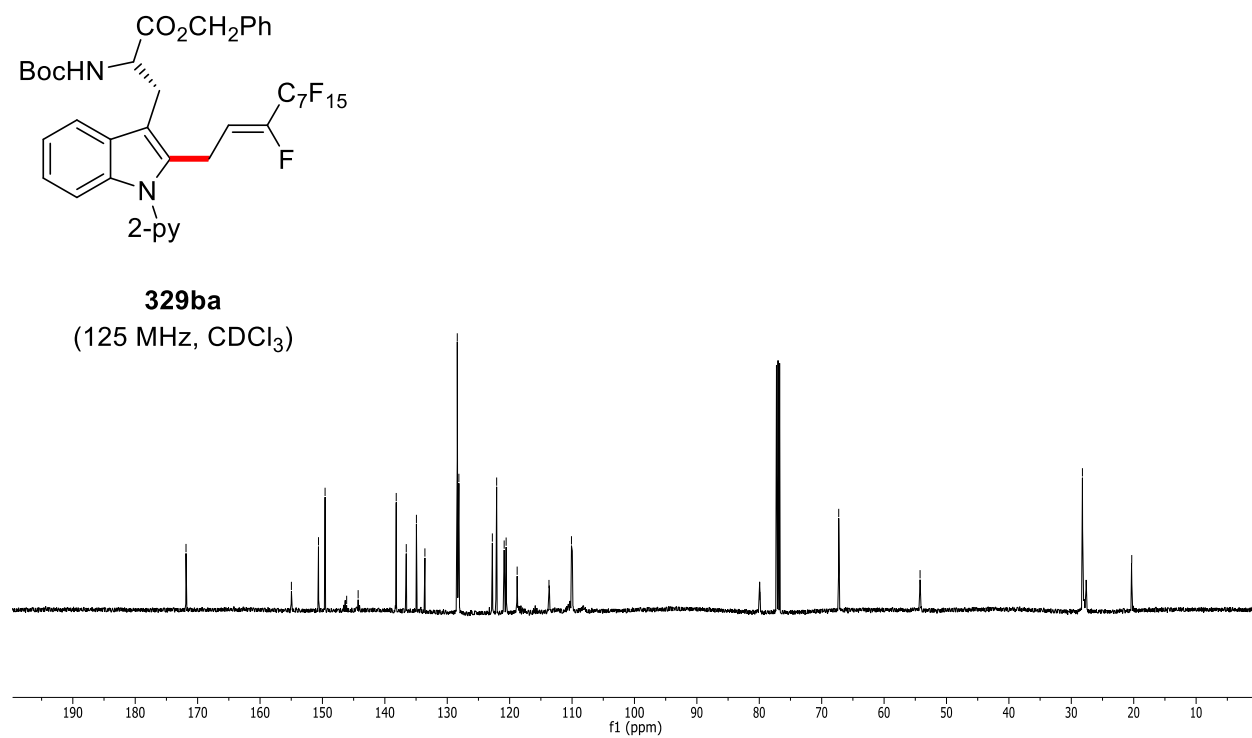
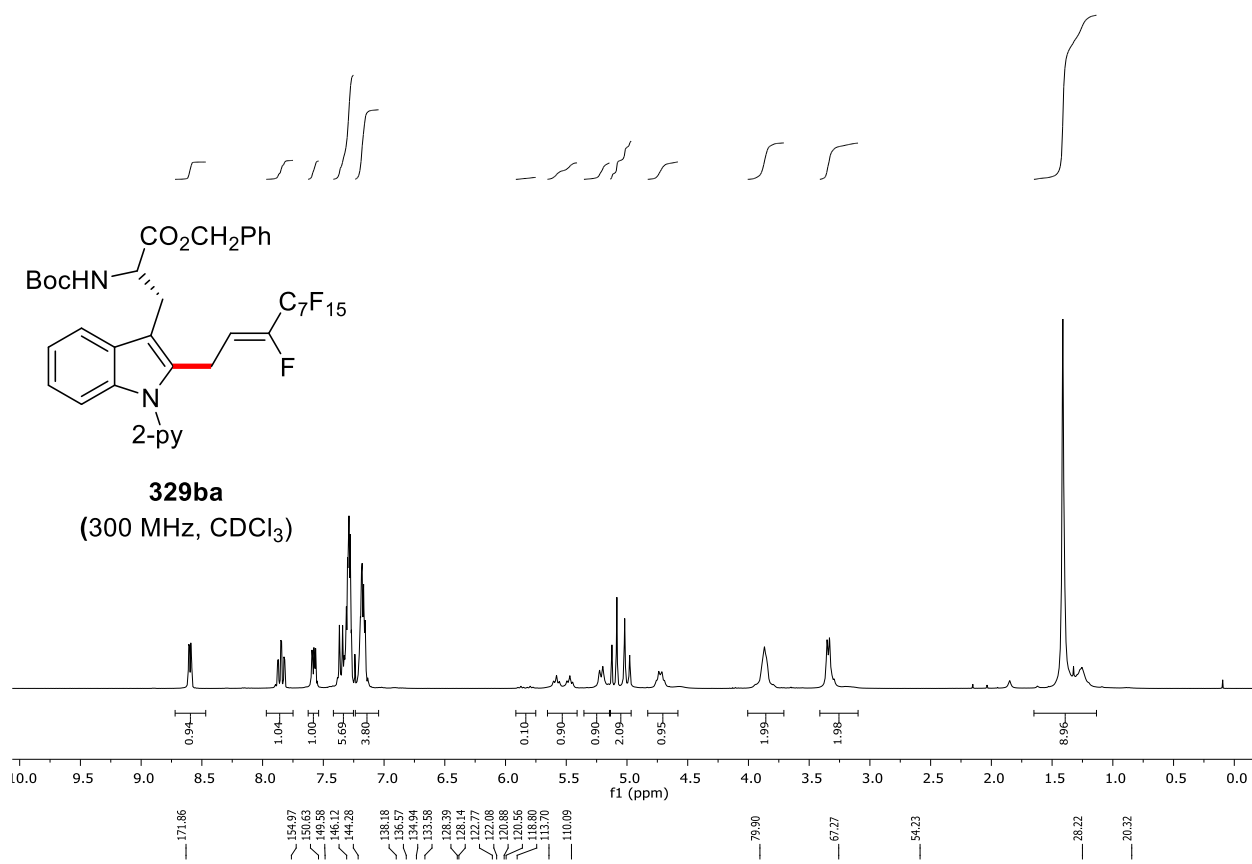


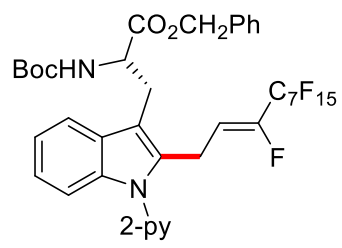




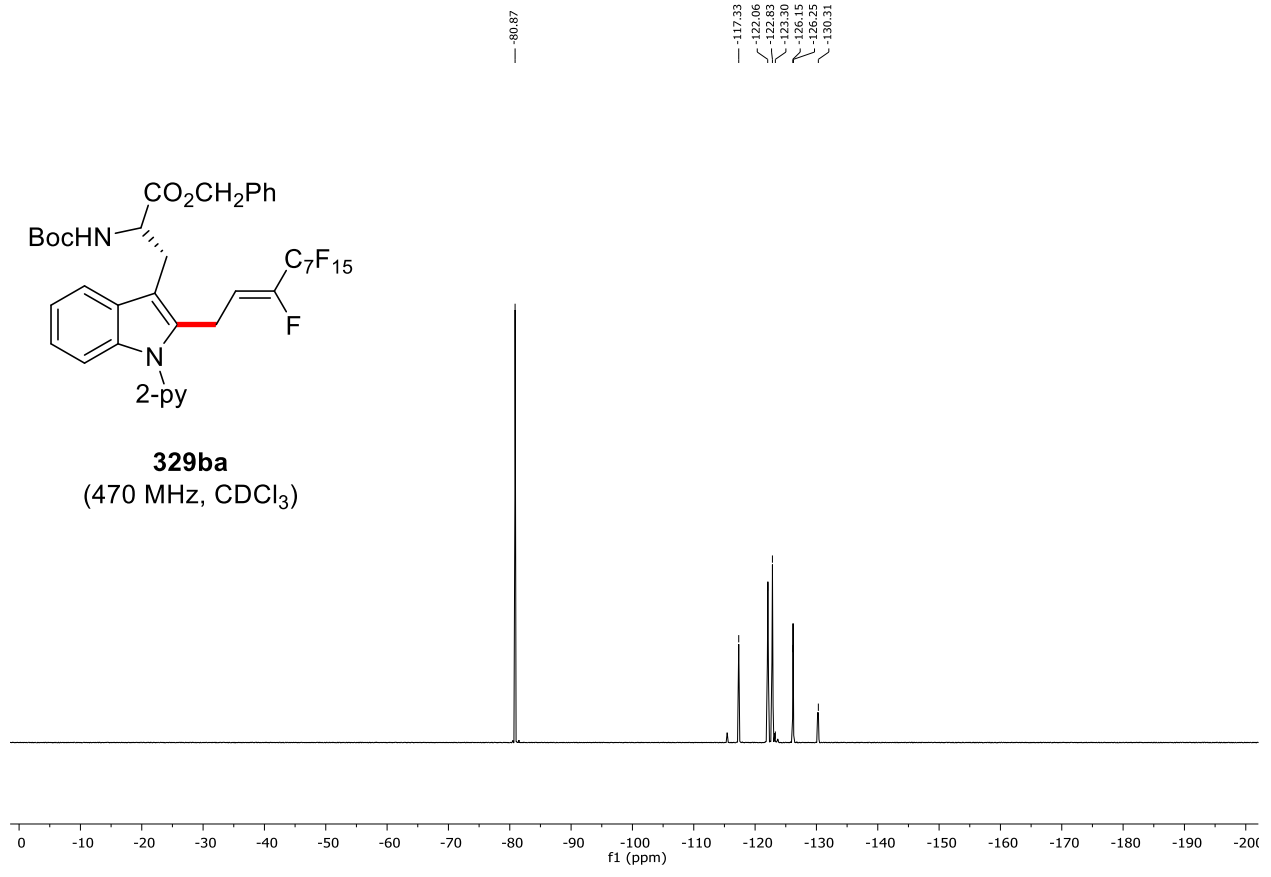
329aa
(470 MHz, CDCl₃)

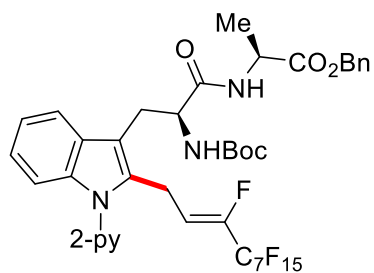




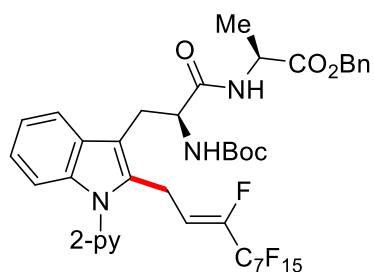
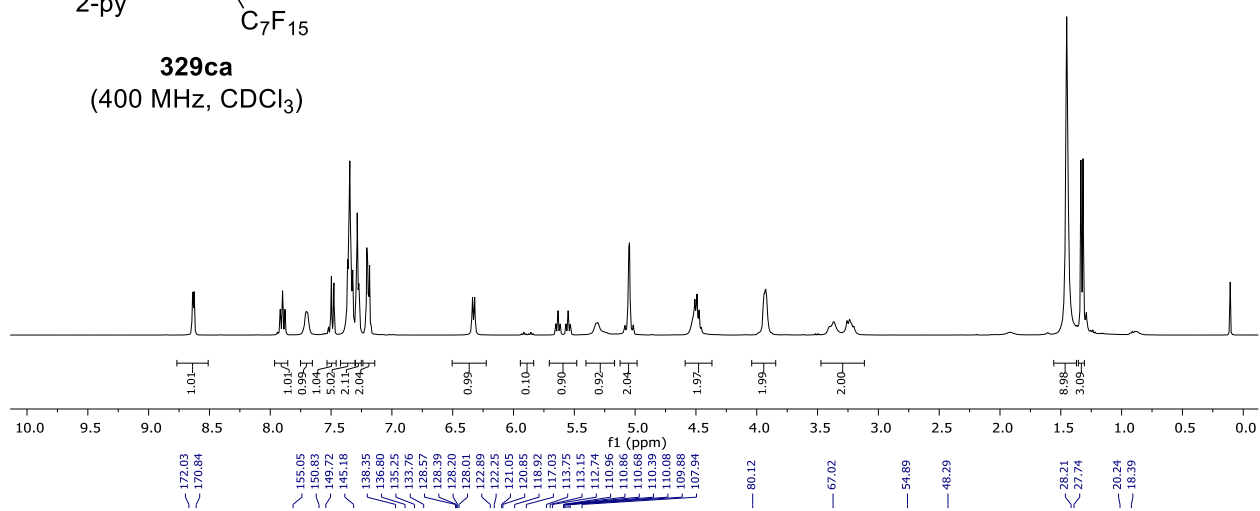


329ba
(470 MHz, CDCl₃)

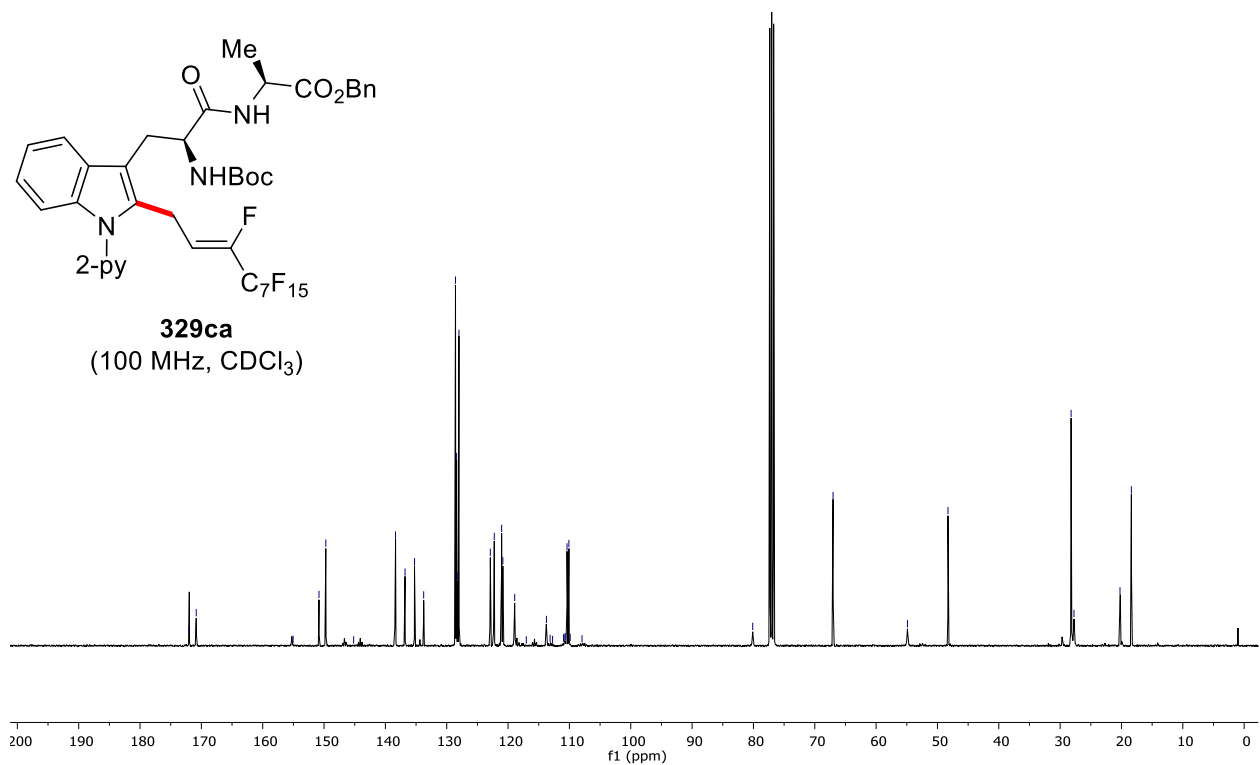


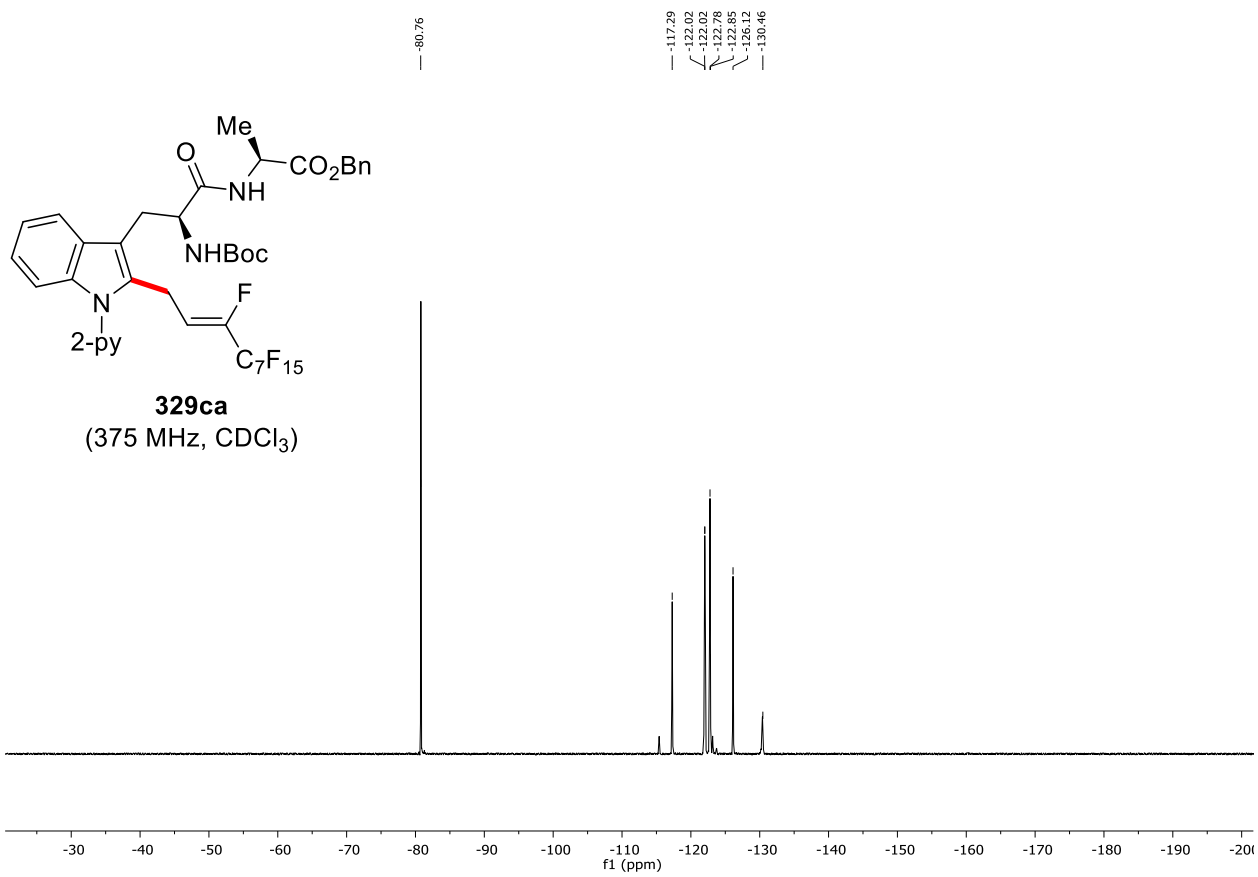


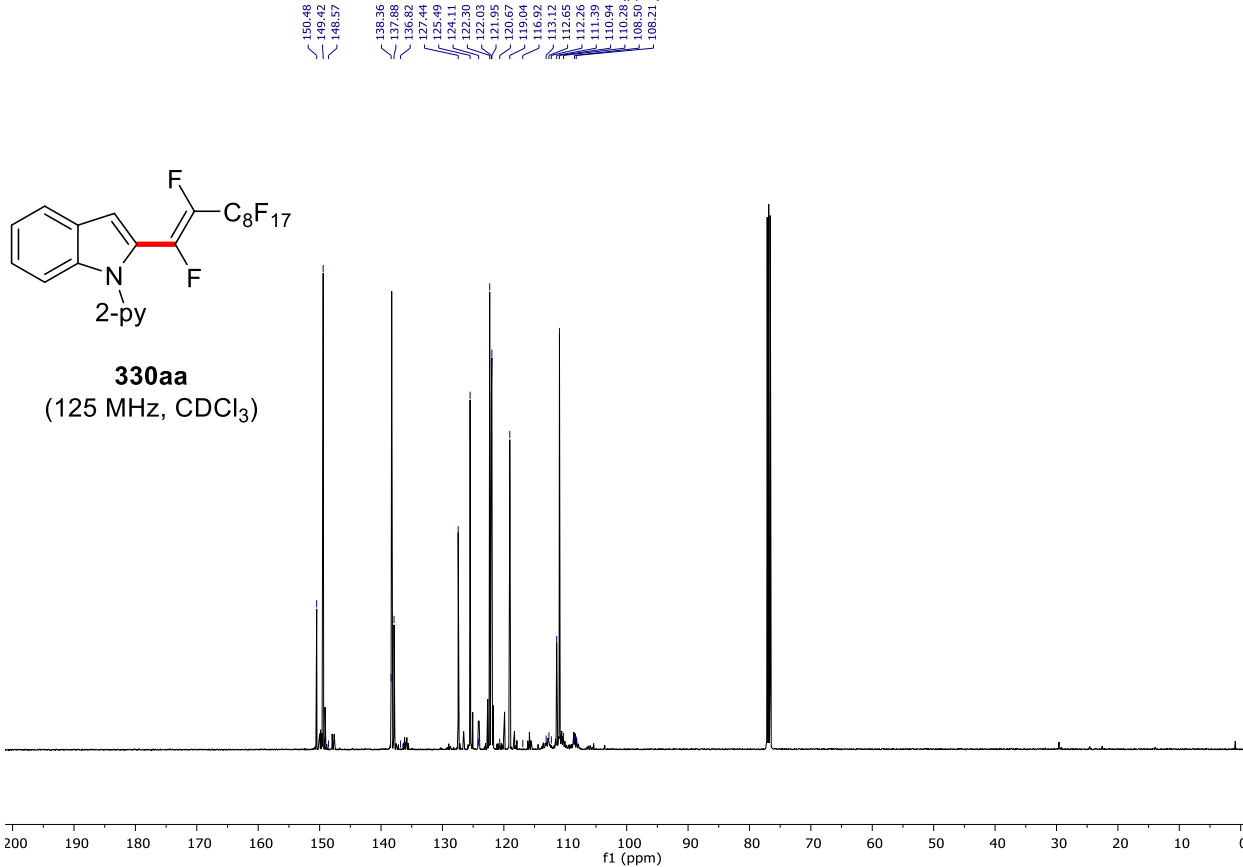
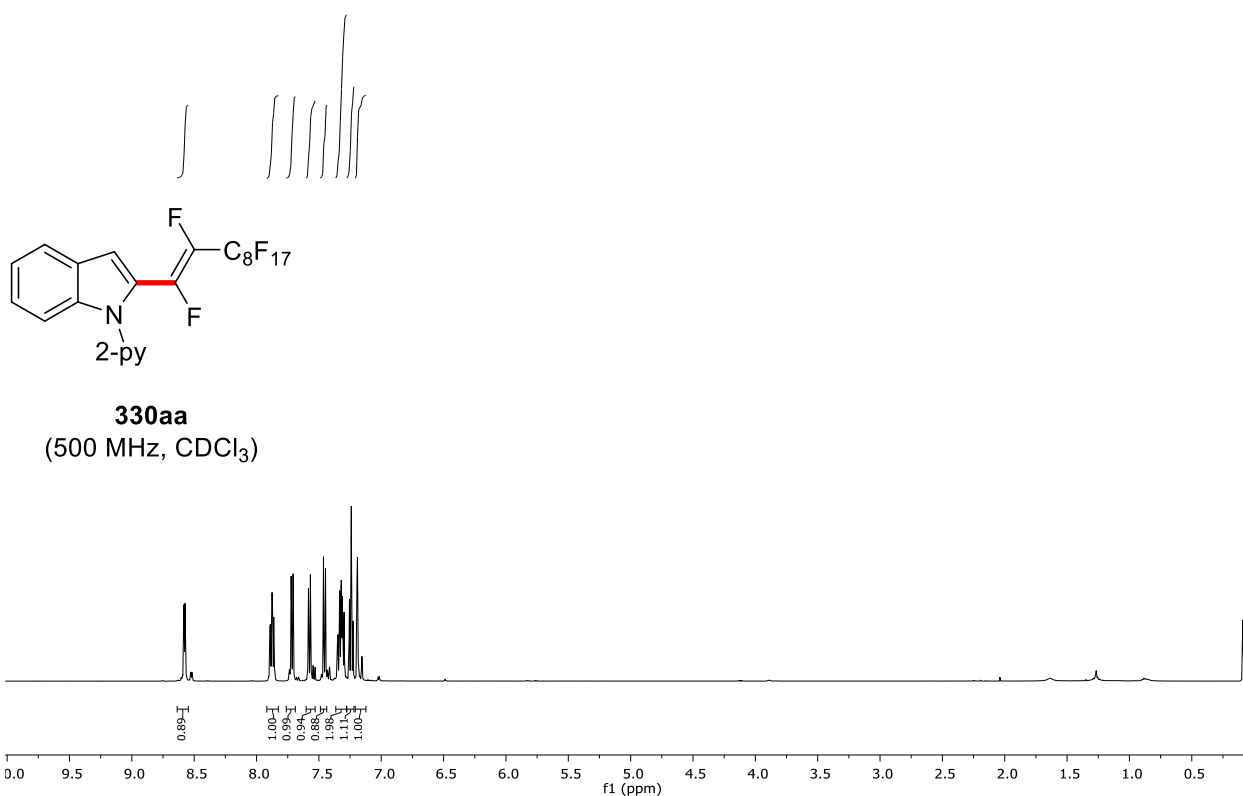
329ca
(400 MHz, CDCl₃)

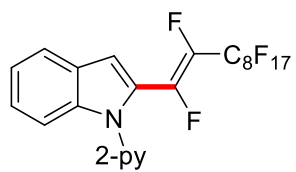


329ca
(100 MHz, CDCl₃)

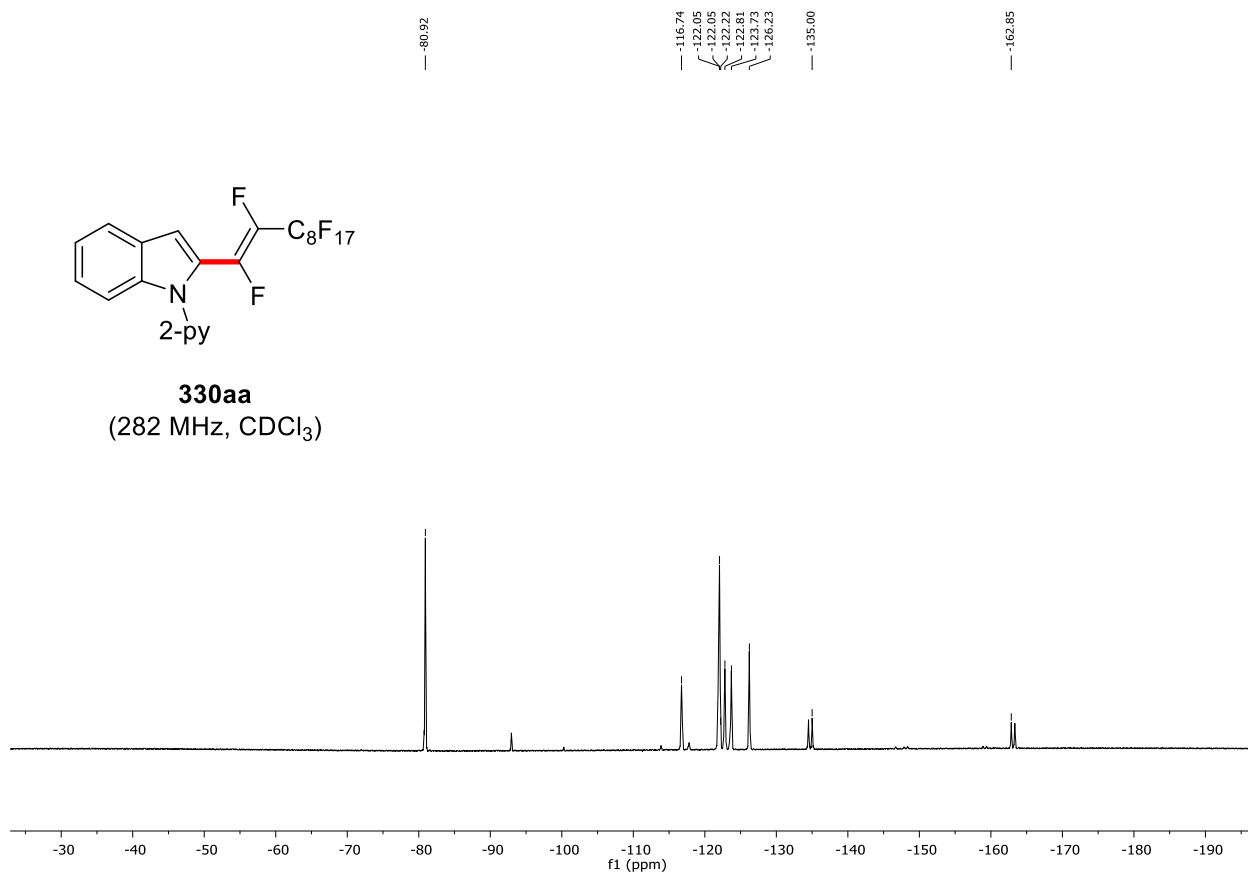


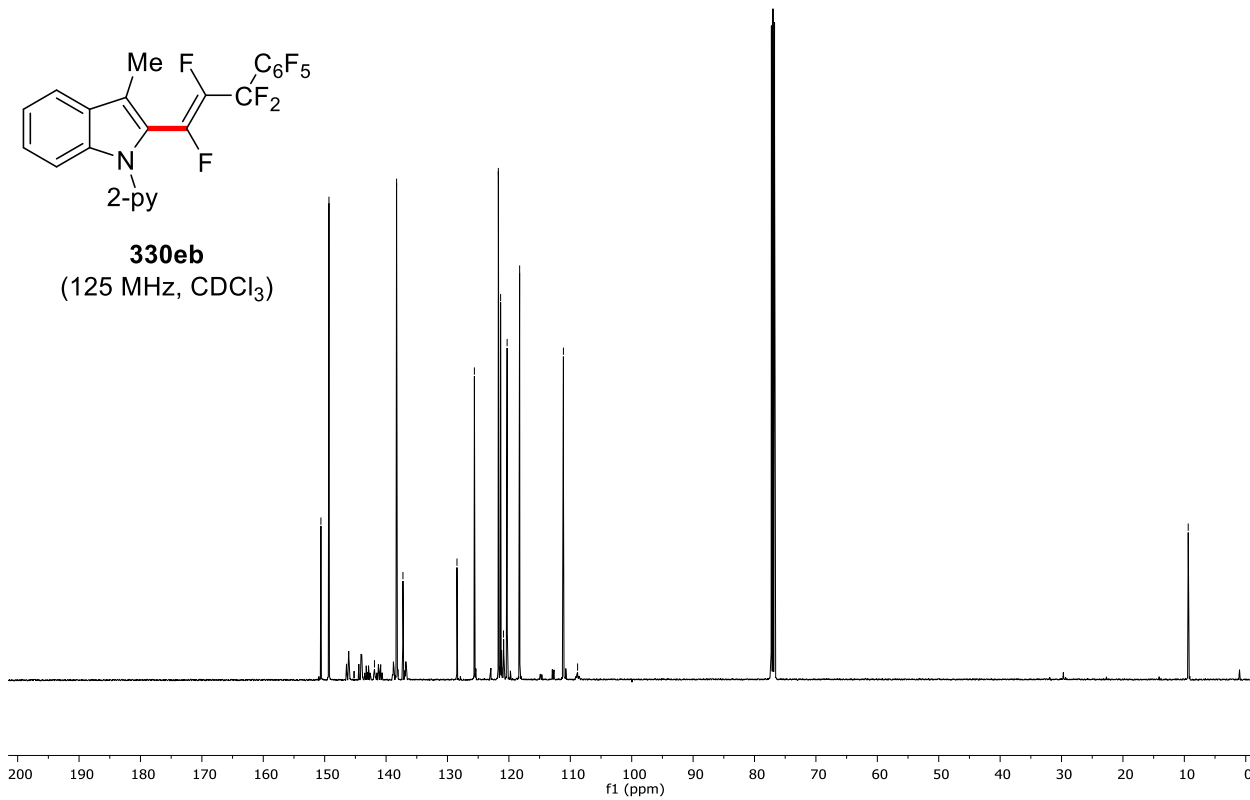
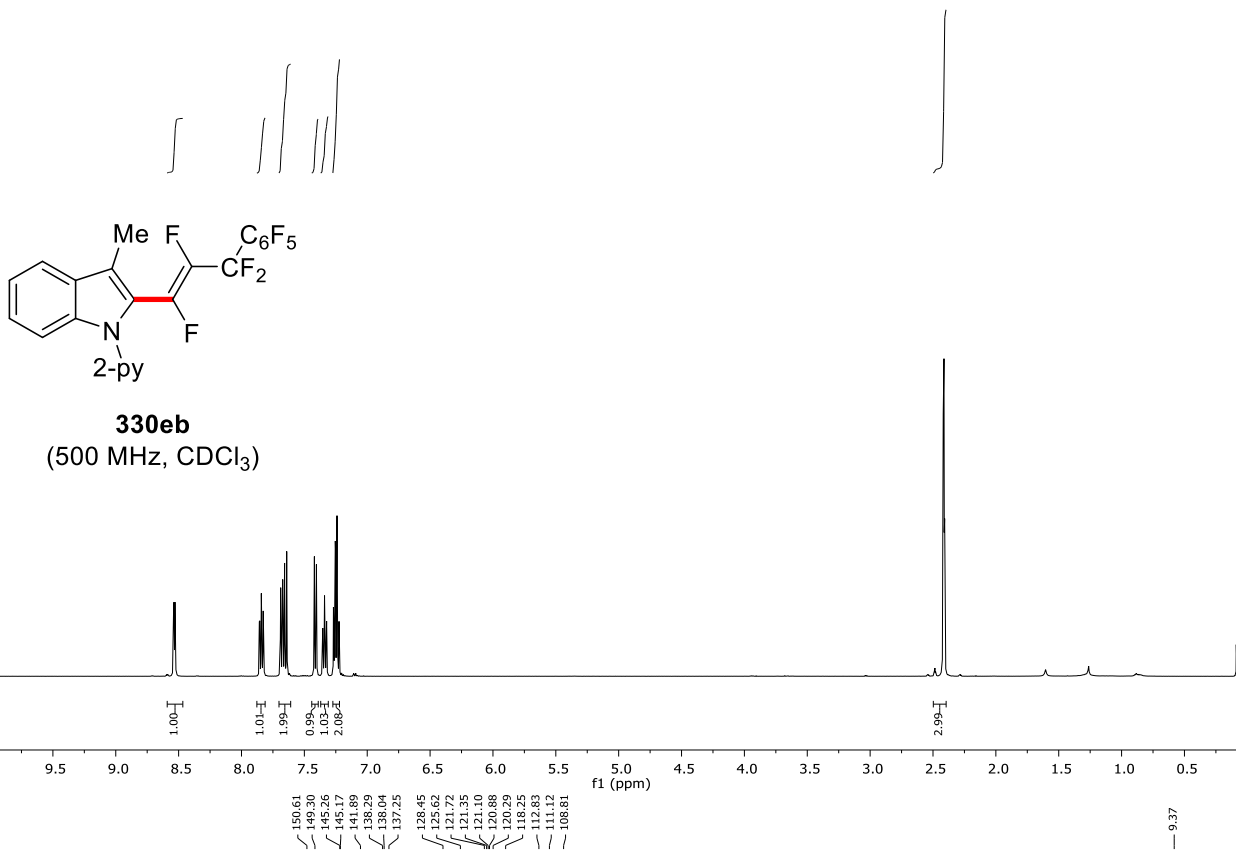


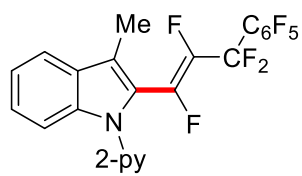




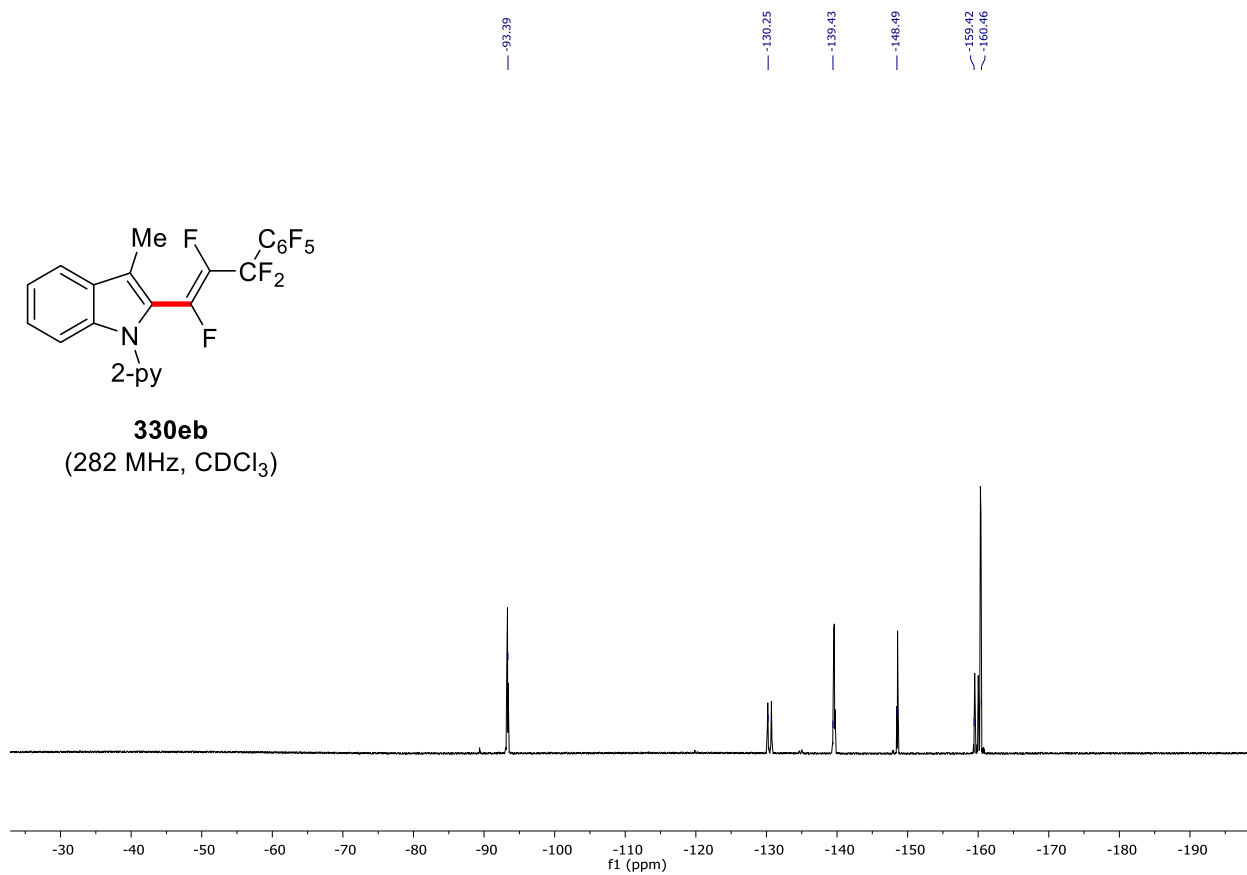
330aa
(282 MHz, CDCl₃)

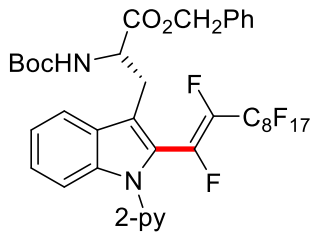




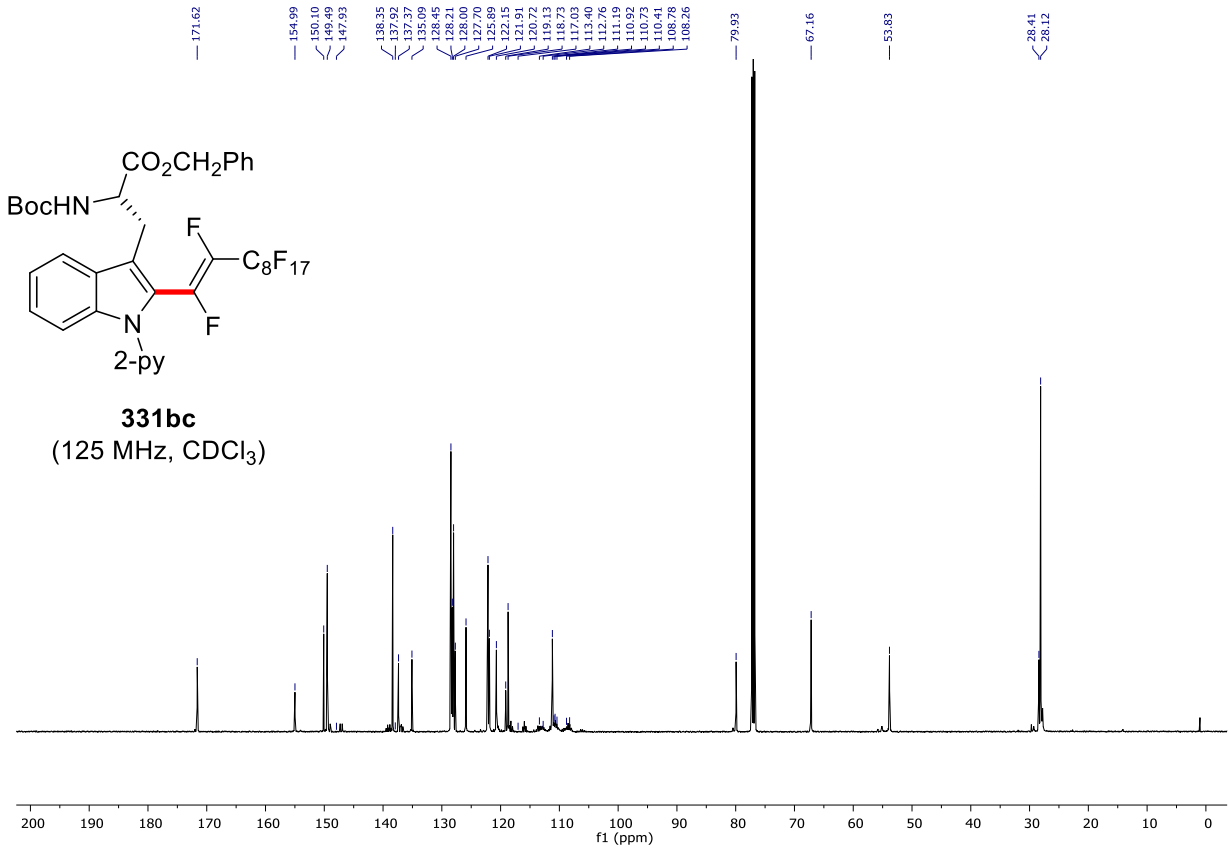
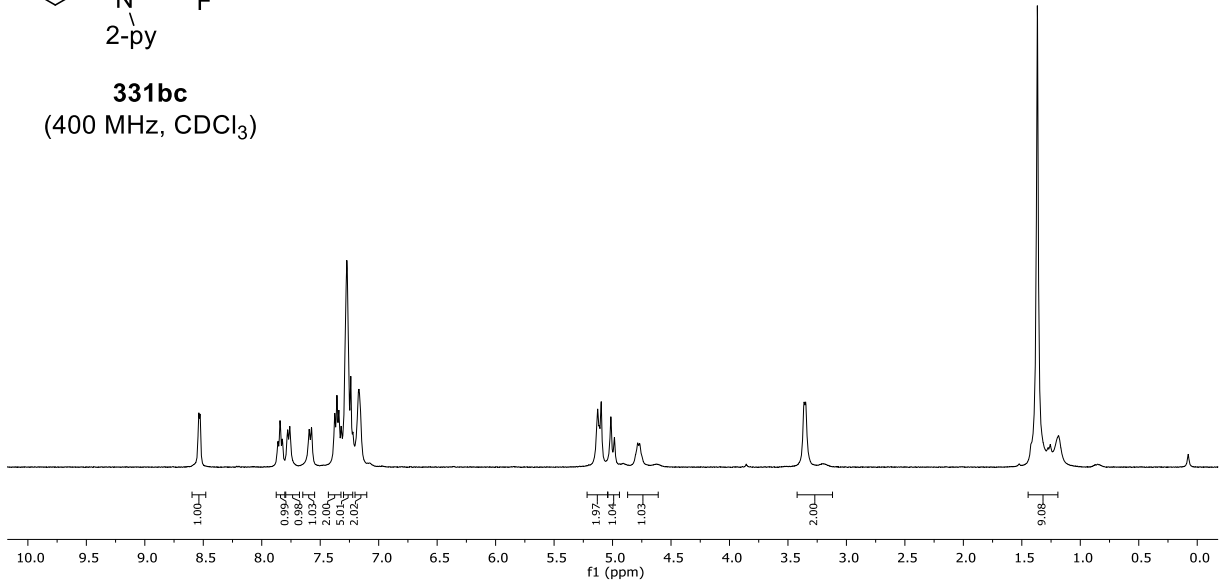


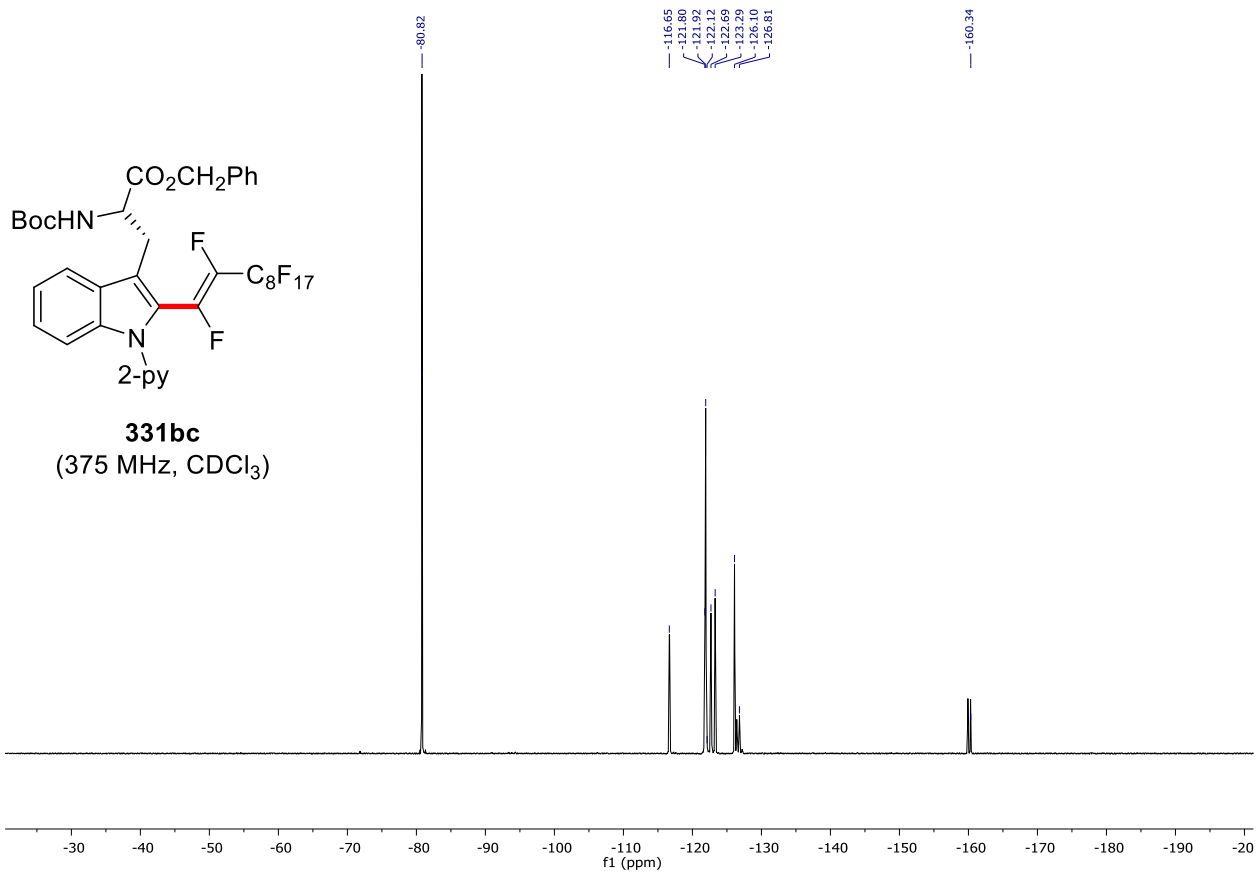
330eb
(282 MHz, CDCl₃)

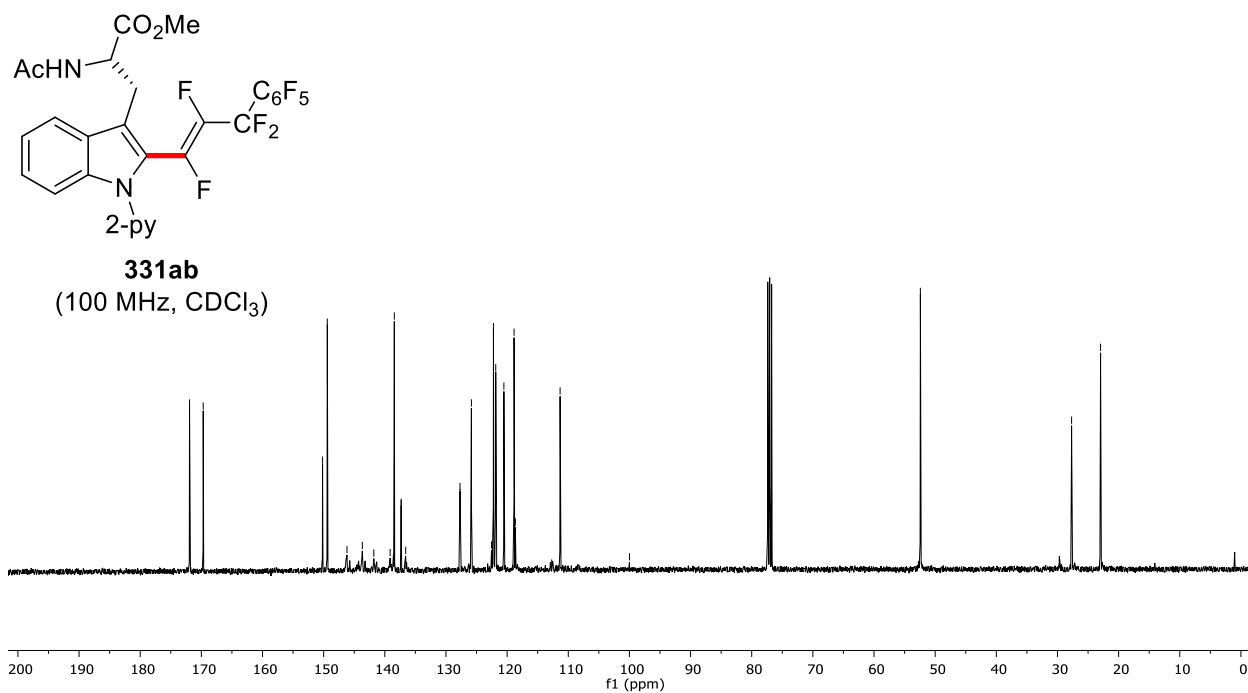
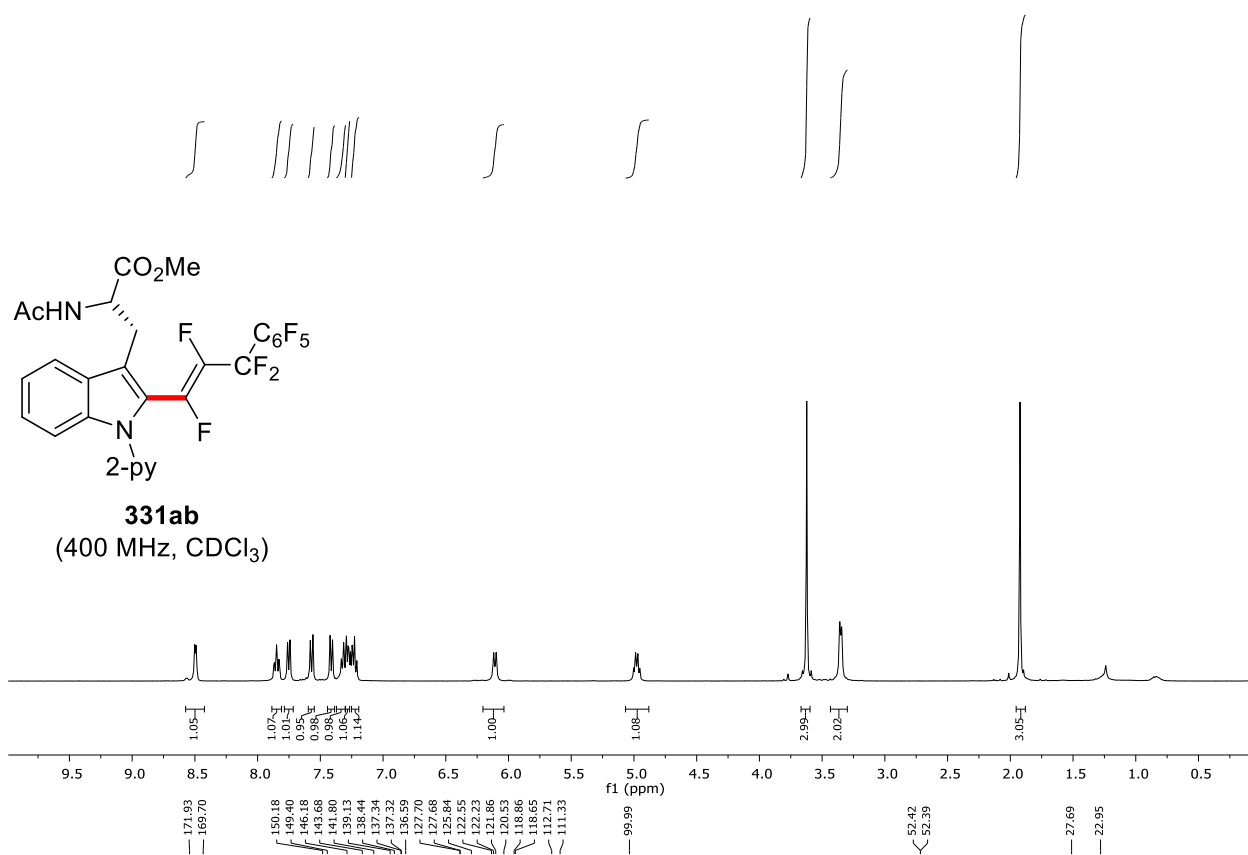


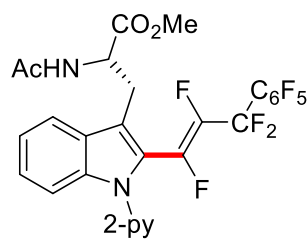


331bc
(400 MHz, CDCl₃)

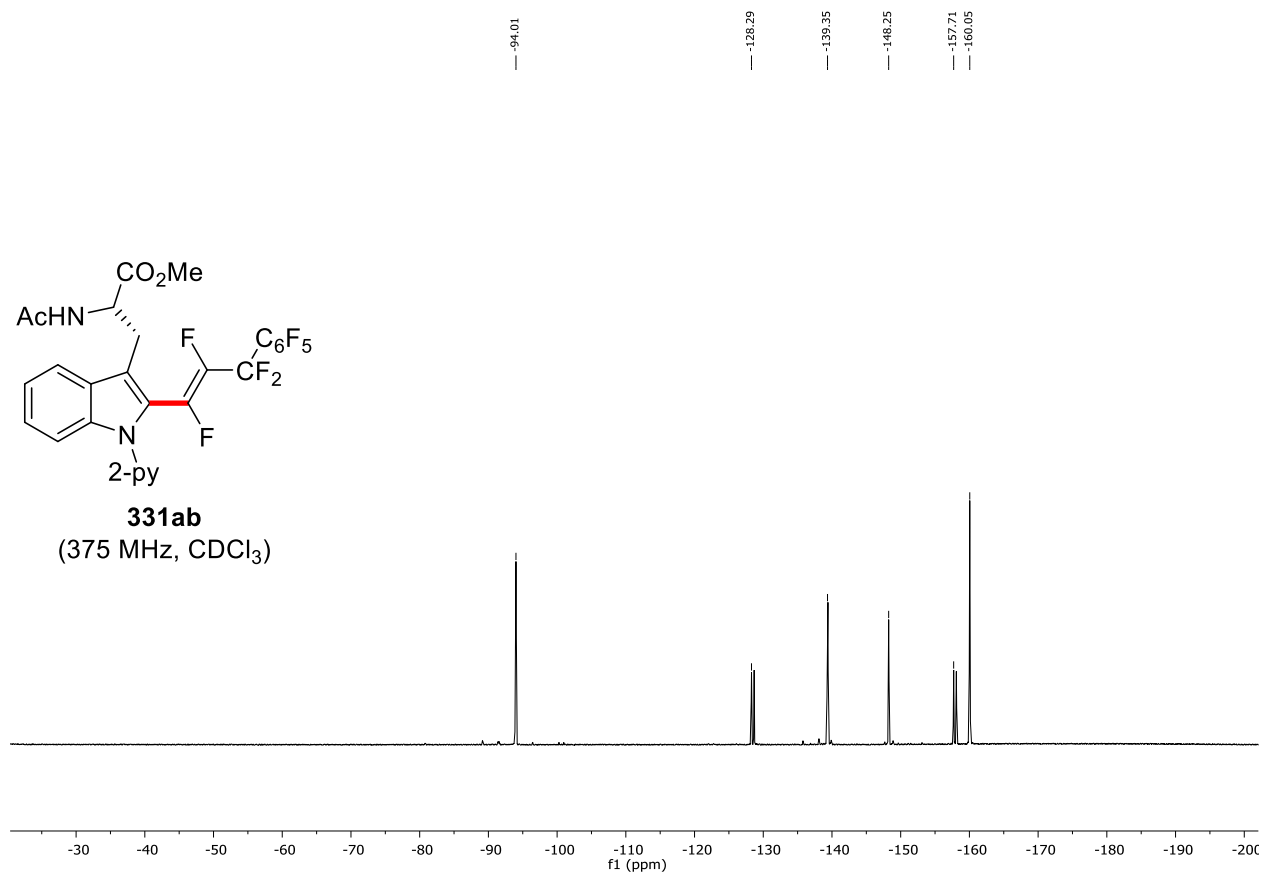


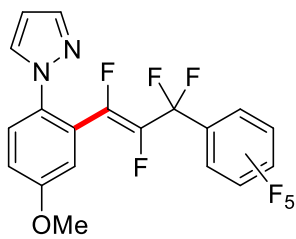




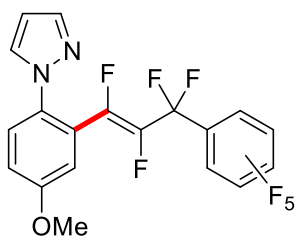
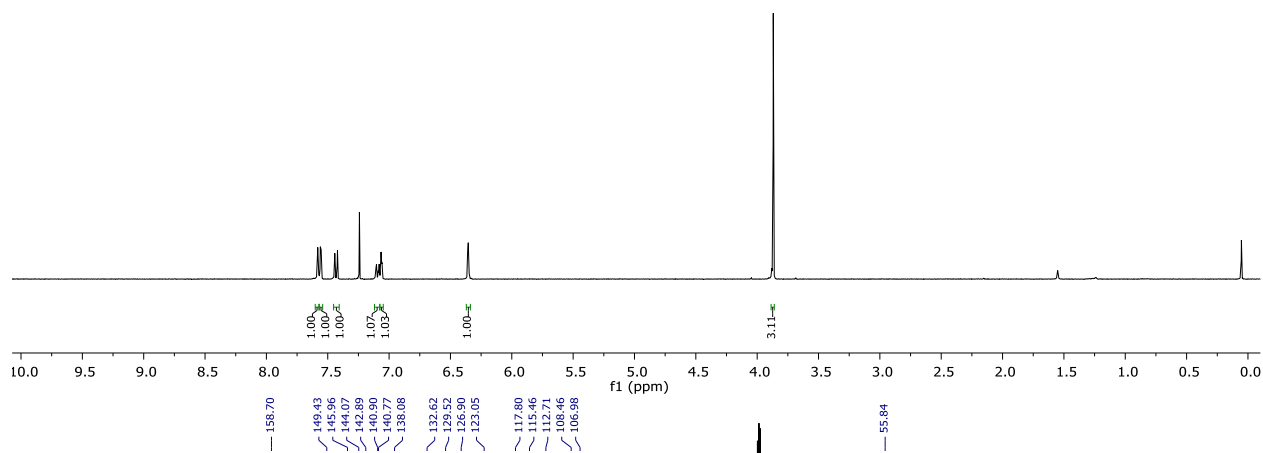


331ab
(375 MHz, CDCl₃)

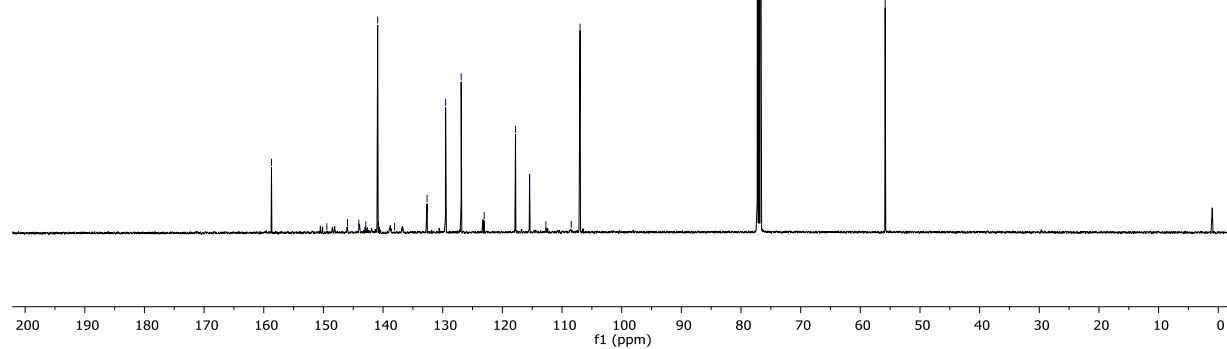


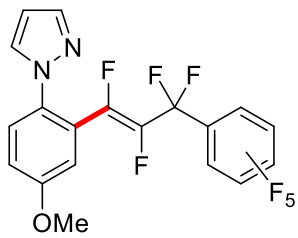


333ab
(400 MHz, CDCl₃)

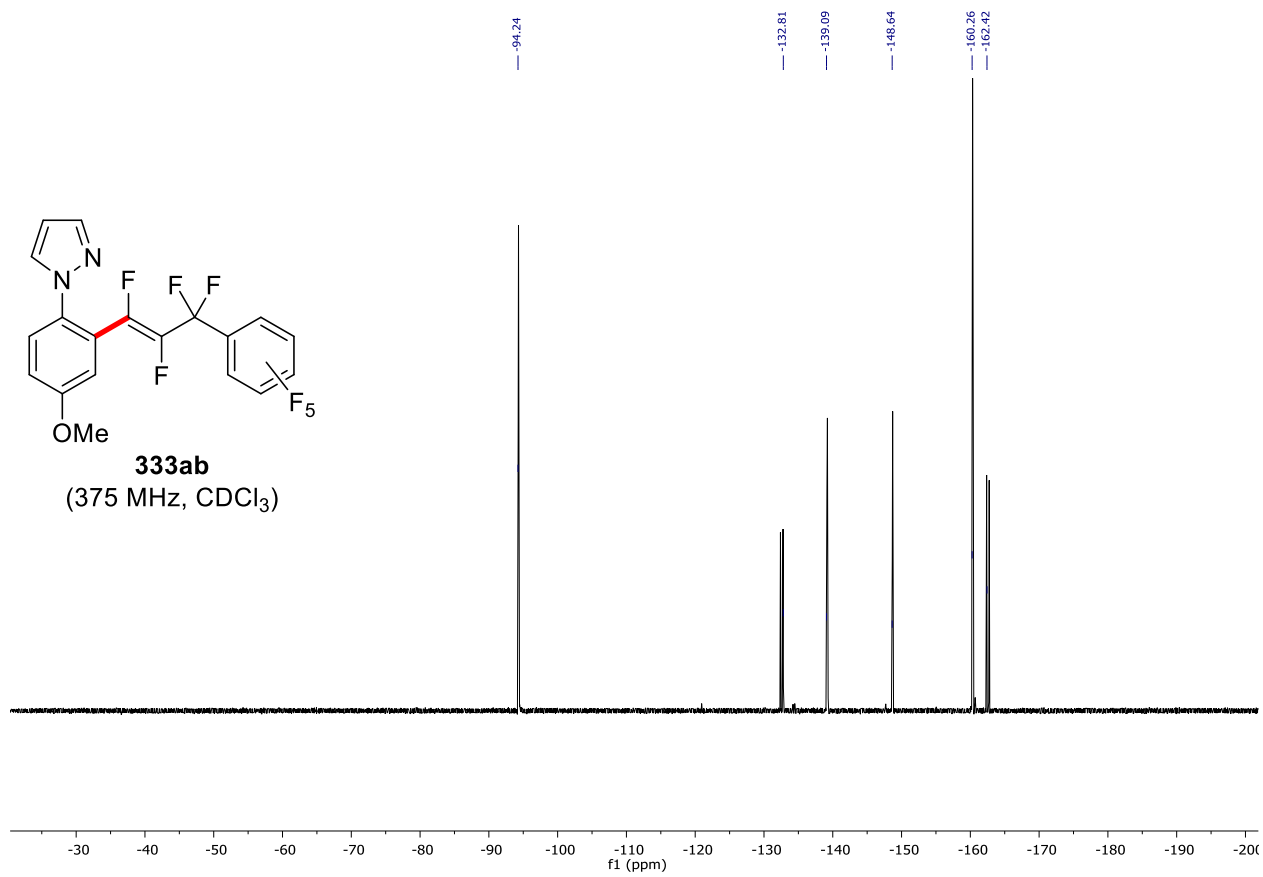


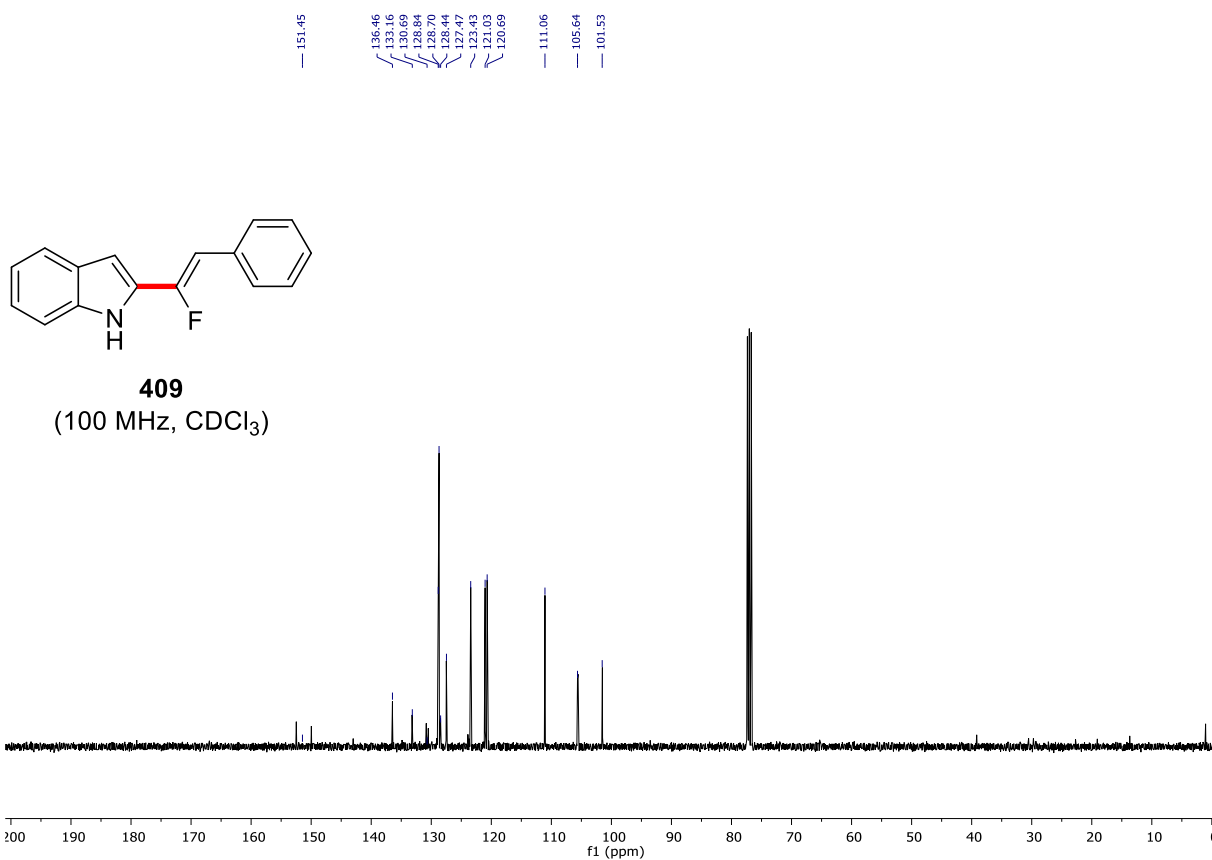
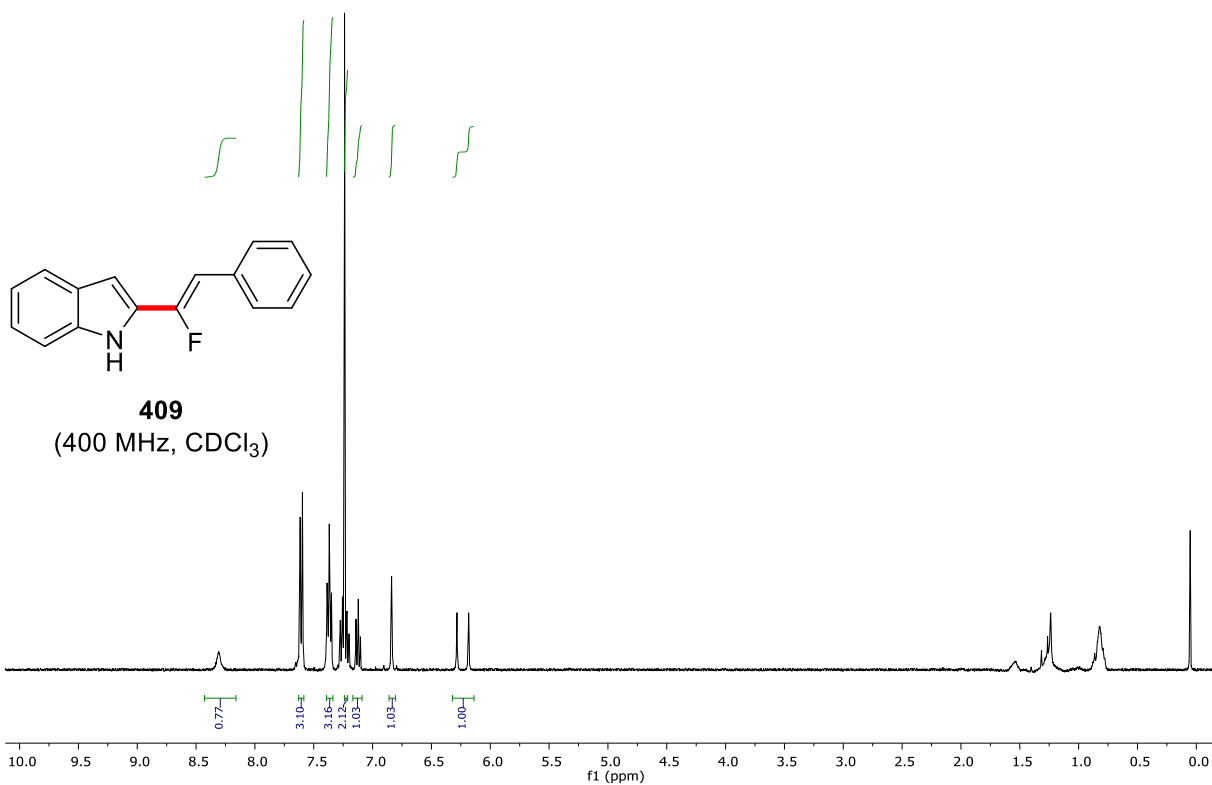
333ab
(125 MHz, CDCl₃)

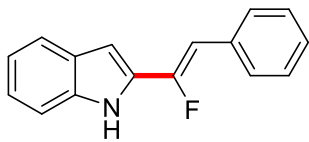




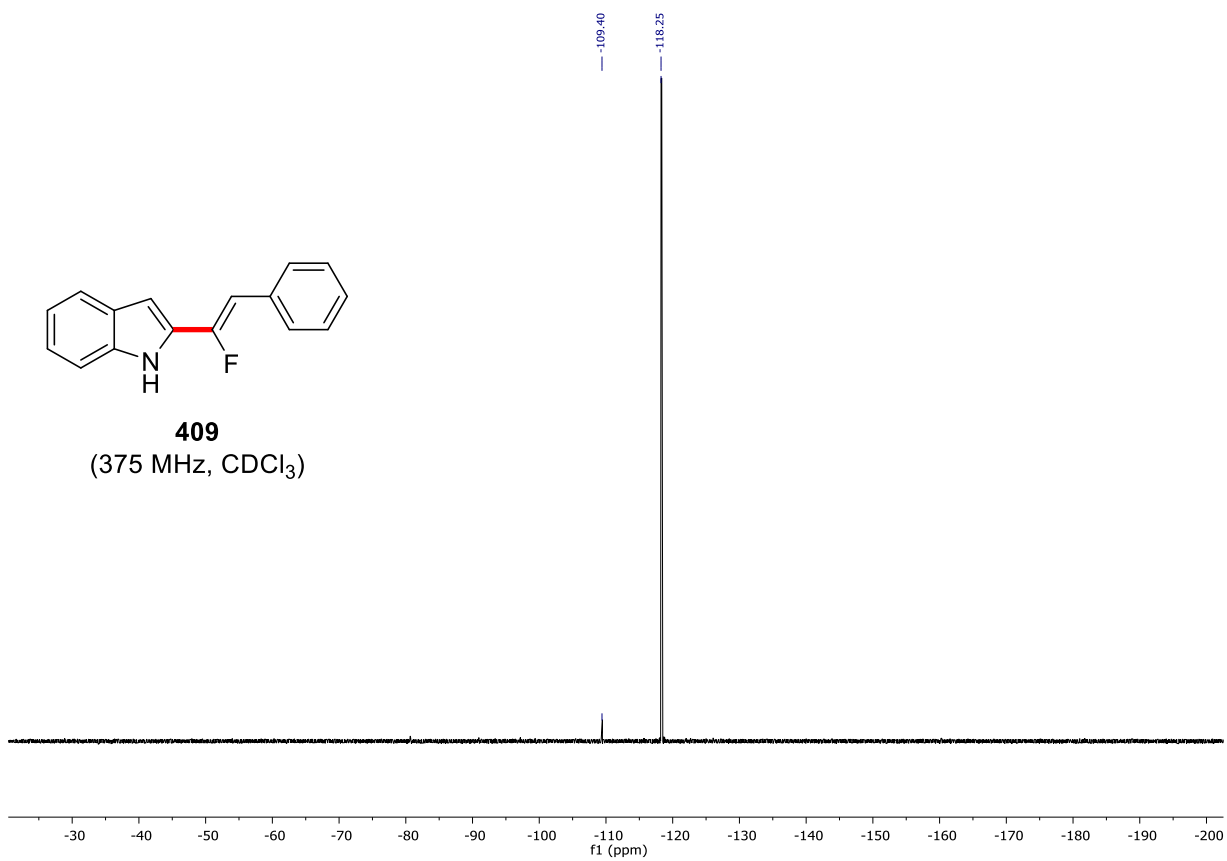
333ab
(375 MHz, CDCl₃)

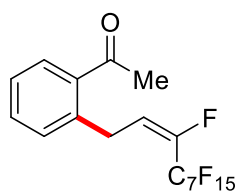




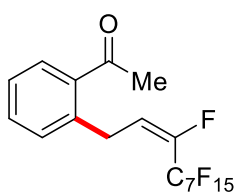
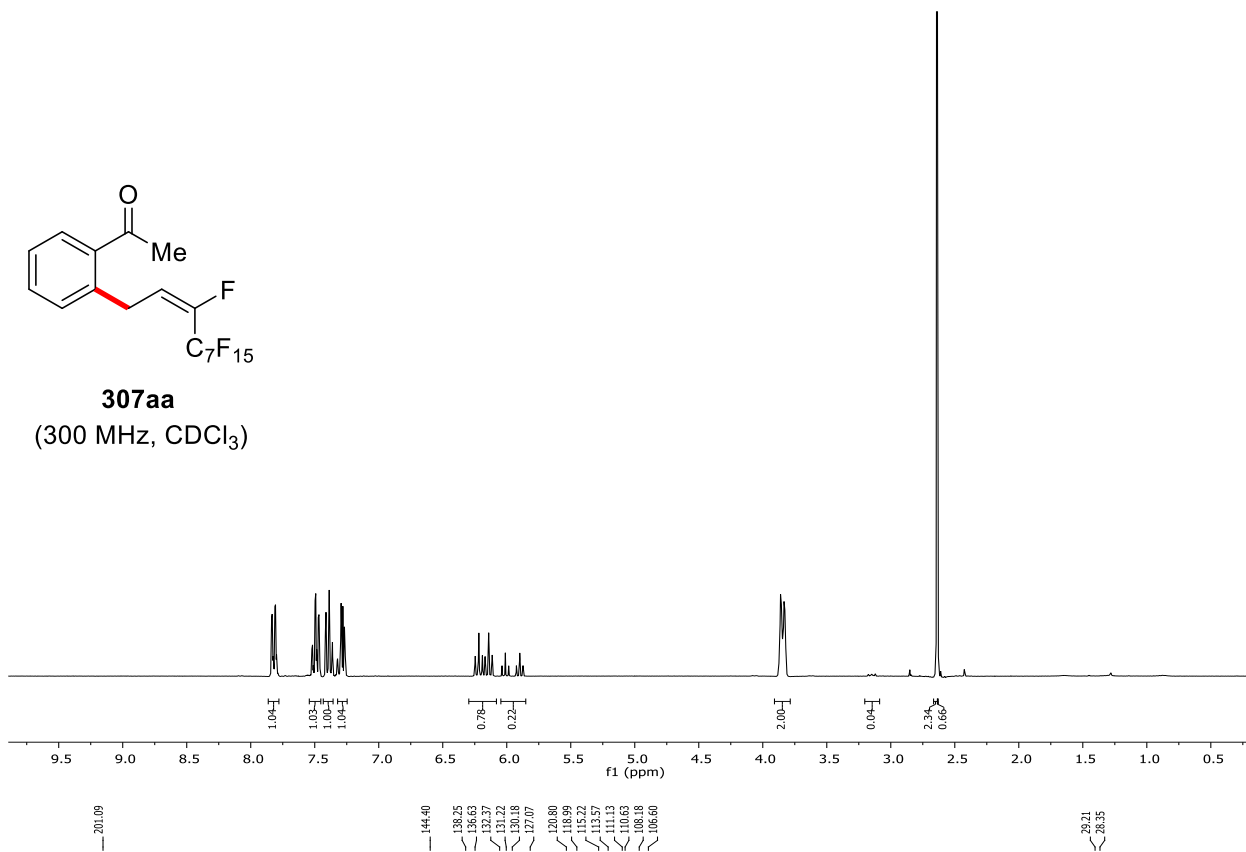


409
(375 MHz, CDCl₃)

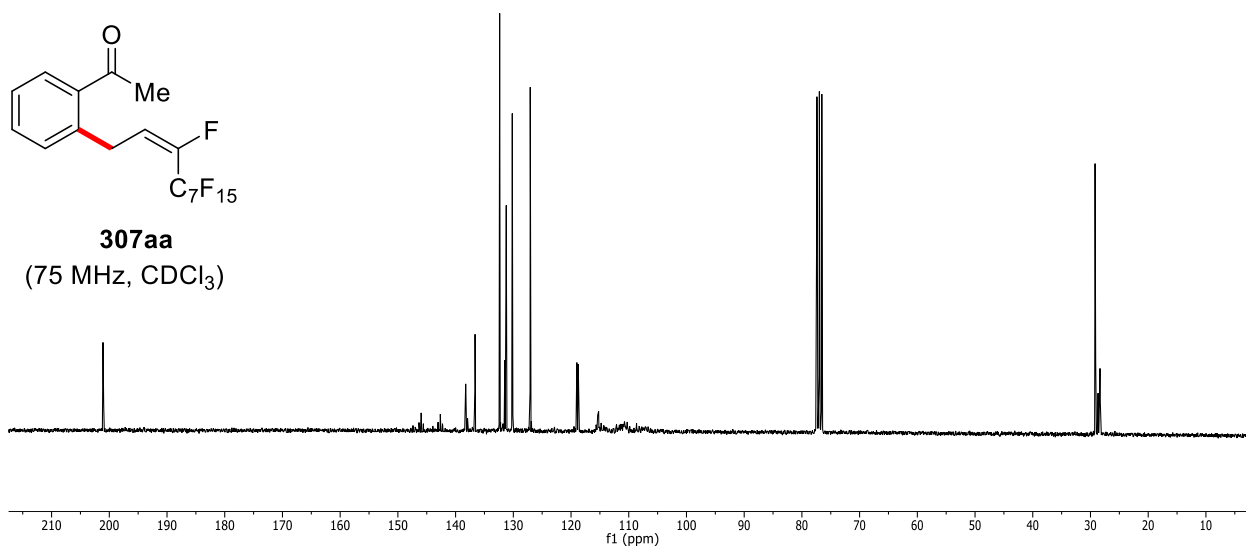


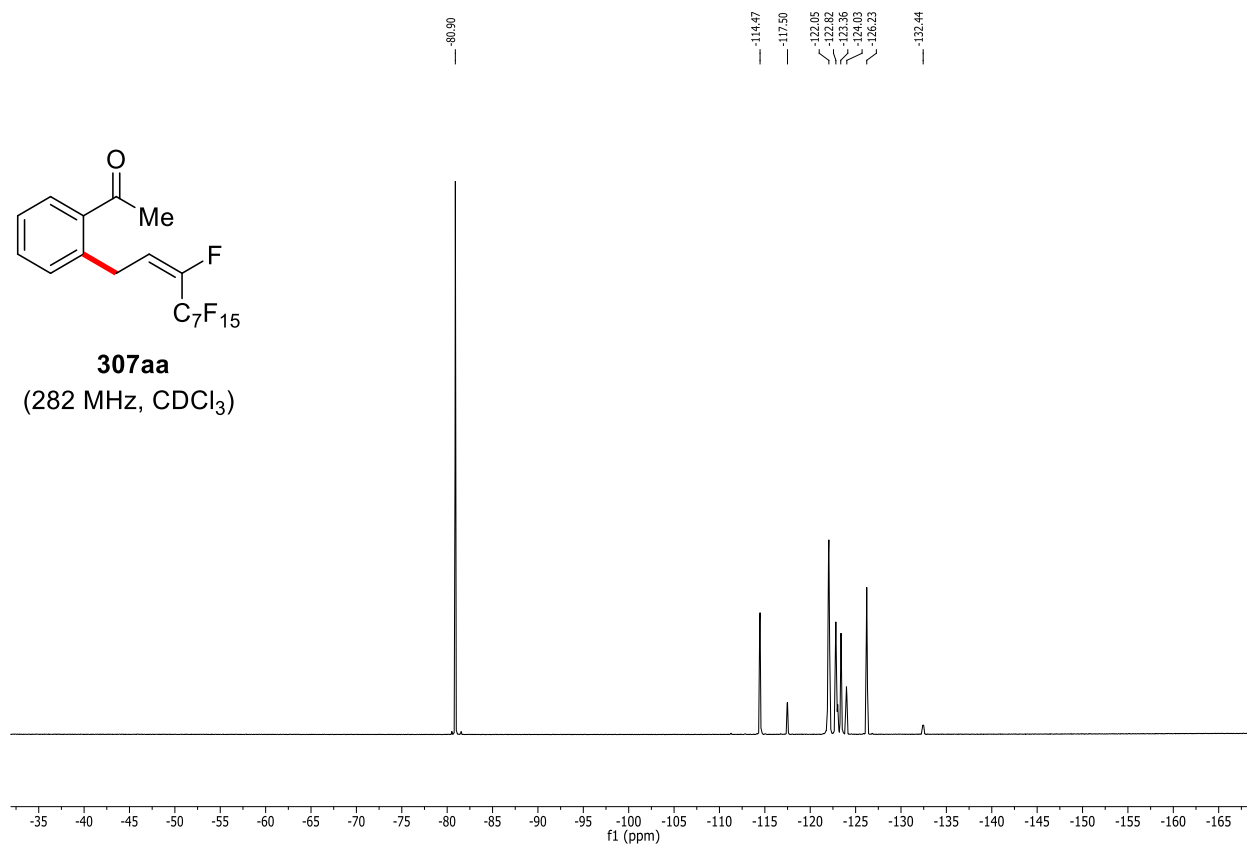
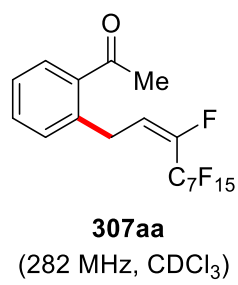


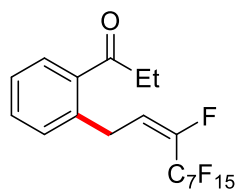
307aa
(300 MHz, CDCl₃)



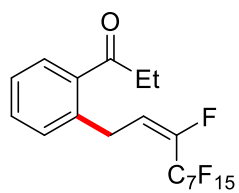
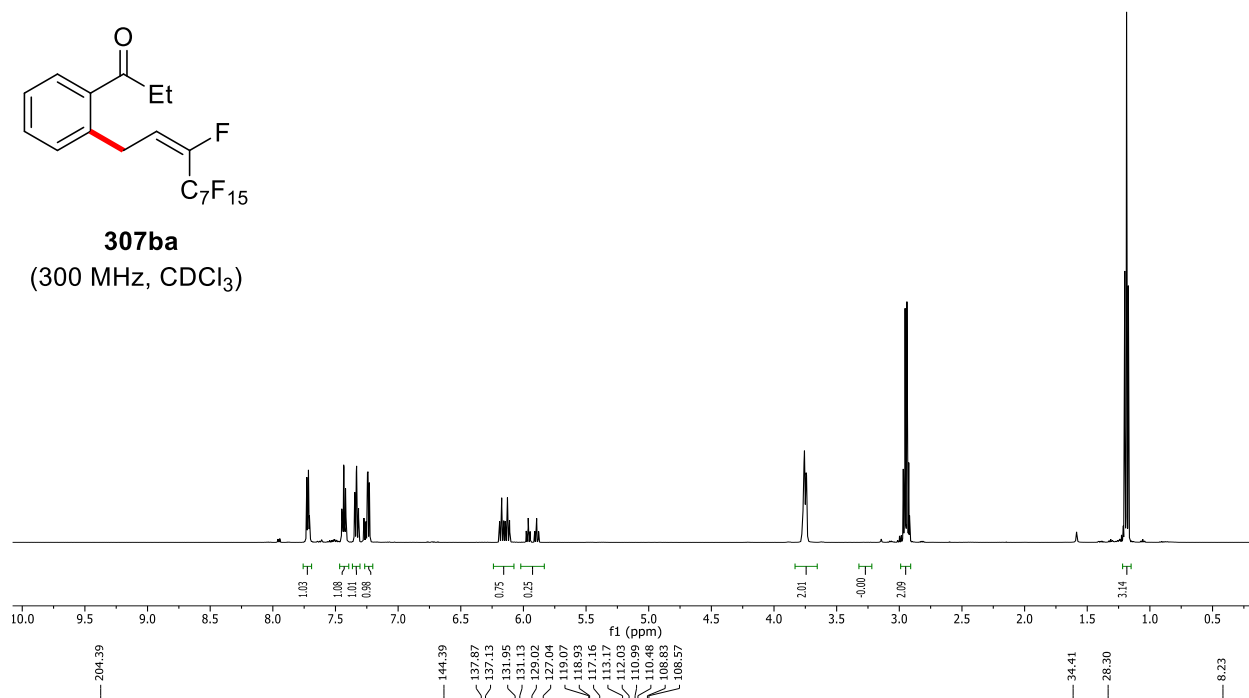
307aa
(75 MHz, CDCl₃)



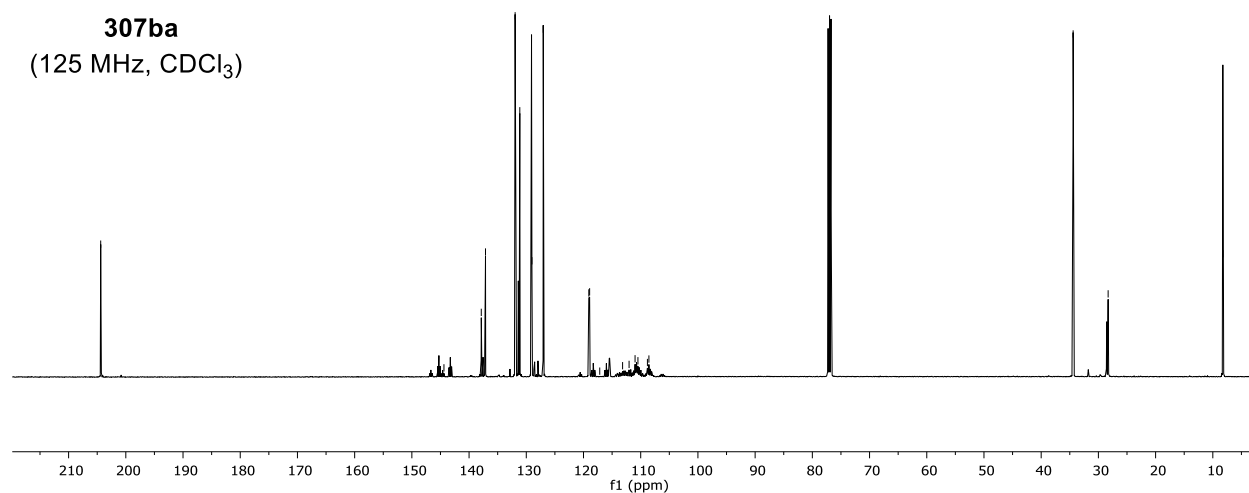


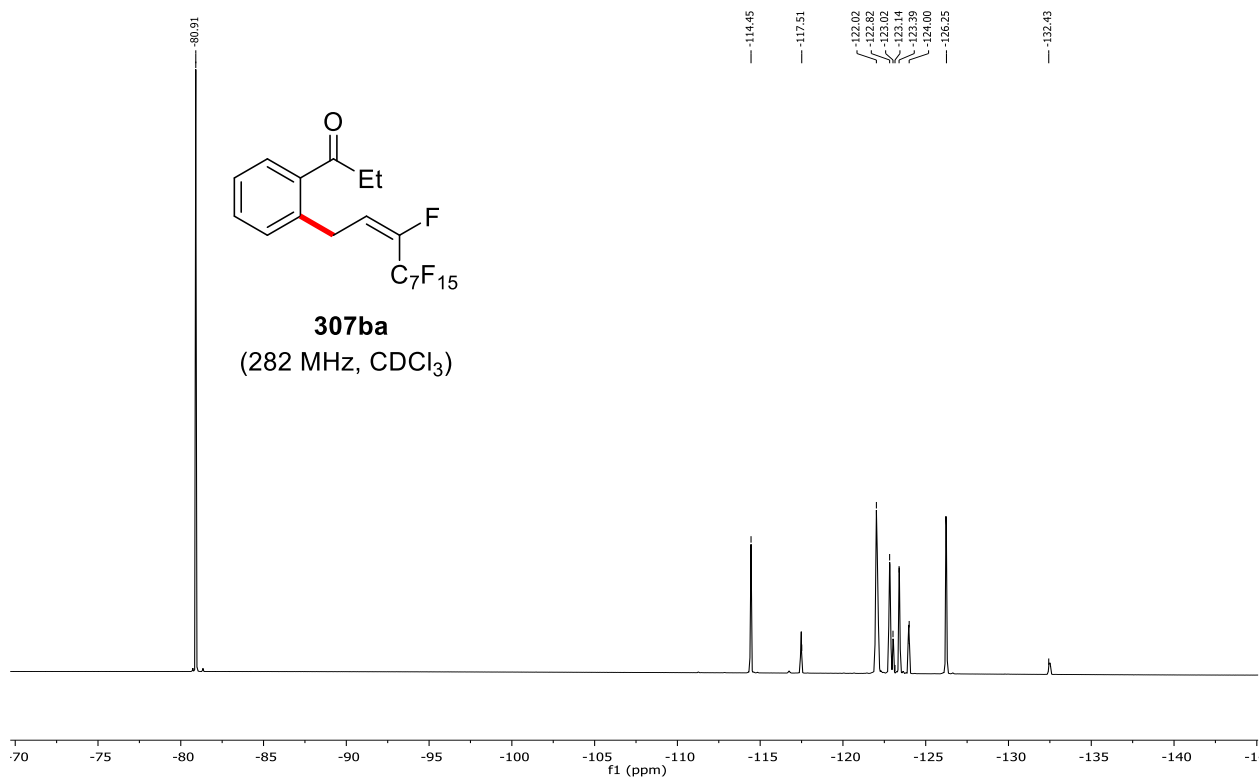


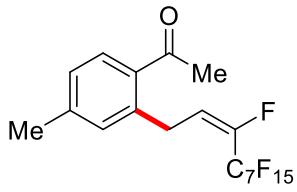
307ba
(300 MHz, CDCl₃)



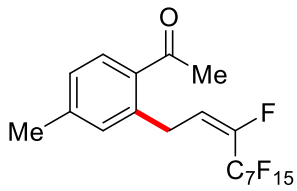
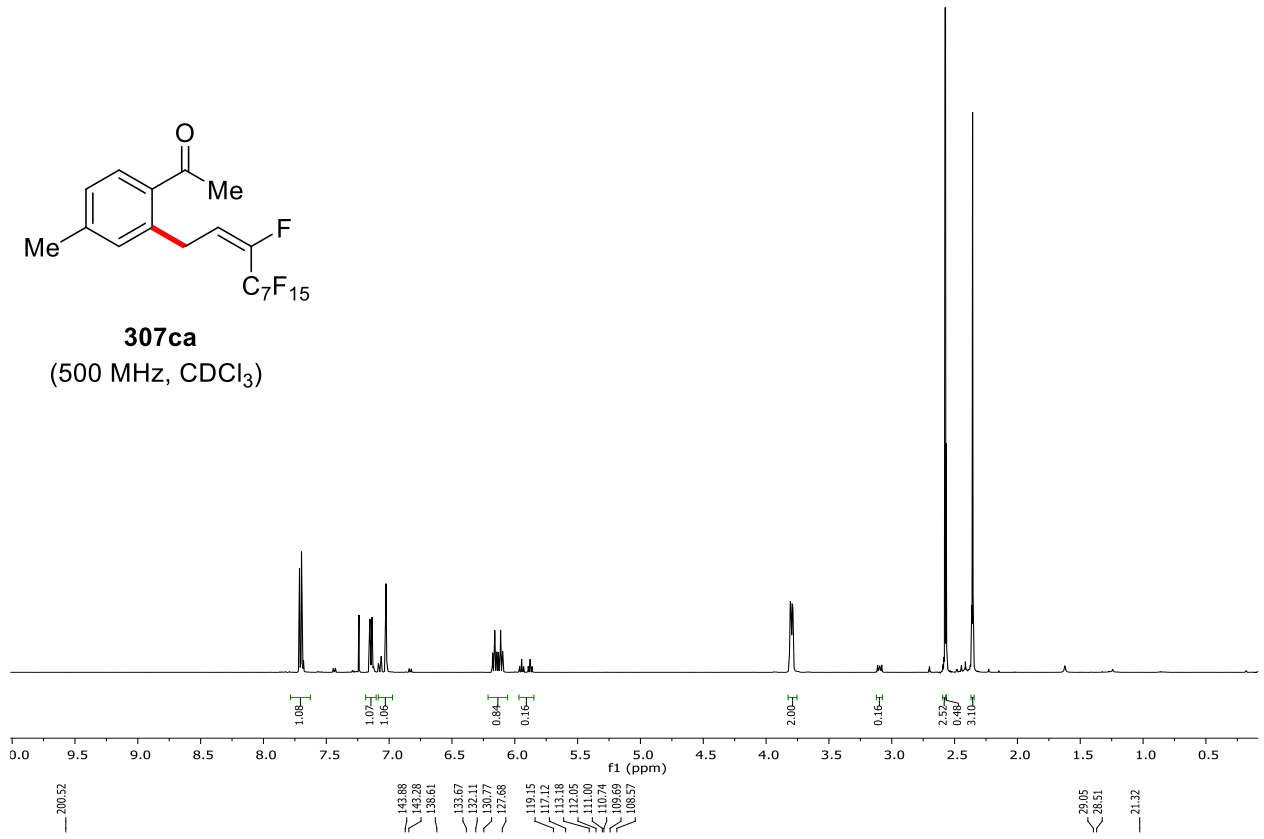
307ba
(125 MHz, CDCl₃)



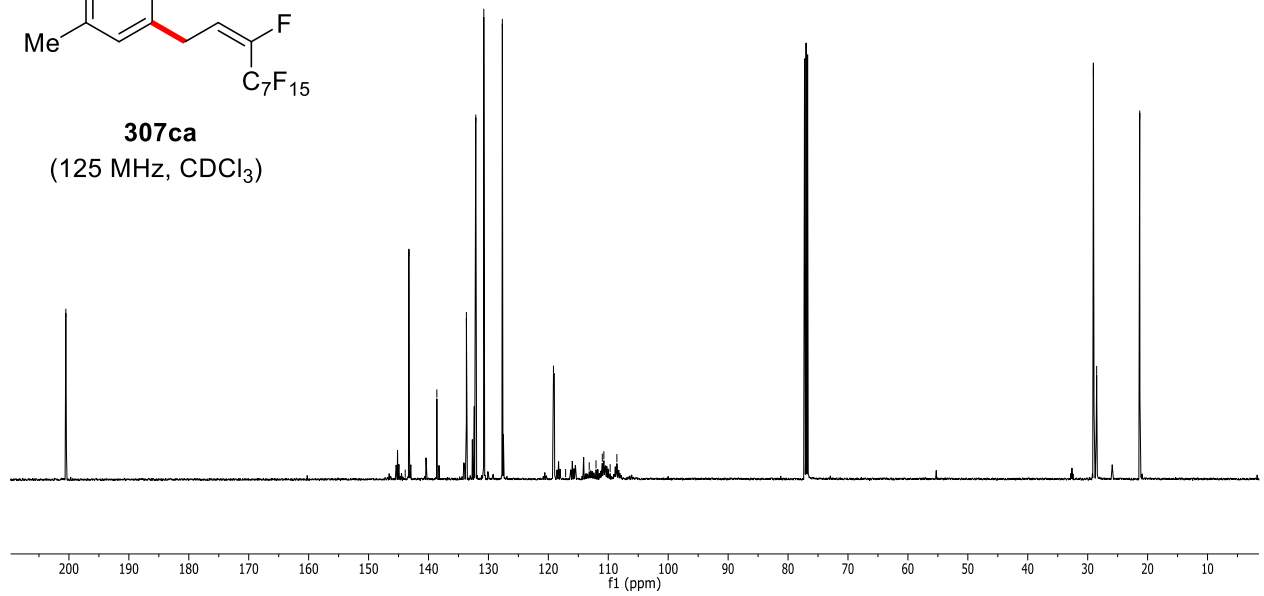


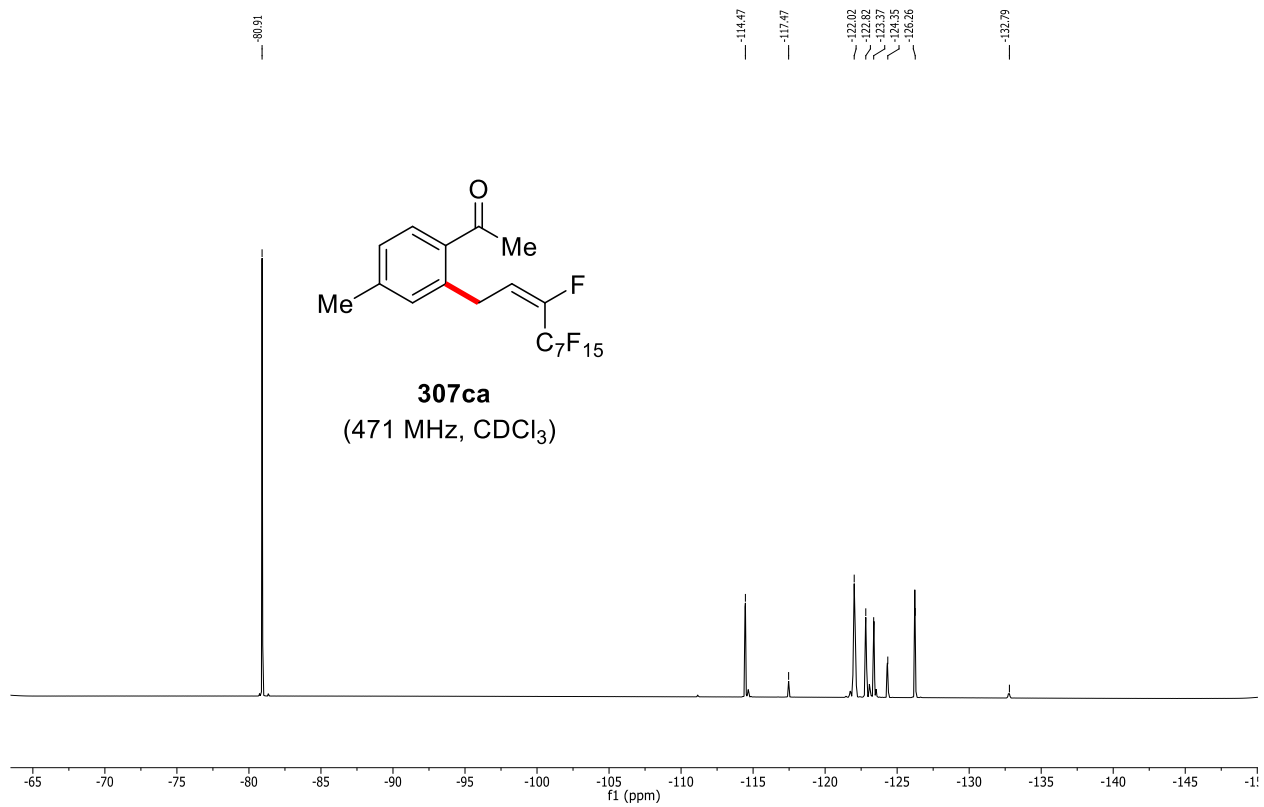


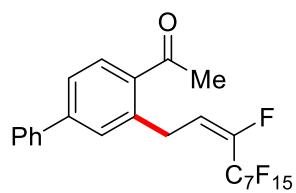
307ca
(500 MHz, CDCl₃)



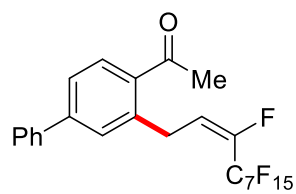
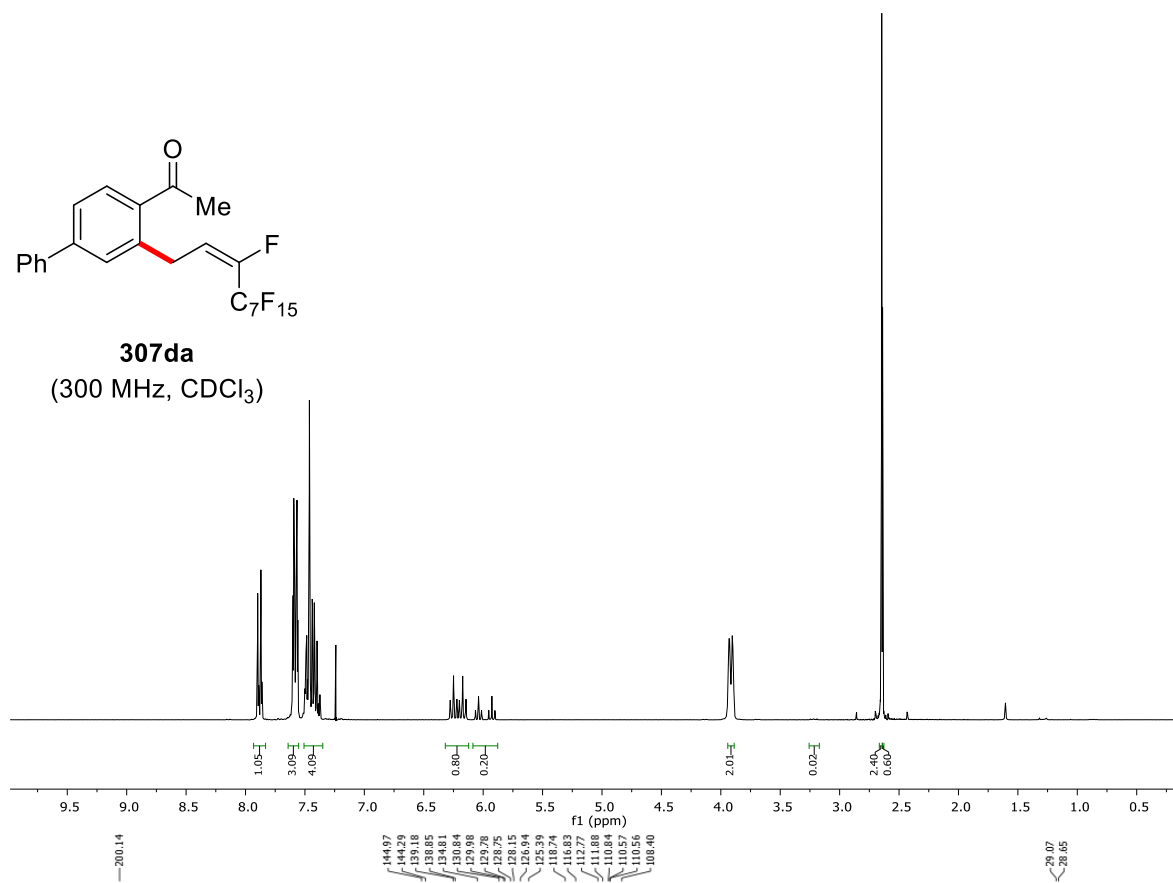
307ca
(125 MHz, CDCl₃)



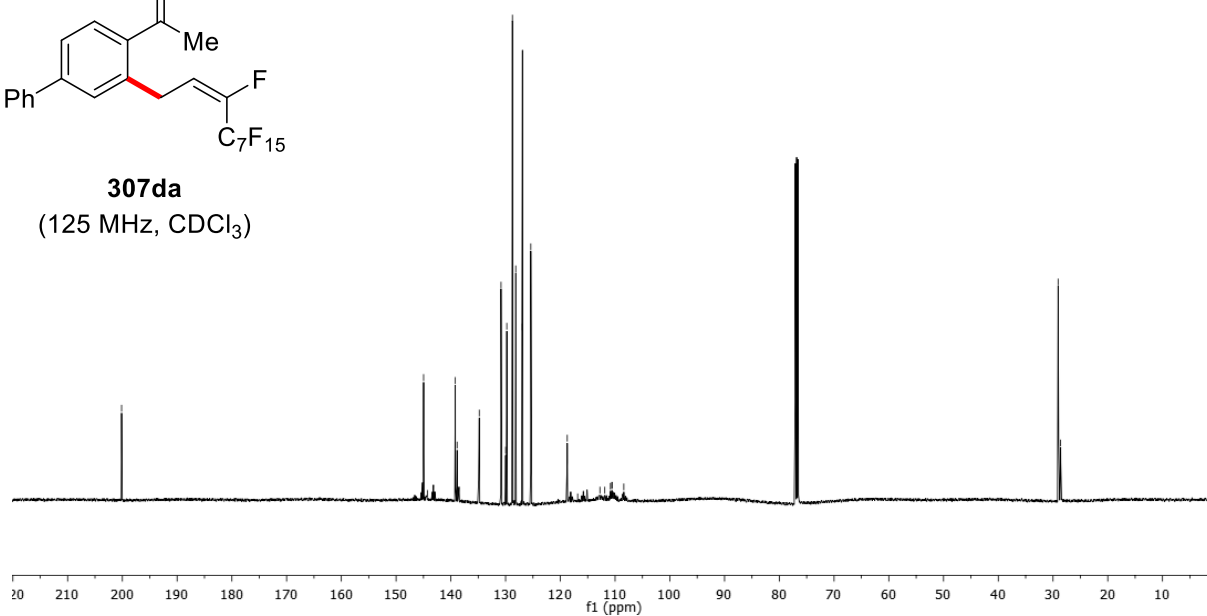


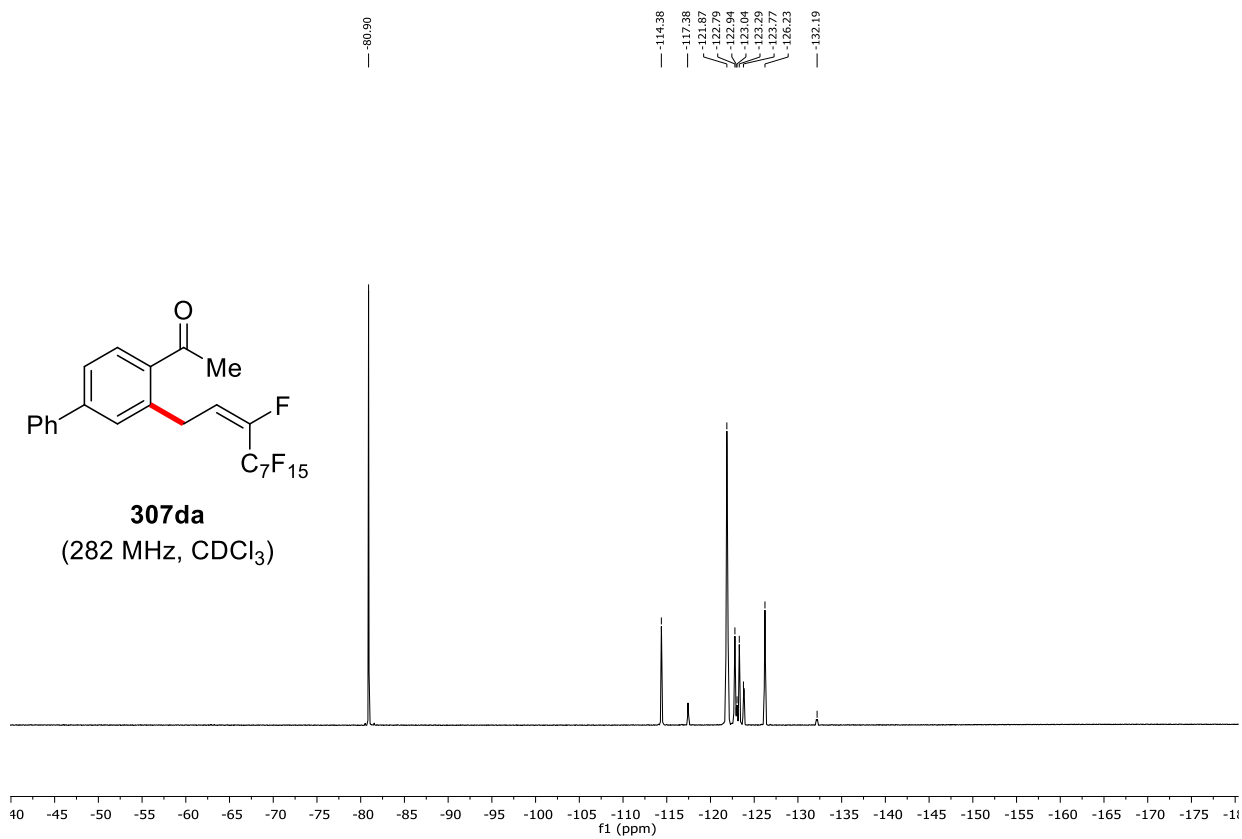


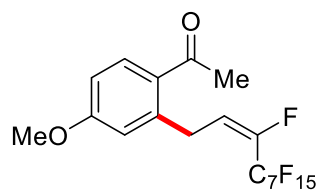
307da
(300 MHz, CDCl₃)



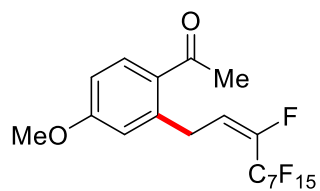
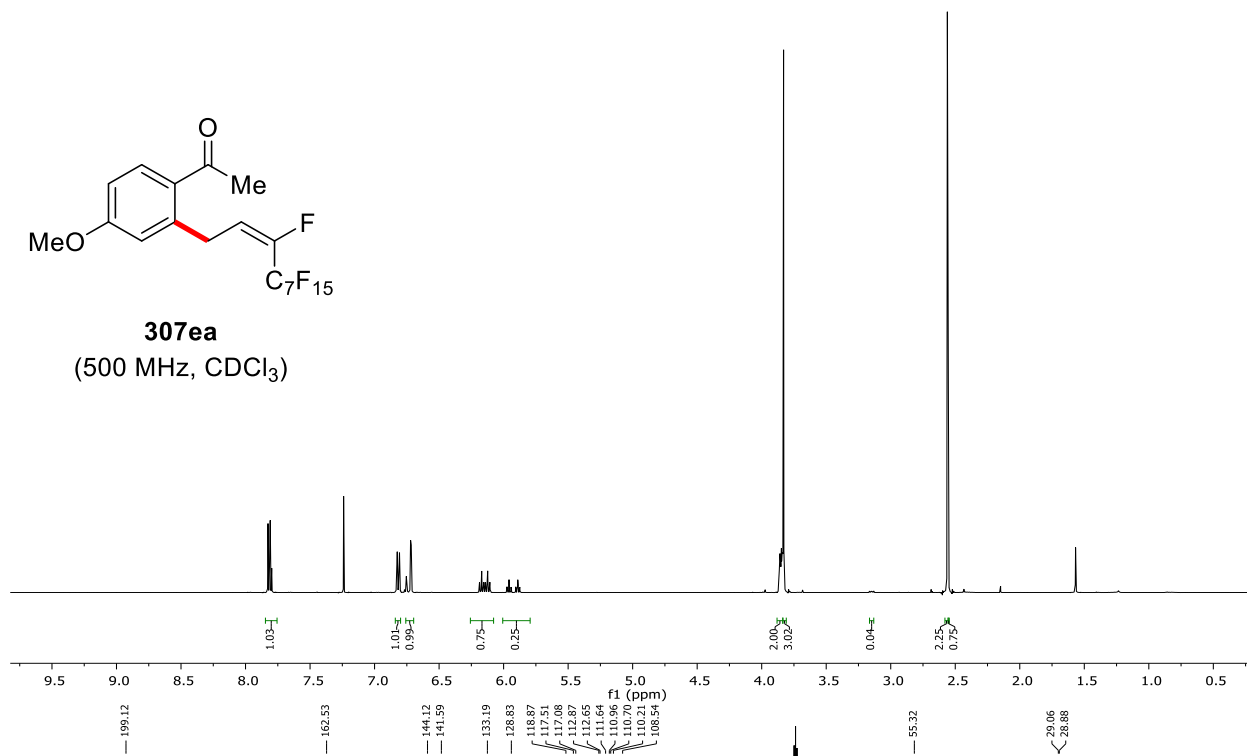
307da
(125 MHz, CDCl₃)



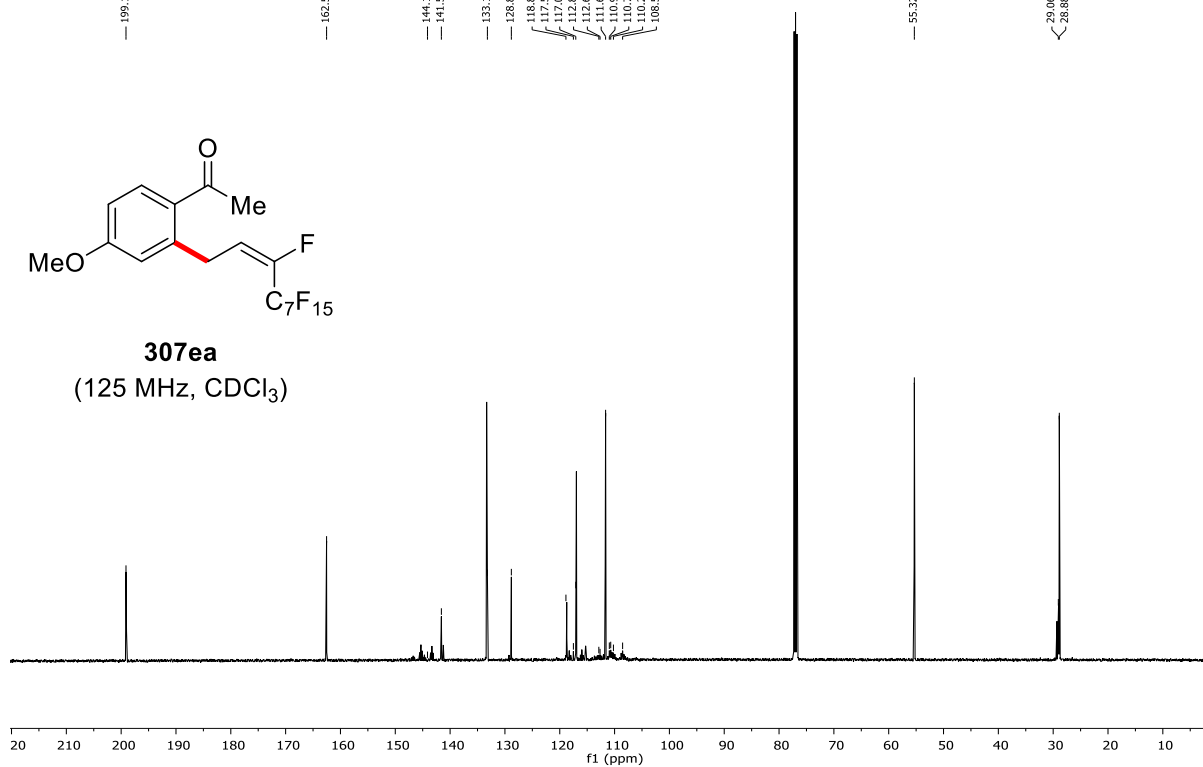


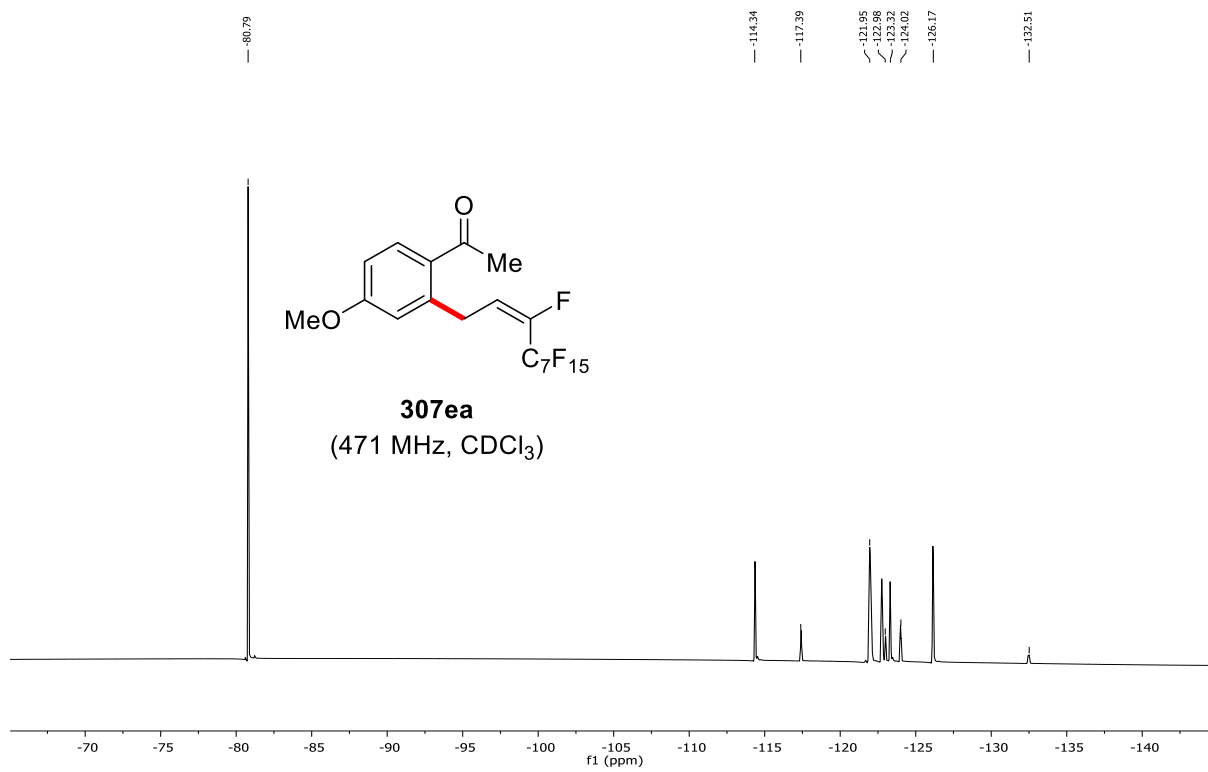


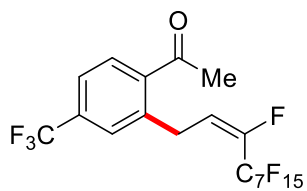
307ea
(500 MHz, CDCl₃)



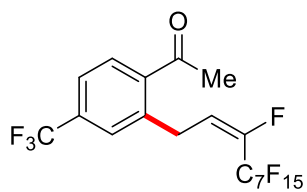
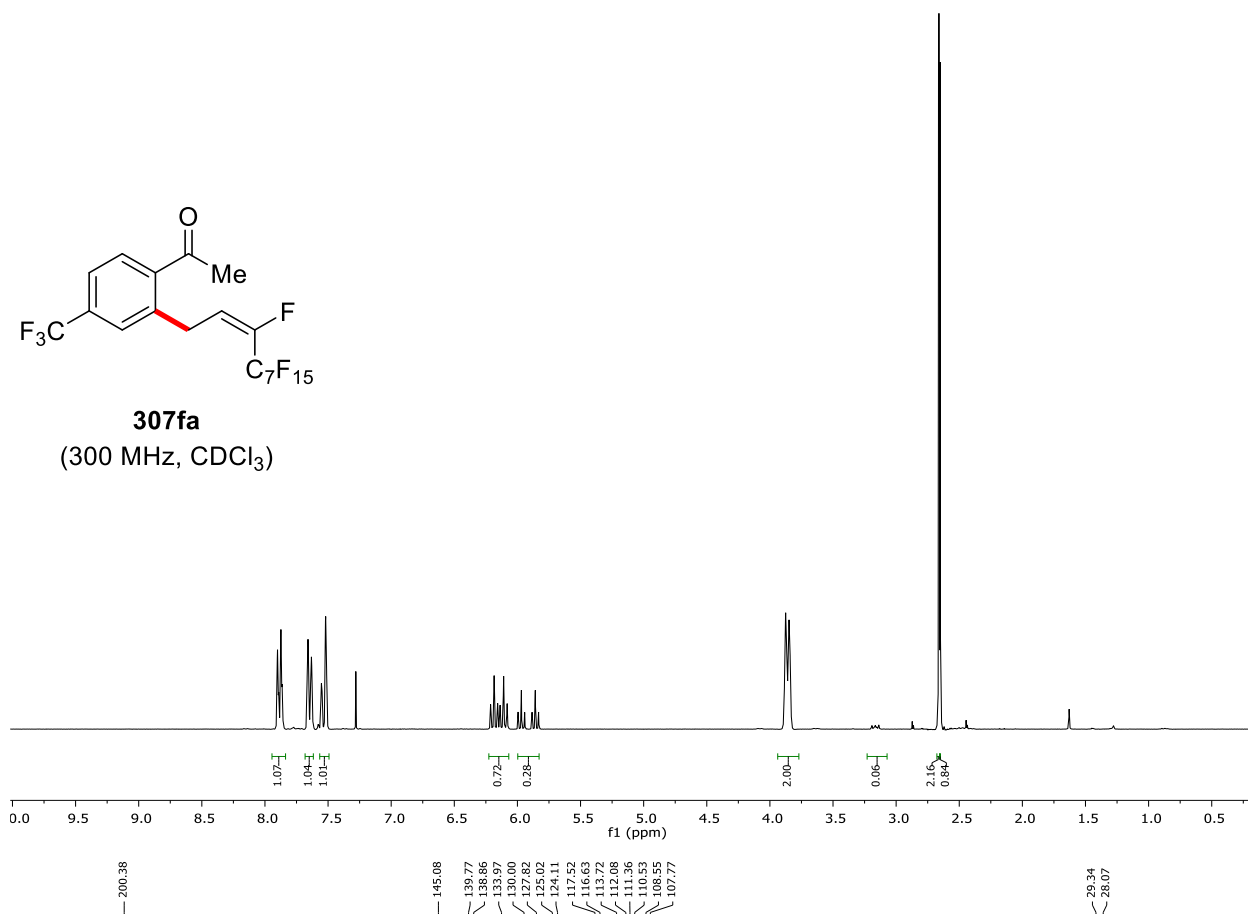
307ea
(125 MHz, CDCl₃)



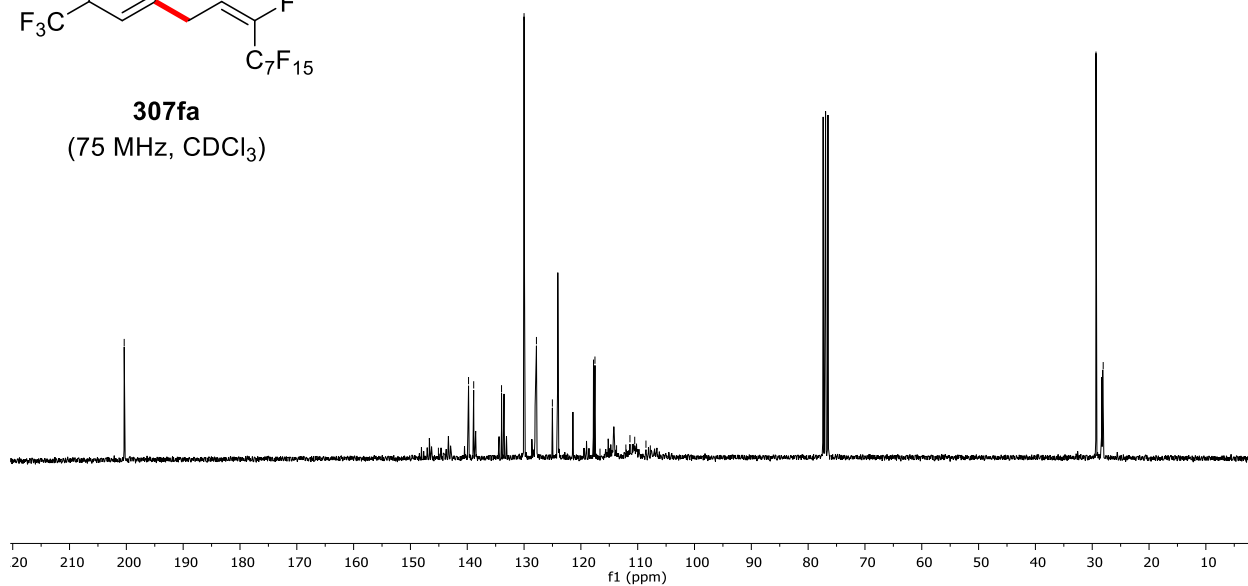


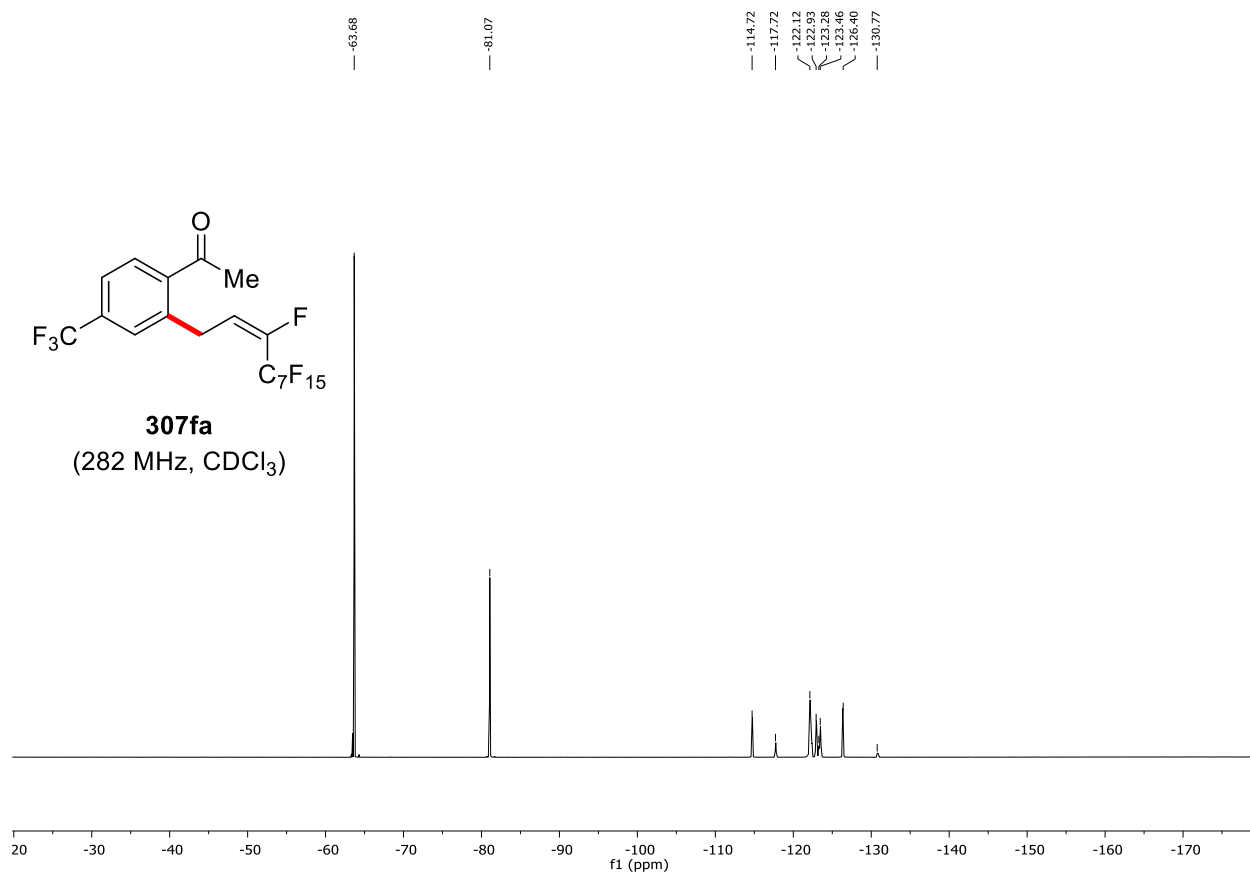


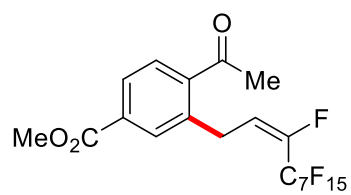
307fa
(300 MHz, CDCl₃)



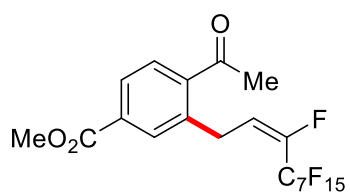
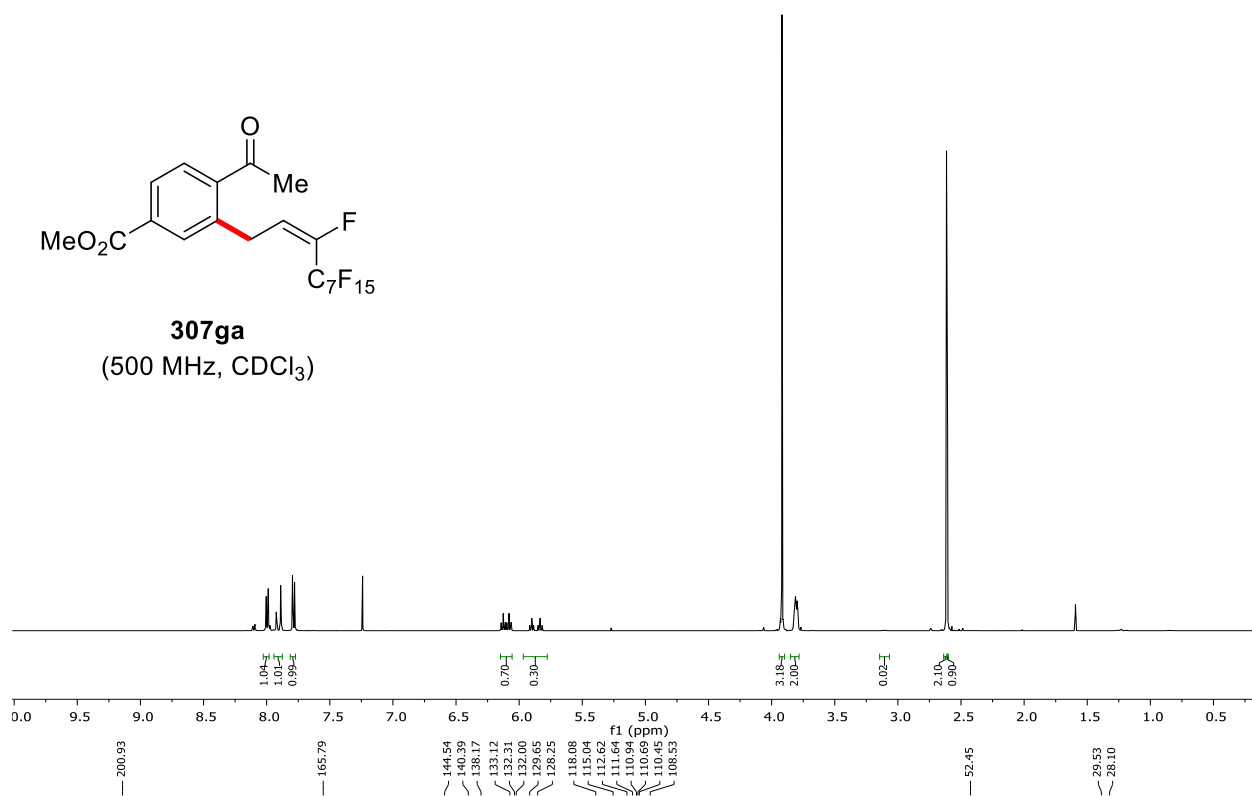
307fa
(75 MHz, CDCl₃)



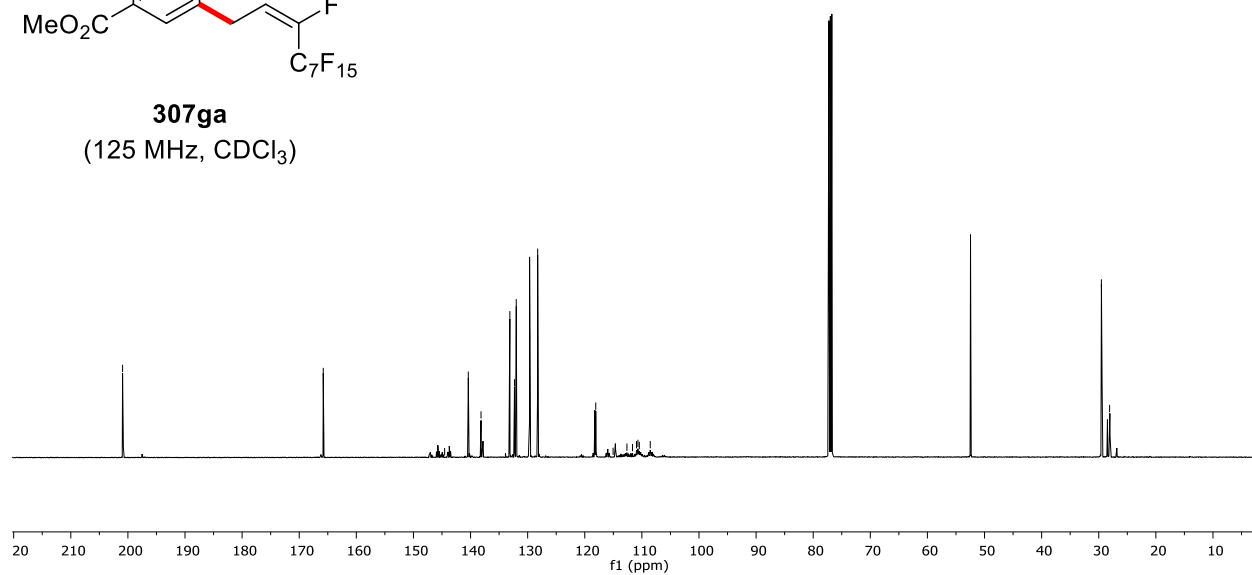


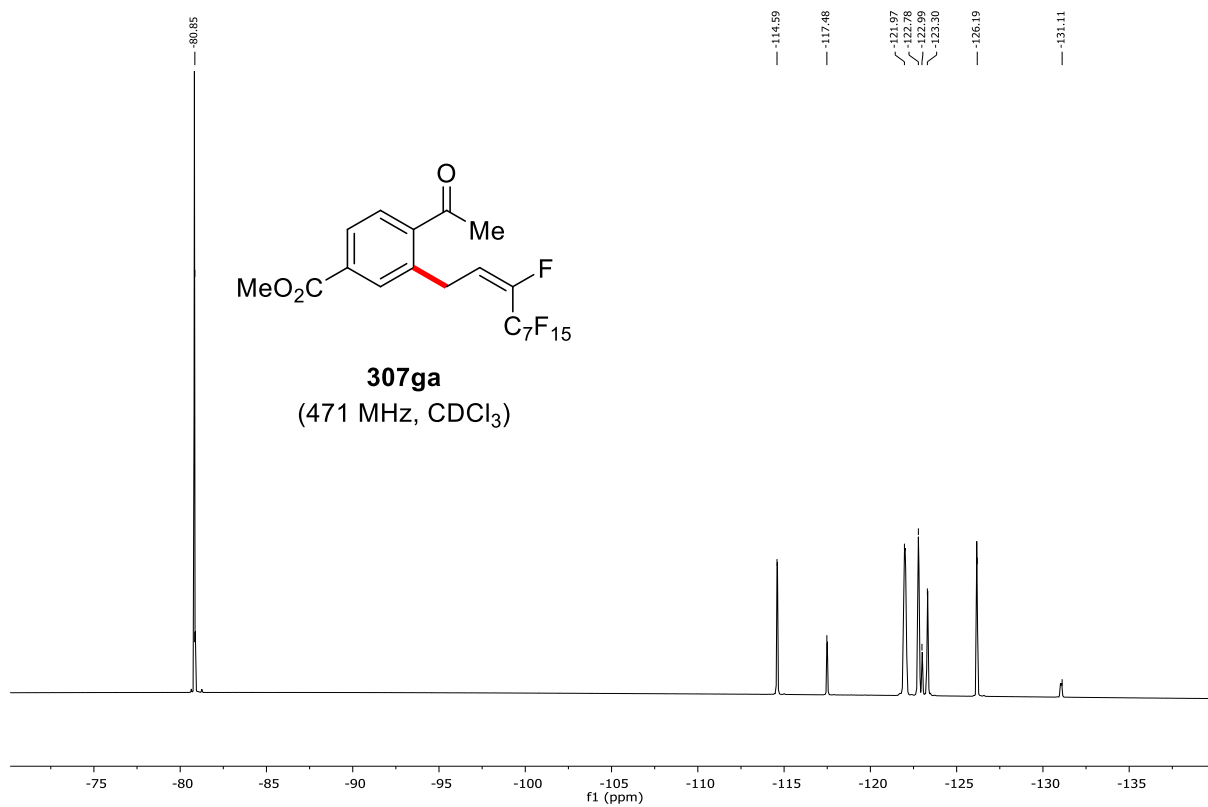


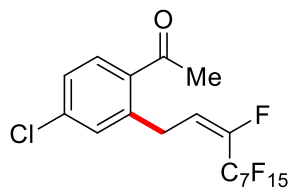
307ga
(500 MHz, CDCl₃)



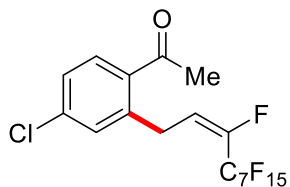
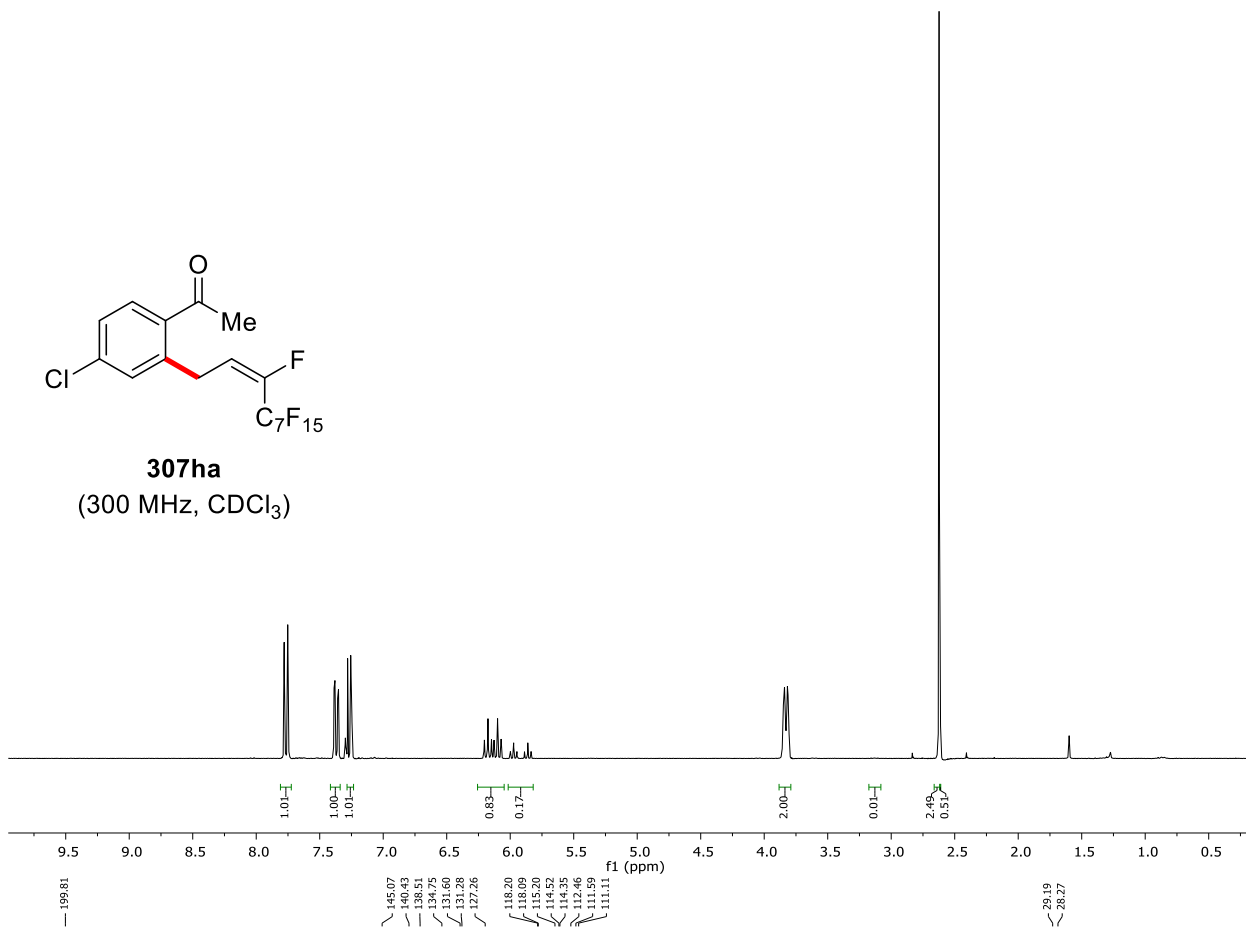
307ga
(125 MHz, CDCl₃)



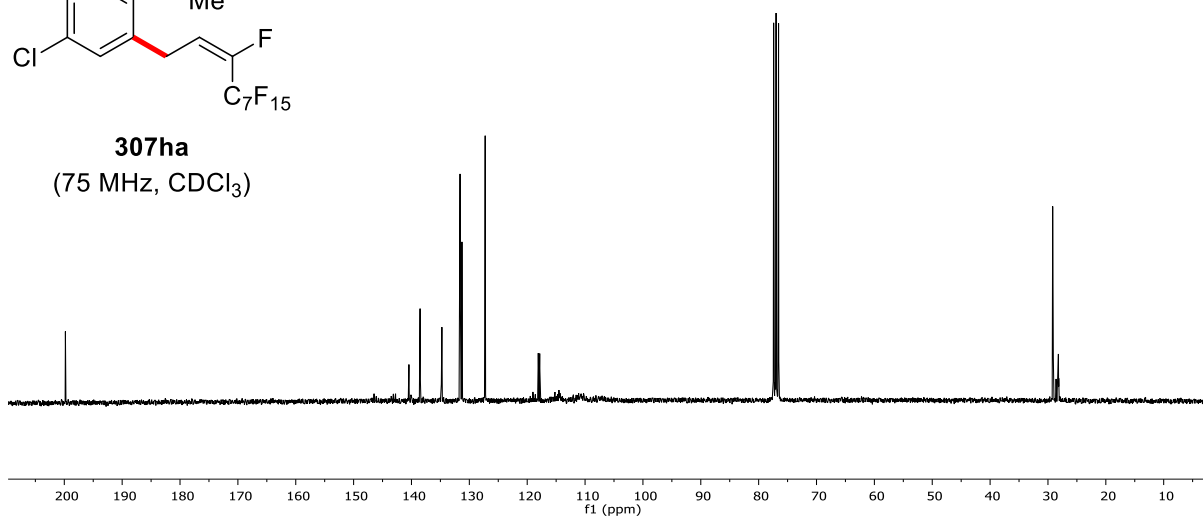


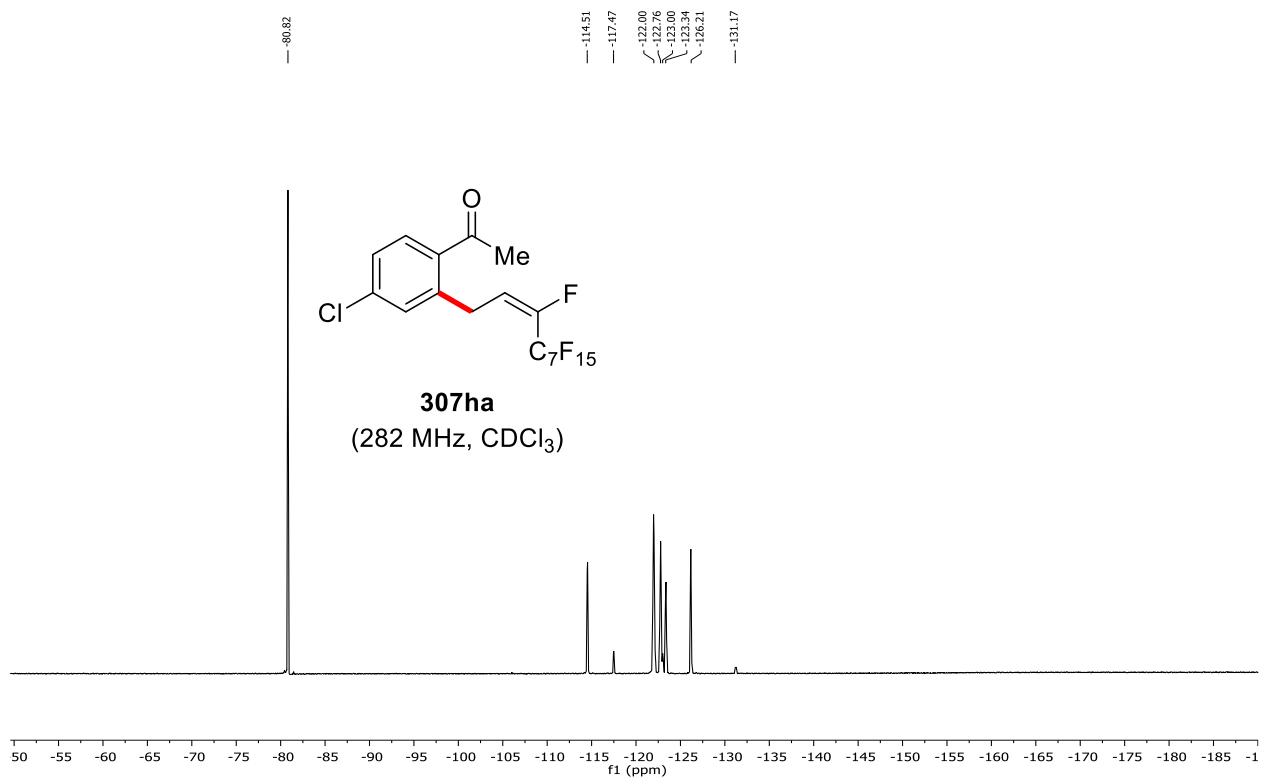


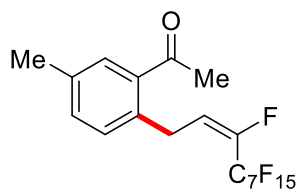
307ha
(300 MHz, CDCl₃)



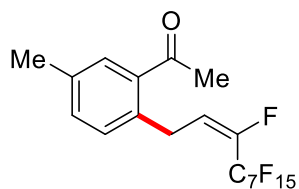
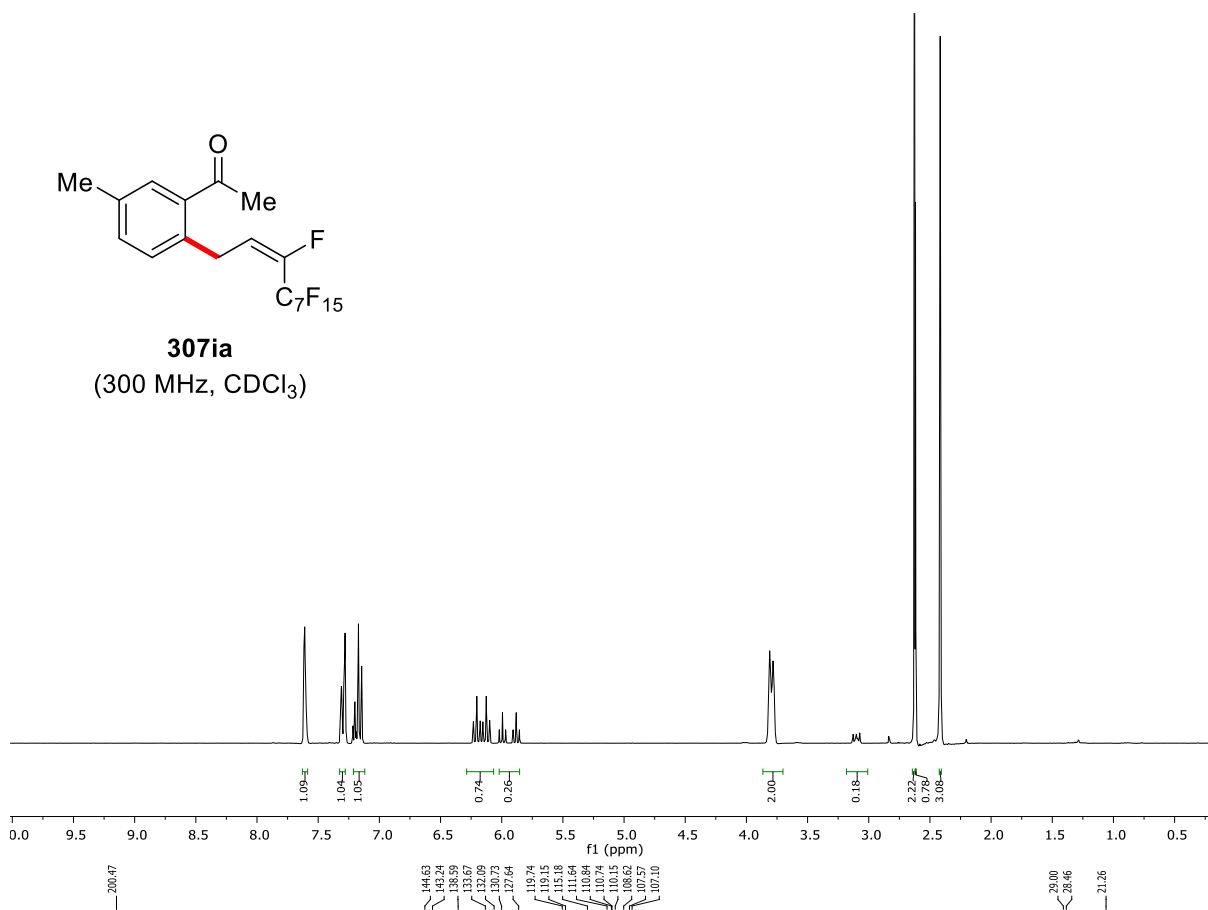
307ha
(75 MHz, CDCl₃)



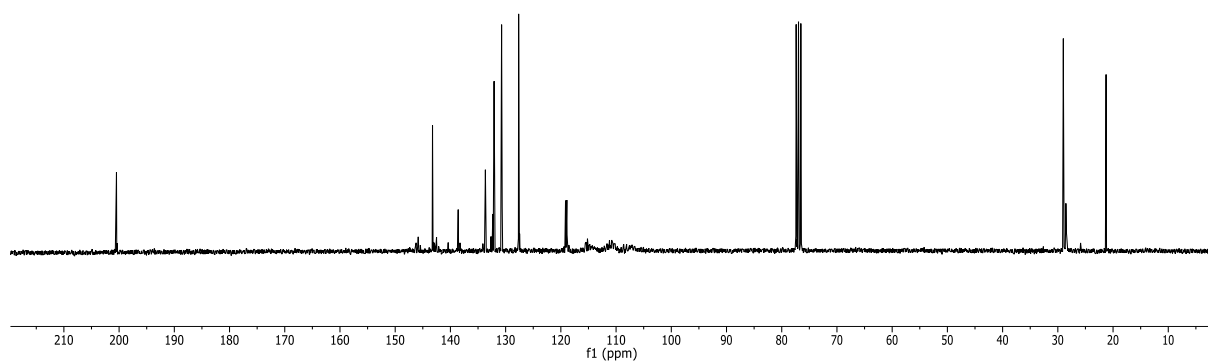


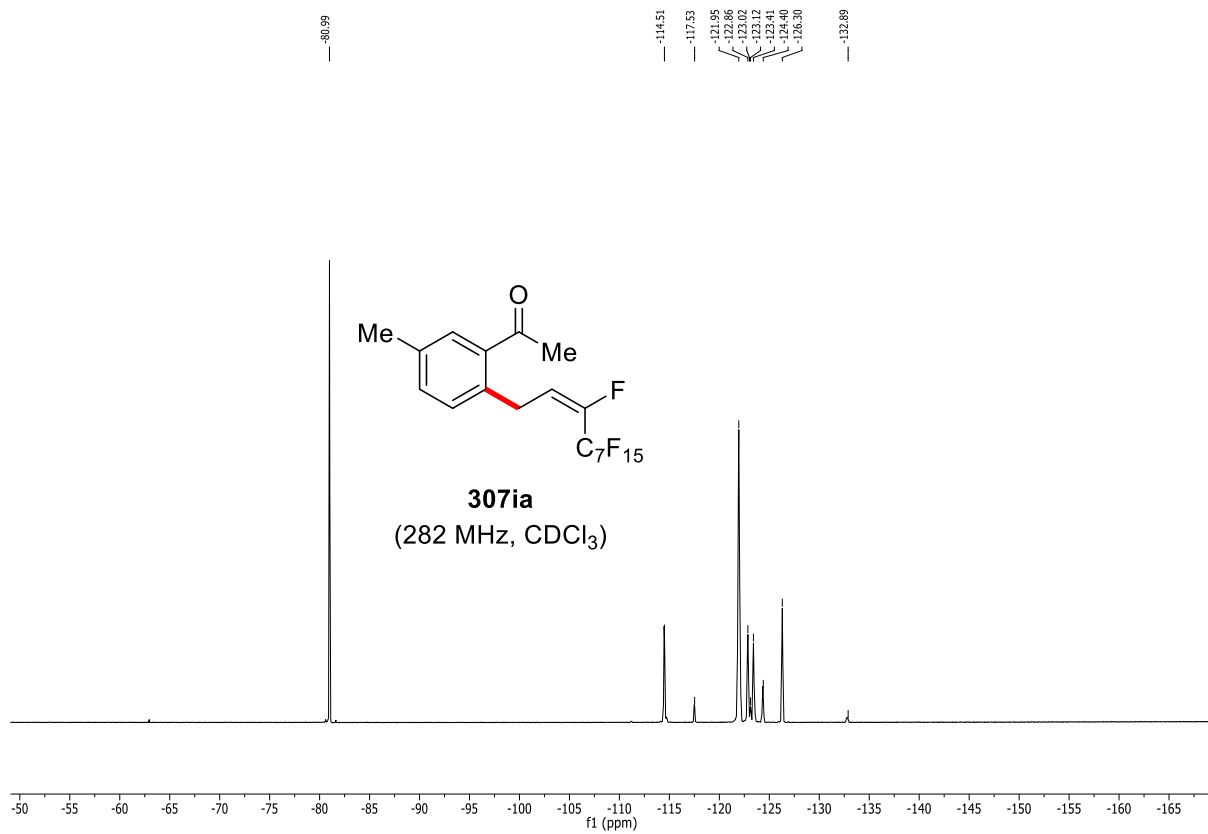


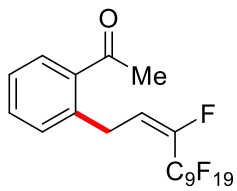
307ia
(300 MHz, CDCl₃)



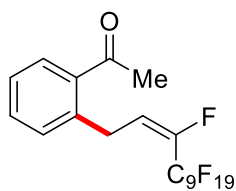
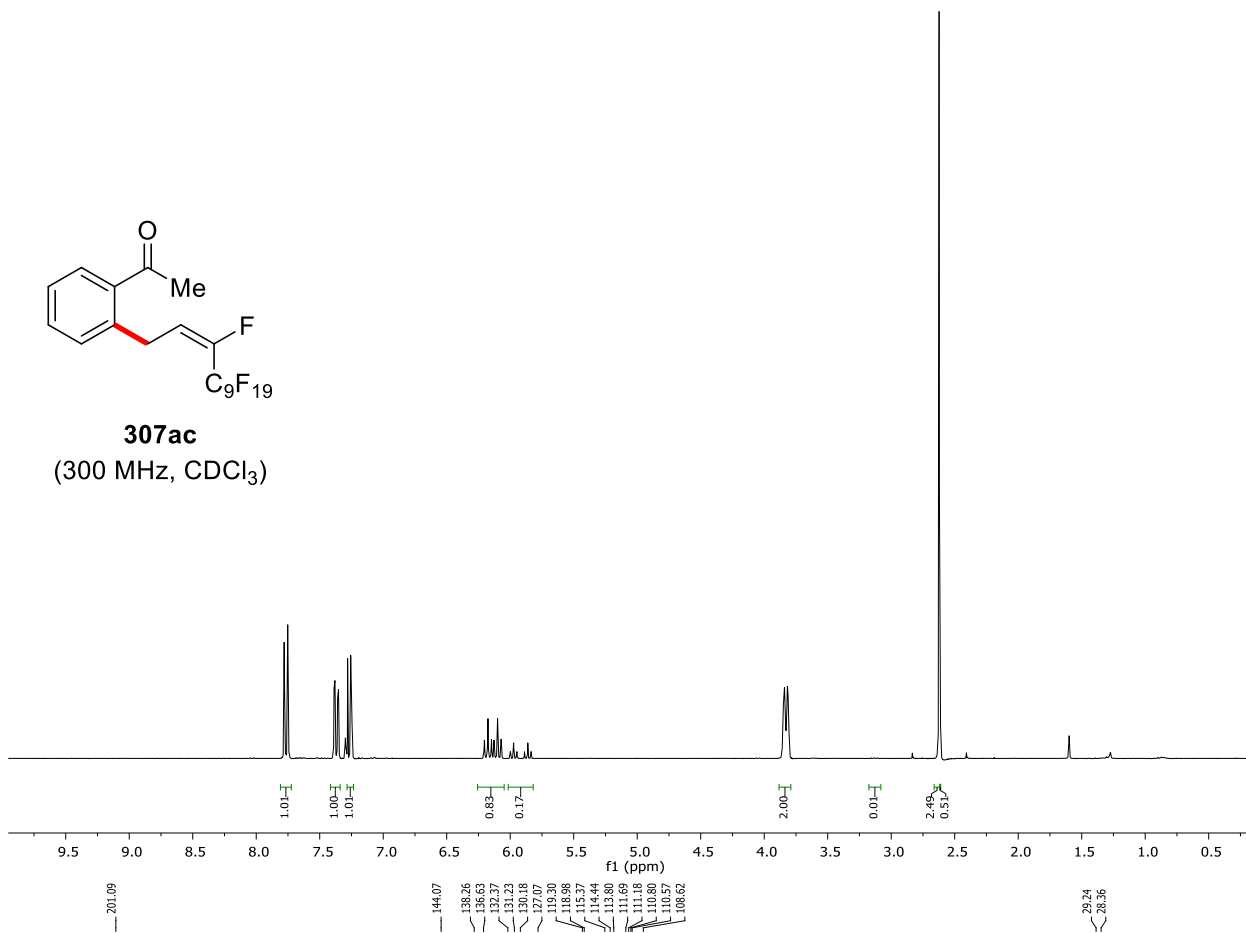
307ia
(75 MHz, CDCl₃)



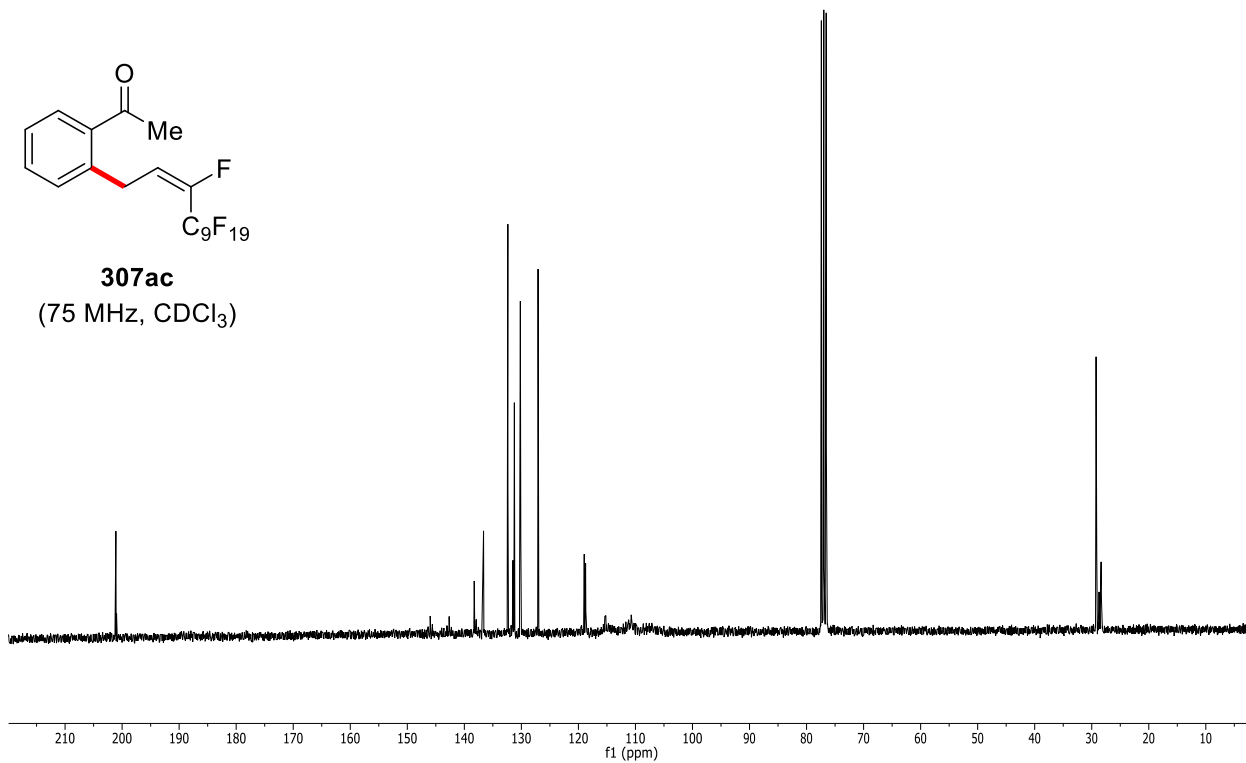


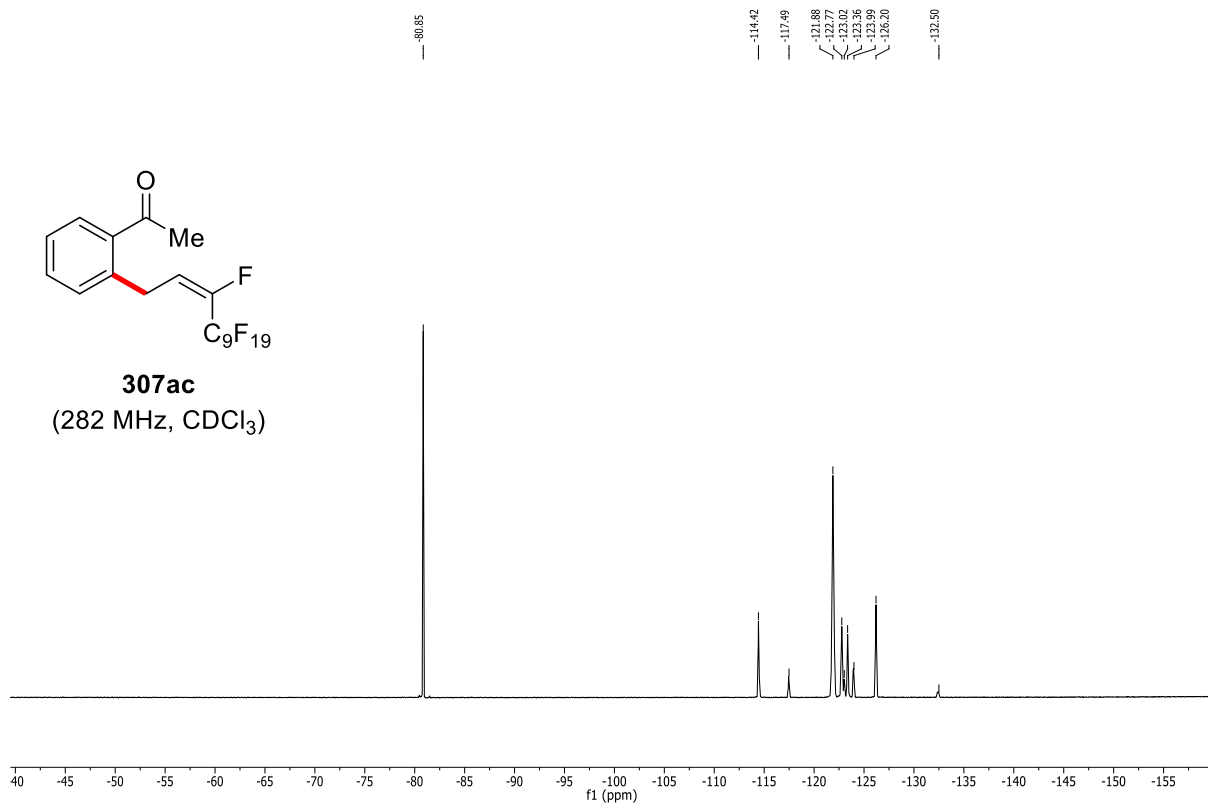


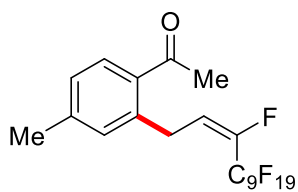
307ac
(300 MHz, CDCl₃)



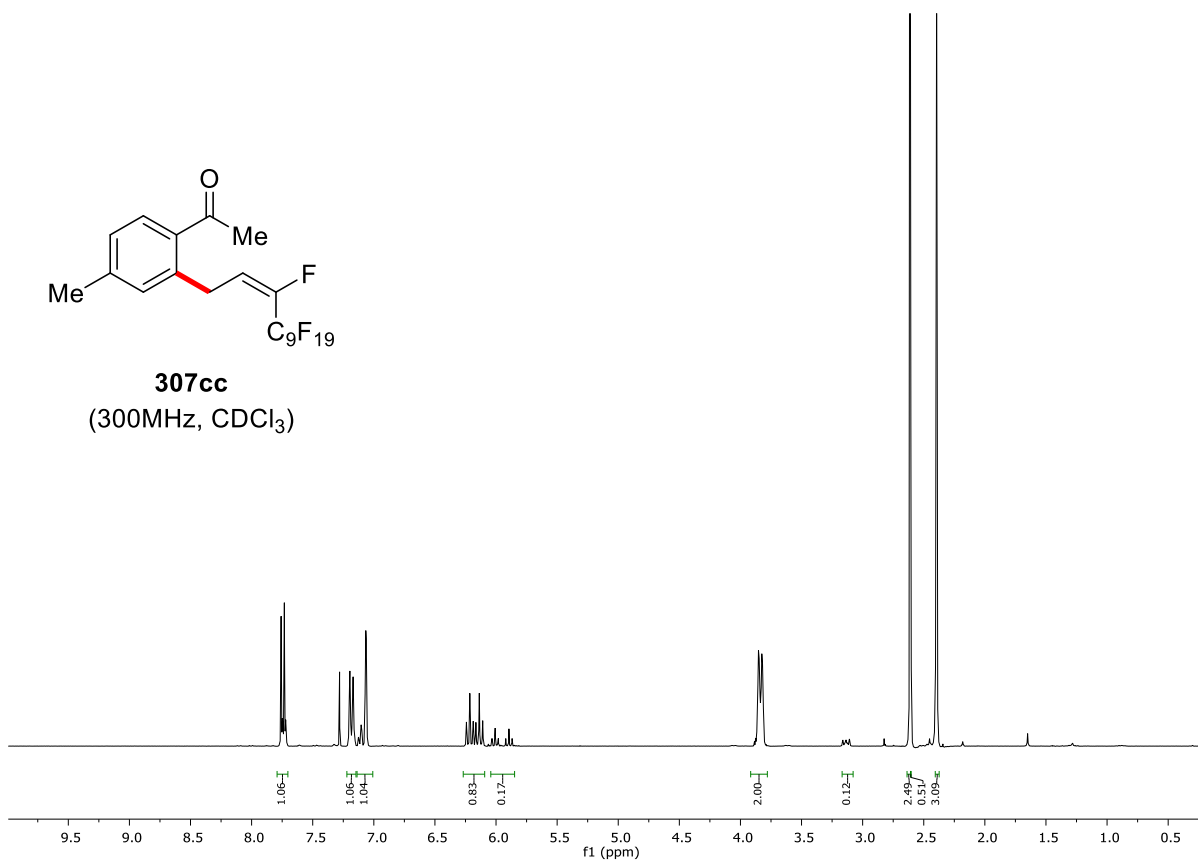
307ac
(75 MHz, CDCl₃)







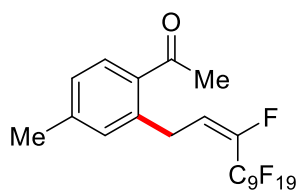
307cc
(300MHz, CDCl₃)



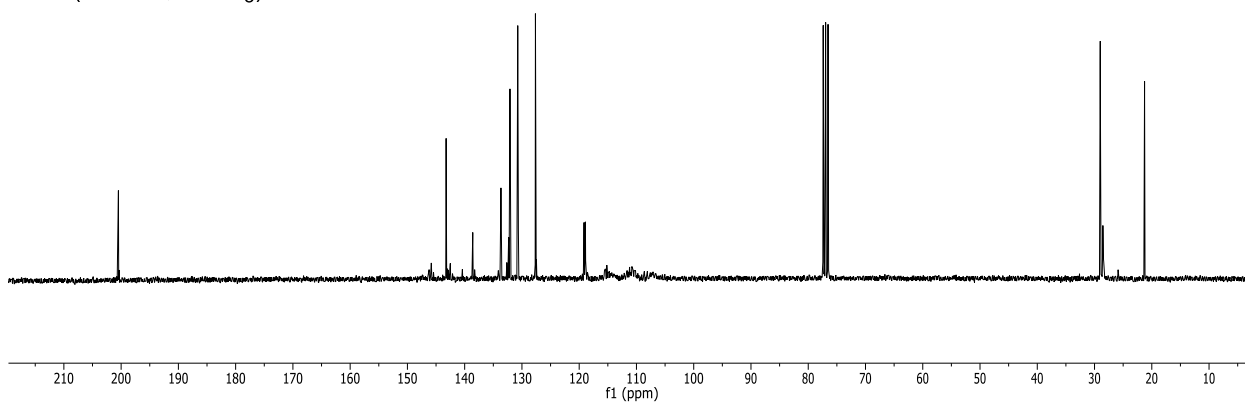
200.47

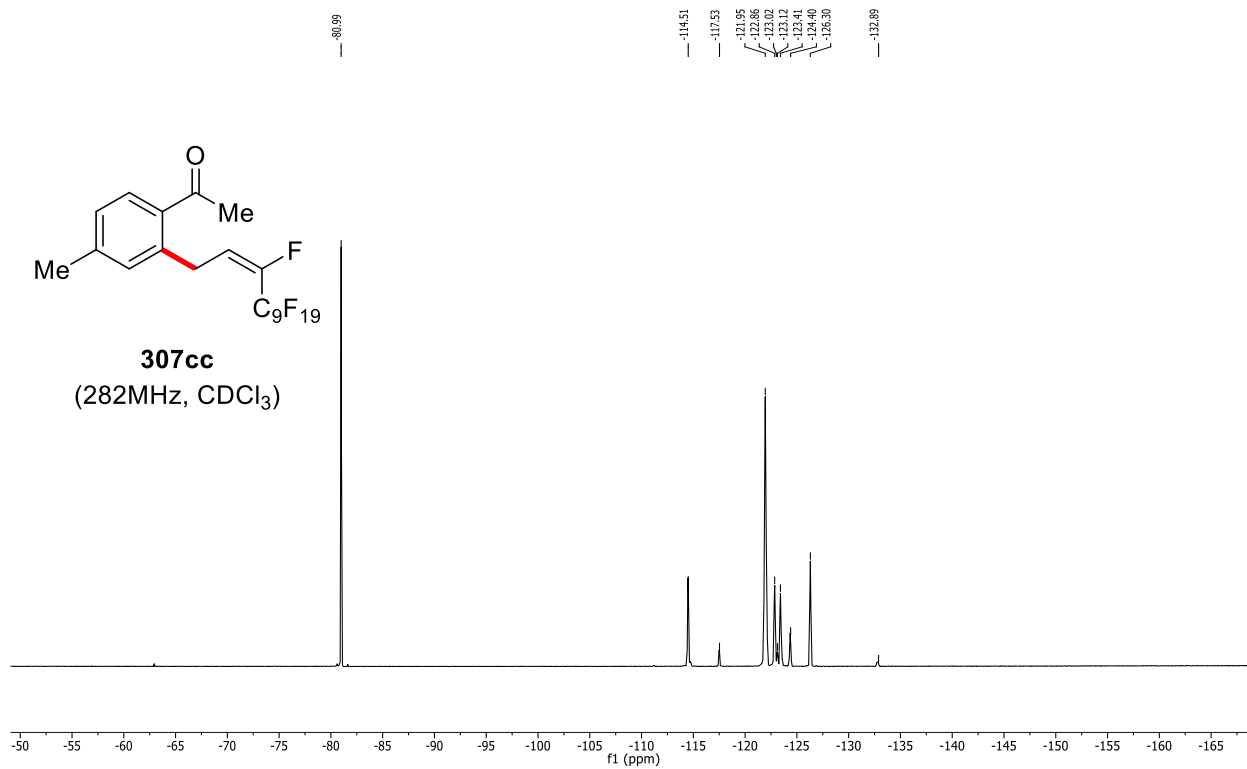
144.63
143.24
138.25
137.87
132.09
130.23
127.64
119.74
119.15
115.18
111.64
110.84
110.74
110.15
108.62
107.57
107.10

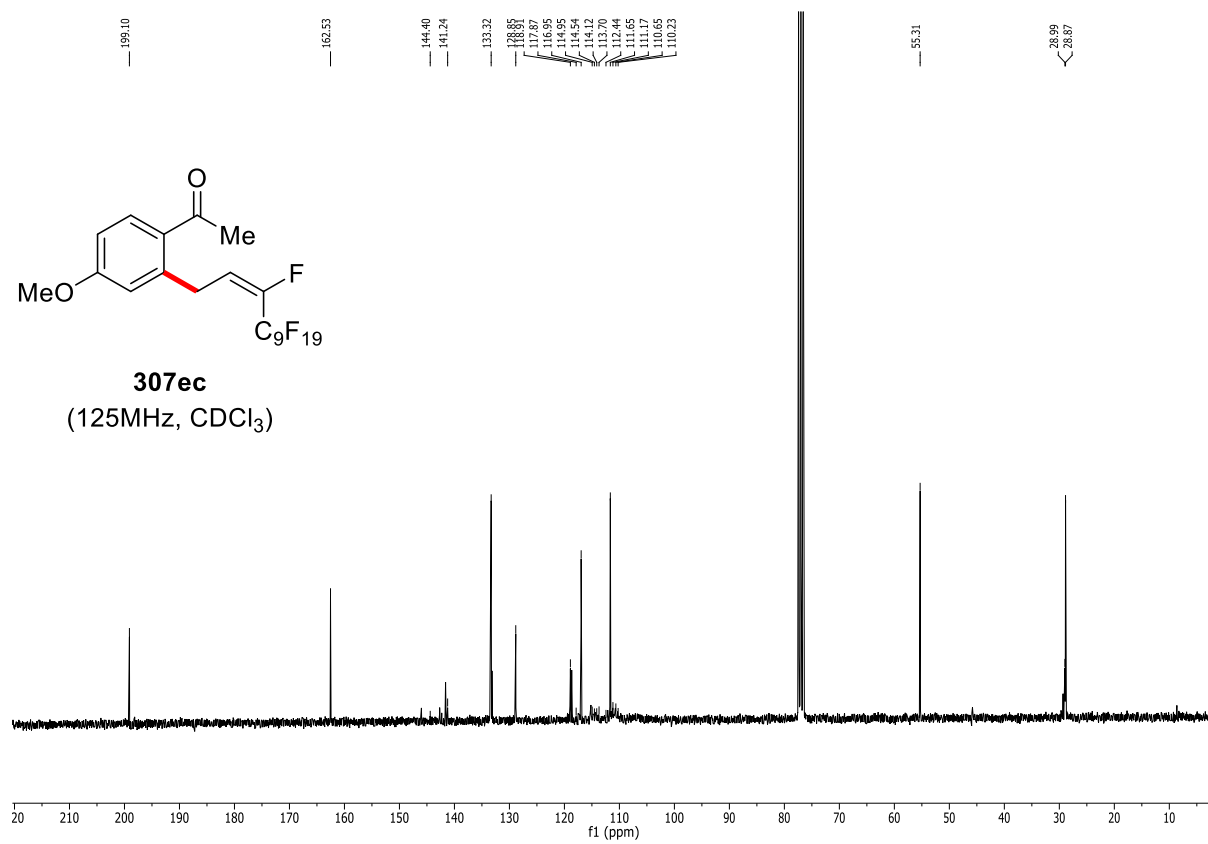
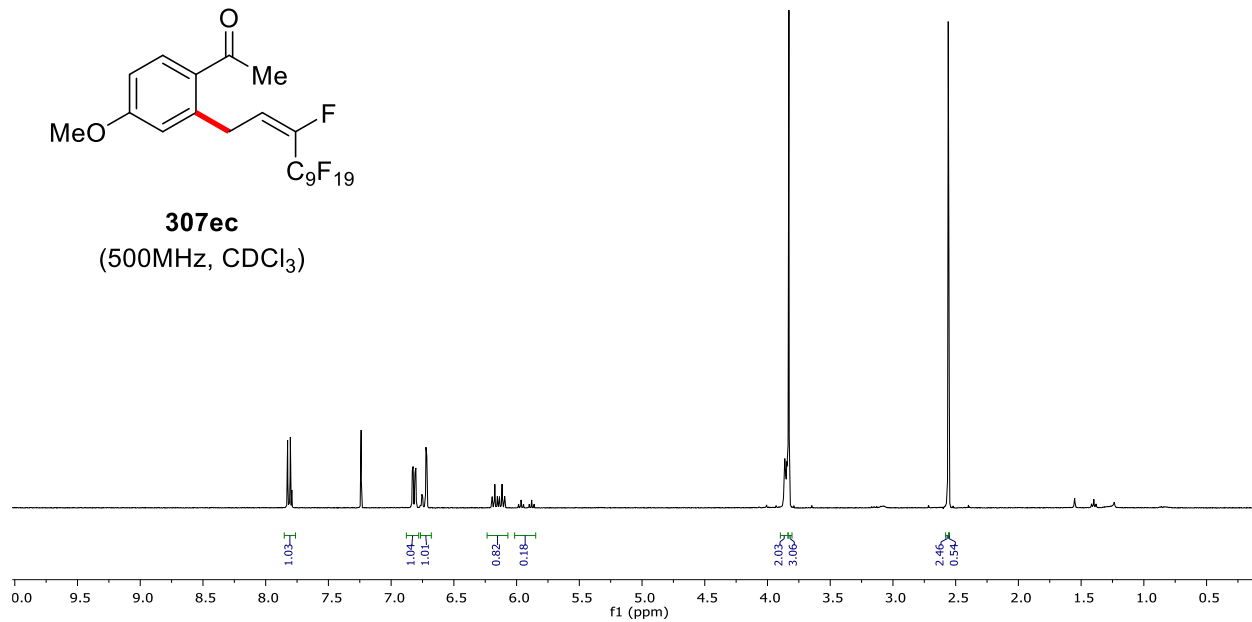
25.00
28.46
21.26

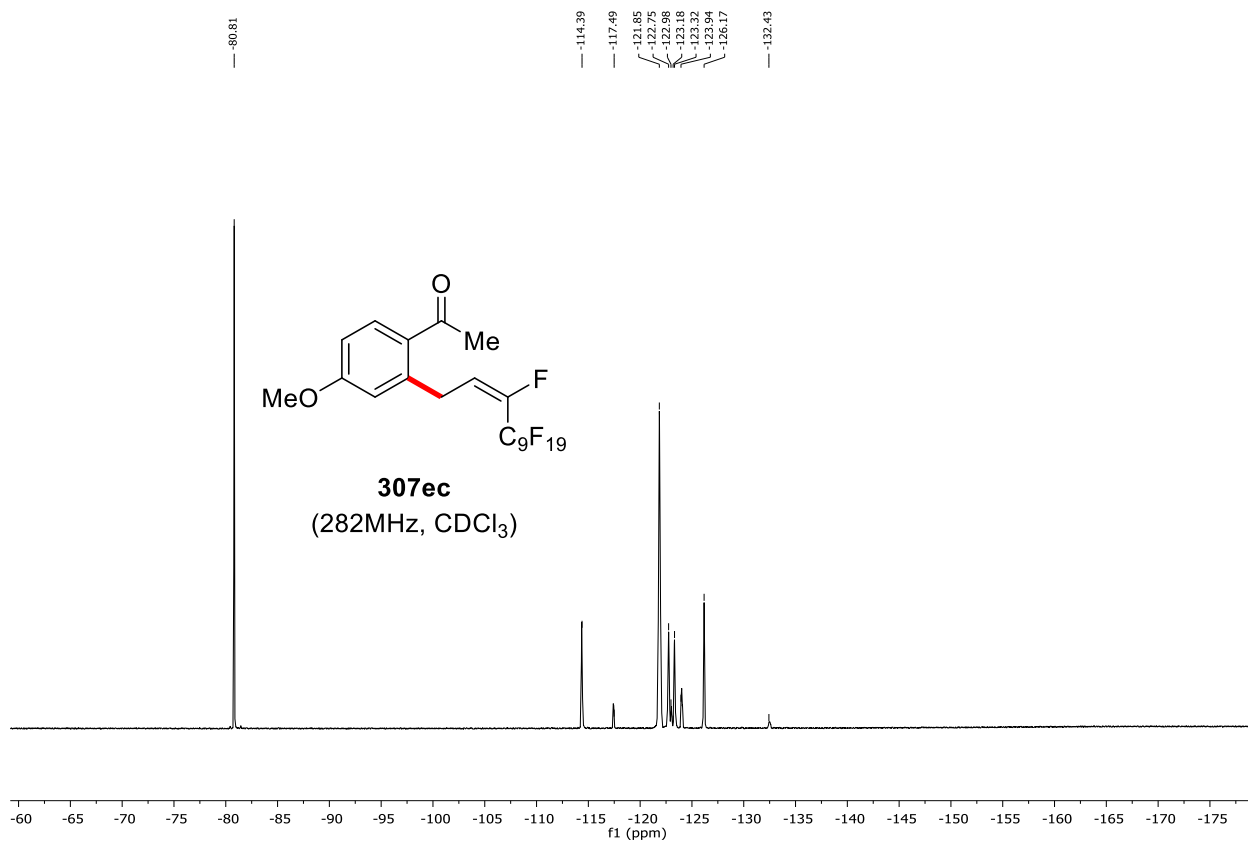


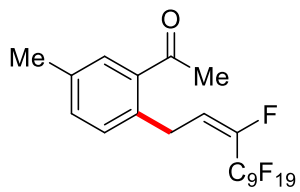
307cc
(75MHz, CDCl₃)



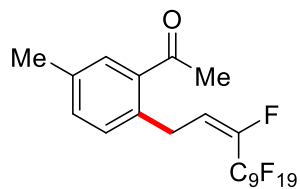
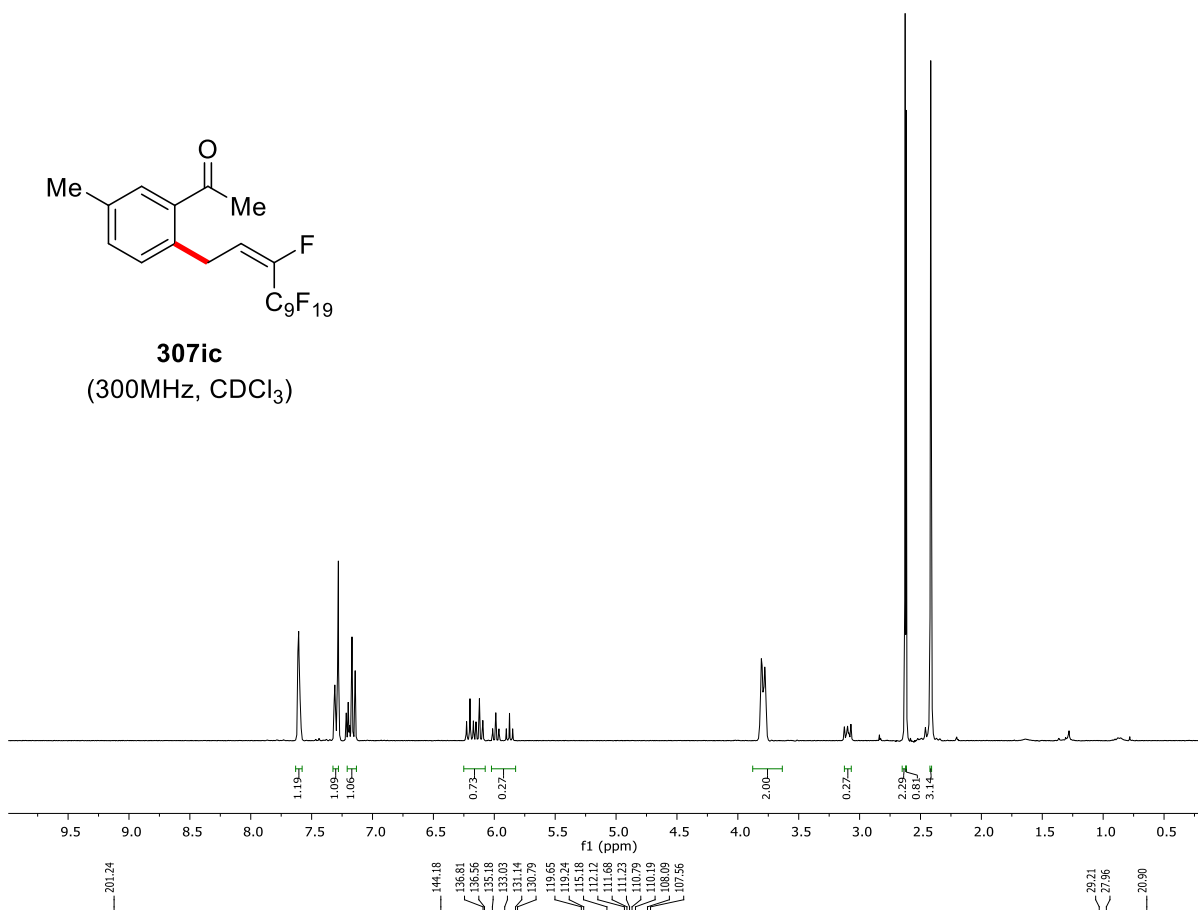




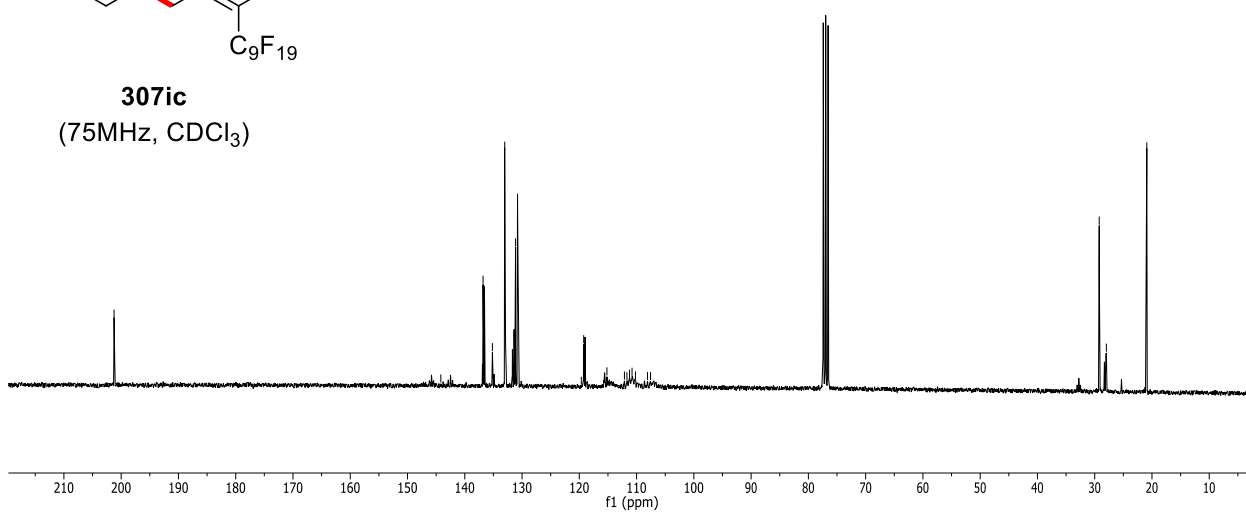


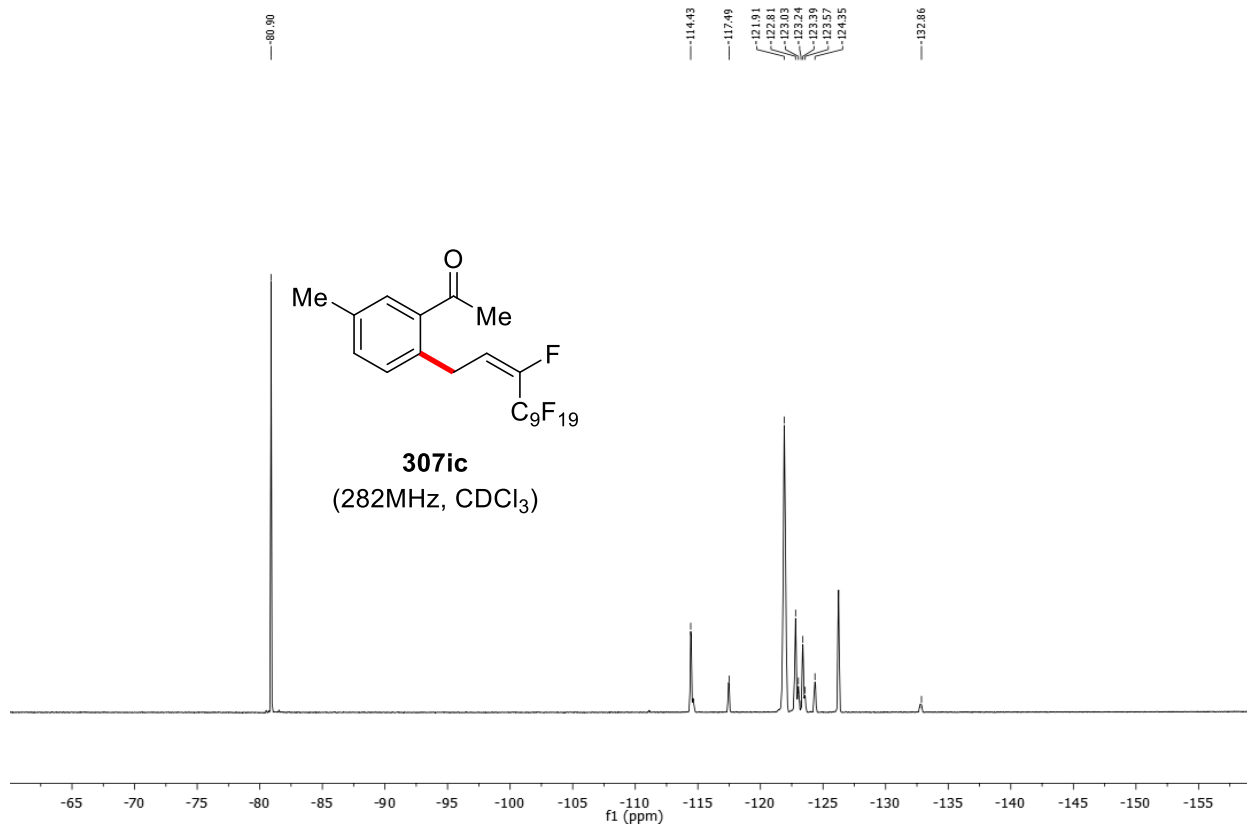


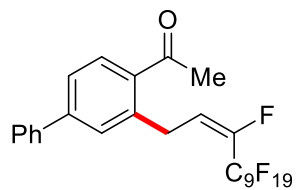
307ic
(300MHz, CDCl₃)



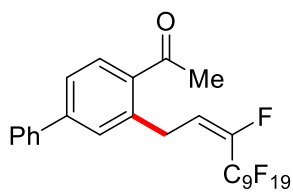
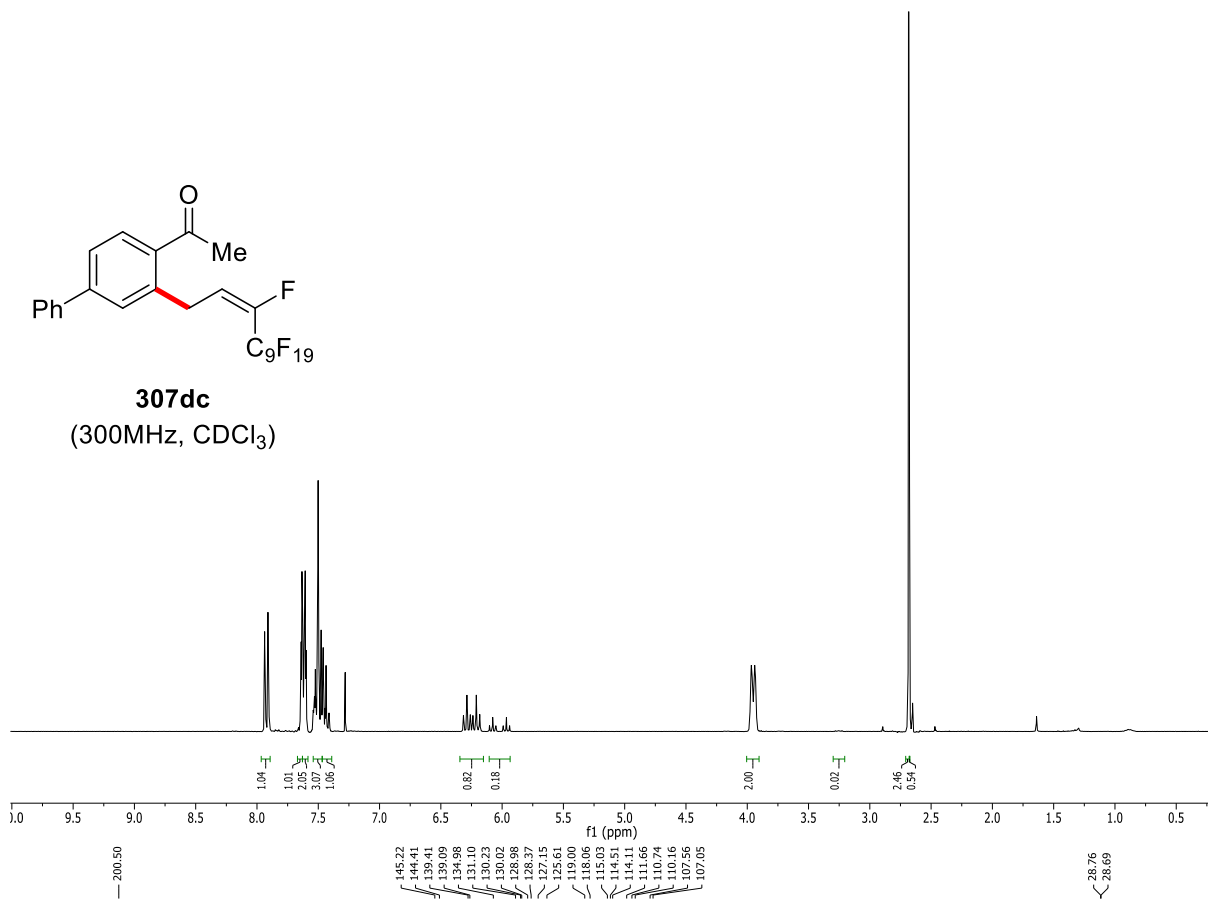
307ic
(75MHz, CDCl₃)



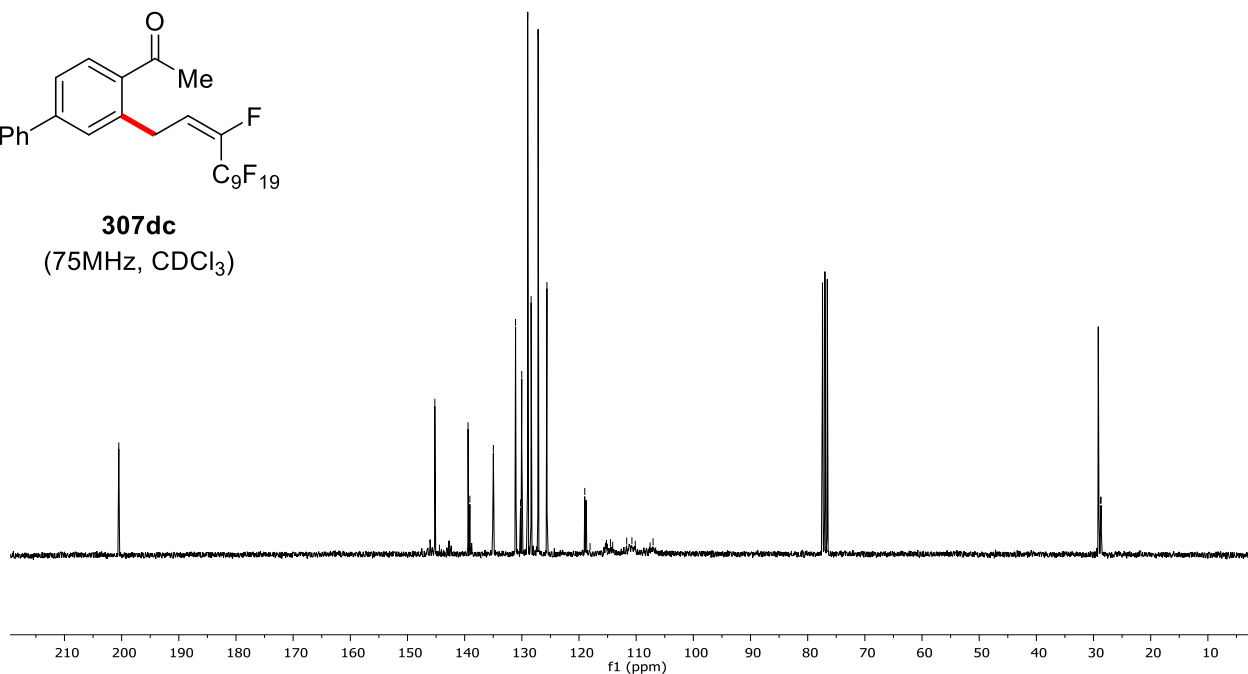


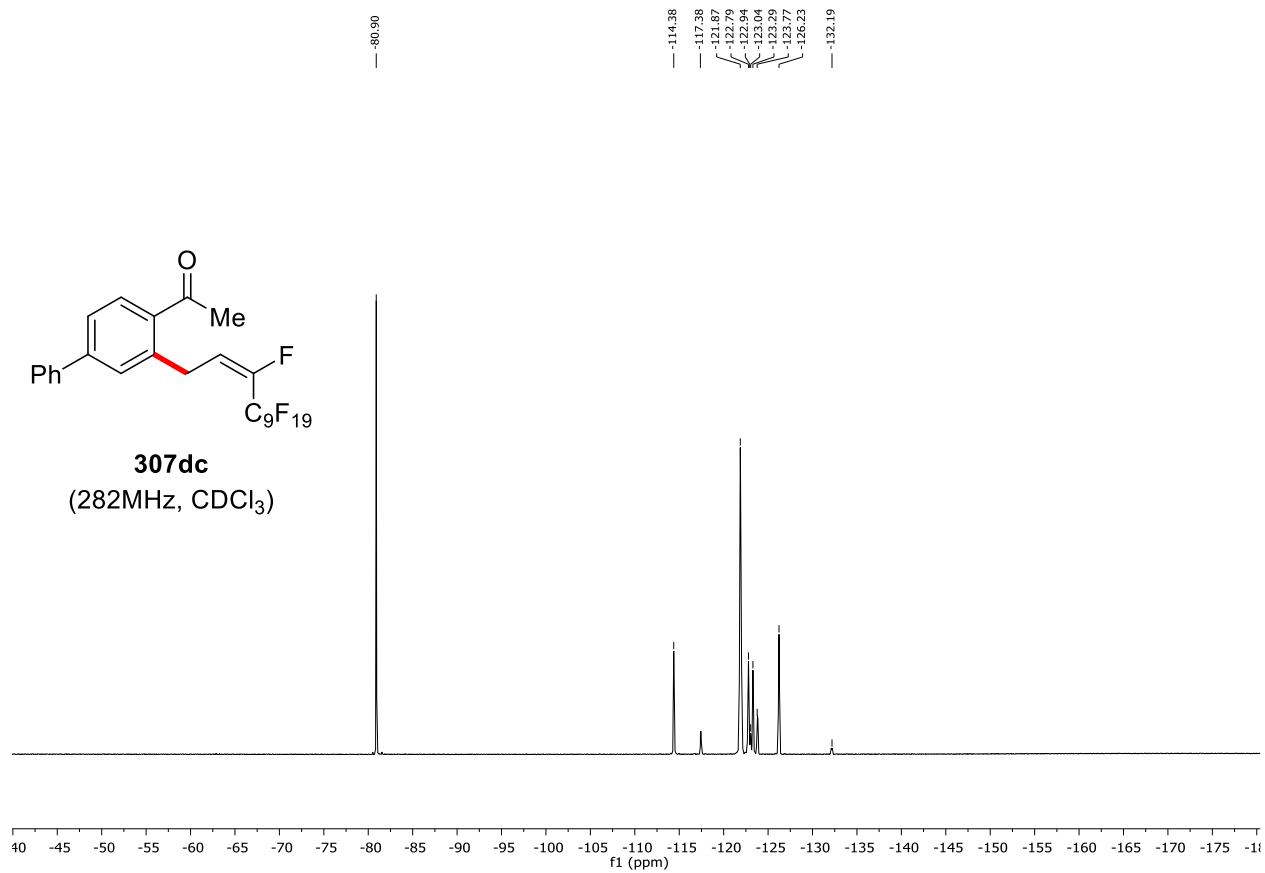


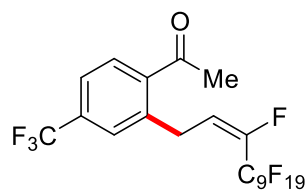
307dc
(300MHz, CDCl₃)



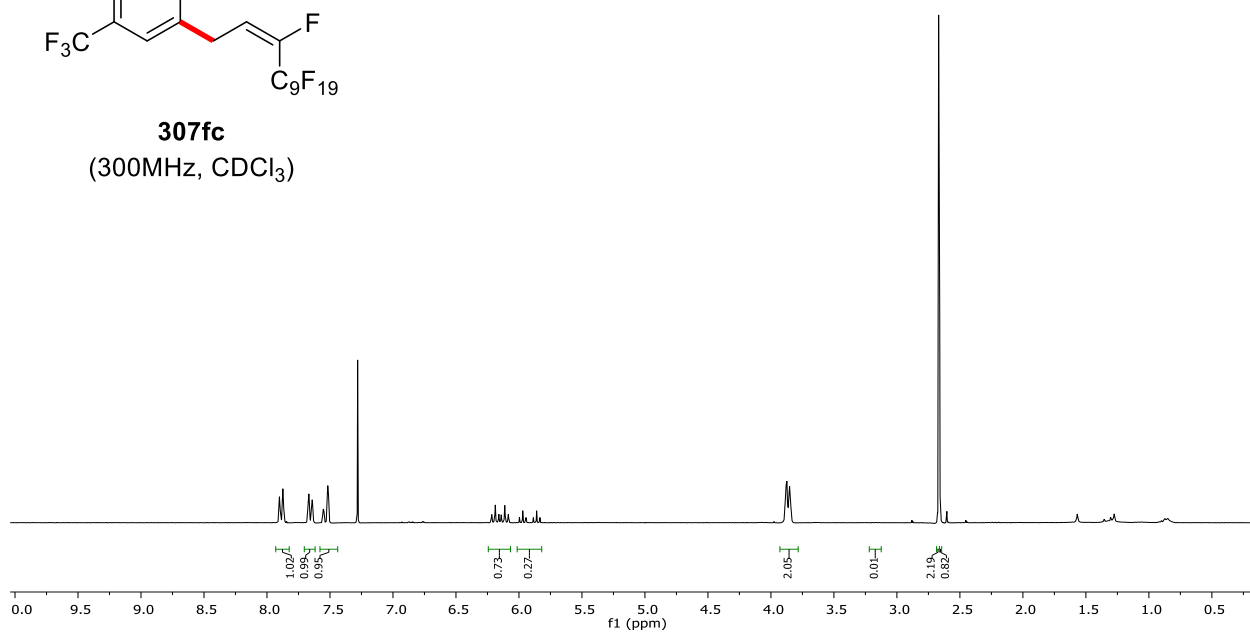
307dc
(75MHz, CDCl₃)







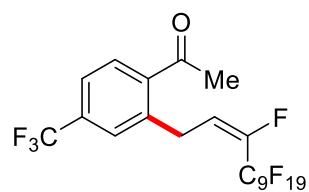
307fc
(300MHz, CDCl₃)



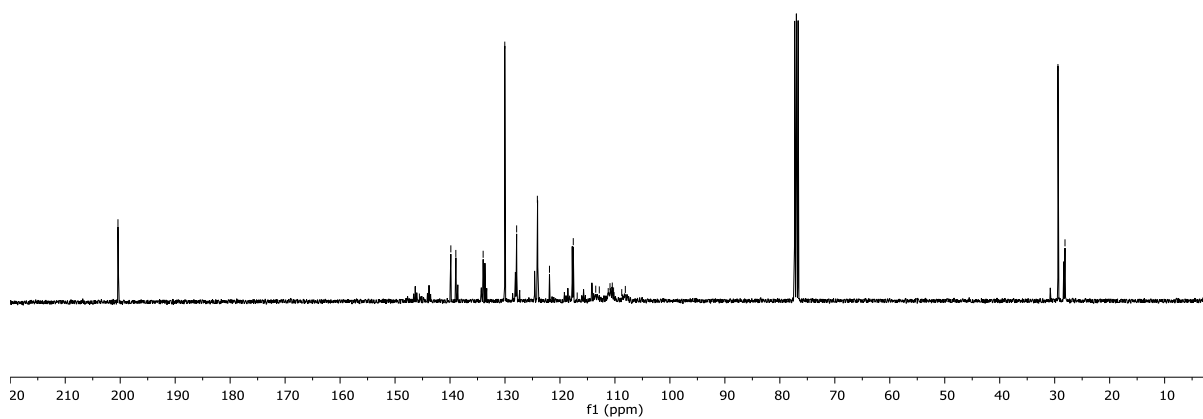
200.41

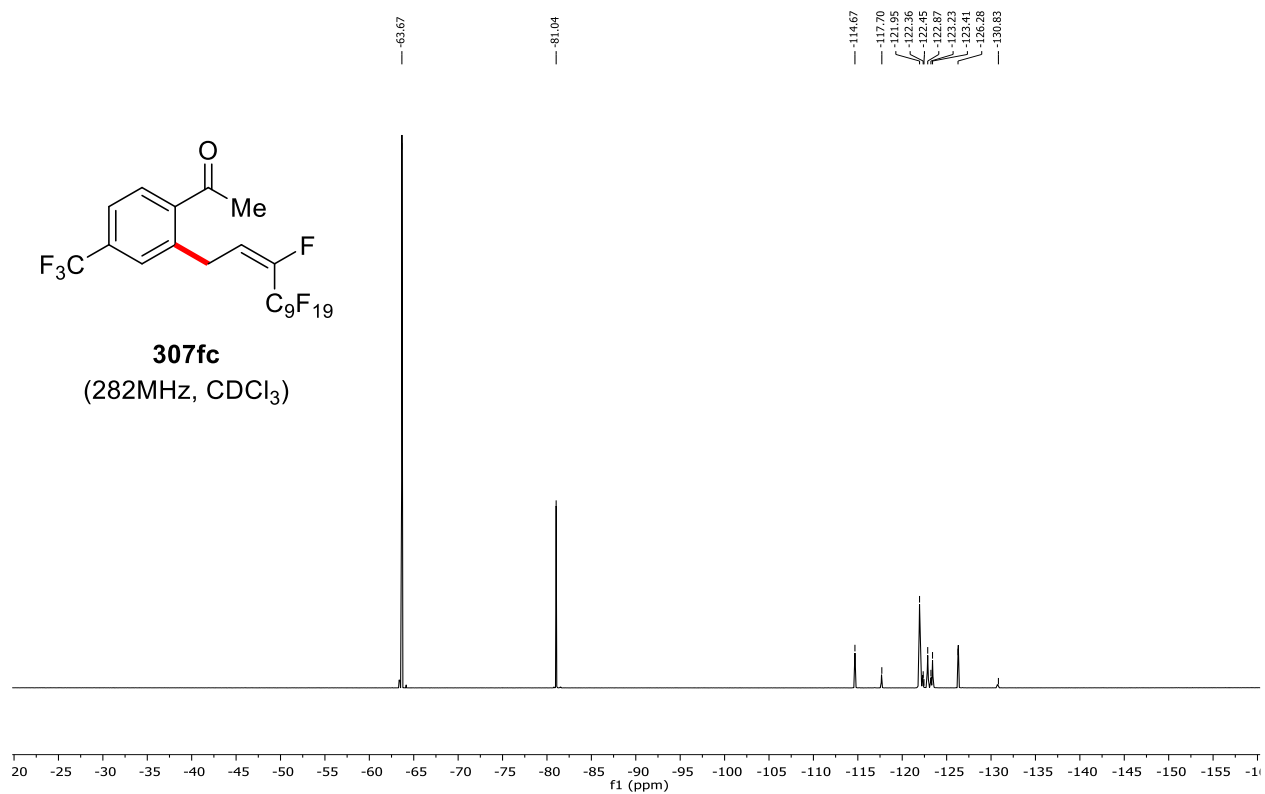
146.57
139.85
138.94
133.98
130.04
127.86
127.11
121.91
117.58
116.87
113.49
112.84
111.22
109.98
110.25
108.76
108.11

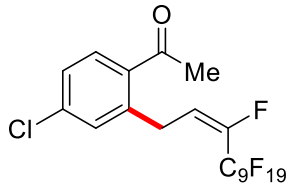
29.41
28.12



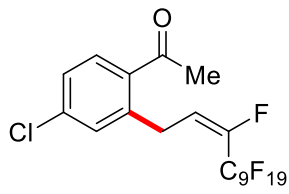
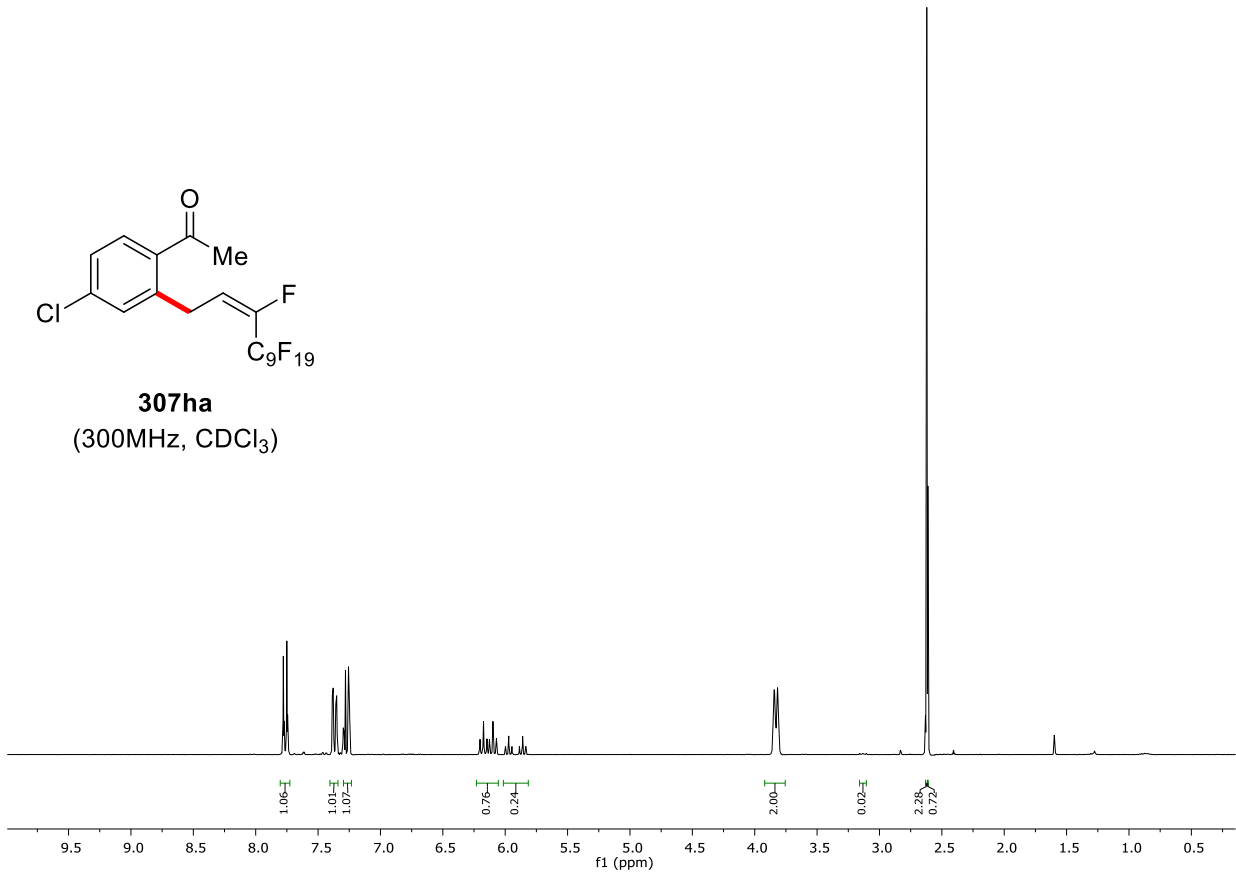
307fc
(100MHz, CDCl₃)



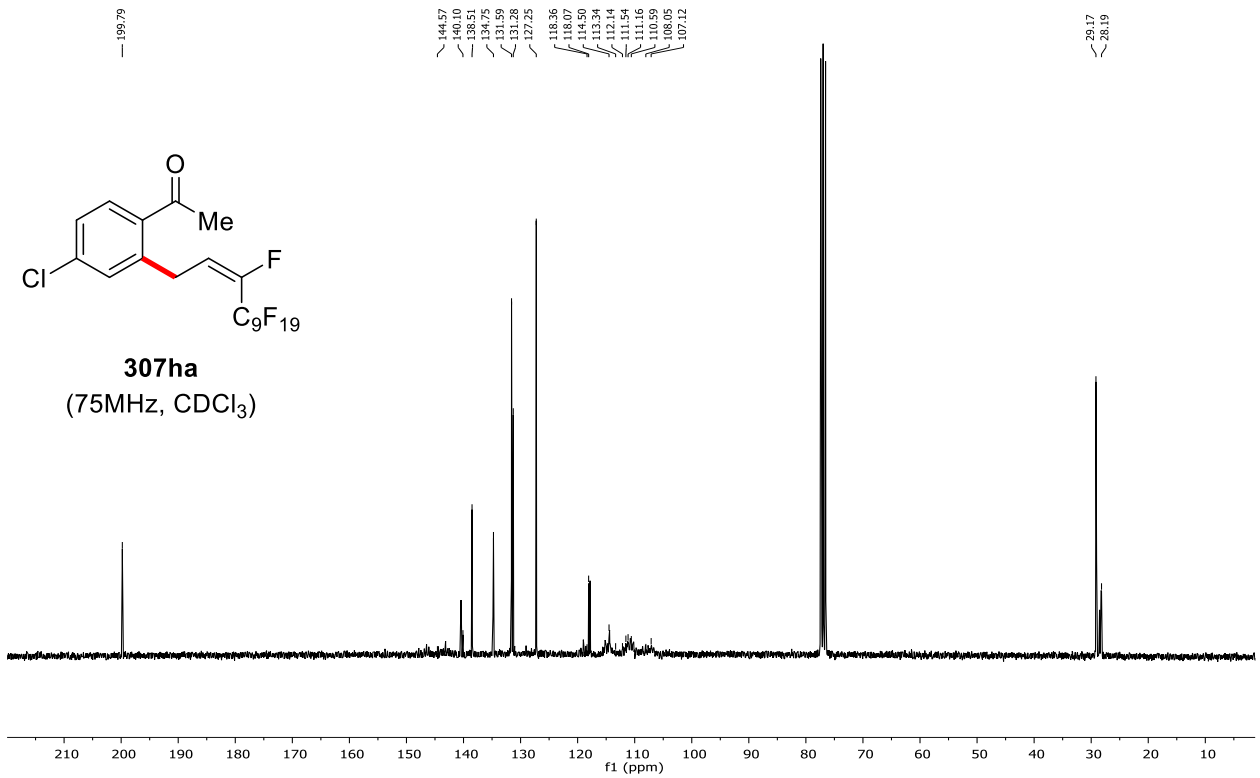


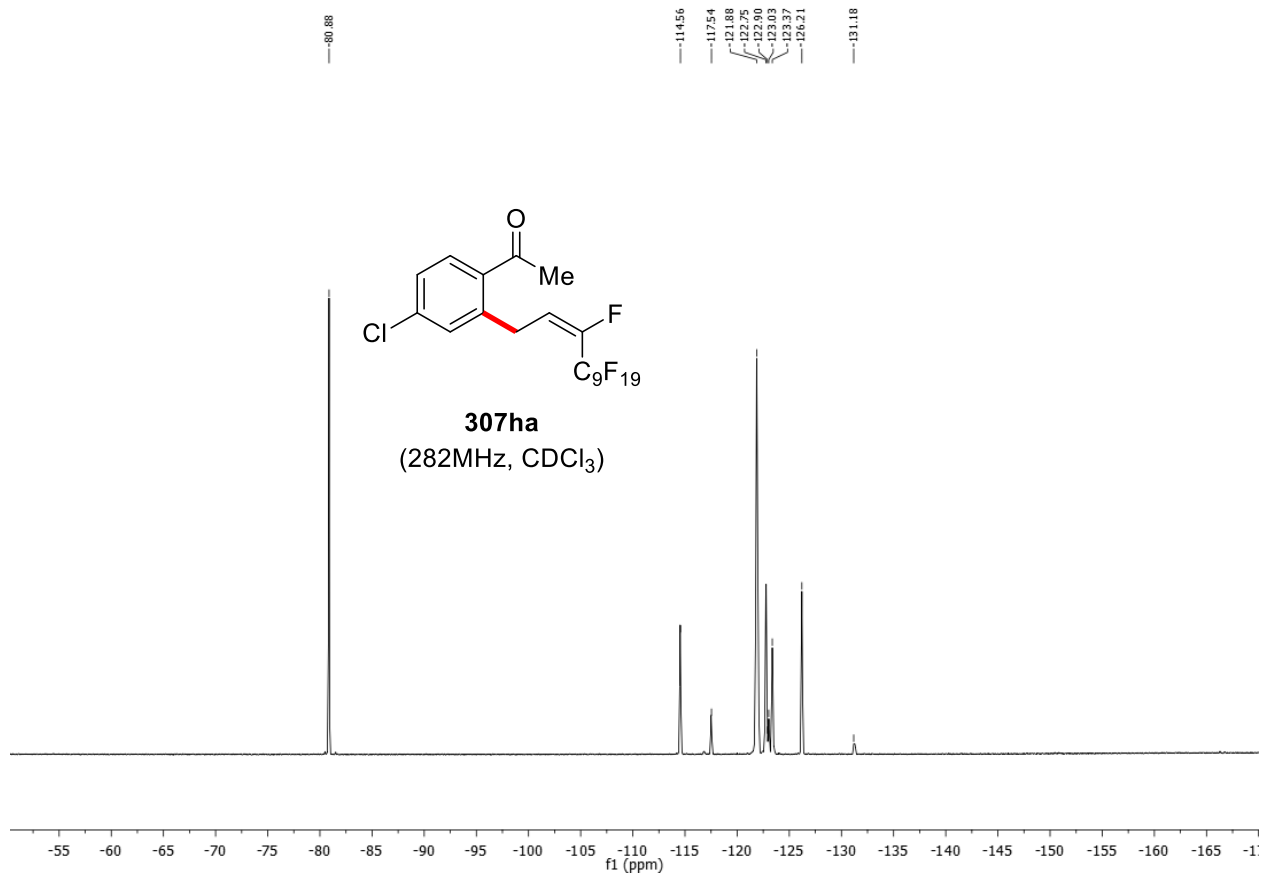


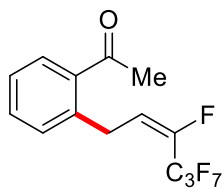
307ha
(300MHz, CDCl₃)



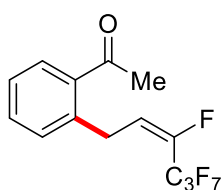
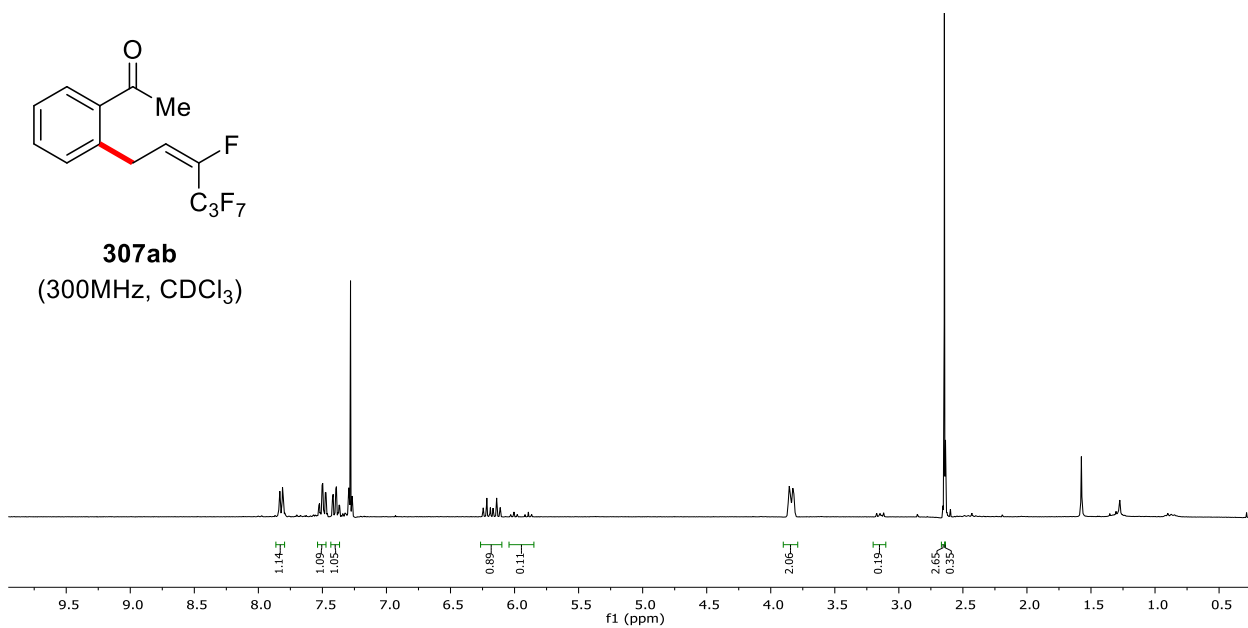
307ha
(75MHz, CDCl₃)



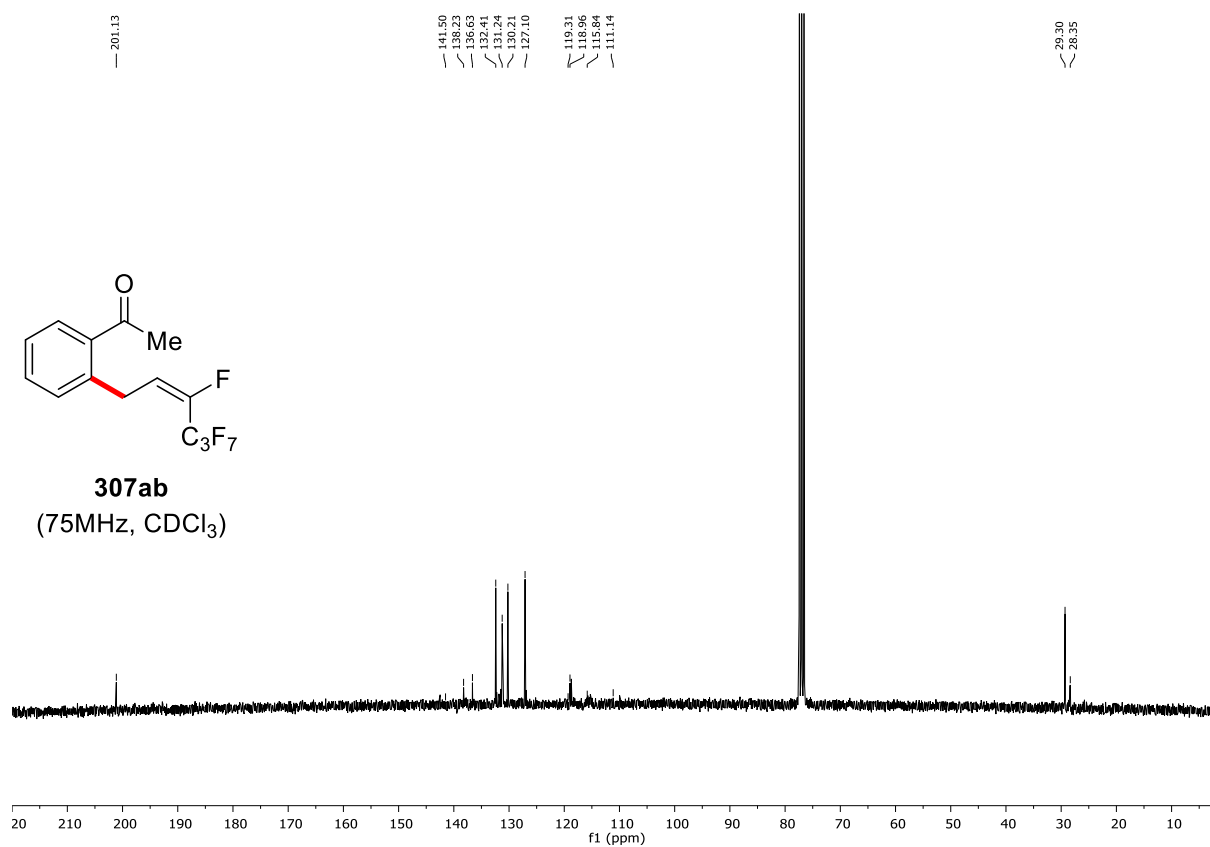


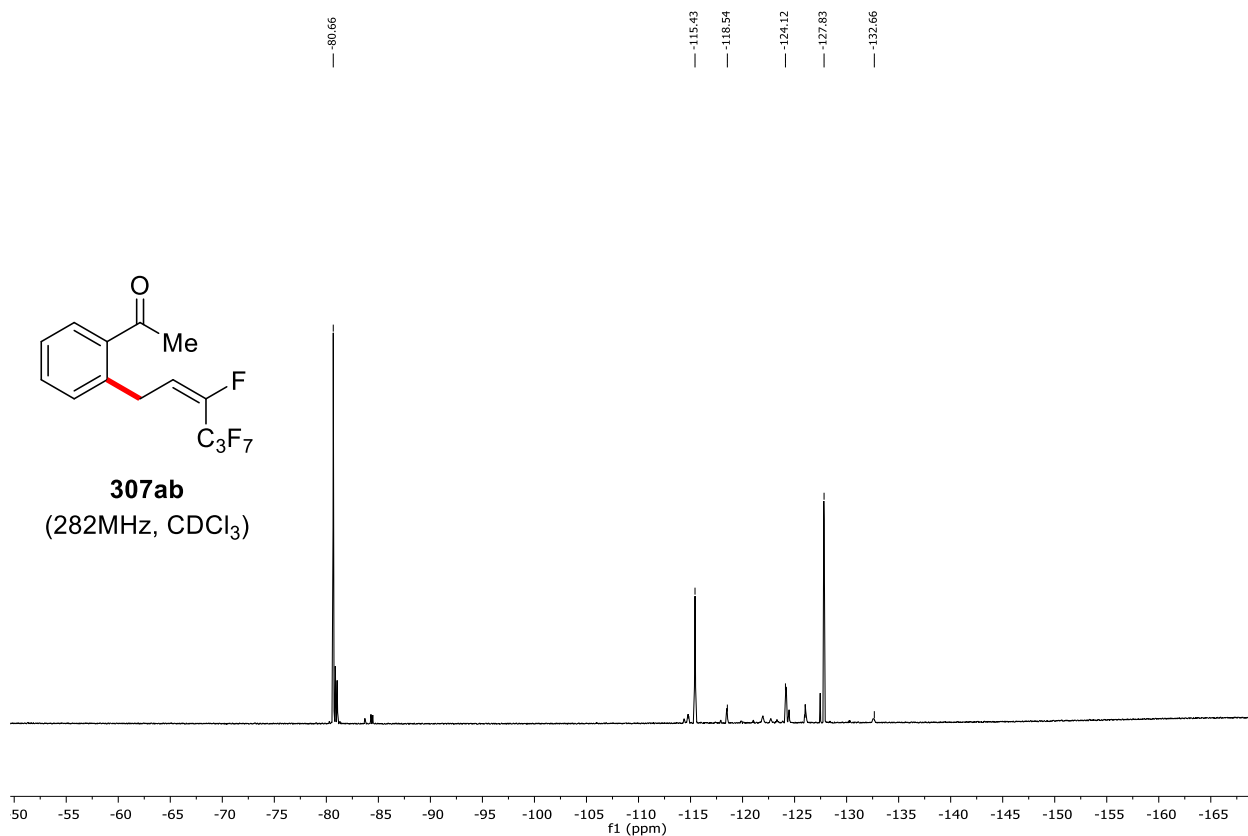


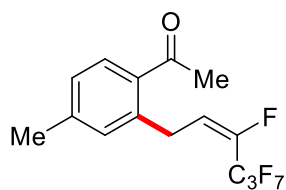
307ab
(300MHz, CDCl₃)



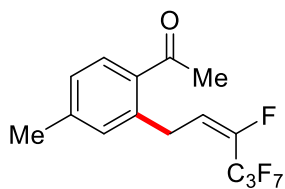
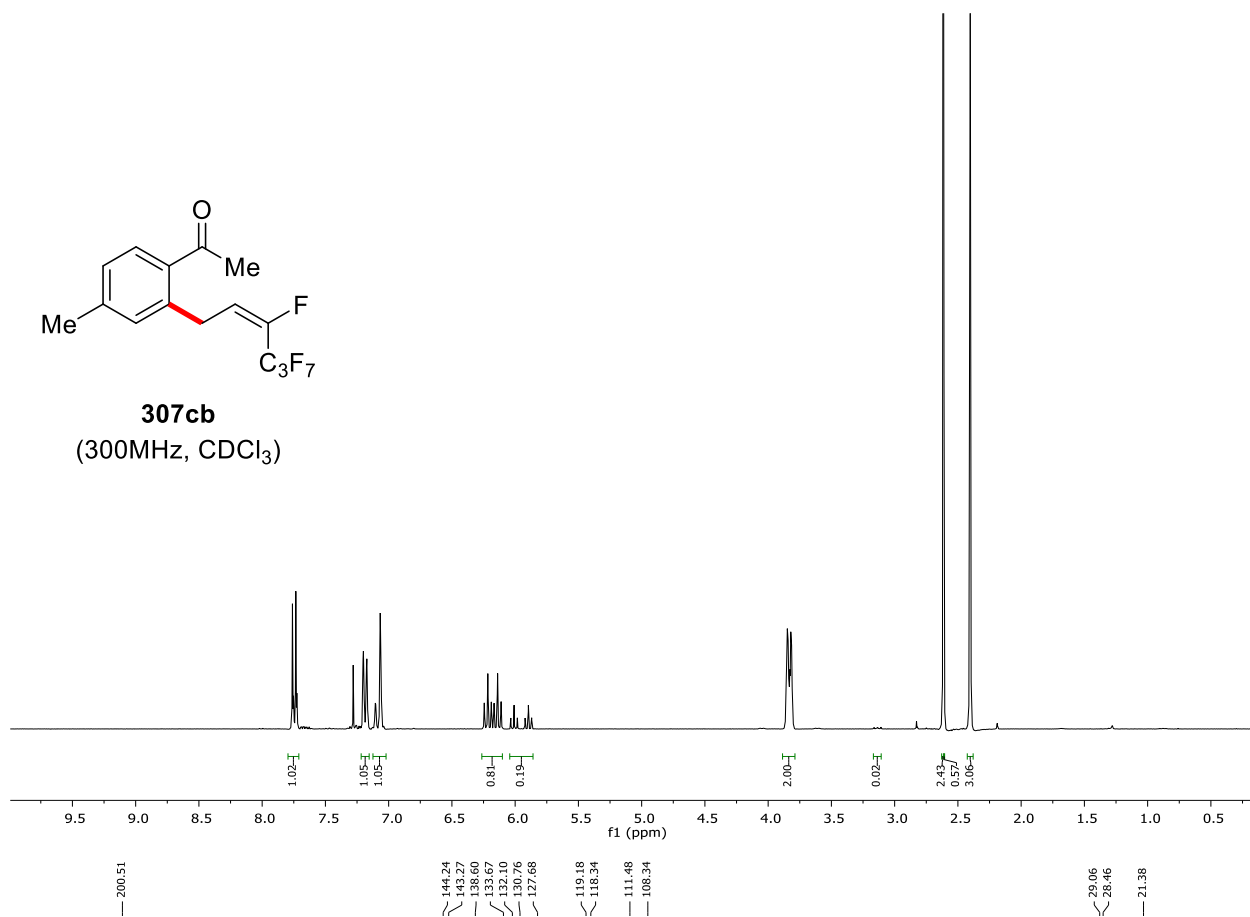
307ab
(75MHz, CDCl₃)



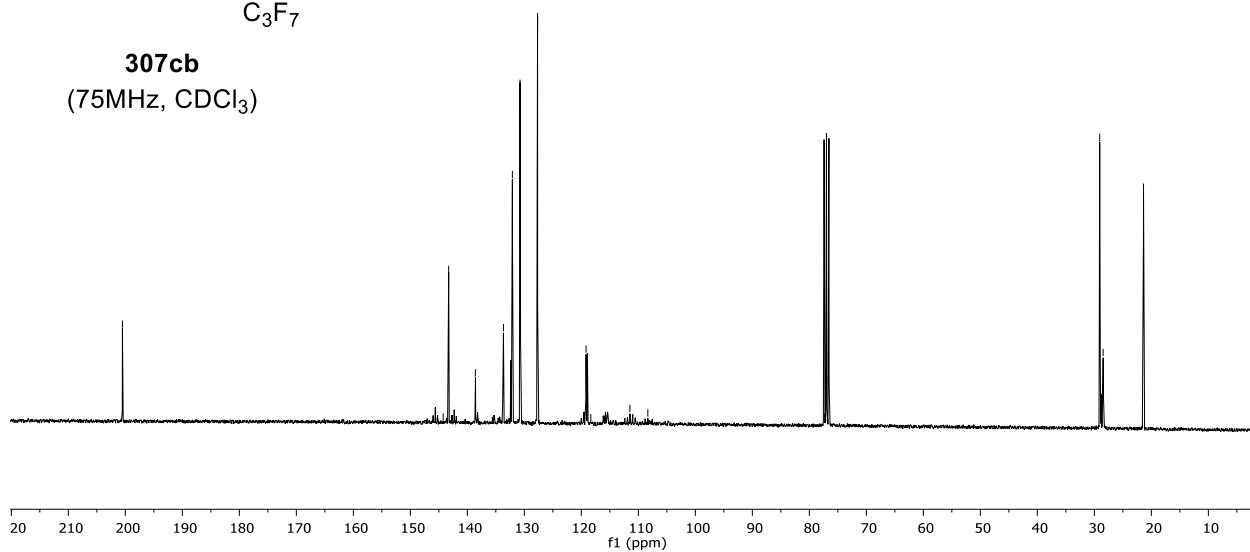


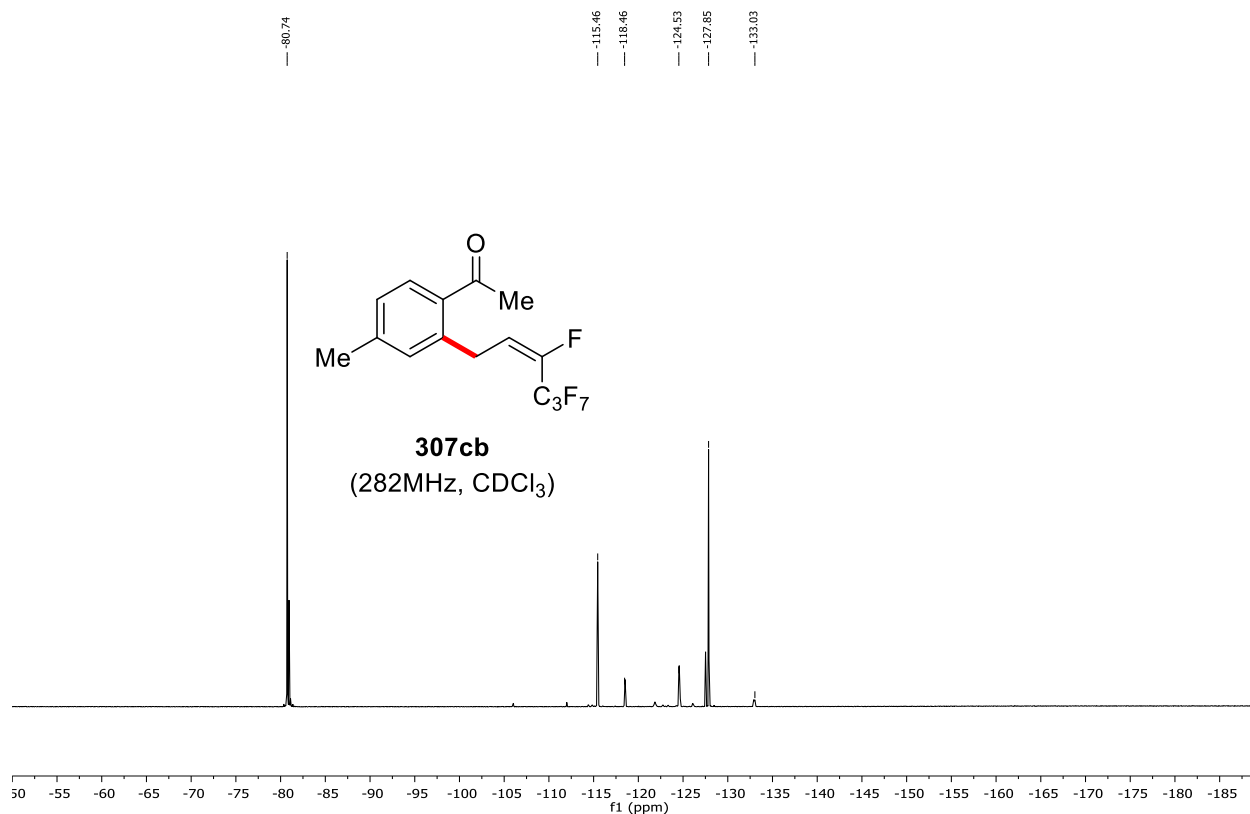


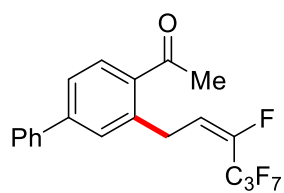
307cb
(300MHz, CDCl₃)



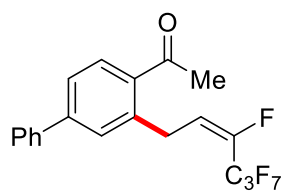
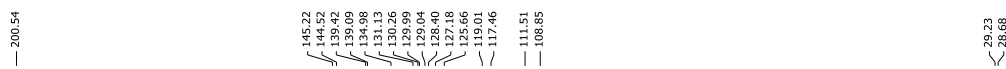
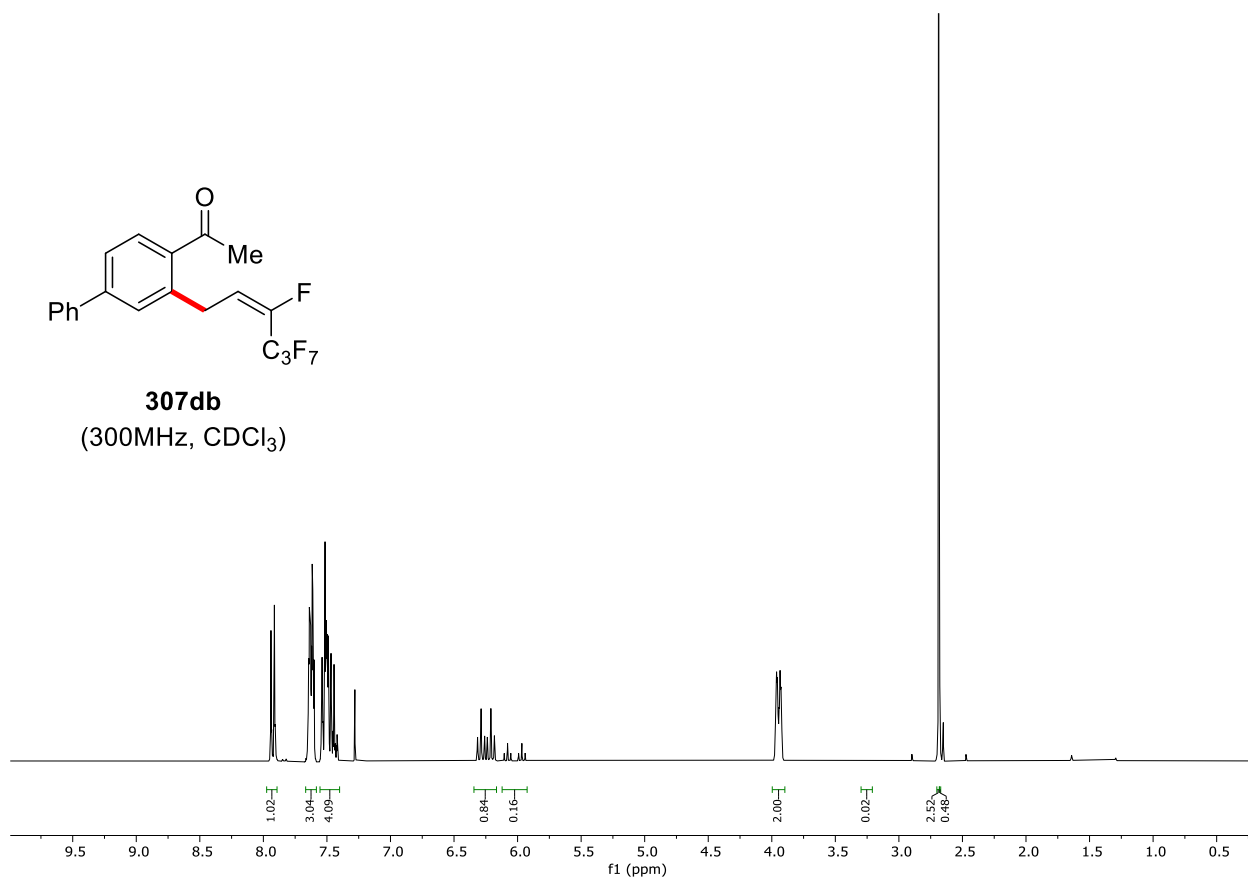
307cb
(75MHz, CDCl₃)



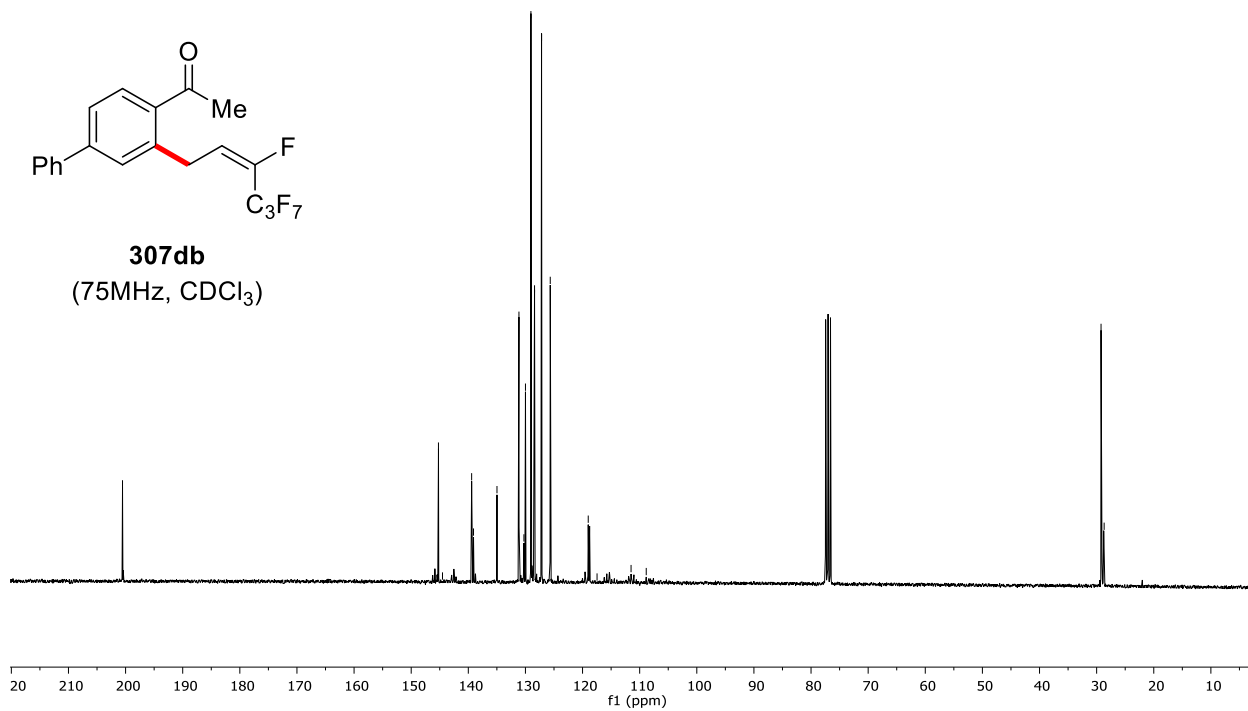


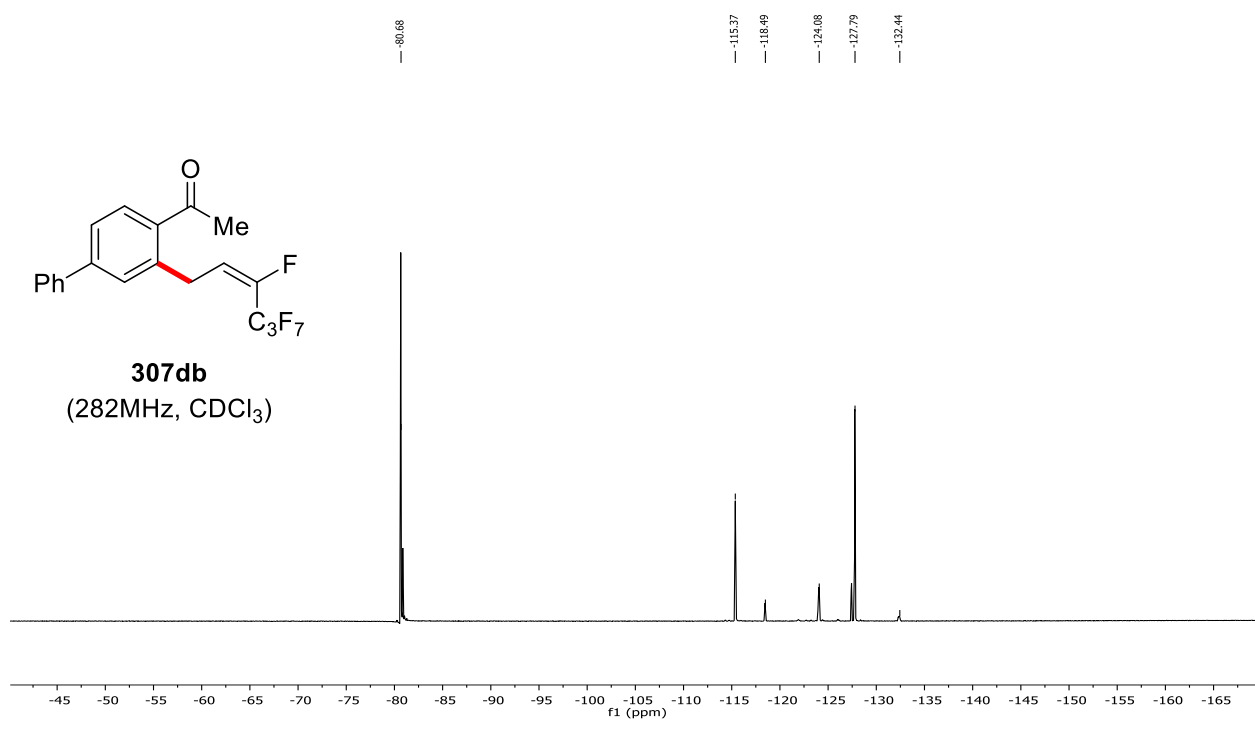


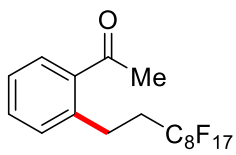
307db
(300MHz, CDCl₃)



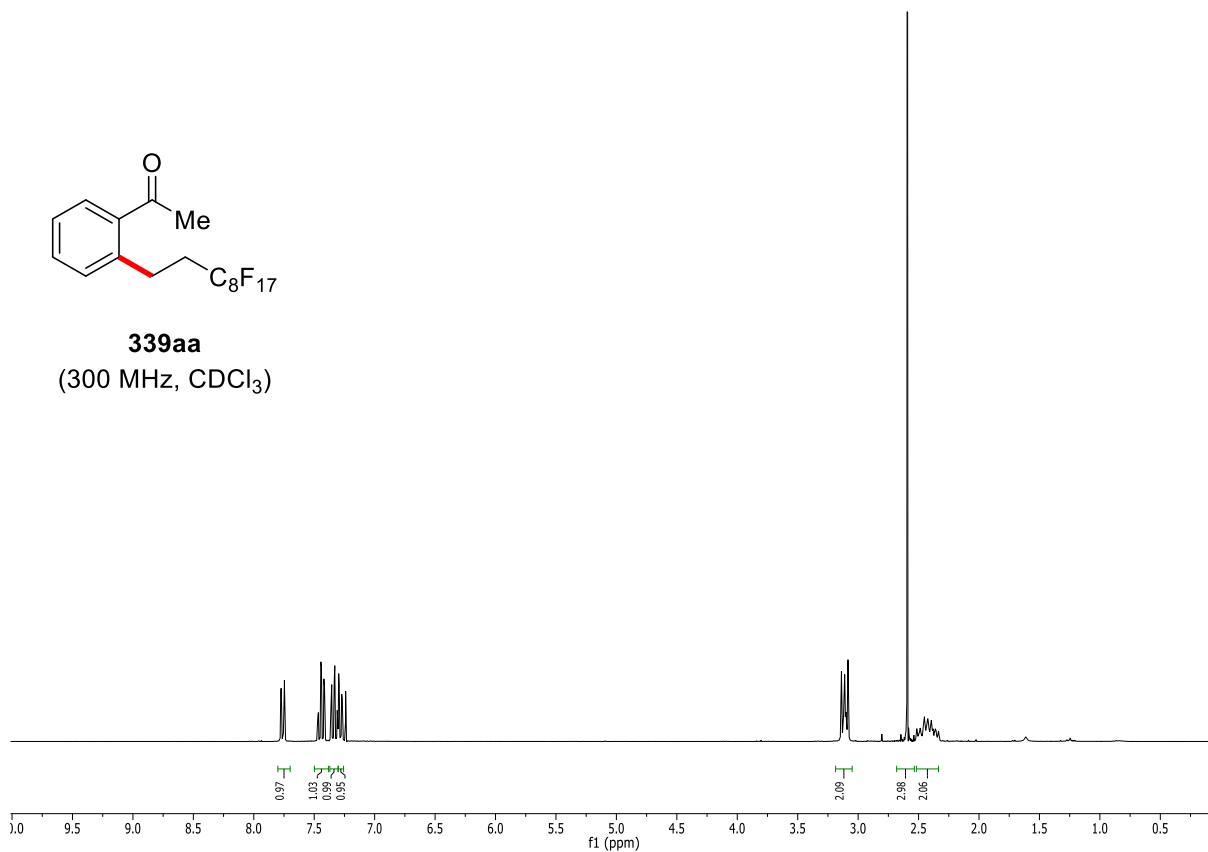
307db
(75MHz, CDCl₃)







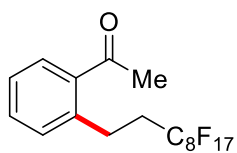
339aa
(300 MHz, CDCl₃)



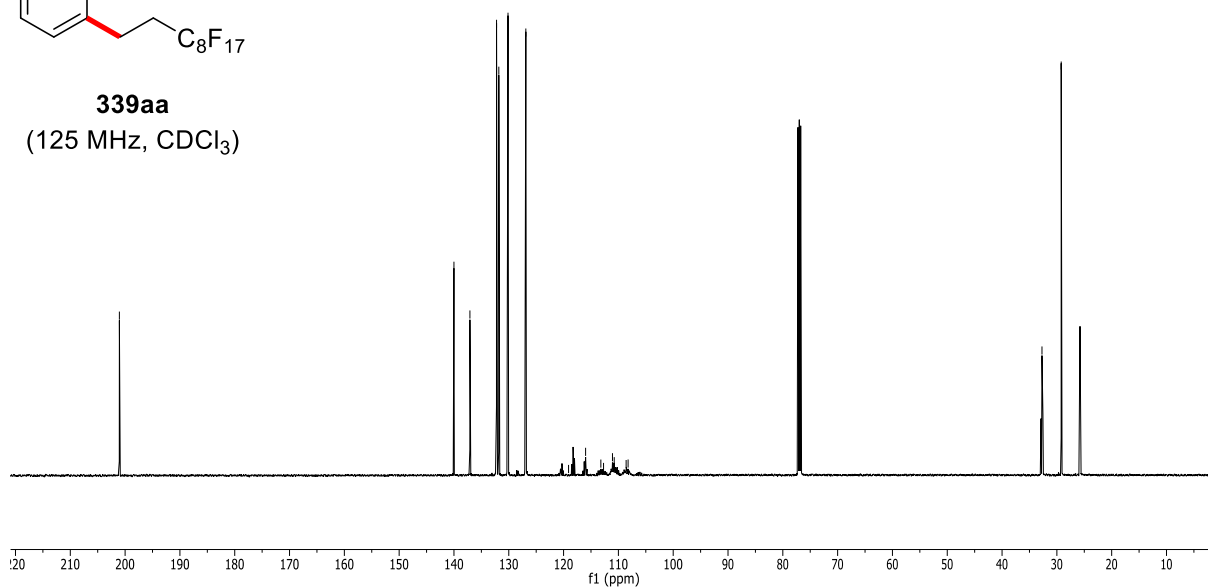
201.04

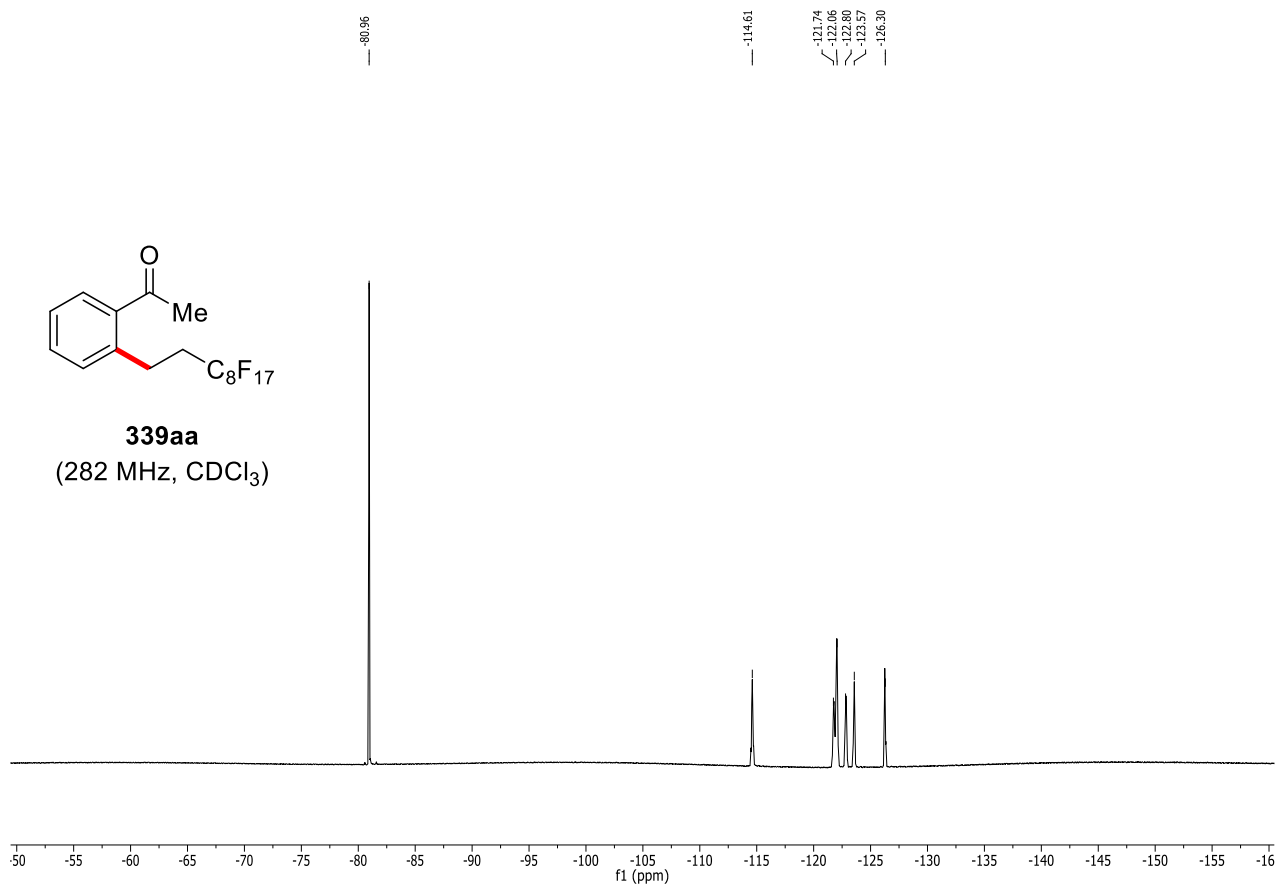
140.01
137.09
132.23
131.62
130.14
126.89
119.09
115.98
113.20
112.71
111.08
110.76
108.39
108.23

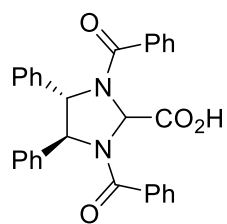
32.72
32.71
25.75



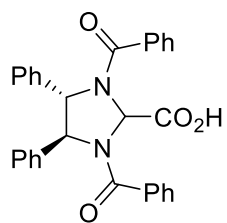
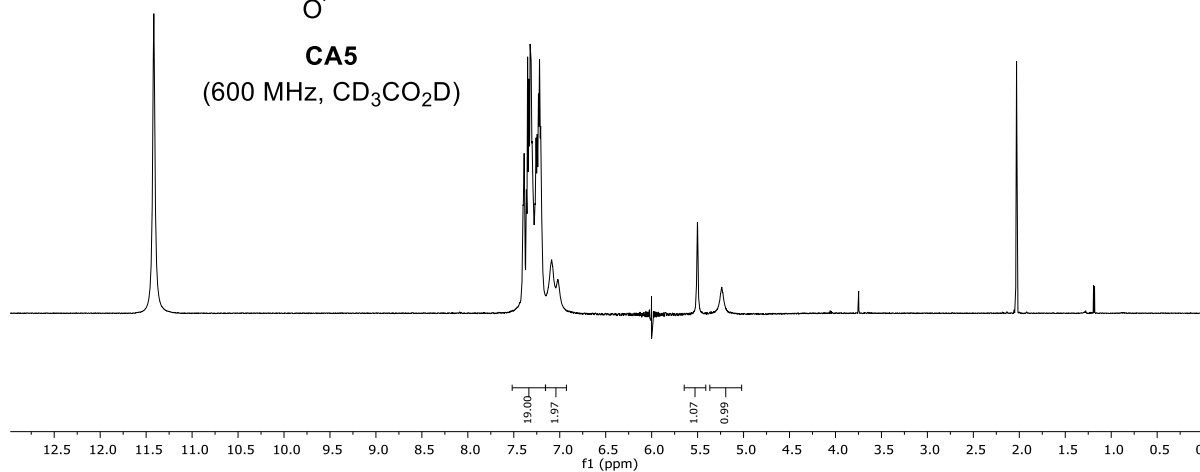
339aa
(125 MHz, CDCl₃)



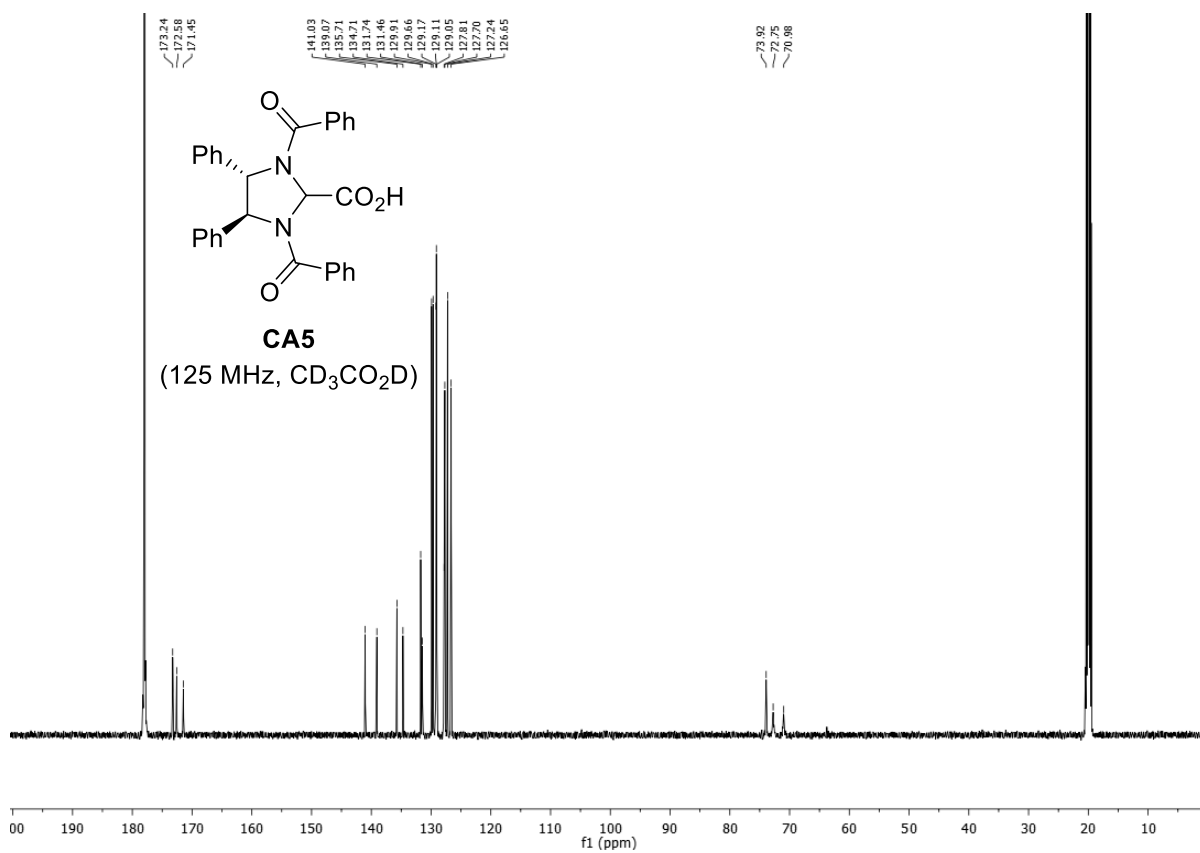


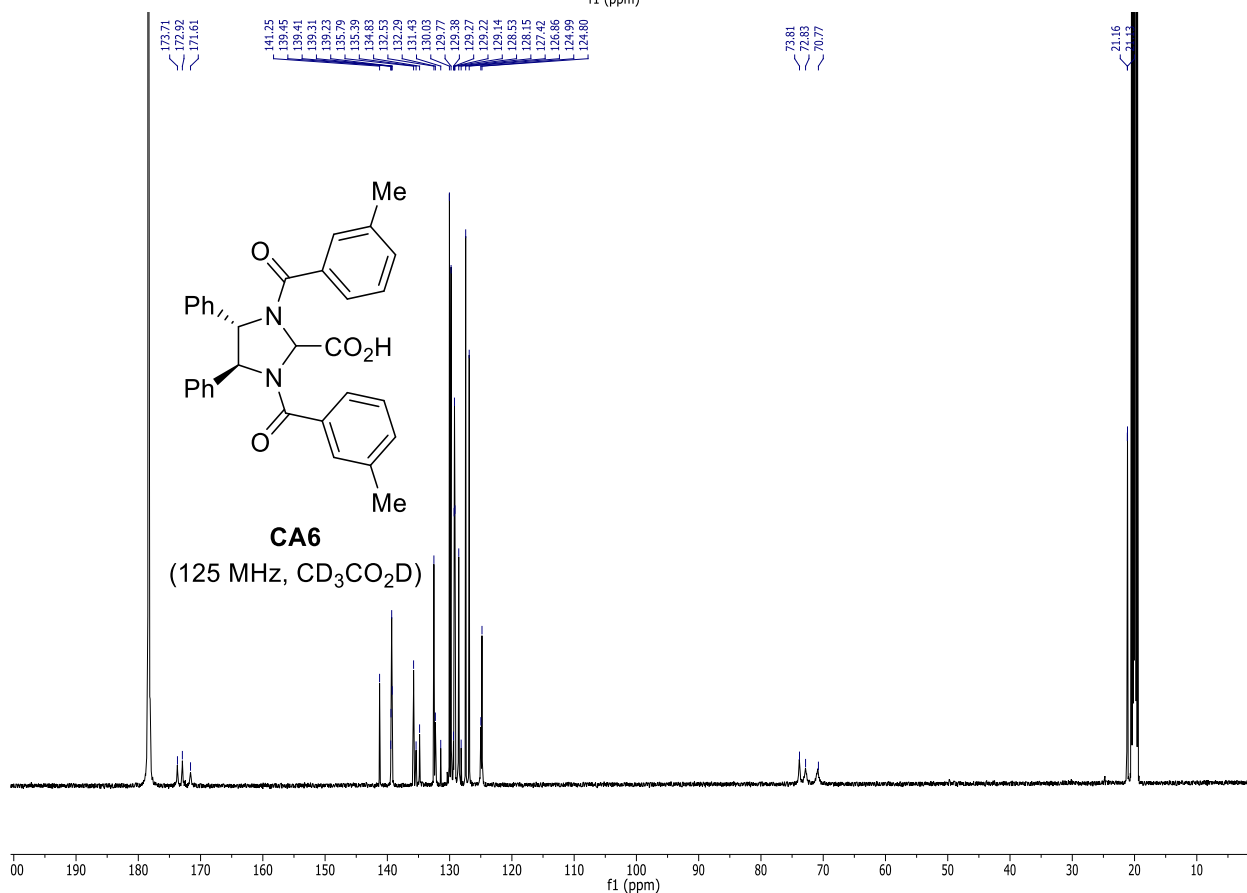
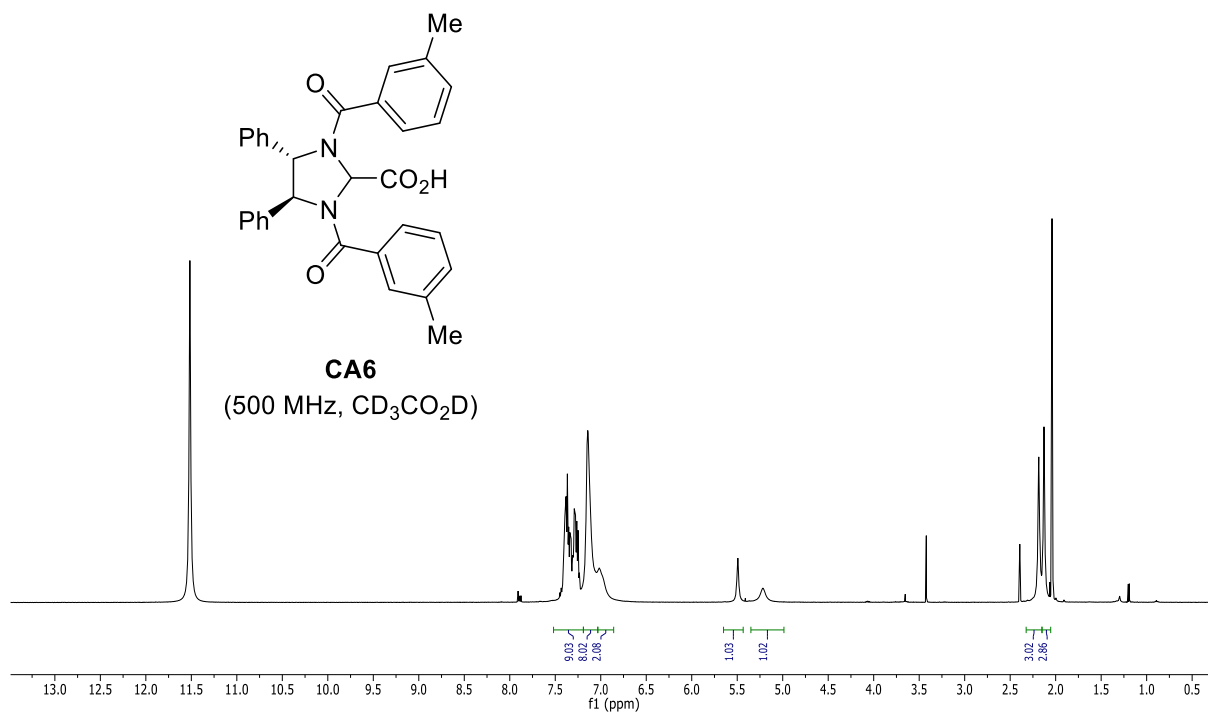


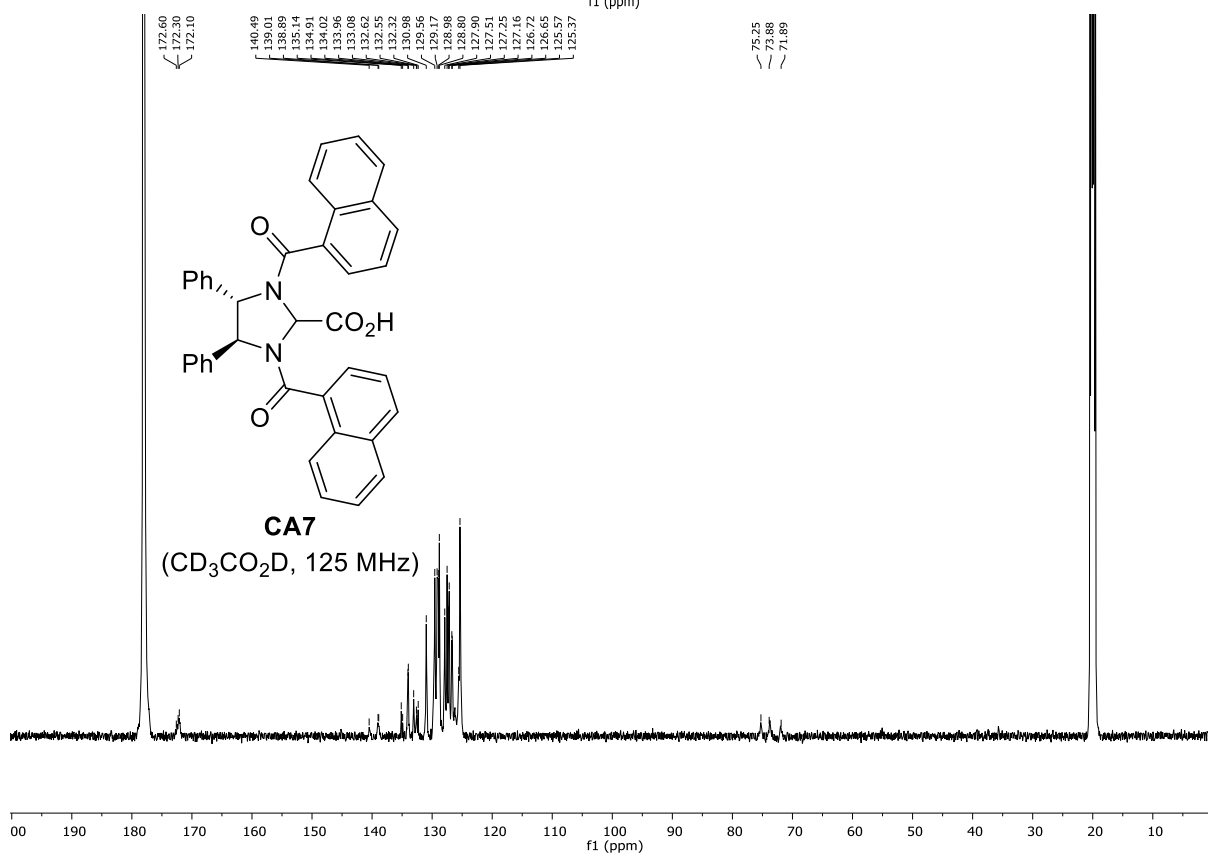
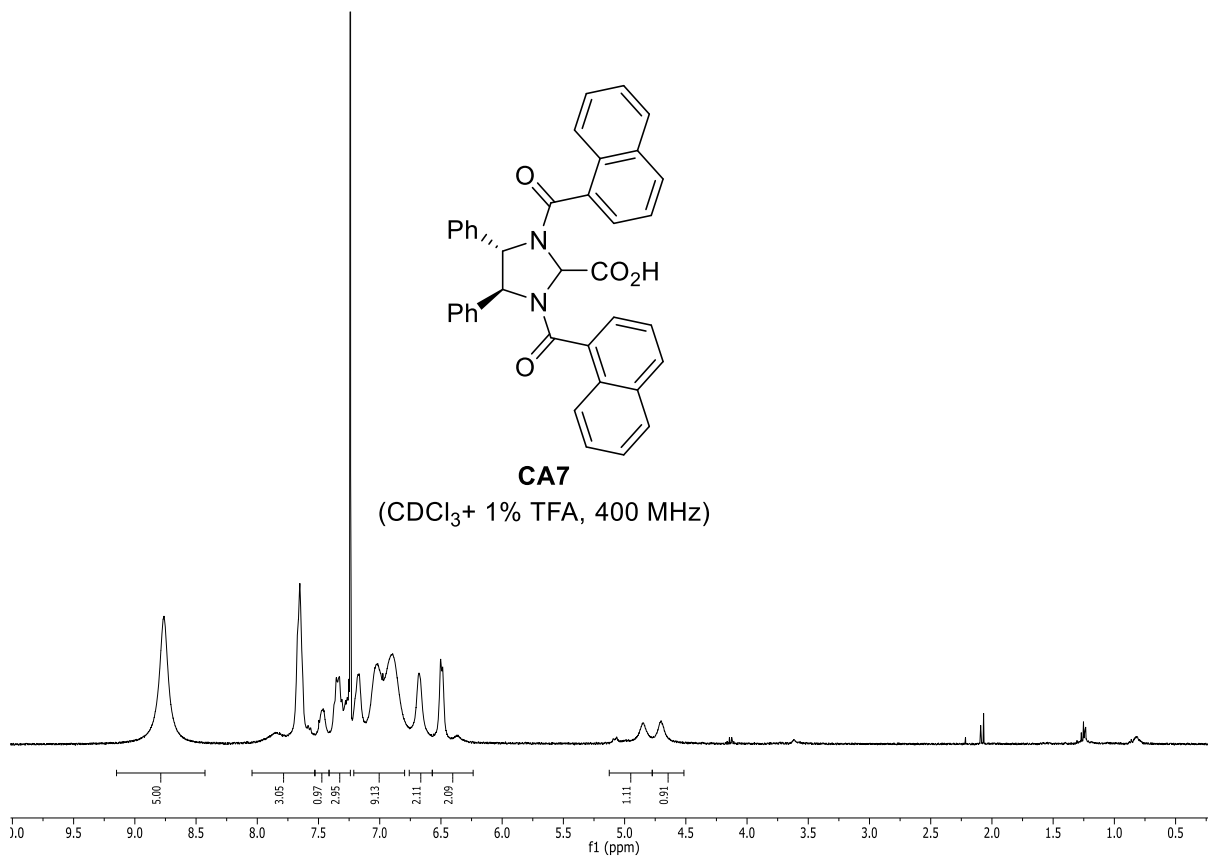
CA5
(600 MHz, CD₃CO₂D)

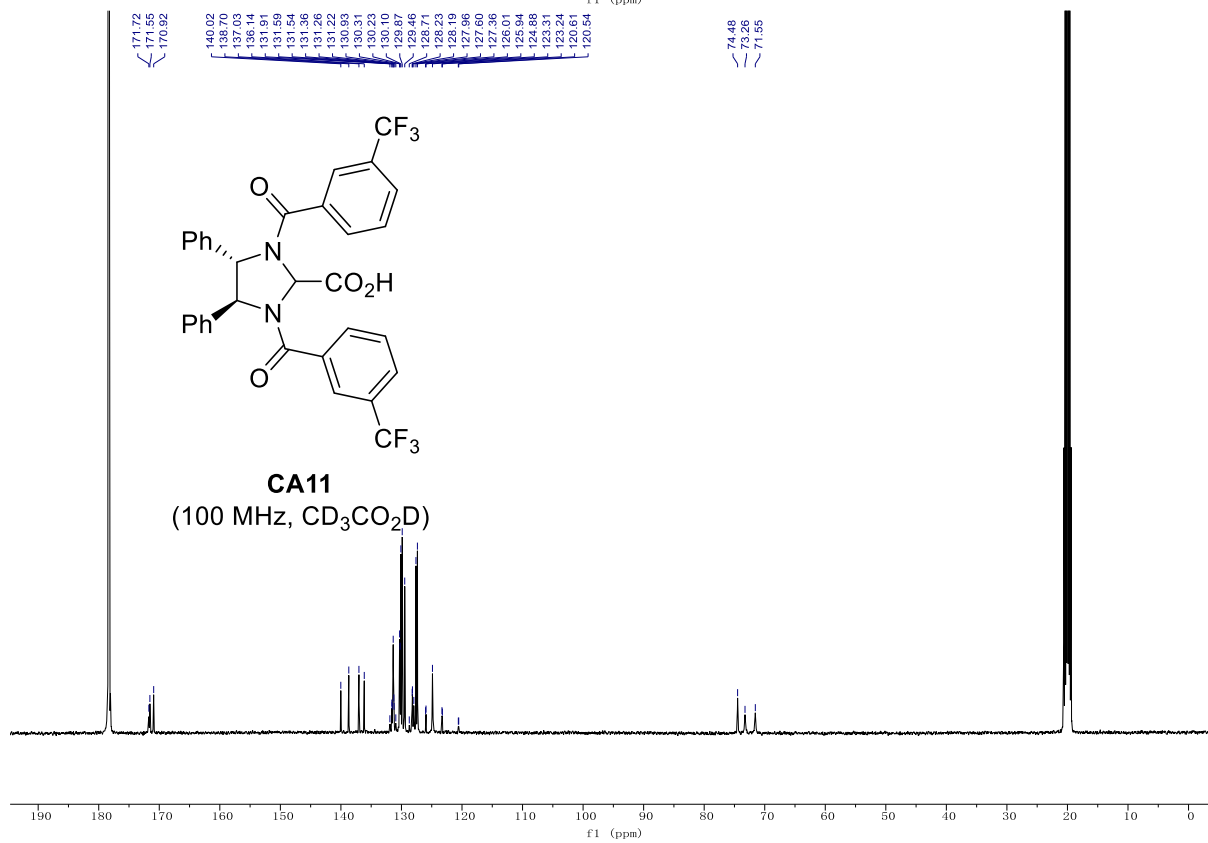
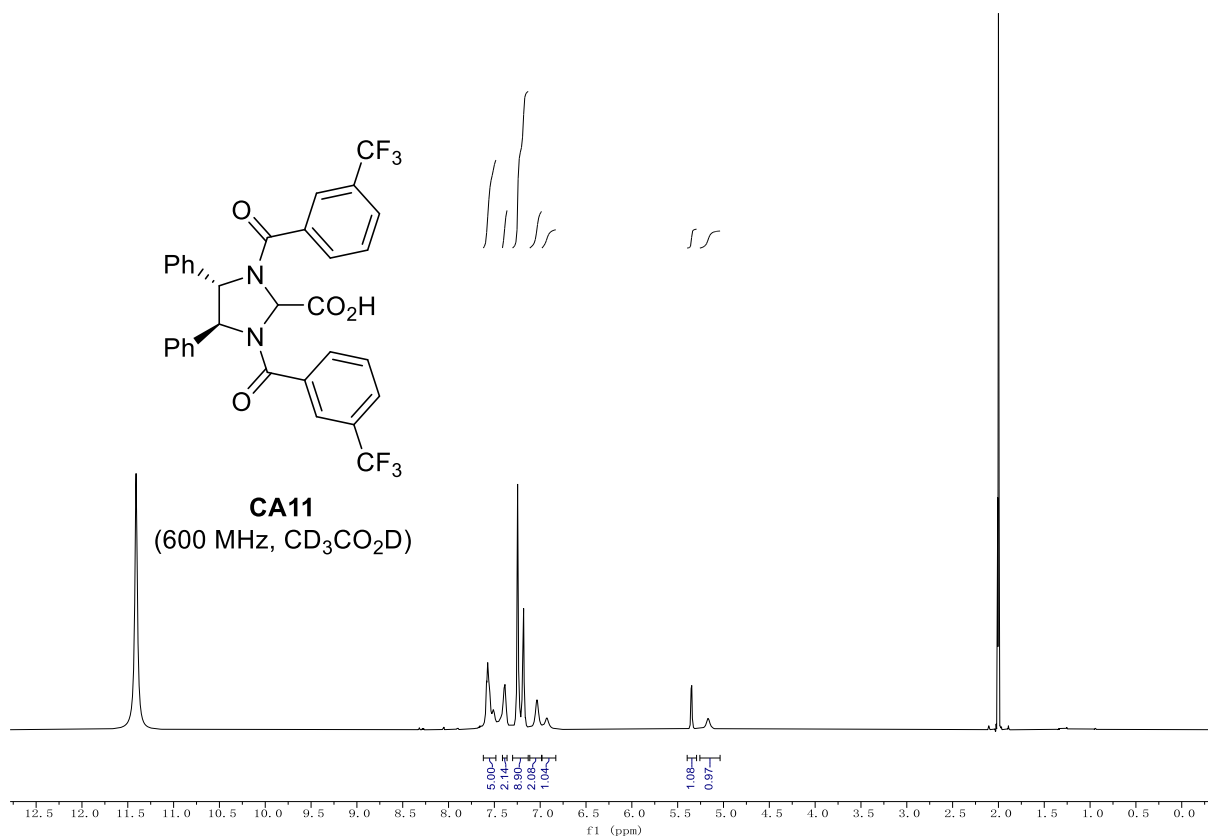


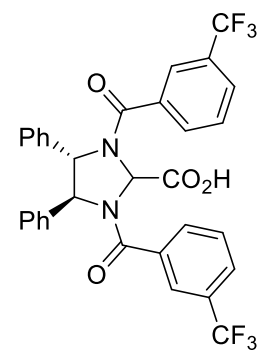
CA5
(125 MHz, CD₃CO₂D)



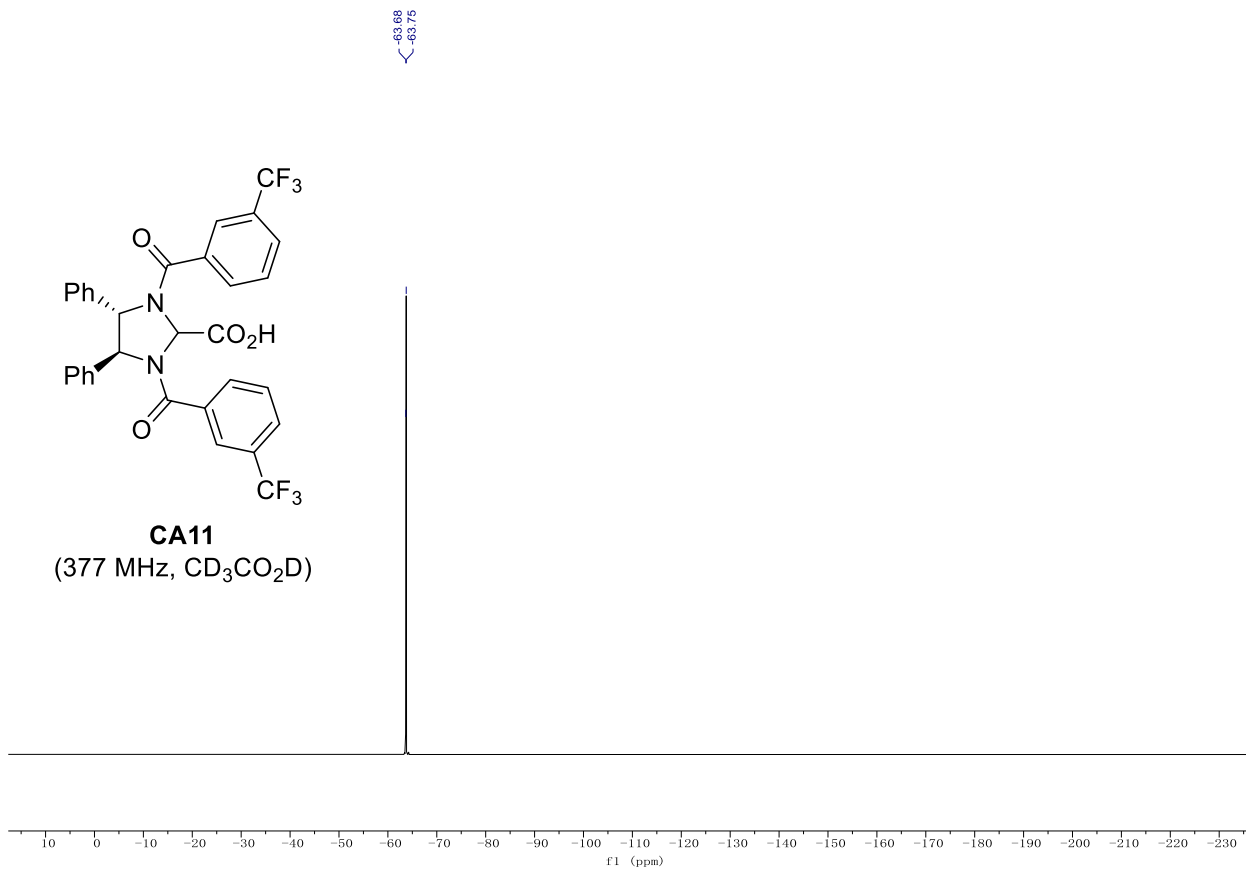


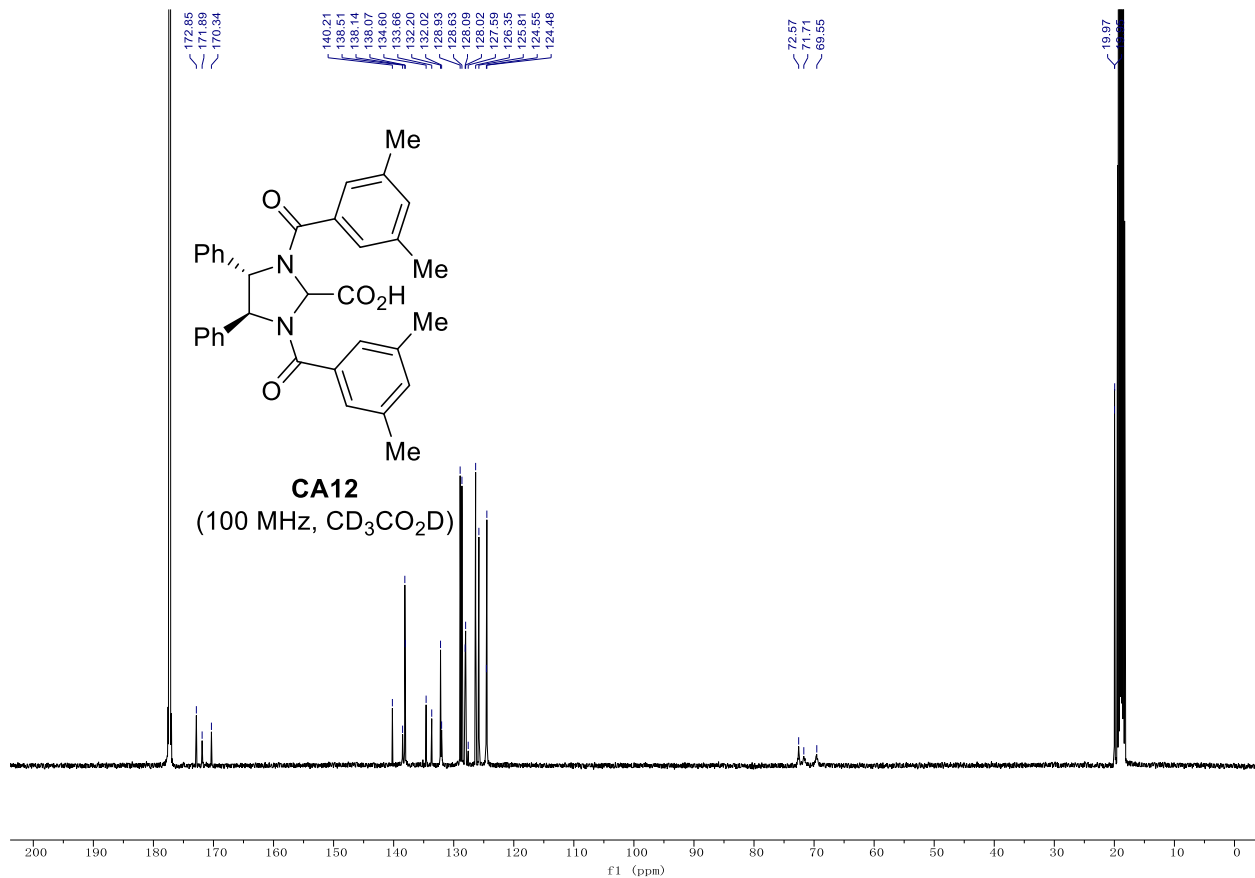
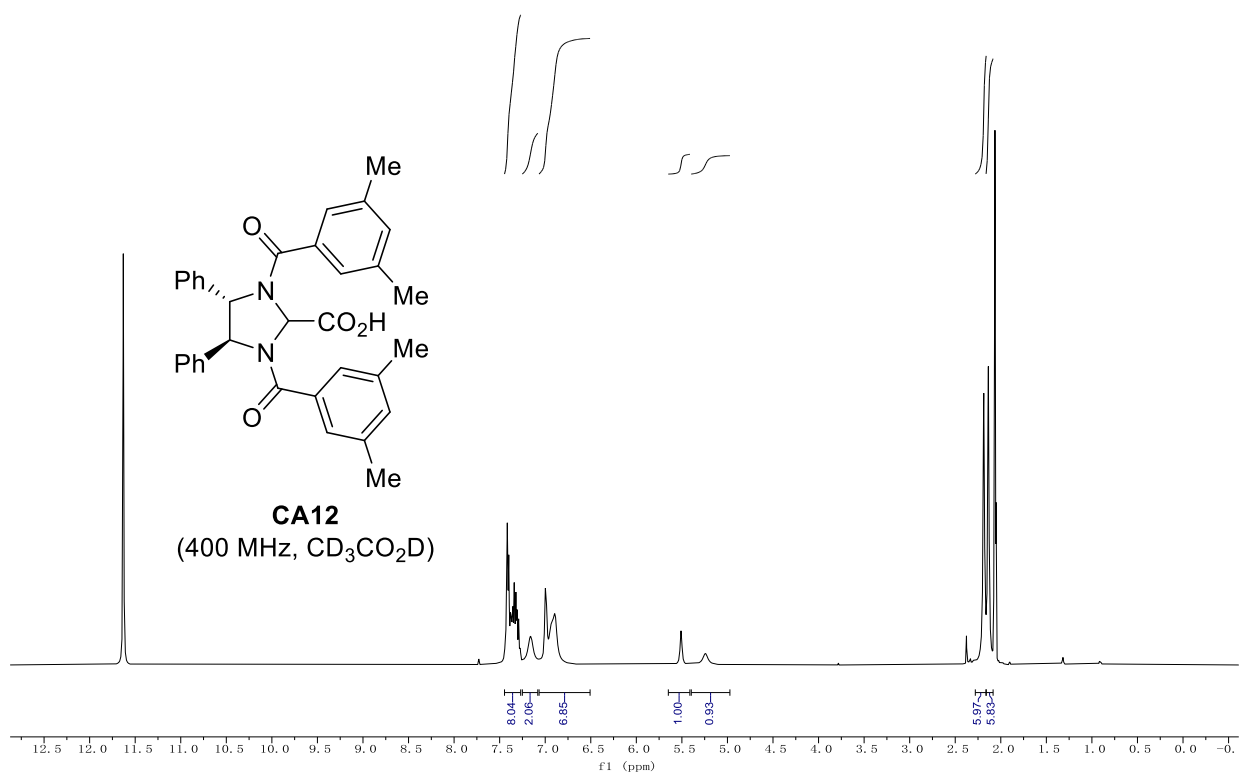


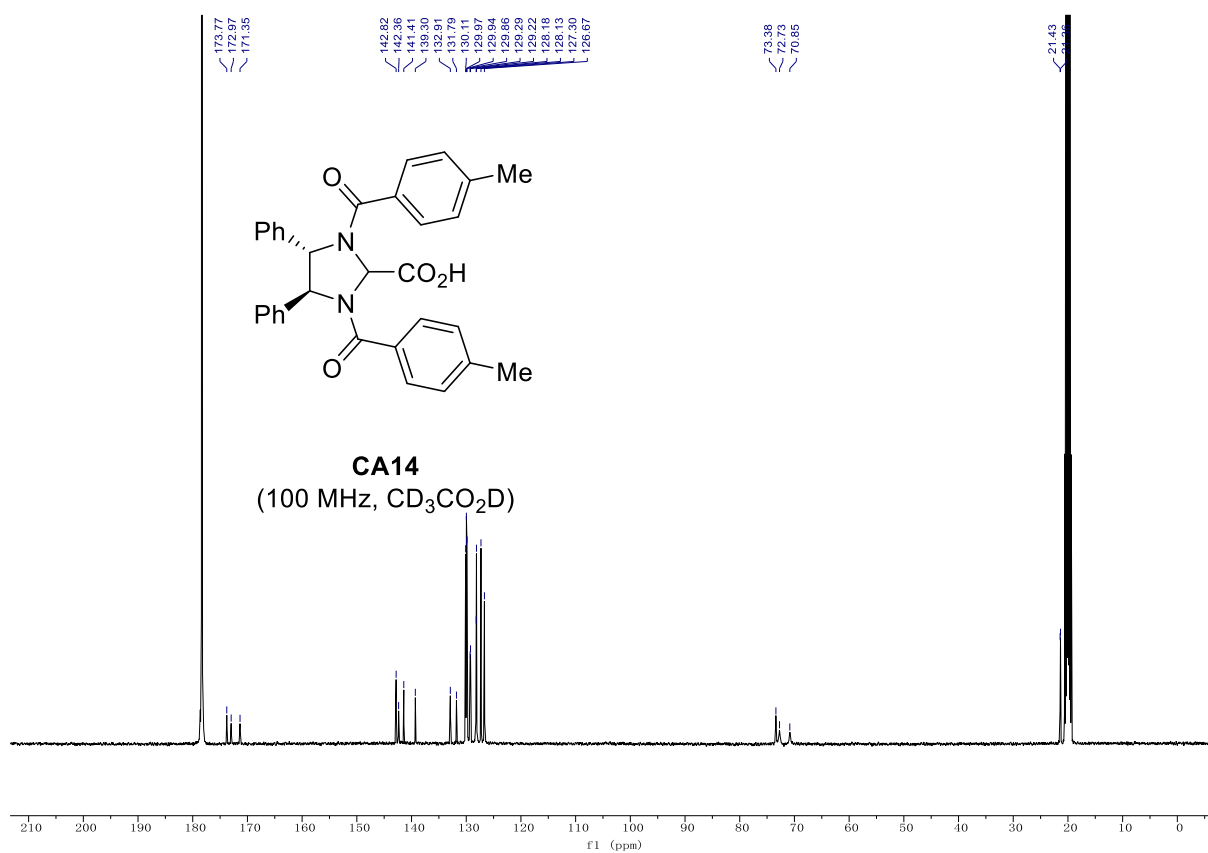
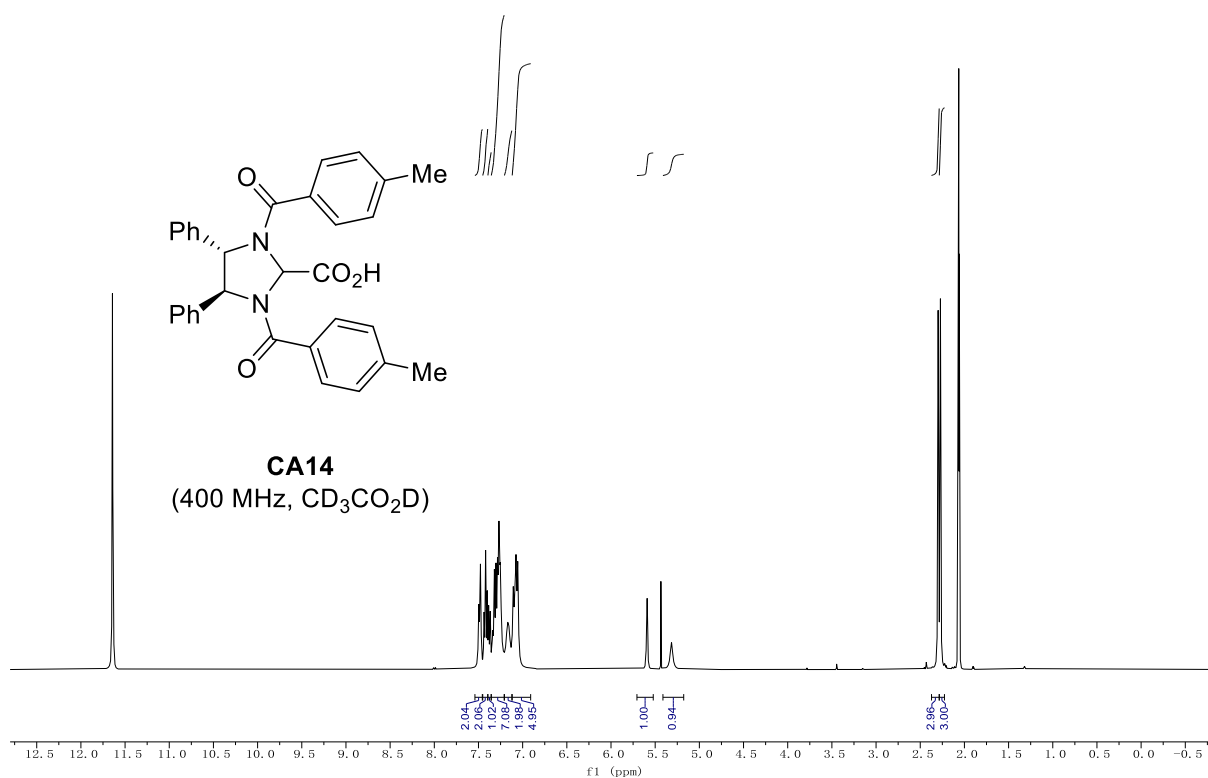


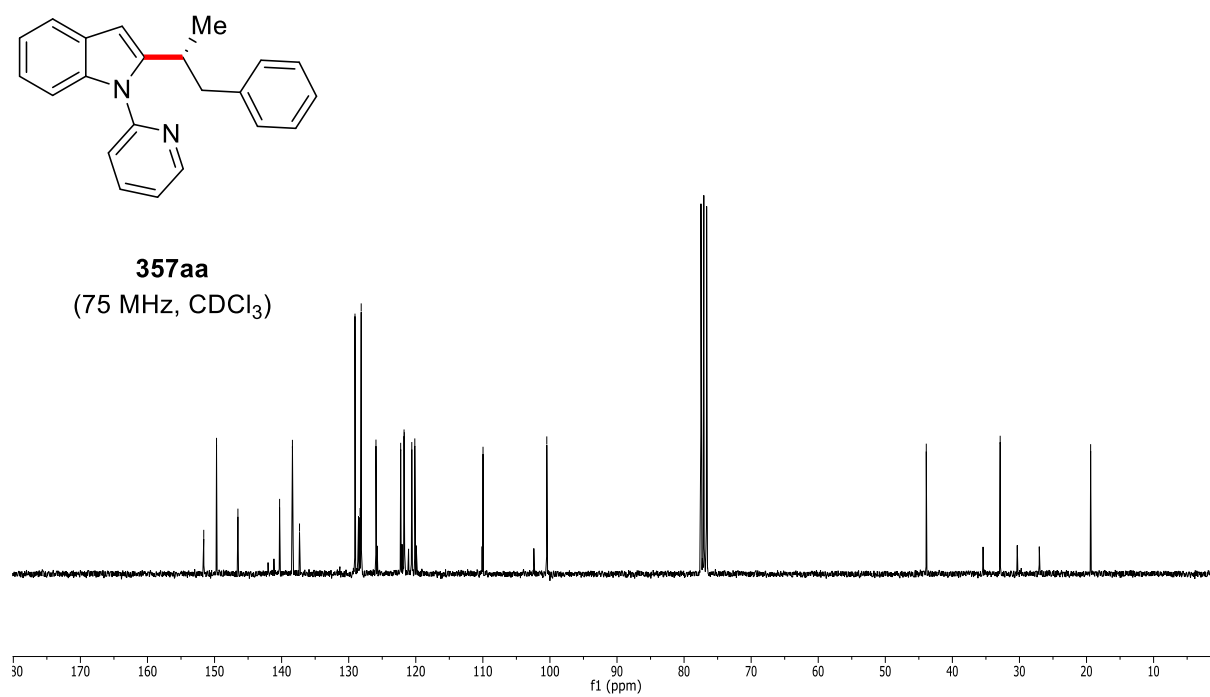
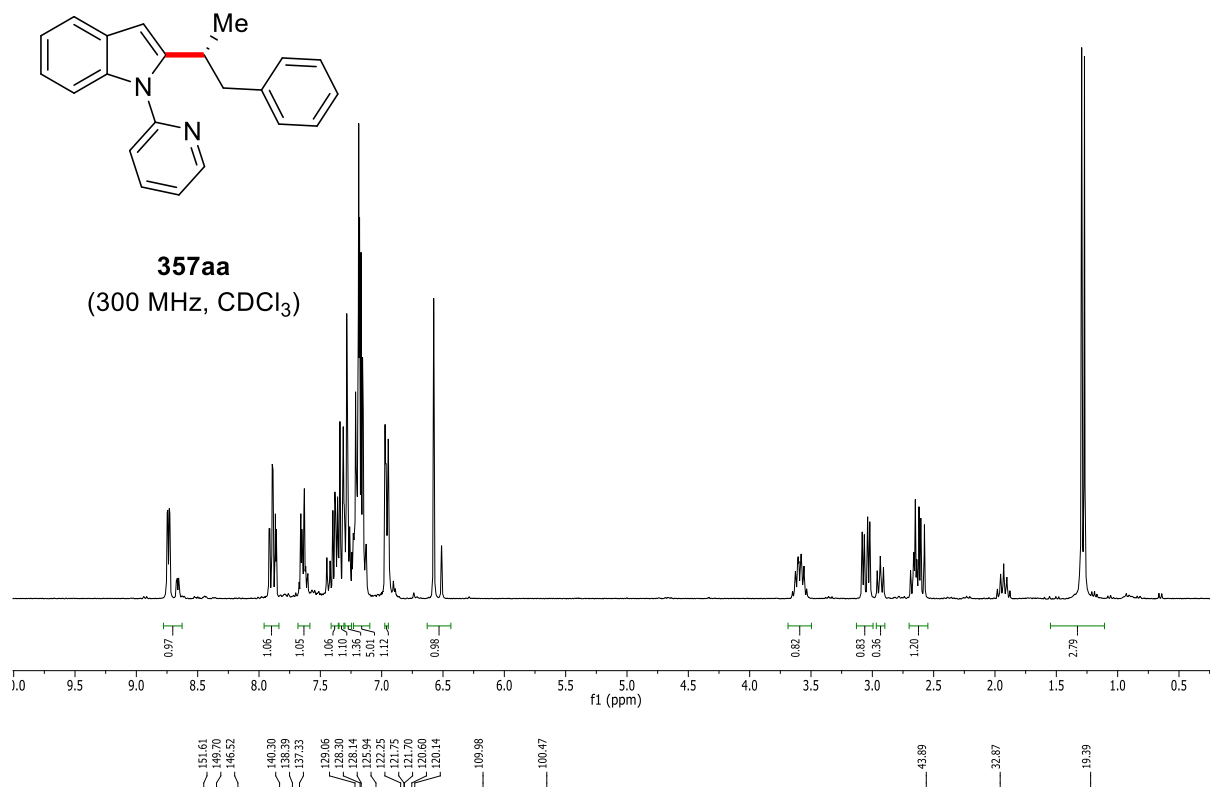


CA11
(377 MHz, CD₃CO₂D)

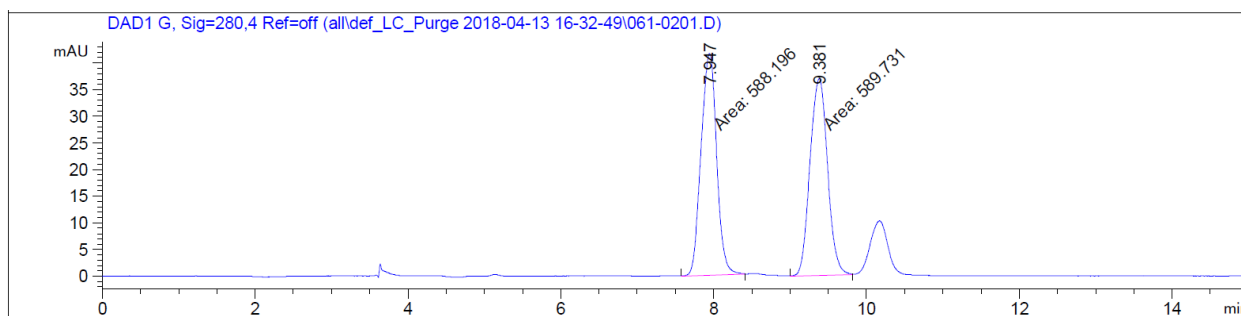




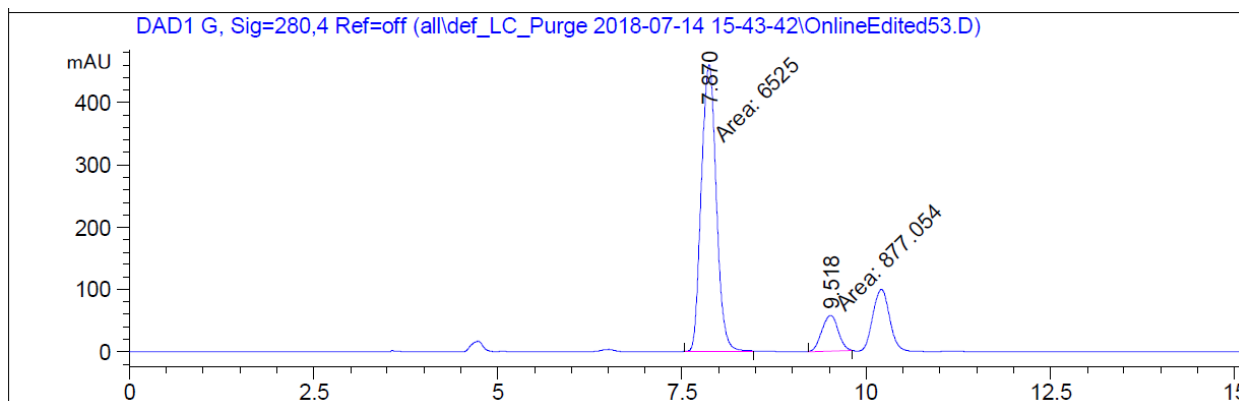




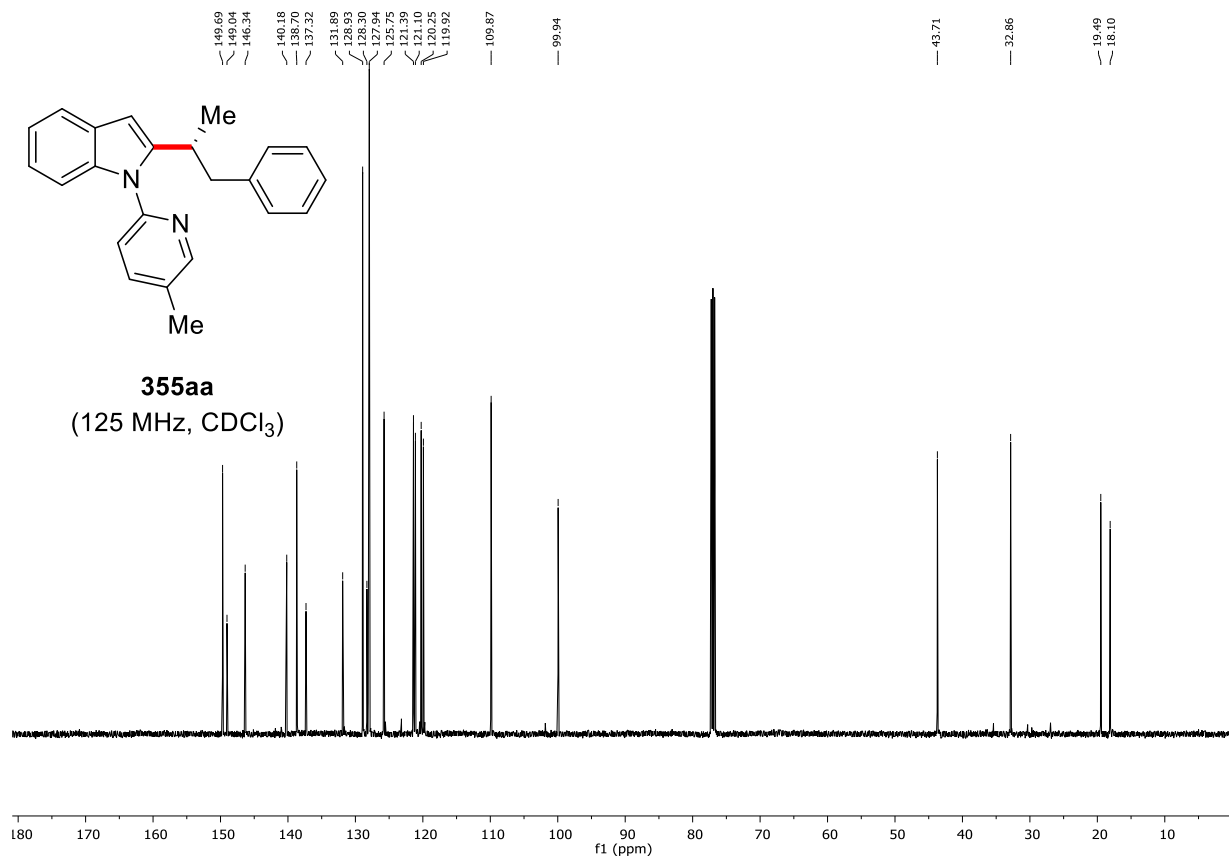
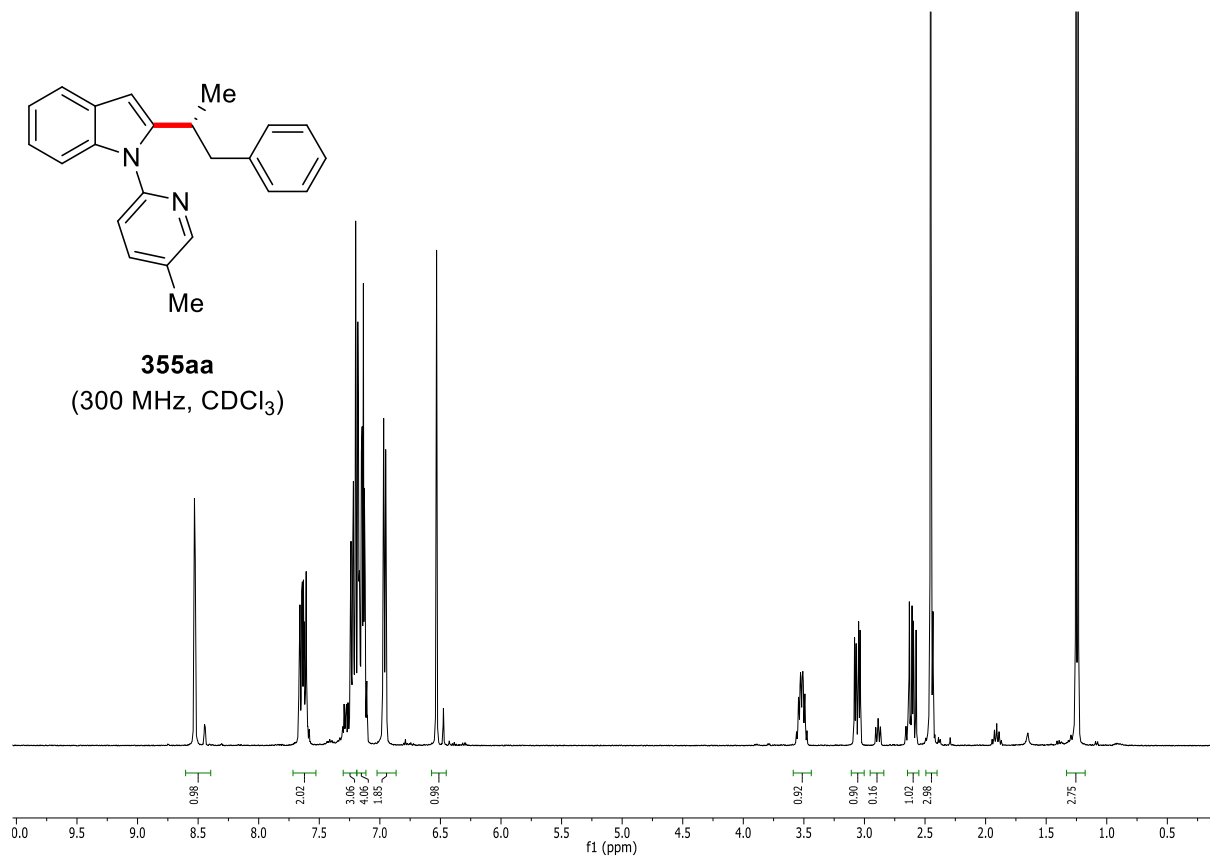
Chiral HPLC of **357aa**:



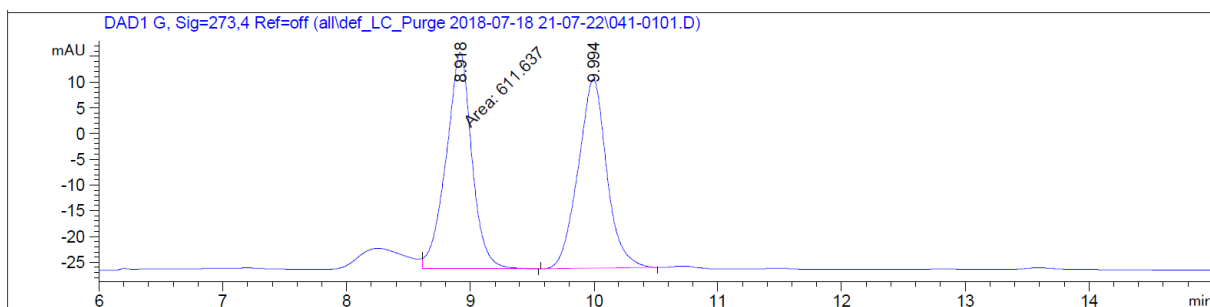
Peak #	RetTime [min]	Type	Width [min]	Area [mAU*s]	Height [mAU]	Area %
1	7.947	MM	0.2355	588.19641	41.62509	49.9348
2	9.381	MM	0.2660	589.73126	36.95060	50.0652



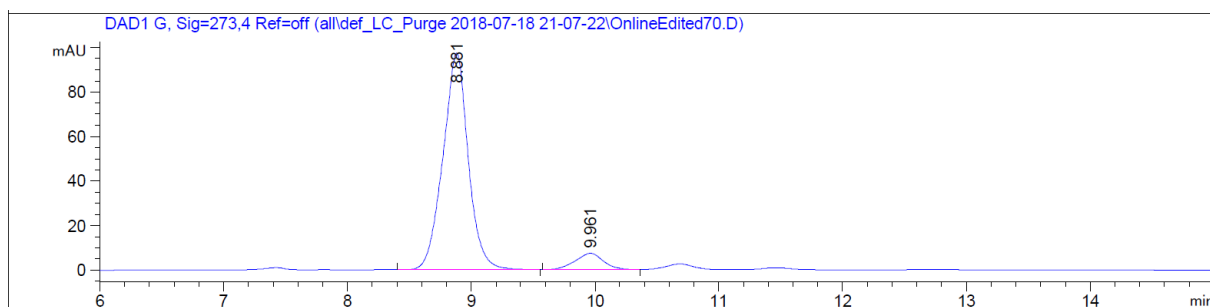
Peak #	RetTime [min]	Type	Width [min]	Area [mAU*s]	Height [mAU]	Area %
1	7.870	MM	0.2362	6525.00391	460.42294	88.1512
2	9.518	MM	0.2552	877.05389	57.27276	11.8488



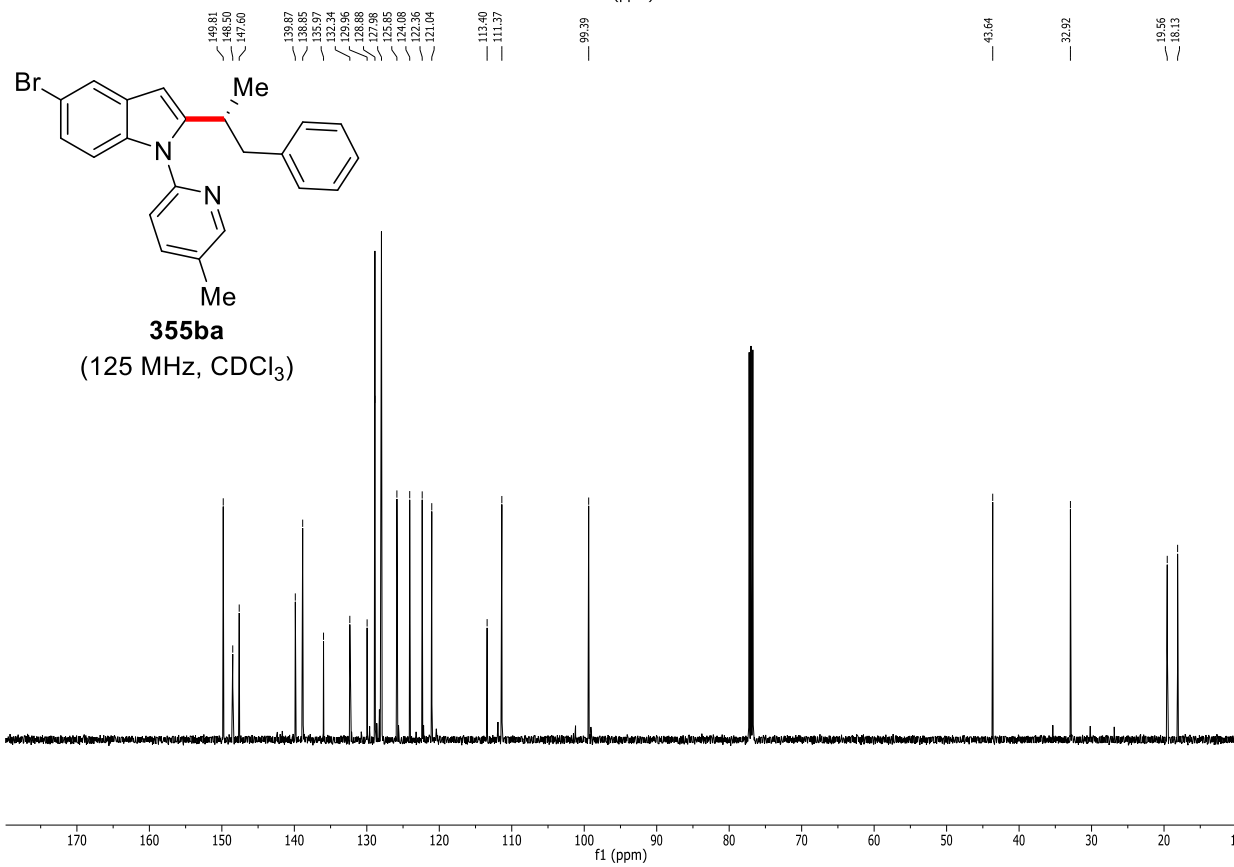
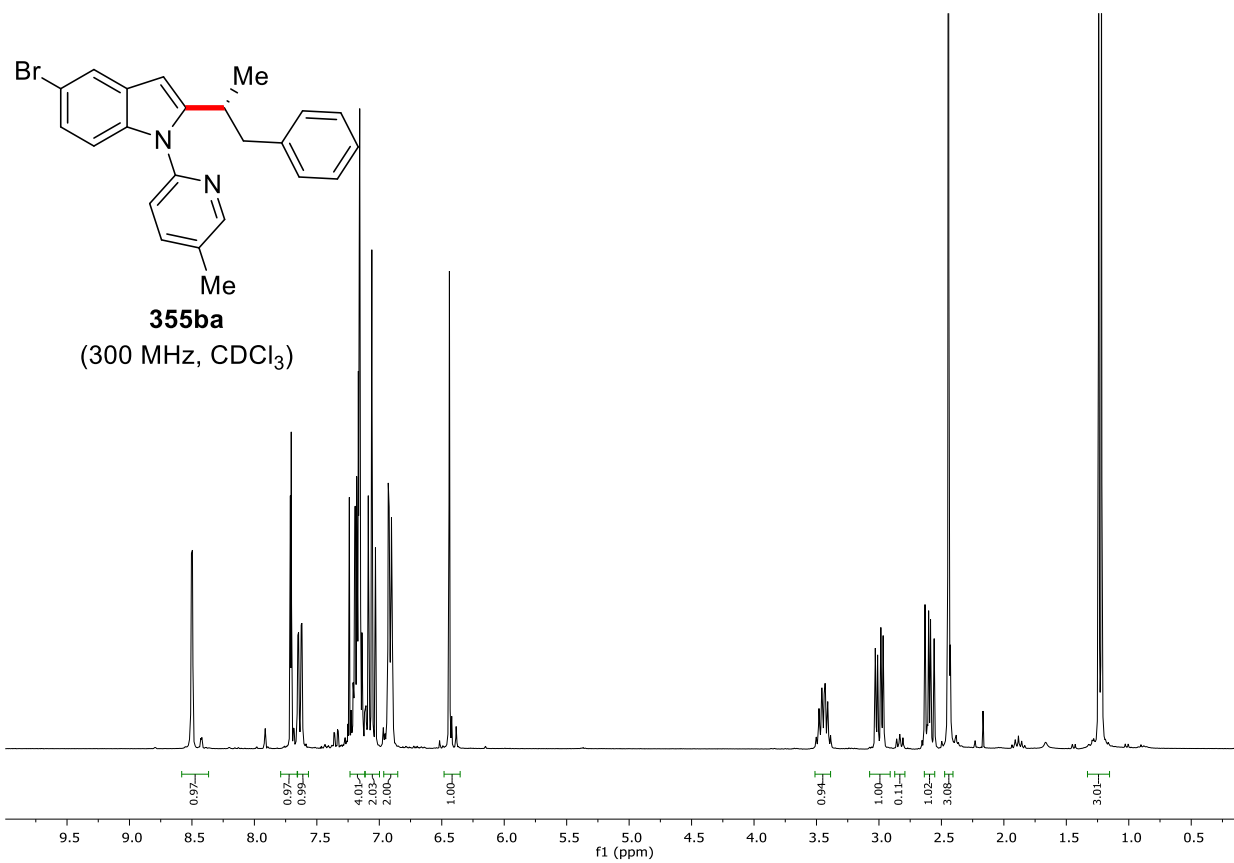
Chiral HPLC of 355aa:



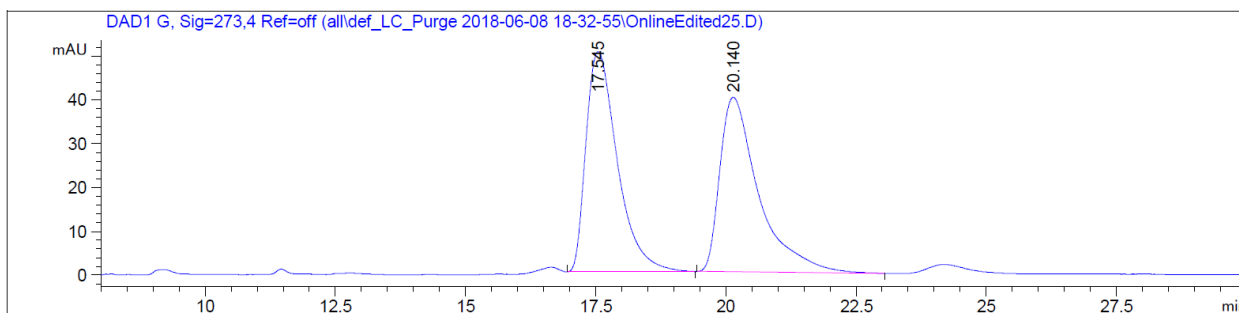
Peak #	RetTime [min]	Type	Width [min]	Area [mAU*s]	Height [mAU]	Area %
1	8.918	FM	0.2419	611.63660	42.14855	50.7977
2	9.994	BB	0.2372	592.42639	36.71786	49.2023



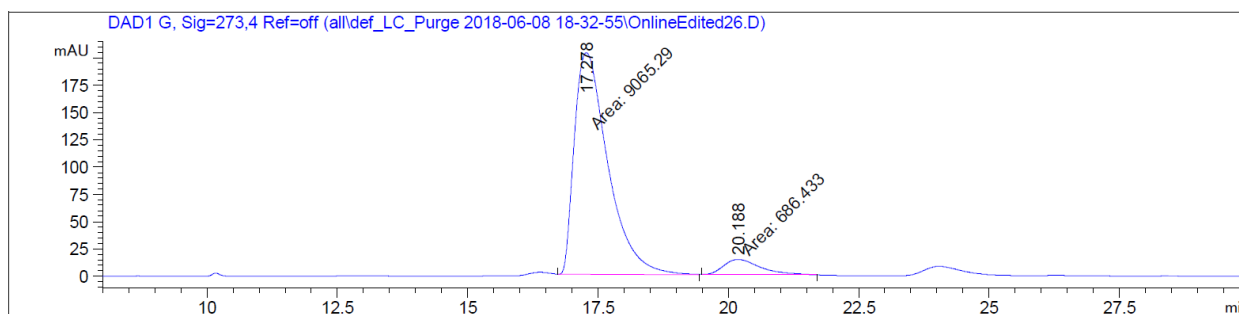
Peak #	RetTime [min]	Type	Width [min]	Area [mAU*s]	Height [mAU]	Area %
1	8.881	BB	0.2064	1380.53003	97.38425	92.3799
2	9.961	BB	0.2261	113.87527	7.29394	7.6201



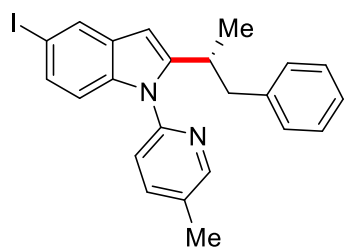
Chiral HPLC of **355ba**:



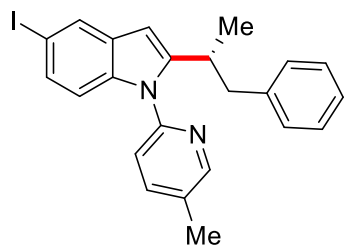
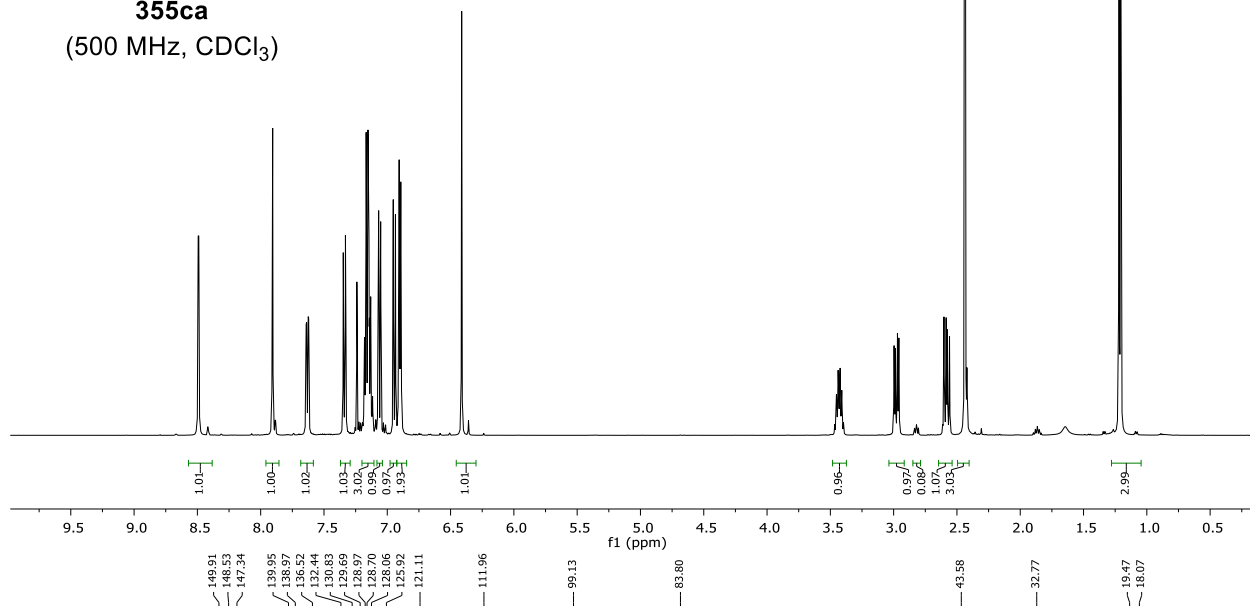
Peak #	RetTime [min]	Type	Width [min]	Area [mAU*s]	Height [mAU]	Area %
1	17.545	BB	0.6281	2103.89453	50.28347	50.3633
2	20.140	BB	0.7387	2073.53882	39.87462	49.6367



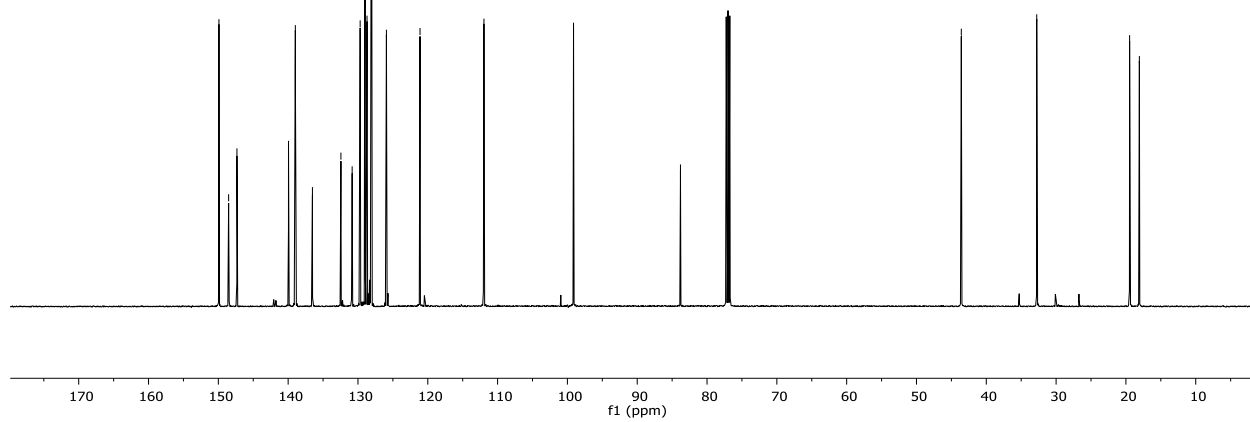
Peak #	RetTime [min]	Type	Width [min]	Area [mAU*s]	Height [mAU]	Area %
1	17.278	MM	0.7439	9065.28809	203.10196	92.9609
2	20.188	MM	0.8185	686.43298	13.97703	7.0391



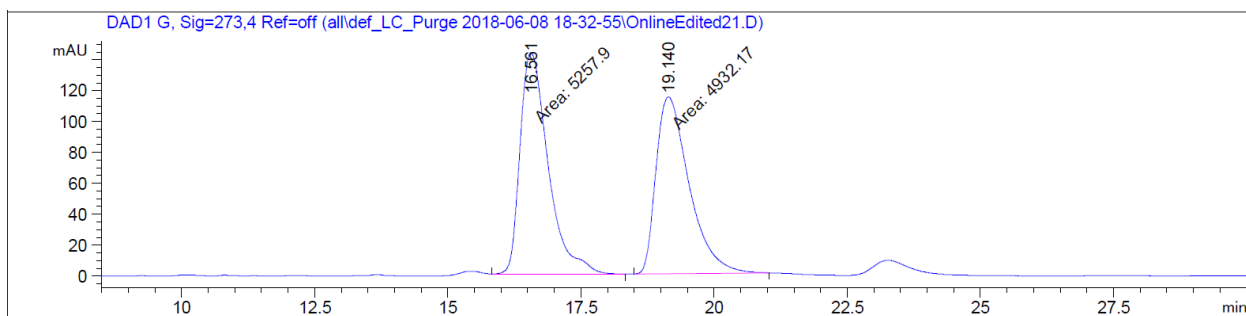
355ca
(500 MHz, CDCl₃)



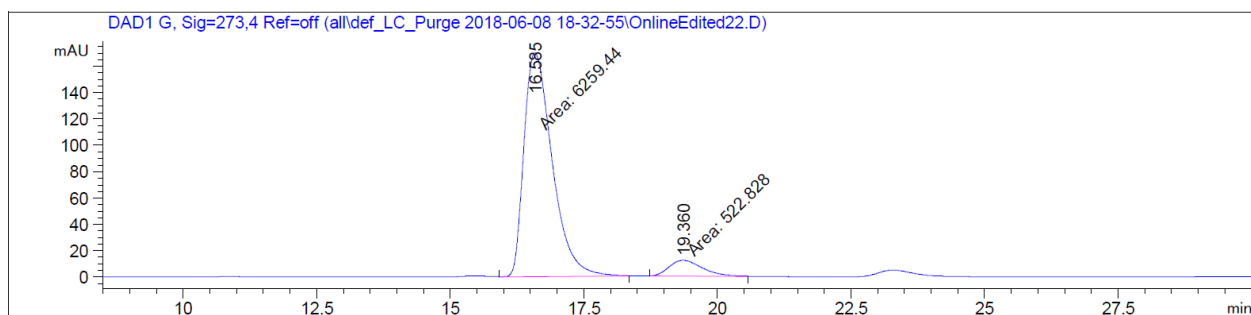
355ca
(125 MHz, CDCl₃)



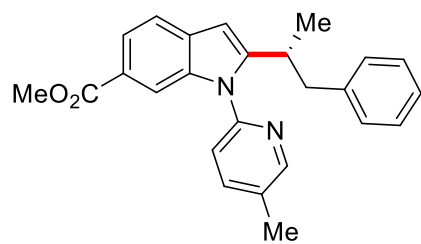
Chiral HPLC of 355ca:



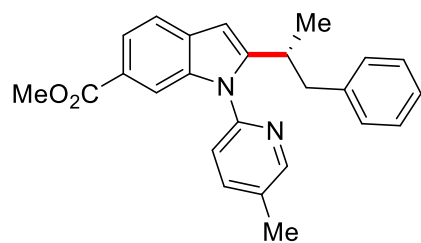
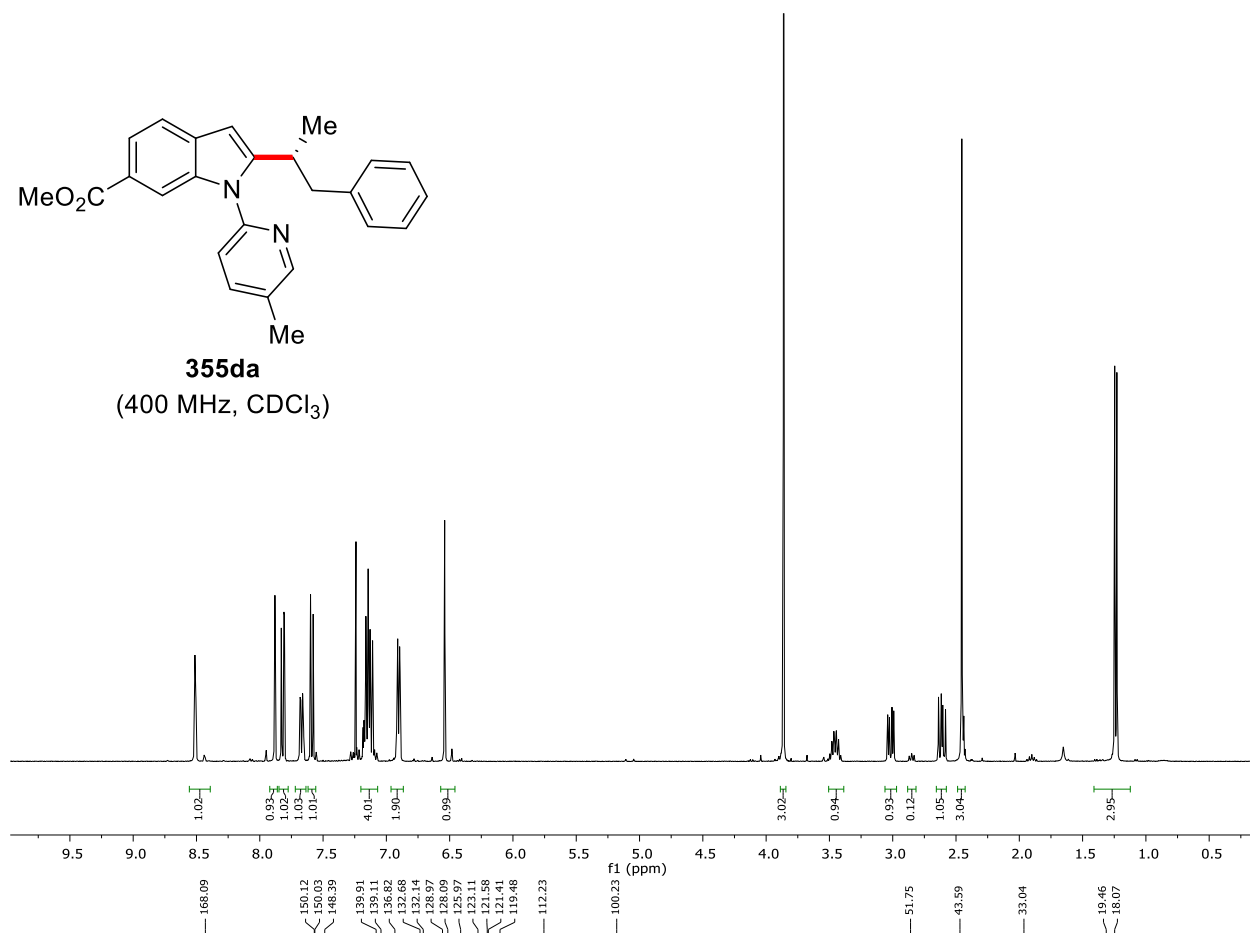
Peak #	RetTime [min]	Type	Width [min]	Area [mAU*s]	Height [mAU]	Area %
1	16.561	MM	0.6121	5257.89502	143.15543	51.5982
2	19.140	MM	0.7197	4932.17480	114.21161	48.4018



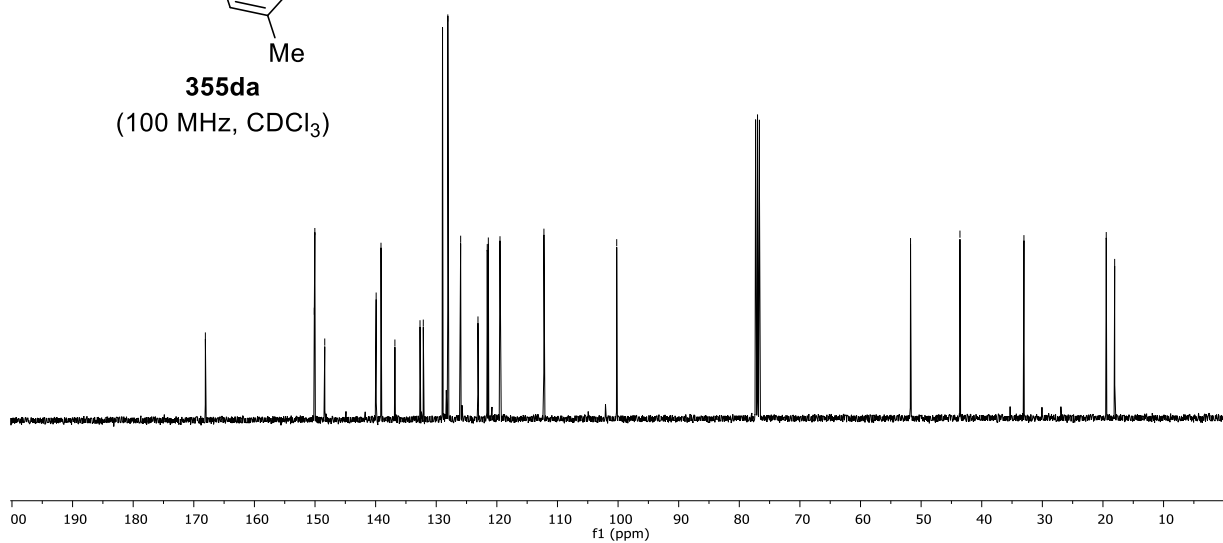
Peak #	RetTime [min]	Type	Width [min]	Area [mAU*s]	Height [mAU]	Area %
1	16.585	MM	0.6133	6259.43994	170.09406	92.2913
2	19.360	MM	0.7212	522.82751	12.08242	7.7087



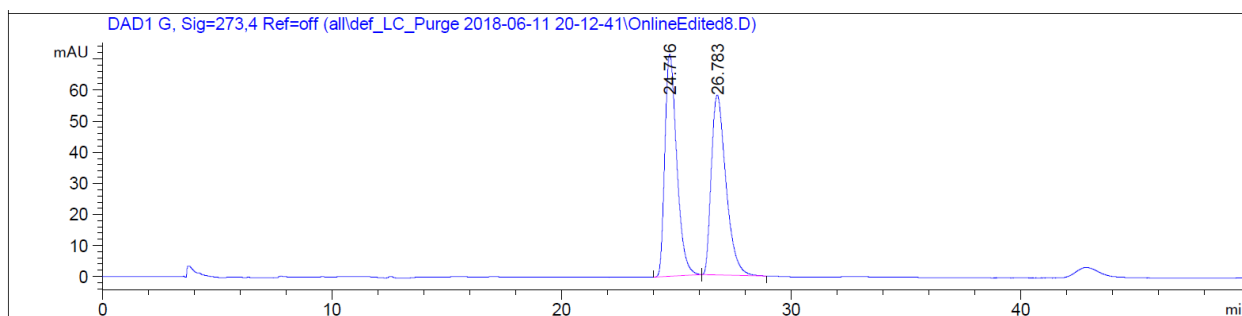
355da
(400 MHz, CDCl₃)



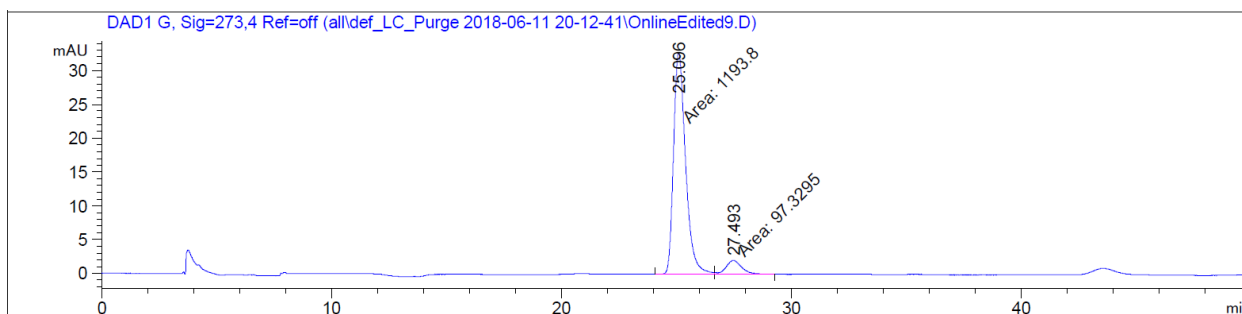
355da
(100 MHz, CDCl₃)



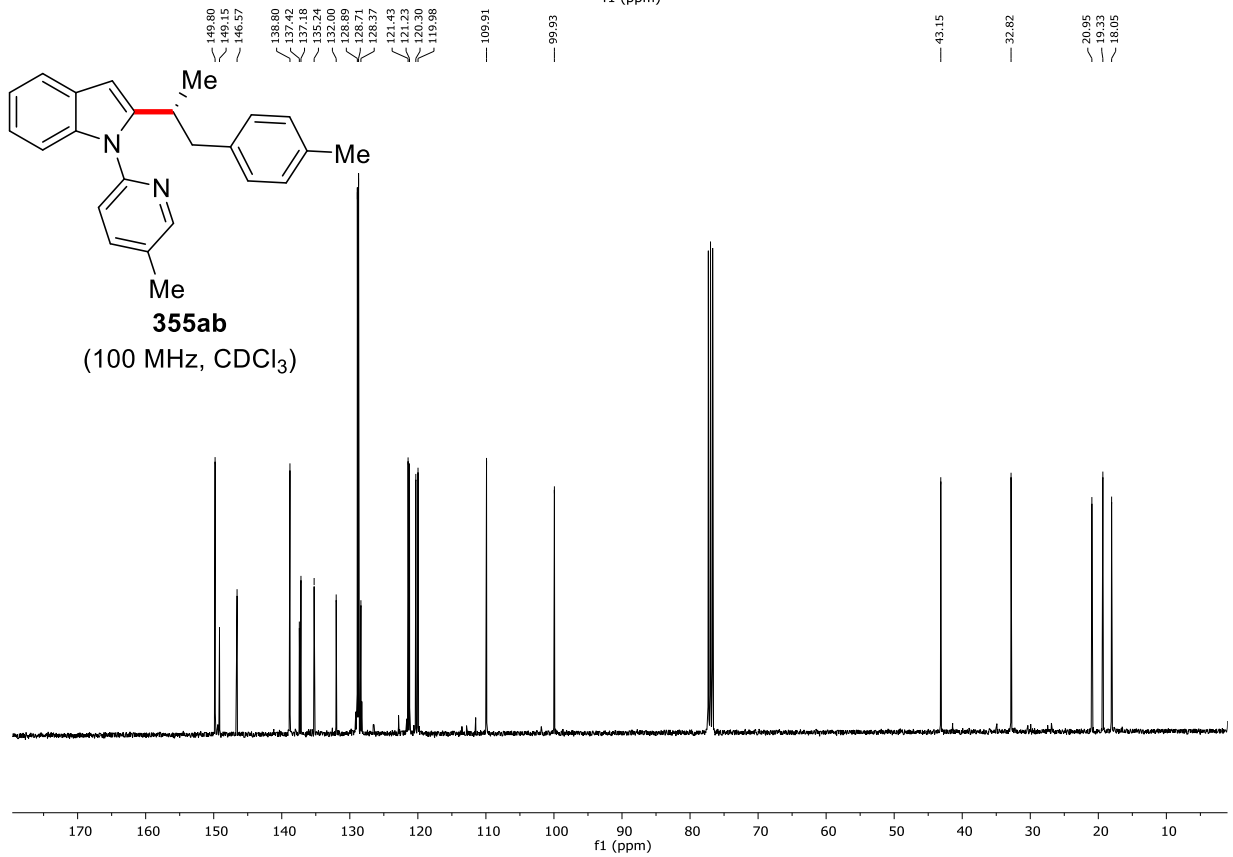
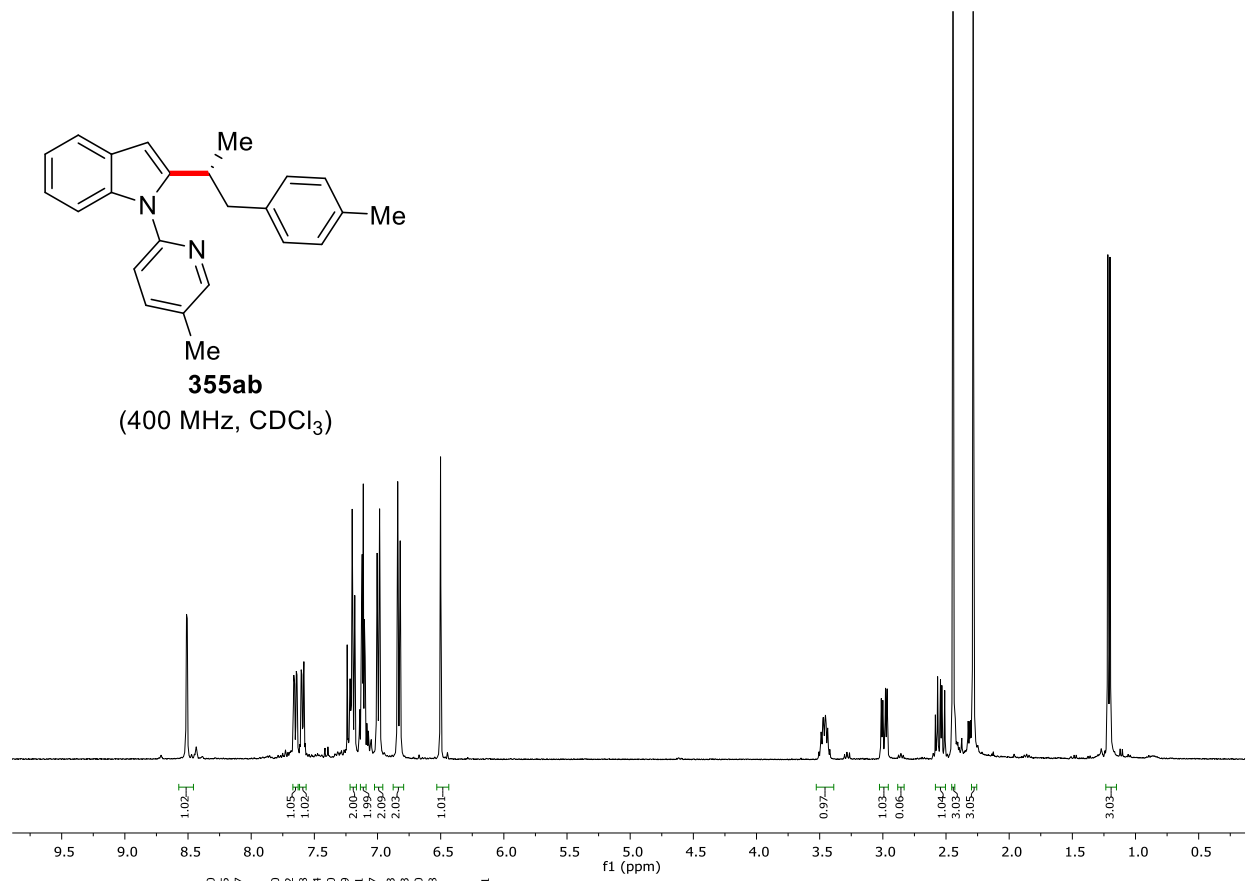
Chiral HPLC of **355da**:



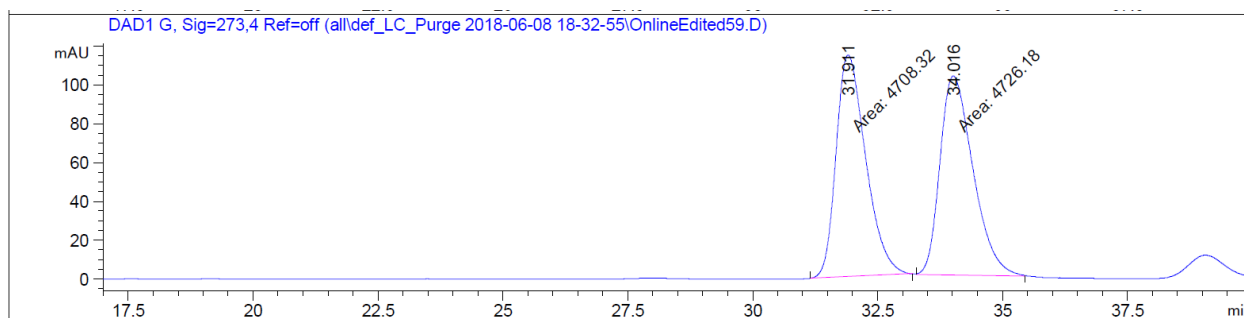
Peak #	RetTime [min]	Type	Width [min]	Area [mAU*s]	Height [mAU]	Area %
1	24.716	BB	0.5522	2575.25684	71.49819	50.0481
2	26.783	BB	0.6626	2570.30273	57.93876	49.9519



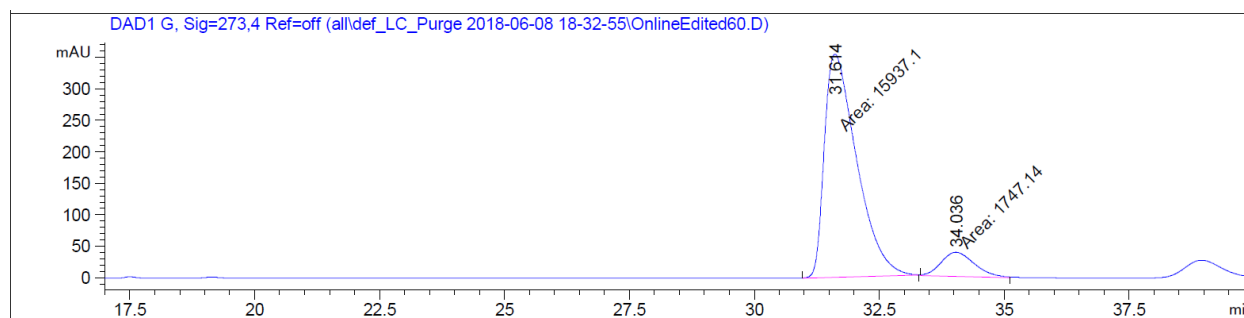
Peak #	RetTime [min]	Type	Width [min]	Area [mAU*s]	Height [mAU]	Area %
1	25.096	MF	0.6066	1193.79517	32.80224	92.4617
2	27.493	FM	0.7956	97.32949	2.03891	7.5383



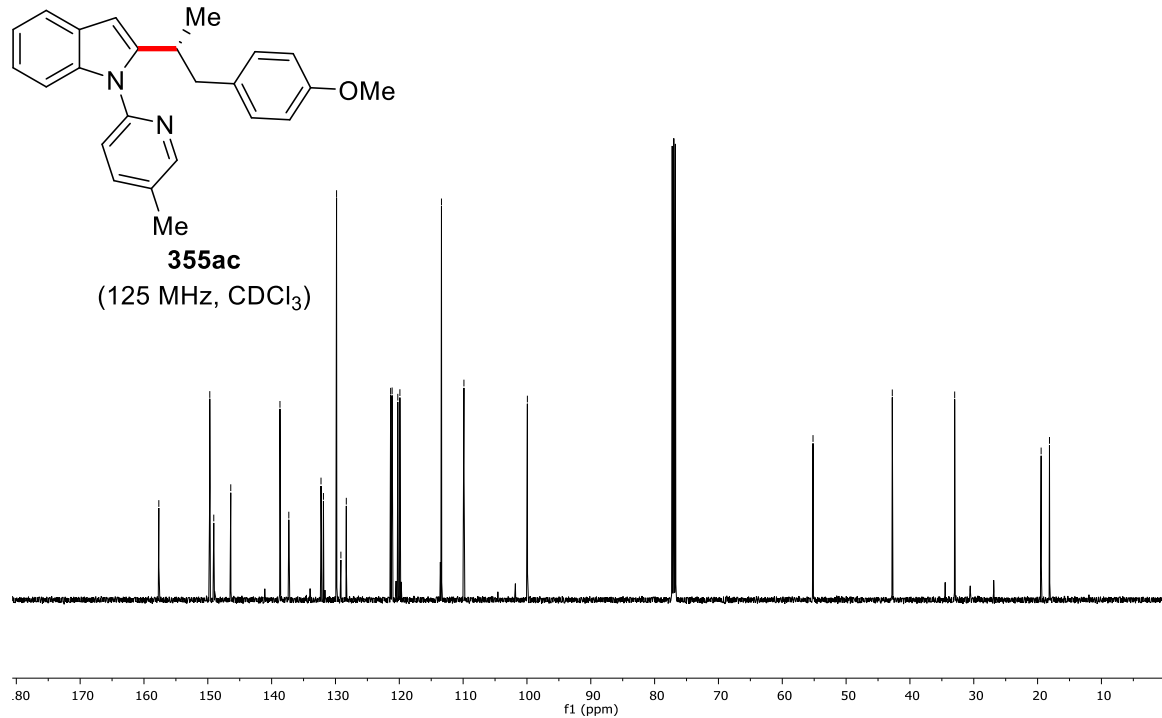
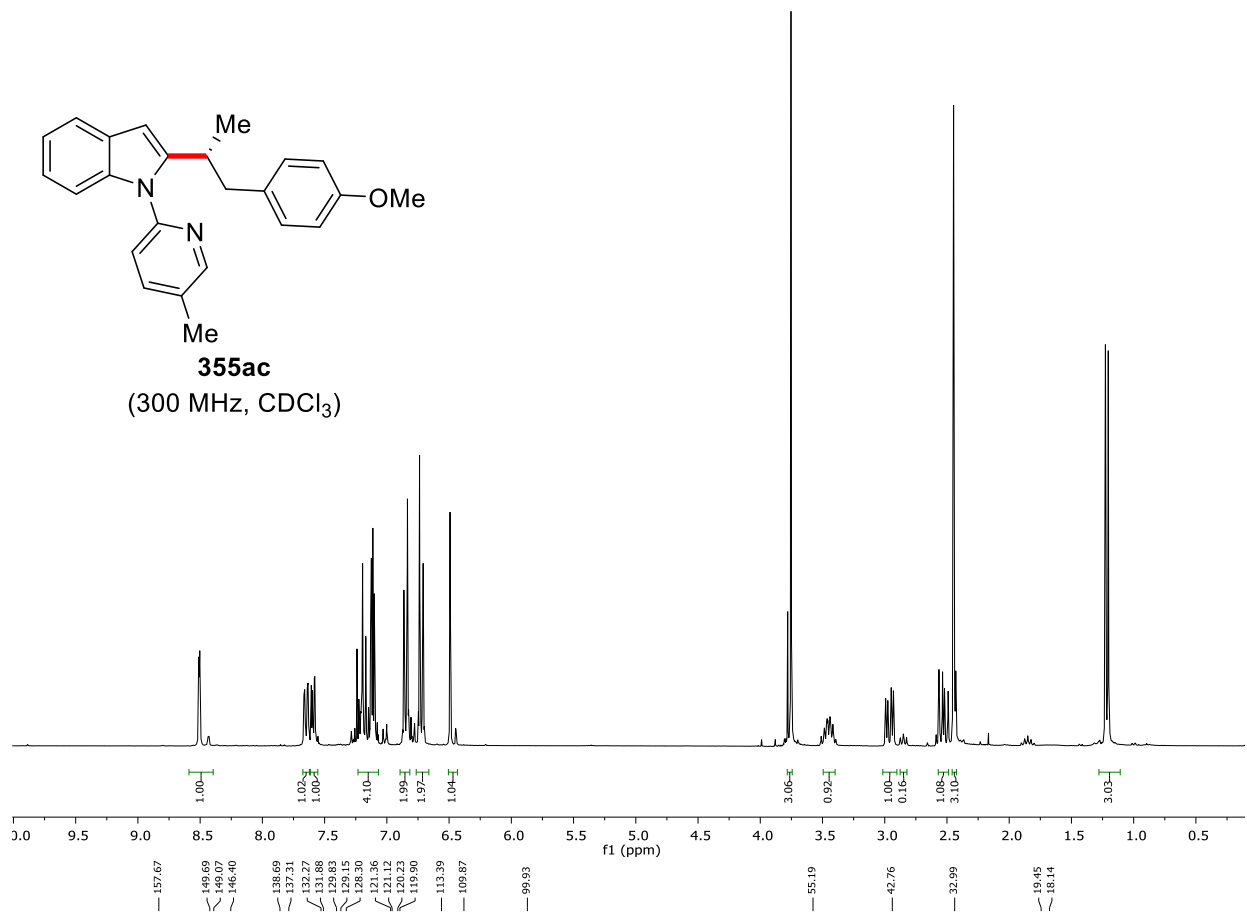
Chiral HPLC of **355ab**:



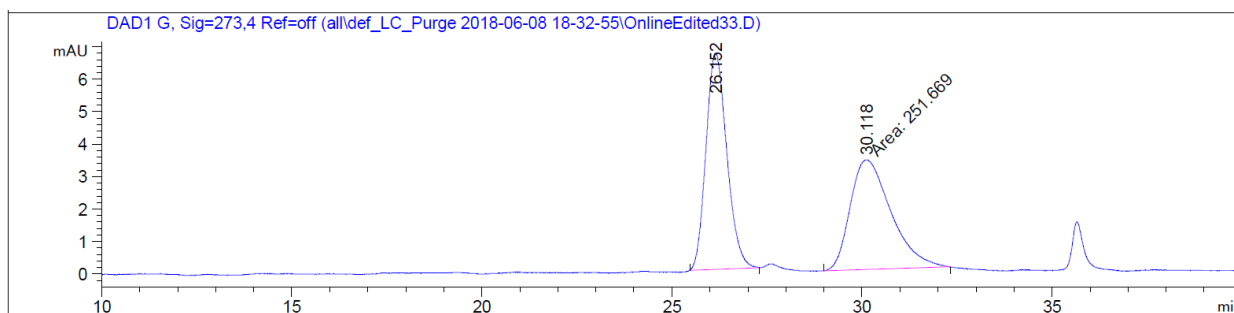
Peak #	RetTime [min]	Type	Width [min]	Area [mAU*s]	Height [mAU]	Area %
1	31.911	BB	0.6290	4741.79736	114.54191	49.9170
2	34.016	BB	0.7005	4757.56152	102.69714	50.0830



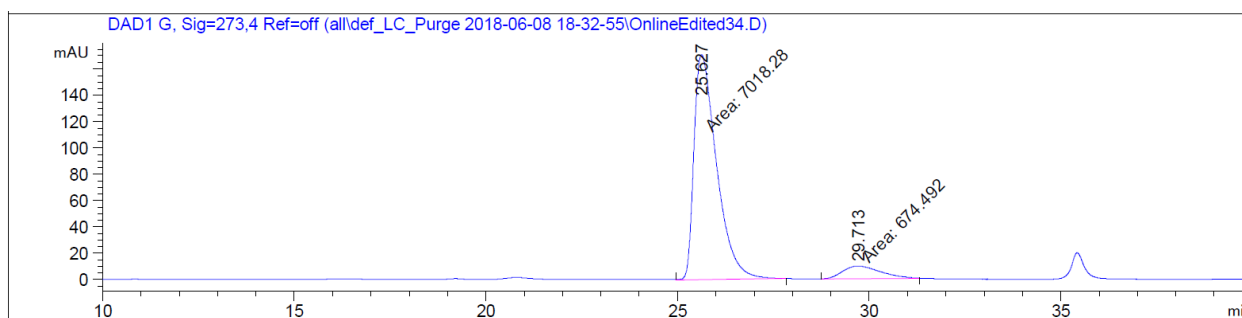
Peak #	RetTime [min]	Type	Width [min]	Area [mAU*s]	Height [mAU]	Area %
1	31.614	MM	0.7493	1.59371e4	354.50583	90.1203
2	34.036	MM	0.7663	1747.13916	37.99726	9.8797



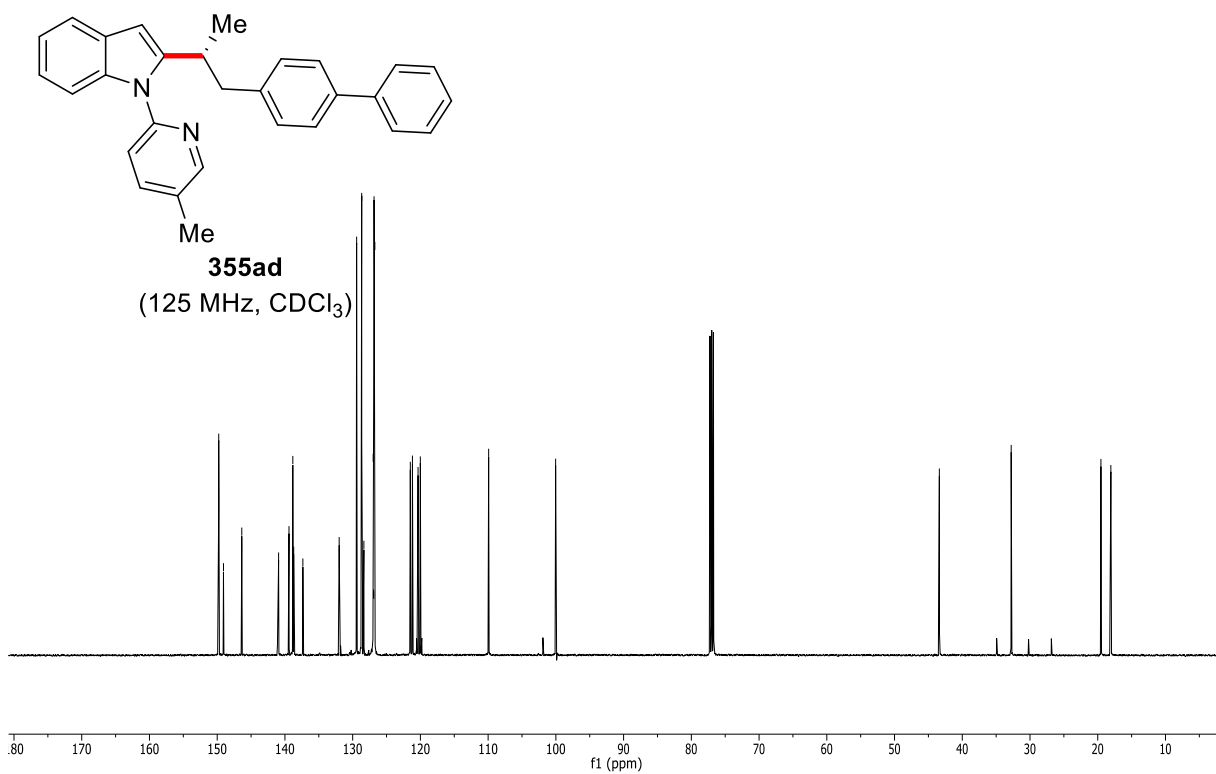
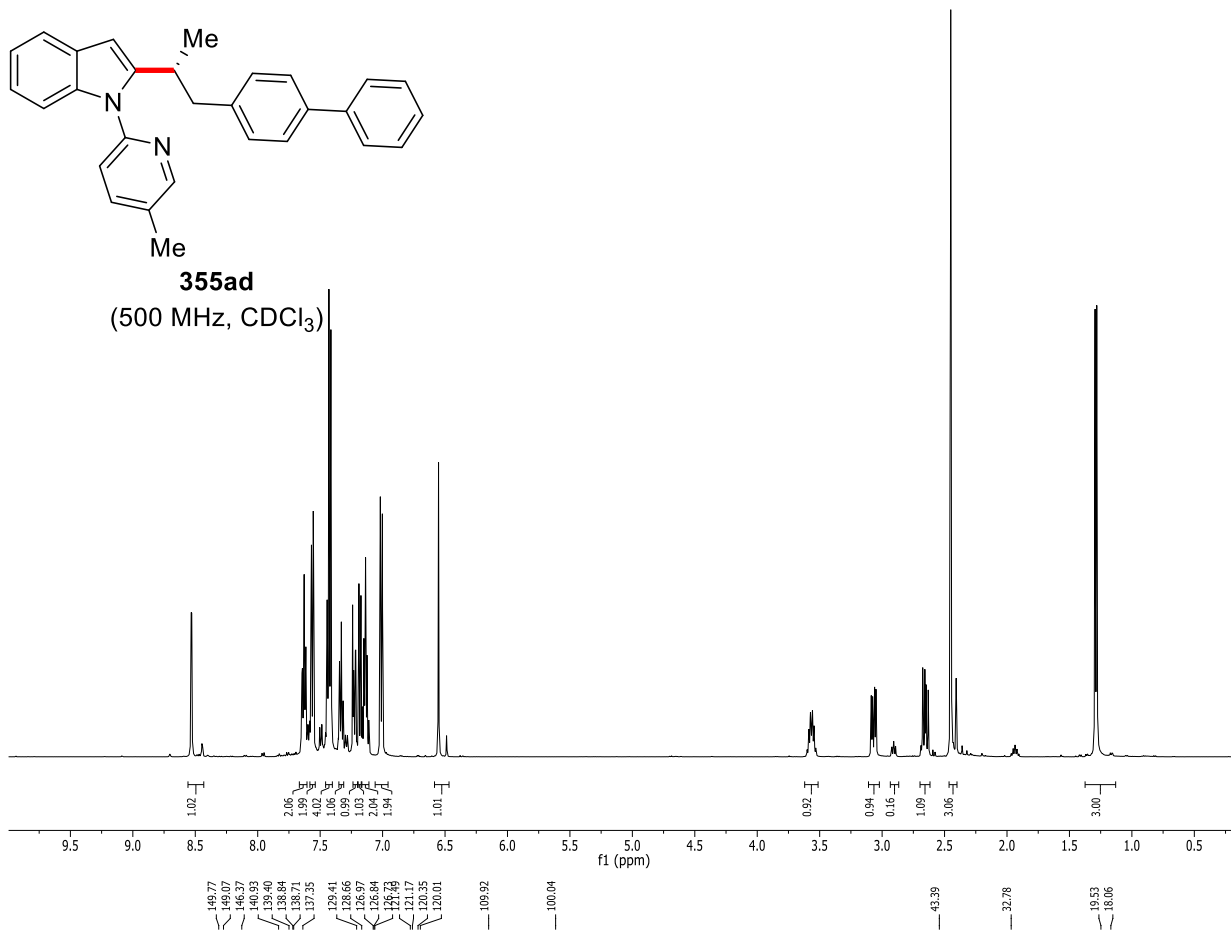
Chiral HPLC of 355ac:



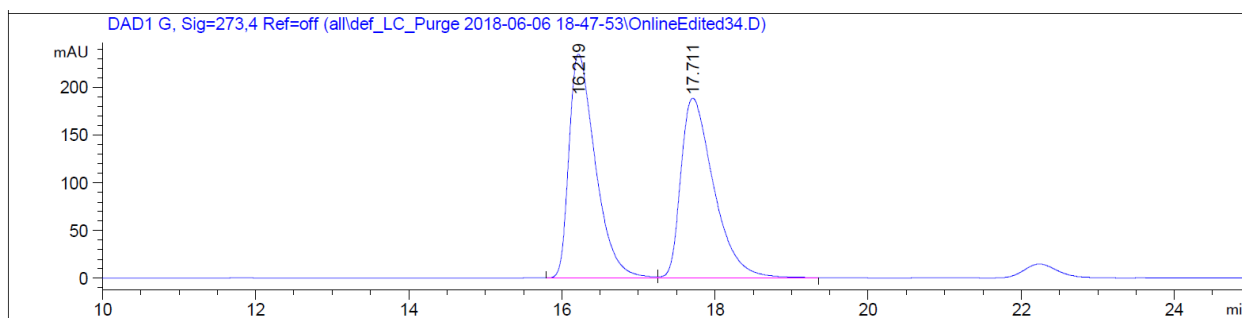
Peak #	RetTime [min]	Type	Width [min]	Area [mAU*s]	Height [mAU]	Area %
1	26.152	BB	0.4814	254.33107	6.66137	50.2631
2	30.118	MM	1.2417	251.66870	3.37793	49.7369



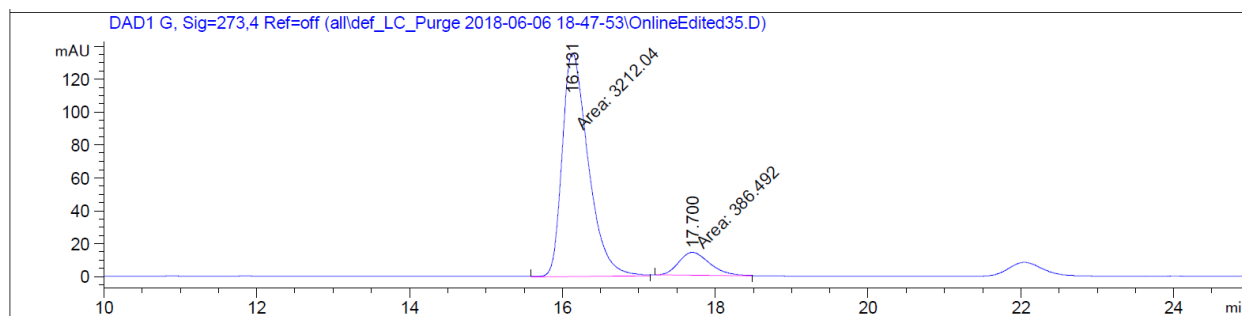
Peak #	RetTime [min]	Type	Width [min]	Area [mAU*s]	Height [mAU]	Area %
1	25.627	MM	0.6841	7018.28076	170.97748	91.2321
2	29.713	MM	1.1670	674.49158	9.63254	8.7679



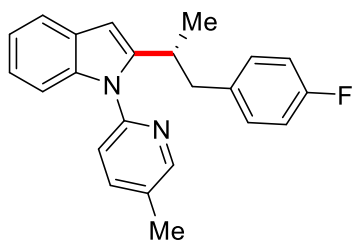
Chiral HPLC of 355ad:



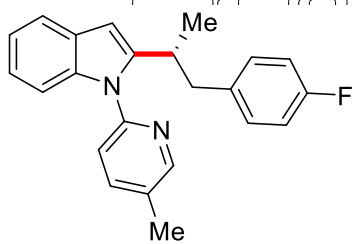
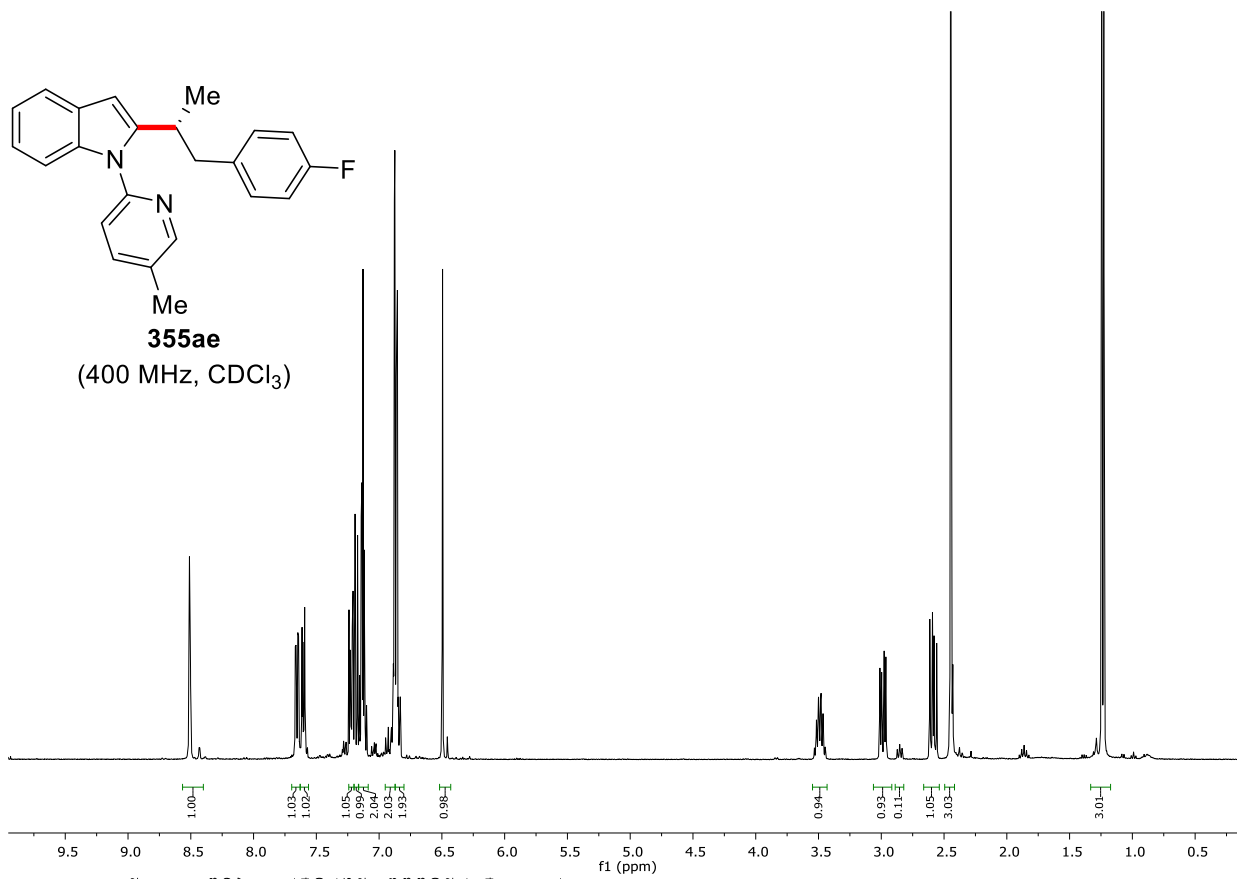
Peak #	RetTime [min]	Type	Width [min]	Area [mAU*s]	Height [mAU]	Area %
1	16.219	BV	0.3659	5600.96582	234.31482	50.0280
2	17.711	VB	0.4562	5594.69434	187.99788	49.9720



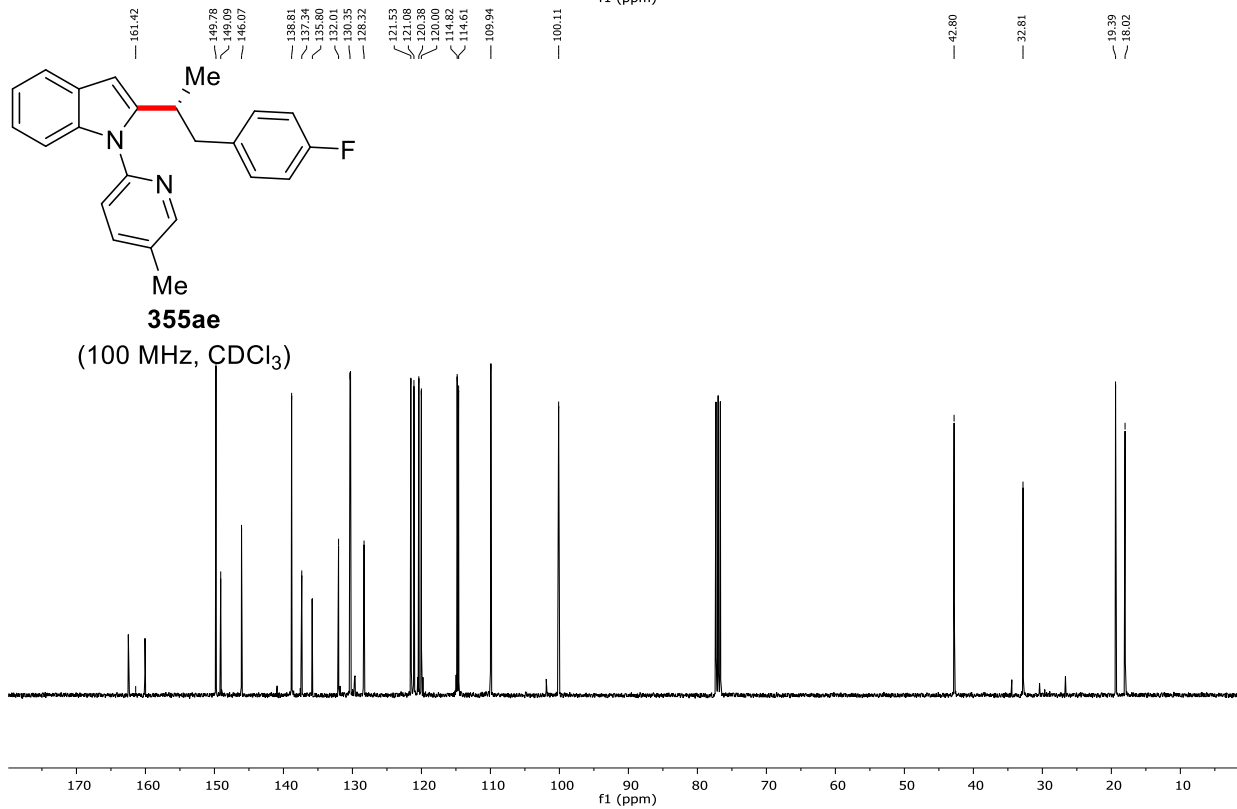
Peak #	RetTime [min]	Type	Width [min]	Area [mAU*s]	Height [mAU]	Area %
1	16.131	MM	0.3943	3212.03906	135.76524	89.2597
2	17.700	MM	0.4647	386.49231	13.86211	10.7403

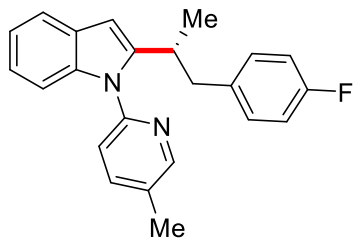


355ae
(400 MHz, CDCl₃)

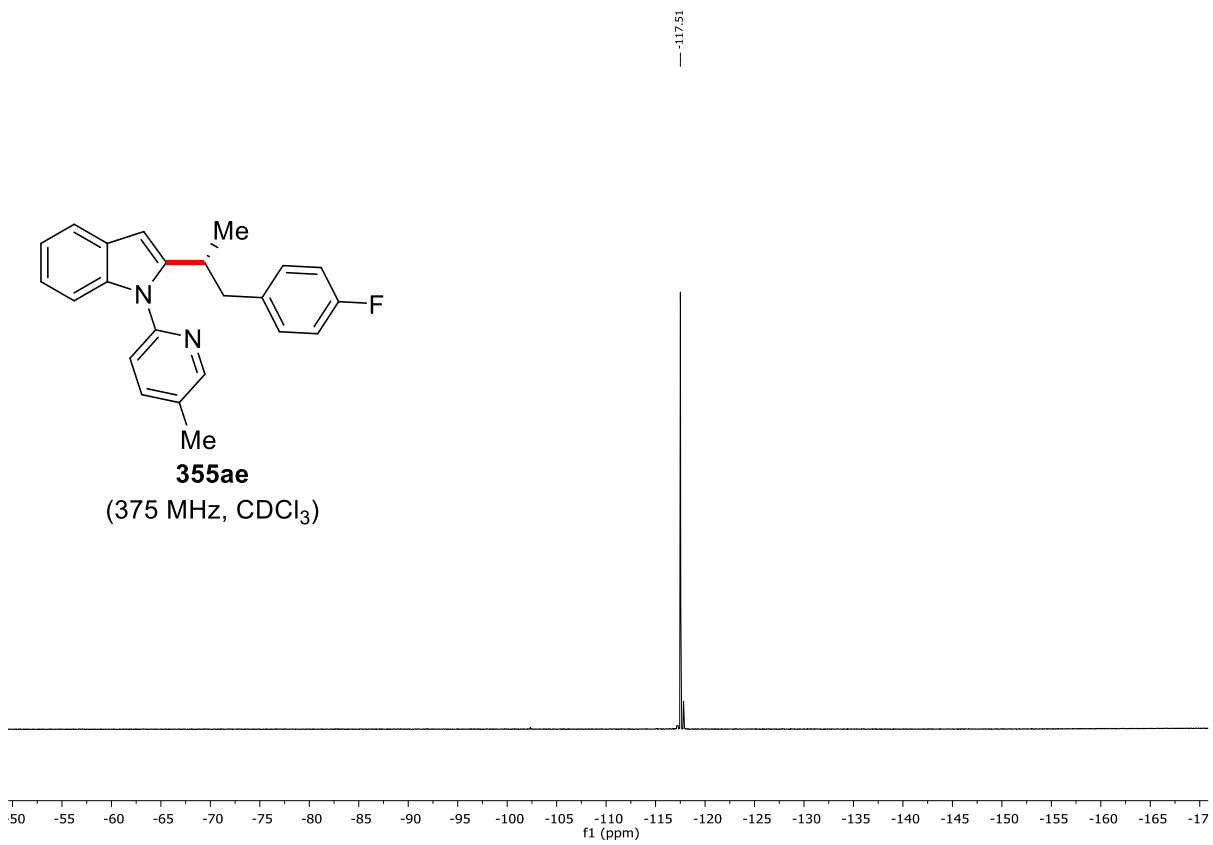


355ae
(100 MHz, CDCl₃)

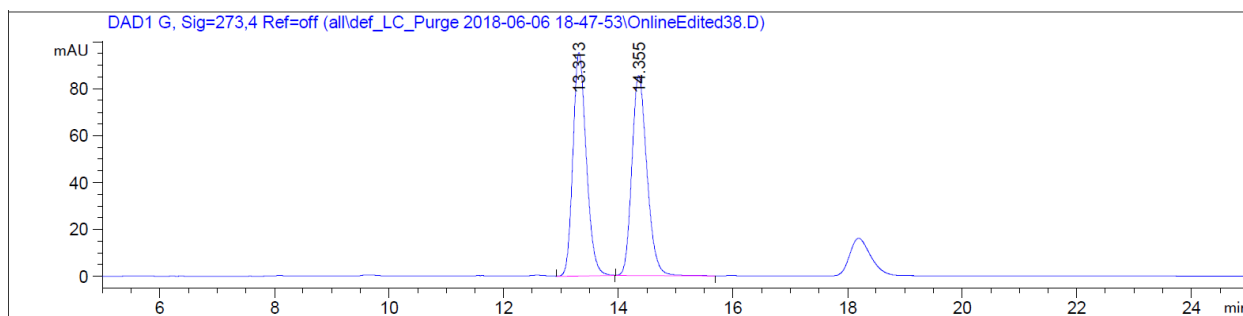




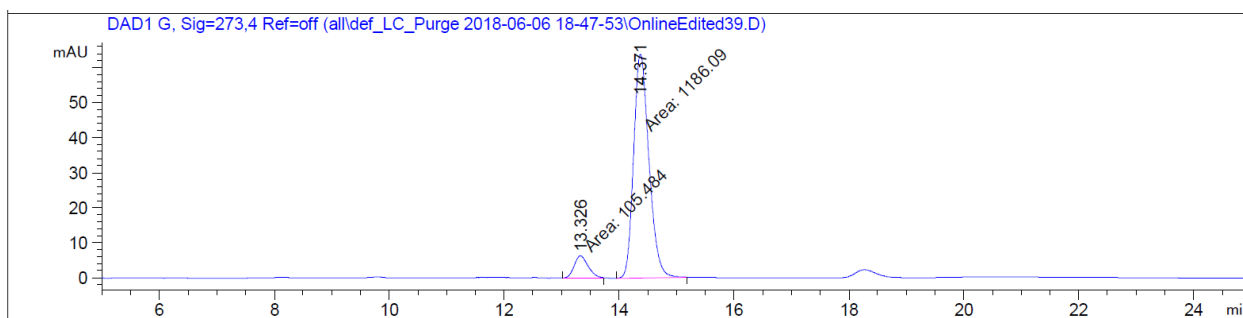
355ae
(375 MHz, CDCl₃)



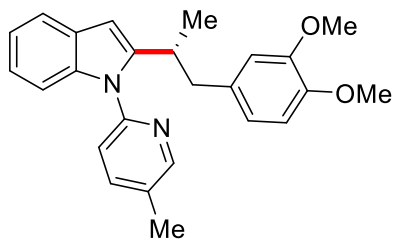
Chiral HPLC of 355ae:



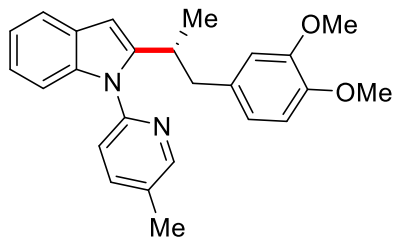
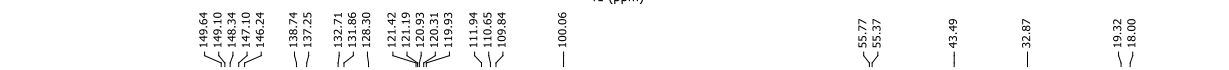
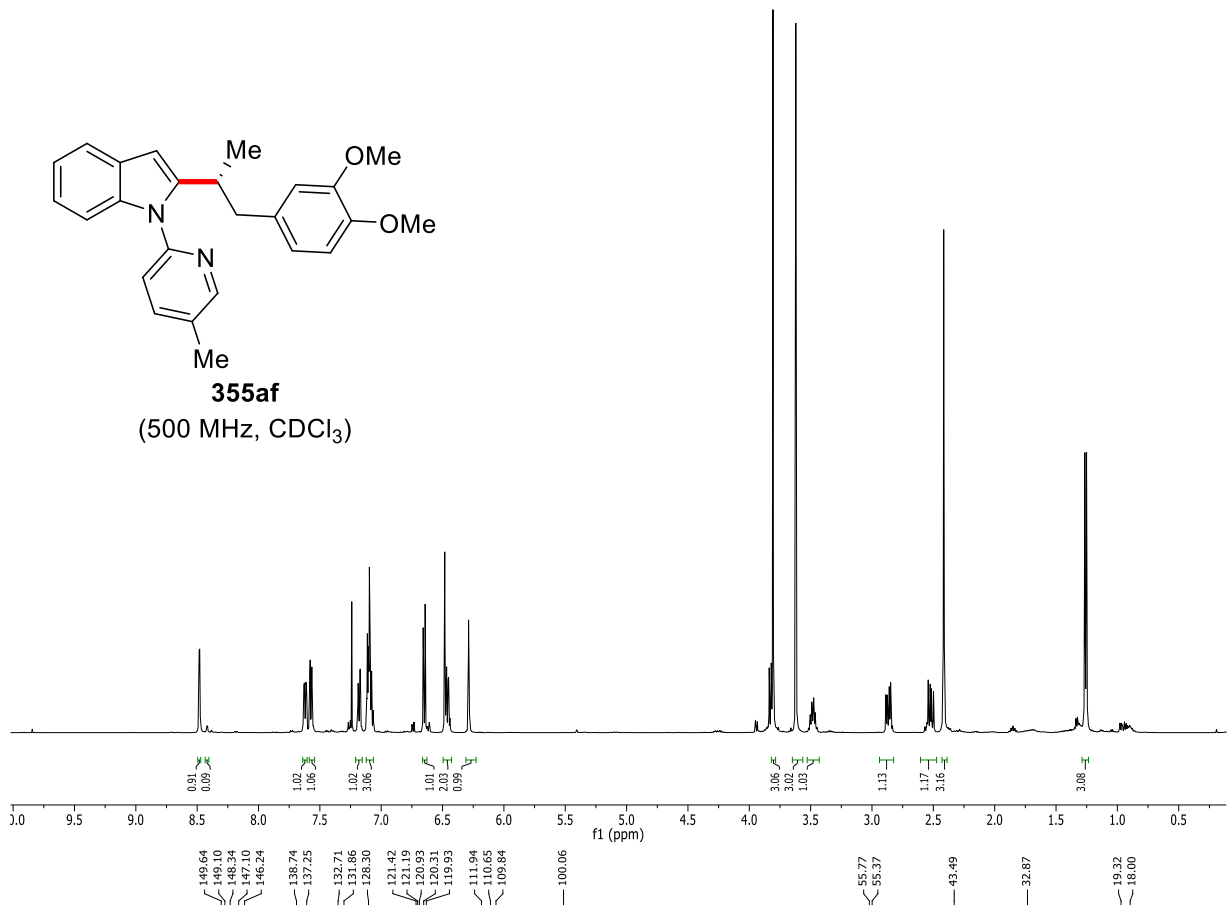
Peak #	RetTime [min]	Type	Width [min]	Area [mAU*s]	Height [mAU]	Area %
1	13.313	BB	0.2489	1542.13428	95.23789	49.8291
2	14.355	BB	0.2796	1552.71533	85.20567	50.1709



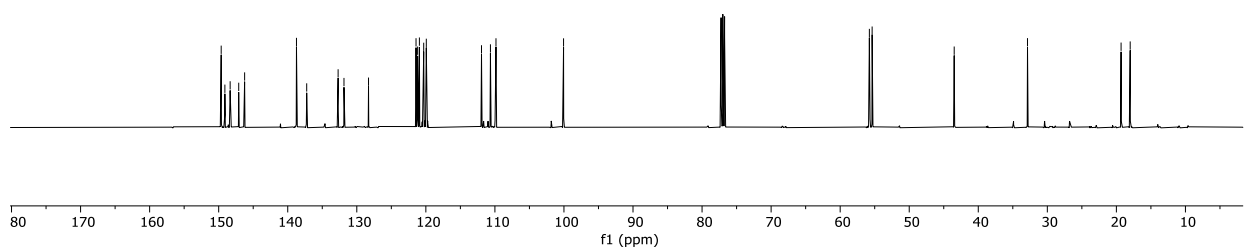
Peak #	RetTime [min]	Type	Width [min]	Area [mAU*s]	Height [mAU]	Area %
1	13.326	MM	0.2797	105.48430	6.28599	8.1671
2	14.371	MM	0.3091	1186.08838	63.94466	91.8329



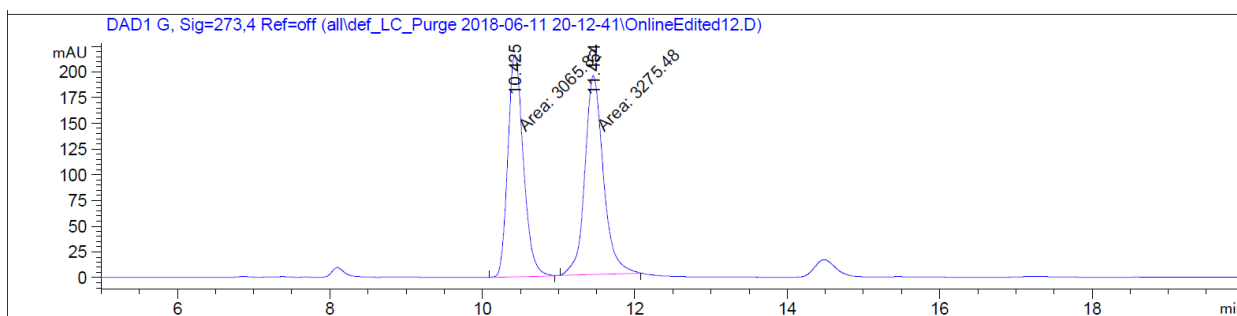
355af
(500 MHz, CDCl₃)



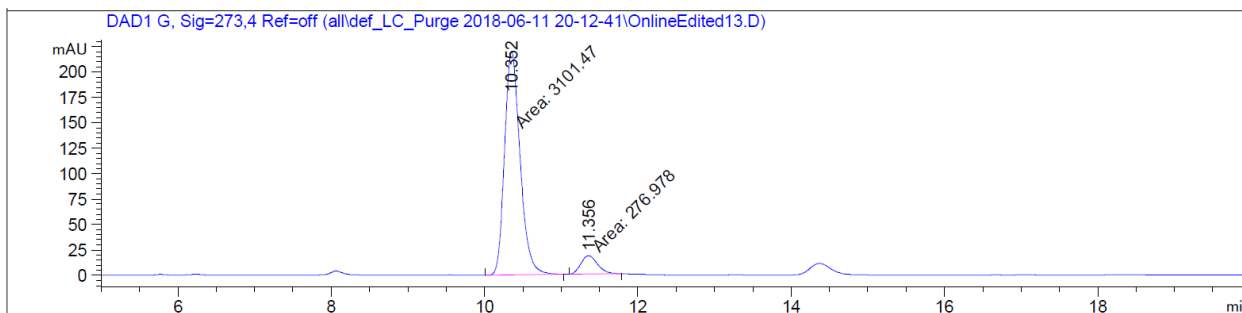
355af
(125 MHz, CDCl₃)



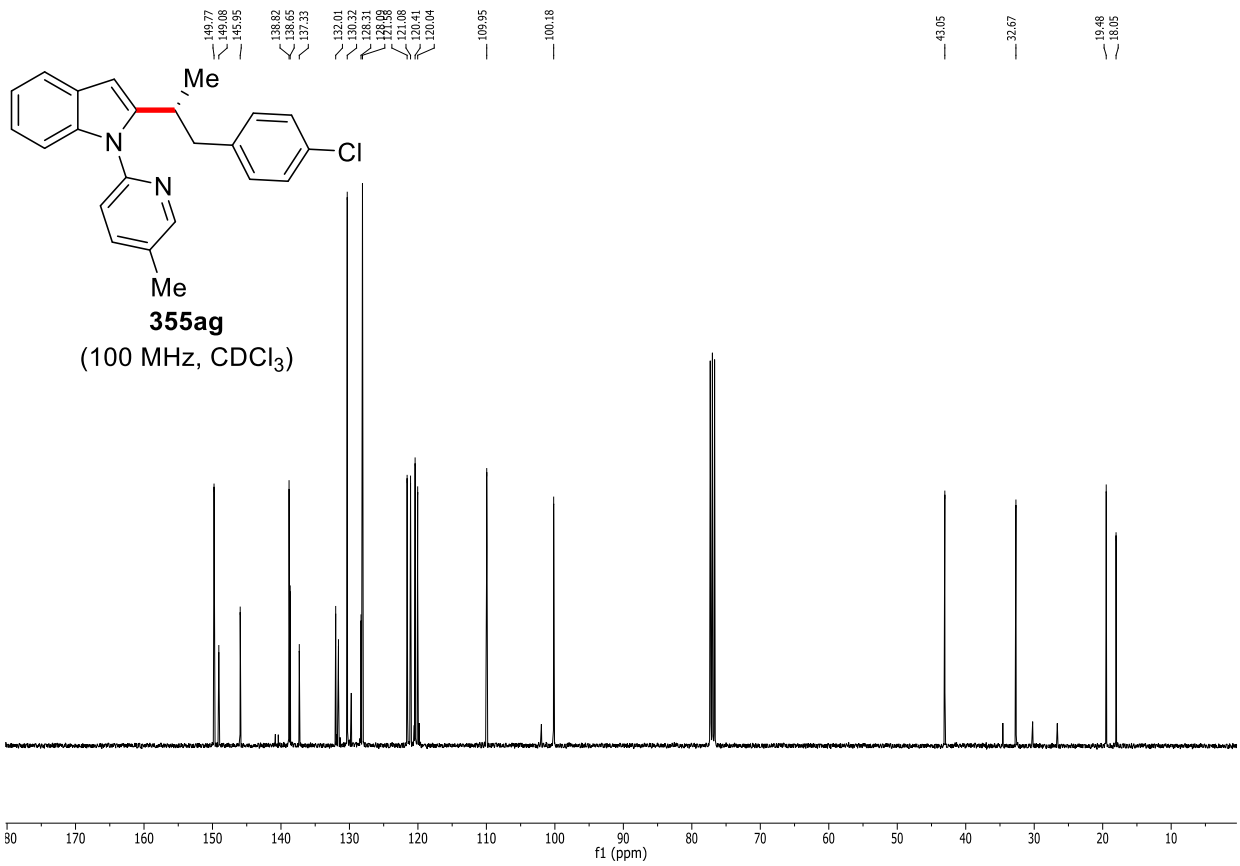
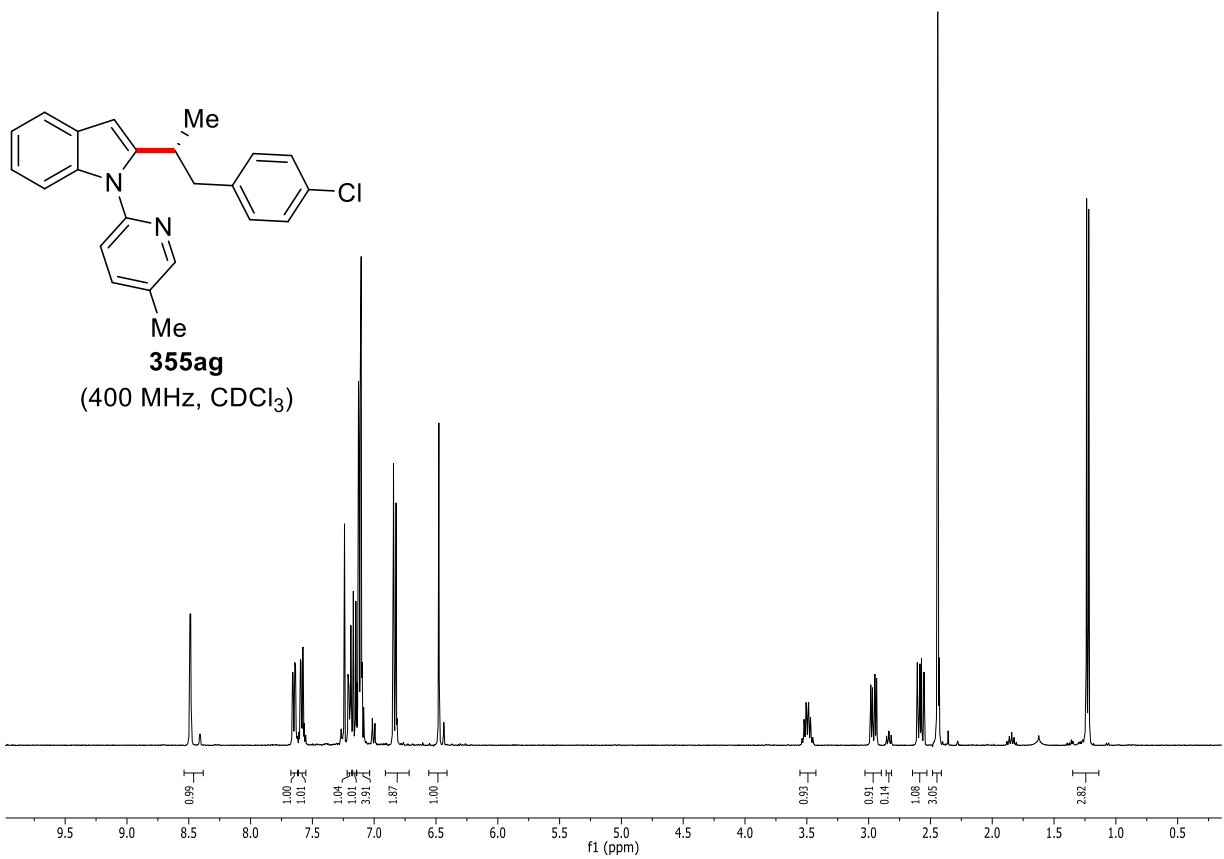
Chiral HPLC of **355af**:



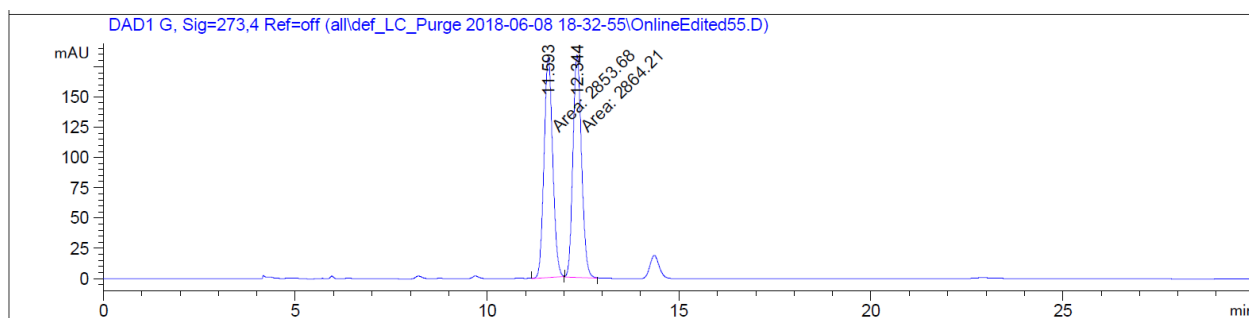
Peak #	RetTime [min]	Type	Width [min]	Area [mAU*s]	Height [mAU]	Area %
1	10.425	MM	0.2363	3065.82056	216.21277	48.3469
2	11.454	MM	0.2824	3275.48120	193.33524	51.6531



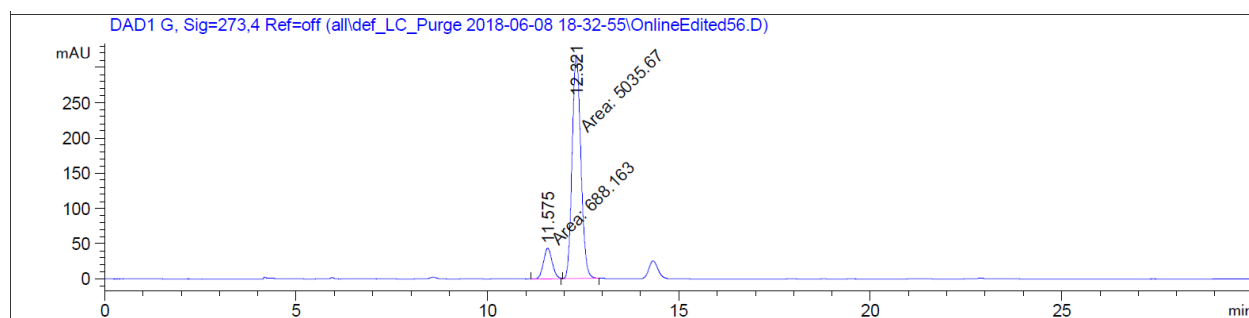
Peak #	RetTime [min]	Type	Width [min]	Area [mAU*s]	Height [mAU]	Area %
1	10.352	MM	0.2348	3101.46777	220.18263	91.8016
2	11.356	MM	0.2548	276.97769	18.11912	8.1984



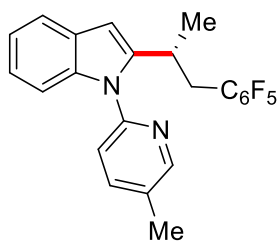
Chiral HPLC of 355ag:



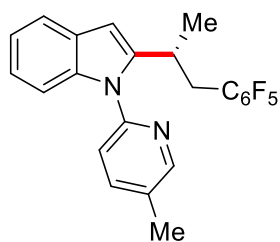
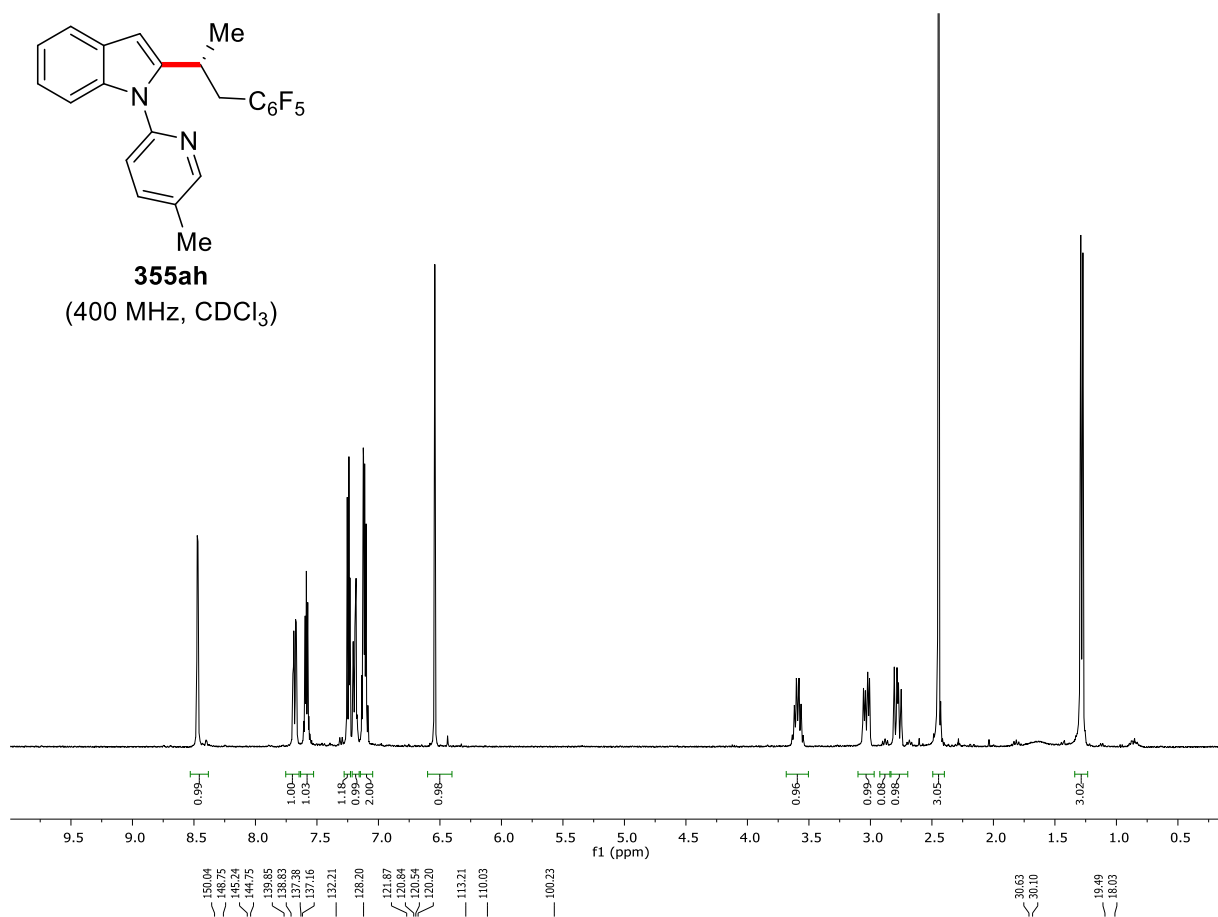
Peak #	RetTime [min]	Type	Width [min]	Area [mAU*s]	Height [mAU]	Area %
1	11.593	MM	0.2626	2853.68335	181.14539	49.9079
2	12.344	MM	0.2601	2864.21436	183.54207	50.0921



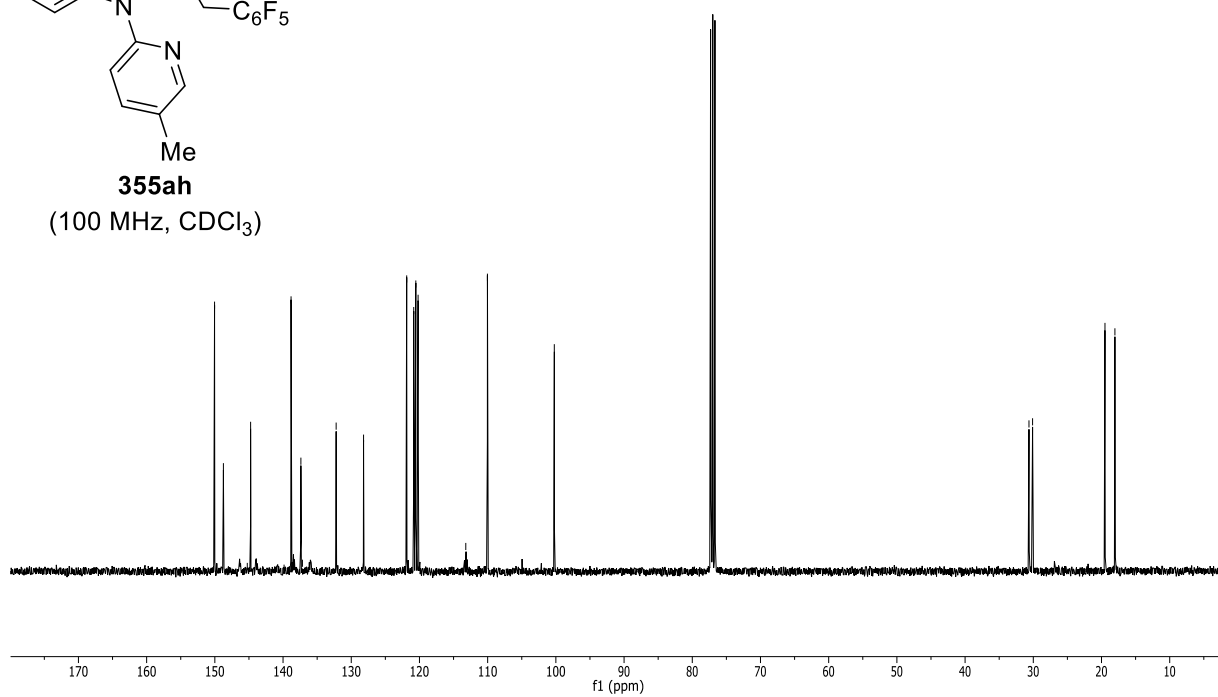
Peak #	RetTime [min]	Type	Width [min]	Area [mAU*s]	Height [mAU]	Area %
1	11.575	MM	0.2650	688.16284	43.27824	12.0228
2	12.321	MM	0.2648	5035.67334	316.90408	87.9772

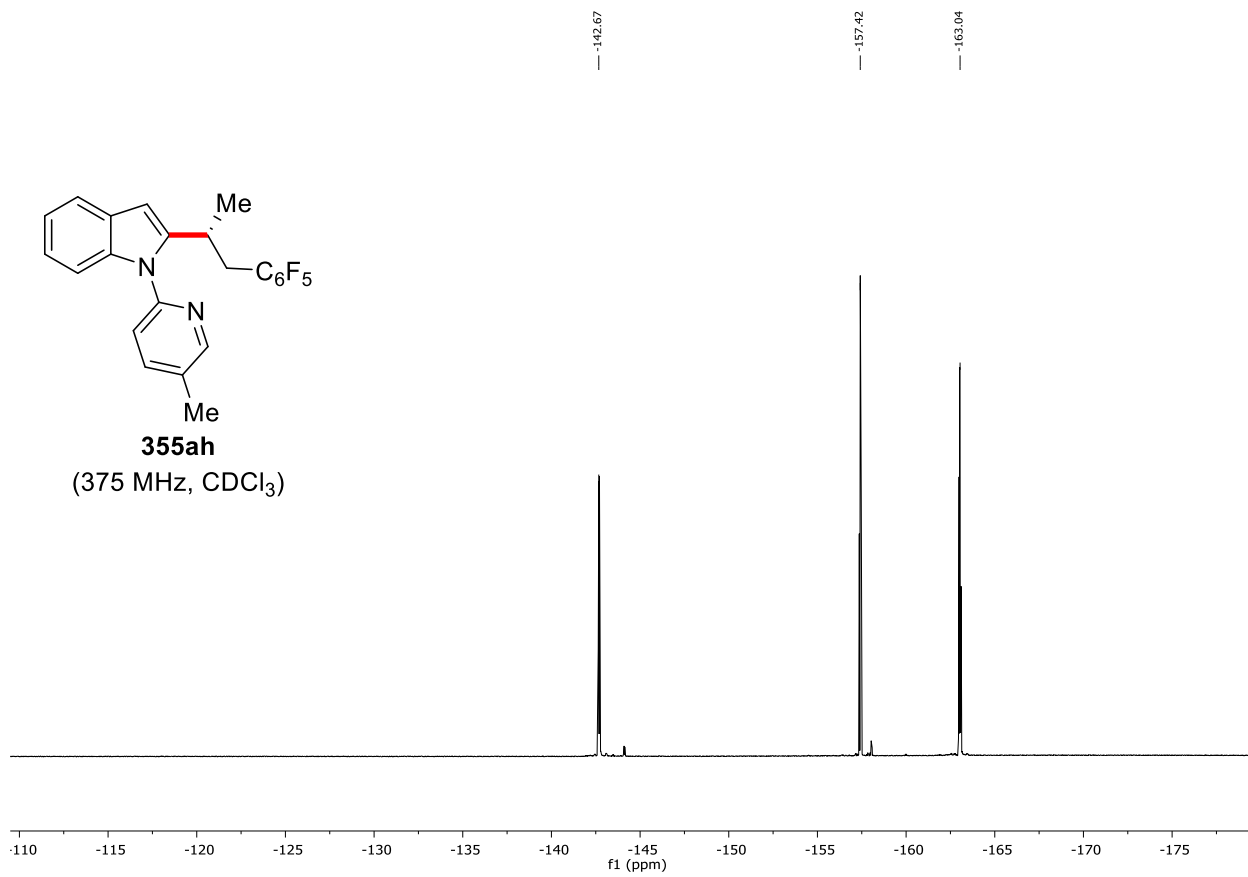


355ah
(400 MHz, CDCl₃)

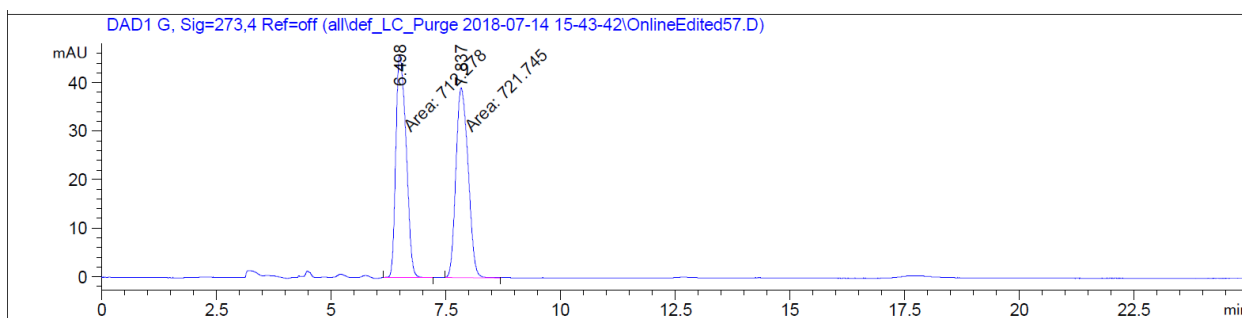


355ah
(100 MHz, CDCl₃)

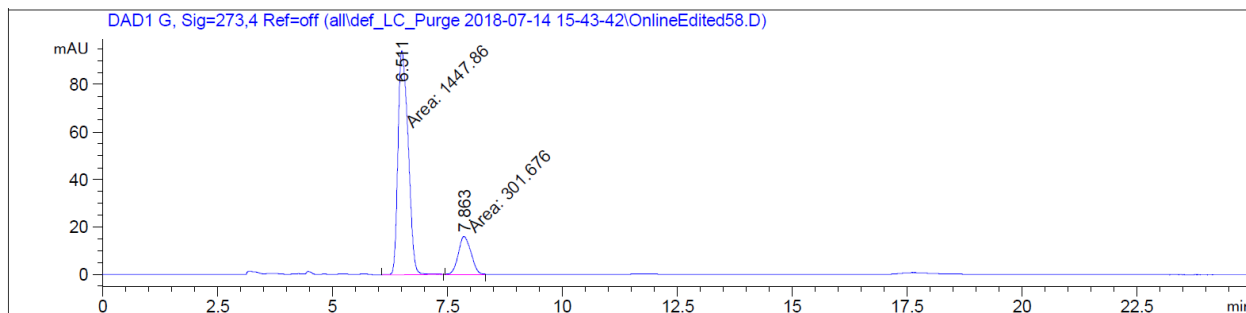




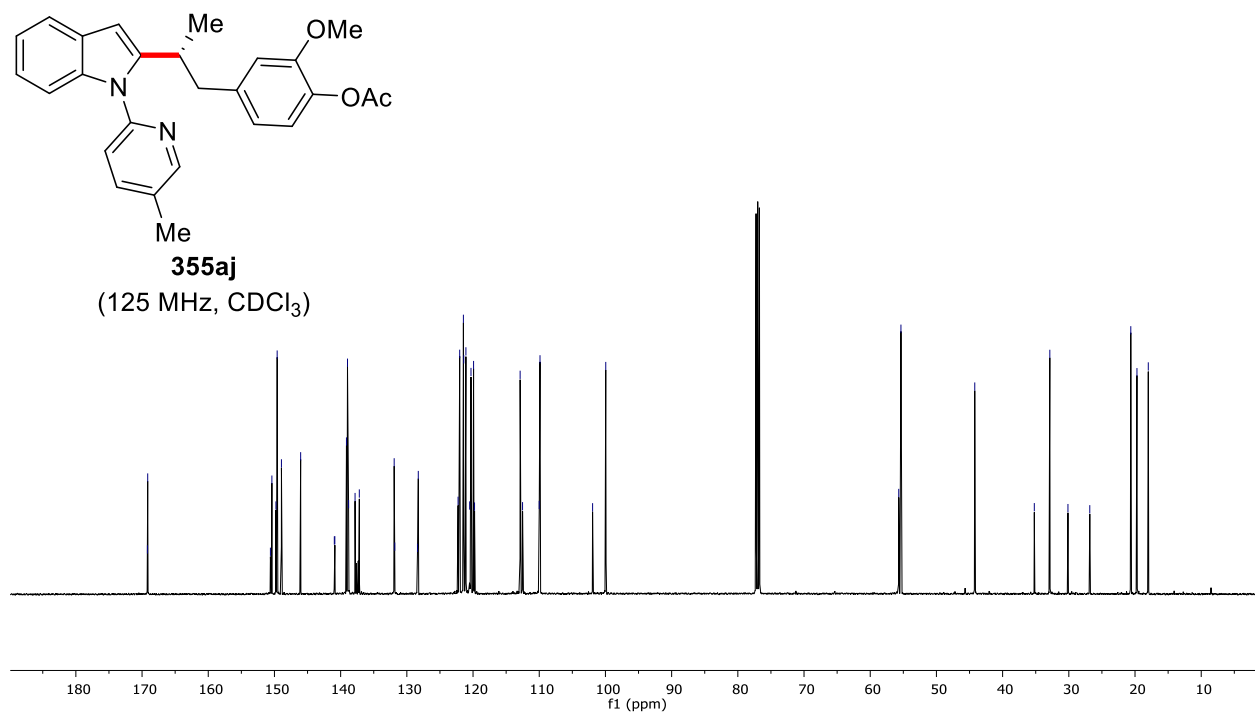
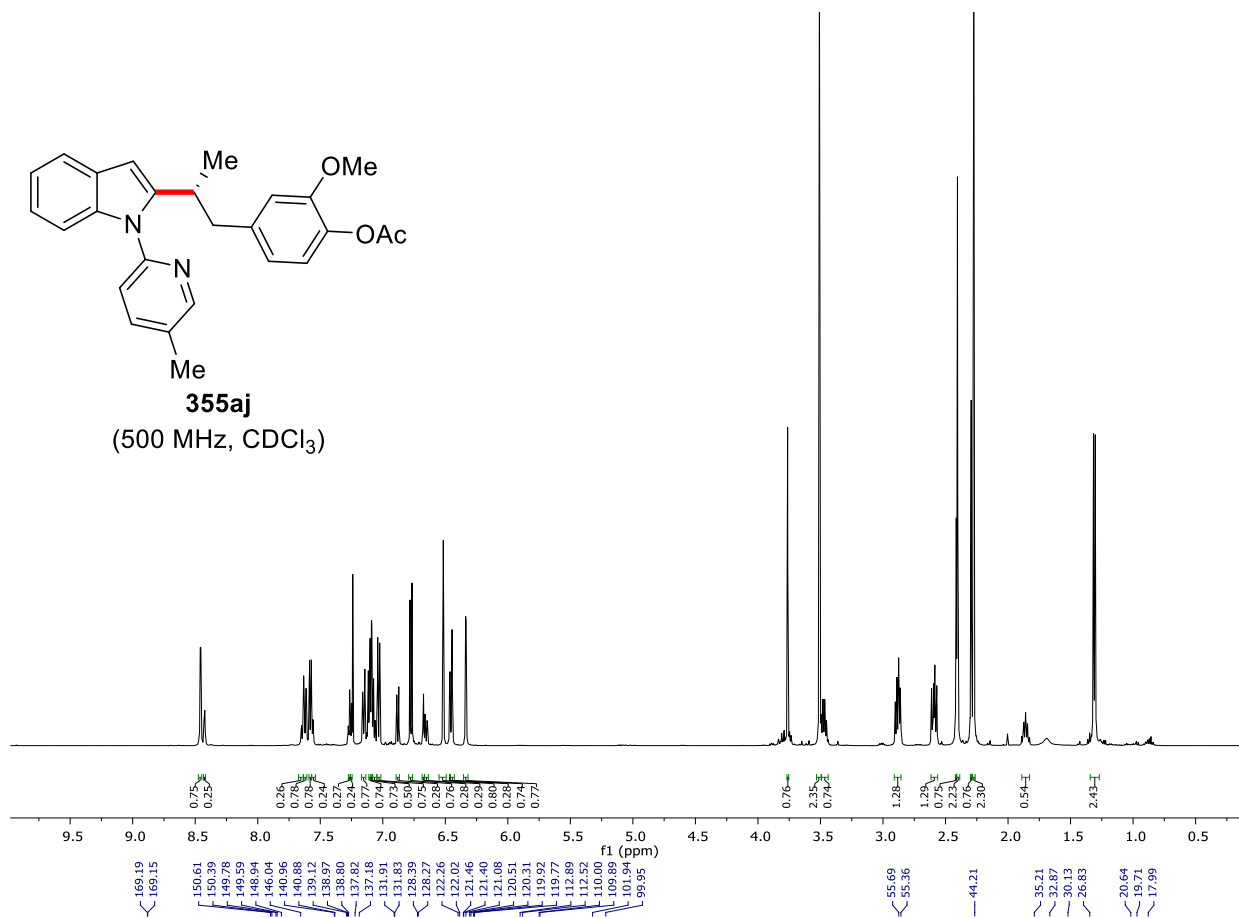
Chiral HPLC of **355ah**:



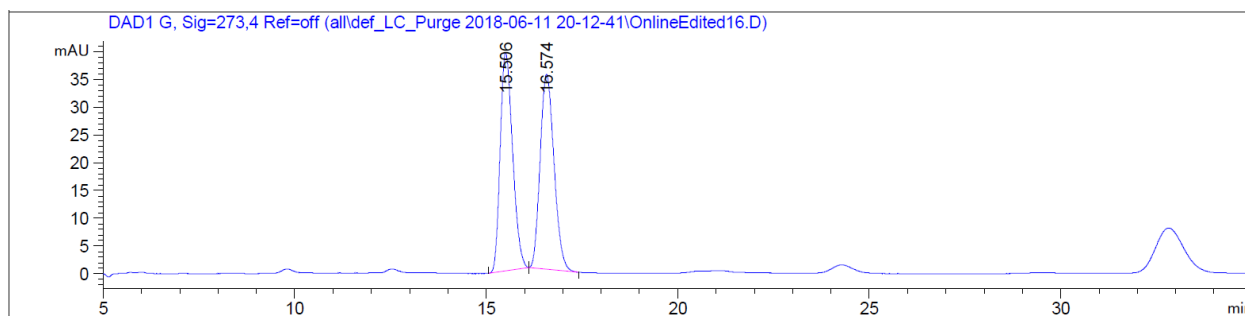
Peak #	RetTime [min]	Type	Width [min]	Area [mAU*s]	Height [mAU]	Area %
1	6.498	MM	0.2591	712.27753	45.82068	49.6699
2	7.837	MM	0.3081	721.74530	39.03794	50.3301



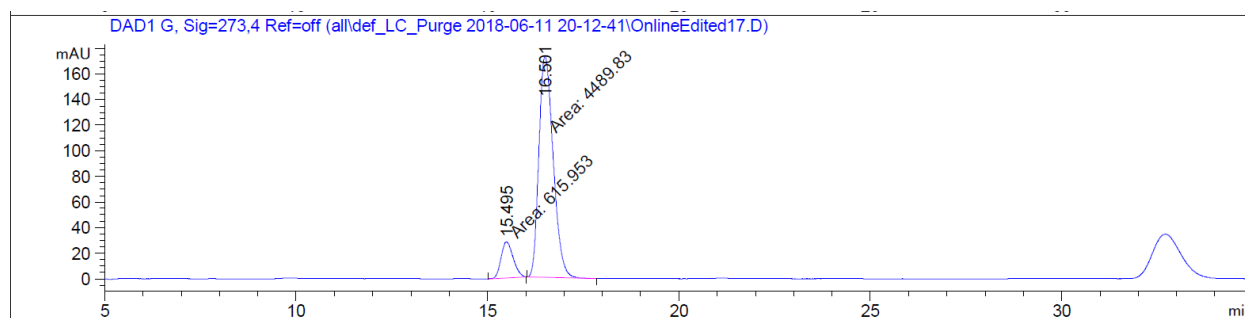
Peak #	RetTime [min]	Type	Width [min]	Area [mAU*s]	Height [mAU]	Area %
1	6.511	MM	0.2556	1447.86475	94.41283	82.7569
2	7.863	MM	0.3156	301.67560	15.93044	17.2431



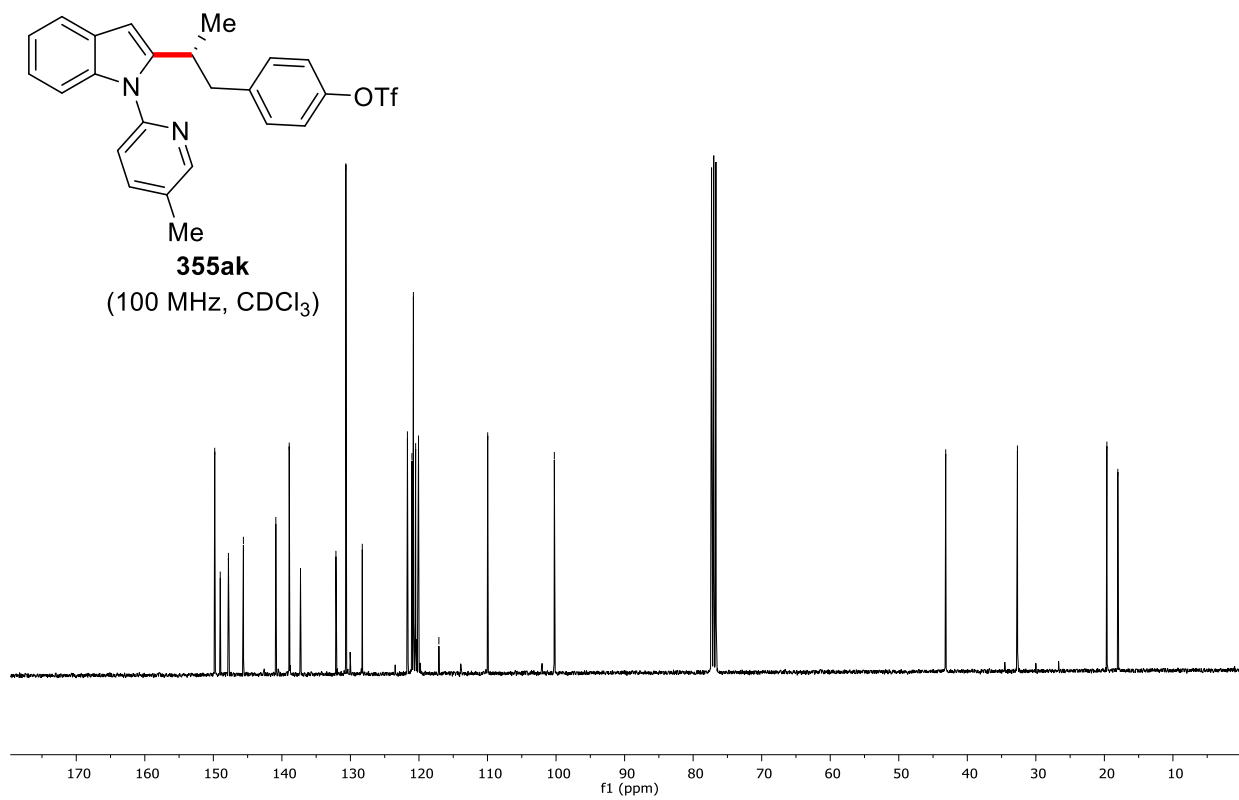
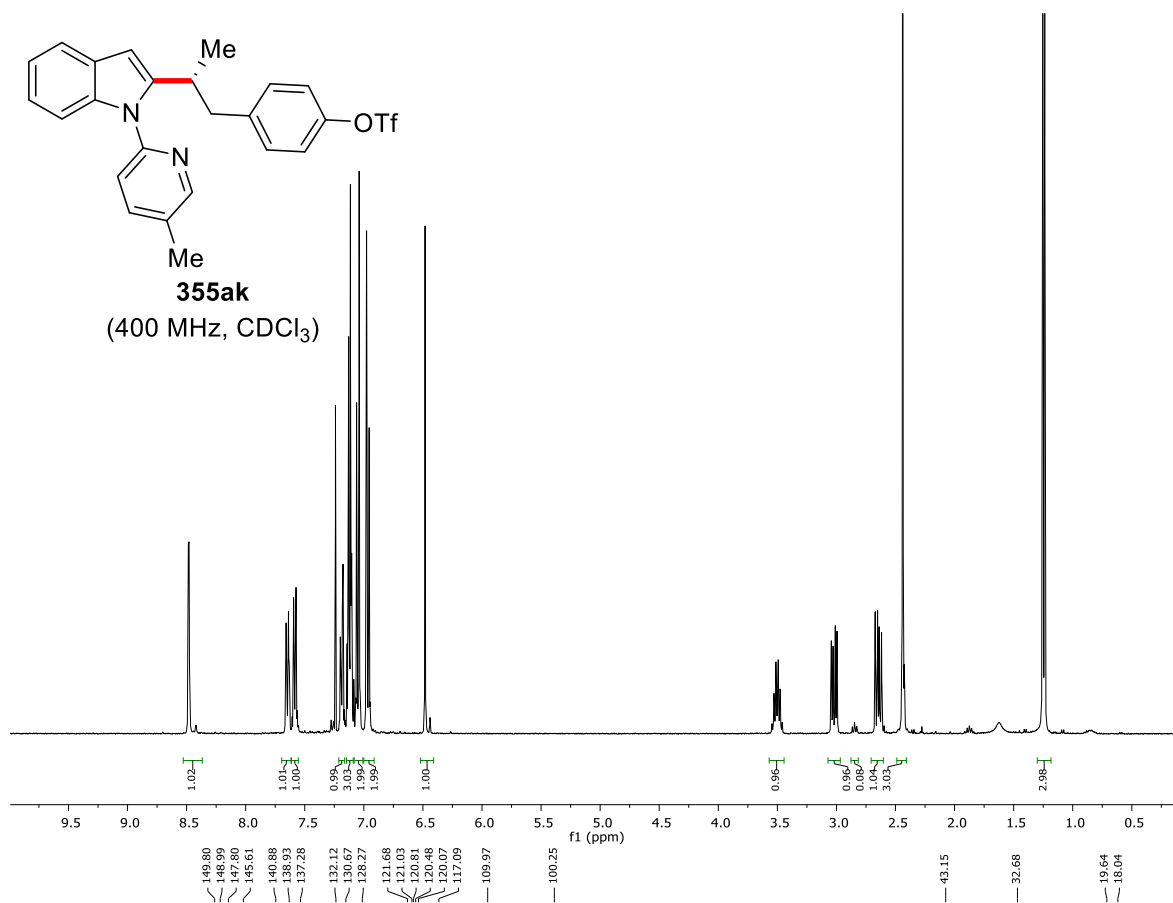
Chiral HPLC of 355aj:

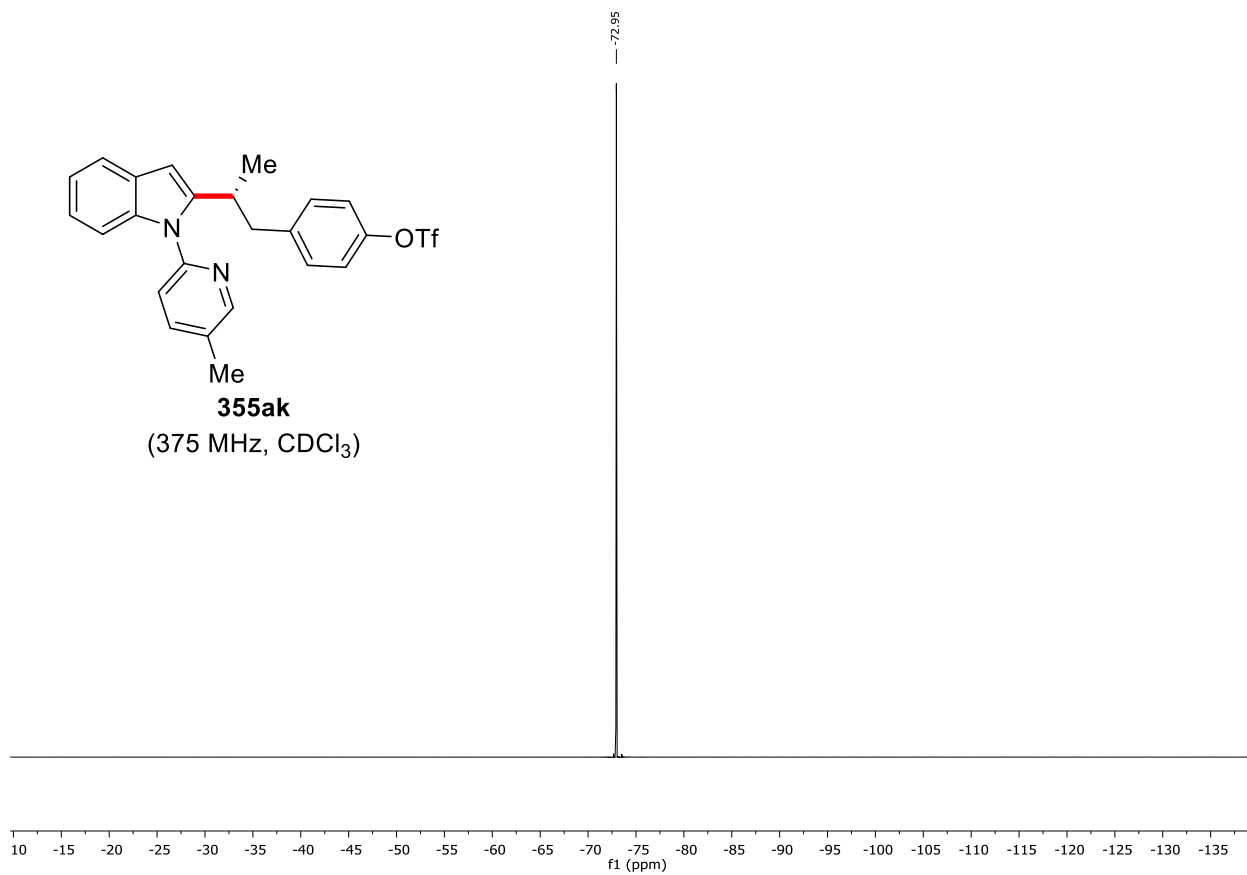


Peak #	RetTime [min]	Type	Width [min]	Area [mAU*s]	Height [mAU]	Area %
1	15.506	BB	0.3480	884.11908	39.36467	49.8972
2	16.574	BB	0.3886	887.76105	35.15716	50.1028

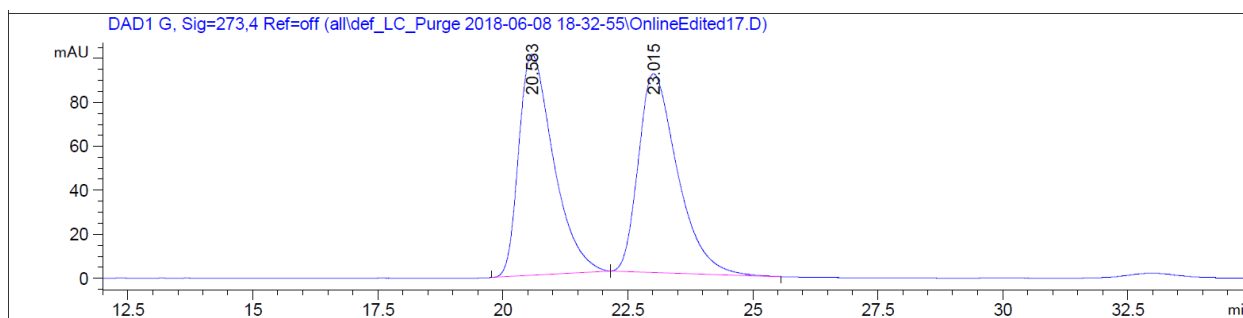


Peak #	RetTime [min]	Type	Width [min]	Area [mAU*s]	Height [mAU]	Area %
1	15.495	MM	0.3685	623.69250	28.21044	12.2205
2	16.501	MM	0.4318	4479.98438	172.92096	87.7795

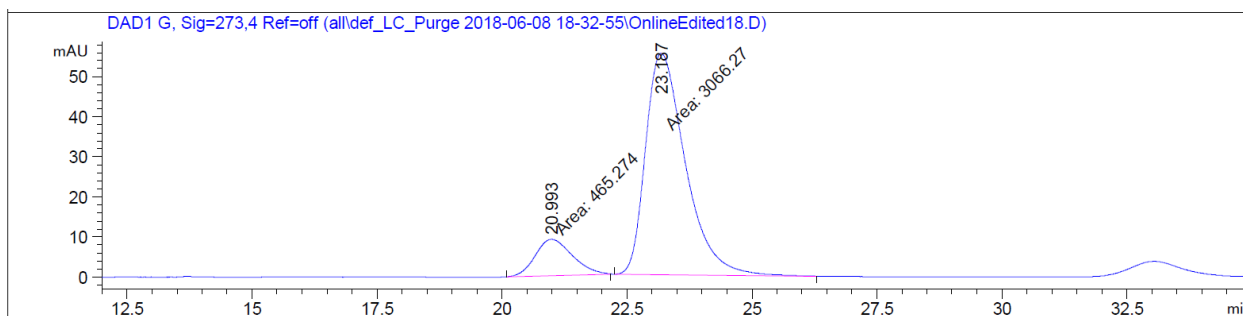




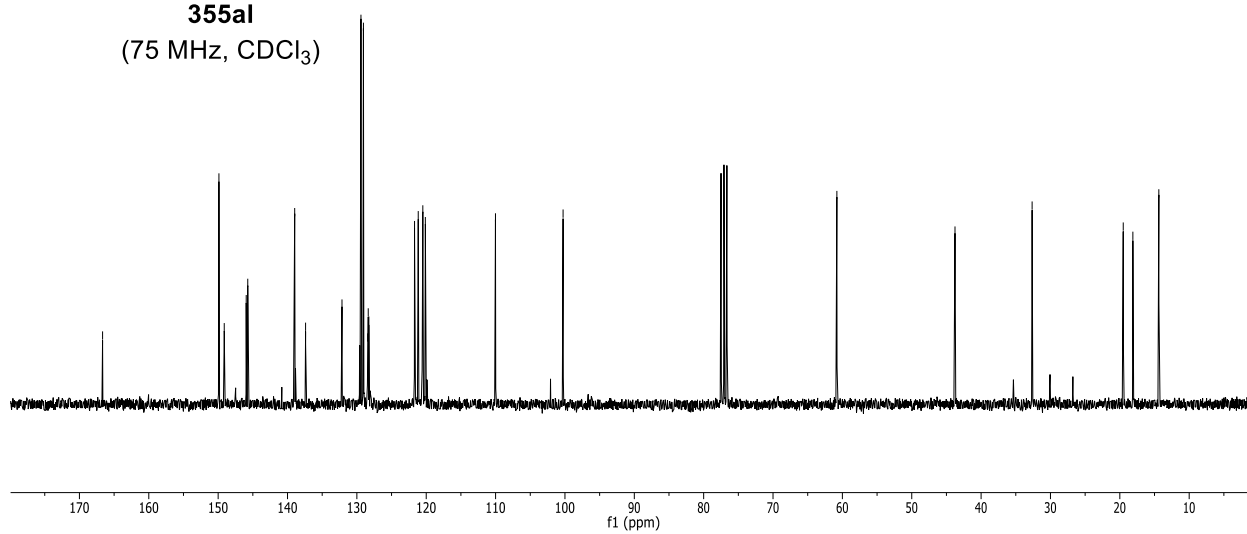
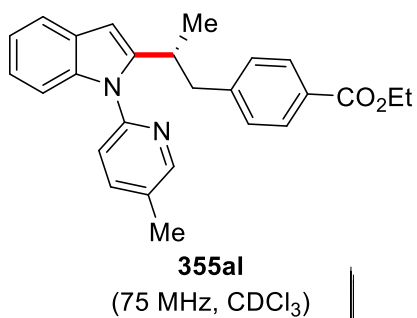
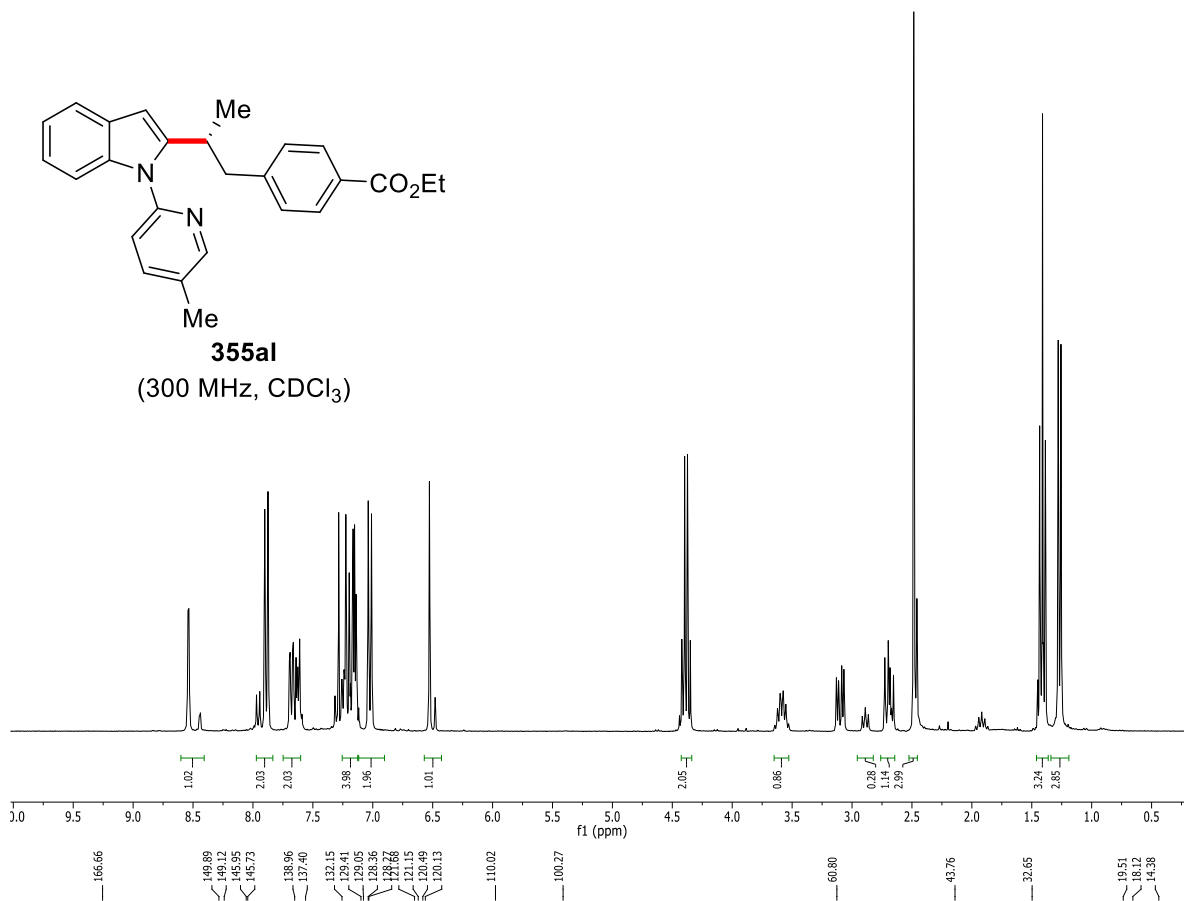
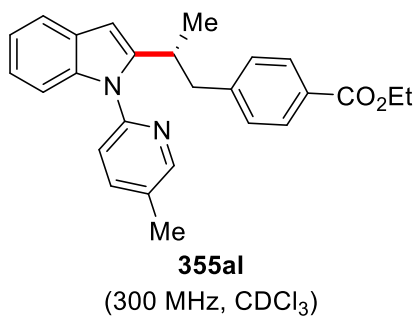
Chiral HPLC of **355ak**:



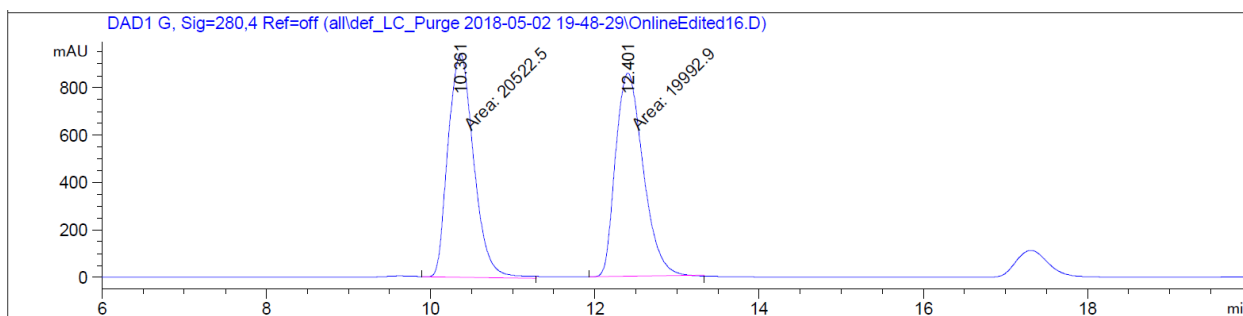
Peak #	RetTime [min]	Type	Width [min]	Area [mAU*s]	Height [mAU]	Area %
1	20.583	BB	0.7153	4857.50391	100.60416	49.6698
2	23.015	BB	0.7870	4922.09814	90.42706	50.3302



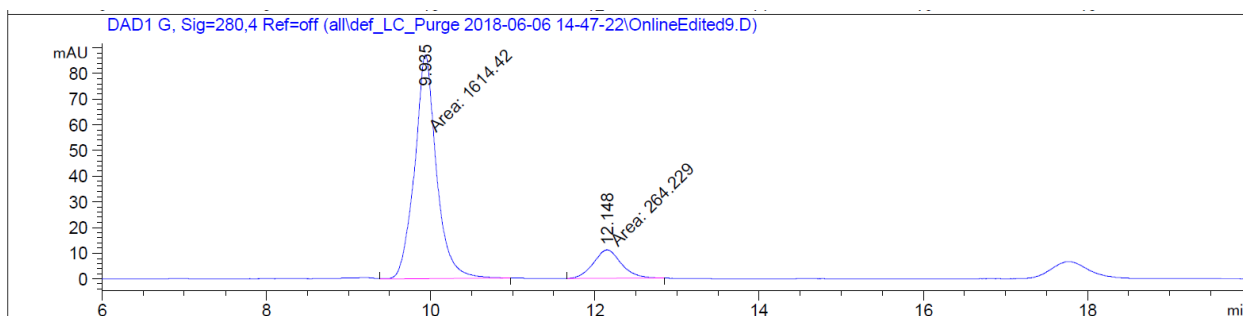
Peak #	RetTime [min]	Type	Width [min]	Area [mAU*s]	Height [mAU]	Area %
1	20.993	MM	0.8571	465.27365	9.04786	13.1748
2	23.187	MM	0.9245	3066.26782	55.27755	86.8252



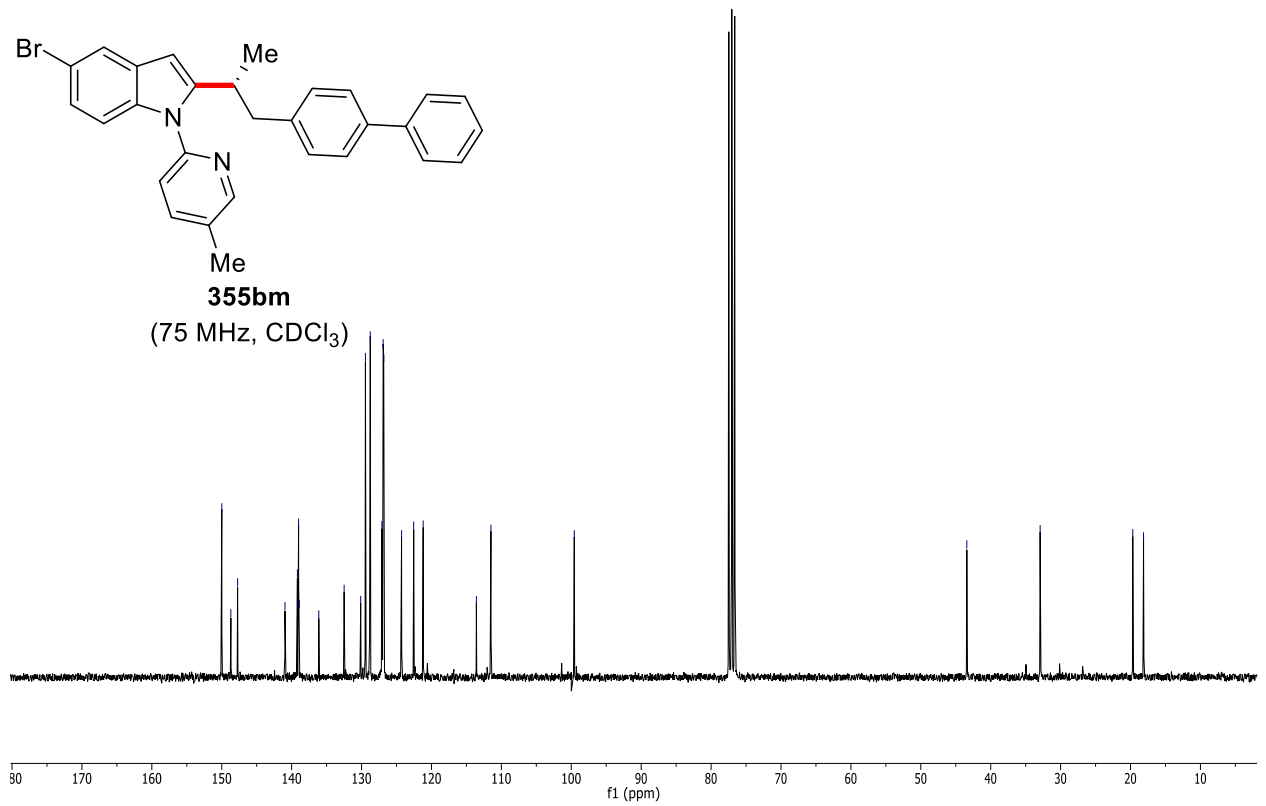
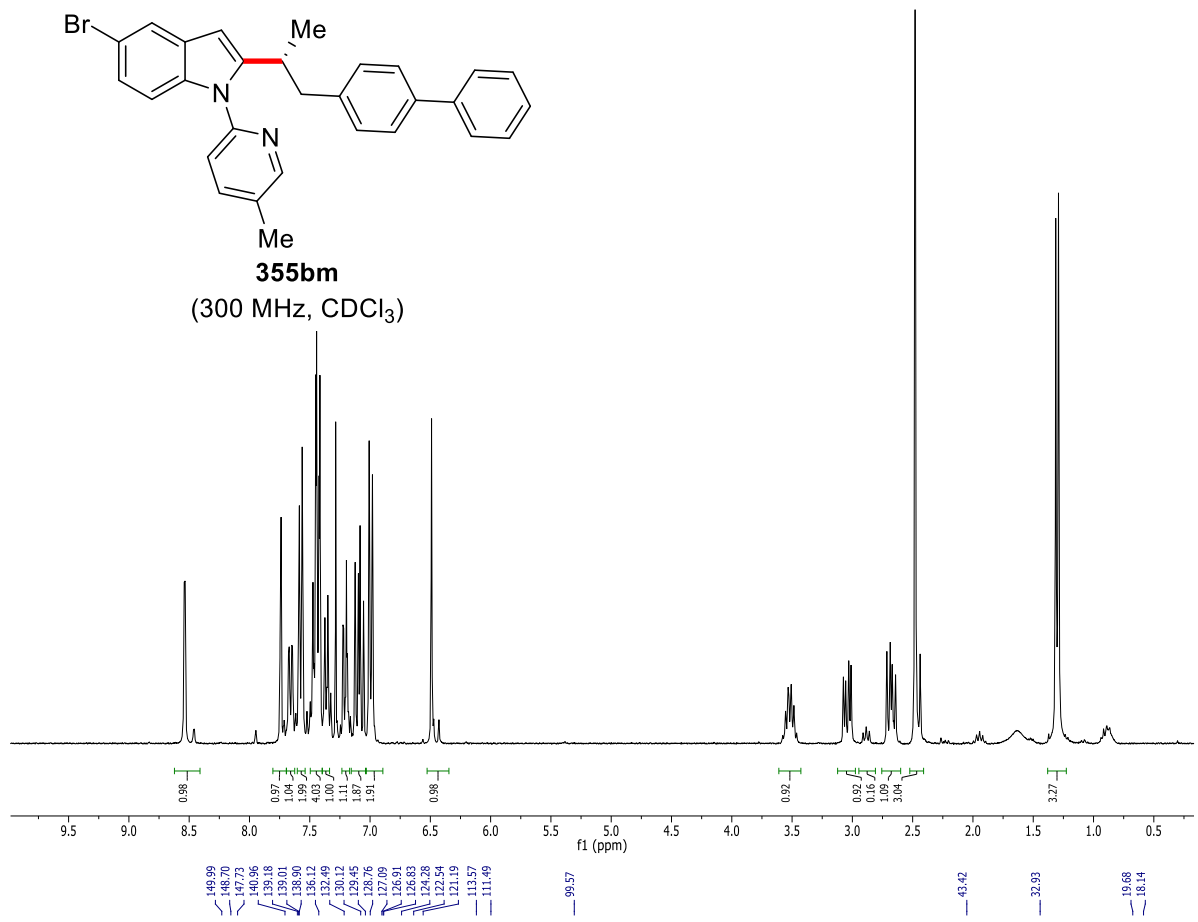
Chiral HPLC of **355a**:



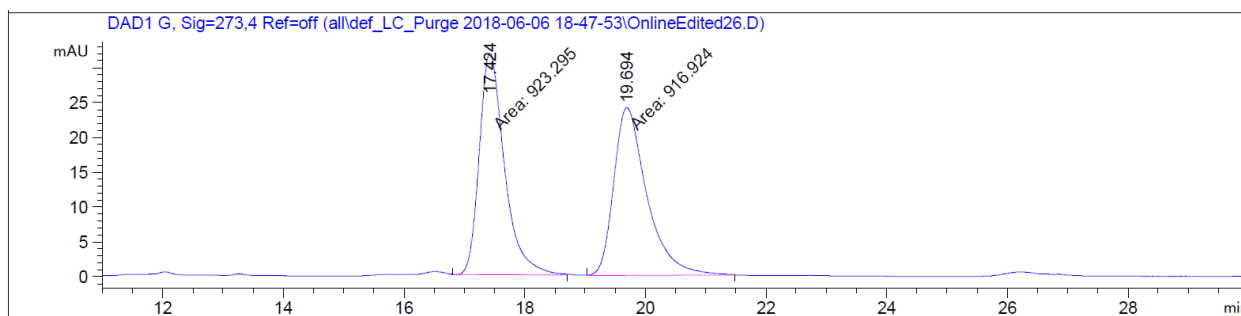
Peak #	RetTime [min]	Type	Width [min]	Area [mAU*s]	Height [mAU]	Area %
1	10.361	MM	0.3621	2.05225e4	944.63037	50.6536
2	12.401	MM	0.3892	1.99929e4	856.14777	49.3464



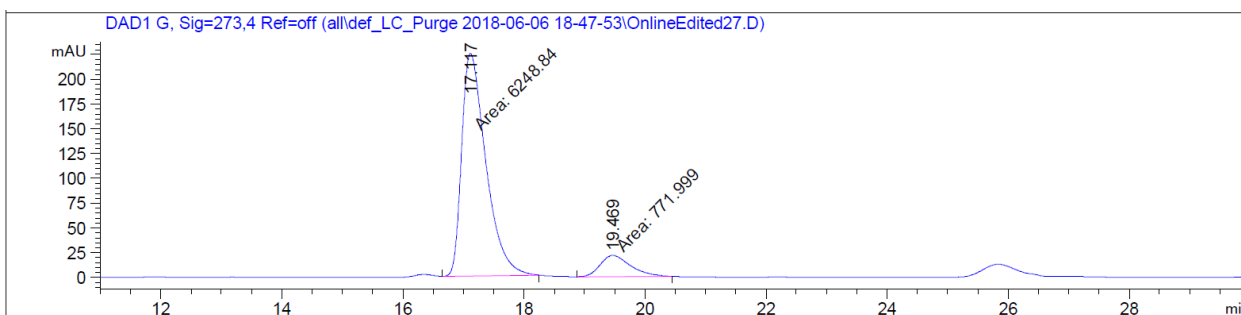
Peak #	RetTime [min]	Type	Width [min]	Area [mAU*s]	Height [mAU]	Area %
1	9.935	MM	0.3088	1614.42334	87.12728	85.9352
2	12.148	MM	0.3964	264.22855	11.10977	14.0648



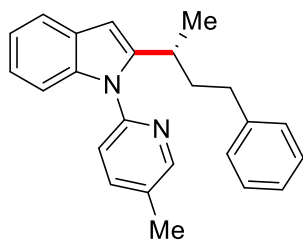
Chiral HPLC of **355bm**:



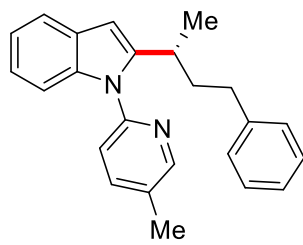
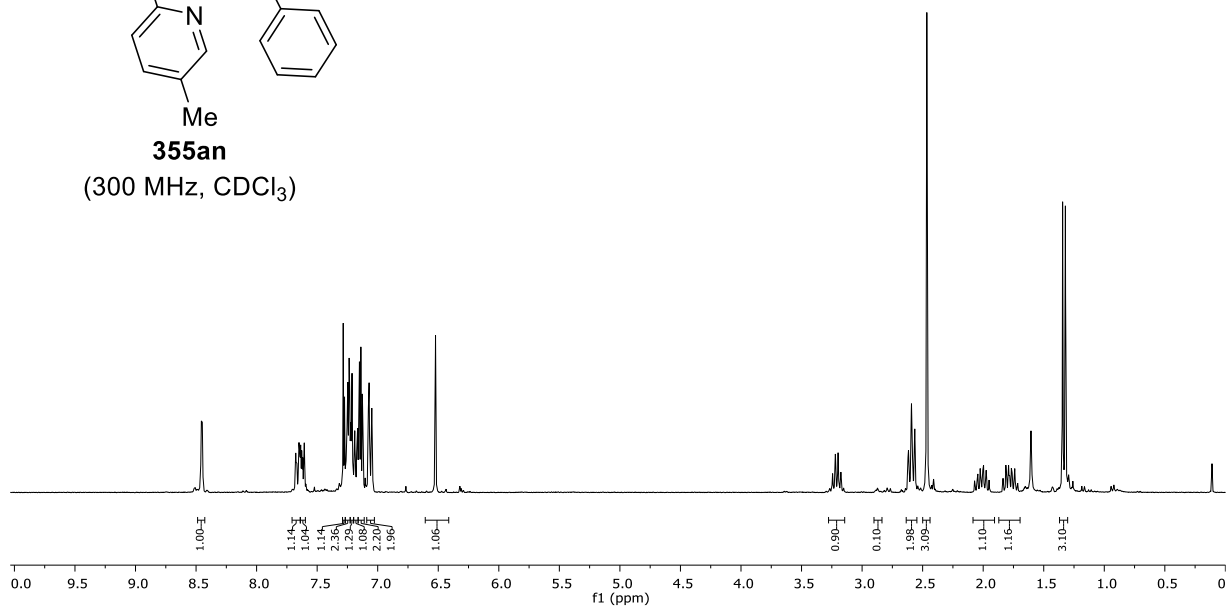
Peak #	RetTime [min]	Type	Width [min]	Area [mAU*s]	Height [mAU]	Area %
1	17.424	MM	0.4840	923.29541	31.79417	50.1731
2	19.694	MM	0.6345	916.92407	24.08637	49.8269



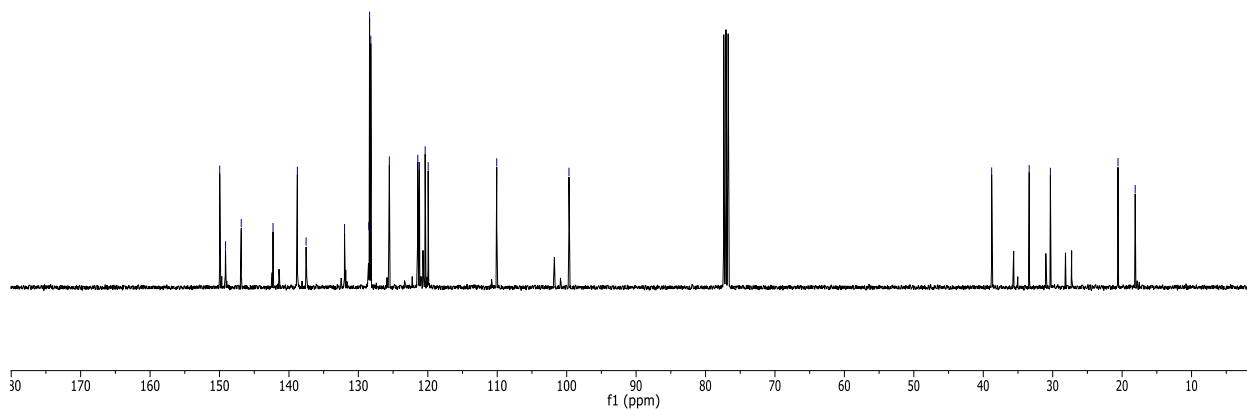
Peak #	RetTime [min]	Type	Width [min]	Area [mAU*s]	Height [mAU]	Area %
1	17.117	MM	0.4632	6248.83594	224.85121	89.0042
2	19.469	MM	0.5937	771.99933	21.67333	10.9958



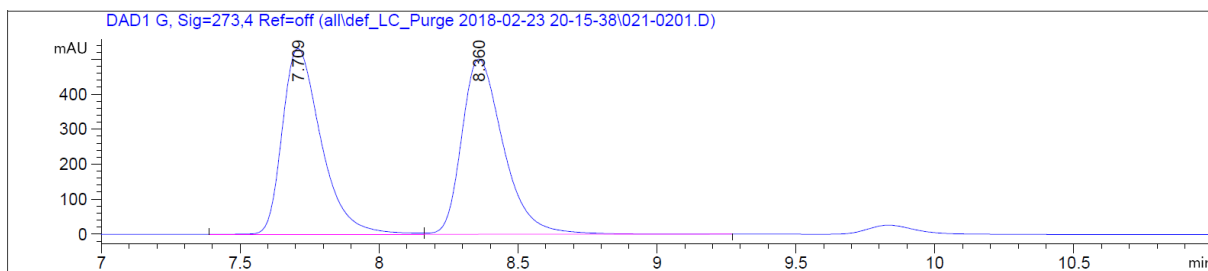
355an
(300 MHz, CDCl₃)



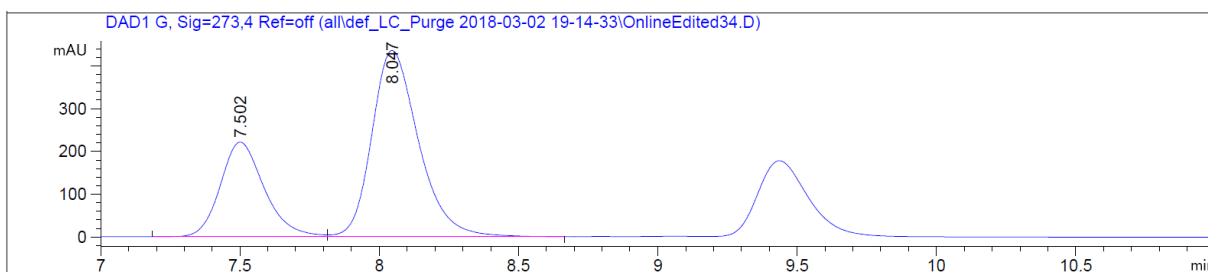
355an
(100 MHz, CDCl₃)



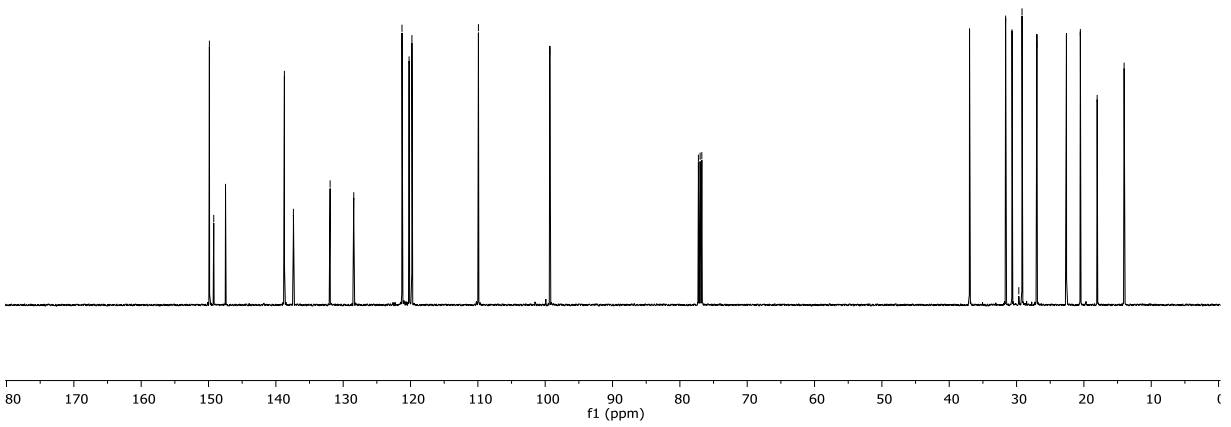
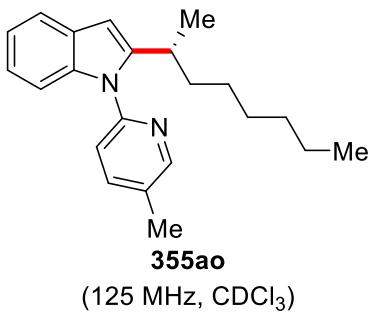
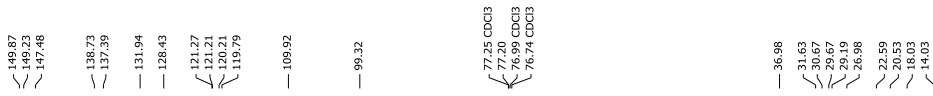
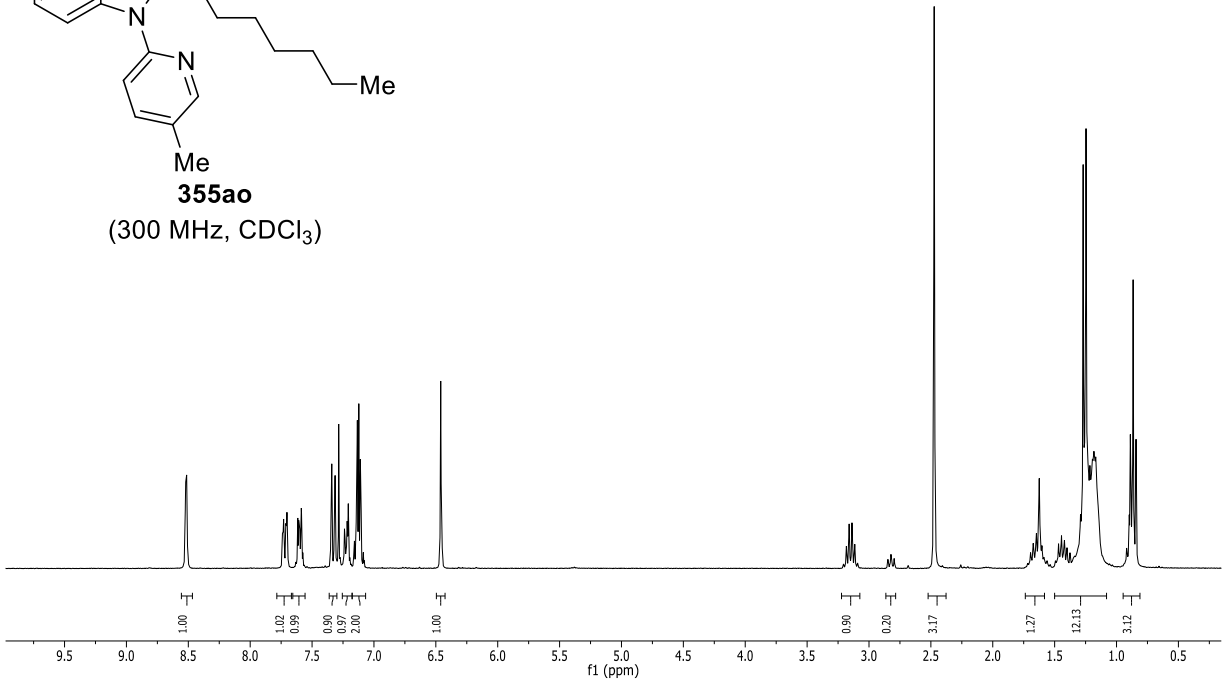
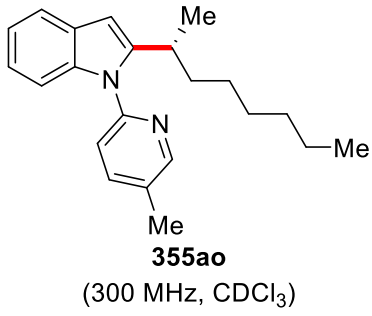
Chiral HPLC of 355an:



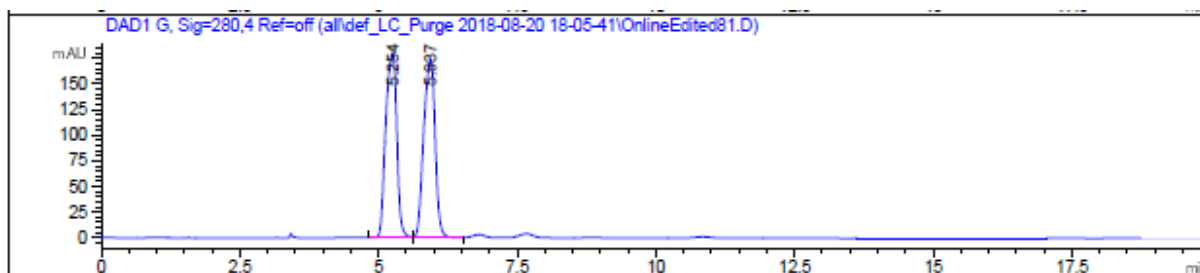
Peak #	RetTime [min]	Type	Width [min]	Area [mAU*s]	Height [mAU]	Area %
1	7.709	BV	0.1483	5158.73682	531.05383	49.7574
2	8.360	VB	0.1594	5209.05127	500.79276	50.2426



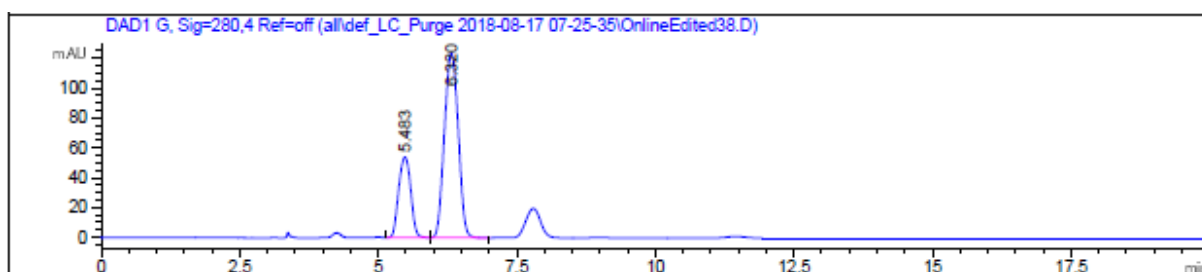
Peak #	RetTime [min]	Type	Width [min]	Area [mAU*s]	Height [mAU]	Area %
1	7.502	BV	0.1658	2422.10693	221.02980	32.2992
2	8.047	VB	0.1791	5076.86377	435.24667	67.7008



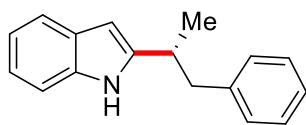
Chiral HPLC of **355ao**:



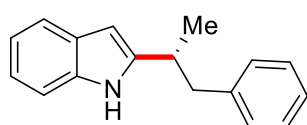
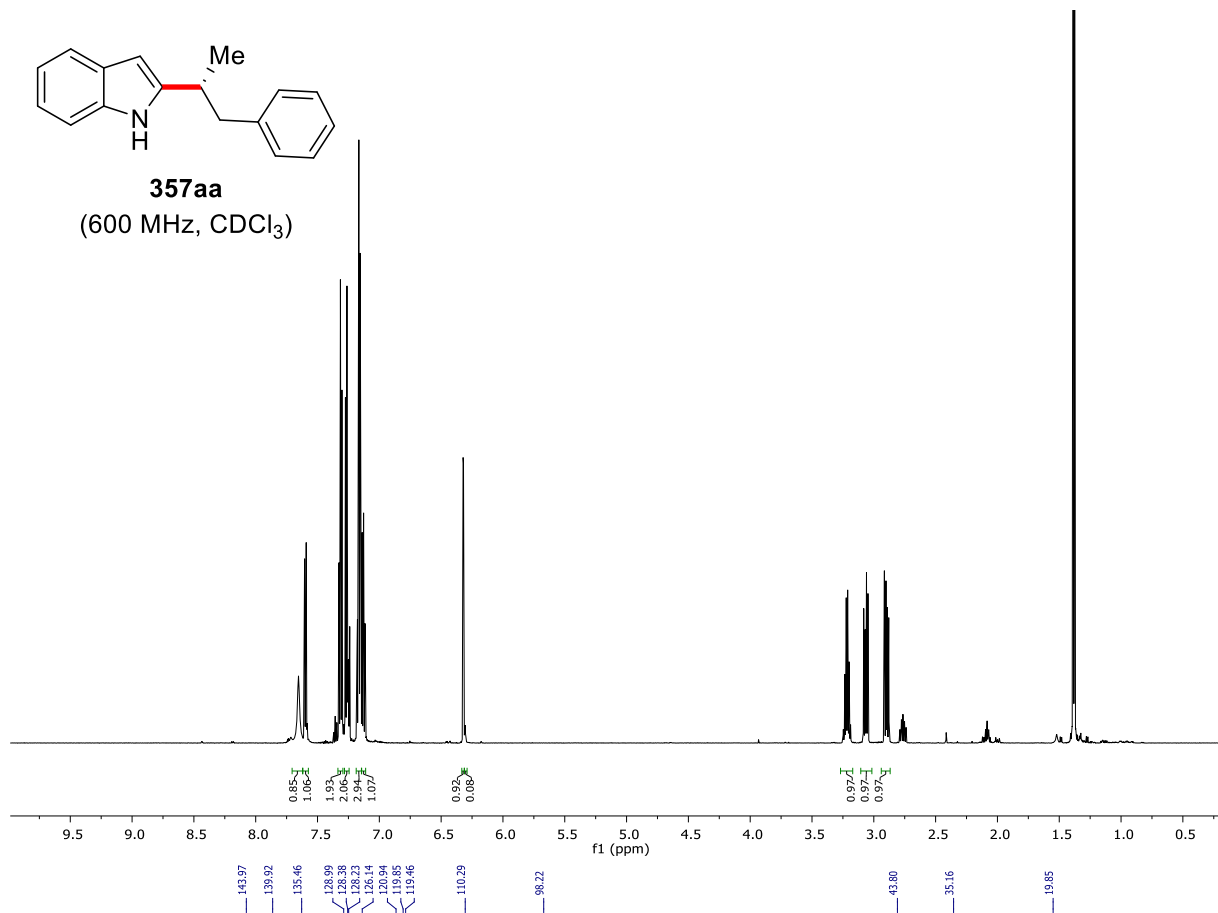
Peak #	RetTime [min]	Type	Width [min]	Area [mAU*s]	Height [mAU]	Area %
1	5.254	BV	0.2299	2502.31396	180.35625	50.2133
2	5.937	VB	0.2341	2481.05249	174.30663	49.7867



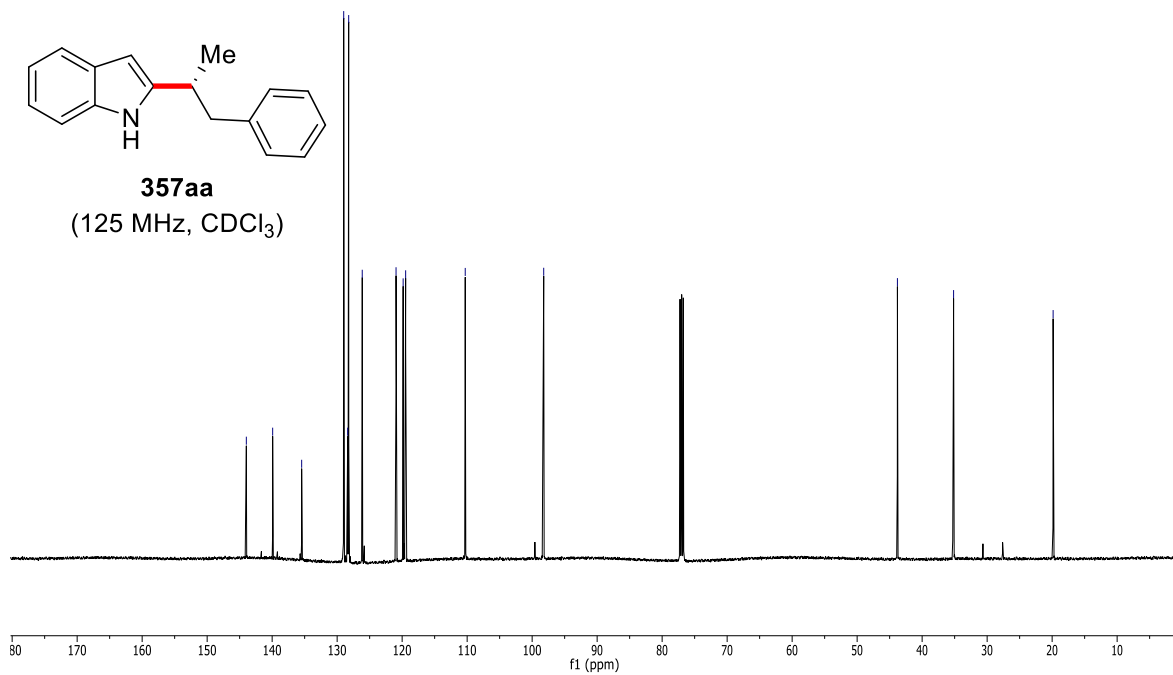
Peak #	RetTime [min]	Type	Width [min]	Area [mAU*s]	Height [mAU]	Area %
1	5.483	BB	0.2527	815.84808	53.86852	27.5697
2	6.320	BB	0.2821	2143.37598	123.76132	72.4303



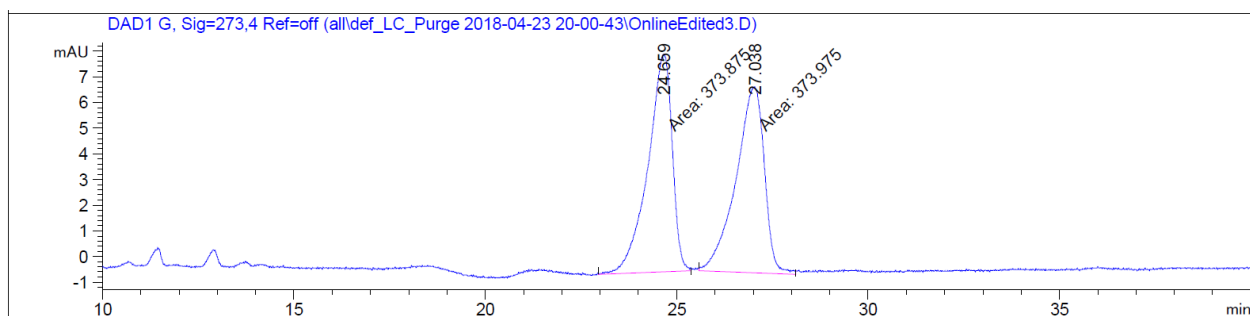
357aa
(600 MHz, CDCl₃)



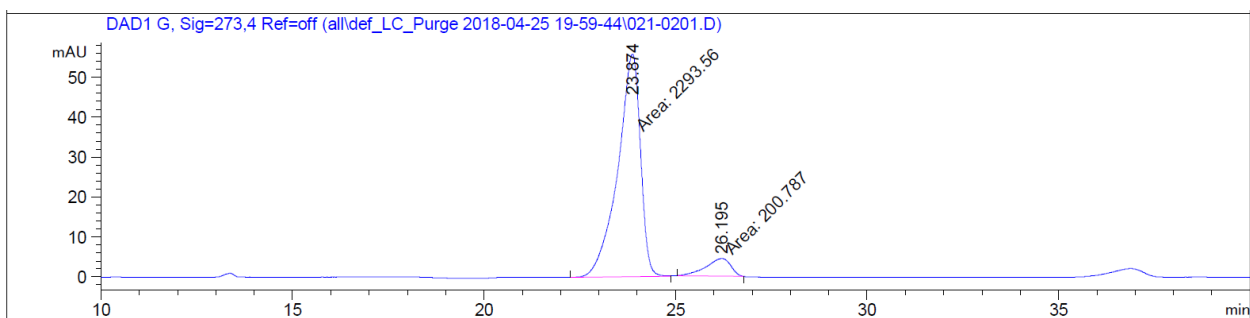
357aa
(125 MHz, CDCl₃)



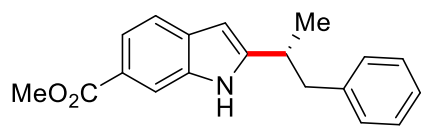
Chiral HPLC of **357aa**:



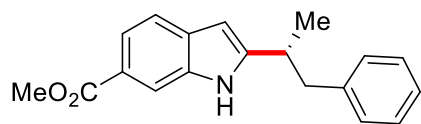
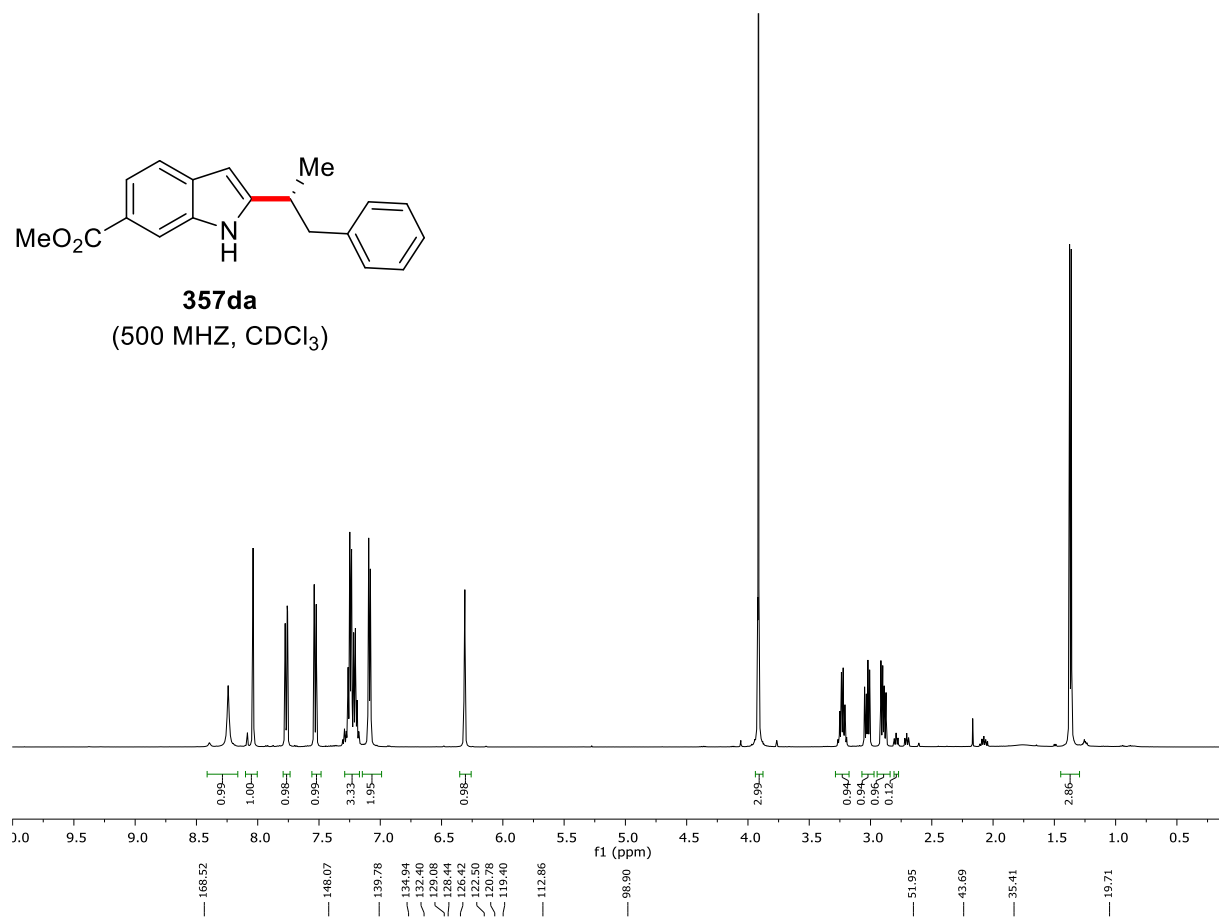
Peak #	RetTime [min]	Type	Width [min]	Area [mAU*s]	Height [mAU]	Area %
1	24.659	MM	0.7355	373.87488	8.47202	49.9933
2	27.038	MM	0.8618	373.97473	7.23236	50.0067



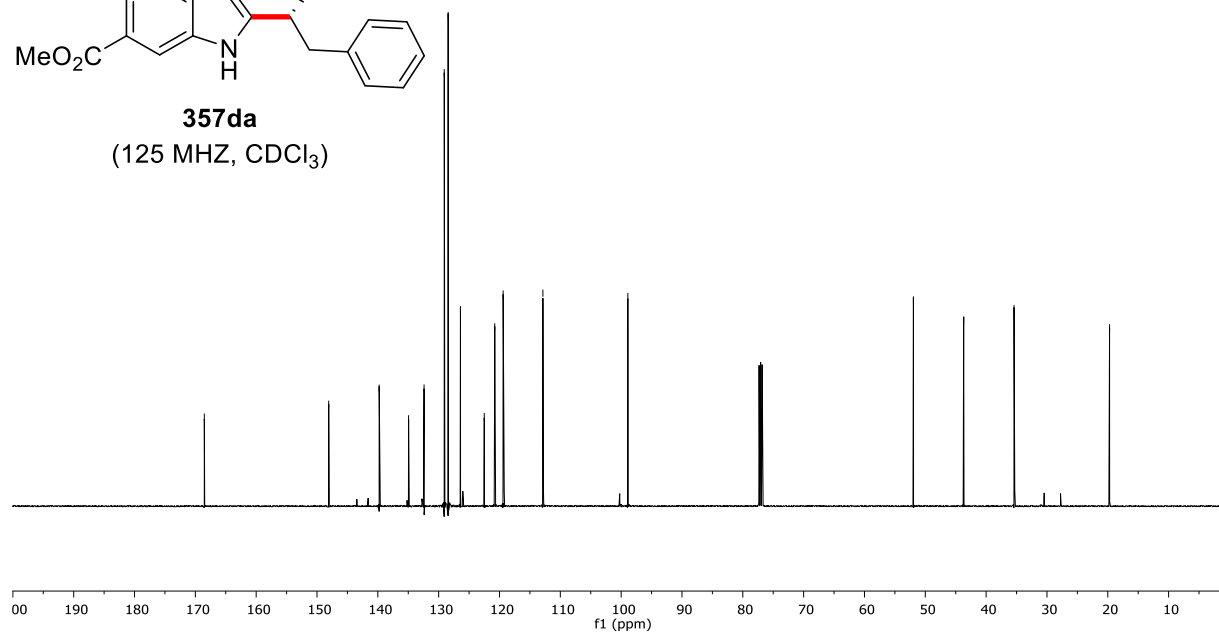
Peak #	RetTime [min]	Type	Width [min]	Area [mAU*s]	Height [mAU]	Area %
1	23.874	MM	0.6858	2293.56128	55.74302	91.9503
2	26.195	MM	0.7572	200.78658	4.41953	8.0497



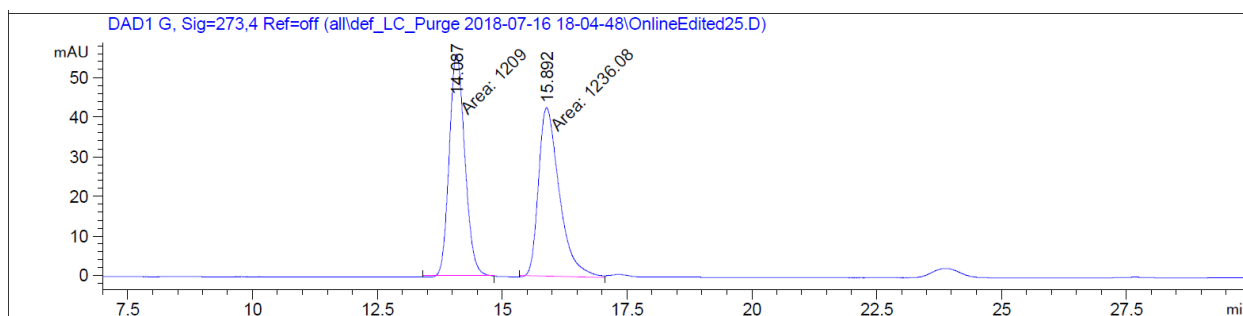
357da
(500 MHz, CDCl₃)



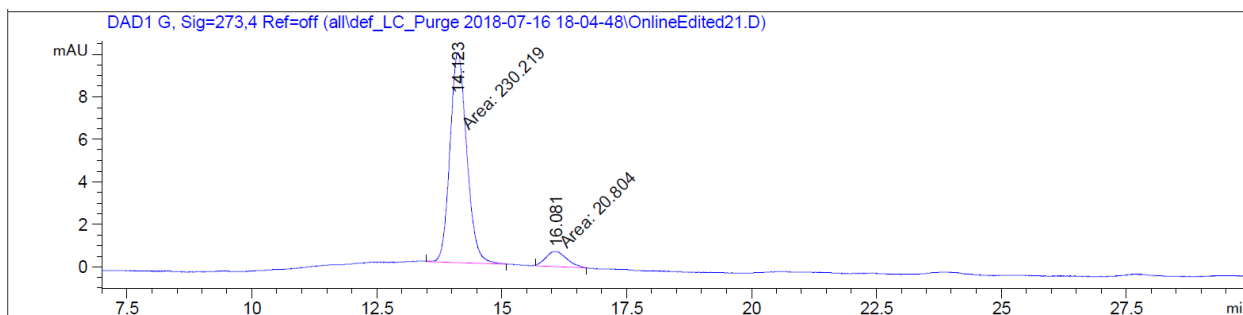
357da
(125 MHz, CDCl₃)



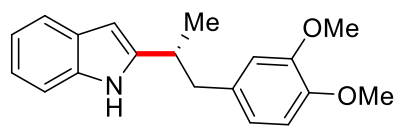
Chiral HPLC of **357da**:



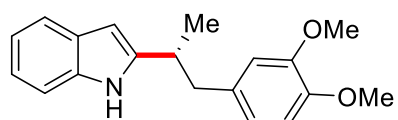
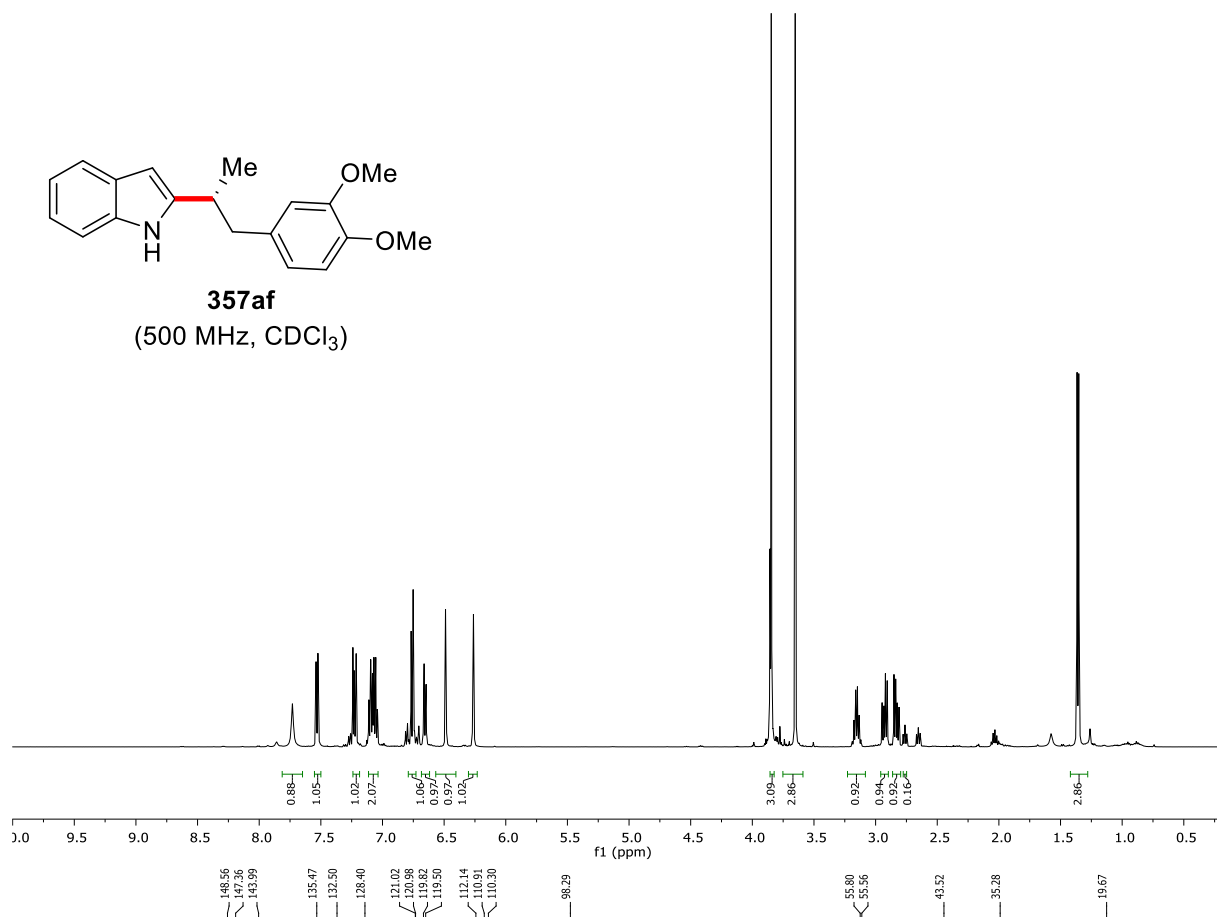
Peak #	RetTime [min]	Type	Width [min]	Area [mAU*s]	Height [mAU]	Area %
1	14.087	MM	0.3604	1208.99988	55.91126	49.4463
2	15.892	MM	0.4848	1236.07727	42.49546	50.5537



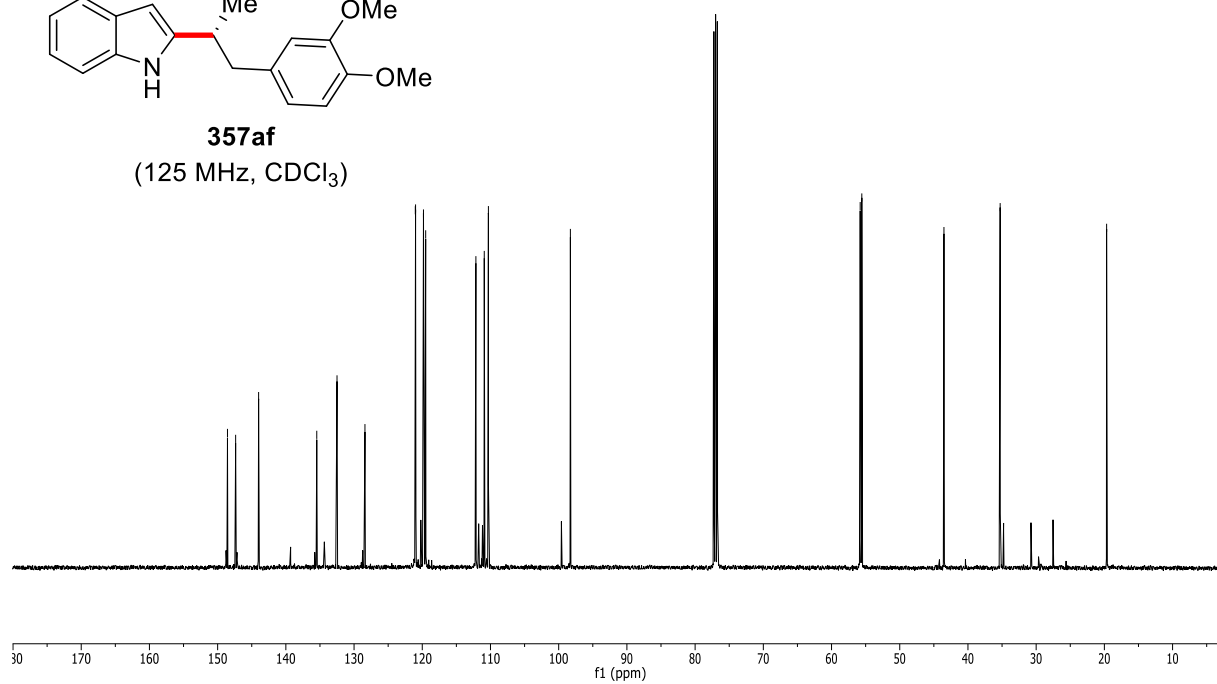
Peak #	RetTime [min]	Type	Width [min]	Area [mAU*s]	Height [mAU]	Area %
1	14.123	MM	0.3880	230.21918	9.88896	91.7123
2	16.081	MM	0.4839	20.80403	7.16477e-1	8.2877



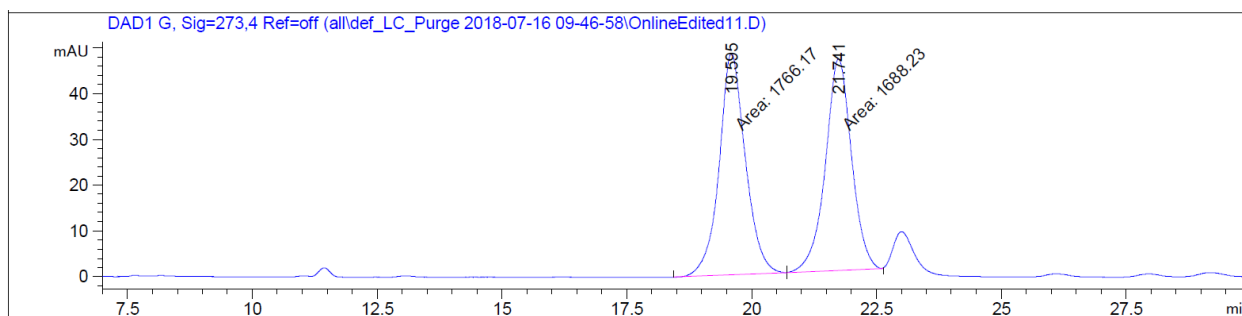
357af
(500 MHz, CDCl₃)



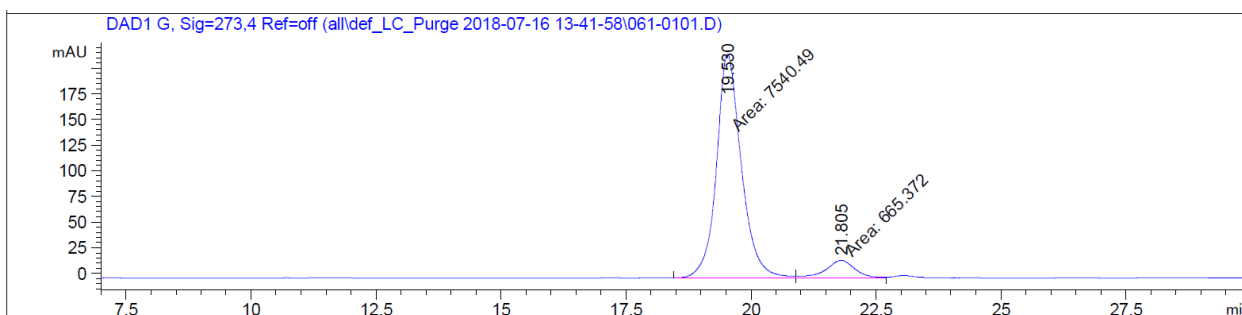
357af
(125 MHz, CDCl₃)



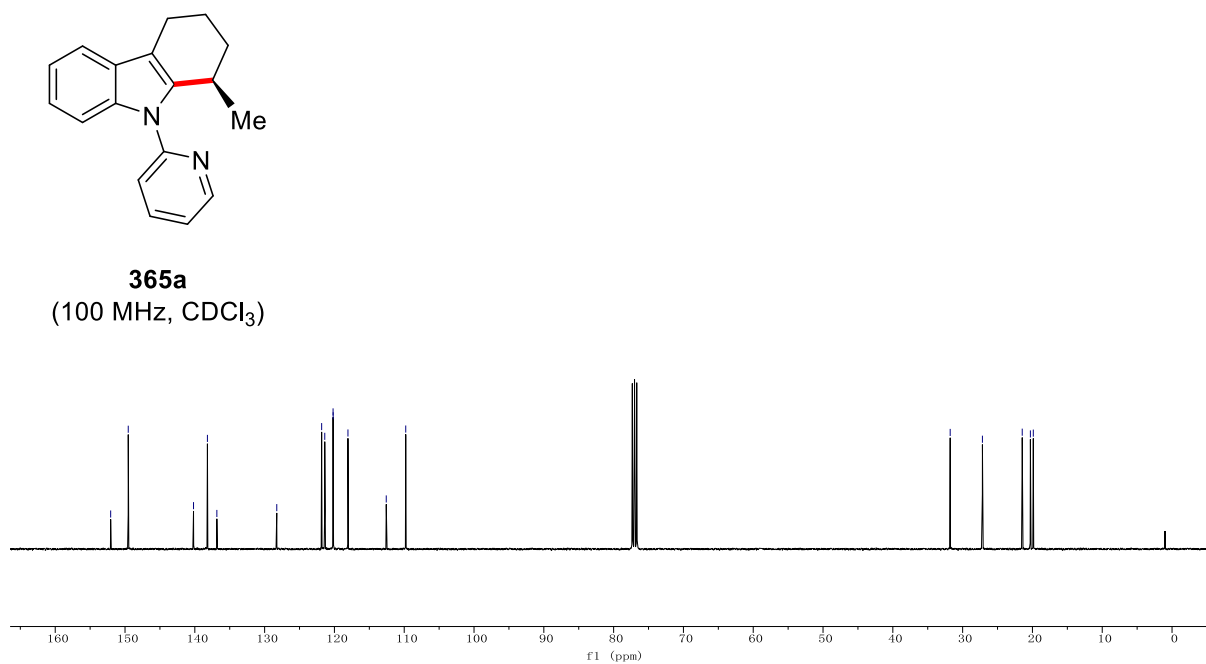
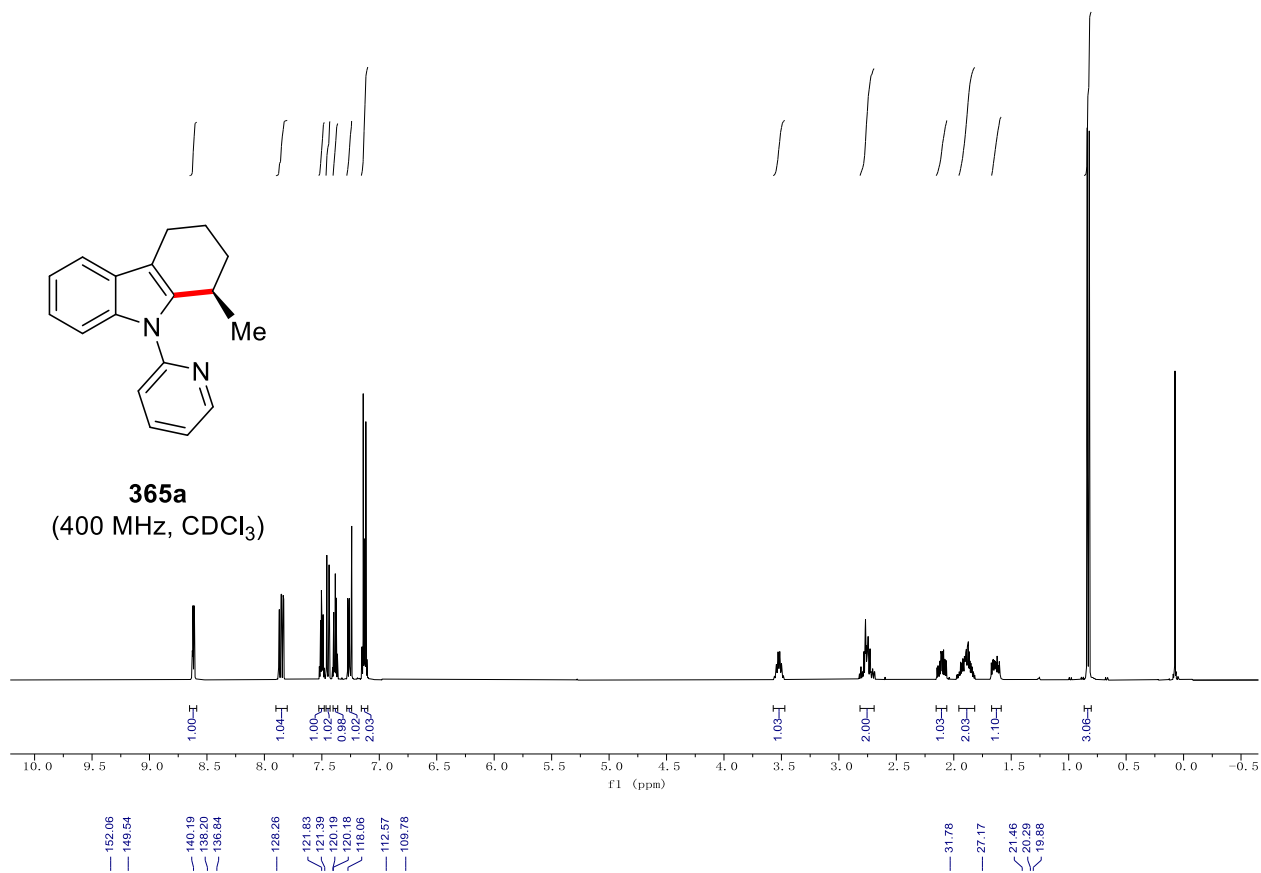
Chiral HPLC of **357af**:



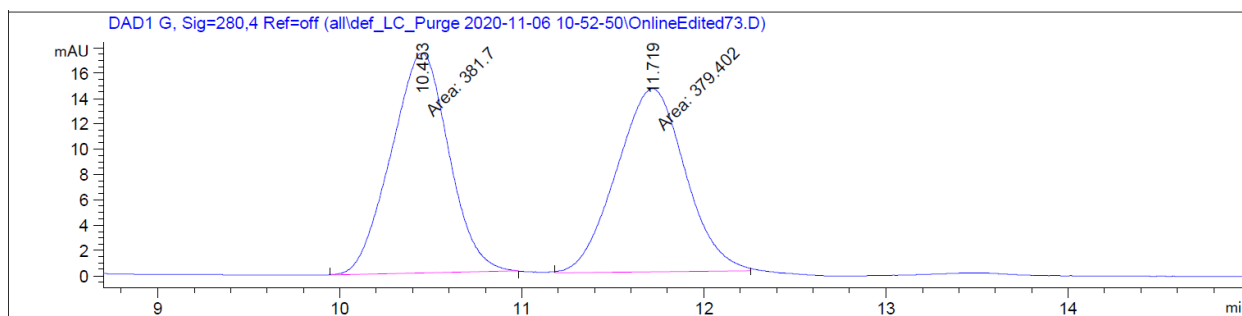
Peak #	RetTime [min]	Type	Width [min]	Area [mAU*s]	Height [mAU]	Area %
1	19.595	MF	0.6082	1766.16919	48.39488	51.1281
2	21.741	FM	0.6084	1688.23096	46.24706	48.8719



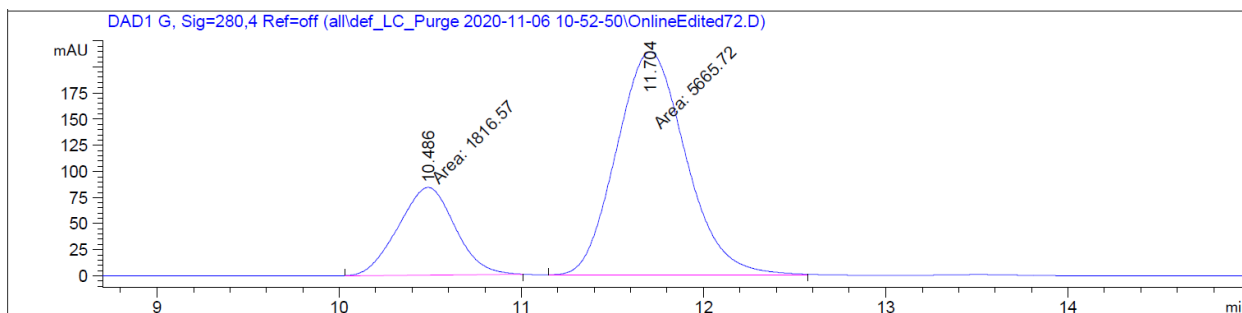
Peak #	RetTime [min]	Type	Width [min]	Area [mAU*s]	Height [mAU]	Area %
1	19.530	MF	0.5763	7540.49170	218.08086	91.8915
2	21.805	FM	0.6555	665.37158	16.91690	8.1085



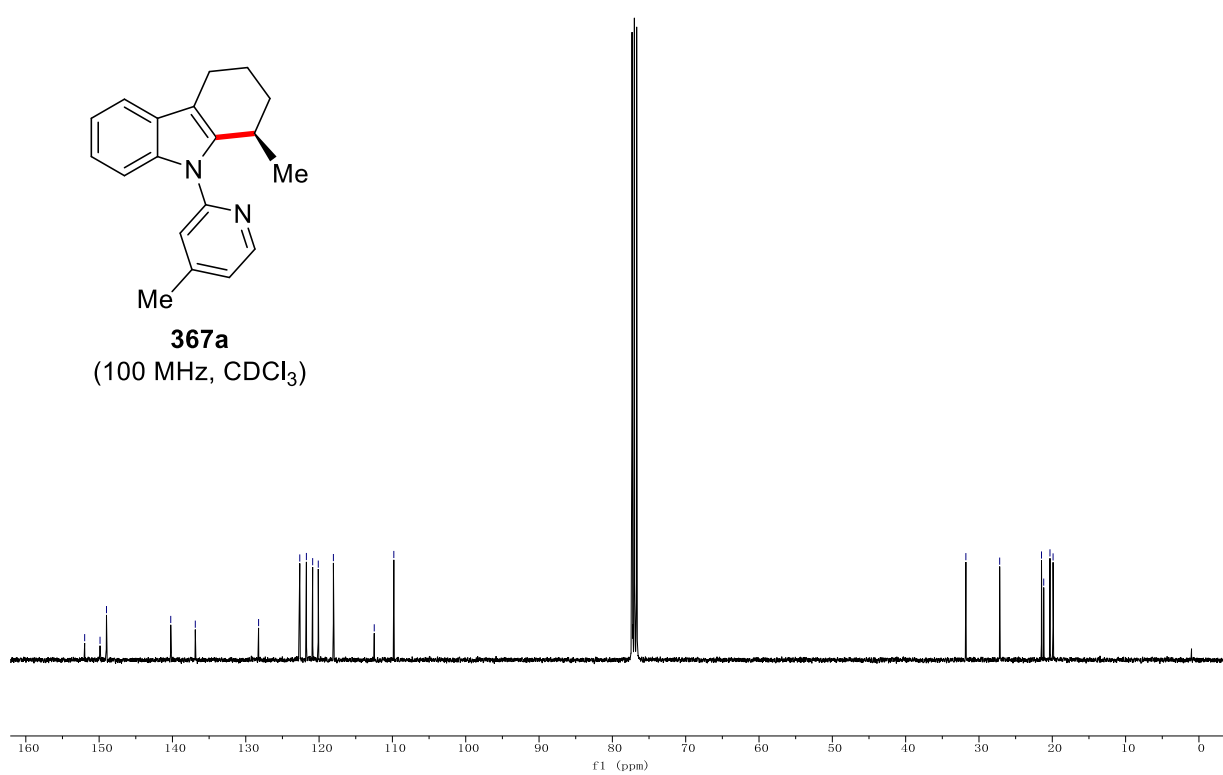
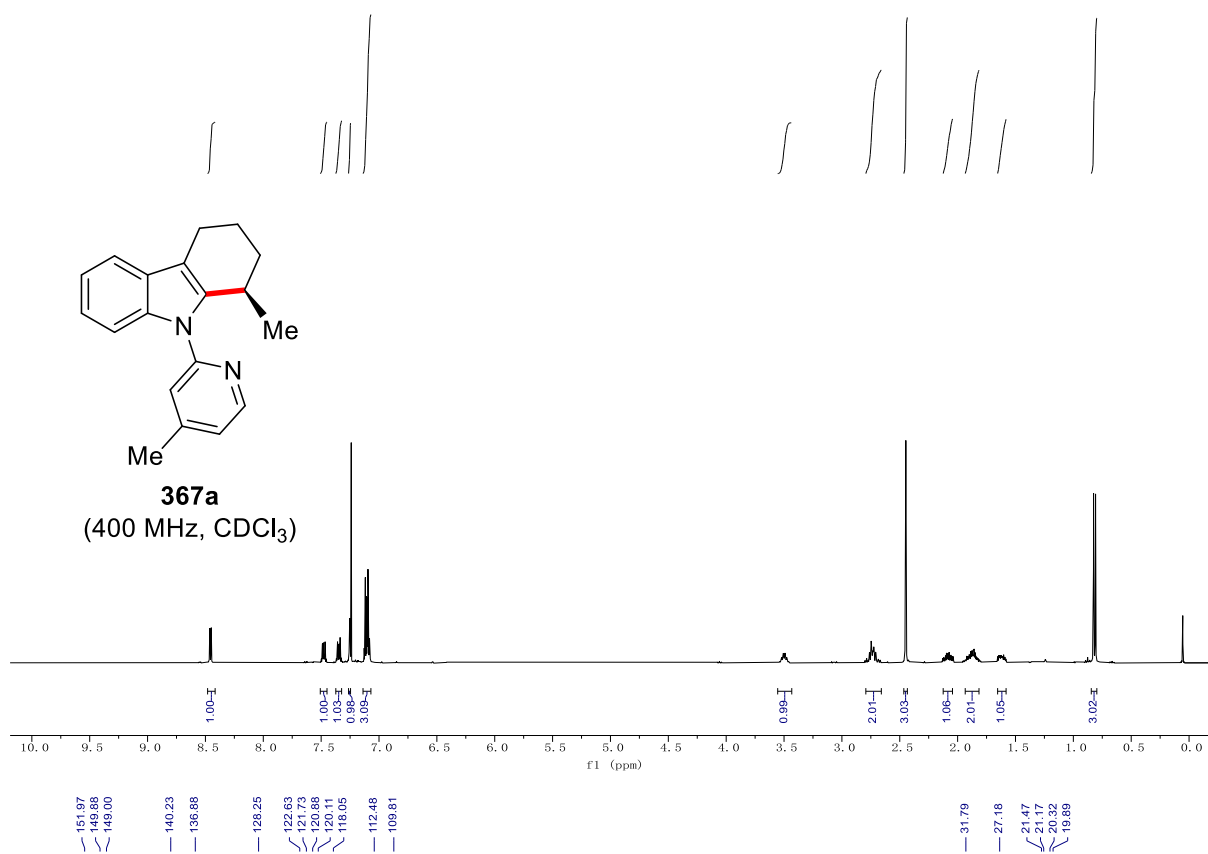
Chiral HPLC of **365a**:



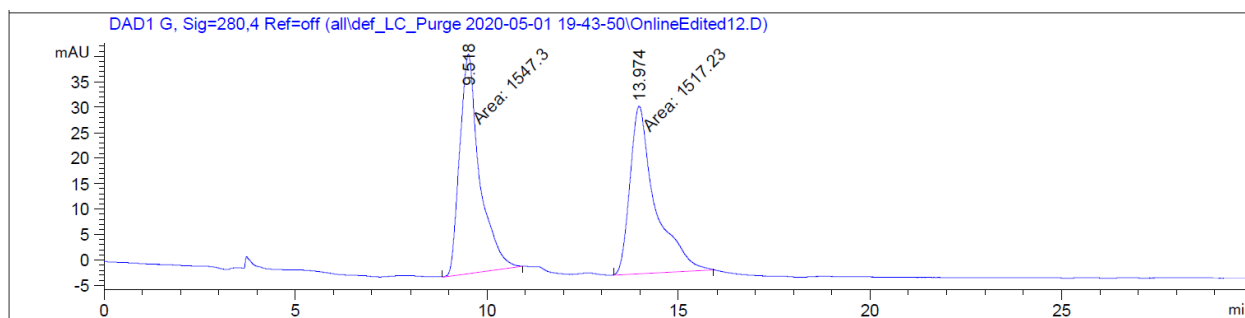
Peak #	RetTime [min]	Type	Width [min]	Area [mAU*s]	Height [mAU]	Area %
1	10.453	MM	0.3665	381.69962	17.35712	50.1509
2	11.719	MM	0.4373	379.40216	14.46167	49.8491



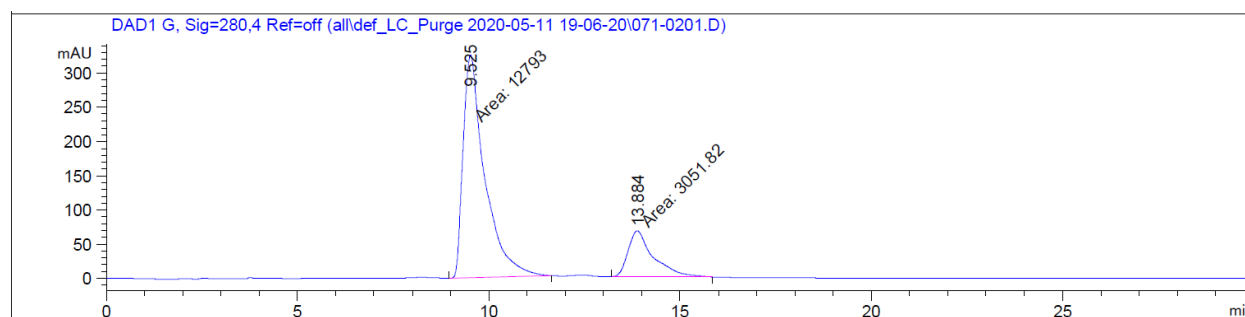
Peak #	RetTime [min]	Type	Width [min]	Area [mAU*s]	Height [mAU]	Area %
1	10.486	MM	0.3609	1816.56604	83.88490	24.2782
2	11.704	MM	0.4418	5665.72119	213.75468	75.7218



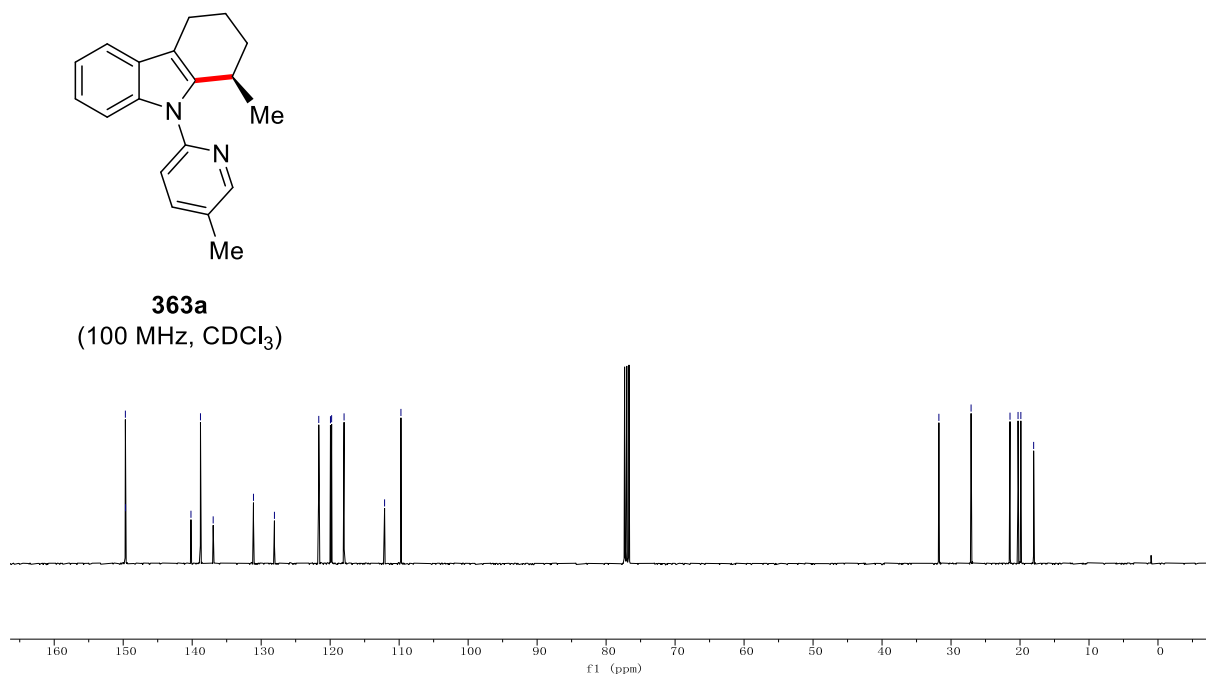
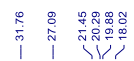
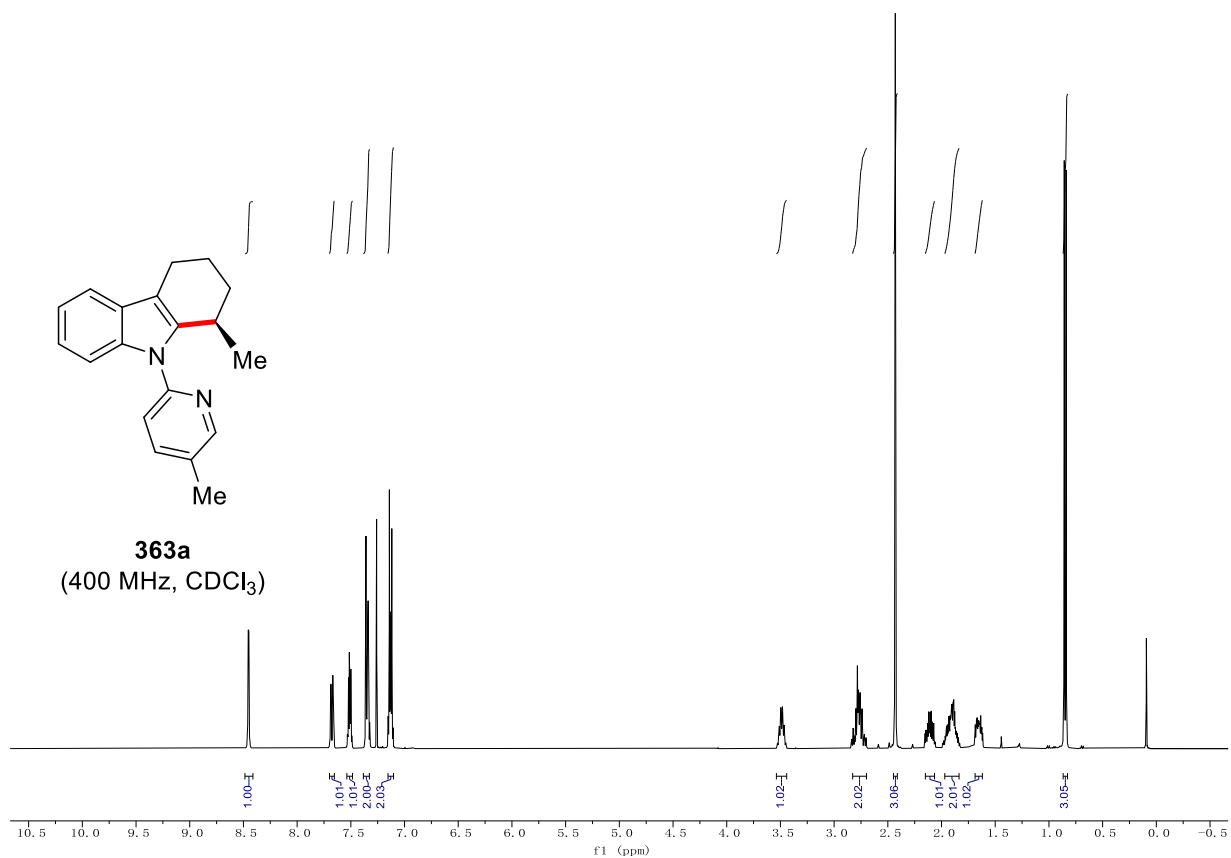
Chiral HPLC of **367a**:



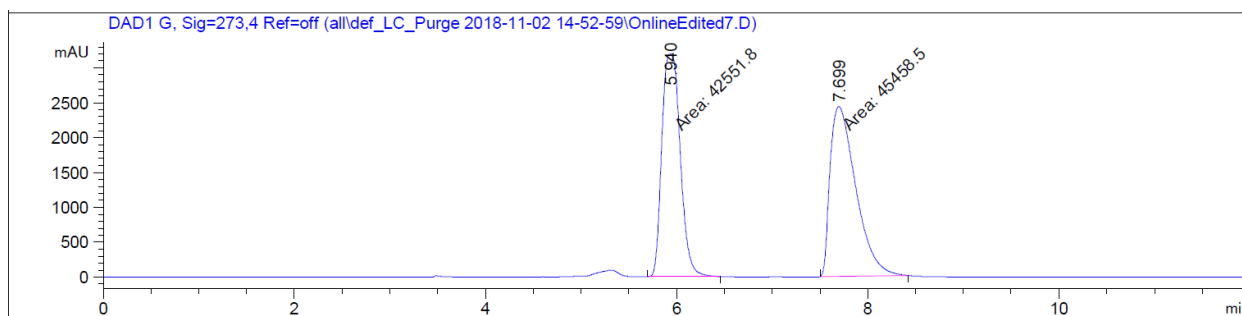
Peak #	RetTime [min]	Type	Width [min]	Area [mAU*s]	Height [mAU]	Area %
1	9.518	MM	0.5983	1547.30481	43.10374	50.4907
2	13.974	MM	0.7677	1517.22803	32.93877	49.5093



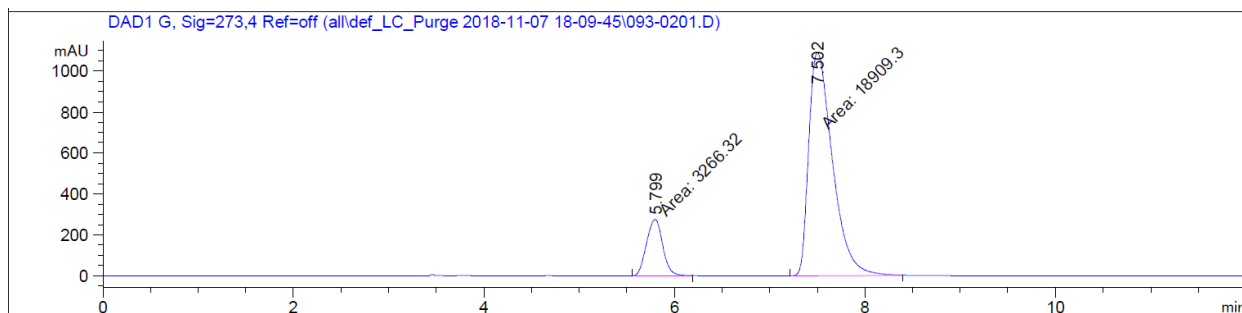
Peak #	RetTime [min]	Type	Width [min]	Area [mAU*s]	Height [mAU]	Area %
1	9.525	MM	0.6555	1.27930e4	325.26505	80.7393
2	13.884	MM	0.7588	3051.82471	67.03014	19.2607



Chiral HPLC of **363a**:



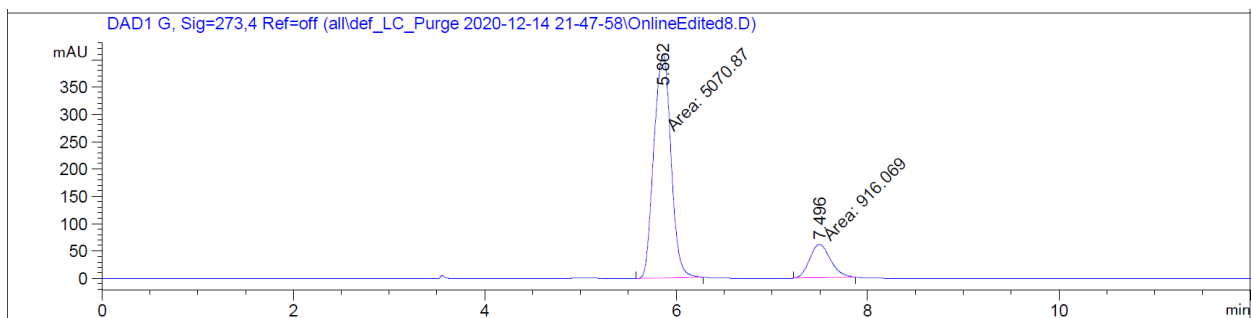
Peak #	RetTime [min]	Type	Width [min]	Area [mAU*s]	Height [mAU]	Area %
1	5.940	MM	0.2220	4.25518e4	3194.78467	48.3486
2	7.699	MM	0.3115	4.54585e4	2432.37988	51.6514



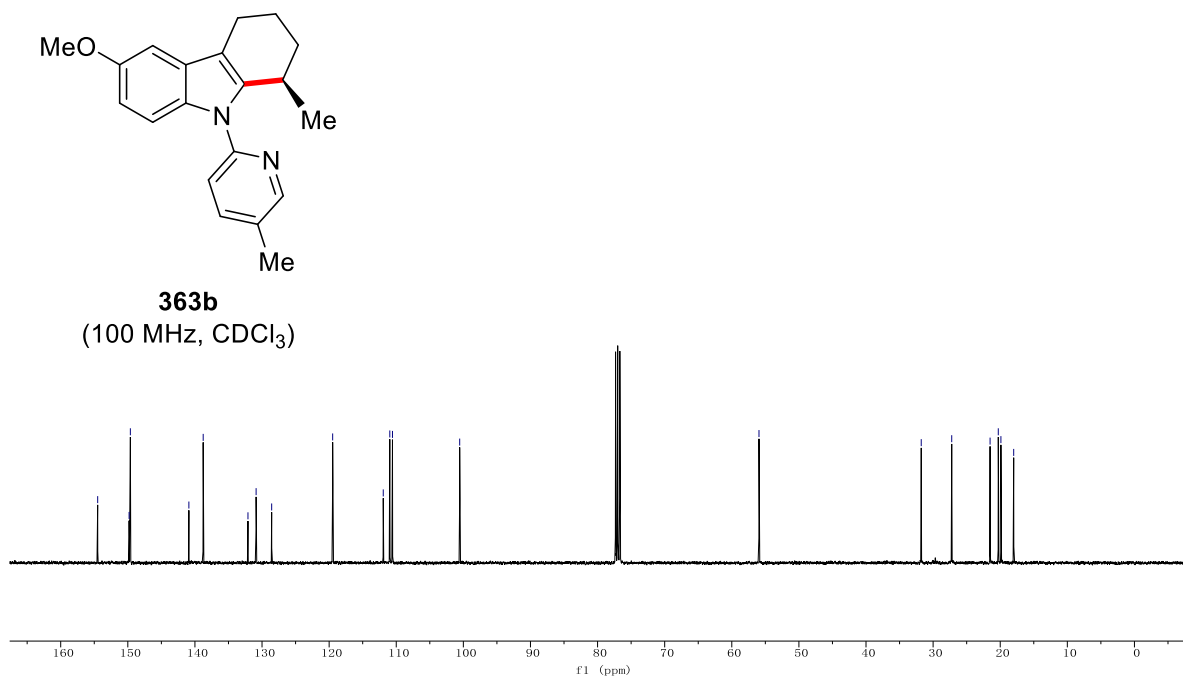
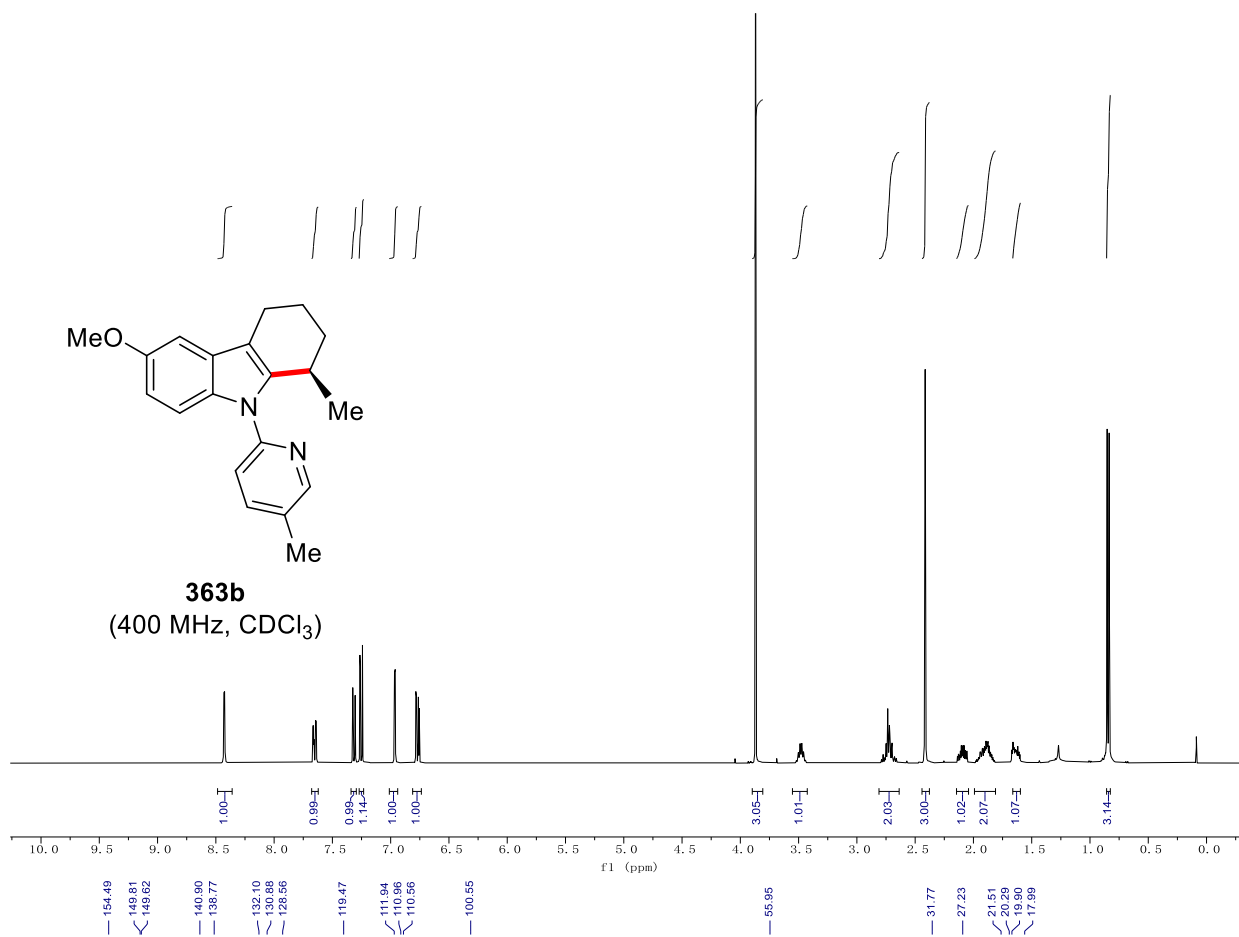
Peak #	RetTime [min]	Type	Width [min]	Area [mAU*s]	Height [mAU]	Area %
1	5.799	MM	0.1976	3266.32373	275.56061	14.7294
2	7.502	MM	0.2889	1.89093e4	1090.78064	85.2706

When *ent*-CA14 was used:

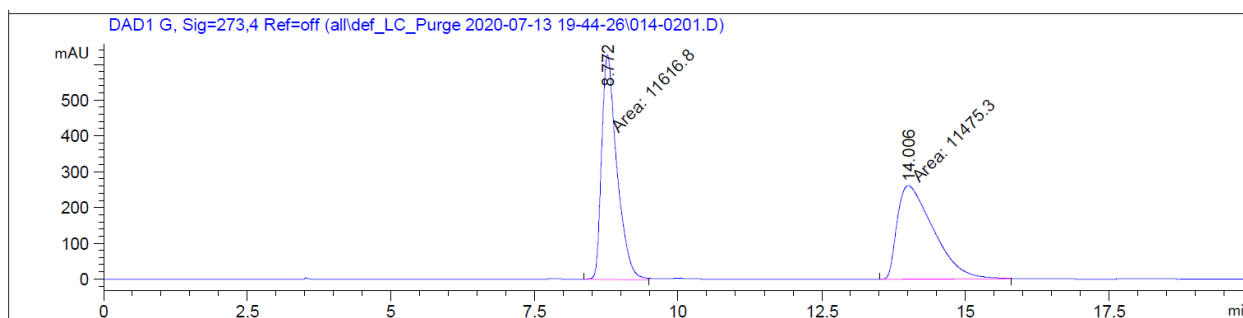
Chiral HPLC of **363a**:



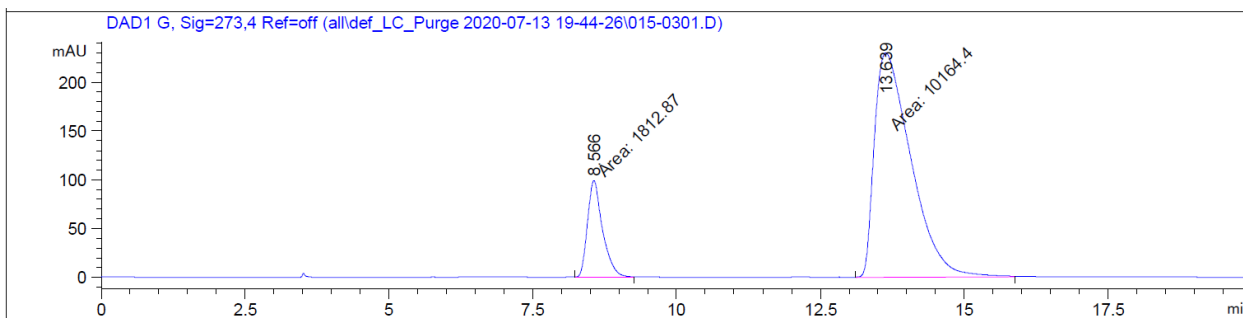
Peak #	RetTime [min]	Type	Width [min]	Area [mAU*s]	Height [mAU]	Area %
1	5.862	MM	0.2063	5070.87109	409.60330	84.6989
2	7.496	MM	0.2507	916.06921	60.90235	15.3011



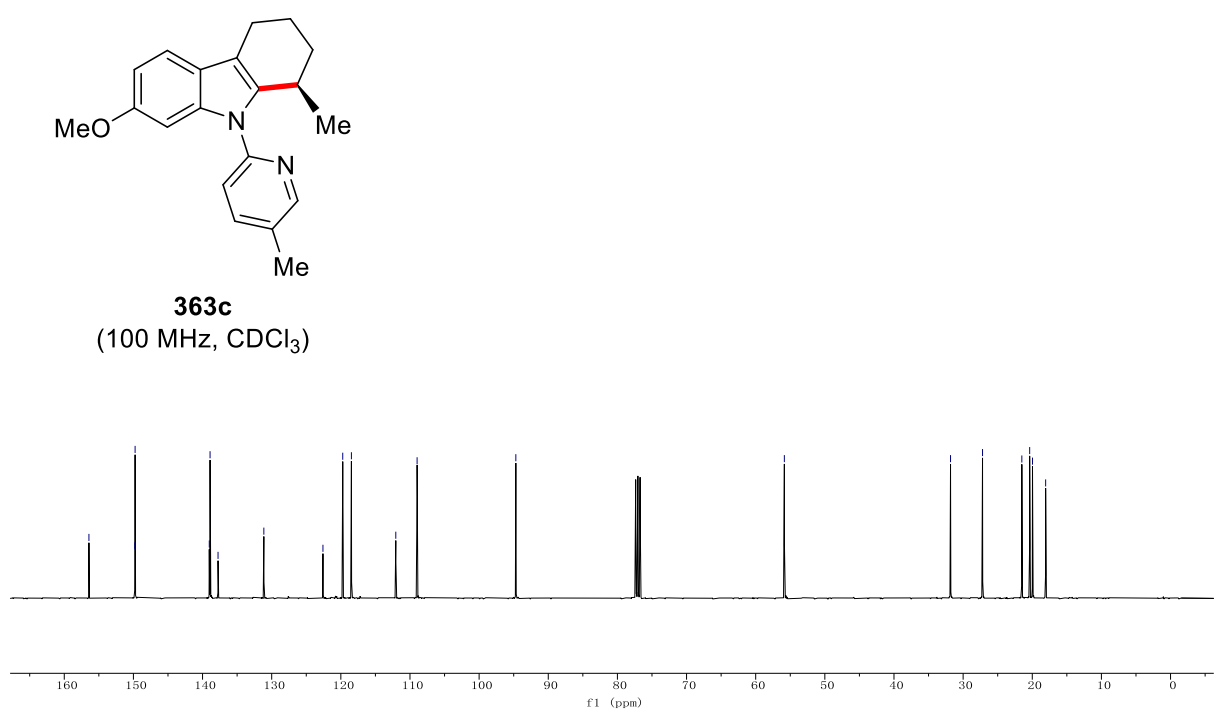
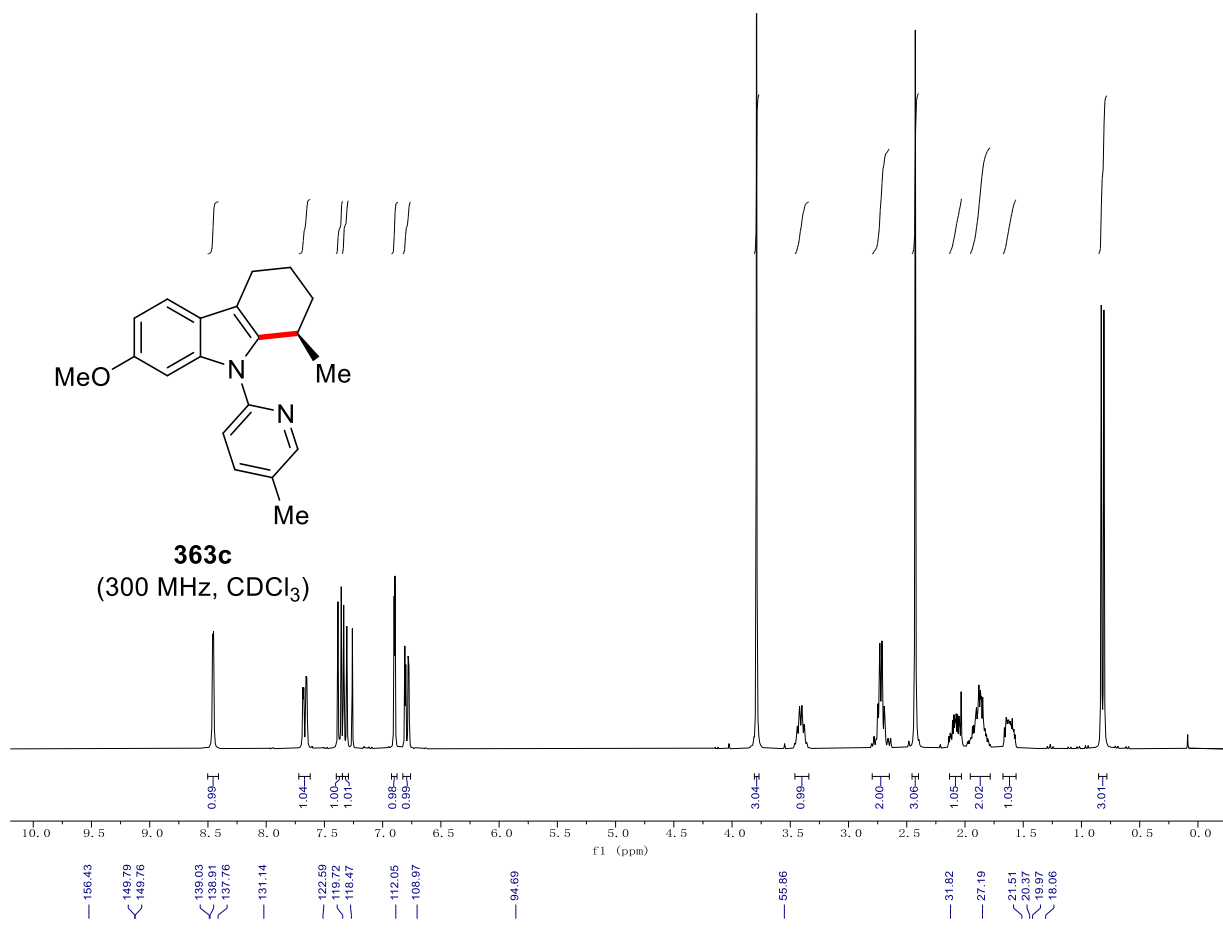
Chiral HPLC of **363b**:



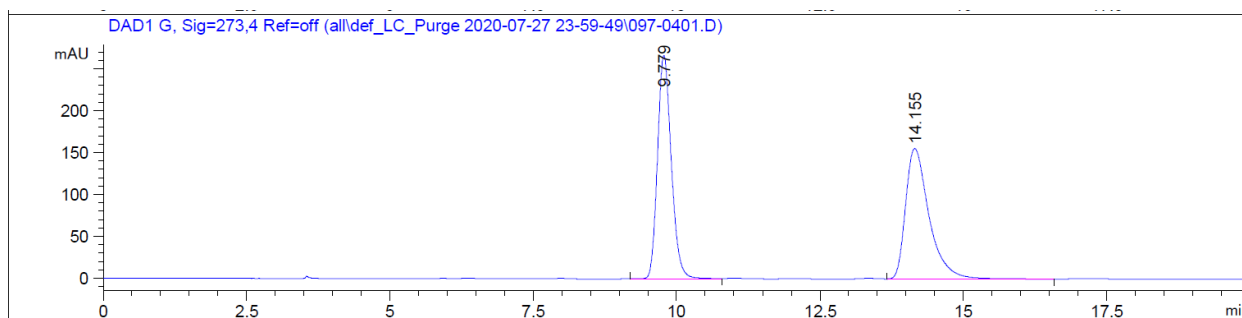
Peak #	RetTime [min]	Type	Width [min]	Area [mAU*s]	Height [mAU]	Area %
1	8.772	MM	0.3088	1.16168e4	626.98230	50.3065
2	14.006	MM	0.7319	1.14753e4	261.32187	49.6935



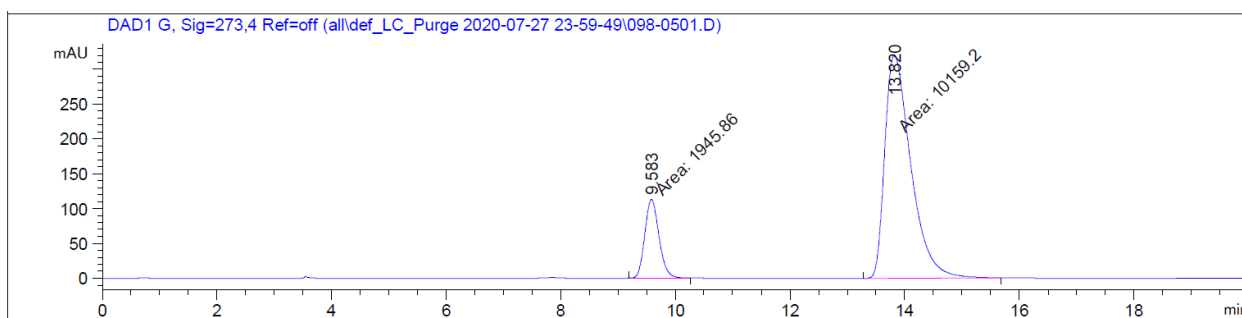
Peak #	RetTime [min]	Type	Width [min]	Area [mAU*s]	Height [mAU]	Area %
1	8.566	MM	0.3051	1812.86841	99.03856	15.1360
2	13.639	MM	0.7363	1.01644e4	230.06743	84.8640



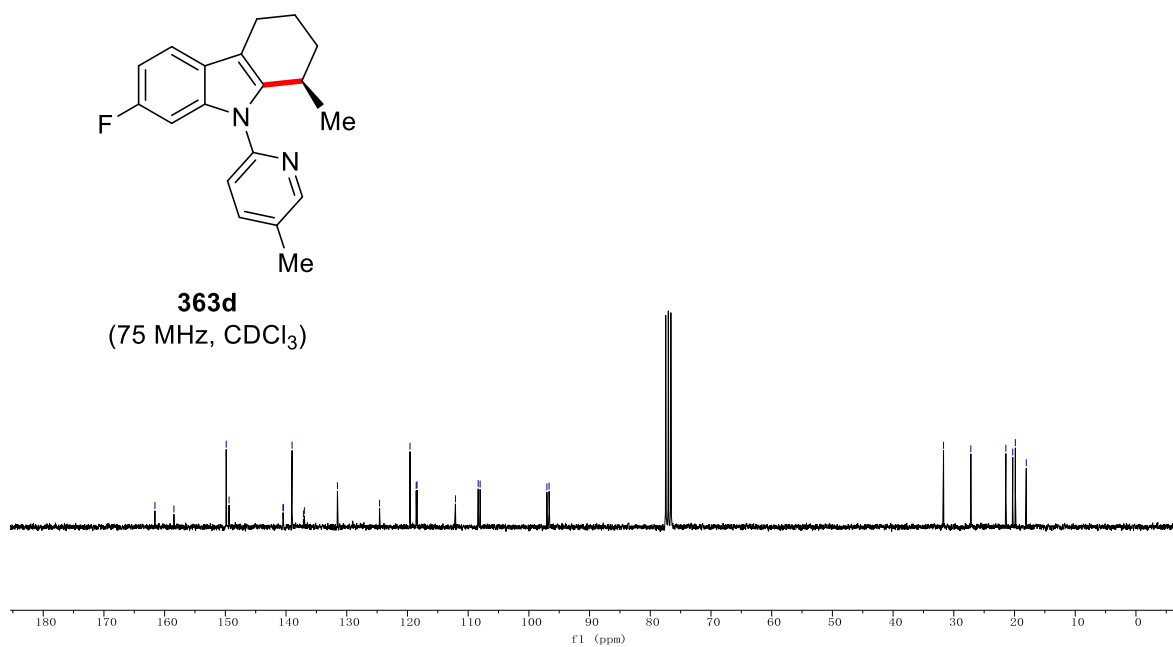
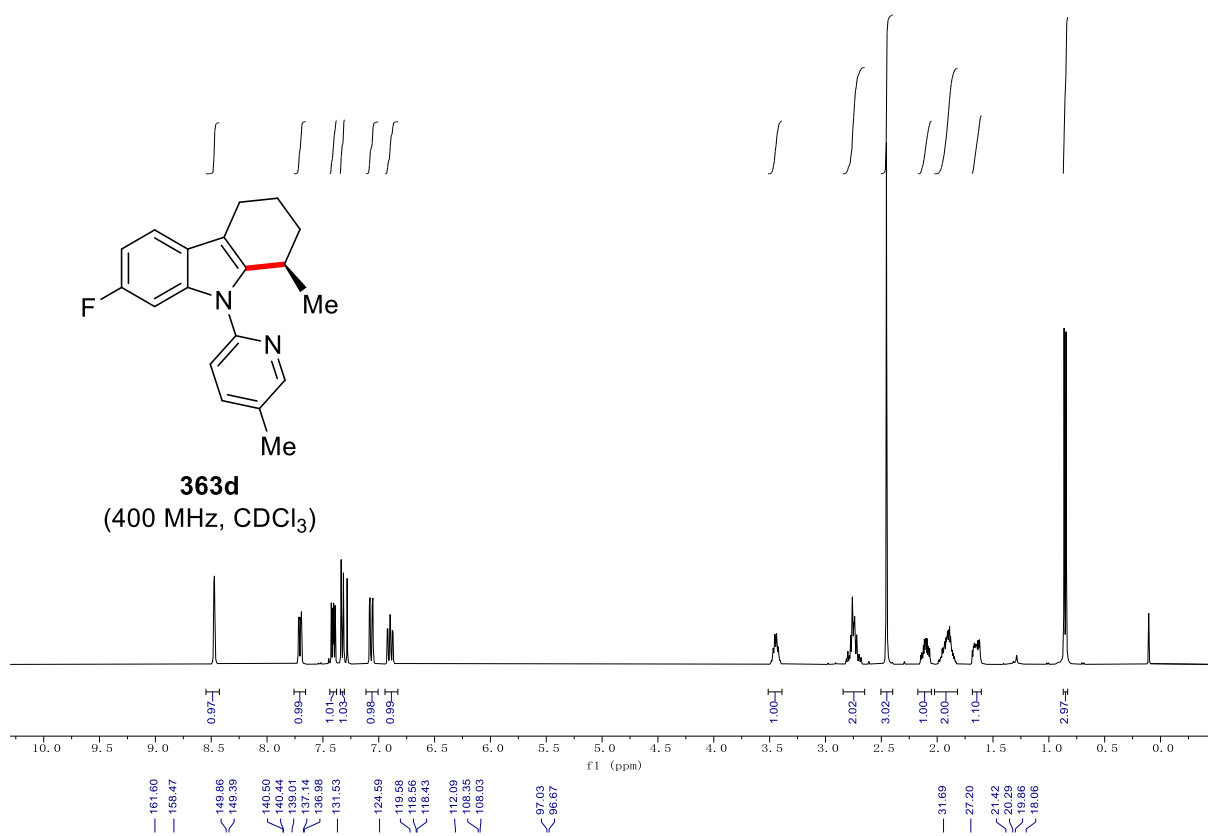
Chiral HPLC of **363c**:

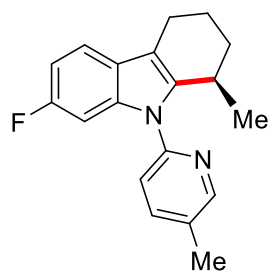


Peak #	RetTime [min]	Type	Width [min]	Area [mAU*s]	Height [mAU]	Area %
1	9.779	BB	0.2576	4441.66455	266.29391	50.0634
2	14.155	BB	0.4321	4430.41992	155.64459	49.9366

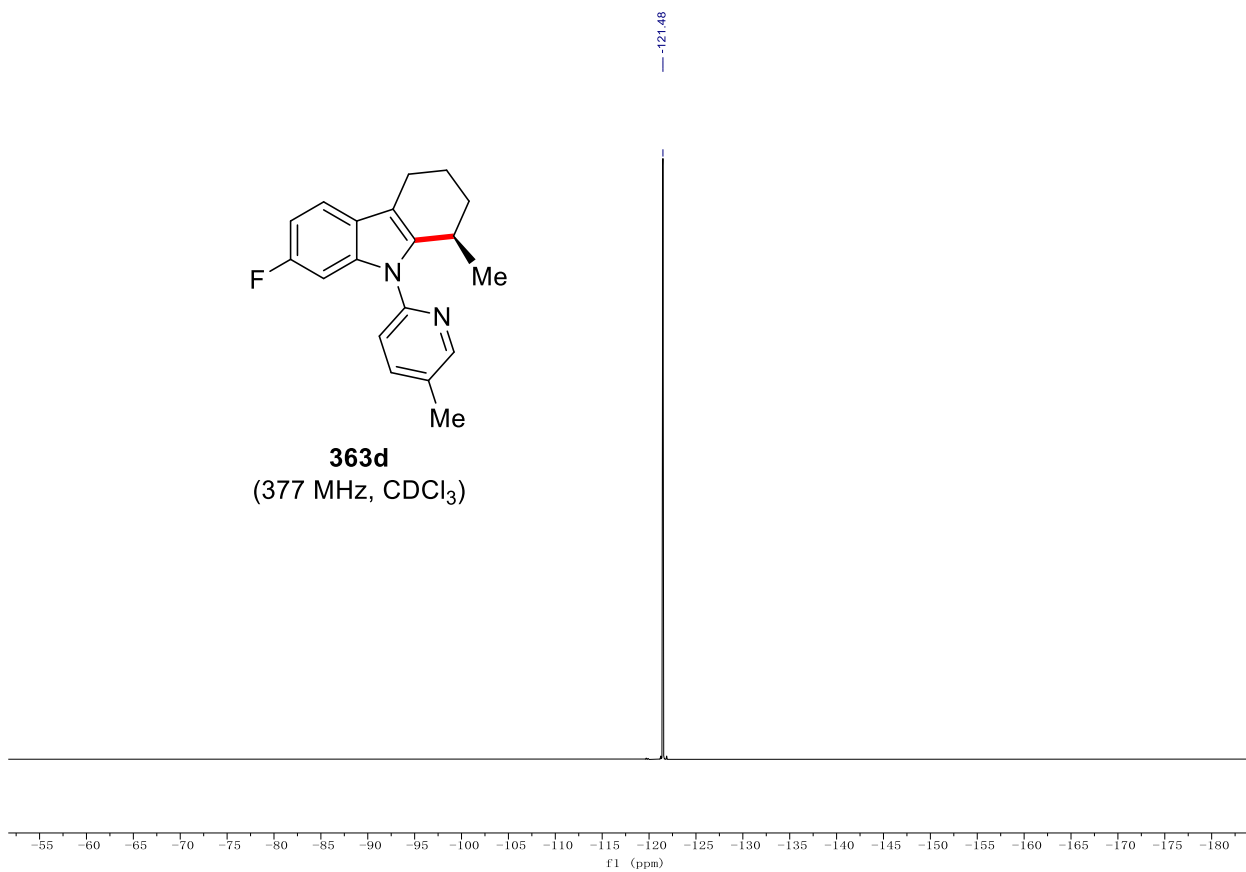


Peak #	RetTime [min]	Type	Width [min]	Area [mAU*s]	Height [mAU]	Area %
1	9.583	MM	0.2870	1945.86218	112.98439	16.0748
2	13.820	MM	0.5277	1.01592e4	320.88641	83.9252

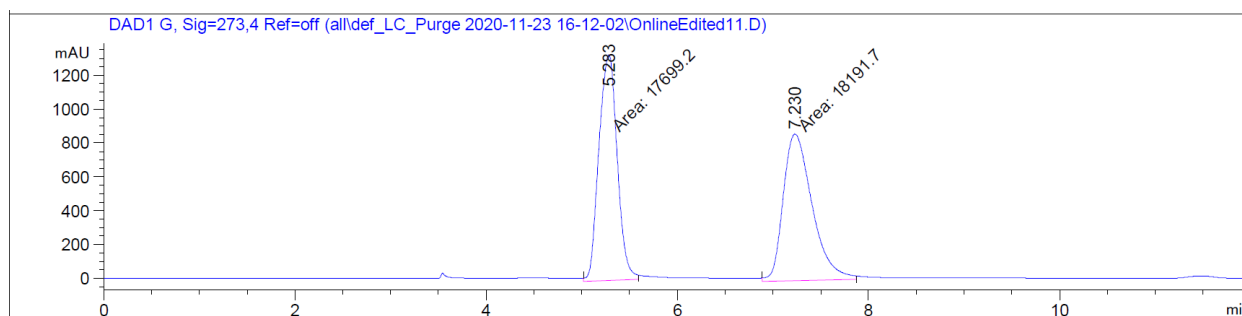




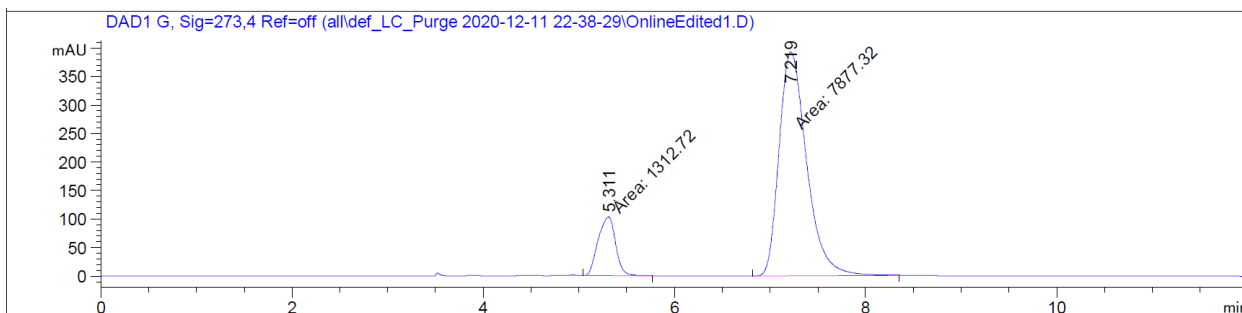
363d
(377 MHz, CDCl₃)



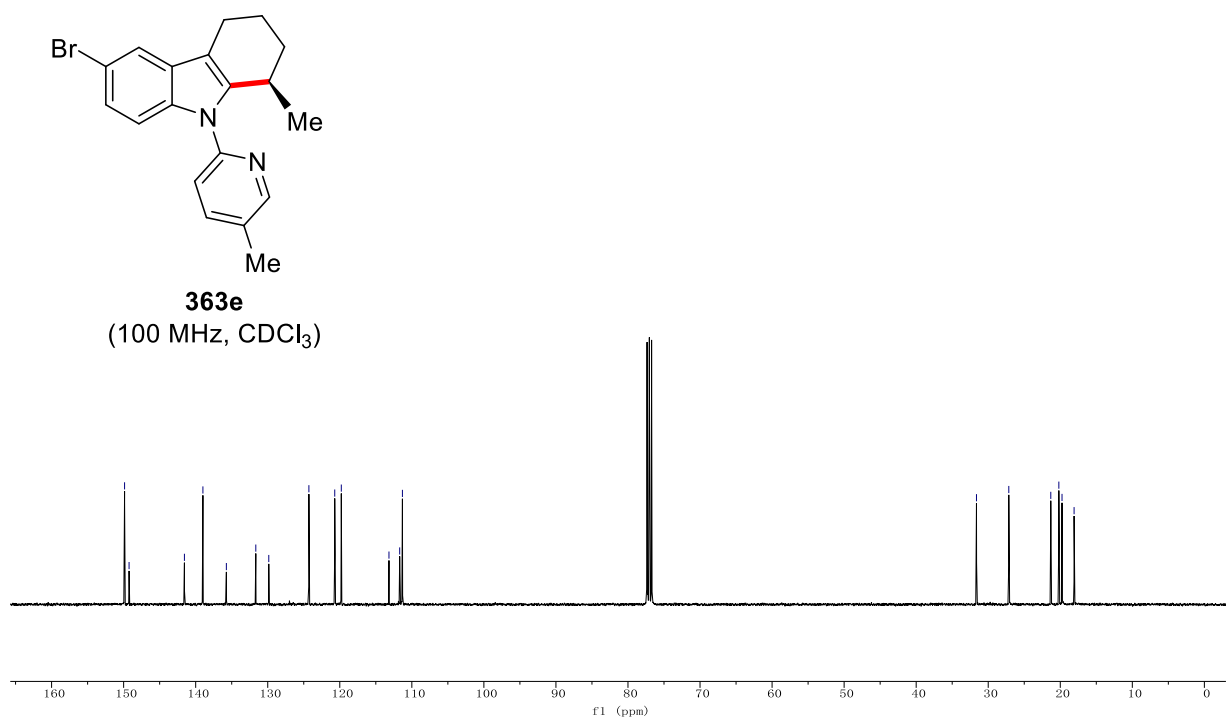
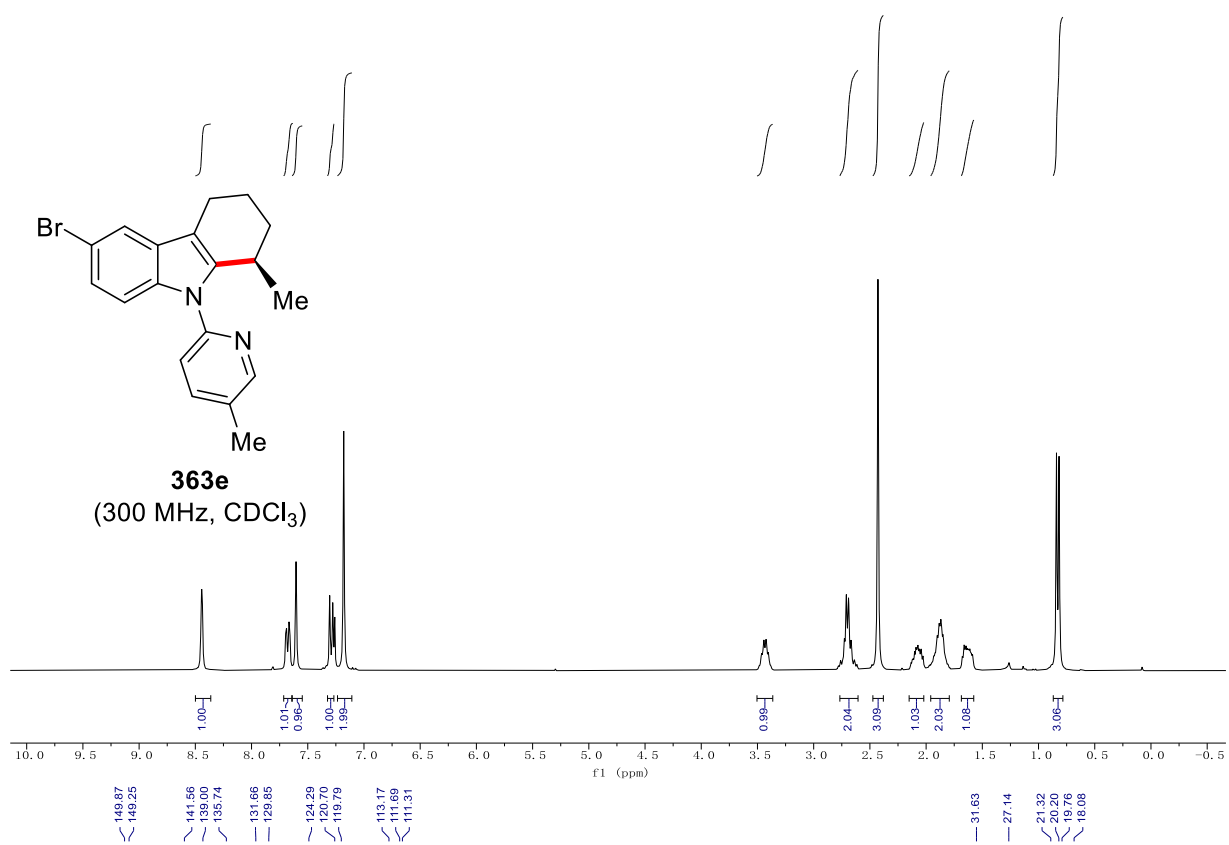
Chiral HPLC of **363d**:



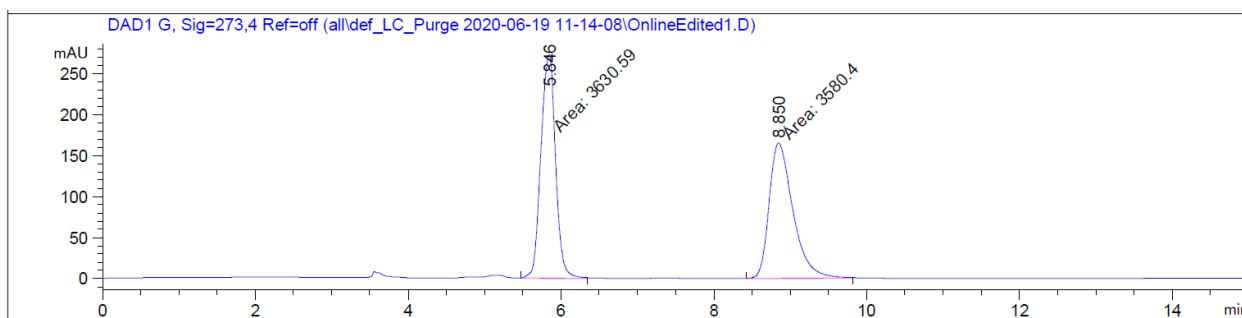
Peak #	RetTime [min]	Type	Width [min]	Area [mAU*s]	Height [mAU]	Area %
1	5.283	MM	0.2214	1.76992e4	1332.59241	49.3139
2	7.230	MM	0.3505	1.81917e4	865.08154	50.6861



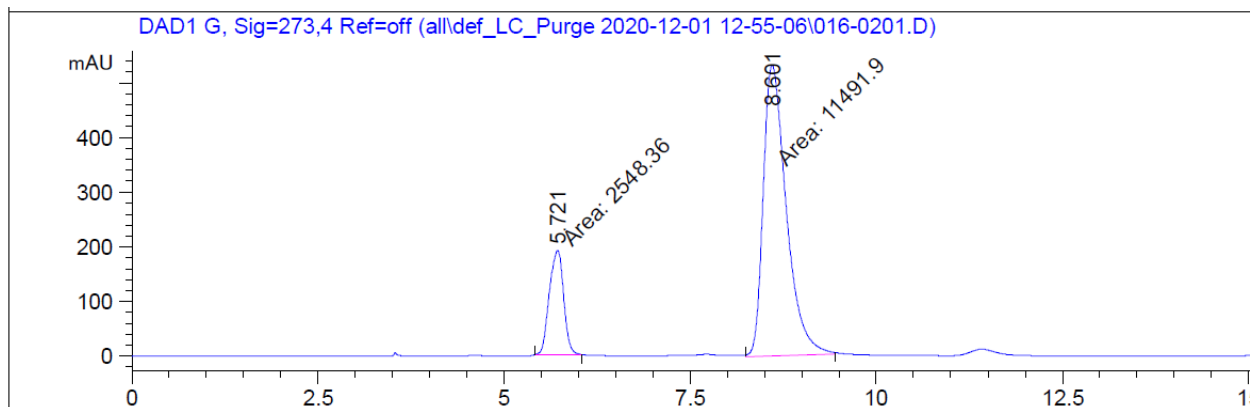
Peak #	RetTime [min]	Type	Width [min]	Area [mAU*s]	Height [mAU]	Area %
1	5.311	MM	0.2118	1312.72412	103.31708	14.2842
2	7.219	MM	0.3337	7877.31885	393.40585	85.7158



Chiral HPLC of **363e**:



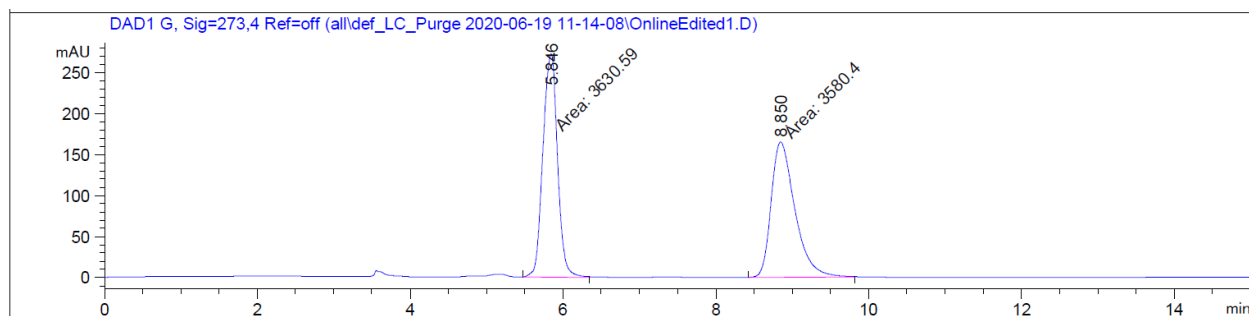
Peak #	RetTime [min]	Type	Width [min]	Area [mAU*s]	Height [mAU]	Area %
1	5.846	MM	0.2217	3630.59351	272.88000	50.3481
2	8.850	MM	0.3607	3580.39746	165.42451	49.6519



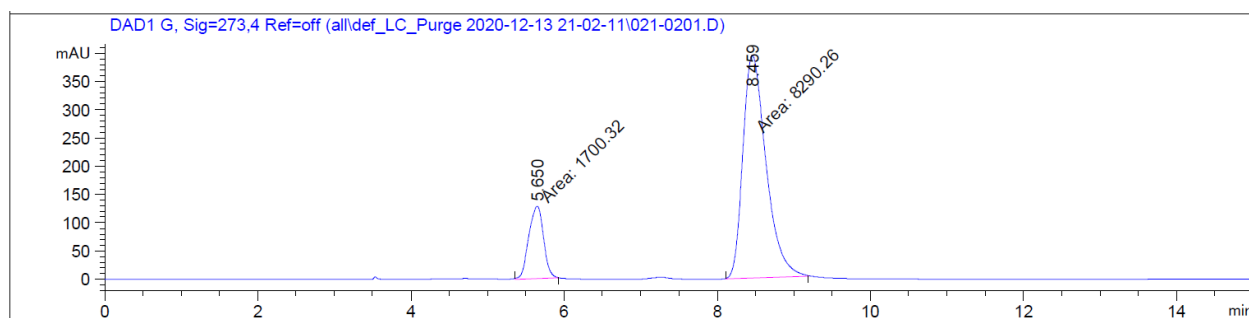
Peak #	RetTime [min]	Type	Width [min]	Area [mAU*s]	Height [mAU]	Area %
1	5.721	MM	0.2223	2548.36377	191.08023	18.1504
2	8.601	MM	0.3594	1.14919e4	532.92352	81.8496

1 mmol scale reaction:

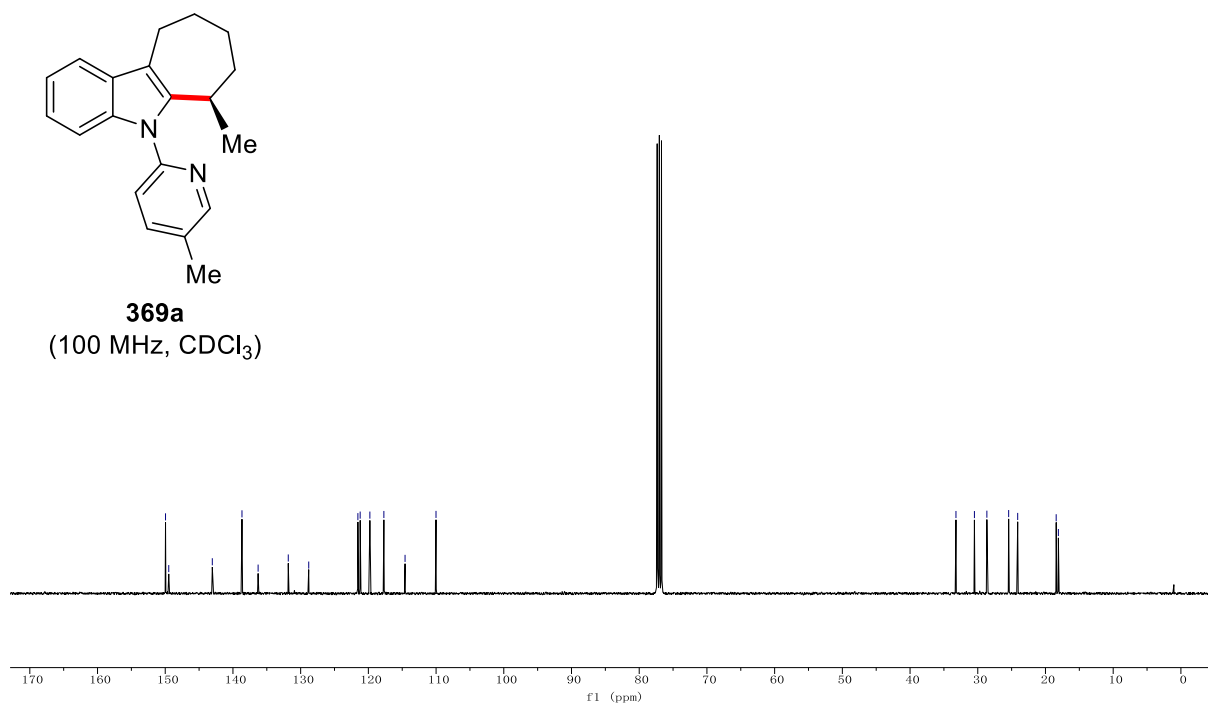
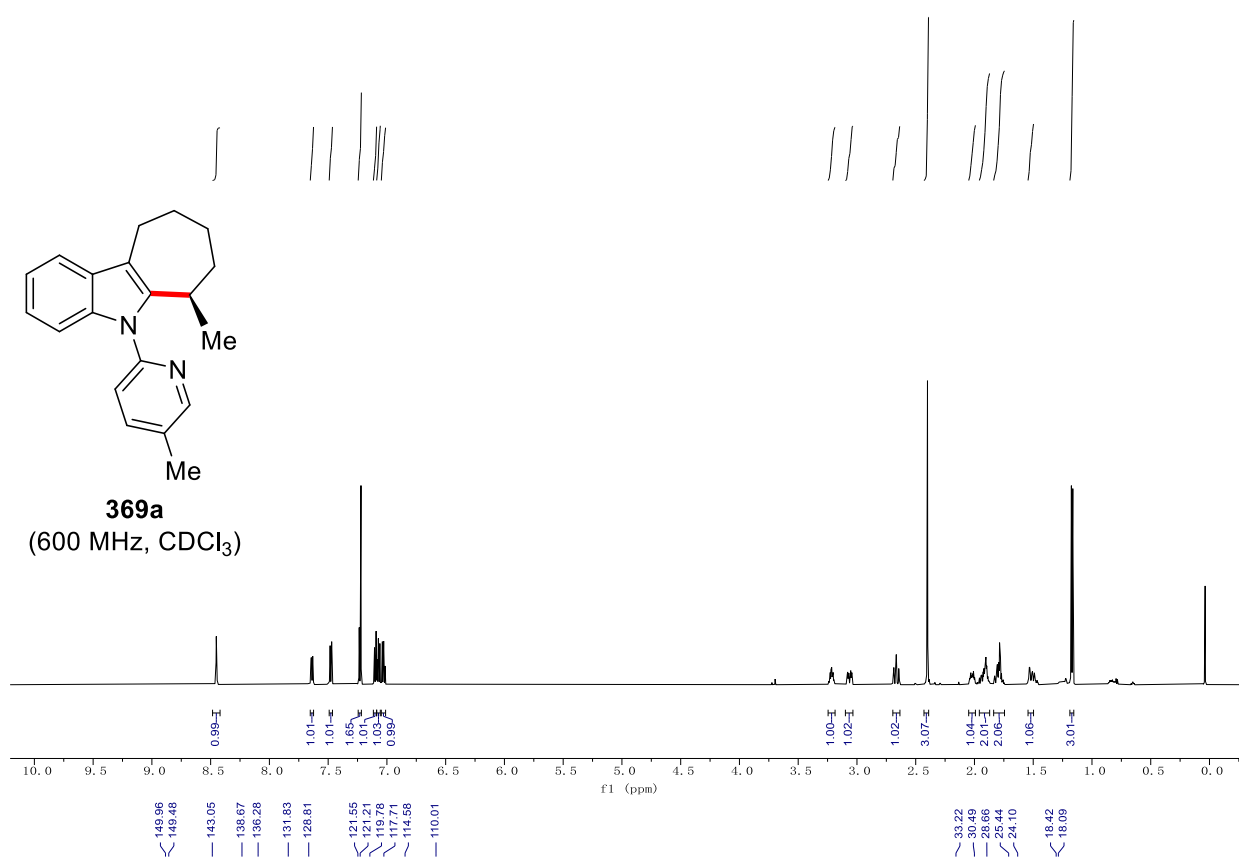
Chiral HPLC of **363e**:



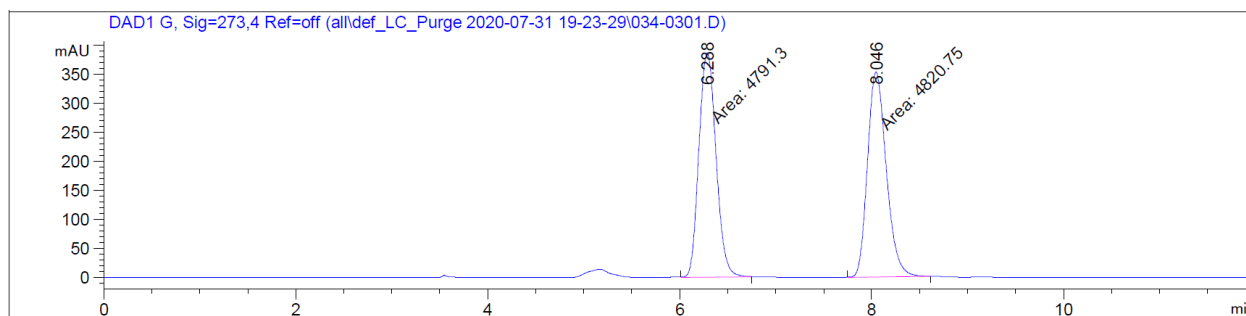
Peak #	RetTime [min]	Type	Width [min]	Area [mAU*s]	Height [mAU]	Area %
1	5.846	MM	0.2217	3630.59351	272.88000	50.3481
2	8.850	MM	0.3607	3580.39746	165.42451	49.6519



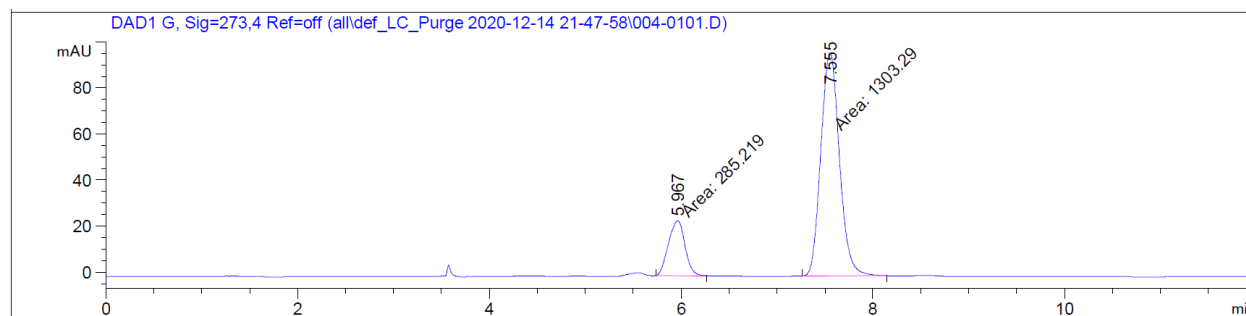
Peak #	RetTime [min]	Type	Width [min]	Area [mAU*s]	Height [mAU]	Area %
1	5.650	MM	0.2219	1700.32336	127.71491	17.0193
2	8.459	MM	0.3504	8290.26270	394.30869	82.9807



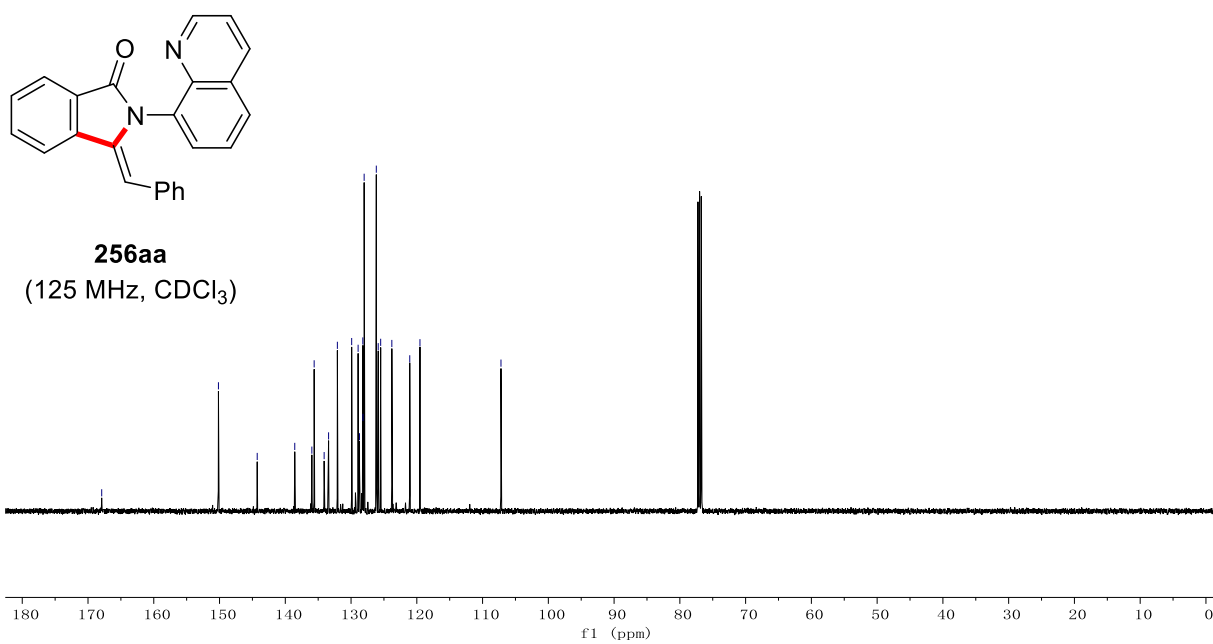
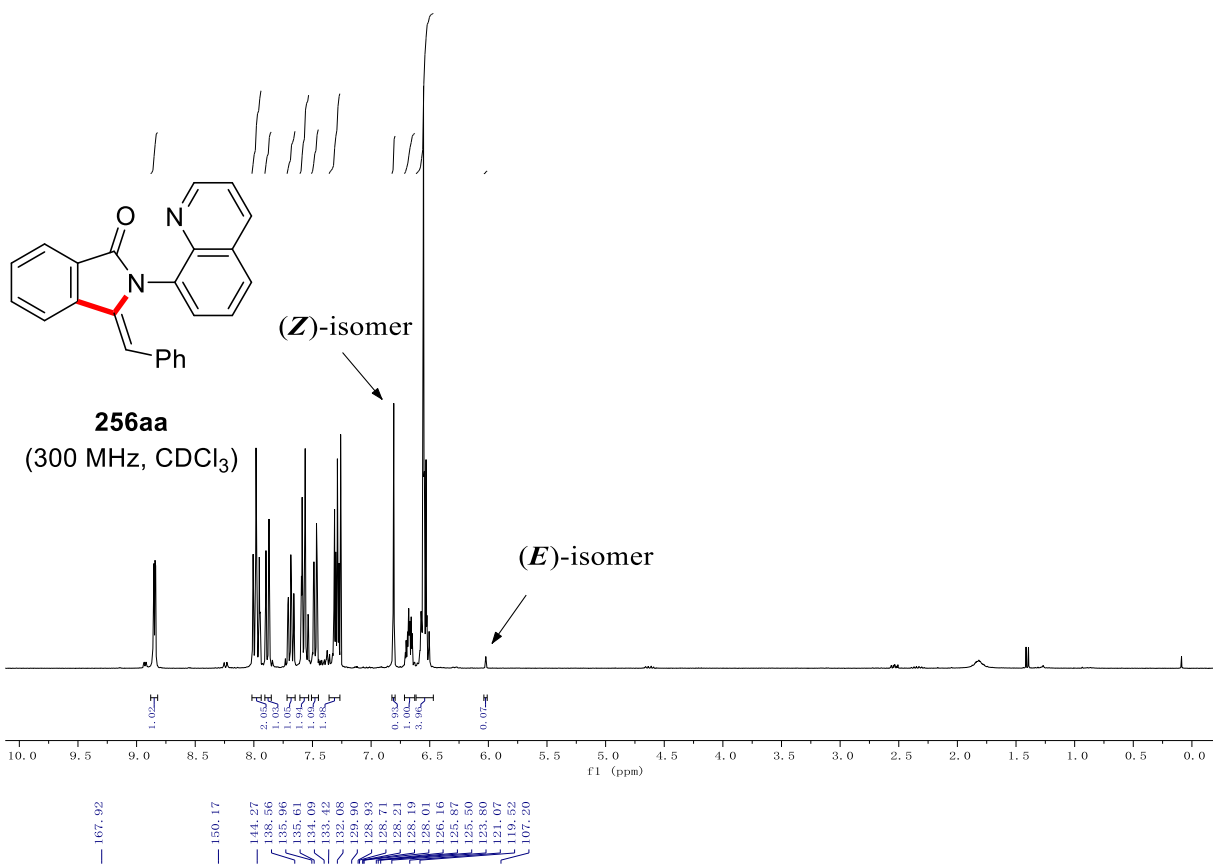
Chiral HPLC of **369a**:

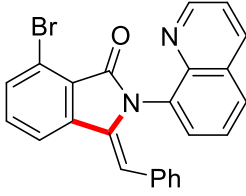


Peak #	RetTime [min]	Type	Width [min]	Area [mAU*s]	Height [mAU]	Area %
1	6.288	MM	0.2062	4791.29688	387.28531	49.8468
2	8.046	MM	0.2268	4820.74707	354.18680	50.1532

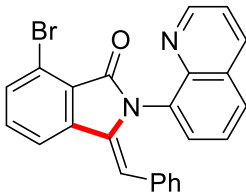
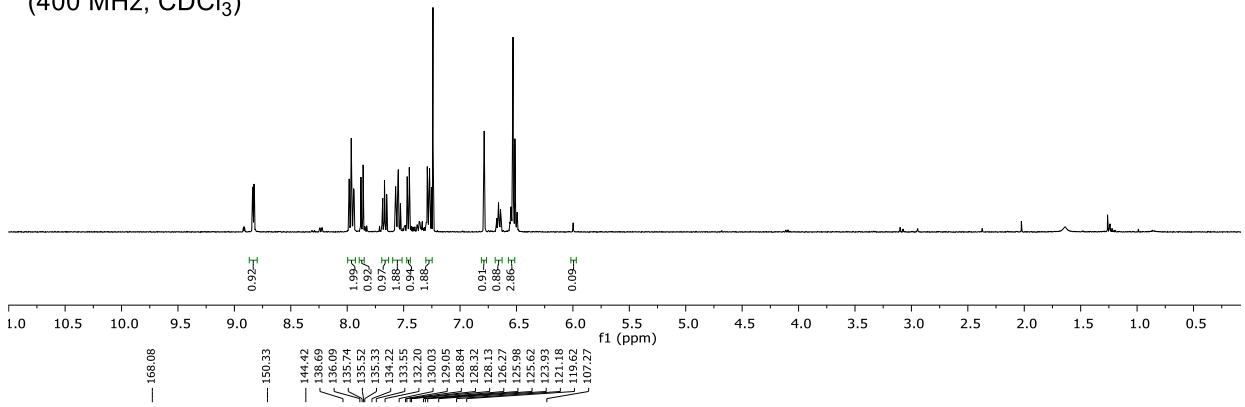


Peak #	RetTime [min]	Type	Width [min]	Area [mAU*s]	Height [mAU]	Area %
1	5.967	MM	0.1995	285.21909	23.83342	17.9552
2	7.555	MM	0.2244	1303.28711	96.80681	82.0448

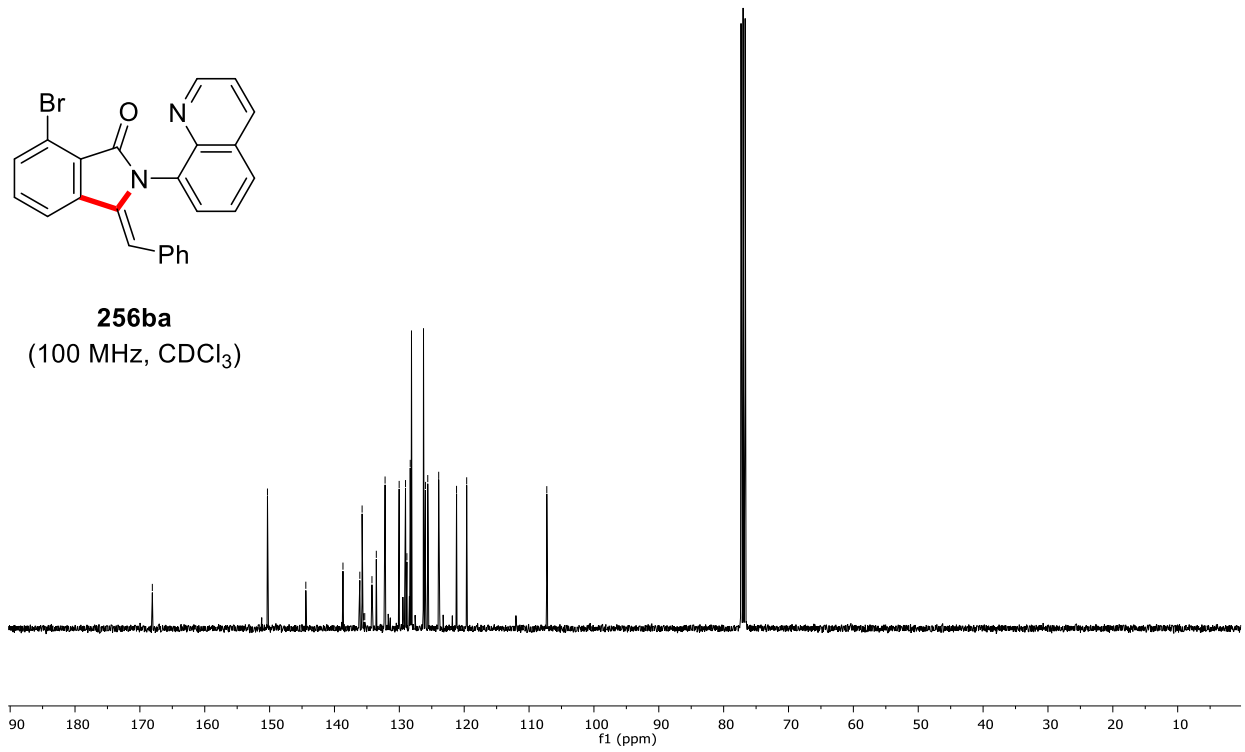


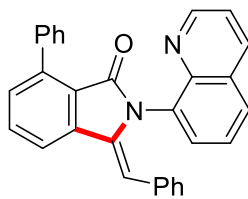


256ba
(400 MHz, CDCl₃)

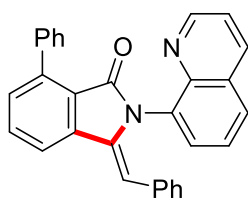
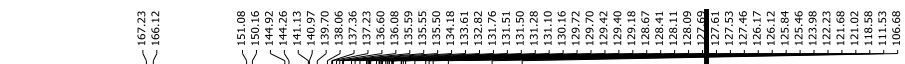
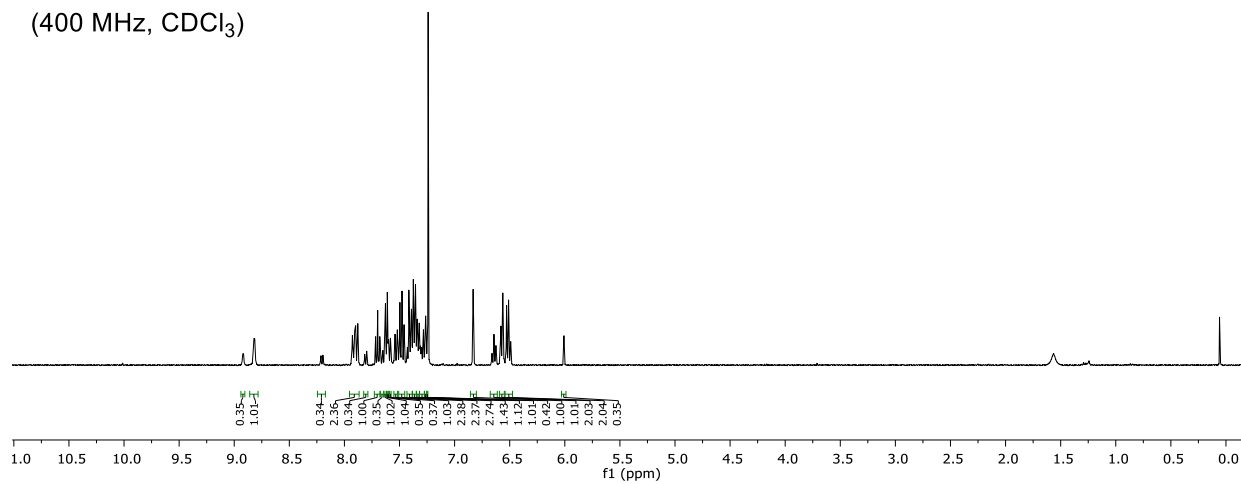


256ba
(100 MHz, CDCl₃)

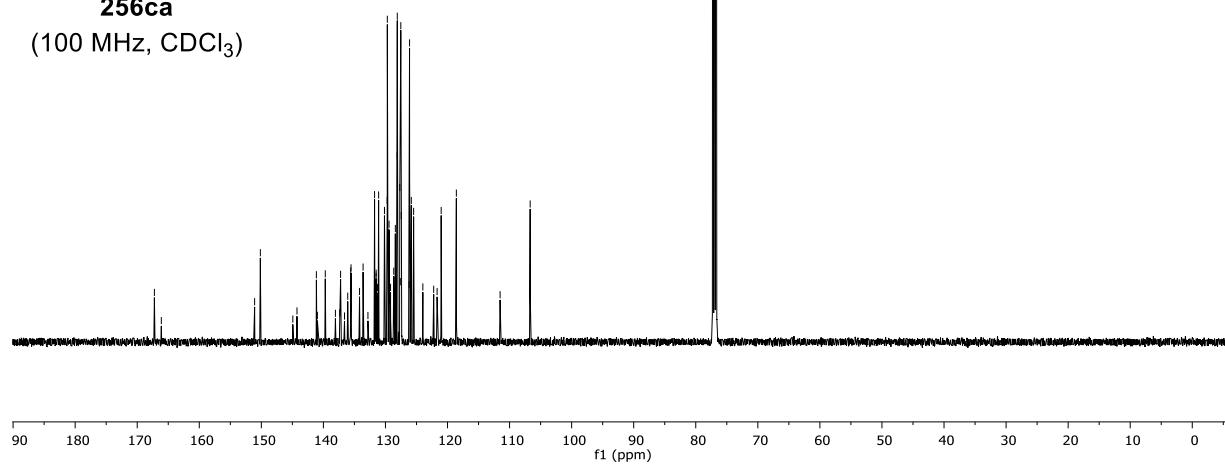


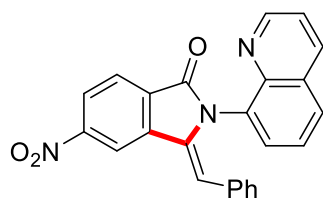


256ca
(400 MHz, CDCl₃)

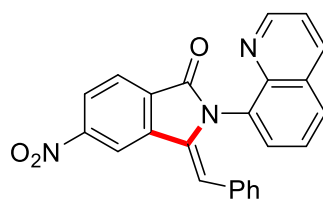
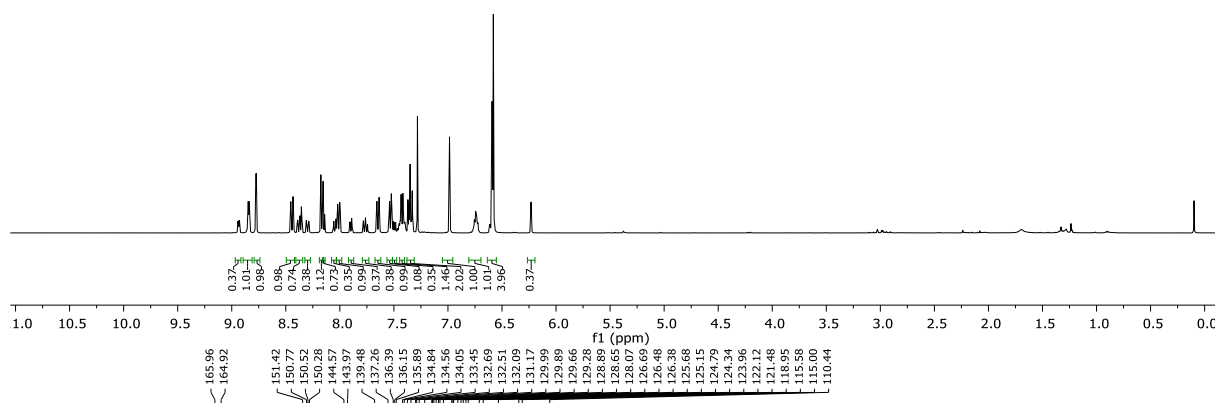


256ca
(100 MHz, CDCl₃)

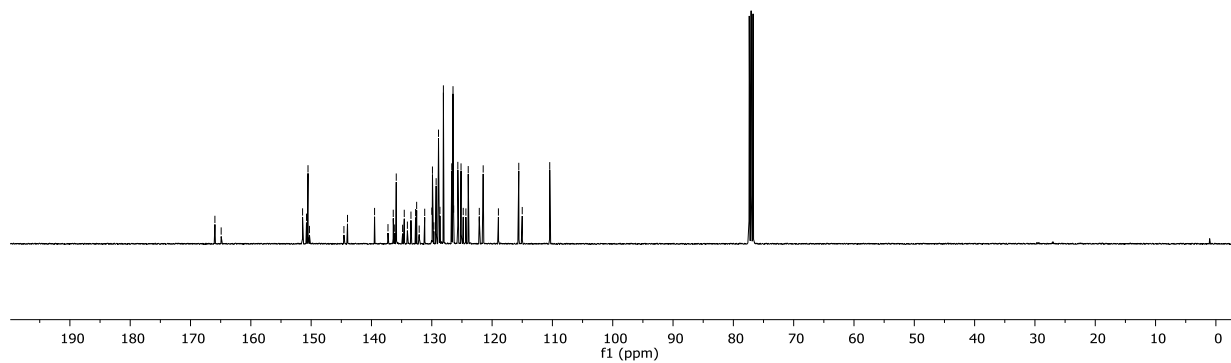


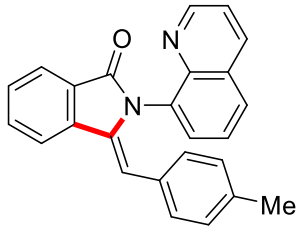


256da
(400 MHz, CDCl₃)

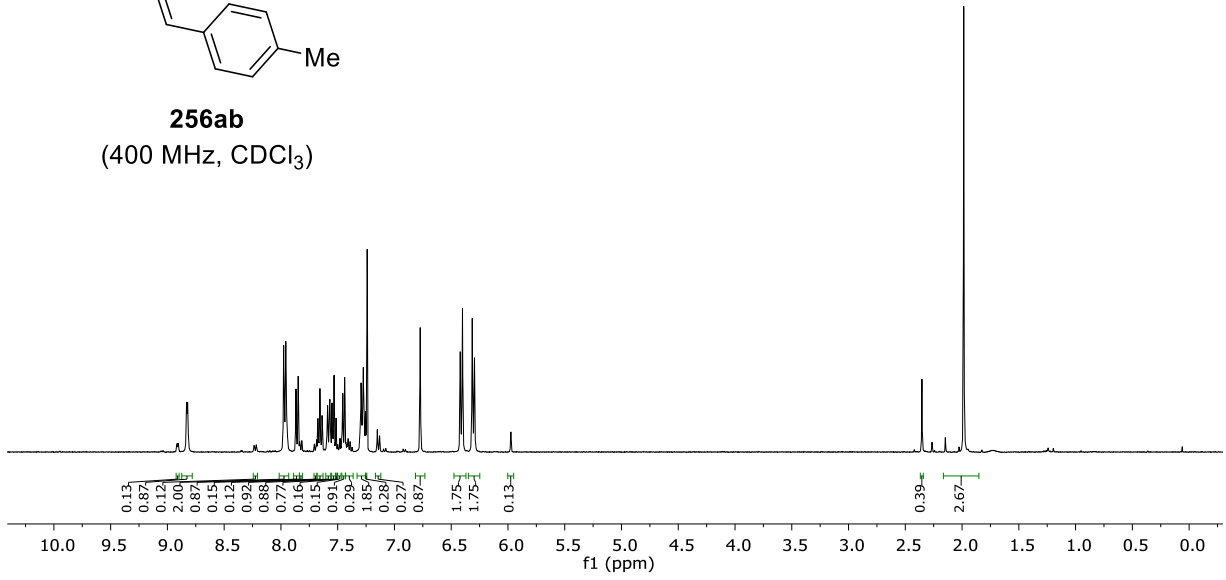


256da
(100 MHz, CDCl₃)

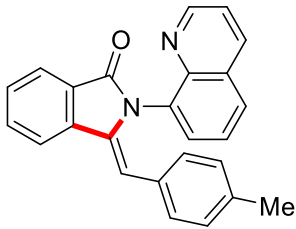




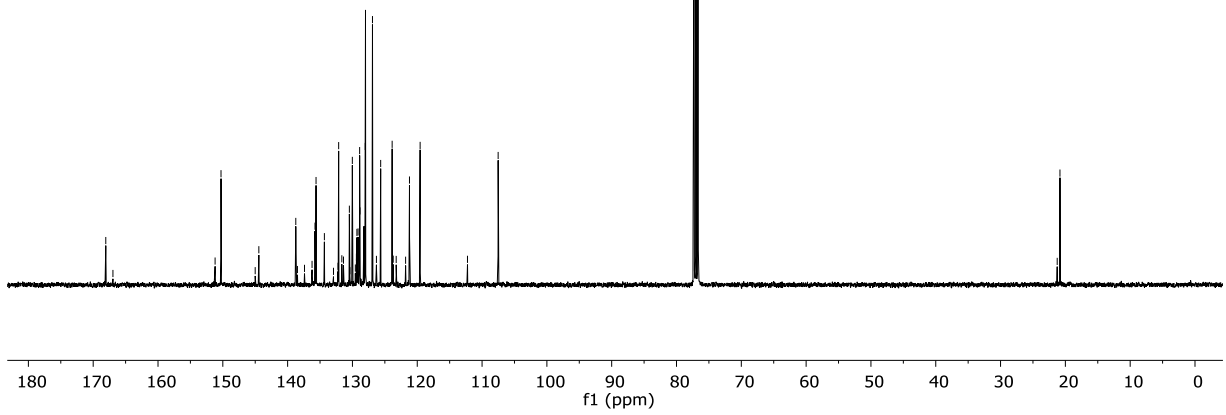
256ab
(400 MHz, CDCl₃)

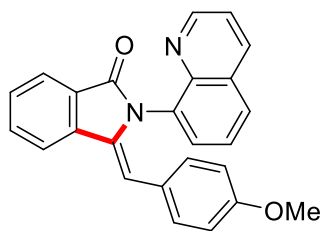


168.06
166.95
151.19
150.28
145.01
144.44
138.74
138.48
137.40
136.23
135.78
135.62
135.56
134.33
132.92
132.23
132.13
131.64
131.38
130.47
130.39
130.02
129.55
129.39
129.31
129.13
128.89
128.83
128.02
127.99
126.91
126.30
125.64
123.87
123.71
123.25
123.25
121.80
121.20
119.56
112.25
107.52
21.26
20.83

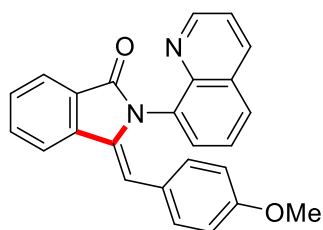
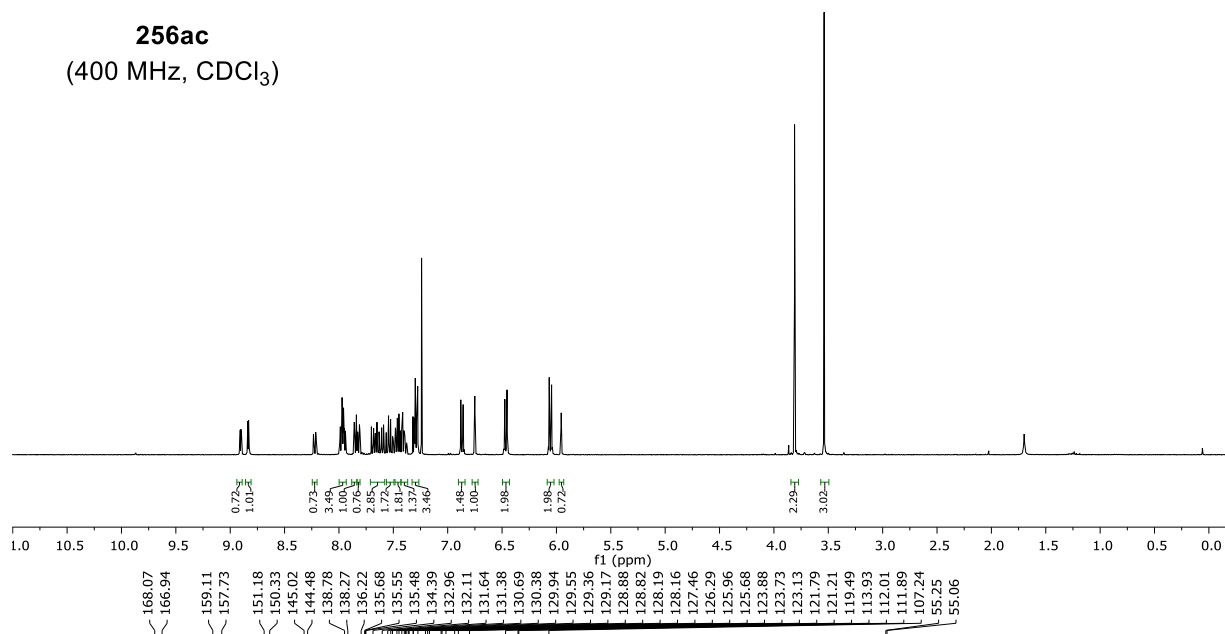


256ab
(100 MHz, CDCl₃)

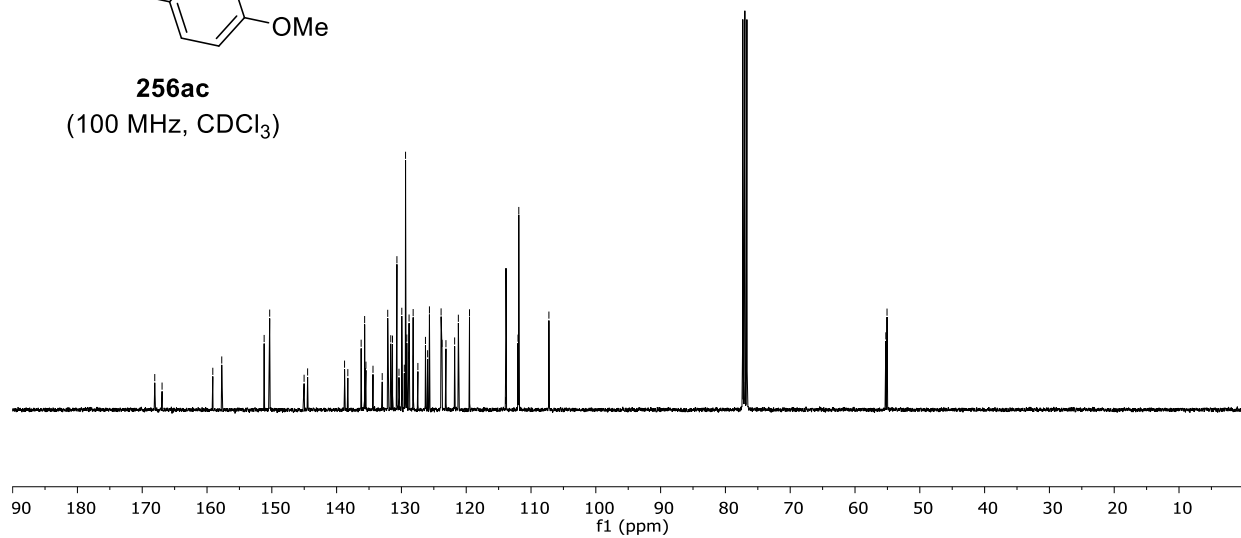


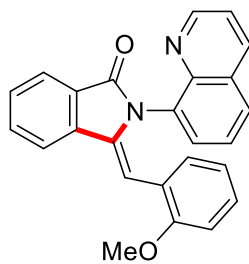


256ac
(400 MHz, CDCl₃)

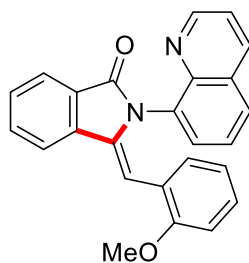
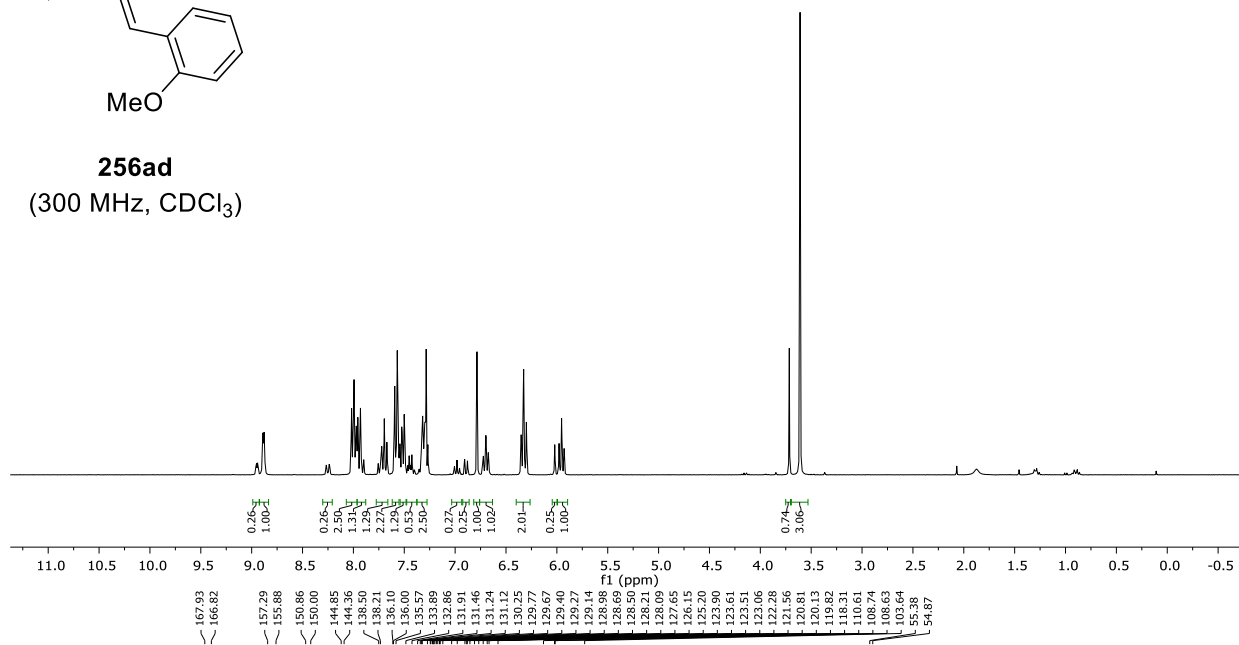


256ac
(100 MHz, CDCl₃)

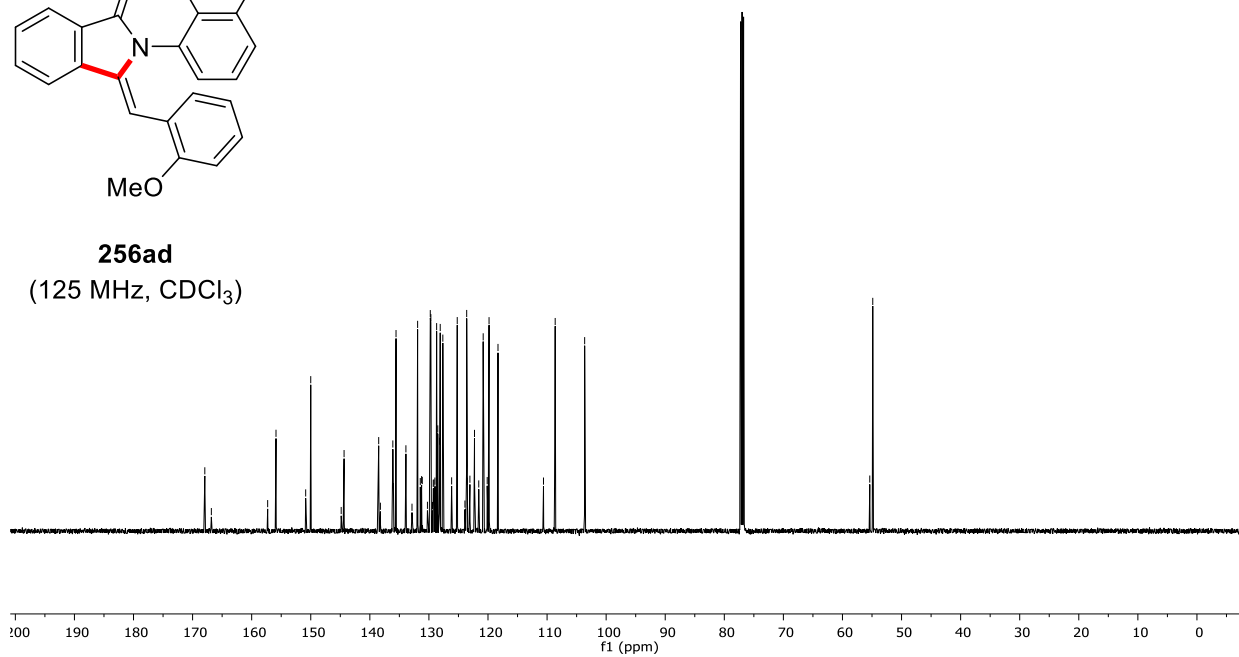


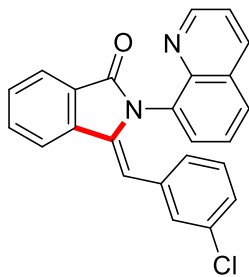


256ad
(300 MHz, CDCl_3)

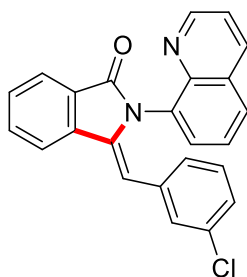
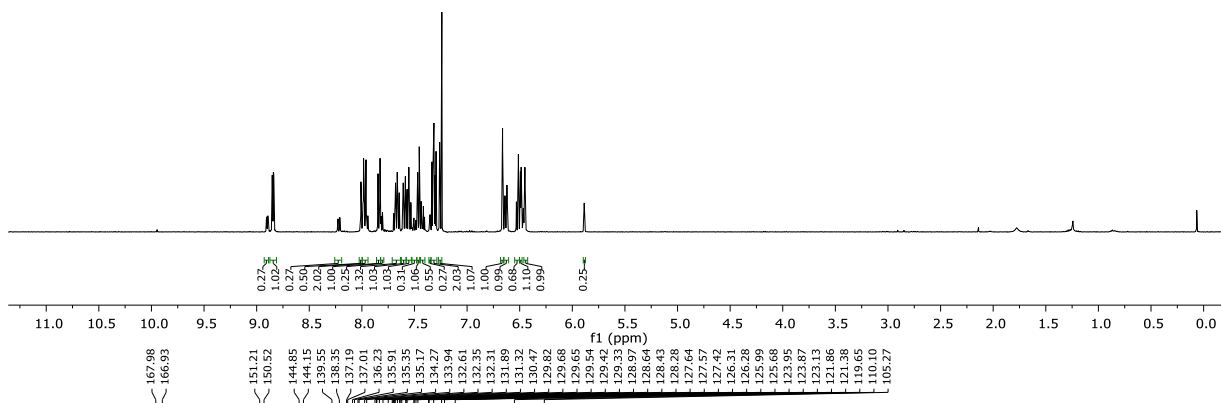


256ad
(125 MHz, CDCl_3)

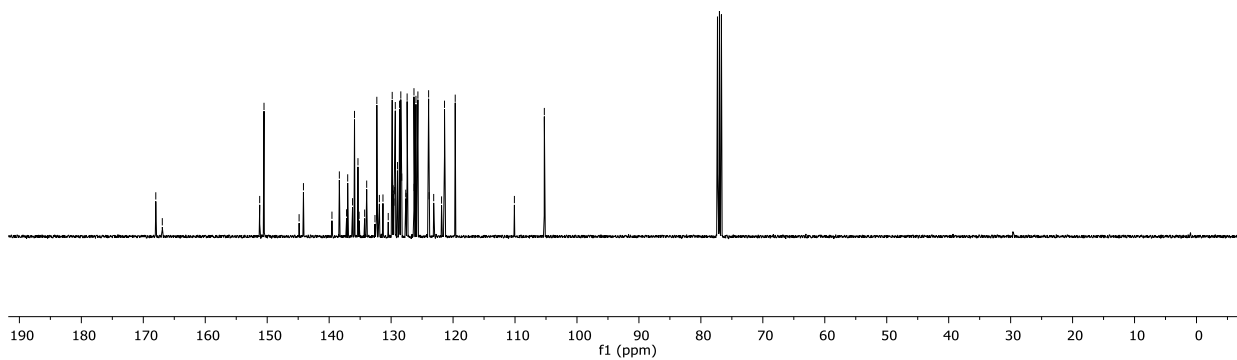


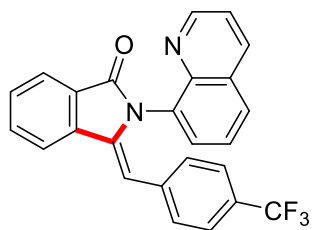


256ae
(400 MHz, CDCl₃)

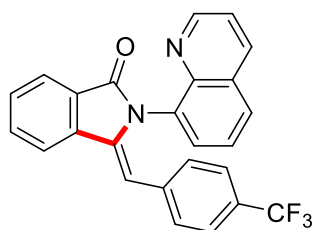
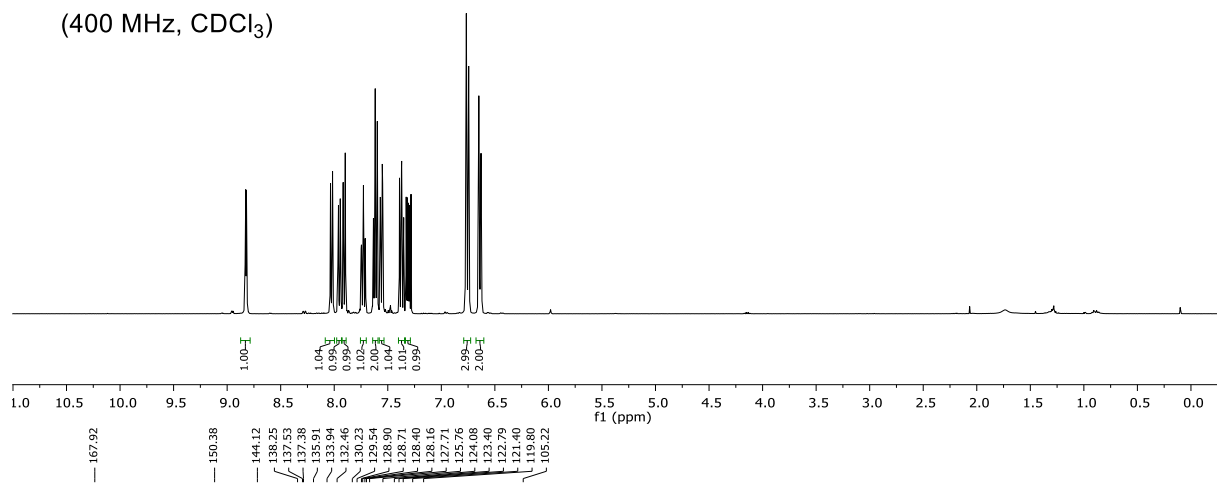


256ae
(100 MHz, CDCl₃)

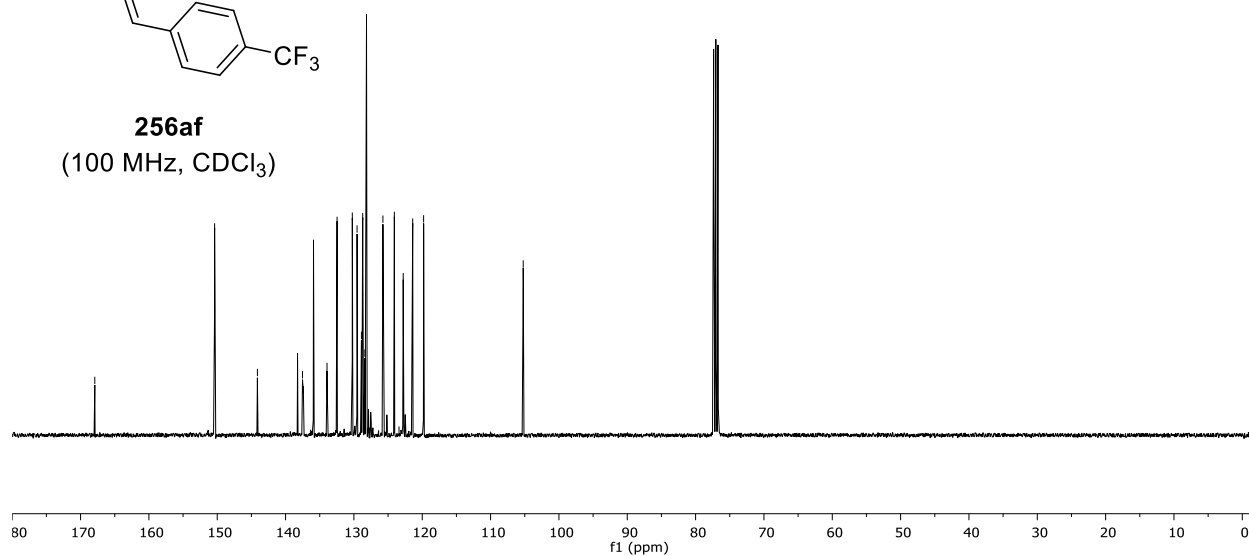


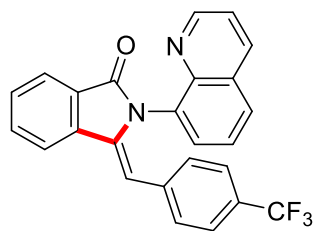


256af
(400 MHz, CDCl₃)



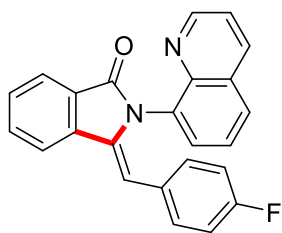
256af
(100 MHz, CDCl₃)



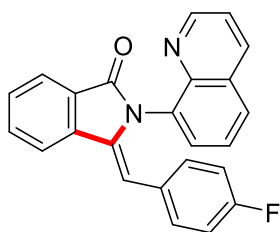
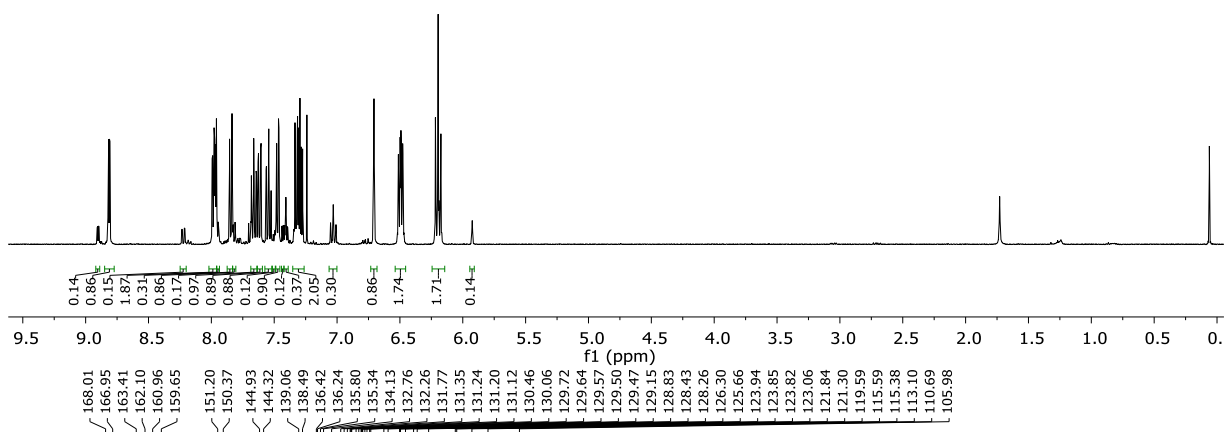


256af
(375 MHz, CDCl₃)

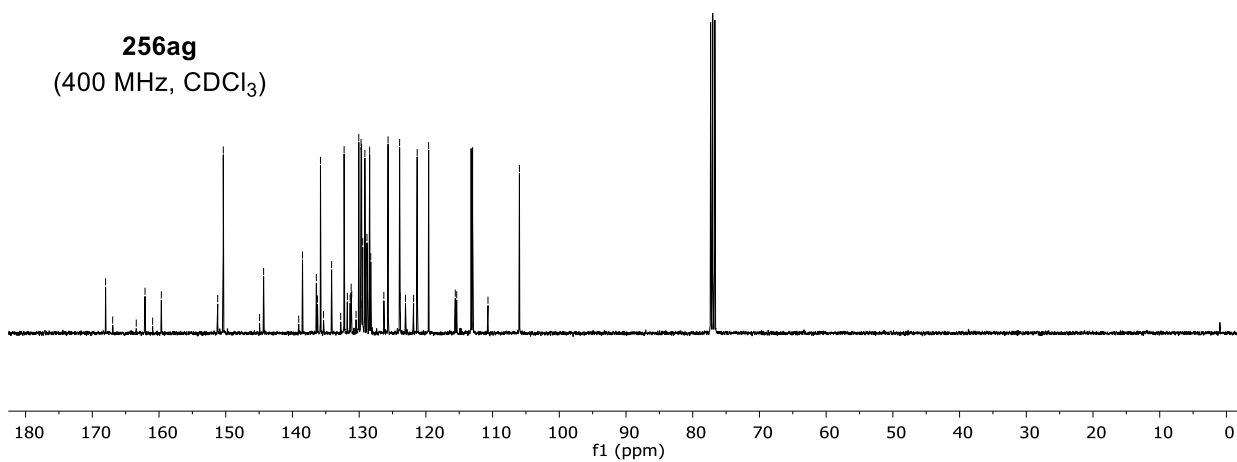


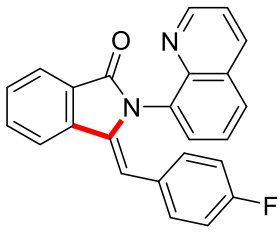


256ag
(100 MHz, CDCl_3)

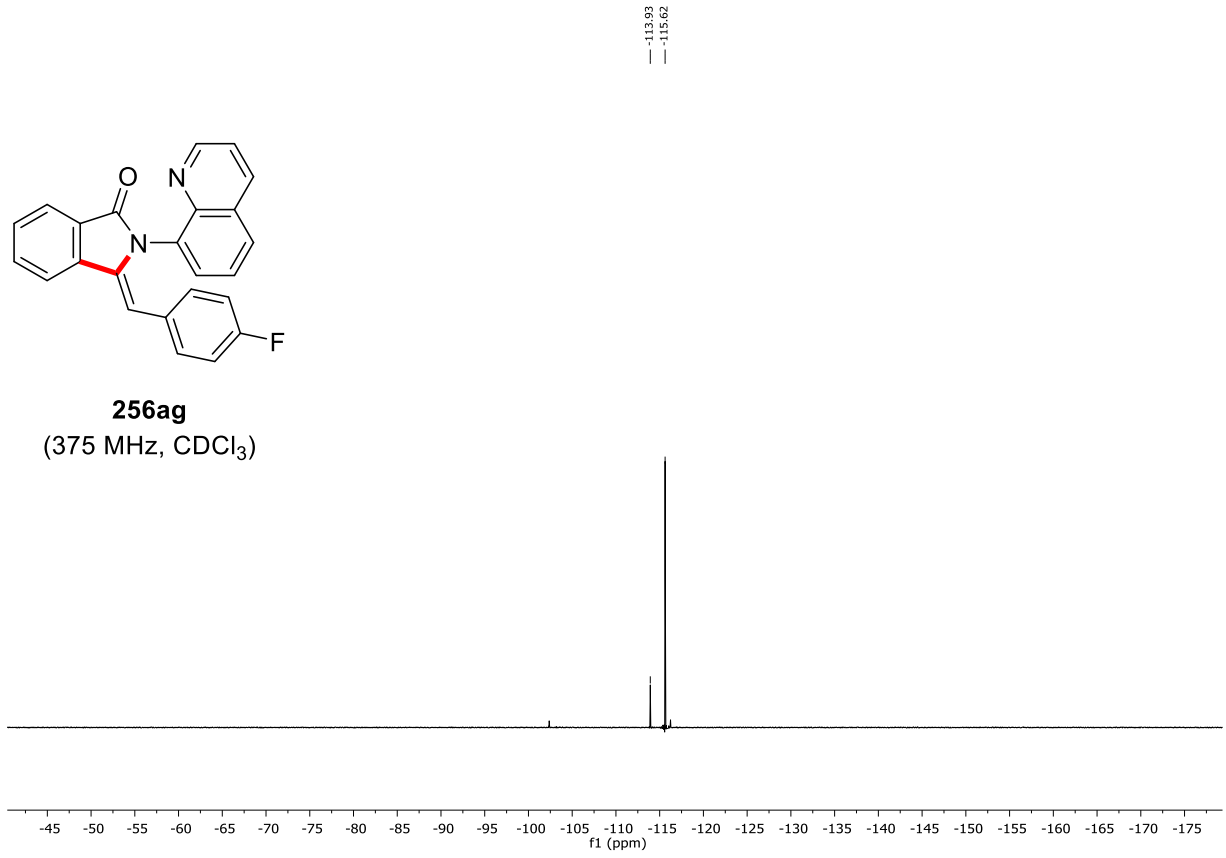


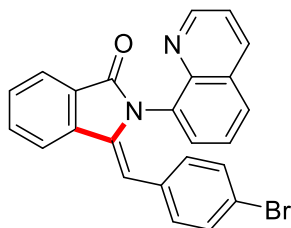
256ag
(400 MHz, CDCl_3)



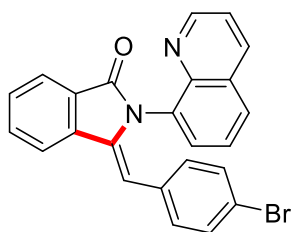
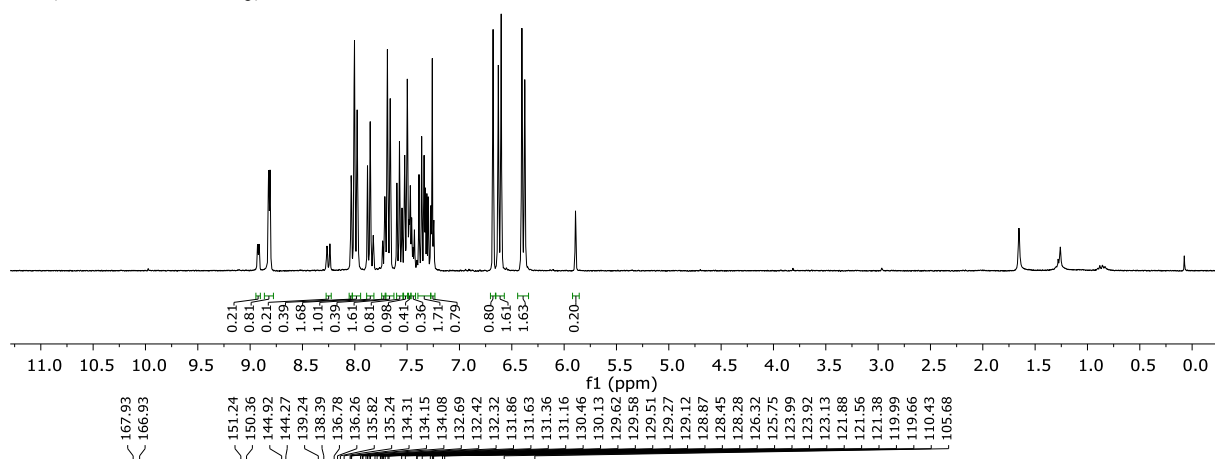


256ag
(375 MHz, CDCl₃)

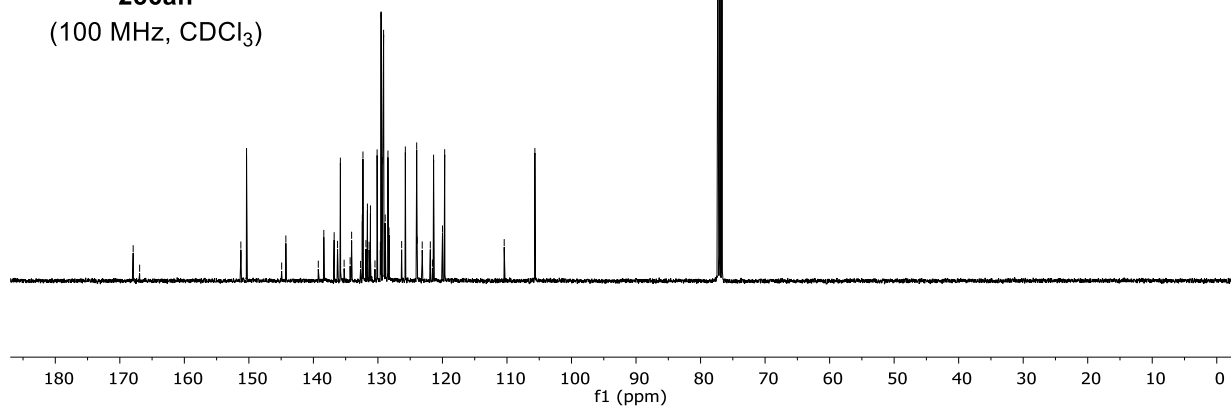


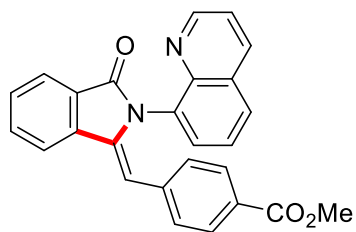


256ah
(400 MHz, CDCl₃)

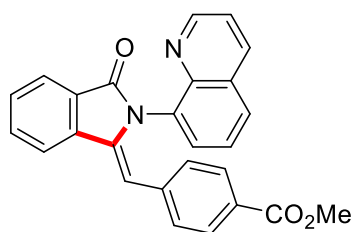
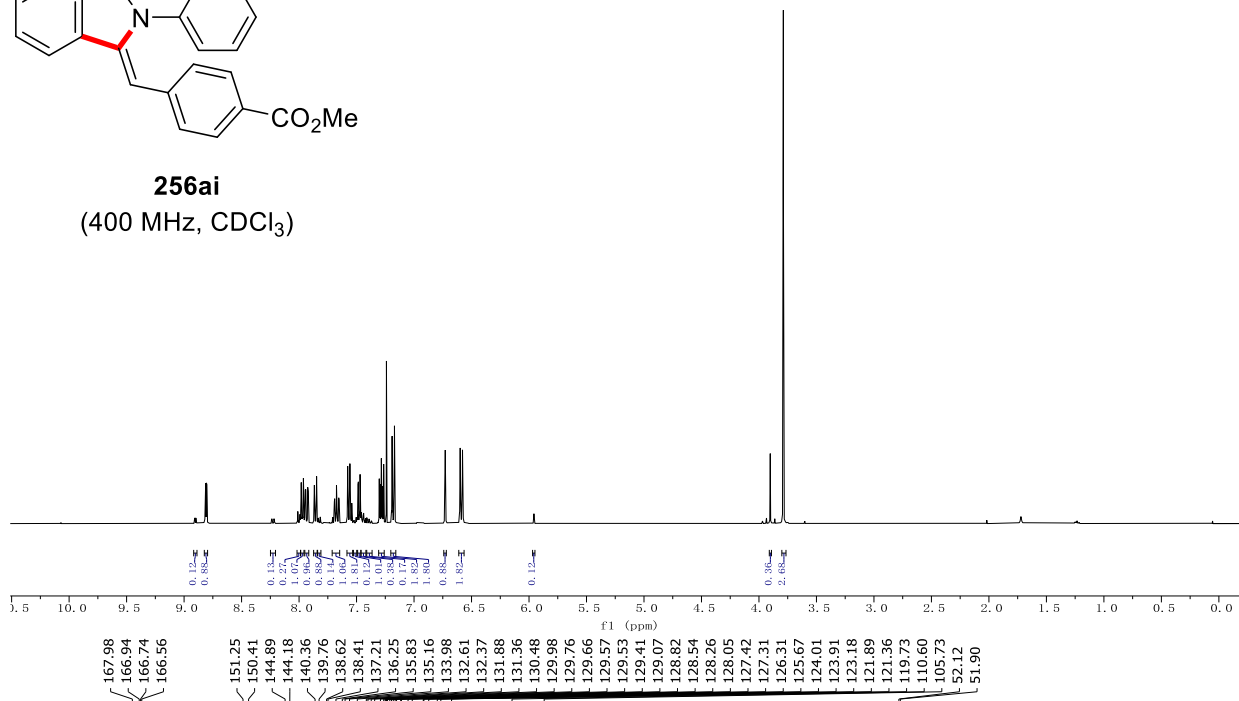


256ah
(100 MHz, CDCl₃)

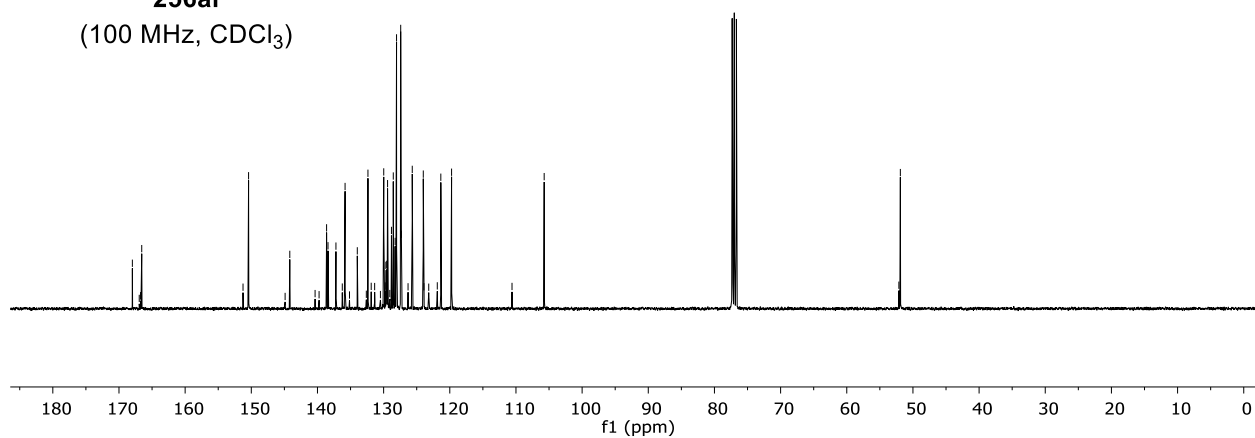


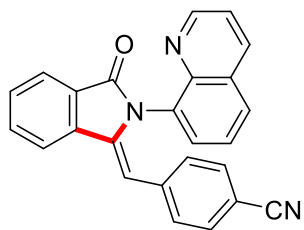


256ai
(400 MHz, CDCl₃)

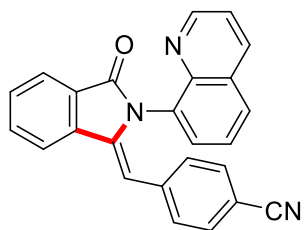
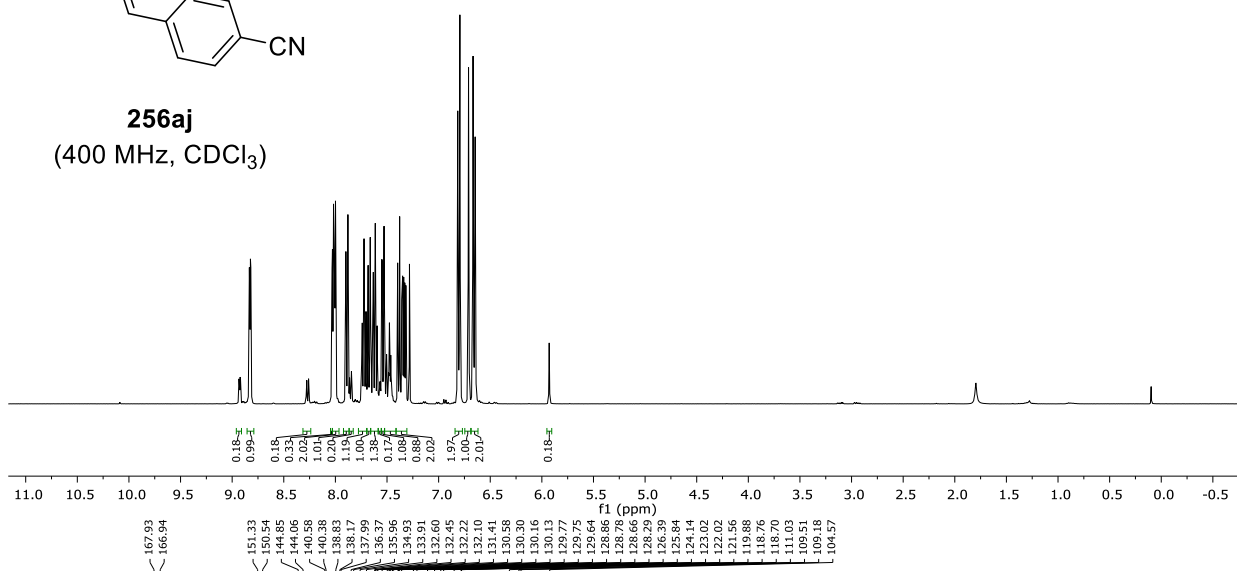


256ai
(100 MHz, CDCl₃)

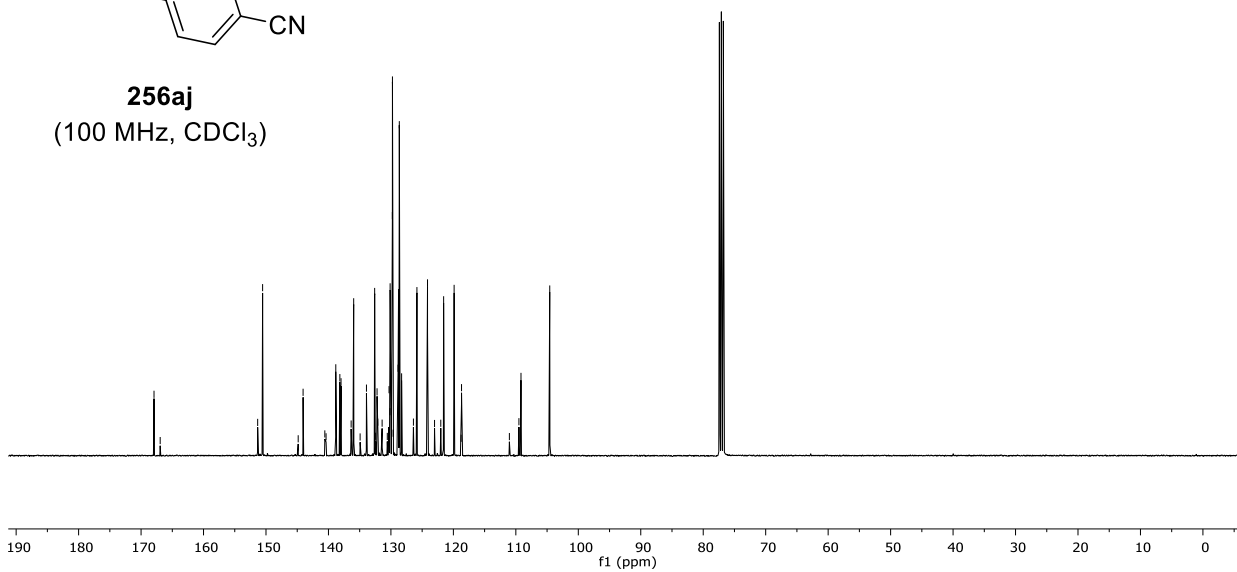


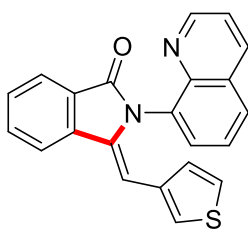


256aj
(400 MHz, CDCl₃)

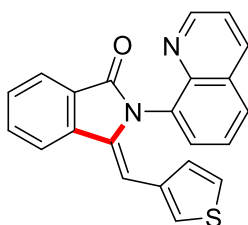
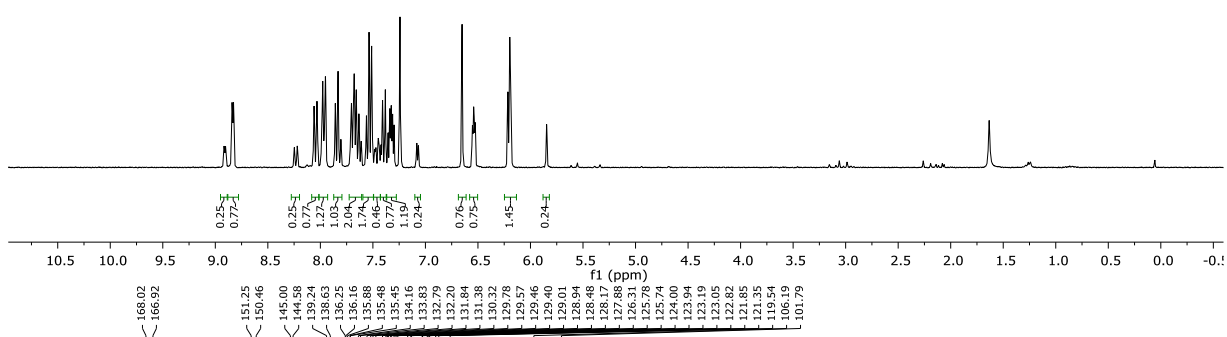


256aj
(100 MHz, CDCl₃)

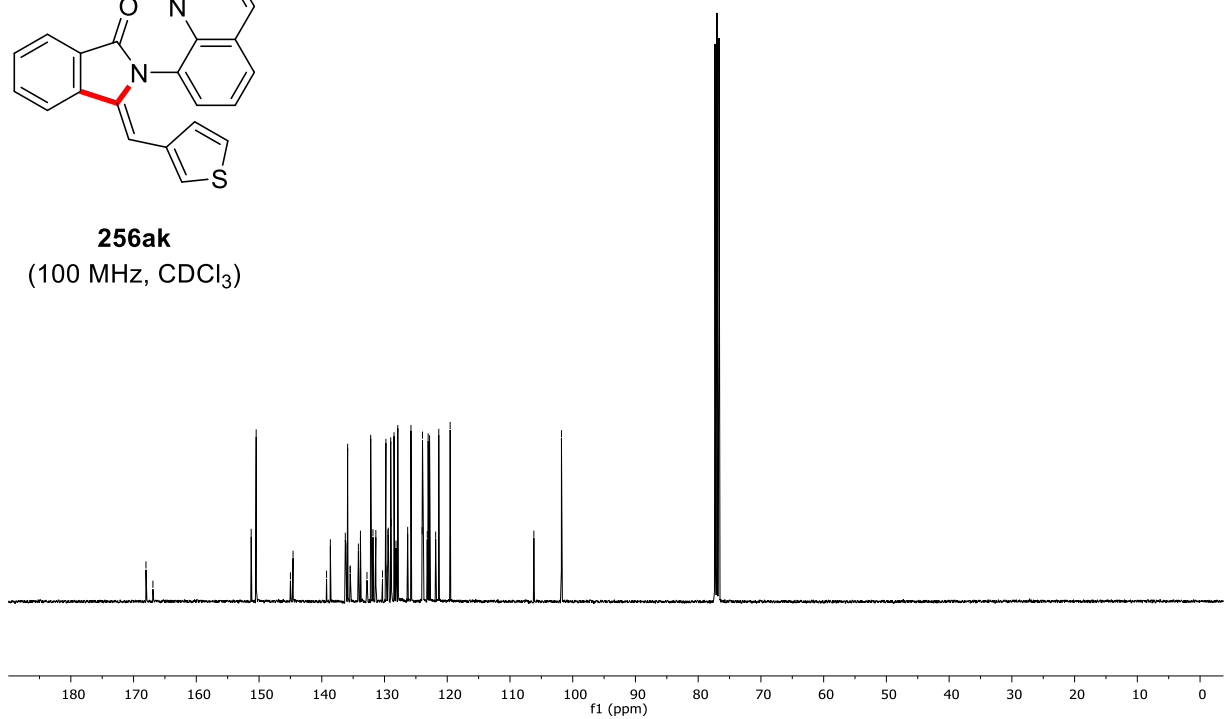


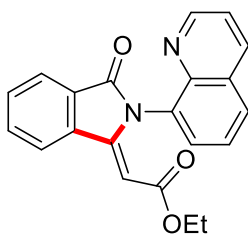


256ak
(400 MHz, CDCl₃)

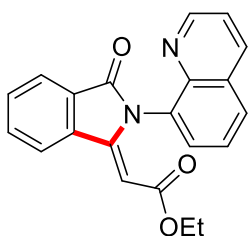
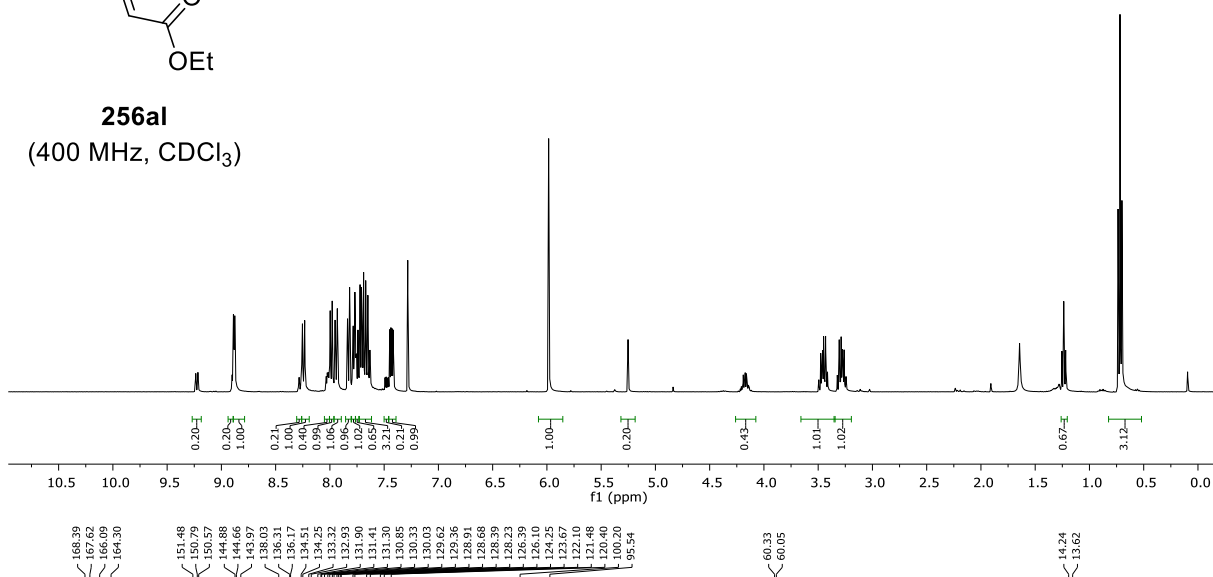


256ak
(100 MHz, CDCl₃)

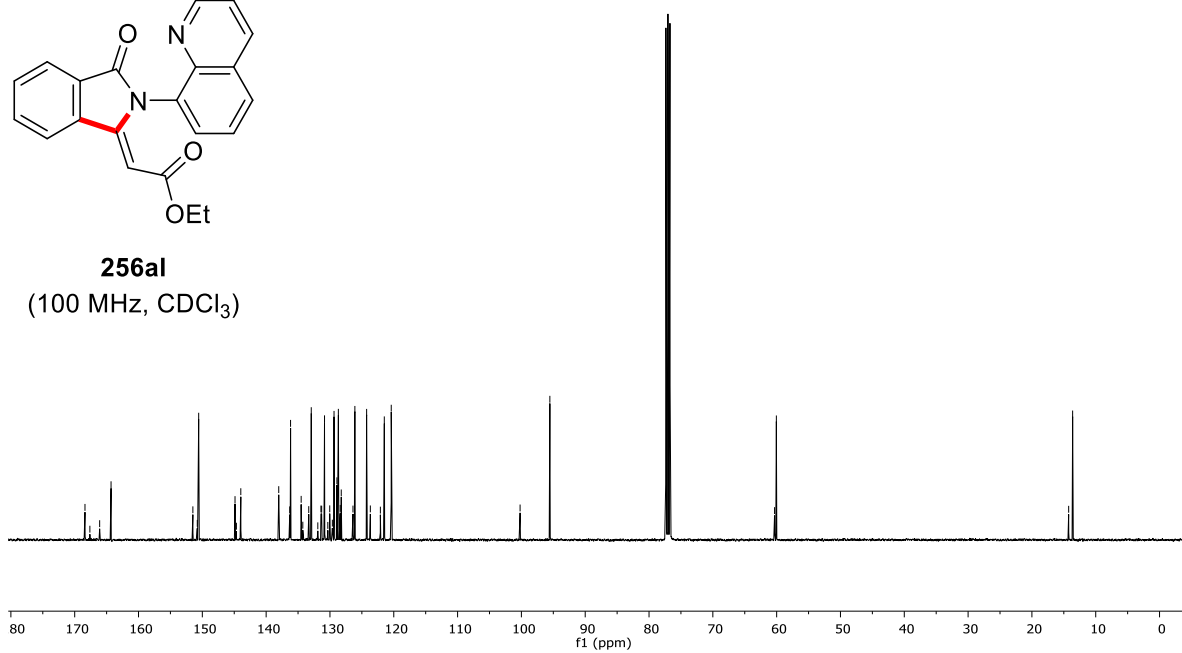


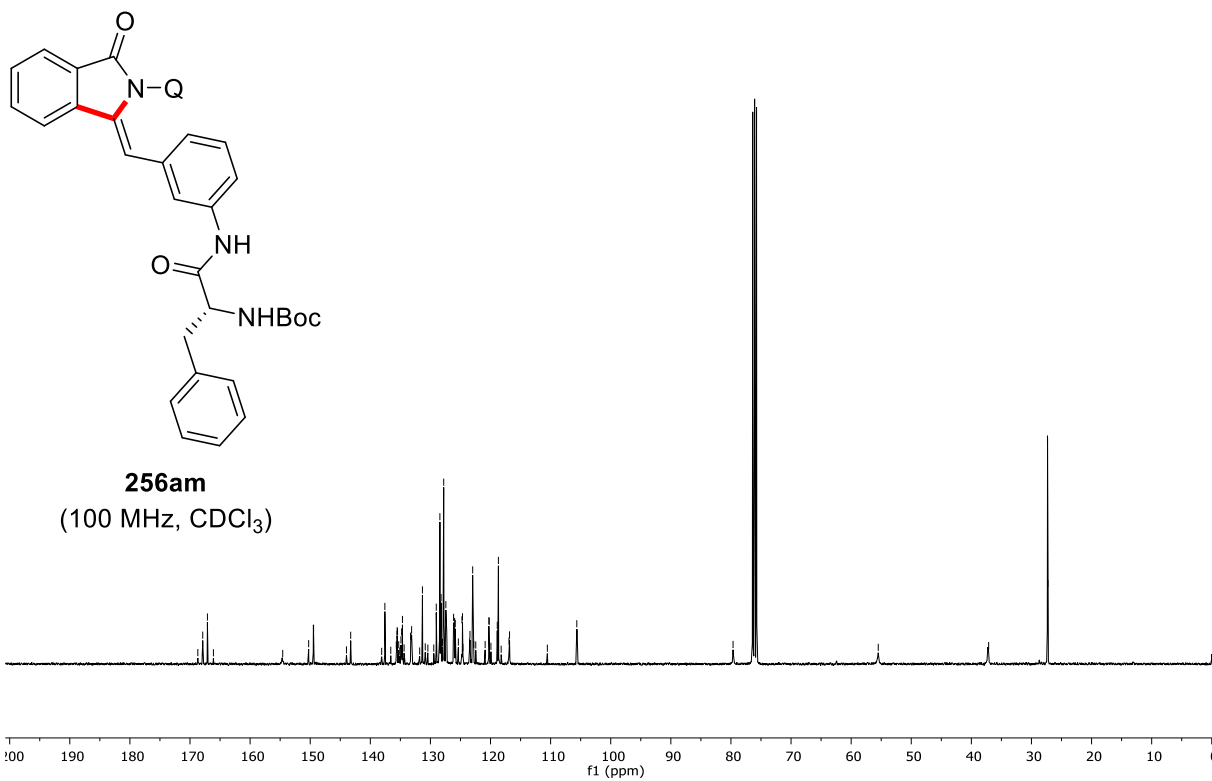
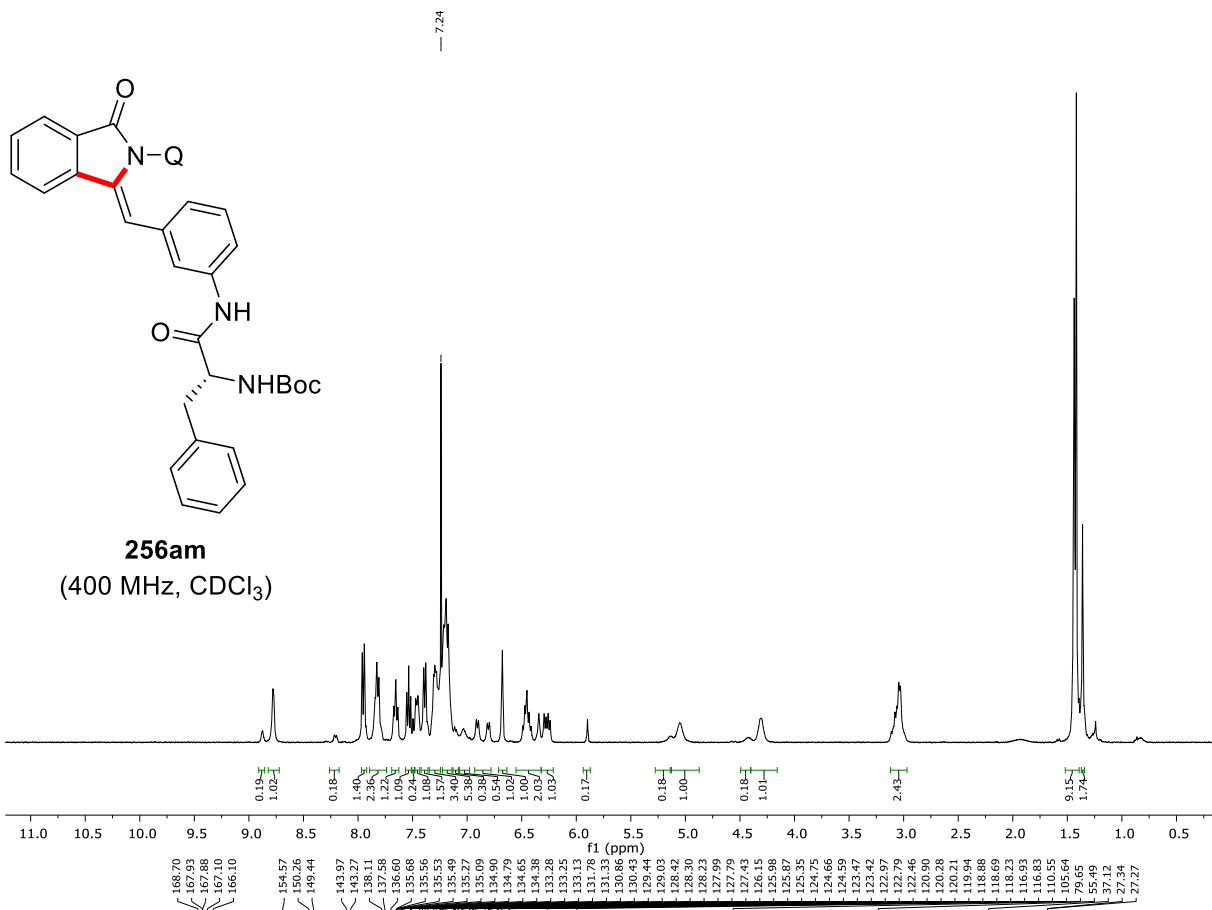


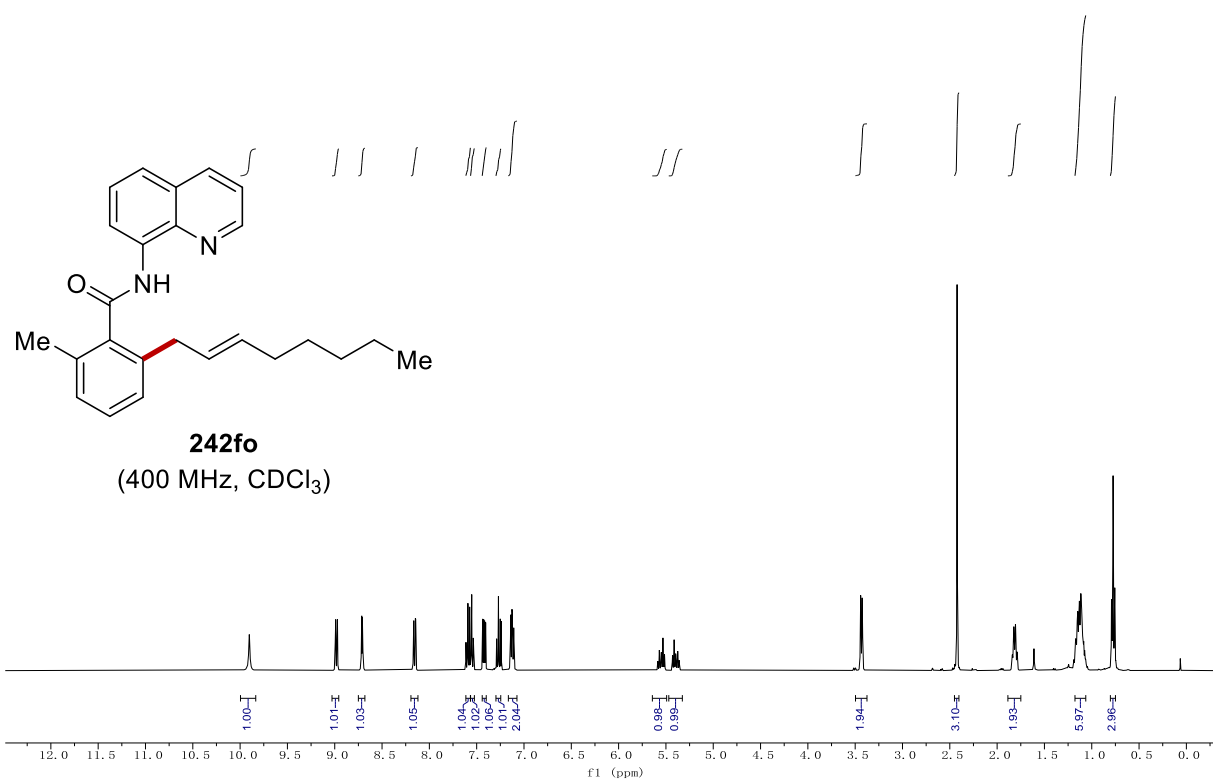
256al
(400 MHz, CDCl₃)



256al
(100 MHz, CDCl₃)

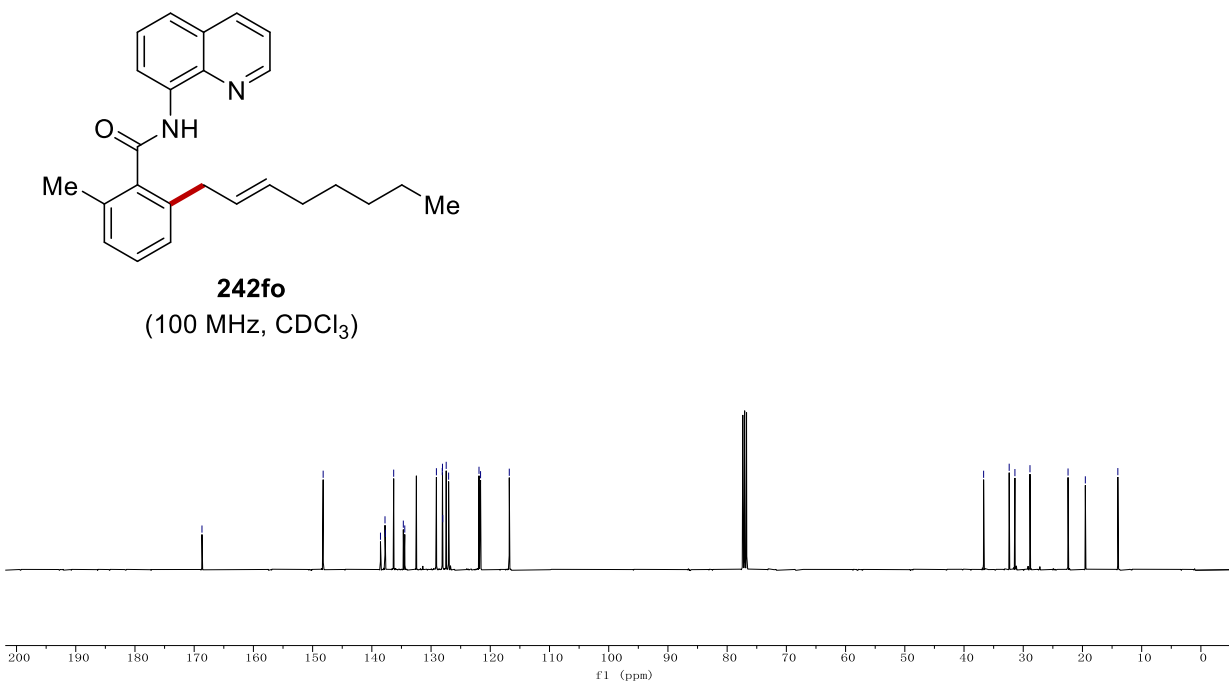


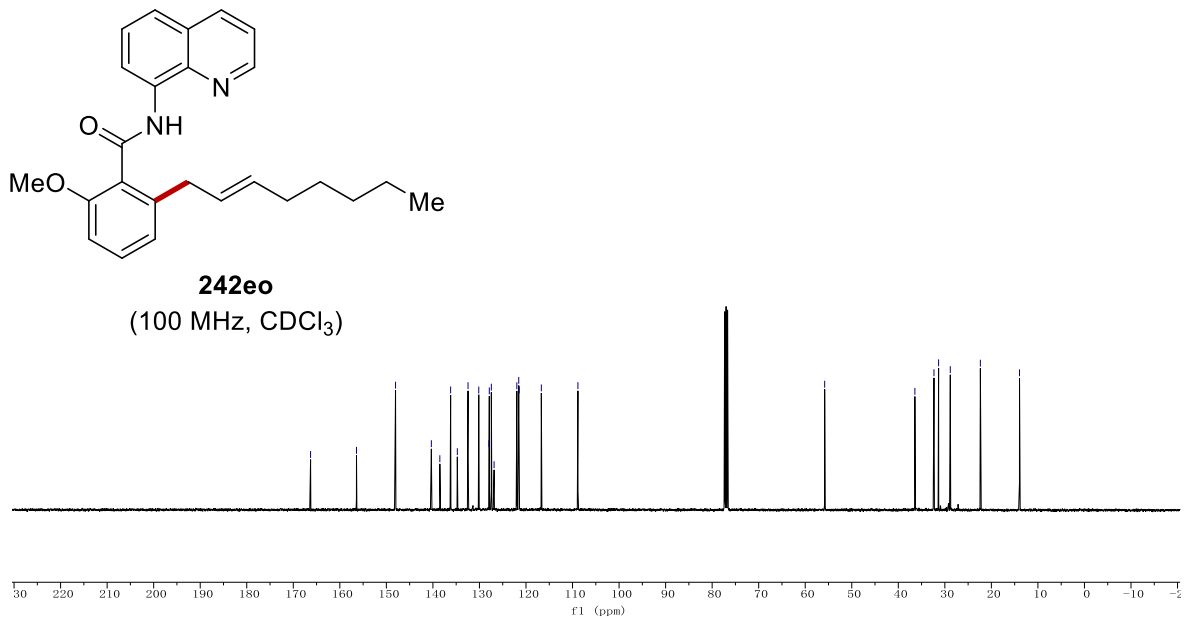
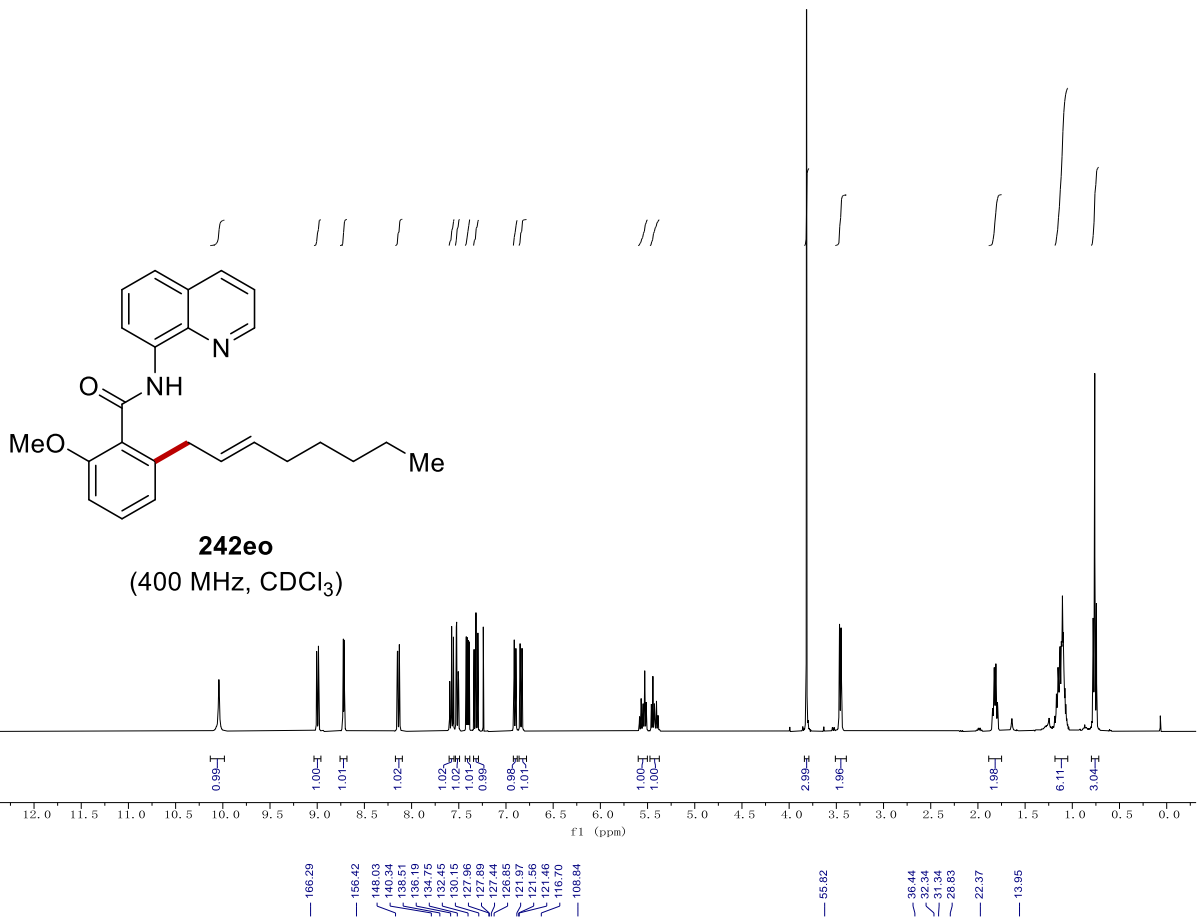


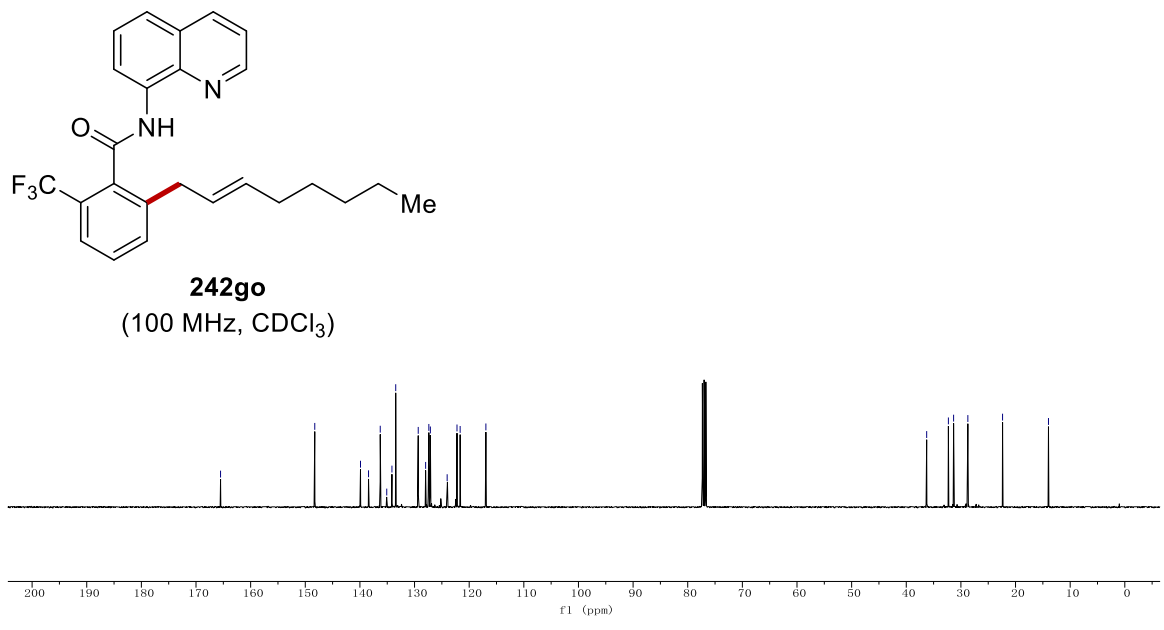
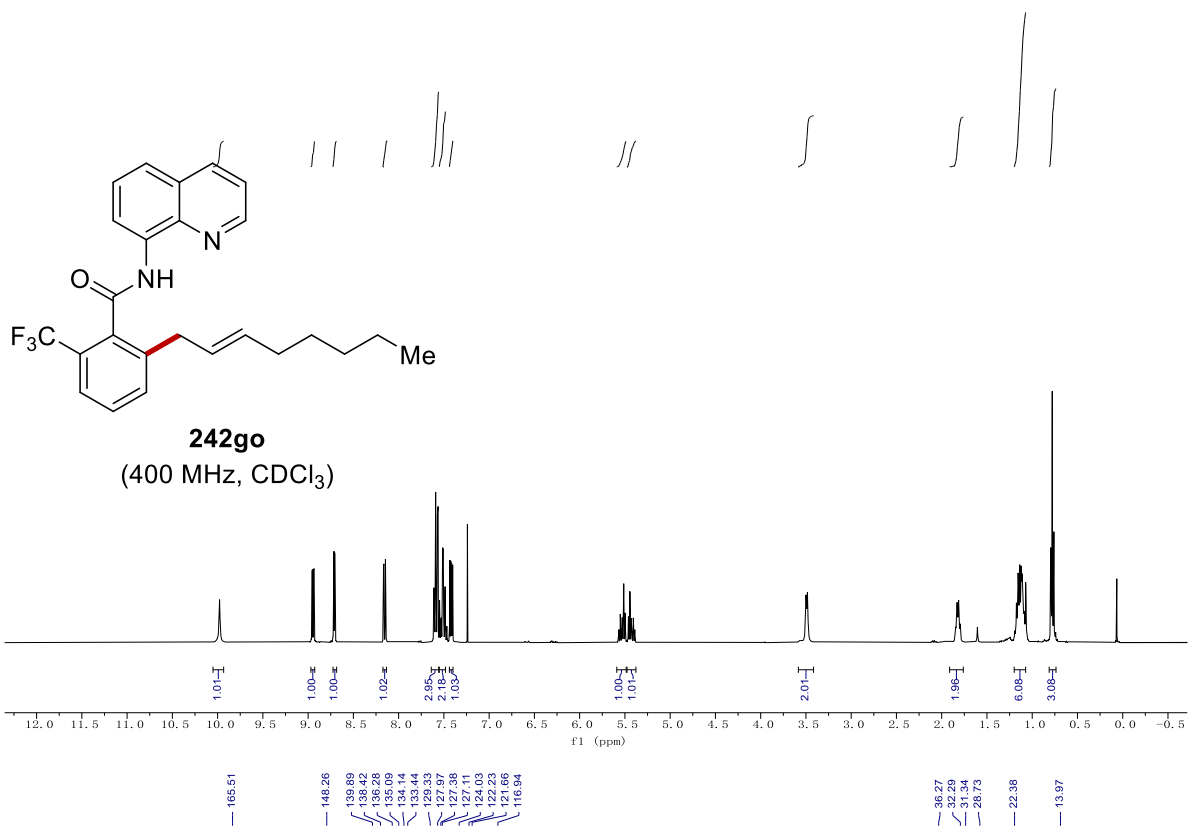


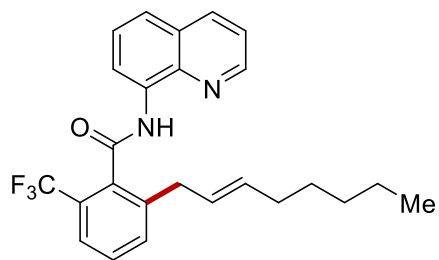
188.69
148.22
138.54
137.78
137.72
136.88
134.68
134.44
129.10
128.10
128.07
128.03
127.74
127.03
121.91
121.84
116.79

36.69
32.37
31.41
28.86
22.44
19.52
14.03

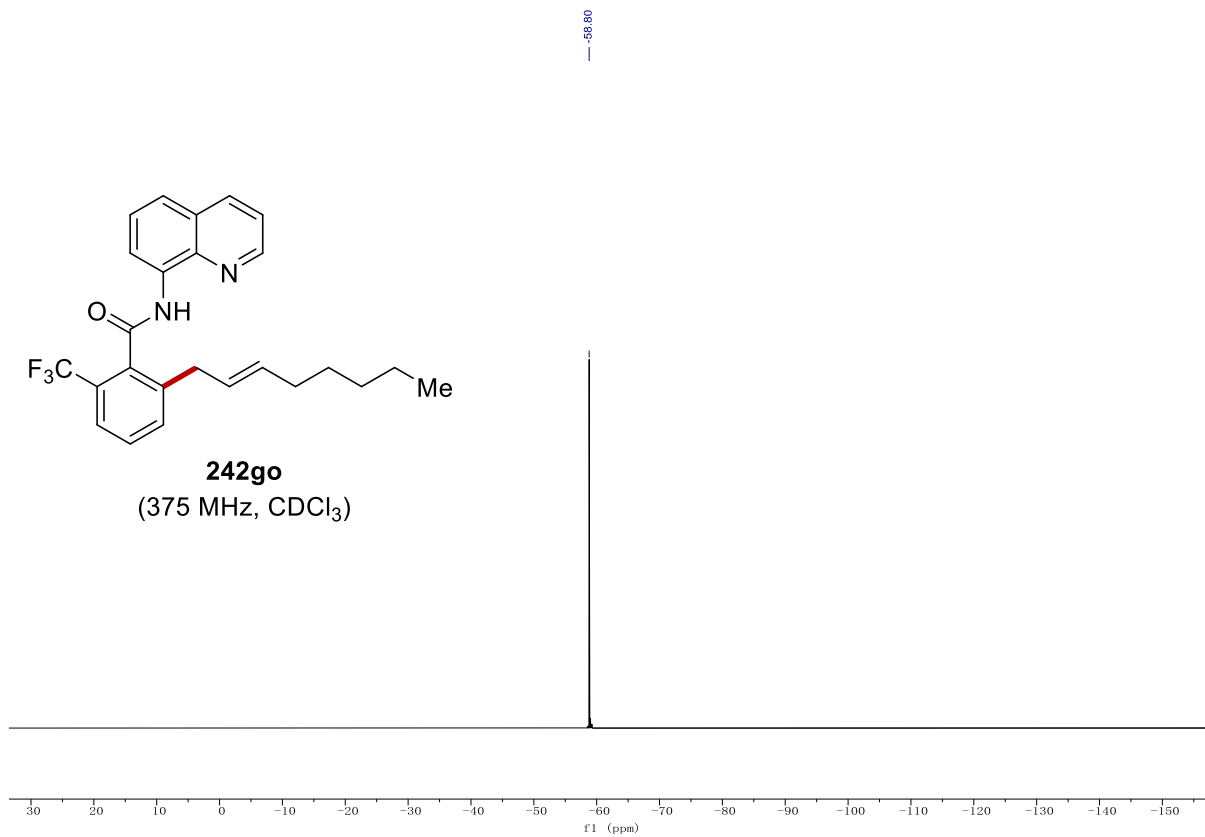


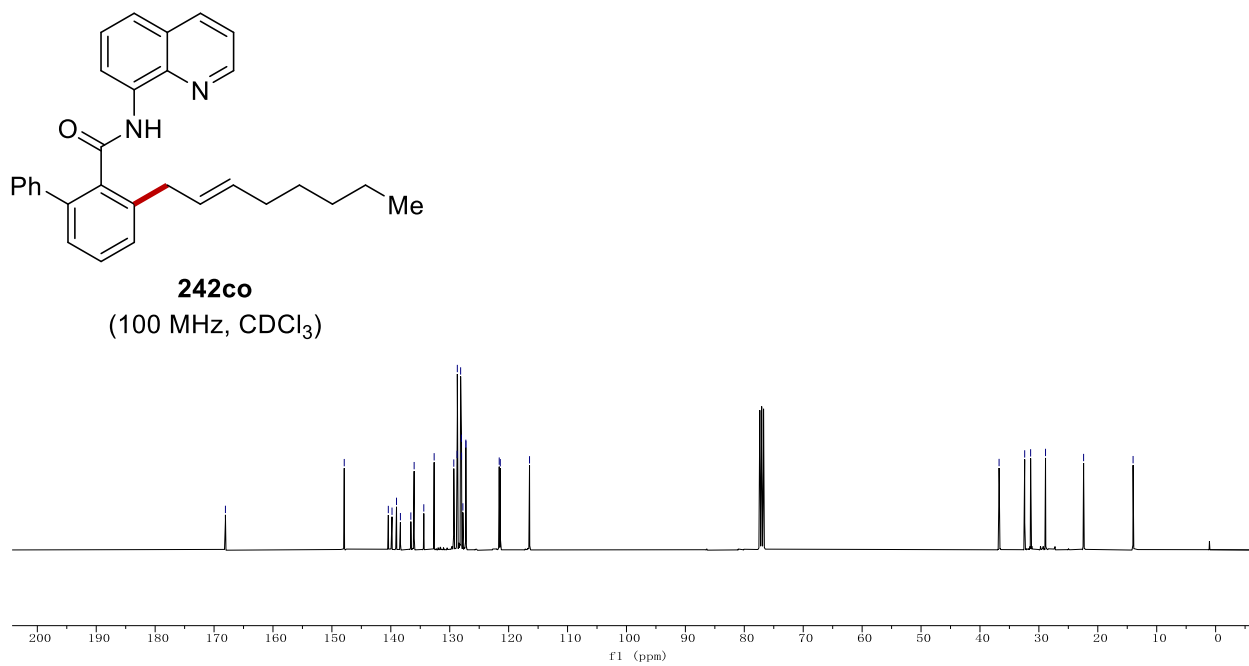
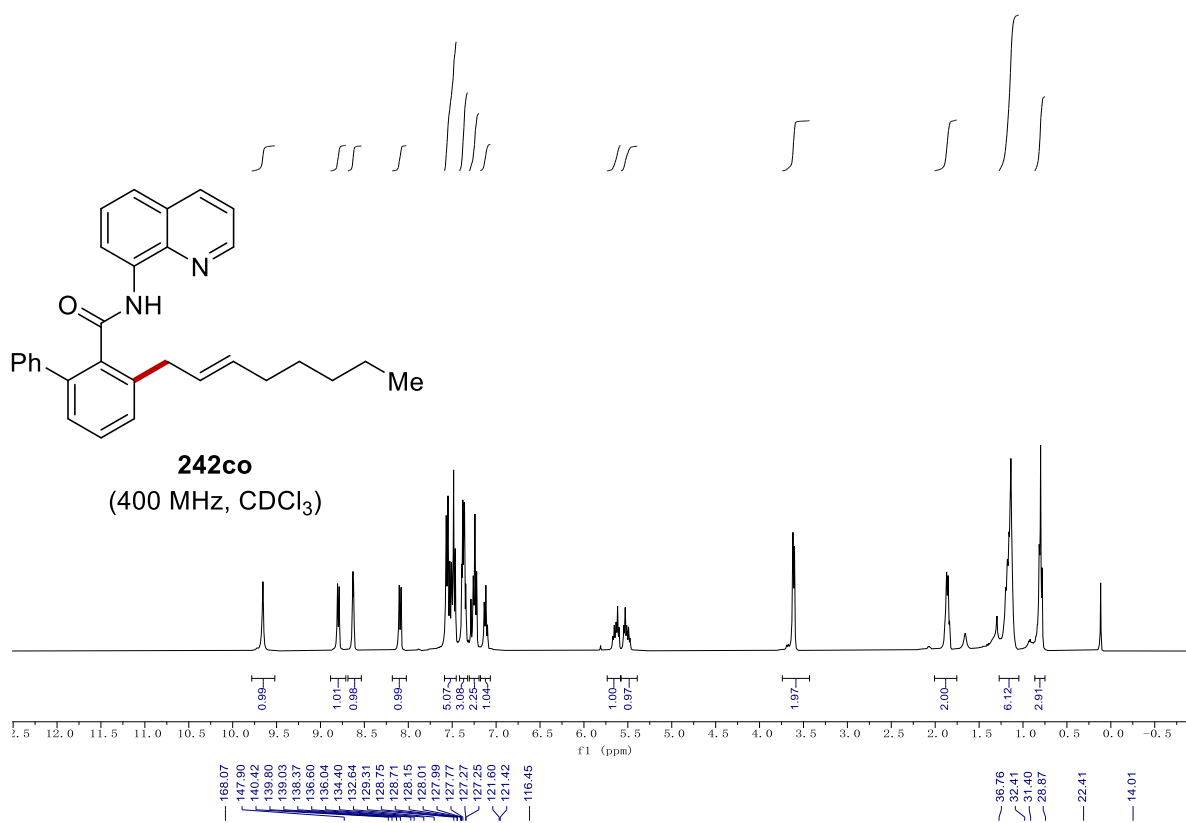


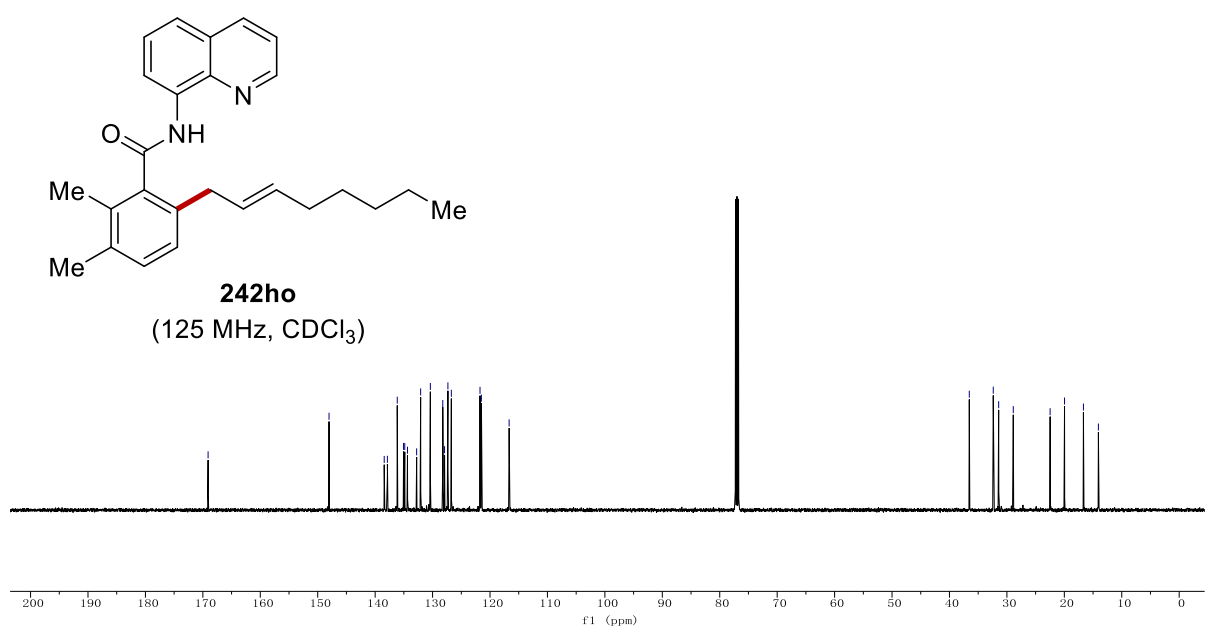
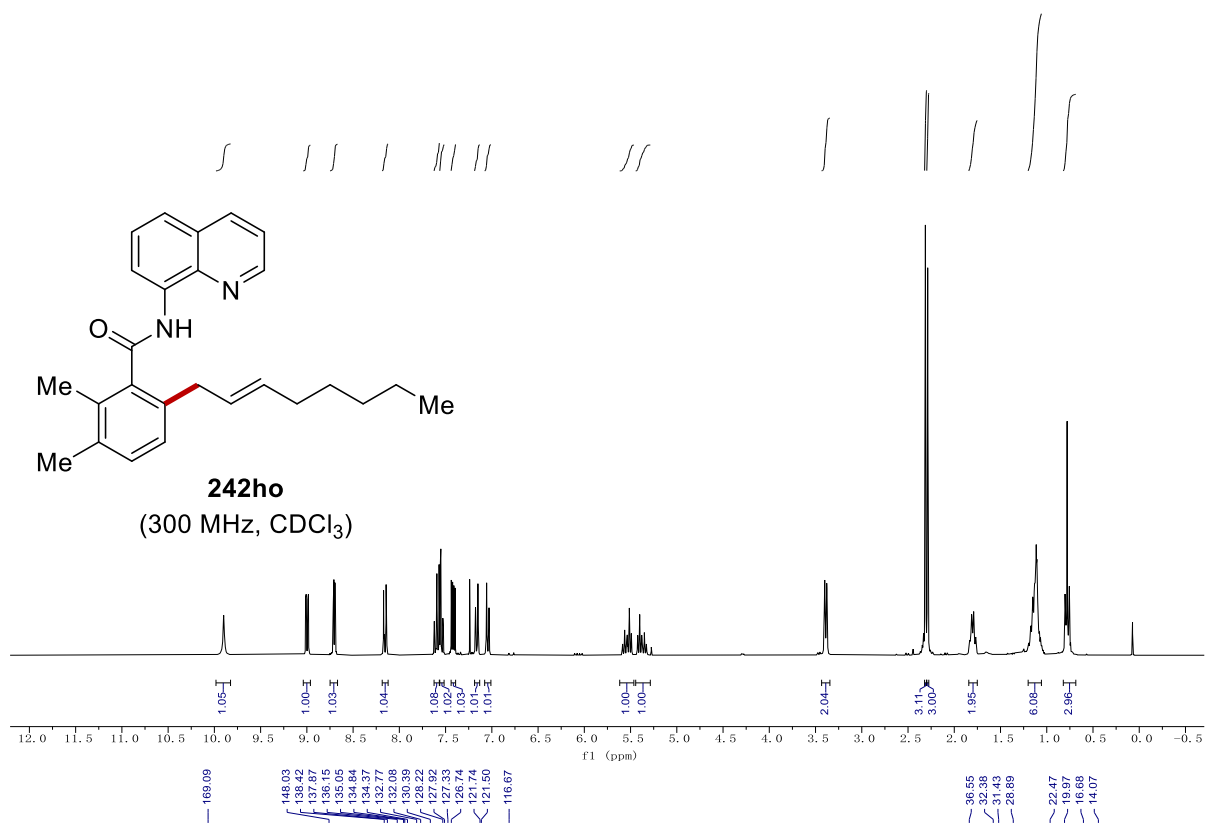


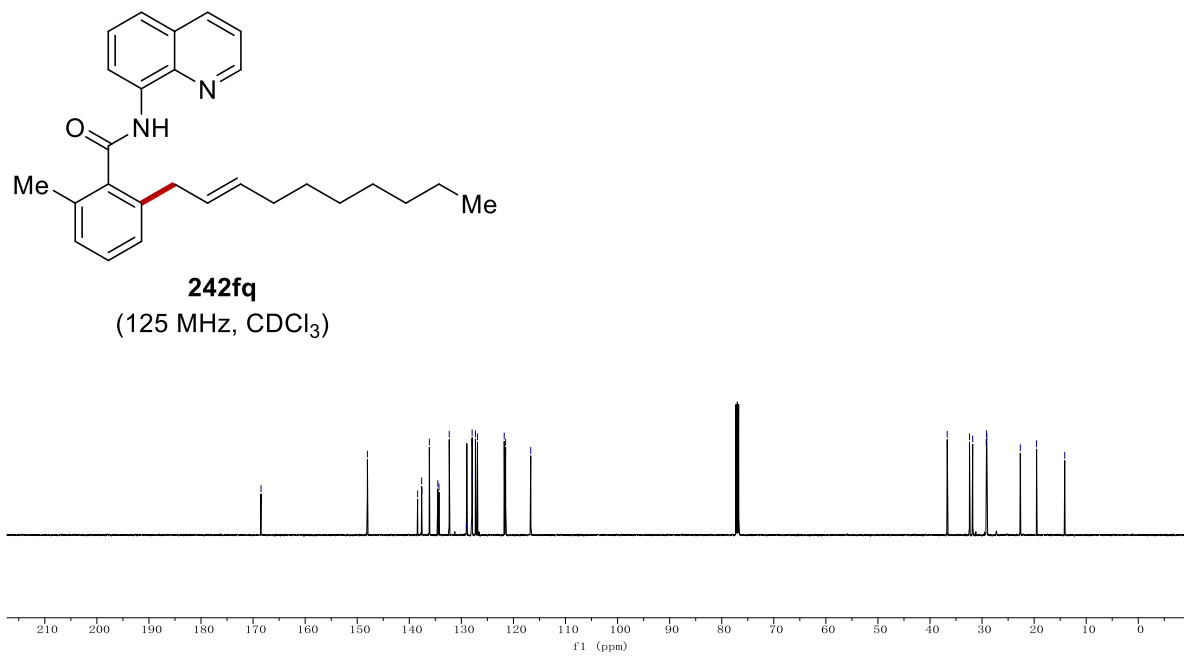
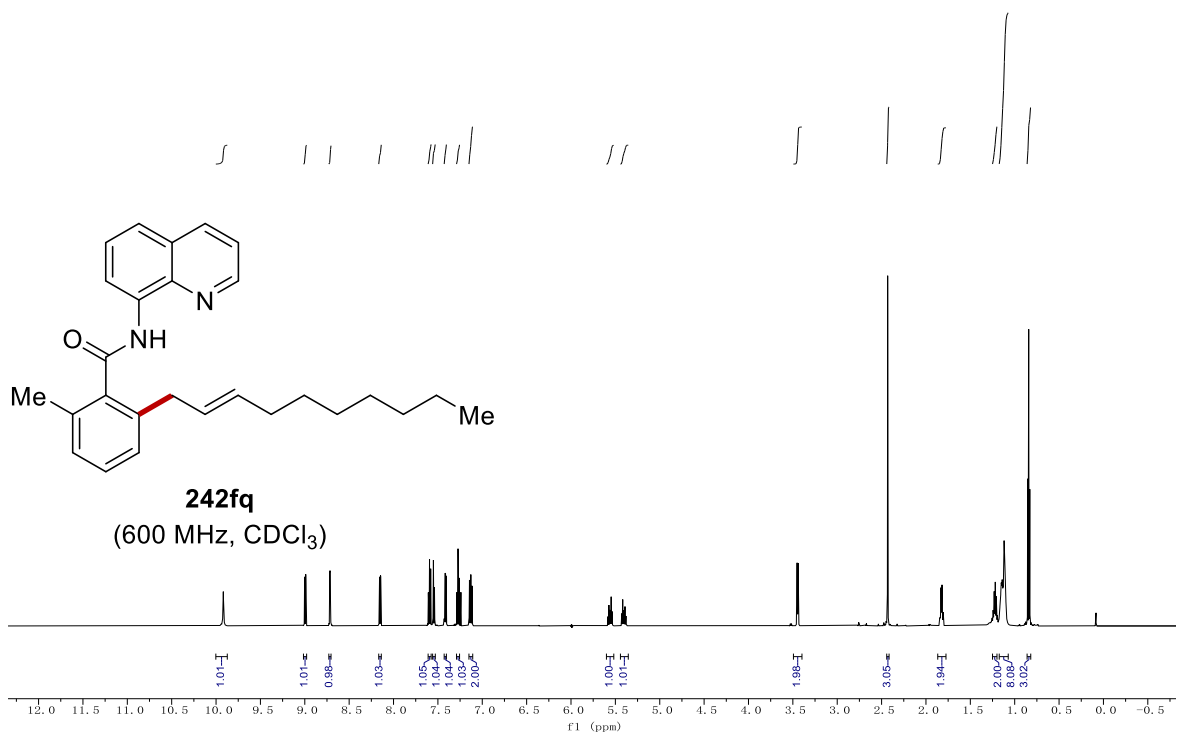


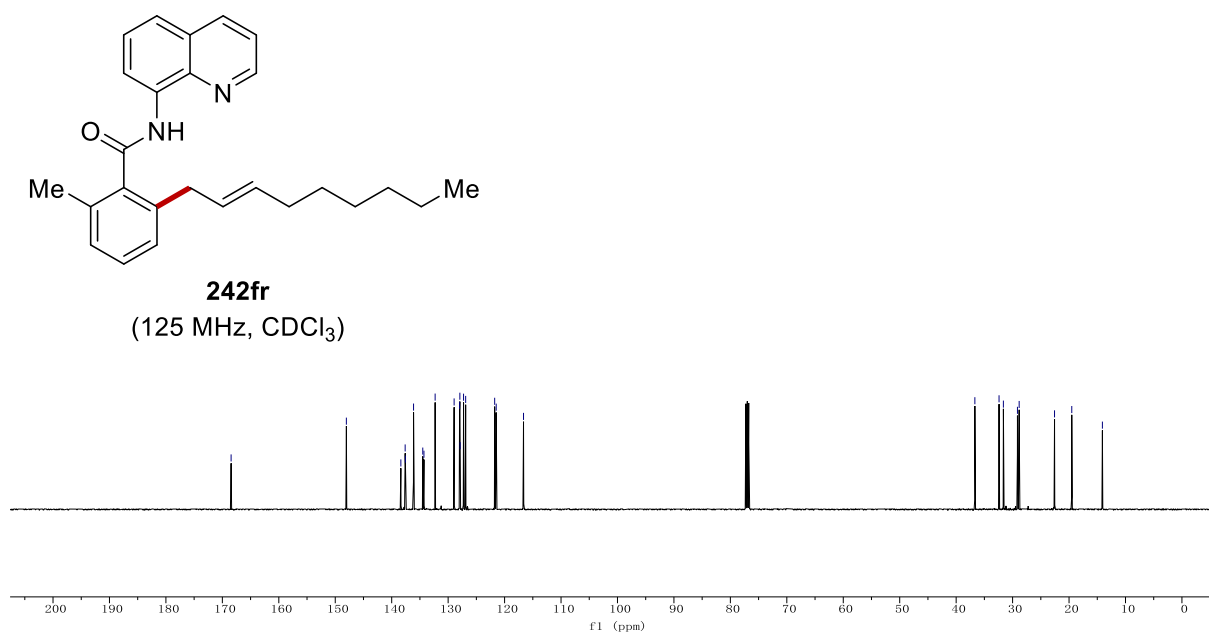
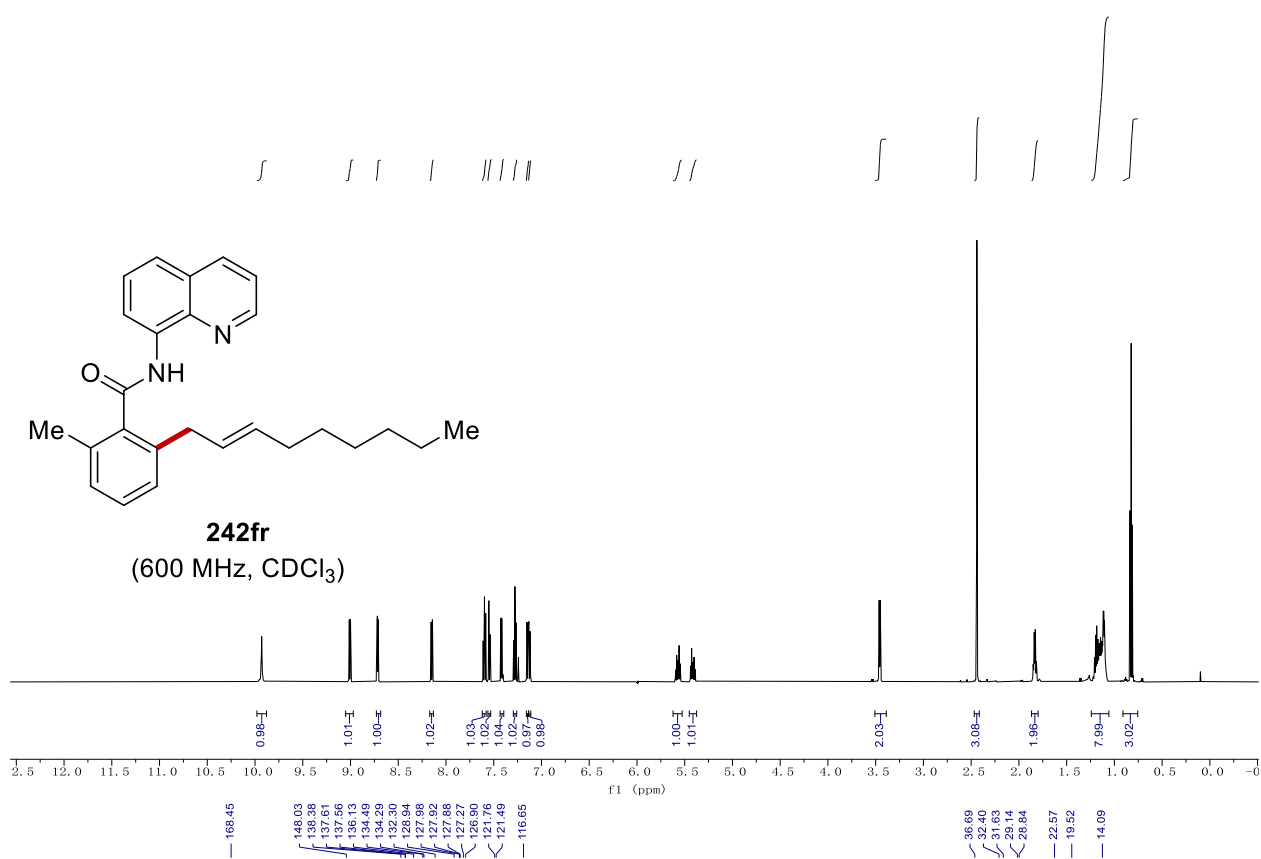
242go
(375 MHz, CDCl₃)

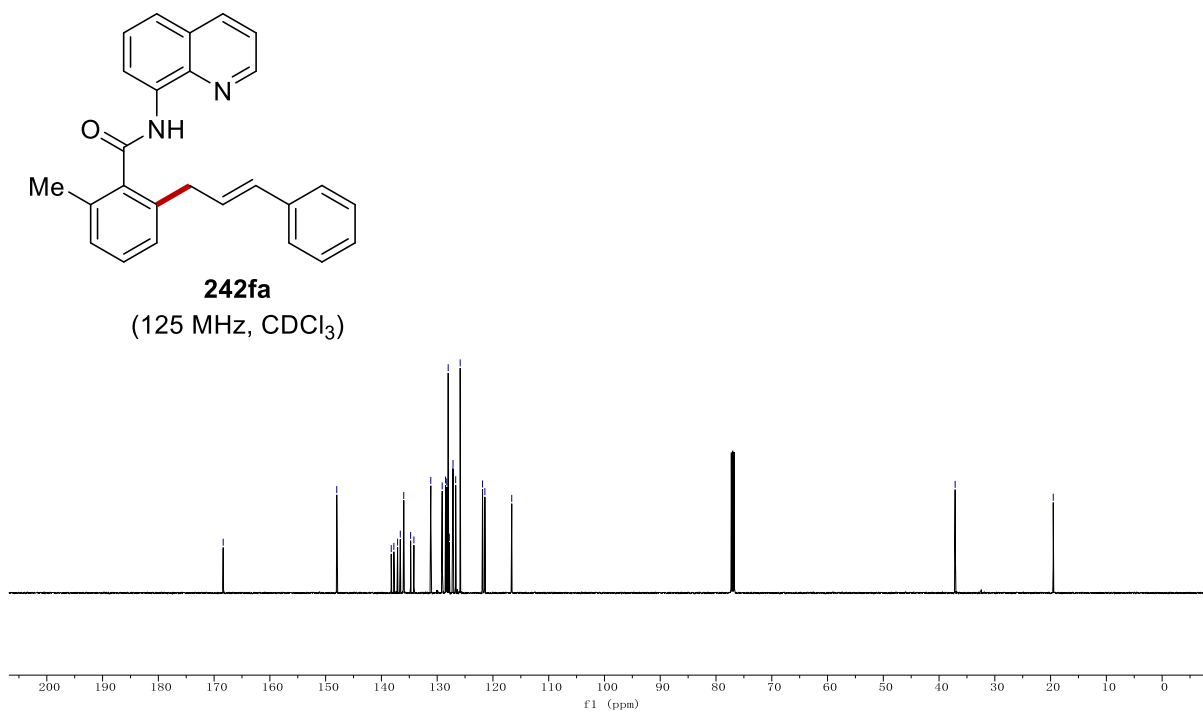
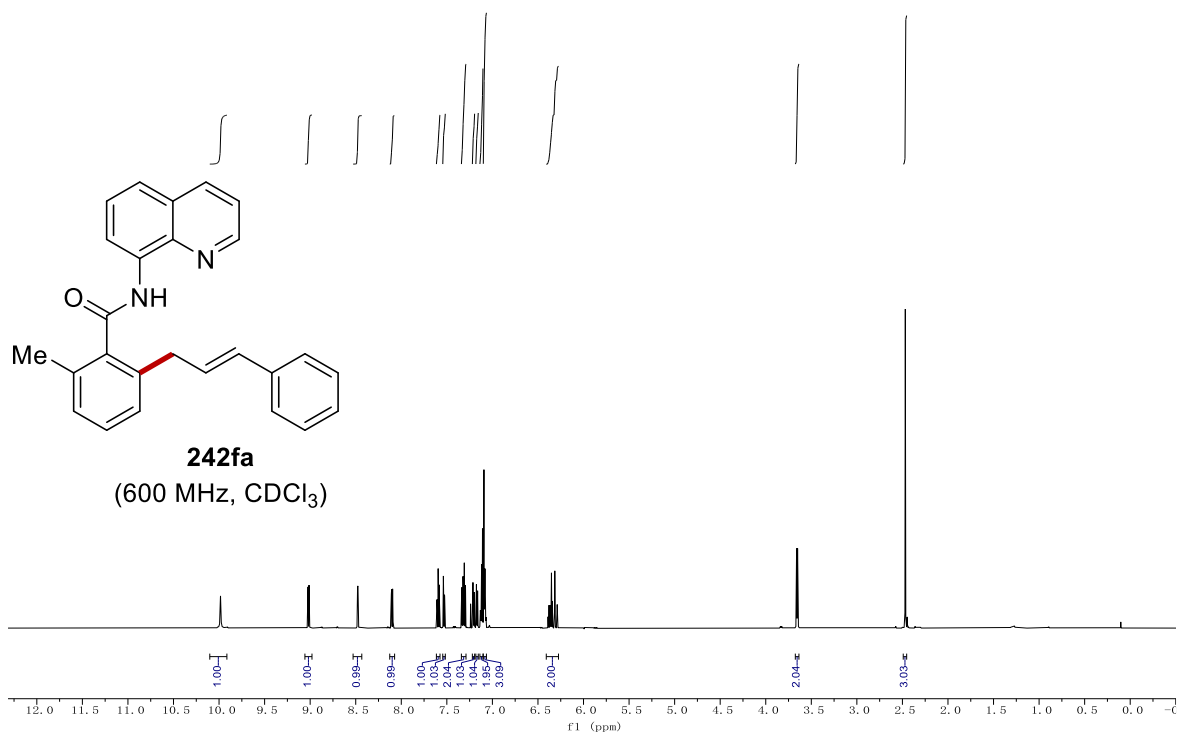


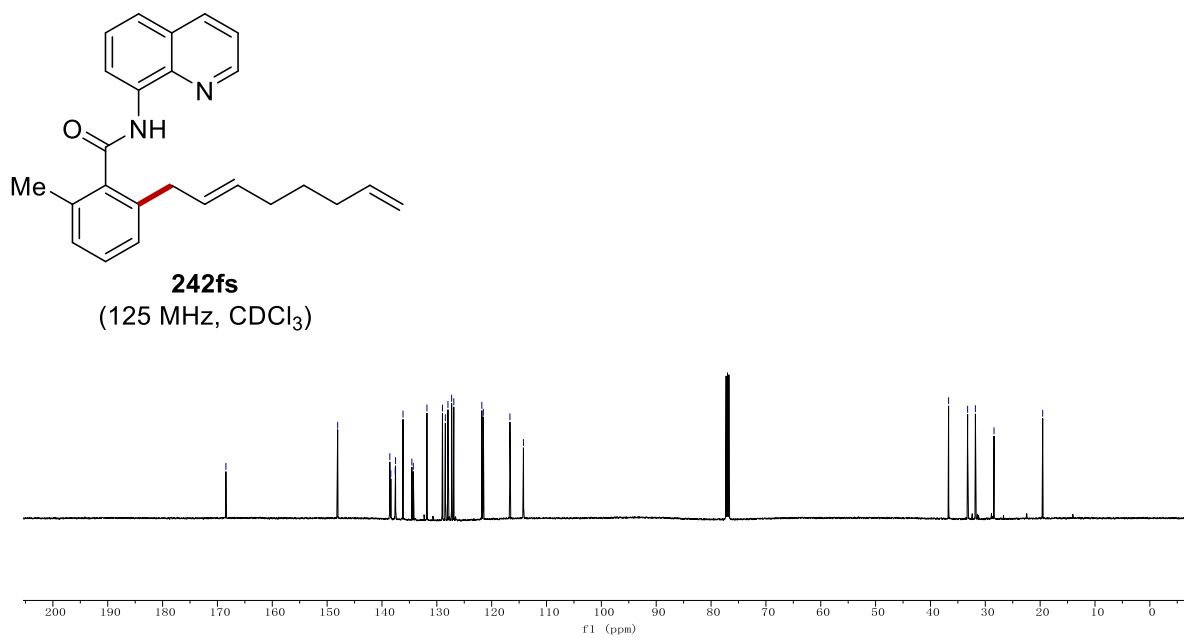
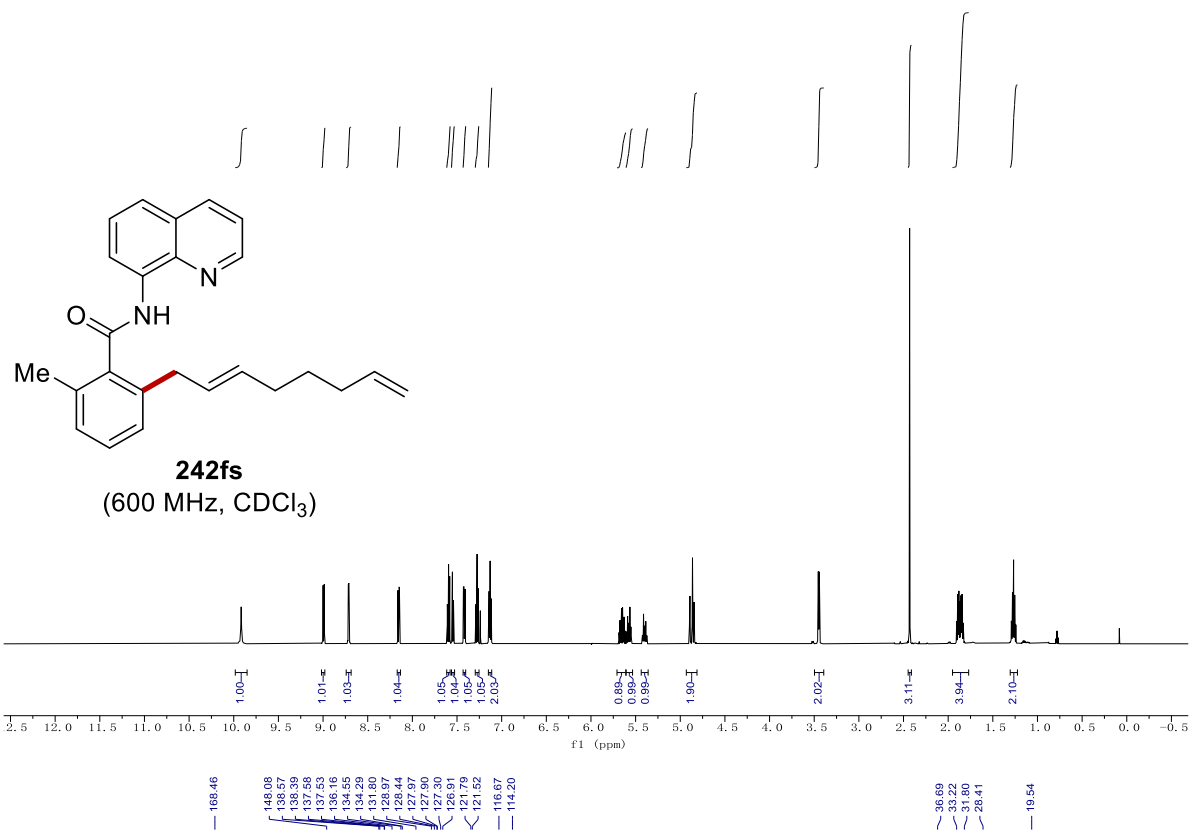


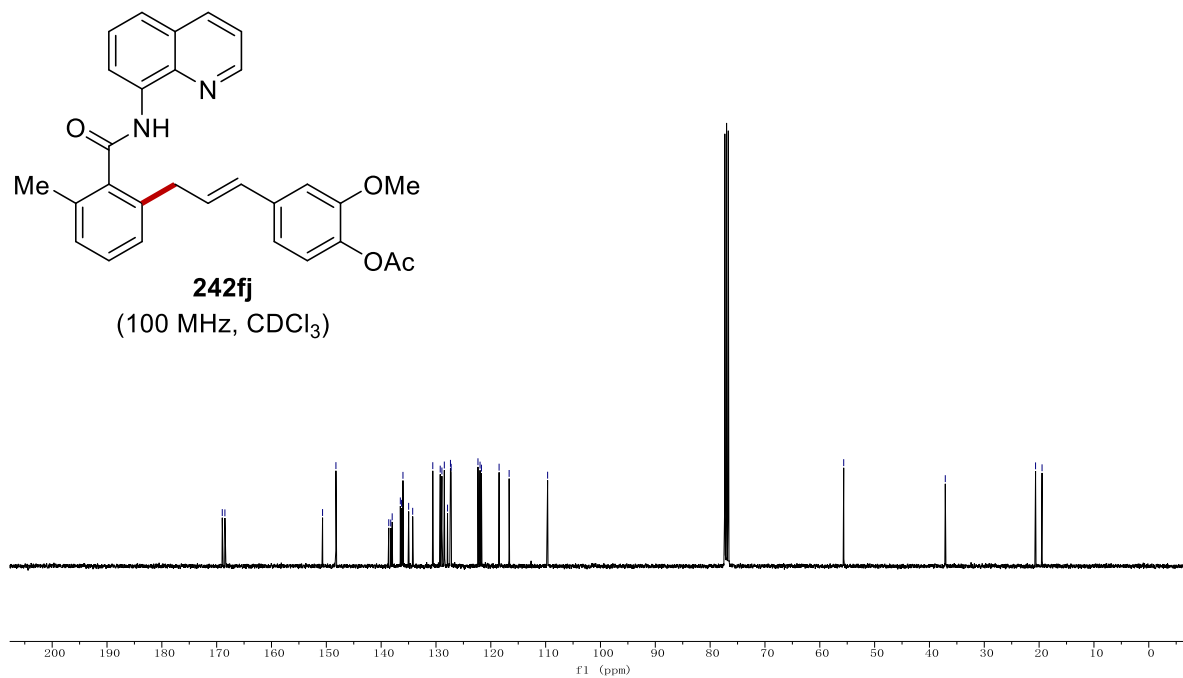
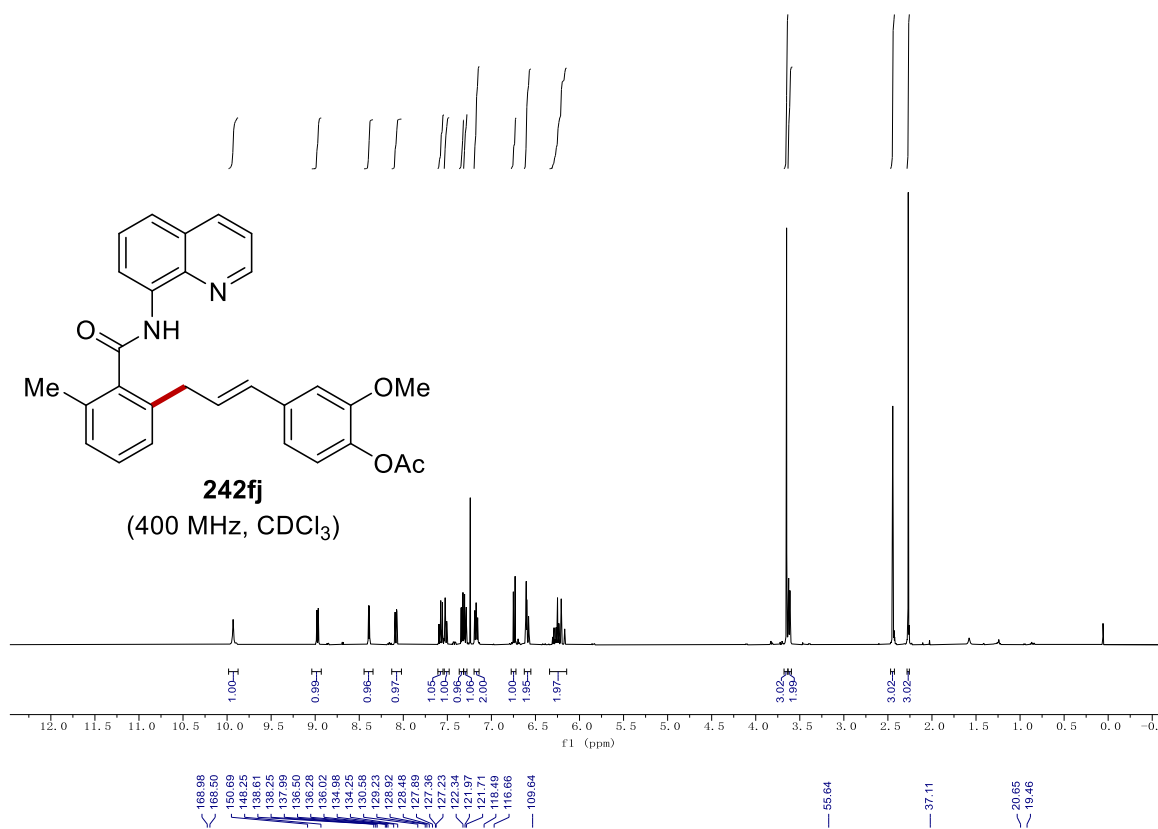


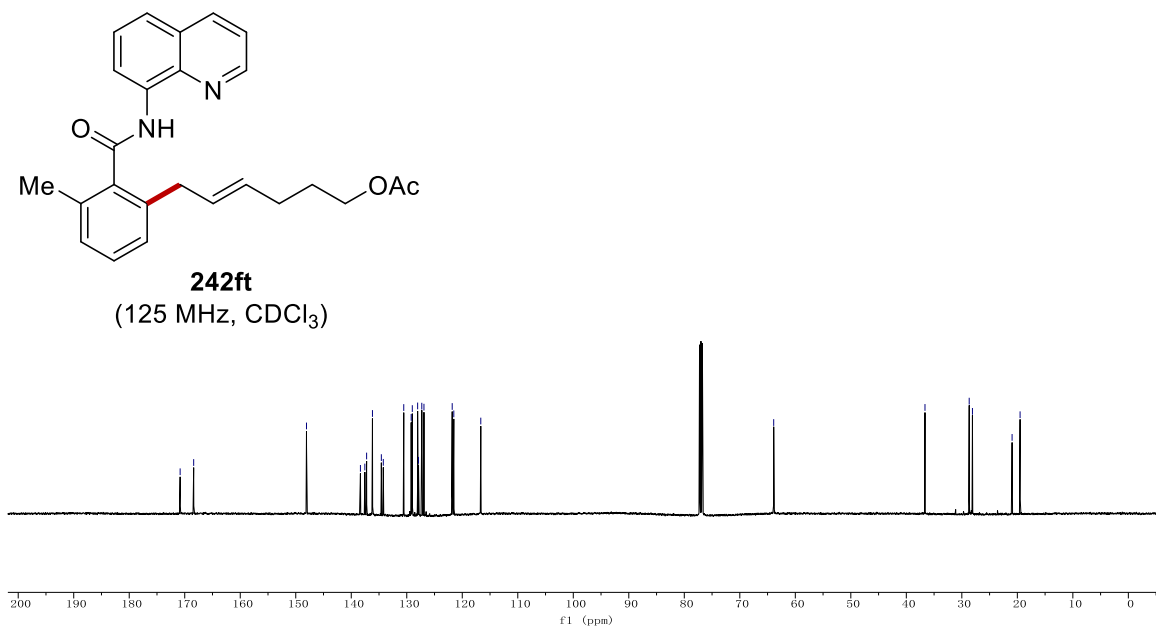
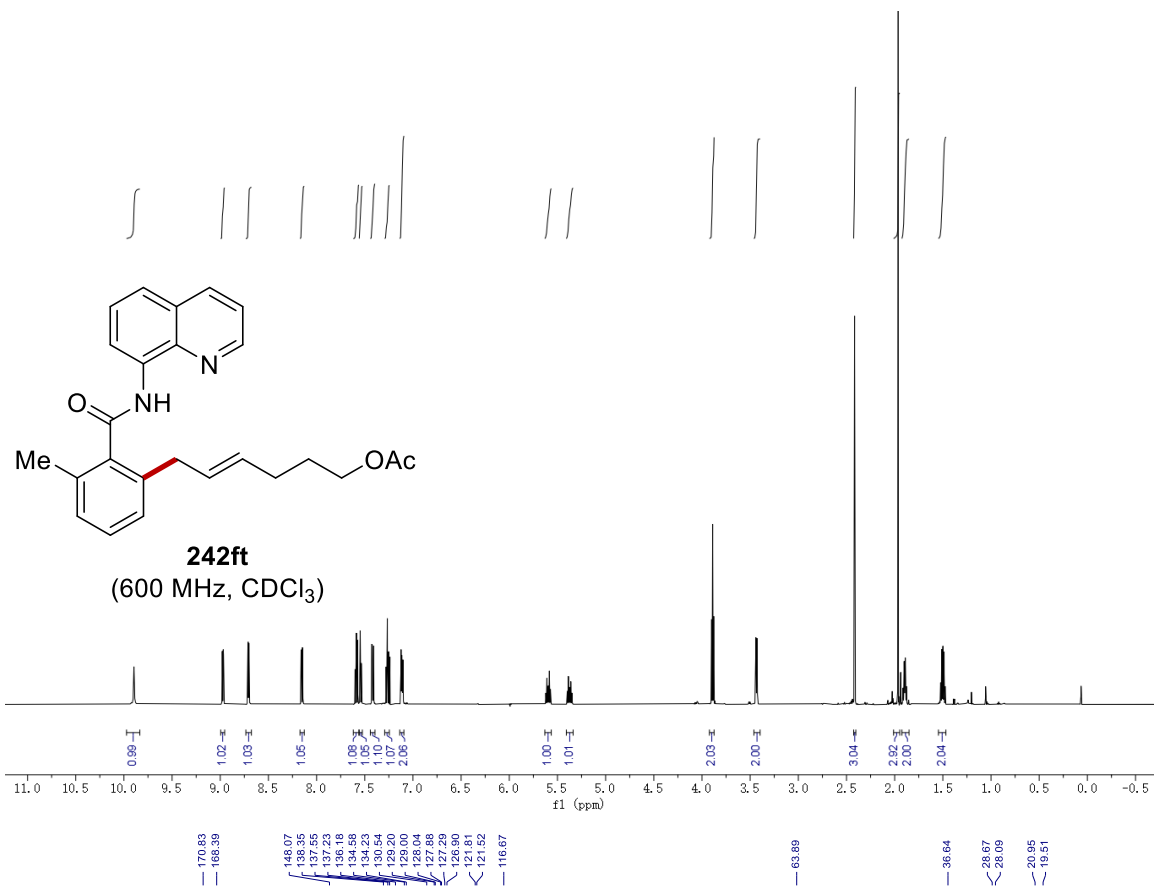


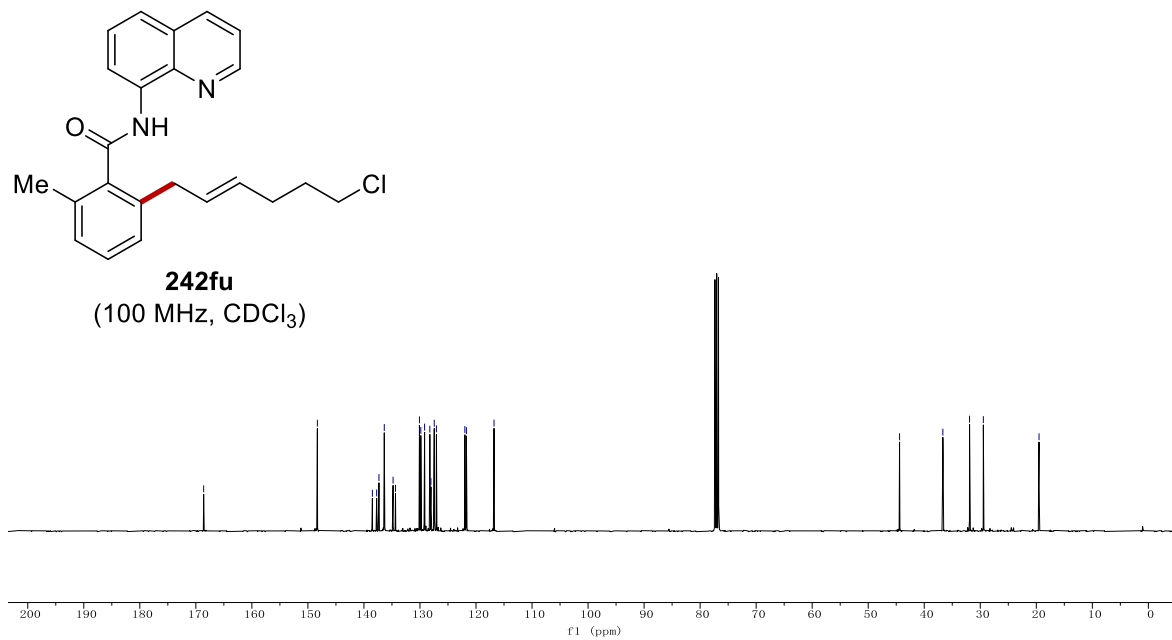
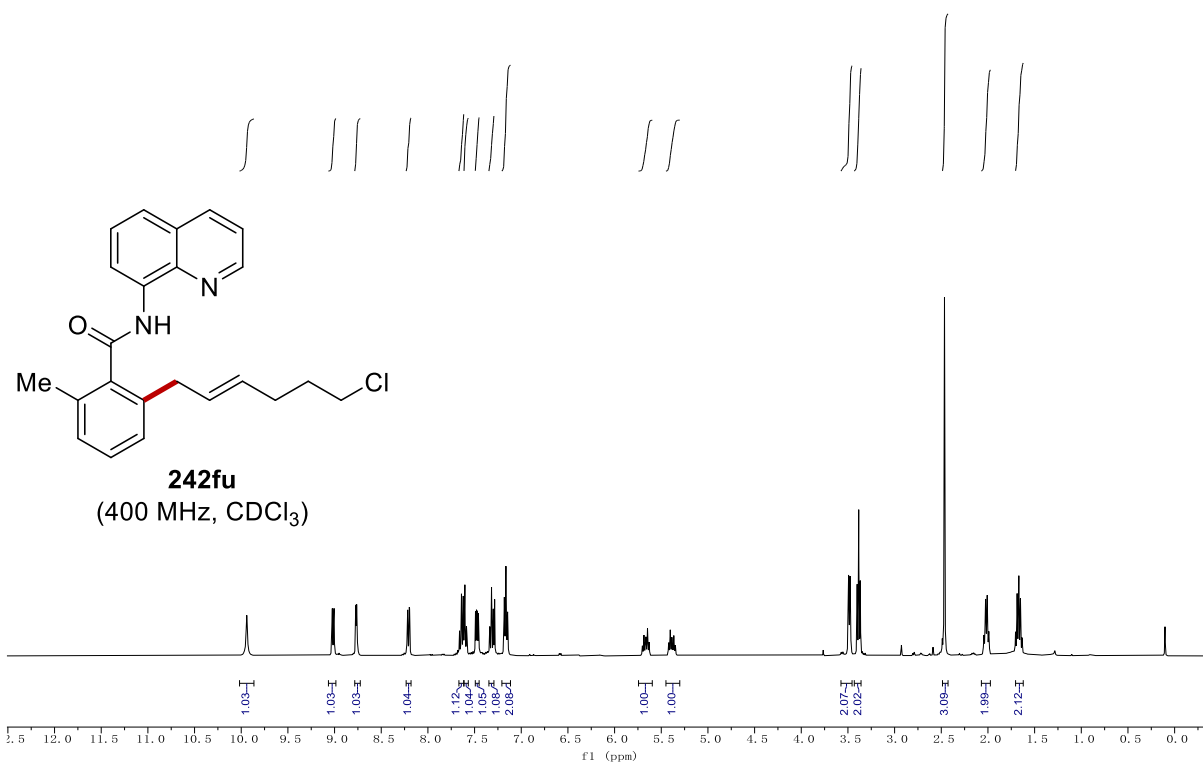


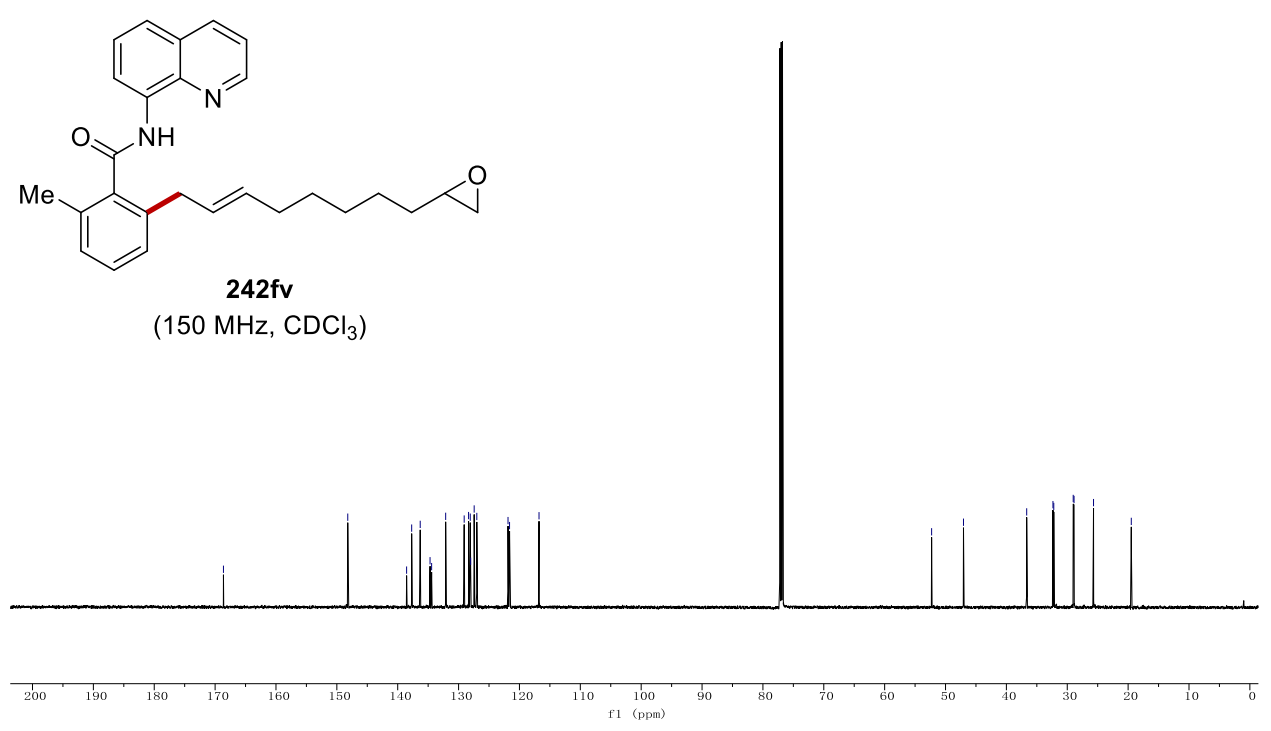
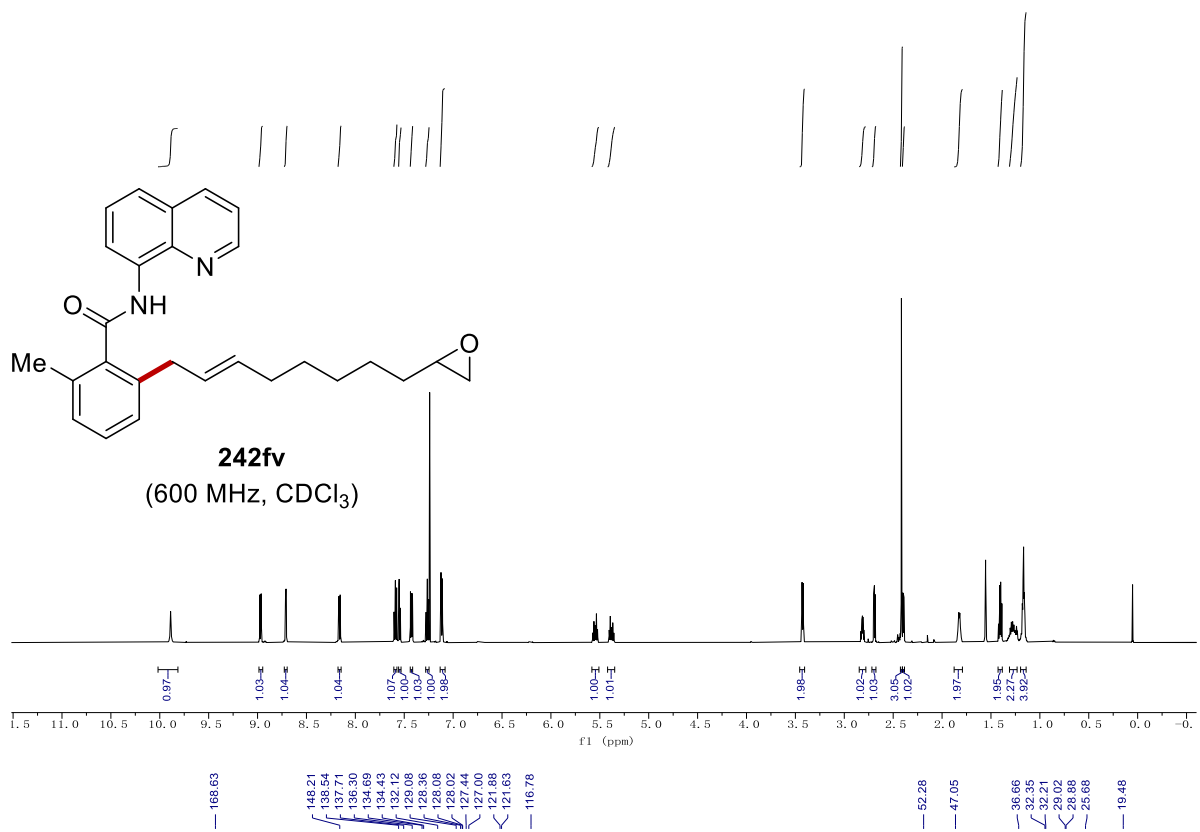


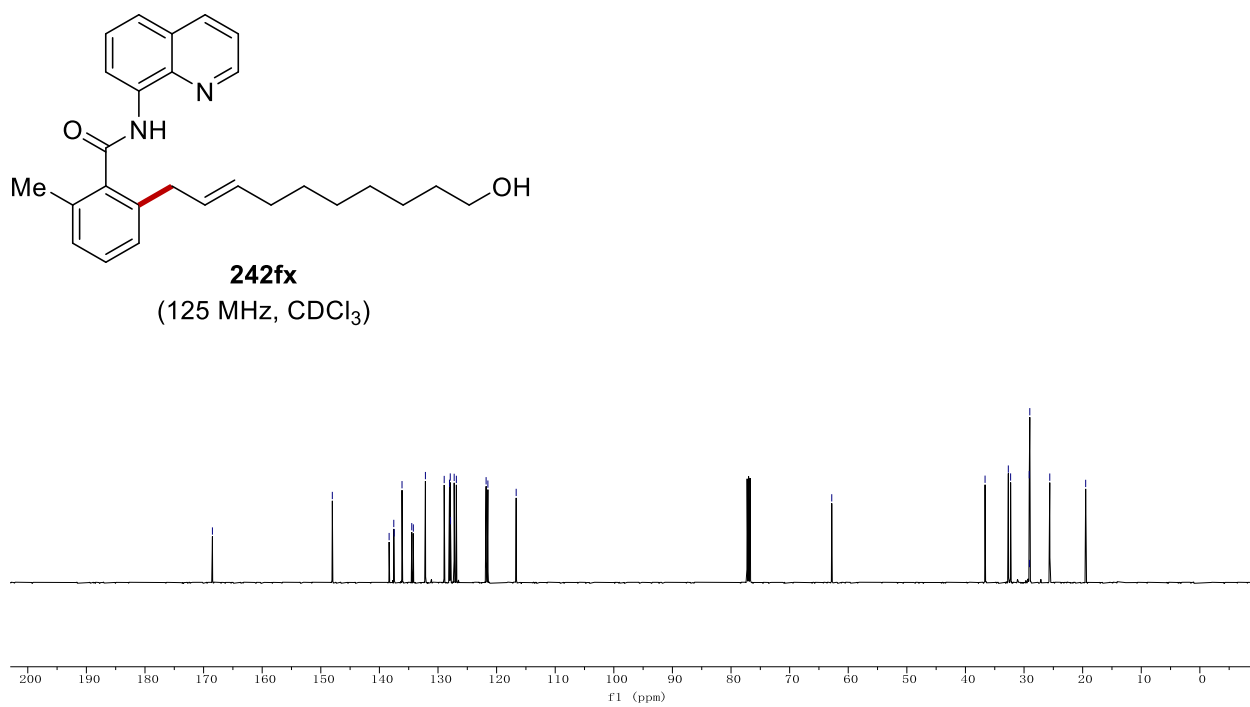
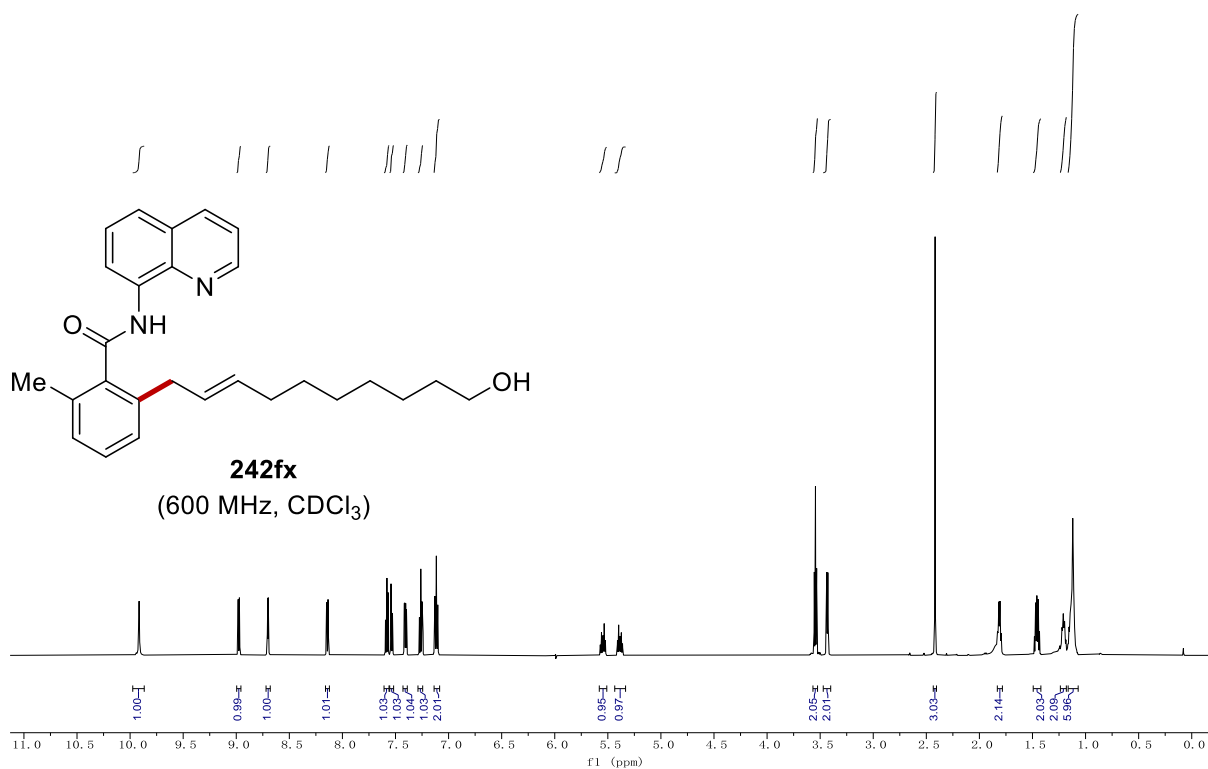


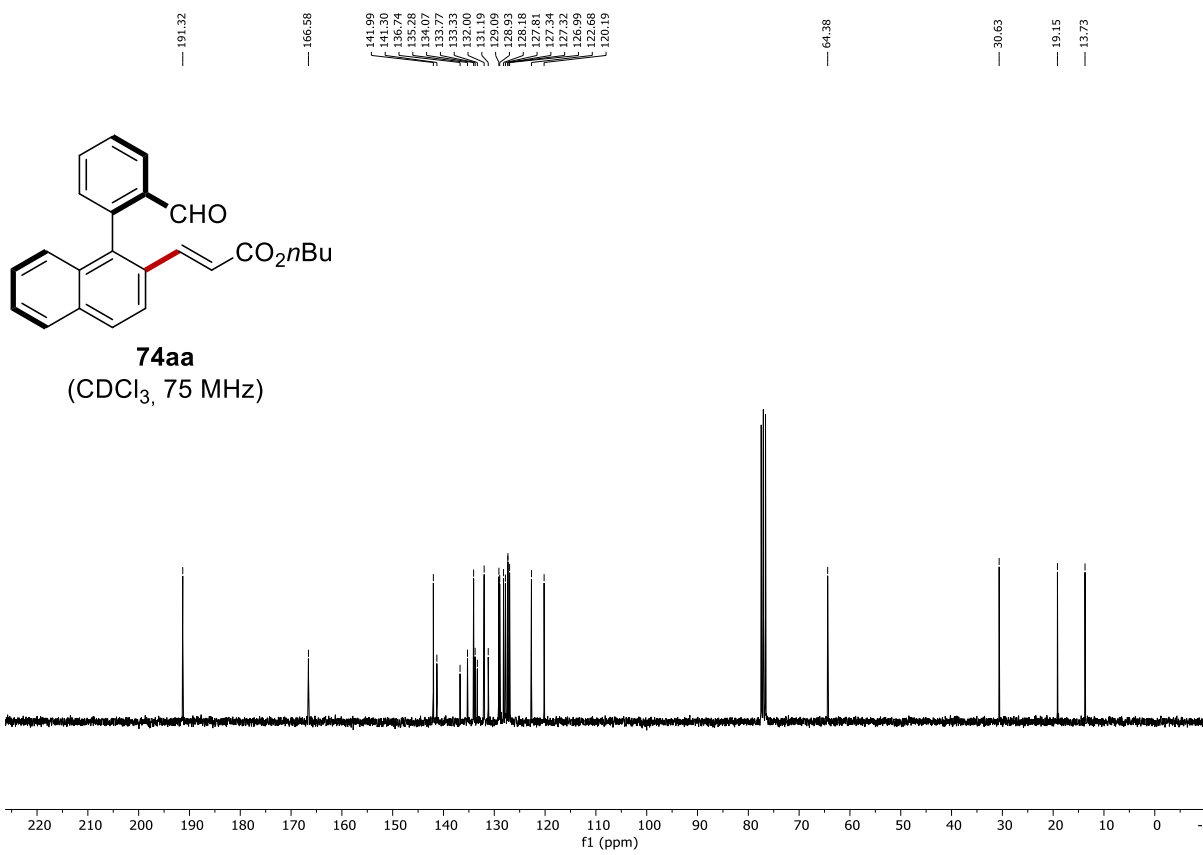
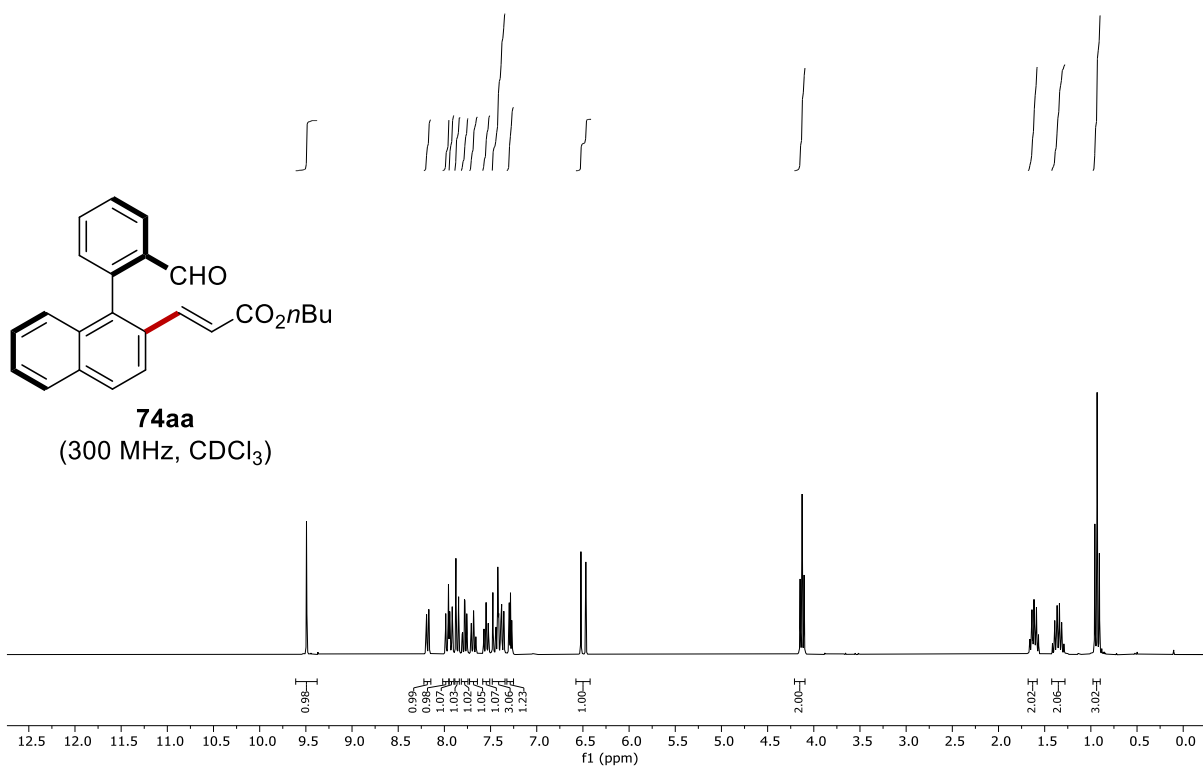




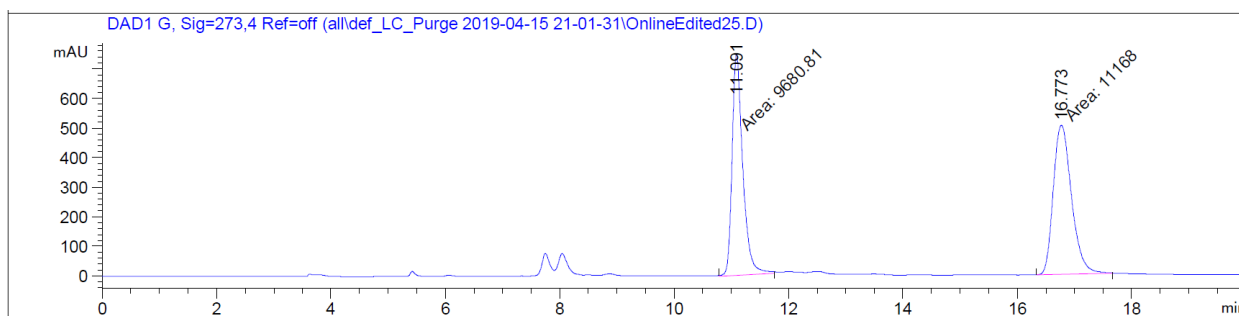




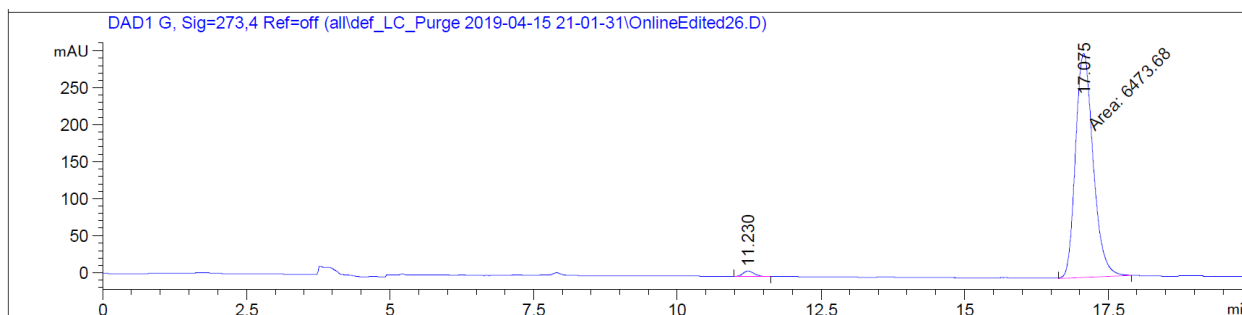




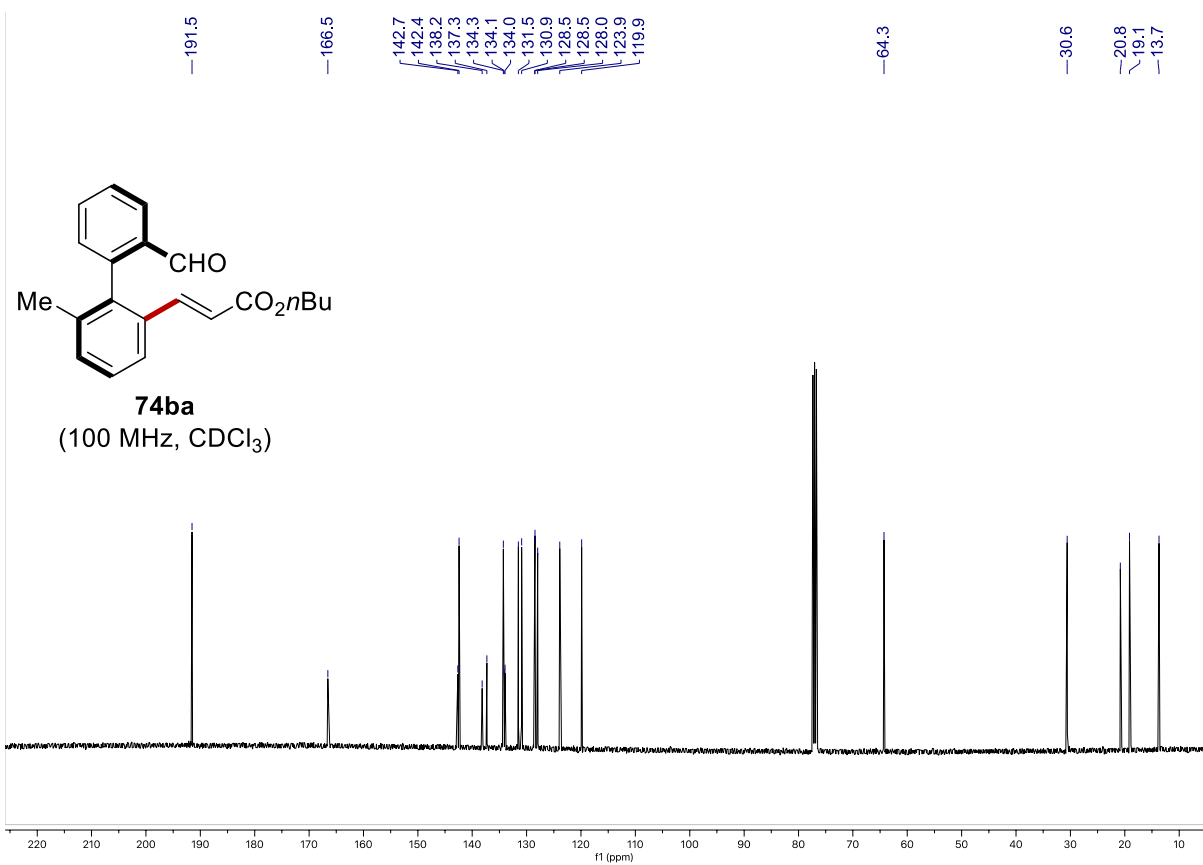
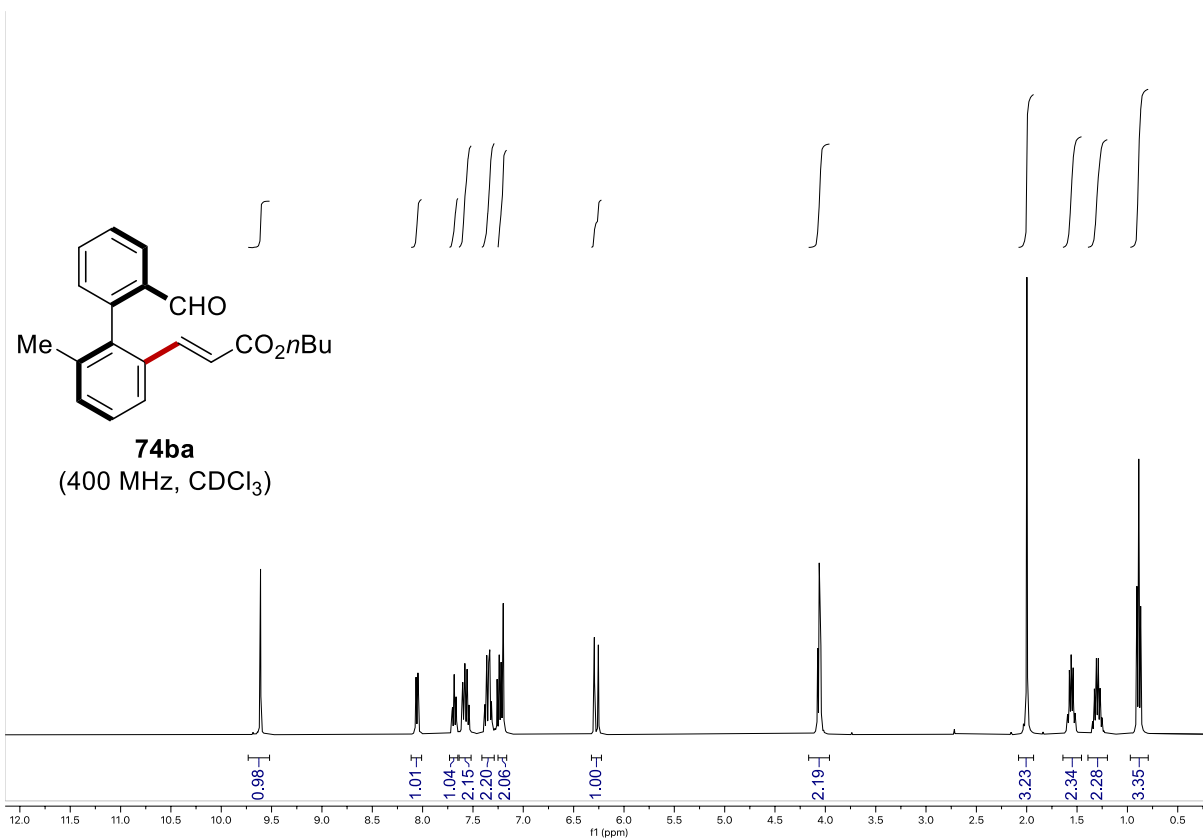
Chiral HPLC of 74aa:



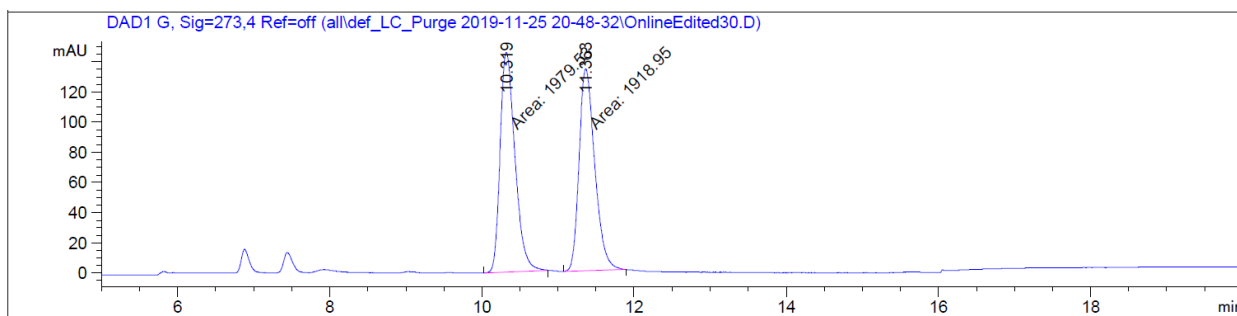
Peak #	RetTime [min]	Type	Width [min]	Area [mAU*s]	Height [mAU]	Area %
1	11.091	MM	0.2156	9680.80762	748.30676	46.4335
2	16.773	MM	0.3693	1.11680e4	503.97537	53.5665



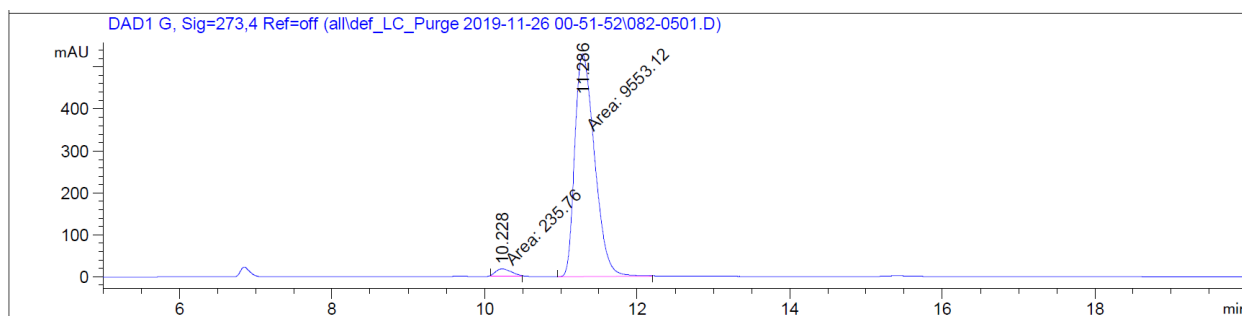
Peak #	RetTime [min]	Type	Width [min]	Area [mAU*s]	Height [mAU]	Area %
1	11.230	BB	0.2030	97.61672	7.20635	1.4855
2	17.075	MM	0.3564	6473.67969	302.74637	98.5145



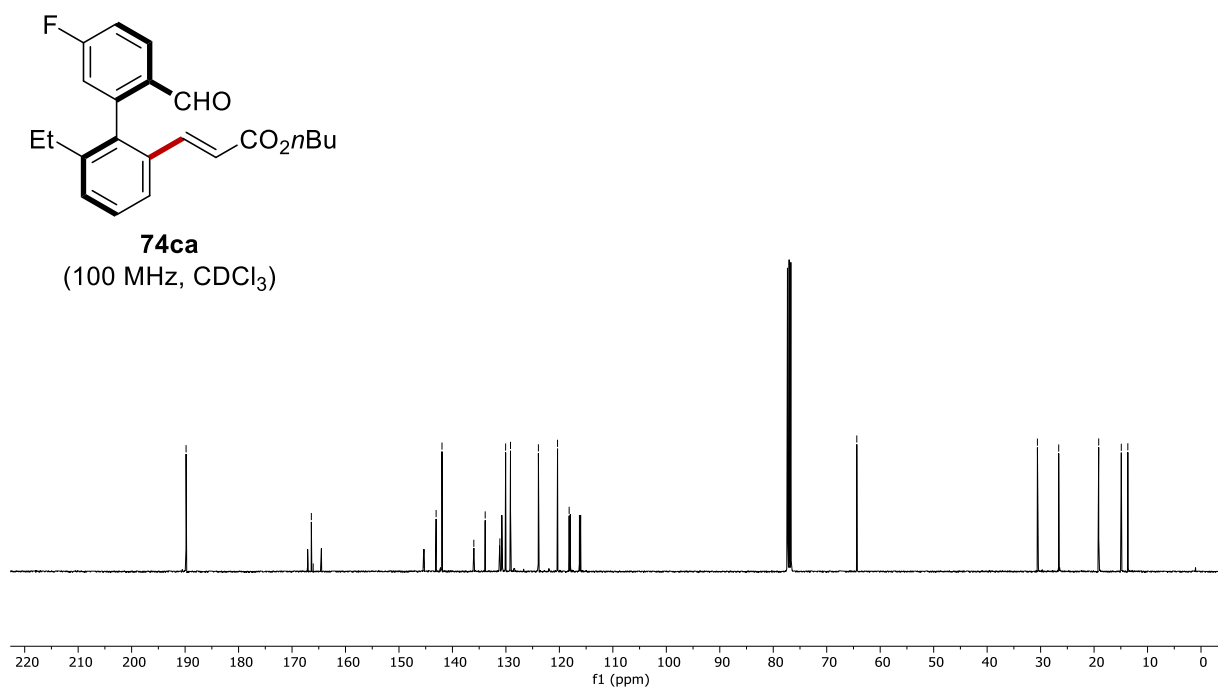
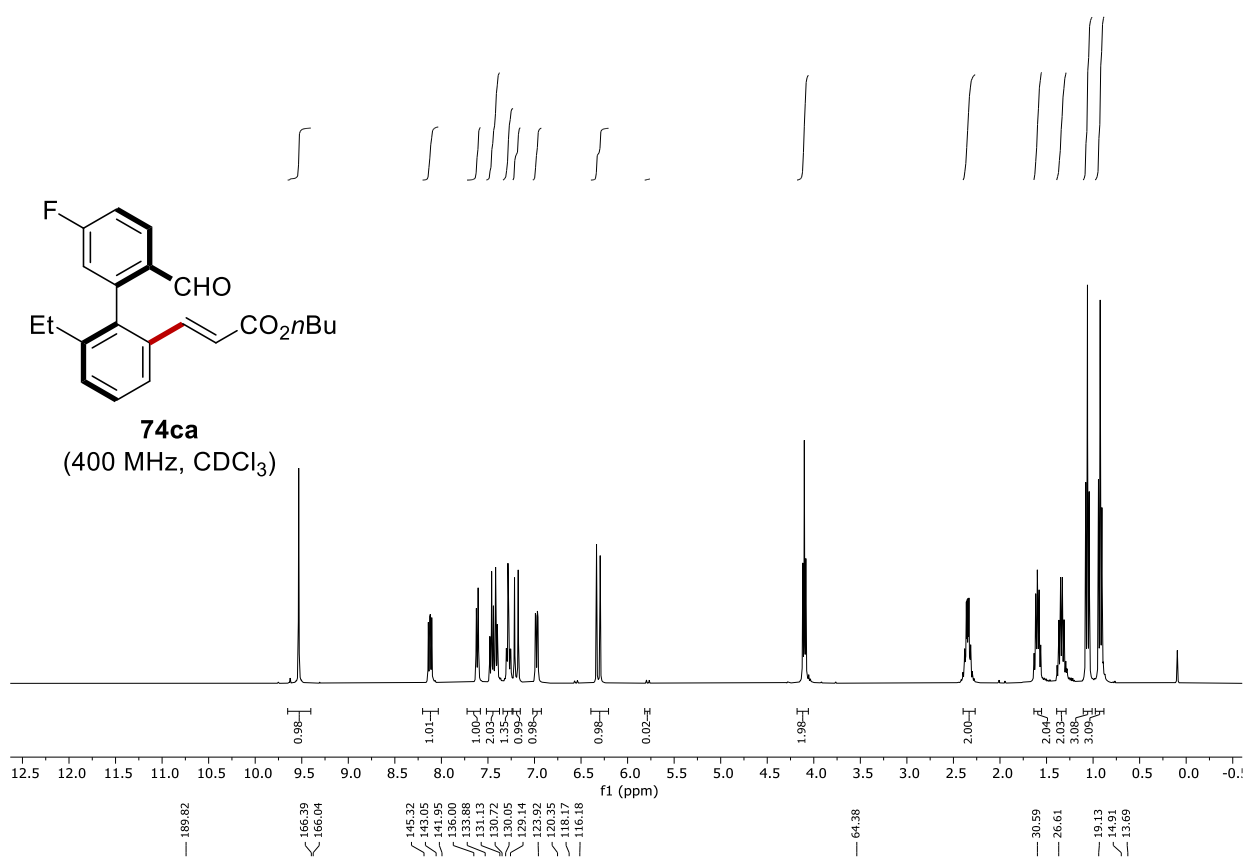
Chiral HPLC of **74ba**:

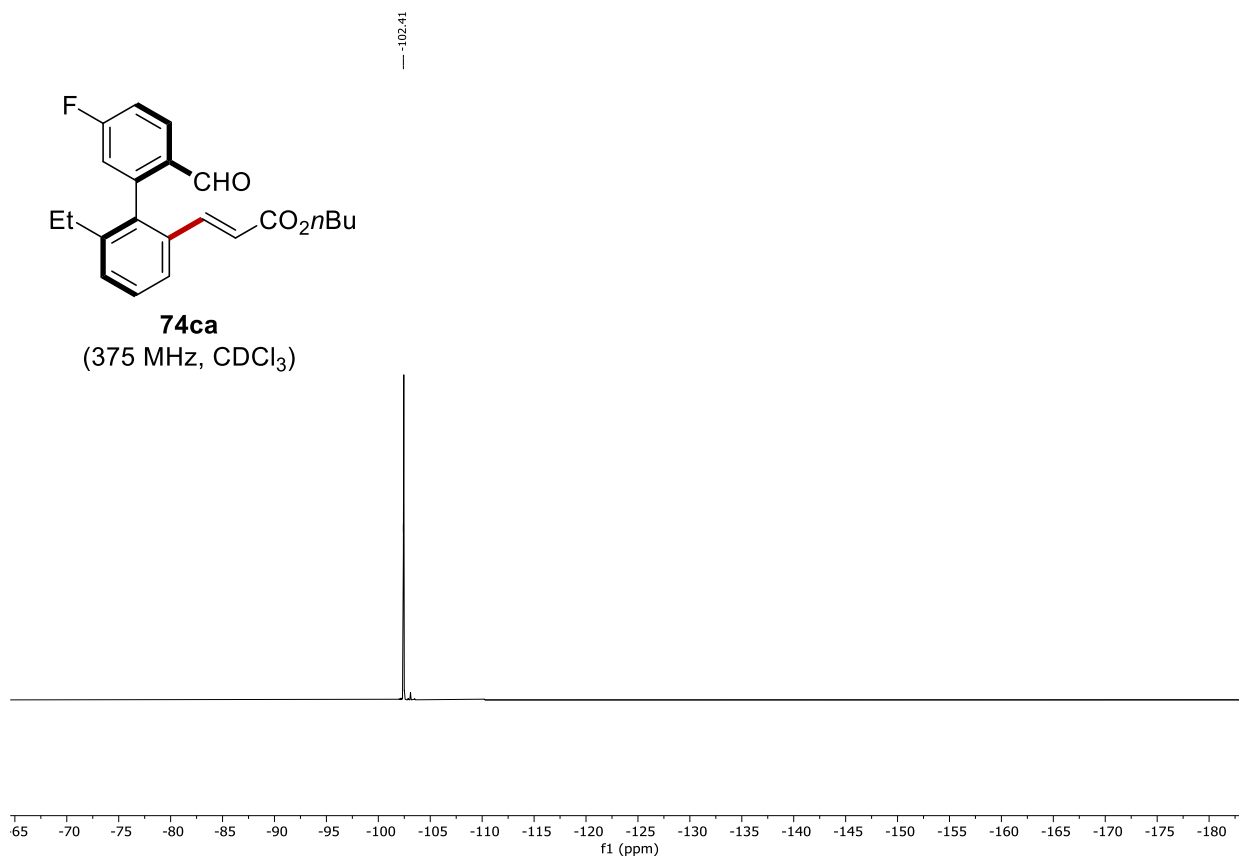


Peak #	RetTime [min]	Type	Width [min]	Area [mAU*s]	Height [mAU]	Area %
1	10.319	MM	0.2265	1979.53455	145.64331	50.7770
2	11.363	MM	0.2386	1918.94910	134.01500	49.2230

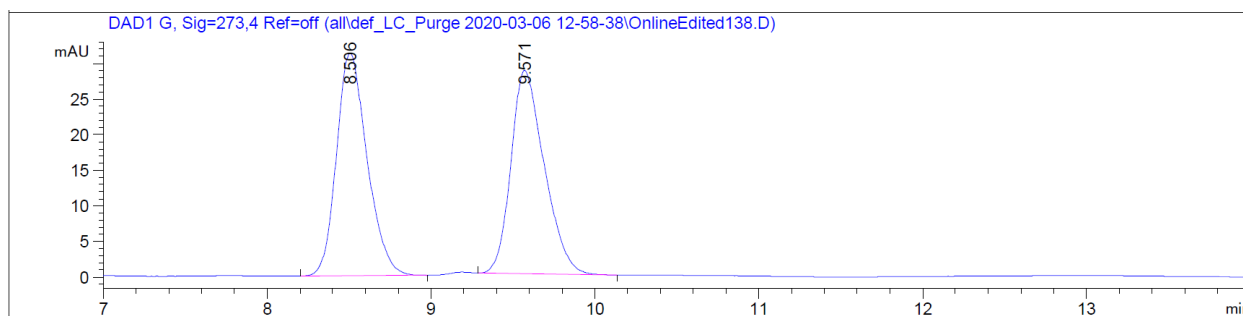


Peak #	RetTime [min]	Type	Width [min]	Area [mAU*s]	Height [mAU]	Area %
1	10.228	MM	0.2335	235.76041	16.82926	2.4085
2	11.286	MM	0.2997	9553.11816	531.20819	97.5915

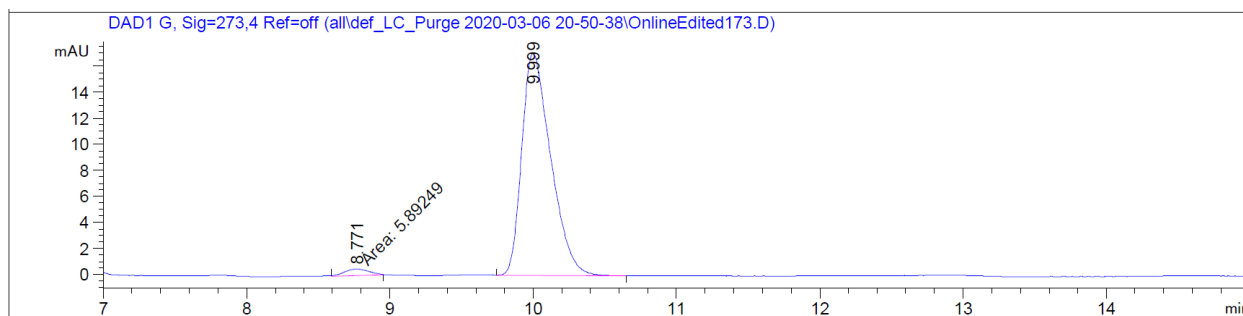




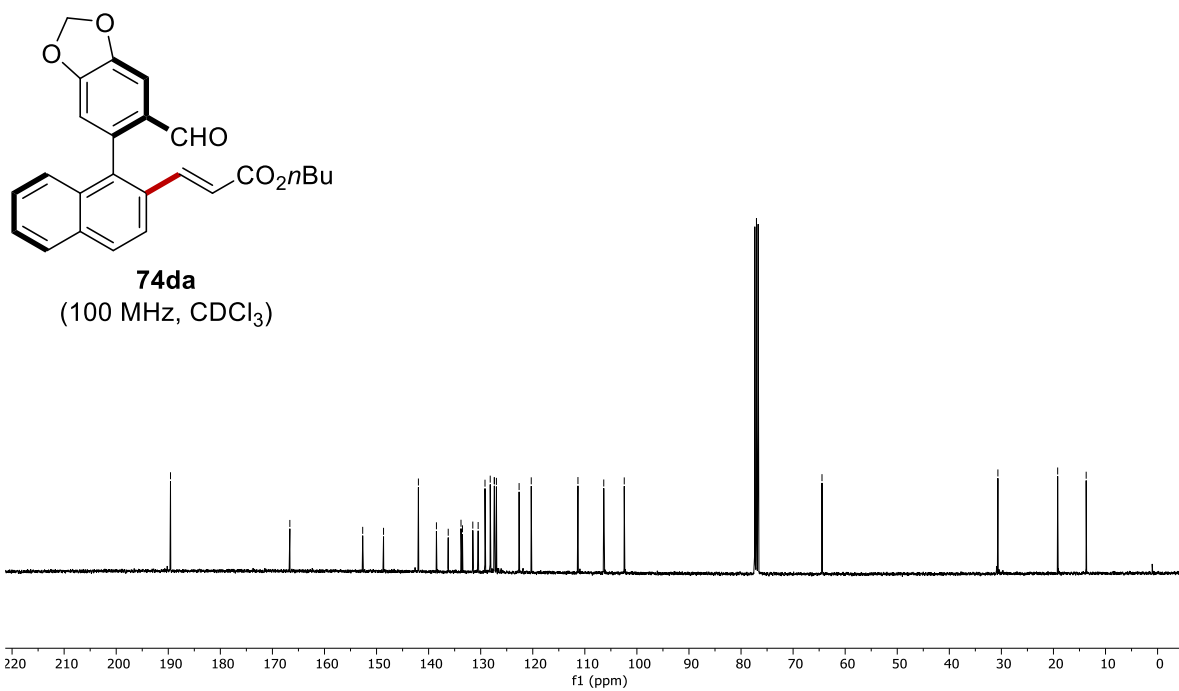
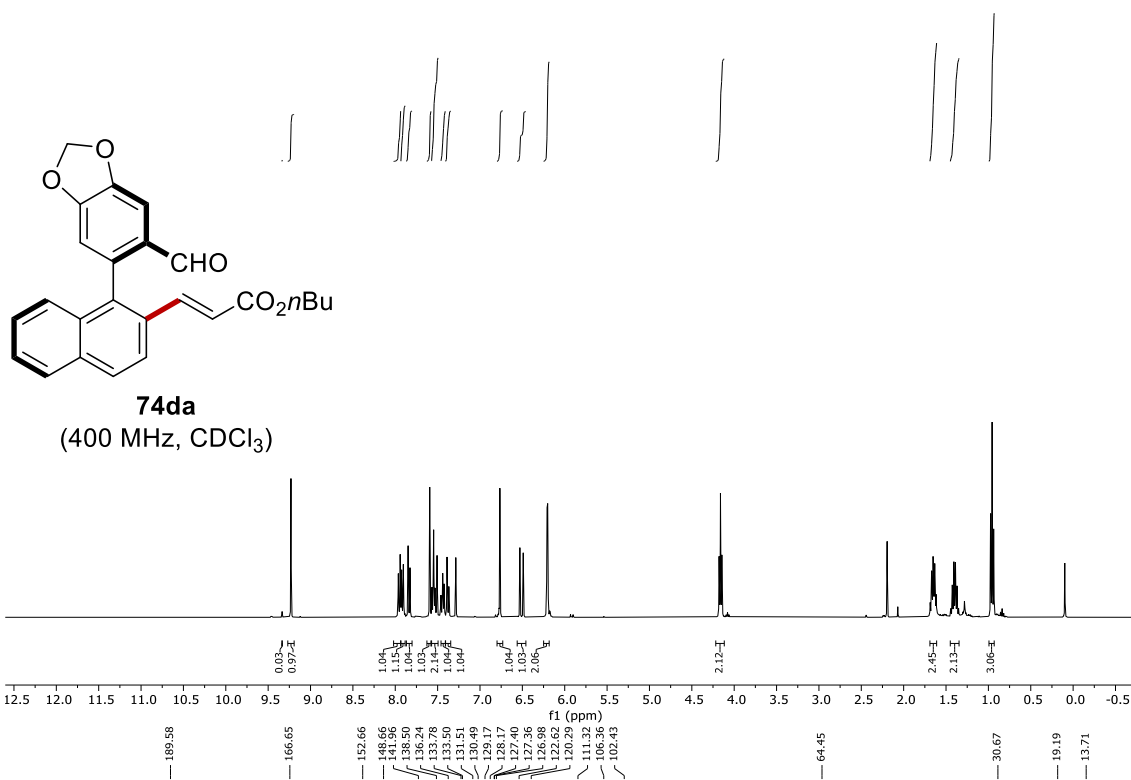
Chiral HPLC of 74ca:



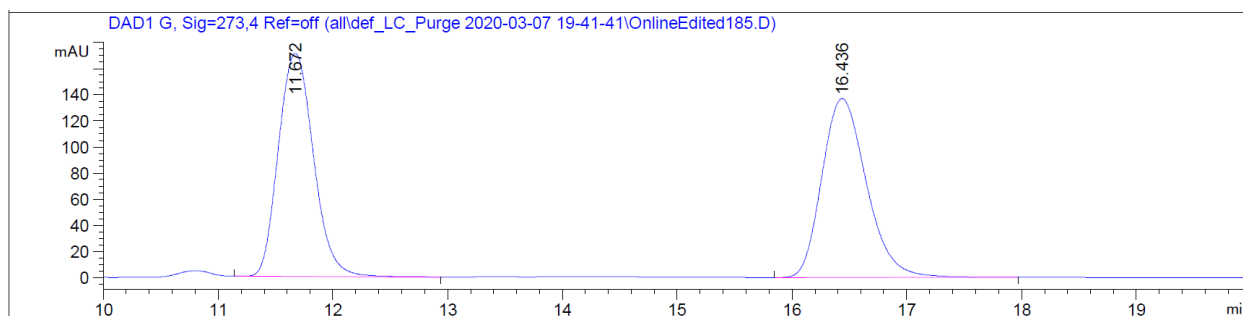
Peak #	RetTime [min]	Type	Width [min]	Area [mAU*s]	Height [mAU]	Area %
1	8.506	BB	0.1965	406.28516	31.27957	50.1652
2	9.571	BB	0.2089	403.60880	28.56208	49.8348



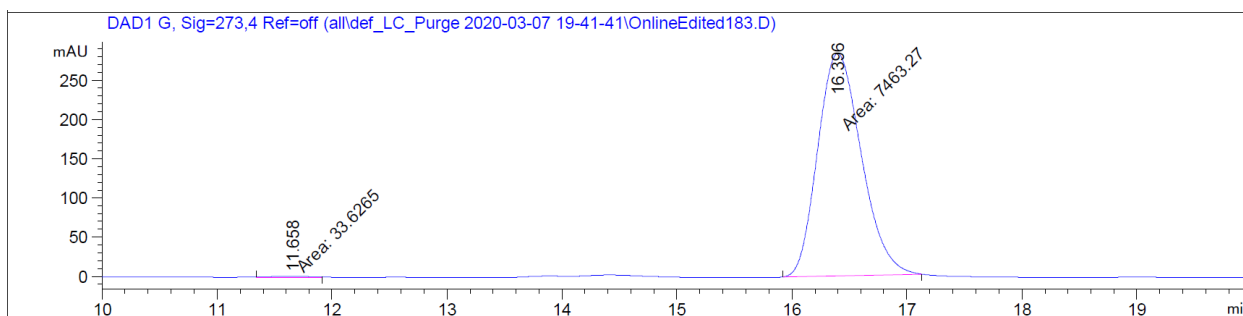
Peak #	RetTime [min]	Type	Width [min]	Area [mAU*s]	Height [mAU]	Area %
1	8.771	MM	0.1947	5.89249	5.04444e-1	2.3997
2	9.999	BB	0.2075	239.65521	17.09557	97.6003



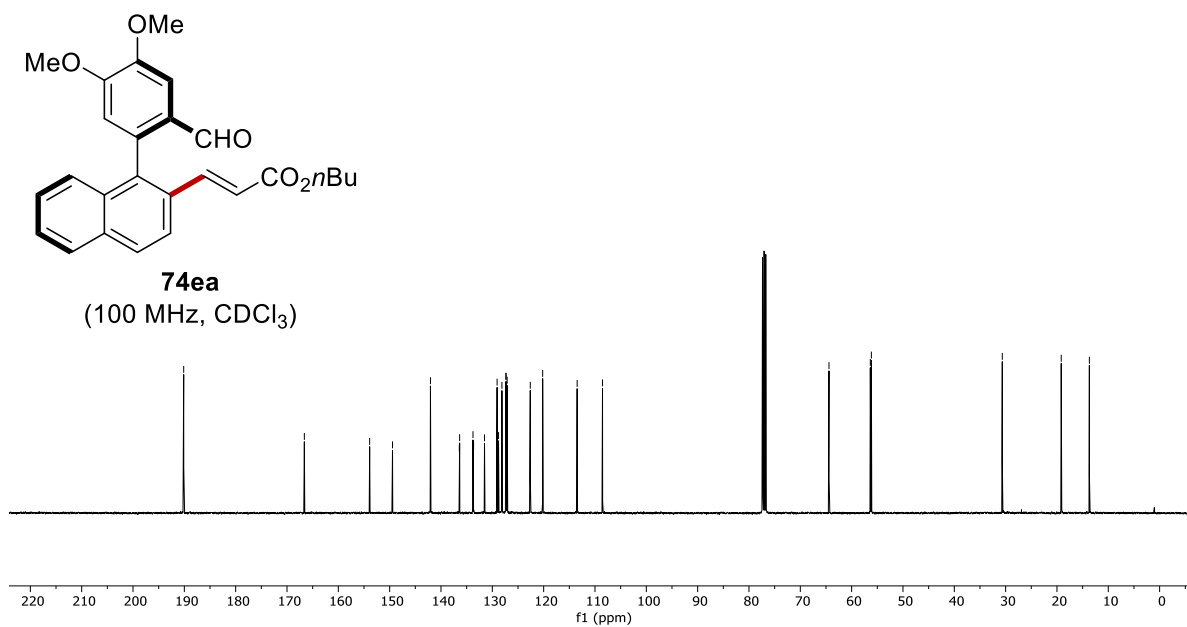
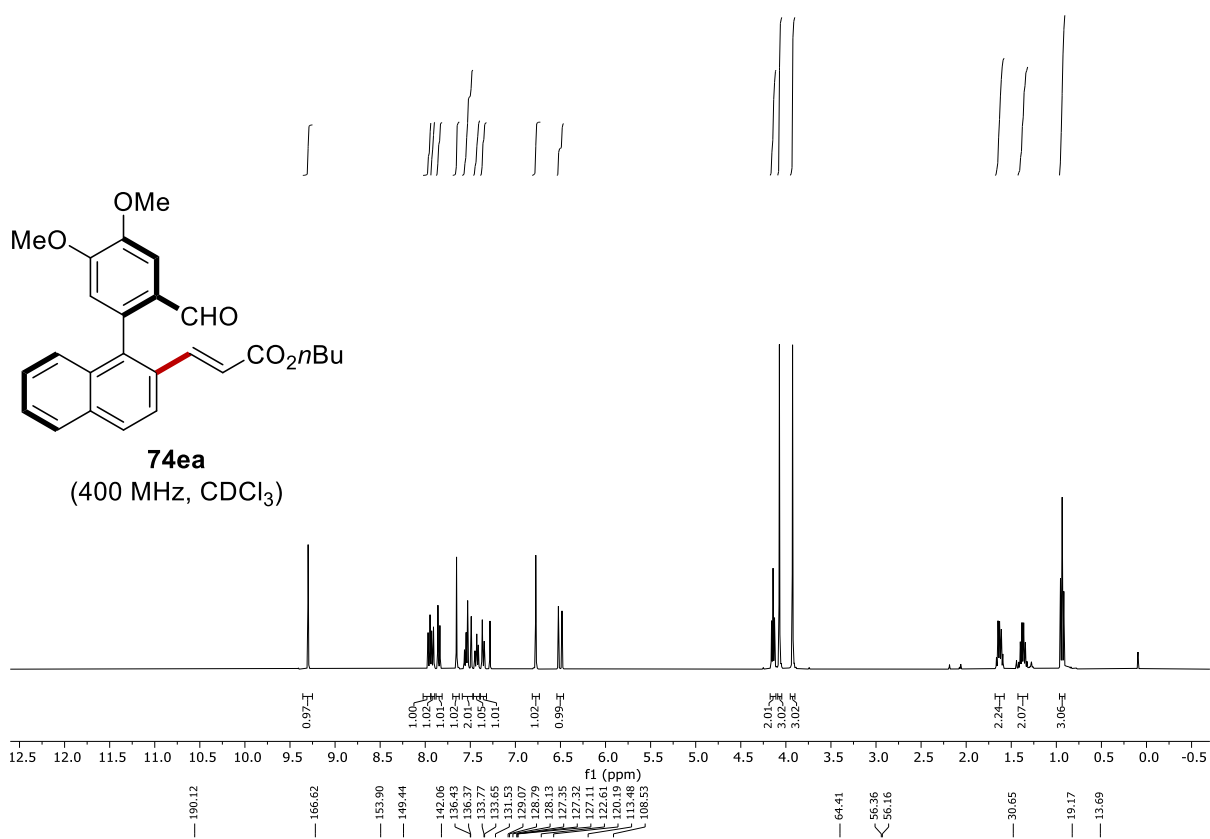
Chiral HPLC of **74da**:



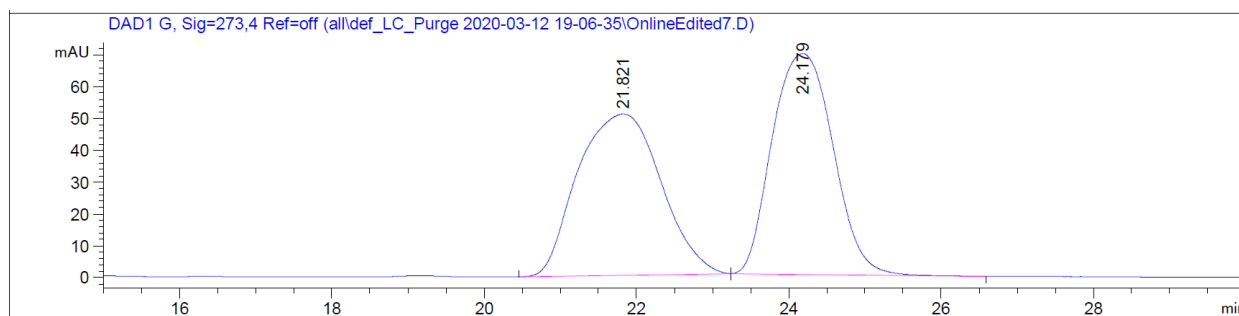
Peak #	RetTime [min]	Type	Width [min]	Area [mAU*s]	Height [mAU]	Area %
1	11.672	BB	0.3381	3626.50928	170.54077	49.5712
2	16.436	BB	0.4186	3689.25098	136.81537	50.4288



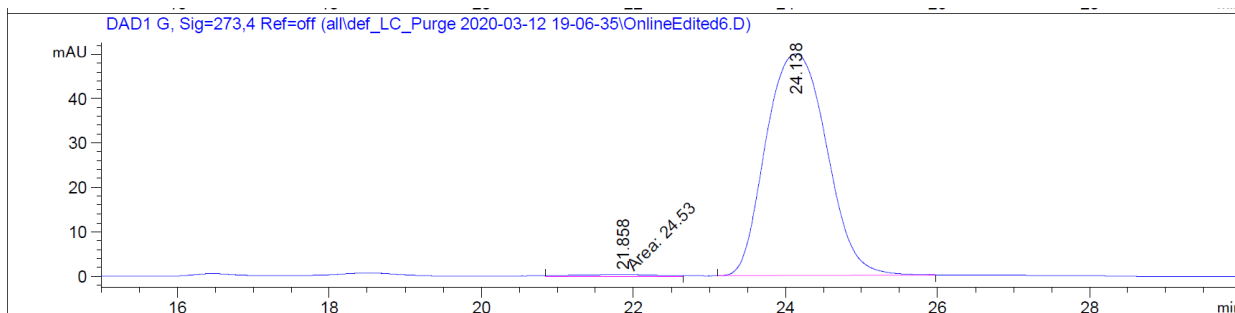
Peak #	RetTime [min]	Type	Width [min]	Area [mAU*s]	Height [mAU]	Area %
1	11.658	MM	0.3962	33.62653	1.41456	0.4485
2	16.396	MM	0.4390	7463.27295	283.31967	99.5515



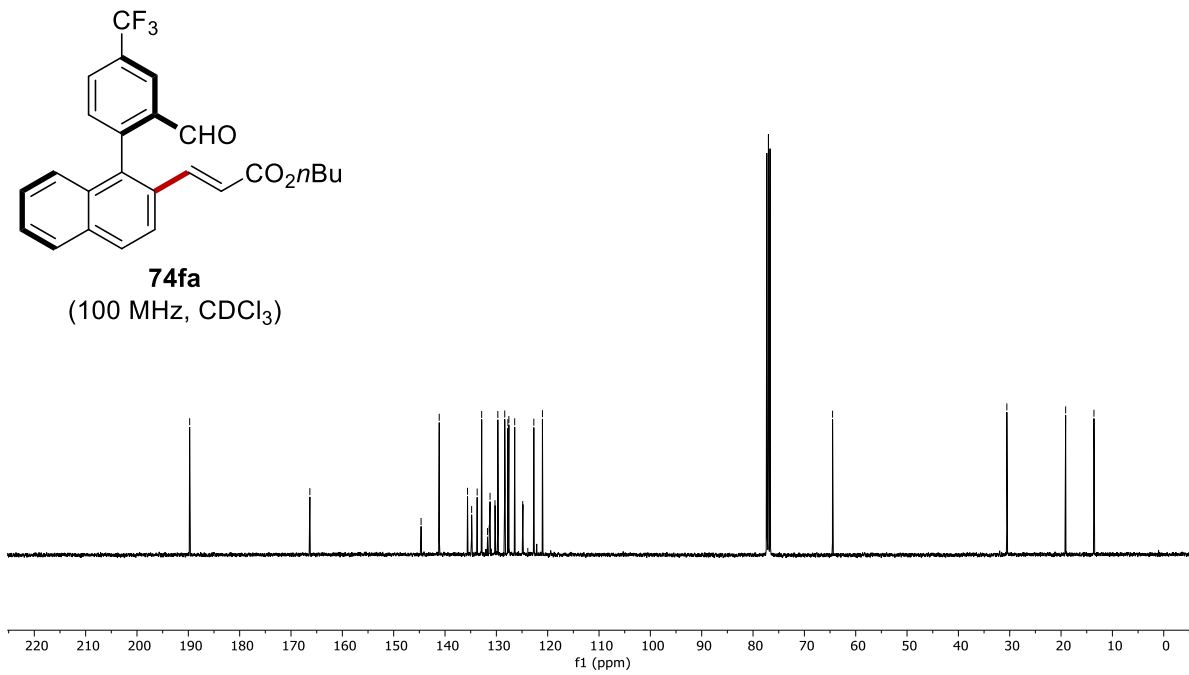
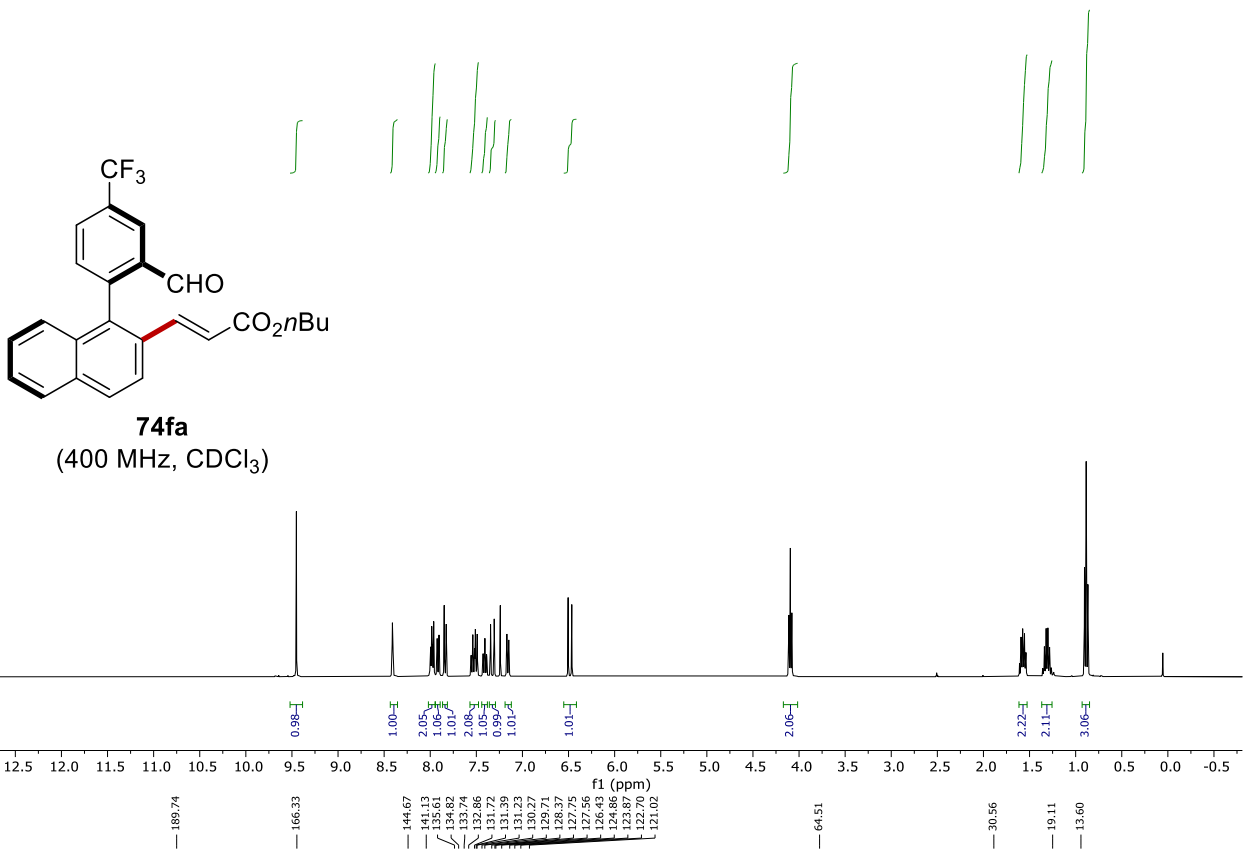
Chiral HPLC of **74ea**:

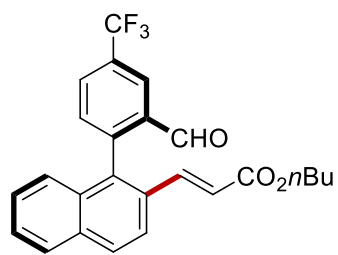


Peak #	RetTime [min]	Type	Width [min]	Area [mAU*s]	Height [mAU]	Area %
1	21.821	BB	0.9015	3842.27759	50.67846	49.8727
2	24.179	BB	0.8866	3861.89331	69.36345	50.1273

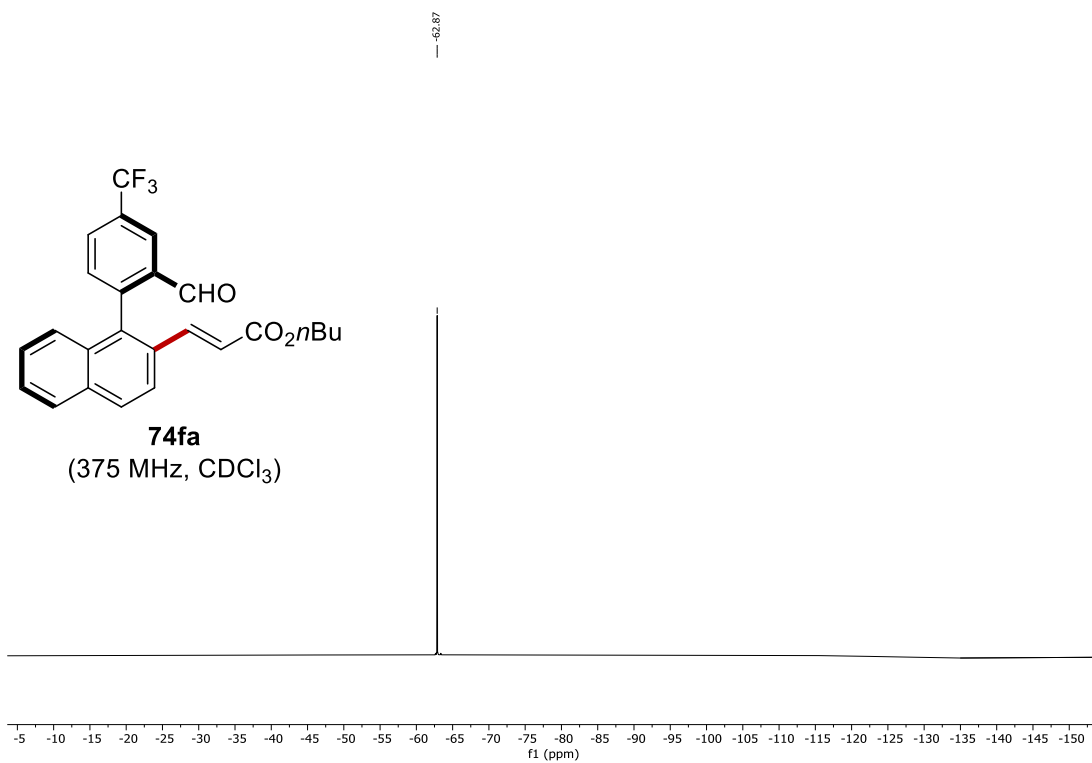


Peak #	RetTime [min]	Type	Width [min]	Area [mAU*s]	Height [mAU]	Area %
1	21.858	MM	1.1642	24.52998	3.51185e-1	0.8768
2	24.138	BB	0.7732	2773.18164	49.99311	99.1232

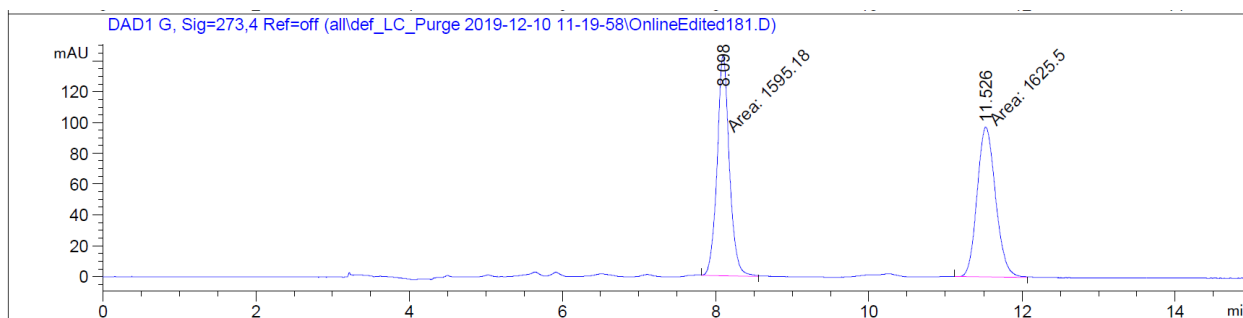




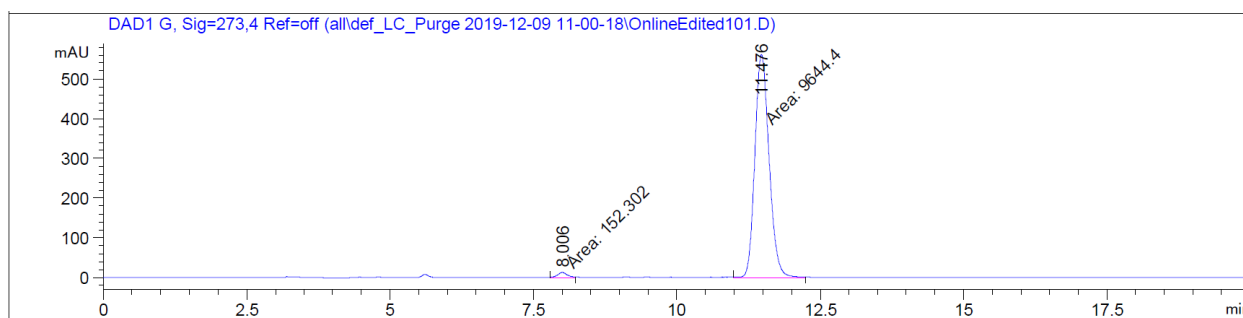
74fa
(375 MHz, CDCl₃)



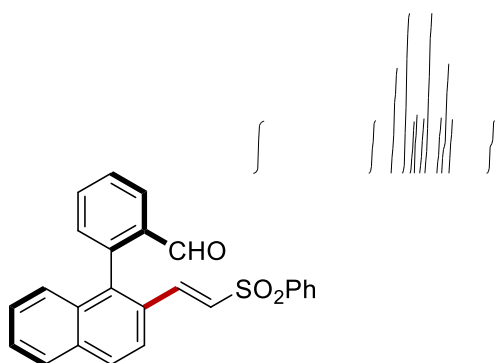
Chiral HPLC of **74fa**:



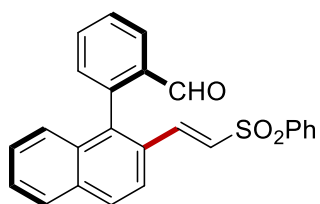
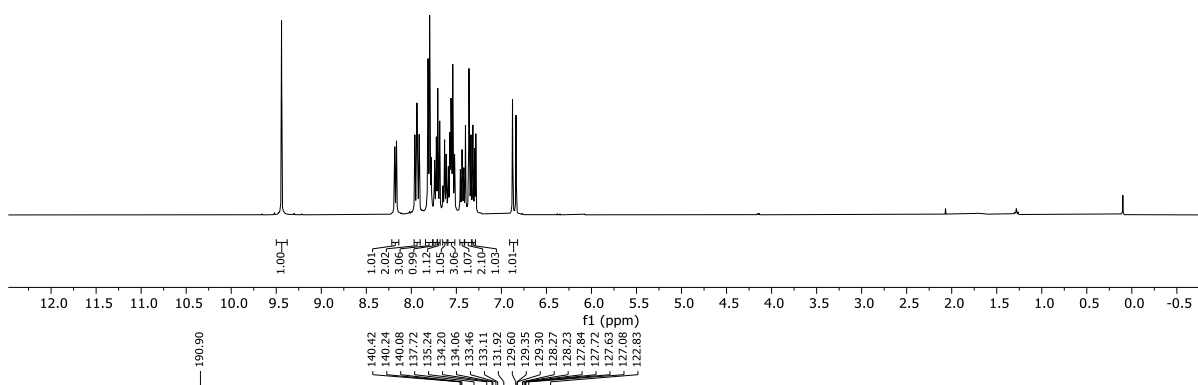
Peak #	RetTime [min]	Type	Width [min]	Area [mAU*s]	Height [mAU]	Area %
1	8.098	MM	0.1856	1595.18274	143.21858	49.5294
2	11.526	MM	0.2785	1625.49817	97.26582	50.4706



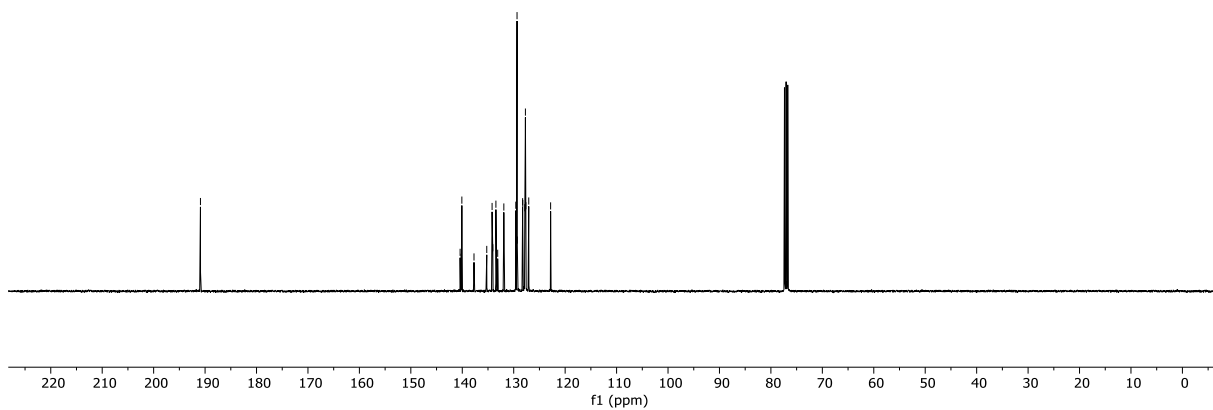
Peak #	RetTime [min]	Type	Width [min]	Area [mAU*s]	Height [mAU]	Area %
1	8.006	MM	0.1963	152.30231	12.92895	1.5546
2	11.476	MM	0.2864	9644.40430	561.29364	98.4454



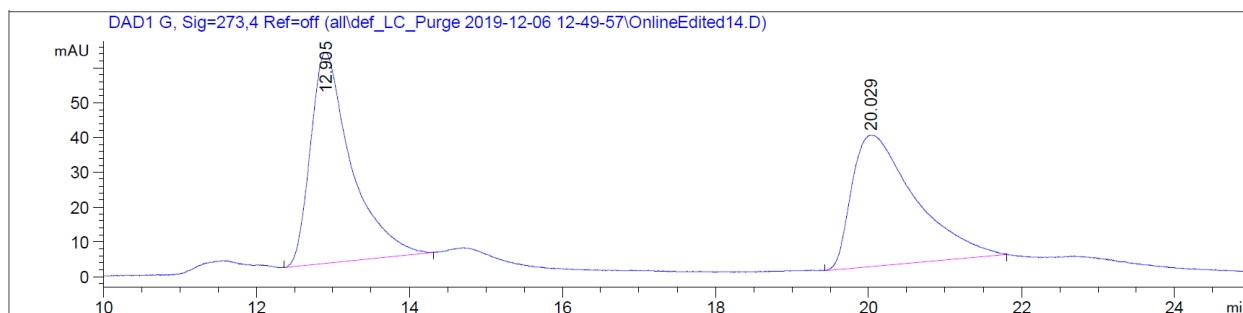
74ab
(400 MHz, CDCl₃)



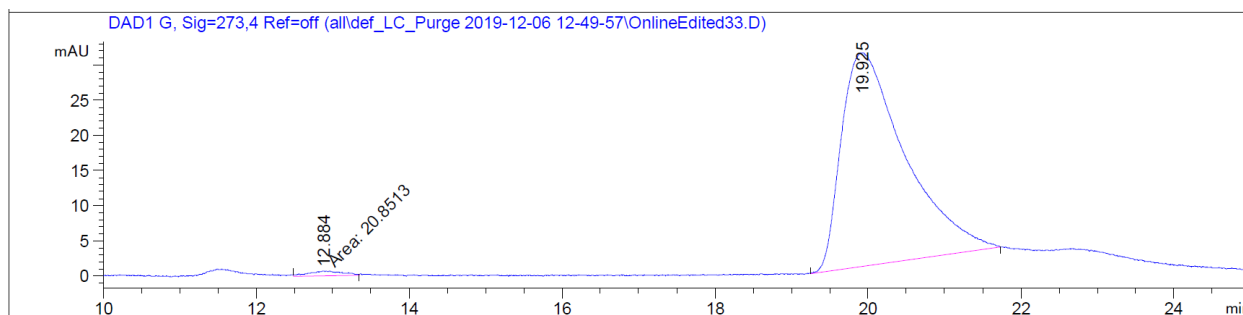
74ab
(100 MHz, CDCl₃)



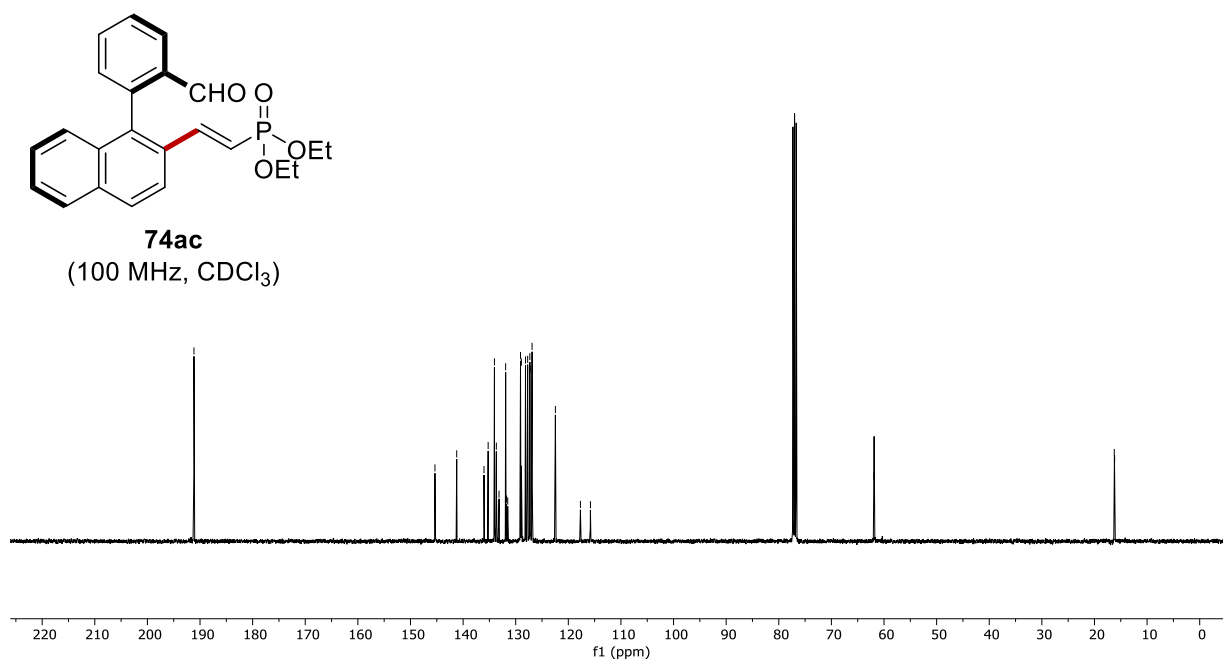
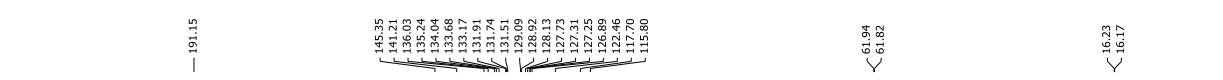
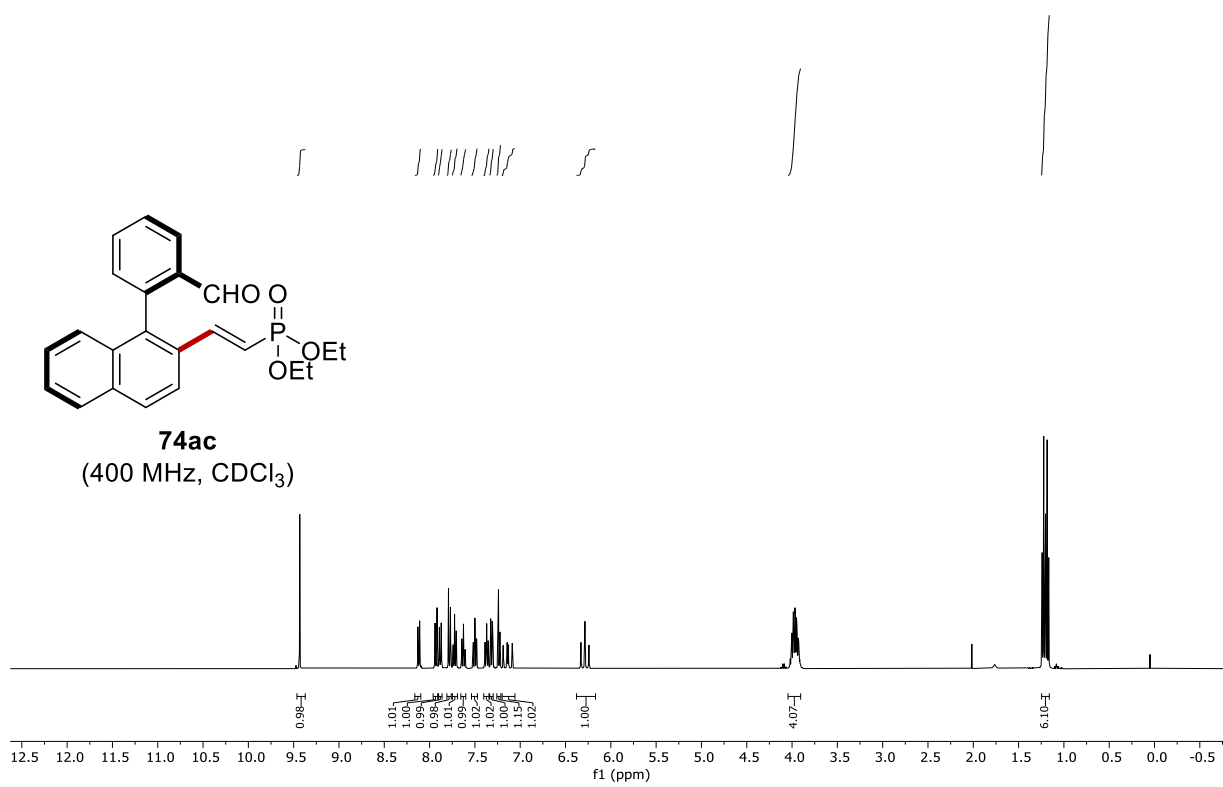
Chiral HPLC of **74ab**:



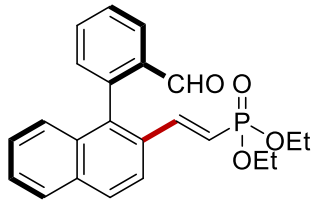
Peak #	RetTime [min]	Type	Width [min]	Area [mAU*s]	Height [mAU]	Area %
1	12.905	BV R	0.4344	2233.30713	60.67965	50.8991
2	20.029	BB	0.6691	2154.41016	37.79290	49.1009



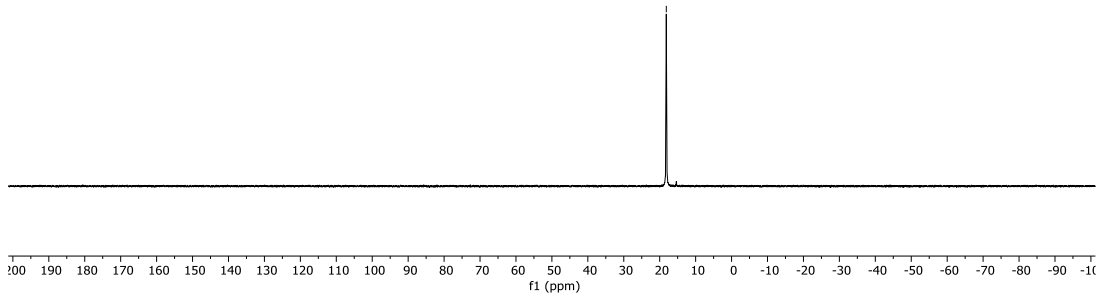
Peak #	RetTime [min]	Type	Width [min]	Area [mAU*s]	Height [mAU]	Area %
1	12.884	MM	0.5092	20.85131	6.82512e-1	1.1735
2	19.925	BV R	0.6788	1755.97766	30.35890	98.8265



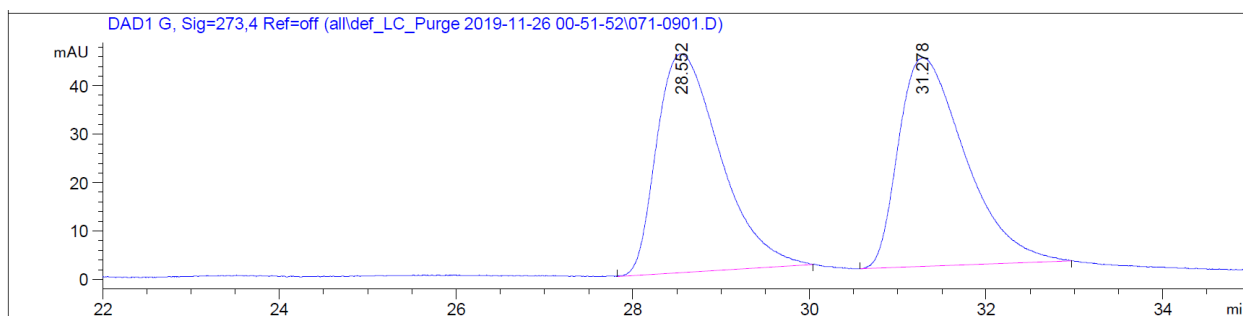
18.17



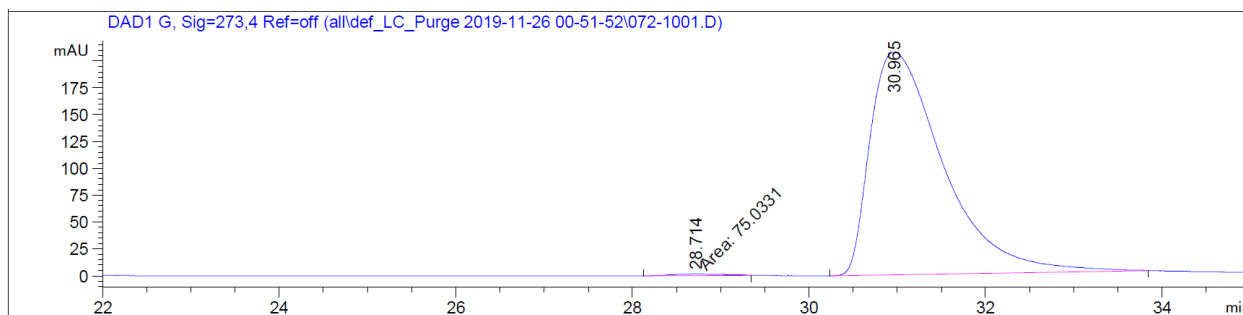
74ac
(160 MHz, CDCl₃)



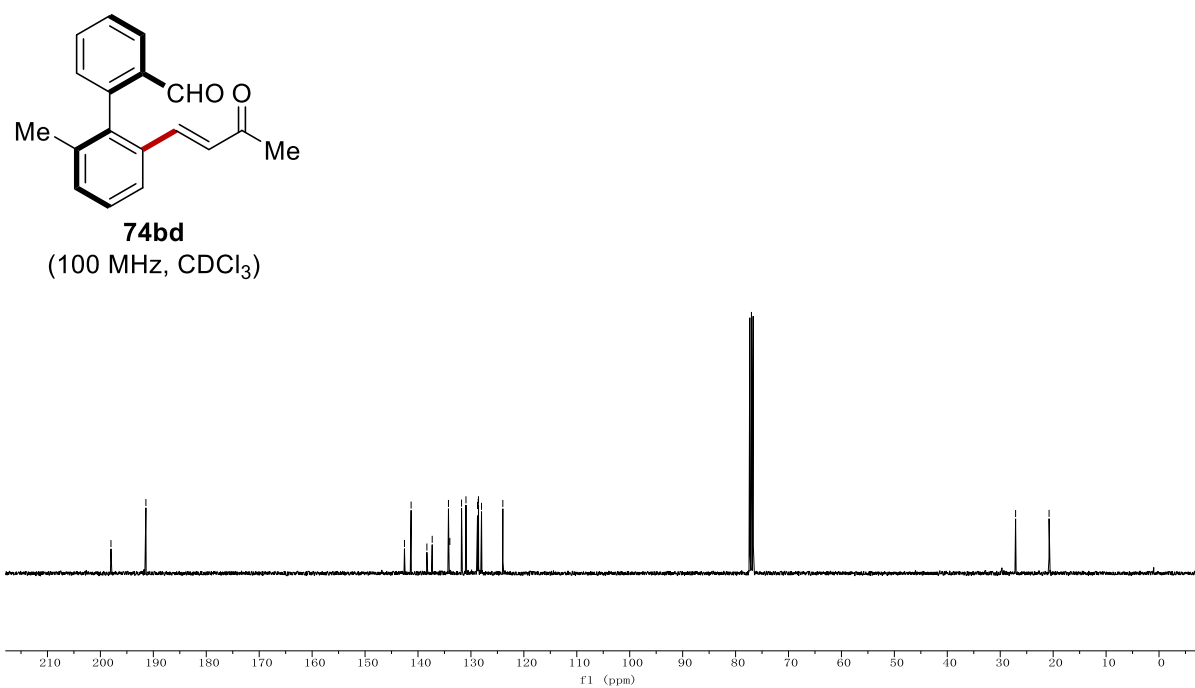
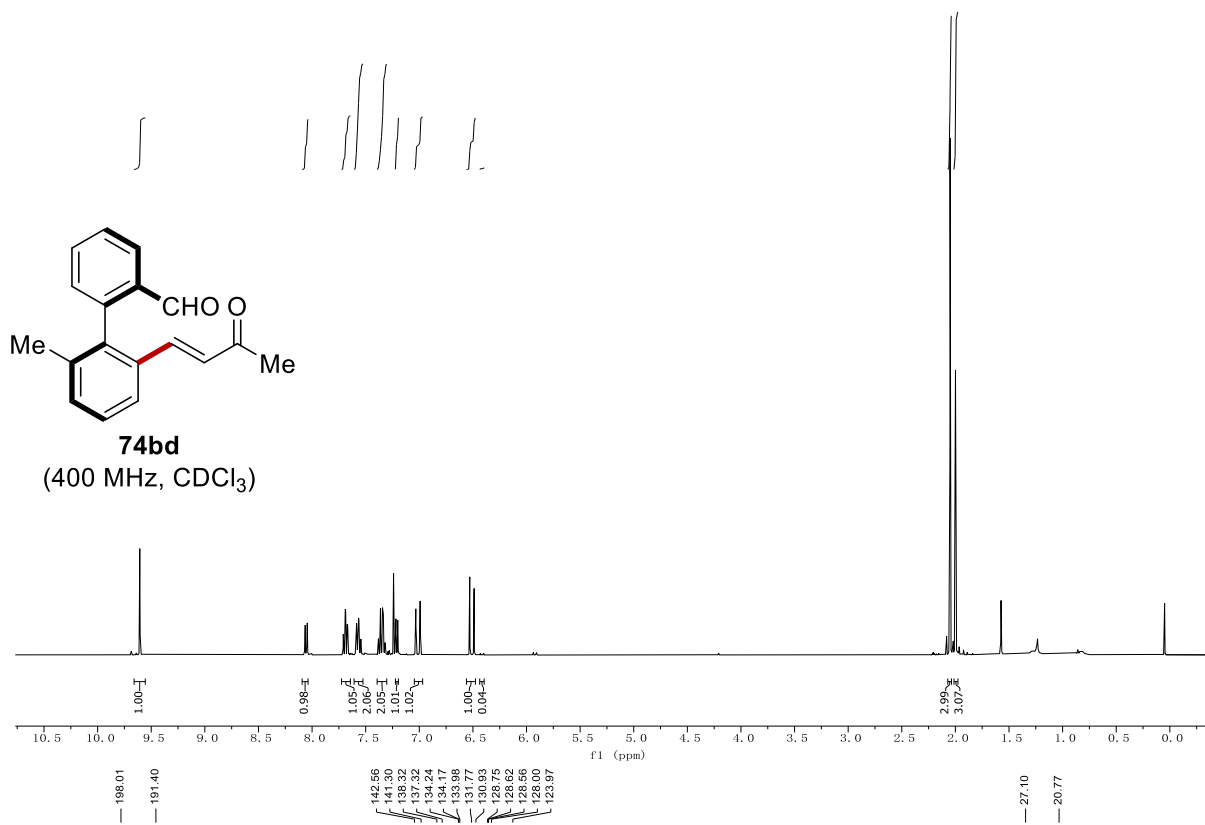
Chiral HPLC of **74ac**:



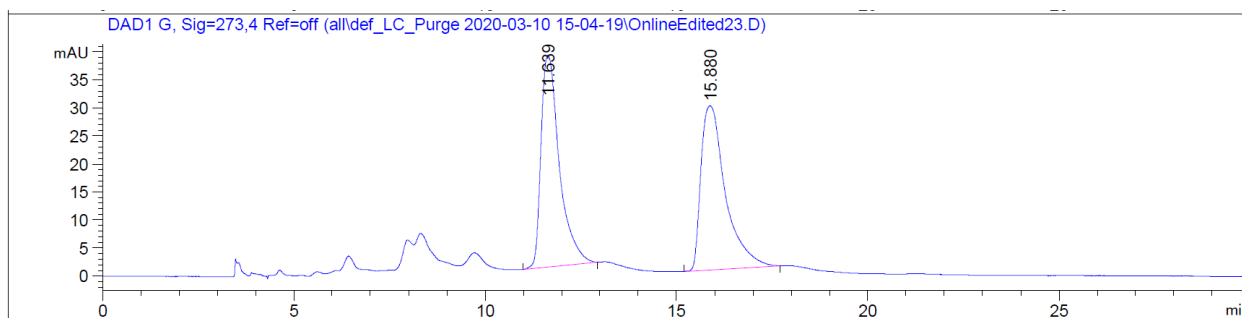
Peak #	RetTime [min]	Type	Width [min]	Area [mAU*s]	Height [mAU]	Area %
1	28.552	BV R	0.5893	2254.54712	45.16977	49.8997
2	31.278	BV R	0.6184	2263.60913	43.12093	50.1003



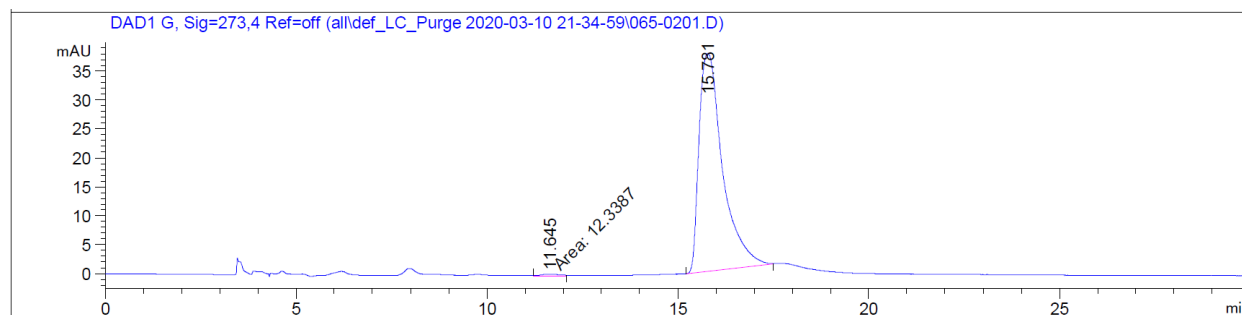
Peak #	RetTime [min]	Type	Width [min]	Area [mAU*s]	Height [mAU]	Area %
1	28.714	MM	0.7017	75.03307	1.78227	0.6230
2	30.965	BB	0.7836	1.19695e4	207.61021	99.3770



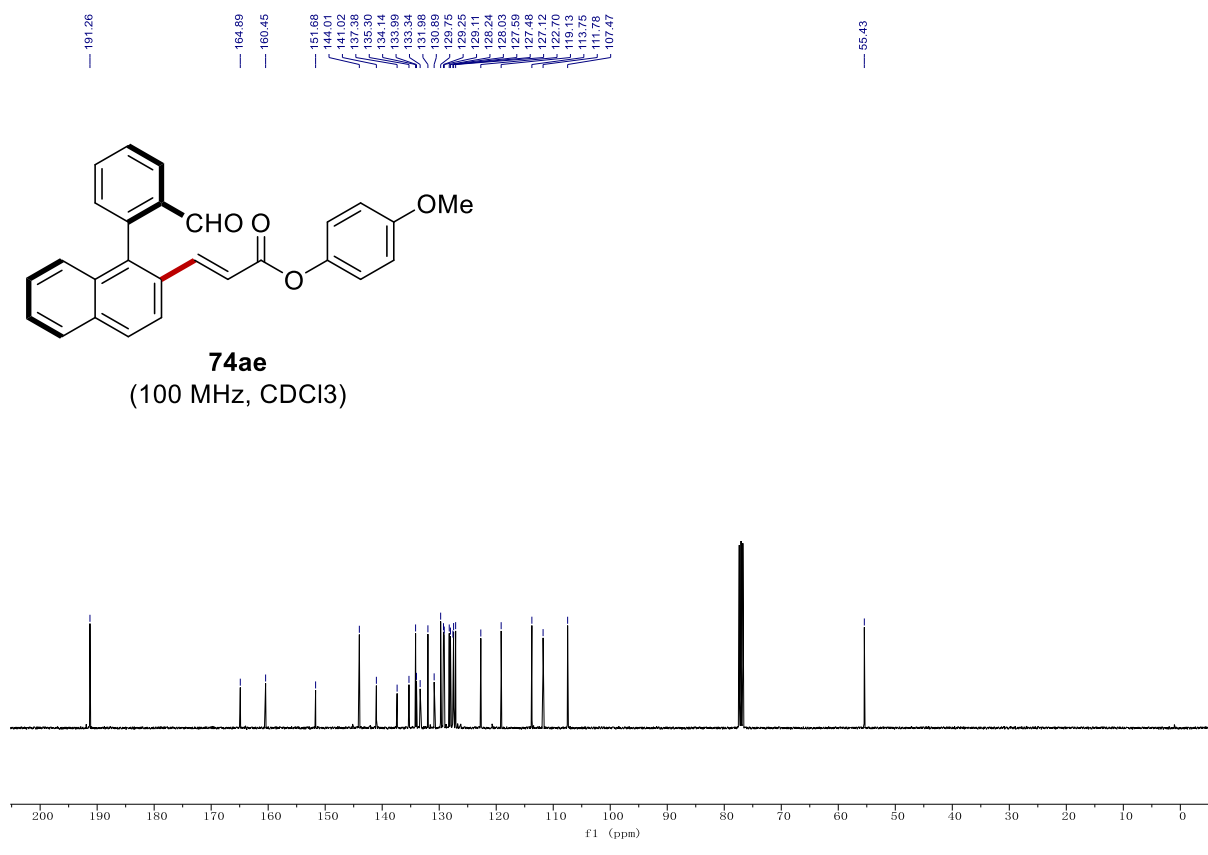
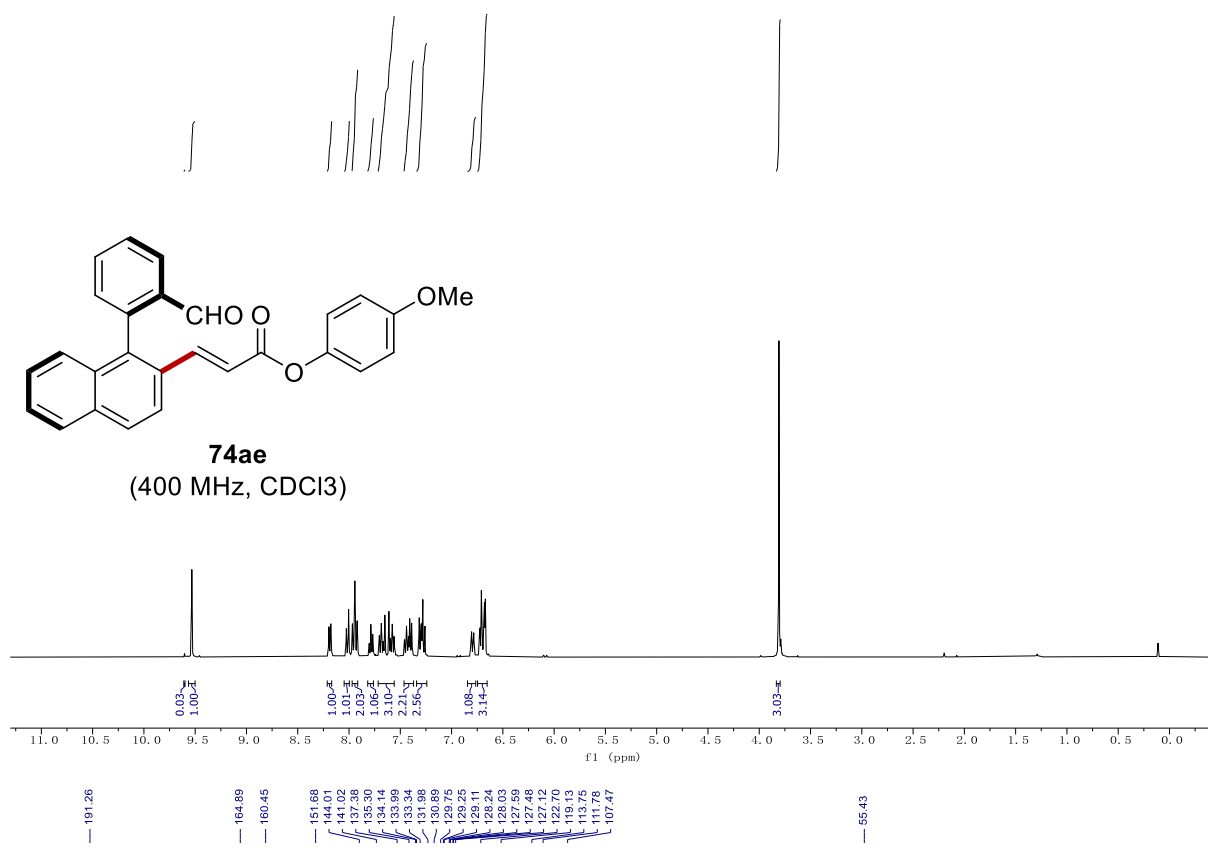
Chiral HPLC of **74bd**:



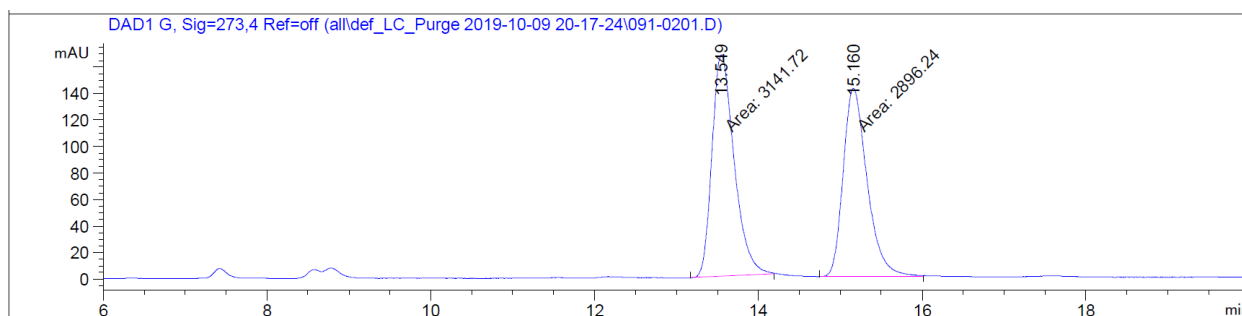
Peak #	RetTime [min]	Type	Width [min]	Area [mAU*s]	Height [mAU]	Area %
1	11.639	BB	0.5085	1260.75012	37.85801	49.2290
2	15.880	BB	0.6688	1300.23975	29.29589	50.7710



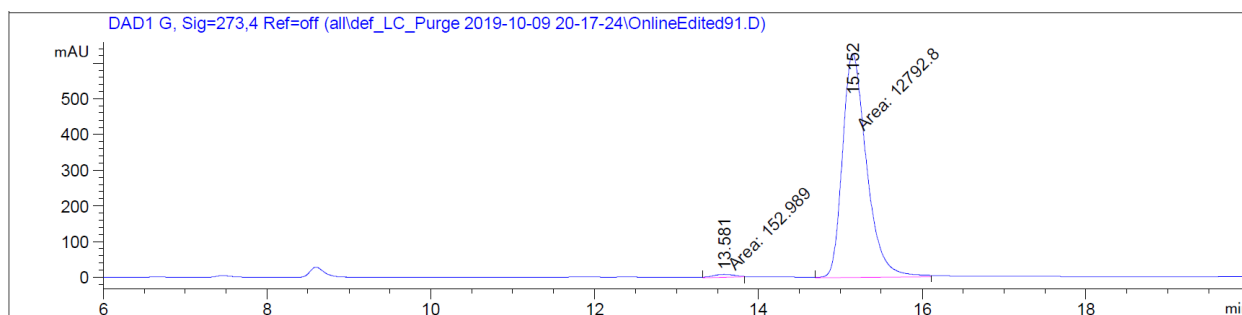
Peak #	RetTime [min]	Type	Width [min]	Area [mAU*s]	Height [mAU]	Area %
1	11.645	MM	0.6017	12.33872	3.41767e-1	0.7612
2	15.781	BB	0.6384	1608.60620	37.65216	99.2388



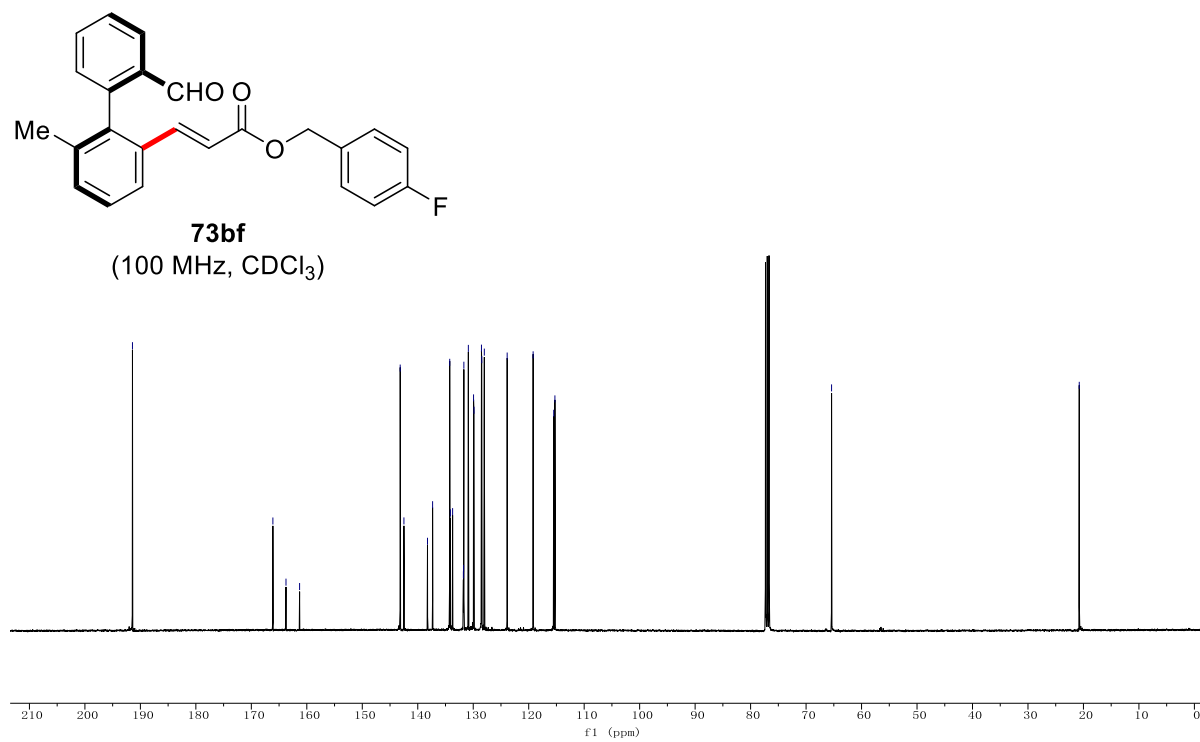
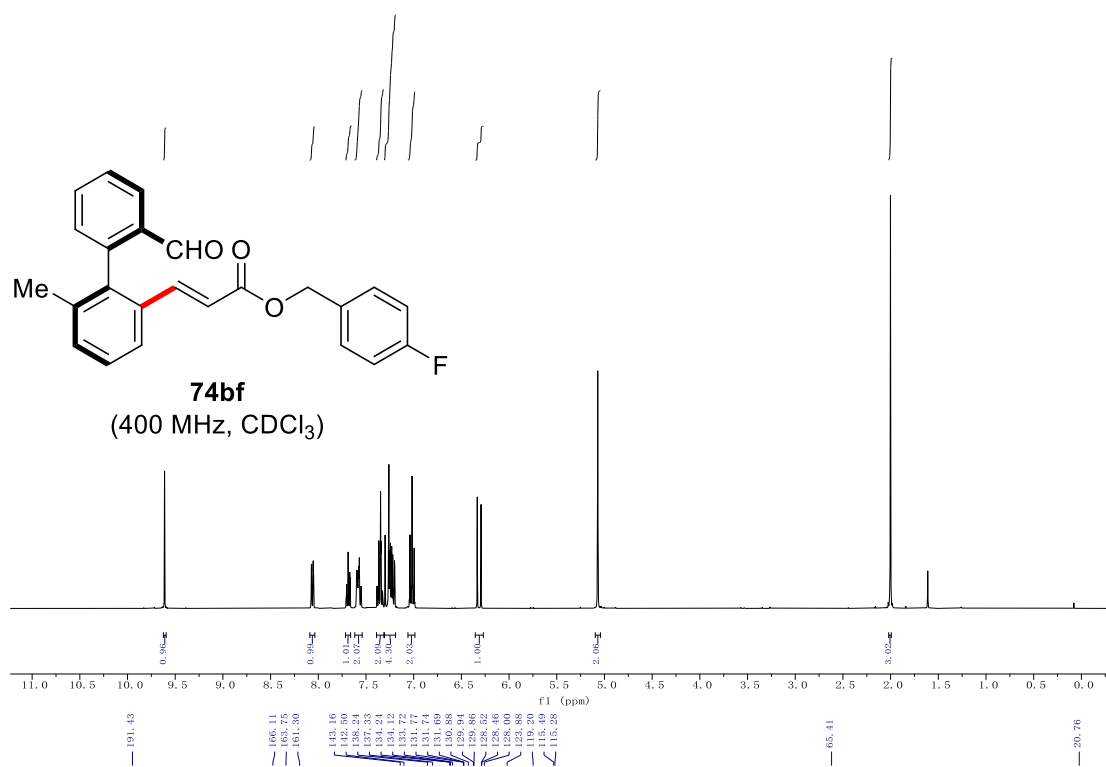
Chiral HPLC of **74ae**:

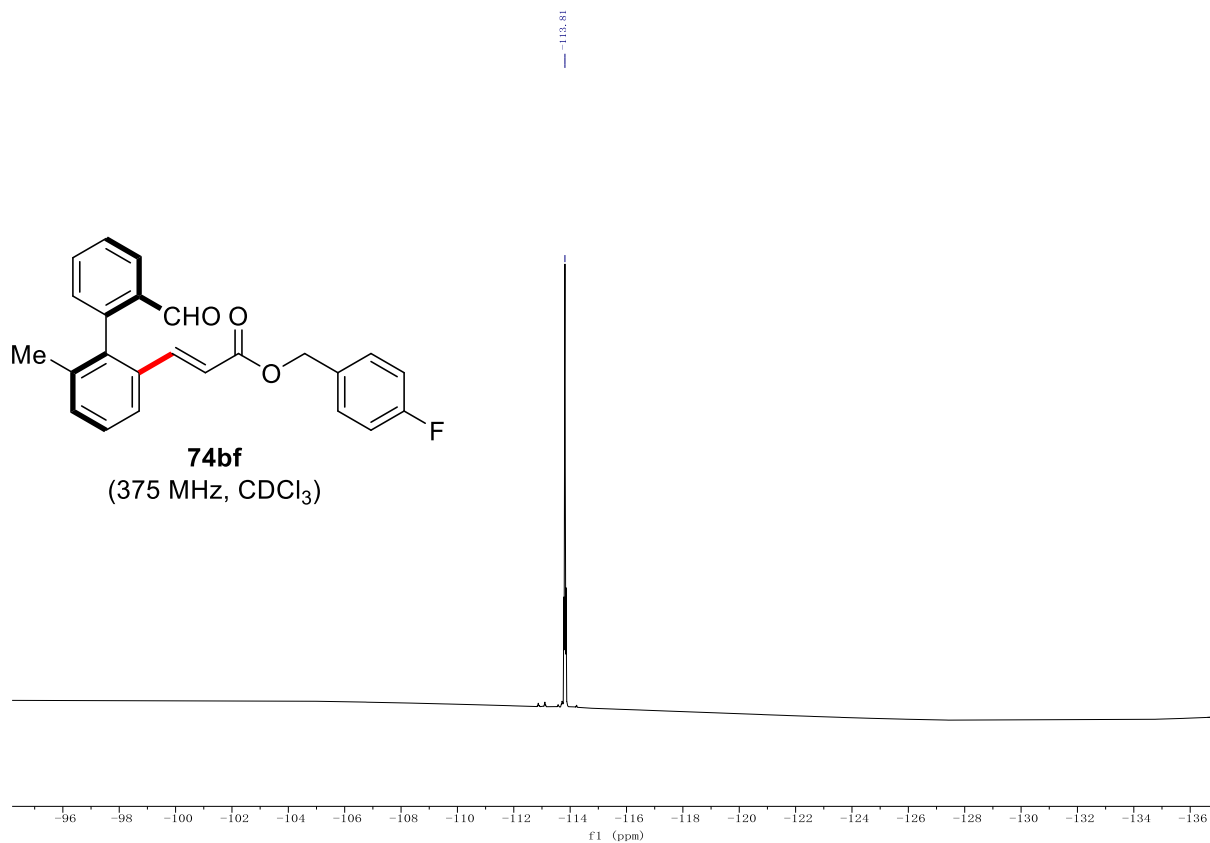


Peak #	RetTime [min]	Type	Width [min]	Area [mAU*s]	Height [mAU]	Area %
1	13.549	MM	0.3134	3141.72144	167.06538	52.0328
2	15.160	MM	0.3397	2896.24219	142.08664	47.9672

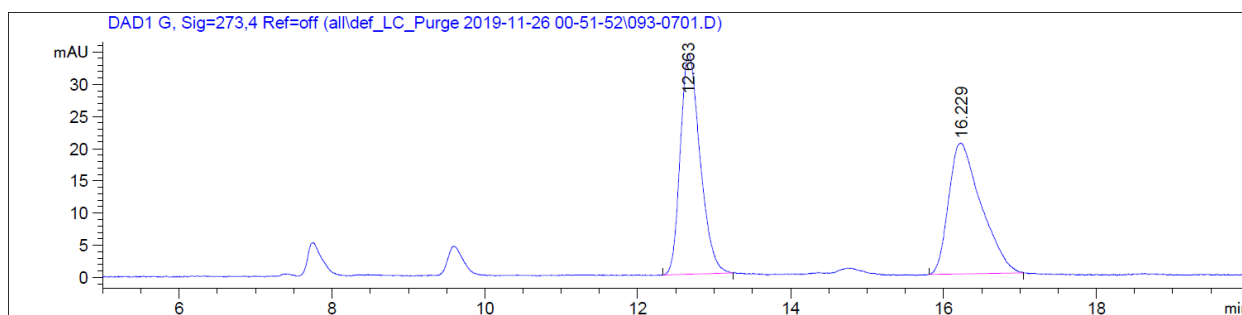


Peak #	RetTime [min]	Type	Width [min]	Area [mAU*s]	Height [mAU]	Area %
1	13.581	MM	0.3040	152.98878	8.38777	1.1818
2	15.152	MM	0.3403	1.27928e4	626.60223	98.8182

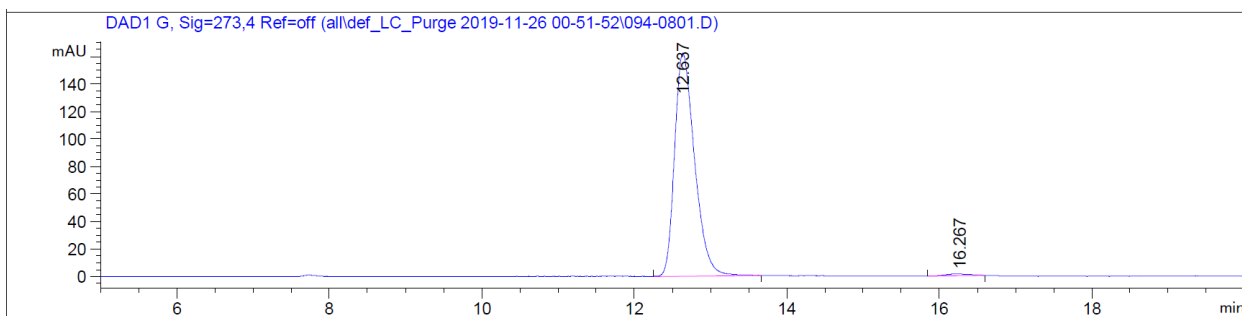




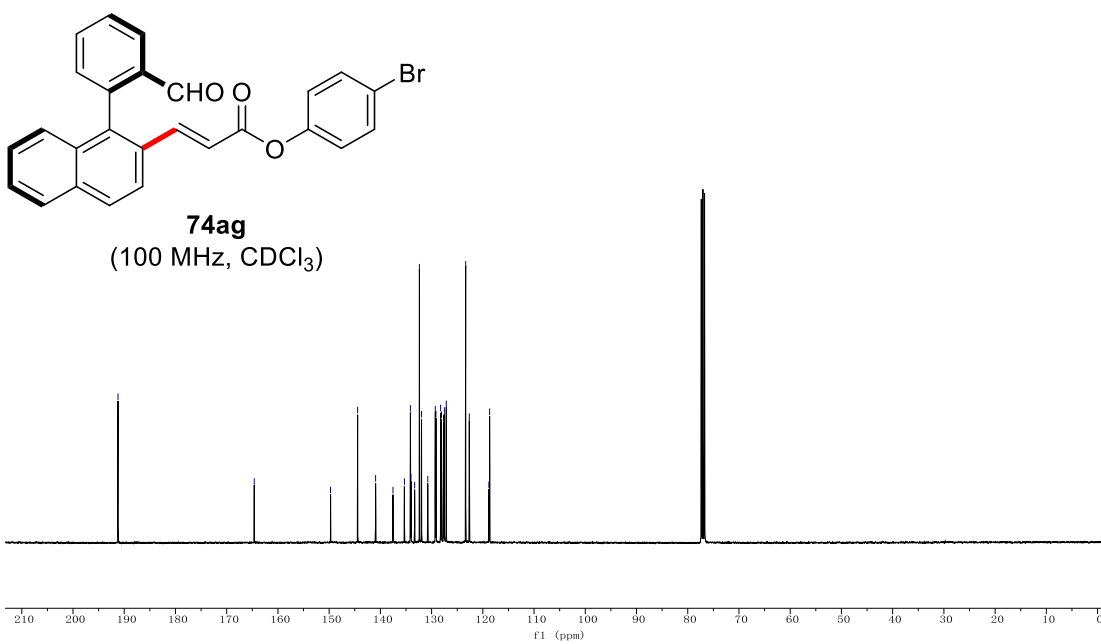
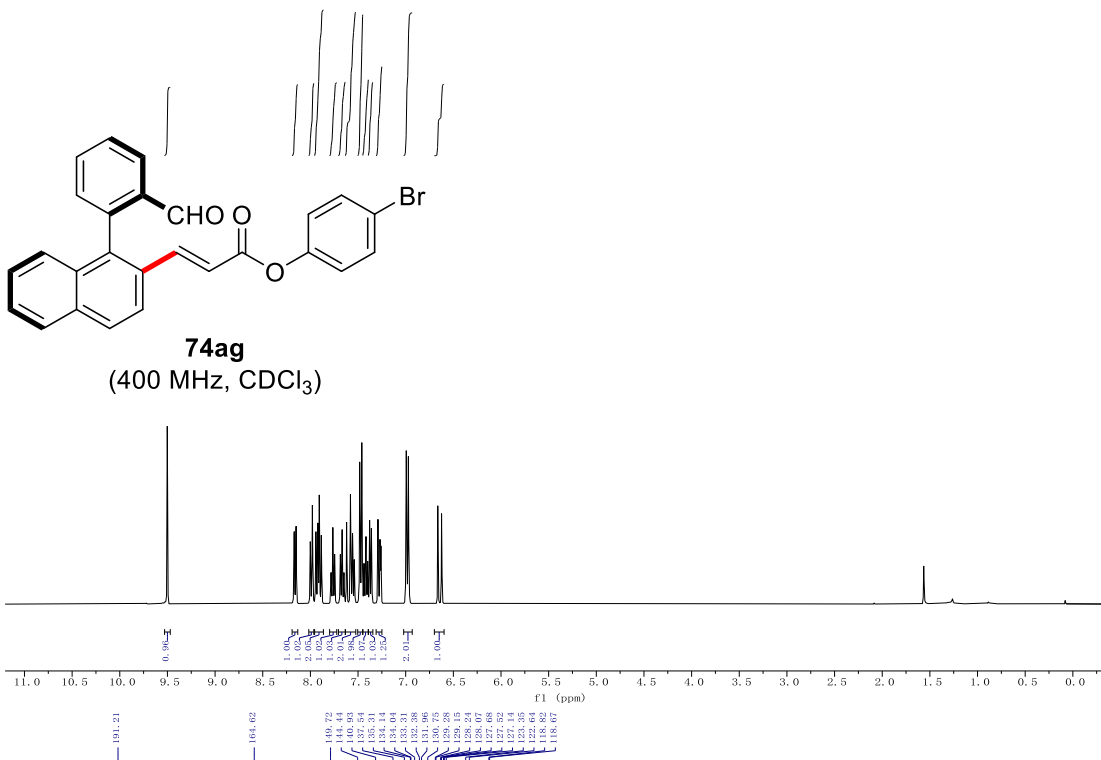
Chiral HPLC of **74bf**:



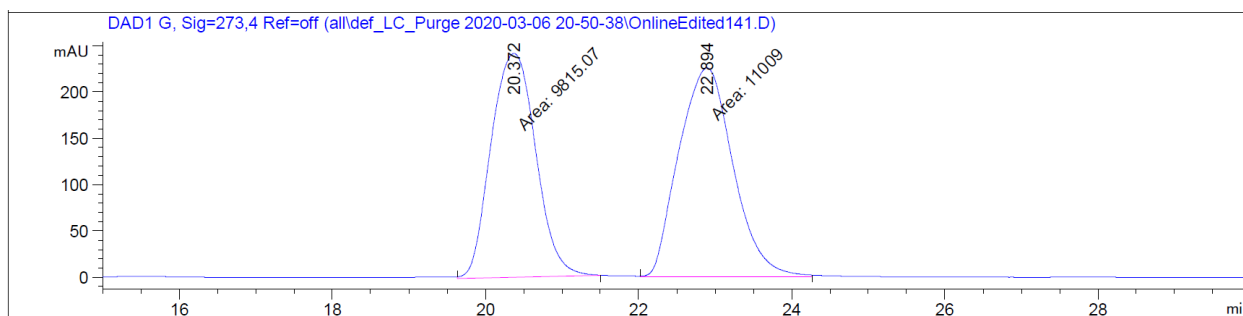
Peak #	RetTime [min]	Type	Width [min]	Area [mAU*s]	Height [mAU]	Area %
1	12.663	BB	0.2546	616.04492	34.28500	50.6977
2	16.229	BB	0.3553	599.08984	20.29773	49.3023



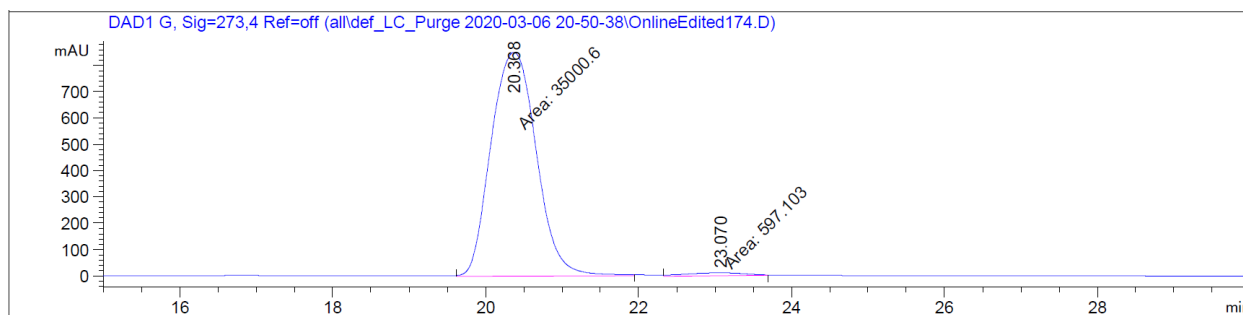
Peak #	RetTime [min]	Type	Width [min]	Area [mAU*s]	Height [mAU]	Area %
1	12.637	BV R	0.2724	2954.47266	162.25336	99.0154
2	16.267	VB R	0.2722	29.38032	1.27799	0.9846



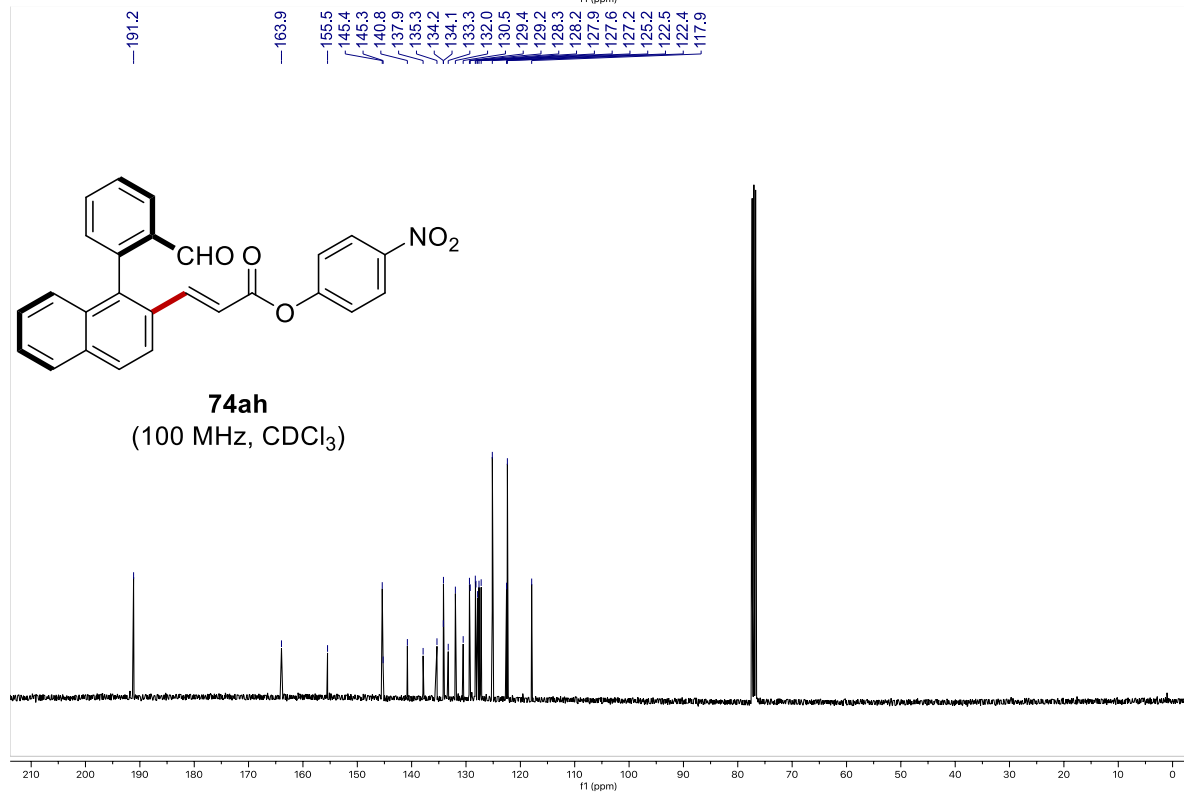
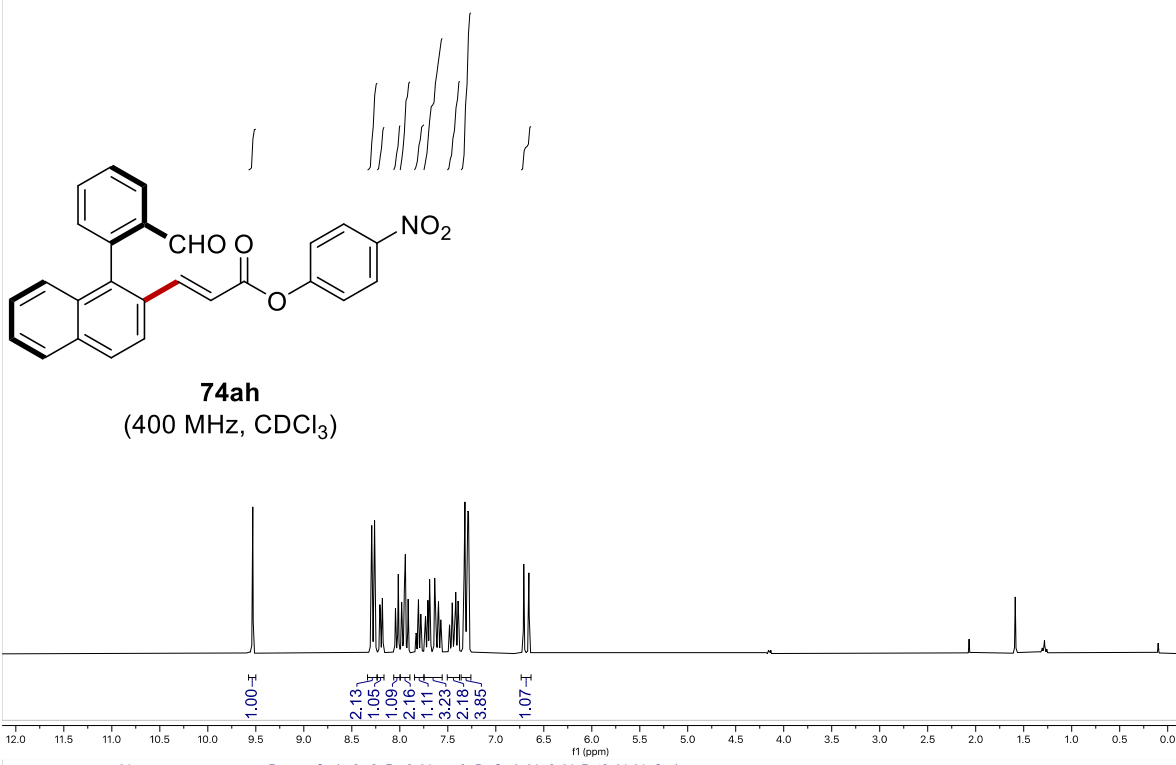
Chiral HPLC of 74ag:



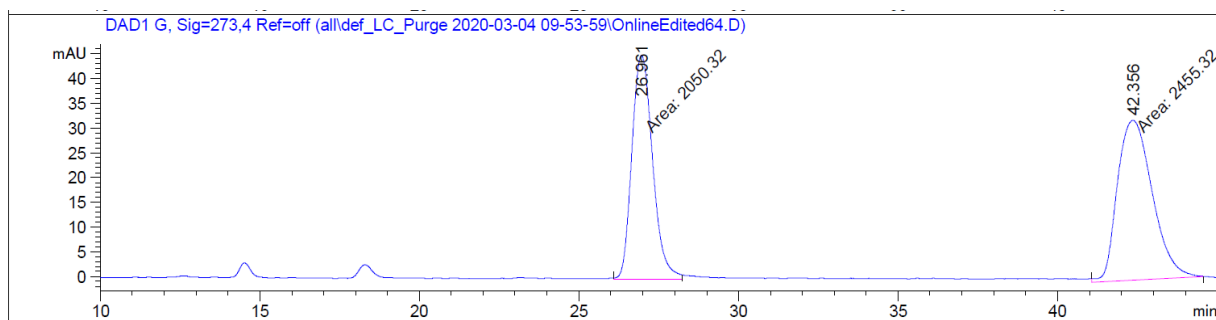
Peak #	RetTime [min]	Type	Width [min]	Area [mAU*s]	Height [mAU]	Area %
1	20.372	MM	0.6771	9815.07031	241.61073	47.1334
2	22.894	MM	0.8160	1.10090e4	224.85251	52.8666



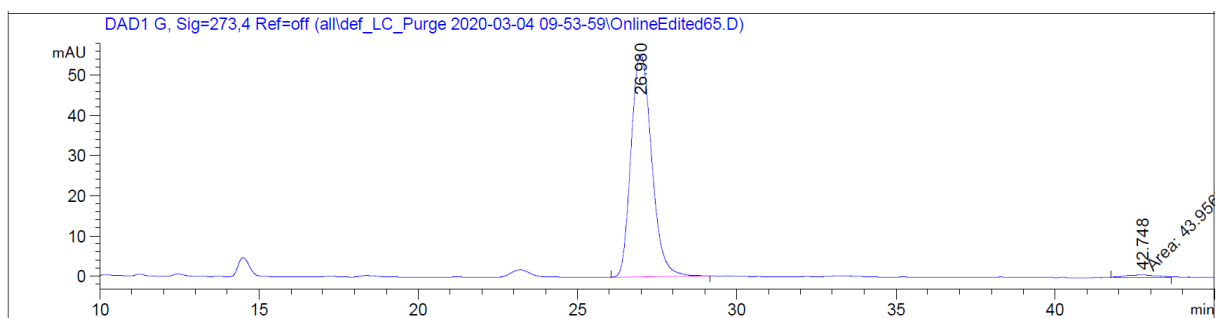
Peak #	RetTime [min]	Type	Width [min]	Area [mAU*s]	Height [mAU]	Area %
1	20.368	MM	0.6857	3.50006e4	850.66534	98.3226
2	23.070	MM	0.6633	597.10272	11.18206	1.6774



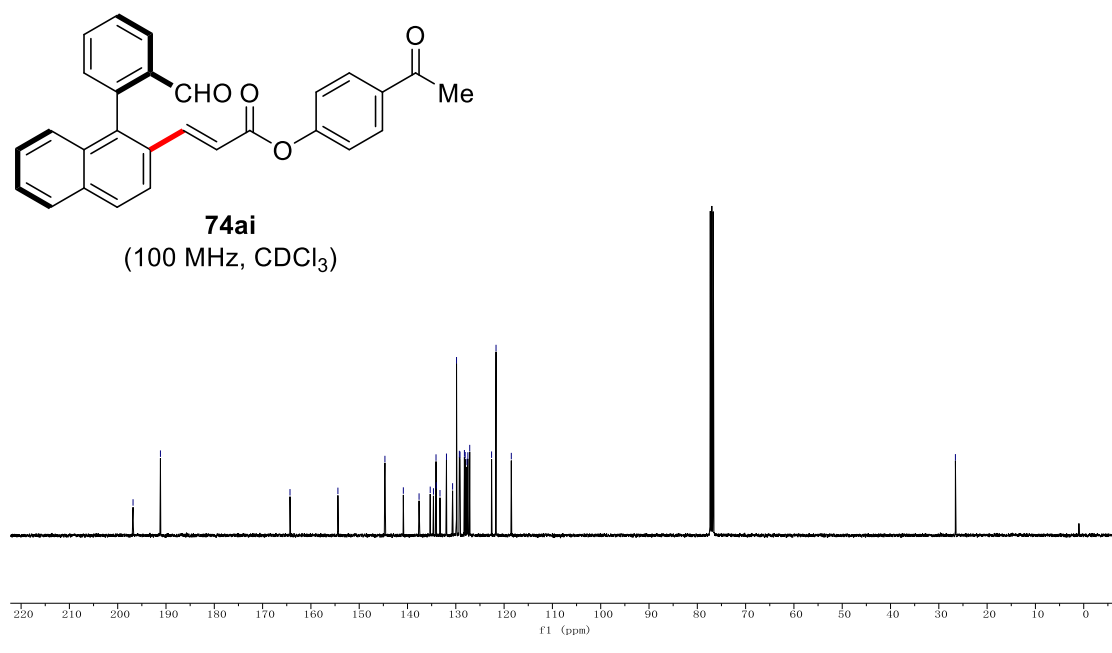
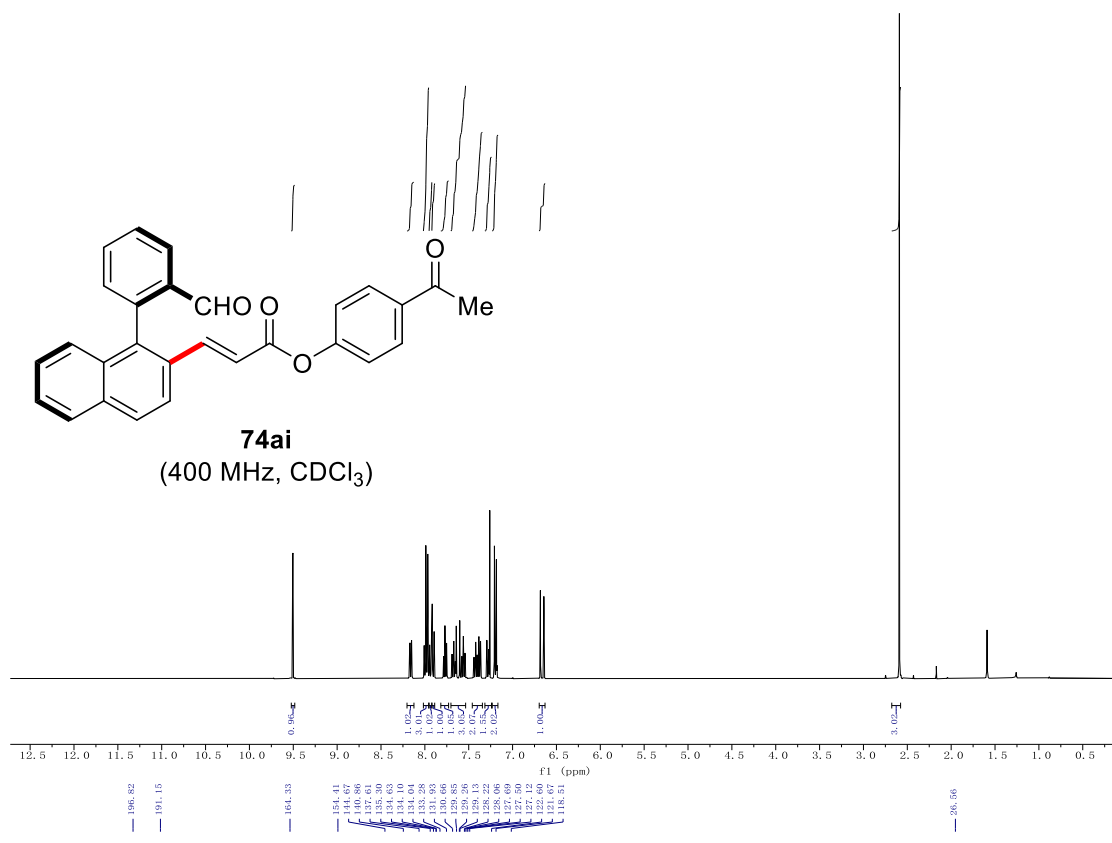
Chiral HPLC of **74ah**:



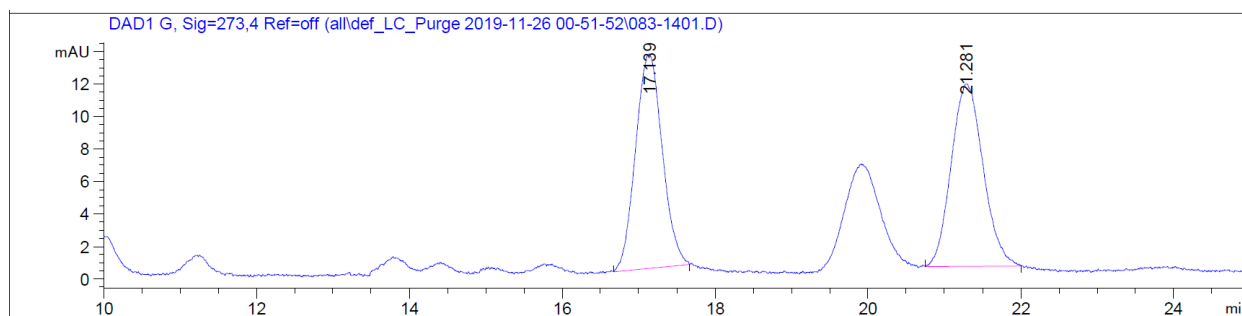
Peak #	RetTime [min]	Type	Width [min]	Area [mAU*s]	Height [mAU]	Area %
1	26.961	MM	0.7543	2050.31958	45.30516	45.5056
2	42.356	MM	1.2667	2455.32104	32.30606	54.4944



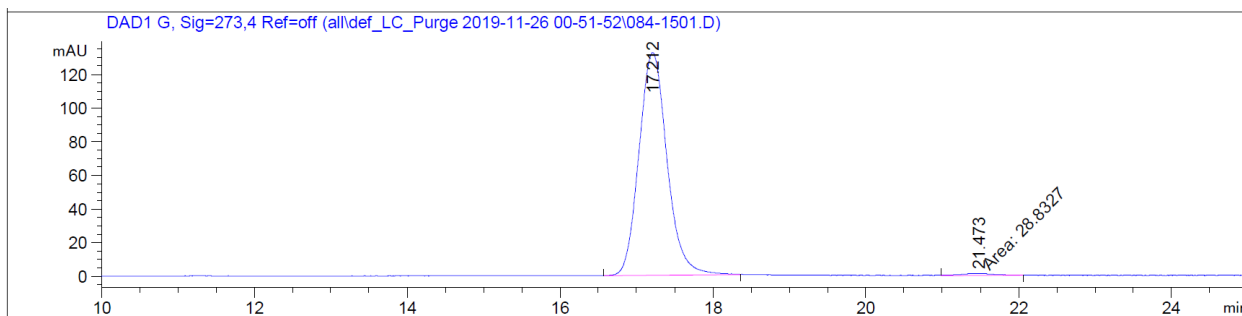
Peak #	RetTime [min]	Type	Width [min]	Area [mAU*s]	Height [mAU]	Area %
1	26.980	BB	0.6919	2494.72827	55.44894	98.2685
2	42.748	MM	1.0945	43.95687	6.69365e-1	1.7315



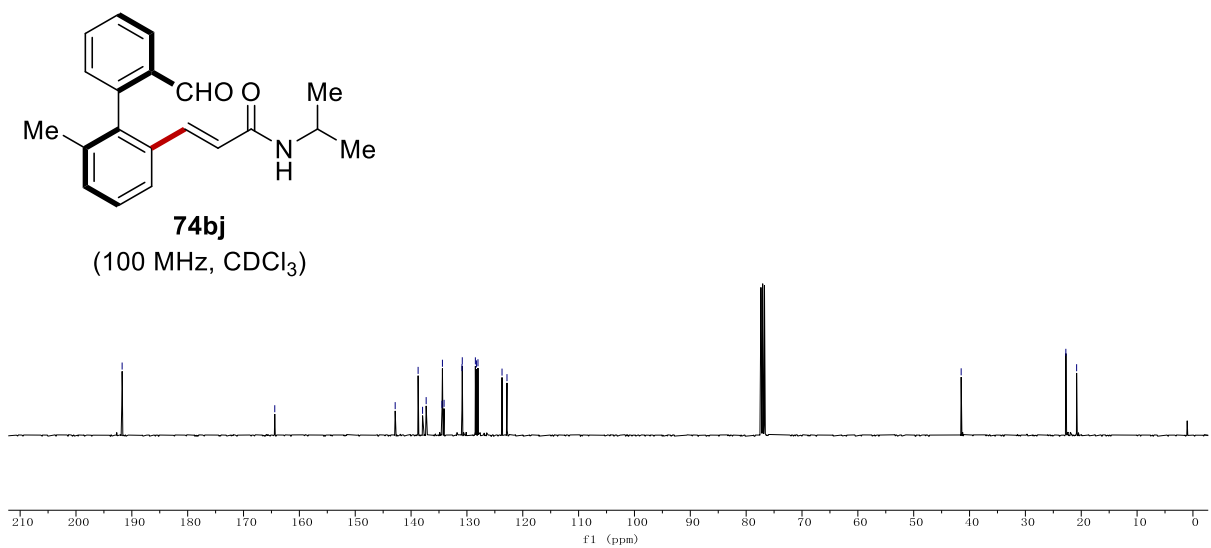
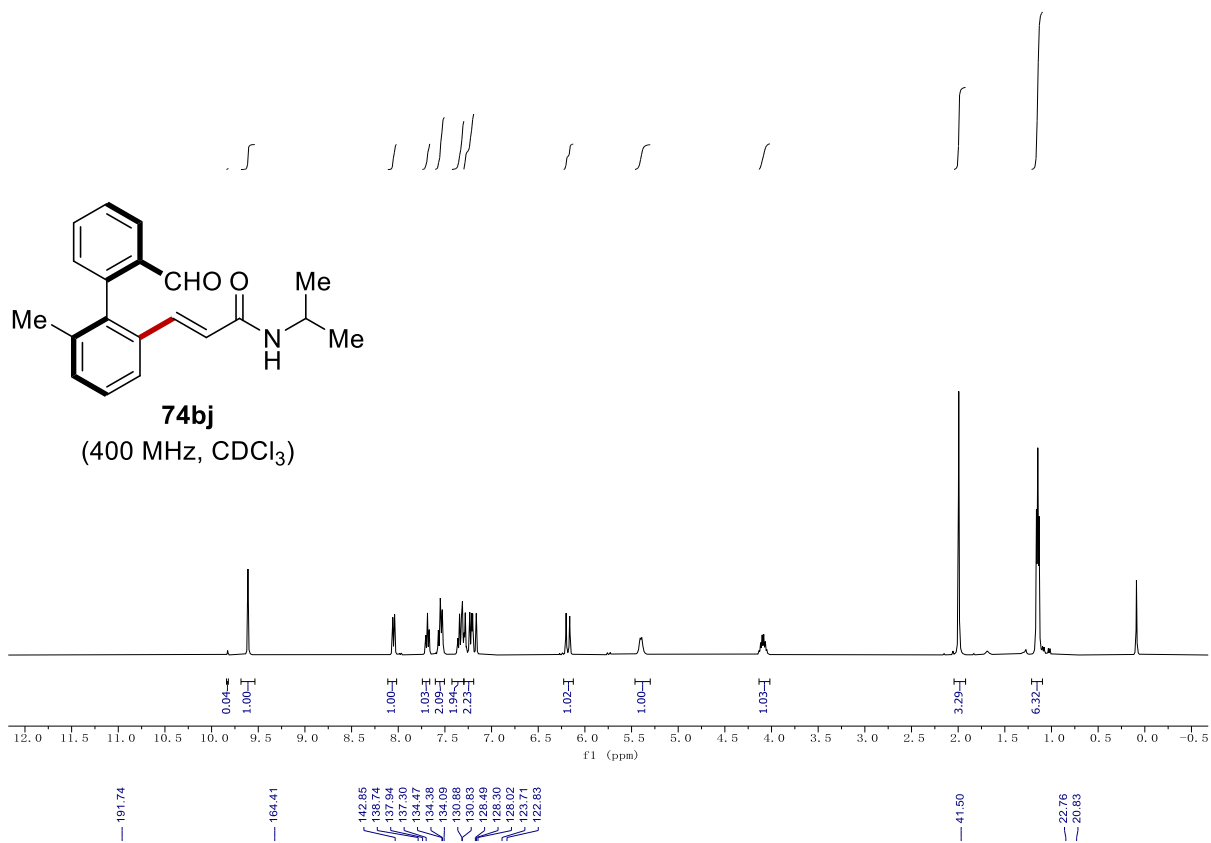
Chiral HPLC of 74ai:



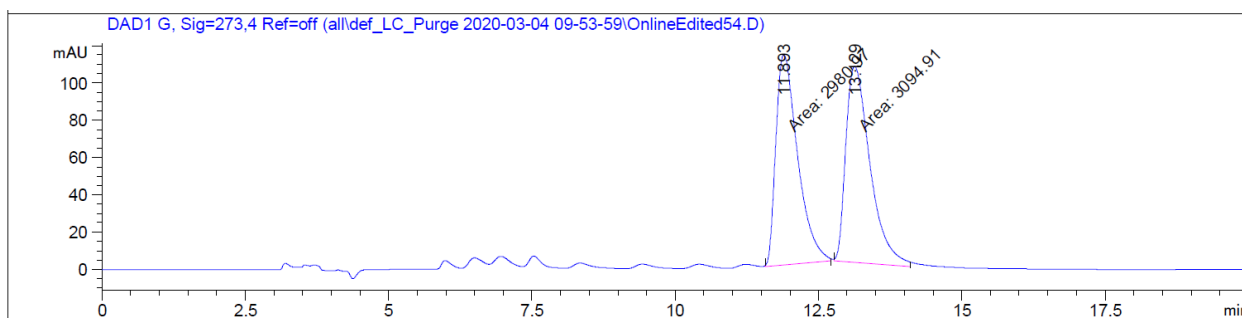
Peak #	RetTime [min]	Type	Width [min]	Area [mAU*s]	Height [mAU]	Area %
1	17.139	BB	0.2886	319.62296	13.19389	49.5082
2	21.281	BB	0.3452	325.97256	11.21191	50.4918



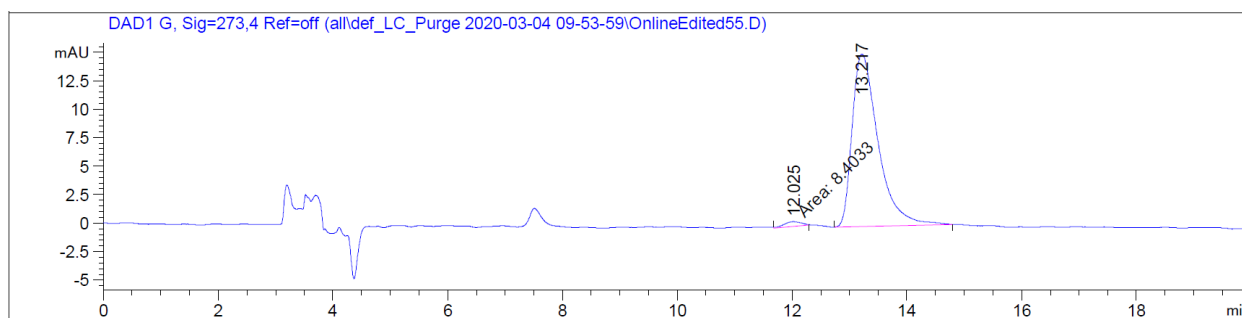
Peak #	RetTime [min]	Type	Width [min]	Area [mAU*s]	Height [mAU]	Area %
1	17.212	BV R	0.3824	3371.56104	132.27379	99.1521
2	21.473	MM	0.4304	28.83274	1.11645	0.8479



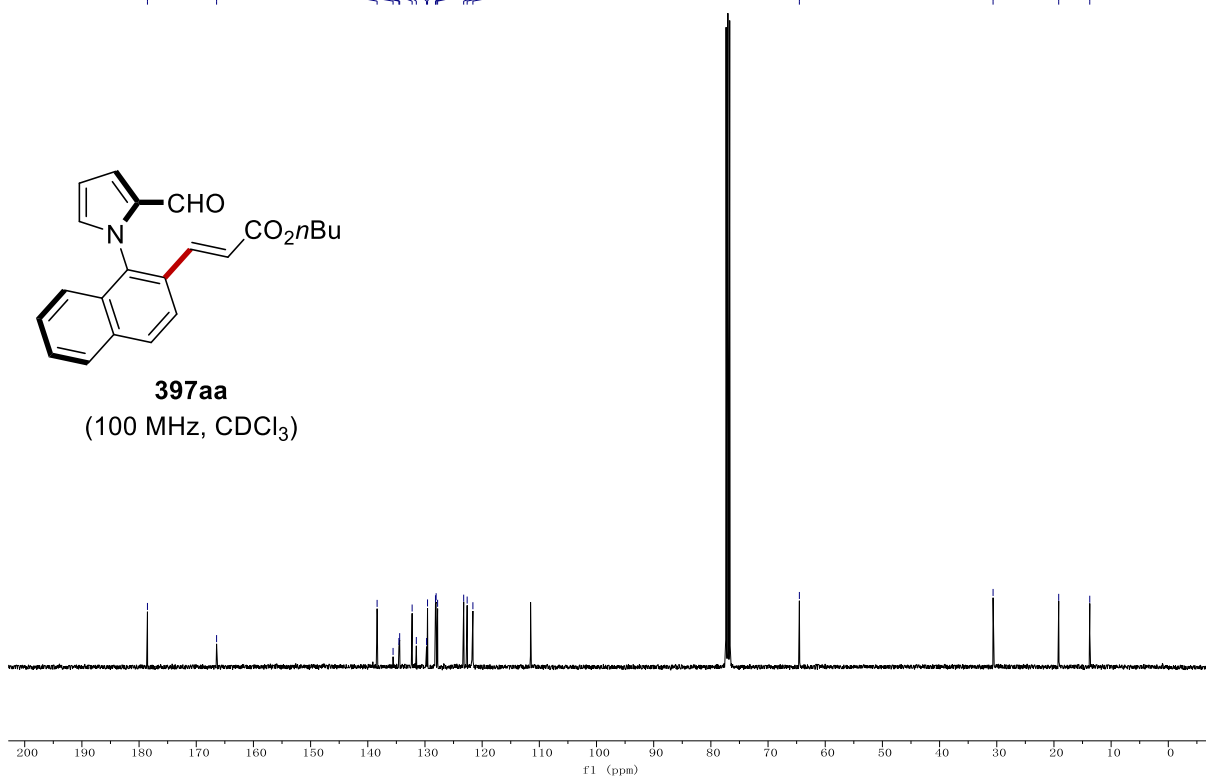
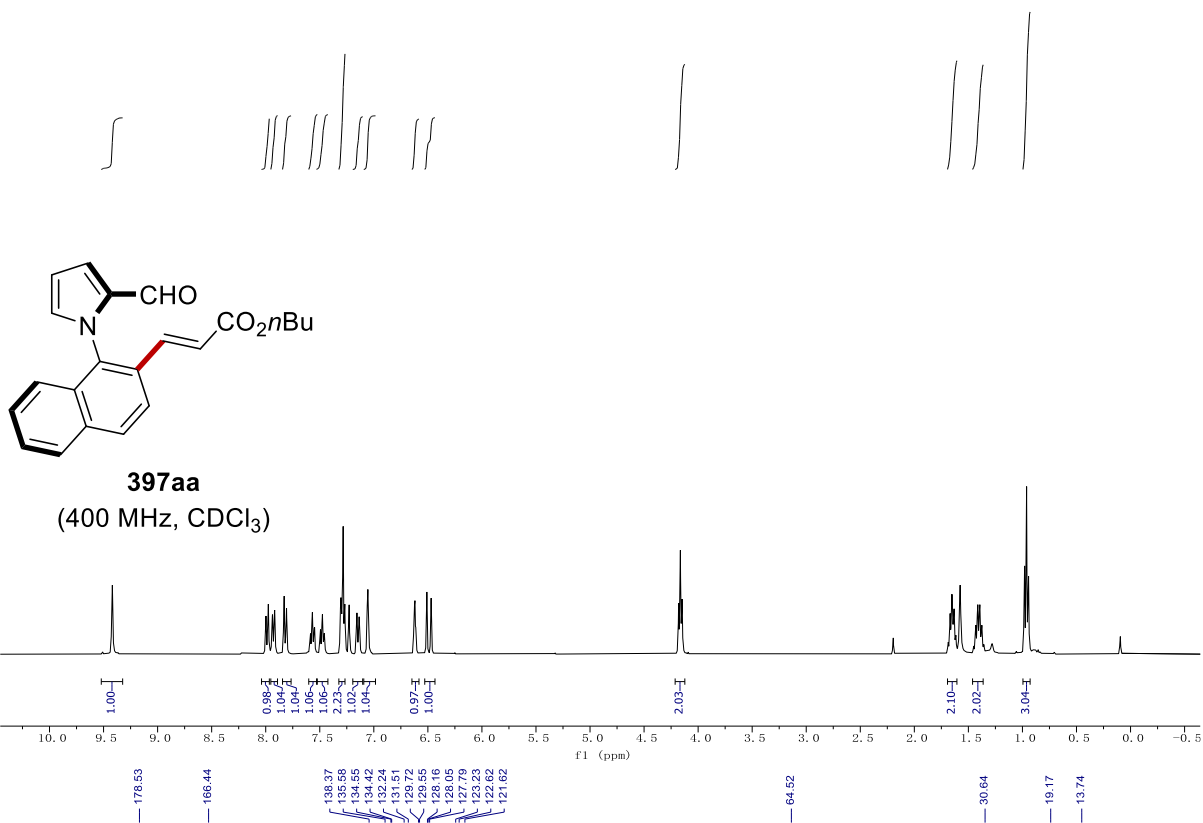
Chiral HPLC of 74bj:



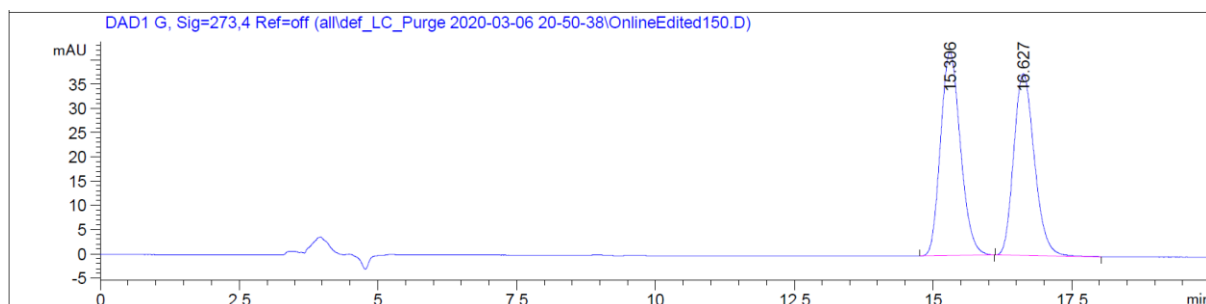
Peak #	RetTime [min]	Type	Width [min]	Area [mAU*s]	Height [mAU]	Area %
1	11.893	MM	0.4406	2980.97485	112.75633	49.0624
2	13.129	MM	0.4903	3094.91162	105.20934	50.9376



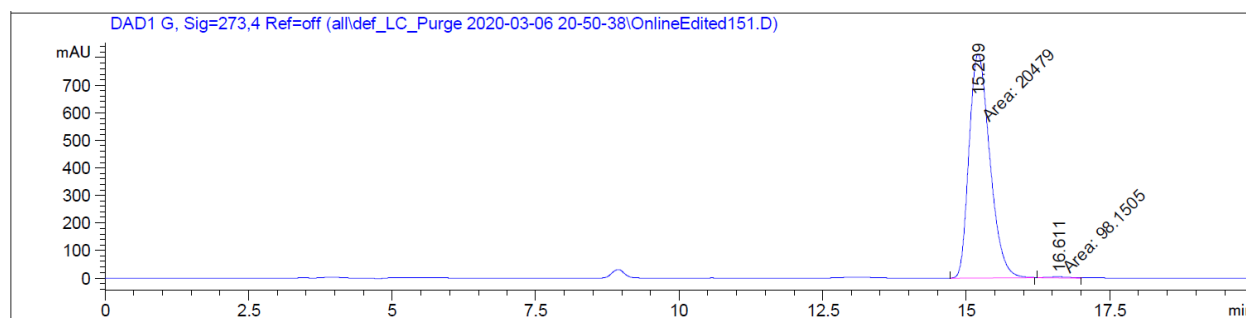
Peak #	RetTime [min]	Type	Width [min]	Area [mAU*s]	Height [mAU]	Area %
1	12.025	MM	0.3340	8.40330	4.19342e-1	1.7344
2	13.217	BB	0.4540	476.10797	15.13699	98.2656



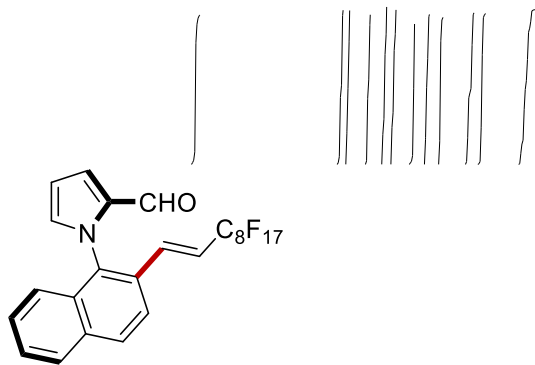
Chiral HPLC of 397aa:



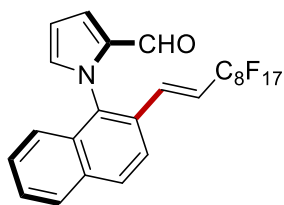
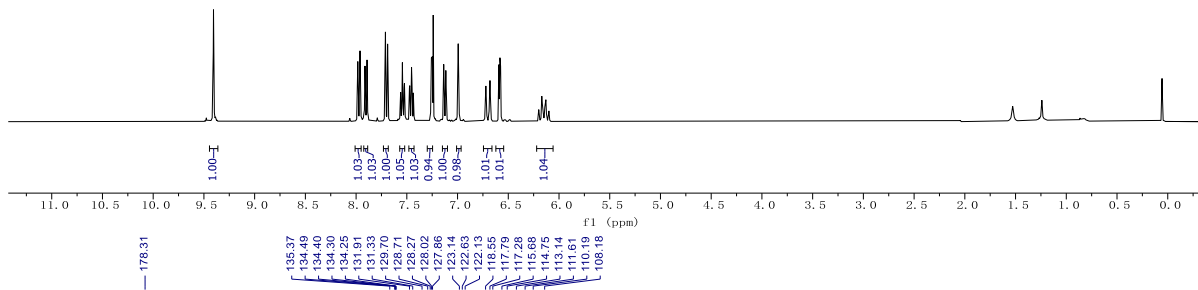
Peak #	RetTime [min]	Type	Width [min]	Area [mAU*s]	Height [mAU]	Area %
1	15.306	BB	0.3872	1047.60132	41.97161	51.8956
2	16.627	BB	0.3998	971.06842	37.53279	48.1044



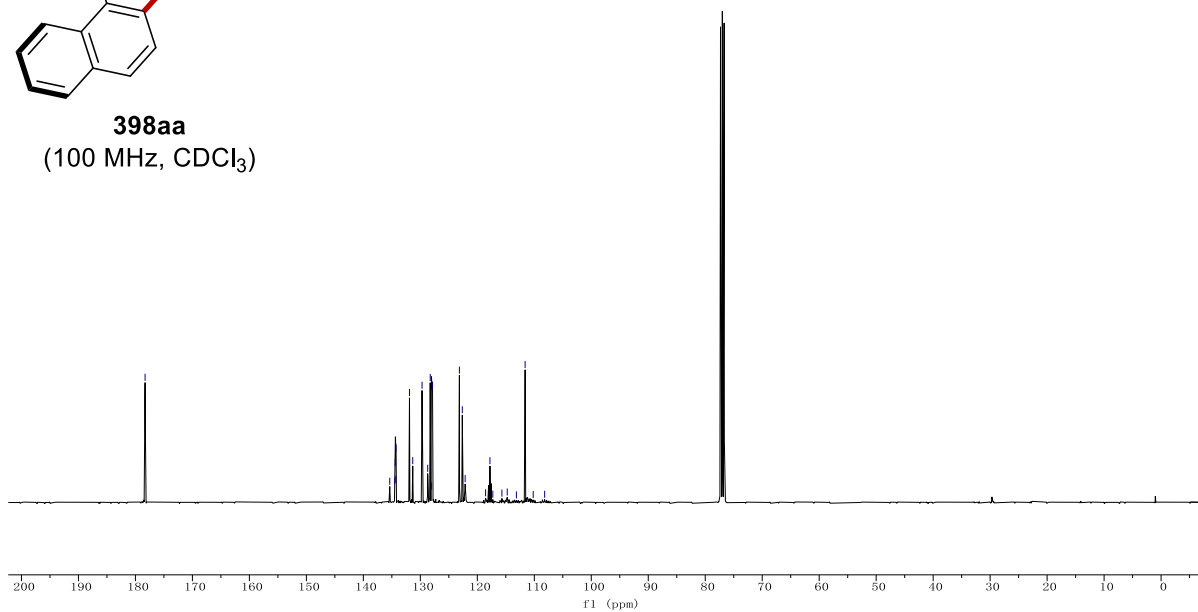
Peak #	RetTime [min]	Type	Width [min]	Area [mAU*s]	Height [mAU]	Area %
1	15.209	MM	0.4203	2.04790e4	812.01709	99.5230
2	16.611	MM	0.4321	98.15052	3.78579	0.4770

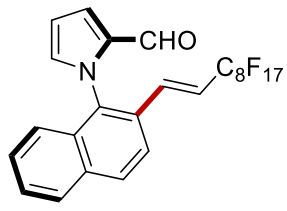


398aa
(400 MHz, CDCl₃)

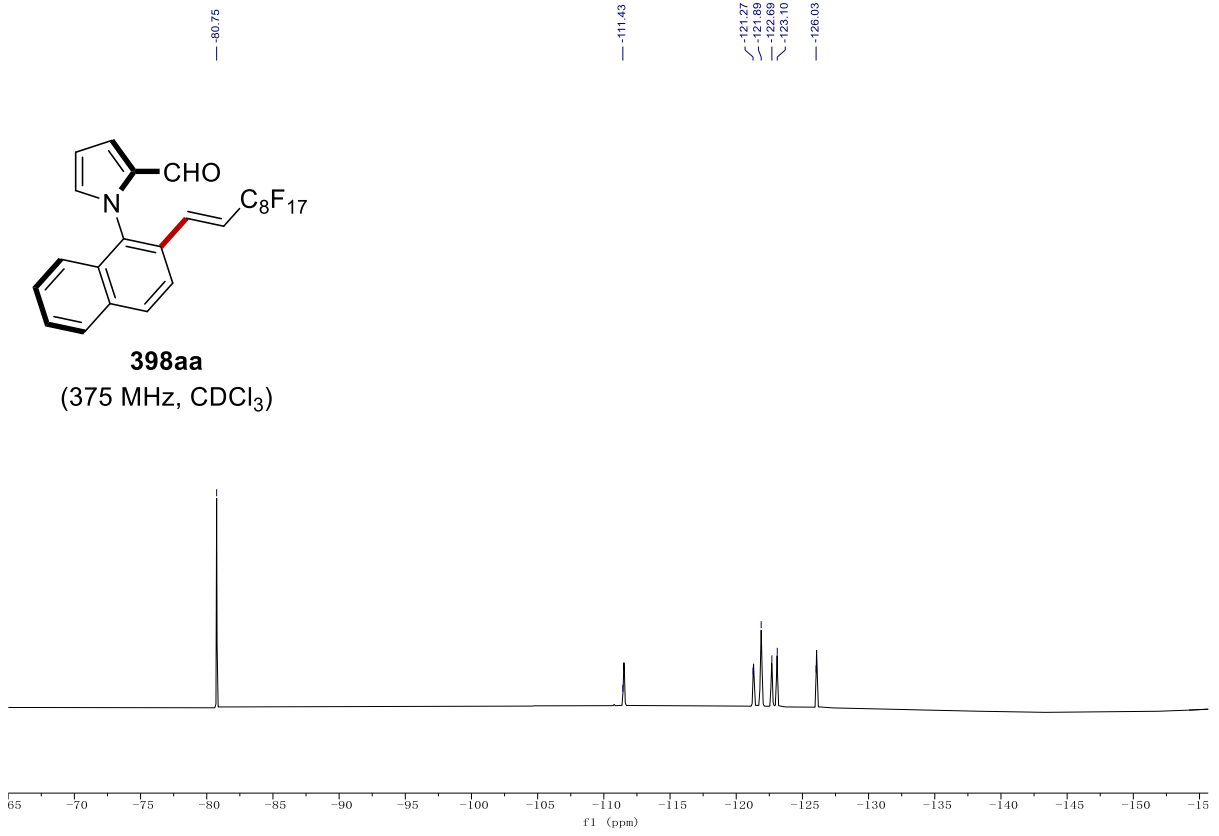


398aa
(100 MHz, CDCl₃)

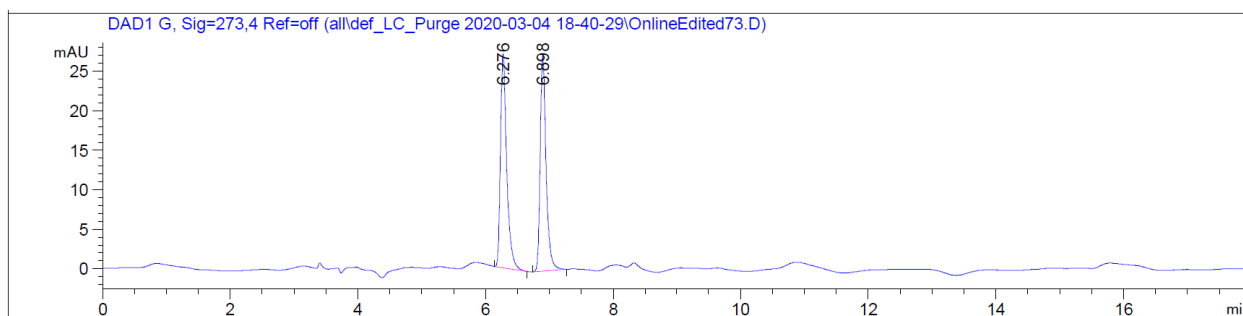




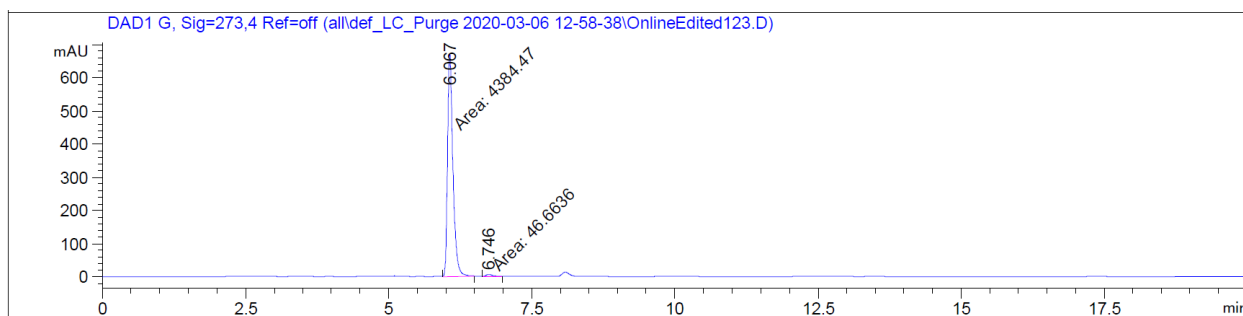
398aa
(375 MHz, CDCl₃)



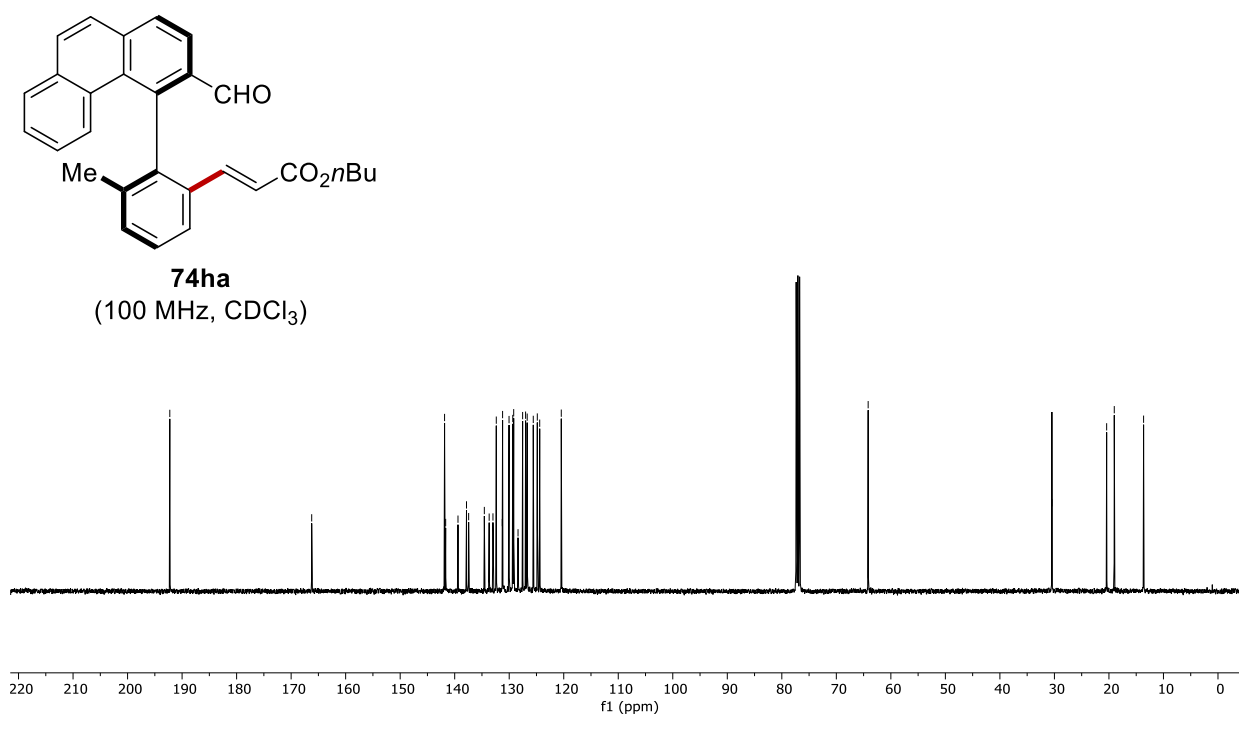
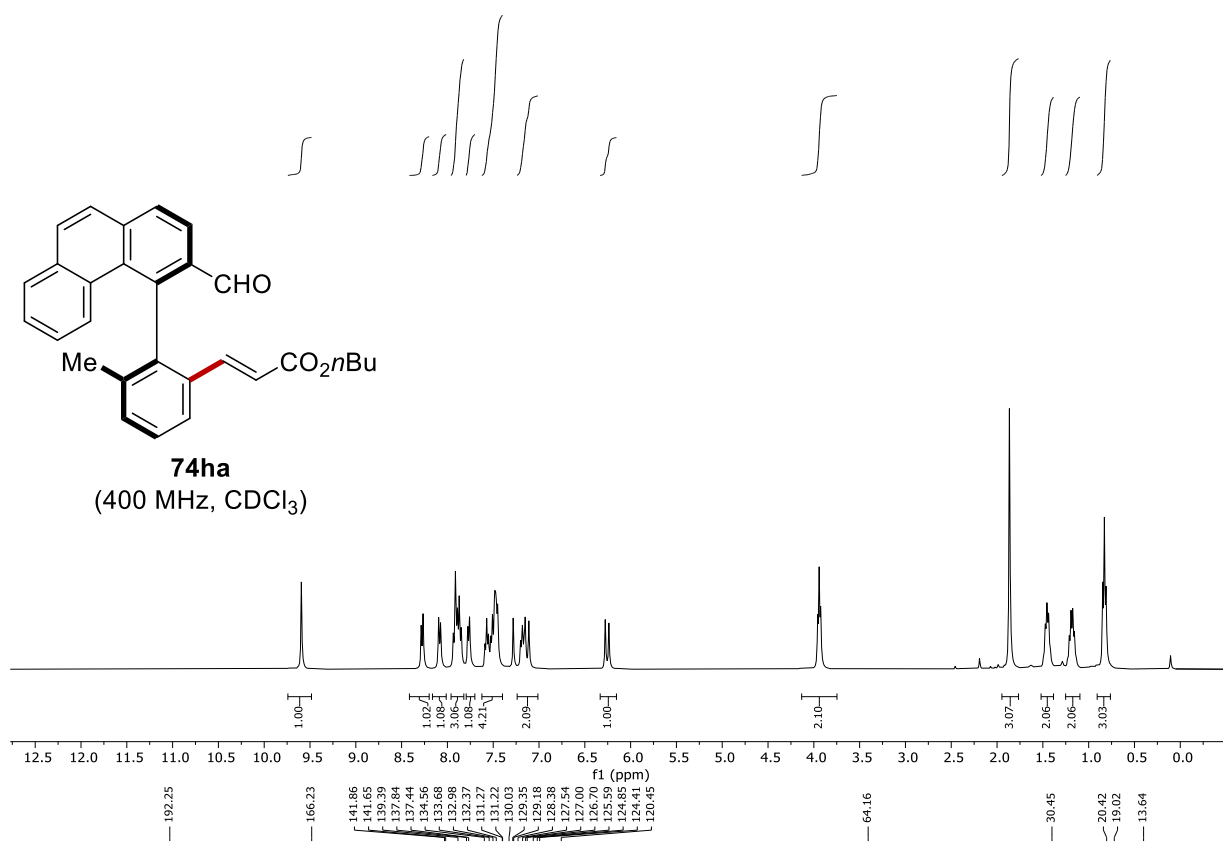
Chiral HPLC of **398aa**:



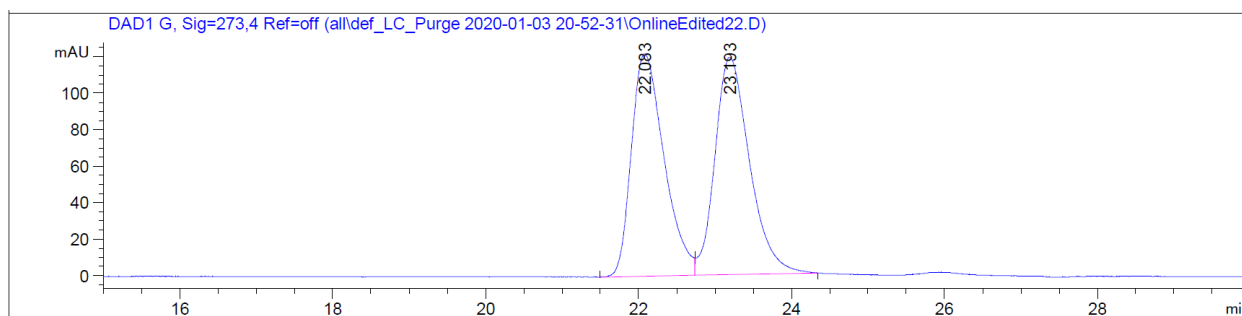
Peak #	RetTime [min]	Type	Width [min]	Area [mAU*s]	Height [mAU]	Area %
1	6.276	BB	0.1008	183.09755	27.10444	51.1153
2	6.898	BB	0.0957	175.10777	27.36011	48.8847



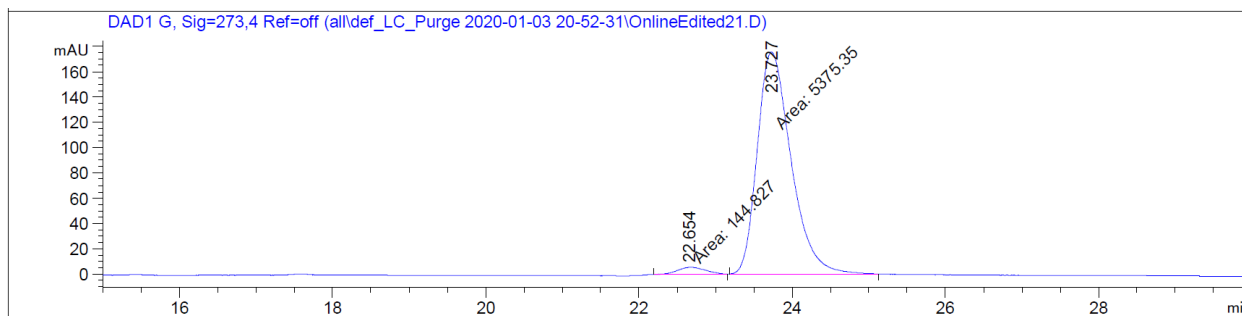
Peak #	RetTime [min]	Type	Width [min]	Area [mAU*s]	Height [mAU]	Area %
1	6.067	MM	0.1086	4384.47314	672.57892	98.9469
2	6.746	MM	0.1356	46.66362	5.73591	1.0531



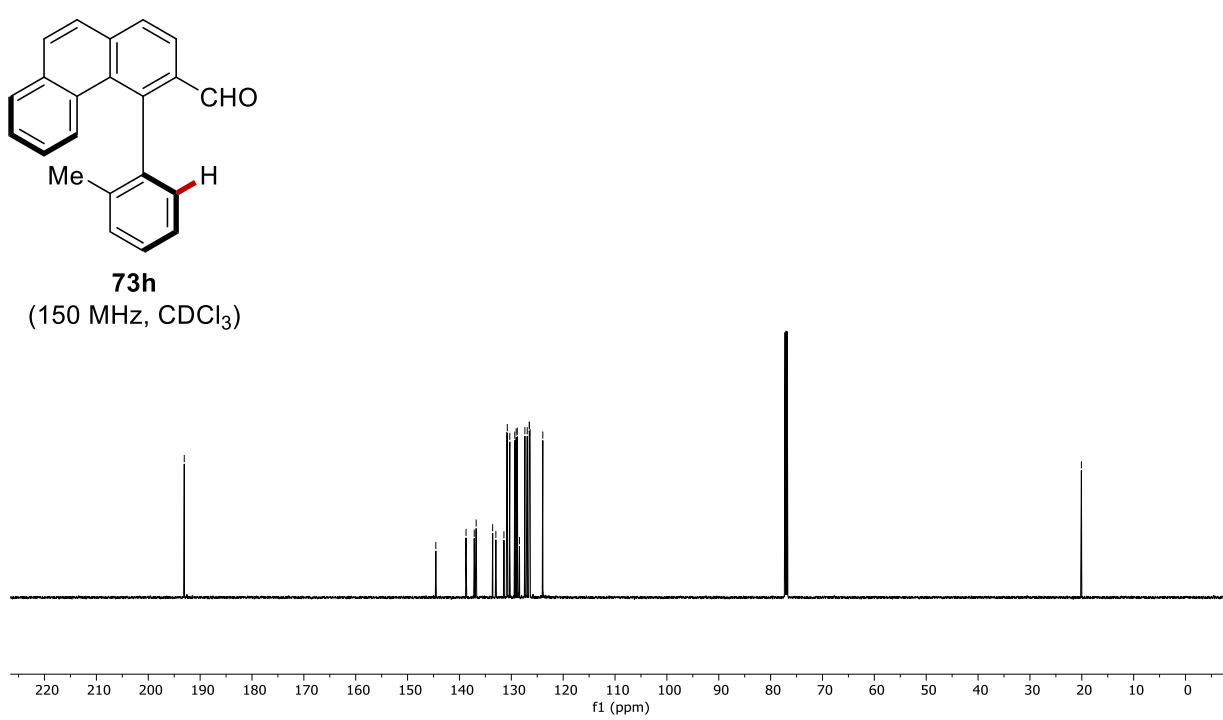
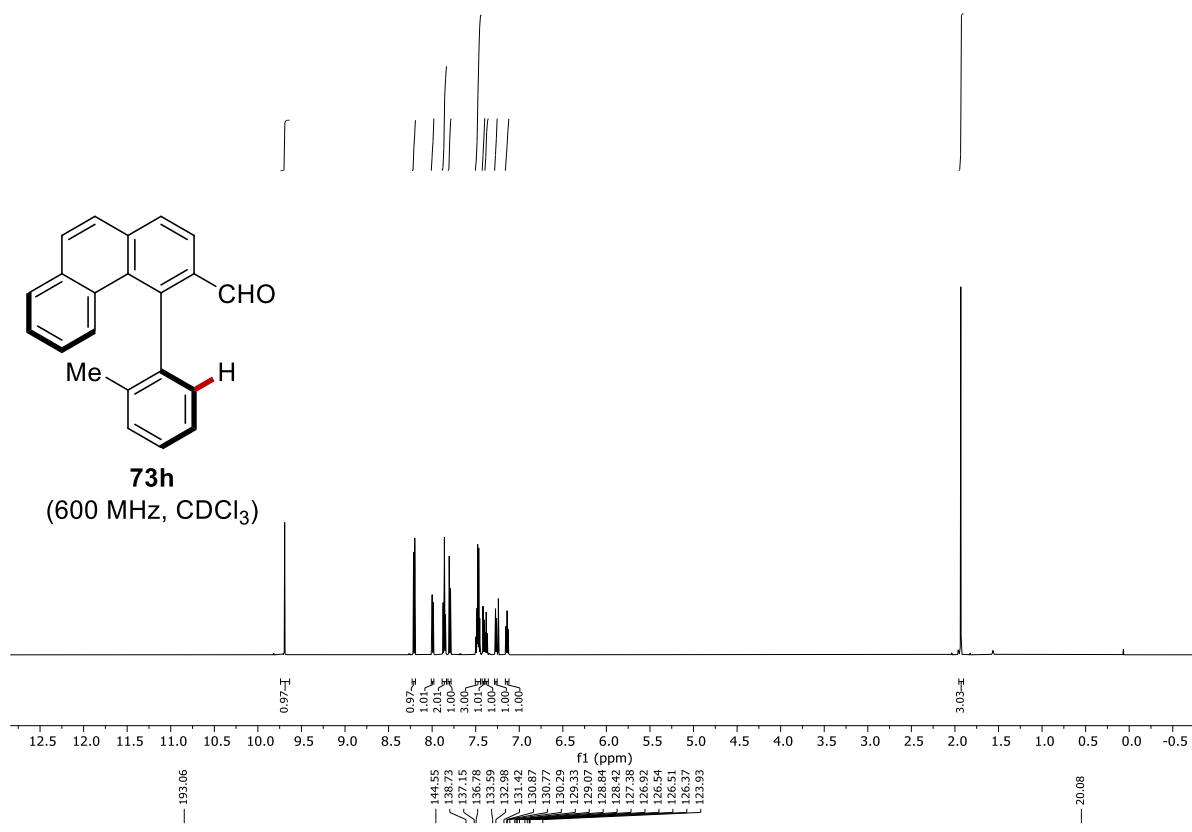
Chiral HPLC of **74ha**:



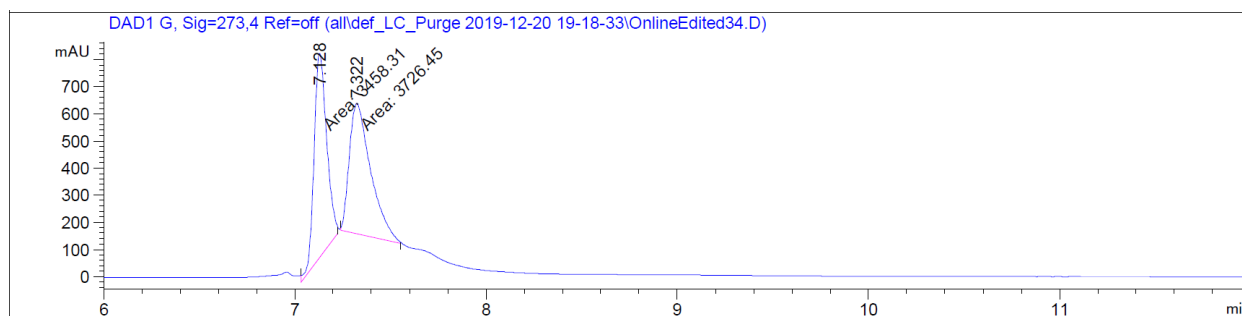
Peak #	RetTime [min]	Type	Width [min]	Area [mAU*s]	Height [mAU]	Area %
1	22.083	BV	0.4136	3627.21289	122.07781	49.1056
2	23.193	VV R	0.4450	3759.34546	119.16909	50.8944



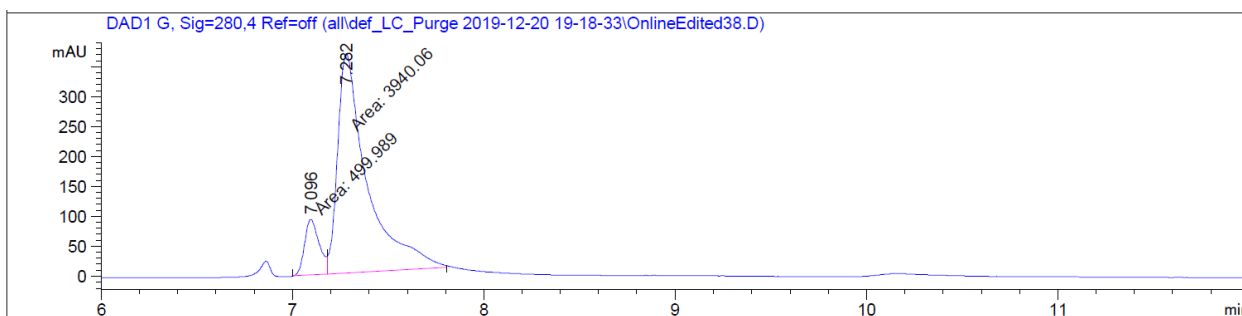
Peak #	RetTime [min]	Type	Width [min]	Area [mAU*s]	Height [mAU]	Area %
1	22.654	MM	0.4270	144.82655	5.65305	2.6236
2	23.727	MM	0.5103	5375.34961	175.55560	97.3764



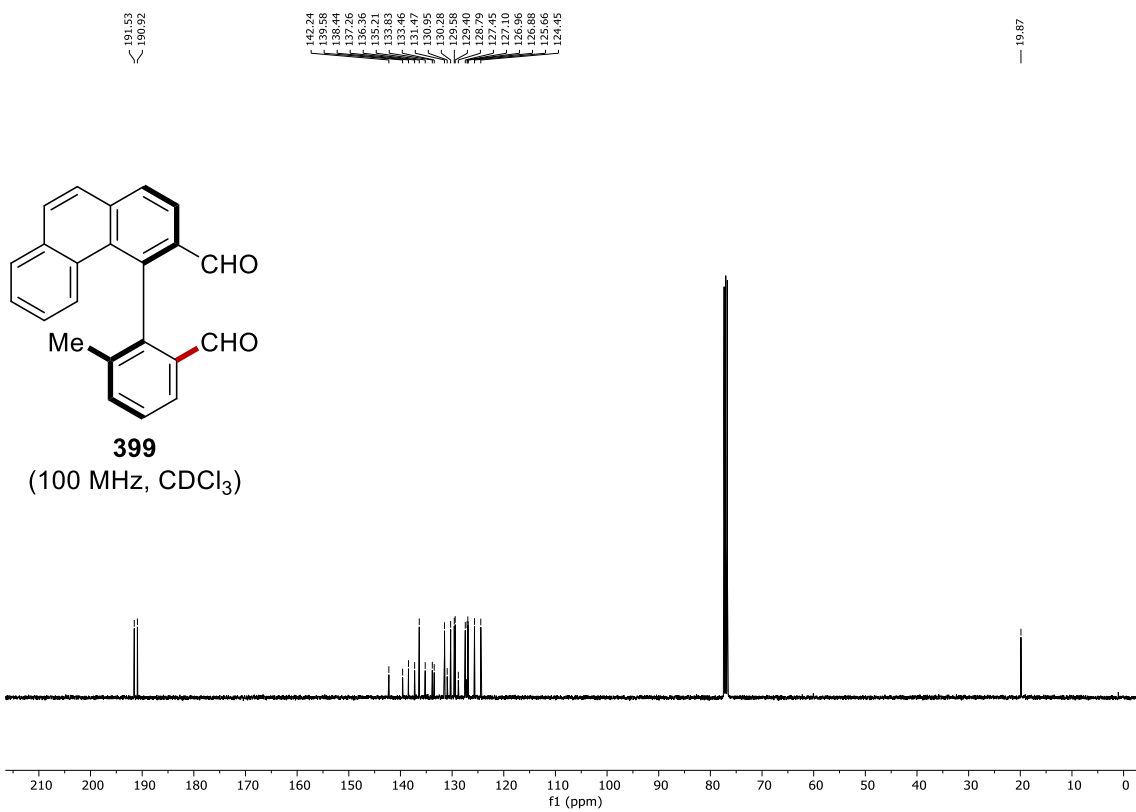
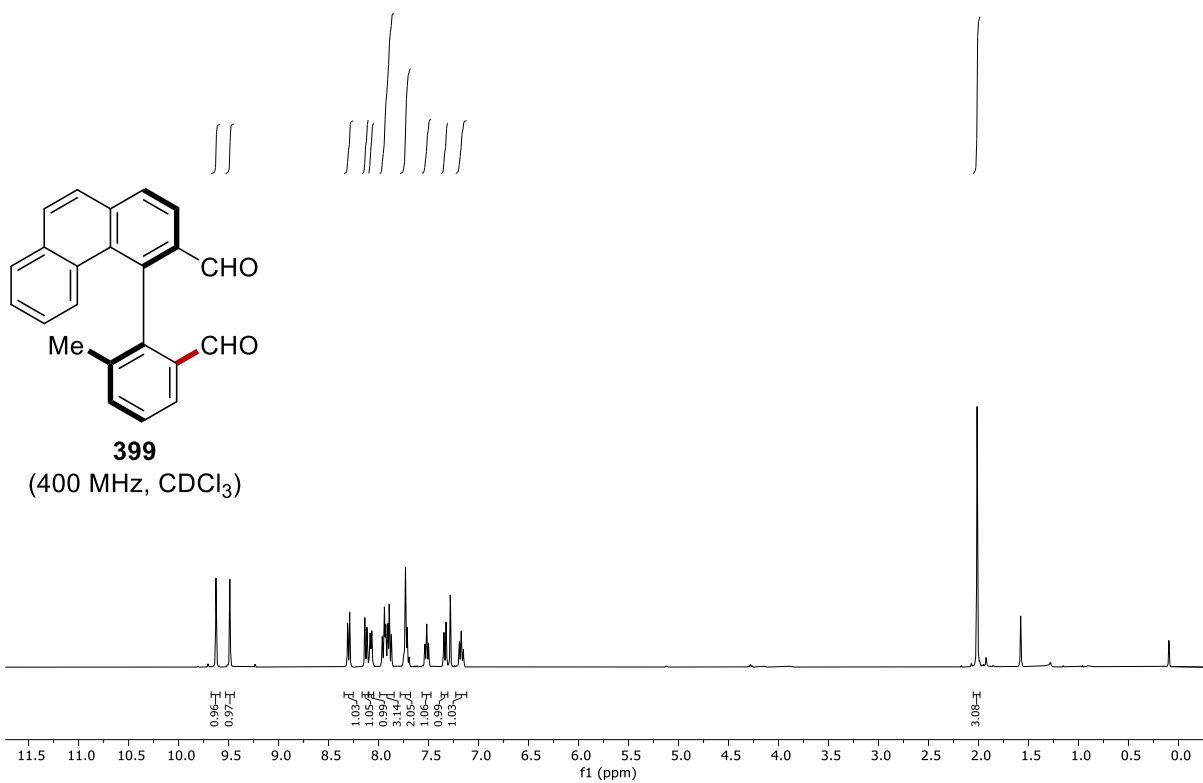
Chiral HPLC of 73h:

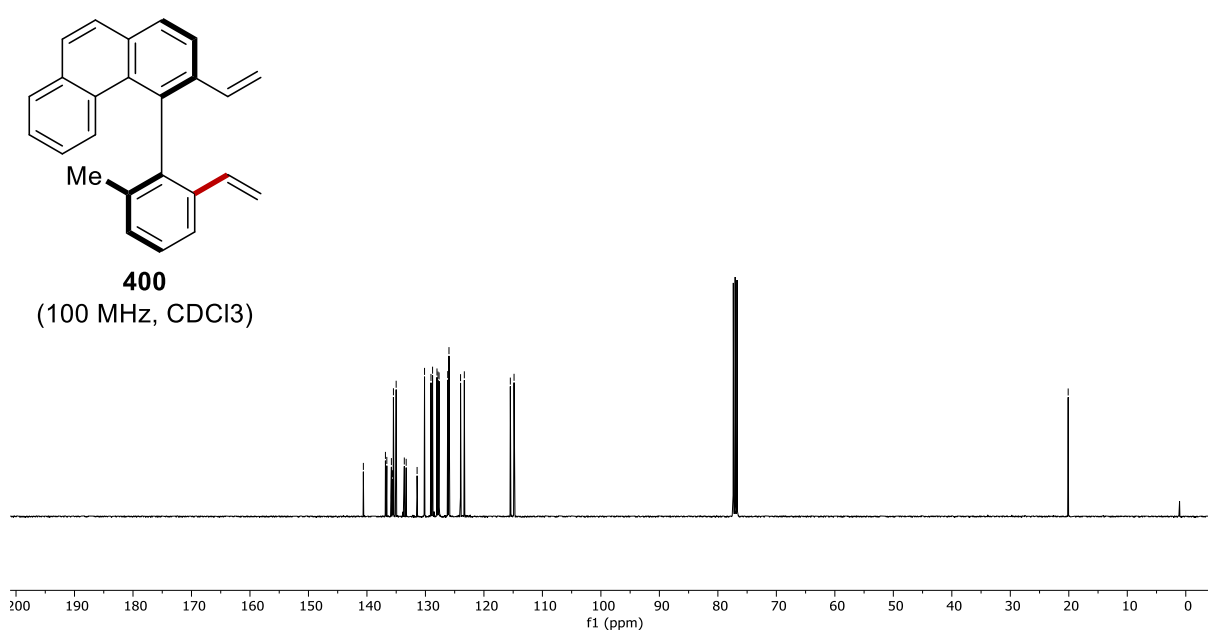
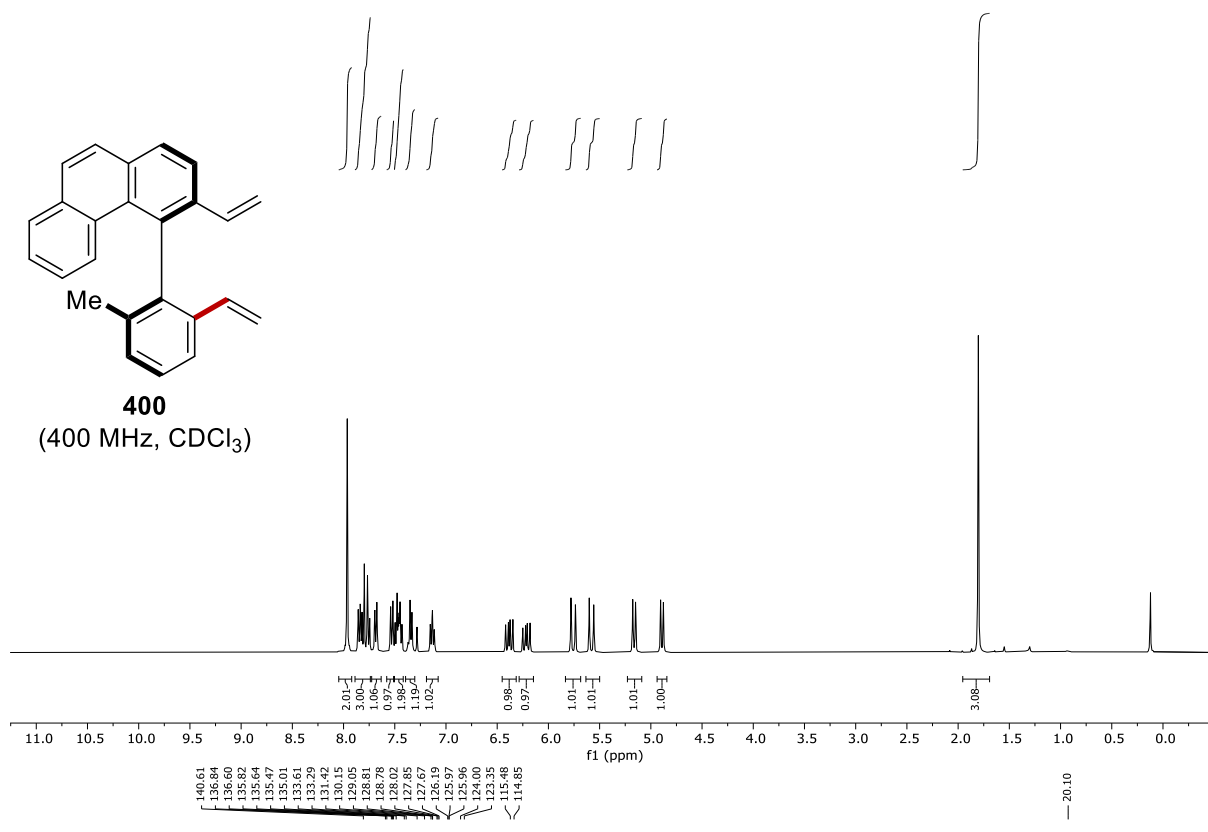


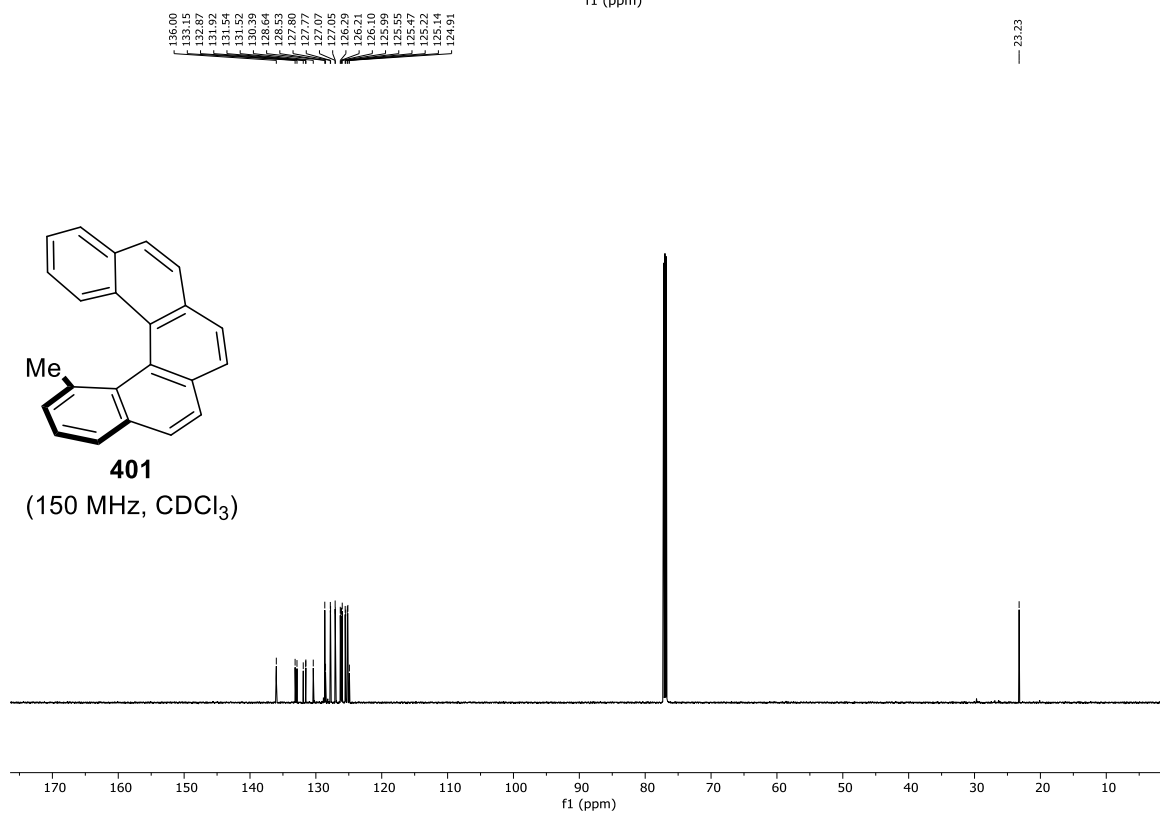
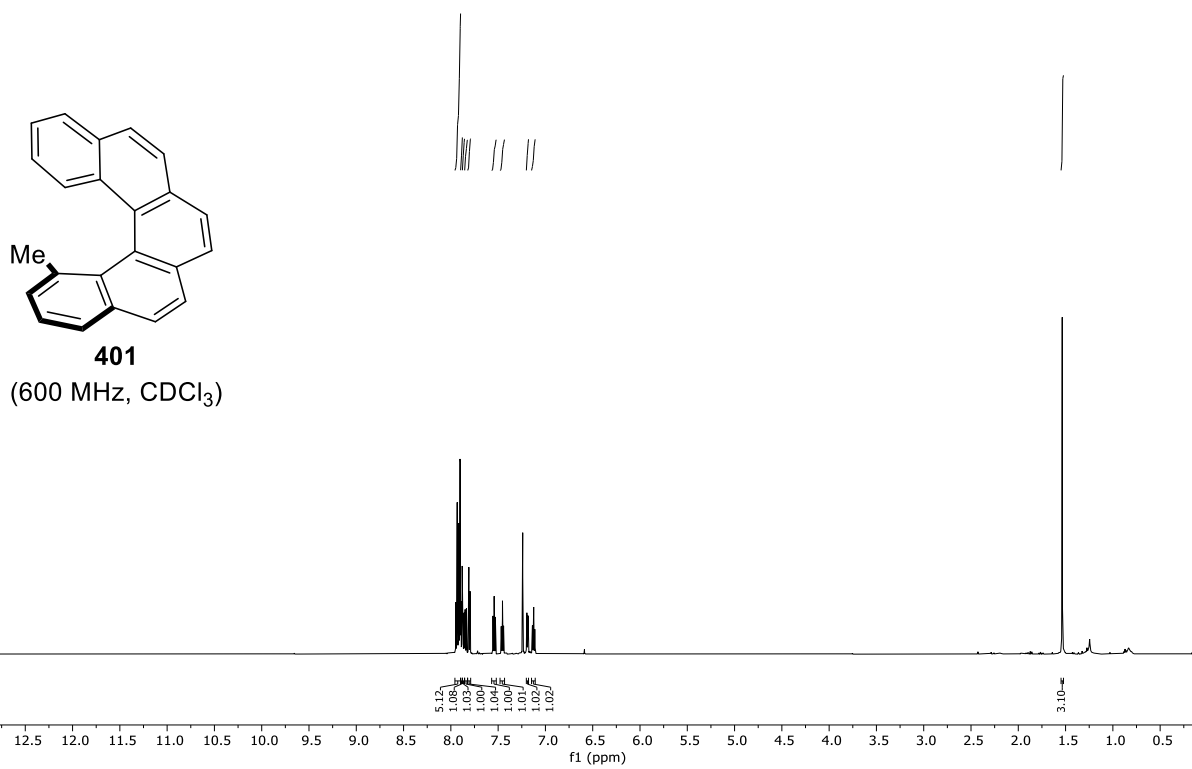
Peak #	RetTime [min]	Type	Width [min]	Area [mAU*s]	Height [mAU]	Area %
1	7.128	MM	0.0762	3458.30835	756.70020	48.1340
2	7.322	MM	0.1294	3726.44995	479.81186	51.8660



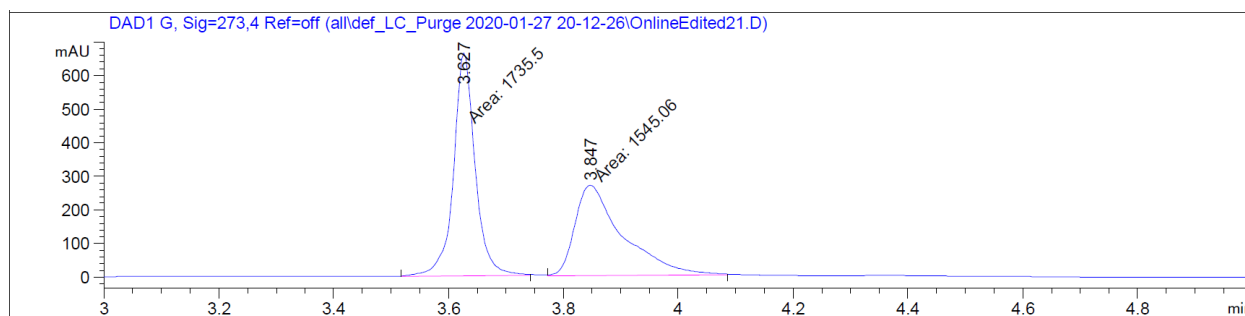
Peak #	RetTime [min]	Type	Width [min]	Area [mAU*s]	Height [mAU]	Area %
1	7.096	MF	0.0895	499.98941	93.06744	11.2609
2	7.282	FM	0.1789	3940.06128	367.04150	88.7391



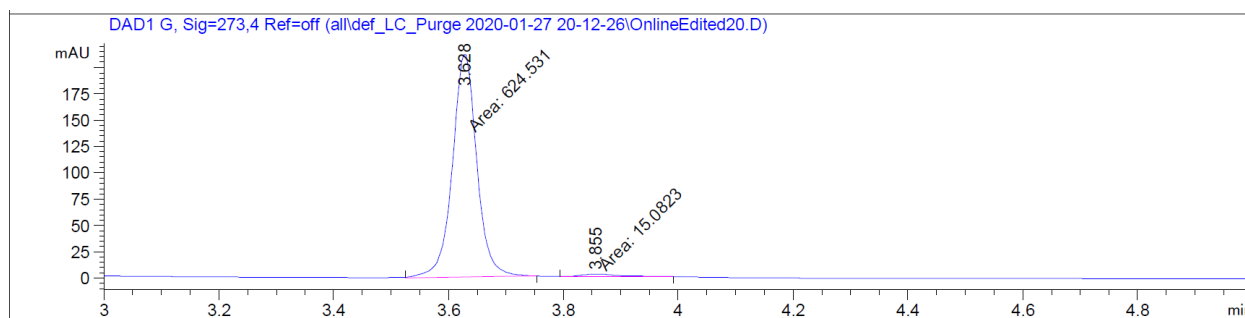




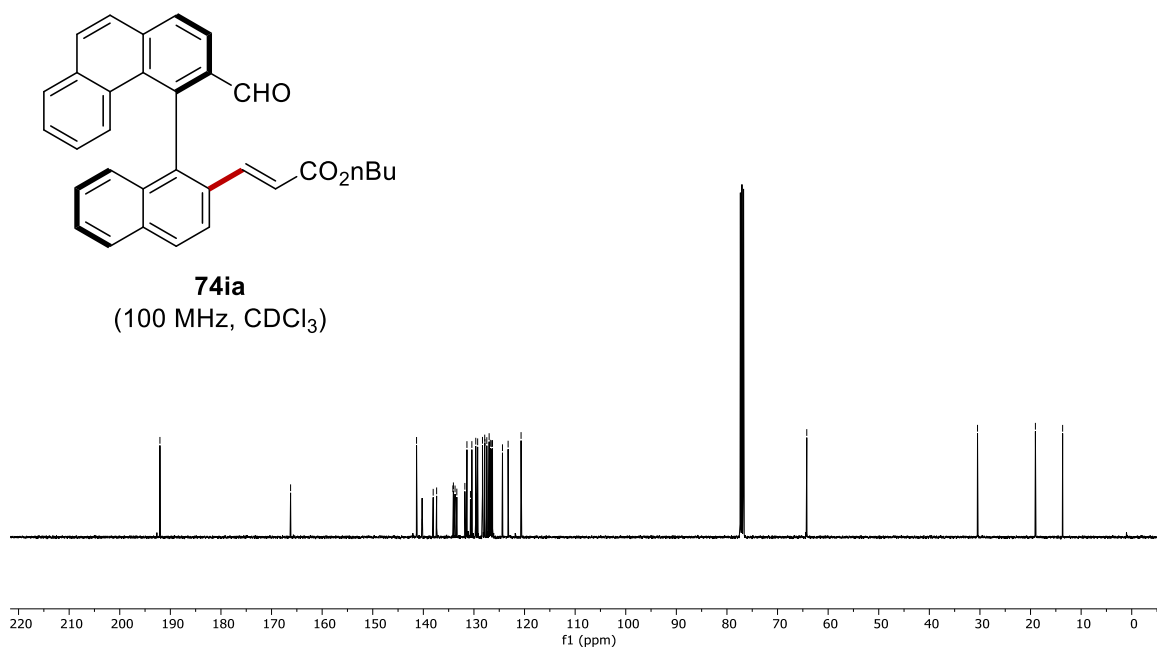
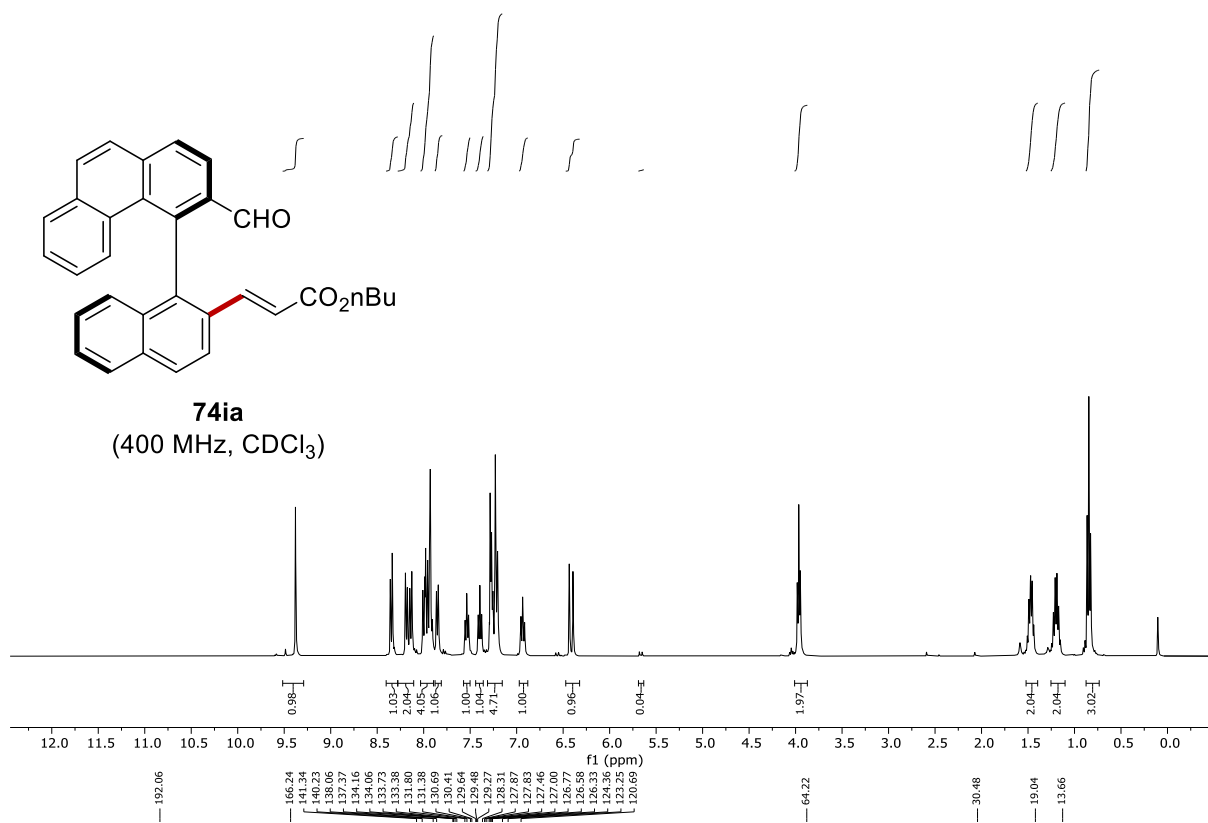
Chiral HPLC of **401**:



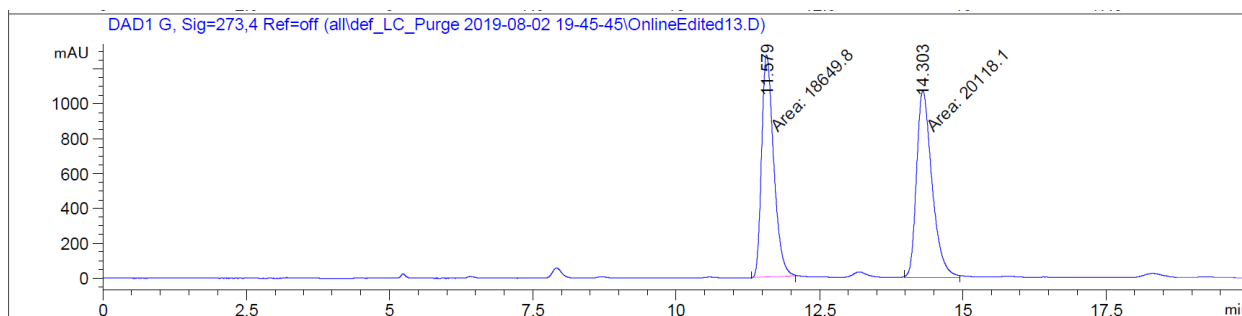
Peak #	RetTime [min]	Type	Width [min]	Area [mAU*s]	Height [mAU]	Area %
1	3.627	MM	0.0435	1735.49817	664.56525	52.9026
2	3.847	MM	0.0956	1545.05713	269.50018	47.0974



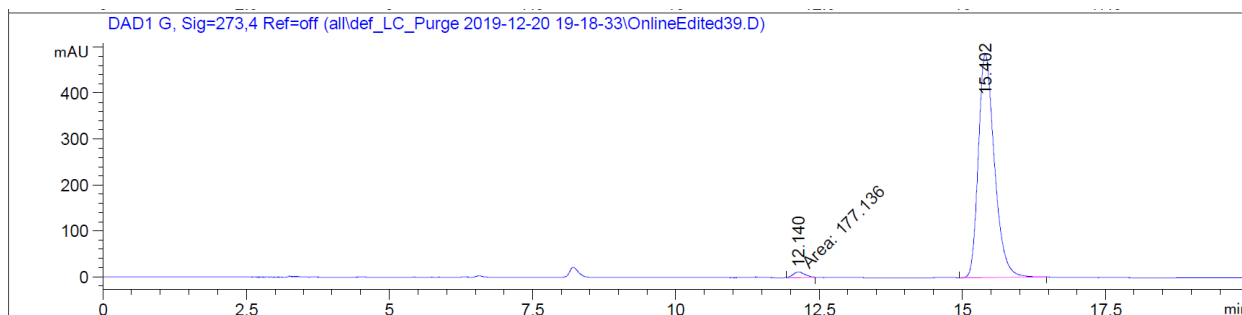
Peak #	RetTime [min]	Type	Width [min]	Area [mAU*s]	Height [mAU]	Area %
1	3.628	MM	0.0491	624.53143	212.18314	97.6420
2	3.855	MM	0.0893	15.08230	2.81371	2.3580



Chiral HPLC of **74ia**:

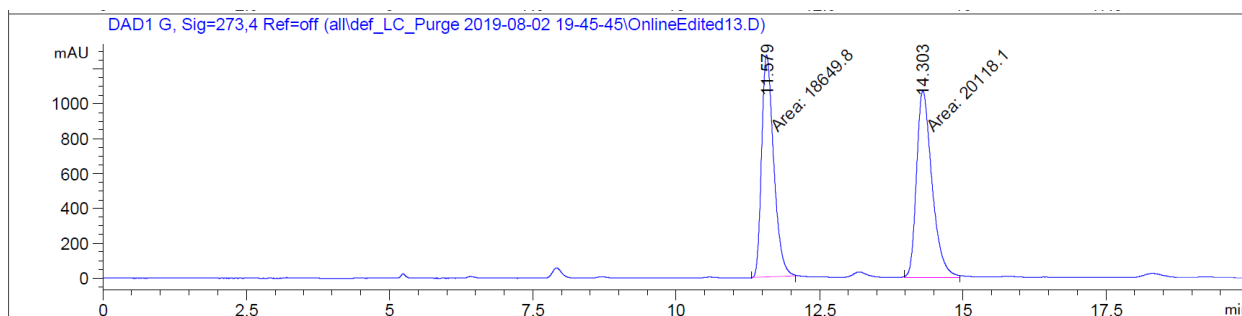


Peak #	RetTime [min]	Type	Width [min]	Area [mAU*s]	Height [mAU]	Area %
1	11.579	MM	0.2440	1.86498e4	1273.93860	48.1064
2	14.303	MM	0.3132	2.01181e4	1070.61853	51.8936

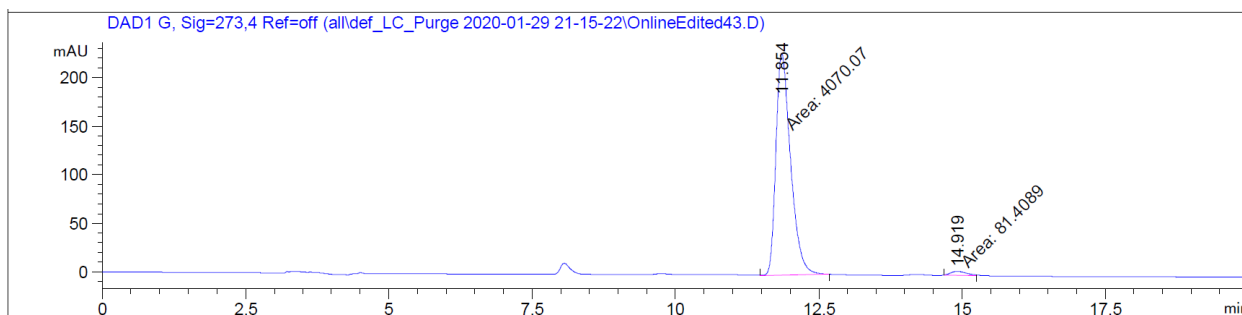


Peak #	RetTime [min]	Type	Width [min]	Area [mAU*s]	Height [mAU]	Area %
1	12.140	MM	0.2389	177.13626	12.35697	1.8337
2	15.402	BB	0.2963	9483.09766	486.68011	98.1663

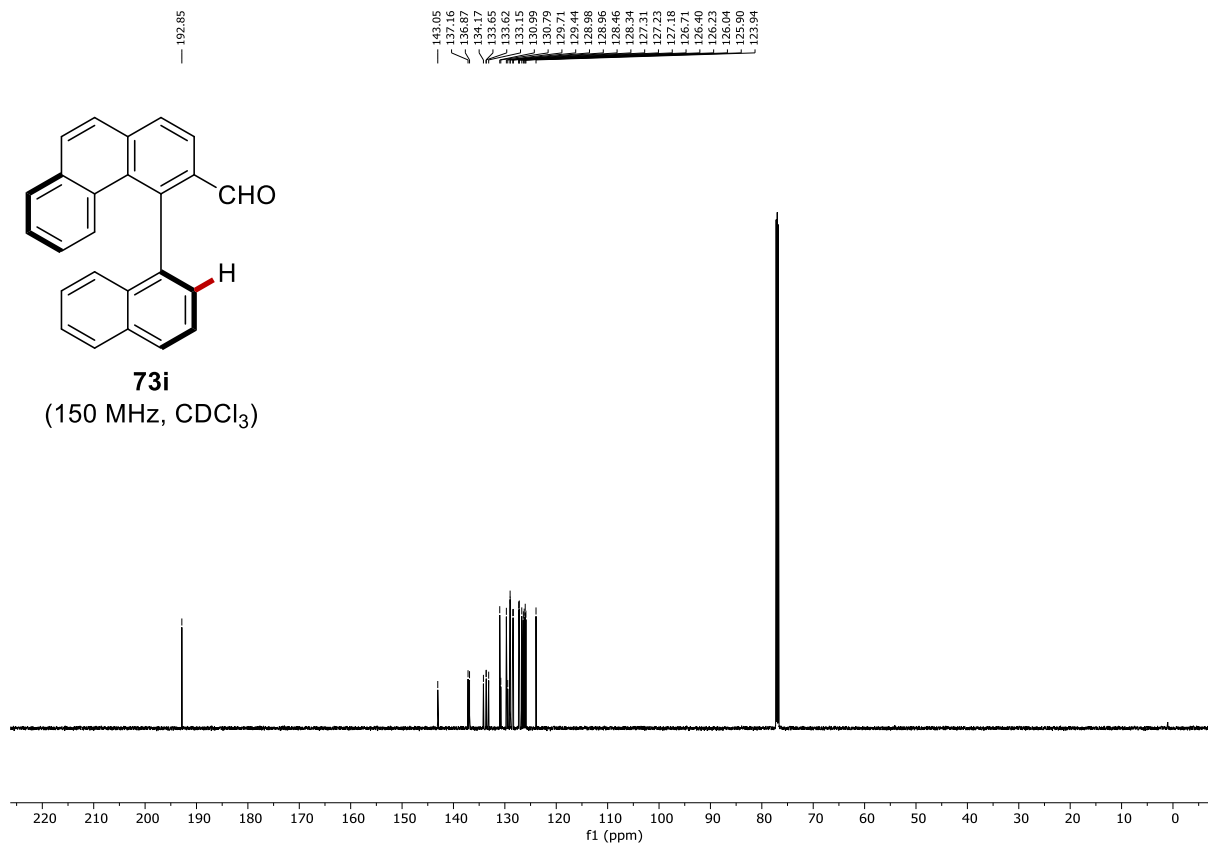
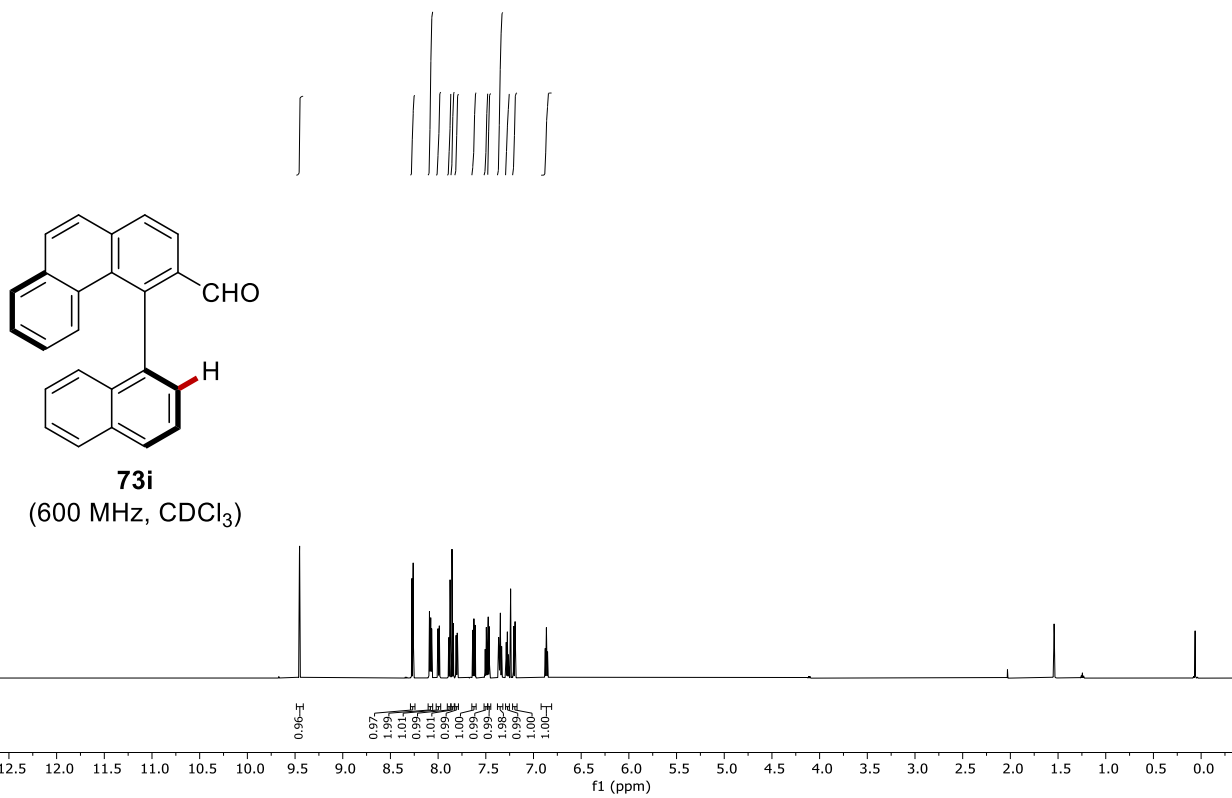
HPLC spectra (-)74ia



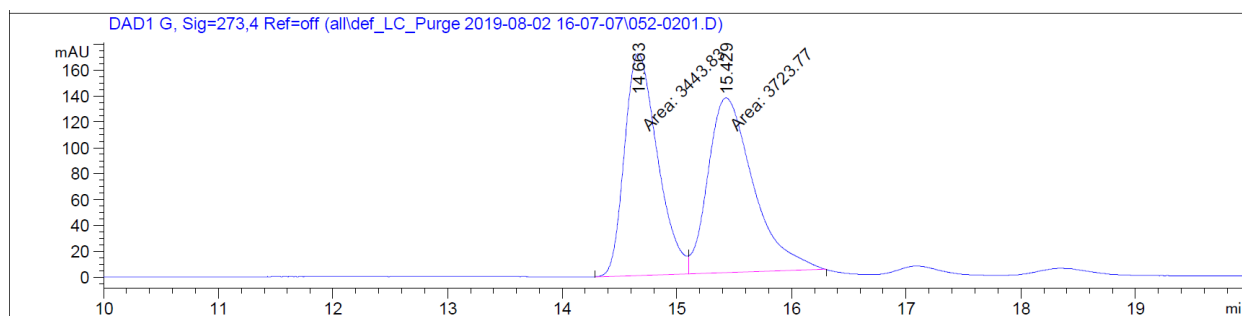
Peak #	RetTime [min]	Type	Width [min]	Area [mAU*s]	Height [mAU]	Area %
1	11.579	MM	0.2440	1.86498e4	1273.93860	48.1064
2	14.303	MM	0.3132	2.01181e4	1070.61853	51.8936



Peak #	RetTime [min]	Type	Width [min]	Area [mAU*s]	Height [mAU]	Area %
1	11.854	MM	0.2967	4070.06567	228.66187	98.0390
2	14.919	MM	0.3266	81.40887	4.15379	1.9610

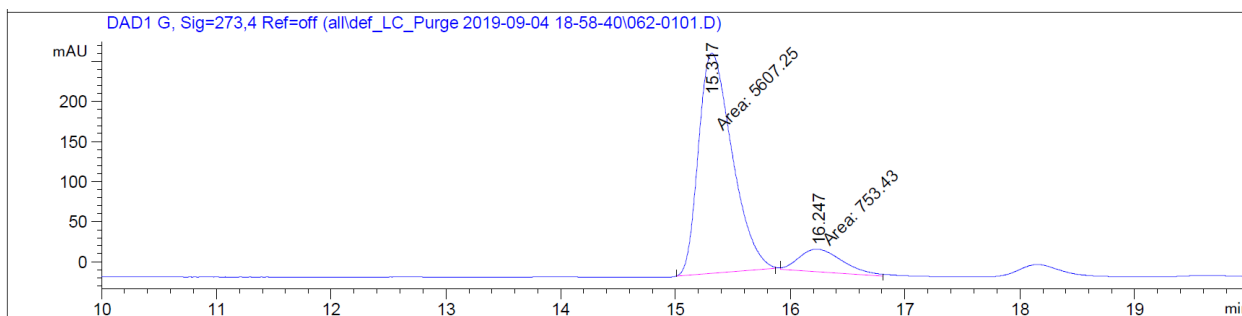


Chiral HPLC of **73i**:

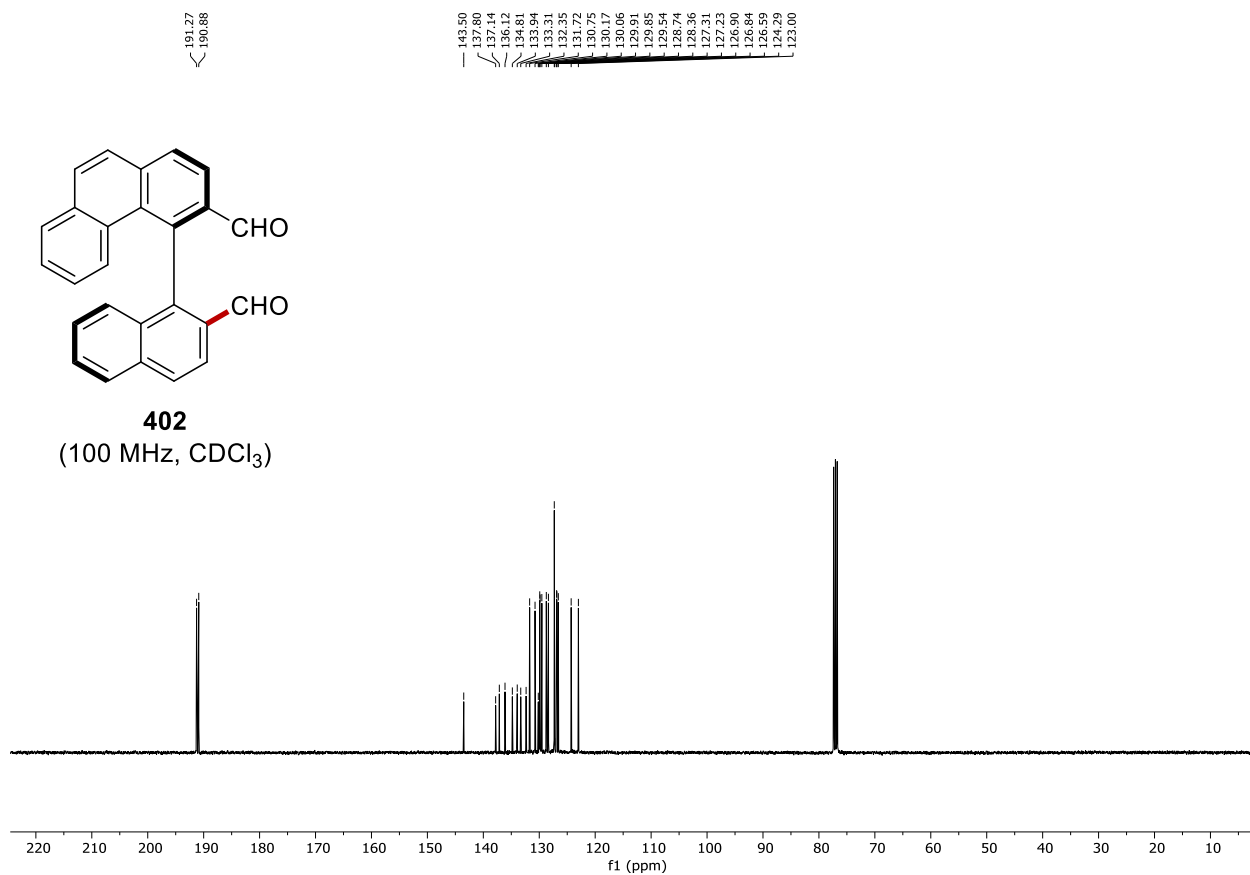
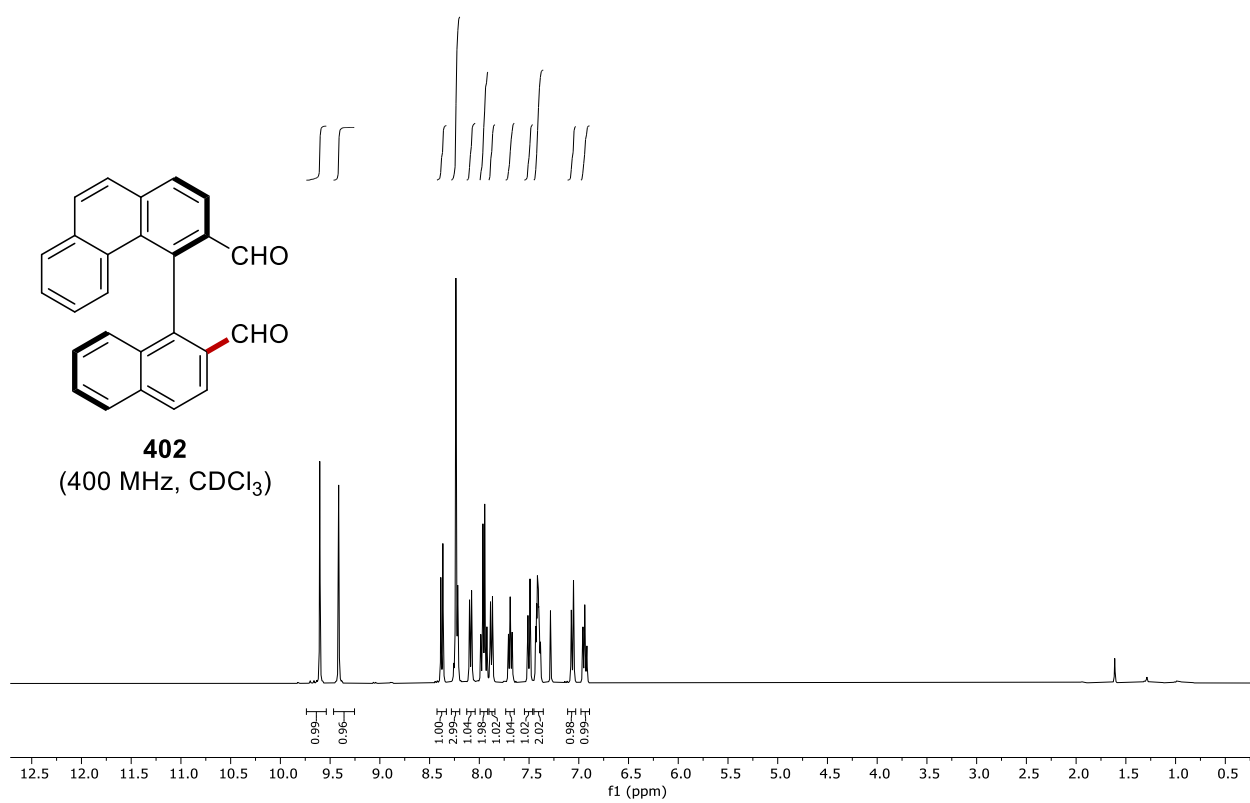


Signal 2: DAD1 G, Sig=273,4 Ref=off

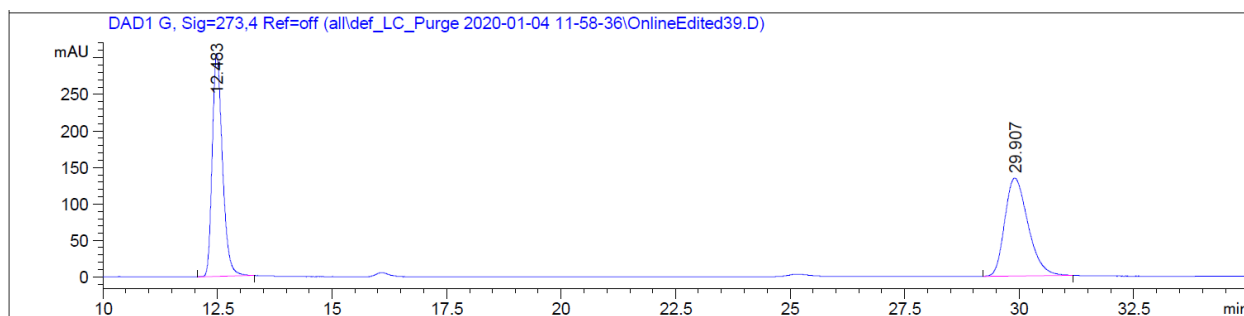
Peak #	RetTime [min]	Type	Width [min]	Area [mAU*s]	Height [mAU]	Area %
1	14.663	MF	0.3346	3443.83179	171.54404	48.0472
2	15.429	FM	0.4595	3723.76880	135.05215	51.9528



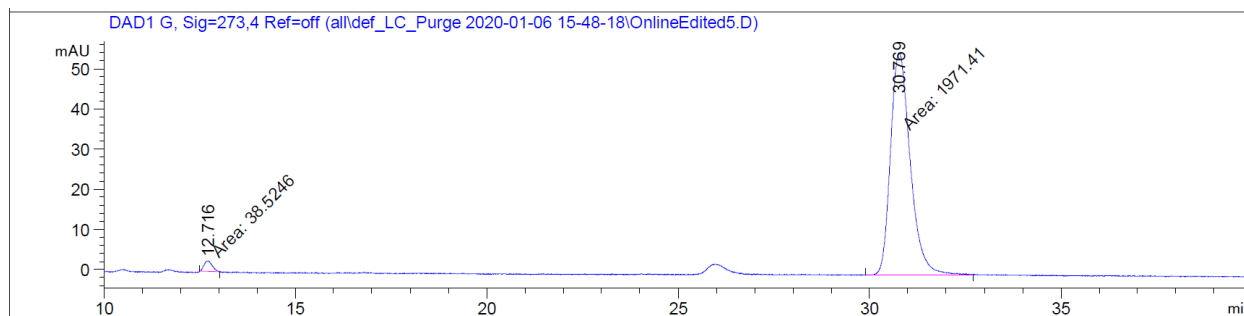
Peak #	RetTime [min]	Type	Width [min]	Area [mAU*s]	Height [mAU]	Area %
1	15.317	MM	0.3426	5678.29395	276.27515	88.2136
2	16.247	MM	0.4445	758.69177	28.44831	11.7864



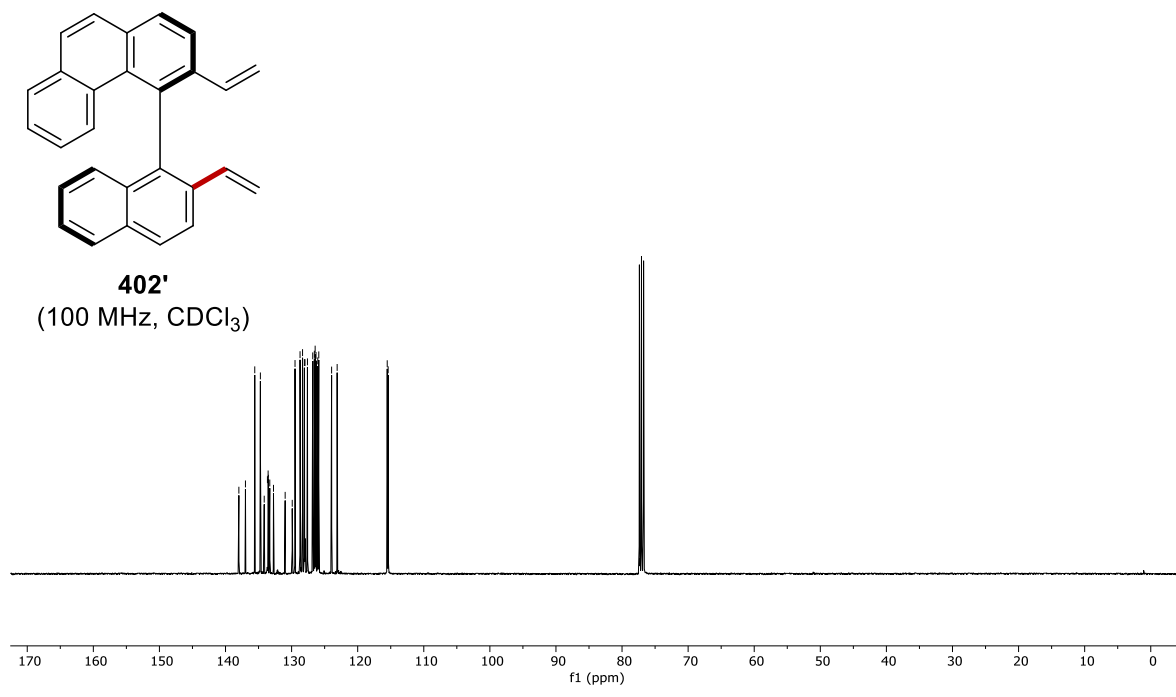
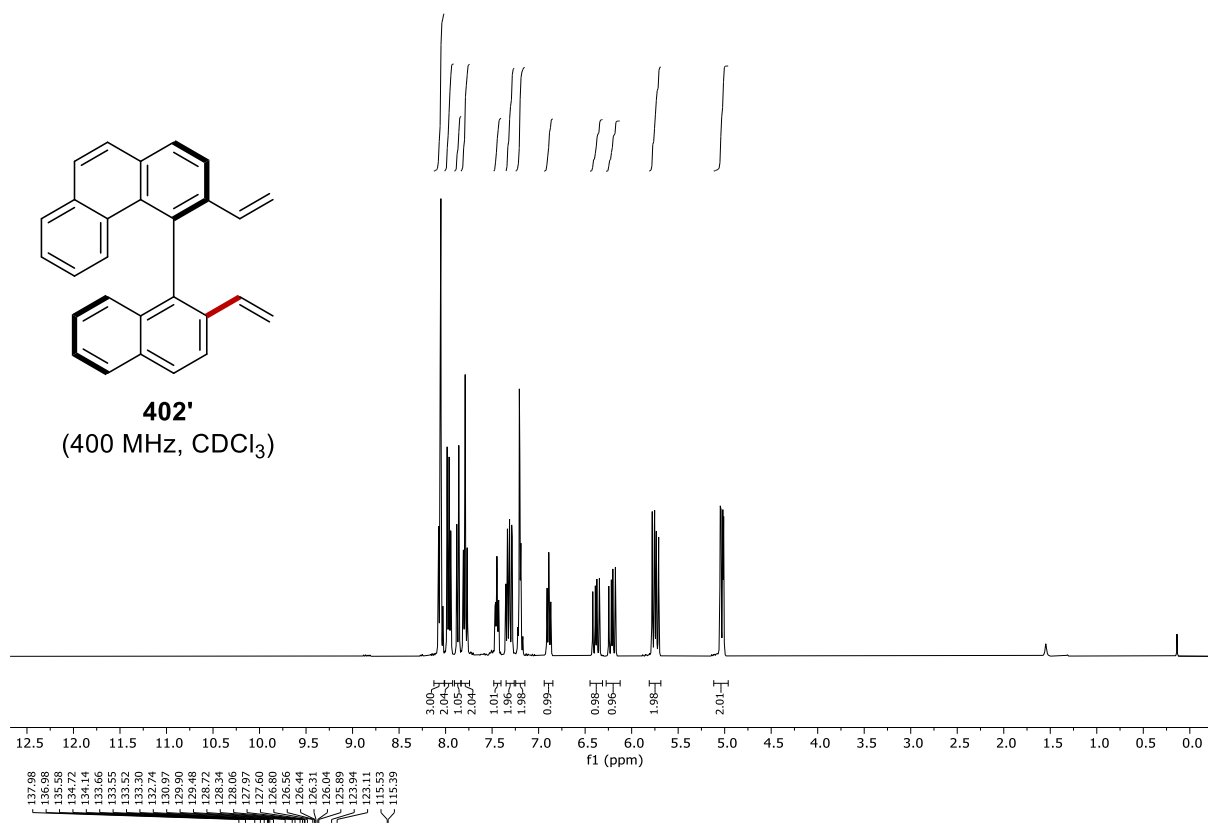
Chiral HPLC of **402**:

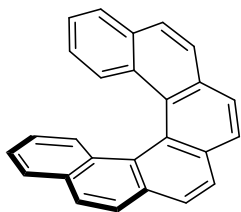


Peak #	RetTime [min]	Type	Width [min]	Area [mAU*s]	Height [mAU]	Area %
1	12.483	VV R	0.2349	4733.96582	305.23483	50.0029
2	29.907	BV R	0.4817	4733.41602	134.13223	49.9971

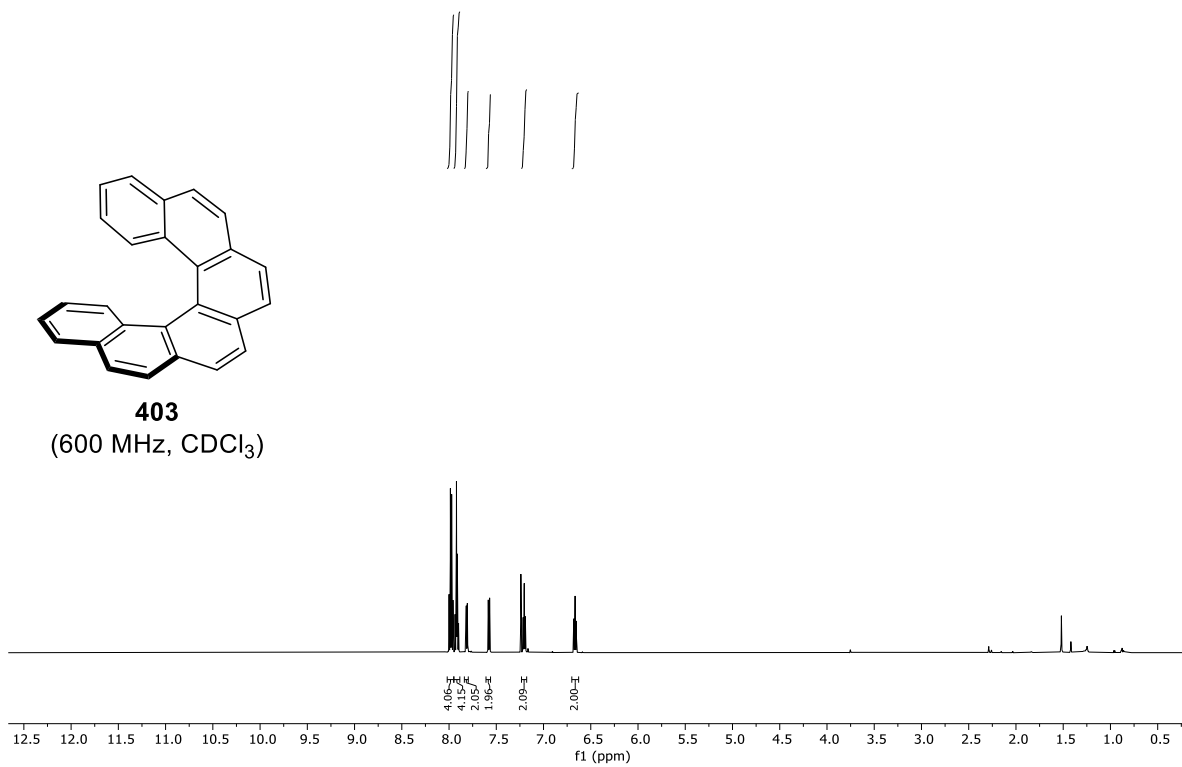


Peak #	RetTime [min]	Type	Width [min]	Area [mAU*s]	Height [mAU]	Area %
1	12.716	MM	0.2465	38.52457	2.60457	1.9167
2	30.769	MM	0.5937	1971.40845	55.33833	98.0833

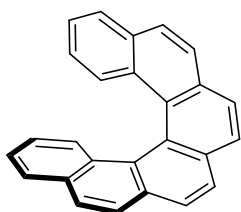




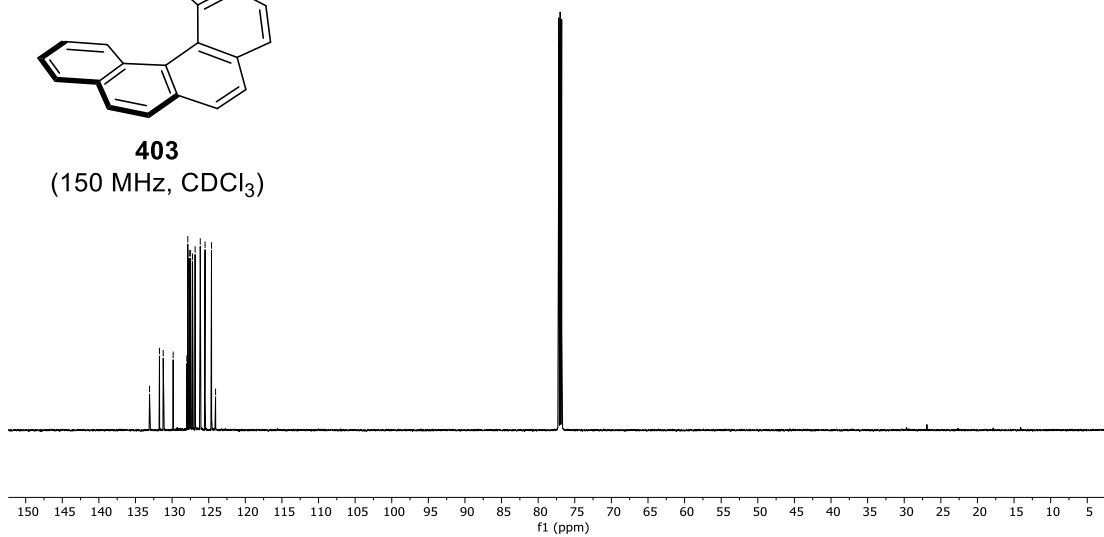
403
(600 MHz, CDCl₃)



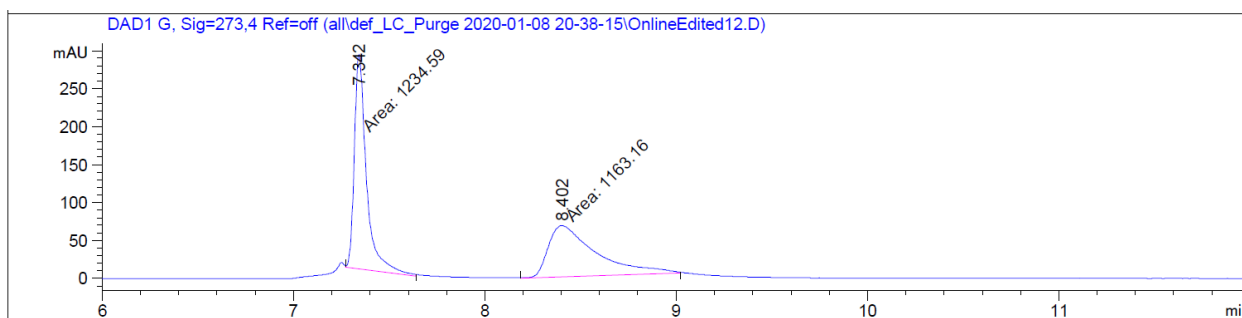
133.08
131.73
131.21
129.85
129.85
127.86
127.65
127.48
127.21
127.21
126.15
125.50
124.62
124.06



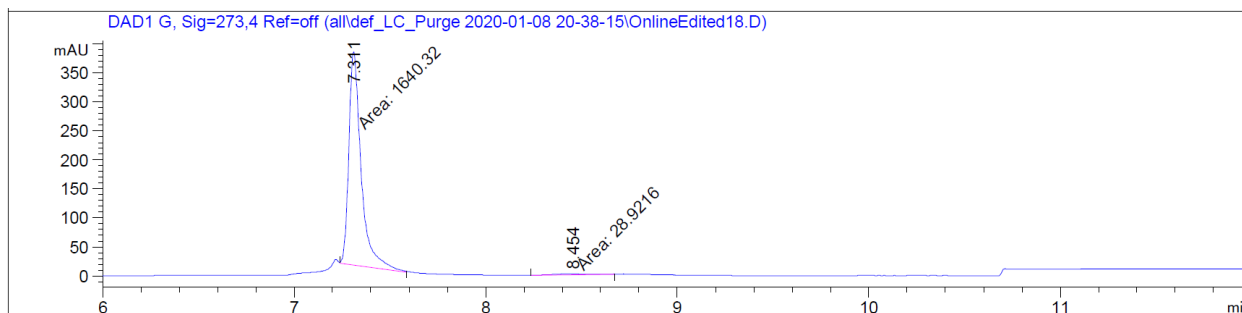
403
(150 MHz, CDCl₃)



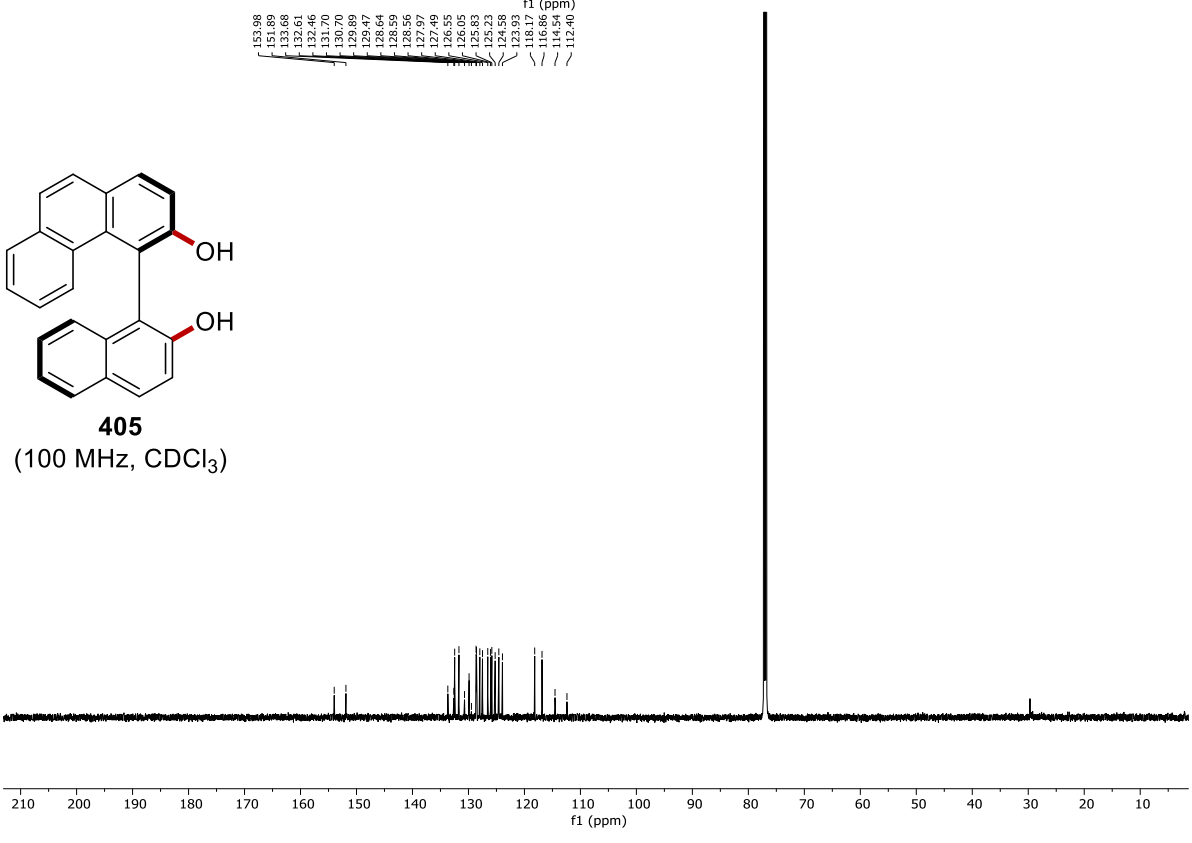
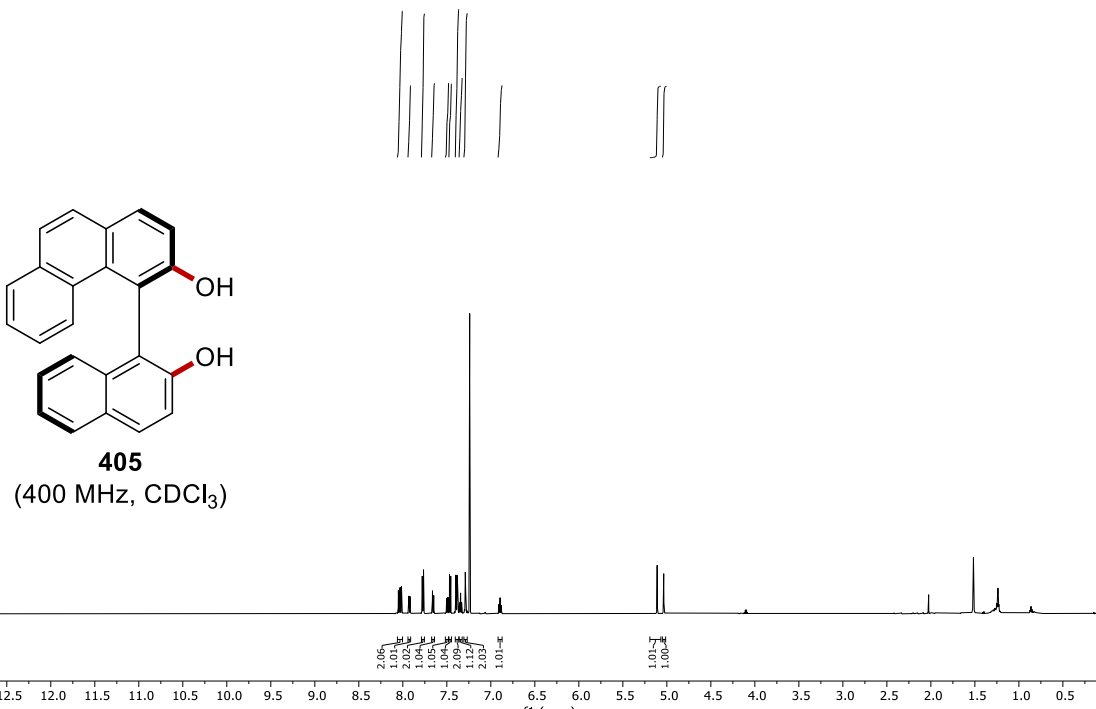
Chiral HPLC of **403**:



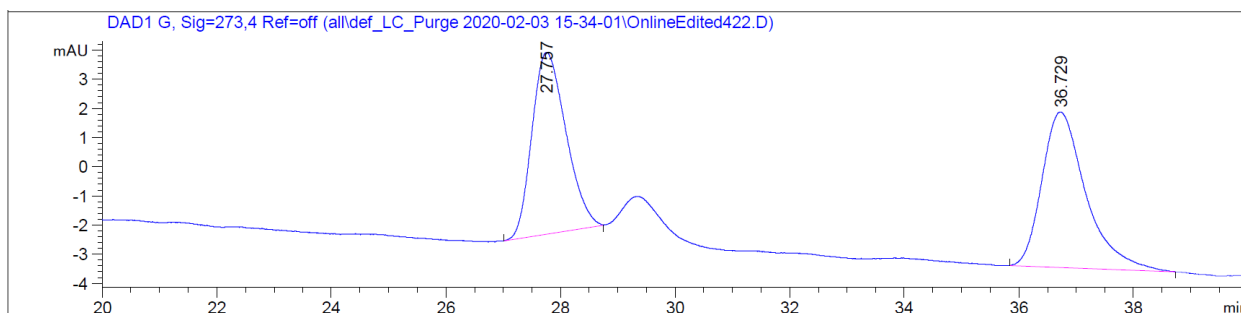
Peak #	RetTime [min]	Type	Width [min]	Area [mAU*s]	Height [mAU]	Area %
1	7.342	MM	0.0728	1234.59485	282.60950	51.4897
2	8.402	MM	0.2878	1163.15759	67.36166	48.5103



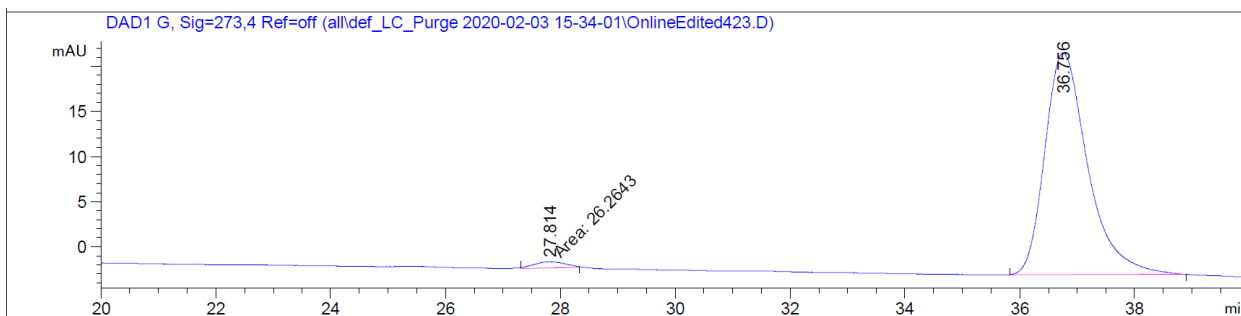
Peak #	RetTime [min]	Type	Width [min]	Area [mAU*s]	Height [mAU]	Area %
1	7.311	MM	0.0743	1640.31567	367.84052	98.2674
2	8.454	MM	0.2429	28.92158	1.98444	1.7326



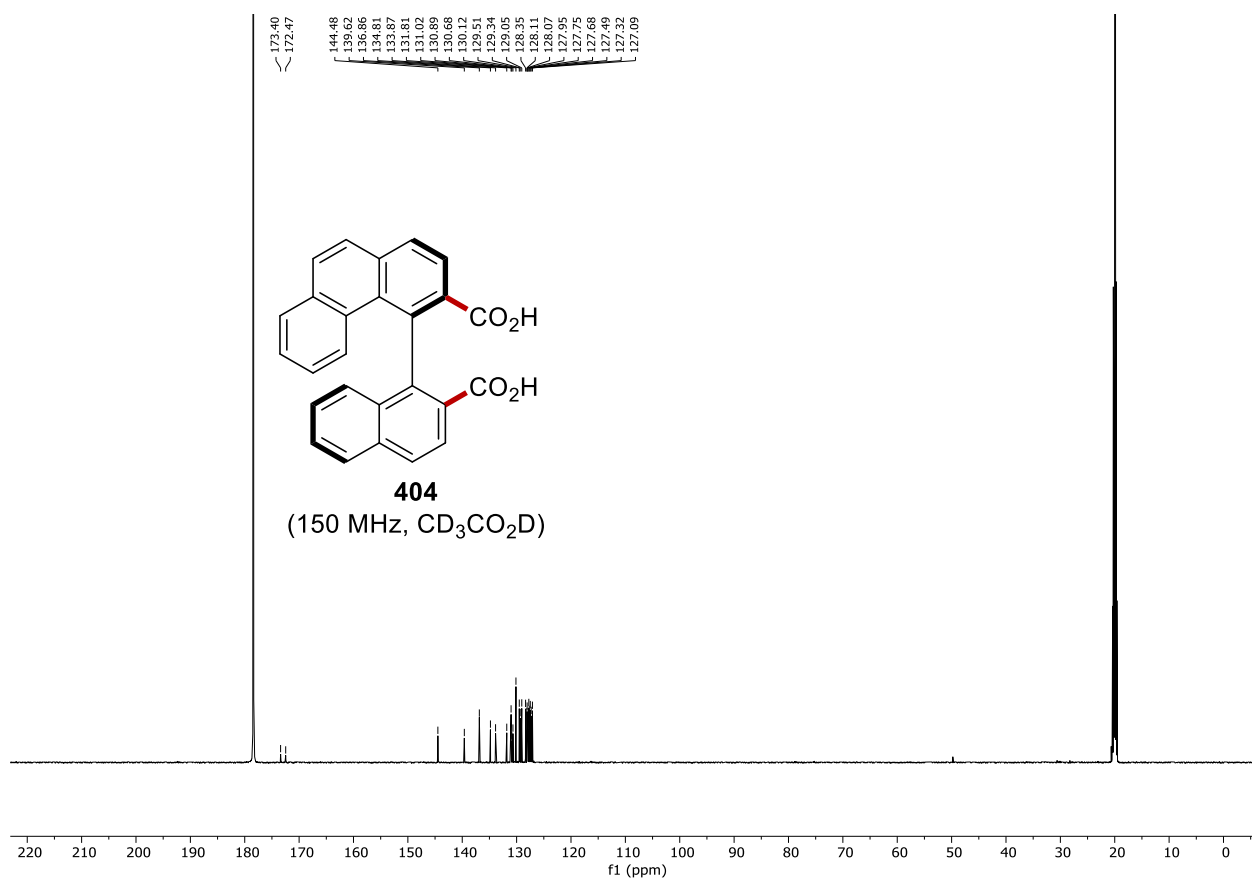
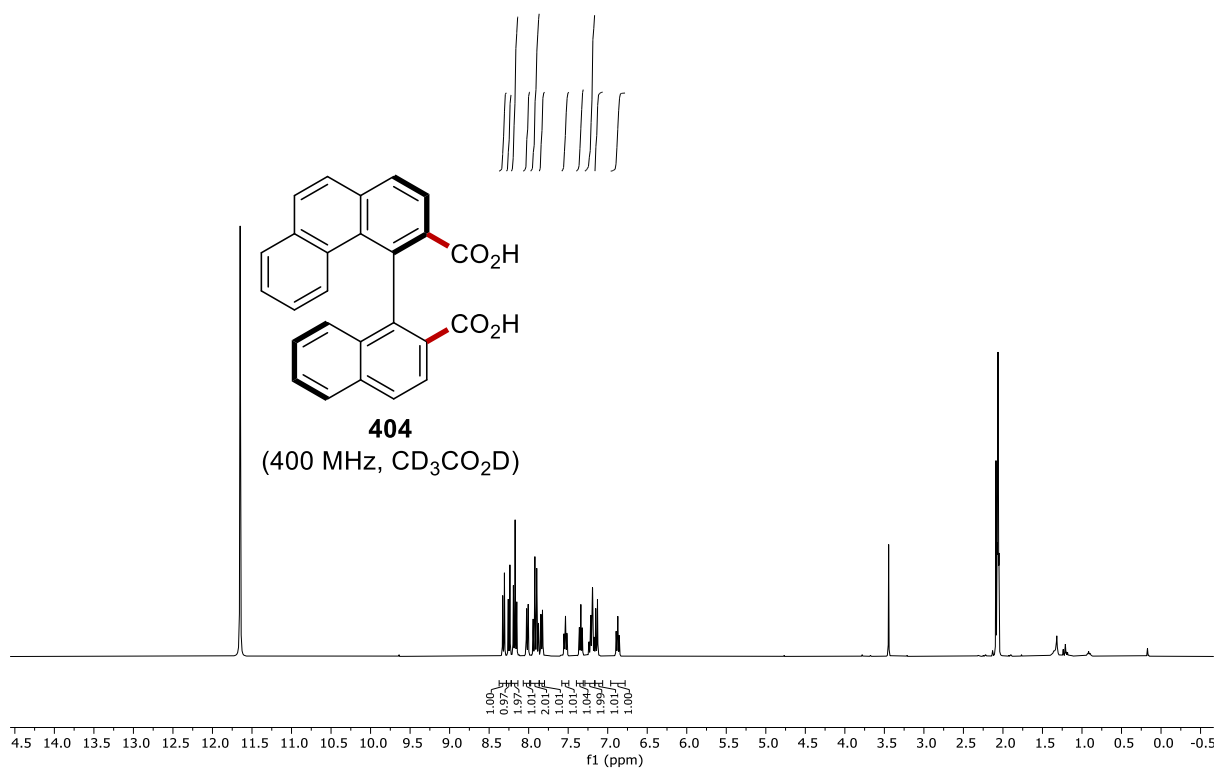
Chiral HPLC of **405**:



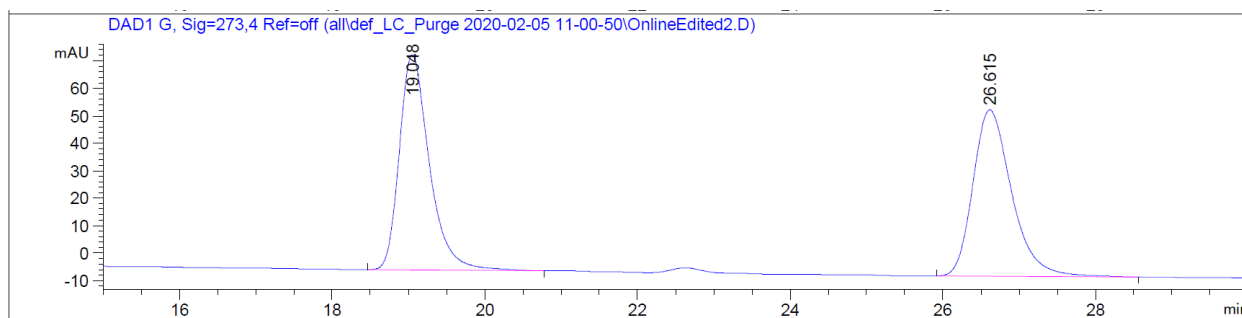
Peak #	RetTime [min]	Type	Width [min]	Area [mAU*s]	Height [mAU]	Area %
1	27.757	BB	0.4912	256.50980	6.23206	47.4281
2	36.729	BB	0.6254	284.32904	5.32964	52.5719



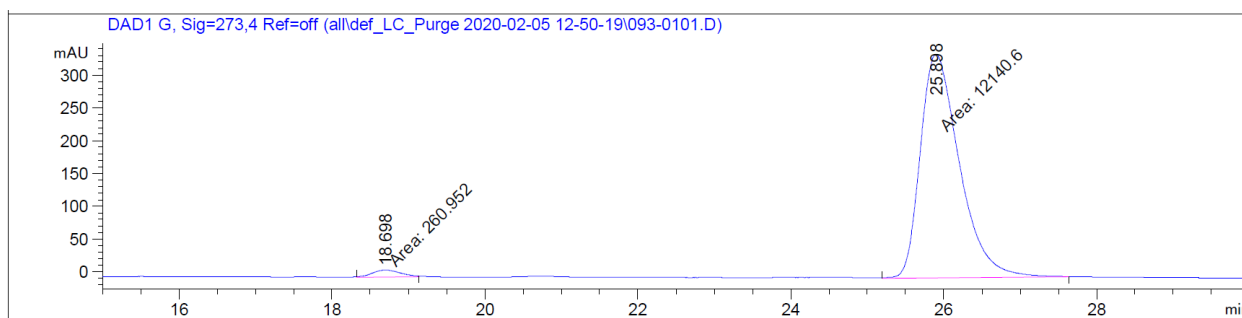
Peak #	RetTime [min]	Type	Width [min]	Area [mAU*s]	Height [mAU]	Area %
1	27.814	MM	0.6388	26.26430	6.85210e-1	2.0200
2	36.756	BB	0.7001	1273.94202	24.60153	97.9800



Chiral HPLC of **404**:



Peak #	RetTime [min]	Type	Width [min]	Area [mAU*s]	Height [mAU]	Area %
1	19.048	BB	0.4143	2144.05420	78.34101	50.1105
2	26.615	BB	0.5291	2134.59570	60.57181	49.8895



Peak #	RetTime [min]	Type	Width [min]	Area [mAU*s]	Height [mAU]	Area %
1	18.698	MM	0.4156	260.95184	10.46387	2.1042
2	25.898	MM	0.5932	1.21406e4	341.10617	97.8958

Erklärung

Ich versichere, dass ich die vorliegende Dissertation in dem Zeitraum von Oktober 2016 bis April 2021 am Institut für Organische und Biomolekulare Chemie der Georg-August-Universität Göttingen

auf Anregung und unter Anleitung von

Herrn Prof. Dr. Lutz Ackermann

selbstständig durchgeführt und keine anderen als die angegebenen Hilfsmittel und Quellen verwendet habe.

Göttingen, den 15.04.2021